I 1103

Vegyészet

ACADÉMIE DE LA RÉPUBLIQUE SOCIALISTE DE ROUMANIE

REVUE ROUMAINE DE CHIMIE

R

REFERÁLVA

TOME 28
N° 1
Janvier 1983

EDITURA ACADEMIEI REPUBLICII SOCIALISTE ROMÂNIA

Rev. Roumaine Chim.

RRCHAX, 28, *1*, p. 1 – 80 (1983), Bucarest

ACADÉMIE DE LA RÉPUBLIQUE SOCIALISTE DE ROUMANIE

COMITÉ DE RÉDACTION

Rédacteur en chef:

I. G. MURGULESCU, membre de l'Académie de la République Socialiste de Roumanie

Rédacteurs en chef adjoints:

A. T. BALABAN et V. EM. SAHINI membres correspondants de l'Académie de la République Socialiste de Roumanie

College de rédaction :

EM. BRATU, ELENA CEAUŞESCU, ECATERINA CIORĂNESCU-NENITZESCU, CR. SIMIONESCU, membres de l'Académie de la République Socialiste de Roumanie; P. SPACU, membre correspondant de l'Académie de la République Socialiste de Roumanie: MARGARETA AVRAM, M. BANCIU, I. HAIDUC, D. I. MARCHIDAN, I. MOLDOVAN, G. NIAC et D. SĂNDULESCU

La Revue Roumaine de Chimie paraît 10 fois par an. Toute commande de l'étranger pour les travaux parus aux Editions de l'Académie de la République Socialiste de Roumanie sera adressée à ILEXIM. Departamentul Export-Import Carte (Livres) Departamentul Export-Import Presă (Revues), P.O.B. 136 — 137, télex 11226 3, str. 13 Decembrie, 79517 Bucarest, Roumanie.

Les manuscrits, les livres et les revues proposés en échange, ainsi que toute correspondance seront envoyés à la rédaction :

REVUE ROUMAINE DE CHIMIE

125, Calea Victoriei, 79717 Bucarest, Roumanie, téléphone 50 76 80

EDITURA ACADEMIEI REPUBLICII SOCIALISTE ROMÂNIA
125, Calea Victoriei, 79717, Bucarest, Roumanie, téléphone 50 76 80

REVUE ROUMAINE DE CHIMIE

ORSZÁGOS MŰSZAKI INFORMÁCIÓS KÖZPONT ÉS KÖNYVTÁR 1883

Tome 28, N° 1 Janvier, 1983

C. MIHART, M. MRACEC and Z. SIMON, Molecular orbital studies for cyclophosphazene derivates. III. Comparison of Fukui and Dewar models. . . 3–13

R. P. VARMA and P. K. JAIN, Studies on behaviour of cobalt and calcium soaps. V. Effect of amines on the conductance behaviour in methanol at 35° . . . . 15–21 R

M. S. SUBHANI, The study of the reaction between TeO_3^{2-} and BrO_3^- ions in solution . . . . 23–26 Bc

S. P. SRIVASTAVA and B.B.L. MATHUR, Kinetics and mechanism of Ag^+ catalysed oxidation of isoleucine by peroxydisulphate ion . . . . 27–32 R

C. I. CHIRIAC, Phenyldichlorophosphite-dimethylformamide. A new reagent for dehydrating aromatic primary amides under mild conditions 33–36

C. I. CHIRIAC, A new convenient method for synthesis of benzoxazoles by a direct condensation reaction . . . . 37–39 R

SOFIA MARCHIDAN, IULIANA VARTIRES and N.D.TOTIR, Determination of trace quantities of the group V-A elements by anodic stripping voltammetry. III. Trace analysis of bismuth 41–44

V. ARMEANU and SANDA VIŞAN, Benzfuroinoxime – an analytical reagent for the microdetermination of uranyl . . . . 45–52 R

V. G. VOICU, Polarographic kinetic study of the oxidation of uranium (V) by vanadium (IV) in sulfuric acid medium 53–56

C. COBIANU and C. PAVELESCU, Deposition kinetics of silicon dioxide from silane and oxygen at low temperature . . . . 57–63 R

MARIA POPESCU and A. DĂNEŢ, Mercury (II) complexes of phenyl-α-pyridyltriazene and *p*-nitrophenyl-α-pyridyl-triazene ; properties and analytical application in a spectrophotometric method 65–74

BOOK REVIEWS 75–80

Rev. Roumaine Chim. 28, *1*, p. 1–80 (1983), Bucarest

Revue Roumaine de Chimie, 28, 1, 3 – 13 (1983)

MOLECULAR ORBITAL STUDIES FOR CYCLOPHOSPHAZENE DERIVATES. III*

COMPARISON OF FUKUI AND DEWAR MODELS

C. MIHART, [a] M. MRACEC, [b] and Z. SIMON [c]

[a] Agronomical Institute of Timişoara, Department of Biochemistry, Calea Aradului, 119, Timişoara, R–1900, Romania

[b] Chemical Research Laboratory, "Solventul" Timişoara, ICECHIM-CCMP, spl. N. Titulescu, 31, Timişoara, R–1900, Romania

[c] Institute of Medicine of Timişoara, Department of Biophysics, spl. T. Vladimirescu, 14, Timişoara, R–1900, Romania

Received April 5, 1981

In order to explain the characteristics of the P–N bond in cyclophosphazenes, HMO calculations are performed by means of the Fukui and Dewar models. The computation data for a series of substituted cyclophosphazenes were compared with the ionisation potentials, the polarographic reduction potentials, the bond lengths, the UV spectral data and some reactivity characteristics. The calculated values are in a satisfactory agreement with the experimental results.

The cyclophosphazenes and their derivatives are of a high theoretical and practical interest, [1,2] due to the chemical stability of the cycles and to a great number of characteristic reactions with wide application in organic chemistry.

In the previous papers, [3,4] we investigated the MO of cyclohalogenotriphosphazenes and some derivates, in order to elucidate the participation of the phosphorus atom in the conjugated system and to have theoretical arguments for the study of the relationship between the electronic structure and the chemical reactivity.

Due to the complex electronic structure of the studied compounds, with a great number of electrons implied in the chemical bonds, we shall begin the MO study in the π approximation, using the Huckel technique, which led to interesting conclusions in the previous papers. [5–10]

The phosphorus atom presents some peculiarities of participation in conjugated systems ; thus three models have been proposed : the antiaromatic, [5–7] the aromatic (Fukui) [8,9] and the Dewar [10] model. The computation performed up to now pointed out that results in good agreement with experimental data were obtained by using the Fukui and Dewar models. [11]

In this paper, the HMO computational results, using the Fukui and the Dewar model, were compared with the experimental data on: ionisation potientials, I(eV), polarographic reduction potentials, $E_{1/2}$(V), bond lengths (A), UV spectral data and some reactivity data.

METHOD AND PARAMETERS

According to the Fukui model, the phosphorus atom participates in the conjugated system with only one hybrid orbital (d_{yz}) and one π electron, while according to the Dewar model, the phosphorus atom participated with two orthogonal d-orbitals (d_{xz} and d_{yz}) and also one π electron. For the phosphorus atom and the other heteroatoms, two sets of parameters were used. The first set for the phosphorus atom was taken from the literature [9,12] (termed as p—L) : $\alpha_P = \alpha - 0.6\beta$ and $\beta_{PN} = 0.9\beta$, and the second set was recommended by Mracec[13] (termed as p—M) on the basis of an optimising procedure using spectral data : $\alpha_P = \alpha - 1.08\beta$ and $\beta_{PN} = 0.9\beta$. The other parameters are listed in table 1.

The computational work was performed on a FELIX C—256 computer, using an adjusted classical OMEGAHMO programme.

TABLE 1

Coulomb and resonance parameters for HMO calculations [12,14,15]

Heteroatom	$\frac{\alpha_x - \alpha}{\beta}$	Bond	β_{xy}/β
—N-(cycle)	0.5	P—N(cycle)	0.9
—$\ddot{C}H_3$(exocyclic)	2.0	P—$\ddot{C}H_3$(exocyclic)	0.6
—$\ddot{F}$ "	3.0	P—$\ddot{F}$ "	0.7
—$\ddot{Cl}$ "	2.0	P—$\ddot{Cl}$ "	0.4
—$\ddot{Br}$ "	1.5	P—$\ddot{Br}$ "	0.3
—$\ddot{O}CH_3$ "	2.0	P—$\ddot{O}CH_3$ "	0.8
—$\ddot{N}H_2$ "	1.5	P—Ar "	0.2
—$\ddot{O}$— "	2.0	P—$\ddot{N}H_2$ "	0.8
—$\ddot{N}$H— "	1.5	P—$\ddot{O}$— "	0.6
		P—$\ddot{N}$H— "	0.8
		O—Ar "	0.8
		NH—Ar	0.8

RESULTS

Figures 1 and 2 reproduce the molecular diagrams calculated with the Fukui and with the Dewar model respectively. Tables 2 and 3 present the frontier orbitals and the π delocalisation energies of the studied compounds, according to the Fukui and Dewar models respectively. Tables 4 — 10 give the correlations between the computed values (ε_{HO}, ε_{LE}, p_{PN}, $\varepsilon_{LE} - \varepsilon_{HO}$ and q_P) and the coresponding experimental data, taken from literature. [1,2] The computed values are listed as pairs, the upper corresponding to the Fukui model and the lower to the Dewar model.

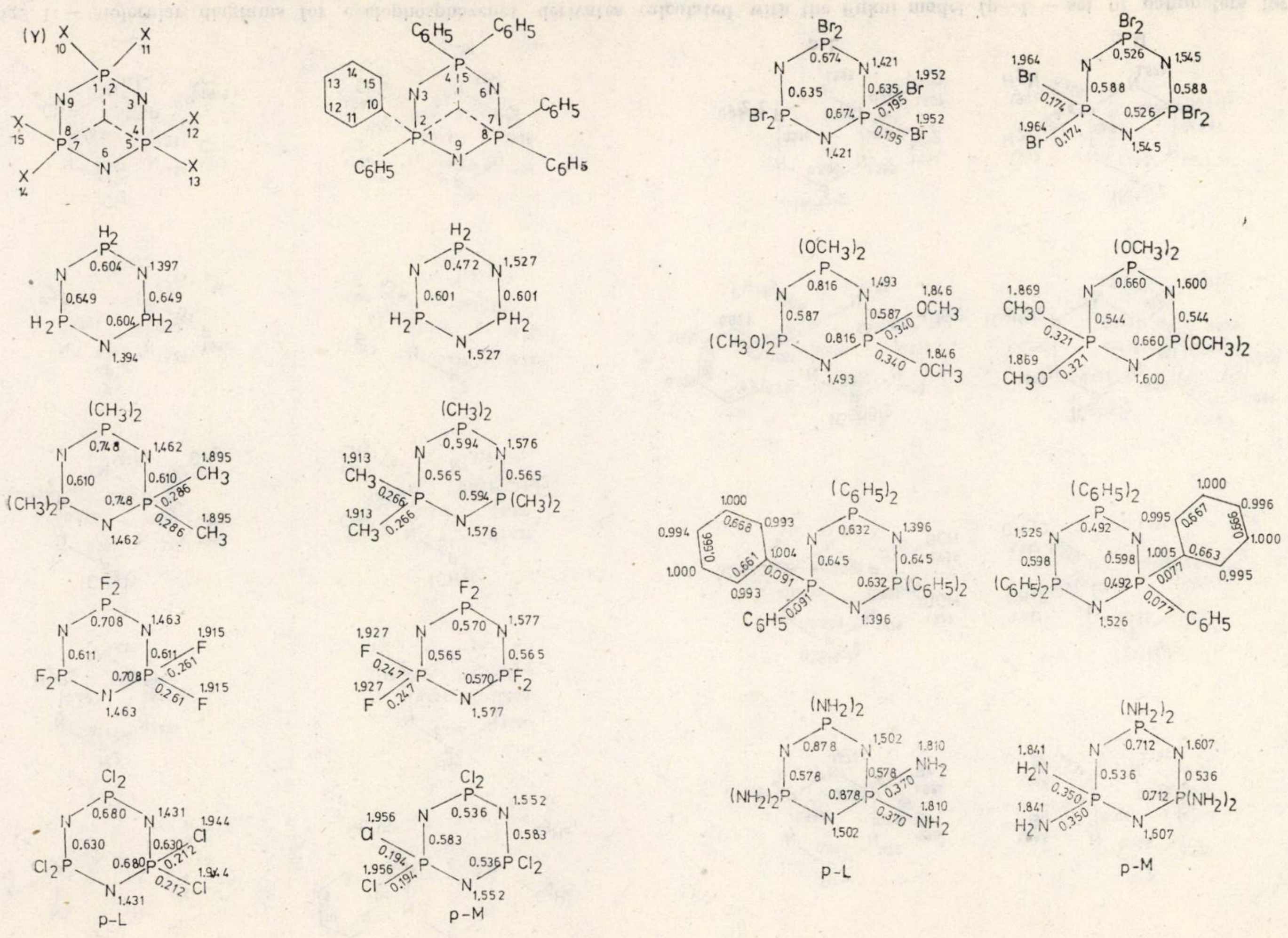
(Y)
p-L
p-M
p-L
p-M

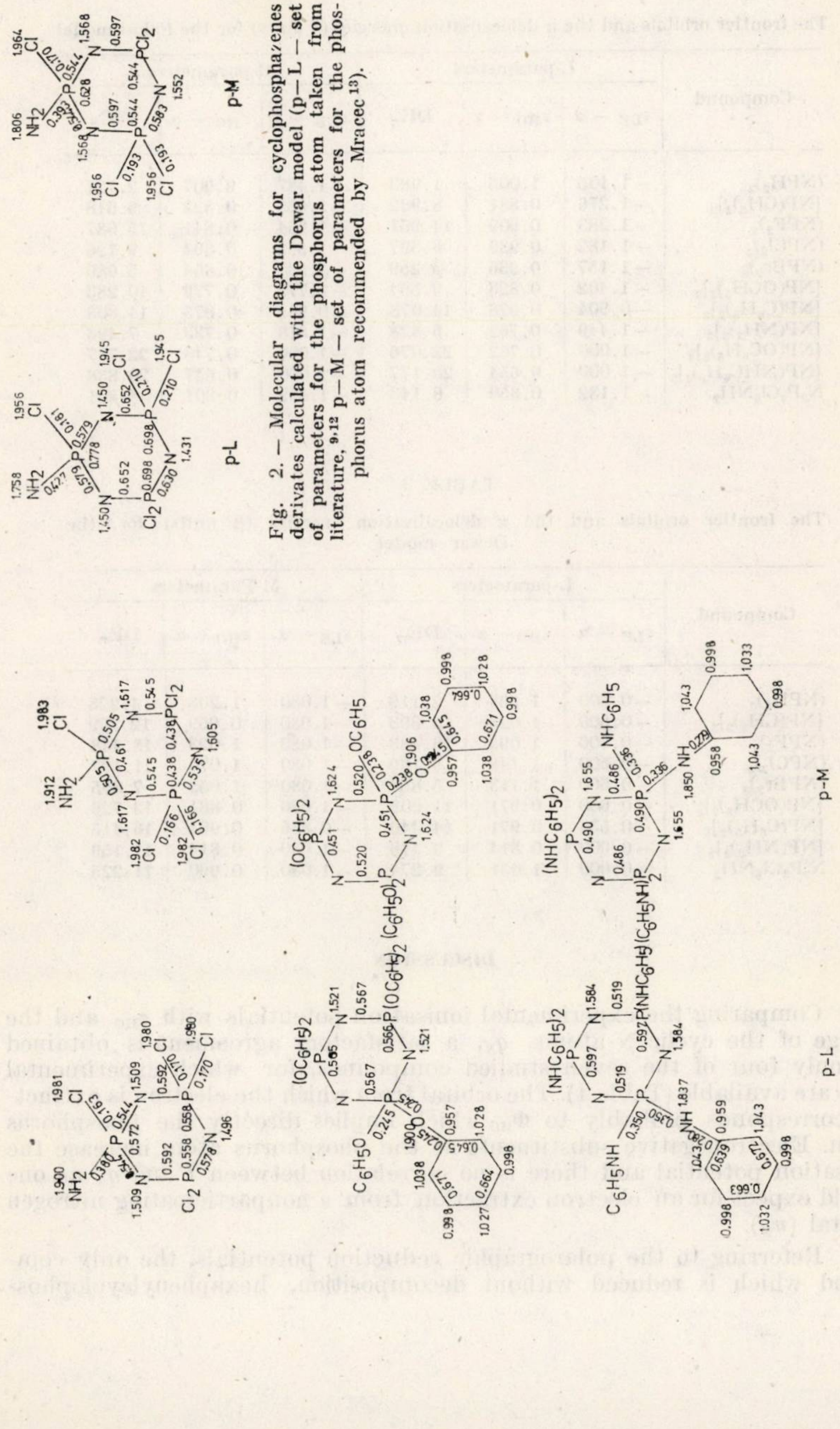
p-L
p-M
NH2
Cl
Cl2
PCl2
(OC6H5)2
OC6H5
C6H5O
(NHC6H5)2
NHC6H5
C6H5NH

Fig. 2. — Molecular diagrams for cyclophosphazenes derivates calculated with the Dewar model (p — L — set of parameters for the phosphorus atom taken from literature, 9,12 p — M — set of parameters for the phosphorus atom recommended by Mracec 13).

TABLE 2

The frontier orbitals and the π delocalisation energies (β units) for the Fukui model

Compound	L-parameters			M-parameters		
	$\varepsilon_{LE} - \alpha$	$\varepsilon_{HO} - \alpha$	DE_π	$\varepsilon_{LE} - \alpha$	$\varepsilon_{HO} - \alpha$	DE_π
$(NPH_2)_3$	−1.105	1.005	1.983	−1.487	9.907	2.721
$[NP(CH_3)_2]_3$	−1.276	0.881	8.902	−1.653	0.822	9.618
$(NPF_2)_3$	−1.283	0.909	14.951	−1.664	0.841	15.687
$(NPCl_2)_3$	−1.182	0.939	8.397	−1.562	0.864	9.126
$(NPBr_2)_3$	−1.157	0.936	5.259	−1.537	0.864	5.986
$[NP(OCH_3)_2]_3$	−1.402	0.823	9.584	−1.775	0.779	10.283
$[NP(C_6H_5)_2]_3$	−0.904	0.928	14.078	−0.961	0.875	14.808
$[NP(NH_2)_2]_3$	−1.449	0.762	6.828	−1.816	0.733	7.496
$[NP(OC_6H_5)_2]_3$	−1.000	0.762	22.076	−1.000	0.746	22.787
$[NP(NHC_6H_5)_2]_3$	−1.000	0.654	20.177	−1.000	0.647	20.838
$N_3P_3Cl_5NH_2$	−1.182	0.850	8.143	−1.562	0.801	8.861

TABLE 3

The frontier orbitals and the π delocalisation energies (β units) for the Dewar model

Compound	L-parameters			M-Parameters		
	$\varepsilon_{LE} - \alpha$	$\varepsilon_{HO} - \alpha$	DE_π	$\varepsilon_{LE} - \alpha$	$\varepsilon_{HO} - \alpha$	DE_π
$(NPH_2)_3$	−0.600	1.336	2.119	−1.080	1.208	4.228
$[NP(CH_3)_2]_3$	−0.600	1.023	10.393	−1.080	0.969	12.309
$(NPF_2)_3$	−0.600	1.095	16.483	−1.080	1.023	18.448
$(NPCl_2)_3$	−0.600	1.148	9.189	−1.080	1.070	11.197
$(NPBr_2)_3$	−0.600	1.113	5.854	−1.080	1.052	7.875
$[NP(OCH_3)_2]_3$	−0.600	0.971	11.905	−1.080	0.881	13.726
$[NP(C_6H_5)_2]_3$	−0.534	0.971	14.340	−0.836	0.964	16.415
$[NP(NH_2)_2]_3$	−0.600	0.814	9.418	−1.080	0.814	11.159
$N_3P_3Cl_6NH_2$	−0.600	1.051	9.274	−1.080	0.990	11.225

DISCUSSION

Comparing the experimental ionisation potentials with ε_{HO} and the charge of the cyclic N-atoms, q_N, a satisfactory agreement is obtained for only four of the seven studied compounds, for which experimental data are available (Table 4). The orbital from which the electron is extracted corresponds probably to Φ_{HO} which implies directly the phosphorus atom. Electronegative substituents at the phosphorus atom increase the ionisation potential and there is no correlation between I and q_N as one would expect for an electron extraction from a nonparticipating nitrogen orbital (n_N).

Referring to the polarographic reduction potentials, the only compound which is reduced without decomposition, hexaphenylcyclophos-

TABLE 4

The correlation between ε_{HO} and the experimental ionisation potentials

Compound	$\frac{\varepsilon_{HO}-\alpha}{\beta}$ $\left(\frac{\text{Fukui}}{\text{Dewar}}\right)$		q_N $\left(\frac{\text{Fukui}}{\text{Dewar}}\right)$		I (eV) (exp.)
	L–p	M–p	L–p	M–p	
$\{NP[N(CH_3)_2]_2\}_3$	0.762 0.814	0.733 0.794	1.595 1.502	1.673 1.607	7.85
$[NP(CH_3)_2]_3$	0.881 1.023	0.822 0.969	1.526 1.462	1.627 1.576	8.35
$[NP(OC_6H_5)_2]_3$	0.762 —	0.746 —	1.521 —	1.624 —	8.83
$[NP(OCH_3)_2]_3$	0.823 0.917	0.779 0.884	1.575 1.493	1.661 1.600	9.29
$(NPBr_2)_3$	0.936 1.113	0.864 1.052	1.472 1.421	1.591 1.545	9.56
$(NPCl_2)_3$	0.939 1.148	0.864 1.070	1.484 1.431	1.599 1.552	10.26
$(NPF_2)_3$	0.909 1.095	0.841 1.023	1.525 1.463	1.628 1.577	11.40

L – p : literature parameters;
M – p : parameters according to Mracec.

TABLE 5

The correlation between ε_{LE} and the polarographic reduction potentials

Compound	$\frac{\varepsilon_{LE}-\alpha}{\beta}$ $\left(\frac{\text{Fukui}}{\text{Dewar}}\right)$		$E_{1/2}$ (V) (exp.)
	L-parameters	M-parameters	
$[NP(C_6H_5)_2]_3$	−0.904 −0.534	−0.961 −0.836	−2.65
$[NP(NHC_6H_5)_2]_3$	−1.000 −1.000	−1.000 −1.000	not reduced
$[NP(OCH_3)_2]_3$	−1.402 −0.600	−1.775 −1.080	”
$(NPF_2)_3$	−1.283 −0.600	−1.664 −1.080	”
$(NPCl_2)_3$	−1.182 −0.600	−1.562 −1.080	”
$(NPBr_2)_3$	−1.157 −0.600	−1.537 −1.080	”

phazene, has a ε_{LE} significantly lower than the other five compounds that are not reduced (Table 5). The lowest empty orbital which accepts the electron in the reduced, phenyl substituted compound corresponds to a combination of the Φ_{LF} of the phosphazenic cycle and the corresponding symmetry combination of the Φ_{LF}'s of the phenyl cycles.

A good concordance is obtained between the bond orders, p_{NP}, and the NP endocyclic and exocyclic bond shortenings (Tables 6 and 7). The

TABLE 6

The correlation between p_{NP} and endocyclic bond lengths NP (Å)

Compound	p_{NP} (Fukui) Dewar		Shortening of bond length (Å)
	L-parameters	M-parameters	
$(NPF_2)_3$	0.563 0.611	0.520 0.565	0.240
$[NP(OC_6H_5)_2]_3$	0.567 —	0.520 —	0.225
$(NPBr_2)_3$	0.589 0.635	0.544 0.588	0.224
$(NPCl_2)_3$	0.583 0.630	0.538 0.583	0.219
$[NP(C_6H_5)_2]_3$	0.599 0.645	0.553 0.598	0.203
r	0.869 0.939	0.823 0.950	

TABLE 7

The correlation between p_{PX} and exocyclic bond lengths P–X (Å)

Compound	p_{PX} (Fukui/Dewar)		Bond	Shortening of bond length (Å)
	L-parameters	M-parameters		
$[NP(C_6H_5)_2]_3$	0.078 0.091	0.070 0.077	P–C	0.066
$(NPBr_2)_3$	0.151 0.195	0.145 0.174	P–Br	0.078
$(NPCl_2)_3$	0.170 0.212	0.116 0.194	P–Cl	0.084
$[NP(OC_6H_5)_2]_3$	0.245 —	0.238 —	P-O	0.178
$(NPF_2)_3$	0.237 0.261	0.230 0.247	P-F	0.192
r	0.903 0.635	0.943 0.660		

TABLE 8

The correlation between $\varepsilon_{LE}-\varepsilon_{HO}$ and wave number (cm^{-1}) for the first maximum in the UV spectra

Compound	$\varepsilon_{LE}-\varepsilon_{HO}$ (− β unit) Fukui (Dewar) L-parameters	M-parameters	λ_{max} (nm)	(log E)	$10^7/\lambda_{max}$ (cm^{-1})
$[NP(C_6H_5)_2]_3$	1.832 1.505	1.836 1.800	266	(3.09)	37 593
$[NP(OC_6H_5)_2]_3$	1.762 —	1.764 —	273 206 259 266 272	(2.89) (4.70) (3.23) (3.31) (3.18)	36 630 48 543 38 610 37 593 36 764
$(NPBr_2)_3$	2.093 1.713	2.401 2.132	200	(4.40)	50 000
$[NP(OCH_3)_2]_3$	2.225 1.517	2.554 1.961	<200		> 50 000
$\{NP[N(CH_3)_2]_2\}_3$	2.211 1.414	2.549 1.874	<200		> 50 000
$[NP(CH_3)_2]_3$	2.157 1.623	2.475 2.049	<200		> 50 000
$(NPCl_2)_3$	2.121 1.748	2.426 2.150	175	(4.00)	57 142
$(NPF_2)_3$	2.192 1.695	2.505 2.103	149	(4.00)	66 934

TABLE 9

Regresional coefficients and r— coefficient for the $\varepsilon_{LE}-\varepsilon_{HO}$ vs. wave number correlations

Model	$\alpha \times 10^4$ (cm^{-1})	$\beta \times 10^4$ (cm^{-1})	r
L-parameters :			
Fukui	−4.07	4.36	0.783
Dewar	−1.63	4.12	0.483
M-parameters :			
Fukui	−0.55	2.39	0.788
Dewar	−4.83	4.92	0.620

TABLE 10

π-electronic change at the phosphorus atom for halogenocyclotriphosphazene derivatives

Compound	L-parameters		M-parameters	
	Fukui	Dewar	Fukui	Dewar
$(NPBr_2)_3$	0.566	0.671	0.436	0.526
$(NPCl_2)_3$	0.577	0.680	0.436	0.536
$(NPF_2)_3$	0.546	0.708	0.437	0.570

shortening of bond lengths is calculated with respect to the sum of monocovalent radii ($R_P = 1.100$, $R_N = 0.700$, $R_C = 0.770$, $R_O = 0.660$, $R_F = 0.640$, $R_{Cl} = 0.990$ and $R_{Br} = 1.140$)[16]. The four correlation coefficients r refer to the following combinations of models and parameters: Fukui, p — L per Dewar, p—L; Fukui, p—M per Dewar, p—M. The best correlations of π-bond orders with the bond length shortenings are obtained with the parameters recommended by Mracec (p—M), with the Dewar model for endocyclic bonds and the Fukui model for exocyclic bonds. For endocyclic bonds an unexpected antiparallelism of p_{NP} and bond shortening is obtained which may be due to peculiarities of the second, in plane, π'-conjugation.

The correlation between the calculated $\varepsilon_{LE} - \varepsilon_{HO}$ difference and the wave number of the first absorption maximum (Table 8) is satisfactory only for the Fukui model (Table 9). The intercept (a) and slope (β) of the regressional equation:

$$\overline{\nu}(\mathrm{cm}^{-1}) = a + \beta(\varepsilon_{LE} - \varepsilon_{HO})$$

are also listed in table 9. The intercept a, calculated for the Fukui model with the parameters recommended by Mracec, is quite small as expected for negligible configuration — interaction effects.

The rate of aminolysis for halogen-substituted cyclotriphosphazenes decreases in the order: $(NP\ Br_2)_3 > (NPCl_2)_3 > (NPF_2)_3$. The π-electronic charges at the phosphorus atom, q_P, are listed in table 10. The order of aminolysis rate is in contradiction with inductive effect of halogens which must be the strongest for the fluorine derivative but agrees with the expectations for the nucleophylic substitution if q_P's calculated with the Dewar-model are considered. This last result agrees with the idea of Moeller and Kokalis, [17] that this reaction implies a nucleophylic attack on the d-orbitals of the phosphorus atom and a flexible, distorted cycle for the transition state of the reaction, enhancing the "PNP-isle" character of the reactive centre.

CONCLUSIONS

The results of the Fukui and Dewar models agree for most of the studied series. The ε_{HO}'s for the highest occupied orbitals are rather low, the ε_{LE}'s for the empty orbitals rather high, the endocyclic P—N π-bond orders and delocalisation energies are appreciable. This suggests an "aromatic" character for these compounds, in good agreement with the fact that the sum of aromaticity constants (Balaban and Simon) [18] is near zero.

It is rather difficult to recommend one of the two models and parameters for the phosphorus atom in the HMO calculations, also because of the reduced number of data available for correlation. The Fukui model with the parameters recommended by Mracec gives the best results in most cases. In hexacyclic phosphazenes, the π-electronic conjugation seems to be extended upon the whole cycle, but transition states for some reactions may imply a distorsion of the cycle with an "PNP insulation" as required by the Dewar model.

The rather satisfactory correlations obtained suggest that consideration also of π-electrons, by Del Re or more elaborated methods, may explain most spectral and reactivity characteristics in this class of heterocycles.

REFERENCES

[*] Part. II. C. Mihart, M. Mracec and Z. Simon, *Anal. Univ. Timișoara, ser. Fiz.—Chim.*, **18**, 161 (1980).

[1] H. R. Allcock, "Phosphorus-Nitrogen Compounds", Academic Press, New York, 1972, chap. 3.

[2] L. S. Haikin and L. V. Vilkov, *Uspekhi Khim.*, **41**, 2224 (1972).

[3] C. Mihart, M. Mracec and Z. Simon, *Anal. Univ. Timişoara, ser. Fiz.— Chim.*, **18**, 71 (1980).

[4] C. Mihart, M. Mracec and Z. Simon, Preprint 2/1981, University of Timișoara, Faculty of Natural Sciences, seria Chimie.

[5] D. P. Graig and N. L. Paddock, *Nature*, **181**, 1052 (1958); *J. Chem. Soc.*, **1962**, 4118.

[6] K. A. R. Mitchell, *J. Chem. Soc. A*, **1968**, 2683; *Chem. Rev.*, **69**, 157 (1969).

[7] S. F. Mason, *Nature*, **205**, 495 (1965).

[8] R. Vîlceanu, A. Balint and Z. Simon, *Nature*, **217**, 61(1968); *Rev. Roumaine Chim.*, **13**, 533 (1968).

[9] K. Fukui, A. Imamura and C. Nagata, *Bull. Chem. Soc. Japan*, **36**, 1450 (1963).

[10] M.J.S. Dewar, E.A.C. Lucken and M.A. Whitehead, *J. Chem. Soc.*, **1960**, 2423.

[11] R. Vîlceanu, A. Balint, Z. Simon and M. Mracec, "Colloques Internationaux du CNRS, nr. 182, Chimie Organique du Phosphore", Paris, 1969, p. 39.

[12] A. Streitwieser, jr., "Molecular Orbital Theory for Organic Chemists", Wiley, New York, 1961, chap. 5.

[13] M. Mracec, "Thesis", University of Timișoara, 1977.

[14] W. P. Purcell and J. A. Singer, *J. Chem. Eng. Data*, **12**, 235 (1967).

[15] Z. Simon, "Biochimie cuantică și intersecțiuni specifice", Ed. Științifică, București, 1973, p. 42.

[16] L. Pauling, "General Chemistry", Third edition, W. H. Freeman and Company, San Francisco, 1970.

[17] T. Moeller and S. G. Kokalis, *J. Inorg. Nuclear Chem.*, **25**, 1397 (1963).

[18] A. T. Balaban and Z. Simon, *Tetrahedron*, **18**, 315 (1962).

Revue Roumaine de Chimie, 28, 1, 15 – 21 (1983

STUDIES ON BEHAVIOUR OF COBALT AND CALCIUM SOAPS. V

EFFECT OF AMINES ON THE CONDUCTANCE BEHAVIOUR IN METHANOL AT 35°

R.P. VARMA and P. K. JAIN
Department of Chemistry, D.A.V. College, Muzaffarnagar-251001, India

Received February 12, 1980
Revised April 10, 1982

The effect of amines (aniline, diethylamine and diethanol-amine) on the conductance behaviour of cobalt and calcium laurates in methanol at 35° has been studied. The CMC of soaps are found to be independent of additive concentration but the same in calcium soap solutions decreases with increasing aniline concentration. The conductance behaviour of calcium soap solutions in the presence of additives is exhibited by a relationship : $\log \lambda = A + B \log C$ for entire range of soap concentration but it is applicable separately below and above CMC of cobalt soap in the presence of aliphatic amines. Constants A and B vary similarly in aniline and diethylamine but show a different behaviour in diethanolamine above CMC for cobalt laurate. Dissociation constant K decreases and molecular conductivity at infinite dilution λ_∞ increases with the addition of aliphatic amines but both the values for cobalt soap show a reverse behaviour in the presence of aniline.

INTRODUCTION

Effect of additives on CMC gives us information on the surface activity and provides a clear understanding of the action of surfactants. It also affords information on the role of additives in concentrated solutions. A considerable effect of small amounts of water or free fatty acids on the size, shape and CMC of surface active agents in non-aqueous solutions has been observed.[1-3] The CMC of transition metal soaps in 1-butanol increases[4] with increasing amounts of water and ethylene glycol but it is independent of aniline concentration. The present communication deals with the study of effect of amines (aniline, diethylamine and diethanolamine) on the conductance behaviour of cobalt and calcium laurates solutions in methanol by determining CMC, dissociation constant and molecular conductance at infinite dilution.

EXPERIMENTAL

Merck of B.D.H. reagent grade chemicals were used. Soaps were prepared in a manner described earlier.[5,6] The procedure and apparatus used to measure the conductance of soap solutions were the same as reported earlier.[7] The reproducibility of measurements was examined by repeating them several times.

RESULTS AND DISCUSSION

Specific conductance, k, increases with increasing aliphatic amines. The increase of k is rapid in lower additions and becomes slow with further increase in aliphatic amine concentration (Fig. 1). However, the specific conductance decreases linearly with aniline concentration. It is also found that k does not vary much at higher diethanolamine and cobalt soap concentration. The plots of k vs. C are characterized by an intersection of two straight lines at CMC without additive. When aniline is added these plots show the same nature but the CMC of calcium soap decreases (from 6.0 to 2.8×10^{-4}M) with increasing aniline concentration. Diethylamine also does not alter the nature of plots for calcium laurate. The plots (Fig. 2) of k vs. C of cobalt laurate are linear and become nonlinear above CMC in the presence of diethylamine. Both the soaps follow this behaviour with the addition of diethanolamine.

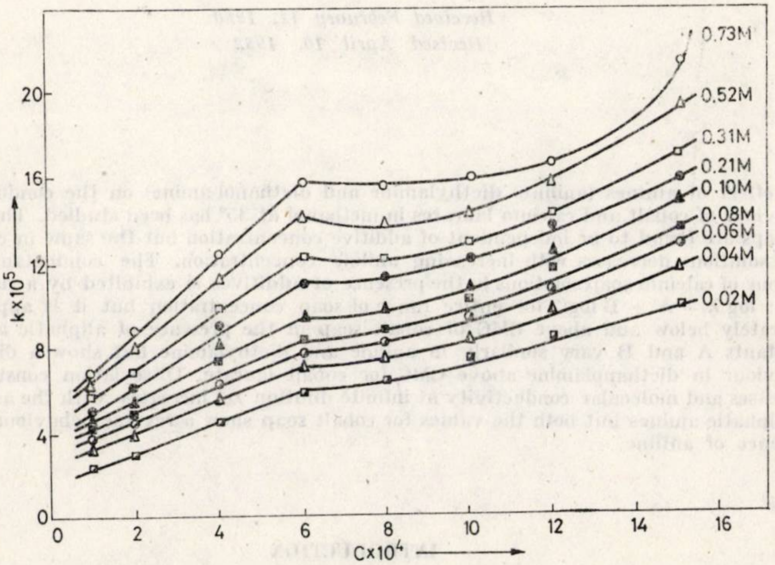

Fig. 1. — Plots of specific conductance. k vs. concentration. C of calcium laurate in methanol in the presence of varying amounts of diethanolamine.

The plots of log λ vs. log C of cobalt soap show an intersection of two straight lines at CMC in the presence of aliphatic amines. The lines are convergent below CMC and are divergent in nature above this concentration in the presence of diethanolamine whereas these are convergent in both the regions in the presence of diethylamine. The plots for calcium soap in aliphatic amines are converging and in aniline are diverging lines (Fig. 3). The linear plots of log λ vs. log C in the presence of varying amounts of additives show a linear relationship

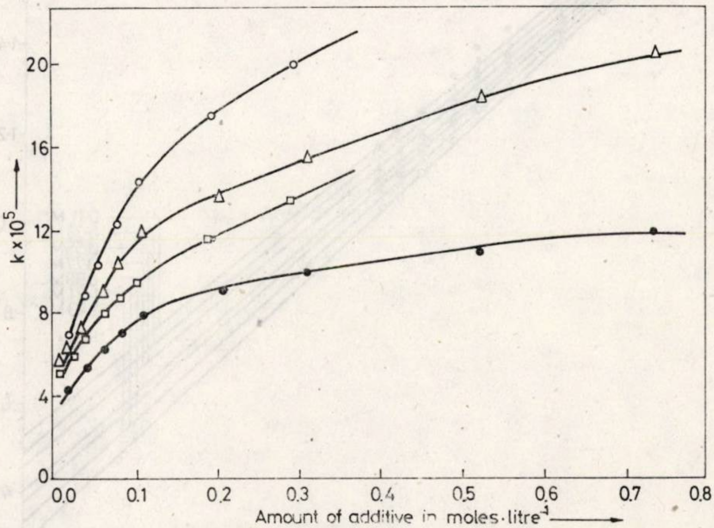

Fig. 2. — Plots of specific conductance, k vs. amount of aliphatic amines (moles/litre) in 0.0004 M soap solutions in methanol.

Cobalt laurate △ diethylamine
□ diethanolamine
calcium laurate ○ diethylamine
● diethanolamine

$$\log \lambda = A + B \log C \tag{i}$$

where A and B are constants.

Constant A (Tables 1 and 2) decreases with increasing additive concentration but the values for cobalt soap increase with increase in amount of diethanolamine above CMC. Constant B (Tables 2 and 3) varies with increasing amount of additives. It is found that these constants for calcium soaps are higher than cobalt soap in the presence of aniline.

Dissociation constant, K, and molecular conductance at infinite dilution, λ_∞ have been evaluated from the following [8,9] expression :

$$C^2\lambda^2 = \frac{K\lambda_\infty^3}{4\lambda} - \frac{\lambda_\infty^2 K}{4} \tag{ii}$$

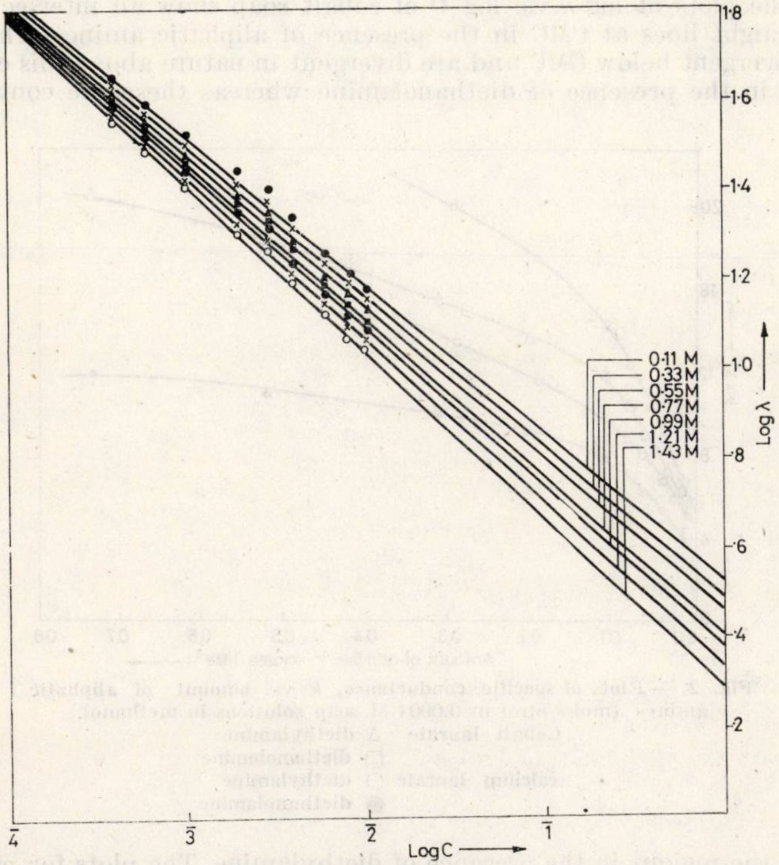

Fig. 3. — Plots of log λ *vs.* log C of cobalt laurate in methanol in the presence of varying amounts of aniline.

TABLE 1

Values of constant A of cobalt laurate in methanol in the presence of varying amounts (moles litre^{-1}) of amines at 35°C

Aniline		Diethylamine			Diethanolamine		
			A			*A*	
Amount	*A*	Amount	below CMC	above CMC	Amount	below CMC	above CMC
0.11	0.53	0.01	0.50	1.04	0.02	0.20	0.061
0.33	0.49	0.02	0.33	1.00	0.04	0.11	0.78
0.55	0.46	0.04	0.22	0.94	0.06	0.01	0.86
0.77	0.41	0.06	0.18	0.89	−0.08	−0.08	0.93
0.99	0.38	0.08	0.11	0.84	0.11	−0.16	1.01
1.21	0.33	0.10	0.02	0.82	0.21	−0.28	1.09
1.43	0.28	0.19	−0.05	0.80	0.31	−0.36	1.13

The plots (Fig. 4) of $C^2\lambda^2$ vs. $1/\lambda$ are linear below CMC. The equation is not found applicable for cobalt laurate solution in the presence of diethanolamine (>0.04 M). The values of K and λ have been evaluated from the slopes and intercepts of the linear $C^2\lambda^2 - 1/\lambda$ plots.

TABLE 2

Values of constants, A and B of calcium laurate in methanol in the presence of varying amounts (moles litre^{-1}) of amines at 35°C

Aniline			Diethylamine			Diethanolamine		
Amount	A	$-B$	Amount	A	$-B$	Amount	A	$-B$
0.11	0.68	0.35	0.01	0.27	0.68	0.02	0.54	0.45
0.33	0.63	0.36	0.02	0.23	0.68	0.04	0.53	0.46
0.55	0.58	0.37	0.04	0.17	0.69	0.06	0.52	0.49
0.77	0.53	0.38	0.06	0.12	0.70	0.08	0.50	0.51
0.99	0.47	0.39	0.08	0.06	0.71	0.11	0.49	0.53
1.21	0.41	0.40	0.10	—0.02	0.71	0.21	0.48	0.55
1.43	0.36	0.41	0.19	—0.10	0.76	0.31	0.47	0.56

TABLE 3

Values of constant, B of cobalt laurate in methanol in the presence of varying amounts (moles litre^{-1}) of amines at 35°C

Aniline		Diethylamine			Diethanolamine		
Amount	A	Amount	A		Amount	A	
			Below CMC	Above CMC		Below CMC	Above CMC
0.11	0.32	0.01	0.48	0.31	0.02	0.56	0.46
0.33	0.33	0.02	0.57	0.34	0.04	0.60	0.43
0.55	0.34	0.04	0.63	0.38	0.06	0.65	0.41
0.77	0.35	0.06	0.66	0.41	0.08	0.69	0.40
0.99	0.36	0.08	0.70	0.44	0.11	0.73	0.38
1.21	0.37	0.10	0.75	0.46	0.21	0.78	0.37
1.43	0.38	0.19	0.79	0.48	0.31	0.81	0.36

Dissociation constant (Table 4) increases with increase in aniline concentration in cobalt soap solution but decreases with increasing amount of other additives in soap solutions. These values of cobalt soap are higher than calcium soap in the presence of the same amount of additives.

Molecular conductance at infinite dilution increases with increase in additive concentration. It is observed that λ_∞ decreases with increasing amount of aniline in cobalt soap solution. A comparison of the values of λ_∞ in the presence of equimolar concentration of additives shows the following order:

Diethylamine > Diethanolamine > Aniline

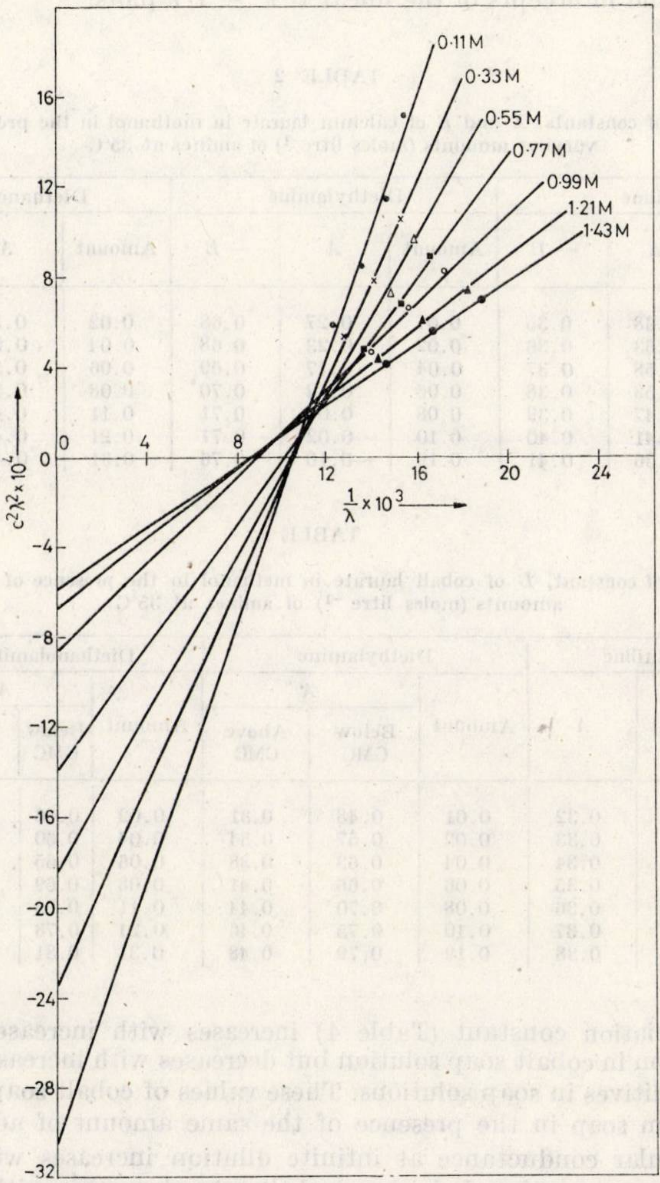

Fig. 4. — Plots of $C^2\lambda^2$ *vs.* $1/\lambda$ of calcium laurate in methanol in the presence of varying amounts of aniline.

ACKNOWLEDGEMENT. The authors are thankful to Dr. K.N. Mehrotra for his keen interest throughout the work and college authorities for providing laboratory facilities. One of the authors (P.K.J.) is grateful to C.S.I.R., New Delhi for the award of research fellowship.

TABLE 4

Values of K and λ_∞ of cobalt and calcium soaps in methanol in the presence of varying amounts (moles litre^{-1}) of amines at 35°C

Aniline			Diethylamine			Diethanolamine		
Amount	$K \times 10^6$	λ_∞	Amount	$K \times 10^8$	λ_∞	Amount	$K \times 10^8$	λ_∞
			Cobalt laurate					
0.11	3.469	49	0.01	25.60	250	0.02	33.95	254
0.33	3.571	47	0.02	13.38	366	0.04	26.14	315
0.55	3.650	45	0.04	7.12	530			
0.77	3.707	44	0.06	5.01	691			
0.99	3.855	42	0.08	3.70	838			
1.21	4.043	40	0.10	3.65	906			
1.43	4.262	39						
			Calcium laurate					
0.11	1.383	94	0.01	18.30	251	0.02	56.18	168
0.33	1.046	94	0.02	7.87	370	0.04	28.84	244
0.55	0.816	94	0.04	2.63	591	0.06	20.59	298
0.77	0.566	98	0.06	0.52	1 100	0.08	17.82	335
0.99	0.268	111	0.08	0.09	2 070	0.11	14.85	388
1.21	0.199	115	0.10	0.01	4 740	0.21	11.91	477
1.43	0.164	116				0.31	10.81	554

REFERENCES

[1] P. Debye and W. Prins, *J. Colloid Sci.*, **13**, 86 (1958).
[2] J. G. Honig and C. R. Singleterry, *J. Phys. Chem.*, **60**, 1108 (1956).
[3] J. G. Honig and C. R. Singleterry, *J. Phys. Chem.*, **58**, 201 (1954).
[4] R. P. Varma and H. K. Bhargava, *J. Indian Chem. Soc.*, **56**, 680 (1979).
[5] R. P. Varma and K. Kumar, *Colloid and Polymer Sci.*, **256**, 266 (1978).
[6] R. P. Varma, H. K. Bhargava and R. Dayal, *Polish J. Chem.*, **30**, 307 (1976).
[7] R. P. Varma and P. K. Jain, *Polish J. Chem.* (Communicated).
[8] R. P. Varma and R. Dayal, *J. Amer. Oil Chem. Soc.*, **53**, 39 (1976).
[9] C. A. Kraus and W. C. Bray, *J. Amer. Chem. Soc.*, **35**, 1315 (1913),

Revue Roumaine de Chimie, 28, 1, 23 – 26 (1983)

THE STUDY OF THE REACTION BETWEEN TeO_3^{2-} AND BrO_3^- IONS IN SOLUTION

M.S. SUBHANI
Department of Chemistry, Faculty of Science, P.O. Box 9480, Benghazi, Libya

Received May 29, 1980
Revised June 30, 1982

The rate of reaction between TeO_3^{2-} ion and BrO_3^- ion was studied at various ionic strengths in solution. The reaction was found to be a second order process. A mechanism is suggested for the reaction. The energy of activation was also evaluated. Studies were also carried out using different dielectric media. From the graphical plot of log K_0 and $1/D$ the values for r and r_{AB} for the activated complex formed $(TeO_3 - BrO_3)^{3-}$ were obtained. On comparison with the theoretical results for the radii of single and double sphere model the single sphere model was found to be the most probable for the activated complex. The electrostatic contributions to the thermodynamic properties for the activated state were also calculated.

INTRODUCTION

Various investigations have been made for the determination of the reaction rate between various simple inorganic ions in solution[1-6] and a number of mechanisms have been suggested. Various workers[5-9] have also carried out studies for the variation of the specific rate constant of the reaction between these inorganic ionic species with the change in the dielectric constants of the medium and ionic strength of the system. Two models, single sphere and double sphere, were proposed for the shape of the activated complex formed during the ionic reaction.

Mathematical relationships relating the radius of the activated complex $r^{\neq}$ or r_{AB} and the rate constant at zero ionic strength (K_0) in different dielectric media (D) were suggested[1] (see equations (1) and (2)

$$\ln k_0 = \ln k_i - \frac{e^2}{2DKT}\left(\frac{(Z_A + Z_B)^2}{r^{\neq}} - \frac{Z_A^2}{r_A} - \frac{Z_B^2}{r_B}\right) \tag{1}$$

$$\ln k_0 = \ln k_i - \frac{Z_A Z_B e^2}{DKT\, r_{AB}} \tag{2}$$

where K_i is the specific rate constant at infinite dielectric of the medium, e, the charge of the electron, Z_A, Z_B, r_A and r_B are the valences and radii of the ions A and B respectively. The energy of activation and other thermodynamic properties for the transition state can be evaluated using expressions reported in the literature.[9-11]

RESULTS AND DISCUSSIONS

Experiments were carried out using the same initial concentration of the reactants for the measurement of the specific rate constants and order of reaction at natural pH. Linear plots were obtained when reciprocal of the concentration of the reactant $(TeO_3^2)^-$ at any interval of time was plotted against time *t*, thus indicating that the reaction between tellarite ion and bromate ion obeys a second order kinetics in solution. The most probable mechanism which can satisfy the above observation can be suggested as an atom transfer from BrO_3^- ion to TeO_3^{2-} ion analogous to that that had been proposed for the sulphite halate ion reactions.[12, 13] The mechanism can be written as follows :

$$TeO_3^{2-} + BrO_3^- \rightarrow TeO_4^{2-} + BrO_2^- \text{ (Slow)} \qquad (3)$$

$$TeO_3^{2-} + BrO_2^- \rightarrow TeO_4^{2-} + BrO^- \text{ (Fast)} \qquad (4)$$

$$TeO_3^{2-} + BrO^- \rightarrow TeO_4^{2-} + Br^- \text{ (Fast)} \qquad (5)$$

The step (3) is regarded as the rate determining step and thus the reaction is expected to follow a second order kinetics.

Measurements for the specific rate constants at various temperatures ranging from 5°C to 50°C were made and a plot between log *K* and reciprocal of temperature in absolute degrees $\left(\frac{1}{T}\right)$ gave a fairly good staight line at a given ionic strength (Fig. 1). From the slope of the plot a value of energy of activation as 63.25KJ/mole was obtained.

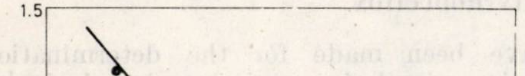

Fig. 1. A plot of log K_{obs} against $\frac{1}{T}$.

Measurements were also made to see the effect of ionic strength and the dielectric of the medium on the rate of reaction between these ions. The results obtained are shown in table 1.

All the plots between square root of ionic strength and the logarithmic function of specific rate constant at a given dielectric of the medium were fairly linear. The value for the log K_0 obtained from the extrapolation to zero ionic strength are summarized in tabel 2.

The plot of log K_0 against $1/D$ is found to be linear (see Fig. 2).

Deviation from linearity at the end of the plot may be due to the preferential association of water molecules with the reacting ions as suggested in the case of other systems.[5,14,15] The linear plot is in accordance with the prediction made in relationships (1) and (2). From the slope, the values of $r^{\neq}$ and r_{AB} were evaluated and are shown in table 3.

TABLE 1

The observed rate constants (K_{obs}) at various ionic strengths in different dielectric media

Dielectric constant D	K_{obs} (M—1 min^{-1}) X 10^3	Ionic strength U
79.8	3.981	0.2
	9.528	0.4
	13.52	0.5
	18.62	0.6
	24.89	0.7
	32.66	0.8
72.1	4.188	0.2
	11.61	0.4
	17.46	0.5
	25.35	0.6
	36.65	0.7
	48.80	0.8
65.5	4.436	0.2
	14.39	0.4
	23.07	0.5
	35.48	0.6
	52.48	0.7
	75.68	0.8
56.3	5.176	0.2
	22.70	0.4
	40.93	0.5
	70.46	0.6
	115.0	0.7
	182.0	0.8
49.2	6.999	0.2
	38.19	0.4
	78.52	0.5
	152.4	0.6
	177.3	0.7
	488.7	0.8

TABLE 2

The values of log K_0 and the reciprocal of dielectric constant ($1/D$)

log K_0	$1/D \times 10^3$
−4.710	12.5
−4.560	13.9
−4.410	15.3
−4.190	17.8
−4.080	20.3

TABLE 3

The theoretical and experimental values for the radii r_{AB} and $r^{\neq}$ for the double and single sphere shape respectively

	Experimental value (A°)	Theoretical value (A°)
r_{AB}	4.615	7.95
$r^{\neq}$	7.130	3.119

TABLE 4

The values for the thermodynamic properties $\Delta G^{\neq}_{es}$, $\Delta H^{\neq}_{es}$ and $\Delta S^{\neq}_{es}$ for the activated state

	$\Delta G^{\neq}_{es}$ (KJ/M)	$\Delta H^{\neq}_{es}$ (J/M)	$\Delta S^{\neq}_{es}$ (KJ/MJ)
Experimental value	7.544	−34.69	−3.139
Theoretical value	7.64	−35.14	−3.183

Theoretical values of $r^{\neq}$ and r_{AB} were obtained by the method reported in the literature,[5,7] using data for the various ionic radii available from the literature.[16-18] The values are also shown in table 3.

On comparison of the theoretical values of $r^{\neq}$ and r_{AB} with those experimentally obtained, it was observed that the most probable shape of the activated complex is of single sphere type.

The data obtained (see table 3) for $r^{\neq}$ were further used to calculate the electrostatic contributions to the thermodynamic properties for the reactants in the activated state. The values are summarized in table 4.

The sign and the changes in the electrostatic contributions to the entropy of activation $(\Delta S_e^{\neq})_s$ can be best interpreted in terms of the description of the initial state of the reactants and the one in the activated state TeO_3^{2-} and BrO_3^- ions can be regarded as doubly and singly negatively charged spheres before the start of reaction as they are at infinite distance from each other. In the activated state the sphere is triply negatively charged with *greater charged density* $(TeO_3 - BrO_3)^{3-}$. The solvent molecules in the neighbourhood of these charged spheres are acted upon by electrostriction. More stronger electrostriction is expected in the activated state than in the initial state of the reactants resulting in a decrease in entropy of activation. Similar arguments can be made for the other thermodynamic properties.

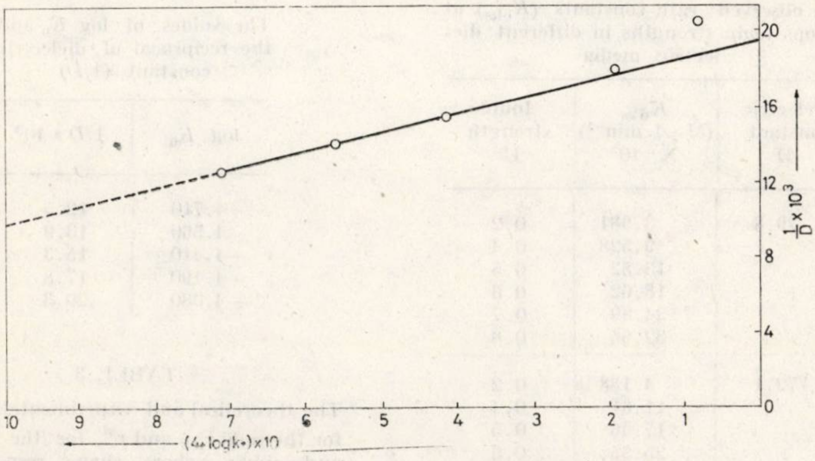

Fig. 2. — A plot of log K_0 against $\frac{1}{D}$.

REFERENCES

[1] K. J. Laidler, "Reaction Kinetics", Pergamon, Oxford, 1963, p. 10.
[2] C. T. Burris and K. J. Laidler, *Trans. Faraday Soc.*, **51**, 1497 (1955).
[3] K. J. Laidler and D. T. Y. Chen, *Trans. Faraday Soc.*, **54**, 1026 (1958).
[4] D.T.Y. Chen and K. J. Laidler, *Canad, J. Chem.*, **37**, 599 (1959).
[5] M. S. Subhani and M.N.H. Iacewala, *J. Sci., Maths.* **1**, 41 (1974).
[6] M. S. Subhani, *Rev. Roumaine Chim* (Accepted for publication).
[7] K. J. Laidler and H. Eyring, *Ann New York acad. Sci.*, **39**, 303 (1940).
[8] E. S. Amis, *J. Chem. Educ.*, **29**, 337 (1952).
[9] K. J. Laidler, "Chemical Kinetics", McGraw Hill, New York, 1965, p. 212., p. 217.
[10] E. S. Amis and J. E. Petts, *J. Amer. Chem. Soc.*, **63**, 2883 (1941).
[11] S. Arrhenius, *Z. Phys. Chem.*, **4**, 226 (1889).
[12] A. C. Nixon and K. B. Krauskopl, *J. Amer. Chem. Soc.*, **54**, 466 (1932).
[13] J. Helperin and H. Taube, *J. Amer Chem. Soc.*, **74**, (1952).
[14] M. S. Subhani and T. Kausar, *Pakistan J. Sci. Ind. Res.*, **18**, 208 (1978).
[15] G. S. Scatchard, *J. Chem. Phys.*, **7**, 657 (1939).
[16] J. Kleinberg, W. J. Argersinger and E. Griswold, "Inorganic Chemistry", D. C. Heath Co., Boston 1965, p. 74.
[17] T. Moeler "Inorganic Chemistry", Wiley, New York, 1960, p. 140.
[18] A. F. Kapusttnsku, *Quart. Rev.*, **10**, 283 (1956).

Revue Roumaine de Chimie, 28, 1, 27 – 32 (1983)

KINETICS AND MECHANISM OF Ag^+ CATALYSED OXIDATION OF ISOLEUCINE BY PEROXYDISULPHATE ION

S.P. SRIVASTAVA and B.B.L. MATHUR *
*Chemical Laboratories, N.R.E.C. College, Khurja (U.P.), India

Received August 20, 1980
Revised July 1, 1982

Ag^+ catalysed oxidation of isoleucine by peroxydisulphate ion in aq. medium has been first oder in $[S_2O_8^{2-}]$, in the catalyst and zeroth order in substrate. However, the first order rate constant decreases with increase in $[S_2O_8^{2-}]$ even at constant K^+ ion concentration and constant ionic strength. The reaction shows negative salt effect of primary exponential type. Different cations have different but small specific inhibitory effects. The different energy parameters are $\Delta E = 13.0 \pm 0.2$ K cal. mole^{-1}, $A = 3.55 \pm 0.07 \times 10^5$ s^{-1}, $\Delta F^{\pm} = 23.5 \pm 0.4$ Kcal mole^{-1}, $\Delta S^{\neq} = -35.25 \pm 0.09$ e.u. Oxidation product has been identified as methyl ethyl acetaldehyde. A mole ratio of 1 : 1 has been found. Allyl acetate shows strong inhibitory effect. A radical mechanism is proposed.

The kinetics and mechanism of the oxidation of various inorganic and organic substrates, by different oxidising agents have received considerable attention in recent years. Peroxydisulphate ion being a milder oxidising agent, has been preferred to others in order to study the various stages of oxidation process. Uncatalysed as well as catalysed oxidation of various substrates by $S_2O_8^{2-}$ ion has been studied by a number of workers and their work has been reviewed by House [1], Wilmarth and Hain. [2]

Survey of the literature has revealed that although the oxidation of a number of aminoacids by different oxidising agents has already been studied by different workers[3-7], no attempt seems to have been made to study the oxidation of isoleucine (an essential aminoacid). Hence a detailed kinetic study of Ag^+ catalysed oxidation of isoleucine by $S_2O_8^{2-}$ has been carried out in aq. medium in order to propose a probable mechanism of its oxidation. The results of these studies are presented in this paper.

MATERIAL AND METHOD

Isoleucine of B.D.H. quality, potassium peroxydisulphate and silver nitrate of B.D.H. Analar grade were used. Double distilled water was used to prepare standard solutions. The progress of the reaction was followed by the same method as reported earlier.[7,8]

Product Analysis — The reaction mixture containing 0.01M isoleucine, 0.05 M $K_2S_2O_8$ and 0.005 M $AgNO_3$ was kept at 45°C for four hours to complete the reaction. As the reaction proceeds, a gas evolves with effervescence which gave a positive test for CO_2. The reaction mixture gave a positive test for NH_4^+. This indicates that oxidation of isoleucine proceeds with oxidative decarboxylation and deamination. The ethereal extract of the reaction mixture gave a positive test of aldehyde.

The oxidation product seems to be methyl ethyl acetaldehyde. The confirmation was brought when 2 : 4· DNP derivative of the reaction product was prepared and characterized by TLC, melting point and I.R. spectrum using authentic sample.

RESULTS AND DISCUSSION

Stoichiometry — One mole of isoleucine is oxidised by one mole of potassium peroxydisulphate.

Kinetik Results

The first order decomposition of peroxydisulphate is appreciable at the experimental temperature. Hence it has been studied simultaneously and accounted for throughout these studies. Kinetic runs carried out in N_2 atmosphere showed no appreciable change in the rate constant or kinetic behaviour due to removal of oxygen. Hence subsequent studies were carried out in the ordinary atmosphere.

The reaction in any particular kinetic run follows first order behaviour in $S_2O_3^{2-}$ as the curve between $\log C$ vs. t is a straight line. However, the first order rate constant decreases with the increase in $[S_2O_8^{2-}]$. Srivastava and Chandra [4] explained this decrease due to the specific inhibitory effect of K^+ ion. But the decrease is observed even when the reaction is carried out at constant K^+ and constant ionic strength. Since the reactions involving $S_2O_8^{2-}$ are very susceptible to trace impurity [9], this decrease may be due to the traces of impurity present even in recrystallized Analar grade $K_2S_2O_8$ used.

TABLE 1

Effect of $S_2O_8^{2-}$ concentration on rate constant at constant K^+ concentration and constant ionic strength

[Isoleucine] = 0.01 M, $[AgNO_3]$ = 0.001M, $\mu = 0.331$, Temp. 33°C

$[S_2O_8^{2-}] \times 10^3$M	10	20	30	40	50
$k_2 \times 10^3$ min^{-1}	8.71	7.55	6.53	5.62	4.75
$k_1 \times 10^3$ min^{-1}	1.16	0.90	0.63	0.42	0.25
$k_r \times 10^3$ min^{-1}	7.55	6.65	5.90	5.20	4 50

where k_1 and k_2 are the first order rate constants in the absence and in the presence of substrate respectively and k_r is the net specific rate of oxidation of isoleucine.

The reaction is zeroth order w.r.t. isoleucine and the first order rate constant is unaffected even by three fold increase in substrate concentration. The rate constant k_r at experimental temperature (33°C) is $11.94 \pm \pm 0.05 \times 10^{-3}$ min^{-1} at 0.031 ionic strength.

Experiments have shown that uncatalysed reaction also proceeds with measurable speed at experimental temperature. The observed rate constant of uncatalysed reaction was found to be 8.2 ± 10^{-3} min^{-1}. The rate of Ag^+ catalysed oxidation has been found to increase with Ag^+ concentration (Table 2). The plot of k_r vs. $[Ag^+]$ is linear (in the conc. range $1 - 3 \times 10^{-3}$M) and follows the equation

$$k_r = 8.4 \times 10^{-3} + 6.5\,[Ag^+]$$

TABLE 2

Effect of Ag^+ concentration on rate constant

$[AgNO_3] \times 10^3$M	1	1.5	2.0	2.5	3.0
$k_2 \times 10^3$ min^{-1}	13.34	17.25	21.60	25.75	30.19
$k_1 \times 10^3$ min^{-1}	1.40	1.95	2.60	3.43	4.19
$k_r \times 10^3$ min^{-1}	11.94	15.30	19.00	22.32	26.00

Table 3 shows that the rate constant decreases with the increase in ionic strength and the plot of log k_r vs. $\mu^{1/2}$ is a straight line, indicating that negative salt effect is of primary exponential type. It is pertinent to mention that Ag^+ catalysed decomposition of $S_2O_8^{2-}$ shows similar effect.

TABLE 3

Effect of ionic strength on rate constant

$[K_2S_2O_8] = 0.01$M, [Isoleucine] $= 0.01$M, $[AgNO_3] = 0.001$M Temp. 33°C

$[K_2SO_4] \times 10^3$M	$k_r \times 10^3$	log k_r	μ	$\mu^{1/2}$
—	11.94	−1.9230	0.031	0.176
5	10.10	−1.9937	0.046	0.214
10	9.10	−2.0410	0.061	0.247
15	8.20	−2.0862	0.076	0.276
20	7.50	−2.1249	0.091	0.302
25	6.85	−2.1643	0.106	0.325

Specific inhibitory effect of different cations which is rather small follows the order

$$Zn^{2+} > Mg^{2+} > Na^+ > K^+$$

The value of $k_r - k_s$ which is a measure of inhibitory effect where k_r and k_s are the rate constants in the absence and in the presence of cations varies linearly with the radius of cation involved and follows the equation

$$(k_r - k_s) \times 10^3 = a - b(r)$$

where a and b are constants and r is the radius of cation.

The reaction has been studied at five different temperatures (33°C—48°C) to evaluate energy parameters. Although these are of little importance, an indication of the trend of reaction can be obtained.[10]

The reaction follows Arrhenius equation and is characterised by large negative value of entropy of activation. The different energy parameters evaluated are $\Delta E = 13.0 \pm 0.2$ Kcal mole, $A = 3.55 \pm 0.07 \times \times 10^5 \text{ sec}^{-1}$, $\Delta F^{\neq} = 28.5 \pm 0.4$ Kcal mole^{-1} $\Delta S^{\neq} = -35.25 \pm 0.09$ (e.u.).

Allyl acetate has a strong inhibitory effect (Table 4) suggesting that the reaction follows radical mechanism.

TABLE 4

Effect of allyl acetate concentration on rate constant

$[K_2S_2O_8] = 0.01M$, [Isoleucine] $= 0.01M$, $[AgNO_3] = = 0.001M$, Temp. 33°C

[Allyl acetate] × 10^3M	—	5	10
$k_2 \times 10^3$ min ^{1}	13.34	3.88	2.10
$k_1 \times 10^3$ min^{-1}	1.40	1.25	1.15
$k_r \times 10^3$ min^{-1}	11.94	2.63	0.95

DISCUSSION

The kinetic data above clearly demonstrate that Ag^+ catalysed oxidation of isoleucine by $S_2O_8^{2-}$ and Ag^+ catalysed decomposition of $S_2O_8^{2-}$ follows similar mechanism involving similar radicals. Further, since the inhibitory effect of allyl acetate is far greater in the case of isoleucine than in self decomposition, it suggests that allyl acetate removes the radical produced from isoleucine and that this radical is also involved in subsequent steps (steps v and vi). Since the uncatalysed oxidation process also occurs at a measurable speed at the temperature of experiment, the total oxidation reaction is a simultaneous reaction consisting of the following reactions: the uncatalysed and Ag^+ catalysed self decomposition of $K_2S_2O_8$ along with uncatalysed and Ag^+ catalysed oxidation of isoleucine. Incidentally all the four reactions are first order in behaviour. It is pertinent to mention that uncatalysed reactions have been found to follow similar kinetic characteristics as the Ag^+ catalysed reactions, pointing to the possibilities of similar radicals being involved in the two cases.

On the basis of the kinetic results and other evidences, the following mechanism is proposed for the Ag^+ catalysed oxidation of isoleucine.

$$\text{(i)} \qquad S_2O_8^{2-} + Ag^+ \underset{k-1}{\overset{k_1}{\rightleftharpoons}} AgS_2O_8^-$$

$$\text{(ii)} \qquad AgS_2O_8^- \xrightarrow{k_2} Ag^{2+} + SO_4^{\cdot -} + SO_4^{2-}$$

(iii)
$$\mathrm{CH_3CH_2CH(CH_3)CH(NH_2)COOH} + $$
$$+ \mathrm{SO_4^{\cdot -}} \xrightarrow{k_3} \mathrm{CH_3CH_2CH(CH_3)CH(NH_4)COO^{\cdot}} + \mathrm{HSO_4^-}$$

(iv)
$$\mathrm{CH_3CH_2CH(CH_3)CH(NH_2)COOH} + $$
$$+ \mathrm{Ag^{2+}} \xrightarrow{k_4} \mathrm{CH_3CH_2CH(CH_3)CH(NH_2)COO^{\cdot}} + \mathrm{Ag^+} + \mathrm{H^+}$$

(v)
$$\mathrm{CH_3CH_2CH(CH_3)CH(NH_2)COO^{\cdot}} + $$
$$+ \mathrm{H_2O} \xrightarrow{k_5} \mathrm{CH_3CH_2CH(CH_3)CHO} + \mathrm{NH_3} + \mathrm{CO_2} + \mathrm{HSO_4^-} + \mathrm{SO_4^{\cdot -}}$$

(vi)
$$\mathrm{CH_3CH_2CH(CH_3)CH(NH_2)COO^{\cdot}} + \mathrm{SO_4^{\cdot -}} + $$
$$+ \mathrm{H_2O} \xrightarrow{k_6} \mathrm{CH_3CH_2CH(CH_3)CHO} + \mathrm{NH_3} + \mathrm{CO_2} + \mathrm{HSO_4^-}$$

Steps (i) and (ii) are in accordance with Beckier, Kijowski[11] and Chattikyan, Beilerian [12]. E.S.R. studies [13] have provided evidence for the existence of $SO_4^{\cdot -}$ radical in peroxy-disulphate reaction. H abstraction in steps (iii) and (iv) from isoleucine molecule is broght about by $SO_4^{\cdot -}$ and Ag^{2+} resulting from the formation of the corresponding radical. H abstraction has been shown to take place in other organic substrates also.[7,8,14] The radical $CH_3CH_2CH(CH_3)CH(NH_2)COO^{\cdot}$ (herein designated as $R^{\cdot}$) then undergoes decarboxylation and deamination in the presence of $S_2O_8^{2-}$ in step (v) and in the presence of $SO_4^{\cdot -}$ in step (vi) to give final product, methyl ethyl acetaldehyde.

Applying the steady state treatment to the radicals $AgS_2O_8^-$, Ag^{2+}, $SO_4^{\cdot -}$, $R^{\cdot}$, the rate expression comes out to be

$$-\frac{d}{dt}[S_2O_8^{2-}] = K\,k_2[Ag^+]\,[S_2O_8^{2-}] + [S_2O_8^{2-}]\sqrt{\frac{Kk_2k_3k_5}{k_6}[Ag^+][R^{\cdot}]}$$

where K is the equilibrium constant of step (i) being mostly to the left. $k_6 \gg k_2$ or k_3 or k_5 because k_6 refers to radical-radical reaction. Hence the second term in the above equation is not kinetically distinguishable and the reaction may apparently show first order behaviour in $S_2O_8^{2-}$ and Ag^+ and zeroth order in substrate as actually found experimentally.

REFERENCES

[1] D. A. House, *Chem. Rev.*, **62**, 185 (1962).

[2] W. K. Wilmarth and A. Hain, "Mechanism of Oxidation by Peroxydisulphate in Peroxide Reaction Mechanism" Wiley, New York, 1961, p. 175.

[3] R. G. R. Bacon, W. J. W. Hanna and D. Stewart, *J. Chem. Soc. C.*, **1966**, 1388.

[4] S. N. Srivastava and G. Chandra, *Indian J. Chem.*, **11**, 773 (1973),

[5] Kamaluddin and M. A. Bèg, *Indian J. Chem.*, **13**, 1167 (1975).
[6] M. Adinarayana, B. Sethuram and N. Rao, *J. Indian Chem. Soc.*, **53**, 877 (1976).
[7] S. P. Srivastava, B. B. L. Mathur and S. K. Singhal, *Kinetika I Kataliz* **19**, 1419 (1978), ibid *Indian J. Chem.*, *16A*, 899 (1978).
[8] S. P. Srivastava and B. B. L. Mathur, *J. Indian Chem. Soc.*, **56**, 991 (1979).
[9] C. V. King and O. F. Steinback, *J. Amer. Chem. Soc.*, **52**, 4779 (1930).
[10] S. P. Srivastava and S. K. Singhal, *J. Indian Chem. Soc.* **46**, 705 (1969).
[11] E. Beckier and W. Kijowski, *Roczniki Chem.*, **14**, 1004 (1934), ibid., **15**, 136 (1935).
[12] O. A. Chattikyan and N. M. Beilerian, *Izvest Akad. Nauk Armiyan S.S.R. Otdel. Khimi Nauk.*, **11**, 13 (1958).
[13] Om. P. Chawla and W. F. Richard, *J. Phys. Chem.* **79**, 2693 (1975).
[14] S. P. Srivastava, H. Singh and A. Kumar, *J. Indian Chem. Soc.*, **52**, 104 (1975).

Revue Roumaine de Chimie, 28, 1, 33 – 36 (1983)

PHENYLDICHLOROPHOSPHITE-DIMETHYLFORMAMIDE. A NEW REAGENT FOR DEHYDRATING AROMATIC PRIMARY AMIDES UNDER MILD CONDITIONS

C. I. CHIRIAC
"P. Poni" Institute of Macromolecular Chemistry
Aleea Gr. Ghica Vodă 41 A Iași, Romania

Received May 9, 1982

Aromatic nitriles are prepared in good yields by a dehydration reaction with the adduct phenyldichlorophosphite-dimethylformamide, under mild condition.

The dehydration of primary amides to the corresponding nitriles is a classical synthesis which uses different reagents as: benzenesulfonyl chloride-pyridine,[1] thionyl chloride-dimethylformamide,[2] cyanuric chloride-dimethylformamide,[3] phosphonitrilic chloride,[4] triphenyl-phosphine-carbon tetrachloride,[5] etc.

RESULTS AND DISCUSSION

A previous communication from this laboratory showed that the phenyldichlorophosphite-dimethylformamide adduct is a useful reagent for the synthesis of 1, 3, 4-oxadiazoles from diaroylhydrazines.[6]

In this work, we have investigated the applicability of the phenyldichlorophosphite in dimethylformamide (DMF) as reagent in the dehydration of primary amides to the corresponding nitriles. Thus by heating at 70 – 80°C one mole of *p*-chlorobenzamide with one mole phenyldichlorophosphite in excess DMF, *p*-chlorobenzonitrile resulted (yield 90%).

The reactive intermediate in this reaction is the adduct of phenyldichlorophosphite with DMF having the structure:

$$[(CH_3)_2N^+ = CH - O - P(Cl)OC_6H_5]^+ Cl^-.^6$$

When we used only 0.5 mole of phenyldichlorophosphite, the yield was 35 – 40%, a situation identical with the synthesis of 1,3,4-oxadiazoles using the same reagent.[6] We have chosen DMF as solvent, because it has a high boiling point and is a very good solvent for the products of reaction.

We supposed, similar as in other cases,[6-9] that this reaction involves two transition states (II) and (III):

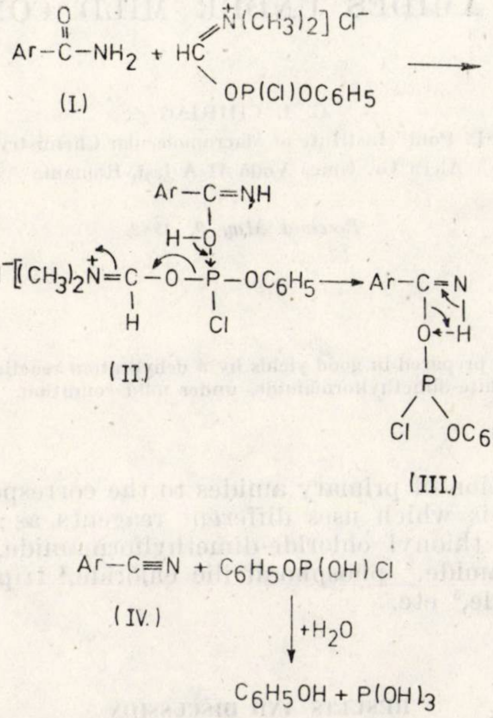

(I.)

(II)

(III.)

(IV.)

In this reaction, $C_6H_5OP(OH)Cl$ which results as by-product, does not affect the reaction, like in other cases.[6,10]

The dehydration reaction of aromatic primary amides takes place also with phenyldichlorophosphite without DMF, but the presence of a good solvent is necessary because the products have aromatic structures with low solubilities. Of course, without solvent, the reaction involves only the transition state of the type (III).

In a typical procedure, one mole of phenyldichlorophosphite was slowly added to a suspension of one mole (I) in DMF. The reaction needs a heating for one hour at 70 – 80°C under stirring. From the obtained solution, the product is precipitated with water and ice, when $C_6H_5OP(OH)Cl$ (by-product) is transformed in $C_6H_5OH, P(OH)_3$, and HCl. The yield of this method ranged from 67 to 90°(Table 1).

Using this adduct between phenyldichlorophosphite and DMF (reactive compound) we obtained the aromatic nitriles presented in table 1.

TABLE 1

Aromatic nitriles obtained from the corresponding amides using the phenyldichlorophosphite-DMF adduct

Aromatic nitriles a)			
	Yield b) %	M.p. c) °C	Reported m.p. d) °C
p-Cl-C_6H_4-CN	90	92–94	93–94 3)
p-$CH_3O-C_6H_4-CN$	81	58–60	59–60 12)
m-Br-C_6H_4-CN	74	37–39	38
p-Br-C_6H_4-CN	79 e)	113–114 e)	113–114 3)
o-Br-C_6H_4-CN	70 e)	51–52 e)	51
p-$CH_3-C_6H_4-CN$	72	57–58	58–59 3)
o-$Cl-C_6H_4-CN$	71	40–42	42–43
2,4-$Cl_2-C_6H_4-CN$	69 e)	60–61 e)	61
m-$Cl-C_6H_4-CN$	67	38–40	39
3,5-$Cl_2-C_6H_4-CN$	68 e)	64–65 e)	64–65

a) The products were identified by comparison of m.p. and IR spectra with authentic samples.
b) Yields calculated on aromatic amides employed.
c) Before recrystallisation.
d) From "Beilsteins Handbuch der Organischen Chemie".
e) After recrystallisation.

EXPERIMENTAL

p-Chlorobenzonitrile

To a suspension of 3.11 g (0.02 moles) *p*-chlorobenzamide in 5 ml DMF, 2.8 ml (0.02 moles) of phenyldichlorophosphite [11] were added under stirring, when the solution became clear and the temperature rose to about 70 – 75°. The solution was heated for one hour at 70–80°C. At the end of reaction, the obtained solution (still warm) was poured into a large volume (40 – 60 ml) of water with ice under stirring, when the desired product precipitated. The solution was treated with 7% NaOH solution till pH = 9 – 10 and the product was collected by filtration, washed with 20 – 25 ml 10% HCl solution, three times with 15 – 20 ml water and dried under vacuum at 40 – 50°C. *p*-Chlorobenzonitrile (2.5 g) was obtained with m.p. 92–94°. yield 90% (calculated on *p*-chlorobenzamide employed).

Anal. Found : C, 61.22 ; H, 2.98 ; N, 10.07%. Calculated for C_7H_4ClN ; C, 61.09 ; H, 2.90 ; N, 10.18%.

Under similar conditions, the other aromatic nitriles (presented in table 1) were prepared in good yields from the corresponding amides.

REFERENCES

[1] P. Oxley and W. F. Short, *J. Chem. Soc.*, **1948,** 1618.
[2] J. C. Thurman, *Chem. Ind.*, **1964,** 752.
[3] G. A. Olah and A. P. Fung, *Synthesis*, **1980,** 658.
[4] J. C. Graham and D. H. Marr, *Canad. J. Chem.*, **50,** 3857 (1972).
[5] W. Yamato and S. Sugasawa, *Tetrahedron Letters*, **47,** 4383 (1970).
[6] C. I. Chiriac, *Rev. Roumaine Chim.*, **27,** 935 (1982).
[7] F. Cramer and M. Winter, *Chem. Ber.*, **94**, 990 (1961).
[8] H. Brederek, *Chem. Ber.*, **92,** 837 (1959).
[9] E. A. Lawton and D. D. McRitchie, *J. Org. Chem.*, **24**, 26 (1959).
[10] C. I. Chiriac, *Rev. Roumaine Chim.*, **26**, 1001 (1981).
[11] H. Tölkmith, *J. Org. Chem.*, **23**, 1682 (1958).
[12] J. H. Hunt, *Chem. Ind.*, **1961**, 1873.

Revue Roumaine de Chimie, 28, 1, 37 – 39 (1983)

A NEW CONVENIENT METHOD FOR SYNTHESIS OF BENZOXAZOLES BY A DIRECT CONDENSATION REACTION

C. I. CHIRIAC

"P. Poni" Institute of Macromolecular Chemistry
Aleea Gr. Ghica Vodă 41 A, Iași, Romania

Received May 9, 1982

Various 2-arylbenzoxazoles were prepared by a direct condensation reaction between *o*-aminophenol and aromatic acids, using phenyldichlorophosphite as reagent at high temperature (145 – 155°C).

The direct synthesis of benzoxazoles from *o*-aminophenol and aromatic acids is difficult to realize. For the synthesis of benzoxazoles by direct condensation reactions, some reagents were used : polyphosphoric acid [1,2] and polyphosphate esters. [3]

RESULTS AND DISCUSSION

The utility of phenyldichlorophosphite as a remarkably effective condensing reagent, particularly for intra- and intermolecular condensations, has been extensively demonstrated in our laboratory.[4,5] Nothing has been reported, however, regarding its effectiveness in intermolecular condensations of *o*-aminophenols with aromatic acids leading to benzoxazoles. In this work, we have investigated the applicability of the phenyldichlorophosphite as a reagent in this field. Thus by heating at 145 – 155°C of one mole of *o*-aminophenol, one mole of benzoic acid and one mole of phenyldichlorophosphite, 2-phenylbenzoxazole resulted (yield 76%). The yield increases with the temperature of reaction. The reaction mixture is a homogeneous solution, because the products are melted over 150°C (the reaction takes place without solvent). During the heating an abundant evolution of gaseous hydrochloric acid was observed. The phenyldichlorophosphite has two reactive groups (two chlorine atoms) and both participate in the condensation reaction at temperatures over 120 – 130°C.

For this reaction, we propose the following mechanism :

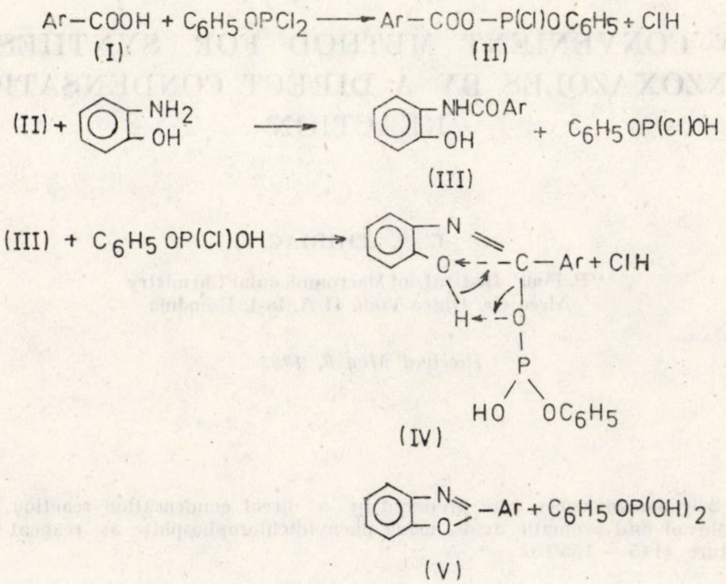
Ar—COOH + C6H5OPCl2 ⟶ Ar—COO—P(Cl)OC6H5 + ClH
(I)
(II)
(II) + NH2 OH ⟶ NHCOAr OH + C6H5OP(Cl)OH
(III)
(III) + C6H5OP(Cl)OH ⟶ N O ← — C — Ar + ClH
H ← O P HO OC6H5
(IV)
N O — Ar + C6H5OP(OH)2
(V)

In this transformation, $C_6H_5OP(OH)_2$ which results as by-product does not affect the reaction, like in other cases.[4,5]

In a typical procedure one mole *o*-aminophenol, one mole aromatic acid and one mole phenyldichlorophosphite are heated under stirring, when the evolution of hydrochloric acid begins and the solution becomes clear. The reaction needs a heating for four hours at 145 – 155°C, after which the final product is separated and purified.

Table 1 shows the benzoxazoles (V) obtained by this procedure.

The large majority of the final products (V) had correct melting points before recrystallisation and the yields ranged from 70 to 84% (Table 1).

In conclusion, by this new direct synthesis we obtained, in high yields, 2-arylbenzoxazoles from *o*-aminophenol and aromatic acids using phenyldichlorophosphite as reagent.

EXPERIMENTAL

2-Phenylbenzoxazole

To 2.18 g (0.02 moles) *o*-aminophenol and 2.44 g (0.02 moles) benzoic acid in a 50 ml three-necked flask, 3 ml (0.02 moles + 10% excess) phenyldichlorophosphite were added under stirring. The obtained suspension is heated with stirring when it becomes clear. After four hours at 145 – 155°C, 10 ml N-methyl-2-pyrrolidone (NMP) were added as solvent at the same temperature. Without NMP, the product crystallises very fast at the end of heating. The obtained solution cooled at 40 – 60°C was poured into a large volume of water with ice (40 – 50 ml) under stirring, then treated with 7% NaOH solution till pH = 9 – 10, The precipitated product was collected by filtration, washed with 15 – 20 ml 10% HCl-solution, three times with 20 – 30 ml water and dried at 40 – 50°C under vacuum. 2t Phenylbenzoxazole (3g) was obtained with m.p. 100 – 102°C (mixed m.p. with pure produc undepressed). Yield 76% calculated on benzoic acid employed.

Anal. Found : C, 79.91 ; H, 4.72 ; N, 7.13%. Calculated for : $C_{13}H_9NO$; C, 80.00 ; H, 4.61 ; N, 7.17%.

Under similar conditions the other benzoxazoles (presented in table 1) were prepared.

TABLE 1

2-Arylbenzoxazoles obtained using phenyldichlorophosphite as reagent

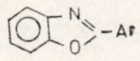 Ar=	Benzoxazoles$^{a)}$		
	Yield$^{b)}$ %	M.p.$^{c)}$ °C	Literature m.p. °C
Phenyl	76	100–102	102–103$^{9)}$
p-Tolyl	79	114–116	115–116$^{9)}$
p-Methoxyphenyl	80	100–102	100–101$^{9)}$
o-Chlorophenyl	72$^{d)}$	70–71$^{d)}$	72$^{10)}$
p-Bromophenyl	84	157–159	158$^{10)}$
p-Chlorophenyl	82	149–151	150–151$^{9)}$
2,4-Dichlorophenyl	71$^{d)}$	119–120$^{d)}$	119$^{10)}$
3,4-Dichlorophenyl	70$^{d)}$	143–144$^{d)}$	144$^{10)}$

[a)] The products were identified by comparison of m.p. and IR spectra with autentic samples.
[b)] Yields calculated on aromatic acid employed.
[c)] Before recrystallisation.
[d)] After recrystallisation.

REFERENCES

[1] J. J. Leavitt, *J. Amer. Chem. Soc.*, **79**, 427 (1957).
[2] D. W. Hein and R. J. Alheim, U.S.2, 985, 661, May 23, 1961 ; *Chem. Abstr.*, **57**, 11.203 (1962).
[3] T. Kanaoka, *Chem. Pharm. Bull. Japan*, **18**, 587 (1970).
[4] C. I. Chiriac, *Rev. Roumaine Chim.*, **26**, 1001 (1981).
[5] C. I. Chiriac, *Rev. Roumaine Chim.*, **27**, 411(1982).
[6] M. A. Phillips, *J. Chem. Soc.*, **1930**, 1409.
[7] H. N. Walborsky and G. E. Niznik, *J. Org. Chem.* **37**, 187 (1972).
[8] E. A. Lawton and D. D. McRitchie, *J. Org. Chem.*, **24**, 26 (1959).
[9] J. Sugita, *Chem. Pharm. Bull.* (*Tokyo*), **12** 1135 (1964) ; *Chem. Abstr.*, **62**, 541 (1965).
[10] N. V. Subba, *Proc. Indian Acad. Sci., Sect.* A, **59**, 396 (1964) ; *Chem. Abstr.*, **62**, 1639 (1965)

Revue Roumaine de Chimie, 28, 7, 41 – 44 (1983)

DETERMINATION OF TRACE QUANTITIES OF THE GROUP V-A ELEMENTS BY ANODIC STRIPPING VOLTAMMETRY. III

TRACE ANALYSIS OF BISMUTH

SOFIA MARCHIDAN*, IULIANA VARTIRES and N. D. TOTIR
Center of Physical Chemistry, Splaiul Independenţei 202, Bucharest 79611, Romania

Received February 26, 1982

A method for determination of bismuth by anodic stripping voltammetry with a detection limit of 2×10^{-9} M has been elaborated. Good results for bismuth (III) on hanging mercury drop electrode using 1 M HCl as supporting electrolyte have been obtained. Large amonts of Cd, Pb, Zn, Ni, Fe, and Cu do not disturb the stripping analysis of bismuth.

Direct determination of bismuth by anodic stripping voltammetry in different supporting electrolyte has been performed by many authors.[1-8]

In this paper a procedure for bismuth trace analysis with a hanging mercury drop electode and the influence of large amounts of Cd, Pb, Zn, Ni, Fe and Cu on stripping analysis is described.

EXPERIMENTAL

Apparatus

The instrumentation and the quartz cell used in this work were described in a previous paper.[9] A hanging mercury drop electrode (HMDE) was used as working electrode and a platinum wire as counter electrode. All the potentials are referred to saturated calomel electrode (SCE) which was used as a reference electrode.

Reagents

Tetradistilled water and Johnson Matthey standard spectrographic reagents weres used for obtaining all the solutions.

A quartz apparatus was used for purifying the mercury.

---

* Deceased on November 25, 1980.

Procedure

The general procedure for anodic stripping analysis has been described previously.[9] As a supporting electrolyte 1 M HCl was used. For the cathodic deposition step, potentials of – 400 mV or – 200 mv *vs.* SCE were used.

Standard Bi^{3+} solutions were prepared by dissolving metallic bismuth in a few milliliters of aqua regia, slowly evaporation of the solution to dryness, repeating the same procedure for the obtained sample by using concentrated HCl and finally dissolving the sample in concentrated hydrochloric acid. The solution so obtained is very stable and can be stored for a long time, in this way being avoided its hydrolisis.

RESULTS AND DISCUSSION

The large number of all the influencing factors which determine the amalgam concentration in the mercury drop and the anodic dissolution of the cations, requires to select the proper experimental conditions for each sample, in order to obtain accurate and reproducible results.

Well defined peaks for Bi^{3+} at $E_p \simeq -65$ mV *vs.* SCE were obtained as can be seen in figure 1.

For a proper selection of the electrodeposition potential, E_d, stripping analysis was performed in the potential range from –150 mV to – 450 mV as can be seen from table 1. There is no large differences between the values of the peak current and therefore it is possible to use any values for deposition potential in the specified range.

The relationship between peak currents and the electrodeposition time τ, ranging from 5 to 20 minutes is presented in table 2. There is a good proportionality between the two values.

The linearity between τ and i_p ranging from 5 to 15 minutes shows that there is no significant diffusion of amalgam into mercury drop for these experimental conditions.

A good sensitivity is obtained by using ten minutes deposition time for $C_{Bi^{3+}} = 10^{-8}$ M and twenty minutes deposition time for $C_{Bi^{3+}} = 10^{-9}$M.

There is a linear dependence between peak current i_p and the concentration of bismuth in the range $10^{-6} - 10^{-9}$ M as is given in table 3.

In our experimental conditions the limit of detection was 2×10^{-9} M Bi^{3+}.

The relative standard deviation was found to be below 2% for $C_{Bi^{3+}} = 1 \times 10^{-7}$ and below 10% for $C_{Bi^{3+}} = 1 \times 10^{-8}$ M.

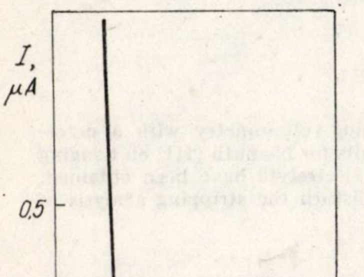

Fig. 1. — Stripping voltammogram of bismuth in 1 M HCl: $\tau = 10$ min; $E_d = -400$ mV; 1. Supporting electrolyte, 1 M HCl; 2. $C_{Bi^{3+}} = 1 \times 10^{-7}$M.

TABLE 1

Dependence of peak current, i_p, on deposition potential, E_d; $C_{Bi^{3+}} = 1 \times 10^{-7}$M

E_d, mV	i_p, μA
-150	0.33
-200	0.32
-250	0.31
-300	0.30
-350	0.29
-400	0.29
-450	0.30

TABLE 2

Dependence of peak current, i_p, on deposition time, τ; $C_{Bi^{3+}} = 1 \times 10^{-7}$ M.

Deposition time τ, min	i_p, μA
5	0.14
10	0.28
15	0.42
20	0.52

TABLE 3

Dependence of peak current, i_p, on Bi^{3+} concentration

$C_{Bi^{3+}}$, M	i_p, μA	E_d, mV τ, min
9.8×10^{-7}	2.32	$\tau = 10$ min $E_d = -400$mV
7.5×10^{-7}	1.75	
5.0×10^{-7}	1.33	
3.0×10^{-7}	0.78	
1.0×10^{-7}	0.25	
9.8×10^{-8}	0.27	$\tau = 10$ min $E_d = -400$mV
7.5×10^{-8}	0.23	
5.0×10^{-8}	0.15	
3.0×10^{-8}	0.09	
1.0×10^{-8}	0.04	
9.8×10^{-9}	0.12	$\tau = 20$min $E_d = -200$mV
7.5×10^{-9}	0.09	
4.0×10^{-9}	0.05	
2.0×10^{-9}	0.03	
1.0×10^{-9}	—	

The influence of some cations on anodic stripping voltammetry of bismuth is given in figure 2. In our experimental conditions at -400 mV electrodeposition potential no interference is observed except for copper as can be seen from curve A. This can be avoided easily by changing the electrodeposition potential from -400 mV to -200 mV as can be seen from part B of the Fig. 2, where the stripping voltammograme of Bi^{3+} cation and the mixture of the Bi^{3+} with all the other cations are identical.

The elaborated method is rapid, direct and sensitive, allowing direct analysis of bismuth from a mixture of cations with a limit of detection of 2×10^{-9} M and a standard deviation below 10%.

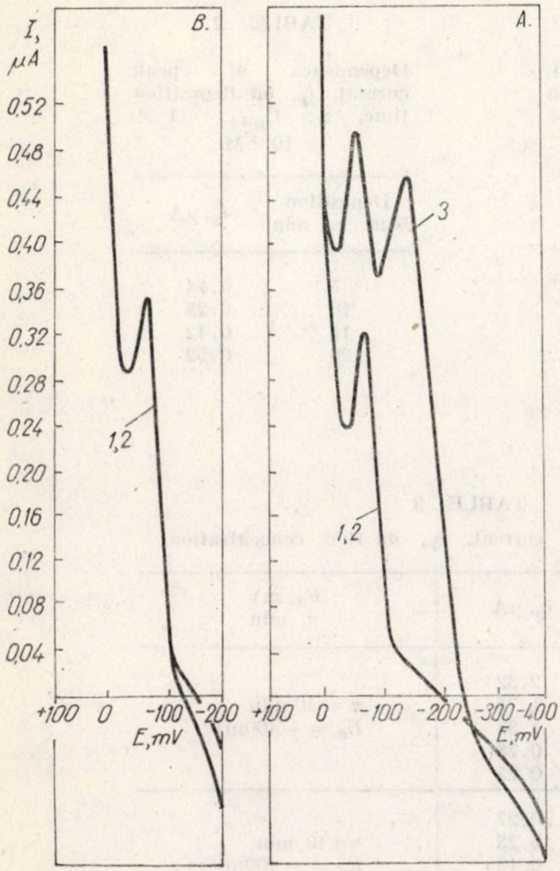

Fig. 2.— Stripping voltammogram of bismuth in the presence of cadmium, lead, zinc, nickel, iron and copper : Curve A, $E_d = -400$ mV ; 1. $C_{Bi^{3+}} = 1 \times 10^{-7}$ M ; 2. $C_{Bi^{3+}}/C_{Cu^{2+}} = 1 : 1$; 3. $C_{Bi^{3+}}/C_{Cu^{2+}} = 1 : 10$. Curve B, $E_d = -200$ mV ; 1. $C_{Bi^{3+}} = 1 \times 10^{-7}$ M ; 2. $C_{Bi^{3+}}/C_{Cd^{2+}}$; $C_{Zn^{2+}}$; $C_{Pb^{2+}}$; $C_{Cu^{2+}}$; $C_{Ni^{2+}}$; $C_{Fe^{3+}} = 1 : 100$.

REFERENCES

[1] G. van Dyck and F. Verbeek, *Z. analyt. Chem.*, **249**, 89 (1970).

[2] H. Z. Brainina and L. N. Kalnisevskaya, *Zavodskaya'Lab.*, **40**, 639 (1964).

[3] I. Sinko and S. Gomiscek, *Analyt. Chim. Acta*, **54**, 253 (1971).

[4] V. F. Toropova, Ju. N. Polyakov and L. N. Soboleva. *Zhur. analit. Khim.*, **27**, 2395 (1972).

[5] N. Velghe and A. Clayers, *J. Electroanalyt. Chem.*, **35**, 229 (1972).

[6] J. J. Vatman and E. G. Cirikizova, *Zavodskaya Lab.*, **34**, 1178 (1968).

[7] V. G. Tiptova-Jakovleva and Ju. A. Figelosou. *Zhur. analit. Khim.*, **27**, 89 (1972).

[8] A. I. Kamenev, E. N. Vinogradova and V. N. Jhryashchevskii, *Zhur. analit. Khim.*, **29**, 40 (1974).

[9] Part I : S. Marchidan, I. Vartires and N. D. Totir, *Rev. Roumaine Chim.*, **25**, 33 (1980), Part II. *Rev. Roumaine Chim.*, **27** 81(1982).

Revue Roumaine de Chimie, 28, 1, 45 – 52 (1983)

BENZFUROINOXIME — AN ANALYTICAL REAGENT FOR THE MICRODETERMINATION OF URANYL

V. ARMEANU and SANDA VIȘAN
Academy of Economic Studies, Piața Romană 6, Bucharest, Romania

Received September 30, 1981

The complex combination formed in the reaction between benzfuroinoxime and the uranyl ion was investigated by spectrophotometrical means. The analytical properties of the complex combinations formed in three solvents (water, ammonia, ethyl alcohol) were found out. The optimal working conditions were specified to determine the uranyl ion with benzfuroinoxime. The behaviours of benzfuroinoxime, acetoinoxime, benzoinoxime and furoinoxime in the presence of the uranyl ion are compared.

1. INTRODUCTION

Benzfuroinoxime was little investigated as an analytical reagent. The literature reports on the complex compound formed by this oxime and the Cu^{2+} ion.[1] In some previous works on the behaviour of some α-hydroxioximes in the presence of uranyl ion,[2-5] the system benzfuroinoxime — uranyl was also investigated. The benzfuroinoxime and the uranyl ions form a yellow compound, soluble in ethyl alcohol, methyl alcohol, ammonia 25 %, but insoluble in benzene, carbon tetrachloride, chloroform, carbon sulphur. This compound was investigated spectrophotometrically with a view to determining the optimal conditions of analysing the uranium present in solution as uranyl ions, with this organic reagent.

2. REAGENTS AND EXPERIMENTAL EQUIPMENT

The synthesis of benzfuroinoxime was carried out according to [1,6] as follows:

— by condensing stoichiometric quantities of benzoic aldehyde and furfurol in boiling alcoholic solution in the presence of KCN.

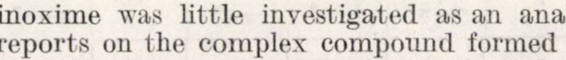

$$C_6H_5-CHO + OHC-C_4H_3O \rightarrow C_6H_5-\underset{OH}{CH}-\underset{O}{\overset{\|}{C}}-C_4H_3O$$

Benzfuroine was recrystallized from methyl alcohol.

— the reaction between benzfuroine and hydroxylamine in aqueous solution of ethyl alcohol.

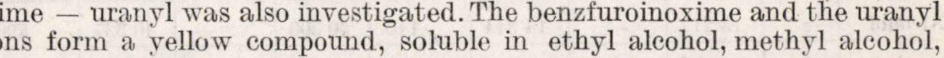

$$C_6H_5-\underset{OH}{CH}-\underset{O}{\overset{\|}{C}}-C_4H_3O + NH_2OH.\,HCl + NaOH \rightarrow C_6H_5-\underset{OH}{CH}-\underset{NOH}{\overset{\|}{C}}-C_4H_3O + NaCl + H_2O$$

The oxime was recrystallized from ethyl alcohol and then characterized by melting point, elementary analysis and IR spectrum.

The uranylacetate used was $UO_2(CH_3COO)_2 \cdot 2H_2O$(UCB). The electronic spectra were recorded by a SPECORD UV – VIS and SPEKOL EK-5 apparatus. The vibrational spectra were recorded in paraffin making use of a SPECORD IR 75 apparatus. The elementary analysis of carbon and hydrogen was carried out by combustion, and the analysis of nitrogen was performed according to the Kjeldahl method, the only one allowing the determination of nitrogen in the oximino group. A SEYBOLD Wien pH-meter with glass electrode was used to measure the pH. The melting point was determined with a Boetius apparatus.

3. RESULTS AND DISCUSSION

Electronic band spectra. The benzfuroinoxime forms with the uranyl ion a yellow-coloured compound; the intensity of the colour varies depending on the solvent and the pH of the solution (Table 1).

TABLE 1

Spectral characteristics of benzfuroinoxime and of the complex compound achieved with uranyl, in various solvent media. The spectra were recorded using the corresponding solvent as reference

Transition Solvent		Benzofuroinoxime				Complex compound			
		E	*K* π→π*	π→π*	→π*	*E*	*K* π→π*	π→π*	n→π*
Ethyl	λ	204 max	–	275 max	335 plateau	200 max	–	266 max	330 plateau
Alcohol	ε	13 217	--	14 344	110	50 200	–	40 337	890
Water	λ	205 max	227 plateau	281 max	345 plateau	204 max	227 plateau	278 max	345 plateau
	ε	7 684	5 480	9 265	150	26 250	12 530	28 660	800
Ammonia	λ	207 max	–	278 max	333 plateau	200 max	– –	281 max	333 plateau
	ε	15 100	–	15 520	390	31 800	–	37 300	1 360

The molecule of benzfuroinoxime contains the following chromophores: the phenyl radical, the radical of furan and the α-hydroxyoximino group. Because of the phenyl radical the electronic spectra have an intense *E* band at λ ~ 205 nm; because of a π → π* transition, a *K* band having a more reduced absorbance appears. The latter can be observed like a shoulder in water, ethyl alcohol and ammonia only, being screened by the *E* band.[7]

The intense band at ~ 275 nm existing in all these three solvents, points out the existence of the chromophore system of the furfurol, having $\lambda_{max} = 270$ nm and $\varepsilon_{max} = 1580\ cm^{-1}\ mol^{-1}\ l^{8}$.

A shoulder appearing in the spectrum at λ ~ 340 nm because of an *n* → π* transition (caused by the unpaired electrons of nitrogen which can conjugate with the furfurol system) proves the existence of the oximino group (: C=NOH).

The complexation of the oxime with uranyl does not cause very important shifts of spectral bands, but only a strong hyperchromic effect awarding the colour to the complex. The *E* band has a slight hypsochromic shift. The *K* band appears at the complex prepared in water only. The $\pi \rightarrow \pi^*$ spectrum bands at $\lambda \sim 270$ nm caused by furan are evidenced. A hypsochromic effect is noticed for the complex combination prepared in ethyl alcohol and water, and a bathochromic effect when the solvent used is ammonia.

The visible spectrum shows shoulders at $\lambda = 330 - 345$ nm.

Subsequent determinations were performed at $\lambda = 340$ nm, the lower limit of the visible spectrum.

Vibrational spectra. The IR spectrum of benzfuroinoxime in paraffin shows the following spectral bands : the ν(OH) band, very large at 3300 cm^{-1}, the ν(C=N) band at 1650 cm^{-1}, δOH(C) at 1495 cm^{-1} (shoulder), δCH(OH) at 1390 cm^{-1} (shoulder), ν(C—OH) at 1030 cm^{-1}, ν(N—O) at 980 cm^{-1}, and the typical spectral bands of the aromatic substituted ring at 690 cm^{-1} and 750 cm^{-1}. The spectral bands of the furan nucleus do not appear clearly because the band at 740 cm^{-1} overlaps that of benzene and the band at 1458 cm^{-1} overlaps the band of paraffin at 1460 cm^{-1}.

The investigations of the complexation reaction with the uranyl ion showed the following :

— the ν(OH) band shifts towards higher wave numbers, about 70 cm^{-1} (because of the disappearance of the intramolecular hydrogen bounds) and its intensity decreases ;

— the ν(C—OH) band is splitted and shows a maximum at 1030 cm^{-1} and another one at 1070 cm^{-1} ;

— in the case of the complex combination prepared in water, the ν(N—O) band is not modified and consequently one concludes that in its molecule the bounding occurs owing to the alcoholic hydroxyl.

The spectra of the complex combinations prepared in ammonia and in aqueous solution of ethyl alcohol are identical with those of the complex prepared in water because, by evaporation, an aqueous solution resulted, out of which the solid complex was obtained by drying.

Experimental conditions. The maximum absorbance of complex combination solutions was observed in the range of pH = 11.5 — 12.5 obtained by adding 15 — 20 cm^3 ammonia 25% in 25 cm^3 of solution.

The concentration of the complex combination being 10^{-3} M the reaction reached the equilibrium after 15 minutes in ethyl alcohol as a solvent, after 1 hour in ammonia and after 2 hours in water. In these solvents the complex combinations are stable for 24 hours.

The maximum quantity of the reagent required in complexation was also determined. The solutions having the same concentration of uranyl at pH $\sim$ 12.5 maintain the same value of absorbency as in molar excess of benzfuroinoxime (40 times more than the quantity of uranyl).

Composition and stability constant. Compositions and stability constants of the complex combinations were determined by means of the Asmus method [9] assuring the optimal working conditions for each solvent at 340 nm. Table 2 presents the working conditions and the plots

TABLE 2

The working conditions used to calculate the compositions and the stability constants of the complex combinations

Solvent	Concentrations		K^{-1}	$\overline{K}^{-1}$	$\overline{K}$	n
	uranyl, M	oxime, M				
Ethyl Alcohol	1.18×10^{-4} 9.88×10^{-5}	5.19×10^{-3} 3.11×10^{-3}	5.19×10^{-3} 4.98×10^{-3}	5.09×10^{-3}	1.96×10^{2}	1
Water	1.18×10^{-4} 9.88×10^{-5}	5.19×10^{-3} 6.23×10^{-3}	1.18×10^{-4} 9.05×10^{-5}	1.04×10^{4}	9.60×10^{3}	2
Ammonia	1.18×10^{-4} 9.88×10^{-5}	5.19×10^{-3} 6.23×10^{-3}	9.88×10^{-4} 8.59×10^{-4}	9.23×10^{-4}	1.08×10^{4}	1

used for calculating the compositions and the stability constants of the complex combinations. The plots are linear for a composition metal : ligand $= n = 1$ in ethyl alcohol and ammonia as a solvent and $n = 1 : 2$ in water.

The combination ratio (n) was checked using the logarithmic method too [10] (Figs 1 and 2).

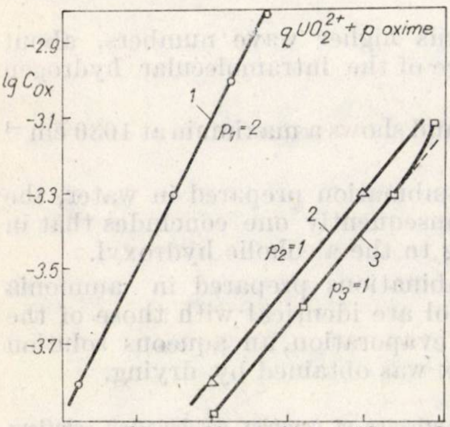

Fig.1. — The logarithmic dependence of the oxime concentration vs. absorbency. Solvents : 1 — water ; 2 — ethyl alcohol ; 3 — ammonia.

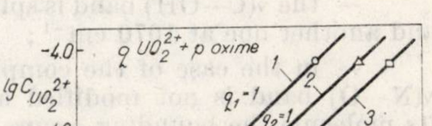

Fig. 2. — The logarithmic dependence of the uranyl concentration vs. absorbency. Solvents : 1 — water ; 2 — ethyl alcohol ; 3 — ammonia.

The complex combination formed in the reaction between benzfuroinoxime and uranyl ion in water as solvent shows the best stability but the absorbencis are low. Therefore, the uranyl ion is better to be determined with benzfuroinoxime in alkaline medium at pH ~ 12 obtained with ammonia 25% when a complex combination with good absorption and stability is formed.

The Bouguer — Lambert-Beer Law. Under optimal working conditions, the uranyl ion can be determined with benzfuroinoxime in maximum concentration of 25 μg UO_2^{2+}/cm^3. The range of validity of the Bouguer — Lambert-Beer law was experimentally found out.

TABLE 3

The range of validity of the Bouguer — Lambert — Beer law

UO_2^{2+} in sample, μg	A	UO_2^{2+} determined, μg	Error, %
62.5	0.042	59.8	−4.3
125.0	0.082	122.7	−1.8
187.5	0.126	191.9	+2.4
312.5	0.199	306.8	−1.8
437.5	0.286	443.6	+1.
500.0	0.325	505.0	+1.0
562.5	0.357	555.4	−1.3
625.0	0.405	630.8	+0.9

With benzfuroinoxime, the uranyl ion can be determined within the range of concentrations of 5 — 25μg UO_2^{2+}/cm^3.

To find out the error of the analysing method the τ criterion was applied to eliminate the uncertain experiments,[11] τ_i being defined as

$$\tau_i = \frac{|\bar{x} - x_i|}{s}$$

x_i — the value of a measurement,
$\bar{x}$ — the mean value of n measurements,
s — the mean square error of a measurement.

The results of experimental measurements are shown in table 4.

For all the eight measurements the condition $\tau_i < \tau_t$ is carried out where $\tau_t = 1.86$. Therefore, the deviations were random and formed in

TABLE 4

Application of τ criterion of elimination of the uncertain experiments

A	UO_2^{2+} determined, μg	Error, δ_i	δ_i^2	τ_i
0.325	505.0	+3.54	12.53	0.77
0.322	50003	−1.16	1.35	0.25
0.320	497.1	−4.40	19.36	0.96
0.325	505.0	+3.54	12.25	0.77
0.320	497.1	−4.40	19.36	0.96
0.324	503.4	+1.90	3.61	0.41
0.319	495.6	−5.90	34.81	1.28
0.327	508.2	+6.70	44.89	1.46

the normal dispersion of the data. Considering the Student distribution to be valid, the errors of the individual experiments and the arithmetic mean value were calculated (Table 5).

TABLE 5

Statistical calculus of errors

Errors of individual value, %		Errors of arithmetic mean value, %	
mean square errors s	probable errors, ε_p	mean errors $s_{\bar{x}}$	probable errors $\varepsilon_{p_{\bar{x}}}$
±0.91	±0.61	±0.32	±0.22

Experimental procedure. The solution containing 125 – 625 μg UO_2^{2+} was introduced into graduated flasks 25 cm^3 ; 5 cm^3 of a solution of benzfuroinoxime 2.7×10^{-2} M was added and the volumetric flask was filled up to a liquid level with ammonia 25%. Absorbencies were read at 340 nm after an hour. The analytical method was of a high precision, the medium error for eight measurements being ± 0.32%.

The structure of the complex combinations. The solutions of the complex combinations were introduced into an electrolytic cell with electrolytic diaphragm separating the anode space from the cathode space. The parameters of the electrolytical process were 6 V and 0.1 A. The solution of the complex combination was first introduced into the anode space. The diffusion of UO_2^{2+} ion in the cathode space did not occur, therefore the complex combination was a neutral one.

On the basis of this finding and the results of the spectrochemical analysis, the following possible structures are suggested :

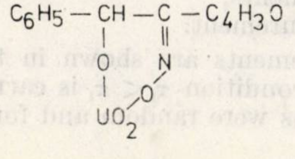

in ammonia

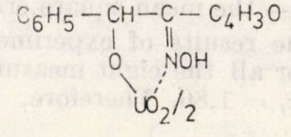

in water

In the case of ethyl alcohol as a solvent the formula of the complex combination is more difficult to be done. Interactions donor – acceptor are possible and as a result, the relatively large absorption at 340 nm occurs. Table 6 compares the behaviour of benzfuroinoxime and other α-hydroxioximes in the presence of the uranyl ion.

The chemical structure of the oximes is related to their analytical behaviours. The α-hydroxioximino group submits the following electronical effects [12]:

– induction electron attractive effect at the simple bond N→OH ;

– electromeric electron attractive effect at the double bond $\overset{\curvearrowright}{C = \ddot{N}} -$, because of the influence of the polar reagents.

TABLE 6

Analytical properties of the complex combinations of uranyl ion with α-hydroxyoximes

Oxime properties	Solvent	Acetoin-oxime	Benzoin-oxime	Benzfuroin-oxime	Furoin-oxime
pH	water	11.5—12.5			
n	water ammonia ethyl alcohol	1 1 1	2 1 1	2 1 1	2 1 1
K^{-1}	alcohol water ammonia	5.79×10^{-2} 4.19×10^{-4} 1.30×10^{-4}	2.32×10^{-3} — 7.19×10^{-4}	5.09×10^{-3} 1.04×10^{-4} 9.23×10^{-4}	1.87×10^{-4} 9.53×10^{-8} 2.16×10^{-6}
K	alcohol water ammonia	1.70×10 2.38×10^{3} 7.68×10^{3}	4.30×10^{2} — 1.40×10^{3}	1.96×10^{2} 9.60×10^{3} 1.08×10^{4}	5.35×10^{3} 1.05×10^{7} 4.63×10^{5}
Excess of reagent, M	ammonia	10	28	40	140
Lambert law, $\mu g UO_2^{2+}/cm^3$	ammonia	10—76.6	5 — 51	5 — 25	2 — 7
Analysis time, h	ammonia	1	0,5	1	0,5
s, %	ammonia	±1.06	±0.92	±0.91	±1.19
ε_p, %	ammonia	±0.71	±0.62	±0.61	±0.80
$s_{\bar{x}}$, %	ammonia	±0.37	±0.33	±0.32	±0.42
$\varepsilon_{p,\bar{x}}$, %	ammonia	±0.25	±0.22	±0.22	±0.28

The organic radicals associated with α-hydroxyoximino groups have the following effects: CH_3 —, electron releaving effect; C_6H_5 — and C_4H_3O —, electron attractive effect. The electron attractive effects of the radicals furyl and phenyl are stronger than the static induction effect of the N—O bond and the electromeric effect of the C=N—bond. Because of these effects the dissociation degree of the oximino group increases especially in alkaline medium when the uranyl ion is present.

3. CONCLUSIONS

The system uranyl — benzfuroinoxime was examined spectrophotometrically. The existence of a complex combination was determined; the structure and the properties of this combination are different in water (neutral), ammonia (pH ~ 12) and ethyl alcohol. The optimal working conditions, the analytical method and the errors affecting the individual values and the arithmetic mean were also determined. Benzfuroinoxime is a reagent having a better reactivity referred to the uranyl ion than benzoinoxime and acetoinoxime.

REFERENCES

[1] F. Feigl, G. Sicher and O. Singer, *Chem. Ber.*, **58**, 2294 (1925).

[2] V. Armeanu, S. Vişan and A. Meghea, *Rev. Chim.* (*Bucureşti*), **28**, 991 (1977).

[3] V. Armeanu, S. Vişan and L. M. Băloiu, *Rev. Chim.* (*Bucureşti*), **28**, 1095 (1977).

[4] V. Armeanu and S. Vişan, *Rev. Roumaine Chim.*, **25**, 867 (1980).

[5] V. Armeanu and S. Vişan, *Rev. Chim.* (*Bucureşti*), to be published.

[6] V. Armeanu and C. Iancu, *Studii şi cercetări de chimie*, Acad. R.P.R. **3**, 423 and 431 (1957).

[7] S. Mager, "Analiză structurală organică", Ed. ştiinţifică şi enciclopedică, Bucureşti, 1979.

[8] L. A. Kazitsina and N. B. Kupletskaia, "Primenenie U. F., I.-K. i Ia. M.R.-spectroscopii v organiceskoi khimii", Izd. Vysshaia Skola, Moskva, 1971.

[9] E. Asmus, U. Hinz, K. Ohls and W. Richley, *Z. analyt. Chem.*, **178**, 104 (1960).

[10] A. Bent and C. French, *J. Amer Chem. Soc.*, **63**, 568 (1941).

[11] * * * "Manualul inginerului chimist", Ed. tehnică, Bucureşti, 1976.

[12] E. Angelescu and F. Cornea, "Probleme teoretice de chimie organică", Ed. didactică şi pedagogică, Bucureşti, 1969.

Revue Roumaine de Chimie, 28, *1*, 53 – 56 (1983)

POLAROGRAPHIC KINETIC STUDY OF THE OXIDATION OF URANIUM(V) BY VANADIUM(IV) IN SULFURIC ACID MEDIUM

V. G. VOICU
Institute of Chemical and Pharmaceutical Researches, Calea Vitan 112, sector 3, Bucharest, Romania

Received July 14, 1981

From the kinetic polarographic currents in the system UO_2^+ and VO^{2+} in sulfuric acid medium, it was established the kinetic constants, which characterize this reaction. So, it was found the rate constant, $k = 6.24 \times 10^3$ l/(mole.s.), the activation energy, $E_a =$ 6.24 kcal/mole, the apparent entropy of activation, $S = 19.08 \pm 0.11$ eu.

The reduction of the uranyl ions in sulfuric acid medium was studied in the literature,[1–6] where the disproportionation of the electrochemical reduction product, the uranium(V) ion – UO_2^+, was considered as having the most important influence upon the shape of the $i - V$ curves.

In 1959 Florence[7] noticed the vanadium interference in uranium determination due to the homogeneous reaction

$$UO^+ + VO^{2+} + 2H^+ = UO_2^{2+} + V^{3+} + H_2O \qquad (1)$$

coupled to the electrochemical step

$$UO_2^{2+} + e^- = UO_2^+ \qquad (2)$$

Such a pattern – first order catalytic wave – is a resolved problem by the theory of dropping mercury electrode polarography.[8] Morachevski and Sakharov[9] proved by amperometric titration the stoichiometry of the redox reaction (1).

Since then, several investigations have tried to use this reaction to develop more sensitive polarographic methods of uranium determination. So, Siniakova[3] gave a method based on catalytic wave determined by vanadium(V) ions, VO_3^-, on the electrochemical reduction (2) in lactic acid media. The optimum vanadium(V) concentration was 0.01 M[10].

A method of uranium determination using the reactions (1) and (2) is applied at CEA – Saclay.[11]

The present work is dealing with the kinetic study of this catalytic reaction in sulfuric media.

EXPERIMENTAL

Uranyl sulfate was a Carlo Erba reagent and vanadium oxide sulfate was a Merck reagent. 10^{-2} *M* solutions of these reagents in tridistilled water were prepared. The concentration of uranyl ions was determined by precipitation of UO_2^{2+}-8-hydroxyquinoline compound [12] and the concentration of VO^{2+} ions was determined by titration with Fe^{2+} in the presence of ferroin.[12]

All the potential values were referred to the saturated calomel electrode (S.C.E.) which was used as reference electrode. Reported current values are average currents corrected for residual currents at given potentials.

The characteristics of the capillary, at 50 cm and zero applied voltage, were $m = 1.62$ mg s^{-1}, $t_1 = 5.47$s and $m^{2/3} t^{1/6} = 1.83$ $mg^{2/3}$ $s^{1/6}$ in 0.1 *M* KCl solution.

Recording of the current-voltage curve was made with a Radelkis polarograph type OH—102. The polarographic cell was constructed following Smoler's design,[13] and was a water-jacketed glass electrolysis cell. The temperature in cell was controlled to 0.1°C by a Hoepler thermostate.

RESULTS AND DISCUSSION

It was admitted that the UO_2^{2+} ion is reduced in a reversible monoelectronic step to UO_2^{+} ($E_{1/2} = -0.2$ V vs S.C.E.), which is relatively stable in a narrow pH range (2.0 — 4.0)[14,15] as the disproportionation is slow.

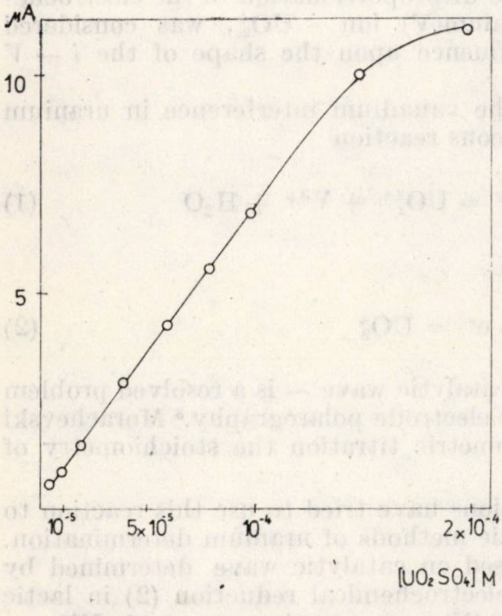

Fig. 1. — UO^{+} oxidation kinetic current height variation with UO_2SO_4 concentration; 10^{-2} *M* $VOSO_4$ and 0.1 *N* H_2SO_4.

Addition of VO^{2+} ions causes an increase of the wave height. A log-log plot of the i/i_d current ratio vs. VO^{2+} concentration has a slope of 0.51. This value has to be one-half for a reaction mechanism of the first order in VO^{2+} ions concentration since the theory gives i as proportional to $[VO^{2+}]^{-1/2}$ for a pseudo-first-order treatment.[8] The limiting current was found to be independent of the mercury column height as is expected when the current is controlled by a catalytic process.[8]

The catalytic currents variation with uranyl ions concentration presented in figure 1 showed a linear variation from 5×10^{-6} *M* to 10^{-4} *M* UO_2SO_4, which can be the basis of a polarographic method of uranium determination.

The rate constant for homogeneous oxidation reaction was calculated on the basis of the reaction layer theory, developed by Brdička and Wiesner [8,16]

$$\bar{i}/\bar{i}_d = 0.81\, k\, [VO^{2+}]\, t_1 \qquad (3)$$

and we found the value $k = (6.24 \pm 0.35) \times 10^3$ l/(mole s) on the system 5×10^{-5} *M* UO_2SO_4, 0.1 *M* H_2SO_4 and $VOSO_4$ ranging between 5×10^{-3} *M* and 7.5×10^{-2} *M*, which was obtained with a relative standard deviation of 5.61 %.

A log-log plot of rate constant vs. sulfuric acid concentration is represented in figure 2. As it can be seen, from 10^{-3} *N* to about 5×10^{-1} *N* H_2SO_4 there is a linear variation with a slope of 2, followed by an independence of the rate constant with sulfuric acid concentration and then another linear variation with a slope of -4, slopes whose values are consistent with the oxidation reaction and UO_2^+ ions disproportionation reaction molecularities.

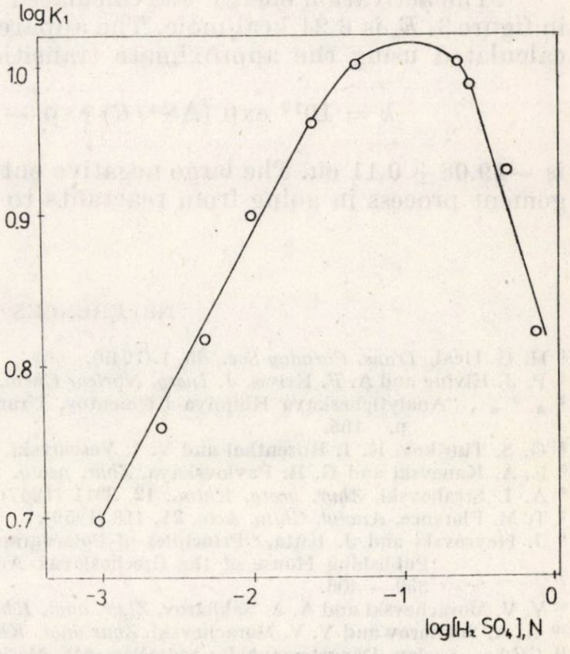

Fig. 2. — Variation of rate constant logarithm for reaction (1) with H_2SO_4 concentration logarithm ; 10^{-4} *M* UO_2SO_4, 3×10^{-2} *M* $VOSO_4$, $t_1 = 5.47$ s.

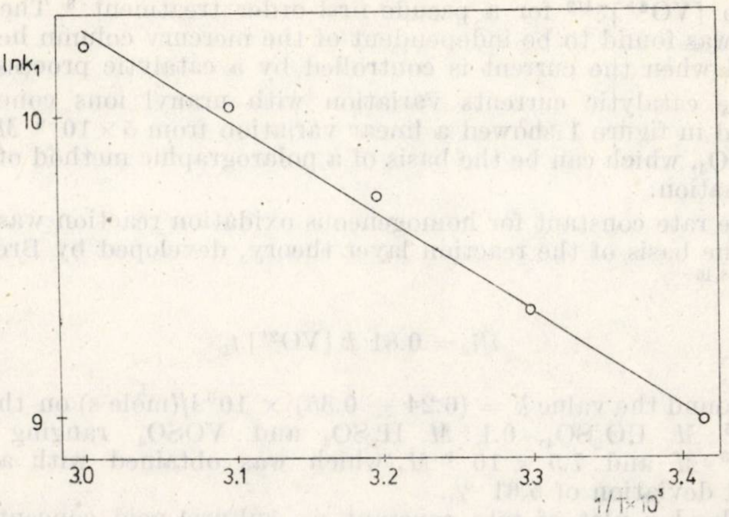

Fig. 3. — Determination of activation energy from the rate constant variation with temperature.

The activation energy was calculated with the Arrhenius plot shown in figure 3. E_a is 6.24 kcal/mole. The apparent entropy of activation, $\Delta S^{\neq}$, calculated using the approximate transition state theory equation

$$k = 10^{13} \exp (\Delta S^{\neq}/R) \exp -[(E_a - RT)/RT] \quad (4)$$

is -19.08 ± 0.11 eu. The large negative entropy is indicative of a rearrangement process in going from reactants to activated state.

REFERENCES

[1] H. G. Heal, *Trans. Faraday Soc.*, **45**, 1 (1949).

[2] P. J. Elving and A. F. Krivis, *J. Inorg. Nuclear Chem.*, **11**, 234 (1959).

[3] * * *, "Analyticheskaya Khimiya Elementov, Uran", Izd. A.N. S.S.S.R., Moskva, 1962, p. 165.

[4] G. S. Tiurikov, K. I. Rozenthal and V. I. Veselovski, *Zhur. fiz. Khim.*, **32**, 1490 (1958).

[5] E. A. Kanevski and G. R. Pavlovskaya, *Zhur. neorg. Khim.*, **5**, 1738, 1964 (1960).

[6] A. I. Strabovski, *Zhur. neorg. Khim.*, **12**, 3311 (1967); and **13**, 406 (1968).

[7] T. M. Florence, *Analyt. Chim. Acta*, **21**, 418 (1959).

[8] J. Heyrovski and J. Kůta, "Principles of Polarography", Chap. XVII — Kinetic Currents, Publishing House of the Czechoslovak Academy of Sciences, Prague, 1965, pp. 339 — 406.

[9] Y. V. Morachevski and A. A. Sakharov, *Zhur. anal. Khim.*, **13**, 83 (1958).

[10] A. A. Sakharov and Y. V. Morachevski, *Zhur anal. Khim.*, **13**, 467 (1958).

[11] CEA — Saclay, Département des radioéléments, Méthode CR 14.

[12] C. L. Wilson and D. W. Wilson, "Comprehensive Analytical Chemistry", Vol. 1 C, Elsevier, Amsterdam, 1962, pp. 614 and 545.

[13] J. Smoler, *Coll. Czech. Chem. Comm.*, **33**, 1036 (1968).

[14] J. Selbin and J. D. Ortego, *Chem. Rev.*, **69**, 657 (1969).

[15] K. A. Kraus, F. Nelson and G. L. Johnson, *J. Amer. Chem. Soc.*, **71**, 2510, 2517 (1949).

[16] R. Brdička and K. Wiesner, *Coll. Czech. Chem. Comm.*, **12**, 39, 139 (1947).

Revue Roumaine de Chimie, 28, 1, 57 – 63 (1983)

DEPOSITION KINETICS OF SILICON DIOXIDE FROM SILANE AND OXYGEN AT LOW TEMPERATURE

C. COBIANU and C. PAVELESCU

Research and Development Center for Semiconductors (CCSITS) Str. Erou Iancu Nicolae 32 B,
R-72996, Bucharest, Romania

Received May 19, 1981

This paper contains an experimental study of the silicon dioxide deposition on silicon substrates as a function of the processing variables in the temperature range 250 to 400° C. The film deposition takes place as a result of the substrate surface reaction between silane and oxygen, both diluted in nitrogen. The analysis of the experimental results proved the heterogeneous character of the deposition reaction and also allowed the evaluation of the reaction order with respect to oxygen and silane, at 400°C corresponding to the maximum deposition rate. Three reaction regions (homogeneous, of the maximum deposition rate and retardated) were delimited as a function of temperature and oxygen/silane mole ratio at constant linear silane flow rate and constant velocity of the total gas flow. The experiments were performed on a continuous type reactor at atmospheric pressure which allowed high deposition rates (0.1 — 3) μm/min.

INTRODUCTION

The deposition of the silicon dioxide films by the silane oxidation was extensively investigated in the temperature range 250 to 500°C.[1-8]

The purpose of this work is to present the reaction kinetics of the silane oxidation on a continuous type reactor at atmospheric pressure. A strong dependence is obtained between all processing variables (temperature, oxygen/silane mole ratio, silane flow rate, linear velocity of the total gas flow) in the process of the low temperature silicon dioxide deposition.

Since these films are deposited at temperatures below the aluminum-silicon eutectic temperature (577°C), they are used to protect the aluminum metallized integrated circuit structures for increasing their reliability.

EXPERIMENTAL

The operating principle of the reactor is shown in Fig. 1. Silane and oxygen, both diluted in nitrogen, have a separate and a laminar flow in the gas distributor (4). The reaction between silane and oxygen takes place at the wafer surface (3) lying on the susceptor (2) heated by resistances (1). The susceptor traverses under the gas distributor with adjustable speed (v). The reactant gases are distributed on an effective area of 77 cm² of the traveling susceptor. The reaction by-products (E) are removed by means of a ventilator.

The gases used were of ultra high purity. There were used 5% silane in argon, nitrogen and oxygen which contained less than 0.0003% water. The gases were passed through 0.5μm Millipore filters. The temperature profile on the susceptor surface was measured by the Technoterm 9500 digital thermometer and it resulted a ± 4°C variation around the set point value. Oxide thickness measurements were made by profilometer method with an Alpha-Step Tencor Instrument and an ellipsometer which also furnished the refractive index of the deposited films. The depositions were performed on p-type silicon substrates that were cleaned before deposition by degreasing in boiled trichloroethylene followed by etching in 5% hydrofluoric acid.

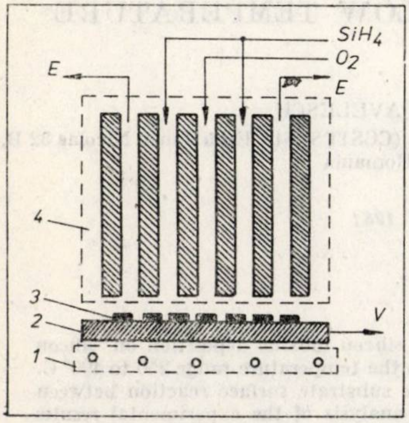

Fig. 1. — Operating principle of the continuous type reactor. 1. heater; 2. susceptor; 3. wafer; 4. gas distributor.

RESULTS

The silicon dioxide films were obtained in the temperature range 250 to 400°C, according to the reaction [2]

$$SiH_4 + O_2 = SiO_2 + 2H_2$$

The effect of the following experimental parameters on the deposition rate was investigated: substrate temperature, oxygen/silane mole ratio, silane flow rate (F_{SiH_4}), linear velocity of the total gas flow (v_F). The last parameter is obtained by dividing the total gas flow rate (in cm^3/min) to the susceptor effective area (in cm^2) on which the gases are distributed.

The effect of the substrate temperature and oxygen/silane mole ratio on the deposition rate

To determine the effect of the oxygen/silane mole ratio on the deposition rate at different temperatures (250 — 400°C), the oxygen flow rate (F_{O_2}) was varied (400 — 1800 cm^3/min) while the silane flow rate and the linear velocity of the total gas flow were kept constant (Fig. 2). An increase-maximum-decrease dependence of the deposition rate on oxygen/silane mole ratio was obtained at all temperatures. It resulted a rapid increase of the maximum deposition rate (about three times) when the substrate temperature increased from 250 to 350°C. Further temperature increase led to a relatively reduced increase of the maximum deposition rate in the temperature range 350 to 400°C. The oxygen/silane mole ratio corresponding to maximum deposition rate increased with temperature increase so that at 400°C this ratio was approximately 12.5/1. At this temperature one can observe a plateau region which consists of a constant silicon dioxide deposition rate when the oxygen/silane mole ratio varies from 12.5/1 to 20/1. At lower temperatures this maximum plateau narrows. The specific feature of this reactor is the high deposition rate obtained. The maximum deposition rate at 250°C for a silane flow rate of 30 cm^3/min is four times higher than the maximum deposition rate obtained on an horizontal reactor at 400°C for a silane flow rate of 38 cm^3/min.[9]

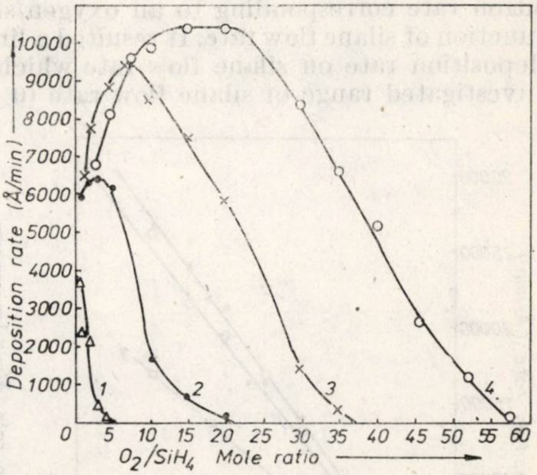

Fig. 2. — Deposition rate vs. oxygen/silane mole ratio.
$F_{SiH_4} = 30$ cm³/min. $v_F = 1.8$ cm/s : 1. $t = 250$°C ; 2. $t = 300$°C ; 3. $t = 350$°C ; 4. $t = 400$°C.

The effect of the silane flow rate on the deposition rate

To evaluate the influence of the silane flow rate on the silicon dioxide deposition rate, two types of experiments were carried out. In the first case, the silane flow rate was varied while the oxygen flow rate, the linear velocity of the total gas flow and the temperature were kept constant as shown in figure 3. Thus, an increase-maximum-decrease dependence of deposition rate on the silane flow rate was obtained. By analysing the two curves with oxygen flow rate as a parameter, it results that the maximum deposition rate is reached at approximately the same oxygen/silane mole ratio of 7/1.

In the second case, the silane flow rate was varied while the oxygen/silane mole ratio, the linear velocity of the total gas flow and temperature were kept constant (Fig. 4). Based on the results of figure 2, oxygen/silane mole ratios of 15/1 and 20/1 were chosen according to a maximum deposition rate. Using the date of figure 3, it was also represented the depo-

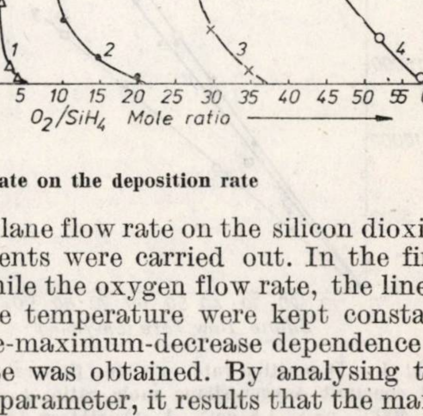

Fig. 3. — Deposition rate vs. silane flow rate. $t = 400$°C, $v_F = 1.8$ cm/s ; 1. $F_{O_2} = 400$ cm³/min ; 2. $F_{O_2} = 200$ cm³/min.

sition rate corresponding to an oxygen/silane mole ratio equal to 15 as a function of silane flow rate. It resulted a linear dependence of the maximum deposition rate on silane flow rate which presented no limitation in the investigated range of silane flow rate (0 – 90 cm^3/min).

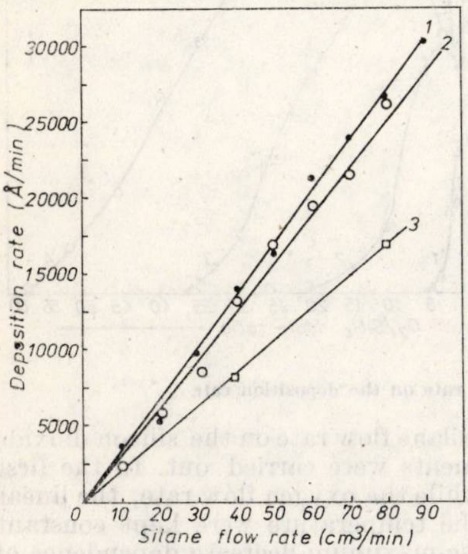

Fig. 4. — Deposition rate vs. silane flow rate at constant oxygen/silane mole ratio. $t = 400°C$, $v_F = 1.8$ cm/s. 1. $O_2/SiH_4 = 15$; 2. $O_2/SiH_4 = 20$; 3. $O_2/SiH_4 = 5$.

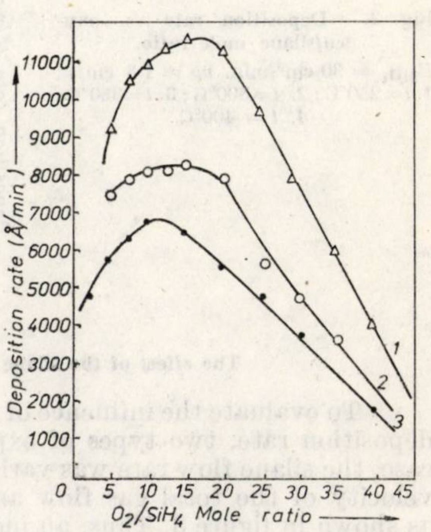

Fig. 5. — Deposition rate vs. oxygen/silane mole ratio at three velocities of total gas flow. $t = 400°C$, $F_{SiH_4} = 30$ cm^3/min. 1. $v_F = 0.9$ cm/s; 2. $v_F = 2.3$ cm/s; 3. $v_F = 3.2$ cm/s.

The effect of the linear velocity of the total gas flow on the deposition rate

To determine the effect of the total gas flow on the deposition rate and uniformity of the layers, the oxygen/silane ratio was varied considering three different values of the linear velocity of the total gas flow (0.9, 2.3 and 3.2 cm/s) as shown in figure 5 where the temperature and silane flow rate were kept constant. The data at 400°C show that the plateau region of the maximum deposition rate as a function of oxygen/silane ratio is well observed only for a value of the linear velocity of flow of 1.7 cm/s (Fig. 2.). In the other flow conditions (Fig. 5), this kinetic region is less characteristic (2.3 cm/s) or even very narrow (0.9 and 3.2 cm/s). At high values of the linear velocity of the total gas flow (over 2.3 cm/s) a high decrease of the maximum deposition rate appeared while the uniformity of the deposited layers was unsatisfactory ($\pm 10\%$ on wafer). We observed that the maximum deposition rate value lowered and shifted a little to smaller values of oxygen/silane mole ratio with the increase of the linear velocity of the total gas flow. We consider that this effect is not only the result of the silane dilution and its decreased residence time on substrate surface but even of a local cooling of the wafer surface, in agreement with the shape of the characteristics obtained at different temperatures according to figure 2.

DISCUSSION

The dependence of the silicon dioxide deposition rate on substrate temperature (Fig. 2) shows that the deposition reaction obeys the heterogeneous reaction theory at a solid surface.

At a given temperature, the decrease of the oxygen/silane mole ratio below a certain value leads to an accelerated process of the silicon dioxide white powder formation. This powder is removed by the exhaust system. The starting point of powder formation fitted with the beginning of the deposition rate decreases from lower oxygen/silane mole ratios for a constant silane flow rate of 30 cm^3/min (Fig. 2). Thus, under these conditions simultaneously with a heterogeneous deposition reaction at the substrate surface, a homogeneous gas phase reaction takes place. This fact allowed the understanding of the results from figure 2 where at an oxygen/silane mole ratio of 5, the deposition rate at 400°C was smaller than that from 350°C. To indicate clearly this phenomenon, the deposition rate is represented as a function of substrate temperature at an oxygen/silane mole ratio of 5 (Fig. 6). At this ratio, in the temperature range from 300 to 350°C, the two reactions (homogeneous and heterogeneous) coexist but the silicon dioxide deposition rate continues to increase with temperature increase and then at higher temperatures (350 – 400°C) the deposition rate begins to decrease. This fact is explained by increasing homogeneous gas phase reaction with temperature increase and therefore decreasing the silane and oxygen available at the substrate surface for heterogeneous deposition reaction. The region in which the deposition rate increases with the oxygen/silane mole ratio increase (Fig. 2) and the two reactions

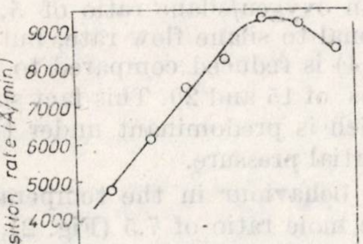

Fig. 6.—Deposition rate vs. deposition temperature. $F_{SiH_4} = 30$ cm^3/s ; $v_F = 1.7$ cm/s ; $O_2/SiH_4 = 5$.

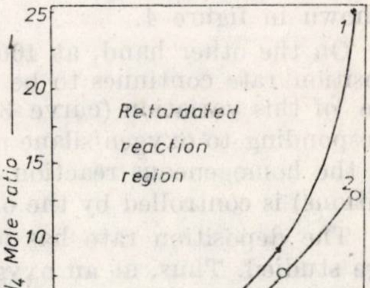

Fig. 7.—Delimitation of the retardated, homogeneous and of the maximum deposition rate (between first two) reaction regions as a function of temperature and oxygen/silane mole ratio. $F_{SiH_4} = 30$ cm^3/min, $v_F = 1.7$ cm/s.

coexist but the homogeneous reaction can be dominant, is called by us the homogeneous reaction region.

Also at a given temperature, over a certain value of oxygen/silane mole ratio, the deposition rate also begins to decrease and finally cancels (retardated region). This phenomenon which appeared at higher oxygen/silane ratios was explained by the retardation effect of the oxygen adsorption on the substrate surface[3].

The above discussion is synthesized in figure 7 where the maximum deposition rate region is situated between the retardated reaction region and homogeneous reaction region. However, the delimitation of these three reaction regions is consistent with the flow conditions specified in figure 7. Therefore, at a given silane flow rate (or nitrogen) the areas occupied by the reaction regions in the (temperature, oxygen/silane mole ratio) plane change as a function of nitrogen (or silane) flow rate. The effect of the linear velocity of the total gas flow was discussed in figure 5. Thus, one can observe a strong correlation between all experimental parameters in the process of flow temperature silicon dioxide deposition by the reaction between diluted silane and oxygen.

At 400°C, the maximum deposition rate plateau corresponding to oxygen/silane ratios between 12 and 20 is well correlated with a zeroth order kinetics with respect to oxygen (the reaction is independent of oxygen flow rate) and first order kinetics with respect to silane. Another argument for this fact is the independence of the deposition rate in oxygen at a given silane flow rate and the linear dependence on silane flow rate, as shown in figure 4.

On the other hand, at 400°C and an oxygen/silane ratio of 5, the deposition rate continues to be proportional to silane flow rate, but the slope of this variation (curve 3 in Fig. 4) is reduced compared to that corresponding to oxygen/silane mole ratios of 15 and 20. This fact shows that the homogeneous reaction rate (which is predominant under these onditions) is controlled by the oxygen partial pressure.

The deposition rate has a specific behaviour in the temperature range studied. Thus, at an oxygen/silane mole ratio of 7.5 (Fig. 2), the reaction takes place in the homogeneous region at 400°C, in the maximum deposition rate region at 350°C, in the retardation region at 300°C and then it is cancelled below 250°C.

CONCLUSIONS

The silicon dioxide deposition kinetics at low temperature (250 – 400°C) on this continuous type reactor presented the particular property of a large range of deposition rates (0.1 – 3) μm/min. The kinetic behaviour is qualitatively similar to those presented on other reactors. A strong dependence was shown between all experimental parameters in the process of the silicon dioxide depposition by the reaction between diluted silane and oxygen.

For a given linear velocity of the total gas flow (2.33 cm/s) and silane flow rate of 30 cm^3/min three regions of the deposition kinetics were delimited as a function of temperature and oxygen/silane mole ratio :

— Retardated reaction region at higher oxygen/silane mole ratios; the deposition rate is controlled by the oxygen adsorption on the substrate surface. At a given temperature, a total inhibition of the reaction is obtained for a certain oxygen/silane mole ratio.

— Homogeneous reaction region; the deposition rate is decreased by the gas phase reaction which plays an important role at lower oxygen/silane mole ratios with temperature increase. For temperatures above 350°C and oxygen/silane mole ratios lower than 5, the homogeneous reaction becomes dominant and is controlled by oxygen partial pressure when silane flow rate is kept constant.

— Maximum deposition rate region; the deposition rate is not lowered either by homogeneous reaction of oxygen adsorption on the surface. At 400°C and a linear velocity of the total gas flow of 2.3 cm/s, for oxygen /silane mole ratios between 12 and 20 it resulted a zeroth order kinetics with respect to oxygen and first order kinetics with respect to silane. The maximum deposition rate region enlarges at higher temperatures.

These results can serve as a starting point in the establishment of the effective mechanism of the silicon dioxide deposition by the reaction between oxygen and silane, which is not known yet.

REFERENCES

[1] N. Goldsmith and W. Kern, *RCA Review*, **28**, 153 (1967).
[2] K. Strater, *RCA Review*, **29**, 618 (1968).
[3] B. J. Baliga and S. K. Gandhy, *J. Appl. Phys.*, **44**, 990 (1973).
[4] W. Kern and R. C. Heim, *J. Electrochem. Soc.*, **117**, 562 (1970).
[5] W. Kern and R. C. Heim, *J. Electrochem. Soc.*, **117**, 568 (1970).
[6] W. Kern and A. W. Fisher, *RCA Review*, **31**, 715 (1970).
[7] M. Shibata and K. Sugawara, *J. Electrochem. Soc.*, **122**, 155, (1970).
[8] M. Shibata, T. Yoshimi and K. Sugawara, *J. Electrochem. Soc.*, **122**, 157 (1975).
[9] E. A. Taft, *J. Electrochem. Soc.*, **126**, 1728 (1979).

Revue Roumaine de Chimie, 28, *1*, 65 — 74 (1983)

MERCURY(II) COMPLEXES OF PHENYL-α-PYRIDYL-TRIAZENE AND *p*-NITROPHENYL-α-PYRIDYL-TRIAZENE; PROPERTIES AND ANALYTICAL APPLICATION IN A SPECTROPHOTOMETRIC METHOD

MARIA POPESCU* and ANDREI DĂNEȚ **
* Institute of Constructions, Bucharest
** Polytechnic Institute, Bucharest

Received May 27, 1981

The paper presents a spectrophotometric determination of Hg(II) using two triazenic compounds such as phenyl-α-pyridyl-triazene and *p*-nitrophenyl-α-pyridyl triazene. The determinations were carried out in aqueous medium and by solvent extraction. The molar coefficients of optic absorption are 24,000 and 31,500 $\mathrm{l\,mol^{-1}\,cm^{-1}}$; the Hg : R combination ratio is 1 : 2 and the conditional instability constant is of the order 10^{-11}. $Hg_2(II)$ and Pd(II) are interfering.

Several spectrophotometric methods to determine Hg(II) ions are suggested in the literature but these are accompanied by numerous interferences.[1]

We found that the triazenic (diazoamino) reagents form chelate compounds extractable in organic solvents, which reduces considerably the interferences.[2,3] Therefore, with this method it was possible to determine Hg(II) traces in waste water,[4] cinnabar ores[5] and air.[6]

Triazenic reagents form with Hg(II) chelate compounds of the type:[7,8,9]

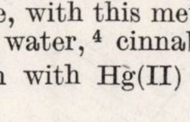

with an Hg/R combination ratio of 1 : 2 and the instability constant of the order $10^{-10} - 10^{-11}$.

This paper reports a spectrophotometric determination of Hg(II) traces both in aqueous and organic phase by using phenyl-α-pyridyl-triazene (DPy) and *p*-nitrophenyl-α-pyridyl-triazene (DPyN) reagents which are very sensitive and selective to Hg(II).

The reagents have been prepared according to the recipes given in the literature.[10]

EXPERIMENTAL

Reagents and instrumentation

Solution of $HgCl_2$ with titre 100 µg Hg(II)/ml, reagent solutions having a concentration of 0.05 % DPy and 0.02% DPyN in EtOH.

Buffer solution of 2M potassium acetate and a solution of 20% sodium potassium tartrate for complexing some easily hydrolyzable ions were used.

To study the interferences of cations and anions, we used titrated solutions of nitrates or sulphates of cations and alkali metal salts of anions such as Li(I), Cu(II), Ag(I), Au(III), Be(II), Mg(II), Ca(II), Sr(II), Ba(II), Zn(II), Cd(II), Hg_2(II), Tl(I, III), UO_2(II), Sn(II), Pb(II), Mn(II), Fe(II, III), Bi(III), Cr(III), Co(II), Ni(II), Rh(III), Pd(II), Ir(IV), Pt(IV), AsO_4^{-3}, SbO_4^{-3}, CrO_4^{-2}, MoO_4^{-2}, WO_4^{-2}, Cl^-, Br^-, I^-, MnO_4^-, SO_4^{-2}, PO_4^{-3}, SCN^-, CN^-, S^{-2}, ClO_4^-, citrate, tartrate, EDTA.

Absorption spectra were measured with SPECORD UV — VIS spectrophotometer using 1 cm cuvettes.

Infrared spectra were recorded on a Perkin Elmer Spectrophotometer 325, the derivatograms on a derivatograph type 2895 F. Paulik — J. Paulik — L. Erdey system, the NMR spectra on VARIAN A-60 A and the X-ray diffraction spectra on a generator TUR-M62 fitted with a diffractometer MZG-3 having a proportional counter.

Absorption Spectra of DPy and DPyN Reagents and Hg(II) Complexes

Figure 1 shows the absorption spectra of a 5.05×10^{-5}M phenyl-α-pyridyl-triazene solution extracted in toluene (curve 1) and of some solutions containing the same amount of reagent and increasing amounts of Hg(II) ranging between 9.96×10^{-7} M and 8.96×10^{-6}M (curves 2 — 10), and Hg(II) in excess (curve 11).

The absorption maximum of the reagent is at $\tilde{\nu} = 29.25 \times 10^3$ cm^{-1}, the absorption maximum of the complex at 27.37×10^3 cm^{-1} and the isosbestic point at 28.25×10^3 cm^{-1}.

The maximum difference between the reagent absorption and the complex absorption is at 25.5×10^3 cm^{-1}, wave number at which most determinations were conducted afterwards.

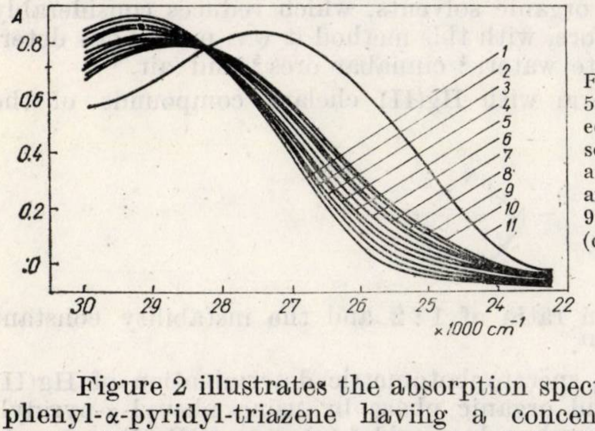

Fig. 1. — Absorption spectra of a 5.05×10^{-5}M DPy solution extracted in toluene (curve 1) and of some solutions containing the same amount of reagent and increasing amounts of Hg(II) ranging between 9.96×10^{-7}M and 8.96×10^{-6}M (curves 2 — 10), and Hg(II) in excess (curve 11).

Figure 2 illustrates the absorption spectra for a solution of *p*-nitrophenyl-α-pyridyl-triazene having a concentration of 8.23×10^{-6} M (curve 1) and increasing amounts of Hg(II) ranging between 1.25×10^{-6} M and 1.25×10^{-5} M extracted in nitrobenzene (curves 2 — 5).

The curves were recorded at a low speed of wavelength augmentation. Even under these recording conditions it was found that the reagent maximum was extremely close to that of the complex, that is at $\tilde{\nu} = 23.25 \times 10^3$ cm^{-1} ($\lambda = 430.1$ nm). By adding Hg(II) only the intensity of the absorption bands increased, this suggesting an interaction between the complex molecules and the solvent polar molecules.[7]

The maximum difference between the reagent absorption and the complex absorption is at 22.5×10^3 cm^{-1}.

The spectra revealed that the two reagents form Hg(II) complexes in which Hg—N bond is polarized in a differentiated way, i.e. the Hg(II) complex with DPyN in nitrobenzene interacts with the solvent molecules, producing a strong polarization of the Hg—N bond, which becomes nearly ionic. The Hg(II) complex with DPy in toluene is a proper complex combination with a covalent interaction between Hg(II) and the donor atoms of the chelate group, as suggested by the bathochromic displacement of the absorption band of the complex versus that of the reagent, and by the increase of its intensity.

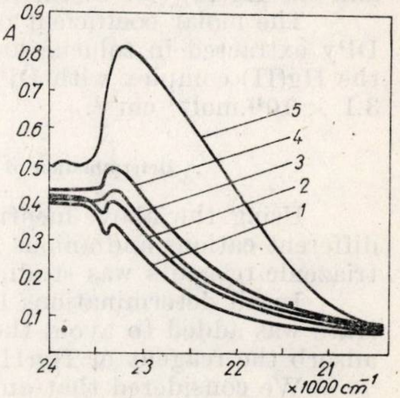

Fig. 2. — Absorption spectra of a 8.23×10^{-6}M DPyN solution extracted in nitrobenzene (curve 1) and of some solutions containing the same amount of reagent and increasing amounts of Hg(II) ranging between 1.25×10^{-6}M and 1.25×10^{-5} M (curves 2 — 5).

Influence of pH on optic absorption

The pH dependence on the optic absorption of Hg(II) complexes with the two reagents illustrated in figure 3, demonstrates that the complex with DPyN, extracted in nitrobenzene, unlike the complex with DPy extracted in toluene, has a constant optic absorption in a limited pH range, such as 6.5 — 8.

All subsequent determinations were effected at pH = 6.5 — 7 using a medium of 0.04 M potassium acetate.

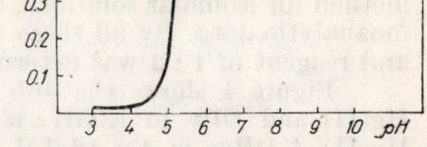

Fig. 3. — pH dependence on the optic absorption.

Operating procedure

Variable quantities of $HgCl_2$ and approximately 7 ml distilled water are introduced in graduated cylinders or separatory funnels of 50 ml, then 2 ml of 2M potassium acetate solution and 1 ml of reagent solution are added. The reaction is fast so that 5 ml of organic solvent for the complex extraction may be immediately added. Shaking is carried out for 1 min. and after the phase separation, the organic extract is spectrophotometrically determined, compared with a blank assay without Hg(II) in 1 cm cuvettes.

In our previous determinations using ^{203}Hg with other triazenic reagents, we found that a simple extraction is sufficient for the complex to pass quantitatively in the organic phase.[2]

Variation of optic absorption with Hg(II) concentration

A linear dependence was obtained between the optic absorption and the Hg(II) concentration within the range of 0.2 — 6 ppm.

The molar coefficient of optic absorption for Hg(II) complex with DPy extracted in toluene has the value 2.4×10^4l. mol^{-1} cm^{-1} and for the Hg(II) complex with DPyN extracted in nitrobenzene has the value 3.1×10^4l.mol^{-1} cm^{-1}.

Determination of Hg(II) in the presence of other ions

Using the above-mentioned operating procedure, the influence of different cations and anions in the determination of Hg(II) with the two triazenic reagents was studied.

In all determinations 1 ml solution of 20% sodium potassium tartrate was added to avoid the formation of some precipitates that might adsorb the reagent or Hg(II) ions on the surface.

We considered that an ion does not interfere when at a maximum admissible ion/Hg(II) ratio we have an error in the determination of Hg(II) concentration lower than 2%.

We found that under the operating conditions mentioned the cations: Zn(II), Cd(II), Tl(I, III), Co(II), Ni(II), Pb(II), Fe(III) and the anions: ClO_4^-, MoO_4^{-2}, WO_4^{-2}, SO_4^{-2}, citrate, tartrate do not interfere up to an ion/Hg(II) ratio of 1000.

Also, Cu(II), Bi(III), Mn(II), Au(III), Rh(III), Pt(IV), Ir(IV), CrO_4^-, SbO_4^{-3}, AsO_4^{-3} ions do not interfere up to a ratio of 500.

Hg_2(II) and Pd(II) cations do interfere and Ag(I) forms a partially extractable complex. Fe(II) and more markedly Sn(II) interfere by reducing Hg(II) to Hg(O).

The oxidizing anions MnO_4^-, $Cr_2O_7^{-2}$ also interfere, by destroying the reagent, S^{-2} ions precipitate Hg(II) as HgS and EDTA, SCN^-, CN^- and I^- interfere due to Hg complexing.

The anions Cl^- and Br^- ions do not interfere up to a ratio of 75 and 5, respectively.

Study on composition of Hg(II) complexes with phenyl-α-pyridyl triazene and p-nitrophenyl-α-pyridyl-triazene

The combination ratio between Hg and reagents was determined by the spectrophotometric titration method,[9] Job's continuous variation method for isomolar solutions, [11] Chriswell's method [12] and from the thermoanalytic data. By all these methods, a combination ratio between Hg and reagent of 1 : 2 was determined.

Figure 4 shows the Job curves obtained for isomolar solution of Hg(II) and DPy in EtOH : $H_2O = 20 : 80$. The sum of concentrations Hg(II) + DPy is 1×10^{-4} M (curve 1); 1.5×10^{-4} M (curve 2) and 2×10^{-4} M (curve 3).

The instability constants of the two complexes were calculated by Job method for non-isomolar solution in aqueous and organic medium; from the flattening degree of Job curves for isomolar solutions and by Chriswell method. [12]

Job curves indicate a conditional instability constant of order 10^{-11} (Table 1).

The experimental data concerning the determination of instability constants of the complexes from the flattening degree of Job curves are shown in table 2.

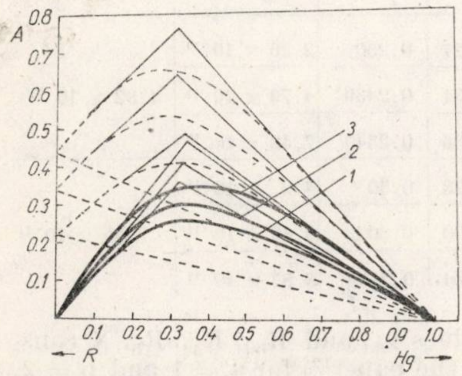

Fig. 4. — The Job curves obtained for isomolar solutions of Hg(II) and DPy in EtOH : $H_2O = 20 : 80$. The sum of concentrations, Hg(II) + DPy is 10^{-4}M (curve 1), 1.5×10^{-4}M (curve 2) and 2×10^{-4} M (curve 3).

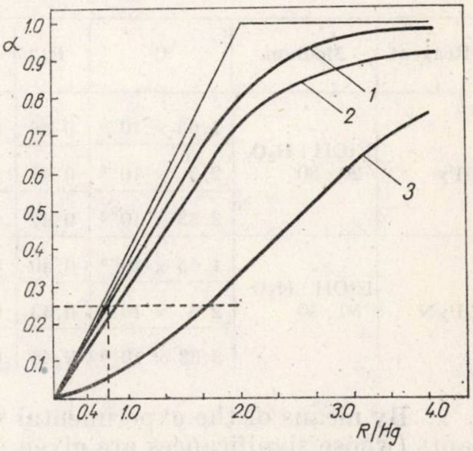

Fig. 5. — Dependence of Hg(II) concentration fraction in DPyN-Hg complex (α) on the molar ratio.

TABLE 1

Experimental data and the values of instability constants obtained from Job curves for non-isomolar solutions

Reagent	Medium	C	ρ	x	K	Km
DPy	EtOH : H_2O 20 : 80 toluene	5×10^{-5}	2	0.54	5.39×10^{-11}	3.35×10^{-11}
		2.5×10^{-5}	4	0.39	1.31×10^{-11}	
DPyN	EtOH : H_2O 50 : 50 nitrobenzene	5×10^{-5}	2	0.53	2.1×10^{-11}	4.85×10^{-11}
		2.5×10^{-5}	4	0.43	7.6×10^{-11}	

To determine the instability constant by Chriswell method, we plotted the fraction of Hg(II) concentrations in the complex (α) dependent on the molar ratio of the reagent and Hg(II) concentrations at different pH values.

At a working pH of 6.5, the complexes are stable and the location of the inflection point cannot be done with precision, therefore, the determinations were carried out at more acid pH values for the DPy-Hg complex and DPyN-Hg complex (Figure 5), pH values where the complexes were partially formed but the curves enable the location of the inflection point at $\alpha_{inf} = 0.25$

TABLE 2

Experimental data and the values of instability constants obtained from Job curve flattening for isomolar solutions

Reagent	Medium	C	E_0	E_1	α	K	Km
DPy	EtOH : H_2O 20 : 80	1.65×10^{-5}	0.36	0.27	0.250	2.26×10^{-11}	4.82×10^{-11}
		2.5×10^{-5}	0.41	0.31	0.2439	4.79×10^{-11}	
		3.33×10^{-5}	0.47	0.36	0.2340	7.42×10^{-11}	
DPyN	EtOH : H_2O 50 : 50	1.65×10^{-5}	0.40	0.28	0.30	4.2×10^{-11}	7.55×10^{-11}
		2.5×10^{-5}	0.43	0.30	0.3023	9.89×10^{-11}	
		3.33×10^{-5}	0.46	0.34	0.2608	8.57×10^{-11}	

By means of the experimental values α_{inf} and R_{inf}, R_A, R_B, X constants (whose significances are given in the paper[12]) for a = 1 and b = 2, the relationships (1) and (2) were checked :

$$\alpha_{inf} = \{[(ab)/(a + b - 1)]^{1/2} - 1\}/(a - 1) \qquad (1)$$

$$R_{inf} = R_A \left[\frac{a/b - (d\alpha/dR)_{inf}}{X\,(d\alpha/dR)_{inf}} \right] + R_B \qquad (2)$$

The data confirm that a = 1 and b = 2, representing the stoichiometry of the complex.

R_{inf} and the graph slope at the inflection point $(d\alpha/dR)_{inf}$ depend upon the formation constant of the complex.

By using the experimental values found, and relations (3) and (4), we calculated the instability constant (Table 3).

TABLE 3

Experimental data and results obtained by applying Chriswell method in determining the instability constants

Reagent	α_{inf}	R_{inf}	$\left(\frac{d\alpha}{dR}\right)_{inf}$	$\left(\frac{\Delta R}{\Delta\alpha}\right)_{inf}$	K (Eq.3)	K (Eq.4)	Km
DPy	0.25	0.62	0.431	2.32	1.19×10^{-11}	2.69×10^{-11}	1.94×10^{-11}
DPyN	0.25	0.58	0.4545	2.20	1.20×10^{-11}	1.05×10^{-11}	1.12×10^{-11}

$$R_{inf} = R_A \left[\frac{1}{K\,C_A^{a+b-1}} \right]^{1/b} + R_B \qquad (3)$$

$$(d\alpha/dR)_{inf} = (a/b)/[X(1/KC_A^{a+b-1})^{1/b} + 1] \qquad (4)$$

Thermoanalytic study of phenyl-α-pyridyl-triazene and p-nitrophenyl-α-pyridyl triazene reagents and their Hg(II) Complexes

The determinations were carried out in static air atmosphere, with dT/dt of 10°C/min; 100 and 200 mg TG sensitivities, DTG 1/10, DTA 1/5 and platinum crucible.

The essential characteristic of these compounds is the partial sublimation of the organic reagent under the influence of heating, this being also observed at other reagents and Hg(II) complex from the same class.[13]

From the calculations presented in Table 4, it appears that the mass loss of Hg(II) complexes at decomposition temperature corresponds to an Hg : R combination ratio of 1 : 2.

After the decomposition a rest of carbon remains in the crucible burning between 400 and 750°C with a high exothermal value indicated by DTA curve.

Infrared spectra

The infrared spectra of the reagent and complexes show the disappearance of the vibration bands characteristic of N—H bond in the spectra of Hg(II) complexes [14,15] and the appearance of a vibration at 480 cm^{-1} characteristic of N—Hg bond.

In the spectra of Hg(II) complexes compared to the reagent spectra it is also found a broadening of the band between 1295 and 1345 cm^{-1} [7] and a negative shift of the $C_6H_5-N=$ vibration bands (Table 5).

NMR spectra

DPy reagent and its complex with Hg(II) have a sufficient solubility in $DMSOd_5$ to make obvious the disappearance of the proton bound to ionic nitrogen in the spectrum of the complex (Figure 6).

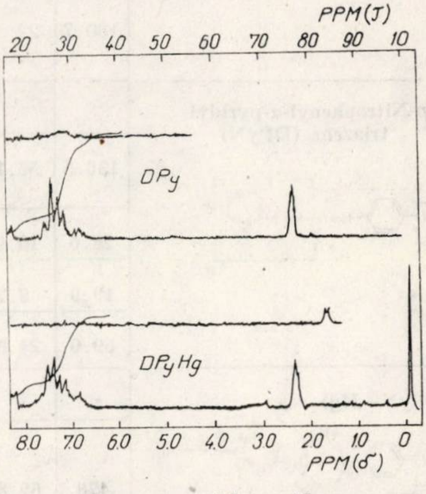

Fig. 6. — NMR spectra for DPy and its complex with $HgCl_2$ in $DMSOd_5$

Aromatic protons appear in the spectrum within the range of 6.7 — 7.7 ppm and the iminic proton at 12.33 ppm.

X-ray diffraction patterns were carried out under the following experimental conditions: CuKα radiation, Ni filtre, the tube supplied at

TABLE 4

Semi-quantitative interpretation of derivatograms

Compound	Molecular mass losses	Loss %	Temp. °C DTG max.	Temp. °C DTA max.	Temp. interval	Remarks
Phenyl-α-pyridyl-triazene (DPy)					25 — 190	
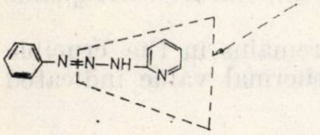	108.9	55	190 endo	190 exo	190	170°mp
	51.5	26			190 — 500	
	37.6	19			500 — 900	
(DPy—Hg)					25 — 170	
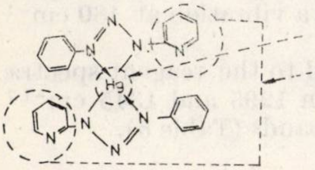	44.5	7.5	200 endo	200 exo	170 — 210	Hg sublimates in complex bet. 170—260 with max. speed at 240°C
	199	33.5	240	240	210 — 260	
	184	31			260 — 340	
	35.6	6			340 — 480	
	130.7	22		620 exo	480 — 900	
p-Nitrophenyl-α-pyridyl-triazene (DPyN)					25 — 220	
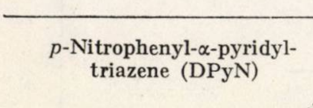	136.5	56.1	220 endo	220 exo		
	26.6	10.9			220 — 360	
	19.9	8.2			360 — 500	
	59.9	24.6			500 — 900	
(DPyN—Hg)					25 — 240	
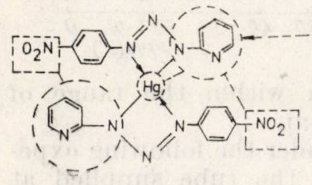	478	69.8	240 endo	240 exo	240	Hg sublimates with a part of the reagent at 240°C
	58.8	8.6			240—380	
	147	21.5			380—900	

TABLE 5

Main absorption bands observed in IR spectra

Compound	τ N–H		τN–Hg	τ C_6H_5–N=					
	(cm^{-1})		(cm^{-1})	(cm^{-1})	(cm^{-1})	Δτ	(cm^{-1})	(cm^{-1})	Δτ
DPy	1 520	3 140	—	1 215		10	1 305		25
DPy–Hg	—	—	480	—	1 205			1 280	
DPyN	1 520	3 180	—	1 235		5	1 320		15
DPyN-Hg	—	—	480	—	1 230		—	1 335	

40 kV and 35 mA, the counter speed of 0.5°/min, impulse scale 1.8 × × 10^5 impulses/min.

From the X-ray diffraction patterns, the interplanar distances "d" and the intensities "I_{obs}" of the most significant diffraction lines were calculated (Table 6).

TABLE 6

X-ray diffraction patterns for reagents and their Hg(II) complexes

DPy		DPy–Hg		DPyN		DPyN–Hg	
dÅ	I_{obs}	dÅ	I_{obs}	dÅ	I_{obs}	dÅ	I_{obs}
11.4	100	11.4	82	13.8	100		
		9.8	100	10.7	86		
8.0	11					10.2	6
7.4	21					9.7	10
		6.22	27	8.4	9		
6.01	100			6.89	45		
		5.68	18	6.71	7		
5.65	25					6.61	10
5.19	40			6.50	9		
		5.01	6			6.28	43
4.97	15			6.01	29		
		4.87	16			5.53	14
4.58	8					5.34	52
4.48	26					5.12	12
		4.20	9			4.84	21
4.14	36			4.76	13		
		3.92	8			4.60	32
3.76	28			4.37	14		
3.72	100					3.80	12
3.60	20			3.468	23		
3.424	11					3.273	100
3.184	31			3.215	63		
		3.106	8	2.759	25		

* Only lines with an intensity higher than 6 are given.

From the table it follows that the conversion of the reagents into Hg(II) complexes is total as no characteristic lines for reagents and $HgCl_2$ appear in the spectrum of the complexes.

All the data presented confirm the structure assumed for the Hg(II) complexes with triazenic reagents.

REFERENCES

[1] S. Chilov, *Talanta*, **22**, 205 (1975).

[2] Gr. Popa and M. Popescu, Paper presented at "National Congress of Chemistry", Bucharest 1978.

[3] Gr. Popa, A. F. Dăneţ and M. Popescu, *Talanta*, **25**, 546 (1978).

[4] Gr. Popa, M. Popescu and A. F. Dăneţ, *Rev. Roumaine Chim.*, **10**, 1427 (1980).

[5] M. Popescu and D. Todor, *Rev. Chim. (Bucureşti)*, **12**, 1182 (1978).

[6] Gr. Popa and M. Popescu, *Rev. Chim. (Bucureşti)*, **5**, 477 (1979).

[7] T. V. Ershova, E. G. Rukhadze and A. P. Terent'ev, *Zhur. obshchei, Khim.*, **39**, 59 (1969).

[8] A. P. Terent'ev, T. V. Ershova and E. G. Rukhadze, *Zhur. obshchei Khim.*, **36**, 1046 (1966).

[9] A. E. Harvey and D. L. Manning, *J. Amer. Chem. Soc.*, **72**, 4488 (1950).

[10] V. O. Lukashevich and E. S. Lisitsyna, *Doklady Akad. Nauk.* S.S.S.R., 172, 2, 345 (1967).

[11] P. Job, *Ann. Chim. (France)*, **9**, 113 (1928).

[12] C. D. Chriswell and A. A. Schilt, *Analyt. Chem.*, **47**, 1623 (1975).

[13] M. Popescu and D. Todor, *Rev. Chim. (Bucureşti)*, **10**, 987 (1978).

[14] K. Nakamoto, "Infrared Spectra of Inorganic and Coordination Compounds", Wiley, New York, 1963.

[15] K. Brodersen and H. J. Becher, *Chem. Ber.*, **89**, 1487 (1956).

Revue Roumaine de Chimie, 28, 1, 75 – 80 (1983)

COMPTES RENDUS

G. E. BAIULESCU, C. PĂTROESCU and R. A. CHALMERS, "*Education and Teaching in Analytical Chemistry*", (Analytical Chemistry Series), John Wiley & Sons Ltd., London, 1982, 190 p.

This book strongly supports the contention that modern analytical chemistry is, multidisciplinary as well as a unified and independent scientific discipline which participates with other sciences in the optimization and development of many processes in modern technology. In the development and training of an analyst, to equip him to tackle the current problems of chemical analysis, the teaching and education he receives play an important role.

This work lays out all the educational requirements in analytical chemistry. It promotes the concept of the analytical chemistry student being "situation-oriented", deliberately encouraged to educate himself. It takes the view that teaching in analytical chemistry plays the role of the catalyst in promoting the process of learning; that teaching is a constituent part of a general education process, carried out in a serious scholarly atmosphere, where the student is taught to think independently and draw from his own ability the capacity to understand, and successfully apply the accumulated experience of his scientific knowledge.

The authors stress their conviction that such education is achieved primarily through the medium of the lecture course, where the necessity lies in logical, sequential presentation of the fundamentals both by the lecturer and by specialist texts; clear, concise wording to the material; the value of audio-visual aids, e.g. blackboard, slides, television; and the succint delivery of the lecture with effective use of the voice. It also advises on the supplementation of the lecture course with suitable reading material, which should be read in relation to the experiments of practical courses.

Readership: teachers and lecturers in analytical chemistry, and all its related disciplines, in universities, polytechnics, technical colleges, and other educational establishments, e.g. adult education centres; and teacher training establishments.

D. I. Marchidan

W. BRUNS, I. MOȚOC and K. F. O'DRISCOLL, "*Monte Carlo Applications in Polymer Science*", (Lecture Notes in Chemistry; Vol. 27). Springer-Verlag, Berlin, 1981, 180 p.

The book consists of four chapters. The first (The Monte Carlo Method and Applications by I. Moțoc and W. Bruns) is dedicated to the principles of Monte Carlo models, with a brief review of Monte Carlo treatment on topics such as hydrophobic interactions, water structure around biomacromolecules, self-replicating macromolecules, reactivity in polymer analogous reactions and binary irreversible copolymerization also included. The references contained in this chapter provide a useful guide to the relevant literature.

Chapters 2 (Monte Carlo Calculation of Sequence Distributions in Polymers by I. Moțoc and K. F. O'Driscoll) and 3 (Polymer Configuration by W. Bruns) represent up-to-date reviews of two important applications of the method in polymer science: calculation of polymer conformation, and calculation of sequence distribution in polymers. These two topics are discussed in detail, and many results obtained by the authors are included.

Chapter 4 (Fortran Programs by W. Bruns and I. Moțoc) describes two computer programs, developed by the authors, to calculate the sequence distribution and polymer conformation by the Monte Carlo technique. The complete listing of the programs and illustrative input/output examples are presented.

This Lecture Notes volume is the first monographic treatment of Monte Carlo applications in polymer science.

The book is meant to meet requirements of the students and teaching people interested in physical chemistry of polymers, as well as of the research workers involved in this field.

D. I. Marchidan

Ion Selective Electrodes, 3, Third Symposium held at Mátrafüred, Hungary, 13 – 15 October, 1980. Edited by E. PUNGOR and I. BUZÁS, Akadémiai Kiadó, Budapest, 1981, 428 pp.

The development of electrochemical sensors selective for one species of ion or even for a variety of specific compounds of critical importance in biomedicine and industrial processes has proved one of the exciting events of the last 15 years. Analytical chemists in particular have been able to profit from the availability of ion-selective electrodes which offer a convenient and rapid means of estimating the concentrations of certain elements which formerly were difficult to determine. The practical results have been enormously beneficial to the laboratory scientist. In addition, the development of the theory of operation of these sensors has led to an increased understanding of membrane behavior in general and of the mechanisms of transfer through membranes important to human physiology. Extensive and detailed studies on the selectivity of these electrodes add much to this understanding and aid materially in increasing the accuracy of analytical determinations of ion concentrations.

The book contains the papers of the third Symposium on Ion-Selective Electrodes held at Matráfüred, Hungary, and summarizes the most recent theoretical and practical results in this field.

Specialists of international reputation have dealt with almost all current theoretical and practical problems of the application of the different systems of ion-selective electrodes.

The volume includes four plenary lectures which only serve as starting points for the discussion rather than being a simple statement of final results, as in common at many conferences. The titles are given below in brackets after the authors' names as follows :

— R.G. Bates' lecture (Thermodynamic Behavior of Ion-Selective Electrodes) reports some of the most important thermodynamic applications of ion-selective electrodes and to outline studies that enable one to establish the suitability of these sensors for thermodynamic measurements, together with the limits of their applicability. The examples cited in the lecture serve to emphasize that ISEs have a vast potential for the aquisition of useful thermodynamic data. For the greatest reliability, however, it is essential that the quality of the electrode response be carefully examined, in order to justify confidence in the results obtained.

— R.P. Buck's lecture (The Impedance Method Applied to the Investigation of Ion-Selective Electrodes) emphasizes the investigation of ISEs using the impedance method. The impedance is a function of the perturbing electrical frequency, temperature, thermodynamic and kinetic parameters, and bathing activities. The direct purpose of the method is the determination and interpretation of the time constants of ISE responses. Most important for the study of ISEs is the interpretation of experimental electrical responses in terms of predicted responses from models of interfacial and bulks, charged-species transport. The impedance method also provides one of several alternative methods for identifying the membrane properties responsible for the potentiometric responses. It must be noticed that the impedance method provides partial tests only in macroscopic terms. It is not possible to deduce microscopic aspects of transport or double layer structure from impedance measurements alone.

— J. Koryta's lecture (Electrolysis at the Interface of Two Immiscible Electrolyte Solutions and its Analytical Aspects) presents the applications of the electrolysis at the interfacial of two immiscible electrolyte solutions (ITIES) to electroanalytical chemistry (stability constant determination, determination of ionophore concentration, assessement of Nernstian behaviour and of response time of ion-selective electrodes) and to biophysics (modelling of membrane processes such as ionophore mediated ion transport and redox-reaction driven ion transport, phospholipid monolayer at ITIES as an analogy of bilayer lipid membrane) show good perspective to this new methodical approach.

— P. Oggenfuss, W. E. Morf, R. J. Funck, H. V. Pham, R. E. Zünd, E. Pretsch and W. Simon's lecture (Transport of Ions through Neutral Carrier Membranes) describes the electrolytic transport of ions on solvent polymeric membranes that contained neutral carriers selective for Li^+, Na^+, K^+, Ca^{2+}, Ba^{2+}, Cd^{2+} and other ions, respectively. Throughout, the measured transport numbers attest a high selectivity in ion permeation. Specific cation transport has been realized even under zero-current conditions. The role of neutral carriers in anion permeation is also discussed.

These lectures end with questions and comments on the problems involved.

Five keynote lectures deal with new research methods : X-ray photoelectron-spectroscopy, the electrochemical behaviour of solid state electrodes, problems of the response time and questions of selectivity and recent improvements.

The application of ion-selective electrodes in continuous monitoring, the use of new sensors as electrodes, physico-chemical investigations on the electrode material; novel trends in instrumentation, theoretical and practical study of the electrodes are the main aspects of the 23 discussion lectures.

The lectures are regarded as initiatives of the discussions. The discussions of the lectures and the Panel Discussion, its main topic being the standardization and classification of ion-selective electrodes, will be of great interest for the scientists engaged in the field.

Iuliana Vartires

PAOLO ARRIGHINI, *Intermolecular Forces and Their Evaluation by Perturbation Theory* (Lecture Notes in Chemistry Series, No. 25), Springer-Verlag, Berlin—Heidelberg—New York, 1981, ix + 243 pp.

Intermolecular forces have been the subject-matter of many books. The reader interested in the methods of their evaluation, however, still cannot find them but scattered as journal papers, mainly because this is a field in full progress. The book of Dr. Paolo Arrighini, of the Pisa University, is the first attempt, to our knowledge, to gather together some of these methods.

In fact, to give the book a unitary character, the author chose to restrict his theoretical treatment to a single method of calculation of the intermolecular forces, i.e. the perturbative one. Even so, the subject was too large to be fitted coherently into a 240-page book and the author confined further the discussion to the case of intermediate- and long-range forces, leaving out the case of short-range forces. Since these act mainly intramolecularly, their neglect does not harm the subject-matter of the book.

Traditionally, the problem of chemical interactions between various species has been approached by variational methods. In spite of their success for various molecular systems, these have the major drawback of evaluating the interaction energy between two atomic partners, which is usually a very small quantity, by a critical subtraction of the energy of the 'complex' from a nearly equal energy of the non-interacting particles. By contrast, the perturbation method allows the direct estimation of this quantity. Moreover, this method provides a natural partitioning of the interaction energy into various contributions which have a physical meaning. This is an appreciable advantage when dealing with large molecules, as is the case with molecules of biological interest. These two great advantages make the perturbation method much more attractive than the variational one, although the author does not claim any superiority for his approach.

After a short review of group theory, the author introduces the symmetry-adapted perturbation theory in a general framework. Since the treatment is only concerned with stationary states, the discussions is restricted to the time-independent equations, emphasizing the role of the partitioning technique in solving secular equations associated with eigenvalue problems and its connections with various perturbative expansions. The very simple case of the $H \ldots H^+$ system is discussed in some detail, mainly to point out the procedure and to define some useful concepts. First-and second-order contributions to the interaction energy between two atoms or molecules are then discussed in detail in two following chapters. As is known, these account, respectively, for the Coulombic (electrostatic) energy and for the polarization and exchange-polarization energies (or, in more familiar terms, induction and dispersion interaction energies, and their less familiar exchange counterparts). Rigorous expressions are given for all the corresponding interaction coefficients. As those who are acquainted with the field would recognize, estimation of the dispersion energy coefficients has been a long-standing, thorny problem in physical chemistry, still unsatisfactorily settled. As a consequence, the author deems it necessary to devote two large sections to this problem, solving it partially by using the Casimir-Polder relation, in which the dispersion energy is orientationally averaged. A critical survey of the results obtained so far using various procedures is also comparatively offered, for systems going from simple ones such as He-He, to reasonably complicated such as ethene-ethene. Another section is devoted to the long-neglected exchange polarization effects.

Without contributing with an absolutely original point of view or with original results, the book has the merit of gathering under a unitary treatment the various methods worked out during the last years to rationalize the intermolecular interactions. A general picture which emerges after reading carefully the book is — in spite of what the author says — a certain superiority of the perturbative approach over the variational one : several aspects of the problem get clearer under this treatment and certainly the results obtained so far for various particular systems justify such a view.

The book can be useful to the numerous researchers interested in intermolecular interactions at a modern theoretical level. Revival of the perturbational methods, long overdue, is certainly with trying on various, more complex systems.

Alex. Butucelea

SALVATORE CALIFANO, VINCENZO SCHETTINO and NATALE NETO, *Lattice Dynamics of Molecular Crystals* (Lecture Notes in Chemistry Series, No. 26), Springer-Verlag, Berlin—Heidelberg—New York, 1981, vi + 309 pp.

The last quarter century has wittnessed an increasing interest in the lattice dynamics of molecular crystals and, as a consequence, both the theoretical and the experimental aspects of the field have known a massive development. Of course, as in any science in progress, several, very different approaches were considered. On the one hand, molecular spectroscopists concentrated their attention upon the perturbations which the crystalline environment induce upon a molecule, in particular upon its vibrational properties. On the other, solid state physicists continued to use increasingly sophisticated variants of the well known Born-von Kármán theory, after having managed in the meantime to extend the lattice dynamical theory from atomic to molecular systems and the group theoretical methods from isolated to crystalline lattices.

Unfortunately, for a long time the two directions ran separately. Spectroscopists and solid state physicists could hardly understand one another; in fact, they did not even bother to read with decent attention the other side's papers. During the last years however some changes have occurred — for the better. A certain overlap has been developing along the years and today any interested researcher in any one of the two fields can, and should, understand with reasonable facility the language of the researcher in the other field.

Publication of this book is a significant step toward this mutual understanding. In the first place, the list of authors includes researchers in both fields. Although the leading author, Professor Califano, of the University of Firenze, Italy, is a well known authority in only one field, molecular spectroscopy, all three have been active lately in both fields. Moreover, the style of the book is coherent from beginning to the end, offering thus the still uninitiated reader the benefit of a unitary language and treatment, with no explicit distinction between the treatment of the two fields.

The introducing chapters are devoted, with increasing complexity, to lattice dynamics, symmetry considerations, and intramolecular potentials. The anharmonic interactions are dealt with in a large chapter, thus recognizing their importance in matters such as the phonon-phonon interactions and, therefore, to mention only a field of practical interest, the thermal expansion of crystals. The formalism used is adapted to treating molecular and lattice vibrations unitarily, in spite of their different nature : the intramolecular potential in the first case and the cubic and higher terms in the expansion of the intermolecular potential in the second. For small anharmonicities the perturbation theory is used to find the corrections to the phonon energies and the lifetimes of the phonon states, whereas for larger ones, perturbation techniques are applied. In this latter case, extensive use is made of the Green's function technique, but a simpler method, the self-consistent phonon (SCP) method, is also described. The closing chapters are devoted to some particular aspects of molecular crystals' spectroscopy, i.e.the two-phonon spectra and the intensity of infrared and Raman bands. Multiphonon processes are particularly important for the information they can give on the intermolecular forces acting in molecular crystals or on the phonon densities of states. The treatment offered by the authors, although limited to two-phonon processes, is rigorous and valuable for the student wishing to pursue further the problem. It is also to be noted that the formalism used in this treatment is coherent to the last detail with that used in the rest of the book (a fact which is difficult enough to manage in many-authored books).

The book, due to its structure, may well be used as a textbook—at the same time introductory and advanced. It obviously is the condensed text of a student course, though managing to remain amazingly clear. It could be used as such by anyone wishing to introduce himself and to penetrate deeply, at the same time, into the very actual problem of the vibrational behaviour of molecular crystals.

Alex. Butucelea

ADVANCES IN STEROID ANALYSIS, Proceedings of the Symposium on the Analysis of Steroids, Eger, Hungary, May 20–22, 1981. Edited by S. Görög, Akademiai Kiado, Budapest, 1982, 552 p.

A wide variety of natural and synthetic compounds of steroid structre has been rigorously characterized following the improvement of analysis techniques.

The practical importance of these compounds is related especially to their remarkable physiological properties. Thus, one can explain why the chemistry handbooks and journals give them special attention, while congresses and symposia present periodically the news in this field. Edited by Dr. S. Görög, the book "Advances in Steroid Analysis" presents remarkable achievements in the field of steroid analysis reported in the 69 communications at the Symposium held between May 20–22, 1981 in Eger – Hungary.

Divided into 9 chapters, the book reviews the modern aspects and new developments of the methods of analysis of some steroid derivatives of biomedical importance.

The first chapter (6 communications) is general; it focuses on the present possibilities of analysing esterogeneous steroids, those of general interest for drug industry, steroidic hormons, anabolized steroids (with implications in drug control), on the pharmaco-kinetics of ethynilestradiol and some of its natural derivatives with endocrine functions.

The second chapter (5 communications) presents the applications and achievements of techniques that are based on specific and nonspecific bonds between steroids and various proteins.

The immunologic methods are thoroughly considered in the third chapter (19 communications) which is divided into two sections: radiometric and enzymatic determinations.

The fourth chapter (6 communications) is devoted to the applications of gas-chromatography to the analysis of steroids from the blood and metabolic products. Methods of extraction, pre-fractionation and derivatization followed by a gas-chromatographic analysis are presented.

The fifth chapter (4 communications) emphasizes the efficiency in steroid analysis brought about by coupling gas-chromatography with mass spectrometry or by the application of some specific techniques prior to gas-chromatographic analysis (enzymatic oxidation, transformation into alkyl-boronic derivatives and isotopic dilution).

The applications of high pressure liquid chromatography are presented in chapter 6 (9 contributions) in two sections: biologic analyses (blood and metabolites) and drug analyses (purity and drug investigations).

The seventh chapter (13 communications; 2 sections) specializes in the problems and techniques of quantitative and qualitative thinlayer chromatography applied to steroids.

Spectral methods are presented in chapter 8 (5 communications) in two sections: UV-visible method and other spectral methods (NMR and spectropolarimetry).

The ninth chapter, the last one (2 communications), presents the applications of polarography in the field of cortico steroids.

The 69 comunication included in the book make up a unitary whole, it covers one of the modern aspects of chemistry – the possibility of analysing the most important natural and synthetic steroids. Therefore it should be recommended to biochemists, analysts and in general to all those dealing with this important class of compounds.

Titus Constantinescu

MACROMOLECULAR CHEMISTRY, Volume 1 – Specialist Periodical Report – Edited by A. D. Jenkins and J. F. Kennedy – The Royal Society of Chemistry, London, 1980, XX + 489 p. ISBN 085–186–840–1.

The opening volume in one of the latest eddition in the "Specialist Periodical Reports" edited by The Royal Society of Chemistry from London is a broad review of the world literature in the general field of macromolecular chemistry, written and edited by the best known English experts in polymer science and technology.

This first volume covers the literature, adequately selected, available to the contributors from January 1977 to December 1978.

After a short introductory chapter, the literature concerning the polymerization chemistry is presented.

Chapter 2 deals with the chain reaction polymerization namely : coordination, cationic, anionic and template polymerization reactions.

The following four chapters cover the particular classes of polymers, such as polysaccharides and glycoproteins, proteins, enzymes, nucleic acids and inorganic polymers.

After a chapter devoted to configuration, the other subjects include physics, physical chemistry and characterization of polymers (five chapters), with details concerning NMR spectroscopy, neutron scattering, polymer crystallization and characterization methods (light scattering and preparative and analytical fractionation), thermodynamics of solutions and mechanics of polymers.

Chapter 15 concerns the engineering and technology of polymers and chapter 16 covers the reactions on polymers and polymer modification.

The following two chapters discuss photo- and photooxidative and thermo- and thermooxidative degradation of polymers.

Chapter 18 reviews the contributions in the field of catalysis achieved by macromolecules and chapter 19 the biomedical application of polymers. The last section (chapter 20) presents the computer applications in polymer science and technology.

The volume denotes a high level editorial effort and so far, has needed contributions of high standard from its authors. Each review also provides a rich source of valuable references in the particular field, i.e. the number of references is closed to 4000. An author index completes the volume.

Adrian Carpov

R. MOHILLA et B. FERENCZ, *Chemical Process Dynamics. La Dynamique des Processus Chimiques*, Ed. Akademiai Kiado, Budapest, 1982, 300 pag.

La dynamique des processus chimiques couvre un domaine commun pour les ingénieurs chimistes et pour ceux qui s'occupent du contrôle des processus. Le but principal des auteurs a été d'étudier le comportement dynamique des unités chimiques à l'aide d'équations fondamentales. La présentation systématique des modèles mathématiques des unités chimiques permettra l'élaboration de modèles aussi pour d'autres unités. Les résultats mathématiques décrivant le comportement dynamique d'opérations chimiques sont applicables directement aux calculs imposés par le contrôle des processus.

L'ouvrage est divisé en quatre parties : généralités, opérations décrites par équations différentielles ordinaires, opérations décrites par équations différentielles partielles et analyse des systèmes de contrôle multiple utilisée dans l'industrie chimique.

Dans la première partie sont présentés les flux généraux permettant de caractériser les opérations unitaires : le flux massique, le flux des différents composants, le flux de chaleur et le flux impulsion. Aussi des opérations unitaires complètement différentes peuvent-elles être décrites par le même système d'équations différentielles, le traitement de la dynamique des processus chimique étant réalisé sur une base uniforme.

Dans le cadre des opérations décrites par équations différentielles ordinaires sont traités les systèmes à flux convectifs (débits de matériel solide et fluide, stockage de liquide et contrôle de niveau, stockage de gaz, processus de mélange, chauffage par injection directe de vapeurs d'eau), systèmes à flux convectifs et de transfert (absorption dans des colonnes à plateaux, extraction, transfert de chaleur en échangeurs, séchage, condensation et évaporation, distillation en colonnes à plateaux) et systèmes combinés (réactions en réacteurs isothermes et dans une série de réacteurs à mélange idéal, réactions en réacteurs polytropiques).

Dans le chapitre suivant sont décrits les modèles pour les processus chimiques, exprimés par équations différentielles partielles : transfert de chaleur en régime non uniforme, flux d'un mélange multicomposant, absorption et extraction en colonnes à remplissage, dynamique d'échangeurs de chaleur, réactions en réacteurs tubulaires isothermes et non isothermes, flux de gaz et de vapeurs dans les conduits.

Dans le dernier chapitre sont analysés différents systèmes de contrôle utilisés dans l'industrie chimique : contrôle avec une variable auxiliaire, contrôle du taux massique de plusieurs fluides et contrôle en cascade.

Malgré la présentation mathématisée, la terminologie est claire et accessible, l'ouvrage étant utile aussi bien aux ingénieurs chimistes, qu'à ceux qui s'occupent du contrôle des processus.

Ana Maria Buricalu

ORSZÁGOS MŰSZAKI INFORMÁCIÓS KÖZPONT ÉS KÖNYVTÁR

NOTE POUR LES AUTEURS

La Revue Roumaine de Chimie publie des articles en anglais, français, russe, allemand ou espagnol. Les auteurs sont priés d'envoyer des articles et des comptes rendus inédits.

Les manuscrits seront dactylographiés à double interligne. La bibliographie, les tableaux et la légende des figures seront placés après le texte.

Si l'article fait partie d'une série numérotée, la partie précédente sera donnée comme première référence.

Chaque article sera précédé d'un résumé comprenant quinze lignes au maximum.

Les références bibliographiques dans le texte seront faites par des exposants sans parenthèses et paraîtront à la fin de l'ouvrage.

Les publications périodiques mentionnées dans la bibliographie seront présentées suivant les prescriptions internationales : le nom de l'auteur précédé de l'initiale du prénom, le titre du périodique abrégé conformément à « Chemical Abstract » et souligné par une ligne, le numéro du tome indiqué par des chiffres arabes et souligné par deux lignes, suivi de la première page de l'article ; à la fin, l'année de la parution sera placée entre parenthèses. Le numéro de la revue ne sera pas indiqué si les pages du volume sont numérotées consécutivement.

Les textes des livres ou traités inclueront : le nom des auteurs, l'initiale du prénom, le titre du livre entre guillemets et sans être souligné, le numéro du tome précédé par l'abréviation « vol. » (ou « Bd. »), le numéro de l'édition, les éditions (the publisher), la localité de la parution du livre, l'année de la parution et la page de la référence précédée(s) par l'abréviation « p » (ou « S »).

Les brevets seront indiqués comme suit : l'auteur ou la firme, le pays et le numéro du brevet, la date et la revue (Chem. Abstr.). Par ex. : M. Jones (to Union Carbide Co.), Brit. Pat. 601 238, 2 sept. 1959 ; cf. *Chem. Abstr.*, **54**, 12808 (1960).

Si la référence n'a pas été lue en original, on indiquera aussi la revue de références consultée.

Les diagrammes seront tracés à l'encre de Chine sur papier calque. Les tableaux et les figures (en nombre strictement nécessaire) ainsi que les courbes dans les figures seront numérotés par des chiffres arabes. Leur explication sera donnée dans la légende des figures. Prière de ne pas inscrire les mêmes données dans les tableaux et les figures. Chaque tableau aura un titre. On indiquera dans le texte la place approximative des tableaux et des figures. Les formules chimiques seront incluses dans le texte ; en outre, elles seront transcrites sur papier calque, à l'encre de Chine.

Les auteurs sont priés d'indiquer les caractères italiques (en soulignant les lettres au crayon), ainsi que tout autre caractère spécial ; les préfixes *ortho, meta, para, cis, trans*, etc. seront soulignés pour indiquer leurs caractères italiques et ne seront jamais écrits avec des majuscules.

Aucune correction à la main ne sera admise sur le manuscrit. Les corrections seront tapées à la machine. Les lettres grecques ou d'autres symboles spéciaux seront insérés à la main à l'encre clairement.

Le manuscrit sera signé par l'auteur.

Le titre-courant aura 50 lettres au maximum.

L'entière responsabilité du contenu des articles appartient aux auteurs.

Sur demande on peut obtenir une note plus complète.

PRINTED IN ROMANIA

TRAVAUX PARUS AUX ÉDITIONS DE L'ACADÉMIE DE LA RÉPUBLIQUE SOCIALISTE DE ROUMANIE

ELENA CEAUŞESCU, **Noi cercetări în domeniul compuşilor macromoleculari** (Nouvelles recherches dans le domaine des composés macromoléculaires), 1981, 536 p.

I. G. MURGULESCU, RODICA VÎLCU, **Introducere în chimia fizică, Vol. III. Termodinamica chimică** (Introduction à la chimie physique, Vol. III, Thermodynamique chimique), 1982, p. 626.

I. G. MURGULESCU, J. PĂUN, **Introducere în chimia fizică, Vol. I. 3. Nucleul atomic, reacţii nucleare, particule elementare** (Introduction à la chimie physique. Vol. I.3. Noyau atomique, réactions nucléaires, particules élémentaires), 1982, 606 p.

ELENA JERCAN, **Analiza cromatografică** (Analyse chromatographique), 1982, 286 p.

I. G. MURGULESCU, TATIANA ONCESCU, E. SEGAL, **Introducere în chimia fizică, Vol. II.2. Cinetică chimică şi cataliză** (Introduction à la chimie physique. Vol. II. 2, Cinétique chimique et catalyse), 1981, 1024 p.

V. DRĂGUŢAN, A. T. BALABAN, M. DIMONIE, **Metateza olefinelor şi polimerizarea prin deschidere de inel a cicloolefinelor** (La métathèse des oléfines et la polymérisation par ouverture annulaire des cyclooléfines), 1981, 254 p.

LYDIA-MARIA VAICUM, **Epurarea apelor uzate cu nămol activ. Bazele biochimice** (L'épuration des eaux résiduelles à boue active. Les bases biochimiques), 1981, 218 p.

I. GĂLĂŢEANU, **Procese şi metode radiochimice în energetica nucleară** (Processus et méthodes radiochimiques dans l'énergétique nucléaire), 1981, 234 p.

OCTAVIAN IORDACHE, **Procese polistocastice aplicate la fenomenele de transfer** (Processus polystochastiques appliqués aux phénomènes de transfert), 1981, 186 p.

CR. SIMIONESCU, VALERIA GORDUZA, **Polimeri biocompatibili şi biologic activi** (Polymères biocompatibles et biologiquement actifs), 1980, 479 p.

ELENA CEAUŞESCU, **Polimerizarea stereospecifică a izoprenului** (La polymérisation stéréospécifique de l'isoprène), 1979, 307 p.

CONST. GH. MACAROVICI, **Analiza chimică cantitativă anorganică** (L'analyse chimique quantitative inorganique), 1979, 457 p.

M. FLORESCU, **Metode ştiinţifice în dezvoltarea industriei chimice moderne** (Méthodes scientifiques dans le développement de l'industrie chimique moderne), 1979, 256 p.

A. T. BALABAN, I. GĂLĂŢEANU, G. GEORGESCU, LIGIA SIMIONESCU, **Compuşi marcaţi şi radiofarmaceutici cu aplicaţii în medicina nucleară** (Composés marqués et radiopharmaceutiques à application en médecine nucléaire), 1979, 495 p.

I. G. MURGULESCU, E. SEGAL, **Introducere în chimia fizică, vol. II.1. Teoria molecular-cinetică a materiei** (Introduction à la chimie physique. Vol. II. 1. La théorie moléculaire-cinétique de la matière), 1979, 1036 p.

S. STERNBERG, FL. DANEŞ, **Termodinamica chimică aplicată** (La thermodynamique chimique appliquée), 1978, 400 p.

I. G. MURGULESCU, V. EM. SAHINI, **Introducere în chimia fizică. Vol. I.2. Structura şi proprietăţile moleculelor** (Introduction à la chimie physique. Vol. I. 2. La structure et les proprietes des molécules), 1978, 604 p.

I. ZUGRĂVESCU, MAGDA PETROVANU, **N-ylid chemistry**, coédition avec McGraw-Hill International Book Company, U.S.A., 1977, 396 p.

I.G. MURGULESCU, **Introducere în chimia fizică. Vol. I.1. Atomi, molecule, legătură chimică** (Introduction à la chimie physique, Vol. I. 1. Atomes, molécules, liaison chimique), 1976, 560 p.

ELENA CEAUŞESCU, **Research work on synthesis and characterization of macromolecular compounds. Contributions**, 1974, 251 p.

CR. SIMIONESCU, VIORICA RUSAN, V. POPA, **Chimia algelor marine** (La chimie des algues marines), 1974, 212 p., 1 pl.

1983 SEP 29

I. P. Informaţia c. 2616

43 426

Lei 40

$ 75 (pour un abonnement annuel)

640 F1103 04 Vegyészet

ACADÉMIE DE LA RÉPUBLIQUE SOCIALISTE DE ROUMANIE

R

REVUE ROUMAINE DE CHIMIE

REFERÁLVA

TOME 28
N° 2
Février 1983

EDITURA ACADEMIEI REPUBLICII SOCIALISTE ROMÂNIA

Rev. Roumaine Chim.

RRCHAX **28**, *2* p. 81 – 190 (1983) Bucarest

ACADÉMIE DE LA RÉPUBLIQUE SOCIALISTE DE ROUMANIE

COMITÉ DE RÉDACTION

Rédacteur en chef :

I. G. MURGULESCU, membre de l'Académie de la République Socialiste de Roumanie

Rédacteurs en chef adjoints:

A. T. BALABAN et V. EM. SAHINI, membres correspondants de l'Académie de la République Socialiste de Roumanie

Collège de redaction:

EM. BRATU, ELENA CEAUȘESCU, ECATERINA CIORĂNESCU-NENITZESCU, CR. SIMIONESCU, membres de l'Académie de la République Socialiste de Roumanie ; P. SPACU, membre correspondant de l'Académie de la République Socialiste de Roumanie : MARGARETA AVRAM, M. BANCIU, I. HAIDUC, D. I. MARCHIDAN, I. MOLDOVAN, G. NIAC et D. SĂNDULESCU

La Revue Roumaine de Chimie paraît 10 fois par an. Toute commande de l'étranger pour les travaux parus aux Editions de l'Académie de la République Socialiste de Roumanie sera adressée à ILEXIM, — Departamentul Export-Import Carte (Livres)/Departamentul Export-Import Presă (Revues), P.O.B. 136–137, télex 11226, 3, str. 13 Decembrie, 79517 Bucarest, Roumanie.

Les manuscrits, les livres et les revues proposés en échange, ainsi que toute correspondance seront envoyés à la rédaction :

REVUE ROUMAINE DE CHIMIE

Calea Victoriei 125, 79717 Bucarest, Roumanie, téléphone 50 76 80

EDITURA ACADEMIEI REPUBLICII SOCIALISTE ROMÂNIA
125, Calea Victoriei 79717 Bucarest, Roumanie, téléphone 50 76 80

REVUE ROUMAINE DE CHIMIE

ORSZÁGOS ... 1883

Tome 28, N° 2 Février, 1983

XU YU XIN, S. MOLDOVEANU and C. I. LEPĂDATU, IR analysis of some oil pollutants in water . . . . 83–89 R
AL. CECAL, Investigation of corrosion kinetics for steel samples in acid media using a method with radioactive tracers (in German) . . . . 91–97 R
A. G. FADNIS and S. K. KULSHRESTHA, Kinetics of ceric ion oxidation of some hexitols in H_2SO_4 medium 99–105
J. ZSAKÓ, MARIA VÁRHELYI and GH. MARCU, Electronic spectra of some *cis*-$Co(en)_2AX]^{2+}$ type complexes 107–114
R. P. VARMA, B. B. BHATNAGAR and P. SINGHAL, Studies on physical properties of alkaline earth metal dodecyl sulphates. I. Conductivity studies of $Ca(DS)_2$ in water-acetone mixtures 115–122 3c
L. FERRARI and M. RUIZ PASTRANA, Study of acid-base catalysis in the reaction of iodine with acetone. I. Catalysis by bases OH^- and HPO_4^{2-} (in Spanish) 123–127
JEAN HERDAN, ALEXANDRU T. BALABAN, NICOLAE NEGOIȚĂ and NICOLETA GRECU, 4-Substituted 2,6-di-*t*-butylphenols and their corresponding aroxyls possessing 4-(1-methylene-imidazolyl), 4-(1-methylene-benzimidazolyl), or 4-(1-sulfonyl-benzimidazolyl) groups 129–137
IOAN A. SILBERG and SIMONA SILBERG, Derivatives of 4-aminomethylthiazole. III. Oxidative cyclizations and dethionations in the series of 1-phenyl-3-(2-aryl-4-thiazolylmethyl)-thioureas 139–145
C. STOICESCU, Kinetics of decarboxylation of β-pyridylacrylic acids 147–150
H. W. LANGFELD and S. IONIȚĂ, Behaviour of some aminonaphtholsulphonic acids in the azo coupling reaction (in German) . . . . 151–167 R
AURORA SALLO, B. DEMIAN and O. EXNER, The kinetic and mechanism of the diazo-coupling reaction of 4-chloro-1-naphthol 169–176
C. LITEANU and R. POPESCU, Study of the behaviour of α, ά-diphenyl-β-picrylhydrazyl free radical in chromatography, as admixture to different stationary phases 177–183
GH. HUBCA, M. GHEORGHIU, CR. OPRESCU and M. DIMONIE, Synthesis and polymerization of polyethylene glycol dimethacrylate. VIII. Relations between structure and reactivity of Polyethylene Glycol Dimethacrylates 185–189

Rev. Roumaine Chim. **28**, *2*, 81–190 (1983) Bucarest

Revue Roumaine de Chimie 28, 2, 83–89 (1983)

IR ANALYSIS OF SOME OIL POLLUTANTS IN WATER

XU YU XIN *, Ş. MOLDOVEANU * and C. I. LEPĂDATU **

* Faculty of Chemical Technology, Bucharest, Romania

** Center of Chemical Physics, Bucharest, Romania

Received December 25, 1981

The IR study of some different oil products has shown the existence of some common absorption bands, but also systematic differences in their spectra, due to the oil predominant composition which may be alkane, cycloalkane or aromatic.

The oil pollutants from water may be quantitatively determined by extraction in CCl_4 followed by an IR spectrophotometric analysis of the extract at a fixed wavenumber (e.g. 2930 cm^{-1}), common to a lot of components. The standardization of the quantitative determinations raises a series of difficulties, among them, the nature of the oil product playing an important role. The differences occurring in the IR spectra (400–4000 cm^{-1}) of some oil pollutants extracted in CCl_4 from water, allow a qualitative and global characterization of the pollutants, in agreement with the choice of standards necessary for their quantitative determination.

The IR spectra of oil products (crude oil or processed products) show a lot of common absorption bands.[1–4] Table 1 gives the absorption maxima between 400 and 4000 cm^{-1} for solutions having equal concentrations (% v/v) in CCl_4 of different types of crude oil, of a synthetic mixture of hydrocarbons (see Table 2), and of *o*-xylene and 2-methylheptane.

As may be seen in table 1, the intense absorption maxima at 2930 cm^{-1} ascribed to the vibrations of $>CH_2$ or $-CH_3$ groups attached to aromatic rings, may allow a global determination of the oil products. This absorption band is common for the majority of hydrocarbon oil components, but its absorption intensity may be obviously different as it can be seen in figure 1.

If the standardization is made with another compound than that to be analyzed (this method is currently used in the analysis of oil pollutants from waters), important systematic errors may therefore occur.

The differences between spectra allow also a global qualitative characterization of the oil pollutants. Both quantitative determination and

TABLE 1

Absorption maxima for solution 1 % vol/vol in CCl_4 (l = 0.62 mm) of different types of crude oil, of a synthetic mixture of hydrocarbons and of *o*-xylene and 2-methylheptane

Compound \ Wavenumber cm^{-1}	3049	3021	2965	2945	2930	2922	2890	2866
Paraffinic oil	0.05	0.07	0.75	0.92	1.69	1.70	1.39	0.455
Naphthenic oil	0.05	0.07	0.72	1.00	1.69	1.52	1.39	0.44
Aromatic oil	0.09	0.17	0.69	0.92	1.69	1.40	1.00	0.32
Synthetic mixture	0.05	0.06	0.455	0.69	1.22	1.06	0.40	0.34
o-Xylene	0.11	0.23	0.39	0.39	0.50	0.45	0.28	0.07
2-Methylheptane	0.02	0.06	0.78	0.60	1.52	1.39	1.52	0.42

Compound \ Wavenumber cm^{-1}	2842	1610	1495	1480	1466	1380	1365	730	691
Paraffinic oil	0.85	0.09	0.30	0.29	0.12	0.17	0.10	0.155	0.125
Naphthenic oil	0.85	0.09	0.30	0.28	0.10	0.17	0.10	0.155	0.125
Aromatic oil	0.85	0.10	0.34	0.28	0.09	0.15	0.06	0.19	0.12
Synthetic mixture	0.485	0.05	0.22	0.18	0.08	0.09	0.04	0.14	0.10
o-Xylene	0.25	0.10	0.21	0.12	0.13	0.06	0.04	0.21	0.05
2-Methylheptane	0.42	0.05	0.09	0.18	0.11	0.14	0.11	0.09	0.04

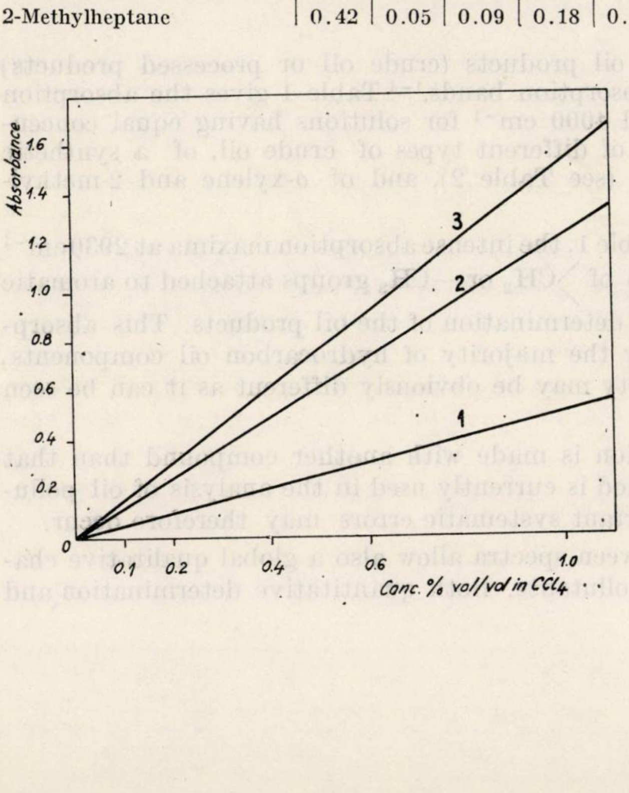

Fig. 1. — Calibration curves (at the same wavenumber) using different standards : 1) *o*-xylene, 2) synthetic mixture, 3) 2-methylheptane.

qualitative characterization need the existence of a reference (standard) with which the sample is compared.

There are two ways to choose the reference for a complex product, as the oil product is,[4] namely:

a) choice as standard a pure hydrocarbon or a synthetic mixture of hydrocarbons having a composition somewhat analogous to an oil product.

b) choice as standard a typical oil product (oil fraction or even crude oil of a specified source) which was previously correctly analyzed.

There are some methods for a relative characterization of a sample if compared with a standard.[5] We shall use a new procedure[6] of qualitative global characterization using the IR spectral data, and a new procedure of standardization for oil pollutants.

THEORY

The qualitative characterization of an oil product may be accomplished taking into account the similitudes and the differences between the IR spectra of the sample and standard.

Let us consider the N-dimensional vector **A**, its components being the absorbance values $\{A_n\}_{n=1,\ldots,N}$ at the corresponding wavenumbers $\{\omega_n\}_{n=1,\ldots,N}$ in the IR spectrum of the standard (chosen by (a) — or (b) — way).

For a certain oil product, the wavenumbers $\{\omega_n\}_{n=1,\ldots,N}$ have generally the absorbances $\{A'_n\}_{n=1,\ldots,N}$, which may be considered as the components of the multidimensional vector **A′**. We may consider **A** as the true value of a multidimensional physical quantity and **A′** the result of a measurement, inherently affected by errors.

The relative error of the n-th component will be

$$e'_n = \frac{A_n - A'_n}{A_n} \tag{1}$$

Because we are interested in the similitude between the components of the spectra, we shall define their relative similitudes as

$$x'_n = |1 - e'_n| = \left|\frac{A'_n}{A_n}\right| = \frac{A'_n}{A_n}, \tag{2}$$

the values A'_n and A_n being always considered as positive and different of zero.

Instead of x'_n, we may use the normed quantities

$$p'_n = \frac{x'_n}{\sum\limits_{i=1}^{N} x'_i}. \tag{3}$$

Every convex function $f : [a, b] \rightarrow \mathbb{R}$, $[a, b] \subset \mathbb{R}$ for

$$\{y_n\}_{n=1,\dots,N},\ y_n \in [a, b]$$

fulfills the Jensen inequality [7] (in a simplified form):

$$\frac{1}{N}\sum_{n=1}^{N} f(y_n) \leqslant f\left(\frac{1}{N}\sum_{n=1}^{N} y_n\right) \tag{4}$$

Taking $y_n = p'_n$ we obtain

$$\frac{1}{N}\sum_{n=1}^{N} f(p'_n) \leqslant f\left(\frac{1}{N}\sum_{n=1}^{N} p'_n\right) \tag{5}$$

Since $\sum_{n=1}^{N} p'_n = 1$, we have

$$\frac{1}{N}\sum_{n=1}^{N} f(p'_n) \leqslant f\left(\frac{1}{N}\right) \tag{6}$$

If the convex function is chosen as

$$f(y) = -y^2, \tag{7}$$

from (6—7), we obtain

$$\sum_{n=1}^{N} (p'_n)^2 \geqslant \frac{1}{N}, \tag{8}$$

the equality being verified only for

$$p'_1 = p'_2 = p'_3 = \dots = p'_n = \frac{1}{N}$$

From (8), it follows that the difference

$$D_1 = \sum_{n=1}^{N} (p'_n)^2 - \frac{1}{N} \tag{9}$$

is always positive or zero and generally characterizes the global difference between standard and sample.

If the components A_n and A'_n are identical, that is the multidimensional vectors **A** and **A′** coincide one follows from (2) and (3), that $p'_n = \frac{1}{N}$ and according to (9), $D_1 = 0$. From (8) we may also obtain:

$$D_2 = \frac{1}{N\sum_{n=1}^{N} (p'_n)^2} \leqslant 1, \tag{10}$$

From (10) and (3), we obtain

$$D_2 = \frac{\left(\sum_{n=1}^{N} x'_n\right)^2}{N \sum_{n=1}^{N} x_n^2} \leqslant 1 \qquad (11)$$

D_2 may also be used to characterize the global difference (or similitude between standard and sample). D_2 multiplied by 100 expresses the percentage similitude between standard and sample. If all $x'_n = \frac{A'_n}{A_n} = k$, from (3) it results that $p'_n = \frac{1}{N}$, and therefore $D_1 = 0$ and $D_2 = 1$. This means that the quantities D_1 or D_2 "recognize" the similitude between sample and standard irrespective if $\{A_n\}_n$ and $\{A'_n\}_n$ spectral absorbances are recorded for different concentrations. (For the case $A'_n = kA_n$, $n = 1, 2, \ldots N$ the number k would represent the dilution).

To apply the expressions D_1 or D_2, one must choose a reference, but there is also the alternative of more references. One knows that the crude oil contains alkanes, cycloalkanes and arenes, and therefore it may be characterized according to its content, which may be predominantly paraffinous, aromatic or naftenic. It may also use three such standards (which may be synthetic) with which the sample is to be compared.

EXPERIMENTAL

In order to determine and characterize the organic part of the waters polluted with oil products, water samples of 500 ml were acidified[4] with 2 ml 50% H_2SO_4, an extraction being then made with two CCl_4 portions of 25 ml. The combined CCl_4 extracts were left to dry for 10 minutes on anhydrous Na_2SO_4.

The experiments made with a third extraction of 25 ml CCl_4 showed an absorbance at 2930 cm^{-1} below 0.03. This means that two extractions are sufficient for our purpose, without supplementary precautions.

The IR spectrum of the dried extract is then recorded between 400 – 4000 cm^{-1}. The IR spectrum was recorded on an IR–75 Specord, Carl Zeiss spectrophotometer using KBr cells of 0.62 mm. The qualitative global characterization of each sample has been made using the expression (10). A synthetic mixture or pure hydrocarbons (*o*-xylene or 2-methylheptane) have been used as standards. The composition of the mixture is given in table 2.

TABLE 2

Composition of the Synthetic Mixtures

Compound	n-Hexane	2-Methyl-heptane	Decaline	Benzene
ml	11.2	11.2	27.6	12.5
Compound	toluene	*o*-xylene	naphthalene	
ml	12.5	12.5	12.2 g	

The same standards were used for quantitative determinations.

The preparation of synthetic standards of water plus organic part has been made as follows : *a* ml of the mixture given in table 2 (or pure hydrocarbon) was stirred for 30 minutes with 1 l distilled water. A sample of 250 ml of the aqueous emulsion, thus obtained, was mixed with 250 ml distilled water in order to obtain the standard with the maximum concentration, and then this one was extracted with CCl_4, according to the procedure earlier described.

The volume of *a* ml was chosen in such a way, that the whole organic amount was emulsioned. It has been concluded from repeated experiments that taking 0.1 ml; 0.05 ml, 0.03 ml of organic part, a linear curve of standardization is obtained if the absorbance at 2930 cm^{-1} is measured. From the emulsion of 0.1 ml mixture, other standards may be afterwards obtained by dilution. The transmittance (subsequently transformed into absorbance) has been read for the wavenumbers given in table 1, which constitute $\{\omega_n\}_{n=1,\ldots,N}$ for the qualitative characterization (see the Theory).

The emulsion used as standard being homogeneous, there are no supplementary problems regarding the accuracy of the proposed method.

RESULTS AND DISCUSSION

The present paper deals with the qualitative characterization and quantitative determinations of the samples of water polluted with oil products or of the samples of water "synthetically" polluted with different types of oils having 0.1 ml organic compounds for 1 liter of water. All samples were compared with synthetic standards, prepared as described, using synthetic mixtures of hydrocarbons or pure *o*-xylene or 2-methylheptane.

The quantitative determinations were performed using 6.4 mm path length cells, due to the low content in organic compounds in water.

Table 3 gives the similarity indices D_2 and the results of the quantitative determinations using as standards either synthetic mixture or pure hydrocarbons, *o*-xylene and 2-methylheptane.

TABLE 3

Similarity indices D_2 and the content of organic compound in polluted waters (ml/l)

Polluted water analysed	Standard					
	Synthetic mixture		*o*-Xylene		2-Methylheptane	
	D_2	ml/l water	D_2	ml/l water	D_2	ml/l water
Synthetic polluted water with 0.1 ml/l paraffinic oil	0.88938	0.138	0.69527	0.338	0.80670	0.112
Synthetic polluted water with 0.1 ml/l naphthenic oil	0.88360	0.136	0.69792	0.330	0.82041	0.110
Synthetic polluted water with 0.1 ml/l aromatic oil	0.88690	0.136	0.78474	0.330	0.71334	0.110
Natural water 1	0.91247	0.008	0.72131	0.020	0.84333	0.010
Natural water 2	0.89921	0.010	0.71341	0.024	0.85211	0.012
Natural water 3	0.89111	0.006	0.74151	0.015	0.83121	0.007

The proposed procedure gives some information concerning the nature of oil products and constitutes a more correct method of their quantitative determination.

REFERENCES

[1] B. T. Brooks, C. E. Bord, S. S. Kurtz Jr. and L. Schmerling, Ed., "The Chemistry of Petroleum Hydrocarbons", Reinhold Pub., New York, 1954.
[2] M. Cruenfeld, *Environ. Sci. & Technol.*, **7**, 636 (1973).
[3] W. Horwitz, Ed., "Official Methods of Analysis of the Association of Official Analytical Chemists", Washington, 1975.
[4] M. Ahmadjian and C. Boer, *Environ. Sci. & Technol.*, **10**, 777 (1976).
[5] K. Van Nes and M. A. Van Westen, "Constitution of Mineral Oils", Elsevier, Amsterdam, 1951.
[6] C. I. Lepădatu, unpublished results.
[7] S. Guiasu and R. Theodorescu, "Teoria matematică a informației", Ed. Academiei R.S.R., București, 1966.

Revue Roumaine de Chimie, 28, 2, 91—97 (1983)

UNTERSUCHUNG DER KORROSIONSKINETIK VON STAHLEN IN SAUREN MEDIEN DURCH ANWENDUNG EINER METHODE MIT MARKIERTEN ATOMEN

AL. CECAL

Facultät für chemische Technologie des polytechnischen Instituts, 71-Splai Bahlui,
6600—Iaşi, Rumänien

Eingegangen am 28. Dezember 1981

Es wurde eine Untersuchung der Kinetik des Korrosionsprozesses der Stähle Rp—3, 15 MoMC—12, 41 MoC—11 und 40 C—10 in HCl, H_2SO_4 und HNO_3 unter verschiedenen experimentellen Bedingungen durchgeführt. Dabei wurde eine radiochemische Methode angewendet, die auf dem Prinzip der isotopischen Verdünnung beruht. Der Ablauf diese Korrosionsreaktionen wurde dargestellt durch die Einführung eines Parameters d sogenennten „Widerstandsgrades (q) der Metallprobe gegenüber der aggressiven Wirku des Korrosionsmittels". Aus den experimentell erhaltenen Daten folgt, dass der Kor sionsprozess dieser Stahlproben in Salzsäure intensiver ist und in Schwefelsäure so in Salpetersäure langsamer verläuft, bei vorgegebener Konzentration. Der Korros prozess ist auch von der chemischen Zusammensetzung jeder der untersu Stahlprobe abhängig.

This paper deals with a study on the kinetics of the corrosion process of son samples of the type: Rp—3, 15 MoMC—12, 41 MoC—41 and 40 C—10 in c media of: HCl, H_2SO_4 and HNO_3 under several experimental conditions. To fo corrosion process a radiochemical method based on the isotopic dilution was The kinetics of these corrosion reactions was described by means of a parame "degree of resistence (q) of the metallic sample against the aggressive mediu From the experimental data, some conclusions concerning the corrosion re in connection with the nature of the steel samples and the aggressive m drawn.

EINFÜHRUNG

Man kennt eine Reihe von Studien über das
Passivitätsverhalten von Metallen mit Hilfe von Radi

Bardeen und Mitarbeiter[7] haben die Korrosion
verschiedenen korrosiven Medien untersucht, indem
der Radioisotope dieser Metalle in der Lösung verfolg
die betreffenden festen Oberfläche aufgetragen wo
wandte markierte Atome an, um den Oxydationsmec
in bestimmten korrosiven Medien verfolgen zu k
andere[9] haben die hemmende Wirkung von Chr

Korrosion der Metalle unter Verwendung von markiertem Chrom untersucht.

Medvedeva und Kolotyrkin [10] haben die Kinetik des Korrosionsprozesses durch Messung der Lösungsaktivität verfolgt, nachdem in die Lösung eine Metallprobestück eingeführt wurde, auf dem vorher markierte Atome aufgetragen worden waren. Darüber hinaus wurden verschiedene weitere Arbeitsvorrichtungen mitgeteilt, mit deren Hilfe man den Korrosionsmechanismus von Metallen mit Hilfe von Radioisotopen verfolgen kann. [11–12]

In dieser Arbeit wurde die Kinetik des Korrosionsprozesses der 4 Stahltypen Rp—3, 15 MoMC—12, 41 MoC—11 und 40 C—10 in den Korrosionsmedien HCl, H_2SO_4 und HNO_3, unter verschiedenen experimentellen Bedingungen untersucht. Dazu wurde eine Variante [13–16] der Analysemethode durch isotopische Verdünnungs [17–22] angewendet. Die radioaktiven Ionen $^{55+59}Fe^{3+}$ erfahren eine isotopische Verdünnung von seiten der nichtradioaktiven Eisenionen, erhalten durch die anodische Auflösung des Metallprobestückes in der korrosiven sauren Lösung, die gleich von Anfang an auch den entsprechenden radioaktiven Tracer enthielt.

EXPERIMENTELLER TEIL

Probestücke der Stahltypen Rp—3, 15 MoMC—12, 41 MoC—11 und 40 C—10 mit 1 cm Durchmesser wurden durch Polieren, Waschen mit Wasser, Entfetten mit Äthylalkohol und Azeton vorbereitet und in einem Ex'kkator gelagert, der P_2O_5 enthielt.

Die chemische Zusammensetzung dieser Proben ist in Tabelle 1 wiedergegeben.

In Falkons wurden je 100 ml korrosive Lösung HCl (1 N ; 0,5 N ; 0,1 N), H_2SO_4 (1 N) und HNO_3 (1 N) und je 20 ml einer Lösung von $^{55+59}FeCl_3$ (10^{-3} M) mit der spezifischen Aktivität von $2 \cdot 10^{-6}$ Ci/ml gefüllt. Somit erhält man 6 Versuchsreihen von je 4 Flakons und zwar 4 Reihen für HCl (für 1 N : 0,5 N und 0,1 N bei 20,5°C und 1N bei 41,1°C) und je eine für H_2SO_4 und HNO_3 (1 N, bei 20,5°C). In diese Flakons wurde je eine zu untersuchende vorbereitete Stahlprobe gegeben, so dass jede Versuchsreihe von 4 Flakons jene 4 verschiedenen Stahltypen enthält.

TABELLE 1

Die chemische Zusammensetzung der untersuchten Stahlproben

Probe	C (%)	Mn (%)	Si (%)	Cr (%)	Mo (%)	W (%)	V (%)
40 C—10	0,43	0,74	0,23	0,97	—	—	—
41 MoC—11	0,45	0,67	0,23	0,95	0,30	—	—
15 MoMC—12	0,17	1,30	0,35	1,04	0,30	—	—
Rp—3	0,76	0,40	0,32	3,80	0,30	18,5	1,20

Bei Kontakt dieser Stahltypen mit dem entsprechenden sauren Medium wurde der Korrosionsprozess ausgelösst.

In vorgegebenen Zeitintervallen wurden aus diesen Lösungen Proben von 1 ml entnommen und in Porzellenschmeltztiegel gefüllt. Nach Verdunsten der Lösungen in den Schmeltztiegeln, mit Hilfe einer Infrarotlampe, wurde die Radioaktivität der verbliebenden Restes in jedem Tiegel gemessen. Die Aktivitätbestimmungen wurden mit einem Geiger-Müller Detektor für β-Strahlen (3 mg/cm²) durchgeführt, der an einen „Orion Decimal Scaler" Zähler angeschlossen wurde.

Um die Abnahme der Aktivität der entsprechenden Proben durch den naturlichen Zerfallprozess des Radioisotope $^{55+59}Fe^{2+}$ zu berücksichtigen, wurden 20 ml $^{55+59}FeCl_3$ Lösung (10^{-3} M) in der oben beschriebenen Weise zu einer Vergleichsprobe verarbeitet. Jedes Mal wenn die spezifische Aktivität R_2 einer Probe (in Puls/min. ml) aus den korrosiven Lösungen, die die Metallprobe enthielten, gemessen wurde, wurde auch die spezifische Aktivität der Vergleichsprobe R_1 (in Puls/min. ml) bestimmt und die Differenz :

$$R = R_1 - R_2 \tag{1}$$

ermittelt wurde.

ERGEBNISSE UND DISKUSSION

In saurem Medium findet gleichzeitig statt die anodische Auflösung der Stahlprobe : [23-62]

$$Fe \rightarrow Fe^{2+} + 2e^-$$

$$Fe^{2+} \rightarrow Fe^{3+} + e^-$$

und die Reduktion der Wasserstoffionen (mit depolarisierender Rolle)

$$3H^+ + 3e^- \rightarrow 3/2\ H_2$$

Damit wächst die Ionenkonzentration von $[Fe^{n+}]$ (wo $[Fe^{n+}] = [Fe^{2+}] + [Fe^{3+}]$) in der Lösung.

Diese nichtradioaktiven Eisenionen wirken als isotopisches Verdünnungsmittel für die von Anfang an im korrosiven System existierenden radioaktiven Ionen $^{55+59}Fe^{3+}$. Infolgedessen fällt die Molarfraktion der radioaktiven Ionen $^{55+59}Fe^{3+}$:

$$x_{^{55+59}Fe^{3+}} = \frac{[^{55+59}Fe^{3+}]}{[^{55+59}Fe^{3+}] + [Fe^{n+}]}, \tag{2}$$

Die spezifische Aktivität jeder aus der korrosiven Lösung entnommenen Probe ist proportional der Konzentration der radioaktiven Ionen $^{55+59}Fe^{3+}$:

$$R_2(\text{Puls/min.ml}) = f(x_{^{55+59}Fe^{3+}}), \tag{3}$$

und mit (2) :

$$R_2(\text{Puls/min.ml}) = f'\left(\frac{1}{[Fe^{n+}]}\right) \tag{4}$$

Zu erwähnen ist, dass gegenüber der Analysenmethode durch isotopische Verdünnung, bei der das isotopische Verdünnungsmittel von aussen zugeführt wird, im Rahmen dieses Verfahrens die entsprechende Verdünnung als Folge eines internen anodischen Lösungsprozesses der Metallprobe staffindet.

Mehr noch, durch die Vermehrung der Restmenge im Schmeltztiehel, verursacht durch die Erhönung der Konzentration von nichtradioaktiven Eisenionen in der Korrosiönslösung, erhält man auch einen teilweisen Schutz seitens dieses Restes gegenüber den β-Strahlen, ausgesandt von den radioaktiven Ionen $^{55+59}Fe^{3+}$, die sich in der aus dem korrosiven Medium genommenen Probe befinden.

Für die quantitative Beschreibung des Korrosionsprozesses wurde ein kinetischer Parameter (q) eingeführt, bezeichnet als „Widerstandsgrad der Metallprobe gegenuber der Wirkung des Korrosionsmittels“ :

$$q(\%) = \frac{R_0 - R}{R_0} \cdot 100, \tag{5}$$

R_0 ist die spezifische Aktivität (Puls/min. ml) der Ausgangslösung, während R ist die spezifische „reine“ Aktivität (Puls/min. ml) einer aus der korrosiven entnommenen Probe zu einem bestimmten Zeitpunkt, berechnet nach (1), darstellt.

Durch die graphische Darstellung der Funktion $q(\%) = f(t)$, erhält man eine Kurve, die in der Tat den zeitlichen Ablauf des berteffenden Korrosionsprozesses beschreibt.

Die Versuche wurden durchgeführt zum Zweck der Klärung des Einflusses von Wesen und Konzentration des aggressiven Mittels, der Zusammensetzung der Metallprobe und der Temperatur des System auf den Ablauf der Korrosionsreaktionen.

Die experimentell gewonnenen Daten wiedergegeben durch die Kurven $q(\%) = f(t)$ sind in Abb. 1 dargestellt.

Betrachtet man den Einfluss der Art des Korrosionsmittels auf den Ablauf der Korrosionsreaktionen stellt man fest, dass zu jedem beliebigen Zeitpunkt die Metallprobe in Salzsäure den kleinsten Widerstandsgrad hat, das heisst, in diesem Medium verläuft die Korrosions jedes untersuchten Stahltypes viel schneller als in Schwefelsäure oder Salpetersäure.

Diese Tatsache kann dadurch erklärt werden, dass Salzsäure die Möglichkeit der Bildung eines Oxyds (oder einer anderen chemischen Verbindung) als Schutz auf der Oberfläche der Stahlprobe sehr klein ist, dann in diesem Medium geht die Verbindung unvermeindbar in lösliches Eisenchlorid über. [27–28]

Die Korrosion in Schwefelsäure verläuft langsamer, denn hier ist die Bildung einiger basischer Verbindungen auf der Kontaktoberfläsche zwischen Metall und Lösung möglich, die schwerer löslich sind. Diese Verbindungen mit einer Schutzrolle können der Form $Fe(OH)_n$ oder $Fe_2(OH)_2(SO_4)_2$ sein.

In Salpetersäure verläuft die Korrosion noch langsamer im Vergleich zu den ersten beiden Fällan, denn hier zeigt sich die Bildung einer braunen Schicht, bestehend aus einem Eisenoxyd mit einer nichtstöichiometrischen Zusammensetzung, die eine schutzende Rolle auf die Metallprobe ausübt gegenüber des weiteren Einflusses des aggressiven Mediums. Weiter ist die Bildung von chemoadsorbierten Sauerstoff zwischen diesem Eisenoxyd und der Metalloberfläche möglich; jener Sauerstoff schlisslich.

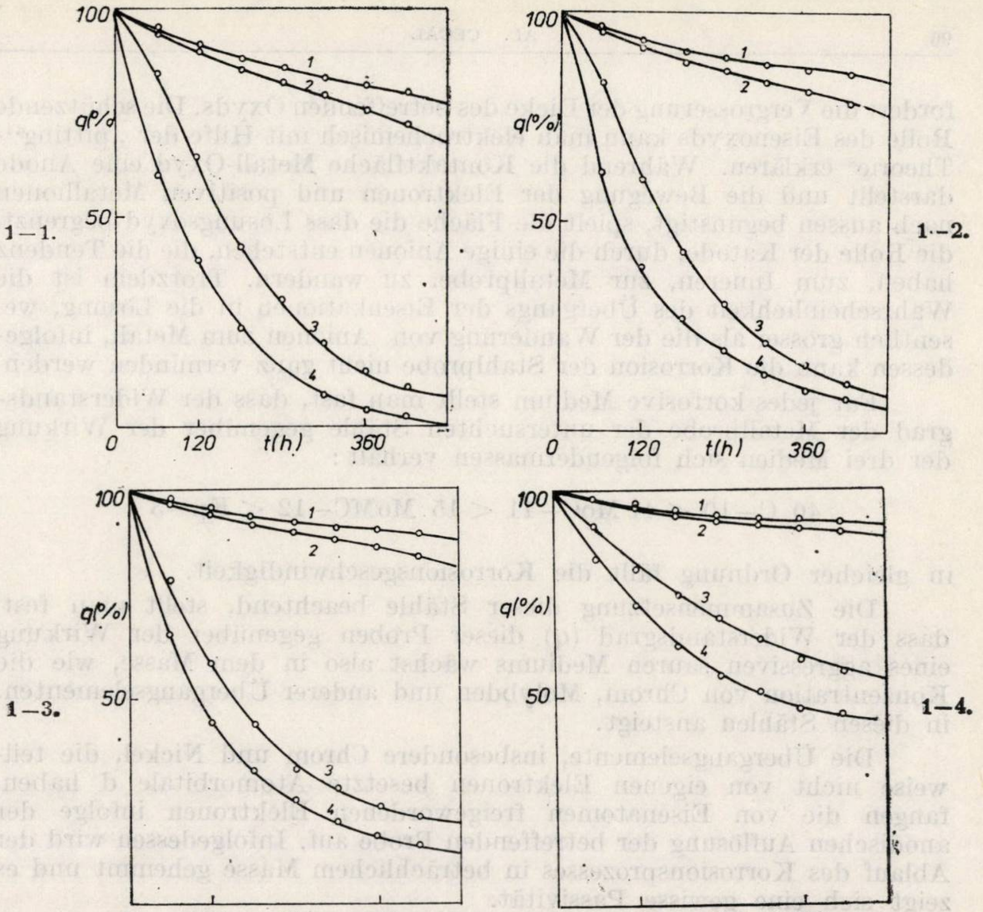

Abb.1 — Die Abwechslung in Zeit des Widerstandsgrades (q) der Stahlprobe von der Wirkung der korrosiven Säuren : *bei 20,5°* 1 — 1. HCl(1 N) ; 1 — 2. HCl (0.5 N) ; 1 — 3. HCl (0,1 N) ; 1 — 4. H_2SO_4 (1 N) ; 1 — 5. HNO_3(1 N) ; *bei* 41,1°C 1 — 6. HCl (1 N). (Die Kurven 1, 2, 3 und 4 entsprechen den Stahlproben von Rp — 3, 15 MoMC — 12, 40MoC — 11 und 40 C — 10)

fordert die Vergrösserung der Dicke des betreffenden Oxyds. Die schützende Rolle des Eisenoxyds kann man elektrochemisch mit Hilfe der „pitting"-Theorie[8] erklären. Während die Kontaktfläche Metall-Oxyd eine Anode darstellt und die Bewegung der Elektronen und positiven Metallionen nach aussen begünstigt, spielt die Fläche die dass Lösungsoxyd begrenzt, die Rolle der Katode, durch die einige Anionen entstehen, die die Tendenz haben, zum Inneren, zur Metallprobe, zu wandern. Trotzdem ist die Wahrscheinlichkeit des Übergangs der Eisenkationen in die Lösung, wesentlich grösser als die der Wanderung von Anionen zum Metall, infolgedessen kann die Korrosion der Stahlprobe nicht ganz verminden werden.

Für jedes korrosive Medium stellt man fast, dass der Widerstandsgrad der Metallprobe der untersuchten Stähle gegenüber der Wirkung der drei Medien sich folgendermassen verhält:

$$40\ \mathrm{C}-10 < 41\ \mathrm{MoC}-11 < 15\ \mathrm{MoMC}-12 < \mathrm{Ep}-3$$

in gleicher Ordnung fällt die Korrosionsgeschwindigkeit.

Die Zusammensetzung dieser Stähle beachtend, stellt man fest, dass der Widerstandsgrad (q) dieser Proben gegenüber der Wirkung eines aggressiven sauren Mediums wächst also in dem Masse, wie die Konzentration von Chrom, Molybden und anderer Übergangselementen, in diesen Stählen ansteigt.

Die Übergangselemente, insbesondere Chrom und Nickel, die teilweise nicht von eigenen Elektronen besetzte Atomorbitale d haben, fangen die von Eisenatomen freigewordenen Elektronen infolge der anodischen Auflösung der betreffenden Probe auf. Infolgedessen wird der Ablauf des Korrosionsprozesses in beträchlichem Masse gehemmt und es zeigt sich eine gewisse Passivität.

Aus den Abbn. 1—1, 1—2 und 1—3 ist ersichtlich, dass in dem Masse wie die Konzentration der Salzsäure in der Lösung fällt, wächst der Widerstandsgrad der Metallprobe gegenüber dem aggressiven Medium, was dadurch erklärt werden kann, dass bei nidrigeren Konzentrationen weniger H^+ — Ionen mit depolarisierender Rolle existieren, infolgedessen der Korrosionsprozess langsamer abläuft.

Mit dem Anwachsen der Temperatur des Systems (Abbn. 1—1 und 1—6) bei gleicher Konzentration des gleichen korrosiven Mediums (HCl), stellt man fest, dass der Korrosionsprozess intensiver abläuft, was auf die Vergrösserung der thermischen Erregung der Moleküle im Reaktionssytem zurückzuführen ist.

LITERATURVERZEICHNIS

[1] K. Schwabe, K. Wagner und C. Weissmantel, *Z. phys. Chem. (Leipzig)*, **206**, 308 (1957).
[2] K. Schwabe, *Chem. Technol.*, **10**, 469 (1958).
[3] R. Dreyer und I. Dreyer, *Z. phys. Chem. (Leipzig)*, **228**, 404 (1965).
[4] I. Dreyer und R. Dreyer, *Z. phys. Chem. (Leipzig)*, **236**, 101 (1967).
[5] J. G. N. Thomas, *Werkst. Korr.*, **19**, 957 (1968).
[6] F. Wormwell und J. G. N. Thomas, *Soc. Chem. Ind. London, Monogr.*, **28**, 365 (1968).
[7] J. Bardeen, W. H. Brattain und W. Shockley, *J. Chem. Phys.*, **14**, 714 (1946).
[8] R. Chan, *Nucleonics*, **9(10)**, 14 (1951).

[9] D. M. Brasher, J. G. Beynon, A. D. Mercer und J. E. Rhoades-Brown, "Proc. 2ème Symp. Européen sur les Inhibiteurs de la Corrosion", 1965 Ferrara, Annali del'Universitá, 1966.

[10] L. A. Medvedeva und Yu. M. Kolotyrkin, *Zhur. fiz. Khim.*, **31**, 2668 (1957).

[11] H. Wroblewa und M. Green, *Electrochim. Acta*, **8**, 673 (1963).

[12] K. H. Lieser, O. Kalvenes und S. Compostella, *Corrosion Sci.*, **4**, 51 (1964).

[13] Al. Cecal, N. Calu und P. Harabor, *Bull. Soc. chim. France*, **1975**, 1076.

[14] Al. Cecal und St. Roşu, *Radiochim. Acta*, **23**, 20 (1976).

[15] Al. Cecal und D. Ciobanu, *Radiochim. Acta*, **28**, 171 (1981).

[16] Al. Cecal, *Isotopenpraxis*, **17**, 328 (1981).

[17] M. Haïssinsky, „La Chimie Nucléaire et ses Applications“, Massons, Paris, 1957.

[18] G. Friedlander, J. W. Kennedy und J. M. Miller, „Nuclear and Radiochemistry“, Wiley, New York, 1964.

[19] K. H. Lieser, „Einführung in die Kernchemie“, Springer Verlag, Berlin, 1967.

[20] H. A. C. Mc Kay, „Principles of Radiochemistry“, Butterworths, London, 1971.

[21] Gh. Marcu, „Chimia elementelor radioactive“, E.D.P., Bucureşti, 1971.

[22] T. Năşcuţiu, „Metode radiochimice de analiză“, E. A., Bucureşti, 1973.

[23] U. R. Evans, „An Introduction to Metallic Corrosion”, Edward Arnold, London 1963.

[24] W. Forker, „Elektrochemische Kinetik“, Akademie Verlag, Berlin, 1966.

[25] M. G. Fontana und R. W. Staehle, „Advances in Corrosion Science and Technology“, Plenum Press, New York, 1970.

[26] L. Antropov, „Theoretical Electrochemistry”, Mir Publ., Moscow, 1972.

[27] U. R. Evans und T. P. Hoar, *J. Electrochem. Soc.*, **99**, 212 (1952).

[28] K. C. Tripathi und K. Schwabe, *Rev. Chim. (Bucureşti)*, **7**, 599 (1962).

Revue Roumaine de Chimie, 28, 2, 99–105 (1983)

KINETICS OF CERIC ION OXIDATION OF SOME HEXITOLS IN H_2SO_4 MEDIUM

A. G. FADNIS* and S. K. KULSHRESTHA

Department of Chemistry, Govt. Science College, Gwalior (M.P.) 474 002
India

Received February 27, 1981

The oxidation of D-mannitol, sorbitol and dulcitol by ceric ion in H_2SO_4 medium is of the first order with respect to oxidant. The dependence of pseudo first order rate constant (k_{obs}) on the substrate concentration suggests the complex formation between the oxidant and substrate. k_{obs} has been found to decrease with sulphuric acid, bisulphate and sulphate ion concentrations, whereas it increases with H^+ and Mn (II) concentrations. A suitable mechanism has been proposed by taking all the observed kinetic and other data into consideration.

INTRODUCTION

Amongst the various metal ion oxidants, ceric ion has been widely employed as a strong oxidant in aqueous acidic solutions.[1] Cerimetry is now a well established analytical technique, since a variety of inorganic species and organic functional groups are readily oxidised.[2]

In order to postulate the mechanism for the oxidation of some hexitoles i.e. D-mannitol, sorbitol and dulcitol by ceric ion in H_2SO_4 medium, we have conducted the present kinetic study.

MATERIALS AND METHOD

MATERIALS

D-mannitol, sorbitol, dulcitol and ceric sulphate (E. Merck) were used without further purifications. Doubly distilled CO_2 free water was used for the preparation of solutions etc. All other commercially available analytical reagents were used.

KINETIC METHOD

The preparation of oxidant and other solutions etc. are the same as described earlier.[3] The kinetic runs have been carried out in the presence of excess of substrate and H_2SO_4 concentrations. The pseudo first order rate constant (k_{obs}) has been calculated as described earlier.[3]

---

* Address for correspondence: Dr. Khirwarkar's Bada, Lohiya Bazar, Gwalior 474 009 (M.P.) India

STOECHIOMETRY

The quantitative estimations of unreacted Ce (IV) indicated that 14.2, 14.2 and 14.3 moles of Ce (IV) are required for complete oxidation of one mole, of D-mannitol, sorbitol and dulcitol respectively. The stoechiometric equation, therefore can be written as :

$$C_6H_{14}O_6 + 14\ Ce(IV) + 6H_2O \rightarrow 6HOOOH + 14\ Ce(III) + 14H^+ \qquad 1(a)$$

Formic acid has been confirmed as end product by mercuric chloride test whereas formaldehyde is confirmed as intermediate product by spot test.[4] The presence of free radicals during the various stages of studies has been confirmed by the polymerisation reaction with acrylanitrile.

In the presence of excess of substrate (under the kinetic conditions) it was found that ~ 2 moles of Ce (IV) are used per mole of hexitol. The respective aldohexose has been confirmed by its usual tests and by preparing its osazone derivative. The stoechiometric equation, therefore can be represented as :

$$C_6H_{14}O_6 + 2\ Ce(IV) \rightarrow C_6H_{12}O_6 + 2Ce\ (III) + 2H^+ \qquad 1(b)$$

RESULTS AND DISCUSSION

The oxidation reaction has been found to be of the first order with respect to Ce (IV) when H_2SO_4 and substrate concentrations are taken in excess. The observed pseudo first order rate constant (k_{obs}) has been found to increase with hexitol concentration (Table 1).

TABLE 1

Dependence of k_{obs} on hexitol concentration

$[Ce(IV)] = 6.0 \times 10^{-3}_{M}$

$[H_2SO_4] = 3.4$ M (A)
1.2 M (B)
2.3 M (C)

[Hexitol] $\times 10^{+2}$ M	$k_{obs} \times 10^4 s^{-1}$		
	D-Mannitol (33°C) (A)	Sorbitol (26°C) (B)	Dulcitol (30°C) (C)
6.6	5.70	7.70	5.84
13.0	10.94	15.34	11.20
20.0	15.62	17.92	17.44
26.0	20.38	20.99	22.12
33.0	24.36	24.12	36.32

The results of substrate dependence of rate (Table 1) suggest the formation of a complex between the substrate and the oxidant prior to the rate determining step as the order with respect to hexitol concentrations is fractional in each case. The observed rate constant (k_{obs}) can be related to the equilibrium constant for the complex formation (K) and the rate constant for the complex disproportionation k_s by the expression :

$$\frac{1}{k_{obs}} = \frac{1}{k_s} + \frac{1}{k_s K[S]} \qquad (2)$$

The values of K (0.96, 8.8 and 0.90 mole^{-1}) and $K_s(100 \times 10^4$, 31.25×10^{-4} and 125×10^{-4} s^{-1}) have been computed for D-mannitol, sorbitol and dulcitol respectively from the steps and intercepts of the linear plots obtained between $\frac{1}{k_{obs}}$ and $\frac{1}{[S]}$

EFFECT OF ACIDITY

Inverse dependence of the k_{obs} on H_2SO_4 concentration has been found. The results of H_2SO_4 variation are given in Table 2.

TABLE 2

Dependence of k_{obs} on H_2SO_4 concentration

$[Ce(IV)] = 6.0 \times 10^{-3}$ M [Hexitol] $= 6.6 \times 10^{-2}$ M

$[H_2SO_4]$ M	$k_{obs} \times 10^4 s^{-1}$		
	D-Mannitol (33°C)	Sorbitol (26°C)	Dulcitol (30°C)
1.20	17.80	7.70	12.67
2.30	10.27	6.29	5.84
3.40	5.99	4.75	4.35
4.50	5.28	3.44	3.78
5.60	3.68	2.10	3.06

H^+ concentration has been varied by keeping HSO_4^- concentrations constant by adding an appropriate quantity of $NaHSO_4$ solution and similarly HSO_4^- concentration has been also varied at constant $[H^+]$ and at constant ionic strength maintained with $NaClO_4$. The results (Table 3) indicate that k_{obs} increases with second power of H^+ and decreases with HSO_4^- concentrations (Table 3).

TABLE 3

Dependence of k_{obs} on H^+ and HSO_4^- concentration

$[Ce(IV)] = 6.0 \times 10^{-3}$ M [Hexitol] $= 6.6 \times 10^{-2}$ M
Temp. = 30°C

$[H^+]$ M	$[HSO_4^-]$ M	$k_{obs} \times 10^4 s^{-1}$		
		D-Mannitol	Sorbitol	Dulcitol
0.50	2.0	0.40	1.20	0.93
1.00	2.0	1.07	3.52	1.67
1.25	2.0	1.96	4.92	2.56
1.50	2.0	3.10	6.93	3.56
1.75	2.0	5.01	8.92	5.01
2.00	2.0	5.30	13.08	8.52
2.30	2.3	1.36	2.03	5.84
2.30	2.5	1.03	1.69	3.08
2.30	2.8	0.74	1.31	1.77
2.38	3.3	0.55	0.88	0.96
2.30	4.3	0.27	0.52	0.51

ACTIVE SPECIES OF Ce(IV)

Ceric ion can form different types of species depending on the nature of acid medium used. Hardwick and Robertson have described various equilibria existing between various active species of Ce (IV) in H_2SO_4 medium.[5] In the present case the neutral covalent species Ce $(SO_4)_2$ can be supposed to be the active species.

Inverse dependence of k_{obs} on H_2SO_4 (Table 2) and increase in rate with the second power of H^+ (Table 3) can be explained by considering the following equilibria.

$$Ce(SO_4)_2 + H_2SO_4 \overset{K_1}{\rightleftharpoons} H_2Ce(SO_4)_3 \overset{K_2}{\rightleftharpoons} Ce(SO_4)_3^{-1} + 2H^+ \qquad (3)$$

The observed decrease in k_{obs} with HSO_4^- (Table 3) and with SO_4^{-2} concentrations (Table 4) can be explained by the following equilibrium, which shows the removal of active species Ce $(SO_4)_2$ by these ions as

$$Ce(SO_4)_2 + HSO_4^- \overset{K_3}{\rightleftharpoons} HCe(SO_4)_3^- \qquad (4)$$

$$Ce(SO_4)_2 + SO_4^{-2} \overset{K_4}{\rightleftharpoons} Ce(SO_4)_3^{-2} \qquad (5)$$

TABLE 4

Dependence of k_{obs} on SO_4^{-2} concentration

$[Ce\,(IV)] = 6.0 \times 10^{-3}$ M $[Hexitol] = 6.6 \times 10^{-2}$ M
$[H_2SO_4]$ = (A) 3.4 M, (B) 1.2 M, (C) 2.3 M
Temp. = 30°C

D-Mannitol (A)		Sorbitol (B)		Dulcitol (C)	
$[SO_4^{-2}]$ M	$k_{obs} \times 10^4$ s^{-1}	$[SO_4^{-2}]$ M	$k_{obs} \times 10^4$ s^{-1}	$[SO_4^{-2}]$ M	$k_{obs} \times 10^4$ s^{-1}
3.5	10.87	1.2	16.24	2.3	5.84
3.6	5.70	1.4	8.12	2.4	5.07
3.8	3.58	1.6	3.68	2.5	3.73
3.9	2.41	1.7	2.58	2.7	3.20
4.0	1.92	1.8	2.05	2.8	1.63

EFFECT OF Mn(II)

The rate constant k_{obs} has been found to increase enormously with the Mn(II) concentration (Table 5). The large catalytic effect due to Mn (II) can be explained by considering the following equilibria between Ce (IV) and Mn (II) as :[6,7]

$$Ce\,(IV) + Mn(II) \rightleftharpoons Mn(III) + Ce(III) \qquad (6)$$

TABLE 5

Dependence of k_{obs} on Mn (II) concentration

$[Ce(IV)] = 6.0 \times 10^{-3}$ M — $[\text{D-mannitol}] = 6.6 \times 10^{-2}$ M

$[H_2SO_4] = 3.4$ M — Temp. = 30°C

$[Mn(II)] \times 10^4$ M	0	1.3	2.6	4.0	5.3
$k_{obs} \times 10^4\ s^{-1}$	3.48	26.34	38.30	46.08	66.33

EFFECT OF TEMPERATURE

The temperature dependence on the rate of the reaction was determined by plotting log k_{obs}, against $1/T$ and the values of activation energies and other Arrhenius parameters computed[8] from the plots are given in Table 6.

A linear isokinetic plot can be obtained (β values 353K) in accordance with Leffler's compensation law[9] from the data given in Table 6. Thus, an identical mechanism for all the three hexitols can be proposed.

TABLE 6

Activation energies and other Arrhenius parameters

Hexitols	ΔE Kcal mole^{-1}	$\Delta S \neq$ Cal/mole-Deg.	$\Delta G \neq$ Kcal mole^{-1}
(A) D-Mannitol	31.88±0.07	27.37±1.67	24.28±1.08
(B) Sorbitol	32.60±0.13	32.60±0.03	31.58±0.08
(C) Dulcitol	26.47±0.07	12.48±0.04	22.63±0.08

MECHANISM

Two types of mechanisms involving the oxidation of organic substrate by ceric ion have been described. In the first type of mechanism a stable coordinated complex is formed between ceric ion and substrate[10,14] which then disproportionates unimolecularly in the slow rate determining step forming Ce (III) and free redical ($\bar{R}$).

$$Ce(IV) + S \overset{K}{\rightleftharpoons} \text{complex} \xrightarrow[\text{slow}]{k_s} Ce(III) + \dot{R} + H^+ \qquad (7)$$

The free radical is then rapidly oxidised to products in a fast step.

$$\dot{R} + Ce(IV) \xrightarrow{\text{fast}} \text{products} \qquad (8)$$

The second mechanism assumes that the substrate is directly oxidised by Ce (IV) as: —

$$Ce(IV) + S \longrightarrow Ce(IV) - S \longrightarrow Ce(III) + \bar{R} + H^+ \qquad (9)$$

Then as in the first mechanism the free radical is rapidly oxidised to products.

In the present reaction, the kinetic evidence for the hexitol—Ce(IV) complex has been obtained (Table 1) and hence the first type of mechanism (eqs 7—8) can be proposed (Scheme I).

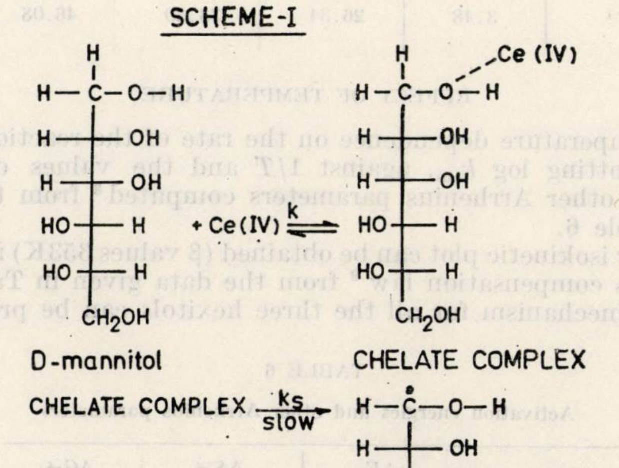
SCHEME-I
H
H—C—O—H
H—OH
H—OH
HO—H
HO—H
CH2OH
+ Ce(IV)
k
H
Ce (IV)
H—C—O—H
H—OH
H—OH
HO—H
HO—H
CH2OH
D-mannitol
CHELATE COMPLEX
CHELATE COMPLEX
ks
slow
H—C—O—H
H—OH
H—OH+H+Ce(III)
HO—H
HO—H
CH2OH
Free Radical
FREE RADICAL + Ce (IV)
fast
H—C=O
H—OH
H—OH + Ce (III)+H+
HO—H
HO—H
CH2OH
MANNOSE

$$C_6H_{12}O_6 + 12\ Ce(IV) + 6H_2O \xrightarrow[fast]{} 6HCOOH + 12\ Ce(III) + 12H^+$$

The magnitudes of '*K*' (the equilibrium constants of the complex formation are not very large in this case. This is not totally unexpected as for the complex formation the hexitol molecule has to compete with the stronger nucleophilic sulphate ion as a ligand for ceric ion.

RATE EXPRESSIONS

The disappearance rate of Ce (IV) with time can now be expressed by considering the proposed mechanistic steps 7—8 as

$$-\frac{\mathrm{d}[\mathrm{Ce(IV)}]}{\mathrm{d}t}=\frac{Kk_s[\mathrm{Ce(IV)}][\mathrm{S}]}{1+K[\mathrm{S}]}=k_{\mathrm{obs}}[\mathrm{Ce(IV)}] \tag{10}$$

The rate expression 10 is identical with 2 which has been used to evaluate K and k_s.

If Ce (IV) is supposed to be present as Ce $(\mathrm{SO_4})_2$ then the rate expression from (3) and (4) can be given as

$$-\frac{\mathrm{d}[\mathrm{Ce(IV)}]}{\mathrm{d}t}=\frac{Kk_s[\mathrm{H_2Ce(SO_4)_3}][\mathrm{S}]}{K_1\mathrm{H_2SO_4}(1+k(\mathrm{S}))}= \tag{11}$$

$$=\frac{Kk_s[\mathrm{Ce(SO_4)_3^{-2}}][\mathrm{S}][\mathrm{H^+}]^2}{k_1k_2[\mathrm{H_2SO_4}](1+K[\mathrm{S}])}= \tag{12}$$

$$=\frac{Kk_s[\mathrm{HCe(SO_4)_3^{-1}}[\mathrm{S}]}{k_3[\mathrm{HSO_4^-}(1+k[\mathrm{S}])}= \tag{13}$$

$$=k_{\mathrm{obs}}[\mathrm{Ce(IV)}]$$

Equilibria (3) and (4) are rapid and hence it can be assumed that $\mathrm{Ce(SO_4)_3^{-2}}$ and undissociated $\mathrm{HCe(SO_4)_3^{-1}}$ and $\mathrm{H_2Ce(SO_4)_3}$ is proportional to Ce(IV). Now these expressions explain the inverse dependence of rate on $\mathrm{H_2SO_4}$ (Table 1) and $\mathrm{HSO_4^-}$ (Table 3) concentrations and increase in rate with the 2nd power of $\mathrm{H^+}$ concentrations (Table 3).

Thus all the kinetic results obtained can be explained by the above mentioned rate expression (10—13) and mechanism steps (7—8).

ACKNOWLEDGEMENT. The authors are thankful to Dr. R. P. Bhatnagar, Professor and Head, School of studies in Chemistry, Jiwaji University, Gwalior (M. P.) for his encouragement and help. One of the authors (SKK) is thankful to U.G.C. (India) for awarding a J. R. Fellowship.

REFERENCES

[1] W. Richardson, "Oxidation in Organic Chemistry", K. Wiberg Ed., Academic Press, New York, 1965 Chap. 4 p. 247.
[2] G. Smith, "Cerate Oxidimetry", G. F. Smith Chemical Company Columbus, Ohio, 1942.
[3] R. P. Bhatnagar and A. G. Fadnis, "Ciencia e Cultura", **30**, 1227 (1978).
[4] F. Fiegal, "Spot Test Inorganic Chemistry", Elsevier Publishing Company, Amsterdam, London, 1966, p. 434.
[5] I. J. Hardwick and E. Robertson. *Canad. J. Chem.*, **29**, 828 (1951).
[6] M. J. Aspray, D. N. Rosseinsky and D. R. Shaw, *Chemy. Ind.*, **1963**, 911.
[7] G. A. Rachmitz, R. G. N. Rao and C. P. Rao, *Analyt. Chem.*, **38**, 1900 (1966).
[8] S. L. Friess, E. S. Lewis and A. Weissberger, "Investigation of Rates and Mechanism of Reaction" Vol. VIII, Part. I, Interscience, New York, 2nd Ed., 1961, p. 201.
[9] J. F. Leffler, *J. Org. Chem.*, **20**, 1202 (1955).
[10] F. R. Duke and G. F. Smith, *Ind. Eng. Chem. Anal. Ed.*, **12**, 201 (1940).
[11] J. S. Littler and W. A. Waters, *J. Chem. Soc.*, **1960**, 2767.
[12] G. Mino, S. Kaizerman and E. Rasmussar, *J. Amer. Chem. Soc.*, **81**, 1494 (1959).
[13] F. R. Duke and R. F. Bromov, *J. Amer. Chem. Soc.*, **73**, 5179 (1951).
[14] C. R. Pottengar and D. C. Johnson, *J. Polymer. Sci. Part A—I*, **3**, 301 (1970).

Revue Roumaine de Chimie, 28, 2, 107–114 (1983)

ELECTRONIC SPECTRA OF SOME *cis*-$[Co(en)_2AX]^{2+}$ TYPE COMPLEXES

J. ZSAKÓ, MARIA VÁRHELYI and GH. MARCU

Faculty of Chemical Technology, "Babeş-Bolyai University", 3400–Cluj-Napoca,
Arany János 11, Romania

Received January 19, 1982

Electronic spectra of 15 complexes of the type *cis*- $[Co(en)_2AX]^{2+}$ (X = Cl, Br, NO_2, A = amines, en = ethylene-diamine) have been recorded. Four absorption bands were observed and their wavelengths were compared with the positions of the same bands of $[Co(NH_3)_5X]^{n+}$ and other $[Co(en)_2AX]^{n+}$ type complexes by using literature data. The first band has the same position as with the corresponding $[Co(NH_3)_5X]^{n+}$ complex, irrespective of the nature of the ligand A. The origin of this transition is discussed in terms of ligand field theory, by taking into account the possibility of Co – X π bond formation.

INTRODUCTION

Electronic spectra of many *cis*-$[Co(en)_2AX]^{2+}$ type complexes of the monoacido-pentammine series (A stands for an amine, X stands for a co-ordinated anion) have been reported in the literature, without any interpretation. In the present paper a number of 15 complexes of the above type have been studied, by recording their absorption spectra in the UV and visible region, between 12 500 and 50 000 cm^{-1} by means of a SPECORD recording spectrophotometer, in aqueous solutions, at room temperature.

By taking into account the literature data concerning the electronic spectra of the above type complexes, as well as of the $[Co(NH_3)_5X]^{2+}$ type, an attempt is made to find out the nature of electronic transitions involved in the formation of different absorption bands.

RESULTS AND DISCUSSIONS

Generally, the absorption spectra in the region investigated exhibit four absorption bands. The first band (*A*) is frequently asymmetric, having a shoulder towards higher wavenumbers. It is strong enough to overlap the crystal field *d* → *d* transitions. If *A* = *o*-anisidine it appears only as an inflexion point. The second band (*B*), and especially the third one (*C*) are marked sometimes only by an inflexion on the absorption curve. In two cases, instead of band C, two inflexions have been observed.

The fourth band (*D*) is situated at the end of the region investigated, viz. at 200–210 nm. The wavelengths of the bands are given in table 1.

As seen, band A is pratically not influenced by the nature of the amine, but it depends on the nature of X. Its wavelength is 520–530 nm, for X = Cl, 540–550 nm for X = Br and only 460–470 nm for X = = NO_2. On the contrary, *B* is not influenced by X (except NO_2), but it depends on the nature of the amine. Band *C* is not influenced by "*A*", but it depends slightly on X. Band *D* has practically a constant position.

TABLE 1

Absorption bands of some *cis*-$[Co(en)_2AX]^{2+}$ type complexes in the visible and UV region *

A	X	λ, nm			
		A	*B*	*C*	*D*
benzylamine	Cl	524*a*	369	233	206
imidazole	Cl	528*a*	369	232*i*	207
pyridine	Cl	530*a*	374	229*i*	203
3,4-lutidine	Cl	538*a*	369	232*i*	208
4-ethyl-pyridine	Cl	525*a*	378	245*i* 222*i*	205
aniline	Cl	526*a*	306	232	207
m-toluidine	Cl	529*a*	308	232	203
p-toluidine	Cl	522*a*	319	231*i*	210
o-anisidine	Cl	515*i*	316	234*i* 216*i*	200
benzylamine	Br	544*a*	388*i*	256	204
aniline	Br	550*a*	300*i*	256	203
m-xylidine	Br	540*a*	297*i*	258	202
pyridine	NO_2	460*s*	339	248	205
β-picoline	NO_2	463*s*	333	243	206
γ-picoline	NO_2	472*s*	339	248*i*	206

* *i* – inflexion point, *a* – asymmetric shape of the band, *s* – symmetric shape of the band.

It is worth mentioning that the same four bands have been reported also by Ablov et al. [1,2] for complexes of the same type with "*A*" – aromatic amines, X = Cl, Br.

It is worth mentioning that 5 of the chloro-complexes given in table 1 have also been studied by Ablov [1] and our results are in quite good agreement with those reported by these authors.

Table 2 presents some literature data concerning the absorption bands of the above type complexes.

As seen, the general picture is the same as in the case of table 1.

The dependence of the position of band A on the nature of the anion X suggests that this is due to the transition of an electron from the highest occupied energy level to an empty antibonding molecular orbital with an important contribution from the ligand X.

In order to give a reliable hypothesis concerning the origin of band *A*, let us consider the energy level diagram [3] and electron configuration of $[Co(NH_3)_6]^{3+}$ and $[Co(NH_3)_5X]^{n+}$ type complexes, by assuming first only Co–X σ bonds.

If an axial NH_3 molecule of the octahedral $[Co(NH_3)_6]^{3+}$ is substituted by an anion forming only σ bonds, the axial bonds will be weakened and the equatorial bonds will be slightly strengthened and the O_h symmetry is lowered to C_{4v}. This leads to the following splitting of the energy levels:

$$T_{1u} \rightarrow A_1 + E, \quad E_g \rightarrow A_1 + B_1, \quad T_{2g} \rightarrow B + E$$

TABLE 2

Literature data concerning the absorption bands of *cis*-$[Co(en)_2AX]^{n+}$ type complexes

A	X	λ, nm				Ref.
		A	*B*	*C*	*D*	
NH_3	Cl	517	361	—	—	4
NH_3	Cl	527	361	230	—	1
H_2O	Cl	517	370	—	—	5
ethylamine	Cl	530	367	228	—	1
benzylamine	Cl	530	368	228	—	1
aniline	Cl	520	305	233	—	1
p-fluoro-aniline	Cl	520	308	233	—	1
p-chloro-aniline	Cl	520	311	233i	218	1
m-toluidine	Cl	520	310	233	—	1
p-toluidine	Cl	520	320	232	—	1
o-anisidine	Cl	520i	330	235i	215	1
o-phenetidine	Cl	520i	330	235i	215	1
p-anisidine	Cl	500—520i	345	223	—	1
NH_3	Br	542	310i	253	—	2
ethylamine	Br	540	305i	257	—	2
m-toluidine	Br	540	310i	257	—	2
p-toluidine	Br	540	320	257	—	2
m-chloro-aniline	Br	540	310i	257	—	2
p-chloro-aniline	Br	540	310	257	—	2
m-bromo-aniline	Br	540	310i	257	—	2
p-bromo-aniline	Br	540	312	257	—	2
p-iodo-aniline	Br	540	320	257	—	2
o-anisidine	Br	540i	315	257	—	2
o-phenetidine	Br	540i	315	257	—	2
p-anisidine	Br	540i	340	257	—	2
pyridine	Br	545	360	244	—	6
β-picoline	Br	540	370	250	—	7
γ-picoline	Br	545	360	240	—	7
NH_3	NO_2	445	—	—	—	8
NH_3	SO_3	463	—	272	—	9
H_2O	SO_3	480	370	285	—	10
NH_3	NCS	500	323	—	—	11
NH_3	OH	495	360	—	—	10

By taking into account these effects, the energy level diagram of $[Co(NH_3)_6]^{3+}$ and $[Co(NH_3)_5X]^{n+}$ can be constructed as given in figure 1. This figure reflects only the general succession of the energy levels, and it ignores the real distances between them. The T_{1u} bonding level is splitted into the A_1 and E bonding levels, A_1 corresponding to an axial, E to two equatorial bonds. Thus A_1 will be above E and consequently the corresponding antiboding A_1^* and E^* level will be disposed reversely. In the case of the $A_1(E_g)$ and $B_1(E_g)$ levels (in parantheses the origin of the orbital is indicated, i.e. its symmetry in O_h field), B_1 represents equatorial bonds and A_1 has a major contribution to the axial bonds. This justifies their succession in figure 1, as well as the order of the corresponding A_1^* and B_1^* levels.

As far as the splitting of the T_{2g} level is concerned, two effects must be taken into account. On the one hand the Co—X bond will be longer than Co—N bond and this lowers the energy of the d_{xz}, d_{yz} orbitals, having E symmetry. On the other hand, the replacement of a neutral molecule by an anion increases the charge density in the direction of the z axis, which will rise the E level. We think the latter effect to be more important than the former one and figure 1 has been constructed on the basis of this assumption.

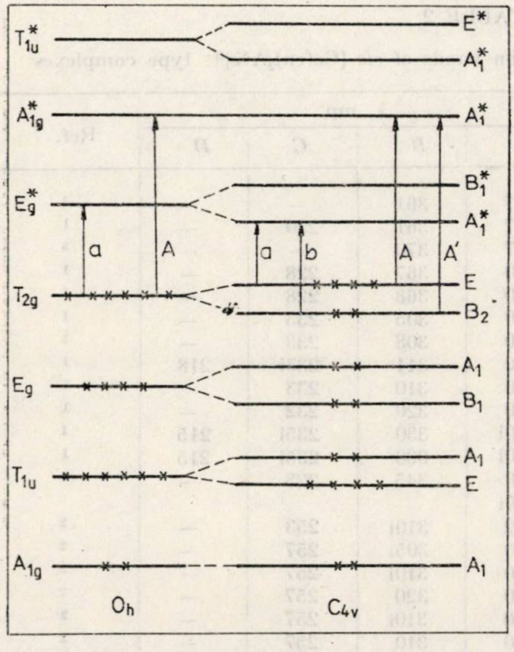

Fig. 1. — Energy level diagram of $[Co(NH_3)_6]^{3+}$ and $[Co(NH_3)_5X]^{2+}$ type complexes by presuming only σ-bonds.

As seen from this figure, the crystal field band a, corresponding to the Laporte forbidden $T_{2g} \rightarrow E_g^*$ transition is splitted in C_{4v} field into at least two bands, a and b, by taking into account only the splitting of the departure level. The first allowed transition $T_{2g} \rightarrow A_{1g}^*$, denoted by A, is also splitted in A and A', corresponding to $E \rightarrow A_1^*$ and $B_2 \rightarrow A_1^*$, respectively.

According to literature data, the first strong band in the spectrum of $[Co(NH_3)_6]^{3+}$ appears at 475 nm[4] and it can be assigned to the transition A. As far as the $[Co(NH_3)_5X]^{n+}$ type complexes are concerned, some spectral data are presented in table 3. This table contains the wavelength of the first strong absorption bands (λ_A) in the order of their increasing values. In some cases the wavelength of the crystal field transitions (λ_a, λ_b) are also given.

From table 3 several interesting conclusions can be drawn. The λ_A values are higher than with $[Co(NH_3)_6]^{3+}$ (except the first two ligands, NO_2^- and SO_3^{2-}) and the weaker the Co—X bond, the higher this λ_A value is, as expected on the basis of figure 1 for the transition A. This allows us to presume that band A is due to the transition $E \rightarrow A_1$.

If the ligand has empty π orbitals, the formation of π type molecular orbitals becomes also possible. This affects the position of the highest occupied level, viz. the non-bonding $E(T_{2g})$ orbitals give with the ligand π orbitals bonding and antibonding $E(\pi)$ molecular orbitals. The stronger this π bond, the lower will be the bonding E (π) level, as compared to the non-bonding $E(T_{2g})$. On the other hand, the stronger this π bond, the shorter will be the Co$-$X bond, and consequently, the higher will be the $A_1^*(A_{1g}^*)$ level.

In the case of weak Co$-$X π bonds, band A corresponds to the transition $E(\pi) \rightarrow A_1^*$, but if the π bond is strong enough, the transition will be $B_2 \rightarrow A_1^*$ and its energy may exceed that of the $T_{2g} \rightarrow A_{1g}^*$ transition of $[Co(NH_3)_6]^{3+}$.

TABLE 3

Spectral data for $[Co(NH_3)_5X]^{n+}$ and $[Co(en)_2AX]^{n+}$ type complexes

X	n	$[Co(NH_3)_5X]^{n+}$				$[Co(en)_2AX]^{n+}$
		λ_a, nm	λ_b, nm	λ_A, nm	Ref	λ_A, nm
NO_2^-	2	—	—	458	15	460
SO_3^{2-}	1	—	—	472	13	471
NCS^-	2	—	—	497	13	500
$C_2O_4^{2-}$	1	—	—	500	14	—
$Cl_2CH \cdot COO^-$	2	—	—	501	16	—
$ClCH_2 \cdot COO^-$	2	—	—	502	16	—
OH^-	2	—	—	503		495
CH_3COO^-	2	—	—	504	16	—
F^-	2	919	646	514	12	—
Cl^-	2	877	657	534	12	524
Br^-	2	922	676	552	12	541
I^-	2	935	724	584	12	—

Thus, the low λ_A values of the NO_2 and SO_3 containing complexes are not surprising, by taking into account the $\pi-$bond formation possibilities.

In the case of the halogeno-complexes, table 3 contains also the crystal field transitions. The increase of λ_b in the order F $<$ Cl $<$ Br $<$ I is in good agreement with figure 1 and with above considerations concerning the influence of X on the position of the energy levels. With λ_a a similar picture is observed with a single inversion, viz. F $>$ Cl$<$ Br $<$ I. This apparently anomalous behaviour of the fluoro complex can be easily explained by π bond formation. The halogen ions, except F^-, possess empty external *d* orbitals, two of them being able to play the rôle of ligand π orbitals. The $E(T_{2g})$ level being transformed into $E(\pi)$ bonding level, its energy becomes lower, which explains the inversion observed with λ_a. Since the π bond formation does not affect the position of B_2, a similar effect is not observed with λ_b. Thus, the λ_a data given in table 3 can be taken for a clear spectroscopic evidence of Co$-$X π bond formation in the $[Co(NH_3)_5X]^{n+}$ type complexes with X $=$ Cl, Br, I.

In the case of $[Co(en)_2AX]^{n+}$ type complexes, ethylenediamine, as well as the ligand A (excepting the aquo-complexes) are co-ordinated to the central Co^{3+} ion through donor nitrogen atoms. Thus, in first approximation, the same local C_{4v} symmetry can be presumed as with $[Co(NH_3)_5X]^{n+}$ type complexes. The presumption seems to be acceptable by taking into account that the λ_A value in the case of $[Co(en)_3]^{3+}$ is almost the same as with $[Co(NH_3)_6]^{3+}$, viz. 467 nm[17]. This means that the position of the band A can be interpreted on the basis of the same energy level diagram presented in figure 1, i.e. one can expect the λ_A value to be practically independent of the nature of the ligand A. Data presented in tables 1 and 2 are consistent with this assumption, which allows to calculate the arithmetical mean of the λ_A values for each ligand X, irrespective to the nature of A. The mean wavelengths $\bar{\lambda}_A$, calculated by using all λ_A values (given in Tables 1 and 2), are given in table 3. It is obvious, that these values are practically the same as with the corresponding $[Co(NH_3)_5X]^{n+}$ complexes, supporting the correctness of the above hypothesis.

As far as the symmetric or asymmetric shape of the band A is concerned, it can be explained on the basis of fig. 1., by taking into account the π bond formation possibilities. If $X = Cl$ and Br, only very weak π bonds are formed and presumably the minimum energy absorption band will imply the transition $E(\pi) \rightarrow A_1^*$, and the energy of the transition $B_2 \rightarrow A_1^*$ will be a little higher. Since the $E(\pi)$ level has 4 electrons and B_2 only 2, the intensity of the band A will be higher than that of A'. Their energy does not differ very much from each other and it is easy to understand that in our working conditions a single, but asymmetric band is obtained in all cases, suggesting the partial overlap of a stronger band and of a weaker one, the former having higher wavelength than the latter.

If $X = NO_2$, the situation is completely different. A strong $Co-NO_2$ π bond is formed and presumably the $E(\pi)$ bonding level becomes much lower than B_2 and only the transition $B_2 \rightarrow A_1^*$ is observed experimentally.

The corresponding λ_A value is even lower than the λ_A value of $[Co(en)_3]^{3+}$ as expected on the basis of the above considerations. The perfectly symmetric shape of the first absorption band of the nitro complexes seems to support the correctness of the above given explanation.

It is worth mentioning that a more rigorous approach leads to a more complicated picture. In the above considerations the π bond formation has been presumed not to modify the molecular symmetry. This is completely true in the case of the halogeno-complexes, the halogen ions (except the F^-) having two empty π orbitals. But in the case of the nitro-complexes NO_2^- has a single empty π orbital, viz. the antibonding three-center molecular orbital of the $O-N-O$ π bond system, since the bonding and the non-bonding MO's are filled. This means that the central ion can use only one of its E orbitals for giving a single π bond. On the other hand, the π bond formation hinders the free rotation of the NO_2 group around the $CO-N$ σ bond, reducing the molecular symmetry to C_{2v}. The situation created is visualized in figure 2, which presents only a part of the energy levels and for simplicity, even the antibonding $B_1^*(\pi)$ level has been omitted. The succession of the energy levels can be presumed by taking into account the strength of the π bond which at one hand diminishes the $Co-N$ distance in the $Co-NO_2$ bond, leading to the strengthening of the axial σ bonds and in some extent to the weakening of the equatorial ones. On the other hand, the delocalization of the $d_{xz}(B_1)$ electrons towards the NO_2 ligand diminishes the energy of the $d_{yz}(B_2)$ electrons, and presumably strengthens the $B_1(T_{1u})$ bond. The energy of the

A_2 (T_{2g}) electrons can be thought to become less than in the absence of the π bond, due to the equatorial dilatation of the molecule.

As seen from figure 2., there are two high occupied levels, with the same number of electrons, and corresponding to energies which presumably do not differ very much from each other. There is a single arrival level.

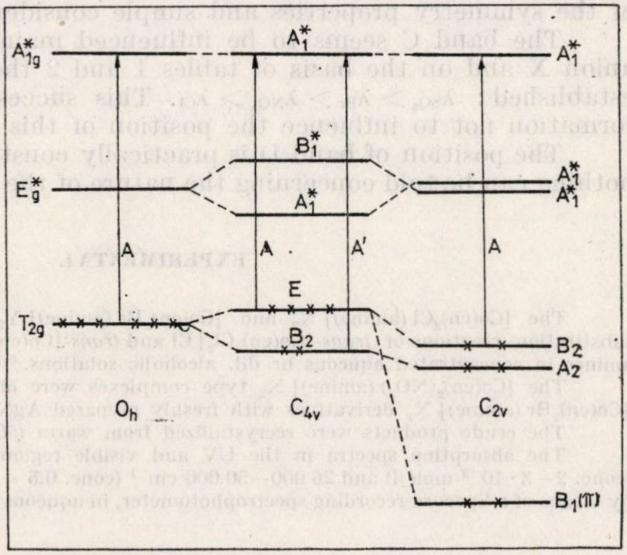

Fig. 2. — Influence of π bond formation on the energy level diagram of $[Co(en)_2A(NO_2)]^{2+}$ type complexes.

In principle, 2 transitions can be imagined, but probably there is very little chance to observe them separately, since practically their energy is almost the same. They can be presumed to occur with the same probability, which might explain the perfectly symmetric shape of the absorption band.

Concerning the position of the absorption band B, its dependence on the nature of the amine A has been observed also by Ablov et al. [1,2]

From tables 1 and 2 it is apparent that the aromatic amines have a completely different behaviour than the other ones. In the case of aromatic amine containing complexes the band B is situated at 300—320 nm, irrespective of the nature of the ligand *X*, but with other amines it appears at about 360—370 nm. The only exception is observed in the case of nitro complexes, the band B being shifted towards the lower wavelengths (330—340 nm). At any rate, this shift shows that besides the nature of the amine A also the π bond formation plays an important part in determination of the position of band B.

Figure 1 suggests for this band an $E(T_{2g}) \rightarrow A_1^*(T_{1u}^*)$ transition. This A_1^* level corresponds to an antibonding orbital formed with the contribution of the axial ligands.

Since in the *cis*-$[Co(en)_2AX]^{n+}$ complexes A is an equatorial ligand, the influence of its nature upon the position of band B remains unexplained. But the above considerations are too simplistic, because the diagram is valid for a C_{4v} local symmetry.

If one presumes the ligand A to have a different behaviour as compared to the amine groups of the ethylenediamine, there is no more reason to accept a C_{4v} symmetry. In fact the complex ion has no symmetry elements and if the ligand A is individualized, even the local symmetry is only C_s. Thus, the construction of energy level diagrams on the basis of the symmetry properties and simple considerations is not possible.

The band C seems to be influenced mainly by the nature of the anion X and on the basis of tables 1 and 2 the following order can be established : $\lambda_{SO_3} > \lambda_{Br} > \lambda_{NO_2} > \lambda_{Cl}$. This succession shows the π bond formation not to influence the position of this band.

The position of band D is practically constant and for the moment nothing can be told concerning the nature of the corresponding transition.

EXPERIMENTAL

The $[Co(en)_2Cl\,(amine)]\,X_2$ and $[Co(en)_2Br\,(amine)]\,Y_2$ complexes were obtained by substitution reactions of *trans*-$[Co(en)_2Cl_2]\,Cl$ and *trans*-$[Co(en)_2Br_2]\,Br$ with the corresponding amines in concentrated aqueous or dil. alcoholic solutions. [6,7]

The $[Co(en)_2(NO_2)\,(amine)]\,X_2$ type complexes were obtained from the corresponding $[Co(en)_2Br\,(amine)]\,X_2$ derivatives with freshly prepared $AgNO_2$.

The crude products were recrystallized from warm (50—60°C) 1—2 % HNO_3.

The absorption spectra in the UV and visible region, between 12 500—26 000 cm^{-1} (conc. $2-3 \cdot 10^{-3}$ mole/l) and 26 000—50 000 cm^{-1} (conc. $0.5 - 2 \times 10^{-4}$ mole/l) were recorded by means of a Specord recording spectrophotometer, in aqueous solutions, at room temperatures.

REFERENCES

1 A. V. Ablov and M. P. Filippov, *Zhur neorg. Khim.*, **2**, 42 (1957).

2 A. V. Ablov and M. P. Filippov, *Zhur. neorg. Khim.*, **2**, 2390 (1957).

3 A. B. P. Lever, "Inorganic Electronic Spectroscopy", Elsevier, Amsterdam, 1968, p. 196.

4 H. Kuroya, *J. Inst. Polytechn. Osaka City Univ.*, **C. 1/1**, 29 (1950). ; *Chem. Abstr.*, **45**, 3240 (1950).

5 J. P. Mathieu, *Bull. Soc. chim. France*, **1936** 463.

6 Cs. Várhelyi and J. Zsakó, *Rev. Roumaine Chim.*, **16**, 1185 (1971).

7 J. Zsakó, Cs. Várhelyi and S. Bleoca, *Acta Chim. Acad. Sci. Hung.*, **70**, 175 (1971).

8 G. L. Amma and B. E. Douglas, *J. Amer. Chem. Soc.*, **84**, 3227 (1962).

9 M. E. Baldwin, *J. Chem. Soc.*, **1961**, 3123.

10 F. Basolo, *J. Amer. Chem. Soc.*, **72**, 4393 (1950).

11 T. Uemura and N. Hirasawa, *Bull. Chem. Soc. Japan*, **13**, 377 (1938).

12 M. Linhard and M. Weigel, *Z. phys. Chem. (Frankfurt)*, (2), 11, 308 (1957).

13 A. Kiss and D. Czeglédy, *Z. anorg. Chem.*, **235**, 407 (1938).

14 D. Czeglédy, *Acta Univ. Szegediensis, Acta Chim.*, **6**, 121 (1938).

15 M. Linhard and M. Weigel, *Z. anorg. Chem.*, **267**, 121 (1951).

16 M. Linhard and M. Weigel, *Z. anorg. Chem.*, **264**, 321 (1951).

17 R. Samuel, A. A. Hafiz Khan and N. Alamad, *Z. Phys. Chem. (Leipzig)*, **B. 22**, 431 (1933).

Revue Roumaine de Chimie, 28, *2,* 115–122 (1983)

STUDIES ON PHYSICAL PROPERTIES OF ALKALINE EARTH METAL DODECYL SULPHATES. I.

CONDUCTIVITY STUDIES OF CALCIUM DODECYL SULPHATE IN WATER-ACETONE MIXTURES

R. P. VARMA, B. B. BHATNAGAR and P. SINGHAL

Chemistry Department, D.A.V. College, Muzaffarnagar-251001, India

Received October 18, 1980
Revised April 10, 1982

Specific conductivity of calcium dodecyl sulphate, $Ca(DS)_2$ has been measured in water-acetone mixtures at different temperatures 35–50°C and the critical micelle concentration obtained from the data is found independent of temperature and composition of the mixture. The conductivity behaviour of $Ca(DS)_2$ is exhibited by an equation $\log\lambda = A + B \log C$. Constant A decreases whereas B increases with increase in acetone concentration in the mixture. The trend in the variation of the constants A and B indicates that the change in the nature of micelles occurs at about 70% acetone. The values of free energy and entropy confirm the dissociation of $Ca(DS)_2$ rather than remaining undissociated molecule below CMC. Dissociation constant, K, molar conductivity at infinite dilution, λ_∞ and heat of dissociation, ΔH°, have been evaluated. The results confirm that the change in the behaviour takes place at about 70% acetone.

INTRODUCTION

The critical micelle concentrations of anionic surfactants have been determined[1] spectrophotometrically and the values have been found considerably lower due to solubilization of dye stuff in the micelle. The micelle formation in aqueous solutions is known to be affected[2] by salt, nature of solvent, temperatures and there have been investigations[3,4] concerning the effect of additive on CMC of anionic surfactant. It is well known that the micellar solutions are influenced by changing the counter ions. Meguro et al.[5] have found the CMC value in order of hydration of counter ions i.e. Li > Na > K. The high frequency conductivity of ionic surfactant has been measured[6] and the data have been determined by Debye Falkenhagen theory. Krafft points of NaDS-bivalent DS mixtures have been determined[7] by electrical conductivity method. Heat of aggregation of NaDS and Na tetra DS in aqueous 1-propanol and aqueous propionic acid has been calculated.[8]

It is found that works on NaDS are readily available but the knowledge about alkaline earth dodecyl sulphates is limited. Therefore, as a part of our work in the mixture of aprotic solvents in which these compounds were not investigated we attempted to study the conductivity behaviour of $Ca(DS)_2$ in water-acetone mixtures at different temperatures, 35—50°C in order to a) determine critical micelle concentration (CMC), b) study the effect of temperature and solvent and c) calculate dissociation constant, K, molar conductivity at infinite dilution, λ_∞, heat of dissociation, ΔH°, free energy, ΔG° and entropy, ΔS° of dissociation.

EXPERIMENTAL

B.D.H. reagent grade calcium chloride and acetone were used. Sodium dodecyl sulphate (NaDS) was obtained from Sigma Chem. Co., U.S.A. Conductivity water was prepared in a glass apparatus and in all cases, freshly distilled (alkaline $KMnO_4$) water was used.

$Ca(DS)_2$ was prepared[9] by adding concentrated aqueous solution of calcium chloride to an aqueous solution of NaDS. The precipitate was filtered and recrystallized from alcohol and then dried in vacuum.

The procedure for the measurement of conductivity of solutions was the same as reported earlier.[10]

RESULTS AND DISCUSSION

Specific conductivity, k (ohm^{-1} cm^{-1}) of $Ca(DS)_2$ solutions in water-acetone mixtures has been measured at different temperatures (35—50°C). The results show that k increases with increasing temperature and surfac-

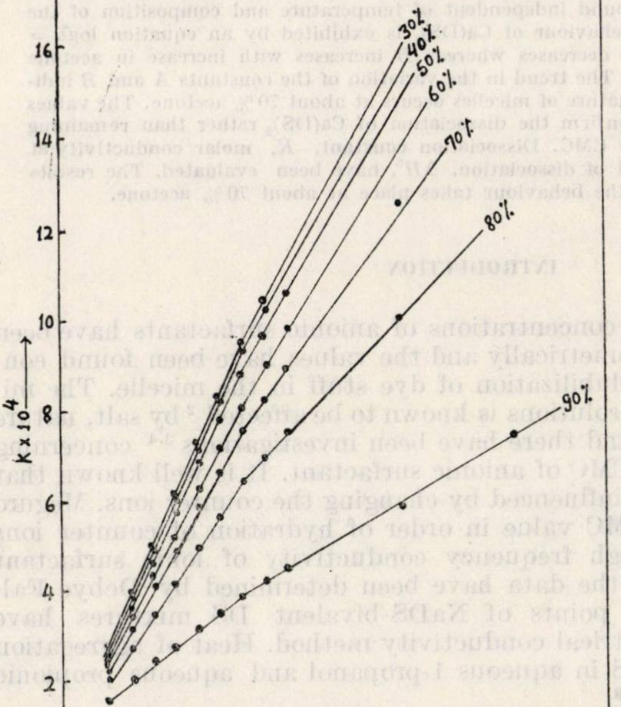

Fig. 1. — Plot of specific conductivity, k (ohm^{-1} cm^{-1}) vs. concentration, C (moles $litre^{-1}$) of $Ca(DS)_2$ at 35°C.

tant concentration. It is observed that the value of k decreases with increase in concentration of acetone in the mixture at all temperatures. The plots (Fig. 1) of specific conductivity vs. surfactant concentration show an intersection of two straight lines at definite concentration 0.008 M, called CMC which is independent of temperature and composition of solvent mixture. The CMC values[11] of calcium valerate, caproate and caprylate in water are 0.010, 0.05 and 0.002 M respectively. These values decrease with increasing chain length but the CMC of $Ca(DS)_2$ does not correspond with the behaviour. This increment in the CMC of $Ca(DS)_2$ is due to presence of aprotic solvent i.e. acetone in the mixture.

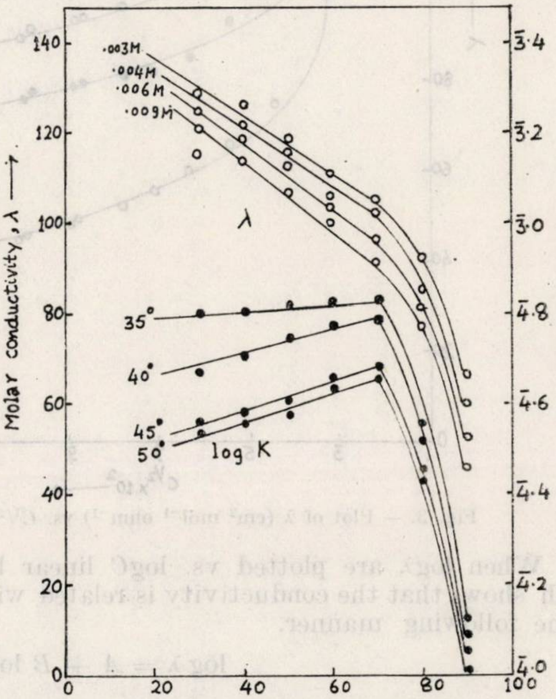

Fig. 2. — Plot of λ ($cm^2\ mol^{-1}\ ohm^{-1}$) and $\log K$ of $Ca(DS)_2$ vs. volume percent of acetone in the mixture at 35°C.

Molar conductivity, λ, calculated from specific conductivity decreases with increasing surfactant concentration and temperature. The plots (Fig. 2) of λ vs. volume percent of acetone in the mixture show that conductivity decreases linearly upto 70% of acetone and then nonlinearly with further increase in acetone content in the system. The plots (Fig. 3) of λ vs. $C^{1/2}$ are concave curves, irrespective of temperature and concentration of acetone. This indicates the weak electrolyte behaviour of $Ca(DS)_2$ in mixed solvents at all temperatures.

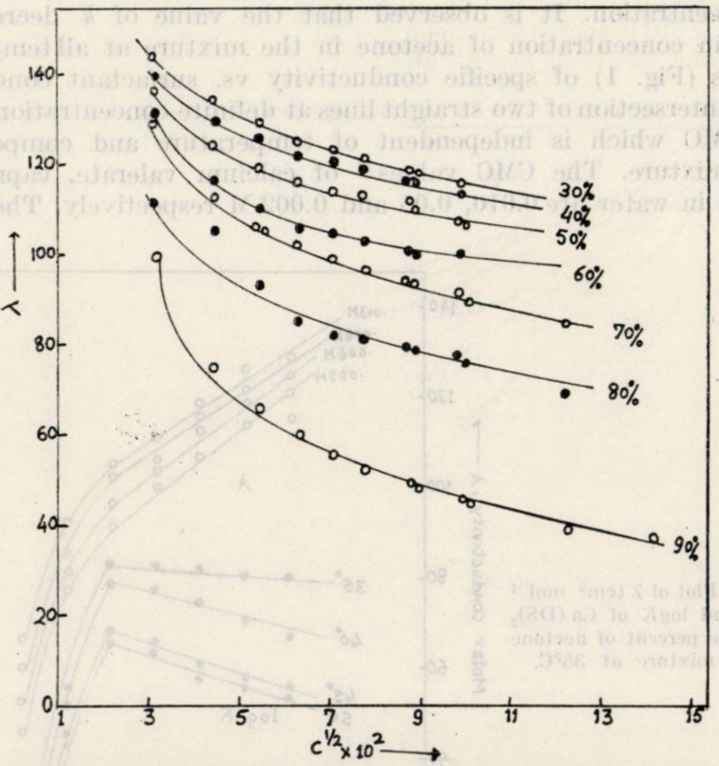

Fig. 3. — Plot of λ (cm^2 mol^{-1} ohm^{-1}) vs. $C^{1/2}$ of Ca $(DS)_2$ at 35°C.

When logλ are plotted vs. log*C* linear lines are obtained (Fig. 4) which shows that the conductivity is related with the soap concentration in the following manner.

$$\log \lambda = A + B \log C \qquad (1)$$

Constants *A* and *B* have been calculated from the intercepts and slopes of the linear plots respectively. Constant *A* (Table 1) decreases

TABLE 1

Constant *A* of $Ca(DS)_2$ in water-acetone mixtures at different temperatures

Volume % of acetone	35°	40°	45°	50°
30	1.905	1.965	1.995	2.020
40	1.885	1.920	1.970	1.995
50	1.860	1.900	1.950	1.975
60	1.755	1.775	1.800	1.810
70	1.660	1.680	1.685	1.690
80	1.510	1.520	1.535	1.540
90	1.065	1.070	1.080	1.150

with increasing concentration of acetone. The difference in successive values of A (10% increase in acetone percentage) indicates that the change in the value of A occurs at about 70% acetone concentration.

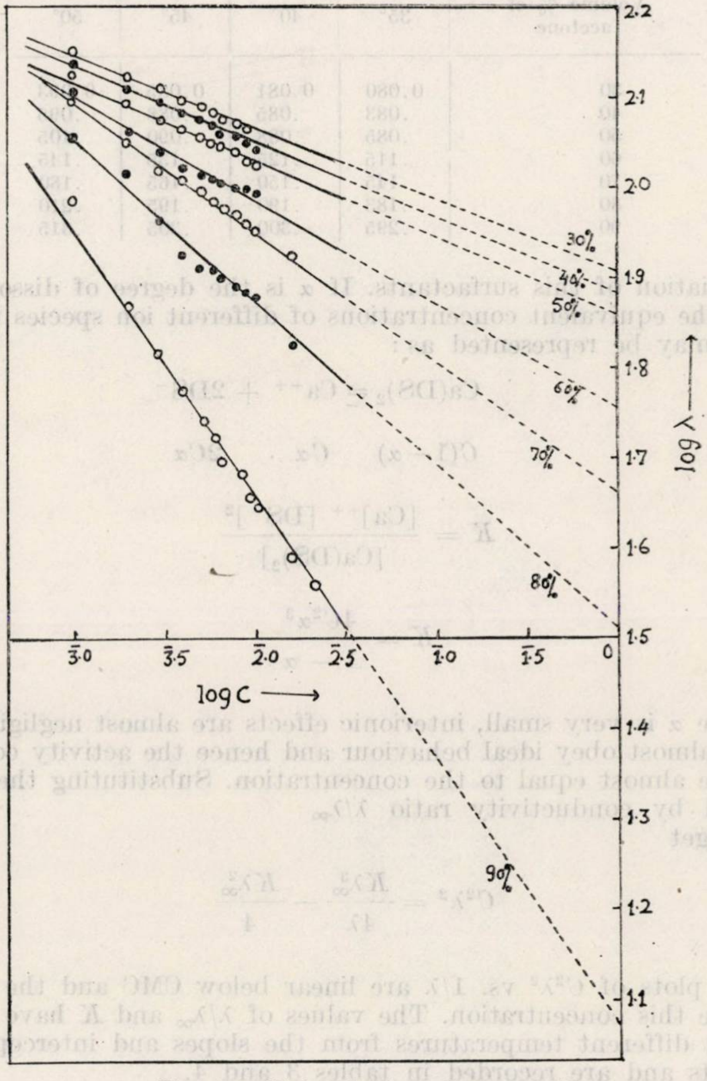

Fig. 4. — Plot of log λ vs. log$C$ at 35°C.

Constant $-B$ (Table 2) increases with increase acetone concentration. It is observed that the values of $-B$ below 70% and above this concentration differ appreciably. This shows that the change of nature of micelles takes place at 70% acetone concentration.

It has been observed that $Ca(DS)_2$ behaves as a weak electrolyte in mixed solvent. Kraus and Brays type expression [12] can be derived for

TABLE 2

Constant, $-B$ of $Ca(DS)_2$ in water-acetone mixtures at different temperatures

Volume % of acetone	35°	40°	45°	50°
30	0.080	0.081	0.085	0.093
40	.083	.085	.088	.095
50	.085	.088	.090	.105
60	.115	.125	.135	.145
70	.145	.150	.165	.180
80	.183	.190	.195	.210
90	.295	.300	.305	.315

the dissociation of this surfactants. If α is the degree of dissociation of $Ca(DS)_2$, the equivalent concentrations of different ion species in dilute solutions may be represented as:

$$Ca(DS)_2 \rightleftharpoons Ca^{++} + 2DS^- \qquad (2)$$

$$C(1-\alpha) \qquad C\alpha \qquad 2C\alpha$$

$$K = \frac{[Ca]^{++}\ [DS^-]^2}{[Ca(DS)_2]}$$

$$K = \frac{4C^2\alpha^3}{1-\alpha} \qquad (3)$$

Since α is very small, interionic effects are almost negligible. Such solutions almost obey ideal behaviour and hence the activity coefficients of ions are almost equal to the concentration. Substituting the value of α, defined by conductivity ratio λ/λ_∞

We get

$$C^2\lambda^2 = \frac{K\lambda_\infty^3}{4\lambda} - \frac{K\lambda_\infty^2}{4} \qquad (4)$$

The plots of $C^2\lambda^2$ vs. $1/\lambda$ are linear below CMC and the equation fails above this concentration. The values of λ/λ_∞ and K have been calculated at different temperatures from the slopes and intercepts of the linear plots and are recorded in tables 3 and 4.

Molar conductivity at infinite dilution (Table 3) increases with increase in temperature and concentration of water in the mixture. It is due to the overall increase in viscosity of the system in which the decrease in viscosity occurs as the acetone content in the solvent increases and the increase in viscosity occurs when the soap is added into it.

Dissociation constant K (Table 4) increases slightly or rather remains constant with increase in acetone concentration upto 70%, but

TABLE 3

Molar conductivity at infinite dilution, $\lambda_\infty \times 10^{-2}$ ($cm^2\ mol^{-1} ohm^{-1}$) of Ca $(DS)_2$ in water-acetone mixtures at different temperatures

Volume % of acetone	35°	40°	45°	50°
30	1.41	1.69	1.93	2.03
40	1.36	1.55	1.87	1.99
50	1.29	1.45	1.79	1.91
60	1.21	1.35	1.58	1.63
70	1.13	1.24	1.42	1.49
80	1.04	1.13	1.26	1.34
90	0.78	0.84	0.92	1.13

TABLE 4

Dissociation constant, $K \times 10^4$ of Ca $(DS)_2$ in water-acetone mixtures at different temperatures

Volume % of acetone	35°	40°	45°	50°
30	6.352	4.738	3.693	3.502
40	6.491	5.512	3.867	3.580
50	6.701	5.672	3.939	3.721
60	6.836	6.010	4.650	4.567
70	6.891	6.022	4.791	4.658
80	3.618	3.385	2.858	2.767
90	1.332	1.244	1.142	1.011

above this concentration there is a sharp fall in the values of K of surfactant at different temperatures. The fall of dissociation constant can be explained due to appreciable decrease in the dielectric constant of the mixture. The plots of log K vs. volume percent of acetone concentration (Fig. 2) show that these are almost linear upto 70% and then become nonlinear with further increase of acetone concentration.

Dissociation constant decreases with increase in temperature which shows the exothermic nature of the surfactant in this solvent. The values of heat of dissociation, ΔH° calculated from the linear plots of log K vs. $1/T$ (Table 5) are negative.

TABLE 5

Values of ΔH°, ΔG° and ΔS° of Ca $(DS)_2$ in water-acetone mixtures at 35°

Volume % of acetone	$-\Delta H^\circ$ (kcal mol^{-1})	$-\Delta G^\circ$ (kcal mol^{-1})	$-\Delta S^\circ$ (cal mol^{-1} deg^{-1})
30	8.145	4.506	11.816
40	7.779	4.492	10.670
50	7.321	4.473	9.247
60	5.491	4.461	3.345
70	5.079	4.456	2.023
80	4.118	4.850	−2.376
90	3.660	5.462	−5.842

The free energy, ΔG° can be calculated from the following relationship :

$$\Delta G^\circ = RT \ln K \qquad (5)$$

Where K is dissociation constant. The values of ΔG° are negative which shows that soap dissociates in dilute solutions. The entropy of dissociation has been calculated (Table 5). These activation parameters show a change at 70% acetone. This confirms that the change in the behaviour takes place at about 70% of acetone concentration.

ACKNOWLEDGEMENTS. The authors record their thanks to Dr. K. N. Mehrotra, Reader at the Department of Chemistry, University of Jodhpur, Jodhpur for his keen interest in the work and to the college authorities for providing laboratory facilities.

REFERENCES

[1] M. Miura and T. Matsumoto, *J. Sci. Hiroshima Univ. Ser.*, **A 21**, 51 (1957).
[2] K. Meguro, T. Kondo and N. Ohba, *Bull. Chem. Soc. Japan*, **30**, 905 (1957).
[3] O. Yoda, K. Meguro, T. Kondo and T. Ino, *Nippon Kagaku Zasshi*, **77**, 905 (1956).
[4] E. D. Goddard, O. Harva and T. G. Jones, *Trans. Faraday. Soc.*, **49**, 980 (1953).
[5] K. Meguro, T. Kondo, O. Yoda, T. Ino and N. Ohba, *Nippon Kagaku Zasshi*, **77**, 1236 (1956).
[6] M. Shirai and B. Tamamushi, *Bull. Chem. Soc. Japan*, **28**, 545 (1955).
[7] M. Yoshikiyo, O. Toshiji and R. Matuura, *J. Colloid Interface Sci.*, **60**, 103 (1977).
[8] B. D. Flockhart and A. R. Ubbelohde, *J. Colloid Sci.*, **8**, 428 (1953).
[9] S. Miyamoto, *Bull. Chem. Soc. Japan*, **33**, 371 (1960).
[10] R. P. Varma and P. Bahadur, *Cellulose Chem. Technol.*, **8**, 27 (1974).
[11] R. P. Varma and P. Bahadur, *Cellulose Chem. Technol.*, **9**, 393 (1975).
[12] C. A. Kraus and W. C. Bray, *J. Amer. Chem. Soc.*, **35**, 1315 (1913).

Revue Roumaine de Chimie, 28, 2, 123–127 (1983)

ESTUDIO DE LA CATÁLISIS ACIDO-BASE EN LA REACCIÓN DE IODACIÓN DE LA ACETONA. I.

CATÁLISIS POR LAS BASES OH^- y $HPO_4^=$.

L. FERRARI y M. RUIZ PASTRANA

Recibido el 3 de noviembre de 1980

Utilizando una técnica fotocolorimétrica, se han estudiado los efectos del pH (en el intervalo 6—11), temperatura y fuerza iónica sobre la velocidad de la reacción de iodación de la acetona. Para pH comprendidos entre 6 y 8 se emplearon disoluciones reguladoras $HPO_3^= / H_2PO_4^-$. Se han determinado las constantes catalíticas k_0, k_{OH^-} y $k_{HPO_4^=}$.

The effects of pH (range 6 —11), temperature and ionic strength on the reaction rate of acetone iodination have been studied using a photocolourimetrical technique. Phosphate buffer was employed in the range of pH 6—8. The catalytic coefficients k_0, k_{OH^-} and $k_{HPO_4^=}$ have been determined.

INTRODUCCIÓN

El estudio cinético de la halogenación de cetonas en medio acuoso y el efecto que ejerce el pH sobre la velocidad de reacción han merecido la atención de numerosos investigadores desde comienzos de siglo [1] hasta nuestros días. [2] Es bien conocido que la reacción es de primer orden respecto de la cetona y de orden cero respecto del halógeno, e independiente de la naturaleza de éste, lo que parece indicar que no interviene en la etapa determinante del proceso.

En la halogenación de la acetona juega un papel esencial su forma enólica, pues la halogenación se produce sobre ésta, y aunque el equilibrio está fuertemente desplazado hacia la forma cetónica (pK $\simeq$ 9) la formación del enol se ve favorecida por la presencia de cualquier especie ácida o básica en el medio. Como el paso de cetona a enol es lento, éste controlorá la velocidad de reacción.

Por consiguiente, las enolizaciones de las cetonas están catalizadas por ácidos y bases en general, y no sólo por el H_3O^+ o el OH^-, habiéndose estudiado exhaustivamente la influencia de las especies AcO^- y AcOH [3 a 7].

EXPERIMENTAL

El estudio de cada reacción se ha efectuado midiendo a intervalo regulares de tiempo la absorción del ión triioduro a 350 nm en un fotocolorímetro Bausch-Lomb, mod. Spectronic—20. Previamente se había comprobado que cumplía la ley de Lambert-Beer en el intervalo de concentraciones utilizado ($[I_3^-] \leqslant 3 \cdot 10^{-5}$ mol dm^{-3}), obteniéndose un valor para el coeficiente de extinción molar $\varepsilon_\lambda = 24480$ dm^3 mol^{-1} cm^{-1}.

Los reactivos empleados fueron: I_2, KI, NaCl, $NaH_2PO_4 \cdot 2H_2O$ y $Na_2HPO_4 \cdot 12\ H_2O$ Panreac "para análisis", acetona Panreac "purísima" y NaOH Merck "para análisis". Como disolvente se utilizó agua bidestilada.

Se ha trabajado entre 20 y 32°, a fuerza iónica constante (0,02 mol dm^{-3}) y en exceso de acetona (entre 10^{-2} y 10^{-3} mol dm^{-3}). El pH (medido en un pH-metro Radiometer, mod. 26) se ha variado entre 6 y 8 con disoluciones reguladoras NaH_2PO_4/Na_2HPO_4. En el intervalo de 8 a 11 los experimentos de realizaron en medios no tamponados.

RESULTADOS Y DISCUSIÓN

a) ECUACIÓN CINÉTICA Y PARÁMETROS TERMODINÁMICOS

Se realizaron una serie de experimentos trabajando en exceso de acetona y a pH = 6,8 (mediante una mezcla reguladora de fosfatos). Así se obtuvo el orden parcial cero respecto del I_3^- (Fig. 1). Con los valores de las pseudoconstantes k' calculados para distintas concentraciones de acetona, y teniendo en cuenta la ecuación

$$k' = k \cdot [C_2H_6CO]^n$$

se determinaron el orden uno respecto de este reactivo y la constante de velocidad k. En la tabla 1 se recogen los valores de k a diferentes temperaturas.

Otra serie de experimentos realizados variando únicamente la fuerza iónica del medio entre 0,02 y 0,08 mol dm^{-3} pusieron en evidencia la no existencia de efecto cinético salino primario.

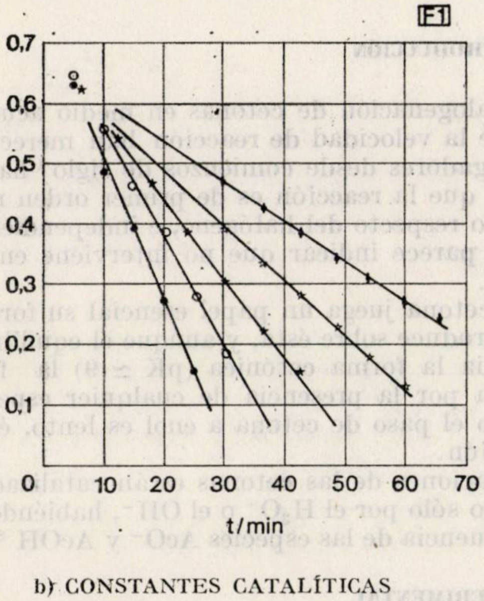

Fig. 1. — Reacción I_3^- -acetona en buffer de fosfatos a 24°. Las rectas absorción/tiempo muestran el orden cero respecto del I_3^- y sus pendientes 7,5 ; 5,7 ; 4,1 ; 2,8 y $2,0 \cdot 10^{-7}$ mol dm^{-3} mol^{-1}, son las pseudoconstantes k' para las concentraciones de acetona 1,94 ; 1,46 ; 0,97 ; 0,73 y $0,49 \cdot 10^{-2}$ mol dm^{-3} respectivamente.

b) CONSTANTES CATALÍTICAS

Si la reacción de iodación de la acetona está catalizada por los ácidos y las bases,[3,7] en nuestras condiciones de trabajo la ecuación catalítica de la constante de velocidad deberá escribirse así:

$$k = k_0 + k_{H^+}[H^+] + k_1[OH^-] + k_2[HPO_4^=] + k_3[H_2PO_4^-]$$

TABLA 1

Variación de la constante de velocidad con la temperatura *)

Condiciones :	T/°C	$k \cdot 10^5$ /min^{-1}
$[I_3^-] = 2{,}86 \cdot 10^{-5}$ mol dm^{-3}		
$[C_2H_6CO]$ entre $0{,}49 \cdot 10^{-2}$ y $1{,}94 \cdot 10^{-2}$ mol dm^{-3}	20	2,7
$J = 0{,}02$ mol dm^{-3}	21	2,9
pH = 6,8	24	3,7
$E_a = 66$ kJ mol^{-1}		
$\Delta H^{\neq} = 64$ kJ mol^{-1}	28	5,6
$\Delta S^{\neq} = -149$ J K^{-1} mol^{-1}	31	6,9
$\Delta G^{\neq} = 108$ kJ mol^{-1}	32	7,8

*) Los coeficientes de correlación oscilaron entre 0,9973 y $0{,}9999_7$ para las constantes de velocidad y fué de 0,9992 en el cálculo de los parámetros termodinámicos.

donde k_0 es la constante de velocidad de la reacción no catalizada — o mejor, catalizada por el disolvente— y los demás términos son los correspondientes a cada uno de los catalizadores presentes. En medios básicos y próximos al neutro las contribuciones de las especies ácidas son despreciables, [8] por lo que la ecuación anterior se reduce a

$$k = k_4 + k_2[HPO_4^=] \tag{1}$$

siendo

$$k_4 = k_0 + k_1[OH^-] \tag{2}$$

Para verificar el cumplimiento de la ecuación (1) y calcular las constantes catalíticas, se realizaron varias series de experimentos manteniendo, en cada uno de ellos, el pH constante pero variando la concentración de $HPO_4^=$ (y, lógicamente la de $H_2PO_4^-$). Las representaciones gráficas de k frente a $[HPO_4^=]$ deberían ser líneas rectas paralelas, cuyas ordenadas en el origen serían las constantes k_4 y la pendiente, k_2. Los resultados para pH comprendidos entre 6 y 8, que se exponen en la tabla 2, confirmaron estas previsiones, obteniéndose para k_2 un valor medio de $6{,}5 \cdot 10^{-4}$ dm^3 mol^{-1} min^{-1}. Mediante una nueva representación de los valores de k_4 frente a $[OH^-]$ (Fig. 2) se determinaron $k_0 = 2{,}3 \cdot 10^{-7}$ min^{-1} y $k_1 = 3{,}8$ dm^3 mol^{-1} min^{-1}.

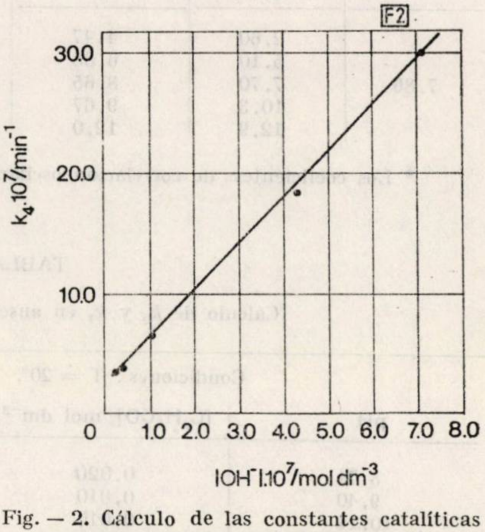

Fig. — 2. Cálculo de las constantes catalíticas k_0 y k_1 en buffer de fosfatos a 20°.

Este estudio se extendió en el intervalo de pH 8 — 11 en ausencia de disoluciones reguladoras, en el que sigue siendo válida la ecuación (2). Así es posible calcular k_0 y k_1, en un intervalo más amplio, con los resultados de la tabla 3.

TABLA 2

Cálculo de las constantes catalíticas k_2 y k_4^-.*

Condiciones : $T = 20°$; $J = 0{,}02$, $[C_2H_6CO] = 0{,}09$; $[I_3^-] = 2{,}86 \cdot 10^{-5}$
(Todas las concentraciones en unidades de mol dm^{-3})

pH	$[HPO_4^=] \cdot 10^3$	$k \cdot 10^6/min^{-1}$	$k_2 \cdot 10^4/dm^3\ mol^{-1}\ min^{-1}$	$k_4 \cdot 10^7/min^{-1}$
6,28	0,29	0,52	6,43	3,16
	0,57	0,69		
	0,86	0,84		
	1,71	1,43		
6,45	0,57	0,68	5,80	3,33
	1,14	0,98		
	1,71	1,33		
	2,29	1,62		
	2,86	2,03		
7,00	1,43	1,54	6,86	6,20
	2,86	2,60		
	4,29	3,79		
	5,71	4,41		
	7,14	5,34		
	8,57	6,63		
7,64	1,74	2,93	6,71	18,4
	2,61	3,75		
	3,49	4,12		
	4,36	4,76		
7,86	2,60	4,47	6,88	30,1
	5,10	6,88		
	7,70	8,65		
	10,3	9,67		
	12,9	12,0		

* Los coeficientes de correlación oscilaron entre 0,9903 y 0,9986.

TABLA 3

Cálculo de k_0 y k_1 en ausencia de disoluciones buffer.

Condiciones : T = 20°, $J = 0{,}02$ mol dm^{-3}

pH	$[C_2H_6CO]$/ mol dm^{-3}	$[I_3^-] \cdot 10^5$/ mol dm^{-3}	$k \cdot 10^3$/ min^{-1}
8,71	0,020	2,00	0,023
9,40	0,010	2,00	0,095
10,11	0,010	0,50	0,41
10,15	0,005	0,50	0,48
10,65	0,002	0,50	1,55
10,88	0,002	0,25	2,63
10,98	0,001	0,25	3,22

Coeficiente de correlación : 0,9970

De la correlación lineal existente entre k y OH^- se obtienen:

$$k_0 = 3{,}0 \cdot 10^{-7} \text{ min}^{-1}$$

$$k_1 = 3{,}4 \text{ dm}^3 \text{ mol}^{-1} \text{ min}^{-1}$$

valores que no discrepan mucho de los calculados anteriormente.

Todos estos resultados son concordantes con un mecanismo de reacción que consta de tres etapas, la primera lenta (transformación de la acetona en el enol o en el ión enolato, según que la reacción no esté catalizada o lo esté por cualquier base B^- respectivamente) y las otras dos rápidas: reacción con I_3^- adicionándose dos átomos de iodo en la forma enólica y posterior pérdida de un ión I^- de ese compuesto intermedio para dar el producto final iodoacetona. La aproximación del estado estacionario a ese mecanismo conduce a expresiones de la ecuación de velocidad de la forma $k[C_2H_6CO]$ y $k'[C_2H_6CO] \cdot [B^-]$, formalmente análogas a las encontradas experimentalmente.

BIBLIOGRAFÍA

[1] A. Lapworth, *J. Chem. Soc.*, **1904**, 30.
[2] L. M. Roshchupkina y Z. P. Sapozhnikova, *Issled. po Elektrokhimii i Korrozii Met.*, **1977**, 95; *Ref. Zhur. Khim.*, **16B**, 1209 (1978).
[3] C. G. Swain, *J. Amer Chem. Soc.*, **72**, 4578 (1950).
[4] (a) T. M. Lowry y I. J. Faulkner, *J. Chem. Soe.*, **1925**, 2883.
(b) H. M. Dawson y E. Spiveyś, *J. Chem. Soc.*, **1930**, 2180.
[5] K. J. Pedersen, *J. Phys. Chem.*, **38**, 590 (1934).
[6] I. Zucker y J. P. Hammett, *J. Amer. Chem. Soc.*, **61**, 2971 (1939).
[7] (a) R. P. Bell y P. Jones, *J. Chem. Soc.*, **1953**, 88.
(b) R. P. Bell y K. Yates, *J. Chem. Soc.*, **1962**, 2225.
[8] M. D. Waddington y J. E. Meany, *J. Chem. Educ.*, **55**, 60 (1978).

Revue Roumaine de Chimie, 28, 2, 129—137 (1983)

4-SUBSTITUTED 2,6-DI-t-BUTYLPHENOLS AND THEIR CORRESPONDING AROXYLS POSSESSING 4-(1-METHYLENE-IMIDAZOLYL), 4-(1-METHYLENE-BENZIMIDAZOLYL), OR 4-(1-SULFONYL-BENZIMIDAZOLYL) GROUPS

JEAN HERDAN,[a] ALEXANDRU T. BALABAN,[b,c] NICOLAE NEGOIȚĂ[d] and NICOLETA GRECU [d]

[a] Institute of Technological Engineering, Research and Refinery Design (ICITPR), Ploiești, Romania
[b] The Polytechnic, Organic Chemistry Department, Bucharest, Romania
[c] Correspondence author
[d] Institute of Nuclear and Engineering Physics (IFIN), Bucharest, Romania

Received May 16, 1982

The preparation of new 2,4,6-trisubstituted phenols **3A** – **E** and **6** is described. They have 2,6-di-t-butyl groups ; **3A** has an imidazole group, the other ones have benzimidazole groups, linked through a methylene bridge (for **3A** – **E**) or a sulfonyl bridge (for **6**). The IR and ^{1}H–NMR spectra, together with elemental analyses, confirm the structures. Oxidation yields persistent aroxyls (**4A** – **E** and **7**) whose ESR spectra and hyperfine coupling constants are described. The antioxidant activity of **6** is lower than of the other phenols described here ; in the autoxidation of tetralin initiated by azo-isobutyronitrile, all phenols **3A** – **E** behave similarly showing good antioxidant activity ; however, in the autoxidation initiated by cupric salts, **3D** has a markedly higher activity as antioxidant, probably owing to chelate formation (**8**).

INTRODUCTION

An earlier paper[1] described the synthesis and spectra (IR, ^{1}H–NMR) of new 2, 4, 6-trisubstituted phenols and of their corresponding aroxyls (including ESR spectra of the latter persistent radicals). In continuation of these investigations we report now the preparation and spectral study of phenols (**3**, **6**) and corresponding aroxyls (**4**, **7**) with 2,6-di-t-butyl substituents and with a heterocyclic group (imidazolyl in **A** or benzimidazolyl in other structures) attached to the 4-position through a methylene (in **3** and **4**) or a sulfonyl bridge (in **6** and **7**).

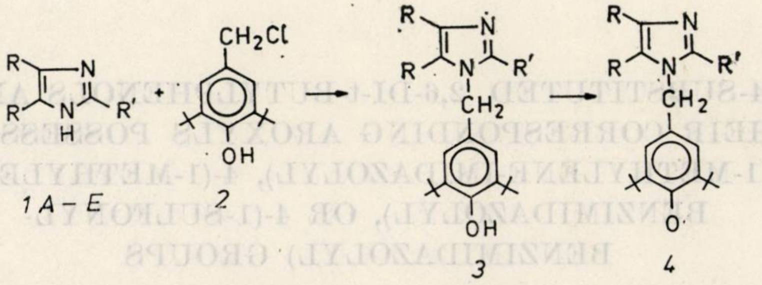

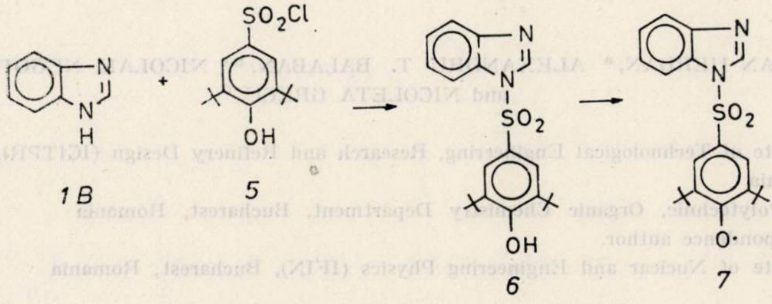

SYNTHESIS, IR AND ^{1}H–NMR SPECTRA

The preparation of phenols **3** was straightforward from 2,6-di-t-butyl-4-chloromethyl-phenol (**2**) and an imidazole or a benzimidazole derivative (**1A**–**E**).

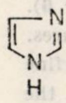
1A

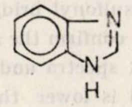
1B

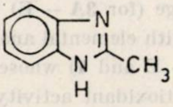
1C

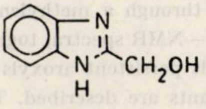
1D

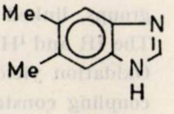
1E

For comparison of ESR hyperfine coupling constants, one sulfonyl derivative **6** was prepared from **1B** and 3,5-di-t-butyl-4-hydroxy-benzenesulfonyl chloride (**5**). In turn, the starting materials **2** and **5** were prepared as follows: **2** was obtained from 2,6-di-t-butylphenol by chloromethylation, and **5** from the same phenol by reaction with chlorosulfonic acid.

The crystalline phenols were characterized by elemental analysis, IR, and ^{1}H–NMR spectra (Tables 1 and 2). Table 2 presents the main IR bands and all peaks but the aromatic multiplets in the ^{1}H–NMR spectra.

In the 60 MHz ^{1}H–NMR spectra, the *m*-standing protons on the phenol ring overlap with the (benz)imidazolic ring (aromatic) proton peaks, so that they are not easily discernible (Table 2). Usually, the 2-imidazolic proton at the CH group flanked by the two nitrogen heteroatoms is distinct from other aromatic proton peaks, but not in **6**. All data from Tables 1–3 confirm the structures of phenols **3** and **6**.

TABLE 1

Melting points and elemental analyses of phenols

Comp.	R	R′	M.p.(°C)	Recryst. from	Formula	N %	
						Calcd.	Found
3A	H	H	126–128	EtOH	$C_{18}H_{26}N_2O$	9.86	9.83
3B	Benzo	H	149–151	EtOH	$C_{22}H_{26}N_2O$	7.29	7.32
3C	Benzo	CH_3	163–165	EtOH–Et_2O	$C_{23}H_{28}N_2O$	7.03	7.07
3D	Benzo	CH_2OH	183–184	EtOH	$C_{23}H_{28}N_2O_2$	6.76	6.89
3E	Me_2-benzo	H	151	EtOH	$C_{24}H_{30}N_2O$	6.79	6.83
6	Benzo	H	228–229	EtOH	$C_{21}H_{24}N_2O_3S$	6.45	6.47

TABLE 2

IR and ^1H–NMR spectral data

Comp.	IR in CCl_4 (cm^{-1})		^1H–NMR spectra in $CDCl_3$ (δ values, ppm)			
	ν (OH)	ν (arom.)	*t*Bu (18 H)	CH_2 (2H)	Aromatic	R′
3A	3650	1587	1,40s	5.05s	6.9 – 7.1 (4H) m	7.50 (1H)s
3B	3653	1610, 1590	1.40s	5.10s	7.0 (2H)s, 7.3 (4H)m	7.82 (1H)s
3C	3658	1608, 1592	1.40s	5.20s	6.9 (2H)s, 7.3–8.0(4H)m	2.60 (3H)s
3D	3652, 3430	1610, 1583	1.35s	5.50s	6.95(1H)s, 7.2–7.8(6H)m	4.80 (2H)d
3E[a]	3650	1609, 1587	1.40s	5.60s	6.35(1H)s, 7.3(2H)d	7.40 (1H)s
6	3652	1610, 1590[b]	1.40s	—	7.0(2H)s, 7.3–7.8(5H)m	c

[a] The two methyl groups in positions 5 and 6 appear at 2.35 ppm (6H)s.

[b] Further IR bands : 1335 (νSO_2 asym.) and 1165 (ν SO_2) sym.).

[c] Overlap between the imidazolic proton and other aromatic peaks.

FORMATION AND ESR SPECTRA OF AROXYLS 4 AND 7

Oxidation of phenols **3A – E** and **6** in benzene solution with lead dioxide leads to the formation of aroxyls **4** and **7**. Their ESR spectra were recorded in degassed solution. Results are presented in Figures 1–3 and in Table 3. The g-values measured with the help of manganese (II) lines is 2.0057 ± 0.0002 for **4A – E**, and 2.0066 ± 0.0002 for **7**. The latter radical has a very simple ESR spectrum, consisting of a triplet

TABLE 3

ESR Spectral data of aroxyls

Comp.	Number of distinct peaks	g	Hyperfine coupling constants (mT)		
			a_{CH_2}	a_{mH}	a_N
4A	27	2.0057	1.15	0.19	0.13
4B	27	2.0057	1.17	0.19	0.133
4C	21	2.0057	1.22	0.19	0.11
4D	27	2.0057	1.15	0.19	0.13
4E	27	2.0057	1.152	0.185	0.132
7	3	2.0066	—	0.18	—

with intensities 1 : 2 : 1 due to the two *m*-protons relative to the aroxyl free radicalic centre. This spectrum gives immediately the hyperfine coupling constant a_{m-H}, and the absence of other splittings is in agreement with the "insulating" properties of sulfonyl groups;[2] the ESR spectrum is presented in Fig. 1.

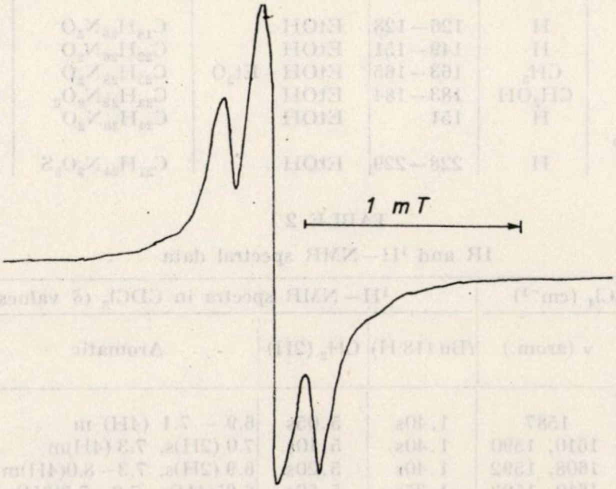

Fig. 1. — Experimental first-derivative ESR spectrum of aroxyl **7** in benzene at room temperature.

Radical **4C** has 21 lines in its ESR spectrum; the experimental and simulated spectra are presented in Fig. 2. All remaining radicals have 27 peaks; since their ESR spectra are similar, we present only two such spectra, experimental and simulated, for **4B** and **4E** (Fig. 3 and 4, respectively).

All radicals **4B** — **E** and **7** can be obtained free of other radicals, and can be conserved in solution without marked decomposition; radical **4A**, however, is usually obtained admixed with another unidentified radical which has approximately the same *g* value and presents only 9 closely spaced lines, overlapping with the central multiplet in the ESR spectrum of **4A**; this impurity radical, whose structure has not been established, lacks apparently the 4—CH_2 group and hence any large couplings; depending on the oxidation conditions and on how long the solution has been conserved before recording its ESR spectrum, this impurity radical can sometimes be the major component of the oxidized mixture.

ANTIOXIDANT ACTIVITY OF PHENOLS 3 AND 6

For determining the antioxidant activity of phenols **3A** — **E** and **6**, the kinetics of oxygen absorption in the autoxidation of tetralin at 60° were studied in the presence of azobis(isobutyronitrile) (10 mmoles/liter) using concentrations of 20 mmoles/ liter of phenols. Results are

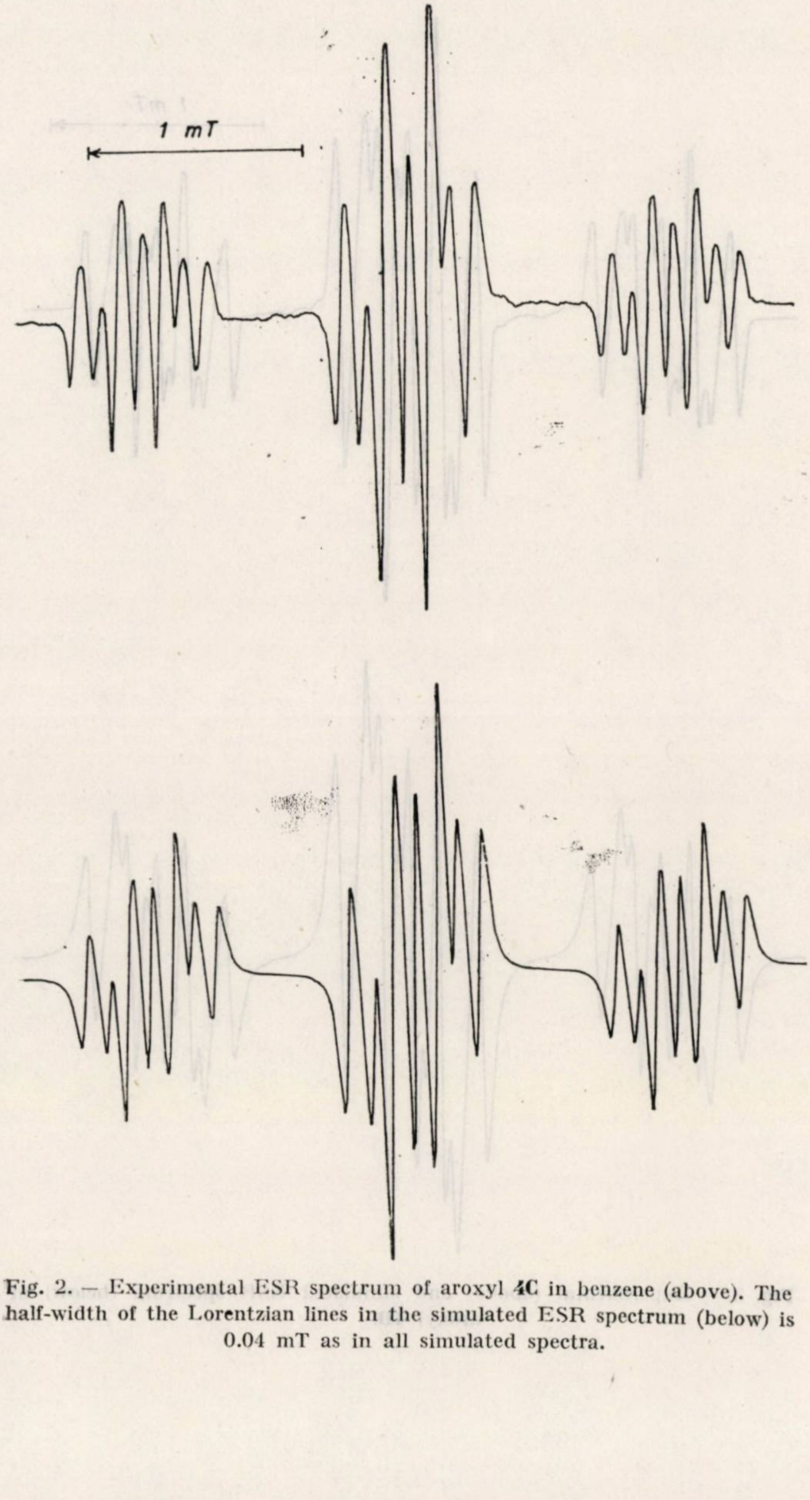

Fig. 2. — Experimental ESR spectrum of aroxyl **4C** in benzene (above). The half-width of the Lorentzian lines in the simulated ESR spectrum (below) is 0.04 mT as in all simulated spectra.

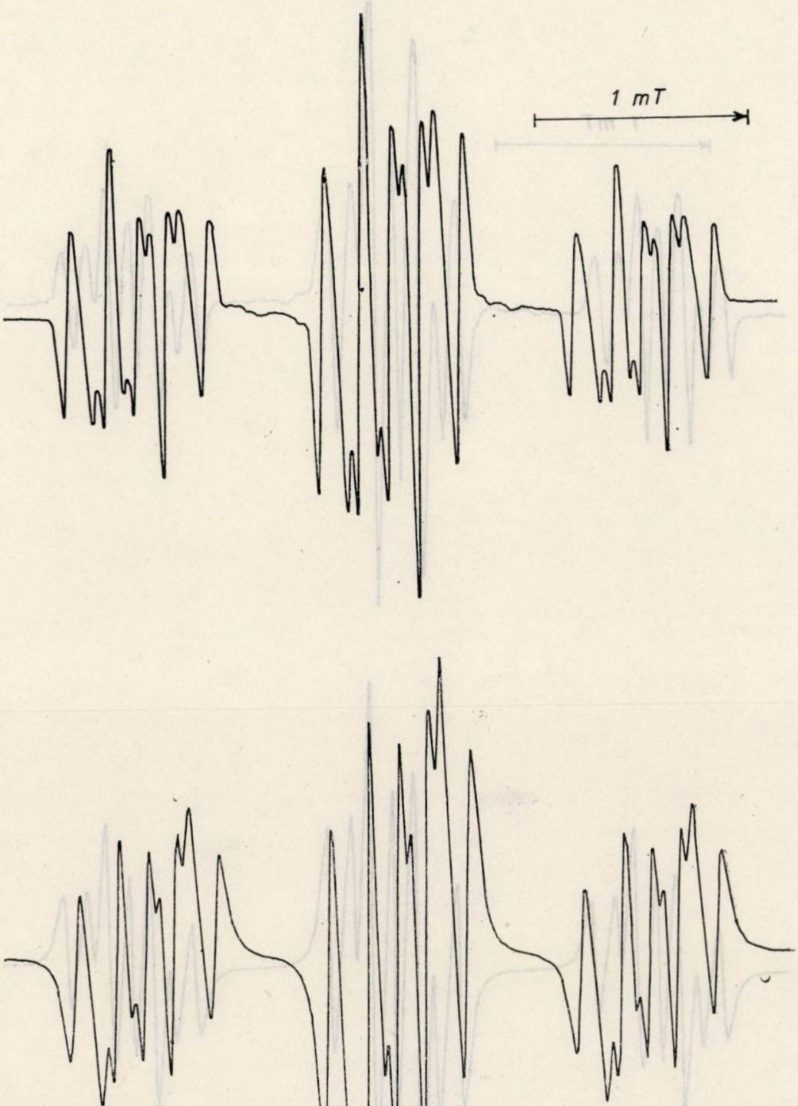

Fig. 3. – Experimental (above) and simulated ESR spectrum (below) of aroxyl **4B**.

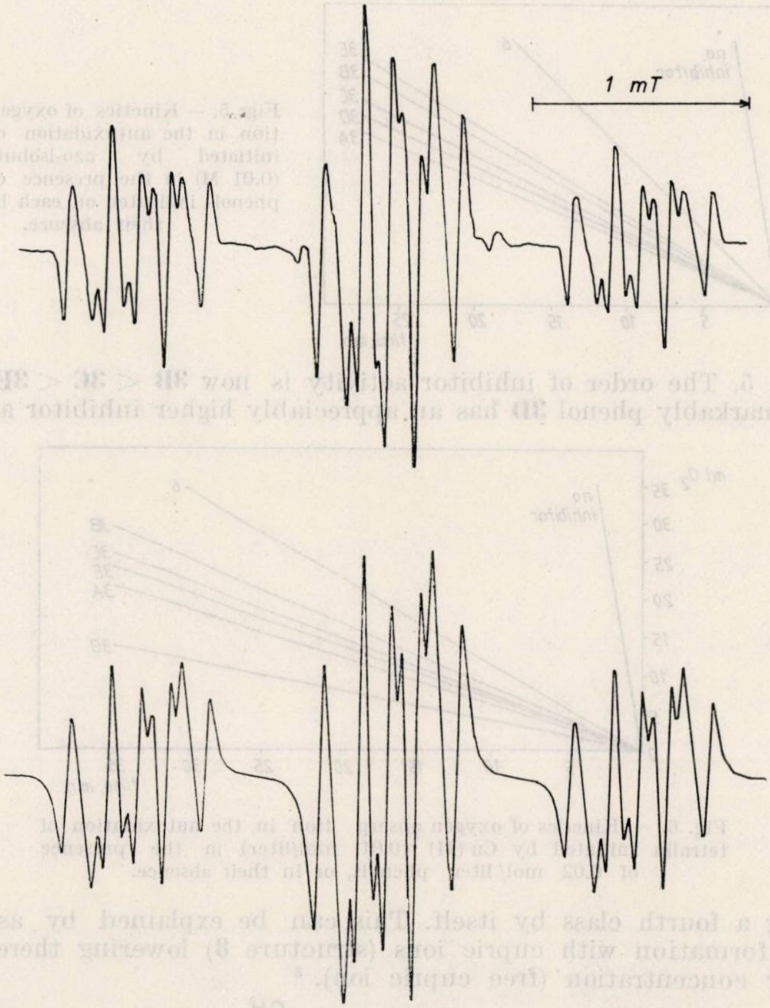

Fig. 4. – Experimental (above) and simulated ESR spectrum (below) of aroxyl **4E**.

presented in Fig. 5. Clearly, the addition of phenols has a retarding effect on the rate of oxygen absorption. The inhibiting effect of phenol **6** (and therefore of aroxyl **7**) is less pronounced than of the other compounds. One can observe the following order of inhibitor activity: **3E** < **3B** < < **3C** < **3D** < **3A**, but these five phenols appear close together in Fig.5 .

On the other hand, when the autoxidation of tetralin at 60° was initiated with Cu(II) stearate in the same concentrations as those described above, the results were different, as shown in Fig. 6. Again, addition of all phenols has a retarding effect. Again, the inhibitor activity is least for **6**, but the activities of the other phenols differ from the pattern shown

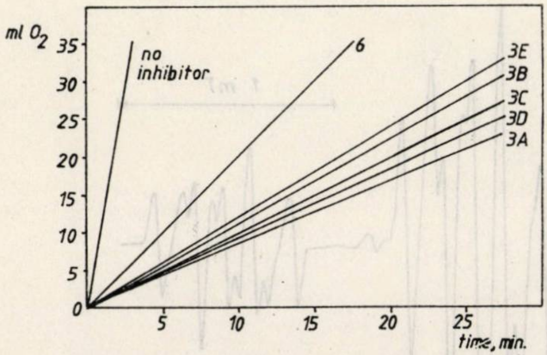

Fig. 5. — Kinetics of oxygen absorption in the autoxidation of tetralin initiated by azo-isobutyronitrile (0.01 M) in the presence of 0.02 M phenols indicated on each line, or in their absence.

by Fig. 5. The order of inhibitor activity is now **3B** < **3C** < **3E** < **3A**, and remarkably phenol **3D** has an appreciably higher inhibitor activity,

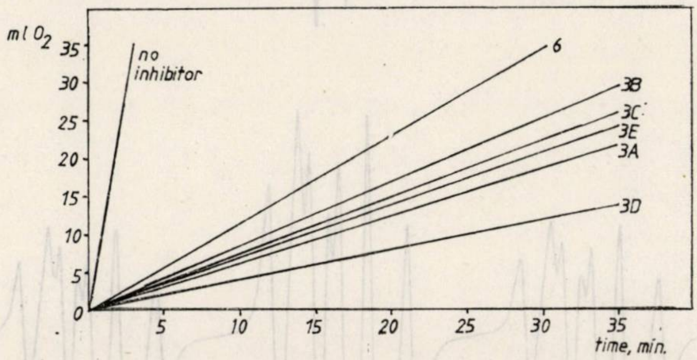

Fig. 6. — Kinetics of oxygen absorption in the autoxidation of tetralin initiated by Cu (II) (0.01 mol/liter) in the presence of 0.02 mol/liter phenols, or in their absence.

forming a fourth class by itself. This can be explained by assuming helate formation with cupric ions (structure **8**) lowering thereby the nitiator concentration (free cupric ion). [3]

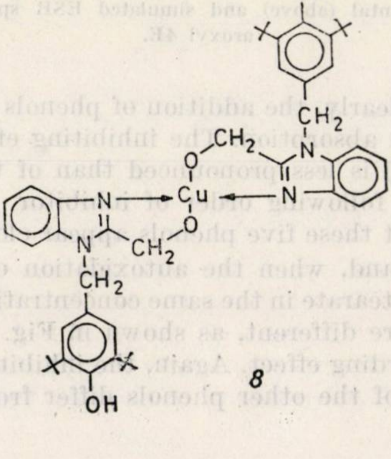

8

EXPERIMENTAL PART

The IR spectra were recorded with a Jena UR–20 spectrophotometer; the ^{1}H–NMR spectra were recorded with a Varian A–60A instrument, and the ESR spectra with a Jeol JES–ME–3X instrument.

Autoxidations were carried out under conditions and in an experimental set-up which were described earlier.[4]

Synthesis of phenols **3**. Equimolar (10 mmol) amounts of (benz)imidazole derivative (**1A** – **E**) and of 2,6-di-t-butyl-4-chloromethyl-phenol (**2**)[5] were dissolved in 50 ml ethanol and treated with 10 mmol of sodium hydroxide solution in 5 ml water. After 5 hrs' refluxation the filtered solution was evaporated and the residue was recrystallized from the solvent indicated in Table 1.

3,5-Di-t-butyl-4-hydroxy-benzenesulfonyl chloride **5** was prepared by chlorosulfonation of 2,6-di-t-butylphenol in chloroform. The product has m.p. 55–60° (crude) and shows IR absorptions at 3630 cm^{-1}, ν(OH); 1230, δ(OH); 1380, ν(SO_2 asym.) and 1180 cm^{-1}, ν(SO_2 sym.).

Phenol **6** was obtained from the chloride **5** and the benzimidazole **1B** under conditions similar to those described above.

For ESR spectra, the oxidations were carried out as described earlier.[1]

ACKNOWLEDGEMENTS. Thanks are expressed to Dr. F. Chiraleu for NMR spectra and to Dr. M. T. Căproiu for simulating ESR spectra.

REFERENCES

[1] J. Herdan, G. Iordache, N. Negoiţă, N. Grecu and A. T. Balaban, *Rev. Roumaine Chim.*, **27**, 69 (1982).

[2] A. T. Balaban and N. Negoiţă, *Rev. Roumaine Chim.*, **17**, 1227 (1972 ; A. T. Balaban, M. T. Căproiu, N. Negoiță and R. Baican, *Tetrahedron Letters*, 4091 (1974); *Tetrahedron*, **33**, 2249 (1977).

[3] B. Lenorcik and W. Mociewski, *Pol. J. Chem.*, **55**, 31 (1981).

[4] J. Herdan, L. Crişan, M. Luca and S. Balin, *Rev. Roumaine Chim.* **27**, 29 (1982).

[5] Ethyl Corp., French Pat. 1 301 518 (1962), cited after: K.–D. Bode, in "Houben-Weyl's Methoden der Organischen Chemie" (ed. E. Müller), vol. VI/1c, Part 2, p. 1042, Thieme, Stuttgart, 1976.

Revue Roumaine de Chimie, 28, 2, 139–145 (1983)

DERIVATIVES OF 4-AMINOMETHYL-THIAZOLE. III[1]

OXIDATIVE CYCLIZATIONS AND DETHIONATIONS IN THE SERIES OF 1-PHENYL-3-(2-ARYL-4-THIAZOLYLMETHYL)-THIOUREAS

IOAN A. SILBERG * and SIMONA SILBERG **

* IECB—"Babeș-Bolyai" University Research Group, Department of Physical Chemistry,
str. Arany Janos 11, R-3400 Cluj-Napoca, Romania
** Pharmaceutical Faculty, str. Ion Creangă 12, R-3400 Cluj-Napoca, Romania

Received June 10, 1982

The oxidative cyclization of the title compounds **1** to the benzothiazoles **5** was carried out under conditions of the Hugershoff reaction and by UV-irradiation in benzene. The cyclization is always accompanied by a dethionation leading to the substituted ureas **2**; under the conditions of the Jacobson reaction there is no benzothiazole formation, but a quantitative and almost instantaneous conversion of **1** into **2**.

The propensity of aryl-thioureas to yield cyclization products belonging to the benzothiazole series, under the action of a large variety of oxidizing agents, is a well established fact.[2] The main ways of effecting such cyclizations consist of treating the aryl-thioureas either with potassium ferricyanide (the Jacobson reaction[3]), or with bromine, or, in a more recent variant, with sulphuryl chloride (Hugershoff's reaction[4-6]). The application of these reaction to 1-phenyl-3-(2-aryl-4-thiazolylmethyl)-thioureas **1**, obtained by us during previous investigations[1] offered new perspectives for our studies in the thiazole series, and provided the opportunity of making a comparison between the various modes of stabilization of the reactive intermediates generated from these thioureas under the action of oxidants. It is to be added that such investigations could contribute to the elucidation of the problem raised by the mass spectra of **1**, which do not show the characteristic M—1 peaks,[1] corresponding, in the mass spectra of usual aryl-thioureas, to the cyclizations yielding cations of benzothiazoles.[7]

The present work reports the results obtained by acting with $K_3[Fe(CN)_6]$ and with SO_2Cl_2 on compounds of the type **1**, as well as by irradiating the latter with UV light.

THE REACTION OF THE THIAZOLE DERIVATIVES OF THIOUREA 1 WITH $K_3[Fe(CN)_6]$

By effecting this process under the conditions which allow the cyclization of most aryl-thioureas to benzothiazoles in good yields, that is, in aqueous-alkaline medium at room temperature, we observed that there is, surprisingly, a quantitative and practically instantaneous conversion of **1** into the thiazole derivative of urea, **2**. A few other cases of partial dethionation under the action of the same reagent,[8] as a side-process in Jacobson cyclizations, can be found in the literature, but they involve almost exclusively alkyl-thioureas and monosubstituted thioureas; hence, the tendency of compounds **1** to give desulphurated derivatives as the only reaction products represents a distinctive features of this group of substituted thioureas.

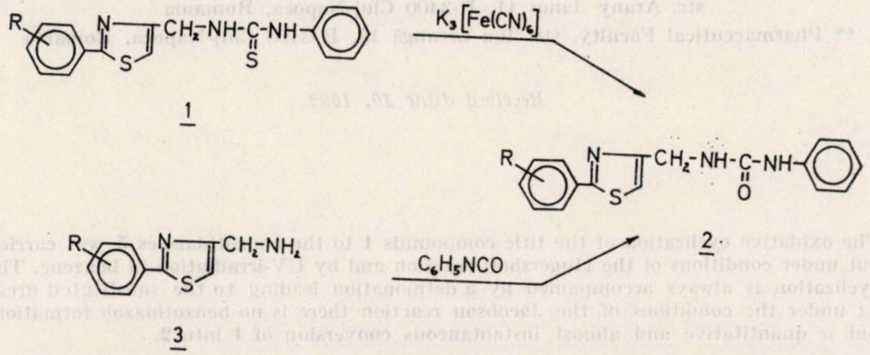

The identity of the 1-phenyl-3-(2-aryl-4-thiazolyl-methyl)-ureas **2** thus obtained was checked by classical analytical tests, as well as by a direct comparison with authentic samples prepared[1] by the addition of 2-aryl-4-aminomethyl-thiazoles **3** to phenylisocyanate.

The marked lability of C—S bonds in the intermediates formed by oxidizing the thioureas **1** represents an intrinsic property and is not due to an interaction of sulphur with iron ions in the system; the experiments described below clearly stress this point of view.

THE REACTION OF 1 WITH SO_2Cl_2

The action of sulphuryl chloride on **1** in chloroform, acetonitrile, or acetic acid at room temperature results in the conversion of the initial compound into two products, a process which can be easily monitored by thin-layer chromatography.

The substance with lower R_f is always the urea derivative **2**, which was formed even when the reaction was carried out in anhydrous media. A much less polar product was obtained in moderate amounts along with **2**; this product was quantitatively separated owing to its solubility in petroleum ether.

In the mass spectrum of the product with higher R_f the molecular ion appears at m/e 323, demonstrating that the new compound was formed by extraction of two hydrogen atoms from the starting substance; the fact that a cyclization product was obtained is also indicated by the abundance of the molecular ion, which represents the base peak of the spectrum, whereas in the case of the initial thiourea the molecular ion had only 50 % relative intensity.[1]

In determining the structure of the product formed in the Hugershoff reaction it is to be taken into account that the species with electrophilic sulphur, which appear in the oxidation of compounds **1**, might generate, in principle, two cyclic structures, **5** and **6**. As shown in the scheme, the formation of compound **5** is the result of an attack at one of *ortho* positions of the benzene ring, in a process belonging to the series of classical benzothiazole cyclizations, whereas product **6** would be formed as a consequence of the increased electron density characteristic of the 5-position of the thiazole ring.

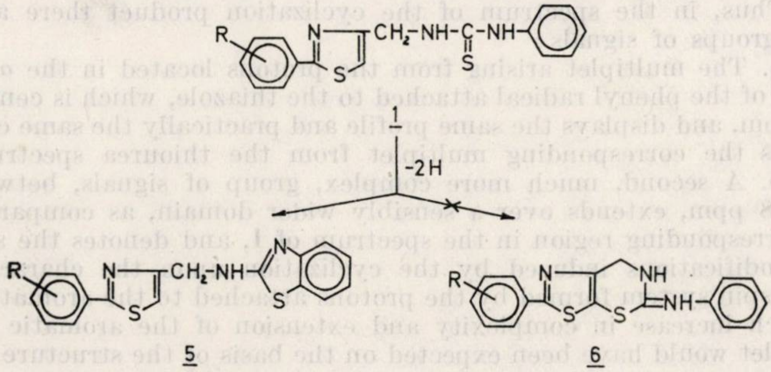

Although in many cases mass spectrometry is a rather inefficient analytical tool for making a distinction between isomeric structures, the formation of almost 30 important fragments from the mass spectrum can be explained under optimal conditions only by starting with the benzothiazole structure **5**. This fragmentation scheme is supported by nine metastable peaks; we emphasize the key fragments at *m/e* 189 and 149,

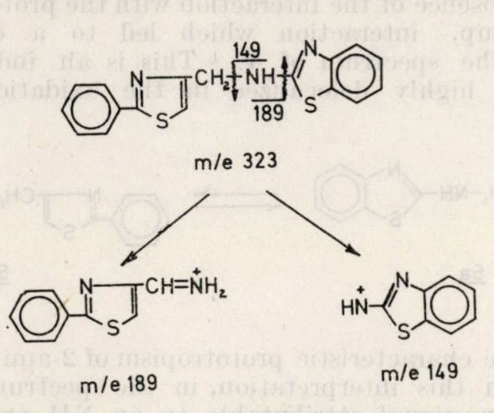

the elimination of SH, characteristic of this heterocycle, and the very marked rise in intensity of the peak at *m/e* 76, indicative of a disubstituted benzene ring, a structural element which appears only in the formulation **5**.

The ^{1}H—NMR spectra led us to an unequivocal decision favouring structure **5**, primarily by comparing the spectrum of **5**, (R=H), with that of the parent thiourea **1** (R=H).[1]

Thus, in the spectrum of the cyclization product there are only three groups of signals:

a. The multiplet arising from the protons located in the *ortho* positions of the phenyl radical attached to the thiazole, which is centered at 7.92 ppm, and displays the same profile and practically the same chemical shift as the corresponding multiplet from the thiourea spectrum.

b. A second, much more complex, group of signals, between 6.8 and 7.8 ppm, extends over a sensibly wider domain, as compared with the corresponding region in the spectrum of **1**, and denotes the substantial modifications induced by the cyclization upon the characteristics of the spin system formed by the protons attached to the aromatic rings. No such increase in complexity and extension of the aromatic protons multiplet would have been expected on the basis of the structure **6**, since the latter contains the same two monosubstituted benzene rings which are encountered in the molecule of the starting thiourea.

c. Finaly, at 4.80 ppm, the methylene group gives rise to a well marked singlet, showing that the interaction with other protons in the molecule are characterized by coupling constants well below 0.5 Hz. The virtual absence of the coupling with the isolated proton from position 5 of the thiazole ring, a phenomenon also observed in the case of the initial thiourea derivatives,[1] represents a particular feature of the NMR spectra of the compounds belonging to this class, especially when compared with the facts observed during the investigations concerning the thiazole derivatives of phenothiazine.[9] However, we wish to point out the conspicuous absence of the interaction with the proton from the neighbouring NH group, interaction which led to a doublet splitting, $J = 5.0$ Hz, in the spectrum of **1**.[1] This is an indication that the iminic proton is highly delocalized in the oxidation product, as a consequence of the characteristic prototropism of 2-amino-benzothiazoles. In agreement with this interpretation, in the spectrum of the cyclized product there is no signal attributable to an NH proton, and, as expected, the treatment with D_2O does not induce any notable change in the spectrum.

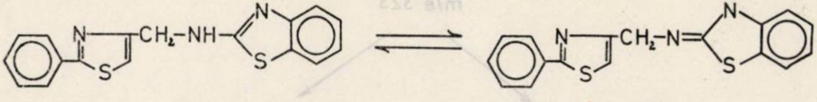

5a 5b

The structure of the cyclization product shows that there is a much more accentuated tendency towards the benzothiazole ring formation, as compared to the ring-closure that would yield compound **6**, with a six-membered 1,3-thiazinic ring. These data might also be interpreted as indications for the fact that positions 5 of the thiazole ring are less reactive than positions *ortho* of the phenyl radical, especially if one takes into account that under the mild experimental conditions used, the formation of the products should be under kinetic control.

PHOTOCHEMICAL TRANSFORMATIONS OF THE THIAZOLE DERIVATIVE OF THIOUREA, 1

Since the irradiation in solution, in the presence of oxygen, represents an efficient method for bringing about cyclization reactions which are difficult to effect by other means, [10] we carried out preliminary investigations on the behaviour of **1** under the action of UV light.

By exposing to intense UV irradiation, at 50–60°, diluted solutions of 1-phenyl-3-(2-phenyl-4-thiazolyl-methyl)-thiourea (**1**, R=H) in anhydrous benzene, and by monitoring the reaction with TLC, we found that, besides abundant tar formation, the main chemical processes which take place are the same as in the case of Hugershoff's reaction *(vide supra)*. Thus, the photochemical process yields the same benzothiazole derivative **5** and substituted urea **2** (R=H in both cases).

We stress once more the outstanding tendency of **1** to undergo dethionation, as well as the clear prevailing of the formation of structure **5** over structure **6**.

As far as the latter aspect is concerned, we find particularly demonstrative the photochemical behaviour of 1-phenyl-3-(2-phenyl-5-chloro-4-thiazolyl-methyl)-thiourea **7**, a compound which should be able to develop, under UV-irradiation, a reactive radicalic center in the position 5 of the thiazole nucleus, by a homolytic cleavage of the C-Cl bond. The photolysis of this bond took place, indeed, as expected, but the radical **8** formed thereby was stabilized almost exclusively by capturing hydrogen atoms from the reaction medium, giving **1** (R=H), instead of being attacked by the sulphur atom of the thiourea group, — thus failing again to yield **6**. By prolonged irradiations we obtained, of course, reaction mixtures which were identical with those formed from **1** under the action of UV light.

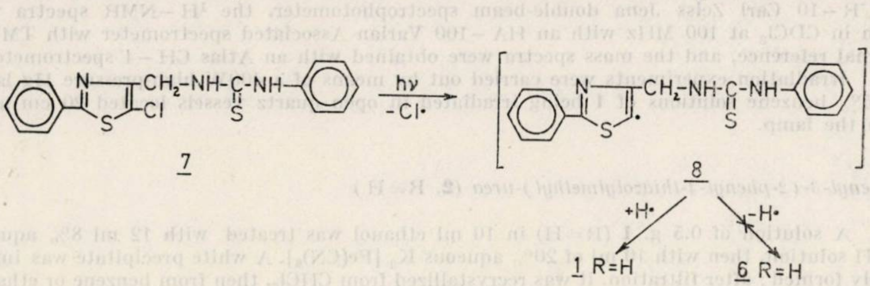

CONCLUDING REMARKS

As already mentioned in a previous report [1] we noted the particular behaviour of the thiazole derivatives of thiourea **1** under electron impact, when the usual cyclization of phenyl-thioureas to benzothiazoles is lacking, as indicated by the absence of M—1 peaks in the mass spectra. The data presented in this paper show that such cyclizations can be performed either by using oxidants (under the conditions of the Hugershoff reaction) or by UV irradiation, but they do not represent a dominant feature of the chemistry of the investigated compounds since other processes are always present, and usually prevail.

The explanation of the observed facts resides in the reaction mechanism, and, although there are tremendous differences between the conditions of the reported experiments, so that the possibilities of formulating definite opinions on the matter are principially limited, we find it of interest to note that the cyclization of **1** to benzothiazoles failed to occur in the mass spectra, where the intermediates are ions (or radical-ions), and under the conditions of the Jacobson reaction, when the aqueous medium clearly favours the formation of polar intermediates. Nevertheless, the cyclization product was obtained by Hugershoff's reaction, *i.e.* under conditions which give more chances to the appearance of neutral radicalic species, and by irradiation, when there are well-grounded reasons to bring in the forefront the radicalic and not the ionic species.

The facts reported here are also pointing out to another peculiarity of the chemical behaviour of the thioureas **1**, namely, the quantitative dethionation under the action of potassium ferricyanide.

EXPERIMENTAL

All melting points are uncorrected. The IR spectra were recorded in KBr pellets with an UR—10 Carl Zeiss Jena double-beam spectrophotometer, the ^1H-NMR spectra were taken in $CDCl_3$ at 100 MHz with an HA—100 Varian Associated spectrometer with TMS as internal reference, and the mass spectra were obtained with an Atlas CH—4 spectrometer.

Irradiation experiments were carried out by means of a 400W high-pressure Hg lamp, the 5% benzene solutions of **1** being irradiated in open quartz vessels located 20 cm apart from the lamp.

1-Phenyl-3-(2-phenyl-4-thiazolylmethyl)-urea (**2**, R=H)

A solution of 0.5 g. **1** (R=H) in 10 ml ethanol was treated with 12 ml 8% aqueous NaOH solution, then with 10 ml of 20% aqueous $K_3[Fe(CN)_6]$. A white precipitate was immediately formed; after filtration, it was recrystallized from $CHCl_3$, then from benzene or ethanol, to give cca. 0.4 g **2** (R=H), m. 197° identical (TLC, IR and mixed m.p.) with an authentic sample.[1]

2-Phenyl-4- [(2-benzothiazolyl-amino)-methyl] -thiazole (**5**, R=H)

A suspension of 0.5 g **1** (R=H), in 10 ml glacial acetic acid was treated at room temperature, under stirring, with 0.2 ml sulphuryl chloride. The stirring was continued for 1 hr, another portion of 0.1 ml SO_2Cl_2 added, the mixture stirred for further 2 hrs, poured in water and rendered alkaline with Na_2CO_3. After overnight standing the white powder was filtered, dried, suspended in 25 ml hot benzene and treated with a few drops of ethanol to get a clear solution; the latter was poured on 250 ml petroleum ether (b. p. 38—41°) and the precipitate was isolated and recrystallized from 30 ml aqueous methanol to yield cca. 0.2 g **2** (R=H), m. 197°, identical with an authentic sample.[1]

The petroleum ether mother liquor obtained after the separation of the urea derivative was evaporated to dryness, the residue recrystallized from aqueous methanol, then from toluene, to give 0.1 g **5** (R=H), m. 172°.

Found : N, 13.08 ; $C_{17}H_{13}N_3S_2$ requires N, 12.99%.

All compounds in the Table were similarly prepared. Acetonitrile and chloroform can also serve as solvents for the above reaction.

TABLE

2-Aryl-4-[(2-benzothiazolyl-amino)-methyl]-thiazoles, **5**

R	m.p. °C	Molecular formula	N%	
			calculated	found
$3-CH_3$	169	$C_{17}H_{15}N_3S_2$	12.45	12.31
$4-CH_3$	178	$C_{17}H_{15}N_3S_2$	12.45	12.78
4−Br	183	$C_{16}H_{12}BrN_3S_2$	10.44	10.35

ACKNOWLEDGEMENTS. Acknowledgement is expressed to Dr. W. Schäffer, Max Planck Institut für Biochimie, München and to Dr. I. Oprean for recording the ^1H-NMR spectra and the mass spectra, to Mrs. E. Hamburg for the IR spectra and to the team of the Microanalytical Laboratory of the Institute of Chemistry, Cluj-Napoca, for the elemental analyses.

REFERENCES

[1] Part II, S. Silberg and I. A. Silberg, *Rev. Roumaine Chim.*, **27**, 69 (1982).

[2] J. M. Sprague and A. H. Land, "Thiazoles and Benzothiazoles" in "Heterocyclic Compounds" (R. C. Elderfield, ed.) vol. 5, p. 484 ; Wiley, New York, 1957.

[3] P. Jacobson, *Ber. dtsch. chem. Ges.*, **19**, 1067 (1886).

[4] A. Hugershoff, *Ber. dtsch. chem. Ges.*, **34**, 3130 (1901).

[5] T. Takahashi and J. Okada, *J. Pharm. Soc. Japan*, **71**, 898 (1951) ; *Chem. Abstr.*, **46**, 8091 (1952).

[6] C. H. F. Allen and J. van Allan, *Org. Synth.*, **22**, 16 (1942).

[7] H. Budzikiewicz, C. Djerassi and D. H. Williams, "Mass Spectrometry of Organic Compounds", Holden-Day Inc., San Francisco, 1967, p. 507.

[8] S. Petersen in "Houben-Weyl's Methoden der organischen Chemie" (E. Müller, ed.) 4th Edition, vol. VIII/3, p. 163 ; Georg Thieme Verlag, Stuttgart, 1952.

[9] S. Silberg, I. A. Silberg and C. Bodea (Part IV of this series), *Rev. Roumaine Chim.*, **27**, 0000 (1982).

[10] A. Schönberg, "Preparative Organic Photochemistry", Springer Verlag, Berlin, 1967, p. 126.

Revue Roumaine de Chimie, 28, 2, 147—150 (1983)

KINETICS OF DECARBOXYLATION OF β-PYRIDYLACRYLIC ACIDS

C. STOICESCU

Chemical and Pharmaceutical Research Institute, 112 Sos. Vitan, Bucharest, Romania

Received September 30, 1981

Kinetic data are reported for the decarboxylation of β-pyridylacrylic acids in quinoline solution, in the presence of copper metal as catalyst. The activation parameters were calculated and the isokinetic temperature was determined. A Hammett correlation with the substituent constants for the aza group of the pyridine nucleus was established.

The decarboxylation reaction of α, β-unsaturated carboxylic acids is a well-known method used for the synthesis of certain vinyl monomers. Although kinetics and mechanism of the decarboxylation reaction were largely investigated, no data have yet been reported on the decarboxylation of β-pyridylacrylic acids. Therefore, we investigated the kinetics of the decarboxylation reaction of β-pyridylacrylic acids in connection with our studies on structure-reactivity relationships in pyridine derivative series. The decarboxylation reaction was followed at temperatures ranging between 190—220°, in quinoline solution, in the presence of copper metal.

RESULTS

The first-order rate constants for the decarboxylation of β-pyridylacrylic acids were calculated by the method of least squares and are listed in Table 1. The activation parameters are presented in Table 2.

TABLE 1

First-order rate constants for the decarboxylation of β-pyridylacrylic acids

Acid	Temp. °C	$k \times 10^5 \cdot s^{-1}$	Standard deviation
2-Pyridylacrylic	190	1.44	0.003
	207	4.10	0.006
	219	7.72	0.004
3-Pyridylacrylic	190	0.68	(0.013)
	207	2.57	0.016
	219	5.73	0.012
4-Pyridylacrylic	190	0.30	(0.004)
	207	1.58	0.003
	219	4.18	0.006

TABLE 2

Activation parameters for the decarboxylation of β-pyridylacrylic acids

Acid	E_{act} kcal/ mole	$\Delta H^{\neq}$ kcal/mole	$\Delta S^{\neq}$ e.u./ mole
2-Pyridylacrylic	25.45	24.85	−27.88
3-Pyridylacrylic	32.21	30.81	−16.41
4-Pyridylacrylic	38.67	37.56	− 3.33

From the slope of the line resulted by plotting $\Delta H^{\neq}$ vs. $\Delta S^{\neq}$, the isokinetic temperature was determined, $T_{iso} = 517$ K (Figure 1).

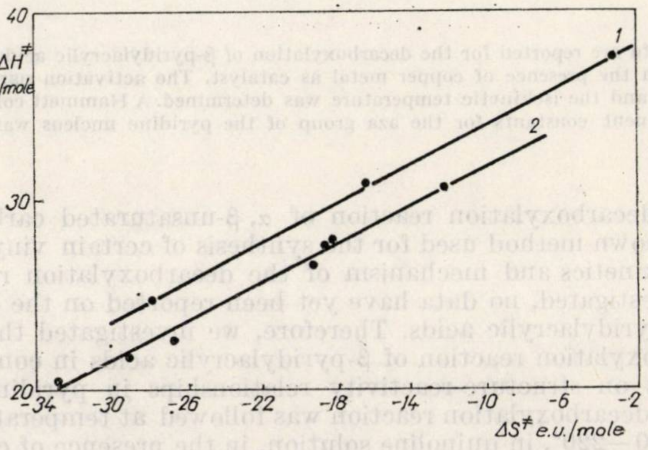

Fig. 1. — Plot of enthalpy vs. entropy of activation for the decarboxylation of β-pyridylacrylic acids (line 1) and β-phenyl- and β-naphthylacrylic acids (line 2) (from ref. 1).

DISCUSSION

Shur and Ishchenko[1] studied the kinetics of decarboxylation of cinnamic, nitrocinnamic, naphthylacrylic and nitronaphthylacrylic acids in quinoline, in the presence of copper metal, at temperatures between 200—230°. Based on the reported data, we calculated the corresponding activation parameters and determined the isokinetic temperature for the phenyl- and naphthylacrylic acid series. The value, $T_{iso} = 518.5$ K was found which being almost identical to that found for the decarboxylation of β-pyridylacrylic acids, confirms that the decarboxylation reaction of both β-aryl- and β-heteroarylacrylic acids takes place by the same mechanism.

According to Cohen[2], the copper-catalyzed decarboxylation of α, β-unsaturated acids in the presence of amines occurs via the electrophilic attack of the Cu(I) ion (present in the reaction mixture or formed *in situ* either by oxidation of copper metal or by reduction of the copper oxide found on the surface of copper metal, as proved by Shur [1]) and results in the formation of a π complex which stabilizes the negative charge which develops by the elimination of carbon dioxide, hence involving an organocopper intermediate (cf. scheme I).

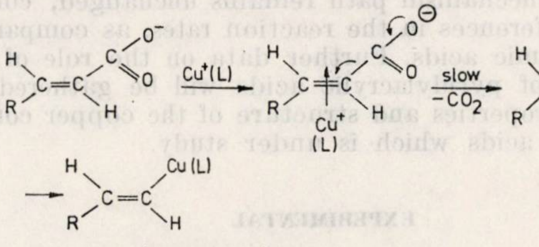

(L=quinoline)

Scheme I

The occurrence of the organocopper intermediates in copper-catalyzed decarboxylations was proved by Nilsson [3] in the decarboxylative coupling of some nitroaromatic acids, as well as by Cairncross *et al.* [4] in the decarboxylation of the copper(I) salts of some aromatic and aliphatic carboxylic acids. Although it is generally admitted that in the uncatalyzed decarboxylation of carboxylic acids, quinoline produces the ionization of the acid, affording the quinolinium salt, followed by the attack of the quinolinium ion at C_α ,[5] we consider that in the copper-catalyzed decarboxylation, quinoline provides a stabilization of the complexed carbanion and increases the rate of the slow step, i.e. the elimination of carbon dioxide. This effect would also account for the linear increase of the rate constant with increasing quinoline concentration on the whole 0–100 % molar range, as reported by Shur [1] for the copper-catalyzed decarboxylation of cinnamic acid, without the occurrence of a plateau or a maximum, such as in the uncatalyzed decarboxylation of salicylic acid in the presence of quinoline, as reported by Dunn .[5] By heating the β-pyridylacrylic acids in quinoline solution within the studied temperature range (190–220°), in the absence of copper metal, no evolvement of carbon dioxide was observed.

We further tried to correlate the kinetic data with the substituent constant for the aza group of the pyridine nucleus as determined by Katritzky [6] from NMR measurements on β-pyridylacrylic acids. A good linear correlation of $\log k/k_0$ (k_0 is the rate constant for the decarboxylation of cinnamic acid), at a temperature of 219°, was found by using the σ values determined for the corresponding pyridinium ions ($r = 0.991$, $S = 0.014$) with a slope $\rho = 0.289$. This result corroborates Katritzky's conclusion that in the case of pyridinium ions, the inductive effects are prevailing over the mesomeric ones. Brown [7] proved that a zwitterion is involved in the transition state of the decarboxylation of 6-substituted pyridine-2-carboxylic acids. A similar zwitterionic mechanism was confirmed by Taylor [8,9] for the decarboxylation of pyridylacetic acids. The Hammett correlation with the substituent constants for the $\geqslant NH^+$ group seems to indicate the occurrence of a zwitterion in the rate-determining step. However, if the specific catalytic effect of copper is taken into account, the formation of the zwitterion is not a prerequisite for decarboxylation, as in the case of picolinic or pyridylacetic acids, at least within the studied temperature interval. Given the well-known ability of pyridine nitrogen to form complexes with most transition metals, it is most probable that such a complex develops in the transition state, which, although the overall mechanism path remains unchanged, could nevertheless explain the differences in the reaction rates, as compared to cinnamic and nitrocinnamic acids. Further data on the role of copper in the decarboxylation of pyridylacrylic acids will be gathered from the examination of the properties and structure of the copper complexes of the above-mentioned acids which is under study.

EXPERIMENTAL

β-Pyridylacrylic acids were prepared and purified according to the methods described in literature : 2-pyridylacrylic acid,[10] m.p. 202°, 3-pyridylacrylic acid,[11] m.p. 223°, 4-pyridylacrylic acid,[12] m.p. 296°. Reagent grade quinoline (Austranal) was distilled before use. Reagent grade powder copper metal was used without further purification.

Decarboxylation was followed by direct measurement of the volume of evolved carbon dioxide collected in a gas buret at room temperature and atmospheric pressure. Temperature control was obtained by immersing the reaction flask in a lagged vapour bath containing a suitable liquid boiling under reflux at atmospheric pressure. The temperature could be maintained constant to ± 0.1°. The values of the rate constant shown in Table 1 are the average of three determinations.

REFERENCES

[1] A. M. Shur and R. I. Ishchenko, *Izvest. V.U.Z. Khim. i khim. Tekhnol.*, **17**, 844 (1974).

[2] T. Cohen and R. A. Schambach, *J. Amer. Chem. Soc.*, **92**, 3189 (1970).

[3] C. Björklund and M. Nilsson, *Acta Chem. Scand.*, **22**, 2585 (1968).

[4] A. Cairncross, J. R. Roland, R. M. Henderson and W. A. Sheppard, *J. Amer. Chem. Soc.*, **92**, 3187 (1970).

[5] A. N. Bourns, J. Buccini, G. F. Dunn and W. Rodewald, *Canad. J. Chem.*, **46**, 3915 (1968).

[6] A. R. Katritzky and F. J. Swinbourne, *J. Chem. Soc.*, **1965**, 6707.

[7] E. V. Brown and R. J. Moser, *J. Org. Chem.*, **36**, 454 (1971).

[8] P. J. Taylor, *J. Chem. Soc. Perkin Trans. II*, **1972**, 1077.

[9] R. G. Button and P. J. Taylor, *J. Chem. Soc. Perkin Trans. II*, **1973**, 557.

[10] C. W. Tullock and S. M. McElvain, *J. Amer. Chem. Soc.*, **81**, 961 (1939).

[11] A. Dornow and W. Schacht, *Chem. Ber.*, **80**, 505 (1947).

[12] M. Kleiman and S. Weinhouse, *J. Org. Chem.*, **10**, 562 (1945).

Revue Roumaine de Chimie, 28, *2*, 151 – 167 (1983)

DAS VERHALTEN EINIGER AMINONAPHTOLSULFOSÄUREN IN DER AZOKUPPLUNGSREAKTION

H.W. LANGFELD und S. IONIŢĂ
Farbstoffunternehmen „Colorom“ Codlea, Rumänien

Eingegangen am 28. Dezember 1981

Anhand einer halbquantitativen chromatographischen Methode wurden bei verschiedenen *p*H-Werten und mit verschieden reaktiven Diazoniumsalzen erhaltene Azokupplungsmassen der technisch oft eingesetzten H-, I- und γ-Säure untersucht. Dabei sind die möglichen Isomere, sowie ihr Anteil am Reaktionsprodukt unter dem Einfluss der angewandten Reaktionsbedingungen festgestellt worden und aufgrund der Ergebnisse, die auch durch *p*K-Bestimmungen unterstützt wurden, gelangt man zu Schlüssen bezüglich der höchsterreichbaren Selektivität der Azokupplung. Es wurden auch bis jetzt weniger behandelte Erscheinungen erklärt, darunter warum in stark saurem Medium die sauer gekuppelten Monoazoderivate der H- und I-Säure leichter in einer von der OH-Gruppe bestimmten Stellung kuppeln, als die freien Aminonaphtolsulfosäuren.

The azocoupling reaction mixtures obtained from the frequently used H-, I- and γ-acids and different reactive diazonium-salts were examined at different *p*H-values by means of a semi-quantitative chromatographic method. The different isomers, as well as their participation in the reaction product under different reaction conditions have been proved. Based on these results which are also supported by *p*K-determinations, conclusions were drawn concerning the highest possible selectivity of the azocoupling reaction. At the same time less studied phenomena could be explained, e.g. why in a strongly acidic medium the acidly coupled monoazoderivatives of the H- and I-acids couple easier, in a position determined by the OH-group, than the free aminonaphtolsulfonic acids.

EINLEITUNG

Die Aminonaphtolsulfosäuren stellen wertvolle Azokupplungskomponenten dar. [1] In der Technologie der Azofarbstoffe haben sich besonders die H-(1,8-Aminonaphtol-3,6-disulfo-), I-(2,5-Aminonaphtol-7-sulfo-) und γ-(2,8-Aminonaphtol-6-sulfo-) Säure durchgesetzt:

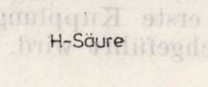

H-Säure

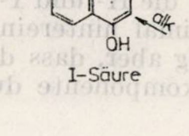

I-Säure

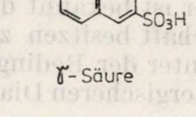

γ- Säure

Die Kinetik der Azokupplung dieser Substanzen entspricht in erster Näherung folgender Gleichung[2]:

$$\frac{d(\mathrm{Az}_{NH_2} + \mathrm{Az}_{OH})}{dt} = [\mathrm{Ar}-\overset{+}{\mathrm{N}}\equiv\mathrm{N}](k_{NH_2}\cdot[\mathrm{HO}-\mathrm{R}-\mathrm{NH_2}] +$$

$$+ k_{OH}\cdot[{}^{-}\mathrm{O}-\mathrm{R}-\mathrm{NH_2}])$$

wobei Az_{NH_2} und Az_{OH} die durch Kupplung in einer von der NH_2, bzw. OH-Gruppe bestimmten Stellung erhaltenen Azoderivate und k_{NH_2}, bzw. k_{OH} die entsprechenden Reaktionsgeschwindigkeitskonstanten darstellen. Der Verlauf der Reaktion hängt in wässerigem Medium von der Konzentration der reaktiven Formen der Kupplungskomponente (freies Amin, bzw. Naphtolat-Ion[3]), also vom *p*H-Wert der Reaktionsmasse, von den *p*K-Werten der funktionellen Gruppen der Kupplungskomponente, sowie vom Verhältnis k_{OH}/k_{NH_2} ab. Da im allgemeinen $pK_{NH_2} \cong 4$ und $pK_{OH} \cong 9$, ergibt sich dass:

— in schwach saurem Medium ($p\mathrm{H} = 4 \ldots 6$) das Aminophenol praktisch total als $\mathrm{HO}-\mathrm{R}-\mathrm{NH_2}$ vorliegt, da die Konzentration des Aminophenolat-Ions unter diesen Bedingungen weniger als 1 % der stöchiometrischen Konzentration ausmacht. Aus diesem Grunde wird in schwach saurem Medium die Bildung des Amino-Azoderivats begünstigt, auch wenn $k_{NH_2} < k_{OH}$ (da $[{}^{-}\mathrm{O}-\mathrm{R}-\mathrm{NH_2}]$ sehr klein ist, folgt das $k_{NH_2}\cdot[\mathrm{HO}-\mathrm{R}-\mathrm{NH_2}] \gg k_{OH}\cdot[{}^{-}\mathrm{O}-\mathrm{R}-\mathrm{NH_2}]$).

— in alkalischem Medium, bei $p\mathrm{H} > 9$, die Konzentrationen der Amino- und Phenolat-Gruppen vergleichbar sind, so dass das Verhälnis der gebildeten isomeren Azoderivate vom Verhältnis der Reaktionsgeschwindigkeitskonstanten k_{OH}/k_{NH_2} abhängig wird. Gewöhnlich ist $k_{OH} \gg k_{NH_2}$, das Verhältnis k_{OH}/k_{NH_2} wird aber durch die Intensivierung der elektrophylen Aktivität der Diazokomponente herabgesetzt. Das heisst dass im alkalischen Medium die Bildung des Hydroxy-Azoderivats wie immer favorisiert wird, dass aber der Anteil des Amino-Azoderivats im Reaktionsgemisch der isomeren Azoprodukte je mehr ansteigt, desto grösser die Reaktivität des Diazoniumsalzes ist.

Wenn die NH_2- und OH-Gruppen in α-Stellungen des Naphtalinkerns haften, muss darüber hinaus das Eintreten der *ortho/para*-Isomerie berücksichtigt werden. Das *ortho/ para*-Verhältnis wird durch die Reaktivität des Diazoderivats, durch die Gegenwart von Basen, sowie durch die Temperatur beeinflusst.[4] Bei der alkalischen Kupplung der I-Säure konnten die zwei Isomere erkannt und getrennt werden.[5] Für die H- und γ-Säure liegen aber keine ähnliche Erkenntnisse vor. Meistens werden als mögliche Kupplungsstellen nur die bei den Formeln von weiter oben durch Pfeile angedeuteten Stellen angegeben.[6–10]

Weiter ist bekannt dass die H- und I-Säure (nicht aber die γ-Säure) die Eigenschaft besitzen zweimal hintereinander zu Disazoderivaten zu kuppeln, unter der Bedingung aber, dass die erste Kupplung sauer und mit der energischeren Diazokomponente durchgeführt wird.[7] Obwohl in solchen Fällen die Synthese des Monoazowischenprodukts bei pH $\doteq$ 2...3 erfolgt (um Bedingungen der maximalen Selektivität der sauren Kupplung zu sichern), ist manchmal neben dem sauer gekuppelten Monoazoderivat auch das Doppelkupplungsprodukt, nicht aber das Monoazoderivat der alkalischen Kupplung festgestellt worden. [8,9] Es ist wie wenn das Monoazoderivat der sauren Kupplung leichter als die freie Aminonaphtolsulfosäure in *ortho/para* gegenüber der OH-Gruppe reagiert, was äusserst interessant ist, da die Einführung eines Arylazo-Restes—ins Molekül des Letzteren (infolge der sauren Kupplung) eine allgemein desaktivierende Wirkung haben müsste. Auf diese Wirkung basiert übrigens die Erklärung der Unmöglichkeit einer zweiten Kupplung mit der H- und I-Säure, falls die erste Kupplung alkalisch durchgeführt wird. [7]

Aus dem bisher Erwähnten ergibt sich die Schwierigkeit der Darstellung von reinen Azoderivaten der H-, I- und γ-Säure, gleichzeitig aber auch die Bedeutung der Erkenntnis sämtlicher möglichen Isomere, sowie ihres Anteils in der Zusammensetzung des Azokupplungsproduktes.

In der vorliegenden Arbeit wird ein Beitrag zur Erläuterung ungeklärter Aspekte der Kupplungsreaktion der drei Aminonaphtolsulfosäuren erbracht, indem die durch Änderung einiger wichtig empfundenen Reaktionsparameter erhaltenen Kupplungsprodukte chromatographisch untersucht werden. Um die Erklärung der dabei gemachten Feststellungen zu stützen, wurden gleichzeitig pK-Bestimmungen durchgeführt.

ERGEBNISSE UND DISKUSSIONEN

1. DURCHGEFÜHRTE AZOKUPPLUNGEN UND MÖGLICHE REAKTIONSPRODUKTE

In der Hauptreihe der Versuche wurde als Azokomponente das 4-Nitrodiazobenzol angewendet, das infolge der genügend grossen (im allgemeinen als durchschnittlich betrachteten [1]) Reaktivität, eine dem gesetzten Ziel entsprechende Selektivität besitzt. Es wurde dabei auch darauf Rücksicht genommen dass das Diazoderivat des 4-Nitroanilins oft zur Darstellung von Monoazozwischenprodukten des untersuchten Typus herangezogen wird. [1, 6, 10–16]

Die Kupplungen wurden bei verschiedenen pH-Werten, zwischen 1 ... 10, unter denselben Bedingungen der Konzentration, der Reagenszugabe, der Temperatur und der Rührung durchgeführt. Die der chromatographischen Analyse unterstellten Proben wurden der Reaktionsmasse nach Erreichen des maximalen Umsatzes entnommen.

Um den Einfluss der elektrophylen Aktivität des Diazoniumsalzes auf die Art und dem Anteilverhältnis der gebildeten Isomere hervorzuheben, wurden gleichzeitig vergleichende Azokupplungen mit Diazobenzol (wenig aktiv) und mit 5-Nitro-2-diazobenzoesäure (sehr aktiv) durchgeführt. Beide Diazoderivate werden technisch eingesetzt. [1] Die Kupplungen mit Diazobenzol erfolgen gewöhnlich in alkalischem Medium, während die mit 5-Nitro-2-diazobenzoesäure in stark saurem, so dass in der vorliegenden Arbeit die vergleichenden Versuche mit dem ersten Diazoderivat bei pH = 8 und die mit dem zweiten bei pH=1 durchgeführt wurden.

Um die Identifizierung der verschiedenen Reaktionsprodukte zu ermöglichen sind weiter hinaus Kupplungen mit azetylierten, bzw. mit Benzolsulfochlorid verersterten N- bzw. O-Acylderivaten der drei Aminonaphtolsulfosäuren durchgeführt worden. Nach anschliessender hydrolytischer Abspaltung der Acylreste sind so in von der NH_2—, bzw. OH-Gruppe bestimmten Stellungen, selektiv gekuppelte Azoderivate erhalten worden.

Gemäss den bekannten Substitutionsregeln des Naphtalinkerns, sowie der praktisch festgestellten Regelmässigkeiten der doppelten Kupplung der Aminonaphtole, müssten sich infolge der Reaktion mit 4-Nitrodiazobenzol folgende Azoderivate bilden:

a) Im Falle der H-Säure:

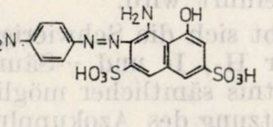

O_2N
N=N
H_2N
OH
HO_3S
SO_3H

I

4-Nitranilin $\xrightarrow{\text{sauer }(o-)}$ H-Säure

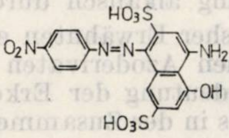

O_2N
N=N
HO_3S
NH_2
OH
HO_3S

II

4-Nitranilin $\xrightarrow{\text{sauer }(p-)}$ H-Säure

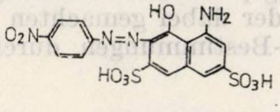

O_2N
N=N
HO
NH_2
HO_3S
SO_3H

III

4-Nitranilin $\xrightarrow{\text{alk.}(o-)}$ H-Säure

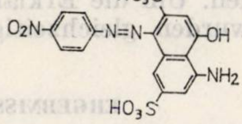

HO_3S
O_2N
N=N
OH
NH_2
HO_3S

IV

4-Nitranilin $\xrightarrow{\text{alk.}(p-)}$ H-Säure

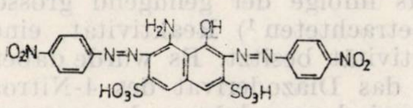

O_2N
N=N
H_2N
OH
N=N
NO_2
HO_3S
SO_3H

V

4-Nitranilin $\xrightarrow{\text{sauer }(o-)}$

H-Säure

4-Nitranilin $\xrightarrow{\text{alk. }(o-)}$

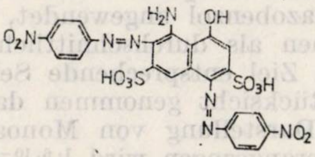

O_2N
N=N
H_2N
OH
HO_3S
SO_3H
N
N
NO_2

VI

4-Nitranilin $\xrightarrow{\text{sauer }(o-)}$

H-Säure

4-Nitranilin $\xrightarrow{\text{alk. }(p-)}$

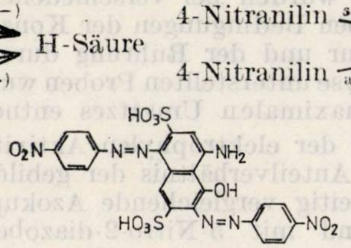

HO_3S
O_2N
N=N
NH_2
OH
HO_3S
N=N
NO_2

VII

4-Nitranilin $\xrightarrow{\text{sauer }(p-)}$

H-Säure

4-Nitranilin $\xrightarrow{\text{alk. }(o-)}$

Das durch Doppelkupplung in den Stellungen 4,5 erreichbare Isomer kann sich infolge sterischer Hinderung nicht bilden.

b) Im Falle der I-Säure:

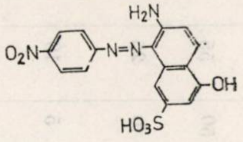
VIII

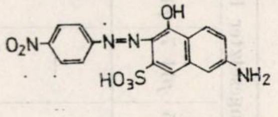
IX

4-Nitranilin $\xrightarrow{\text{sauer}}$ I-Säure 4-Nitranilin $\xrightarrow{\text{alk. } (o-1)}$ I-Säure

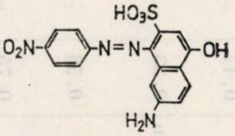
X

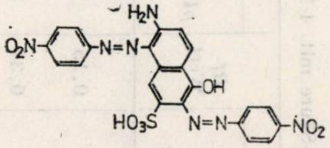
XI

4-Nitranilin $\xrightarrow{\text{alk. } (p)}$ I-Säure

4-Nitranilin $\xrightarrow{\text{sauer}}$ I-Säure

4-Nitranilin $\xrightarrow{\text{alk. } (o-)}$ I-Säure

Das 1,8-Doppelkupplungsprodukt kann sich aus sterischen Gründen nicht bilden.

c) Im Falle der γ-Säure

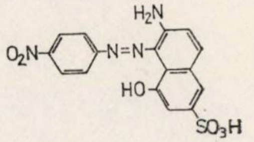
XII

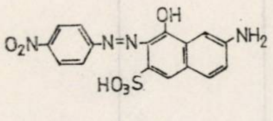
XIII

4-Nitranilin $\xrightarrow{\text{sauer}}$ γ-Säure 4-Nitranilin $\xrightarrow{\text{alk. } (o-)}$ γ-Säure

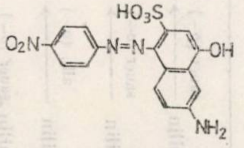
XIV

4-Nitranilin $\xrightarrow{\text{alk. } (p)}$ γ-Säure

Infolge der Wasserstoffbindung zwischen den *peri*-ständigen OH- und Azo-Gruppen, welche die Acidität der ersten stark reduziert, kann das Monoazoderivat XII nur unter aussergewöhnlichen (in 2,5 N NaOH-Lösung [11]), in der vorliegenden Arbeit nicht erreichten Bedingungen gekuppelt werden. Die Bildung eines Disazoderivats der γ-Säure wurde deswegen nicht angenommen.

Durch Einsatz von Diazobenzol, bzw. 5-Nitro-2-diazobenzoesäure als Diazokomponente bilden sich analoge Azoderivate.

2. DIE CHROMATOGRAME

Es wurden Dünnschichtchromatograme auf Silicagel G der Firma „Merck" — Darmstadt/BRD. durchgeführt. Als Fliessmittel diente ein vorerst bei Trennungen von ähnlichen Substanzen geprüftes ternäres Gemisch *n*-Butanol/Äthanol/ wässr. Ammoniak 25 % (3 : 1 : 1). [12]

Die Chromatograme wurden halbquantitativ ausgelegt, aufgrud eines bekannten Verfahrens. [13,14]

Die angewendeten Identifizierungskriterien der Azokupplungsprodukte werden im experimentellen Teil ausführlich beschrieben.

3.1. Chromatograme der Kupplungsprodukte der H-Säure

Die Ergebnisse der chromatographischen Trennung werden in den Tabellen 1, 2, und 3 zusammengefasst. Sie führen zu folgenden Schlüssen :

— Im Kupplungsprozess der H-Säure können sich, abhängig von den Reaktionsbedingungen, sämtliche sieben Isomere bilden. Dass das Disazoderivat VII in den Chromatogramen nicht festgestellt wurde, ist auf die in der Arbeit angewandte Kupplungstechnik zurückzuführen. Wenn die bei $pH = 1$ gewonnene Reaktionsmasse (mit einem 10 %-igen Gehalt an Azoderivat II) anschliessend auf $pH = 8$ gebracht worden wäre, dann hätte sich unter einem leichten Überschuss an 4-Nitrodiazobenzol, mit Sicherheit auch das Disazoderivat VII gebildet, da dieses das Produkt der alkalischen Kupplung des Azoderivats II darstellt.

TABELLE 2

Chromatographische Trennung der Kupplungsprodukte der H-Säure mit Diazobenzol

Die Substanz	Farbe der Flecke		*Rf*-Wert	Anteil in % umgesetzter H-Säure $pH = 8$
	in saurem Medium	in alkalischem Medium		
Anilin $\xrightarrow{\text{alk. }(o-)}$ H-Säure	rot	rot		80
Anilin $\xrightarrow{\text{sauer }(o-)}$ Anilin $\xrightarrow{\text{alk. }(o-)}$ H-Säure	blau	blau	0,52	10
Anilin $\xrightarrow{\text{alk. }(p-)}$ H-Säure	rot	rötlich-blau	0,60	10

— Die grösste Selektivität der Reaktion ist in stark saurem Bereich festzustellen, aber auch bei $pH = 1$ bildet sich nicht nur das o-NH_2-Kupplungsprodukt (Azoderivat I). Der Anteil des *para*-Isomers steigt mit dem pH relativ an (bei $pH = 1$: 10% *para*, $85 + 5 = 90$% *ortho*; bei $pH = 3$: 5% *para*, $30-55 = 85$% *ortho*).

Das Disazoderivat V ist bei $pH = 1$ ebenfalls feststellbar (trotzdem sich unter denselben Bedingungen das Monokupplungsprodukt in einer durch die OH-Gruppe bestimmten Stellung nicht bildet).

— Die Selektivität der alkalischen Kupplung ist gering und wird auch von der Reaktivität des Diazoderivats beeinflusst.

— Die Reaktionsmasse der Kupplung mit Diazobenzol enthält in kleineren Mengen Disazoderivate und auch weniger p-OH-Monoazoderivat.

— Dem gegenüber, falls die NH_2-Gruppe vorher acyliert wird, kann eine sehr grosse Selektivität erreicht werden (Tabelle 3). Bei Anwendung eines Diazoderivats mit geringer Elektrophylität wird so die ausschliessliche Bildung des o-OH-Kupplungsproduktes möglich.

TABELLE 3

Chromatographische Trennung der Kupplungsprodukte der N-Azetyl-H-Säure mit 4-Nitrodiazobenzol

Die Substanz	Farbe der Flecke		*Rf*-Wert	Anteil in % umgesetzten N-Azetyl-H-Säure $pH = 7 \ldots 8$
	in saurem Medium	in alkalischem Medium		
4-Nitranilin $\xrightarrow{\text{alk. } (o-)}$ N-Azetyl-H-Säure	rot	rot	0,55	82
4-Nitranilin $\xrightarrow{\text{alk. } (p-)}$ N-Azetyl-H-Säure	dunkel-rot	rötlich-blau	0,63	18

3.2. Chromatograme der Kupplungsprodukte der I-Säure

Aus den in der Tabelle 4 zusammengefassten Ergebnissen geht hervor dass die I-Säure sich gegenüber der H-Säure verschieden verhält:

— In stark saurem Bereich, bei $pH = 1$, bildet sich in grösserem Masse Disazoderivat (20%, gegenüber nur 5% bei den H-Säure), ohne dass dabei, ähnlich wie bei der H-Säure, das in einer von der OH-Gruppe bestimmten Stellung gekuppelte Monoazoderivat festzustellen wäre. Daraus folgt dass die einheitliche Darstellung des o-NH_2-Monokupplungsproduktes der I-Säure auf grössere Schwierigkeiten stösst (Diese sind unter besonderen Bedingungen überwindbar: grosse Acidität des Reaktionsmediums, Anwendung eines Diazoniumsalzes mit hoher elektrophyler Aktivität, Reaktantenzugabe so geregelt dass ein Diazoderivatüberschuss, sei es auch nur zeitweilig und lokal, vermieden wird).

— Andererseits, überwiegen schon bei $pH = 5$ die durch Kupplung in einer von der OH-Gruppe bestimmten Stellung erhaltenen Azoderivate. Bei $pH = 5$ ist der Anteil des *para*-Kupplungsproduktes mit 4-Nitranilin noch unbedeutend, er vergrössert sich aber mit dem Anstieg des pH-

Wertes. Bei $pH = 10$ ist das Substitutionsverhältnis *ortho/para* gleich 1,2 gegenüber von 3,5 im Falle der H-Säure und 3,4 in dem der γ-Säure (Tabellen 1, bzw. 7). So wie die Kupplungsergebnisse mit 5-Nitro-2-diazobenzoesäure zeigen (Tabelle 5), wird das *ortho/ para*-Verhältnis zusätzlich von der Aktivität des Diazoderivats stark beeinflusst.

Das besondere Verhalten der I-Säure ist die Folge der gegenseitigen Verstärkung des Orientierungseffektes der Gruppen OH und NH_2:

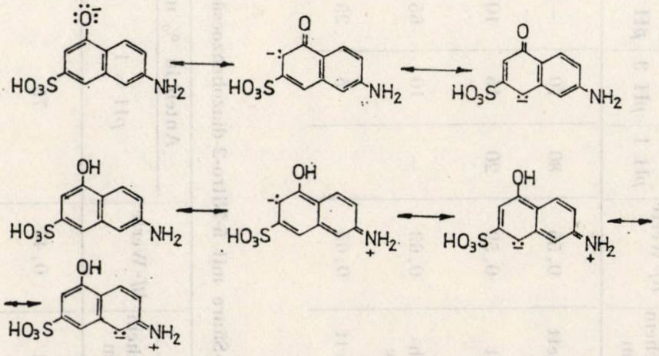

was im Falle der H- und γ-Säure nicht möglich ist. Eine ähnliche Erklärung ist von anderen Autoren für das Verhalten der „Dioxy-I"-Säure (1,6-Dihydroxynaphtalin-3-sulfosäure) gegeben worden[15].

Eine einheitliche Darstellung des *o*-OH-Monokupplungsproduktes der I-Säure gelingt nur in schwach saurem Bereich und nur unter vorheriger Blockierung der einsamen Elektronen der NH_2-Gruppe, z.B. durch Acylieren.

3.3. Chromatograme der Kupplungsprodukte der γ-Säure

Die in der Tabelle 7 zusammengefassten Ergebnisse erlauben folgende Schlüsse:

— in stark saurem Medium ($pH = 1$) wird das in *ortho*-Stellung gegenüber der NH_2-Gruppe gekuppelte Azoderivat rein erhalten.

— Die in einer von der OH-Gruppe bestimmten Stellung gekuppelten Azoderivate bilden sich schon bei $pH = 3$, aber sie überwiegen nur im alkalischen Bereich. Bei $pH = 8$ ist der Anteil des *o*-NH_2-Kupplungsproduktes unbedeutend, so dass unter diesen Bedingungen die Kupplung nur noch unter dem Einfluss der OH-Gruppe stattfindet (wobei der Anteil des *para*-Isomers nur bei $pH = 10$ 20% erreicht). Das *ortho/ para*-Substitutionsverhältnis nähert sich dem der H-Säure.

Der Unterschied gegenüber der I-Säure ist darauf zurückzuführen dass sich die Gruppen OH und NH_2 in ihrer Wirkung gegenseitg aufheben.

— Es ist in keinem der Versuche das Doppelkupplungsprodukt erhalten worden, was mit den Kenntnissen über das spezifische Verhalten der γ-Säure[1] übereinstimmt.

4. BESTIMMUNGEN VON *p*K-WERTEN

Es wurden die pK_{NH_2} — und pK_{OH}—Werte de H—, I— und γ-Säure, sowie der Azoderivate I (4-Nitranilin $\xrightarrow{\text{sauer } (o-)}$ H-Säure) und VIII (4-Nitranilin $\xrightarrow{\text{sauer}}$ I-Säure) potentiometrisch bestimmt.

In der Literatur werden ebenfalls potentiometrisch bestimmte *p*K-Werte der H-Säure erwähnt.[2] Weiter wird der spektrometrisch bestimmte pK_{OH}-Wert der 2-(4-Nitrobenzolazo)-1-Amino-8-naphtol-3,6-disulfosäure (Azoderivat I) erwähnt.[8] Die eigenen Ergebnisse stimmen gut mit diesen Literaturangaben überein. Für die I- und γ-Säure, sowie für das Azoderivat VIII konnten, mangels entsprechender Daten aus der Literatur, nicht Vergleiche gemacht werden.

Die in der Tabelle 8 zusammengefassten Ergebnisse erlauben folgende wichtigere Schlüsse :

— Die Anwesenheit von zwei SO_3H-Gruppen im Molekül der H-Säure bewirkt eine Abnahme der Basizität der NH_2-Gruppe und, implizite, eine merkliche Senkung des pK_{NH_2}-Wertes gegenüber der I- und γ-Säure. Aus diesem Grunde kann in stark saurem Medium die H-Säure auch mit mittelmässig aktiven Diazoniumsalzen gekuppelt werden. Gleichfalls ist der Selektivitätsbereich der in einer durch die NH_2-Gruppe bestimmten Stellung erfolgten Kupplung bei der H-Säure breiter als bei der I-Säure.

— Die pK_{OH}-Werte der drei Aminonaphtolsulfosäuren sind weniger differenziert, aber auch in ihrem Fall ist der pK_{OH}-Wert der H-Säure der niedrigste (was dem Säureverstärkungseffekt der Sulfogruppen zuzuschreiben ist).

— Die pK_{NH_2} — und pK_{OH}-Werte der I- und γ-Säure sind ihrerseits eine Folge der spezifischen Wechselwirkung der Gruppen NH_2, OH und SO_3H. Zum Beispiel, im Falle der γ-Säure bedingt die 2-stellige NH_2-Gruppe eine Erhöhung der Elektronendensität beim 6-stelligen Kohlenstoffatom an dem die SO_3H-Gruppe haftet, was zur Herabsetzung des Elektronenanziehenden Effekts dieser Gruppe gegenüber der OH-Gruppe führt. Die Folge ist eine Erniedrigung der Basizität der NH_2-Gruppe, gleichzeitig aber auch der Azidität der OH-Gruppe, was sich in einem kleinen pK_{NH_2}-Wert, bzw. einem grösseren pK_{OH}-Wert der γ-Säure, gegenüber der I-Säure (bei der die drei Gruppen anders zusammenwirken) äussert.

— Die Einführung eines Arylazorestes in einer Stellung die die Bildung der Wasserstoffbindung zur OH-Gruppe (wie z.B. im Falle der γ-Säure) nicht ermöglicht, bewirkt eine plötzliche Senkung des pK_{OH}-Wertes : von 8,25 auf 6,20 beim Azoderivat I, bzw. von 8,60 auf 5,15 beim Azoderivat VIII. Diese Erhöhung der Acidität der OH-Gruppe erklärt warum die Azoderivate I und VIII in saurem Medium leichter in einer von dieser Gruppe bestimmten Stellung kuppeln, als die ungekuppelte H- bzw. I-Säure. Der Effekt ist desto ausgesprochener, desto stärker die Gruppen OH und Arylazo zusammenwirken. Berücksichtigt man einerseits den niedrigen pK_{OH}-Wert des Azoderivats VIII und andererseits den hohen pK_{NH_2}-Wert der eigentlichen I-Säure, ist zu erwarten dass die Doppelkupplung dieser Aminonaphtolsulfosäure auch in stark saurem Bereich, schwer zu vermeiden ist.

SCHLUSSFOLGERUNGEN

Die Ergebnisse dieser Arbeit ermöglichen folgende Schlüsse, die als Ergänzung der allgemeinen Kenntnisse über die Azokupplung der H-, I- und γ-Säure zu betrachten sind:

1. Alle drei Aminonaphtolsulfosäuren kuppeln auch in *para*-Stellung zu den α-stelligen NH_2- und OH-Gruppen. Bei der Monokupplung der H- und γ-Säure überschreitet der Anteil des *para*-Isomers im Kupplungsproduktengemisch nicht 20%. Demgegenüber kann im Falle der I-Säure der Anteil bis auf 40% ansteigen, was in der Technik negative Folgen hat, da das *para*-Kupplungsprodukt uninteressant ist.[1] Das *ortho*/*para*-Substitutionsverhältnis wird vom pH-Wert und von der Reaktivität des Diazoniumsalzes beeinflusst und zwar sinkt es beim Anstieg dieses Parameters, wobei der Effekt ausgesprochener bei der I-Säure zur Wirkung kommt.

Die *para*-Isomere bilden sich auch bei der doppelten Kupplung der H- und I-Säure.

2. Die grösste Kupplungsselektivität wird in saurem Medium erreicht. Ein reines Produkt resultiert nur im Falle der γ-Säure. Bei der H-Säure ist unter diesen Bedingungen die Bildung des sauer gekuppelten *para*-Isomers möglich. Wenn Diazoniumsalze mit mittelmässiger Reaktivität angewendet werden, kann aber der Anteil dieses Isomers stark herabgesetzt werden.

Hinzu kommt noch im Falle der H-Säure, und noch mehr im Falle der I-Säure die gleichzeitige Bildung des Disazoderivats. Dass in stark saurem Medium die zweite Kupplung leichter im Vergleich zur ersten Kupplung in *ortho*/*para*-Stellung gegenüber der OH-Gruppe erfolgt kann erklärt werden durch die Erhöhung der Acidität dieser Gruppe infolge der Wechselwirkung mit dem Elektronenanziehenden Arylazorest. Da der Effekt im Falle der I-Säure ausgeprägter zur Wirkung kommt, ist die reine Darstellung des sauer gekuppelten Monoazoderivats nur unter schwierigen Bedingungen, bei hoher Acidität und unter Anwendung eines Diazoderivats mit hoher Reaktivität, das bei diesen Bedingungen noch kupplungsfähig ist (da der pK_{NH_2}-Wert der I-Säure grösser ist wie der der H-Säure).

3. In alkalischem Medium ist die Selektivität der Kupplung gering. Praktisch werden alle möglichen Isomere erhalten. Es überwiegen aber de *o*/*p*-OH-Kupplungsprodukte, deren Anteil in Produktengemisch mit der Abnahme der Reaktivität des Diazoniumsalzes ansteigt.

Die Selektivität wird stark erhöht wenn die einsamen Elektronen der NH_2-Gruppe blockiert werden, z.B. durch Acylieren. Wenn ein Diazoderivat mit geringer Reaktivität angewendet wird erhält man bei der Kupplung mit N-acylierter H-Säure fast nur *o*-OH-Azoderivat. Die leuchtende Nuance der durch Kupplung der N-Azetyl-H-Säure mit Diazobenzol, *p*-Diazotoluol oder *p*-Diazoazetianilid erhaltenen Monoazoderivate, kann nicht nur durch die (infolge des Ersatzes der NH_2- mit der $NHCOCH_3$-Gruppe) eingetretene hypsochrome Verschiebung der Farbe erklärt werden, so wie es gewöhnlich geschieht,[16] sondern gleichzeitig durch die grössere Reinheit des Kupplungsproduktes, da die Bildung der (durch *o*/*p*-NH_2-, bzw. *p*-OH-Kupplung erhaltenen) Isomere mit unbeständiger, vom *p*H-Wert abhängiger Nuance, stark eingeschränkt wird.

Im Falle der γ-Säure ist im Bereich oberhalb *p*H = 8, die Kupplungsselktivität befriedigend (Der Anteil des *p*-OH-Isomers ist gering und die *o*-NH_2-Kupplung unbedeutend).

Demgegenüber erreicht aber die Selektivität der Kupplung mit N-Acetyl-I-Säure einen äusserst niederen Stand, da der Anteil des *p*-OH-Isomers sehr gross wird.

4. Im *p*H-Bereich 4 ... 7,5 ist die Kupplungsselektivität im allgemeinen gering. Im Falle der H- und γ-Säure sollte dieser Bereich vermieden werden.

Das schwach saure Reaktionsmedium ermöglicht aber im Falle der I-Säure die Darstellung des *o*-OH-Kupplungsproduktes mit zufriedenstellender Ausbeute bei geringstem Gehalt an *p*-Isomer. Wenn dazu die NH_2-Gruppe acyliert wird, erreicht die Selektivität ein Maximum, weil auch die Bildung des *o*-NH_2-Azoderivats vermieden wird.

So lassen sich die reineren, durch Kupplung mit N-substituierter I-Säure (N-Phenyl-, Benzoyl-, Naphtimidazolyl-, Triazolyl-, Thiazolyl-I-Säure-, Di-I-Säure, Scharlach-Säure u.s.w.[17]) erreichten Nuancen, sowie die Bevorzugung der Reihenfolge Acylierung- alkalische Kupplung in jeder technischen Synthese die diese zwei Reaktionen einschliesst,[18] erklären.

Dass im Falle der I-Säure die *o*/*p*-OH-Kupplung schon in schwach saurem Medium gegenüber der NH_2-Kupplung überwiegt ist auf die Wechselwirkung zwischen den zwei Gruppen, die sich im Orientierungseffekt gegenseitig verstärken, zurückzuführen.

EXPERIMENTELLER TEIL

Durchführung der Azokupplungen

Es wurden chemisch-reine Substanzen folgender Herkunft eingesetzt: H-und γ-Säure — „Schuchardt" — München/B.R.D., I-Säure — „Chemapol" — Prag/Tschechoslowakei, 4-Nitranilin — „Loba-Chemie" — Wien, Fischamend/Österreich, Anilin — „U.C.B." — Brüssel/Belgien. Die 5-Nitro-2-aminobenzoesäure war technisches Produkt, konz. 98 %, der Firma „Bayer" — B.R.D. und wurde durch Umkristallisieren aus Äthanol bis auf Schmp. 280°C gereinigt. Die N-Acylderivate der H-, I- und γ-Säure sind durch Behandlung mit Essigsäureanhydrid nach einem bekannten Verfahren[19] dargestellt worden. Ebenfalls nach einem bekannten Verfahren ist die Veresterung mit Benzolsulfochlorid der drei Aminonaphtolsulfosäuren erfolgt.[20]

Die Diazotierung des Anilins und 4-Nitranilins wurde mit Natriumnitrit in wässerig-mineralsäurem Medium nach bekannten Verfahren durchgeführt worden.[21] Die 5-Nitro-2-aminobenzoesäure wurde in fein dispergierter Form in wässeriger Salzsäure (3 Äquivalente) diazotiert.[22]

Die Azokupplungen erfolgten bei sechs verschiedenen pH-Werten. Das Diazoniumsalz und die Kupplungskomponente wurden gleichzeitig in eine wässerige Pufferlösung eingeführt, wobei ununterbrochen kontrolliert wurde dass sich kein wesentlicher Überschuss der Reaktionspartner, auch nur zeitweilig und lokal, einstellt (Probe mit H-Säurelösung für die Feststellung der Diazokomponente, bzw. mit 4-Nitrodiazobenzollösung für die Kupplungskomponente). Das Molarverhältnis der Komponenten war in allen Fällen 1 : 1 und die Zusammensetzung der Pufferlösungen folgende[23]:

*p*H = 125 ml 0,2 M KCl, 67 ml 0,2 M HCl, verdünnt auf 100 ml

*p*H = 350 ml 0,1 M KH-Phtalat, 22,3 ml 0,1 M HCl, verdünnt auf 100 ml
*p*H = 550 ml 0,1 M KH-Phtalat, 22,6 ml 0,1 M NaOH, verdünnt auf 100 ml
*p*H = 750 ml 0,1 M KH_2OU_4, 20,1 ml 0,1 M NaOH, verdünnt auf 100 ml
*p*H = 850 ml 0,1 M KH_2PO_4, 46,1 ml 0,1 M NaOH, verdünnt auf 100 ml
*p*H = 1050 ml 0,1 M KCl und H_3PO_3, 43,7 ml 0,1 M NaOH, verdünnt auf 100 ml.

Die Zuflussmenge der Reaktionspartner entsprach der Reaktionsgeschwindigkeit (welche erwartungsgemäss einen wesentlichen Anstieg von *p*H = 2 zu *p*H = 10 zeigte). Die Kupplungstemperatur ist in allen Fällen, durch äussere Kühlung, innerhalb 5... 15°C gehalten worden und die Volumina derart eingestellt dass die durchschnittliche Endkonzentration der Azoderivate 10^{-2} Mol/l ausmachte. Die Reaktionsdauer bis zum maximalen Umsatz schwankte zwischen weiten Grenzen : 24 h bei *p*H = 2 bis 3/4 h bei *p*H = 10

Zwecks Freilegung der durch Acylieren blockierten Gruppen OH und NH_2 sind die Kupplungsreaktionsmassen der N-, bzw. O-Acylderivate der H-, I- und γ-Säure mit Natronlauge bis zu einem Gehalt von 5...6 % freiem NaOH behandelt worden, anschliessend zum Sieden erhitzt und 1 h bei Siedetemperatur gerührt.

Die Synthese der bei *p*K-Bestimmungen eingesetzten reinen Azoderivate I und VIII erfolgte nach einem geänderten Verfahren, durch Einführen der 4-Nitrodiazobenzollösung in die feine Suspension der Aminonaphtolsulfosäure, bei *p*H = 0,5 ... 1 und der Temperatur von ~5°C, und mit einer solchen Geschwindigkeit dass ein auch nur geringer Überschuss des Diazoderivats ausgeschlossen wurde. Dabei spielte der Umsatz keine Rolle, sondern bloss das Vermeiden der Nebenproduktebildung.

Durchführung und Auslegung der Chromatograme

Als Trägermaterial diente auf 5×20 cm-Glasplatten aufgezogenes Silicagel G—„Merck". Die Vorbereitung der Platten erfolgte mit Hilfe einer automatischen Schichtaufziehvorrichtung Typ 05—304 der Firma „Labor Müszeripari Müvek" — Esztergom/Ungarn. Die Schichtdicke betrug 0,5 mm. Die Aktivierung fand durch 30—60 Min.-langem Erhitzen auf 100—110°C in der Etuve statt.

Auf der Platte sind 5 μl Kupplungsmasse, entsprechend $2 \cdot 10^{-5}$g Azoderivatmischung, aufgetragen worden. Die Entwicklung erfolgte in geschlossenem Glasgefäss, durch die aufziehende Methode. Als Fliessmittel wurde das ternäre Gemisch *n*-Butanol : Äthanol : wässr. Ammoniak 25 % (3 : 1 : 1) [12] angewendet. Die erreichte Trennung war genügend gut. Nur im Falle der Isomerenpaare IX—X und XIII—XIV sind die Rf-Werte weniger differenziert gewesen, der grosse Farbunterschied der Flecke in alkalischem Medium ermöglichte aber eine klare Erkennung der Individuen.

Die Bestimmung der chromatographisch getrennten und entsprechend den weiter unten beschriebenen Kriterien identifizierten Azoderivate, erfolgte halbquantitativ durch die Methode des visuellen Vergleiches der Fleckflächen. [13,14] Die Eichflecke sind durch chromatographische Entwicklung (unter denselben Bedingungen) von titanometrisch genau dosierten wässerigen Lösungen der reinen Azoderivate erhalten worden. Diese wiederum sind folgendermassen dargestellt worden :

— die Azoderivate I und VIII entsprechend der oben beschriebenen Arbeitsweise ;

— das Azoderivat XII durch Ausfällen des Kupplungsproduktes der γ-Säure bei *p*H = 1

— die Azoderivate III, IV, IX, X, XII und XIV durch Kupplung bei *p*H = 8 der N-Acetylderivate der H-, I- und γ-Säure, anschliessender hydrolytischer Abspaltung der Acetylgruppe und fraktionierter Fällung der *ortho-* und *para*-Kupplungsprodukte durch eine bekannte Methode. [5]

— die Disazoderivate V, VI und XI durch Kuppeln der Monoazoderivate I und VIII mit 4-Nitranilin in Überschuss, bei *p*H = 8. Die Trennung der Disazoderivate V und VI erfolgte durch fraktionierte Fällung mit Natriumchlorid.

Durch Vergleich der Fleckflächen mit Hilfe einer Desaga-Schablone ist die prozentuelle Zusammensetzung berechnet worden, die in Gewichtsprozente der in der Reaktion umgesetzten und im Fleck enthaltenen Aminonaphtolsulfosäure ausgedrückt wurde. Bezüglich dem Azoderivat II ist durch Differenz geschlossen worden.

Die Genauigkeit der angewandten Methode ist nicht gross (Fehlergrenze zwischen ±25 %),[13] sie konnte aber durch Summieren der Prozente noch verbessert werden und genügt so dem vorgesetzten Ziel dieser Arbeit.

Identifizierungskriterien

Es sind folgende Kriterien berücksichtigt worden:

— Die Azoderivate I, II, VIII und IX müssen identisch sein mit denen die durch Kupplung der O-Benzolsulfonylderivate der H-, I- und γ-Säuren und anschliessender hydrolitischer Spaltung der Estergruppe, hergestellt worden sind. Weil bei Azokupplungen von einfachen α-Naphtylaminsulfosäuren eine Verringerung des *ortho/para*-Verhältnisses mit dem Anstieg des *p*H-Wertes festgestellt worden ist,[4] muss eine Änderung des Verhältnisses der Azoderivate I und II in der selben Richtung angenommen werden.

— Die Azoderivate III, IV, IX, X, XII, XIV müssen identisch sein mit den durch Kupplung der N-Azetylderivate der H-, I- und γ-Säuren und anschliessender hydrolitischer Abspaltung des Acylrestes, hergestellten Substanzen. Dabei unterscheiden sich die *para*- wesentlich von den *ortho*-Isomeren, indem sie beim Übergang vom sauren zum alkalischen Medium ihre Farbe stark bathochrom ändern (Infolge der Wasserstoffbrücke zur Azogruppe sind die *o*-OH-Gruppen bedeutend weniger sauer). Die *para*-Isomere sind auch leichter löslich. [5]

— Die Disazoderivate V und VI stellen die möglichen Kupplungsprodukte des Monoazoderivats I dar. Ihr quantitatives Verhältnis muss sich ähnlich dem der Kupplungsprodukte der α-Naphtolsulfosäuren ändern bzw. verringern mit dem Anstieg des *p*H-Wertes.[4] Das *para*-Isomer VI, müsste eine Farbvertiefung beim Übergang vom sauren zum alkalischen Medium erfahren, der dunklen Farbe wegen ist aber der Unterschied im Chromatogram schwer erkennbar.

Das Disazoderivat VII kann deduktiv durch Ausschluss erkannt werden, da sämtliche Disazoprodukte II, III und VII bedeutend dunkler sind als die Monoazoderivate. Ähnlich kann, sehr leicht das Disazoderivat XI, von den Azoderivaten VII, IX und X unterschieden werden.

Bestimmung der pK-Werte

Die potentiometrischen Bestimmungen wurden mit Hilfe eines Titrierautomaten AT2 der Firma „VEB MLW Prüfgerätewerk Medingen"—Freital/DDR durchgeführt, wobei 100 ml 0,01-molare Lösung der analysierten Substanz mit einer 0,1 N-NaOH-Lösung titriert wurde. Die Messungen erfolgten mit einer GA 50-Glaselektrode gegen eine gesättigte Kalomelelektrode.

Die Ergebnisse wiedergeben den Durchschnitt von sechs Messungen. Die Reproduktibilität der Titrierkurven schwankte dabei zwischen ± 0,05 *p*H-Einheien.

Vor dem Einsatz wurden die Azoderivate I und VII weitgehend gereinigt durch Auflösen in Wasser bei *p*H = 7 . . . 7,2 und einer Temperatur von 80°C, dann Ausfällen mit der Mindestmenge NaCl und langsamer Kühlung (Abstellen des Rührers). Der Niederschlag wurde am Filter noch mit 10%-iger NaCl-Lösung gewaschen.

LITERATUR

[1] L. Floru, H. W. Langfeld und C. Tărăbăşanu-Mihăilă, „Coloranţi azoici", Ed. tehnică, Bucureşti, 1981, S. 142, 279, 341.

[2] H. Zollinger und C. Wittwer, *Helv. Chim. Acta*, **35**, 1209 (1952).

[3] H. Zollinger und W. Büchler, *Helv. Chim. Acta*, **34**, 591 (1951).

[4] O. A. Stamm und H. Zollinger, *Helv. Chim. Acta*, **40**, 1105, 1955 (1957)

[5] Z. J. Allan und J. Podstata, *Coll. Czech. Chem. Comm.*, **26**, 1862 (1961); *Chem. Abstr.*, **56**, 5898 (1962).

[6] L. Floru, F. Urseanu, C. Tărăbăşanu und R. Palea, „Chimia şi tehnologia intermediarilor aromatici şi a coloranţilor sintetici", Ed. didactică şi pedagogică, Bucureşti, 1980, S. 325.

[7] H. Zollinger, „Azo and Diazo Chemistry", Interscience Publishers, New York, 1961, S. 263.

[8] A. Demian, I. Ipsilanti und W. Schmidt, *Studii şi Cercetări Sti. Chim. Baza Cercet. Sti. Acad. R.P.R. Timişoara*, **1958**, 117.

[9] l. cit., [1] S. 374.

[10] Ullmann's „Enzyklopädie der technischen Chemie", vol. IX, Urban u. Schwarzenberg, München, 1963, S. 92.

[11] Z. J. Allan und J. Podstata, *Coll. Czech. Chem. Comm.*, **25**, 1337 (1960); Bundesdeutsches Pat. 842821 (1949), Sandoz; *Chem. Zentr.*, **1954**, 10819; Bundesdeutsches Pat. 842977 (1949), Sandoz; *Chem. Abstr.*, **45**, 9272 (1951).

[12] H. W. Langfeld und I. Dan, *Rev. Chim. (Bucureşti)*, **29**, 873 (1978).

[13] J. K. Kirchner (Editor A. Weissberger), „Thin-Layer Chromatography Technique of Organic Chemistry“, vol. XII, Interscience Publishers, New York 1967, S. 87, 147, 187, 209.

[14] V. Pelloni-Tamaş und F. Iohan, „Cromatografia în strat subţire“, Ed. tehnică, Bucureşti, 1971, S. 131.

[15] H. Zollinger, *Helv. Chim. Acta*, **33**, 538 (1950).

[16] H. R. Schweitzer, „Künstliche organische Farbstoffe und ihre Zwischenprodukte“, Springer-Verlag, Berlin 1964, S. 458; K. Venkataraman, „The Chemistry of Synthetic Dyes“, I. Band, Academic Press, New York, 1952, S. 480–495.

[17] * * * „Colour Index“, Edited by Society of Dyers and Colourists/England and American Association of Textile Chemists and Colourists, IV. Band, 1971, S. 4791, 4792, 4799–4802, 4805.

[18] H. Zollinger, *Angew. Chem.*, **73**, 126 (1964); Bundesdeutsches Pat. 1019025 (1954); H. Sanielevici und L. Floru, „Sinteza intermediarilor şi a coloranţilor“, Ed. Didactică şi pedagogică, Bucureşti 1971, S. 341.

[19] H. E. Fierz-David und L. Blangey, „Grundlegende Operationen der Farbenchemie“, Springer-Verlag, Wien, 1952, S. 259.

[20] l. cit., [1] S. 369.

[21] l. cit., [19] S. 240, 242.

[22] J. Havlik, W. Schmidt und A. Toth („Colorom“ Codlea), Rumänisches Pat. 77261 (1979).

[23] W. M. Clark und H. A. Lubs, *J. Biol. Chem.*, **25**, 479 (1916).

Revue Roumaine de Chimie, 28, 2, 169–176 (1983)

THE KINETICS AND MECHANISM OF THE DIAZO-COUPLING REACTION OF 4-CHLORO-1-NAPHTHOL

AURORA SALLO[a], B. DEMIAN[a] and O. EXNER[b]

[a] Chemical Research Centre, B-dul M. Viteazul 24, 1900 Timișoara, Romania
[b] Institute of Organic Chemistry and Biochemistry Flamingovo 2, 166 10 Praha 6, Czechoslovakia

Received December 25, 1981

In the present paper the diazo-coupling reaction of 4-chloro-1-naphthol with nine substituted benzenediazonium tetrafluoroborates has been investigated. The resulted kinetic data were analyzed using extrathermodynamic relationships (i.e., isokinetic, isoparametric with σ and T^{-1} and Yukawa-Tsuno equations) fair correlations being obtained. The above correlations were compared with the corresponding ones resulted by means of our previously obtained data for reactions of the same type. The results argue for the association of a water molecule in a cyclic transition state structure. The water molecule assists the proton transfer, explaining in this way the deviations of the most electron attracting and electron releasing substituents from the isoentropic relationship.

INTRODUCTION

The systematic study of the diazo-coupling reaction was started by Zollinger [1] who concluded : i) the diazo-coupling reaction is an electrophilic substitution; ii) the electrophilic species i.e. the diazonium cation, is characterized by relatively low reactivity and high selectivity; iii) the coupling component, i.e., phenols or aromatic amines, reacts as phenoxides or free amines, respectively; iv) the structure of the transition state (of the rate determining step — the electrophilic attack) is closely related to the "benzodienonic sigma complex"; v) the step following the electrophilic attack (sometimes associated to the rate determining step [2]) is the proton elimination.

Some coupling reactions (for example, *ortho*-hydroxy and *ortho*-amino) possess certain characteristic features as compared with the general pattern detailed above. On the basis of the kinetic study [3] of the diazo-coupling with 1-naphthol-3-sulfonic acid, one may suggest the following structure for the transition state :

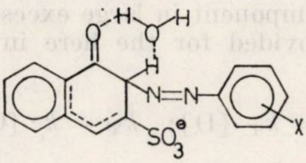

(1)

The main argument for the above cyclic six-membered structure originates in the large difference [3] of activation entropies for *para*- and *ortho*-coupling.

Investigating the diazo-coupling with 1-naphthol-4-sulfonic acid, Demian [4] suggests a reaction mechanism implying a variable association of a water molecule to the transition state.

This paper studies the kinetics of the diazo-coupling of 4-chloro-1-naphthol with nine substituted benzenediazonium tetrafluoroborates. This reaction takes place exclusively in the *ortho* position to the hydroxy group. The resulted kinetic data are correlated with extrathermodynamic relationships [5,6] and compared with the data obtained for previously investigated reactions of the same type. [4,7]

RESULTS AND DISCUSSION

The here investigated reaction

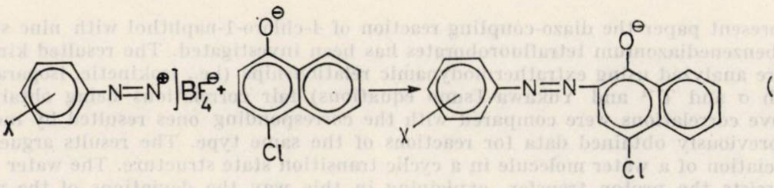

(2)

(D) (C) (Az)

$$X = m,\ p{-}NO_2;\ m,\ p{-}Cl;\ m,\ p{-}CH_3;\ m,\ p{-}OCH_3;\ H;$$

follows the kinetic equation:

$$\frac{d\,[Az]}{dt} = k\,[D]\,[C] \tag{3}$$

where [ ] denotes the concentration; we mention that [C] is conditioned by the equilibrium (4) as:

$$Cl{-}C_{10}H_6{-}OH \rightleftarrows Cl{-}C_{10}H_6{-}O^{\ominus} + H^{\oplus} \tag{4}$$

$$[C] = \frac{K_a\,c_i}{K_a + [H^+]} \tag{5}$$

where: K_a is the acidity constant of naphthol, c_i the initial concentration of naphthol, and $[H^+]$ is the concentration of hydronium ions.

Using the naphthol component in large excess, the pseudomonomolecular conditions were provided for the here investigated kinetics:

$$\frac{d\,[Az]}{dt} = k_{\Psi}\,[D];\quad k_{\Psi} = k \cdot [C] \tag{6}$$

where k_{Ψ} is the pseudo-first-order rate constant.

By combining relations (3), (5) and (6) the bimolecular rate constants k were calculated

$$k = \frac{k_{\Psi}\,(K_a + [\mathrm{H}^+])}{K_a\, c_i} \qquad [1 \cdot \mathrm{mol}^{-1} \cdot \mathrm{s}^{-1}] \qquad (7)$$

and listed in table 1.
From k values obtained at four temperatures (see Table 1) the activation parameters displayed in table 2 resulted. [8]

When processing our kinetic data (reaction series A) within the framework of correlation analysis, reference will be made to similar diazo-coupling reactions into the 2-position of the naphthalene nucleus, viz. that with 1-hydroxynaphthalene-4-sulfonic acid [4] (reaction series B) and with 1-aminonaphthalene-4-sulfonic acid [7] (reaction series C) as coupling components. Note, however, that the conditions were not strictly identical, since in the reaction series A the solvent was 50 % methanol and the anion was BF_4^-.

The kinetic data were processed in terms of the isokinetic relationship [6] (IKR) on the one hand, and in terms of the Hammett equation [5] and its extensions, [9,10] on the other one. A preliminary test of the IKR was made by plotting $\Delta H^{\neq}$ *vs* $\Delta G^{\neq}$ according to Krug, Hunter and Grieger. [11] In our reaction series A the substituents $4-\mathrm{NO}_2$ and $3-\mathrm{NO}_2$ deviated significantly from the linear dependence, in the series B the same behaviour was observed with $4-\mathrm{NO}_2$ and $4-\mathrm{OCH}_3$. The anomalous behaviour of these substituents was confirmed by a plot of log k *vs* substituents constants [12] σ° : within the series A and B the substituents $4-\mathrm{NO}_2$ and $4-\mathrm{OCH}_3$ were off the line whereas in the C series only $4-\mathrm{OCH}_3$. The behaviour of the 4-methoxy group can be accounted for either by variable direct conjugation or by specific solvation in water solution. On the contrary, we have no straightforward explanation for the deviations of the $4-\mathrm{NO}_2$ group which belongs usually to the well-behaved substituents.

The statistical treatment of the IKR was carried out by a method [13] based on the least squares condition in the coordinates log k *vs* T^{-1}. In this concept, the existence of IKR is equivalent to the condition that the Arrhenius lines intersect in the point of coordinates (β^{-1}, y_0) as :

$$\log k_{ij} = y_0 + b_i\,(T_j^{-1} - \beta^{-1}) \qquad (8)$$

For the reasons discussed in some detail elsewhere [6,13] we preferred to take all rate constants with the same weight, irrespective of their experimental errors estimated from individual kinetic runs. The most important statistics are listed in table 3.
The precision of IKR is given by the standard deviation s_0, or by the standard deviations s_∞ or s_S which would be operative if the reaction series were isoenthalpic or isoentropic, respectively. The standard devia-

TABLE 1

Values of the rate constant k

Substituent	t°C	pH	n^a	k^b	s^c
1	2	3	4	5	6
$p-NO_2$	18.4	2.97	6	$5.075 \cdot 10^7$	$0.012 \cdot 10^7$
	22.4	2.97	5	$7.000 \cdot 10^7$	$0.077 \cdot 10^7$
	26.5	2.97	5	$11.610 \cdot 10^7$	$0.210 \cdot 10^7$
	28.8	2.97	5	$16.360 \cdot 10^7$	$0.770 \cdot 10^7$
$m-NO_2$	18.4	2.52	4	$5.210 \cdot 10^7$	$0.320 \cdot 10^7$
	22.4	2.52	5	$7.640 \cdot 10^7$	$0.320 \cdot 10^7$
	26.8	2.52	5	$10.300 \cdot 10^7$	$0.320 \cdot 10^7$
	28.8	2.52	5	$14.990 \cdot 10^7$	$0.110 \cdot 10^7$
$p-Cl$	18.6	3.97	4	$2.638 \cdot 10^6$	$0.098 \cdot 10^6$
	22.2	3.97	5	$2.906 \cdot 10^6$	$0.170 \cdot 10^6$
	26.2	3.97	5	$4.000 \cdot 10^6$	$0.138 \cdot 10^6$
	29.0	3.97	4	$5.110 \cdot 10^6$	$0.072 \cdot 10^6$
$m-Cl$	18.6	3.79	5	$6.040 \cdot 10^6$	$0.010 \cdot 10^6$
	22.4	3.79	5	$8.210 \cdot 10^6$	$0.320 \cdot 10^6$
	26.2	3.79	6	$10.300 \cdot 10^6$	$0.450 \cdot 10^6$
	28.8	3.79	4	$11.610 \cdot 10^6$	$0.680 \cdot 10^6$
H	18.4	4.93	4	$2.720 \cdot 10^5$	$0.360 \cdot 10^5$
	23.0	4.93	4	$3.015 \cdot 10^5$	$0.361 \cdot 10^5$
	26.2	4.93	6	$4.450 \cdot 10^5$	$0.140 \cdot 10^5$
	29.0	4.93	5	$5.610 \cdot 10^5$	$0.200 \cdot 10^5$
$p-CH_3$	19.0	5.26	5	$1.332 \cdot 10^5$	$0.098 \cdot 10^5$
	22.5	5.26	4	$1.685 \cdot 10^5$	$0.259 \cdot 10^5$
	26.2	5.26	6	$2.047 \cdot 10^5$	$0.095 \cdot 10^5$
	29.0	5.26	5	$2.764 \cdot 10^5$	$0.249 \cdot 10^5$
$m-CH_3$	19.0	5.28	4	$1.815 \cdot 10^5$	$0.075 \cdot 10^5$
	22.6	5.28	4	$2.593 \cdot 10^5$	$0.087 \cdot 10^5$
	26.2	5.28	5	$3.527 \cdot 10^5$	$0.126 \cdot 10^5$
	29.0	5.28	5	$4.192 \cdot 10^5$	$0.348 \cdot 10^5$
$p-OCH_3$	18.6	5.75	5	$2.960 \cdot 10^4$	$0.010 \cdot 10^4$
	22.8	5.75	3	$3.323 \cdot 10^4$	$0.036 \cdot 10^4$
	26.5	5.75	4	$5.610 \cdot 10^4$	$0.500 \cdot 10^4$
	29.0	5.75	4	$7.401 \cdot 10^4$	$0.447 \cdot 10^4$
$m-OCH_3$	18.6	4.95	5	$5.130 \cdot 10^5$	$0.550 \cdot 10^5$
	23.0	4.95	5	$6.510 \cdot 10^5$	$0.200 \cdot 10^5$
	26.2	4.95	5	$9.060 \cdot 10^5$	$0.310 \cdot 10^5$
	29.0	4.95	4	$11.650 \cdot 10^5$	$0.82 \cdot 10^5$

[a] n — the number of values used in the calculation of the mean value of the rate constant according to equation (7)

[b] k — in l. $mol^{-1} \cdot s^{-1}$

[c] s — standard deviation

tion s_{00} refers to original Arrhenius lines (without any isokinetic constraint) and serves as an estimate of overall experimental error. The salient feature of the data is that IKR is accepted as a useful empirical relationship since the statistic Ψ (relating s_0 to the variance between individual reactions as expressed by s_R) is significantly lower than 0.1. The IKR is also valid within the limits of experimental error according to the confidence level α (relating s_0 to s_{00}). An unfavourable feature of the series A as compared to B and C is lower experimental accuracy (s_{00}), i.e. the error in k is corresponding to 8 % in A, 3 % in B and 2 % in C. The series B and C are clearly isoentropic since s_S is the lowest of the standard deviations; this conclusion is insensitive to two reactions eliminated (i.e., $4-NO_2$ and $4-OCH_3$, substrates) from B. The values of isokinetic temperature β are of no chemical meaning, they should be actually infinite. On the other hand, reaction A is probably isoentropic, too, but the isoenthalpic hypothesis cannot be firmly rejected. The picture becomes still more confused if the two nitro derivatives are not excluded; in such cases one is forced

TABLE 2

Activation parameters

Substituent	H_{298}, cal mol^{-1}	S_{298}, cal $mol^1 grd^{-1}$
$p-NO_2$	18480	40.1
$m-NO_2$	15830	31.1
$p-Cl$	10680	7.4
$m-Cl$	10630	9.0
H	11760	6.6
$p-CH_3$	11130	3.0
$m-CH_3$	14200	14.2
$p-OCH_3$	15490	14.8
$m-OCH_3$	12810	11.5

TABLE 3

Statistics of the isokinetic relationship

Reaction series	A	A without $3-NO_2$ $4-NO_2$	B without $4-NO_2$ $4-OCH_3$	C
Standard deviations 10^4				
s_{00}	401	376	139	82
s_0	440	348	137	98
s_∞	447	371	220	275
s_S	519	341	133	98
s_R	11775	7795	10712	12959
Isokinetic temperature				
β, K	118	1144	5188	−3860
Validity of IKR: ψ	0.037	0.045	0.013	0.008
α	>0.25	>0.25	>0.25	>0.25

to choose the isoenthalpic hypothesis as the simplest one (it means in fact that the precision of the data does not allow to evaluate the differences in enthalpies). Our opinion is that the lowered precision is the only important difference between the series A and B and C respectively; otherwise all the statistics are very similar.

The treatment in terms of the Hammett-type equations was carried out for all temperatures together. If substituent and temperature are both varied, the general form of the correlation equation is the isoparametric relationship [10,14] with σ and T^{-1} as independent variables:

$$\log k_{ij} = -\beta \rho_0 (\sigma_i - \vartheta)(T_j^{-1} - \beta^{-1}) \tag{9}$$

The isokinetic temperature β has the same meaning as above and ϑ represents the extrapolated value of σ constant which should make the reactivity independent of temperature. Equation (9) differs from equation (8) only by the requirement that the slopes b_i are proportional to substituent constants σ. From various sets of constants, [12] the best results were obtained with standard constants σ^0 for all substituents except $4-OCH_3$ for which the value 0.28 was used (derived from dissociation constants in water [12]) stressing in this way the importance of hydration processes. The 4-nitro substituent was omitted in all series, although this was not necessary in series C. The statistics listed in table 4 reveal again the greater similarity of the series B and C than of B or C as compared to A (see particularly the values of ϑ and β). In our opinion the main reason is again the lower precision within series A combined with a worse adherence to the linear correlation equation. In all the cases the isoparametric relationship is adequate and its standard deviation (s_{ISOP}) is lower than for independent correlations at each separate temperature (s_{LFER}). The similarity of the three reaction series is revealed most distinctly in the reaction constant ρ_{25} valid for 25°C, whereas the values of ρ_0 of $\beta\rho_0$ are immaterial as products of a far reaching extrapolation; similarly, the values of ϑ represent extrapolations that cannot be reached experimentally.

An alternative set of σ constants can be obtained from the Yukawa-Tsuno treatment [9] as

$$\sigma = \sigma^0 + r(\sigma^+ - \sigma^0) \tag{10}$$

where the adjustable parameter r expresses the variable conjugation of substituent with the reaction center. Our data do not allow a precise treatment since r is determined mainly by the substituent $4-OCH_3$ and hence estimated very roughly. Even so, the essential similarity of the three series is confirmed by the r values in table 4. The direct conjugation seems to be of minor importance, if present at all. The precision of the whole Yukawa-Tsuno treatment in series A and C is slightly lower than in series B.

TABLE 4

Statistics of the isoparametric relationships with σ, T^{-1}

Reaction series	A	B	C
		without $4-NO_2$	
a) σ^0 constants and -0.28 for $4-OCH_3$			
ρ_{25}	3.33	3.96	3.35
ϑ	−13.0	3.26	2.32
βK	55	−4071	−40260
$-\beta\rho_0 K$	−224	1103	994
standard deviations:			
s_{ISOP}	0.088	0.151	0.092
s_{LFER}	0.092	0.158	0.094
b) Yukawa-Tsuno σ constants			
ρ_{25}	3.36	3.63	3.29
r	0.20	0.43	0.26
ϑ	−9.84	4.01	2.32
standard deviations:			
s_{ISOP}	0.138	0.065	0.100
s_{LFER}	0.148	0.067	0.108

CONCLUSIONS

The results of the correlation analysis are compatible with an essentially common mechanism of the three series implying a sigma complex transition state. The association of a water molecule in a cyclic structure may assist in proton transfer, this effect being probably responsible for characteristic deviations of the most electron attracting and most electron releasing substituents. For instance, in the case of 4-nitro substituent, the demand for the proton transfer assistance is reduced and the association of water molecule is less tight; this results in a less ordered transition state and higher entropy, and accordingly the isoentropic relationship is violated.

EXPERIMENTAL SECTION

4-Chloro-1-naphthol was prepared from 1-naphthol, by halogenation with sulfuryl chloride in chloroform, [15] and subsequent recrystallization from chloroform (m.p. of 120 – 121°C, as mentioned in the literature [15]). The aromatic amines were purified by recrystallization and vacuum distillation. The diazotation of the amines and the preparation of benzenediazonium tetrafluoroborates were performed according to ref. [16–18]

The acidity constant of 4-chloro-1-naphthol was spectrophotometrically [19] determined in 50% water/ methanol borax buffer solutions, (ionic strength $I - 0.25$), $pK = 9.79 \pm 0.1$.

The concentration of the 4-chloro-1-naphthol solutions was $5 \cdot 10^{-3}$ mol/l, while the concentration of benzenediazonium tetrafluoroborates was about $5 \cdot 10^{-5}$ mol/ l. Citrate-HCl and citrate – NaOH [20] in 50% v/v water-methanol were used as buffer solutions ($I = 0.25$). The pH of the naphthol solutions was selected in such a way that the value of the rate constant k_{Ψ} (equation (6)) should be at least two order of magnitude greater than the rate constant of the parallel thermal decomposition reaction of the diazonium salt. [21]

The pH measurements were performed with a precision pH – meter MV85 Pracitronic – DDR, calibrated with 50% v/v aqueous methanol buffer, as recommended in ref. [22]

The kinetics of the diazocoupling reactions was followed spectrophotometrically at $\lambda = \lambda_{max}$ of the formed azo dye.

The kinetic runs were accomplished in the thermostated cell of a UNICAM SP – 800 spectrophotometer provided with the SP – 820 and SP – 870 accesories, the exit signal being recorded with a Philips PM 8100 recorder. The temperature in the cell was measured by a mercury thermometer of ± 0.1°C precision.

The pseudo first-order-rate constant, k_{Ψ}, was determined by linearization (the method of least squares [23]) of log ($E_{\infty} - E$) *vs t*, k_{Ψ} being the slope of regression line. Four or six runs were performed at each temperature.

REFERENCES

[1] H. Zollinger, "Azo and Diazo Chemistry", Interscience Publishers, New York, 1961, p.221.

[2] H. Zollinger, in "Advances in Physical Organic Chemistry", V. Gold, Ed., vol. 2, Academic Press, London, 1964, p. 163.

[3] O. A. Stamm and H. Zollinger, *Helv. Chim. Acta,* **11**, 1955 (1957).

[4] B. Demian, *Bull. Soc. chim. France,* **1973**, 769.

[5] L. P. Hammett, "Physical Organic Chemistry", 2nd Ed., Mc Graw Hill, New York, 1970, p. 347.

[6] O. Exner, *Progr. Phys. Org. Chem.*, **10**, 411 (1973).

[7] B. Demian, O. Exner and A. Sallo, *Coll. Czech. Chem. Comm.*, in press.

[8] S. W. Benson, "Foundations of Chemical Kinetics", Mc Graw Hill, New York, 1960.

[9] Y. Yukawa, Y. Tsuno and M. Savada, *Bull. Chem. Soc. Japan*, **39**, 2279 (1966).

[10] O. Exner, *Coll. Czech. Chem. Comm.*, **39**, 515 (1974).

[11] R. R. Krug, W. G. Hunter and R. A. Grieger, *J. Phys. Chem.*, **80**, 2335 (1976).

[12] O. Exner, in "Correlations Analysis in Chemistry-Recent Advances", N. B. Chapman and J. Shorter Eds., Plenum Press, New York, 1976, p. 439.

[13] O. Exner, *Coll. Czech. Chem. Comm.*, **37**, 1425 (1972); O. Exner and V. Beranek, *Coll. Czech. Comm.*, **38**, 781 (1973).

[14] V. A. Palm and B. I. Istomin, *Reacts. Sposobnost Org. Soedin.*, **6**, 427 (1969).

[15] H. Kast, *Ber. dtsch. chem. Ges.*, **44**, 1337 (1911).

[16] Houben-Weyl, "Methoden der organischen Chemie", vol. 10/3, Georg Thieme Verlag, Stuttgart, 1965, p. 37.

[17] E. W. Dürfurt and G. Balz, *Ber. dtsch. chem. Ges.*, **60**, 116 (1927).

[18] H. E. Fierz-David and L. Blangey, "Grundlagen Operationen der Farben-Chemie" Springer-Verlag, Wien, 1943, p. 240.

[19] A. Albert and E. P. Searjeant, "Ionization Constants of Acid and Bases", Wiley, New York, 1962, p. 69.

[20] I. I. Lurie, "Spravochnik po Analiticheskoi Khimii", Izd. Khimia, Moscow, 1967, p. 224.

[21] D. F. DeTar and A. A. Ballentine, *J. Amer. Chem. Soc.*, **78**, 3916 (1956).

[22] J. J. Lagowski, "The Chemistry of Non-Aqueous Solvents", Academic Press, London, 1966, p. 113.

[23] A. G. Worthing and J. Gaffner, "Prelucrarea datelor experimentale", Ed. Tehnică, București, 1959, p. 225 (Translation from English).

Revue Roumaine de Chimie, 28, 2, 177–183 (1983)

STUDY OF THE BEHAVIOUR OF α, α-DIPHENYL-β-PICRYLHYDRAZYL FREE RADICAL IN CHROMATOGRAPHY, AS ADMIXTURE TO DIFFERENT STATIONARY PHASES

CANDIN LITEANU * and RADU POPESCU **

* Department of Chemical Technology, University of Cluj-Napoca, str. Arany Janos 11, Cluj-Napoca, Romania
** Romanian Institute of Research, Development and Design for Refineries, Bd. Republicii 291, Ploiești, Romania

Received March 8, 1982

A study has been performed in order to determine the influence of complexing agent addition to chromatographic stationary phase. The experiments were performed with polyethyleneglycol – 400 (PEG – 400) and silicone oil QF – 1 as stationary phases to which α, α-diphenyl-β-picrylhydrazyl (DPPH) was added. We found a stabilization of the stationary phase and the possibility to separate some compounds more difficult to separate under normal conditions.

I. INTRODUCTION

In the last years several papers were published dealing with the experiments in which it was tried to modify the retention parameters by adding to the chromatographic stationary phase some modifiers which, by their characteristics, have the capacity to influence the chromatographic separation of some compounds which are difficult to separate under normal conditions. Thus, the idea appeared of using organic admixture, nitrocompounds especially, which have the possibility to form unsteady complexes with some components of the mixture to be analysed, by increasing the distance among the components or even changing the elution order in the chromatographic column.

Thus, mention should be made of those papers in which their authors used 2,4,7-trinitrofluorenone [1–5] in admixture to different stationary phases studying its complex with anilines, amines, hydrocarbons, heterocycles and other substances. Maczec [6] used tritolylphosphate in admixture with trinitrophenetole, while other researchers [7,8] noticing the advantages of interactions in the separation of aromatic hydrocarbons used different combinations as fluorene and picric acid or dibutylphthalate and picric acid and others.

Cvetanovic [9] studied the behaviour of olefines in the presence of 1,3,5-trinitrobenzene, and Castells [10] used gas-liquid chromatography to study the complexing process at 60°C of some 1,3,5-trinitrobenzene disolved in dinonylphthalate with a series of hydrocarbons.

Starting from the real statement that the addition of complexing agents to the chromatographic stationary phase has a positive influence on the separation from a mixture containing components more difficult to separate under ordinary conditions and based on the studies concerning the phenomena taking place at gas — liquid interface, [11,12] we studied α, α-diphenyl-β-picrylhydrazile as free radical (it will be still written as DPPH), capable of forming complex combinations with different organic substances. The study has been performed in order to determine the influence of complexing agent addition to chromatographic stationary phase, when this is distributed in a very small amount on the surface of the solid support, as well as the variation of the retention parameters from the chromatographic column against the increase of the quantity of the simple stationary phase or with the addition of complexing agent. The study has been performed with the help of the retaining indices. [13]

II. APPARATUS AND PROCEDURE

The experiments were performed on a chromatographic column of 150 cm long and 5 mm internal diameter, packed with kieselgur with grains of 0.2 to 0.3 mm on which the stationary phase was placed as such or containing the complexing agent. Nitrogen was the carrier gas at a flow rate of 25 cc/min. Working temperature was 70°C and 100°C.

One used as stationary phases polyethyleneglycol—400 (PEG—400) and silicone oil QF—1 to which one added in compliance with its solving capacity 20% DPPH calculated for the amount of stationary phase that was processed. The concentration of the stationary phase on the support was 3%, 6%, 10%, 15% and 20% so that a rather wide range of concentrations was covered. As it has been already mentioned the complexing agent was a supplementary amount.

The substances used for the determinations were the following: n-hexane, n-octane hexene-1, octene-1, cyclohexene, benzene, toluene, chloroform, carbon tetrachloride, acetone methyl alcohol and ethyl alcohol.

The samples where introduced with a Hamilton syringe and did not exceed 0.5 µl.

III. EXPERIMENTAL RESULTS

The DPPH free radical was obtained by syntheses and was purified by several recrystallyzations from acetone. [14] It contains three nitro groups and a free electron at one of the nitrogen atoms having the following structural formula:

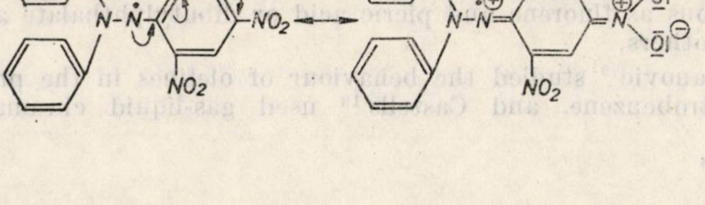

Its dissolution in the stationary phases leads to a stabilisation of the stationary phase, a fact underlined by the thermogravimetric analysis which shows that the solutions of complexing agents in stationary phase are more stable from a thermal point of view than the stationary phases without addition. This is illustrated by figures 1 and 2 in which one can see that this type of stationary phase can be used at higher temperatures, which increases its uses. One can estimate that inter and intramolecular interactions existing in PEG—400 are replaced by strong intermolecular interactions probably by the formation of some hydrogen bridges.

The interactions established between DPPH and the organic substances used in the experiments are emphasized in the graphs from figures 3 and 4. As it has been already mentioned one used in the determination the retention indices, taking n-hexane and n-octane as reference.

Generally, the curves drawn for DPPH solution in polyethylene glycol—400, or in silicone oil QF—1 are above the curves for solvents without DPPH addition, a fact which shows that between this one and the studies compounds take place interactions which are weaker or stronger depending on the structure of each compound.

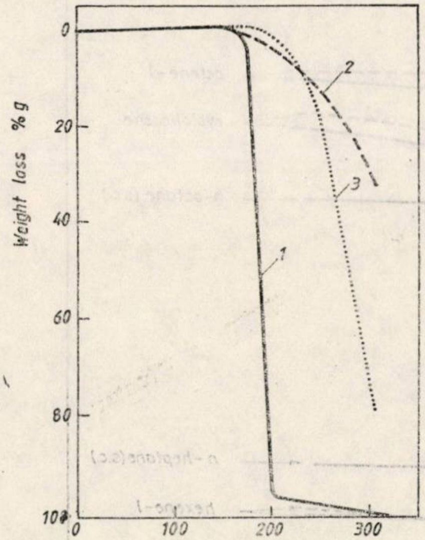

Fig. 1. — Comparison of thermogravimetric analyses of PEG—400, DPPH and its solution in PEG—400 : 1. —— PEG—400 ; 2. — — — DPPH ; 3. ··· PEG + 20% DPPH.

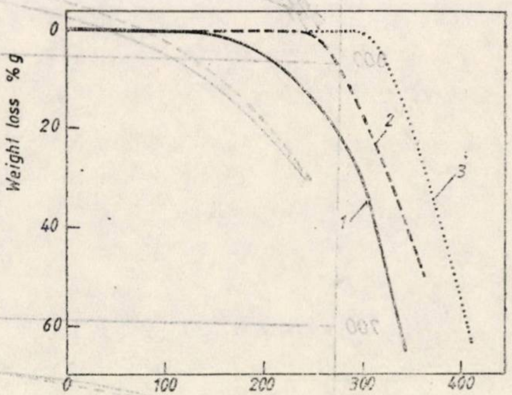

Fig. 2. — Comparison of thermogravimetric analyses of QF—1 oil, DPPH and its solution in QF—1 : 1. —— DPPH ; 2. — — — QF—1 ; 3. ··· QF—1+20% DPPH.

Only chloroform shows different behaviour, the values for this one in PEG—400 solution with DPPH being below the values for the pure solvent. When working with silicone oil QF—1 at low concentrations of the stationary phase, a series of reversals of the values for the retention indices are taking place in the case of the chlorinated or oxygenated

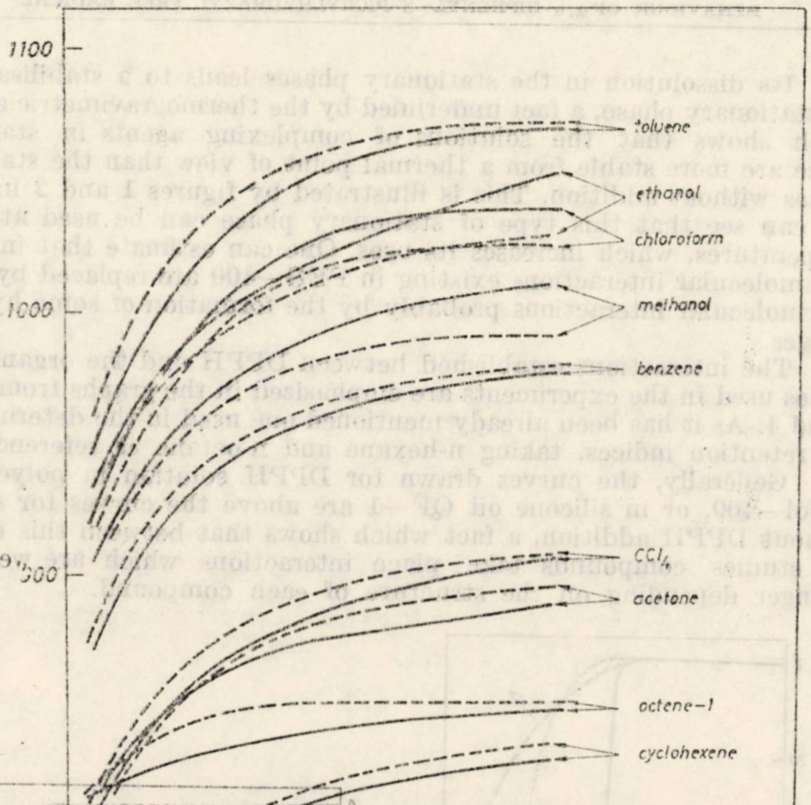

Fig. 3. — Comparison of retention indices obtained when using PEG−400 as stationary phase, or its solution with 20% DPPH: —— PEG − 400; — — — PEG−400 + 20% DPPH.

compounds. This in important because by an adequate choice of the quantity of stationary phase one can achieve separations by changing the order of components elution. Thus, there are conditions to change the relation between the factors which have a contribution to retention.

Temperature is another factor which has an influence upon the separation. The data obtained for silicon oil QF$-$1 with DPPH addition

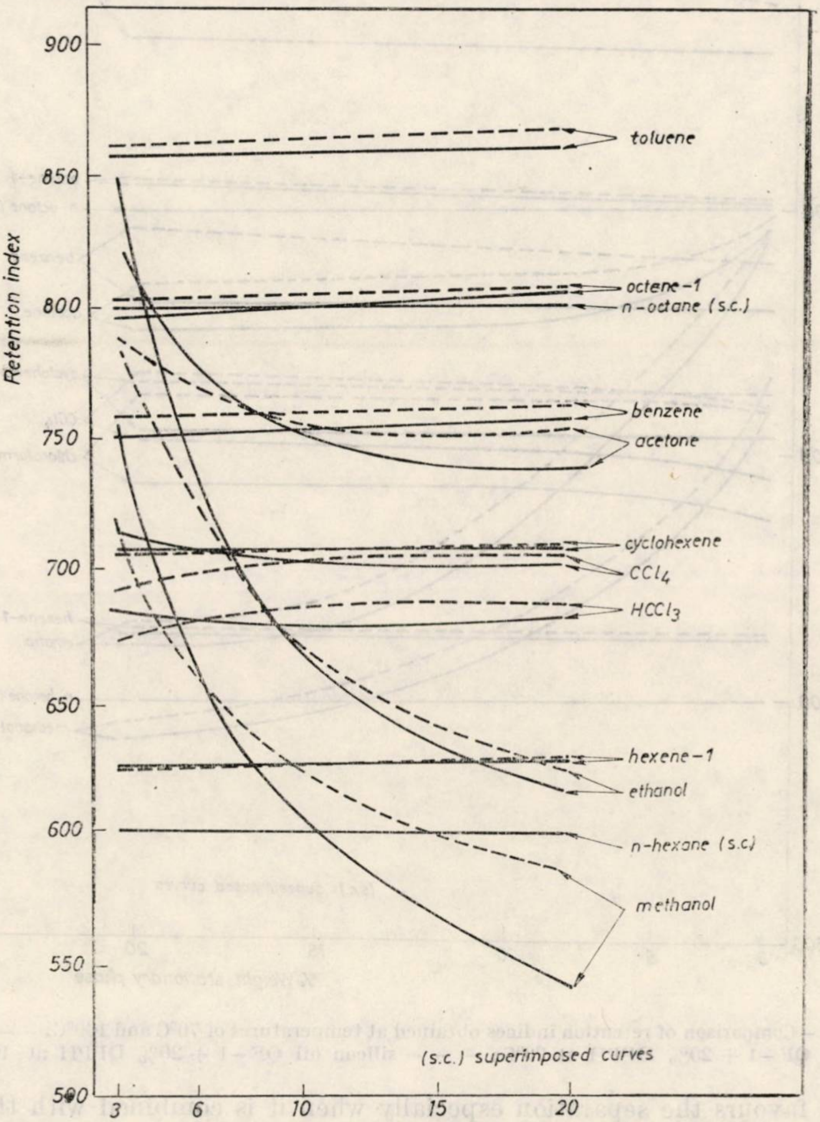

Fig. 4. – Comparison of retention indices obtained when using as stationary phase QF$-$1 silicon oil, or with DPPH addition : —— QF$-$1 ; – – – QF$-$1 + 20% DPPH.

are given in figure 5, where the solid lines represent the curves for a temperature of 70°C, while the dotted lines represent the curve for a temperature of 100°C. One can notice that the work at different temperatures favours the separation especially when it is combined with the use of complexing agents. This shows the large number of possibilities of combinations achieved by the use of stationary phases containing complexing agents in the chromatographic separation of blends of several compounds.

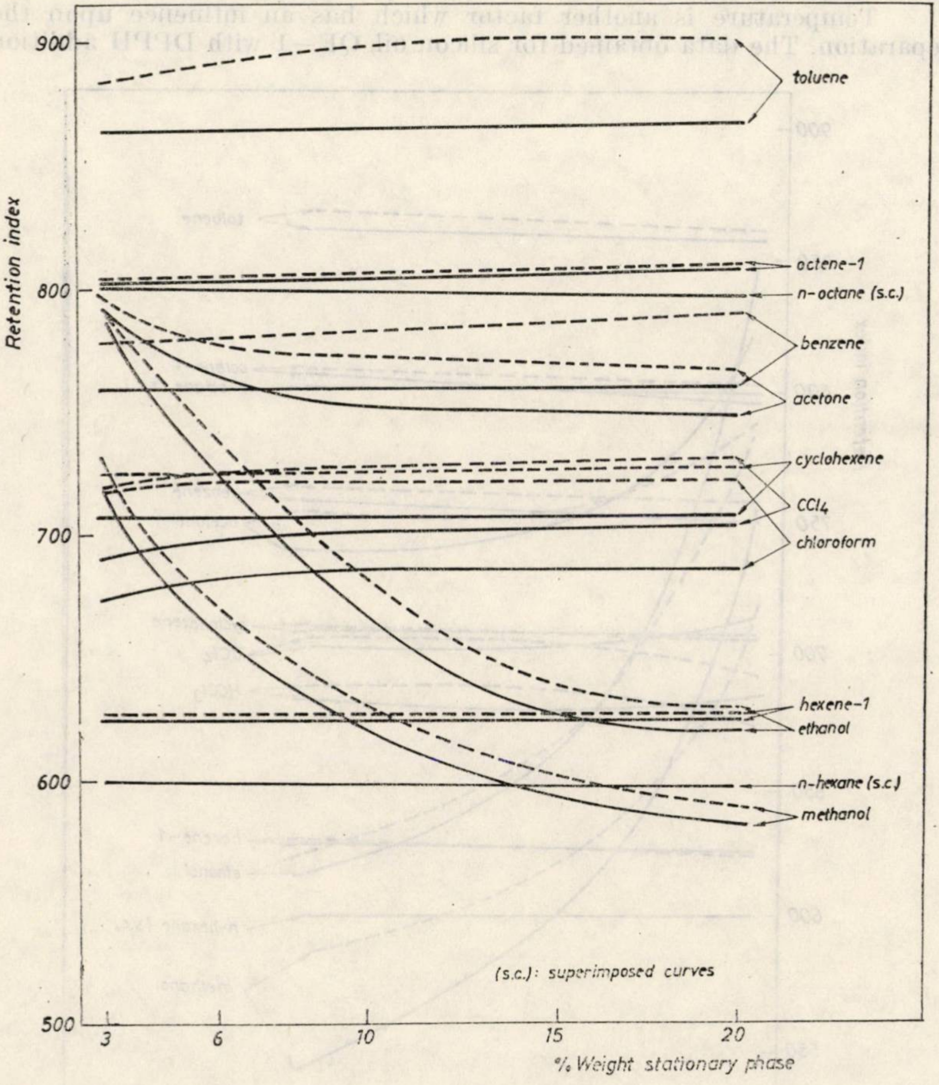

Fig. 5. – Comparison of retention indices obtained at temperatures of 70^{0}C and 100^{0}C: —— silicon oil QF–1 + 20% DPPH at 70^{0}C; – – – silicon oil QF–1 + 20% DPPH at 100°C.

REFERENCES

[1] Y. V. Tewary, D. E. Martire and J. P. Sheridan, *J. Phys. Chem.*, **74**, 2345 (1970).

[2] C. W. P. Crowne and M. F. Harper, *J. Chromatog.*, **61**, 7 (1971).

[3] A. R. Cooper, C. W. P. Crowne and P. G. Farell, *Trans. Faraday Soc.*, **63**, 447 (1967).

[4] A. R. Cooper, C. W. P. Crowne and P. G. Farrell, *Trans. Faraday Soc.*, **62**, 2725 (1966).

[5] E. B. Call, A. J. Neale and T. J. Rawlings, *J. Chem. Soc.*, **1962**, 4900.

[6] A. O. S. Maczec and C. S. G. Phillips, *J. Chromatog.*, **29**, 15 (1967).

[7] P. G. Farrell and J. V. Westwood, *J. Chem. Soc. (B)*, **1970**, 1518.

[8] P. D. Gardner, R. L. Brandon, N. J. Nix and I. Y. Chang, *J. Amer. Chem. Soc.*, **81**, 3413 (1959).

[9] R. J. Cvetanovic, F. J. Duncan and W. E. Falconer, *Canad. J. Chem.*, **42**, 2410 (1964).

[10] R. C. Castells, *Chromatographia*, **6**, (2), 57 (1973).

[11] J. Serpinet, *J. Chromatog.*, **68**, 9 (1972).

[12] B. G. Belenki, A. I. Rusanov and L. D. Turkova, J. Chromatog., **80**, 147 (1973).

[13] O. Piringer and E. Tătaru, "Cromatografia în fază gazoasă", Ed. tehnică, București, 1969.

[14] J. B. Hendrickson, D. J. Cram and G. S. Hammond, "Chimie organică", Ed. științifică și enciclopedică, București 1976, p. 853.

Revue Roumaine de Chimie, 28, *2*, 185–189 (1983)

SYNTHESIS AND POLYMERIZATION OF POLYETHYLENE GLYCOL DIMETHACRYLATE. VIII[1]

RELATIONS BETWEEN STRUCTURE AND REACTIVITY OF POLYETHYLENE GLYCOL DIMETHACRYLATES

GH. HUBCA, M. GHEORGHIU, CR. OPRESCU and M. DIMONIE

Polytehnical Institute of Bucharest, Laboratory of
Macromolecular Technology, Calea Victoriei 149, Bucharest, Romania

Received September 30, 1981

This paper deals with the dependency of polyethylene glycol dimethacrylate reactivity on the length of polyetheric chain. It is shown that the monomer reactivity increases on polyetheric chain length, fact determined by oligomeric chain flexibility increase and by the increase of its free rotation.

The study of homo — and copolymerization processes of ethylene dimethacrylate, diethylene glycol dimethacrylate, triethylene glycol dimethacrylate and tetraethylene glycol dimethacrylate [2-4] showed that :

1. Rate of homopolymerization reaction and limit conversion increase from ethylene dimethacrylate to tetraethylene glycol dimethacrylate.

2. Kinetic characteristics of homopolymerization process are similar to those of methyl methacrylate. At conversions close to zero the polymerization rate is proportional to the first power of monomer concentration and 0.5 as against initiator concentration.

3. Overall activation energy decreases from ethylene dimethacrylate to tetraethylene glycol dimethacrylate.

4. Values of copolymerization constants of the mentioned monomers by styrene increase from ethylene dimethacrylate to tetraethylene glycol dimethacrylate.

From the above mentioned data it results that the reactivity of polyethylene glycol dimethacrylate is determined by polyetheric chain length, increasing together with it.

In order to emphasize the way the length of polyetheric chain influences monomer reactivity it is necessary to study the topochemistry of polymerization process.

The situation of mobility of the two reactive species existing at one time in the system (Figure 1) is the following:

a) Macroradicals are inserted in the tridimensional polymer network just after their forming.

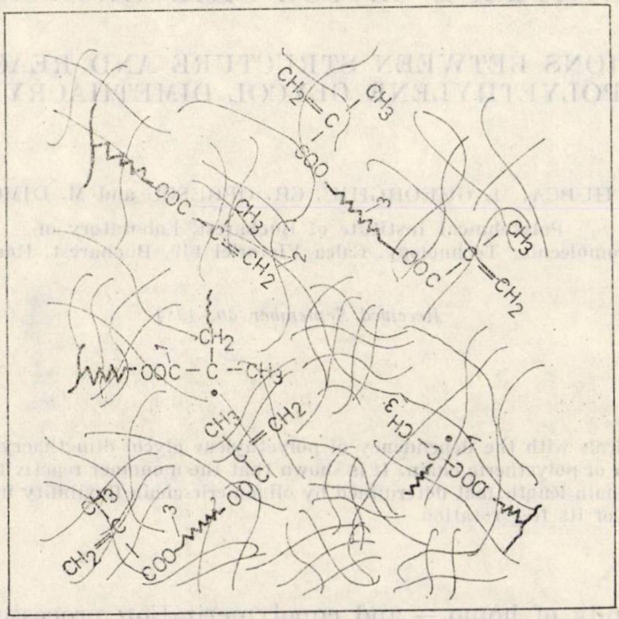

Fig. 1. — Topochemistry of polymerization process: 1 — rising macroradicals; 2 — double bonds connected to tridimensional network; 3 — free monomer molecules.

b) Double bonds exist both in unreacted monomer and at the end of side branches of polymer network, but their mobility is completely different.

Degrees of freedom of macroradicals and double bonds fixed in polymer network are generally reduced and depend on oligomeric chain length.

For this reason together with the formation of tridimensional network the main development way of polymerization is monomer diffusion through polymer network eyes.

The length of polyethylene glycol chain between the two methacrylic groups, in other words the size of monomer molecule, influences monomer reactivity and diffusion processes by opposite direction effects. So this factor has a determinate action on polymerization process development.

The smaller polyetheric chain length the denser the tridimensional network is but monomer molecule mobility is larger.

At the same time a long polyetheric chain has as effect the decrease of interactions between terminal methacrylic groups, increase of their freedom degrees and by this, their reactivity increase.

This complex influence is different along polymerization as it results from our experimental data, mentioned before.

On the whole, the favourable effect of polyetheric chain length on monomer reactivity increase and formation of a more loose network of tridimensional polymer exceeds the negative effect of monomer diffusion decrease because of its sizes increase.

In order to show directly the influence of oligomeric chain length on monomer reactivity, ^1H-NMR spectra have been recorded for liquid monomers (Figure 2). Signals have been assigned by model analyses, from the simplest molecules to the most complicated ones. Thus the signals occurring in the ethylene dimethacrylate spectrum in the field between 330 and 387 Hz, were assigned to the two vinyl protons, and the signal occurring between 105 and 137 Hz, where stape is of a doublet with allyl link with link constant $j = 1$ Hz, was assigned to CH_3 groups. Analysing the spectra corresponding to the four monomer studied we notice that signals assigned to vinyl protons and CH_3 groups occur at the same chemical displacement.

In the ethylene dimethacrylate spectrum, the signal which occurs at a displacement of $\delta = 4.47$ ppm was assigned to protons in ethylene group ($-CH_2-CH_2-$).

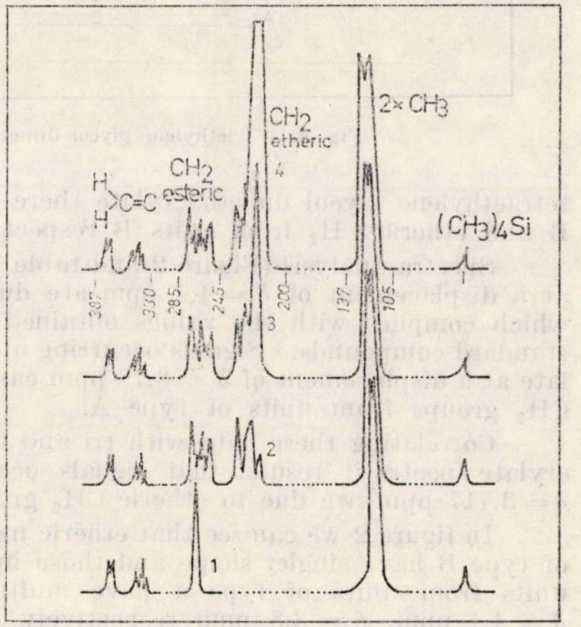

Fig. 2. – ^1H-NMR spectra of liquid monomers; solvent = $CDCl_3$ TMS – internal = $(CH_3)_4Si$; t = 37°C, 1 – ethylene dimethacrylate, 2 – diethylene glycol dimethacrylate, 3 – triethylene glycol dimethacrylate, 4 – tetraethylene glycol dimethacrylate.

Considering the number of ethylene groups increased together with oligomeric chain length, in order to observe the position of various CH_2 groups in diester molecule we gave them, conventionally, various names. We called ethylenic unit linked directly by esteric groups, unit of type A, and ethylenic units between the two ether bridges, units of type B. In units of type A, we shall have two kinds of CH_2 groups, directly linked to esteric groups, which we shall call esteric CH_2 and the groups linked directly to etheric groups we shall call etheric CH_2 of type A.

In units B the methylene groups are identical and we shall call them etheric CH_2 of type B.

It results that in ethylene dimethacrylate we shall have a unit of type A and two esteric methylenic groups, in diethylene glycol dimethacrylate two ethylenic units of type A and two CH_2 types: esteric CH_2 and etheric CH_2. In triethyleneglycol dimetharylate (Figure 3) and

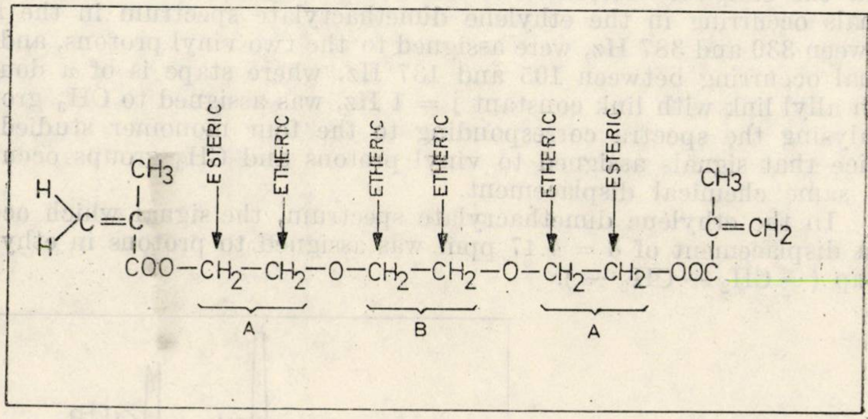

Fig. 3. – Triethylene glycol dimethacrylate structure.

tetraethylene glycol dimethacrylate there occur ethylenic units of type B and etheric CH_2 from units B respectively.

Spectra analysis (Figure 2 and table 1) show that signals occurring at a displacement of $\delta = 4.4$ ppm are due to esteric CH_2 groups, fact which complies with the values obtained for esteric CH_2 groups from standard compounds. [5] Signals occurring at diethylene glycol dimethacrylate at a displacement of $\delta = 3.78$ ppm cannot be assigned but to etheric CH_2 groups from units of type A.

Correlating these data with tri and tetra ethylene glycol dimethacrylate spectra it results that signals occurring at a displacement of $\delta = 3.717$ ppm are due to etheric CH_2 groups from units B.

In figure 2 we can see that etheric methylenic protons in sequences of type B have singlet shape and those in esteric CH_2 and etheric CH_2 units from units of type a have multiplet shape centered around $\delta = 4.4$ ppm, $\delta = 3.8$ ppm respectively (Table 1).

The above presented data show that CH_2 groups in polyeteric chain are not identical. Analysis of signal shape led to the conclusion that sequences of type A are pseudorigid, while sequences of type B show a strong free rotation. This means that the decrease of etheric ethylenic group number (sequences of type B) will have as result the increase of molecule rigidity and, at the same time, they will decreases the possibility of macroradicals to meet the non-reacted double bonds.

TABLE 1

The values of chemical displacement of polyethylene glycol dimethacrylates in ^1H-NMR spectra

Group / Monomer	$H_1H_2C=C<$		CH_2 esteric δ (ppm)	etheric CH_2		$2 \times CH_3$ δ (ppm)
	δH_1 (ppm)	δH_2 (ppm)		$\delta (CH_2)_A^*$ (ppm)	$\delta (CH_2)_B^{**}$ (ppm)	
Ethylene dimethacrylate	6.217	5.568	4.47	—	—	1.98
Diethylene glycol dimethacrylate	6.150	5.562	4.32	3.78	—	1.97
Triethylene glycol dimethacrylate	6.200	5.565	4.438	3.83	3.717	2.00
Tetraethylene glycol dimethacrylate	6.200	5.565	4.370	3.82	3.717	2.00

* $\delta (CH_2)_A$ = chemical displacement for $-CH_2-$ group in the unit of type A
** $\delta (CH_2)_B$ = chemical displacement for $-CH_2-$ group in the unit of type B

This fact, remarked also by Korolev, [6,7] explains the lower reactivity of ethylene dimethacrylate and, of high reactivity of tetraethylene glycol dimethacrylate respectively.

At the same time, as shown at the beginning, in the case of ethylene dimethacrylate the obtained tridimensional polymer presents the highest network density, reason for which monomer diffusion to rising macroradical is most difficult. Together with oligomeric chain increase, products with lesser and lesser network density are obtained in which the monomer diffusion is easier. Due to this fact the limit conversion increases from ethylene dimethacrylate to tetraethylene glycol dimethacrylate.

CONCLUSIONS

Reactivity of polyethylene glycol dimethacrylates is determined by oligomeric chain length being higher as its length is greater. This fact is due to the increase of oligomeric chain flexibility and of possibilities of its free rotation, fact emphasized by ^1H-NMR spectra, as well as to tridimensional network density which is more loose as the distance between the double bonds is larger.

These factors make the monomer diffusion towards active centers easier and increase the non-reacted double bond possibilities to meet the rising macroradicals, thus contributing to polymerization rate and limit conversion increase.

REFERENCES

[1] Part VII, A. Caragheorgheopol, H. Căldăraru, Gh. Hubca, Cr. Oprescu and M. Dimonie, *Rev. Roumaine Chim*, **27**, 969 (1982).

[2] Part. IV, Gh. Hubca, Cr. Oprescu, Gh. Drăgan and M. Dimonie, *Rev. Roumaine Chim.*, **27**, 433 (1982).

[3] Part. V. Gh. Hubca, Gh. Drăgan, Cr. Oprescu and M. Dimonie *Rev. Roumaine Chim.* **27**, 585 (1982).

[4] Part. VI. Gh. Hubca, Cr. Oprescu, A. Caragheorgheopol, H. Căldăraru, D. Racoţi and M. Dimonie, *Rev. Roumaine Chim.*, **27**, 569 (1982).

[5] D. H. Williams and I. Fleming, "Spectroscopic Methods in Organic Chemistry", Mc Graw — Hill, London 1966.

[6] G. V. Korolev, B. R. Smirnov and A. B. Bolhovitimov, *Vysokomol. Soedinenyia*, **4**, 1660 (1962).

[7] G. V. Korolev, L. I. Mahonina and A. A. Berlin, *Vysokomol. Soedinenyia*, **3**, 198 (1961).

NOTE POUR LES AUTEURS

La Revue Roumaine de Chimie publie des articles en anglais, français, russe, allemand ou espagnol. Les auteurs sont priés d'envoyer des articles et des comptes rendus inédits.

Les manuscrits seront dactylographiés à deux intervalles. La bibliographie, les tableaux et la légende des figures seront placés après le texte.

Si l'article fait partie d'une serie numérotée, la partie précédente sera donnée comme première référence.

Chaque article sera précédé d'un résumé comprenant quinze lignes au maximum.

Les références bibliographiques dans le texte seront faites par des exposants sans parenthèses et paraîtront à la fin de l'ouvrage.

Les publications périodiques mentionnées dans la bibliographie seront présentées suivant les prescriptions internationales : le nom de l'auteur précédé de l'initiale du prénom, le titre du périodique abrégé conformément à « Chemical Abstracts » et souligné par une ligne, le numéro du tome indiqué par des chiffres arabes et souligné par deux lignes, suivi de la première page de l'article : à la fin, l'année de la parution sera placée entre parenthèses. Le numéro de la revue ne sera pas indiqué si les pages du volume sont numérotées consécutivement.

Les textes des livres ou traités inclueront : les noms des auteurs, les initiales du prénom, le titre du livre entre guillemets et sans être souligné, le numéro du tome précédé par l'abréviation « vol » (ou « Bd »), le numéro de l'édition, les éditions (the publisher), la localité de la parution du livre, l'année de la parution et la page de la référence précédée(s) par l'abréviation « p » (ou « S »).

Les brevets seront indiqués comme suit : l'auteur ou la firme, le pays et le numéro du brevet, la date et la revue *(Chem. Abstr.)*. Par ex. : M. Jones (to Union Carbide Co.), *Brit. Pat.* 601 238, 2 Sept. 1959, *Chem. Abstr.* **54**, 12808 (1960).

Si la référence n'a pas été lue en original, on indiquera aussi la revue de références consultée.

Les diagrammes seront tracés à l'encre de Chine sur papier calque. Les tableaux et les figures (en nombre strictement nécessaire) ainsi que les courbes dans les figures seront numérotés par des chiffres arabes. Leur explication sera donnée dans la légende des figures. Prière de ne pas inscrire les mêmes données dans les tableaux et les figures. Chaque tableau aura un titre. On indiquera dans le texte la place approximative des tableaux et des figures. Les formules chimiques seront incluses dans le texte : en outre, elles seront transcrites sur papier calque, à l'encre de Chine.

Les auteurs sont priés d'indiquer les caractères italiques (en soulignant les letttres au crayon), ainsi que tout autre caractère spécial : les préfixes *ortho*, *meta*, *para*, *cis*, *trans*, etc. seront soulignés pour indiquer leurs caractères italiques et ne seront jamais écrits avec des majuscules.

Aucune correction à la main ne sera admise sur le manuscrit. Les corrections seront frappées à la machine. Les lettres grecques ou autres symboles spéciaux seront insérés à la main à l'encre clairement.

Le manuscrit sera signé par l'auteur.

Le titre-courant aura 50 lettres au maximum.

L'entière responsabilité du contenu des articles appartient aux auteurs.

Sur demande on peut obtenir une note plus complète.

PRINTED IN ROMANIA

NOTE POUR LES AUTEURS

La Revue Roumaine de Chimie publie des articles en anglais, français, russe, allemand ou espagnol. Les auteurs sont priés d'envoyer des articles et des comptes rendus inédits.

Les manuscrits seront dactylographiés à deux intervalles. La bibliographie, les tableaux et la légende des figures seront placés après le texte.

Si l'article fait partie d'une série numérotée, la partie précédente sera donnée comme première référence.

Chaque article sera précédé d'un résumé comprenant quinze lignes au maximum.

Les références bibliographiques dans le texte seront faites par des exposants sans parenthèses et paraîtront à la fin de l'ouvrage.

Les publications périodiques mentionnées dans la bibliographie seront présentées suivant les prescriptions internationales : le nom de l'auteur précédé de l'initiale du prénom, le titre du périodique abrégé conformément à « Chemical Abstracts » et souligné par une ligne, le numéro du tome indiqué par des chiffres arabes et souligné par deux lignes, suivi de la première page de l'article ; à la fin, l'année de la parution sera placée entre parenthèses. Le numéro de la revue ne sera pas indiqué si les pages du volume sont numérotées consécutivement.

Les textes des livres ou traités incluront : les noms des auteurs, les initiales du prénom, le titre du livre entre guillemets et sans être souligné, le numéro du tome précédé par l'abréviation « vol » (ou « Bd »), le numéro de l'édition, les éditions (the publisher), la localité de la parution du livre, l'année de la parution et la page de la référence précédée(s) par l'abréviation « p » (ou « S »).

Les brevets seront indiqués comme soit : l'auteur ou la firme, le pays et le numéro du brevet, la date et la revue (*Chem. Abstr.*). Par ex. : M. Jones (to Union Carbide Co.), *Brit. Pat.* 804228, 2 Sept. 1959, *Chem. Abstr.* 54, 12808 (1960).

Si la référence n'a pas été lue en original, on indiquera aussi la revue de références consultée.

Les diagrammes seront tracés à l'encre de Chine sur papier calque. Les tableaux et les figures (en nombre strictement nécessaire) ainsi que les courbes dans les figures seront numérotés par des chiffres arabes. Leur explication sera donnée dans la légende des figures. Prière de ne pas inscrire les mêmes données dans les tableaux et les figures. Chaque tableau aura un titre. On indiquera dans le texte la place approximative des tableaux et des figures. Les formules chimiques seront incluses dans le texte ; en outre, elles seront transcrites sur papier calque, à l'encre de Chine.

Les auteurs sont priés d'indiquer les caractères italiques (en soulignant les lettres au crayon), ainsi que tout autre caractère spécial ; les préfixes ortho, méta, para, cis, trans, etc. seront soulignés pour indiquer leurs caractères italiques et ne seront jamais écrits avec des majuscules.

Aucune correction à la main ne sera admise sur le manuscrit. Les corrections seront frappées à la machine. Les lettres grecques ou autres symboles spéciaux seront insérés à la main à l'encre, clairement.

Le manuscrit sera signé par l'auteur.

Le titre courant aura 30 lettres au maximum.

L'entière responsabilité du contenu des articles appartient aux auteurs.

Sur demande on peut obtenir une note plus complète.

PRINTED IN ROMANIA

TRAVAUX PARUS AUX ÉDITIONS DE L'ACADÉMIE DE LA RÉPUBLIQUE SOCIALISTE DE ROUMANIE

ELENA CEAUŞESCU, **Noi cercetări în domeniul compuşilor macromoleculari** (Nouvelles recherches dans le domaine des composés macromoléculaires), 1981, 536 p.

I. G. MURGULESCU, RODICA VÎLCU, **Introducere în chimia fizică, Vol. III. Termodinamica chimică** (Introduction à la chimie physique, Vol. III, Thermodynamique chimique), 1982, 624 p.

I. G. MURGULESCU, J. PĂUN, **Introducere în chimia fizică, Vol. I. 3. Nucleul atomic, reacţii nucleare, particule elementare** (Introduction à la chimie physique. Vol. I. 3. Noyau atomique, réactions nucléaires, particules élémentaires), 1982, 606 p.

ELENA JERCAN, **Analiza cromatografică** (Analyse chromatographique), 1982, 286 p.

I. G. MURGULESCU, TATIANA ONCESCU, E. SEGAL, **Introducere în chimia fizică. Vol. II. 2. Cinetică chimică şi cataliză** (Introduction à la chimie physique. Vol. II 2. Cinétique chimique et catalyse), 1981, 1024 p.

V. DRĂGUŢAN, A. T. BALABAN, M. DIMONIE, **Metateza olefinelor şi polimerizarea prin deschidere de inel a cicloolefinelor** (La métathèse des oléfines et la polymérisation par ouverture annulaire des cyclooléfines), 1981, 254 p.

LYDIA-MARIA VAICUM, **Epurarea apelor uzate cu nămol activ. Bazele biochimice** (L'épuration des eaux résiduelles à boue active. Les bases biochimiques), 1981, 218 p.

I. GĂLĂŢEANU, **Procese şi metode radiochimice în energetica nucleară** (Processus et méthodes radiochimiques dans l'énergetique nucléaire), 1981, 234 p.

OCTAVIAN IORDACHE, **Procese polistocastice aplicate la fenomenele de transfer** (Processus polystochastiques appliqués aux phénomènes de transfert), 1981, 186 p.

CR. SIMIONESCU, VALERIA GORDUZA, **Polimeri biocompatibili şi biologic activi** (Polymères biocompatibles et biologiquement actifs), 1980, 479 p.

ELENA CEAUŞESCU, **Polimerizarea stereospecifică a izoprenului** (La polymérisation stéréospécifique de l'isoprène), 1979, 307 p.

CONST. GH. MACAROVICI, **Analiza chimică cantitativă anorganică** (L'analyse chimique quantitative inorganique), 1979, 457 p.

M. FLORESCU, **Metode ştiinţifice în dezvoltarea industriei chimice moderne** (Méthodes scientifiques dans le développement de l'industrie chimique moderne), 1979, 256 p.

A. T. BALABAN, I. GĂLĂŢEANU, G. GEORGESCU, LIGIA SIMIONESCU, **Compuşi marcaţi şi radiofarmaceutici cu aplicaţii în medicina nucleară** (Composés marqués et radiopharmaceutiques à application en médecine nucléaire), 1979, 495 p.

I. G. MURGULESCU, E. SEGAL, **Introducere în chimia fizică, vol. II. 1. Teoria molecular cinetică a materiei** (Introduction à la chimie physique. Vol. II. 1. La théorie moléculaire-cinétique de la matière), 1979, 1036 p.

S. STERNBERG, FL. DANEŞ, **Termodinamica chimică aplicată** (La thermodynamique chimique appliquée), 1978, 400 p.

I. G. MURGULESCU, V. EM. SAHINI, **Introducere în chimia fizică, Vol. I. 2. Structura şi proprietăţile moleculelor** (Introduction à la chimie physique. Vol. I. 2. La structure et les propriétés des molécules), 1978, 604 p.

I. ZUGRĂVESCU, MAGDA PETROVANU, **N-ylid chemistry**, coédition avec McGraw-Hill International Book Company, U.S.A., 1977, 396 p.

I. G. MURGULESCU, **Introducere în chimia fizică. Vol. I. 1. Atomi, molecule, legătură chimică** (Introduction à la chimie physique, Vol. I. 1. Atomes, molécules, liaison chimique), 1976, 560 p.

ELENA CEAUŞESCU, **Research work on synthesis and characterization of macromolecular, compounds. Contributions**, 1974, 251 p.

CR. SIMIONESCU, VIORICA RUSAN, V. POPA, **Chimia algelor marine** (La chimie des algues marines), 1974, 212 p., 1 pl.

1983 SEP 22

ISSN 0035—4090

I. P. Informaţia c. 2652

43 426

Lei 40
$ 70 (pour un abonnement annuel)

F 1103

Vegyészet

ACADÉMIE DE LA RÉPUBLIQUE SOCIALISTE DE ROUMANIE

REFERÁLVA

REVUE ROUMAINE DE CHIMIE

TOME 28

N° 3

Mars 1983

EDITURA ACADEMIEI REPUBLICII SOCIALISTE ROMÂNIA

Rev. Roumaine Chim.

RRCHAX, **28**, *3*, p. 191–296 (1983), Bucarest

ACADÉMIE DE LA RÉPUBLIQUE SOCIALISTE DE ROUMANIE

COMITÉ DE RÉDACTION

Rédacteur en chef :

I. G. MURGULESCU, membre de l'Académie de la République Socialiste de Roumanie

Rédacteurs en chef adjoints :

A. T. BALABAN et V. EM. SAHINI, membres correspondants de l'Académie de la République Socialiste de Roumanie

Collège de rédaction :

EM. BRATU, ELENA CEAUŞESCU, ECATERINA CIORĂNESCU-NENITZESCU, CR. SIMIONESCU, membres de l'Académie de la République Socialiste de Roumanie; P. SPACU, membre correspondant de l'Académie de la République Socialiste de Roumanie; MARGARETA AVRAM, M. BANCIU, I. HAIDUC, D.I. MARCHIDAN, I. MOLDOVAN, G. NIAC et D. SĂNDULESCU

La Revue Roumaine de Chimie paraît 10 fois par an. Toute commande de l'étranger pour les travaux parus aux Editions de l'Académie de la République Socialiste de Roumanie sera adressée à ILEXIM – Departamentul Export-Import Carte (Livres)/Departamentul Export-Import Presă (Revues), P.O.B. 136 – 137, télex 11226, 3, str. 13 Decembrie, 79517 Bucarest, Roumanie

Les manuscrits, les livres et les revues proposés en échange, ainsi que toute correspondance seront envoyés à la rédaction :

REVUE ROUMAINE DE CHIMIE

125, Calea Victoriei, 79717 Bucarest, Roumanie, téléphone 50 76 80

EDITURA ACADEMIEI REPUBLICII SOCIALISTE ROMÂNIA
125, Calea Victoriei, 79717 Bucarest, Roumanie, téléphone 50 76 80

REVUE ROUMAINE
DE
CHIMIE

ORSZÁGOS MŰSZAKI INFORMÁCIÓS KÖZPONT ÉS KÖNYVTÁR 1983

Tome 28, N° 3 Mars, 1983

V. BRÂNZOI and S. STERNBERG, Polarization behaviour of copper in $CH_3OH + H_2SO_4$ solution . . . . 193—200 R

A. DABROWSKI, M. JARONIEC and J. K. GARBACZ, Discussion of the liquid adsorption model involving multilayer formation, surface heterogeneity and nonideality of the bulk solution . . . . 201—210

C. LUCA, A. POPA, N. BÎLBĂ and GH. MIHĂILĂ, Inclusion compounds of perhydrotriphenylene with higher *n*-alcohols . . . . 211—216

P. BAHADUR, A. GUPTA and P. LATA, Conductance behaviour of cationic surfactants in alkanols . . . . 217—223 Bc

D. NEGOIU and ILEANA GHELASE, Complex compounds of Cd(II) with acetone selenosemicarbazone . . . . 225—234

I. HAVLIK und R. BACALOGLU, Nucleophilic substitutions in the 1,3,5-triazine. IX. Kinetics and Mechanism of the reaction between 2,4-dichloro-6-phenylazophenylamino-1,3,5-triazine with 4-amino-azobenzene (in German) . . . . 235—242

SIMONA SILBERG, IOAN A. SILBERG and CORNEL BODEA, Derivatives of 4-aminomethyl-thiazole. IV. Thiazole derivatives of phenothiazine . . 243—247

MIRCEA V. DIUDEA, Phenazathionium cations. V. Reactions of 10-(3-phenothiazinylidene)-phenothiazinium cations and their complexes with copper and iron chlorides . . . . 249—261

V. P. KUDESIA and C. B. SHARMA, Effect of structure on the reactivity in the oxidation of aliphatic alcohols by chlorine dioxide . . . . 263—266

FLORENTINA C. GEORGESCU, E. G. GEORGESCU, F. CHIRALEU, E. I. GEORGESCU and I. ZUGRĂVESCU, Pyridinium-ylids. IV. Reactions of carbanion-monosubstituted 4-phenyl-pyridinium-ylids with activated olefins (in French) . . . . 267—274

SOFIA MARCHIDAN, IULIANA VARTIRES, I. TĂNASE and N. D. TOTIR, Determination of trace quantities of cobalt by anodic stripping voltammetry and alternating current polarography . . . . 275—280 R

M. S. SUBHANI, Radiation chemistry of iodate anion in aqueous solution . . 281—286 R

MINODORA LECA and MARIA ENACHE, Determination of polymer partial solubility parameters by gas-liquid chromatography . . . . 287—291 Bc

BOOK REVIEWS . . . . 293—296

Rev. Roumaine Chim. **28,** *3,* 191—296 (1983), Bucarest

Revue Roumaine de Chimie, 28, *3*, 193–200, (1983)

POLARIZATION BEHAVIOUR OF COPPER IN $CH_3OH + H_2SO_4$ SOLUTION

V. BRÂNZOI and S. STERNBERG
Department of Physical Chemistry and Electrochemistry, National
Institute of Chemistry, Bucharest, Str. Polizu 1, Romania

Received September 16, 1981

Using the potentiodynamic method, the polarization behaviour of copper has been studied under a variety of environmental conditions. In dilute solutions of H_2SO_4 in CH_3OH at room temperature, copper may dissolve at rates limited by a diffusion-controlled current; increasing the acid concentration results in an increased tendency for passivation. Lowering the temperature promotes the establishment of passivity. The analysis of the current-potential curves led to some discussions concerning the mechanism of electrochemical dissolution of copper.

The mechanical properties of copper are weaker than those of many metals or alloys and even of its own alloys. Nevertheless, copper has been widely applied in industry owing to its good chemical stability in many corrosive media and high electric and thermal conductivity. This paper was undertaken in an attempt to analyse the polarization behaviour of copper in $CH_3OH + H_2SO_4$ (in various H_2SO_4 concentrations) taking into account the great economic importance of metal corrosion in organic liquids. Today, the number of organic systems used in technology has cosiderably increased.

The present paper reports on the polarization behaviour of copper in $CH_3OH + xMH_2SO_4$ solutions ($x = 0.25$; 0.5; 0.75; ....10M) at 0°C and 25°C.

EXPERIMENTAL

For the experimental determinations, the potentiodynamic technique was used plotting the potentiodynamic polarization curves by means of a Tacussel assembly. A schematical representation of the device for plotting the polarization curves and of the working cell were presented in an earlier paper. [1] Before each determination, the cylindrical copper electrode was mechanically polished with emery paper of varied granulation up to mirror lustre, degreased in benzene, washed with acetone, dried and then immersed, for two minutes, in nitric acid, 20% at 25°C. After immersion the electrode was washed in methyl alcohol and then fixed in the working cell. The solution to be tested was deaerated with purified argon for one hour before each determination, argon bubbling continuing throughout the experiment.

The working electrode was always measured with respect to the saturated calomel electrode and was represented graphically as a function of the current appearing in the external circuit. Thus, the anodic or cathodic polarization curves were obtained in terms of the direction of the working electrode potential.

EXPERIMENTAL RESULTS

Figures 1 and 2 show that up to concentrations of 5 MH_2SO_4 and at a temperature of 20°C, copper has a region of active dissolution followed

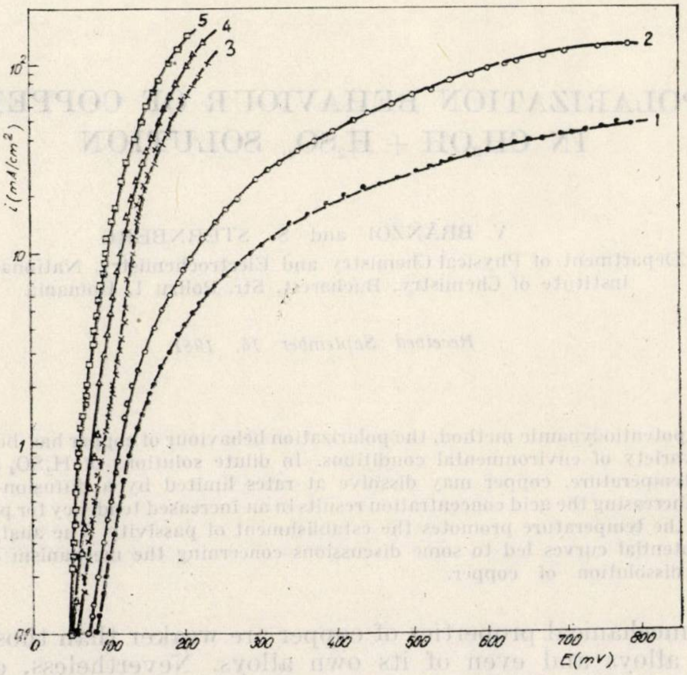

Fig. 1. – Anodic polarization curves of copper in CH_3OH + + H_2SO_4 at 25°C : (1) Cu + $CH_3OH \cdot 1{,}5M\ H_2SO_4$; (2) Cu + + CH_3OH + 1M H_2SO_4 ; (3) Cu + CH_3OH + 0.75 M H_2SO_4 ; (4) Cu + CH_3OH + 0.5M H_2SO_4 ; (5) Cu + CH_3OH + 0.25 M H_2SO_4.

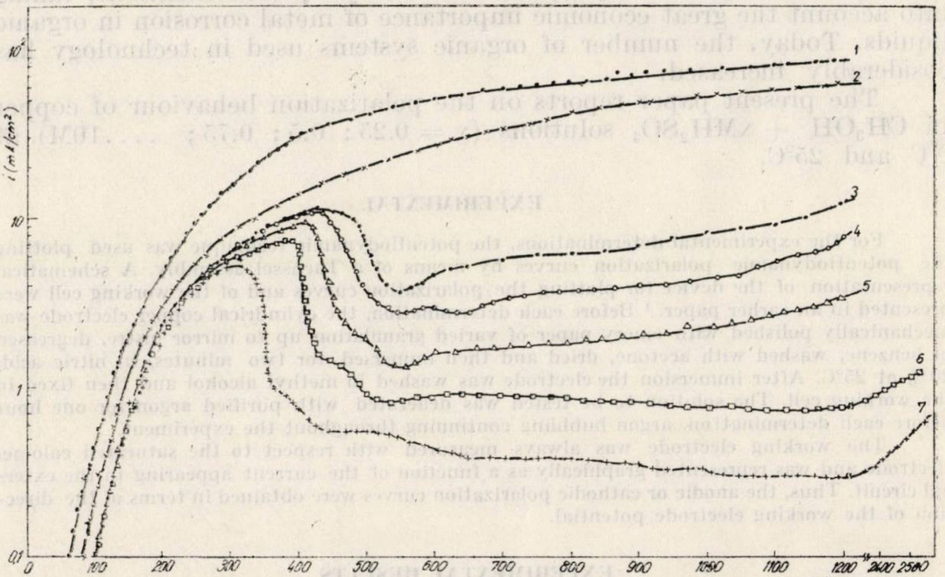

Fig. 2. – Anodic polarization curves of copper in CH_3OH + H_2SO_4 at 25°C : (1) Cu + CH_3OH+ + 3M H_2SO_4 ; (2) Cu + CH_3OH + 4M H_2SO_4 ; (3) Cu + CH_3OH + 5M H_2SO_4 ; (4) Cu+ + CH_3OH + 6M H_2SO_4 ; (5) Cu + CH_3OH + 7M H_2SO_4 ; (6) Cu + CH_3OH + 9M H_2SO_4 ; (7) Cu + CH_3OH + 10M H_2SO_4.

by a transpassive dissolution, controlled by the mass transfer of the soluble corrosion products on the surface of the electrode in solution.

Increase of the sulfuric acid concentration above 5 M leads to the appearance of passivity. Thus, it can be seen that the higher the sulfuric acid concentration, for a given temperature, the more pronounced is the passive region. Decrease of the temperature to 0°C promotes an increased tendency to passivation (Fig. 3.). Analysis of the polarization curves shows that between 4 and 5 MH_2SO_4, copper passes from active dissolution with current densities controlled by diffusion to a passive behaviour indicating the formation of an oxide film. The region of active dissolution is greater at lower sulfuric acid concentrations. This can be explained in that solubility of the corrosion products decreases with increase in sulfuric acid concentration on the one hand and, on the other, that the possible formation of the oxide film augments with increase in the water quantity (water concentration increases with H_2SO_4 concetration). It has been shown that in anhydrous and deaerated organic media, water plays a decisive role, in formation of the passive film, as it furnishes the necessary oxygen for the oxide.[2-4] In agreement with Latimer,[5] the free enthalpy of CuO_2 is -34.98 kcal. The free enthalpy was calculated for the following reaction using the thermodynamic relations

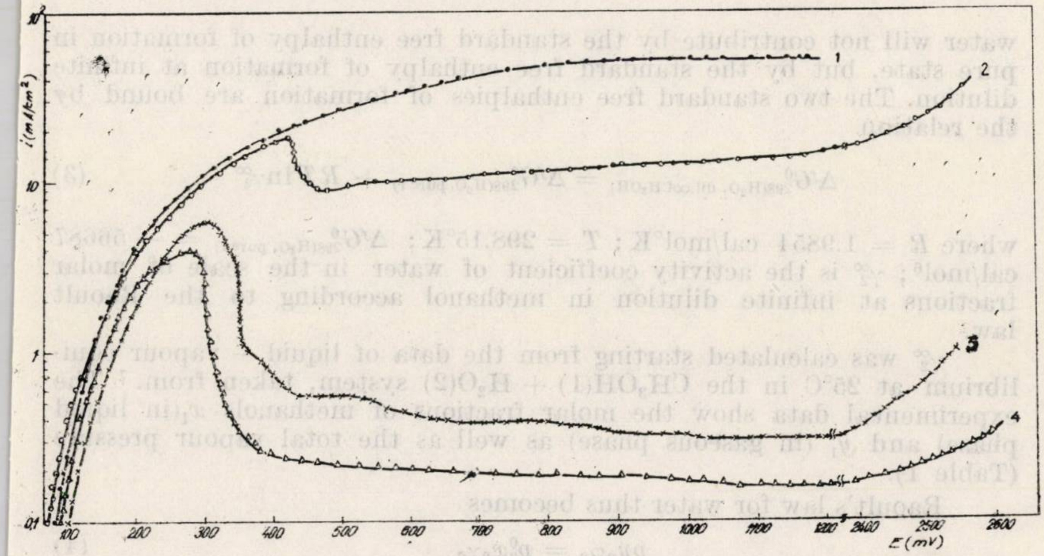

Fig. 3. — Anodic polarization curves in $CH_3OH + H_2SO_4$; (1) Cu + CH_3OH + 1.5 M H_2S at 25°C ; (2) Cu + CH_3OH + 1.5 M H_2SO_4 at 0°C ; (3) Cu + CH_3OH + 10M H_2SO_4 at 25°C ; (4) Cu + CH_3OH + 10M H_2SO_4 at 0°C.

$$2Cu + H_2O \rightarrow Cu_2O + 2H^+ + 2e \qquad (1)$$

As the reaction medium is a very dilute water solution in methanol, an infinite dilute solution is preferred as standard state for water. In this case, in relation $a_{H_2O} = x_{H_2O} \cdot \gamma_{H_2O}$, γ_{H_2O} may be taken as $= 1$.

Thus, for calculating the standard free enthalpy of the reaction, $\Delta^r G^0_{298}$, from the standard free enthalpies of $\Delta^f G^0_{298,i}$ formation of the i participants to the reaction

$$\Delta^r G^0_{298} = \sum_i^n \nu_i \Delta^f G^0_{298,i} \tag{2}$$

water will not contribute by the standard free enthalpy of formation in pure state, but by the standard free enthalpy of formation at infinite dilution. The two standard free enthalpies of formation are bound by the relation

$$\Delta^f G^0_{298(\mathrm{H_2O,\ dil.\infty CH_3OH})} = \Delta^f G^0_{298(\mathrm{H_2O,\ pure\ 1})} + RT\ln\gamma_2^\infty \tag{3}$$

where $R = 1.9854$ cal/mol°K; $T = 298.15$°K; $\Delta^f G^0_{298(\mathrm{H_2O,\ pure\ 1})} = -56687$ cal/mol[6]; γ_2^∞ is the activity coefficient of water in the scale of molar fractions at infinite dilution in methanol according to the Raoult law.

γ_2^∞ was calculated starting from the data of liquid — vapour equilibrium at 25°C in the $CH_3OH(1) + H_2O(2)$ system, taken from.[7] The experimental data show the molar fractions of methanols x_1(in liquid phase) and y_1 (in gaseous phase) as well as the total vapour pressure (Table 1).

Raoult's law for water thus becomes

$$py_2\varphi_2 = p_2^0 x_2 \gamma_2 \tag{4}$$

where y_2 and x_2 are the water molar fractions in vapours and in liquid respectively, φ_2 is the fugacity coefficient of water in vapours, γ_2 the fugacity coefficient of water in liquid (according to Raoult's law), p_2^0 is the vapour pressure of pure water, and $(py_2\varphi_2)$ is the fugacity of water in the vapour phase.

As $p_2^0 = \lim\limits_{x_2\to 1} p$, or $p_2^0 = \lim\limits_{x_1\to 0} p$, its value can be found directly from table 1. It was thus found

$$p_2^0 = 23.7\ \text{Torr} \tag{5}$$

TABLE 1

Values of molar fractions of methanol x_1 (in liquid phase), y_1 (in gaseous phase) and total vapour pressure p

x_1	0	0.0873	0.1900	0.3417	0.4943	0.6919	0.8492	1.0000
y_1	0	0.4187	0.6187	0.7350	0.7934	0.8822	0.9384	1.00
p(torr)	23.7	37.5	53.0	69.8	82.3	98.5	112.0	124.0

As $p \ll 1$ atm, it may be considered that the vapours are an ideal mixture of perfect gases, so that

$$\varphi_2 = 1 \tag{6}$$

Substituting x_2, y_2, p_2^0, φ_2, in equation (4), the following results

$$\gamma_2 = \frac{p(1 - y_1)}{23.7(1 - x_1)} \tag{7}$$

With relation (7) and p, y_1, x_1 values in table 1, the following dependence $\gamma_2(x_1)$, shown in table 2 results.

TABLE 2

γ_2 values as a function of x_1

x_1	0.0873	0.1900	0.3417	0.4943	0.6919	0.8492
γ_2	1.008	1.053	1.186	1.419	1.589	1.930

By definition the γ_2^∞ value looked for will be

$$\gamma_2^\infty = \lim_{x_1 \to 1} \gamma_2 \tag{8}$$

For facilitating extrapolation at infinite dilution, the model of regular solutions is used,[8] according to which $\gamma_2 \sim x_1^2$, thus substituting direct extrapolation (8) by extrapolation

$$\ln \gamma_2^\infty = \lim_{x_1 \to 1} \left(\frac{\ln \gamma_2}{x_1^2} \right) \tag{9}$$

The values of the extrapolated function, $\ln\gamma_2/x_1^2$, are calculated by means of the data in table 2 and are shown in table 3.

TABLE 3

Values of the $\ln\gamma_2/x_1^2$ function

x_1	0.0873	0.1900	0.3417	0.4943	0.6919	0.8492
$\ln\frac{\gamma_2}{x_1^2}$	1.009	1.431	1.461	1.432	0.967	0.912

Graphic extrapolation of the data in table 3 leads, according to eqution (9) to

$$\ln \gamma_2^\infty = 0.88 \tag{10}$$

By substituting this value in equation (4)

$$\Delta^f G^0_{298(\mathrm{H_2O,\ dil.\infty CH_3OH})} = -56687 + 1.9854.298.15.0.88 = -56165 \text{ cal/mol} \tag{11}$$

The standard free enthalpy of the reaction can now be calculated according to equation (2). The value of the equilibrium potential for the formation of cuprous acid (Cu_2O), in keeping with reaction (1) is

$$E^0 = \frac{-\Delta G^0_{\text{reaction}}(1)}{0.239\ \mathrm{ZF}} + \frac{\Delta G_{\text{mixture}}}{0.239\ \mathrm{ZF}} \tag{12}$$

$$E^0 = \frac{-(\Delta^f G^0_{Cu_2O} - \Delta^f G^0_{(H_2O,\ \text{dil.}\infty CH_3OH)}}{0.239\,ZF} + \frac{RT \ln a_{H_2O}}{0.239\,ZF} \tag{13}$$

The values of the molar fractions of water for various solutions and also the equilibrium potentials $E^0_{Cu_2O/Cu}$, calculated on the basis of relation (13) are given in table 4.

TABLE 4

The calculated values of the molar function X_{H_2O}, of $E^0_{Cu_2O/Cu}$ equilibrium potential and the experimental values of the E_A potential

Solution	X_{H_2O}	$E_{Cu_2O/Cu}$ mV SCE	E_A mV SCE
$CH_3OH + 5M\ H_2SO_4$	$4.48 \cdot 10^{-2}$	257.2	265
$CH_3OH + 6M\ H_2SO_4$	$5.4 \cdot 10^{-2}$	251.0	260
$CH_3OH + 7M\ H_2SO_4$	$6.33 \cdot 10^{-2}$	253.0	260
$CH_3OH + 9M\ H_2SO_4$	$8.21 \cdot 10^{-2}$	249.3	254
$CH_3OH + 10M\ H_2SO_4$	$9.16 \cdot 10^{-2}$	247.5	250

The table shows that the values of the equilibrium potential $E_{Cu_2O/Cu}$, are very close to the values of E_A potential (the potential from which the oxide formation reaction is thermodynamically possible)[9] thus suggesting that the passivation reaction can well be associated with Cu_2O formation. The absence of passivity in more dilute H_2SO_4 solutions in methanol can be attributed, on the one hand, to increase in the solubility of the corrosion products, and on the other to an insufficient quantity of water for formation of the Cu_2O film.

The tendency of copper to passivation in $CH_3OH + 1.5N\ H_2SO_4$ solution at 0°C can be attributed to the reduced solubility of the corrosion products at low temperatures. Moreover, increase in the stability of the passive film with the decrease of temperature is due to the same cause. In more dilute solutions of H_2SO_4 in methanol, considered to be strongly ionized, the active dissolution region is broader (up to very high currents) and the anodic Tafel slopes have 40 mV values, in agreement with the results in, [10] obtained for copper in aqueous solutions of sulfuric acid. It may therefore be concluded that the active dissolution of copper in H_2SO_4 methanol solutions takes place according to a mechanism similar to that in the H_2SO_4 aqueous solutions by a two-step charge transfer as follows

$$\mathrm{Cu} \overset{\text{rapid}}{\rightleftarrows} \mathrm{Cu}^+ + \mathrm{e} \tag{14}$$

$$\mathrm{Cu}^+ \xrightarrow{\text{slow}} \mathrm{Cu}^{2+} + \mathrm{e} \tag{15}$$

Cu^+ ions are considered to be adsorbed on the electrode surface and their concentration on the surface to depend on the potential.

According to [11] and postulating that there is no Cu^+ loss by diffusion, the equation of the current density for the two-step charge transfer is :

$$i = 2\frac{\exp[-(\alpha_1 + \alpha_2)F] - \exp[(2 - \alpha_1 - \alpha_2)F\eta]}{\frac{1}{i_{01}}\exp[(1 - \alpha_2)F\eta] + \frac{1}{i_{02}}\exp(-\alpha_1 F\eta)} \tag{16}$$

where α_1 and α_2 are the transfer coefficients for (14) and (15) respectively, i_{01} and i_{02} are the densities of the exchange current for the two steps. Considering $i_{01} \gg i_{02}$, $\alpha_1 = \alpha_2 = \alpha = 0.5$ and intermediate values for η, the first term of numerator and denominator can be neglected, then equation (16) is reduced to

$$i = -2i_{02}\exp[(2 - \alpha)F\eta] \tag{17}$$

This equation presupposes anodic Tafel slopes of 39mV, that is in good agreement with our experimental results. Small deviations from 40mV cannot be excluded at very high current densities but this also is in keeping with equation (17) and confirms once more the existence of the two-step charge transfer mentioned above.

Analysis of the curves of anodic polarization in figures 2 and 3 shows that the transpassive region begins at very high anodic potentials (over 2V). Optical study of the copper electrodes subjected to anodic dissolution in the transpassive region evidenced the formation of a poorly adhesive, dark-coloured porous film, on the electrode surface. This film, formed during transpassive dissolution, is made up of Cu_2O[5,12,13] the same as the oxide layer in the passive region except that during passivity a thin, adhesive and compact CuO_2 layer is formed, whereas in the transpassive region the film is much thicker, porous and less adhesive. This can be explained as follows : increase in the anodic potential to very high values (as already shown, the transpassive region begins at very high anodic potentials) increases the conductibility of the oxide film formed in the passive region, resulting in the subsequent oxidation of copper through this film.

The new cuprous oxide layer is formed on the surface of the Cu_2O film in the passive region (due to its increased conductibility) so that its properties differ from those of the former.

Thus, it may be concluded that dissolution in the transpassive region takes place at very high anodic potentials, due to the adhesive compact Cu_2O layer in the passive region.

Finally, the anodic films has a structure formed of two parts :

— a thin adhesive, compact Cu_2O layer in contact with the metal, that determines the electrochemical behaviour of the copper electrode;

— another thicker, porous and less adhesive Cu_2O layer, formed over the surface of the former, that influences the polarization behaviour of the copper electrode to a less extent.

CONCLUSIONS

In methanol solutions of sulfuric acid up to 5 M H_2SO_4 and at 25°C, copper has a region of active dissolution followed by a transpassive dissolution controlled by the mass transfer of soluble corrosion products on the surface of the electrode in solution.

The region of active dissolution is larger for more dilute H_2SO_4 solutions in methanol.

The kinetic parameters of corrosion determined by polarization curves (anodic Tafel slopes of 40 mV and subunit reaction order) plead for the active dissolution of copper by a two-step charge transfer :

$$Cu \overset{\text{rapid}}{\rightleftarrows} Cu^+ + e$$

$$Cu^+ \longrightarrow Cu^{2+} + e$$

Cu^+ ions are adsorbed on the electrode surface and their concentration on the surface depends on the potential.

Increase of sulfuric acid concentration over 5M leads to the appearance of passivity. Thermodynamical calculations furnish evidence of the formation of cuprous oxide (Cu_2O) producing the passive film.

Diminution of temperature increases the tendency to passivation of copper in the methanol solutions of sulfuric acid. For the same H_2SO_4 concentration but at low temperatures, a larger passive range and lower values are obtained for the critical current density of passivation and the current density of passivation.

REFERENCES

[1] V. Brânzoi, *Bull. Inst. Polytech. Bucharest, series Chimie-Metalurgie*, **3**, 21 (1978).
[2] F. Mansfeld, *J. Electrochem. Soc.*, **120**, 188 (1973).
[3] F. Mansfeld, *J. Electrochem. Soc.*, **118**, 1412 (1971).
[4] T. Tousek, *Corrosion Sci.*, **12**, 15 (1972).
[5] W. Latimer, "Oxidation Potentials", Prentice Hall LONDON 1952.
[6] "Selected Values of Chemical Thermodinamic Properties National Bureau of Standards Circular 500".
[7] W. B. Kogan and W. B. Fridman, "Handbuch der Dampf-Flussigkeits Gleichgewichte", Veb Deutscher Verlag Der Wissenschoften, Berlin, 1961.
[8] J. Hildebrand and R. Scott, "Regular Solutions", Prentice-Hall, Englewood Cliffs, New Jersey, 1962.
[9] T. S. De Gromoboy and L. L. Shreir, *Electrochim. Acta*, **11**, 7, 895 (1966).
[10] E. Mattson and J. O'M. Bockris, *Trans. Faraday Soc.*, **55**, 1586, (1959).
[11] P. Delahay, "Double Layer and Electrode Kinetics", "Interscience Pubs., LONDON, 1965.
[12] K. Kinoshita, D. Landolt, R. H. Muller, and C. W. Tobias, *J. Electrochem. Soc.*, **117**, 1246 (1970).
[13] K. Kinoshita, Ph. D. Thesis, University of California, Berkeley, UCRL-19051, Sept. (1969).

Revue Roumaine de Chimie, 28, 3, 201–210 (1983)

DISCUSSION OF THE LIQUID ADSORPTION MODEL INVOLVING MULTILAYER FORMATION, SURFACE HETEROGENEITY AND NONIDEALITY OF THE BULK SOLUTION

A. DABROWSKI *, M. JARONIEC * and J. K. GARBACZ **
*Institute of Chemistry, M. Curie — Skłodowska University, 20031 Lublin, Poland
** Institute of Chemistry, N. Copernicus University, 87100 Toruń, Poland

Received March 26, 1981

Analytical equations for multilayer adsorption from binary nonideal liquid mixtures on energetically heterogeneous solid surfaces are discussed. One of these equations, derived for quasi-gaussian energy distribution, is examined by applying the experimental excess adsorption data available from the literature. According to this equation the model calculations, illustrating the effect of adsorbent heterogeneity and nonideality of the bulk solution, are performed and discussed.

INTRODUCTION

The monolayer adsorption of liquid mixtures on solid surfaces has been discussed by many authors (see references in the reviews [1–3]). They considered the adsorption from binary and multicomponent liquid mixtures on energetically homogeneous and heterogeneous solid surfaces. Theoretical considerations were made for ideal and nonideal bulk and surface phases.

In contrast to the extensive literature concerning the monolayer adsorption from liquid mixtures, the multilayer adsorption from solutions onto solid surfaces has been comparatively little investigated; usually, the studies concern the bilayer and multilayer adsorption on homogeneous solid surfaces (see references in the paper [4]). In the reference [4] a simple model for multilayer adsorption from multicomponent liquid mixtures on homogeneous and heterogeneous solid surfaces has been discussed. Taking into account in this model the recent theoretical isotherms for monolayer liquid adsorption onto heterogeneous solid surfaces, [5] the new equations for multilayer adsorption may be derived.

In this paper the analytical equations for multilayer adsorption from binary liquid mixtures on heterogeneous solid surfaces have been discussed. One of these equations, derived for quasi-gaussian energy distribution, has been examined by using the experimental adsorption data available from literature. Moreover, according to this equation the theoretical excess isotherms have been calculated for different adsorption parameters.

THEORETICAL

Let us consider r-layer adsorption from binary mixture $1 + 2$ on an energetically heterogeneous solid surface by assuming the following:

(a) adsorbent surface is energetically heterogeneous,

(b) bulk phase is ideal or nonideal,

(c) surface phase is ideal,

(d) total number of molecules in each adsorbed layer is constant, and

(e) molecular sizes of both components are identical. According to the paper [4] the general equation for the mole fraction of 1-st component in the surface phase may be expressed as follows:

$$x_{1,t}^{s} = \frac{1}{r}\,\theta_{1,t}^{(1)} + \frac{1}{r}\sum_{k=2}^{r} \theta_{1}^{(k)} \tag{1}$$

where $x_{1,t}^{s}$ is the mole fraction of 1-st component in the surface phase for a heterogeneous solid surface, $\theta_{1,t}^{(1)}$ and $\theta_{1}^{(k)}$ are the mole fractions of 1-st component in 1-st and k-th adsorbed layer, respectively, and r is the total number of adsorbed layers. The mole fraction $\theta_{1}^{(k)}$ is defined by the following equation:

$$\theta_{1}^{(k)} = L_{12}^{(k)} a_{12} / (1 + L_{12}^{(k)} a_{12}) \tag{2}$$

where

$$L_{12}^{(k)} = \prod_{1=k}^{r} K_{12}^{(1)} \tag{3}$$

$$L_{12}^{(r)} = K_{12}^{(r)} \tag{4}$$

$$a_{12} = a_1 / a_2 \tag{5}$$

and

$$a_i = f_i x_i^{1} \qquad \text{for } i = 1{,}2. \tag{6}$$

In the above a_i, x_i^1 and f_i are the activity, mole fraction and activity coefficient of the i-th component in the bulk phase, respectively, and $K_{12}^{(k)}$ is the equilibrium constant describing the exchange of a molecule of 1-st component from $(k + 1)$-layer with a molecule of 2-nd component from the k-th adsorbed layer.

Substituting in equation (1) the different equations of monolayer liquid adsorption on heterogeneous solid surfaces for $\theta_{1,t}^{(1)}$, we can obtain new expressions describing the multilayer liquid adsorption.

The majority of monolayer isotherms for adsorption from binary liquid mixtures on heterogeneous solid surfaces may be divided into two main groups. The first group contains equations which for $m = 1$ lead to Everett's adsorption isotherm,[1] where m is the heterogeneity parameter changing from zero to unity. This parameter characterizes the shape of the energy distribution function.[3,5] The most important isotherm equations belonging to the first group are the following :

$$\theta_{1,t}^{(1)} = \frac{(L_{12}^{1}\, a_{12})^{m}}{1 + (L_{12}^{1} a_{12})^{m}} \tag{7}$$

$$\theta_{1,t}^{(1)} = \frac{L_{12}^{(1)} a_{12}}{[1 + (L_{12}^{1}\, a_{12})^{m}]^{1/m}} \tag{8}$$

and

$$\theta_{1,t}^{(1)} = \left[\frac{L_{12}^{(1)}\, a_{12}}{1 + L_{12}^{(1)} a_{12}} \right]^{m} \tag{9}$$

Equation (7) has been derived for symmetrical energy distribution,[6-8] equation (8) has been obtained for Tóth's slightly asymmetrical distribution,[9] however, equation (9) relates to exponential distribution.[10]

The isotherm equations belonging to the other group are special cases of the exponential adsorption isotherm :[11]

$$\theta_{1,t}^{(1)} = \exp \left[\sum_{p=1}^{P} \beta_p \left(\ln \frac{a_{12}}{L_0} \right)^{p} \right] \tag{10}$$

where β_p for $p = 1, 2, \ldots, P$ and L_0 are the parameters of equation (10). From equation (10) the following adsorption isotherms may be obtained :

$$\theta_{1,2}^{(1)} = (a_{12}/L_0)^{\beta_1} \tag{11}$$

$$\theta_{1,t}^{(1)} = \exp \left[\beta_2 \left(\ln \frac{a_{12}}{L_0} \right)^{2} \right] \tag{12}$$

$$\theta_{1,t}^{(1)} = \exp \left[\beta_p \left(\ln \frac{a_{12}}{L_0} \right)^{p} \right] \tag{13}$$

where β_2 and β_p are smaller than zero. Equations (11) and (12) relate to Freundlich and Dubinin-Radushkevich gas adsorption isotherms, respectively.[3] Equations (10) — (11) are defined for $a_{12} < L_0$, however, for $a_{12} \geqslant L_0$ the value of $\theta_{1,t}^{(1)}$ is assumed to be unity.

The isotherm equations (7) — (13) may be used to describe the mole fraction of 1-st component in 1-st adsorbed layer. Applying these isotherms in equation (1) we obtain the equations for multilayer liquid adsorption on heterogeneous solid surfaces.

RESULTS AND DISCUSSION

Extensive model calculations have been performed for the following adsorption isotherm:

$$x^s_{1,t} = 0.5\,\frac{(L^{(1)}_{12}a_{12})^m}{1+(L^{(1)}_{12}a_{12})^m} + 0.5\,\frac{K^{(2)}_{12}a_{12}}{1+K^{(2)}_{12}a_{12}} \tag{14}$$

Equation (14) has been obtained by combining the equations (1), (2), (4) and (7) for $r = 2$ (bilayer adsorption). According to equation (3) the constant $L^{(1)}_{12}$ is equal to:

$$L^{(1)}_{12} = K^{(1)}_{12}\,K^{(2)}_{12} \tag{15}$$

Moreover, the model calculations have been made for regular bulk phase. For such model of the bulk phase, the variable a_{12} may be expressed as follows:

$$a_{12} = x^l_{12}\exp(q - 2qx^l_1)\,;\qquad x^l_{12} = x^l_1/x^l_2 \tag{16}$$

where q is the constant characterizing molecular interactions in the bulk regular solution.

The total adsorption excess of 1-st component is defined as follows:

$$n^e_1 = n^s_t(x^s_{1,t} - x^l_1) \tag{17}$$

where n^s_t is the capacity of the surface phase.
The adsorption excess in the k-th adsorbed layer is equal to:

$$n^{e(k)}_1 = n^s(\theta^{(k)}_1 - x^l_1) \tag{18}$$

where

$$n^e_1 = \sum_{k=1}^{r} n^{e(k)}_1 \tag{19}$$

and

$$n^s_t = rn^s \tag{20}$$

Figures 1 — 4 show the theoretical excess adsorption isotherms calculated for different parameters q and m. All calculations have been made for $K^{(1)}_{12} = 5.0$ and $K^{(2)}_{12} = 1.25$.

Figures 1 — 2 show the influence of the heterogeneity parameter m on the adsorption excesses n^e_1, $n^{e(1)}_1$ and $n^{e(2)}_1$; the calculations were made for $q = 0$ (Fig. 1), and 2.0 (Fig. 2). The part A of each figure shows the adsorption excesses $n^{e(1)}_1$ (the solid lines) and $n^{e(2)}_1$ (the dashed line) as functions of x^l_1. However, the part B of each figure presents the total adsorption excess n^e_1, which is sum of $n^{e(1)}_1$ and $n^{e(2)}_1$.

For energetically homogeneous solid surfaces ($m = 1$) the excess adsorption isotherm is U-shaped, whereas, for strongly heterogeneous

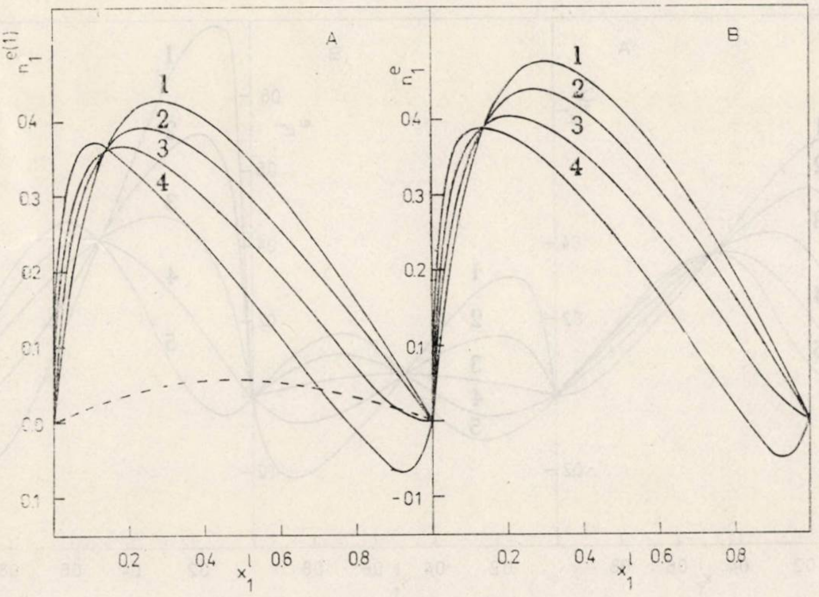

Fig. 1. — The excess adsorption isotherms $n_1^{e(1)}$ (the solid lines in part A), $n_1^{e(2)}$ (the dashed line in part A) and n_1^e (the solid lines in part B) calculated for $q = 0$ and $m = 1.0$ (1), 0.8 (2), 0.6 (3) and 0.4 (4).

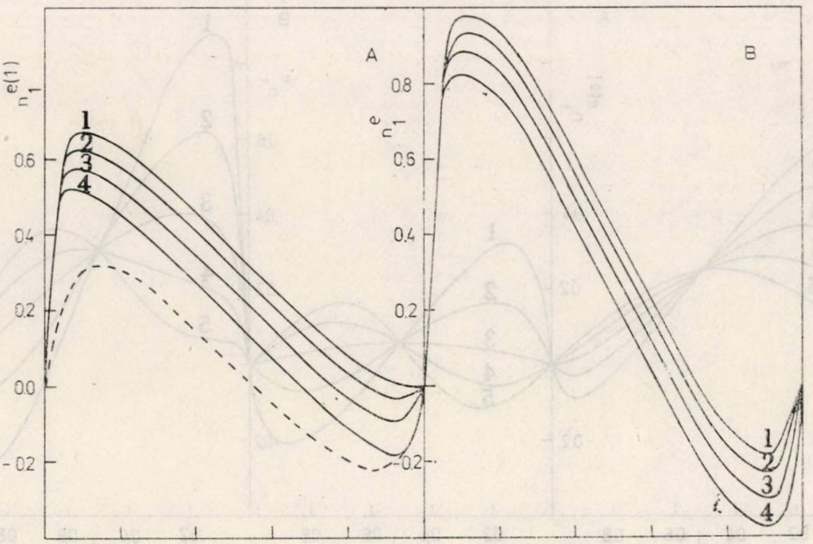

Fig. 2. — The excess adsorption isotherms $n_1^{e(1)}$, $n_1^{e(2)}$ and n_1^e calculated for $q = 2$ and different values of m. The labelling and parameters are as in Fig. 1.

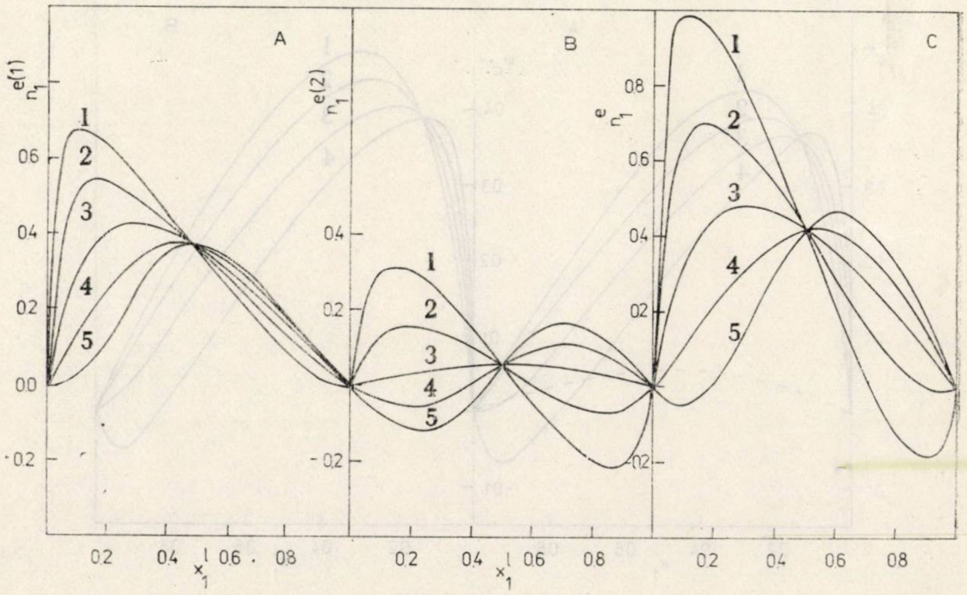

Fig. 3. — The excess adsorption isotherms $n_1^{e(1)}$ (part *A*), $n_1^{e(2)}$ (part *B*) and n_1^e (part *C*) calculated for $m = 1$ and $q = 2$ (1), 1(2), 0(3), -1 (4) and -2 (5).

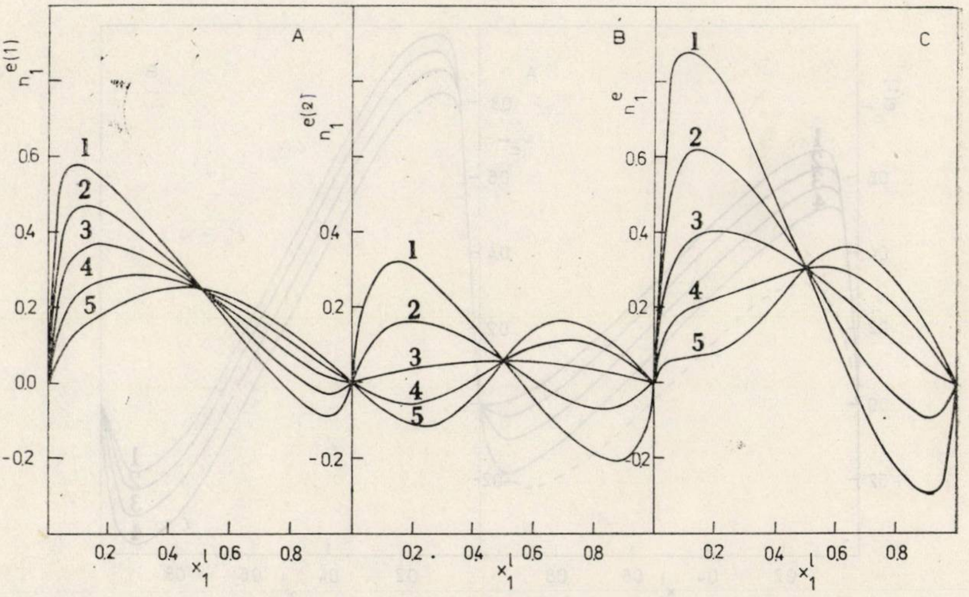

Fig. 4. — The excess adsorption isotherms $n_1^{e(1)}$, $n_1^{e(2)}$ and n_1^e calculated for $m = 0.6$ and different values of *q*. The labelling and parameters are as in Fig. 3.

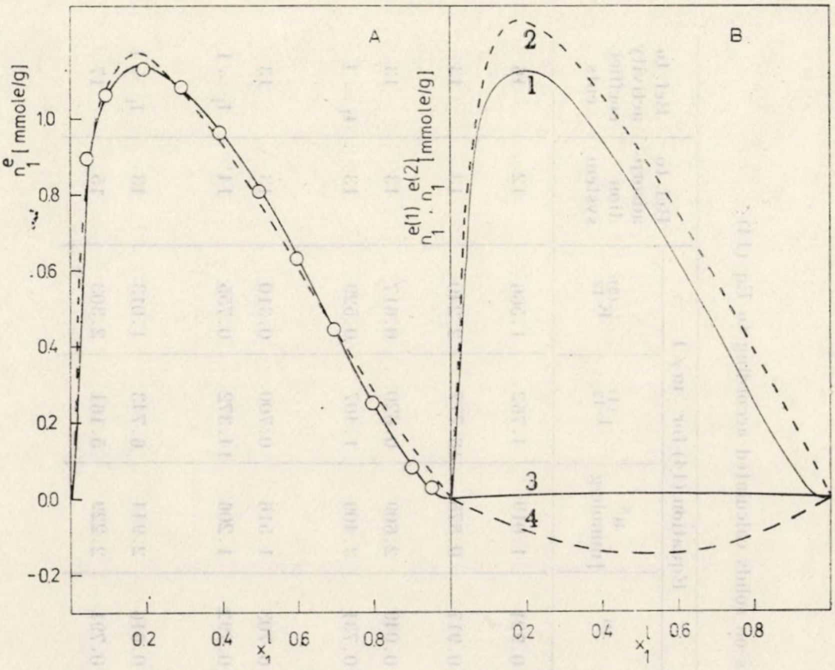

Fig. 5. — The excess isotherms n_1^e (part A), $n_1^{e(1)}$ (the curves 1 and 2) and $n_1^{e(2)}$ (the curves 3 and 4) for adsorption of pyridine from ethanol on charcoal at 293 K. The theoretical isotherms, calculated according to equation (14) for $m \neq 1$ (the solid lines) and $m = 1$ (the dashed lines) are compared with the experimental points (circles).

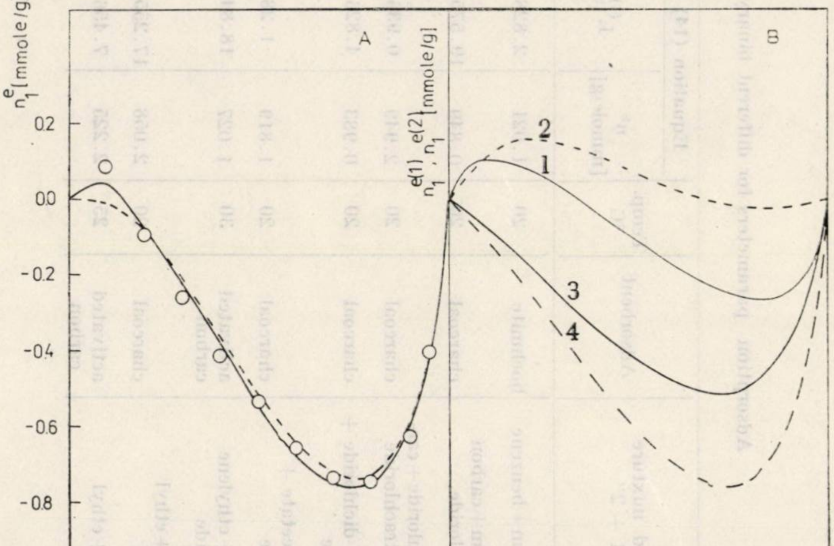

Fig. 6. — The excess isotherms for adsorption of methyl acetate from benzene on charcoal at 293 K. The labelling is as in Fig. 5.

solid surfaces the S-shape isotherm may be obtained (see Fig. 1A). For ideal bulk phase ($q = 0$) the excess isotherm $n_1^{e(2)}(x_1^l)$ is U-shape. In the case of ideal bulk phase the influence of the parameter m on the total adsorption excess n_1^e is most significant.

For regular bulk phase showing the positive deviation from Raoult's law, the S-shape excess isotherms are obtained for $n_1^{e(1)}$, $n_1^{e(2)}$ and n_1^e (see Fig. 2).

Figures 3 and 4 show the theoretical excess isotherms $n_1^{e(1)}$ (part A), $n_1^{e(2)}$ (part B) and n_1^e (part C) calculated for different values of q and the fixed values of m; the heterogeneity parameter m is equal to 1.0 (Fig. 3) and 0.6 (Fig. 4). Since the parameter q influences significantly on both excesses, $n_1^{e(1)}$ and $n_1^{e(2)}$, the total adsorption excess is dependent upon composition of both adsorbed layers.

Equation (14) has been examined by using the experimental excess adsorption isotherms available from literature.[12-15] The equilibrium constants $L_{12}^{(1)}$ and $K_{12}^{(2)}$ and the parameter n_t^s have been calculated by assuming $m = 1$(homogeneous surface) and $m \neq 1$ (heterogeneous solid surface). These adsorption parameters are summarized in table 1. It follows from table 1 that the values of n_t^s evaluated for $m = 1$ and $m \neq 1$ are similar; it means that energetic heterogeneity of the adsorbent surface changes very small the surface phase capacity. This conclusion is in a good agreement with our earlier studies.[11] However, values of the equilibrium constants are more dependent upon the heterogeneity parameter m. Especially, the constant $L_{12}^{(1)}$ is sensitive on a change in the value of m.

Figures 5 — 6 show the experimental excess adsorption data (circles) with comparison to the theoretical isotherms calculated for the parameters from table 1 (part A). The solid line in the part A of each figure is calculated for $m \neq 1$, whereas, the dashed line is plotted for $m = 1$. The part B of each figure shows the adsorption excesses $n_1^{e(1)}$ and $n_1^{e(2)}$ calculated for $m \neq 1$ (the solid lines) and $m = 1$ (the dashed lines).

It follows from table 1 and figures 5 — 6 that equation (14) is a good approximation of the experimental data and it is very useful for determining the heterogeneity parameter, the surface phase capacity and the equilibrium constants characterizing formation of first and second adsorbed layers.

REFERENCES

[1] D. H. Everett, in "Colloid Science", Specialist Periodical Reports, vol. 1, ed. D. H. Everett, The Chemical Society, London, 1973, chap. 2.

[2] A. C. Brown and D. H. Everett, in "Colloid Science", Specialist Periodical Reports, vol. 2, ed. D. H. Everett, The Chemical Society, London, 1975, p. 52 — 100.

[3] M. Jaroniec, A. Patrykiejew and M. Borówko, in "Progress in Surface and Membrane Science", vol. 14, Academic Press, New York, 1980.

[4] M. Jaroniec, J. Ościk and A. Deryło, *Monatsh.*, **112**, 175 (1981).
[5] M. Borówko and M. Jaroniec, *Rev. Roumaine Chim.*, **25**, 475 (1980).
[6] A. Dabrowski, J. Ościk, W. Rudziński and M. Jaroniec, *J. Colloid and Interface Sci.*, **69**, 287 (1979).
[7] A. Dabrowski and M. Jaroniec, *J. Colloid and Interface Sci.*, **73**, 475 (1980).
[8] M. Jaroniec, *J. Res. Inst. Catalysis, Hokkaido Univ.*, **26**, 155 (1978).
[9] A. Patrykiejew, M. Jaroniec, A. Dabrowski and J. Tóth, *Croat. Chemica Acta*, **53**, 9 (1980).
[10] M. Jaroniec and A. Patrykiejew, *J. Chem. Soc. Faraday I*, **76**, 2486 (1980).
[11] J. Ościk, A. Dabrowski, M. Jaroniec and W. Rudziński, *J. Colloid and Interface Sci.*, **56**, 403 (1976).
[12] J. J. Kipling and D. B. Peakall, *J. Chem. Soc.*, **52**, 4828 (1956).
[13] A. Blackburn and J. J. Kipling, *J. Chem Soc.*, **52**, 2373 (1957).
[14] S. Sircar and A. L. Myers, *J. Phys. Chem.*, **74**, 2828 (1970).
[15] F. E. Bartell and S. K. Sloan, *J. Amer. Chem. Soc.*, **51**, 1643 (1929).
[16] J. J. Kipling and D. B. Peakall, *J. Chem. Soc.*, **54**, 3899 (1958).
[17] V. C. Smith and R. L. Robinson, *J. Chem. Eng. Data*, **15**, 391 (1970).

Revue Roumaine de Chimie, 28, *3*, 211–216 (1983)

INCLUSION COMPOUNDS OF PERHYDROTRIPHENYLENE WITH HIGHER n-ALCOHOLS

C. LUCA, A. POPA, N. BÎLBĂ and GH. MIHĂILĂ
Department of Chemical Technology, Polytechnic Institute, Splai Bahlui 71, Iași, Romania

Received December 10, 1981

The paper deals with a study of the inclusion compounds of perhydrotriphenylene with aliphatic alcohols, $C_8 - C_{18}$, having even-numbered chain carbon atoms, by IR spectroscopy, thermal analysis and X-ray difraction. The inclusion compounds perhydrotriphenylene — n-alcohols have higher thermal stabilities than individual components and belong to the hexagonal system. The n-alcohols are found to be associated as dimers in the channels of perhydrotriphenylene.

INTRODUCTION

The equatorial isomer *anti-trans-anti-trans-anti-trans* of perhydrotriphenylene (PHTP), I_a and I_b, forms stable channel-like inclusions compounds with hydrocarbons, esters, monocarboxylic acids, macromolecules etc. [1-3] The investigations concerning these compounds have been developed considerably, referring especialy to their structures and applications.

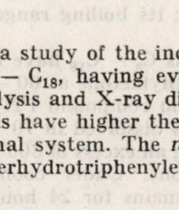

I_a

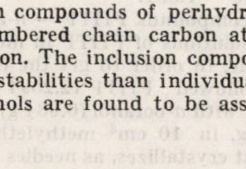

I_b

Using IR spectroscopy, thermal analysis and X-ray difraction, the inclusion compounds of PHTP with aliphatic alcohols, $C_8 - C_{18}$, having even-numbered chain carbon atoms, have been investigated.

EXPERIMENTAL

PHTP has been synthetized by catalytic hydrogenation of dodecahydrotriphenylene, obtained from tetraline and 1,4-dichlorobutane, in the presence of anhydrous aluminium trichloride, using the method indicated by Farina. [4,5]

The above reaction generates a mixture of 10 stereoisomers [5] from which, by treating with n-heptane, the *anti-trans-anti-trans-anti-trans* isomer is separated as a crystalline inclusion

compound, PHTP — *n*-heptane. Heating this product under a pressure as low as 2.10^{-5} mm Hg, the *anti-trans-anti-trans-anti-trans* isomer of perhydrotriphenylene (PHTP), I_a and I_b, is obtained.

The employed *n*-alcohols : 1-octanol, 1-decanol, 1-dodecanol, 1-hexadecanol and 1-octadecanol, delivered by Merck Co., were of chromatographic grade. Methylethylketone employed as solvent was of chromatographic grade too ; its boiling range was 79 — 81 °C and its refractive index 1.380 — 1.381.

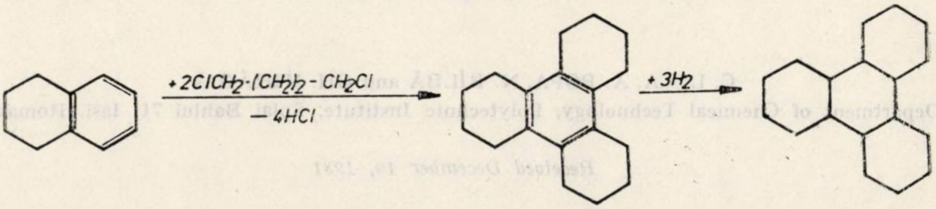

The inclusion compounds PHTP — *n*-alcohols C_8 — C_{18} have been prepared by crystallization in saturated solutions of PHTP in methylethylketone at 60 — 70°C and *n*-alcohols respectively. For example, in order to get the inclusion compound PHTP — *n*-octanol, the next procedure has been followed : PHTP (2.2594 g) was dissolved in 70 cm³ methylethylketone at 60 — 70 °C and mixed with *n*-octanol (0.984 g), using an excess of 300%, in pure state or dissolved, without heating, in 10 cm³ methylethylketone. Under cooling to room temperature, a yellow-white product crystallizes, as needles. It remains for 24 hours in contact with mother liquor for a complete crystallization of the inclusion compound. The crystalls formed are filtered, washed with methylethylketone and dried in air to constant weight. One got ~1.8 (~88%) inclusion compound PHTP — *n*-octanol.

The IR spectra of the inclusion compounds were carried out in KBr pellets, using a Perkin-Elmer 577 spectrophotometer.

Thermal analyses were carried out with a derivatograph MOM Budapest, under a heating rate of 10°/min. and sensitivity 1/3, using ignited α-alumina as reference material.

The crystalline structure of the products was analysed on an X-ray difraction apparatus TUR M-61 Dresden, using the K_{α_1} radiation of copper (with nickel filter).

RESULTS AND DISCUSSION

In the preparation of the inclusion compounds PHTP — *n*-alcohols, methylethylketone was employed as solvent, because it dissolves both PHTP and *n*-alcohols but does not form inclusion compounds with PHTP.

On experimental way it was observed that utilization of certain excess of *n*-alcohol led to obtainment of pure inclusion compound, without excess of PHTP, the yield being about 90%. This excess must be larger in the case of *n*-alcohols with shorter chain (about 300% for 1-octanol), since their solubility in methylethylketone is greater. In the case of *n*-alcohols with longer chains, the excess of *n*-alcohol must be smaller (about 5 — 10% for 1-octadecanol).

The excess of C_{12} — C_{18} *n*-alcohols from crystalls was removed by their washing with methylethylketone.

The characteristics of the PHTP — *n*-alcohols inclusion compounds prepared are summarized in table 1.

The data concerning the elemental analysis show that the weight ratios, PHTP/*n*-alcohols, do not depend on the length of the included *n*-alcohol ; these are about constant and equal to 10. Comparison of the weight ratios, PHTP/*n*-alcohols, obtained with weight ratios, PHTP/*n*-carboxy-

TABLE 1

Characterization of the inclusion compounds PHTP — *n*-alcohols

Inclusion compound	Yield, %,	Elemental analysis, %			Weight ratio, PHTP / *n*-alcohol	Weight ratio, PHTP / *n*-alcohol
		C	H	O		
PHTP — octanol	87.6	86.72	12.21	1.07	10.42	5.52
PHTP — decanol	88.2	86.87	12.24	0.89	10.26	6.60
PHTP — dodecanol	88.9	86.96	12.27	0.77	10.15	7.69
PHTP — hexadecanol	89.6	87.13	12.28	0.59	10.18	10.03
PHTP — octadecanol	91.1	87.18	12.30	0.52	10.37	11.41

lic acids, in the inclusion compounds PHTP-*n*-carboxylic acids [1], for which the found value is 10.3, points out that these ratios depend insignificantly on the functional group nature. On the contrary, the weight ratios PHTP/*n*-alcohols depend much on the length of *n*-alcohol molecule included, from 5.52 for C_8 up to 11.41, having a linear dependence, Figure 1.

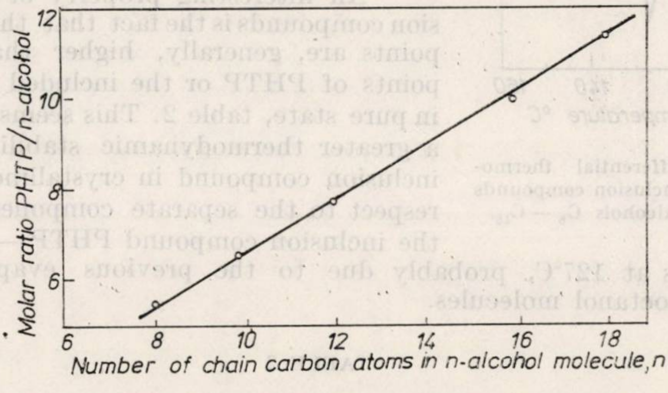

Fig. 1. — Molar ratio PHTP/*n*-alcohol against the number of chain carbon atoms in included *n*-alcohol molecule.

The inclusion compounds PHTP — *n*-alcohols exhibit identical IR spectra.

The region 800 — 1400 cm^{-1}, characteristic of PHTP presents the following absorption bands: 832s, 896s, 918m, 938m, 960w, 978m, 1046m, 1068w, 1102w, 1127w, 1168m, 1205s, 1260w, 1284m, 1290w, 1322w, 1334w, 1346m and 1360w. These absorption bands are identical or very close to those attributed for PHTP by Farina and Audisio. [5] In this region, the inclusion compounds PHTP — *n*-alcohols exhibit only one more absorption band at 715 — 720 cm^{-1}, the other bands being identical.

Transparency of PHTP in the region between 700 — 750 cm^{-1} allows accurate analyses of the PHTP — *n*-alcohols inclusion compounds, using the characteristic rocking, $\gamma_{CH_2} r$, 715 — 720 cm^{-1}, proper to methylenic groups of *n*-alcohols chains.

In contrast to PHTP, in the region between 3200 — 4000 cm^{-1}, in IR spectra of the PHTP— *n*-alcohols inclusion compounds, only one absorption band, characteristic of valence vibrations of hydroxylic groups, appears at about 3490 cm^{-1}. Appearance of this absorption band points out that the respective *n*-alcohols are found in the channel of inclusion compounds associated as dimers.

The thermal stability of the inclusion compounds PHTP — *n*-alcohols C_8 — C_{18} was studied by differential thermal analysis. Rewritten differential thermograms for studied compounds are plotted in Figure 2. In the temperature region of 120 — 160°C in all cases, an endothermic peak is evidenced, which corresponds to inclusion compound fusion and which advances continuously towards higher temperatures, as chain length of the guest molecule increases.

An interesting property of these inclusion compounds is the fact that their melting points are, generally, higher than melting points of PHTP or the included compounds in pure state, table 2. This seems to indicate a greater thermodynamic stability for the inclusion compound in crystalline state with respect to the separate components, except the inclusion compound PHTP — *n*-octanol, which melts at 127°C, probably due to the previous evaporation of included *n*-octanol molecules.

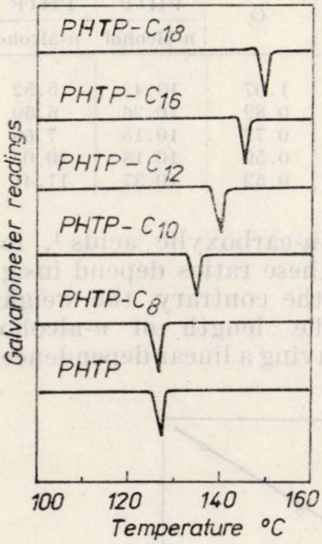

Fig. 2. — Differential thermograms of the inclusion compounds PHTP — *n*-alcohols C_8 — C_{18}.

TABLE 2

Melting points of the *n*-alcohols C_8 — C_{18} and the corresponding inclusion compounds with PHTP (M.p. of pure PHTP = 128°C)

Inclusion compound	Melting point, °C			
	n-alcohol	Inclusion compound by method ;		
		DTA (incipient)	DTA (peak)	Visual
PHTP — octanol	—16	—	127	126.5
PHTP — decanol	7	128.0	135	134.0
PHTP — dodecanol	23	133.5	141	140.5
PHTP — hexadecanol	49 . . . 50	138.5	146	146.5
PHTP — octadecanol	58.5	144.0	149.5	150.0

Comparison of the melting points of inclusion compounds PHTP— *n*-alcohols C_8 — C_{18} with those found in literature[1] for the inclusion compounds PHTP — *n*-monocarboxylic acids, figure 3, points out that they depend substantially on the included molecule length and less on the functional group. For a certain length of the included molecule chain, the thermal stability of the inclusion compounds PHTP-*n*-monocarboxylic acids is greater than that of the inclusion compounds PHTP — *n*-alcohols.

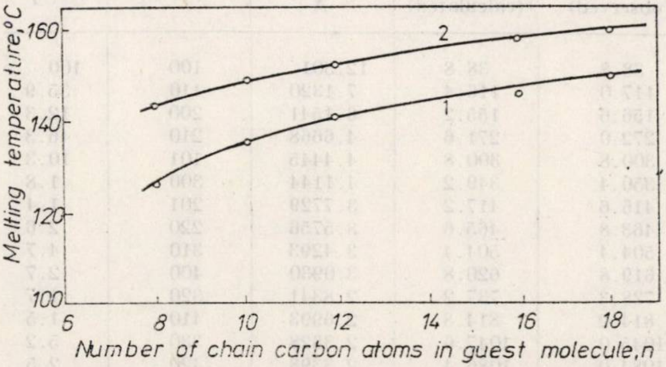

Fig. 3. — Melting point of the inclusion compounds of PHTP against the number of chain carbon atoms in the guest molecule : 1 — *n*-alcohol ; 2-*n*-carboxylic acid.

Determination of cyrstalline structure of the inclusion compounds PHTP — *n*-alcohols $C_8 - C_{18}$, was carried out by röentgenographic analysis, using the $Cu_{k\alpha_1}$ radiation ($\lambda = 1.5405$ A°). PHTP crystallizes in monoclinical system[1], its unit cell corresponding to the values: $a = 19.59 \pm 0.07$, $b = 15.39 \pm 0.06$, $c = 5.36 \pm 0.03$ Å, $\beta = 109.7 \pm 0.3$ and $V = 1522 \pm 0$ Å^3.

The inclusion compounds PHTP — *n*-alcohols $C_8 - C_{18}$ exhibit identical X-ray difraction spectra. Absence of the diffraction line $d = 7.60$Å, proper to PHTP[1] shows that the obtained products are in pure state.

Using the analytical method of indexation, from the relation

$$\sin^2\theta_{hkl} = A(h^2 + hk + k^2) + C.l^2$$

where, $A = \lambda^2/3a^2$ and $C = \lambda^2/4c^2$, for the case of $(hk0)$ lines one gets the correspondence between the observed θ_{hk0} and calculated θ_{hk0} and the more frequent ratio of $\sin^2\theta_{hkl}$ is 3, characteristic of the hexagonal system. For the range of θ between 2 — 23°, the observed and calculated values of $\sin\theta_{hkl}$, interplanar distances observed, assumed Miller's indices and relative intensities proper to reflexions for the inclusion compounds PHTP — *n*-alcohol C_{16} are listed in table 3. Analytical processing of the experimental data shows that the inclusion compounds PHTP — *n*-alcohols $C_8 - C_{18}$ crystallize in the hexagonal system.

TABLE 3

X-Ray difraction data of the inclusion compounds PHTP — hexadecanol, radiation CuK_{α_1}

$\sin^2\theta \times 10^4$ (observed)	$\sin^2\theta \times 10^4$ (calculated)	$d_{observed}$, Å	$h\,k\,1$	I/I_1
38.8	38.8	12.301	100	100
117.0	116.4	7.1320	110	35.9
156.6	155.2	6.1541	200	12.3
272.0	271.6	4.6668	210	46.3
300.8	300.8	4.4445	101	10.3
350.4	349.2	4.1144	300	1.8
416.6	417.2	3.7729	201	1.4
463.8	465.6	3.5756	220	2.6
504.4	504.4	3.4293	310	4.7
619.8	620.8	3.0930	400	2.7
738.3	737.2	2.8341	320	1.7
814.2	814.8	2.6993	410	1.5
1045.0	1047.6	2.3828	330	5.2
1084.0	1086.4	2.3398	420	2.5
1204.0	1202.8	2.2201	510	1.3
1346.6	1348.4	2.0988	421	1.7
1434.0	1435.6	2.0342	430	1.9

CONCLUSIONS

From the experimental results presented above, the following conclusions may be drawn:

1. PHTP forms inclusions compounds with *n*-alcohols $C_8 - C_{18}$; the weight ratios PHTP/*n*-alcohol are about 10 and the molar ratios PHTP/*n*-alcohols vary between 5.52 and 11.41.

2. The inclusion compounds PHTP — *n*-alcohols $C_8 - C_{18}$ exhibit a higher thermal stability than that of the individual components.

3. The *n*-alcohols $C_8 - C_{18}$ are found to be associated as dimers in the channels of PHTP, ν_{OH} being about 3490 cm^{-1}.

4. All the inclusion compounds PHTP — *n*-alcohols are strictly isomorphous to one another and belong to the hexagonal system.

REFERENCES

G. Allegra, M. Farina, A. Immirazi, A. Colombo, U. Rossi, R. Broggi and G. Natta, *J. Chem. Soc.* (*B*), **1967**. 1020.

[2] C. Luca and V. Ababi, *Materiale plastice*, **13**, 89 (1976).

[3] M. Farina, G. Allegra and G. Natta, *J. Amer. Chem. Soc.*, **86**, 516 (1964).

[4] M. Farina, *Tetrahedron Letters*, **1963**, 2097.

[5] M. Farina and G. Audisio, *Tetrahedron*, **26**, 1827 (1970).

Revue Roumaine de Chimie, 28, *3* 217—223 (1983)

CONDUCTANCE BEHAVIOUR OF CATIONIC SURFACTANTS IN ALKANOLS

P. BAHADUR, A. GUPTA and P. LATA
Chemistry Laboratories, D.A.V. College, Muzaffarnagar-25 1001, India

Received February 27, 1981

Conductance measurements of some quaternary ammonium type cationic surfactants showed the existence of micelles in a few lower aliphatic alcohols. The behaviour was ascribed by an empirical equation and law of mass action applied for the dissociation of surfactants. Various useful thermodynamical parameters were evaluated.

INTRODUCTION

Micelle formation of cationic surfactants in aqueous [1] and non-aqueous [2] (solvents of low dielectric constants eq.benzene) media has been reviewed. Gopal and Singh [3] have observed micells of hexadecyl-trimethyl-ammonium bromide in formamide. Some investigations on cationic surfactant micelles in alkanol-water,[4-7] alkanol-hydrocarbon [7] and acetone-water [4] have also been reported in literature. Micelle formation by anionic soaps and detergents in alkanols has been observed but such data on cationic surfactants are rather scarce. This paper deals with the conductance behaviour of some quaternary ammonium halide solutions in a few alkanols.

EXPERIMENTAL

The surfactants used : decyl-trimethylammonium bromide (De TAB an Eastman Kodak Chemical), tetradecyl-and hexadecyl-trimethyl-ammonium bromide (TTAB, HTAB Sigma products) and dodecylpyridinium chloride (DPC) were recrystallized and their purity was checked by observing no minima in surface tension curves. AnalaR grade organic solvents and all pyrex glass apparatus were used. The conductances measurements, in the absence of moisture traces were made using a conductivity meter at a constant temperature.

RESULTS AND DISCUSSION

Figure 1 reveals micelle formation (CMC) of alkyl quaternary ammonium halides in different alkanols (methanol, propanol-1, propanol-2 and butanol-1) at 40°C. All these plots (specific conductance vs. concentration) are not smooth and show a break at a point indicating the probable formation of micelle ; the values of CMC thus obtained are recorded in

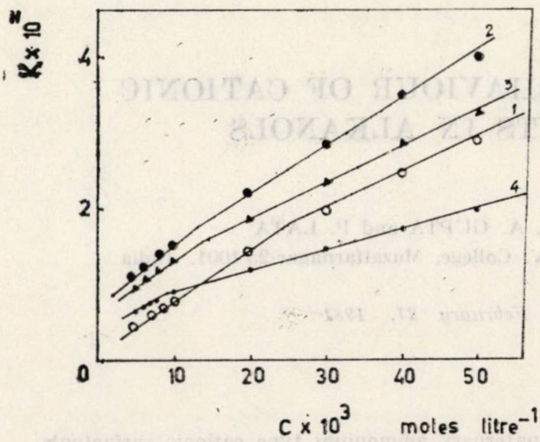

Fig.1. — Specific conductances vs. concentration for dodecyl pyridinium chloride in different alkanols at 40°C.

1. Methanol ; 2. — propanol-1 ; 3 — propanol-2 ; 4. — butanol-1.
$x = 4$ for methanol
$x = 5$ for propanol-1, propanol-2, butanol-1.

TABLE 1

Values of CMC, conductance constants and thermodynamic parameters for cationic surfactants in alkanols at 40°C

Alkanols	CMC $\times 10^3$	A	B	λ_∞	$k \times 10^4$	$-\Delta G_D$ k.cal.	$-\Delta G_A$ k.cal.
DeTAB							
PrOH-1	35.00	0.420	0.380	33.84	38.40	3.46	7.68
PrOH-2	35.00	—	—	—	—	—	7.68
Butanol-1	30.00	$\bar{1}.940$	0.490	33.33	9.10	4.36	7.60
DPC							
PrOH-1	13.50	0.350	0.420	54.54	10.08	4.29	8.86
PrOH-2	13.50	0.260	0.425	126.60	1.18	5.63	8.86
Butanol-1	8.50	$\bar{1}.940$	0.500	172.00	0.28	6.52	9.18
TTAB							
PrOH-1	3.15	0.565	0.275	38.37	12.76	4.15	10.66
PrOH-2	3.15	0.870	0.200	37.90	31.60	3.58	10.66
Butanol-1	2.80	0.010	0.370	24.61	5.28	4.69	10.56
HTAB							
PrOH-1	0.90	0.950	0.185	55.69	7.09	4.51	12.22
PrOH-2	0.90	0.465	0.295	38.38	8.08	4.43	12.22
Butanol-1	0.70	0.230	0.280	—	—	—	12.28

tables 1 and 2. The CMC decreases with the increase of carbon atoms in the hydrophobic chain of the surfactant and in the alkanols as well, used as solvent and exhibit the order :

DeTAB > DPC > TTAB > HTAB

Further on, the CMC of these surfactants shows an increase with increase in temperature within the range studied. The same CMC has been determined using viscometric data (to be communicated).

The molecular conductivity (λ), obtained in the usual manner from the specific conductivity data, decreases as the concentration of the

TABLE 2

Values of CMC, conductance constants and thermodynamic parameters for cationic surfactants in methanol.

Temp.	CMC × 10^3	A	B	$\lambda\infty$	$-\Delta G_D$ k.cal.	$-\Delta S_D \times 10^3$ k.cal.	$-\Delta G_A$ k.cal.	$\Delta S_A \times 10^3$ k.cal.
DeTAB								
35°C	48.00	1.560	0.205	107.70	1.86	5.84	7.94	33.96
40°C	51.00	1.585	0.210	118.50	1.92	5.56	7.98	33.51
45°C	54.00	1.600	0.215	123.10	2.03	5.13	8.04	33.21
50°C	57.00	1.620	0.220	134.00	2.15	4.68	8.10	32.88
DPC								
35°C	22.50	1.570	0.125	70.28	1.16	77.96	8.86	40.65
40°C	25.00	1.585	0.155	83.73	1.42	75.89	8.88	40.06
45°C	27.00	1.610	0.165	92.35	1.56	74.25	8.92	39.56
50°C	30.00	1.625	0.170	114.00	2.23	71.03	8.92	38.95
TTAB								
35°C	3.10	1.720	0.110	114.30	2.51	26.02	11.28	48.51
40°C	3.40	1.725	0.115	121.60	2.63	25.20	11.36	47.99
45°C	3.70	1.730	0.120	132.10	2.78	24.34	11.42	47.42
50°C	4.00	1.755	0.125	145.10	3.06	23.10	11.50	46.93
HTAB								
35°C	0.80	2.040	0.105	278.20	3.25	26.58	12.94	69.51
40°C	1.00	2.060	0.110	286.50	3.36	25.82	12.88	68.21
45°C	1.25	2.080	0.115	318.50	3.57	24.76	12.80	66.89
50°C	1.50	2.090	0.120	335.60	3.68	24.01	12.76	65.73

urfactant solution increases. The nature of decrease seems to be due to the tendency of the surfactants to form aggregate at higher concentration. The conductance behaviour (Fig. 2) for all the surfactant — solven systems was depicted by an equation [8]

$$\log \lambda = A + B \log C$$

where A and B are constants.

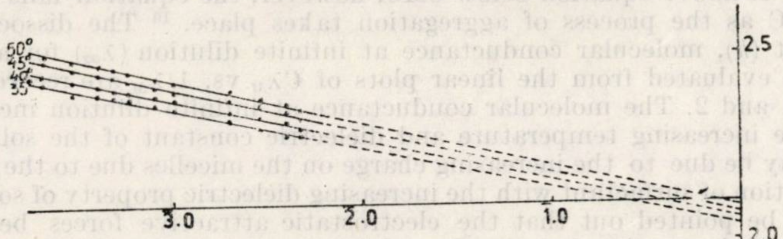

Fig. 2. — Plot of log molecular conductance vs. concentration for hexa decyl trimethyl ammonium bromide in methanol at different temperatures (35 — 50°C).

The *A* values (i.e. $\lambda_{C=1}$ obtained from the extrapolation of $\log\lambda$ vs. $\log C$ plots for zero values of $\log C$) in alkanols at diferent temperatures have been calculated and are given in tables 1 and 2. It may be pointed out that it is not possible to prepare the surfactant solution of such a high concentration in alkanols. Thus the *A* values signify the limiting molecular conductance and have got theoretical importance. These values show an increase with temperature.

The values of constant *B* (i.e. the slope of the plots of $\log\lambda$ vs. $\log C$) are given in tables 1 and 2. The increasing trend in *B* values with temperature also confirms the temperature dependence of CMC [8].

The energy changes during the process of dissociations and association are evaluated following some usual treatments. The behaviour of these surfactants in alkanols may be presumed as weak electrolytes, the expression for their dissociation may be derived following Kraus and Bray treatment [9].

$$RX \rightleftharpoons R^{+} + X^{-}$$

$$C(1-\alpha) \qquad C\alpha \; C\alpha$$

where R represents the quaternary alkyl radical and X the halogen. The dissociation constant may be given by

$$k = \frac{C\alpha^{2}}{1-\alpha}$$

where α is the dissociation degree and k the dissociation constant. Since α for such systems may be taken very small, interionic effects may be treated as negligible. Thus, considering α as $\lambda_{M/\lambda_{\infty}}$.

$$C\lambda_{M} = \frac{k\lambda_{\infty}^{2}}{\lambda_{M}} - k\,\lambda_{\infty}$$

The plots of $C\lambda_M$ vs. $1/\lambda_M$ are found linear (Fig. 3) only for the data within a limited range of concentration (below CMC). This shows the validity of above equation below CMC, however, the equation fails above the CMC as the process of aggregation takes place. [10] The dissociation constant (k), molecular conductance at infinite dilution (λ_∞) for all the systems evaluated from the linear plots of $C\lambda_M$ vs. $1/\lambda_M$ are recorded in tables 1 and 2. The molecular conductance at infinite dilution increases with the increasing temperature and dielectric constant of the solvents. This may be due to the increasing charge on the micelles due to the easier dissociation of surfactant with the increasing dielectric property of solvent. It may be pointed out that the electrostatic attractive forces between positive and negative ions in the solvent increases with the decreasing dielectric constant of the solvent and thus such solvents have a small dissociating influence. The values of dissociation constant for all the systems reported in table 1 are also in agreement with this explanation. On the other hand the micelle formation occurs more easily in the solvents of low dielectric constant showing the trend BUOH $>$ PrOH $>$ MeOH.

Thus the role of dielectric constant is not only the significant factor in micelle formation. It appears that the micelle formation depends on the nature and interaction of solute solvent species.

The heats of dissociation for all the surfactants ($C_{10} - C_{16}$) in methanol obtained from the linear plots of log k vs. $1/T$ (Fig. 4) are -3.66, -25.77, -10.52 and -11.44 for C_{10}, C_{12}, C_{14} and C_{16} surfactants respectively.

The free energy for the dissociation process, ΔG_D was evaluated from the expression :

$$\Delta G_D = -RT \ln k_A$$

where k_A is equilibrium constant for association process thus

$$\Delta G_D = -RT \ln \frac{1}{k_D}$$

$$= RT \ln k_D$$

where k_D is the equilibrium constant of dissociation process, i.e. dissociation constant.

Now for aggregation process, when counter-ions are bound to the micelle, the standard free energy of micellization (per mole of monomer) ΔG_A for the phase separation model is given by the expression :[11]

$$\Delta G_A = 2RT \ln \mathrm{CMC}_M$$

where CMC_M is expressed as a mole fraction where the total number of moles present at the CMC is equal to the sum of moles of solvent and surfactant. Tables 1 and 2 show the free energy for the dissociation and micellization process for all the systems.

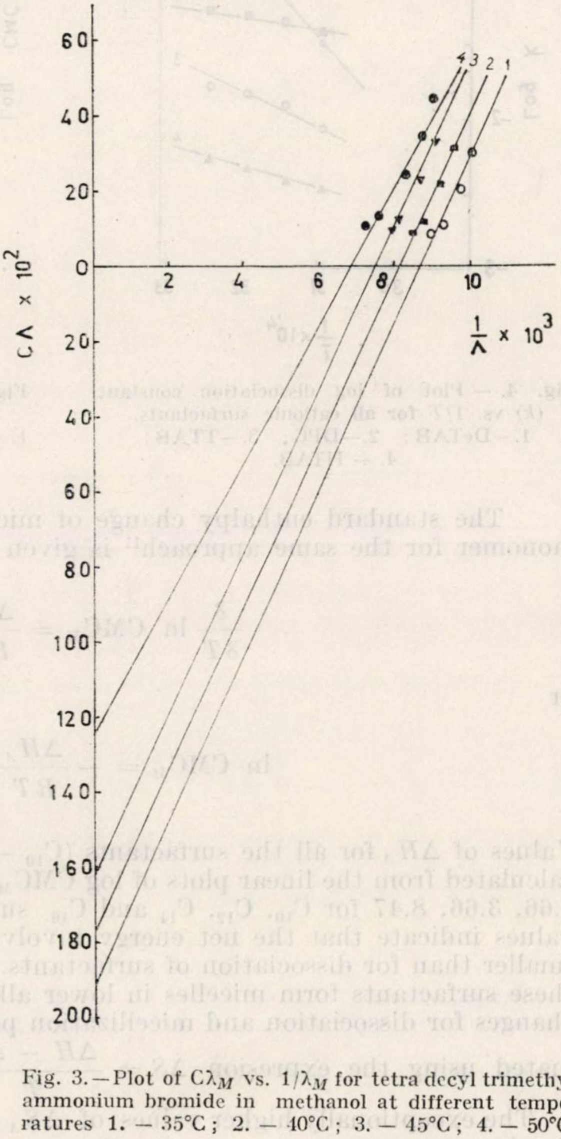

Fig. 3. — Plot of $C\lambda_M$ vs. $1/\lambda_M$ for tetra decyl trimethyl ammonium bromide in methanol at different temperatures 1. — 35°C ; 2. — 40°C ; 3. — 45°C ; 4. — 50°C.

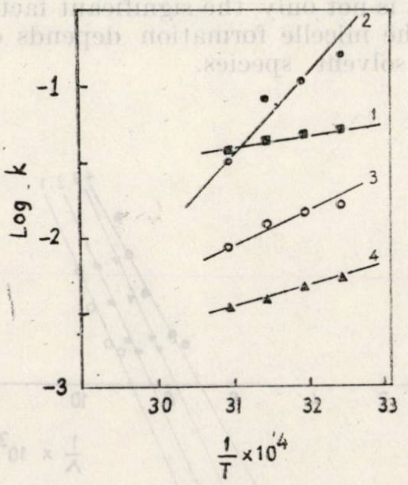

Fig. 4. — Plot of log dissociation constant (k) vs. $1/T$ for all cationic surfactants.
1.—DeTAB; 2.—DPC; 3.—TTAB; 4. — HTAB.

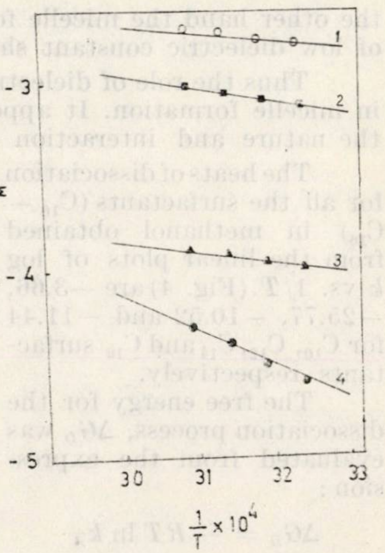

Fig. 5. — Plot of log CMC$_M$ vs. $1/T$ for all cationic surfactants.
1. — DeTAB; 2. — DPC; 3. — TTAB; 4. — HTAB.

The standard enthalpy change of micellization (ΔH_A) per mole of monomer for the same approach[11] is given by:

$$\frac{\delta}{\delta T} \ln \text{ CMC}_M = \frac{\Delta H_A}{RT^2}$$

or

$$\ln \text{ CMC}_M = -\frac{\Delta H_A}{RT} + C$$

Values of ΔH_A for all the surfactants ($C_{10} - C_{16}$) in methanol have been calculated from the linear plots of log CMC$_M$ vs. $1/T$ (Fig. 5) and are 2.52, 3.66, 3.66, 8.47 for C_{10}, C_{12}, C_{14} and C_{16} surfactants respectively. These values indicate that the net energy involved in micellization process is smaller than for dissociation of surfactants. Thus it seems probable that these surfactants form micelles in lower alkanols. The standard entropy changes for dissociation and micellization process ΔS_D and ΔS_A were evaluated using the expresion $\Delta S = \dfrac{\Delta H - \Delta G}{T}$ and are reported in table 2. The exceptionally higher values of ΔS_A than ΔS_D favour the micellization process.

ACKNOWLEDGEMENT. Authors are grateful to CSIR for the awards of research fellowships to AG and PL.

REFERENCES

[1] E. W. Anacker, In "Cationic Surfactants", Ed. E. Jungermann, Marcel Dekker, New York, 1969, p. 203.
[2] A. Kitahara, *ibid.* p. 289.
[3] R. Gopal and J. R. Singh, *Kolloid Z.U.Z. Polymer*, **239**, 699 (1972).
[4] S. Miyagishi, *Bull. Chem. Soc. Japan*, **47**, 2972 (1974); **48**, 2349 (1975); **49**, 34 (1976).
[5] H. N. Singh, S. Singh and D. S. Mahalwar, *J. Colloid and Interface Sci.*, **59**, 386 (1977).
[6] L. R. Singh, P. Bahadur and S. N. Srivastava, *Rev. Roumaine Chim.*, **22**, 1145 (1977).
[7] P. Bahadur, A. Gupta and P. Bahadur, *Gazz. chim. Ital.* (Communicated).
[8] R. P. Varma and P. Bahadur, *Indian J. Chem.*, **10**, 1189 (1972).
[9] C. A. Kraus and W. C. Bray, *J. Amer. Chem. Soc.*, **35**, 1315 (1913).
[10] R. P. Varma and K. Kumar, *Colloid Polymer Sci.*, **256**, 269 (1978).
[11] G. F. J. Russel, *J. Colloid Interface Sci.*, **40**, 174 (1972).

Revue Roumaine de Chimie, 28, 3, 225–234 (1983)

COMPLEX COMPOUNDS OF Cd(II) WITH ACETONE SELENOSEMICARBAZONE

D. NEGOIU and ILEANA GHELASE
Faculty of Chemical Technology,
Polytechnical Institute of Bucharest,
1, Polizu Street, 78126-Bucharest, Romania

Received May 6, 1981

Complex compounds of Cd(II) with acetone selenosemicarbazone (Hsesac) of $[(CdClHsesacH_2O)_2]Cl_2$, $[CdCl(Hsesac)_2]$ $Cl \cdot 0.5H_2O$, $[(CdI_2Hsesac)_2]$, $[CdI_2(Hsesac)_2]$, $[\{Cd(CH_3COO)(CH_3COOH)(sesac)\}_2]$, $[CdCH_3COO(sesac)$ $(Hsesac)]$. $0.5H_2O$ and $[Cd(sesac)_2]$ type have been synthetized. The compounds were characterized by elemental chemical analysis, molecular weight determinations, molar electric conductivity determinations, thermal analysis, as well as visible, ultraviolet and infrared spectra. The coordination mode of ligands has been established. The structural formulae have been assigned for all of the synthetized complex compounds.

INTRODUCTION

The first studies on the application of selenosemicarbazones as ligands in complex compounds with metal ions have been reported in 1968 by Ablov et al. [1,2] Since then, two complex compounds of cobalt [1], one of zinc and one of nickel [3] with acetone selenosemicarbazone have been mentioned in literature.

As a contribution to this field of investigation, the present study is concerned with the ability of cadmium ions to form complex compounds with acetone selenosemicarbazone.

RESULTS AND DISCUSSION

In synthetizing the complex compounds, the optimal molar ratio metal ion : ligand has been studied, as well as the influence of solvent, concentration, temperature, pH of reaction medium, and of the nature of anions present. The influence of some external factors such as : air, light, humidity, over the stability of the synthetized compounds has also been observed.

Through the interaction of cadmium chloride, $CdCl_2 \cdot 2.5H_2O$, with acetone selenosemicarbazone (Hsesac) under 1 : 1 and 1 : 2 molar ratios, in saturated ethyl alcohol solution at $pH = 7$ and room temperature, two solid, white-pink, complex compounds $[(CdClHsesac\,H_2O)_2]Cl_2$ and $[CdCl(Hsesac)_2]$ $Cl.0.5H_2O$ have been obtained.

Under the same conditions, cadmium iodide, CdI_2, also forms two complex compounds of a white-pink colour, of the $[(CdI_2Hsesac)_2]$ and $[CdI_2(Hsesac)_2]$ type.

When the cadmium salt is an acetate, $Cd(CH_3COO)_2 \cdot 2H_2O$, the complex compounds obtained under the above mentioned conditions are of the type: $[\{Cd(CH_3COO)(CH_3COOH)(sesac)\}_2]$ — with a yellow-greenish colour — and $[CdCH_3COO(sesac)(Hsesac)].0.5H_2O$ — with a white, slightly yellowish colour.

If the experimental conditions are modified — by raising the pH value of the reaction medium by adding ammonia and appropriately diluting the reacting solutions — the anion of the cadmium salt (acetate) is completely eliminated from the coordination sphere of complex compounds. When the molar ratio Cd : Se is 1 : 1 or 1 : 2, in alcoholic solutions at pH = 10.5 a lemon yellow, microcrystalline compound $[Cd(sesac)_2]$ is obtained.

From the above mentioned data it follows that the cadmium ion presents a good complexing capacity with the acetone selenosemicarbazone; the syntheses are reproducible (Table 1).

The complex compounds obtained are solid crystalline substances, with characteristic X-ray powder diffractograms[4]. Their solubility in methyl or ethyl alcohol is rather low, and they are almost insoluble in nitrobenzene, toluene, chloroform or benzene. They are sensible to ether. Under prolonged influence of sunlight, air, humidity or heat the complex compounds decompose forming cadmium selenide (Fig. 1). How-

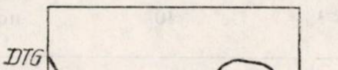

Fig. 1. — Thermal analysis curves for complex compound $[\{Cd(CH_3COO)(CH_3COOH)(sesac)\}_2]$

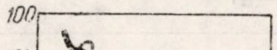

Fig. 2. — Electronic reflectance spectra of compounds: 1. $[(CdClHsesacH_2O)_2]Cl_2$, 2. $[CdCl(Hsesac)_2]Cl \cdot 0.5H_2O$, 3. $[CdI_2(Hsesac)_2]$, 4. Acetone selenosemicarbazone.

ever, if these factors are eliminated, the compounds can be stored for a long time.

Molecular weight determinations with a spectrophotometric method[5] of ultraviolet absorption have shown that the synthetized complex compounds are monomers or dimers.

Molar electric conductivity measurements have proved that complex compounds of cadmium with acetone selenosemicarbazone are either electrolytes of 1 : 1 or 1 : 2 type, or, in most cases, non-electrolytes (Table 2). Some non-electrolytes compounds— (3), (4), (5) in Table 2 — exhibit some electric conductivity in methanolic solutions. This is probably due to an interaction between the complex compound and the solvent[6].

TABLE 2

Molar electric conductivity of complex compounds of cadmium with acetone selenosemicarbazone (in methanolic solutions)

COMPLEX COMPOUNDS	Concentration mol/l	Molar electric conductivity $\Omega^{-1}.cm^2.mol^{-1}$	Type of electrolyte
$[(CdClHsesacH_2O)_2]Cl_2$	$1.63 \cdot 10^{-4}$	178	1 : 2
$[CdCl(Hsesac)_2]Cl \cdot 0.5H_2O$	$1.82 \cdot 10^{-4}$	88	1 : 1
$[(CdI_2Hsesac)_2]$	$2.31 \cdot 10^{-4}$	40	non-electrolyte
$[CdI_2(Hsesac)_2]$	$1.99 \cdot 10^{-4}$	45	non-electrolyte
$[\{Cd(CH_3COO)(CH_3COOH)(sesac)\}_2]$	$2.54 \cdot 10^{-4}$	46	non-electrolyte
$[CdCH_3COO(sesac)(Hsesac)] \cdot 0.5H_2O$	$5.90 \cdot 10^{-4}$	17	non-electrolyte
$[Cd(sesac)_2]$	$4.99 \cdot 10^{-4}$	8	non-electrolyte

Electronic reflectance spectra of complex compounds of cadmium with acetone selenosemicarbazone do not show any absorption bands in the visible range (Fig. 2). In ultraviolet range the compounds exhibit a characteristic absorption band of the ligand at 275 — 305 nm. This band has been attributed to an $n \rightarrow \pi^*$ transition of the lone electron pairs of selenium.[7]

In ultraviolet absorption electronic spectra the "characteristic band of the ligand" is situated at 286 — 288 nm. Since it is not influenced by coordination, it has been possible to use this absorption band for spectrophotometric determination of the molecular weight of the synthetized complex compounds.[5]

The presence of an intense absorption band at 240 — 245 nm has been attributed to $\pi \rightarrow \pi^*$ electrons transitions of the two conjugated $\rangle C{=}N-$ double bonds which are stabilized when acetone selenosemicarbazone coordinates as a bidentate ligand, at the selenium atom and at the hydrazine nitrogen atom, according to structure (1). The shape of ultraviolet absorption electronic spectra proves that this mode of coordi-

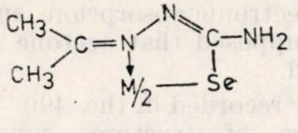

(1)

nation of the ligand with selenium is present in complex compounds: $[\{Cd(CH_3COO)(CH_3COOH)(sesac)\}_2]$, $[CdCH_3COO(sesac)(Hsesac)].0.5H_2O$ and $[Cd(sesac)_2]$ (Fig. 3). In ethanolic solutions of the free ligand,[7] the band which is attributed to the $\pi \rightarrow \pi^*$ transition in the $\rangle C{=}N{-}$ double bond is situated at 212 nm.

In the case of the complex compounds of the type: $[(CdClHsesacH_2O)_2]Cl_2$, $[CdCl(Hsesac)_2]Cl.\ 0.5H_2O$ and $[(CdI_2Hsesac)_2]$, in the 240 – 245 nm range of electronic absorption spectra only inflections of a higher intensity are observed (Fig. 4). This behaviour suggests

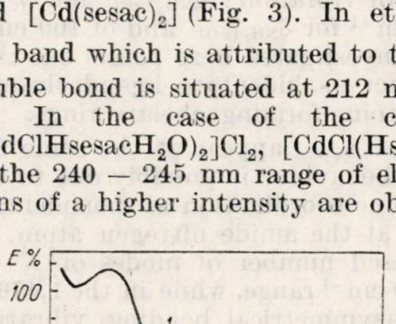

Fig. 3. — Ultraviolet absorption electronic spectra of compounds:
1. $[\{Cd(CH_3COO)(CH_3COOH)(sesac)\}_2]$,
2. $[CdCH_3COO(sesac)(Hsesac)] \cdot 0.5H_2O$,
3. $[Cd(sesac)_2]$, 4. Acetone selenosemicarbazone

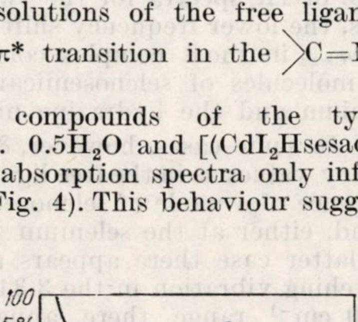

Fig. 4. — Ultraviolet absorption electronic spectra of compounds:
1. $[(CdClHsesacH_2O)_2]Cl_2$,
2. $[CdCl(Hsesac)_2]Cl \cdot 0.5H_2O$,
3. $[(CdI_2Hsesac)_2]$, 4. $[CdI_2(Hsesac)_2]$,
5. Acetone selenosemicarbazone.

that in these compounds some weak chelate rings are formed, the acetone selenosemicarbazone coordinating as a bidentate ligand according to the structure (2).

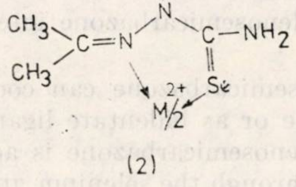

(2)

The situation is entirely different in the case of the complex compound $[CdI_2(Hsesac)_2]$, which shows no inflection point in the 240 – 245 nm range of the electronic absorption spectrum (Fig. 4, curve 4). In this case it may be supposed that acetone selenosemicarbazone acts as a monodentate ligand.

Vibrational spectra recorded in the 400 — 4,000 cm^{-1} range have confirmed the above types of structures suggested by the ultraviolet absorption electronic spectra (Table 3).

The largest frequency shifts are recorded in the 1,700 — 400 cm^{-1} range of IR spectra for the two modes of vibration : $\delta_{NH_2\,twist.}$ and $\nu_{C=Se}$. Thus, the lower frequency shift of 125 cm^{-1} for $\delta_{NH_2\,twist.}$ and of 100 cm^{-1} for $\nu_{C=Se}$ in most complex compounds investigated here points out that the molecules of selenosemicarbazone act as bidentate ligand through selenium and the hydrazine nitrogen atom, forming chelate rings.

In some cases, however, $\delta_{NH_2\,twist.}$ and $\nu_{C=Se}$ appear at the same frequency values as in the free ligand. This behaviour is possibly due to the existence of a mode of selenosemicarbazone coordination as monodentate ligand, either at the selenium atom, or at the amide nitrogen atom. In the latter case there appears an increased number of modes of N–H stretching vibration in the 3,340 – 3,100 cm^{-1} range, while in the 1,476 – 1,480 cm^{-1} range there appears the asymmetrical bending vibration of the isopropylidene group ($\delta_{as\ CH_3}$).

Vibration spectra have also been used to establish the role of water molecules, as coordination or crystallization water.[8,9] The presence of crystallization water — which has also been proved chemically by drying in an desiccator under vacuum over P_2O_5 in the dark – in compounds: $[CdCH_3COO(sesac)(Hsesac)] \cdot 0.5H_2O$ and $[CdCl(Hsesac)_2]Cl \cdot 0.5H_2O$ is revealed by the existence of wide absorption bands in the domains of ν_{NH} stretching vibrations and of skeleton vibrations at low frequencies. Likewise, the somewhat higher values of δ_{NH_2} bending vibration, which occur with these compounds, point out to the possibility of a superposition of the δ_{H-OH} and δ_{NH_2} vibrations. The presence of coordinated water in the compound $[(CdClHsesacH_2O)_2]Cl_2$ is revealed by the existence of a $\delta_{H_2O\ wagg.}$ vibration mode, at 735 cm^{-1}.

CONCLUSIONS

The infrared and the ultraviolet absorption electronic spectra have shown that, in complex compounds of the cadmium ion with acetone selenosemicarbazone, the selenium atom and the atoms of hydrazine or amide nitrogen of the selenosemicarbazone interact with the Cd(II) ion forming σ bonds.

The acetone selenosemicarbazone can coordinate with the Cd(II) ion either as monodentate or as bidentate ligand. The monodentate coordination of acetone selenosemicarbazone is achieved through σ bonds of the L→M type, either through the selenium atom, or through the amide

TABLE 3

Characteristic IR frequencies (in cm^{-1}) and their assignment

Crt. no.	ν_{NH}	$\nu_{C=N}$	δ_{NH_2}	δ_{N-H} + ν_{C-N}	δ_{CH_3}	ν_{N-C-N}	ν_{N-N}	δ_{NH_2} *twist.*	$\nu_{C=Se}$	δ_{H_2O} coordinated	Low frequencies
1.	Acetone selenosemicarbazone 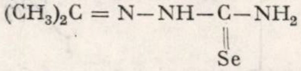 $(CH_3)_2C=N-NH-\underset{\underset{\textstyle Se}{\Vert}}{C}-NH_2$										
	3340vs 3200vs 3120vs	1650m	1605vs	1525vs 1275vs 1197s	1475s 1435vs 1375s	1115vs	1030m	865m	775s	—	615vs 575vs 535s 495m
2.	$[Cd(sesac)_2]$										
	3415m 3290s 3115m	1625m	1590m	1520s 1300m 1270s	1435w 1368w	1160w	1018w	740m	675m	—	—
3.	$[CdCH_3COO(sesac)(Hsesac)] \cdot 0.5H_2O$										
	3360m 3255s 3145s wide	1625s	1610s	1520s 1328m 1305m 1270m	1435s 1375m	1180w 1115w	1020w	860vw 740m	770w 675m	—	625w 580w 480w wide
4.	$[\{Cd(CH_3COO)(CH_3COOH)(sesac)\}_2]$										
	3390m 3260m 3160m very wide	1610s	1575vs	1540vs 1280m	1435s 1350m	1110w	1030w	740m	675m	—	—
5.	$[CdCl(Hsesac)_2]Cl.0.5H_2O$										
	3300m wide 3180m 3120m	1650w	1610s	1535s 1280m	1435m 1375w	1165w 1115w	1015w	860vw 730w	770w 685w	—	615w 580w wide
6.	$[(CdClHsesacH_2O)_2]Cl_2$										
	3305m 3220s 3130s	1625vs	1568s	1540m 1280m	1430m 1368m	1170m 1120w	1020vw	745m	683m	735w	600m 545m 515m
7.	$[CdI_2(Hsesac)_2]$										
	3330s 3285s 3200vs 3100s	1650w	1605vs	1535vs 1280m 1265m	1480m 1435m 1375m	1120m	1025w	860w	771m	—	607m 562m
8.	$[(CdI_2Hsesac)_2]$										
	3340m 3280m 3190s 3105m	1620s	1560m	1543m 1275m	1480w 1430m 1370m	1160m 1115w	1030w	860vw 743w	773w 675w	—	610w 535m 475w wide

Description of absorption: vs=very strong, s=strong, m=medium, w=weak, vw=very weak.

nitrogen atom, in the complex compounds: $[CdCl(Hsesac)_2]\ Cl\cdot 0.5H_2O$ and $[CdI_2(Hsesac)_2]$, according to structures (3) and (4).

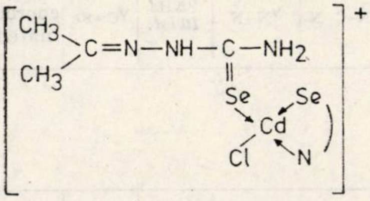
CH3
CH3
C=N—NH—C—NH2
Se
Se
Cd
Cl
N
+

(3)

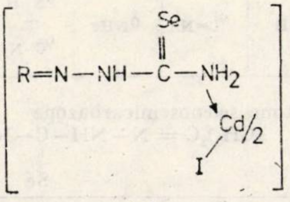
Se
R=N—NH—C—NH2
Cd/2
I

(4)

In the complex compound $[Cd(sesac)_2]$ acetone selenosemicarbazone coordinates as a bidentate ligand, according to structure (1).

Some types of complex compounds – $[CdCl(Hsesac)_2]Cl.0.5H_2O$ and $[CdCH_3COO(sesac)(Hsesac)].0.5H_2O$ – have been synthetized containing two molecules of selenosemicarbazone, each coordinated differently to the same Cd(II) ion, according to structures (3) and (5).

It has also been proved, by spectrophotometrical method, that some complex compounds of Cd(II) with acetone selenosemicarbazone – $[(CdClHsesacH_2O)_2]Cl_2$ and $[\{Cd(CH_3COO)(CH_3COOH)\ (sesac)\}_2]$ – are

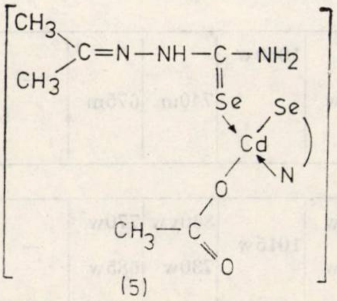
CH3
CH3
C=N—NH—C—NH2
Se
Se
Cd
N
O
CH3—C
O

(5)

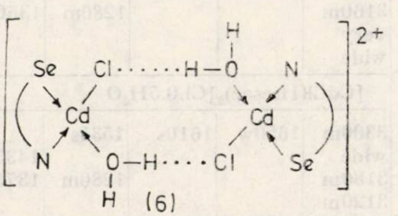
H
2+
Se
Cl·····H—O
N
Cd
Cd
N
O—H····Cl
Se
H

(6)

dimers, according to structures (6) and (7), or are binuclear complex compounds – $[(CdI_2Hsesac)_2]$ – as represented by structure (8).

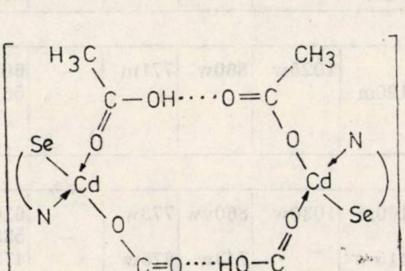
H3C
CH3
C—OH····O=C
Se
O
O
N
Cd
Cd
N
O
O
Se
C=O····HO—C
H3C
CH3

(7)

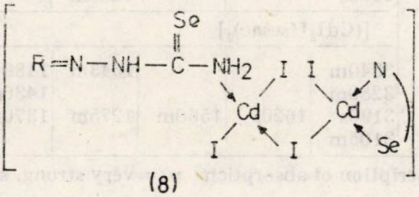
Se
R=N—NH—C—NH2
I
I
N
Cd
Cd
I
I
Se

(8)

EXPERIMENTAL DATA

I. Synthesis of the complex compounds

1. $[(CdClHsesacH_2O)_2]Cl_2$: 1.14 g $CdCl_2 \cdot 2.5H_2O$ and 0.89 g Hsesac, freshly triturated, are mixed with 2 cm^3 ethyl alcohol for 20 minutes (pH = 7). The resulting precipitate is vacuum filtered in a filtering crucible, then washed with 2 cm^3 ethyl alcohol, gradually added and is dried, in the dark and in the presence of air. The yield is 94%.

2. $[CdCl(Hsesac)_2]Cl.0.5H_2O$: 0.57 g $CdCl_2 \cdot 2.5H_2O$ and 0.89 g Hsesac are mixed with 2 cm^3 ethyl alcohol for 30 minutes (pH = 7). Other 5 cm^3 ethyl alcohol are then added and the resulting suspension is vacuum filtered in a filtering crucible. It is washed with 40 drops of water and 50 drops of ethyl alcohol and dried. The yield is 88%.

3. $[(CdI_2Hsesac)_2]$: To 0.89 g Hsesac, 1.83 g CdI_2 is added. The powders are mixed, then 7 cm^3 ethyl alcohol are gradually added. The resulting suspension is mixed for 45 minutes (pH = = 7), then filtered. The precipitate is washed with 50 drops of ethyl alcohol and dried. The yield is 61%.

4. $[CdI_2(Hsesac)_2]$: To 0.91 g CdI_2 powder, 0.89 g Hsesac, freshly triturated, is added. The powders are mixed, then 2 cm^3 ethyl alcohol are added and the homogenization is continued other 20 minutes To the resulting paste another 6 cm^3 ethyl alcohol are added (pH = 7). The resulting suspension is mixed for other 5 minutes, then filtered. The precipitate obtained by filtering is washed with 20 drops of water and 50 drops of ethyl alcohol, and then dried.The yield is 87%.

5. $[\{Cd(CH_3COO)(CH_3COOH)(sesac)\}_2]$: To 0.80 g $Cd(CH_3COO)_2.2H_2O$ there are added 0.53 g Hsesac. The two substances are thoroughly mixed and moistened with 0.4 cm^3 ethyl alcohol. By mixing for 20 minutes, an homogeneous paste is obtained, which gradually solidifies. Other 4 cm^3 ethyl alcohol are added (pH = 7). The resulting suspension is mixed for a few minutes and then filtered. The precipitate, separated on a filter plate, is washed with 50 drops of ethyl alcohol, and dried. The yield is 57%.

6. $[CdCH_3COO(sesac)\ (Hsesac)].\ 0.5H_2O$: To 0.40 g $Cd(CH_3COO)_2.\ 2H_2O$ and 0.53 g Hsesac, 1.5 cm^3 ethyl alcohol is added (pH = 7) and the homogenization continues until an abundant uniform paste is formed. Other 4 cm^3 ethyl alcohol are added, the suspension is stirred for a few minutes, and then filtered. The resulting precipitate is washed with 50 drops of ethyl alcohol, gradually added, and afterwards dried. The yield is 59%.

7. $[Cd(sesac)_2]$: 0.40 g $Cd(CH_3COO)_2 \cdot 2H_2O$ and 0.53 g Hsesac are thoroughly mixed with 3 cm^3 ethyl alcohol. Then 1.5 cm^3 of 25% ammonia solution is dropwise added (pH = = 10.5). There appears immediately an abundant precipitate, of a yellowish-lemon colour. The precipitate is left 10 minutes, occasionally stirring the suspension, then filtering it. The filtrated precipitate is first washed with 20 drops of water, then with 20 drops of ethyl alcohol, the solvents being gradually added. The product is then dried. The yield is 81%.

II. Apparatus

For molar electric conductivity measurements, a conductometer of the IRME type (Romania) has been used, its cell constant being $c = 0.30738$ cm^{-1}. CARLO ERBA methyl alcohol for electronic use, 99.9% purity and 0.05% H_2O, was used as solvent.

Electronic reflectance spectra have been recorded on a VSU-1 spectrophotometer Carl Zeiss-Jena (East Germany), using magnesium oxide as reference substance.

Ultraviolet absorption electronic spectra were recorded on a double beam Beckman DK-2A spectrophotometer (USA) using quartz cells with optic path of 1 cm. Absolute ethyl alcohol has been used as solvent.

IR spectra were recorded on an UR 10 Carl Zeiss-Jena spectrophotometer (East Germany). Solid samples have been used as KBr pellets, 1 mg substance /300 mg KBr.

For the thermal analysis of the compounds, a derivatograph of MOM-type (Hungary) has been used. The curves were recorded in air, at temperatures ranging between 20°C — 500°C ; the heating rate was of 5°C/min. The standard sample was Al_2O_3 ; the working sample was of 0.4 g.

REFERENCES

[1] A. V. Ablov, N. V. Gerbeleu and A. M. Romanov, *Zhur. neorg. Khim.*, **13**, 787 (1968).

[2] A. V. Ablov, N. V. Gerbeleu and A. M. Romanov, *Zhur. neorg. Khim.*, **13**, 3024 (1968).

[3] A. V. Ablov, N. V. Gerbeleu, A. M. Romanov and V. M. Vlad, *Zhur. neorg. Khim.*, **16**, 1357 (1971).

[4] I. Ghelase, Doctoral Dissertation, Polytechnical Institute of Bucharest, 1979.

[5] I. Pogany and M. Banciu, "Metode fizice în chimia organică", Ed. Ştiinţifică, Bucureşti, 1972 p. 162.

[6] Iu. N. Kukushkin, P. G. Antonov, K. I. Dubonos and L. V. Konovalov, *Zhur. neorg. Khim.*, **18**, 3017 (1973).

[7] D. Negoiu and I. Ghelase, *Bul. Inst. Polit. Bucureşti, Seria Chim.— Metal.*, **43**, 27 (1981).

[8] K. Nakamoto, "Infrakrasnye spektry neorganicheskih i koordinatsionnykh soedinenii", Izd. Mir, Moscow, 1966, p. 214, 215.

[9] M. Dinculescu, Doctoral Dissertation, Polytechnical Institute of Bucharest, 1977.

Revue Roumaine de Chimie, 28, 3, 235–242 (1983)

NUCLEOPHILE SUBSTITUTIONEN IN DER 1,3,5-TRIAZINREIHE. IX[1].

KINETIK UND MECHANISMUS DER REAKTION DER 2,4-DICHLOR-6-PHENYLAZOPHENYLAMINO-1,3,5-TRIAZINE MIT 4-AMINOAZOBENZENEN

I. HAVLIK* und R. BACALOGLU**
* Chemie-Forschungszentrum
Bd. Mihai Viteazul 24, Timişoara
** Laboratorium für Organische Chemie, Technische Hochschule „Traian Vuia",
str. Bocşa 6, Timişoara

Eingegangen am 4. Dezember 1981

Die Kinetik und der Mechanismus der Reaktion der 2,4-Dichlor-6-phenylazophenylamino-1,3,5-triazine mit 4′-substituierten 4-Aminoazobenzenen wurde konduktometrisch untersucht. Es wurde ein Additions-Eliminierungs-Mechanismus festgestellt, wobei als langsame Etappe ein nucleophiler Angriff – bei kleinen Wasserkonzentrationen – und eine langsame Eliminierung des Chloridions – bei großen Wasserkonzentrationen – gilt. Eine Ausnahme bildet 4-Amino-4′-nitroazobenzen, wo eine Umkehrung der langsamen Etappen festgestellt werden kann, und zwar eine Eliminierung des Chloridions bei kleinen Wasserkonzentrationen und ein nucleophiler Angriff bei großen Wasserkonzentrationen.

The kinetics and mechanism of 2,4-dichloro-6-phenylazophenylamino-1,3,5,-triazine with 4′-substituted 4-aminoazobenzene have been studied by conductimitry. An addition-elimination mechanism with a slow nucleophilic attack at low water concentrations, and with a slow chloride ion elimitation at high water concentrations, has been demonstrated. The reaction of 4-amino-4′-nitrobenzene is an exception. An inversion of the slow steps takes place: the chloride ion elimination is the slow step at small water concentrations, and the nucleophilic attack at higher ones.

In einer vorangehenden Arbeit dieser Reihe[1] wurden die Reaktionen des Cyanurchlorids mit 4′-substituierten 4-Aminoazobenzenen – eine Modellreaktion für die erste Phase der Synthese von reaktiven Triazinfarbstoffen – untersucht. Die symmetrischen und asymmetrischen Disubstitutionsreaktionen wurden an denselben Modellreaktionen untersucht. Die erhaltenen Ergebnisse stellen den Inhalt vorliegender Arbeit dar.

ERGEBNISSE UND DISKUSSION

Die Kinetik der Reaktion der 2,4-Dichlor-6-phenylazophenylamino-1,3,5-triazine mit 4′-substituierten 4-Aminoazobenzenen wurde in wäßrigem Dioxan durch Verfolgung der Leitfähigkeit der Lösung untersucht (Molverhältnis 4-Aminoazobenzen/Dichlortriazin – 10-12/1 ; pseudoerste Ordnung in bezug auf die Dichlortriazine).

Die erhaltenen Konstanten zweiter Ordnung der Synthesereaktion einiger symmetrischer 2-Chlor-4,6-di(phenylazophenylamino)-1,3,5-triazinderivate mit verschiedenen Substituenten am aromatischen Ring sind in Tabelle 1 zusammengefaßt.

Innerhalb der Grenzen der experimentellen Fehler (ca. 7 – 10 %), hängen die Geschwindigkeitskonstanten zweiter Ordnung nicht von dem Verhältnis der Reagenzien ab, was eine Katalyse durch das aromatische Amin, sowie eine Autokatalyse (Tabelle 1, Nr. 4 – 6) ausschließt.

TABELLE 1

Geschwindigkeitskonstanten der Reaktion :

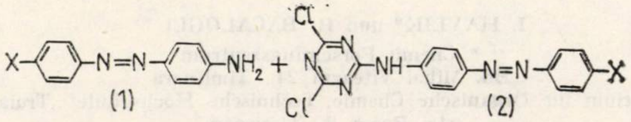

in wäßrigem Dioxan (40 Vol. % Wasser), bei 80,4°C

X	σ_p[2]	pK_a[3]	Molverhältnis (1)/(2)	$k_2 \cdot 10^2$ l/mol. sec	k_2^m/k_2*)
NO_2–	+0,778	1,88	11,2	15,5	63,9 (177,5^e)
CH_3CO–	+0,502	2,16	11,7	7,97	204,5
Cl–	+0,227	2,24	10,8	9,46	267,6
H–	0	2,50	10,6	11,1*)	345,9 (4110^e)
H–	0		15,7	9,7**)	
H–	0		20,5	10,0**)	
CH_3–	–0,170	2,56	12,1	12,0	400,8
HO–	–0,370	2,74	11,8	13,0	516,9
$(CH_3)_2N$–	–0,830	3,06	10,6	18,7	784,5

*) k_2^m – die Konstanten zweiter Ordnung für die Monosubstitution des Cyanurchlorids mit denselben 4′-substituierten 4-Amino-azobenzenen in wäßrigem Dioxan (45/55 Vol/Vol) und bei 35,1°C. Die mit *e* bezeichneten Werte entsprechen Verhältnis zwischen den bei 35,1°C extrapolierten Konstanten zweiter Ordnung der Dikondensationsreaktion.

**) Durchschnitt $10{,}26 \cdot 10^{-2} \pm 0{,}74 \cdot 10^{-2}$ l/mol. sec

Den 4′-substituierten 4-Aminoazobenzenen kommt in der langsamen Stufe oder in einem raschen Vorgleichgewicht die Rolle der nucleophilen Agenzien zu. Dies geht aus den guten Hammett-Korrelationen lg k auch mit den pK_a-Werten hervor (mit Ausnahme des 4-Amino-4′-nitroazobenzens) :

$$\lg k_2 = -0{,}964 - 0{,}270\,\sigma \qquad r = 0{,}996$$

$$\lg k_2 = -1{,}900 + 0{,}379\ \mathrm{p}K_a \qquad r = 0{,}988$$

In Tabelle 2 sind die RG-Werte der Reaktion der 4′-substituierten 4-Aminoazobenzene mit 2,4-Dichlor-6-phenylazophenyl-1,3,5-triazinen, die am aromatischen Ring Nitro- und Dimethylamino-Gruppen tragen, angegeben. Mit Ausnahme der 4-Amino-4′-nitroazobenzene wurde auch in diesem Fall eine gute Hammett-Korrelation zwischen den lg k und den pK_a-Werten gefunden:

$$(H_3C)_2N\text{-}\quad \lg k = -1{,}165 - 0{,}513\,\sigma \qquad r = 0{,}999$$

$$\lg k = -2{,}934 + 0{,}717\ pK_a \qquad r = 0{,}990$$

$$O_2N\text{-}\quad \lg k = -0{,}866 - 0{,}471\,\sigma \qquad r = 0{,}993$$

$$\lg k = -2{,}498 + 0{,}661\ pK_a \qquad r = 0{,}987$$

TABELLE 2

Die Geschwindigkeitskonstanten der Reaktion

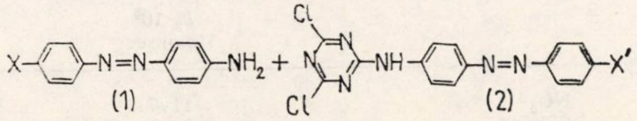

im wäßrigem Dioxan (40 Vol. % Wasser) bei 80,4°C (Für die σ_x – und pK_a – Werte, siehe Tabelle 1)

X′	X	$k_2 \cdot 10^2$ l/mol·sec	k_2^a/k_2^s *)	k_2^{ma}/k_2^{ms} **)
$(CH_3)_2N$–	O_2N–	9,4	0,606	0,0675
	CH_3CO–	3,83	0,408	0,111
	Cl–	5,25	0,555	0,172
	H–	6,75	0,608	0,262
	CH_3–	8,45	0,708	0,328
	HO–	10,1	0,776	0,458
	$(CH_3)_2N$–	18,7	1,000	1,000
O_2N–	O_2N–	15,5	1,000	1,000
	CH_3CO–	8,0	0,516	1,646
	Cl–	10,5	0,677	2,556
	H–	14,1	0,910	3,879
	CH_3–	16,8	1,083	4,858
	HO–	18,2	1,174	6,788
	$(CH_3)_2N$–	35,2	2,271	14,819

*) Das Verhältnis zwischen den Reaktionsgeschwindigkeiten der Entstehung des asymmetrisch und symmetrich substituierten triazins, im Falle der Reaktion der 4′-substituierten 4-Aminoazobenzole mit 2,4-Dichlor-6-phenylazophenyl-1,3,5-triazinen, die am aromatischen Ring eine NO_2– und $(CH_3)_2$ N-Gruppe tragen.

**) Das Verhältnis zwischen den Monosubstitutionskonstanten des 4-Aminoazobenzols bzw. des 4-Amino-4′-dimethylaminobenzols, bzw. des 4-Amino-4′-nitroazobenzols – vorangehende Mitteilung[1] – bei 35,5°C in Dioxan-Wasser 55/45 Vol/Vol.

Dies deutet wiederum auf die nucleophile Rolle der 4-Aminoazobenzene im Prozeß.

Tabelle 3 enthält die Geschwindigkeitskonstanten zweiter Ordnung der Reaktionen des 4-aminoazobenzens mit kernsubstituierten 2,4-Dichlor-6-phenylazophenylamino-1,3,5-triazinen. Außer der mit der Dimethylaminogruppe substituierten Verbindung, weisen alle anderen Verbindungen eine fast konstante Reaktionsgeschwindigkeit auf. Die Hammett-Korrelierung:

$$\lg k_2 = -0{,}952 + 0{,}029\sigma \qquad r = 0{,}956$$

TABELLE 3

Die Geschwindigkeitskonstanten der Reaktion

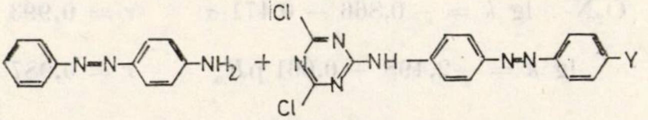

in wäßrigem Dioxan (40 Vol H_2O/100 Vol. Dioxan) bei 80,4°C (für σ_p-Werte, siehe Tabelle 1)

Y	$k_2 \cdot 10^2$ l/mol.sec
NO_2-	11,7
CH_3CO-	11,5
CL–	11,5
H–	11,1
CH_3-	11,1
HO–	10,8
$(CH_3)_2N-$	6,75

TABELLE 4

Der Einfluß der Polarität des Lösungsmittels auf die Reaktionen

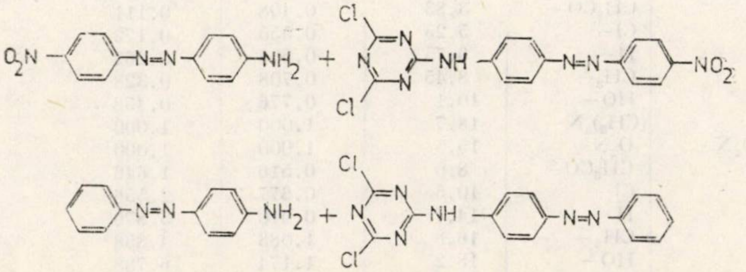

(1)

(2)

bei 80,4°C

Vol. % H_2O im Dioxan	H_2O-Konz. mol/l	E_T*)	Y**)	$k_2 \cdot 10^2$ l/mol·sec (1)	$k_2 \cdot 10^2$ l/mol·sec (2)
11,1	6,17	47	−1,86	4,75	—
21,0	11,66	49,2	−0,75	8,80	—
30,0	16,68	50,9	0,02	12,0	2,3
35,0	19,44	51,6	0,39	14,0	3,9
40,0	22,23	52,3	0,72	15,0	11,0
45,0	25,00	53,0	1,05	24,0	12,0
49,2	27,35	53,5	1,31	32,0	13,0
55,0	30,53	54,6	1,54	—	15,0
60,0	33,30	55,6	1,81	—	20,0

*) Werte aus Arbeit[4] oder extrapoliert nahe den Angaben dieser Arbeit.

**) Werte aus Arbeit[5] oder extrapoliert nahe den Angaben dieser Arbeit.

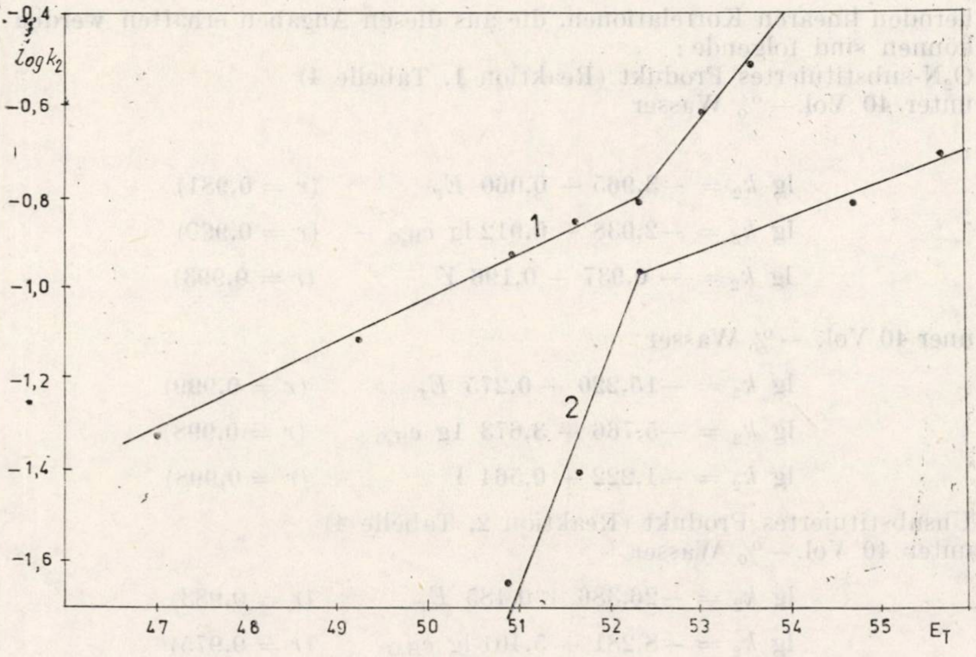

Abb.1. — Veränderung der Geschwindigkeitskonstanten zweiter Ordnung in Abhängigkeit vom E_T — Parameter: 1 — für die Reaktion (1); 2 — für die Reaktion (2).

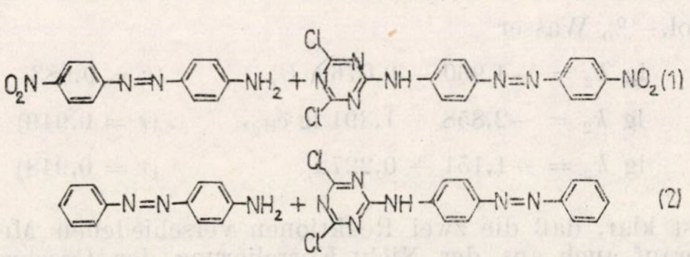

beweist, daß die Substituenten des Benzenkerns praktisch keinen Einfluß auf die Reaktionsfähigkeit des Triazine haben. Daraus folgt, daß die Übertragung der elektronischen Effekte der Substituenten durch die Azo- und Amino-Gruppen auf den Triazinring unbedeutend ist.

Aus Tabelle 4 geht der Einfluß der Zusammensetzung des Lösungsmittels auf die Reaktionsgeschwindigkeit in zwei verschiedenen Fällen hervor. Es handelt sich um die Reaktion des 4-Amino-azobenzens mit dem von ihm abgeleiteten monosubstituierten Derivat und des 4-Amino-4′-nitroazobenzens mit dem entsprechenden monosubstituierten Derivat.

In Abbildung 1 ist die Veränderung des Logarithmus der Geschwindigkeitskonstanten mit einem für die Polarität des Lösungsmittels kennzeichnenden Parameter— E_4^T —dargestellt.

Es ist offensichtlich, daß beide Reaktionen zwei Gebiete mit verschiedenen linearen Korrelationsanstiegen umfassen, und zwar eines unter 40 Vol.— % Wasser in Dioxan und eines über diesem Wert. Die annä-

hernden linearen Korrelationen, die aus diesen Angaben erhalten werden können sind folgende:
O_2N-substituiertes Produkt (Reaktion 1, Tabelle 4)
unter 40 Vol.–% Wasser

$$\lg k_2 = -3{,}965 + 0{,}060\ E_T \qquad (r = 0{,}981)$$

$$\lg k_2 = -2{,}038 + 0{,}912 \lg c_{H_2O} \qquad (r = 0{,}990)$$

$$\lg k_2 = -\ 0{,}937 + 0{,}196\ Y \qquad (r = 0{,}993)$$

üner 40 Vol. – % Wasser

$$\lg k_2 = -15{,}220 + 0{,}275\ E_T \qquad (r = 0{,}999)$$

$$\lg k_2 = -5{,}766 + 3{,}673 \lg c_{H_2O} \qquad (r = 0{,}998)$$

$$\lg k_2 = -1{,}222 + 0{,}564\ Y \qquad (r = 0{,}998)$$

Unsubstituiertes Produkt (Reaktion 2, Tabelle 4)
unter 40 Vol.–% Wasser

$$\lg k_2 = -26{,}386 + 0{,}485\ E_T \qquad (r = 0{,}983)$$

$$\lg k_2 = -8{,}281 + 5{,}401 \lg c_{H_2O} \qquad (r = 0{,}975)$$

$$\lg k_2 = -1{,}698 + 0{,}964\ Y \qquad (r = 0{,}976)$$

über 40 Vol.–% Wasser

$$\lg k_2 = -4{,}960 + 0{,}0762\ E_T \qquad (r = 0{,}983)$$

$$\lg k_2 = -2{,}858 + 1{,}391 \lg c_{H_2O} \qquad (r = 0{,}949)$$

$$\lg k_2 = -1{,}151 + 0{,}227\,Y \qquad (r = 0{,}948)$$

Es ist klar, daß die zwei Reaktionen verschiedenen Mechanismen folgen, worauf auch aus der Nicht-Korrelierung der Geschwindigkeitskonstanten des 4-Amino-4′-nitroazobenzens mit den Hammett-Parametern oder der pK_a-Werte mit den Geschwindigkeitskonstanten der anderen substituierten 4-Aminoazobenzene geschlossen werden kann.

Die Aktivierungsparameter der beiden oben beschriebenen Reaktionen sind in Tabelle 5 zusammengefaßt.

Werden die erhaltenen Ergebnisse mit jenen für die Monosubstitutionsreaktion erhaltenen verglichen, wo ähnliche Veränderungen der Reaktionsfähigkeit bei Wasserkonzentrationen im Dioxan von unter und über 30 % festgestellt werden können, kann man folgende Schlüsse ziehen:

Im Falle der Reaktion des Monosubstitutionsproduktes des Cyanurchlorids mit 4-Amino-4′-nitroazobenzen (Reaktion 1, Tabelle 4 und 5) weist die graphische Darstellung der Abhängigkeit der Wasserkonzentration dieselbe Form auf wie jene, die für die Monosubstitution des Cyanurchlorids mit 4-Amino-4′-nitroazobenzen erhalten wurde.[1] In letzterem Fall wurden für kleine Wasserkonzentrationen folgende Proportionalitätskoeffizienten der $\lg k_2$-Korrelierungen gefunden: 0,098 (für

E_T), 0,968 (für c_{H_2O}) und 0,252 (für Y), während für große Wasserkonzentrationen 0,190 (für E_T), 2,313 (für c_{H_2O}) und 0,386 (für Y) gefunden wurden. Wir können also annehmen, daß es sich um einen ähnlichen Mechanismus handelt, der bei großen Wasserkonzentrationen einem langsamen nucleophilen Angriff (1) und bei kleinen Wasserkonzentrationen einer langsamen Eliminierung des Chlors (2) aus dem gebildeten Zwischenprodukt entspricht :

TABELLE 5

Scheinbare Aktivierungsparameter für die Reaktionen

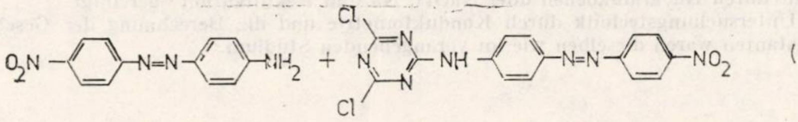

(1)

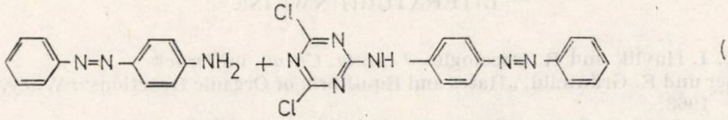

(2)

in wäßrigem Dioxan (40 Vol. % H_2O).

t °C	$k_2 \cdot 10^2$ l/mol·sec	$\Delta S^{\neq}$ cal/mol°K	$\Delta H^{\neq}$ kcal/mol
	Für Reaktion(1)		
50,5	8,07	−48,24	4,35
60,0	10,00		
69,1	12,20		
80,4	15,50		
	Für Reaktion (2)		
51	2,50	−29,83	11,10
60	3,68		
68,5	6,16		
80,4	11,10		

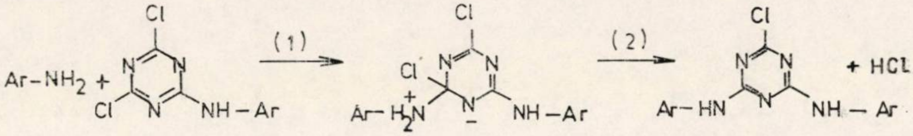

Im Falle der Reaktionen der restlichen Arylamino-1,3,5-triazine entsprechen die Proportionalitätsfaktoren der Korrelationen mit den Polaritätsparametern des Lösungsmittels sowie den scheinbaren Aktivierungsparametern einer langsamen Stufe des nucleophilen Angriffs bei kleinen Wasserkonzentrationen. Diese Feststellung kann leicht erklärt werden, wenn wir die Abnahme der Reaktionsfähigkeit des Dichlorarylamino-1,3,5-triazins im Vergleich zu der des Cyanurchlorids in betracht ziehen.

BESCHREIBUNG DER VERSUCHE

Die Azofarbstoffe wurden in den meisten Fällen durch Diazotierung und Kupplung synthetisiert und durch wiederholte Kristallisation gereinigt.[3] Die mono- und disubstituierten Derivate des Cyanurchlorids wurden aus Cyanurchlorid und Aminozofarbstoffen hergestellt und durch IR–, UV–und ^{1}H-NMR-Spektroskopie charakterisiert. Ihre Reinheit wurde durch Schmelzpunktbestimmungen und Dünnschichtchromatographie[6] geprüft. Das Dioxan p.a. Merck wurde durch Rückflußkochen über NaOH, Na und Rektifikation[1] gereinigt.

Die Untersuchungstechnik durch Konduktometrie und die Berechnung der Geschwindigkeitskonstanten waren dieselben wie im vorangehenden Studium.[1]

LITERATURHINWEISE

[1] VIII. Mitt. I. Havlik und R. Bacaloglu, *J. prakt. Chem.*, im Druck.

[2] J. E. Leffler und E. Grünwald, „Rates and Equilibria of Organic Reactions“, Wiley, New York, 1963.

[3] I. Havlik, A. Toth, C. Csunderlik und R. Bacaloglu, *Rev. Roumaine Chim.*, im Druck.

[4] Ch. Reichard und K. Dimroth, *Forsth. Chem. Forsch.*, **11**, 1 (1968).

[5] M. Charton, *Chem. Tech.*, **5**, 245 (1975).

[6] I. Havlik, C. Csunderlik und R. Bacaloglu, *Rev. Roumaine Chim.*, im Druck.

Revue Roumaine de Chimie, **28**, *3*, **243**—247 (1983)

DERIVATIVES OF 4-AMINOMETHYL-THIAZOLE. IV[1]

THIAZOLE DERIVATIVES OF PHENOTHIAZINE

SIMONA SILBERG *, IOAN A. SILBERG ** and CORNEL BODEA ***

* Pharmaceutical Faculty, str. Ion Creangă 12, R-3400 Cluj-Napoca Romania
** IECB-"Babeș-Bolyai" University Research Group, Department of Physical Chemistry str. Arany Janos 11, R-3400 Cluj-Napoca, Romania
*** Institute of Chemistry, str. Donath 65—103, R-3400 Cluj-Napoca, Romania

Received June 10, 1982

The synthesis and physico-chemical characterization of new thiazole derivatives of phenothiazine are presented.

The encouraging results obtained by linking the thiazole ring and the nitrogen mustard moiety [2] prompted us to investigate the preparation and properties of another group of compounds, in which the thiazole is attached to the phenothiazine nucleus, a structural element which is encountered in the molecule of a great number of substances of well established therapeutical value.[3]

From the preparative point of view, our researches were stimulated by the feasibility of syntheses for the thiazole derivatives of phenothiazine by condensing 2-aryl-4-chloromethyl-thiazoles with 10-unsubstituted phenothiazines; the compounds thus obtained present interesting structural analogies with some phenothiazine drugs, which possess antihistaminic properties and act on the central nervous system.

In a few instances, there were reports in the literature on compounds containing both the thiazole and the phenothiazine rings in the molecule;[4] however, they present only slight similitudes to the class of the phenothiazine drugs, and were obtained by essentially different synthetic routes.

It may be of interest to recall that all phenothiazine drugs belonging to the above mentioned categories contain a side-chain, with two or three carbon atoms attached to the phenothiazine heterocyclic nitrogen, the opposite end of the chain being always linked to another nitrogen atom; the latter is very often involved, in its turn, in a heterocyclic structure. When the two nitrogen atoms are separated by only two carbon atoms, as shown in the schematic formulation **1**, the antihistaminic action is the prevailing one.

The biological activity is conditioned by the lack of chain branching at the level of C_α and is often enhanced by a branching at C_β (see for example the structure of promethazine [3]).

An examination of the formula **2**, which describes the structure of the thiazole derivatives of phenothiazine herewith reported, shows that these compounds fulfil the basic structural requirements for the manifestation of biological activity, while presenting a series of specific features which could entail the appearance of new facets in their pharmacological behaviour.

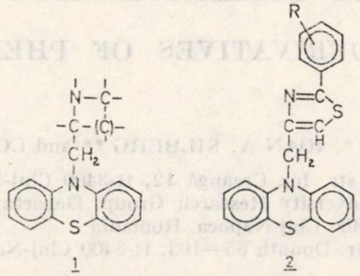

Taking into account the moderate reactivity of position 10 in phenothiazines, we decided to make use of the procedure recommended for attaching amino-alkyl side-chains, namely, by converting the phenothiazine into its sodium derivative and by refluxing the latter with halomethylthiazoles **3** in toluene.[3,4] The reaction products were reluctant to crystallization and had to be converted, for a better characterization, into hydrochlorides. By recrystallizing the latter from *o*-dichlorobenzene, an interesting thermochromy was observed: the gold-yellow leaflets of the hydrochlorides were dissolved on heating, yielding yellow solutions; with increasing temperature, the colour gradually vanished, and the boiling solutions were colourless. On cooling, the yellow colour reappeared and at room temperature the golden crystals of the hydrochloride separated. These phenomena, obviously connected with the reversible dissociation of the hydrochlorides, took place, unfortunately, at too high a temperature to allow a convenient spectrophotometrical monitoring of the process; however, electronic spectra demonstrated that the thiazole ring nitrogen represents the site of the protonation.[5]

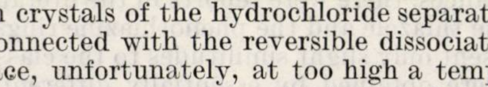

The hydrochlorides of compounds **2** turn green on exposure to air, showing the usual sensitivity towards oxidation of the phenothiazine derivatives. Another example of typical phenothiazine behaviour is the conversion of **2** into the 5,5-dioxides **4** on treatment with H_2O_2 in boiling acetic acid; crystalline, easily isolable compounds were thus obtained. Their structure was checked by independent synthesis, condensing the 4-chloromethyl-thiazoles **3** with the sodium derivative of phenothiazine-5,5-dioxide.

The IR spectra supported the structure assigned to the above mentioned compounds; there is no NH vibration, as expected for 10-substituted phenothiazines, and the bands of the SO_2 groups are conspicuous in the case of the dioxides **4.**

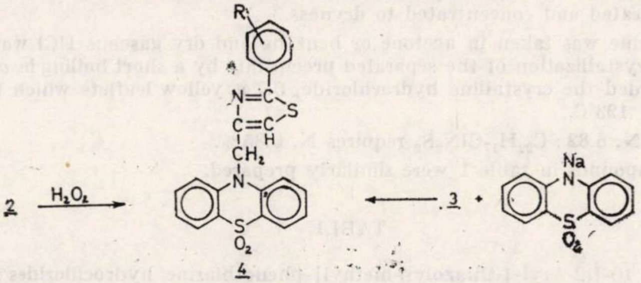

In the ^1H-NMR-spectra, besides the multiplets arising from the protons located on the benzenic rings in the molecule, one can easily identify the signals of the protons from position 5 of the thiazole ring, on the high-field edge of the aromatic multiplet, and the signals of the CH_2 groups, at 5.35 ppm in **2a** and 5.60 ppm in the 5,5-dioxide **4a.** The low position of the latter is to be noted as well as the long-range deshielding induced by the conversion of the sulphide linkage of **2** into the strong electron-withdrawing SO_2 group.

The methylene protons and the isolated one in position 5 of the thiazole form an AX_2 system, as shown by the reciprocal splitting in doublets and triplets, respectively, with $J_{AX} = 1.0$ Hz. As the CH_2 group bridges the two heterocyclic nuclei and is involved in their electronic interactions,[5] and because in the spectra of similar compounds, reported in this series of papers, *e.g.* the urea-,[6] thiourea-,[6] and benzothiazole derivatives of thiazole,[1] the couplings between C-5 and CH_2 protons are virtually absent, we carried out a double resonance experiment on this system, which removed any doubt as to the validity of our interpretation given above.

The striking differences between the magnitudes of the *cisoid* allylic (benzylic) couplings noted above point out to an important change in conformation in the case of the phenothiazine derivatives, as compared with other compounds, in which the side-chain nitrogen of the 4-aminomethyl-thiazole constellation is not involved in rigid cyclic structures. This conclusion is in excellent agreement with other physical and chemical properties of our compounds, as will be shown in a further report, and led to a better understanding of the mechanism of *in vitro* and metabolic degradation of phenothiazine drugs.

EXPERIMENTAL

Melting points are uncorrected. The IR spectra were recorded on a double-beam UR-10 Carl Zeiss Jena spectrophotometer, in KBr pellets; the ^1H-NMR spectra were obtained in $CDCl_3$ solutions at 60 MHz by means of a Varian A-60A spectrometer.

10-[(2-Phenyl-4-thiazolyl)-methyl] -phenothiazine hydrochloride (2, R=H) (2a)

A mixture of 1 g phenothiazine and 1 g finely powdered NaOH in 250 ml anhydrou toluene was concentrated by distillation to cca. 50 ml while water was azeotropically removed one gram 2-phenyl-4-chloromethyl-thiazole (**3**, R=H) was added and the mixture refluxed fo 3 hrs. The alkalies were removed by washing the toluene solutions with water, then the organi layer was separated and concentrated to dryness.

The residue was taken in acetone or benzene and dry gaseous HCl was bubbled in th solution. A recrystallization of the separated precipitate by a short boiling in *o*-dichlorobenzen (see text) afforded the crystalline hydrochloride, 0.7 g, yellow leaflets which turn greenish o standing, m.p. 193°C.

Found : N, 6.82 ; $C_{22}H_{17}ClN_2S_2$ requires N, 6.85%.

The compounds in table 1 were similarly prepared.

TABLE 1

10-[(2-Aryl-4-thiazolyl)-methyl]-phenothiazine hydrochlorides **2**

R	m.p.°C	Molecular formula	N%	
			Calc.	Found
3—CH_3	189	$C_{23}H_{19}ClN_2S_2$	6.63	6.58
4—CH_3	196	$C_{23}H_{19}ClN_2S_2$	6.63	6.79
4—Br	175—7	$C_{22}H_{16}BrClN_2S_2$	5.74	5.40

10-[(2-Phenyl-4-thiazolyl)-methyl] -phenothiazine -5,5-dioxide (4, R=H) (4a)

a. A solution of 0.5 g **2a** in 25 ml glacial acetic acid was treated with H_2O_2 in portions of 2 ml each at 30 min. intervals while maintaining the mixture under a gentle refluxing. By adding water dropwise until persistent cloudiness and slow cooling, 0.3 g of white glittering crystals separated. After a recrystallization from aqueous acetic acid, m.p. 164°C.

Found : N, 7.02 ; $C_{22}H_{16}N_2O_2S_2$ requires N, 6.93 %

b. A suspension of 2.3 g phenothiazin-5,5-dioxide and 0.4 g finely powdered sodium amide in 15 ml xylene was refluxed for 30 min., then treated dropwise with a solution of 2.2 g **3** (R = H) in 10 ml xylene. The mixture was refluxed for 3 hrs, then cooled, treated with water, the xylene layer separated, dried on Na_2SO_4 sicc., filtered and diluted with a double volume of petroleum ether. After filtration and recrystallization from ethanol of the precipitate, 2.1 g white needles, m.p. 164°, were obtained ; no depression of the m.p. upon admixture with the substance obtained above, under *a*.

The compounds in table 2 were similarly prepared.

TABLE 2

10-[(2-Aryl-4-thiazolyl)-methyl]-phenothiazin-5,5-dioxides, **4**

R	m.p.°C	Molecular formula	N %	
			Calc.	Found
3—CH_3	173	$C_{23}H_{19}ClN_2O_2S_2$*	6.16	6.33
4—CH_3	187	$C_{23}H_{19}ClN_2O_2S_2$*	6.16	6·27
4—Br	115	$C_{22}H_{16}BrN_2O_2S_2$	5.78	5.62

* Hydrochlorides

ACKNOWLEDGEMENTS. The authors express their gratitude to Dr. Ing. M. Elian for recording the ^{1}H-NMR spectra and to Mrs. E. Hamburg for the IR spectra. The elemental analyses were carried out by the team of the Microanalytical Laboratory of the Institute of Chemistry, Cluj-Napoca.

REFERENCES

[1] Part III, I. A. Silberg and S. Silberg, *Rev. Roumaine Chim.*, **27** (1982).
[2] I. Simiti and S. Silberg, Papers presented before the National Congress of Pharmacy, Bucharest, 1968, p. 34.
[3] E. Schenker and H. Herbst, *Progr. Drug Res.* **5**, 269 (1963).
[4] C. Bodea and I. A. Silberg, *Adv. Heterocyclic Chem.* **9**, 322 (1968).
[5] S. Silberg, Ph. D. Thesis, Institute of Chemistry, Cluj-Napoca, 1974.
[6] S. Silberg and I. A. Silberg (Part II of this series), *Rev. Roumaine Chim.*, **27** (1982).

Revue Roumaine de Chimie, 28, *3*, 249–261 (1983)

PHENAZATHIONIUM CATIONS. V.

REACTIONS OF 10-(3-PHENOTHIAZINYLIDENE)-PHENOTHIAZINIUM CATIONS AND THEIR COMPLEXES WITH COPPER AND IRON CHLORIDES

MIRCEA V. DIUDEA
Chemical-Pharmaceutical Research Institute, R-3400 Cluj-Napoca, Fabricii Str. 126, Romania

Received October 25, 1981

The synthesis and physico-chemical properties of some complexes of the green cation of phenothiazine [G^+=10-(3-phenothiazinylidene)-phenothiazinium cation] and its aryl derivatives with copper and iron chlorides, and also the chemical behaviour of these compounds in both ionic and radicalic type reactions are described. Thus, both C-derivatives and N-derivatives of 3,10′-diphenothiazine were obtained; among the last ones, the 10, 10′, 3′, 10″ — triphenothiazines represent a new class of *oligo*-phenothiazines. All compounds described in the experimental part are new substances.

1. INTRODUCTION

Our previous papers of this series[1–4] summarized, based on pertinent literature data and personal experiments, the dual behaviour of phenazathionium cations in reactions with nucleophilic reagents, leading to either S-derivatives (kinetic control) or C-derivatives (thermodynamic control). We pointed out the role of concentrations of the active species: phenazathionium cations and nucleophilic reagents, as well as the role of the nucleophilicity (besides pH, temperature, reaction time, solvent and other parameters) in driving the reactions on a certain way or another and stated the real conditions for obtaining C-polysubstituted phenothiazine derivatives in position 3,7 and even 1,9, with sulphide bridge oxidized or not. We also stated that the C-monosubstitution (in positions 3 or 1), in the phenothiazine chemistry necessarily involves the disproportionation of phenothiazinyl cation-radicals and the absence of any oxidant. We created such conditions using complexes of phenothiazinyl (10-unsubstituted) and of diphenothiazinyl cation-radicals with copper halides. In the papers mentioned before and in others [5, 6] we showed that such complexes are stable substances that can be transformed, by ionic or radicalic mechanisms depending on reaction partners and conditions, in well-defined C-monosubstituted derivatives.

This paper deals with the synthesis of some complexes of the green cation of phenothiazines (the famous "green product" marked by us $G^{+, 6}$), and its aryl derivatives and with their physico-chemical characterization and it also suggests a scheme of chemical behaviour of G^+ in reactions developed by ionic and radicalic mechanisms.

2. COMPLEXES OF G^+ CATIONS WITH COPPER AND IRON CHLORIDES

Many papers reported the appearance of a green colour in the processes involving the phenothiazine species S and T (see[7]) in solutions containing water.[7–14] Due to the failure in isolating the "phantom compound" (neither by concentration nor by chromatography on alumina) different structures that can justify its chemical and physico-chemical behaviour, were proposed.

The controversy has been eliminated by the unambiguous synthesis [15,16] of 3,10′-diphenothiazine (**4** – see Scheme 1) and subsequent oxidation with T1(III)-acetate in acetonitrile. The green solution thus obtained showed absorption maxima in visible spectrum at about 450 and 630 nm, values that agree with the absorption maxima reported by other authors [8–14] for the "green product".

Previously, Tsujino et al. [17–22] obtained 3,10′-diphenothiazine (**4**), in anhydrous conditions, by oxidizing phenothiazine with acetic anhydride or iodine. By treating **4** with H_2SO_4 conc. a reddish colour was observed with an ESR spectrum consistent with a triplet state (biradical).[17,20] On diluting with water, the colour became green and its absorption maxima were those of the green cation [G^+ = 10-(3-phenothiazinylidene)-phenothiazinium]. The authors mentioned before succeeded [22] in isolating G^+ in solid state, as $G^+ClO_4^-$ and G^+(5-oxide)ClO_4^- by oxidizing 3.10′-diphenothiazine-5′-oxide with $HClO_4$ 60%.

We remind that in the pioneering period of phenothiazine chemistry, Kehrmann and Vessely,[23] on mixing the alcoholic solutions of phenothiazine and of $FeCl_3$ (see also) [24] had isolated a compound of formula $(C_{12}H_8NSCl)_2Fe(II)Cl_2$.

We succeeded [6] in isolating a complex of formula $G^+Cu(I)Cl_2^-$(**1**—Scheme 1), well crystallized and relatively stable, on treating the complex $(SH^{\dot{+}})_2Cu(II)Cl_4^{2-}$ (see)[25] with $NaHCO_3$ in acetonic medium. In this case the deprotonation of $SH^{\dot{+}}$ species to neutral radical $S^{\cdot}$ and its dimerization to 3,10′-diphenothiazine (**4**), followed by rapid oxidation of the latter by Cu(II) existing in the system took place.

According to Kehrmann's [23] idea we tried to obtain the complex **1** starting just from phenothiazine and $CuCl_2$ in ethanolic solutions. [26] In this way we succeeded in obtaining, in a single step, a compound identical to that described above and in the same way the complex G^+ $Fe(II)Cl_3^-$(**2**—Scheme 1) was prepared.

Scheme 1

$$\text{Phenothiazine} + MCl_n \longrightarrow SH^{\dot{+}} + M^{n-1}Cl_n^-$$

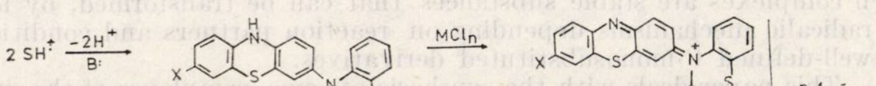

4. X=H
5. X=NO_2

1. M=Cu, n=2, X=H
2. M=Fe, n=3, X=H
3. M=Cu, n=2, X=NO_2

In the ethanolic mother solutions we revealed [26] (by TLC) the presence of 1-and-3-chlorinated phenothiazines and it is likely that the cited authors [23] had obtained a compound (of type **2**) impurified with chlorophenothiazines before.

By treating **1** and **2** with $NaNO_2$ in polar solvent [4] we obtained 7-nitro-3,10′-diphenothiazine **(5)**, which we oxidized with an acetonic $CuCl_2$ solution, thus isolating the complex 7-nitro-G^+ $Cu(I)Cl_2^-$**(3)**.

The complexes **1**, **2** and **3** were characterized by elemental analysis, and visible and IR spectra (see experimental part). The ESR signals of **1** and **2**, on polycrystalline sample are of isotropic type and characterized by the following values: $\Delta H = 15.0$ Gauss **(1)**[6] and 116.5 Gauss **(2)**; $g = 2.0069082$ **(1)**[6] and 2.0150502 **(2)**. These data suggest a radicalic state for G^+ ($G^+ \leftrightarrow G^{+}_{\cdot}$) in such complexes (state favoured by a possible charge transfer: $M \xrightarrow{n-1} G^+$, see below) and also the existence of Cu(I) and Fe(II) ions.

3. REACTIONS OF G+ CATIONS AND THEIR COMPLEXES WITH COPPER AND IRON CHLORIDES

The cations of type G^+ can participate into reactions in which they manifest both ionic and radicalic characteristics, the last ones acquired by charge transfer (Scheme 2).

3.1. *The ionic pathway*. The G^+ cation is stable only in acid medium. In 96% H_2SO_4 the green colour turns into golden-red, [26] due to the protonated species $GH^{++} \leftrightarrow GH^{+\,+}_{\cdot\,\cdot}$, giving an ESR signal consistent with a triplet state [17,20] (see above). The deprotonation occurs by adding some drops of water, the colour returning into the characteristic green:

$$GH^{++} \underset{+H^+}{\overset{-H^+}{\rightleftarrows}} G^+$$

proves the establishment of a fast equilibrium between the protonated and deprotonated forms, as well as the fact that the GH^{++} [3-(10-phenothiazinyl)- phenazathionium dication] is a strong acid ($pK_a - 2.9$). [17,20] In more diluted solutions of strong acids (HCl, H_2SO_4,) the colour remains green.

At neutral or alkaline pH, in polar solvent, G^+ undergoes the attack of nucleophiles X^-(X :) in positions 3,7 and 1,9 (of 10-unsubstituted phenothiazine nucleus) forming C-substituted derivatives; after such nucleophilic attacks the bond $C_3—N_{10'}$ can be preserved or, on the contrary, splitted.

The positive charge of G^+ seems to be distributed between the atom $N_{10'}$ (with the doublet involved in the extended conjugation) and the N-unsubstituted phenothiazine nucleus, with high values in positions 3,7 (see also the spin density distribution for $SH^{+}_{\cdot}$ species). [27] The access of nucleophile to position 3 is sterically hindered by the large volume of 10′-coupling phenothiazine nucleus, so that the position 7 remains the most favoured. The positions 1,9 can be also substituted, in conditions of thermodynamic control (see [3]), after the positions 3,7 were occupied.

When the nucleophile is H_2O, the attack in position 3 results in breaking the bond C_3-$N_{10'}$, with formation of T^+ cation (finally phenothiazine) and probably 3-hydroxy-phenothiazine (see [15,16]), species able, together

Scheme 2

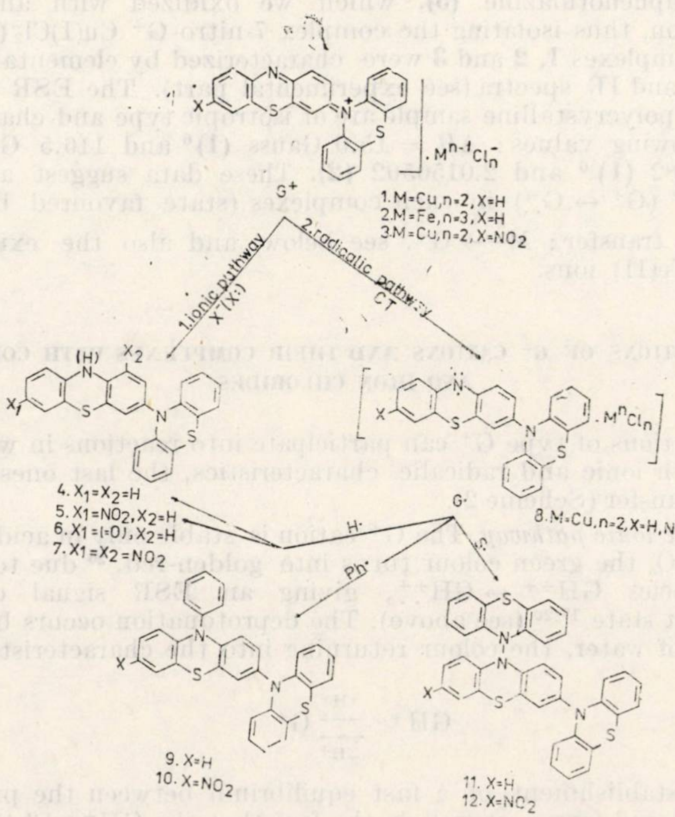
G+
.Mn-1Cln-
1.M=Cu,n=2,X=H
2.M=Fe,n=3,X=H
3.M=Cu,n=2,X=NO2
1.ionic pathway X-(X:)
2.radicalic pathway CT
(H) X2
X1
4. X1=X2=H
5. X1=NO2,X2=H
6. X1=(=O),X2=H
7. X1=X2=NO2
.MnCln
8.M=Cu,n=2,X=H,NO2
G·
H·
Pb·
9. X=H
10. X=NO2
11. X=H
12. X=NO2

with 7-hydroxy-3,10′-diphenothiazine (possible present by attack of H_2O in position 7), to reduce the G^+ cation to the unoxidized dimer **4**, the hydroxylated species turning into the corresponding quinones. It is the case of G^+ hydrolysis, reaction in which the following species were isolated :[17,20] phenothiazine (3%); phenothiazin-3-one (5%); 3,10′-diphenothiazine **4** (40%) and 3,10′-diphenothiazin-7-one **6** (30%).

We performed the hydrolysis of G^+ (from **1**) in the presence of hydrazine, thus isolating [26] the dimer **4** (27.95%), dimeric phenothiazinone **6** (26.70%) and phenothiazine and phenothiazin-3-one revealed qualitatively by TLC. The isolating of dimer **4** is difficult due to its fast oxidation to G^+ by several species from the system (e.g. T^+) [15] or by atmospheric oxygen and subsequent hydrolysis of G^+, reactions that occur just on alumina column. In the presence of Cu(II), the dimer **4** is rapidly oxidized to G^+.

When the nucleophile is different to H_2O(e.g. NO_2^-), the principal products isolated were the dimers 7- and 1(9)-substituted (as unoxidized forms, as the nucleophilic substitution followed by 3 (or 1)-10 prototropism equalizes the reduction of G^+). Thus we obtained 7-nitro-3,10′-diphenothiazine **(5)**[4] and 1 (or 9), 7-dinitro-3,10′-diphenothiazine **(7)**.

No reactions of G^+ in which the 10′-coupling phenothiazine nucleus and sulfidic bridges 5 or 5′ could be substituted, were related (although 3,10′-diphenothiazin-5(or 5′)-oxides have been isolated,[22] probably in another way). Attempts to oxidize G^+ at sulfur led us only to phenothiazinones.

3.2. *The radicalic pathway*. In the complexes of type **1** — **3**, the G^+ cations show radicalic character, revealed by ESR (see above), the radicalic mesomeric structure prevailing by charge transfer (CT) from metal to G^+ :

$$G^{+}_{\cdot\cdot}M^{(n-1)}Cl_n^- \xrightarrow{CT} G\cdot M^{(n)}Cl_n$$

transfer "at demand" in the presence of radicalic partners. The spin density will be maximum in atom N_{10}(cf. S.).[27]

We succeeded for the first time to couple the radical G.(3,10′-diphenothiazin-10-yl, from **8)** with the radical Ph. (phenyl) by melting a mixture of **1** and $SnPh_4$. Thus we obtained 10-phenyl-3,10′-diphenothiazine (**9**, X = H) and similarly 7-nitro-10-phenyl-3,10′-diphenothiazine (**10**, X = NO_2), starting from **3** (Scheme 2). In chromatographic separation of 10-phenyl-dimers we revealed the dimers **4** and **5** (by TLC, comparison with authentic samples[26]) — compounds which are generated simultaneously, by coupling the radicals G· and H·.Taking into account the capability of radicalic coupling of G· as well as the possible existence and reaction of monomeric radical S·[15,16,26-28] we also succeeded in première, the coupling of these two radicals, obtaining a trimer : 10, 10′, 3′, 10″ — triphenothiazine (**11**, X = H) and indirectly, the 7-nitro-trimer (**12**, X = NO_2 — Scheme 2).

3.3. *Triphenothiazines and complexes of di- and tri-phenothiazines with $CuCl_2$*. As previously shown, the coupling 3,10′ is a major reaction pathway of phenothiazinyl radicals,[15-21] in these positions the spin densities being the highest.[7,16,27] The possibilities of generating the free radicals $S\cdot(S^{+}_{\cdot})$ include in addition to electro- and photochemical methods[16] a wide range of reagents :[26] transitional metals in high oxidizing states,[28-36] common oxidants (iodine, acetic anhydride, H_2SO_4 conc., $KMnO_4$, $POCl_3$ etc.)[17-21,28,37] or complex oxidants,[38,39] hydroperoxides,[27,40,41] charge transfer complexes[10,42,43] or stable organic radicals (e.g. diphenylpicrylhydrazyl, tri-tret-butylphenoxyl),[28] in reactions of redox or homolytic type (H. extracting).

The 3,10′ coupling generates C—N bonds, relatively stable, the resulted dimers of type **4** being stabilized by oxidation to G^+ (when the coplanarity of the two phenothiazine nuclei is not sterically hindered) so that the process becomes irreversible. This is the case previously reported by us, in preparing the complex $G^+Cu(I)Cl_2^-$ **(1)** from the complex $(SH^{+}_{\cdot})_2$ $Cu(II)Cl_4^{2-}$ in the presence of the bases. In this system, in addition to the pair $G^+CuCl_2^-$, there are radicals S·(or phenothiazine, by coupling with H·) and the complex acid $HCuCl_2$. Using an acetonic solution of $KMnO_4$ (see [26,28]) we reached an optimum concentration of species S· in the green solution, making possible the charge transfer:

$$G^+Cu(I)Cl_2^- \xrightarrow{CT} G{\cdot}Cu(II)Cl_2$$

and the coupling 10, 10′ of the two radicals. The resulting trimer is rapidly oxidized, the oxidized species forming a complex **13** [10, 10′, 3′, 10″-triphenothiazinyl tetrachlorocuprate (II)] with the anion $Cu(II)Cl_4^{2-}$ also present in the system (Scheme 3) and the colour turns into dark blue.

Scheme 3

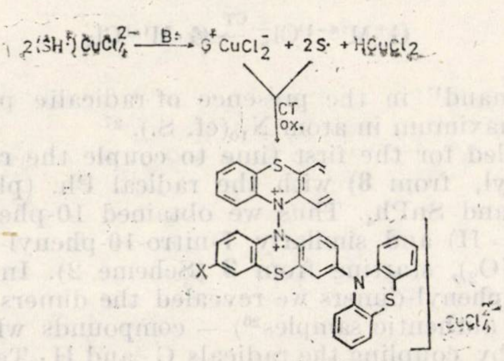

13. X=H
14. X=

In working conditions, **13** was isolated as a dark blue powder, relatively stable, soluble in chloroform, acetone, DMF. We remind that Jackson and Patel [28] had previously reported a blue colour resulting from mixing the acetonic solutions of phenothiazine and DPPH, with a λ max. at about 660 nm (for comparison see the experimental part, Table 1).

By nitrating **13** with $NaNO_2$ we obtained the trimer **12**, the subsequent oxidation with $CuCl_2$ leading to the complex **14**[7′-nitro-10, 10′, 3′, 10″ — triphenothiazinyl tetrachlorocuprate (II)] analogous with **13**.

The hydrolysis of **13** (in the presence of hydrazine) allowed us to isolate the trimer **11**, a greenish-white powder which (as will be shown below) contains both N—N bond (coupling of type 10, 10′) and C—N bond (coupling of type 3, 10′). We mention that Tsujino [19] reported some trimers and tetramers (molecular weight: 618 and 814), in reactions of which mean product was 3, 10′-diphenothiazine (**4**), the dimer 10, 10′ being not reported.

Previously we have pointed out that $CuCl_2$ is able to oxidize the di- and tri-phenothiazines and, in addition, to complex the resulting species, forming solid, coloured and relatively stable complexes: **1**, **3**, **13** and **14**. Now we add that the 10-phenyl-3, 10′-diphenothiazine (**9**) gives a green colour if treated with $CuCl_2$ in polar solvent; by analogy with other com-

TABLE 1

Visible absorption maxima of di- and tri-phenothiazine complexes with $CuCl_2$

Compound	Solvent	Absorption maxima a) $\tilde{\nu}$ — $cm^{-1} \times 1000$ b) λ — nm			ε_M*
G+-dichlorocuprate(I) **1**	ethanol	a) 22.08 b) 452.898		a) 15.08 b) 629.722	
	acetone	a) 21.92 b) 456.204		a) 15.69 b) 637.348	$1.67 \cdot 10^4$
	chloroform	a) 21.84 b) 457.875		a) 15.40 b) 649.35	$1.71 \cdot 10^4$
	KBr pellet	a) 21.44 b) 466.417		a) 15.00 b) 666.66	
7-Nitro-G+-dichloro-cuprate(I) **3**	acetone	a) 23.12 b) 432.525	a) 22.16 b) 451.263	a) 15.61 b) 640.614	
	chloroform	a) 23.12 b) 432.525	a) 22.03 b) 453.926	a) 15.47 b) 646.412	
10-Phenyl-G++-tetra-chlorocuprate(II) **15**	acetone		a) 16.21 b) 616.903	a) 14.88 b) 672.043	
	chloroform		a) 16.08 b) 621.890	a) 14.63 b) 683.526	
10, 10′, 3′, 10″ — Triphenothiazinyl tetrachlorocuprate(II) **13**	acetone			a) 14.96 b) 668.449	
	chloroform			a) 14.57 b) 686.341	$6.8 \cdot 10^4$
7′-Nitro-10, 10′, 3,′ 10″ — triphenothiazinyl tetrachlorocuprate (II) **14**	acetone			a) 14.64 b) 683.060	
	chloroform			a) 14.43 b) 693.000	
10, 10′—Diphenothiazinyl tetrachlorocuprate (II) **16**	chloroform			a) 14.32 b) 698.324	$7.05 \cdot 10^3$

* calculated for the longest wavelength

plexes isolated by us[6,26] we propose the structure **15** for the green compound of **9** (not isolated because of lack of substance). In opposition with **9**, the nitroderivative **10** does not yield a green colour by treating with $CuCl_2$, possibly because of the increasing redox potential by introducing the nitro group in position 7 (*para* to the nitrogen).

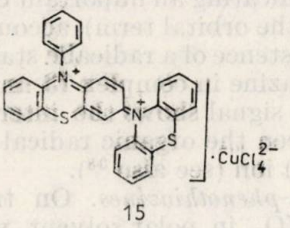

15

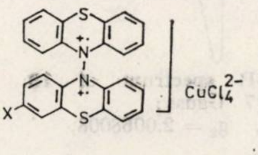

16. X=H
17. X=NO$_2$(unoxidized)

The analysis of electronic spectra of the complexes **1**, **3**, **13** – **15** and of the complex 10, 10′-diphenothiazinyl-tetrachlorocuprate (II), **16**(see[6]) allowed us to correlate the structures of these *oligo*-phenothiazines: the compounds containing only C–N bonds showed maxima analogous to that of the G^+ cation (**1**, **3** and **15**) and the compounds with N–N bonds have an absorption similar to that of the dication-10, 10′ (**13**, **14** and **16** – see Table 1, experimental part). The cation 10-phenyl-G^{++} (**15**) appears to be situated at the limit between the two groups; it loses the characteristic band of G^+ at about 450 nm and in addition, it shows the band at about 630 nm splited in two bands: one with a hypsochrome shift (at about 620 nm) and one with a batochrome shift (at about 680 nm) approaching of the maxima of the N–N coupled group. We estimate that the benzenic ring from position 10 tends to a position coplanar to the system *para*-conjugated from **15** (see the second absorption maximum), with the participation of π-electrons to the extended conjugation, although in unoxidized form **10**, the benzenic ring does not influence the position of maximum absorption (see below), in conformity with a twisted position (about 65 to 70°, see [44]). Based on these data we also concluded that the $C_{3'} - N_{10''}$ coupling phenothiazine nucleus participates in a small degree to the extended conjugation (with a possible rotation around this bond), observation supported also by the fact that this bond does not split in the presence of concentrated H_2O_2, while the bond $C_3 - N_{10'}$, strongly involved in the extended conjugation into G^+, is splitted under such circumstances.

From Table 1, a solvatochromism of these complexes is observed. The batochrome shift of λ max. along with the decreasing of solvent polarity shows the existence of intimate ion pairs, stabilized by intramolecular charge transfer.

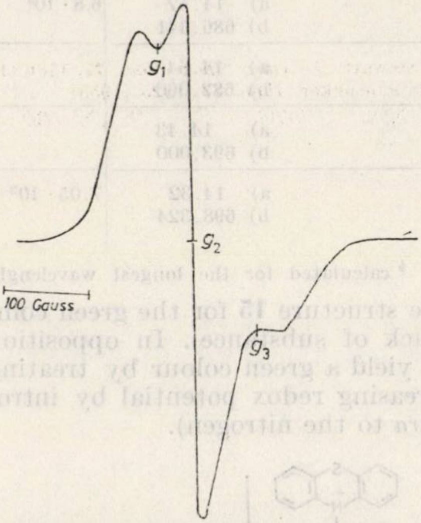

Figure 1. – ESR spectrum of **13**. $\Delta H = 36.233477$ Gauss; $g_1 = 2.0102191$, $g_2 = 2.0068008$, $g_3 = 1.9941198$.

The ESR signal (polycrystalline sample – see fig.) supports the existence of the N–N bond from the blue cation **13** [characteristics and aspect different from those of complex **1** but similar to those of complex **16**(see[6]): $g_1 = 2\cdot0102191$, $g_2 = 2.0068008$; $g_3 = 1.9941198$ and $\Delta H = 36.23347$ Gauss for **13** and $g = 2.0072521$ and $\Delta H = 33.12775$ Gauss for **16**, the splitting of the latter signal being more diminished].

We consider that the g_2 value (indicating an important contribution of the orbital term) accounts for the existence of a radicalic state of phenothiazine in complex **13** and, in total, the signal shows the interactions between the organic radical and copper (II) ion (see also [38]).

3.4. *Nitroderivatives of di- and tri-phenothiazines.* On treating the complexes **1**–**3**, **13**, **15** and **16** with $NaNO_2$, in polar solvent, we obtained the corresponding nitroderivatives (as unoxidized species): **5**[4], **7**, **10**, **12** and **17**[4]. Some theoretical and practical aspects concerning the nitration of phenothiazines with $NaNO_2$ were discussed in a previous paper;[4] in addition, we stress here that the result of such reactions is the monosubstitution, irrespective if the mechanism involves a disproportion or if it is of "half-regeneration" type (see [16]). The synthesis of these nitroderivatives enabled us to elucidate the different structures of the obtained *oligo*-phenothiazines. On comparing the visible absorption maxima of the nitroderivatives **5**, **10**, **12** and **17** with the signal of 3-nitrophenothiazine (Table 2) we revealed that: *i*) the C—N coupling nuclei show free rotation around this bond (in the case of **5**, **10**, and **12**), the almost coincidence of the absorption maxima positions of these compounds with that of the reference compound showing that the nuclei in question do not participate in an extended conjugation with the central phenothiazine nucleus and *ii*) the N—N coupling nuclei show a batochrome shift of the absorption (almost identical for **12** and **17**) suggesting a free rotation and possible mesomeric interactions.

TABLE 2

Visible absorption maxima of some nitrophenothiazines in $CHCl_3$

Compound	Absorption maxima a) $\tilde{\nu}$ — $cm^{-1} \times 1000$ b) λ — nm
3-Nitrophenothiazine	a) 22.24 b) 449.640
7-Nitro-3,10′-diphenothiazine **5**	a) 22.32 b) 448.280
7-Nitro-10-phenyl-3,10′-diphenothiazine **10**	a) 22.16 b) 451.263
3-Nitro-10,10′-diphenothiazine **17**	a) 19.68 b) 508.130
7′-Nitro-10,10′,3′,10″-triphenothiazine **12**	a) 19.76 b) 506.072

The fact that the nitroderivative **12** (and similarly **10** and **17**) do not yield *aci*-nitro colours [7,26] points out the absence of iminic proton (NH band is absent in IR) and implicitly the presence of the substituent to $N_{10'}$.

The splittings of the nitroderivatives **7**, **10** and **12** under electronic impact revealed, besides other aspects, the presence of nitro groups only on the polysubstituted phenothiazine nucleus and confirmed, once more, the trimer character of **12** [m/e = 638 (M^+), 592, 394, 198, 196]. The presence in position 1 (or 9) of a nitro group in **7** was indicated by the peak M^+-17 (participation to a McLafferty type rearrangement — see[1]).

In **conclusion**, the cation G^+ and its aryl derivatives do not represent inert, final compounds but reactive species, which can participate to different nucleophilic substitution reactions (nitrations, oxidations etc.) and the radicalic species resulted from charge transfer (with the participation of metalic partners from complexes) can form N—C and N—N bonds by radicalic couplings. The syntheses of 10-phenyl-3,10′-diphenothiazines and 10-phenothiazinyl-3,10′-diphenothiazines (tri-phenothiazines) fully illustrate the preparative possibilities of these reactions starting from the G^+ cation and are reported for the first time in literature by this paper.

ACKNOWLEDGEMENT is expressed to Prof. Dr. Valer Fărcăşan and to Prof. Dr. Ionel Haiduc of the Faculty of Chemical Technology of "Babeş-Bolyai" University, Cluj-Napoca, for their helpful discussions and to Conf. Dr. Georgeta Lupuţiu, of the I.M.F. Cluj-Napoca, for the assistance in achieving and interpreting the mass spectra.

EXPERIMENTAL

Melting points are uncorrected.

IR spectra were recorded on an UR-10 Carl Zeiss Jena spectrometer on KBr pellets, UV-Vis spectra were recorded on a Specord Carl Zeiss Jena spectrophotometer, mass spectra on a Varian-MAT 111 spectrometer. A JEOL spectrometer was used for ESR spectra. The eemental analyses were performed in the Microanalytical Laboratory of the Chemical Technollogy Faculty, "Babeş-Bolyai" University, Cluj-Napoca.

G^+-dichlorocuprate (I). [*10-(3-phenothiazinylidene)-phenothiazinium dichlorocuprate (I)*] (**1**) — A suspension of 3 g (4.97 mmoles) of phenothiazinyl tetrachlorocuprate (II) [25] in 50 ml of acetone was stirred for 10 min. with 10 g (119.04 mmoles) of $NaHCO_3$. The reaction mixture became green. The green solution was filtered and by a slow concentration 0.2 g of **1**, black crystals, were separated. The initial reaction mass was extracted again with 3 × 25 ml of acetone and the extract yielded, upon dilution with ligroine a further fraction of 0.53 g of **1**; total yield 0.73 g (55.42%), m.p. (decomp.) 143 — 4°C.

General procedure for G^+ complexes with copper and iron chlorides.— A solution of 5 g (25.09 mmoles) of phenothiazine in 50 ml of acetone was added, under stirring, to a solution of chloride ($M^n Cl_n$, M = Cu or Fe; $n = 2$ or 3 — molar ratio; 1 : 3.5) in 100 ml of ethanol. The reaction mixture turned from brown to green and within 10 minutes a black precipitate was formed. It was filtered off and washed with a small amount of ethanol. For **1** and **2** the results are tabulated as follows:

	Compound	Amount from 5 g of phenothiazine	%	m.p. (decomp.) °C	C	H	N	Cl	M
1	($C_{24}H_{15}Cl_2CuN_2S_2$)	4.11	61.82	143—4	a) 54.39 b) 55.87	2.85 3.28	5.28 5.44	13.38 13.59	11.98 11.61
2	($C_{24}H_{15}Cl_3FeN_2S_2$)	2.39	41.87	231—3	a) 51.69 b) 49.91	2.71 2.39	5.02 5.33	19.07 19.45	10.01 10.42

IR spectrum : no NH band

a) calculated
b) found

7-Nitro-G^+-dichlorocuprate (I) [*7-Nitro-10-(3-phenothiazinylidene)-phenothiazinium dichlorocuprate (I)*] (**3**). *Procedure a)* — A mixture of 1 g (1.88 mmoles) of **1** and 5g (72.47 mmoles) of $NaNO_2$ in 150 ml of acetone was stirred for 15 minutes at room temperature, the colour turning from green to brown. The brown solution of **5** (identical TLC to an authentical sample[4]) was filtered and stirred for 10 minutes with a solution of 1.3 g (7.63 mmoles) of

$CuCl_2.2H_2O$ in 100 ml of acetone. The reaction mixture became dark green. On diluting with ligroine 0.53 g (49.03 %) of **3**, dark green powder, were separated from the green solution.

Procedure b) — A solution of 4g (7.17 mmoles) of **2** in 300 ml of DMF was stirred for 15 minutes with 20 g (289.87 mmoles) of $NaNO_2$. The reaction mixture turned from green to brown; it was then poured into water and the brown precipitate of **5** thus formed was filtered off. It was extracted in acetone and the solution stirred for 10 minutes with a saturated acetonic solution of 6g (35.17 mmoles) of $CuCl_2.2H_2O$. On diluting with ligroine 3.11 g (75.44 %) of **3** were separated. A small amount of **3** was purified by extracting in chloroform and reprecipitation with ligroine: m.p. (decomp.) over 198°C.

$C_{24}H_{14}Cl_2CuN_3O_2S_2$, N %, calcd.: 7.308, found: 7.21

Cu %, calcd.: 11.05, found: 10.78

IR spectrum: no NH band.

10-Phenyl-3,10'-diphenothiazine (**9**). A mixture of 5g (9,43 mmoles) of **1** and 10g (21.18 mmoles) of $SnPh_4$ was melted, under stirring, for 45 minutes at 150 — 170°C. The reaction mass was extracted in CCl_4, diluted with ligroine and the low soluble components (e.g. **4**, identical TLC to an authentical sample [6]) filtered off. The filtrate was chromatographed on alumina, eluent CCl_4, then ligroine. The first major fraction separated, on slow concentration, 1.19 g (26.70 %) of **9**, white powder turning greenish, m.p. 230 — 1°C, slightly soluble in acetone.

$C_{30}H_{20}N_2S_2$, N %, calcd.: 5.93, found: 6.31

Mass spectrum: m/e = 472 (M^+), 395, 198, 197.

IR spectrum: no NH band

7-Nitro-10-phenyl-3,10'-diphenothiazine (**10**). A mixture of 3.5 g (6.09 mmoles) of **3** and 5g (10.59 mmoles), of $SnPh_4$ was melted, under stirring, for 30 minutes at 150 — 170°C. The reaction mass was extracted in warm CCl_4 (on cooling, the unreactioned $SnPh_4$ or its dimer was separated) and chromatographed on alumina, eluent CCl_4, then ligroine. The second fraction separated, on slow concentration, 1.33 g of **10** (42.19 %), orange powder, m.p. 235°C, slightly soluble in acetone.

$C_{30}H_{19}N_3O_2S_2$, N %, calcd.: 8.118, found: 7.98

Mass spectrum: m/e = 517 (M^+), 487, 471, 440, 394, 198, 196.

IR spectrum: no NH band

10, 10', 3', 10''-triphenothiazinyl tetrachlorocuprate (II) (**13**). *Procedure a)* A mixture of 15 g (24.85 mmoles) of phenothiazinyl tetrachlorocuprate (II) [25] and 15g (178.55 mmoles) of $NaHCO_3$ was stirred for 30 minutes, in 600 ml of $CHCl_3$. The dark green solution of G^+ was filtered and treated, under stirring, with 250 ml of saturated acetonic solution of $KMnO_4$. The colour turned into blue; the solution was filtered and diluted with ligroine. The dark blue precipitate thus obtained was filtered off and washed with a small amount of ligroine. The blue powder was disolved in $CHCl_3$ and reprecipitated with ligroine: 3.52 g (35.44 %) of **13**, blue powder, m.p. (decomp.) about 194°C, was obtained.

Procedure b) A solution of 0.5 g (0.84 mmoles) of **11** in 100 ml mixture of benzen-ligroine (1 : 1) was treated, under stirring, with 0.86 g (5.04 mmoles) of $CuCl_2. 2H_2O$ (molar ratio 1 : 6) in saturated acetonic solution. The precipitate thus obtained was filtered off, washed with benzene, extracted in $CHCl_3$ and chromatographed on alumina, eluent benzene, then $CHCl_3$. The resulted dark blue solution was concentrated, then diluted with ligroine: 0.37 g (54.95 %) of **13**, blue powder, identical IR, UV-Vis and m.p. to the compound prepared according to a) was obtained.

$C_{36}H_{23}Cl_4CuN_3S_3$, N %. calcd.: 5.258, found: 5.62

IR spectrum: no NH band

10, 10', 3', 10''-Triphenothiazine (**11**). A solution of 3g (3.75 mmoles) of **13** in 150 ml of DMF and 150 ml of benzene was treated, under stirring, with 30 % hydrazine hydrate until the colour turned from blue to light-yellow. The mixture was diluted with excess of water, the organic layer separated and chromatographed on alumina, eluent benzene-ligroine, then benzene-chloroform. The third fraction, on concentration and subsequent dilution with ligroine separated 0.68 g (30.63%) of **11**, white powder turning greenish, m.p. about 230°C, slightly soluble in acetone.

$C_{36}H_{23}N_3S_3$, N %, calcd. : 7.076, found : 7.27

IR spectrum: no NH band

7′-Nitro-10, 10′, 3′, 10″-triphenothiazine (**12**). A suspension of 10 g (12.5 mmoles) of **13** in 200 ml of DMF was stirred for 15 minutes with 30 g (434.81 mmoles) of $NaNO_2$. The colour turned from blue into reddish-brown. To the reaction mixture 800 ml of CCl_4 were added and diluted with excess of water. The organic layer was separated, dried, then diluted with ligroine and the slightly soluble components filtered off. The filtrate was chromatographed on alumina, eluent CCl_4, and finally a few drops of $CHCl_3$ were added. The second fraction separated, on concentration and subsequent dilution with ligroine, 1.42 g (17.76%) of **12**, brownish-violet powder, m.p. (rezin.) about 194°C, slightly soluble in acetone.

$C_{36}H_{22}N_4O_2S_3$, N %, calcd. : 8.70, found : 8.62

Mass spectrum: m/e = 638 (M^+), 592, 394, 198, 196

IR spectrum: no NH band

7′-Nitro-10, 10′, 3′, 10″-triphenothiazinyl tetrachlorocuprate (II) (**14**).

Procedure a) A suspension of 0.5 g (0.78 mmoles) of **12** in **15** ml of a mixture of acetone and CCl_4 (1 : 1) was added, under stirring, to 20 ml of a saturated acetonic solution of $CuCl_2$. The resulting solution was diluted with ligroine and the precipitate filtered off. This precipitate was extracted in $CHCl_3$, concentrated and again diluted with ligroine, thus separating 0.29 g (43.87%) of **14**, dark blue powder, m.p. (decomp.) about 210°C.

Procedure b) A suspension of 2 g (2.50 mmoles) of **13** in 100ml of DMF was stirred for 15 minutes with 5 g (72.47 mmoles) of $NaNO_2$. The mixture reaction turned from blue into reddish-brown, then it was poured into water. The brown precipitate (containing **12**) was filtered off, extracted in acetone and added under stirring to a saturated acetonic solution of 3 g (17.59 mmoles) of $CuCl_2.2H_2O$. The colour turned again into dark blue, the solution was diluted with ligroine and the resulting precipitate filtered off. It was then extracted in $CHCl_3$, concentrated and again diluted with ligroine, thus separating 1.45 g (68.64 %) of **14**, identical IR, UV-Vis and m.p. to the compound prepared according to a).

$C_{36}H_{22}Cl_4CuN_4O_2S_3$, N %, calcd. : 6.60, found : 6.91

IR spectrum: no NH band.

1(9),7-Dinitro-3, 10′-diphenothiazine (**7**) A suspension of 2 g (3.48 mmoles) of **3** in 200 ml of acetone was stirred for 15 minutes with 10 g (144.94 mmoles) of $NaNO_2$. The colour turned from green into brown ; the solution was filtered and diluted with excess of water. The brown precipitate thus obtained was filtered off, extracted in CCl_4 and purified by chromatography on alumina, eluent CCl_4. The first fraction separated, on concentration and subsequent dilution with ligroine, 0.26 g (15.40 %) of **7**, brown powder, m.p. 143°C.

$C_{24}H_{13}N_4O_4S_2$, N %, calcd. : 11.52, found : 11.31

Mass spectrum: m/e = 486 (M^+), 469, 440, 394, 198, 196.

IR spectrum (KBr ; cm^{-1}) : 3330, ν (NH).

REFERENCES

[1] Part IV, M. V. Diudea, *Rev. Roumaine Chim.*, **26**, 887 (1981).

[2] I. A. Silberg and M. V. Diudea, *Rev. Roumaine Chim.*, **25**, 1229 (1980). (Part I).

[3] I. A. Silberg and M. V. Diudea, *Rev. Roumaine Chim.*, **25**, 1239 (1980).

[4] M. V. Diudea, *Rev. Roumaine Chim.*, **26**, 725 (1981).

[5] I. A. Silberg, V. Fărcăşan and M. V. Diudea, *J. prakt. Chem.*, **318**, 353 (1976).

[6] M. V. Diudea and I. A. Silberg, *J. prakt. Chem.*, **324**, 769 (1982).

[7] C. Bodea and I. A. Silberg, *Adv. Heterocycl. Chem.*, **9**, 322 (1968); (A. R. Katritzky and A. J. Boulton, ed.) Academic Press, New York.

[8] J. P. Billon, *Bull. Soc. Chim. France,* **1961**, 1923.

[9] D. J. Cavanaugh, *J. Amer. Chem. Soc.*, **81**, 2507 (1959).

[10] R. Foster and P. Hanson, *Biochim. Biophys. Acta,* **112**, 482 (1966).

[11] R. Knoesel, B. Gebus and J. Parrod, *Bull. Soc. Chim. France,* **1971**, 4471.

[12] H. J. Shine and E. E. Mach, *J. Org. Chem.*, **30**, 2130 (1965).

[13] M. Kamiya, T. Mitsui and Y. Akahori, *Bull. Chem. Soc. Japan,* **46**, 1577 (1973).

[14] H. D. Burrows, J. Diaz da Silva, B. Ventura and Maria Isabel, *Excited States Biol. Mol. Proc. Int. Conf.*, **1974**, 116 (pub. 1976); *Chem. Abstr.*, **87**, 5071 (1977).

[15] P. Hanson and R. O. C. Norman, *J. Chem. Soc. Perkin Trans.* II, **1973**, 264.

[16] P. Hanson, *Adv. Heterocycl. Chem.*, **27**, 126 (1980); (A. R. Katritzky and A. J. Boulton, ed.) Academic Press, New York.

[17] Y. Tsujino, *Tetrahedron Letters,* **1968**, 2545.

[18] Y. Tsujino, *Tetrahedron Letters,* **1969**, 763.

[19] Y. Tsujino, *Tetrahedron Letters,* **1968**, 4111.

[20] Y. Tsujino, *Nippon Kagaku Zasshi,* **90**, 809 (1969); *Chem. Abstr.*, **71**, 101795 (1969).

[21] S. Sugita and Y. Tsujino, *Japan,* 74, 45, 392; *Chem. Abstr.*, **83**, 79267 (1975).

[22] Y. Tsujino, K. Nishikida and T. Naito, *Nippon Kagaku Zasshi,* **91**, 1080 (1970); *Chem. Abstr.*, **74**, 125598 (1971).

[23] F. Kehrmann and O. Vessely, *Ber. dtsch. chem. Ges.*, **34**, 4172 (1901).

[24] S. C. J. Olivier and W. P. Combé, *Rec. Trav. Chim.*, **68**, 526 (1950).

[25] M. V. Diudea and I. A. Silberg, *Romanian Patent Application,* 79, 933.

[26] M. V. Diudea, Doctorate Dissertation, Institute of Chemistry, Cluj-Napoca, 1979.

[27] M. F. Chiu, B. C. Gilbert and P. Hanson, *J. Chem. Soc. B.*, **1970**, 1700.

[28] C. Jackson and N. K. D. Patel, *Tetrahedron Letters,* **1967**, 2255.

[29] B. Guigan, J. R. Dellar and W. D. Phillips, *Ger. Offen,* 2, 250, 364 (1971); *Chem. Abstr.*, **79**, 94464 (1973).

[30] C. Finzi, *Giorn. Chim. Ind. Appl.*, **9**, 176 (1927); *Chem. Zentr. II,* 933 (1927).

[31] L. Pesci, *Gazz. Chim. Ital.*, **46(I)**, 103 (1916); *Chem. Zentr. I,* 936 (1916).

[32] D. Clarke, B. C. Gilbert and P. Hanson, *J. Chem. Soc. Perkin Trans. II,* **1977**, 517.

[33] S. A. Alkaitis, G. Beck and M. Grätzel, *J. Amer. Chem. Soc.*, **97**, 5723 (1975).

[34] Y. Sato, M. Kinoshita, M. Sano and H. Akamatu, *Bull. Chem. Soc. Japan,* **40**, 2539 (1967).

[35] M. H. Litt and J. Radović, *J. Phys. Chem.*, **78**, 1750 (1974).

[36] J. Selbin, D. G. Durrett, H. J. Sherrill, G. R. Newkome and M. Collins, *J. Inorg. Nuclear Chem.*, **35**, 3467 (1973).

[37] B. A. Arbuzov and D. K. Yarmukhametova, *Izvest. Akad. Nauk S.S.S.R. Otdel. Khim. Nauk,* **1962**, 1405.

[38] J. Selbin and H. J. Sherrill, *J. Chem. Soc. Chem. Commun.*, **1973**, 120.

[39] B. K. Bandlish and H. J. Shine, *J. Org. Chem.*, **42**, 561 (1977).

[40] A. L. Buchachenko, *Opt. Spektrosk.*, **13**, 795 (1962).

[41] S. M. Kavun and A. L. Buchachenko, *Zhur. Fiz. Khim.*, **42**, 818 (1968).

[42] I. A. Silberg, Doctorate Dissertation, Institute of Chemistry, Cluj-Napoca, 1970.

[43] W. E. Geiger, Jr. and A. H. Maki, *J. Phys. Chem.*, **75**, 2381 (1971).

[44] D. Clarke, B. C. Gilbert and P. Hanson, *J. Chem. Soc. Perkin Trans. II,* **1975** 1078.

Revue Roumaine de Chimie, 28, *3*, 263–266 (1983)

EFFECT OF STRUCTURE ON THE REACTIVITY IN THE OXIDATION OF ALIPHATIC ALCOHOLS BY CHLORINE DIOXIDE

V.P. KUDESIA and C. B. SHARMA
Water Pollution Laboratory, D.N. College, Meerut-2, India

Received March 20, 1981

The effect of structure on the reactivity in the oxidation of some primary and secondary aliphatic monohydric alcohols by chlorine dioxide has been investigated in detail. The relative thermodynamic activation parameters for the reactions of methanol, ethanol, *n*-propanol, *n*-butanol, isobutanol, propan-2-ol, and butan-2-ol with chlorine dioxide have been calculated. The results exhibit that the oxidation mechanism of aliphatic alcohols by chlorine dioxide is the same in all cases. The entropy of activation is the main controlling factor and the variation of activation energy is relatively unimportant.

The introduction of substituents into a parent molecule produces definite changes in the reaction velocity, which can frequently be correlated with the electronic properties of the substituent group ; a substituent alters the availability of the electrons at the seat of the reaction. Such studies have been made in the oxidation of glycols,[1] substituted benzaldehydes,[2–4] aliphatic monohydric alcohols,[5] and aliphatic aldehydes[6] by chromic acid, oxidation of glycols by lead tetraacetate[7] and periodic acid,[8–10] oxidation of substituted toluenes[11] and substituted benzaldehydes[12] by permanganate, oxidation of olefines by perbenzoic acid,[13] oxidation of aliphatic alcohols[14] and aliphatic aldehydes[15] by tertiary butyl hypochlorite and oxidation of alcohols by chlorine.[16]

An idea of the properties of activated complex is essential for knowing the effect of substituent on reactivity. The activated complex is to be regarded as an ordinary molecule possessing all the usual thermodynamic properties. The free energy, heat, and entropy of activation is related to the potential energy and probability changes.[17]

Price and Hammett[18, 19] and Fitzpatrick and Gettler[20] have studied the formation of semicarbazones and oximes of several carbonyl compounds. They calculated the relative entropies, enthalpies and free energies of activation related to that of acetone by using the following equations :

$$\Delta S^{\neq} - \Delta S_s^{\neq} = \frac{\partial}{\partial T}\left(RT\ln\frac{k}{k_s}\right) \tag{1}$$

$$\Delta H^{\neq} - \Delta H_s^{\neq} = RT^2\frac{\partial}{\partial T}\left(\ln\frac{k}{k_s}\right) \tag{2}$$

$$\Delta G^{\neq} - \Delta G_s^{\neq} = -RT\ln\frac{k}{k_s} \tag{3}$$

In all these equations symbols with subscripts refer to the standard substance, those without subscripts to the compound in question.

The relative thermodynamic activation parameters for the reactions of some aliphatic primary and secondary alcohols with chlorine dioxide in absence and in presence of perchloric acid, relative to that of methanol have been calculated by using the equations [21]

$$\Delta\Delta G^{\neq} = -2.303RT\log(k/k_s) \tag{4}$$

$$\Delta\Delta H^{\neq} = -2.303\text{R}\,\frac{\log(k/k_s)_{T_2} - \log(k/k_s)_{T_1}}{1/T_2 - 1/T_1} \tag{5}$$

$$\Delta\Delta S^{\neq} = 2.303R\,\frac{T_2\log(k/k_s)_{T_2} - T_1\log(k/k_s)_{T_1}}{T_2 - T_1} \tag{6}$$

These equations have been obtained from equations (1) to (3). An attempt has been made to establish a correlation between the structure of organic molecule and reaction rate on the basis of the data presented in tables 1 and 2.

TABLE 1

Reaction of monohydric alcohols with ClO_2 in absence of perchloric acid : energy of activation ; relative entropy ; enthalpy and free energy of activation[a]

Alcohol	E_{Arr} kJ	$\Delta\Delta S^{\neq}$ $J.K^{-1}$	$\Delta\Delta H^{\neq}$ kJ	$\Delta\Delta G^{\neq}$ kJ(at 25°C)	$\Delta\Delta G^{\neq}$ kJ (at 25°C)
Methanol	64.48	—	—	—	—
Ethanol	61.21	5.65	− 3.22	− 1.55	− 1.51
n-Propanol	55.85	1.72	− 8.53	− 8.12	− 8.08
n-Butanol	51.82	12.47	−12.51	− 9.49	− 9.41
Isobutanol	46.22	27.09	−18.04	−10.16	− 9.87
Propan-2-ol	44.76	30.77	−19.55	−10.58	−10.25
Butan-2-ol	44.12	31.11	−20.14	−11.04	−10.75

[a] Concentrations : [Alcohol] = 0.150M ; $[ClO_2]$ = 0.0030M ; $\mu = 0.2$

TABLE 2

Reaction of monohydric alcohols with ClO_2 in presence of perchloric acid : energy of activation ; relative entropy ; enthalpy and free energy of activation[a]

Alcohol	E_{Arr} k.J.	$\Delta\Delta S^{\neq}$ $J.K^{-1}$	$\Delta\Delta H^{\neq}$ k.J.	$\Delta\Delta G^{\neq}$ k.J. (at 25°C)	$\Delta\Delta G^{\neq}$ k.J. (at 35°C)
Methanol	58.53	—	—	—	—
Ethanol	54.71	7.20	−3.47	− 1.38	− 1.30
n-Propanol	49.11	5.69	− 9.32	− 7.70	− 7.66
n-Butanol	47.10	6.91	−11.29	− 9.37	− 9.28
Isobutanol	44.00	16.08	−14.36	− 9.70	− 9.53
Propanol-2-ol	42.66	18.25	−15.70	−10.41	−10.25
Butan-2-ol	41.16	21.98	−17.21	−10.83	−10.58

[a] Concentrations [Alcohol]= 0.150 M ; (ClO_2) = 0.0030M ; $(HClO_4)$ = 0.030 M ; $\mu = 0.2$

EXPERIMENTAL

All the chemicals used were either of Merck (C.P.) or B.D.H. (Analar) grade or of comparable purity. Water was purified by passing through an ion exchanger and distillation from alkaline $KMnO_4$. Chlorine dioxide was prepared by Bray's method.[22]

The kinetics of the reactions of methanol, ethanol, *n*-propanol, *n*-butanol, isobutanol, propan-2-ol and butan-2-ol with chlorine dioxide in absence and in presence of perchloric acid have been studied at 25° and 35°C according to the method [23] described earlier in absence of light and the initial rates (k_0) have been calculated.

RESULTS AND DISCUSSION

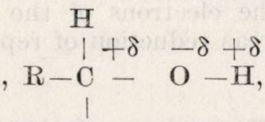

In alcohol molecules, $R-\underset{|}{\overset{\displaystyle H}{\overset{|}{C}}}\overset{+\delta}{\ }-\overset{-\delta}{O}-\overset{+\delta}{H}$, both the C—O and O—H bonds are polarised with negative end of the bond dipoles at oxygen. Moreover, the oxygen has two unshared pairs of electrons. These are the features that determine the chemical reactions of the saturated alcohols.[24]

The data (Table 1) indicate that in absence of perchloric acid, the rate of reaction increases regularly with the substitution of methyl group for hydrogen, i.e., the reaction rate of methanol $<$ ethanol $<$ $<$ *n*-propanol $<$ *n*-butanol $<$ isobutanol $<$ propan-2-ol $<$ butan-2-ol. The reaction rate is also in the same order (Table 2) in presence of perchloric acid. This is the expected order for electron release at the C—H bond of the carbinol group, since the methyl group will tend to increase the electron density at the carbon atom by their general inductive effect, 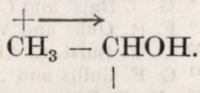 $\overset{+\!\longrightarrow}{CH_3 - \underset{|}{C}}HOH$.

The polarizability of the molecule increases with the number of electrons in the molecule and with their distance from the nucleus . Thus by increasing hydrocarbon chain length, the attarctive forces resulting from the polarizability of the molecule increase. Since chlorine dioxide is electron attracting, the increase in chain length facilitates the formation of alkyl hypochlorite, which in turn increases the rate of the reaction.

It appears that the dielectric constant of the alcohols also plays a role on the rates of reactions. The increasing order of the dielectric constant is methanol $>$ ethanol $>$ *n*-propanol $>$ *n*-butanol $>$ isobutanol $>$ $>$ propan-2-ol $>$ butan-2-ol.

The enthalpy may be considered to reside in the bond energies. A decrease in ethalpy is a driving force for a reaction. It appears that enthalpy is a rate controlling factor in absence of perchloric acid. Entropy is a measure of the probability for the existence of a given state. The ability of a process to take place with an increase in entropy is a driving force that causes the process to take place. In absence of perchloric acid, the negative entropy shows an erratic trend, in presence of perchloric acid, the negative entropy again shows an erratic trend. The direction and extent of a reaction are determined by two driving forces, (i) the tendency to react in a state of lowest enthalpy, and (ii) the tendency to react in a state of highest entropy. Perhaps both entropy and enthalpy of activation are the main rate controlling factors. While studying the mechanism of chlorine oxidations of ethylene and methylated ethylene glycols, Kudesia [25] inferred the increase in reactivity with the substitution of methyl group for hydrogen entirely due to an entropy effect. A similar idea was also proposed by Kudesia and Sharma, [26] while studying the mechanism of oxidation of aliphatic monohydric alcohols by tertiary butyl hypochlorite and again supported by Kudesia *et al.*[27] in the reactions of alcohols by chlorine. According to them, the entropy of activation is the main controlling factor and the variation of activation energy is relatively unimportant.

Steric condition in the transition state is, however, a factor that influences the activation energy. Any structural feature that leads to the greater repulsion among the electrons of the bonding orbitals increases the activation energy, whereas reduction of repulsive forces decreases the activation energy.

ACKNOWLEDGEMENT. The authors are thankful to the College authorities for providing research facilities and U.G.C. (India) for awarding research fellowship to one of us (C.B. Sharma).

REFERENCES

[1] A. C. Chatterji and S. K. Mukherjee, *Z. phys. Chem. (Leipzig)*, **210**, 166, 255 (1959).
[2] E. Lucchi, *Boll. Sci. Facolta Chim. Ind., Bolonga, II*, **208**, 333 (1940).
[3] E. Lucchi, *Gazz. Chim. Ital.*, **71**, 729, 751 (1941).
[4] E. Lucchi, *Boll. Sci. Facolta Chim. Ind., Bolonga*, **2**, 165, 176 (1941).
[5] A. C. Chatterji and V. Antony, *Z. phys. Chem. (Leipzig)*, **210**, 50, 103 (1959).
[6] J. Lal, Ph. D. Thesis, Lucknow University (1966).
[7] J. P. Cordner and K. H. Pausacker, *J. Chem. Soc.*, **1953**, 102.
[8] G. J. Buist and C. A. Bunton, *Ibid.*, **1954**, 1406 *Ibid.*, **1957**, 4580.
[9] F. R. Duke and V. C. Bulgrin, *J. Amer. Chem. Soc.*, **76**, 3803 (1954).
[10] G. J. Buist, C. A. Bunton and J. H. Miles, *J. Chem. Soc.*, **1957**, 4567, 4575.
[11] C. F. Cullis and J. W. Ladbury, *J. Chem. Soc.*, **1955**, 555.
[12] K. B. Wiberg and R. Stewart, *J. Amer. Chem. Soc.*, **77**, 1786 (1955).
[13] B. M. Lynch and K. H. Pausacker, *Ibid.*, **77**, 1525 (1955).
[14] V. P. Kudesia and B. K. Sharma, *Indian J. Chem.*, **19A**, 82 (1980).
[15] S. C. Sharma, Ph. D. Thesis, Meerut University (1978).
[16] S. Kant, Ph. D. Thesis, Meerut University (1979).
[17] J. Hine, "Physical Organic Chemistry", McGraw-Hill, London, 1956, p. 85.
[18] F. P. Price and L. P. Hammett, *J. Amer. Chem. Soc.*, **63**, 2387 (1941).
[19] L. P. Hammett, "Physical Organic Chemistry", McGraw-Hill, London, 1940, p. 118.
[20] F. W. Fitzpatrick and J. D. Gettler, *J. Amer. Chem. Soc.*, **78**, 530 (1956).
[21] M. S. Newman "Steric Effects in Organic Chemistry", Wiley, New York, 1956, p. 566.
[22] W. C. Bray, *Z. phys. Chem.*, **54**, 569 (1906).
[23] V. P. Kudesia and C. B. Sharma, *React. Kinet. Catal. Lett.*, (communicated) (1981).
[24] C. R. Noller, "Chemistry of Organic Compounds", W. B. Saunders, Philadelphia, 1965, p. 142.
[25] V. P. Kudesia, *Rev. Roumaine Chim.*, **20**, 1065 (1975).
[26] V. P. Kudesia and B. K. Sharma, *Acta Ciencia Indica*, **3**, 116 (1977).
[27] V. P. Kudesia, S. Kant, S. K. Srivastava and D. Prakash, *Ibid.*, **5**, 85 (1979).

Revue Roumaine de Chimie, **28**, *3*, 267–274 (1983)

PYRIMIDINIUM-YLURES. IV[1]

LES RÉACTIONS DE QUELQUES 4-PHÉNYL-PYRIMIDINIUM-YLURES CARBANION-MONOSUBSTITUÉS AVEC DES OLÉFINES ACTIVÉES

FLORENTINA C. GEORGESCU[a], E. G. GEORGESCU[b], F. CHIRALEU[b],
E. I. GEORGESCU[a] et I. ZUGRĂVESCU[c]

[a] Centre de Recherches, 1 str. Uzinei, Rm. Vîlcea, Roumanie
[b] Centre de Chimie Organique, Bucarest, Roumanie
[c] Institut Polytechnique, Iassy, Roumanie

Reçu le 23 décembre 1981

On a étudié les réactions de cycloaddition [3 + 2] dipolaires de quelques 4-phényl-pyrimidinium-ylures carbanion-monosubstitués avec des esters de l'acide maléique et fumarique, mettant en évidence la *cis*-stéréospécificité de ces réactions.

The [3 + 2] dipolar cycloaddition reactions of carbanion-monosubstituted 4-phenyl-pyrimidinium-ylides with esters of the maleic and fumaric acids are investigated, the *cis*-stereospecificity of these reactions being proved.

Les réactions des cycloimmonium-ylures avec des oléfines activées isomères *cis-trans* ont été peu étudiées jusqu'à présent. Les données de la littérature[2–5] montrent que, dans la majorité des cas, les cycloimmonium-ylures se comportent comme des dipôles 1,3 dans les réactions de cycloaddition. La majorité des dipôles 1,3 réagissant d'une manière *cis*-stéréospécifique avec des oléfines isomères *cis-trans*.[3–7] Pourtant, dans la littérature on trouve encore peu d'indications[3,5] concernant la stéréochimie des réactions des cycloimmonium-ylures avec des oléfines activées isomères *cis-trans*.

Pour obtenir de nouvelles données concernant la stéréochimie de ces réactions, nous avons étudié les réactions de quelques 4-phényl-pyrimidinium-1-benzoylméthylures **2**[8,9] avec des esters de l'acide maléique et fumarique.

Le caractère de dipôle 1,3 des 4-phénylpyrimidinium-1-benzoylméthylures **2a** et **2b**, obtenus[8] par la déhydrobromuration en milieu alcalin des sels quaternaires **1a** et **1b**, a été démontré[9] par l'isolement des cycloadducts **3a** et **3b**, respectivement **4a** et **4b**, par suite des réactions avec le diméthylacétylènedicarboxylate et respectivement le propyolate d'éthyle. Dû à la faible stabilité, de ces ylures les réactions de cycloadditions ont été effectuées « in situ » par le traitement des sels quaternaires respectifs[8] dans l'acétonitrile avec le dipolarophyle en présence de triéthylamin ou dans le propylène oxyde utilisé comme solvant et accepteur d'acide, une méthode élargie par nos recherches.[1,9,10]

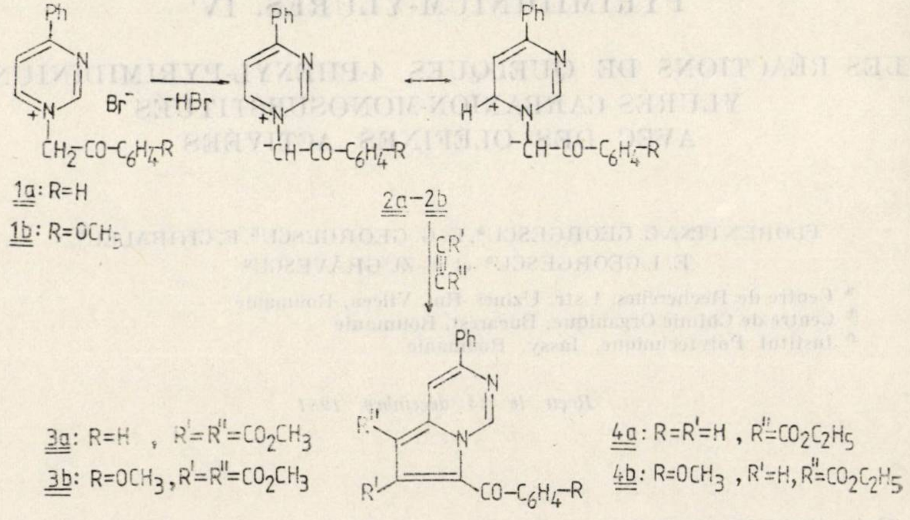
Ph
N
Br⁻
−HBr
H
CH₂−CO−C₆H₄−R
CH−CO−C₆H₄−R
2a−2b
CR'
CR"
R'
R"
CO−C₆H₄−R

1a: R=H

1b: R=OCH₃

3a: R=H , $R'=R''=CO_2CH_3$

3b: $R=OCH_3$, $R'=R''=CO_2CH_3$

4a: R=R'=H , $R''=CO_2C_2H_5$

4b: $R=OCH_3$, R'=H, $R''=CO_2C_2H_5$

Par la réaction des 4-phénylpyrimidinium-ylures **2a** et respectivement **2b**, obtenues « in situ » sous l'action de propylène oxyde, avec l maléate d'éthyle on a obtenu les cycloadducts **5a** et **5b**. Les mêmes 4 phénylpyrimidinium-ylures **2a** et respectivement **2b**, par le traitemen avec le fumarate d'éthyle dans les mêmes conditions, ont conduit à la formation d'autres deux cycloadducts **6a** et respectivement **6b**.

Tenant compte des analyses chimiques et spectrales, on a attribu à deux cycloadducts une structure de tétrahydropyrrolo [1,2-c]pyrimidine

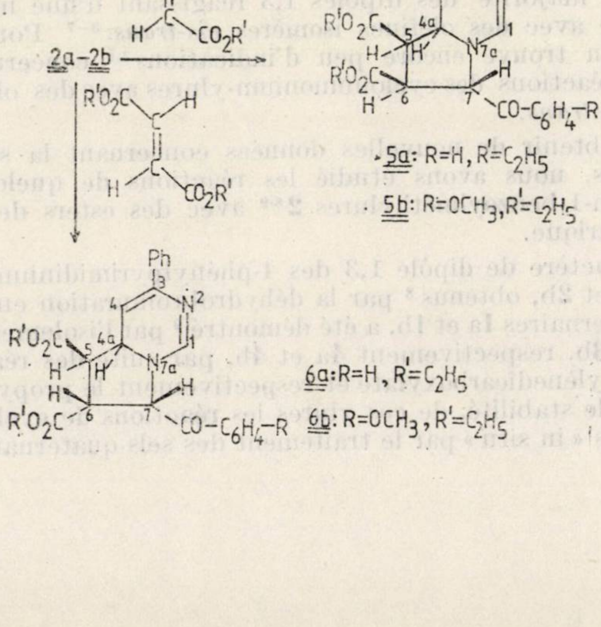
H
CO₂R'
H
CO₂R'
2a−2b
R'O₂C
H
H
CO₂R'
Ph
3
N
2
4
4a
1
5
7a
6
7
R'O₂C
H
CO−C₆H₄−R

5a: R=H, $R'=C_2H_5$

5b: $R=OCH_3$, $R'=C_2H_5$

6a: R=H , $R'=C_2H_5$

6b: $R=OCH_3$, $R'=C_2H_5$

Pour confirmer la structure de tétrahydropyrrolo [1,2-c] pyrimidine, ttribuée aux cycloadducts, le 4-phénylpyrimidinium-1-(*p*-méthoxyénzoyl) méthylure (**2b**), formée « in situ » dans les mêmes conditions, a té traité avec le maléate de méthyl, respectivement avec le fumarate le méthyl, obtenant deux cycloadducts **7** et respectivement **8**, avec des ropriétés physiques distinctes. La déhydrogénation des deux cycloadlucts stéréoisomères **7** et resp. **8**, effectuée en présence de Pd 30 % en charon, a conduit au 3-phényl-5-6-dicarbométhoxy-7-(*p*-méthoxybenzoyl) yrrolo [1, 2-c]pyrimidine (**3b**). Ce produit a le point de fusion, les specres IR et ¹H—RMN identiques à ceux du cycloadduct obtenu par la réacion de 4-phénylpyrimidinium-1-(*p*-méthoxybenzoyl)méthylure (**2b**) avec a diméthylacéthylène-dicarboxylate.[9]

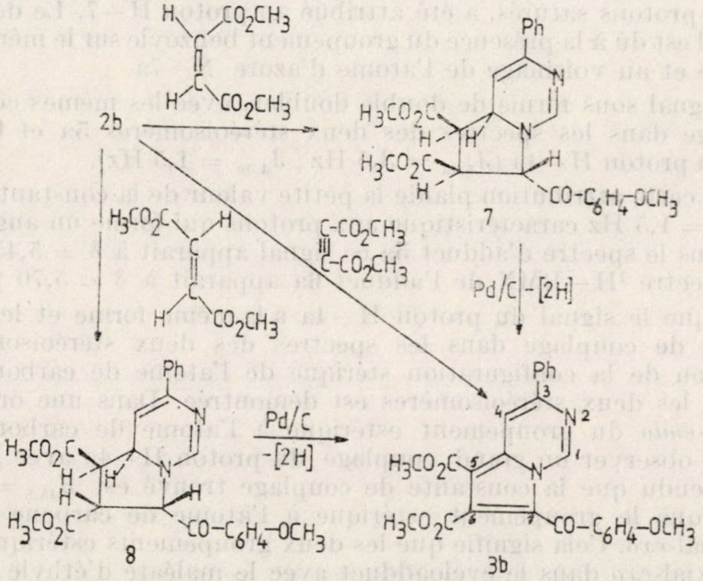

Les réactions de cycloaddition des 4-phénylpyrimidinium-ylures **2a** et respectivement **2b** avec des esters de l'acide maléique et fumarique ont été effectuées aussi par le traitement des sels quaternaires respectives avec l'oléfine, dans l'acétonitrile en présence de triéthylamine.

Attendu que dans les réactions des 4-phénylpyrimidinium-ylures **2a** et **2b** avec des esters maléiques et fumariques on a obtenu des produits avec des propriétés physiques distinctes on a démontré que la réaction est stéréosélective.

La structure et la configuration des adducts stéréoisomères ont été établies tenant compte des analyses chimiques et spectrales.

Considérant comme signifiants les spectres des adducts stéréoisomères **5a** et **6a**, on remarque que le spectre IR du produit **5a** présente une bande d'absorption intense à 1730 cm^{-1} correspondant aux deux groupements carbonyle estérique équivalents et une bande d'absorption à 1690 cm^{-1} correspondant au groupement carbonyle cétonique. Dans le spectre IR du produit **6a** on remarque les deux bandes d'absorption correspondant aux groupements carbonyle estériques à 1730 cm^{-1} et une bande d'absorption caractéristique au groupement carbonyle cétonique à 1685 cm^{-1}.

Les signaux des spectres ^1H-RMN ont été attribués tenant compte des déplacements chimiques et des constantes de couplage. Les valeurs des constantes de couplage ont été corrélées avec les valeurs appréciées par les relations d'entre la variation de la constante de couplage et les angles dièdres formés par les protons respectifs. Les estimations des angles dièdres ont été faites à l'aide des modèles moléculaires de Dreiding.

Par la comparaison des spectres ^1H-RMN des cycloadducts stéréoisomères **5a** et **6a** on observe que le signal à $\delta = 5{,}92$ ppm a la même forme et le même déplacement chimique. Ce signal, le plus déblindé de la région des protons saturés, a été attribué au proton H—7. Le déblindage de ce signal est dû à la présence du groupement benzoyle sur le même atome de carbone et au voisinage de l'atome d'azote N—7a.

Le signal sous forme de double doublet, avec les mêmes constantes de couplage dans les spectres des deux stéréoisomères **5a** et **6a**, a été attribué au proton H—4a ($J_{5,4a} = 3{,}5$ Hz ; $J_{4,4a} = 1{,}5$ Hz).

Pour cette attribution plaide la petite valeur de la constante de couplage $J_{4,4a} = 1{,}5$ Hz caractéristique aux protons qui forme un angle dièdre de 90°. Dans le spectre d'adduct **5a** ce signal apparaît à $\delta = 5{,}45$ ppm et dans le spectre ^1H-RMN de l'adduct **6a** apparaît à $\delta = 5{,}70$ ppm.

Puisque le signal du proton H—4a a la même forme et les mêmes constantes de couplage dans les spectres des deux stéréoisomères, la conservation de la configuration stérique de l'atome de carbone voisin C—5 dans les deux stéréoisomères est démontrée. Dans une orientation équatorial-*endo* du groupement estérique à l'atome de carbone C—5, on devrait observer un grand couplage du proton H—4a avec le proton H—5. Attendu que la constante de couplage trouvé est $J_{4a,5} = 3{,}5$ Hz, il résulte que le groupement estérique à l'atome de carbone C—5 est orienté axial-*exo*. Cela signifie que les deux groupements estériques seront orientés axial-*exo* dans le cycloadduct avec le maléate d'éthyle **5a** ; dans le cycloadduct avec le fumarate d'éthyle **6a** le groupement estérique lié à l'atome de carbone C—5 sera orienté axial-*exo* et le groupement estérique lié à l'atome de carbone C—6 sera orienté axial-*endo*.

Le signal sous forme de double doublet à $\delta = 4{,}92$ ppm ($J_{4a,5} = 3{,}5$ Hz ; $J_{5,6} = 5$ Hz) dans le spectre du cycloadduct **6a** a été attribué au proton H—5.

Les déplacements chimiques des signaux des protons H—4a et H—5 dans les spectres ^1H-RMN des deux cycloadducts justifient les attributions respectives.

Ainsi, en concordance avec les données expérimentales les déplacements chimiques des signaux H—4a et H—5 doivent être plus grands dans le spectre du cycloadduct formé avec l'ester fumarique 6a dû au déblindage produit par la position d'un groupement carbéthoxy à l'atome de carbone C—6.

Le signal du proton H—6 n'est pas toujours mis en évidence dans les spectres ^1H-RMN dû à la superposition des signaux des groupements éthyle ou méthyle. Dans les spectres où le signal apparaît (les spectres des produits **5**a et **5**b) le déplacement chimique et les constantes de couplage sont en concordance avec les attributions respectives.

Tenant compte de l'analyse comparative des spectres ^1H-RMN des cycloadducts stéréoisomères **5**a et **6**a, on a attribué la structure I aux produits **5**a, **5**b et **7** obtenus par la réaction de cycloaddition [3 + 2] dipolaire des 4-phénylpyrimidinium-ylures **2**a et **2**b avec des esters maléiques et la structure II aux produits **6**a, **6**b et **8** obtenus par la réaction de cycloaddition [3 + 2] dipolaire des mêmes ylures **2**a et **2**b avec des esters maléiques.

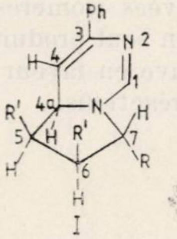

I

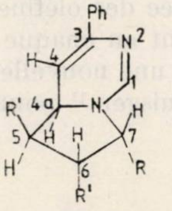

II

$R = -COC_6H_5, -COC_6H_4OCH_3$

$R' = -CO_2C_2H_5, -CO_2CH_3$

L'analyse des valeurs des constantes de couplage dans les deux séries de cycloadducts, qui ont les structures générales I et II, fournit de nouveaux arguments pour les structures attribuées.

Ainsi, dans les spectres ^1H-RMN on remarque que la valeur de la constante de couplage d'entre les protons H—6 et H—7 est plus grande pour le cycloadduct formé avec le fumarate d'éthyle ($J_{6,7} = 7{,}5$ Hz) et plus petite pour le cycloadduct formé avec le maléate d'éthyle **5**a ($J_{6,7} = 6$ Hz).

Sur des modèles stériques Dreiding on remarque que dans le cycloadduct **5**a le proton H—6 orienté axial-*endo* et le proton H—7 orienté axial-*exo* forme un angle dièdre qui dépasse un peu plus 120° qui, conformément à l'équation Karplus correspond à une constante de couplage $J_{6,7}$ d'env. 6—7 Hz. Le proton H—5 orienté équatorial-*endo* et le proton H—6 orienté axial-*endo* forme un angle dièdre d'env. 20° qui correspondra à une constante de couplage $J_{5,6} = 6-7$ Hz. Mais dans le cas des substituants volumineux pareil aux substituants carbéthoxy, apparaissent des phénomènes de répulsion et une torsion de la molécule qui conduisent à l'agrandissement de l'angle dièdre d'entre les protons H—5 et H—6 jusqu'à 40°, ce qui correspond à un amoindrissement de la constante de couplage à 4—5 Hz. La valeur de la constante de couplage $J_{5,6} = 5$ Hz dans le spectre RMN du cycloadduct **5**a concorde avec la valeur résultée par la relation Karplus dans le sens de la torsion de la molécule.

Dans le cycloadduct **6**a, le proton H—6 orienté équatorial-*exo* et le proton H—7 orienté axial-*exo* forment un angle dièdre de presque 0°, ce qui correspondra à une constante de couplage d'env. 7, 5 Hz.

Dû à l'empêchement stérique d'entre le groupement estérique orienté axial-*endo* lié à l'atome de carbone C—6 et le groupement benzoyle orienté équatorial-*endo* lié à l'atome de carbone C—7, apparaît une torsion de la molécule qui conduit à un agrandissement de l'angle dièdre d'entre le proton H—5 orienté équatorial-*endo* et le proton H—6 orienté équatorial-*exo* jusqu'à env. 140°. Cette valeur correspond à une constante de couplage de 7 — 8 Hz.

Les valeurs des constantes de couplage $J_{6,7} = 7{,}5$ Hz et $J_{5,6} = 7{,}5$ Hz observées dans le spectre ^{1}H—RMN sont en concordance avec ces considérations.

Tenant compte des données présentées on peut affirmer que la réaction de cycloaddition [3 + 2]dipolaire des 4-phényl-pyrimidinium-benzoylméthylures **2a** et **2b** avec des oléfines activées isomères *cis-trans* est *cis*-stéréospécifique, obtenant en chaque cas un seul produit de réaction. Ces données représentent une nouvelle épreuve en faveur du mécanisme concerté proposé par Huisgen [11] pour ces réactions.

PARTIE EXPÉRIMENTALE

Les sels quaternaires de 4-phénylpyrimidinium **1a** et resp. **1b** ont été obtenus par la réaction de 4-phénylpyrimidine avec le ω-bromocétophénone et resp. ω-brom-*p*-méthoxyacétophénone d'après le procédé décrit dans un travail antérieur.

Les points de fusion ne sont pas corrigés. Les spectres IR ont été enregistrés sur un spectromètre Perkin-Elmer 621 et les spectres ^{1}H-RMN ont été enregistrés sur un spectromètre Varian A-60A.

Les réactions des 4-phénylpyrimidinium-1-bénzoylemëthylures **2***a et* **2***b avec des esters de l'acide maléique et fumarique ; procédés généraux.* a. A une suspension de 10 mmoles de sel quaternaire **1a** resp. **1b** dans 50 ml propylène oxyde on ajoute 11 mmoles d'ester maléique ou fumarique. On agite le mélange réactionnel 10 jours à la température ambiante. On évapore une partie du solvant. Après le refroidissement on filtre et on recristallise le produit obtenu.

b. A une suspension de 10 mmoles de sel quaternaire **1a** resp. **1b** dans 50 ml d'acétonitrile on ajoute 11 mmoles d'ester maléique ou fumarique. On ajoute goutte-à-goutte, sous agitation, 11 mmoles (1,5 ml) de triéthylamine. On agite le mélange encore 2—3 heures à la température ambiante et le mélange est porté à reflux pendant 8 heures. On chasse la plupart du solvant. Après le refroidissement on filtre le produit obtenu et on lave à l'eau sur la filtre pour chasser le bromhydrate de la triéthylamine. On recristallise le produit obtenu.

3-Phényl-cis-5,6-dicarbéthoxy-7-bénzoyl-4a, 5, 6, 7-tétrahydropyrrolo [1,2 — c] pyrimidine (**5a**) : cristaux aciculaires blancs ; p. f. = 158—159°C (en éthanol) ; rend. 65%. Analyse pour $C_{26}H_{26}N_2O_5$: *calculé:* C 69,95, H 5,82, N 6,28% ; *trouvé:* C 69,90, H 5,68, N 6,30%. Spectre IR(KBr) : 1730 cm^{-1} ($\nu_{C=0}$ estérique) ; 1690 cm^{-1} ($\nu_{C=0}$ cétonique). Spectre ^{1}H—RMN (CDCl$_3$, δ, ppm) : 1,15 et 1,19 (2 tr., 6H, 2CH$_3$ des groupements carbéthoxy), 3,60 (d.d., 1 H, H—6, $J_{5,6} = 5$ Hz, $J_{6,7} = 6$Hz), 4,10 et 4,15 (2 q, 4H, 2CH$_2$ des groupements carbéthoxy) 4,92 (dd, 1H, H—5, $J_{5,6} = 5$ Hz, $J_{4a,5} = 3{,}5$ Hz), 5,46 (dd, 1 H, H—4a, $J_{4a,5} = 3{,}5$ Hz, $J_{4,4a} = 1{,}5$ Hz), 5,93 (d, 1H, H—7, $J_{6,7} = 6$Hz), 7,11 — 7,40 et 7,48 — 7,73 (2m, 10H, des protons aromatiques), 8,05 — 8,25 (m, 2H, les protons H—2′ et H—6′ du groupement phényl de la position 3).

3-Phényl-cis-5, 6-dicarbéthoxy-7-(p-méthoxybenzoyl)-4a,5,6,7-tétrahydropyrrolo [1, 2-c] pyrimidine (**5b**) : cristaux aciculaires blancs ; p.f. = 149 — 152°C (dans de l'éthanol) ; rend.

72 %. Analyse pour $C_{27}H_{28}N_2O_6$: *calculé:* C 68,06 ; H 5,88 ; N 5,88 % ; *trouvé:* C 67,96 ; H 5,82 ; N 5,90 %. Spectre IR(KBr) : 1730 cm^{-1} ($\nu_{C=0}$ estériques), 1690 cm^{-1} ($\nu_{C=0}$ cétonique). Spectre ^{1}H−RMN (CDCl$_3$, δ, ppm) : 1,05 et 1,15 (2 tr. 6H, 2CH$_3$ des groupements carbéthoxy), 3,57 (dd, 1H, H−6, $J_{5,6}$ = 5Hz, $J_{6,7}$ = 6 Hz), 3,90 (s, 3H du groupement OCH$_3$), 4,05 et 4,12 (2q, 4H, 2 CH$_2$ des groupements carbéthoxy), 4,98 (dd, 1H, H−5,$J_{5,6}$ = 5Hz, $J_{4a,5}$=3,5Hz), 5,48 (dd, 1H, H−4a, $J_{4a,5}$=3,5 Hz, $J_{4,4a}$=1,5 Hz), 5,93 (d, 1H, H−7, $J_{6,7}$ = 6,0 Hz), 6,90−7,70 et 7,88 − 8,40 (2m, 11H, des protons aromatiques).

3-Phényl-trans-5,6-dicarbéthoxy-7-benzoyl-4a,5,6,7-tétrahydropyrrolo [1,2-c] pyrimidine (**6**a) : cristaux blancs : p.f. = 139 − 142°C (en éthanol) ; rend. 21 %. Analyse pour $C_{26}H_{26}N_2O_5$: *calculé:* C 69,95, H 5,82 N 6,28 % ; *trouvé:* C 69,85, H 5,95, N 6,40 %. Spectre IR(KBr) : 1730 cm^{-1} et 1685 cm^{-1} ($\nu_{C=0}$ estériques), 1665 cm^{-1} ($\nu_{C=0}$cétonique). Spectre ^{1}H−RMN (CDCl$_3$, δ, ppm) : 0,98 et 1,24 (2 tr., 6H, 2CH$_3$ des groupements carbéthoxy), 3,60−4,40 (m, 5H, H − 6+ + 2CH$_2$ des groupements carbéthoxy), 5,30 (dd, 1H, H−5, $J_{5,6}$ = 7,5 Hz, $J_{4a,5}$ = 3,5 Hz) 5,70 (dd, 1H, H−4a, $J_{4a,5}$= 3,5 Hz, $J_{4,4a}$=1,2 Hz), 5,92 (d.14, H−7, $J_{6,7}$ = 7,5 Hz), 7,46 − − 7,77 et 8,00 − 8,53 (2m, 12H, des protons aromatiques).

3-Phényl-trans-5,6-dicarbéthoxy-7-(p-méthoxybenzoyl)-4a,5,6,7-tétrahydropyrrolo [1,2-c] pyrimidine (**6**b) : cristaux jaunes p.f. = 164 − 166°C (en éthanol) ; rend. 31,5 %. Analyse pour $C_{27}H_{28}N_2O_6$: *calculé:* C 68,06, H 5,88, N 5,88 % ; *trouvé:* C 68,12,H 5,96, N 6,02 %. Spectre IR(KBr) : 1740 cm^{-1} et 1710 cm^{-1} ($\nu_{C=0}$ estériques), 1665 cm^{-1} ($\nu_{C=0}$ cétonique). Spectre ^{1}H−RMN (CDCl$_3$, δ, ppm) : 1,04 et 1,22 (2 tr. 6 H, 2CH$_3$ des groupements carbéthoxy), 3,73− − 4,46 (m, 8H, H−6+ CH$_3$ du groupement OCH$_3$ + 2CH$_2$ des groupements carbéthoxy), 5,12 (dd, 1H, H−5, $J_{5,6}$= 7,5 Hz. $J_{4a,5}$= 3,5 Hz), 5,68 (dd, 15H, H−4a, $J_{4a,5}$ = 3,5 Hz, $J_{4,9}$ = = 1,5 Hz), 5,93 (d.1H, H−7, $J_{6,7}$= 7,5 Hz), 7,12 (d, 2H, les protons H−3′ et H−5′ du groupement benzoyle), 7,35 − 7,63 et 7,76 − 8,00 (2m, 5H, des protons aromatiques), 8,20 (d.2H, H−2′ et H−6′ du groupement benzoyle).

3-Phényl-cis-5,6-dicarbométhoxy-7-(p-méthoxybenzoyl)-4a,5,6,7-tétrahydropyrrolo [1,2-c] pyrimidine (**7**) : cristaux aciculaires blancs ; p.f. =185− 185°C (dans de l'éthanol) ; rend. 29 %. Analyse pour $C_{25}H_{24}N_2O_6$: *calculé:* C 66,96, H 5,35, N 6,25 % ; *trouvé:* C 66,87, H 5,32, N 6,37 %. Spectre IR(KBr) : 1730 cm^{-1} ($\nu_{C=0}$ estériques) ; 1690 cm^{-1} ($\nu_{C=0}$ cétonique). Spectre ^{1}H−RMN (CDCl$_3$, δ, ppm) 3,56 − 4,00 (m, 10H, H−6 + 2CH$_3$ des groupements carbométhoxy + CH$_3$ du groupement OCH$_3$), 4,99 (dd, 1H, H−5, $J_{5,6}$= 5Hz, $J_{4a,5}$= 3,5 Hz), 5,49 (dd, 1H, H−4a, $J_{4a,5}$= 3,5 Hz, $J_{4,4a}$ = 1,5 Hz), 5,94 (d, 1H, H−7, $J_{6,7}$ = 6 Hz), 7,07 (d, 2H, H−3′ et H−5′ du groupement benzoyle), 7,21 − 7,50 (m, 5H, des protons aromatiques), 7,61 − 7,83 (m, 2H, H−2′ et H−6′ du groupement phényle de la position 3), 8,24 (d, 2H, H−2′ et H−6′ du groupement benzoyle).

3-Phényl-trans-5,6-dicarbométhoxy-7-(p-méthoxybenzoyl)-4a,5,6,7-tétrahydropyrrolo [1,2-c] pyrimidine (**8**) : cristaux blancs ; p.f. = 178 − 179°C (en éthanol) ; rend. 24,5 %. Analyse pour $C_{25}H_{24}N_2O_6$: *calculé:* C 66,96, H 5,35, N 6,25 % ; *trouvé:* C 67,05, H 5,40, N 6,40 %. Spectre IR(KBr) : 1730 cm^{-1} et 1710 cm^{-1} ($\nu_{C=0}$ estériques) : 1665 cm^{-1} ($\nu_{C=0}$ cétonique). Spectre ^{1}H−RMN (CDCl$_3$, δ, ppm) : 3,20−4,25 (m, 10H, 2CH$_3$ des groupements carbométhoxy + CH$_3$ du groupement OCH$_3$ + H−6), 5,15 (dd, 1H, H−5, $J_{5,6}$ = 7,5 Hz, $J_{4a,5}$ = 3,5 Hz), 5,62 (dd, 1H, H−4a, $J_{4a,5}$= 3,5 Hz, $J_{4,4a}$=1,5 Hz), 5,92 (d, 1H, H−7, $J_{6,7}$=7,5 Hz), 7,16 (d, 2 H, H−3′ et H−5′ du groupements benzoyle) 7,41 − 7,80 et 7,93 − 8,56 (2m, 9H, des protons aromatiques).

3-Phényl-5,6-dicarbométhoxy-7-(p-méthoxybenzoyl)-pyrrolo [1,2-c] pyrimidine (**3**b)[8] : cristaux aciculaires blancs ; p.f. = 152−154°C (dans du chloroforme/éther). Analyse pour $C_{25}H_{20}N_2O_6$: *calculé:* C 67,56, H 4,50, N 6,30 % ; *trouvé* : C 67,73, H 4,97, N 6,43 %. Spectre IR(KBr) : 1735 cm^{-1} et 1705 cm^{-1} ($\nu_{C=0}$ estériques), 1620 cm^{-1} ($\nu_{C=0}$ cétonique). Spectre ^{1}H−RMN (CDCl$_3$, δ, ppm) : 3,44 et 3,92 (2s, 6H, 2 CH$_3$ du groupement carbométhoxy), 3,88 (s, 3H, CH$_3$ du groupement OCH$_3$), 6,95 (d, 24, H−3′ et H−5 du groupement benzoyle), 7,36− − 7,53 (m, 3H, H−3′, H−4′ et H−5′ du groupement phényl de la position 3), 7,75 (d, 2H, H−2′ et H−6′ du groupement benzoyle), 8,00 − 8,20 (m, 2H, H−2′ et H−6′ du groupement phényl de la position 3), 8,53 (d, 1H, H−4), 10,07 (d, 1H, H−1, $J_{1,4}$ = 1,5 Hz).

RÉFÉRENCES

[1] F. Georgescu, E. I. Georgescu, F. Chiraleu et I. Zugrăvescu, *Rev. Roumaine Chim.* (sous presse).

[2] I. Zugrăvescu et M. Petrovanu, « Chimia N-ilidelor », Ed. Academiei, București, 1974.

[3] R. Huisgen, R. Grashey et E. Steingruber, *Tetrahedron Letters*, **1963**, 1441.

[4] R. Huisgen, *Rev. Real. Acad. Ciencias Exactas, Fisicas y Naturales (Madrid)*, **65**, 293 (1978).

[5] M. Petrovanu, I. Druţă et Mai Van Tri, *Rev. Roumaine Chim.*, **23**, 781 (1978).

[6] R. Huisgen, *Angew. Chem.*, **75**, 741 (1963).

[7] R. Huisgen, *J. Org. Chem.*, **33**, 2291 (1968).

[8] I. Zugrăvescu, F. Georgescu, F. Chiraleu, P. Filip et E. I. Georgescu, *Rev. Chim. (București)*, **31**, 11(1980).

[9] F. Georgescu, F. Chiraleu, E. I. Georgescu et I. Zugrăvescu, *Rev. Roumaine Chim.*, **26**, 879 (1981).

[10] E. I. Georgescu, I. Druţă et M. Petrovanu, *Rev. Roumaine Chim.*, **26**, 109 (1981).

Revue Roumaine de Chimie, **28**, *3*, 275–280 (1983)

DETERMINATION OF TRACE QUANTITIES OF COBALT BY ANODIC STRIPPING VOLTAMMETRY AND ALTERNATING CURRENT POLAROGRAPHY

SOFIA MARCHIDAN*, IULIANA VARTIRES, I. TĂNASE and N. D. TOTIR
Center of Physical Chemistry, Splaiul Independenţei 202, Bucharest 79611, Romania

Received June 22, 1982

A method for determination of cobalt in the concentration range $10^{-6} - 10^{-9}$ M with a standard deviation below 10 % by using anodic stripping voltammetry and alternating current polarography has been elaborated. Good sensibility and reproductibility for cobalt analysis on hanging mercury drop electrode using 0.1 M NH_4OH + 0.1 M NH_4Cl in presence of dimethylglyoxime have been obtained.

In order to analyse trace amounts of cobalt from different samples an analytical method is needed, which should fulfil at least two main characteristics namely a standard deviation below 10 % in the concentration range $10^{-6} - 10^{-10}$ M and a very good selectivity.

There are papers in the literature regarding determination of trace quantities of cobalt by using different electrochemical methods.[1–10]

In this paper a method for cobalt determination with a good sensitivity and selectivity by using 0.1 M NH_4OH+0.1 M NH_4Cl in presence of dimethylglyoxime is described.

EXPERIMENTAL

Apparatus

EG & G Princeton Applied Research Model 384 – 4 microprocessor based polarographic analyzer working in the concentration range 0.001 ppb to 9999 ppm was used for anodic stripping voltammetry measurements. The instrument, equipped with an RE 0082 digital plotter, is able to give, at the same time, the experimental curves. As working electrode a 303 SMDE model was used.

All the measurements in alternating current were performed by using a Tacussel potentiostat type PRT 20-2A and a Tacussel pulse generator and recorder.

Reagents

All reagents used were of high purity without further purification. Standard solutions were prepared from tetradistilled water and p.a. chemicals respectively. All the solutions were prepared just before measurements and stored in a Pyrex glass vessel.

---

* Deceased on November 25, 1980

Procedure

The quartz cell was thoroughly cleaned with 1 : 1 concentrated nitric acid and sulphuric acid and then rinsed with tetradistilled water.

The oxygen was removed from the solution by passing purified argon bubbles for 30 minutes. After that the working electrode was polarized at a certain potential values, followed by the recording of the anodic stripping voltammogram, of the supporting electrolyte. By using the standard addition method the cobalt concentration of the samples was determined.

RESULTS AND DISCUSSION

Although the anodic stripping voltammetry of cobalt is very difficult, it can be noticed from the literature that if the experimental conditions are properly selected the cobalt analysis is possible with a relatively good precision (Fig. 1).

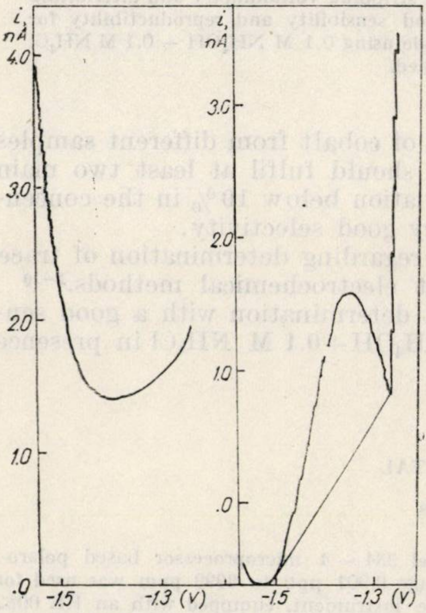

Fig. 1. Stripping voltammogram of cobalt in 0.5 M KCl + 0.1 M KSCN : $\tau = 5$ min ; $E_d = -1625$ mV ; $C_{Co^{2+}} = 5 \times 10^{-7}$ M.

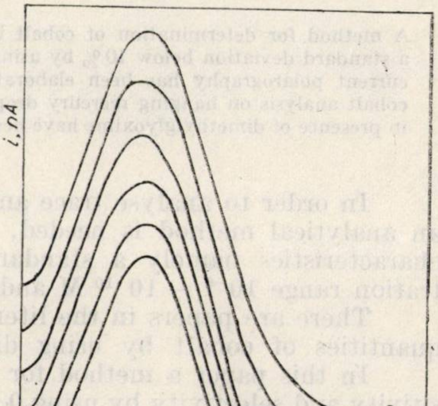

Fig. 2. Alternating current polarographic waves obtained for different concentrations of Co^{2+} : 1.1×10^{-5}M ; 2.2×10^{-5} M ; 3.3×10^{-5} M ; 4.4×10^{-5} M ; 5. 5×10^{-5} M ; 6.6×10^{-5}M ; $\nu = 30$ Hz ; $\Delta E = 40$ mV.

It has been established that there is a good proportionality between peak current density i_p and the cobalt concentration $C_{Co^{2+}}$. The dependence of peak current i_p of cobalt in the concentration range $10^{-6} - 10^{-8}$ M is given in table 1.

TABLE 1

Dependence of peak current i_p on cobalt concentration

$C_{Co^{2+}}$, M	i_p, nA	$C_{Co^{2+}}$, M	i_p, nA
4.0×10^{-6}	53.40	1.0×10^{-6}	21.09
3.5×10^{-6}	51.40	5.0×10^{-7}	13.41
3.0×10^{-6}	50.30	1.2×10^{-7}	10.48
2.5×10^{-6}	46.30	7.0×10^{-8}	9.97
2.0×10^{-6}	40.13	5.0×10^{-8}	8.95
1.5×10^{-6}	30.08	2.0×10^{-8}	7.79

Among supporting electrolytes, described in the literature for alternating current polarography, only KSCN and the mixture NH_4OH 0.1 M and NH_4Cl 0.1 M give good results. Unfortunately, in the case of KSCN the peaks current obtained are very wide in a potential range of 400 — — 500 mV which shows a very low selectivity (Fig. 2.). By changing the amplitude and frequency no increase of the sensitivity was noticed (Figs. 3 and 4).

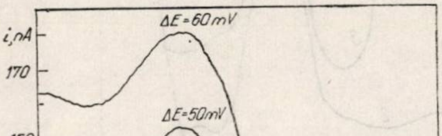

Fig. 3. Influence of amplitude on the peak current. ν = 100 Hz.

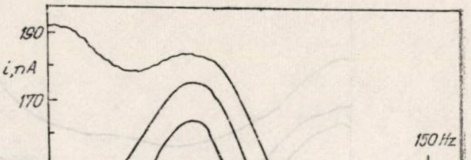

Fig. 4. Influence of frequency on the peak current. $\Delta E = 40$ mV.

The results obtained in the case of the mixture NH_4OH 0.1 M and NH_4Cl 0.1 M and 0.01 % dimethylglyoxime are given in Fig. 5. The results obtained initially in sample without dimethylglyoxime show a relatively low sensitivity.

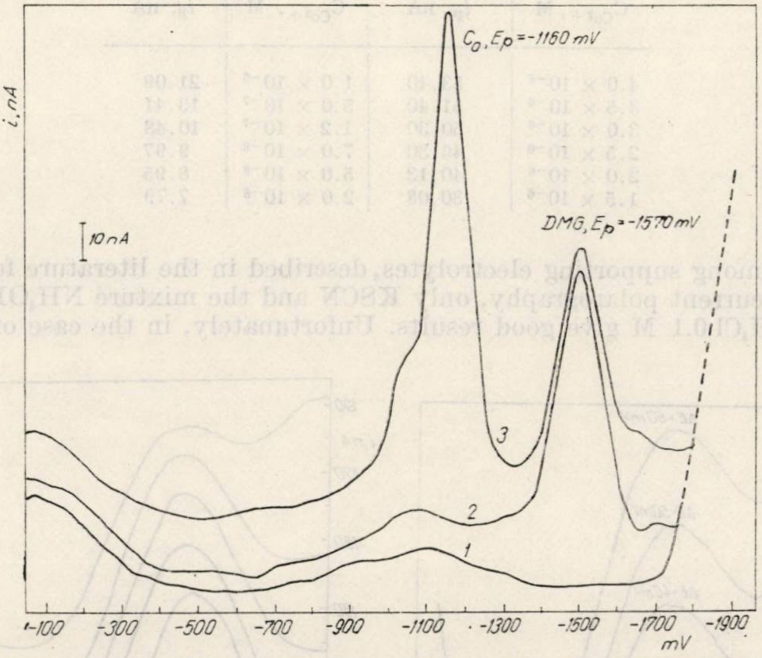

Fig. 5. Alternating current polarogram of cobalt in $NH_4OH + NH_4Cl +$ + dimethylglyoxime. *1* — Supporting electrolyte (0.1 M $NH_4OH +$ + 0.1 M NH_4Cl). *2* — Supporting electrolyte + 0.01 % dimethylglyoxime. *3* — Supporting electrolyte + 0.01 % dimethylglyoxime + 1.5×10^{-4} M Co^{2+}.

In order to increase the sensitivity in the supporting electrolyte, an alcoholic solution of 0.01 % dimethylglyoxime was added, obtaining a higher sensitivity of the method.

As can be seen in figure 5, dimethylglyoxime gives a peak at —1570 mV but compared with the cobalt peak from —1160 mV, the potential range is higher with 400 mV in the negative direction, allowing the cobalt analysis without difficulties.

In comparison with the results obtained in the KSCN case, for this system the selectivity is much better, the peak current being only 200 mV wide.

After selecting all the convenient working parameters, the calibration curves were obtained in the concentration range $10^{-5} - 10^{-6}$ M Co^{2+} the results obtained being presented in figures 6 and 7.

Among the other cations only zinc interferes with cobalt determination, this being avoided by changing the experimental conditions in a proper way. By increasing the alternating signals from 30 Hz to 500 Hz for an amplitude of 6 MV it is possible to separate Co from Zn (Fig. 8).

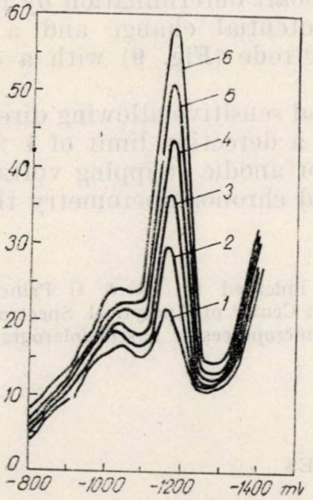

Fig. 6. Alternating curent polarographic waves for cobalt in 10^{-6} M concentration range : *1.* 0.5×10^{-6} M Co^{2+} ; *2.* 1.5×10^{-6} M Co^{2+} : *3.* 4.0×10^{-6} M Co^{2+} ; 4. 6.0×10^{-6} M Co^{2+} : 5. 7.5×10^{-6} M Co^{2+} ; 6. 8.5×10^{-6} M Co^{2+}.

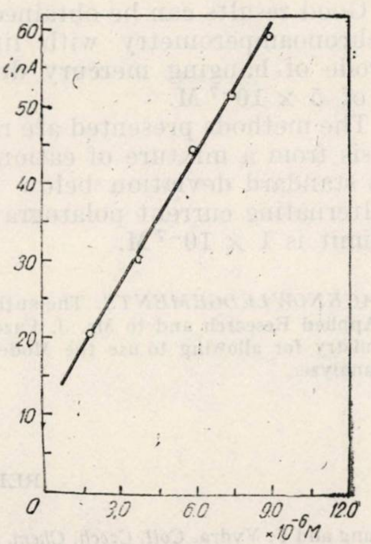

Fig. 7. Calibration curves for cobalt analyses by alternating current polarography.

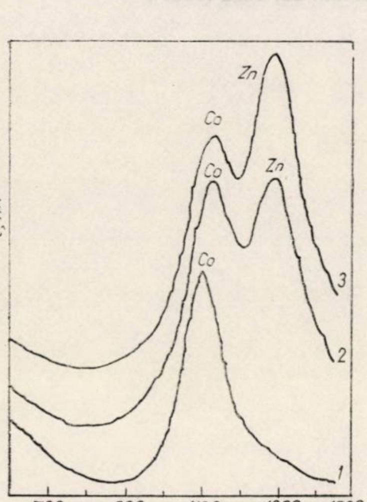

Fig. 8. Separation of cobalt from zinc by alternating current polarography. $\Delta E = 6$ mV; $\nu = 500$ Hz. 1. 5×10^{-5} M Co^{2+}; 2. 5×10^{-5} M $Co^{2+} + 1 \times 10^{-4}$ M Zn^{2+}; 3. 5×10^{-5} M $Co^{2+} + 5 \times 10^{-4}$ M Zn^{2+}.

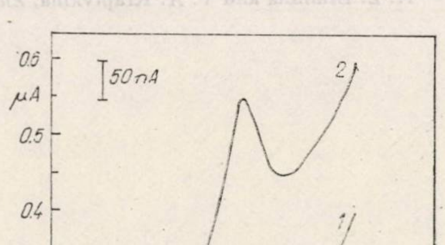

Fig. 9. Chronoamperometry for cobalt determination. 1. Supporting electrolyte; 2. 5×10^{-7} M Co^{2+}.

Good results can be obtained for cobalt determination by using also the chronoamperometry with linear potential change and a working electrode of hanging mercury drop electrode (Fig. 9) with a detection limit of 5×10^{-7} M.

The methods presented are rapid and sensitive allowing direct cobalt analysis from a mixture of cations with a detection limit of 1×10^{-4} M and a standard deviation below 10% for anodic stripping voltammetry. For alternating current polarography and chronoamperometry the detection limit is 1×10^{-7} M.

ACKNOWLEDGEMENTS. The authors are indebted to EG & G Princeton Applied Research and to Mr. J. Fazekas from Center of Analytical Spectrochemistry for allowing to use the Model 384-4 microprocessor based polarographic analyzer.

REFERENCES

[1] L. Loung and F. Vydra, *Coll. Czech. Chem. Comm.*, **40**, 2961 (1974).
[2] M. J. Abdulah and L. G. Rayle, *Analyt. Chim. Acta*, **58**, 283 (1972).
[3] P. Nanghiot, *J. Electroanalyt. Chem.*, **7**, 50 (1964).
[4] E. Temmerman and F. Verbeek, *Analyt. Chim. Acta*, **50**, 505 (1970).
[5] P. Nanghiot, *J. Polarog. Soc.*, **11**, 45 (1965).
[6] P. Nanghiot, *J. Electroanalyt. Chem.*, **14**, 197 (1967).
[7] K. Z. Brainina, *Talanta*, **18**, 513 (1971).
[8] E. Itabashi, *J. Electroanalyt. Chem.*, **91**, 339 (1978).
[9] B. K. Hovsepian and I. Shain, *J. Electroanalyt. Chem.*, **12**, 397 (1966).
[10] K. Z. Brainina and T. A. Krapivkina, *Zhur. analit. Khim.*, **22**, 1382 (1967).

Revue Roumaine de Chimie, **28**, *3*, 281–286 (1983)

RADIATION CHEMISTRY OF IODATE ANION IN AQUEOUS SOLUTION

M. S. SUBHANI
Faculty of Science, University of Garyounis P. O. Box No. 9480 Benghazi, Libya

Received January 29, 1981

Steady state radiolytic studies of aqueous solution of iodate ion have been carried out. The radiation chemical yields $G(-IO_3^-)$, $G(IO_4^-)$, $G(IO^-)$, $G(O_2)$, and $G(H_2)$ were measured and the values 10.92 ± 0.12, 7.21 ± 0.23, 3.43 ± 0.12, 0.85 ± 0.05! and $0.47 \pm$ $\pm\ 0.05$ were found.

The following mechanism for the radiolytic decomposion of iodate ion has been proposed:

$$IO_3^- + e_{aq}^- \rightarrow IO_2 + 2OH^-$$

$$IO_3^- + OH \rightarrow IO_3 + OH^-$$

$$IO_2 + IO_3^- \rightarrow IO_4^- + IO$$

$$2IO \rightleftarrows I_2O_2$$

$$2IO_3 \rightleftarrows I_2O_6$$

$$I_2O_2 + H_2O \rightarrow IO^- + IO_2^- + 2H^+$$

$$I_2O_6 + H_2O \rightarrow IO_3^- + IO_4^- + 2H^+$$

$$IO_2^- + IO_3^- \rightarrow IO_4^- + IO^-$$

$$IO_3^- + H_2O_2 \rightarrow O_2 + H_2O + IO_2^-$$

$$IO_2^- + H_2O_2 \rightarrow O_2 + H_2O + IO^-$$

$$IO^- + H_2O_2 \rightarrow O_2 + H_2O + I^-$$

INTRODUCTION

The pulse radiolysis and flash photolysis of IO_3^- anions in aqueous solution give rise to transient absorption in the region 300 nm to 800 nm[1]. The band peaking at 490 nm was assigned to IO, [1,2] the absorption bands peaking at 380 nm and 715 nm are reported as due to the transient species IO_3 and IO_2 respectively .[1] The pulse radiolysis and flash photolysis studies of oxybromine and oxychlorine anions have given rise to similar species.[3-7] The species IO_3, IO and IO_2 are suggested to be produced most likely by the following processes [1]

$$e_{aq}^- + IO_3^- \rightarrow IO_2 + 2OH^- \quad (1)$$

$$IO_3^- + OH \rightarrow IO_3 + OH^- \quad (2)$$

$$IO_2 + IO_3^- \rightarrow IO_4^- + IO \quad (3)$$

Data regarding the decay of these species, the end products and the overall mechanism for their formation, are not available in the literature. In this paper the results for the investigation of steady state radiolysis of aqueous solution of iodate ion are presented which will provide detailed information on the chemistry of IO_3, IO_2 and IO.

EXPERIMENTAL

All solutions were prepared from water which had been redistilled from acid deichromate and alkaline permanganate. Chemicals were of A.R. grade. Sodium hypoiodite was prepared by the method reported in the literature. [8] All solutions were saturated with N_2 or N_2O gas by the usual bubbling procedure reported elsewhere. [9] Ci^{60} gamma ray source was used and the arrangements for the irradiation of the samples were the same as described before. [6,10]

ANALYSIS

The gaseous products were analysed chromatographically [6]. Hypoiodite ion was measured spectrophotometrically at $\lambda_{max} = 365$ nm using PYE UNICAM SP1800 Spectrophotometer as reported in the literature.[8]

Mixtures of hypoiodite, iodate and periodate were analysed by the following method.

(a) Iodate + Periodate ions

To an aliquot of the solution 5 to 6 drops of 5% ethanol were added and the mixture was allowed to stand for a couple of minutes to make sure that all the hypoiodite present in the mixture was destroyed. Then, to this solution dilute sulphuric acid was added so that the pH of the solution was brought between 7 and 8.

A bicarbonate buffer was used to keep the pH around 7. To this solution at pH = 7 1M solution of KI was added. Under these conditions only IO_4^- oxidizes I^-. The amount of triodide ion produced was measured spectrophotometrically at 350 nm with $\varepsilon_{I_3^-} = 25{,}700\ M^{-1}\,cm^{-1}$. [11]

(b) Iodate ion

The solution from (a) was brought to lower pH = 4 with potassium hydrogen phthalate buffer. At this pH iodate ion produced from periodate and the original iodate ion present in the mixture react with iodide ion producing more triiodide ion which is measured spectrophotometrically again at 350 nm. The difference in absorption between (b) and (a) corresponds to the triiodide ion produced due to the total iodate ion in the mixture, which of course includes the iodate resulted from periodate in (a).

The original iodate was estimated by subtracting twice the absorption measured in (a) from that measured in (b).

(c) Hypoiodite + Iodate + periodate ions

An aliquot of the solution was added to potassium iodide solution in (a) followed by dilute sulphuric acid to make the hydrogen ions concentration 0.2M. Under these conditions all three oxyanions oxidize iodide to I_3^- and this tri iodide ion was determined as described above.

In all these tests solutions were measured against reagent blanks.

RESULTS AND DISCUSSIONS

(a) Nitrogen saturated system

Steady state radiolysis of aqueous solution of iodate ion at pH 13.4 ± 0.1 was performed to measure the end products formed and the disappearance yield of iodate ion. The yield/dose plots for iodate ion periodate ion, hypoiodate ion, hydrogen and oxygen were found to be fairly linear. The radiation chemical yields for these species obtained from the slope of the yield/dose plots are summarized in table 1.

$$H_2O \rightsquigarrow OH,\ e_{aq}^-\ H, H_2O_2, H_2 \qquad (4)$$

The species e_{aq}^- and OH radical are reacting with IO_3^- anion in the following way

$$IO_3^- + e_{aq}^- \rightarrow IO_2 + 2OH^- \qquad (1)$$

$$IO_3^- + OH \rightarrow IO_3 + OH^- \qquad (2)$$

as reported in the literature.[1] The species IO_2 is reported to react with IO_3^- by reaction (3)

$$IO_2 + IO_3^- \rightarrow IO_4^- + IO \qquad (3)$$

TABLE 1

The measured radiation chemical yield in the steady state radiolysis of nitrogen saturated aqueous solutions of IO_3^- ion.

$[IO_3^-] = 10^{-3} - 5 \times 10^{-3}M$

$pH = 13.4 \pm 0.1$

$G(IO_3^-) = 10.92 \pm 0.12$

$G(IO_4^-) = 7.21 \pm 0.22$

$G(IO^-) = 3.43 \pm 0.12$

$G(O_2) = 0.85 \pm 0.05$

$G(H_2) = 0.47 \pm 0.05$

The radiolysis of aqueous solution gives rise to the species given in equation (4).

The transient species IO_3 and IO decay by second order.[1,12] The decay of IO_3 was also reported to be independent of IO_3^- anion concentration. Similar observations are reported in the decay of ClO, ClO_3 IO.[1,5,6,7,12] Thus dimerization reactions (5) and (6).

$$2IO \rightleftharpoons I_2O_4 \qquad (5)$$

and

$$2\,IO_3 \rightleftharpoons I_2O_6 \qquad (6)$$

may be taking place similar to that observed in case of ClO.[5]

The species I_2O_2 and I_2O_6 most probably react with water producing IO_2^- and IO_4^- ions by reactions (7) and (8)

$$I_2O_2 + H_2O \rightarrow IO^- + IO^- + 2H^- \qquad (7)$$

$$I_2O_6 + H_2O \rightarrow IO_3^- + IO_4^- + 2H^+ \qquad (8)$$

IO^- and IO_4^- have been identified as among the end products in the system (see table 1) IO_2^- anion can react in two possible ways (10) and (11) in this system.

$$IO_2^- + IO_2 \rightarrow IO_3^- + IO^- \qquad (9)$$

$$IO_2^- + IO_3^- \rightarrow IO_4^- + IO^- \qquad (10)$$

The observed yield of IO_4^- (see table 1) suggests that under these conditions most of the IO_2^- anions are being converted to IO_4^- through reaction (10).

Oxygen is observed as one of the gaseous end products in additions to hydrogen. This is most probably produced by reactions (11), (12) and (13). Similar to those reported for the oxychlorine and oxybromine systems [3,5,6,7]

$$IO_3^- + H_2O_2 \rightarrow IO_2^- + H_2O + O_2 \qquad (11)$$

$$IO_2^- + H_2O_2 \rightarrow IO^- + H_2O + O_2 \qquad (12)$$

$$IO^- + H_2O_2 \rightarrow I^- + H_2O + O_2 \qquad (13)$$

H_2O_2 is produced during the interaction of gamma radiations with H_2O as shown in reaction (4).

The expected radiation chemical yields $G(-IO_3^-)$, $G(IO_4^-)$, $G(IO^-)$, $G(O_2)$ and $G(H_2)$ can be obtained by taking into account the mechanism based on the above mentioned reactions during the radiolysis of iodate ion in water.

They are as follows

$$G(-IO_3^-) = 0.5\ G_{OH} + 2.5 G_R + 0.33\ G_{H_2O} \qquad (14)$$

$$G(IO^-) = G_R \qquad (15)$$

$$G(IO_4^-) = 1.5\ G_R + 0.5\ G_{OH} \qquad (16)$$

$$G(O_2) = G_{H_2O_2} \qquad (17)$$

$$G(H_2) = G_{H_2} \qquad (18)$$

where $G_R = G_{e_{aq}^-} + G_H$

Substituting values of G_{OH}, G_R, $G_{H_2O_2}$, G_{H_2} obtained from the literature[13] under the experimental conditions employed, the values for $G(-IO_3^-)$, $G(IO^-)$, $G(IO_4^-)$, $G(O_2)$ $G(H_2)$ are 10.7 3.6, 6.9, (0.88 and 6.45 respectively). The observed yields in nitrogen saturated system are in good agreement with the theoretically calculated yields (see table 1), thus supporting the above mentioned mechanism for the radiolysis of iodate ion.

(b) N_2O Saturated system

Steady state radiolysis of N_2O saturated aqueous solution of iodate ion was also carried out at pH 13.4 ± 0.1. The yield/dose plots for the disappearance yield of iodate ion and for the formation of hypoiodite ion periodate ion, oxygen and hydrogen were almost linear and the radiation chemical yields obtained from the slope of these plots are shown in table 2.

Under these conditions N_2O will scavenage all the e_{aq}^- as the reaction of N_2O with e_{aq}^-.[1,13] Thus reaction (1) will be insignificant in this case and the product IO_2 will not be available for reaction (3) and the species IO_2 is in fact not observed under these conditions as reported in the literature.[1] In the absence of reactions (3), reactions (5), (7), (9), and (10) do not take place thus reducing the reactions, and products and their yields. On this basis the calculated G values for IO_4^-. IO_3^-, IO^-, O_2 and H_2 can be written as

TABLE 2

The observed radiation chemical yields in the steady state radiolysis of N_2O saturated aqueous solutions of IO_3^- ion.

$[IO_3^-] = 10^{-3} - 5\times10^{-3}M$
$pH = 13.4 \pm 0.1$
$G(-IO_3^-) = 3.65 \pm 0.11$
$G(IO_4^-) = 3.21 \pm 0.11$
$G(IO_4^-) = 3.21 \pm 0.11$
$G(IO^-) = 0.00$
$G(O_2) = 0.85 \pm 0.05$
$G(H_2) = 0.46 \pm 0.05$

$$G(-IO_3^-) = 0.5(G_R + G_{OH}) + 0.33\ G_{H_2O_2} \qquad (19)$$

$$G(IO_4^-) = 0.5\ (G_R + G_{OH}) \qquad (20)$$

$$G(IO^-) = \text{Zero} \qquad (21)$$

$$G(O_2) = G_{H_2O_2} \qquad (17)$$

$$G(H_2) = G_{H_2} \qquad (18)$$

On substitution of primary radiation chemical yield G_R, G_{OH}, $G_{H_2O_2}$ and G_{H_2} from literature,[13] the yields obtained for IO_3^-, IO_4^-, IO^-, O_2 and H_2 are 3.54, 3.25, zero, 0.88 and 0.45 respectively. The experimentally observed values are in good agreement with the theoretical values (see table 2). Thus all these observations support the idea that the following mechanism is the most likely mechanism for the radiolytic decomposition of iodate ion in aqueous solution.

$$H_2O \rightsquigarrow OH_2,\ e^-_{aq}\ H,\ H_2,\ H_2O_2,\ H_2 \qquad (4)$$

$$IO_3^- + e^-_{aq} \rightarrow IO_2 + 2OH^- \qquad (1)$$

$$IO_3^- + OH \rightarrow IO_3 + OH^- \qquad (2)$$

$$IO_2 + IO_3^- \rightarrow IO_4^- + IO \qquad (3)$$

$$2IO \rightleftharpoons I_2O_2 \qquad (5)$$

$$2IO_3 \rightleftharpoons I_2O_6 \qquad (6)$$

$$I_2O_2 + H_2O \rightarrow IO_2^- + IO^- + 2H^+ \qquad (7)$$

$$I_2O_6 + H_2O \rightarrow IO_4^- + IO_3^- + 2H^+ \qquad (8)$$

$$IO_2^- + IO_3^- \rightarrow IO_4^- + IO^- \qquad (10)$$

$$IO_3^- + H_2O_2 \rightarrow O_2 + H_2O + IO_2^- \qquad (11)$$

$$IO_2^- + H_2O_2 \rightarrow O_2 + H_2O + IO^- \qquad (12)$$

$$IO^- + H_2O_2 \rightarrow O_2 + H_2O + I^- \qquad (13)$$

REFERENCES

[1] O. Amichai and A. Treinin, *J. Phys. Chem.*, **74**, 830 (1970).

[2] M. S. Subhani, Rev. Roumaine Chim. (Accepted for publication)

[3] G. V. Buxton and F. S. Dainton, *Proc. Roy. Soc.*, **A304**, 441 (1968).

[4] O. Amichai, G. Gzapski and A. Treinin, *Israel J. Chem.*, **7**, 351 (1969).

[5] G. V. Buxton and M. S. Subhani, *J. Chem, Soc. Faraday Trans.*, **68**, 958 (1972).

[6] G. V. Buxton and M. S. Subhani, *J. Chem. Soc Faraday Trans.*, **68**, 947 (1972).

[7] G. V. Buxton and M. S. Subhani, *J. Chem., Soc. Farady Trans.*, **68**, 970 (1972).

[8] O. Haimouich and A. Treinin, *J. Phys. Chem.*, **71**, 1941 (1967).

[9] M. S. Subhani, *Rev. Roumaine Chim.*, **23**, 1619 (1978).

[10] M. S. Subhani and A. F. El-Messmar, (Submitted for publication) *J. Natural Science.*

[11] R. L. Augustin ed., "Oxidation", Marcel Deker, New York, 1948, p. 1.

[12] M. S. Subhani, *Rev. Roumaine Chim.* (Accepted for publication).

[13] G. V. Buxton, *Radiation Reserach Rev.*, **1**, 209 (1968).

Revue Roumaine de Chimie, 28, *3*, 287–291 (1983)

DETERMINATION OF POLYMER PARTIAL SOLUBILITY PARAMETERS BY GAS-LIQUID CHROMATOGRAPHY

MINODORA LECA and MARIA ENACHE,
Polytechnic Institute of Bucharest, Chemistry Department, Bld. Republicii No. 13, Romania

Received December 23, 1981

Using polymers as stationary phases and injecting volatile compounds having known structure, belonging to some homologus series, as a function of polymer structure, the gas-liquid chromatography can be used to determine the partial and the total solubility parameters of polymers.

The solubility parameter concept, developed by Hildebrand[1] based on regular solution theory, is extensively used — especially in the paint and laquer industry — to predict the polymer solubility in various solvents and solvent mixtures as well as their adhesion.

Following Hildebrand, the solubility parameter δ is the square root of the cohesive energy density:

$$\delta = \left(\frac{\Delta U^V}{V}\right)^{1/2} = \left(\frac{\Delta H^V - RT}{V}\right)^{1/2}, [(\mathrm{cal/cm^3})^{1/2}] \qquad (1)$$

where ΔU^V is the internal energy of vaporization, V — the molar volume, ΔH^V — the heat of vaporization, R — the gas constant and T — the temperature. Therefore, the solubility parameter can be easily determined from the heat of vaporization and the molar volume at 25°C if the compounds can be vaporized.

Different compounds can be solved one into another if their solubility parameters are equal or sufficiently close. Some exceptions were however noted which initially had no explanation.

In 1967 Hansen[2,3] showed that the cohesive energy of a compound representing the sum of three contributions: due to the dispersion forces ΔU_d^V, dipol-dipol and dipol-induced dipol (polar) forces ΔU_p^V and hydrogen bonding ΔU_h^V — when the substance can develop all the forces cited above — the total solubility parameter can be written:

$$\delta = (\delta_d^2 + \delta_p^2 + \delta_h^2)^{1/2} \qquad (2)$$

where δ_d is the solubility parameter due to dispersion forces, δ_p is due to the polar one and δ_h is due to hydrogen bonding. The compounds can be dissolved one into another when all the three solubility parameters are equal or very close. The main problem is to differentiate the three types of intermolecular forces to be able to determine the corresponding partial solubility parameters.

This problem has been solved for micromolecular compounds : δ_d was determined on the homomorph principle basis[4] — the polar compound homomorph is a nonpolar molecule having about the same size and shape as that of the polar one and can be determined from the homomorphism charts[2] or by gas liquid chromatography.[5, 6]

δ_h can be calculated using the data obtained by IR spectroscopy :[3]

$$\delta_h = \left(\frac{5000.n}{V} \right)^{1/2} \tag{3}$$

where 5000 is the internal energy of vaporization, expressed in cal, corresponding to a mol of —OH groups, n — the number of —OH groups in the compound and V — the molar volume. The difference, calculated with relation (2), is due to the polar forces.

The total solubility parameters of polymers are given in the literature as ranges of values and not as a definite value, especially when the solubility method is used to determine them. Also, the partial solubility parameters are not given but the solubility parameters of their solvents divided into three clases : weak polar, moderate polar and strong polar.[7]

The solubility parameters of nonvolatile compounds, as are the polymers, cannot be determined using relation (1).

The Hildebrand theory, combined with the Flory-Huggins[8] one, give the following relation between the partial molar heat of mixing of solvent $\overline{H}_1^M$ and the solubility parameters of the two compounds (δ_1 — solvent, δ_2 — polymer) :

$$\overline{H}_1^M = V_1 \, \varphi_2^2 \, (\delta_1 - \delta_2)^2 \tag{4}$$

where V_1 is the molar volume of the solvent and φ_2 — the volume fraction of polymer. This relation has been obtained for the mixing of nonpolar compounds. It can be extended for polar interaction too, but only when the two components of the mixture have nearly equal polar interaction[9].

$\overline{H}_1^M$ can be determined accurately by gas-liquid chromatography.

For infinite dilution condition the partial molar heat of mixing of the solvent $\overline{H}_1^\infty$ can be simplified to :

$$\overline{H}_1^\infty = V_1(\delta_1 - \delta_2)^2 \tag{5}$$

Using polymers as stationary phases and injecting suitable volatile compounds the solubility parameters of polymers can be determined if δ_1 is known. Injecting hydrocarbons, dispersion intermolecular interaction forces are only possible. From $\overline{H}_1^\infty$ thus determined δ_d for polymers can be deduced. For polar polymers, injecting compounds having similar structure, the total solubility parameters can be determined. The solubility parameters due to the polar forces can be determined using relation (2) simplified in the form : $\delta = (\delta_d^2 + \delta_p^2)^{1/2}$.

To increase the result accuracy the solubility parameters of polymers were not determined from $\overline{H}_1^\infty$ of some polymer-solvent pairs, as we did in an earlier paper, [10] but compounds belonging to some homologous series were injected, the $\overline{H}_1^\infty$ values were determined ; they were represented in terms of δ_1, and the obtained straight line was extrapolated to $\overline{H}_1^\infty = 0$, a value for which, according to relation (5), $\delta_1 = \delta_2$.

EXPERIMENTAL PART

Polystyrene Toporex of common application having $\overline{M}_v = 1.69 \times 10^5$, polyethyleneoxide having $\overline{M}_n = 40\,000$ and a series of ethyleneoxide-propyleneoxide copolymers — Pluronics — having surface action : Pluronic L 72, Pluronic L 64 and Pluronic F 68 were used as stationary phases on Chromosorb P 100 — 120 mesh as support. The columns, 1m length and 6 mm o.d., were conditioned for 8 hours in carrier gas using flow rates between 5 and 20 ml/min.

Flame ionization detector with argon as carrier gas was used. The column was thermostated for at least 40 min et each temperature.

The following normal hydrocarbons were injected : heptane, octane, nonane, decane. Benzene, toluene and p-xylene were also injected, on polystyrene only. The injected quantities were 0.2 — 0.4 μl and methane was used as noninteracting substance.

Specific retention volumes V_g were computed from the relation :

$$V_g = (t_r F/m)\, J_2^3\, (760/p_0) \tag{6}$$

where t_r is the net retention time, F — the flow rate at 273.16 K (760 mm Hg), m — the mass of polymer and J_2^3 is given by the relationship :

$$J_2^3 = \frac{3}{2}\, [(p_i\,/\,p_0)^2\ - 1]\ /\ [(p_i/p_0)^3 - 1] \tag{7}$$

where p_i and p_0 are the inlet and outlet pressures respectively.

RESULTS AND DISCUSSION

The heat of vaporization of the injected compound from the stationary phase $\Delta\overline{H}_{s\to v}$ can be straightforwardly determined from gas-chromatographic data, using the relation :

$$\Delta\overline{H}_{s\to v} = R[\mathrm{d} \ln V_g/\mathrm{d}\,(1/T)] \tag{8}$$

where the quantities have the known meanings.

The partial molar heat of mixing of the solvent at infinite dilution

$\Delta\overline{H}_{1\to s} = \overline{H}_1^\infty$ is related to $\Delta\overline{H}_{s\to v}$ by the relation :

$$\overline{H}_1^\infty = \Delta\, H_{1\to v} - \Delta\overline{H}_{s\to v} \tag{9}$$

where $\Delta H_{1\to v}$ is the heat of vaporization of the injected compound at the column temperature.

$\Delta \overline{H}_{s\to v}$ can be determined experimentally from the slope of the best straight line through a plot of the logarithm of the specific retention volume vs. the reciprocal of the absolute temperature as determined by the linear regression method. $\Delta H_{1\to v}$ are given in the literature and can be calculated at the column temperature. Therefore, $\overline{H}_1^\infty$ can be determined at the column temperature using relation (9).

The heat of vaporization decreasing and the molar volume increasing with increasing temperature, the solubility parameters of compounds decrease with increasing temperature. Assumig the same variation of δ for polymers and micromolecular compounds, $\overline{H}_1^\infty$ can be correlated with δ_1 at 25°C and δ_2 for polymers can be determined at the same temperature. As a matter of fact the variation of solubility parameters with temperature is expected to be smaller for polymers than for solvents because of the relatively small thermal expansion coefficient of polymers and the δ_2 values a little bit larger than those obtained in this way.

The studied polymer-solvent systems are given in table 1 together with the column medium temperature, heat of vaporization from the stationary phase of the injected substances, and partial molar heat of mixing of the solvent at infinite dilution.

TABLE 1

The studied systems, the medium column temperature, the heat of vaporization from the stationary phase, the partial molar heat of mixing of the injected compounds, and the resulted solubility parameters

System	$\overline{T}$, K	$\Delta \overline{H}_{s\to v}$, cal/mol	$\overline{H}_1^\infty$, cal/mol	δ_2 (cal/cm^3)$^{1/2}$
PS$-C_7H_{16}$	478.1	4580	850	7.25
PS$-C_8H_{18}$		5410	1030	
PS$-C_9H_{20}$		6470	1340	
PS$-C_{12}H_{26}$		9560	2300	
PS$-C_6H_6$	478.1	4120	1080	8.65
PS$-C_6H_5CH_3$		5710	600	
PS$-C_6H_4(CH_3)_2$		6960	370	
PEO$-C_7H_{16}$	339.7	6240	1850	7.39
PEO$-C_8H_{18}$		6540	2550	
PEO$-C_9H_{20}$		6740	4180	
PL 72$-C_6H_{14}$	339.7	5270	1800	6.06
PL 72$-C_7H_{16}$		6130	2110	
PL 72$-C_8H_{18}$		7200	2170	
PL 72$-C_9H_{20}$		8340	2330	
PL 64$-C_7H_{16}$	339.7	6770	1410	6.50
PL 64$-C_8H_{18}$		7770	1530	
PL 64$-C_9H_{28}$		8840	1770	
PF 68$-C_7H_{16}$	339.7	5610	2390	7.28
PF 68$-C_8H_{18}$		6040	2910	
PF 68$-C_9H_{20}$		6200	4080	

PS$-$polystyrene; PEO$-$polyethyleneoxide; P-Pluronic.

Representing $\overline{H}_1^{\infty}$ in terms of δ_1 for the polymer-solvens pairs belonging to the same homologous series and extrapolating the straight line to $\overline{H}_1^{\infty} = 0$ the values given in the fifth column of the table 1 were obtained.

A solubility parameter due to the dispersion forces of 7.25 (cal/cm^3)$^{1/2}$ was obtained for polystyrene. The total solubility parameter — 8.65 (cal/ /cm^3)$^{1/2}$ — is in good agreement with the literature data at 25°C, which for polystyren are in the range of 8.5 to 9.3, (one paper only indicating 9.7 (cal/cm^3)$^{1/2}$,[7] and with that obtained in paper.[10] Having δ and δ_d for polystyrene a value of 4.72 (cal/cm^3)$^{1/2}$ results for the solubility parameter due to the polar forces (interaction between π electrons of the benzene rings).

For PEO, PL 72, PL 64, and PF 68 the solubility parameters due to the dispersion forces were only obtained. The values of δ_d increase with increasing ethyleneoxide content, as can be seen from table 1, reaching the value 7. 39 (cal/cm^3)$^{1/2}$ for PEG.

The values of δ_d obtained for pluronics were correlated with another very important property of those surfactants — the hydrophile-lipophile balance (HLB) — which predicts the possibilities of their uses. A linear relation exists between δ_d and HLB values, given by the equation :

$$\mathrm{HLB} = -104.75 + 18.38\ \delta_d \tag{10}$$

Introducing the δ_d value for PEO in equation (10) a HLB value of 31.1 was obtained.

CONCLUSIONS

Using polymers as stationary phases and selecting adequate compounds for injection, the gas-liquid chromatography became an accurate and fast method to determine the solubility parameters due to dispersion forces and also the total solubility parameters of polymers which do not give hydrogen bonds. The method offers the possibility to differentiate between the solubility parameters due to the dispersion and that due to polar forces, allowing a more judicious selection of solvents.

REFERENCES

[1] J. H. Hildebrand and R. L. Scott, "The Solubility of Non-Electrolytes", 3rd ed., Dover, New York, 1949.
[2] C. M. Hansen, *J. Paint Technol.*, **39**, 104; 505 (1967).
[3] C. M. Hansen and K. Skaarup, *J. Paint Technol.*, **39**, 511 (1967).
[4] A. Bondi and D. J. Simkin, *A. I. Ch. E. J.*, **3**, 473 (1957).
[5] M. Leca, M. Surmeian and L. Groswald-Cremer, *Rev. Chim. (București)* **30**, 172 (1979).
[6] M. Leca, *Rev. Roumaine Chim.*, in press.
[7] J. Brandrup and E. H. Immergut, "Polymer Handbook", Interscience, New York, 1976.
[8] I. Mândru and M. Leca, "Chimie macromoleculară și coloidală", Ed. Didactică și Pedagogică București, 1977.
[9] R. C. Nelson, R. W. Hemwall and G. D. Edwards, *J. Paint Technol.*, **42**, 636 (1970).
[10] M. Leca, L. Groswald-Cremer and M. Surmeian, *Mat. Plastice*, **16**, 114 (1979).

Revue Roumaine de Chimie, 28, 3, 293–296 (1983)

COMPTES RENDUS

HANS RICKERT "Electrochemistry of Solids", An Introduction, Springer-Verlag, Berlin, Heidelberg, New York, 1982, 240 p.

The 7th volume of Inorganic Chemistry Concepts, titled "Electrochemistry of Solids", is the completely revised and extended version of the German edition "Einführung in die Elektrochemie fester Stoffe" which appeared in 1973. Since then, the subject of the electrochemistry of solids has developed further and a large number of new solid electrolytes have been discovered. With the help of solid electrolytes, i.e. solid ionic conductors, galvanic cells are constantly being built for thermodynamic or kinetic investigations and for technical applications. Though the book takes these new developments into consideration, its main aim is to provide an introduction to the electrochemistry of solids, emphasizing the principles of the subject but not attempting to present a complete account of the existing literature.

The volume is organized in 12 chapters. The chapters have been thus written that most of them can be read independently of each other.

After the first chapter, the introduction, the second chapter, "Disorder in Solids" treats on the irregularities in the structure of crystals, i.e. on the lattice defects.

Under real conditions, all ordered compounds, crystalline metal-non metal compounds, exhibit deviations from a regular crystal structure which are of great importance, particularly for the understanding of thermodynamic and kinetic properties of crystalline compounds.

The third chapter, "Examples of Disorder in Solids" deals with a few typical examples of disorder in solids and defects disorder equilibria. Between them the classical examples for compounds with a Schottky-type disorder are alkali halides, whereas those of the Frenkel-type are silver halides such as silver chloride and silver bromide. Important examples of occurrence of defect associates, especially of complex formation between anion and cation vacancies, are the so-called F′-centres present in alkali halides below certain temperatures. Examples for compounds with predominant electronic conduction like zinc oxide, copper (I) oxide are considered too. As a qualitative rule it is found that an excess of electron defects, and therefore electron defect conduction, occurs particularly in oxides, sulfides and halides where the cations show a tendency to increase their valency. In the other case the electronic conduction exhibited is mainly due to free electrons.

The fourth chapter, "Thermodynamic Quantities of Quasi-Free Electrons and Electron Defects in Semiconductors" discusses the thermodynamic quantities of quasi-free electrons and electron defects, in particular the electrochemical potential $\bar{\eta}_e$ and chemical potential $\bar{\mu}$, both considered with respect to a single particle. The relation between these quantities and the concentrations of the quasi-free electrons and electron defects are presented. In the course of the treatment of phase boundaries or surfaces, the terms work function, Volta potential and Galvani or macropotential are also discussed.

The fifth chapter, "An Example of Electronic Disorder. Electrons and Electron Defects in α-Ag_2S" is concerned with an instructive example to discuss electronic disorder in solid compounds of α-Ag_2S. The conductivity of α-silver sulfide being in equilibrium with metallic silver is about 20 times higher than of α-Ag_2S which has been equilibrated with sulfur because the concentration of the free electrons varies also by a factor of about 20. The thermodynamic activity of the electrons in α-Ag_2S is however possible to explain their behaviour quantitatively if the electrons are assumed to be degenerate thus making the use of Fermi-Dirac statistics necessary.

The sixth chapter, "Mobility, Diffusion and Partial Conductivity of Ions and Electrons" discusses the diffusion of ions and electrons in a concentration or activity gradient and their transport in an electric field. These two processes are often superimposed in which case it is more appropriate to speak of transport in an electrochemical potential gradient. The expressions to be derived are valid for the fluxes of each of the various types or ions and electrons separately. The discussion is divided into

a) a phenomenological treatment in which the transport processes are described in terms of experimentally measurable quantities such as diffusion coefficients, mobilities, partial conductivities or Onsager coefficients, and

b) a statistical treatment in which the quantities involved in the phenomenological treatment are related to atomistic quantities.

The seventh chapter, "Solid Ionic Conductors, Solid Electrolytes and Solid-Solution Electrodes", in the first part contains a compilation of solid electrolytes – solid ionic conductors – according to the type of mobile ion which causes the ionic conductivity characteristic of the particular class of solid materials. The second part gives an account of mixed conductors which can be used as electrodes, the so-called solid-solution electrodes.

The eight chapter, "Galvanic Cells with Solid Electrolytes for Thermodynamic Investigations" presents the thermodynamic investigations involving galvanic cells with solid electrolytes which permit the determination of : Gibbs reaction energies, chemical potentials, activities or partial pressures, reaction enthalpies and reaction entropies obtained from investigations of temperature dependencies. The galvanic cells with solid electrolytes may be treated from two different points of view : a) that due to Helmholtz, in which the maximum available work done by the cell during the cell reaction is considered ; b) that due to Nernst, in which single electrode potentials are considered, these then being summed to give the total emf of the galvanic cell.

The ninth chapter, "Technical Applications of Solid Electrolytes – Solid-State Ionics" is a review on some or all of these applications given by several authors. There are discussed a number of examples like, sensors, fuel cells and electrolyzers, batteries with solid electrolytes, chemotronic building units, coulometers and time switches, analogous memories etc.

In the tenth chapter, "Solid-State Reactions" is considered in some detail diffusion-controlled solid-state reactions, taking as the first example the formation of tarnishing layers on metals which has been treated quantitatively by C. Wagner. A reaction of this type is only possible if defects migrate within the volume of a solid. Then a type of reaction involving formation of double salts and double oxides in solid-state reactions has been treated ; this process is also made possible by the migration of defects.

The eleventh chapter, "Galvanic Cells with Solid Electrolytes for Kinetic Investigations" is concerned with the use of galvanic cell with solid electrolytes for kinetic studies in solid and at surface and phase boundaries of solids. Kinetic investigation of such type of galvanic cells containing solid auxiliary electrolytes, which exhibit virtually pure ionic conductivity, does not only provide thermodynamic information via the emf but also allows direct determination of reaction rates via measurements of the current flow within a suitably constructed cell. The combination of rate measurements (via electric currents) with measurements of thermodynamic quantities (via emf's) often permits the analysis of kinetic processes.

In the twelfth chapter, the last one, "Non-Isothermal Systems. Soret Effect, Transport Processes, and Thermopowers" are discussed the effects which are observed if the solid compounds are subject to a temperature gradient like a) changes of concentrations, i.e. changes in stoichiometry or in the activities of the components along the sample ; b) transport processes which involve the migration of one or several components of solid and c) electric potential differences which result from a temperature gradient. These three phenomena may be quantitatively treated using the equation of irreversible thermodynamics, the principle of which is also, discussed.

Both the qualities of contents and the graphic presentation make the 7th volume of "Inorganic Chemistry Concepts", titled : "Electrochemistry of Solids", by Hans Rickert a very valuable reference source for scientists and graduate students who require an approach that will familiarize them with this field.

Iuliana Vartires

H. C. FREYHARDT (Editor), "Growth and Properties", the II-nd volume in the series Crystals-Growth, Properties and Applications (Springer-Verlag Berlin – Heidelberg – New York, 1980, 197 pages).

The second volume in Springer's series "Crystals-Growth, Properties and Applications" includes four papers dealing with crystal growth and properties of some synthetic crystals.

The first paper ("The Growth of Synthetic and Imitation Gems" by Kurt Nassau and Julia Nassau, 50 pages, 153 references) presents the status of preparation methods used for synthetic and imitation gems as diamond, emerald, sapphires of different colours, several types of quartz, spinel, chrysoberyl, rutile, strontium titanate, yttrium aluminium and gadolinium gallium garnets, and others. The specific properties of these materials, allowing their use as synthetic imitation gems are described. A brief outline of the fundamentals of gemology is also included, and the differences between synthetic and imitation gems are detailed.

The second paper ("The Growth of Large Crystals from the Vapour Phase", by Erich Schönherr, 68 pages and 145 references) demonstrates various methods which lead to large single crystals starting from vapour phase. These methods can be used either for the preparation of materials which evaporate congruently, or sublimate with dissociation, or can be grown by chemical transport.

This paper is a good experimental introduction in the field of crystal growth from the vapour phase. The techniques and equipment used are described in detail, in order to allow them to be employed for the growth of large crystals of new materials.

The third paper ("Crystal Growth from the Melt. Experimental Investigation of Kinetics and Morphology", by Dmitrij E. Ovsienko and Gennadij A. Alfintsev, 51 pages and 76 references) presents the authors' experience in the investigation of kinetics, morphology and mechanisms of crystal growth from the melt; likewise the relations between these data and melting entropy are discussed.

The fourth paper ("Morphology and Physical Properties of Gamma Iron Oxide", by Allan Morrish, 27 pages and 146 references) reviews the present data on the gamma iron oxide, which is the most widely used material for magnetic recording. The preparation methods are discussed, including Fe_3O_4 conversion to $\gamma - Fe_2O_3$, in correlation with crystallographic and magnetic properties. The properties of gamma iron oxide with different cation substitutes are considered, and some directions for further research on this important material are suggested.

All papers are written in a remarkably clear and concise manner. The great amount of experimental data (much of them selected from the authors' own work) and the extensive bibliographic references increase the usefulness of this book to all those working in fields of crystal growth and characterization.

Dorel Crişan

"Polymer networks", KAREL DUŠEK Editor, with contributions by M. Adam, J. Bestide, S. Candau, A. Coniglio, M. Delsanti, J. E. Mark, D. Stauffer and A. J. Staverman, Springer-Verlag, Berlin, 1982, 164.

The 44th volume in the Advances in Polymer Science of Springer-Verlag is a collection of four review papers dedicated to Prof. Manfred Gordon with the occasion of his 65th birthday taking into account his great contribution to gelation and networks science. As the first stage of polymer science was represented by studies on relationship between properties and molecular structure in dilute polymer solutions, the actual point of view on polymer networks reffers to the same relationship in solid polymers and concentrated solutions. This position was progressively adopted as being the more realistic for practical ends. The above mentioned four contributions are the following:

"The use of model polymer networks to elucidate molecular aspects of rubberlike elasticity" (J. E. Mark) reviews intra- and inter-molecular aspects of mechanical properties, as effects of network chain length distribution, cross-link functionality and dangling chains, on the one hand, and strain-induced crystallization, networks containing repeating chains, on the other hand, respectively. This review shows how a selectively prepared "model" elastomers can be used to elucidate the dependence of a variety of elastomeric properties on network structure.

"Structural, elastic and dynamic properties of swollen polymer networks" (S. Candau, J. Bastide and M. Delsanti) reviews some recent developments in the physics of gels, due both to the new methods of synthesis and to the modern techniques for the study of microscopic properties of gels. The conclusion emphasis the important progress made in understanding of the static and dynamic properties of swollen networks and describes possible future developments.

"Properties of phantom networks and real networks" (A. J. Staverman), takes into consideration the theory of phantom networks by James (1947) and elaborated by Duiser and Staverman (1965) and by Flory (1976) which generally lead to the frontfactor equation for the elastic free energy.

"Gelation and critical phenomena" (D. Stauffer, A. Coniglio and M. Adam) reviews the critical behaviour of sol-gel phase transition in general terms of critical exponents or scaling laws adopted for all kind of phase transitions. This modern point of view is compared with the classical approach (Flory-Stockmayer type theory) used by chemists.

In fact, all this collection constitutes the intermediate connection between the classical and actual vision on polymer morphology which reffers also to the atomic and small-molecular compounds not only the macromolecular compounds. For this reason, the book appears as interesting both for polymer chemists and for physicists working in material science field.

Gheorghe Drăgan

"Guide-lines to planning atomic spectrometric analysis", B. Magyar, Akademiai Kiado, Budapest, 1982, 273 + X.

This monography is the fourth volume in the Studies in Analytical Chemistry series edited by E. Pungor (Budapest), W. Simon (Zürich) and J. Inczédy (Veszprèm). The theoretical and experimental discussions on atomic spectra include ultraviolet, visible and also X-rays. In fact, the book is constituted on the following contents:

Chapter 1 (Introduction) explains the historical development of the atomic absorption (AAS) and atomic emission spectrometry (AES) and their actual place as elemental analysis.

Chapter 2 (The electromagnetic radiation) deals with the theoretical and phenomenological aspects of electromagnetic radiation (wave and corpuscular nature, generation and absorption laws).

Chapter 3 (The profile of atomic emission and absorption lines) plays a key role for calibration of AAS curves, discussing the main causes of spectral lines broadening.

Chapter 4 (Atomic spectra and electronic structure) discusses in suggestive and original fashion the electronic structure of free atoms or in external magnetic field. This topic is important in atomic spectrometry for spectral lines, atomic and/or ionic species identification so that an appropriate nomenclature is necessary. The actual one needs further perfections to enrich this end in better conditions.

Chapter 5 (Characteristics of atom reservoirs and their influences upon the sensitivities of determinations by AAS and AES) discusses in detail the sensitivity of determination by AAS and AES. This is partly written like a scientific paper because the majority of the experimental results is published for the first time in this book.

Chapter 6 (Spectrometric measurement of atomic absorption and emission) discusses the experimental principles of measurement and calibration of AAS curves. The background compensation in AAS, especially the polychromatic beam method and the Absorption Zeeman-Effect Atomic Absorption (A-ZE/AA), are also discussed.

The seven Appendices physical constants, spectrometric data, sensitivities and detection limits are compiled.

Although the book is intended primarily for students as an solid introduction to the atomic spectrometry, it should also be useful for experienced analysts who need more information on their results.

Gheorghe Drăgan

NOTE POUR LES AUTEURS

La Revue Roumaine de Chimie publie des articles en anglais, français, russe, allemand ou espagnol. Les auteurs sont priés d'envoyer des articles et des comptes rendus inédits.

Les manuscrits seront dactylographiés à double interligne. La bibliographie, les tableaux et la légende des figures seront placés après le texte.

Si l'article fait partie d'une série numérotée, la partie précédente sera donnée comme première référence.

Chaque article sera précédé d'un résumé comprenant quinze lignes au maximum.

Les références bibliographiques dans le texte seront faites par des exposants sans parenthèses et paraîtront à la fin de l'ouvrage.

Les publications périodiques mentionnées dans la bibliographie seront présentées suivant les prescriptions internationales : le nom de l'auteur précédé de l'initiale du prénom, le titre du périodique abrégé conformément à « Chemical Abstracts » et souligné par une ligne, le numéro du tome indiqué par des chiffres arabes et souligné par deux lignes, suivi de la première page de l'article ; à la fin, l'année de la parution sera placée entre parenthèses. Le numéro de la revue ne sera pas indiqué si les pages du volume sont numérotées consécutivement.

Les textes des livres ou traités inclueront : le nom des auteurs, l'initiale du prénom, le titre du livre entre guillements et sans être souligné, le numéro du tome précédé par l'abréviation « vol. » (ou « Bd. »), le numéro de l'édition, les éditions (the publisher), la localité de la parution du livre, l'année de la parution et la page de la référence précédée(s) par l'abréviation « p » (ou « S »).

Les brevets seront indiqués comme suit : l'auteur ou la firme, le pays et le numéro du brevet, la date et la revue *(Chem. Abstr.)*. Par ex. : M. Jones (to Union Carbide Co.), Brit. Pat. 601 238, 2 Sept. 1959 ; cf. *Chem. Abstr.*, **54**, 12808 (1960).

Si la référence n'a pas été lue en original, on indiquera aussi la revue de références consultée.

Les diagrammes seront tracés à l'encre de Chine sur papier calque. Les tableaux et les figures (en nombre strictement nécessaire), ainsi que les courbes dans les figures seront numérotés par des chiffres arabes. Leur explication sera donnée dans la légende des figures. Prière de ne pas inscrire les mêmes données dans les tableaux et les figures. Chaque tableau aura un titre. On indiquera dans le texte la place approximative des tableaux et des figures. Les formules chimiques seront incluses dans le texte ; en outre, elles seront transcrites sur papier calque, à l'encre de Chine.

Les auteurs sont priés d'indiquer les caractères italiques (en soulignant les lettres au crayon), ainsi que tout autre caractère spécial ; les préfixes *ortho. meta, para, cis, trans,* etc. seront soulignés pour indiquer leurs caractères italiques et ne seront jamais écrits avec des majuscules.

Aucune correction à la main ne sera admise sur le manuscrit. Les corrections seront tapées à la machine. Les lettres grecques ou d'autres symboles spéciaux seront insérés à la main à l'encre clairement.

Le manuscrit sera signé par l'auteur.

Le titre-courant aura 50 lettres au maximum.

L'entière responsabilité du contenu des articles appartient aux auteurs.

Sur demande on peut obtenir une note plus complète.

PRINTED IN ROMANIA

TRAVAUX PARUS AUX ÉDITIONS DE L'ACADÉMIE DE LA RÉPUBLIQUE SOCIALISTE DE ROUMANIE

ELENA CEAUȘESCU, **Noi cercetări în domeniul compușilor macromoleculari** (Nouvelles recherches dans le domaine des composés macromoléculaires), 1981, 536 p.

I. G. MURGULESCU, RODICA VÎLCU, **Introducere în chimia fizică, Vol. III. Termodinamica chimică** (Introduction à la chimie physique, Vol. III, Thermodynamique chimique), 1982, p. 624.

I. G. MURGULESCU, J. PĂUN, **Introducere în chimia fizică, Vol. I. 3. Nucleul atomic, reacții nucleare, particule elementare** (Introduction à la chimie physique. Vol. I. 3. Noyau atomique, réactions nucléaires, particules élémentaires), 1982, 606 p.

ELENA JERCAN, **Analiza cromatografică** (Analyse chromatographique), 1982, 286 p.

I. G. MURGULESCU, TATIANA ONCESCU, E. SEGAL, **Introducere în chimia fizică, Vol. II. 2. Cinetică chimică și cataliză** (Introduction à la chimie physique. Vol. II. 2. Cinétique chimique et catalyse), 1981, 1024 p.

V. DRĂGUȚAN, A. T. BALABAN, M. DIMONIE, **Metateza olefinelor și polimerizarea prin deschidere de inel a cicloolefinelor** (La métathèse des oléfines et la polymérisation par ouverture annulaire des cyclooléfines), 1981, 254 p.

LYDIA-MARIA VAICUM, **Epurarea apelor uzate cu nămol activ. Bazele biochimice** (L'épuration des eaux résiduelles à boue active. Les bases biochimiques), 1981, 218 p.

I. GĂLĂȚEANU, **Procese și metode radiochimice în energetica nucleară** (Processus et méthodes radiochimiques dans l'énergétique nucléaire), 1981, 234 p.

O. IORDACHE, **Procese polistocastice aplicate la fenomenele de transfer** (Processus polystochastiques appliqués aux phénomènes de transfert), 1981, 186 p.

CR. SIMIONESCU, VALERIA GORDUZA, **Polimeri biocompatibili și biologic activi** (Polymères biocompatibles et biologiquement actifs), 1980, 479 p.

CONST. GH. MACAROVICI, **Analiza chimică cantitativă anorganică** (L'analyse chimique quantitative inorganique), 1979, 457 p.

ELENA CEAUȘESCU, **Polimerizarea stereospecifică a izoprenului** (La polymérisation stéréospécifique de l'isoprène), 1979, 307 p.

M. FLORESCU, **Metode științifice în dezvoltarea industriei chimice moderne** (Méthodes scientifiques dans le développement de l'industrie chimique moderne), 1979, 256 p.

A. T. BALABAN, I. GĂLĂȚEANU, G. GEORGESCU, LIGIA SIMIONESCU, **Compuși marcați și radiofarmaceutici cu aplicații în medicina nucleară** (Composés marqués et radiopharmaceutiques à application en médecine nucléaire), 1979, 495 p.

I. G. MURGULESCU, E. SEGAL, **Introducere în chimia fizică, vol. II. 1. Teoria molecular cinetică a materiei** (Introduction à la chimie physique. Vol. II. 1. La théorie moléculaire-cinétique de la matière), 1979, 1036 p.

S. STERNBERG, FL. DANEȘ, **Termodinamica chimică aplicată** (La thermodynamique chimique appliquée), 1978, 400 p.

I. G. MURGULESCU, V. EM. SAHINI, **Introducere în chimia fizică. Vol. I. 2. Structura și proprietățile moleculelor** (Introduction à la chimie physique. Vol. I. 2. La structure et les propriétés des molécules), 1978, 604 p.

I. ZUGRĂVESCU, MAGDA PETROVANU, **N-ylid chemistry**, coédition avec McGraw-Hill International Book Company, U.S.A., 1977, 396 p.

I. G. MURGULESCU, **Introducere în chimia fizică. Vol. I. 1. Atomi, molecule, legătură chimică** (Introduction à la chimie physique, Vol. I. 1. Atomes, molécules, liaison chimique), 1976, 560 p.

ELENA CEAUȘESCU, **Research work on synthesis and characterization of macromolecular compounds. Contributions**, 1974, 251 p.

CR. SIMIONESCU, VIORICA RUSAN, V. POPA, **Chimia algelor marine** (La chimie des algues marines), 1974, 212 p., 1 pl.

1983 SEP 2 9

ISSN 0035—4090

I. P. Informația c. 2720

43 426

Lei 40. —

$ 75 (pour un abonnement annuel)

F 1103

Veggészet

ACADÉMIE DE LA RÉPUBLIQUE SOCIALISTE DE ROUMANIE

REFERÁLVA

REVUE ROUMAINE DE CHIMIE

R

TOME 28

N° 4

Avril 1983

EDITURA ACADEMIEI REPUBLICII SOCIALISTE ROMÂNIA

Rev. Roumaine Chim.

RRCHAX, 28, 4, p. 297–428 (1983), Bucarest

ACADÉMIE DE LA RÉPUBLIQUE SOCIALISTE DE ROUMANIE

COMITÉ DE RÉDACTION

Rédacteur en chef:

I. G. MURGULESCU, membre de l'Académie de la République Socialiste de Roumanie

Rédacteurs en chef adjoints:

A. T. BALABAN et V. EM. SAHINI, membres correspondants de l'Académie de la République Socialiste de Roumanie

Collège de rédaction:

EM. BRATU, ELENA CEAUŞESCU, ECATERINA CIORĂNESCU-NENITZESCU, CR. SIMIONESCU, membres de l'Académie de la République Socialiste de Roumanie ; P. SPACU, membre correspondant de l'Académie de la République Socialiste de Roumanie : MARGARETA AVRAM, M. BANCIU, I. HAIDUC, D. I. MARCHIDAN, I. MOLDOVAN, G. NIAC et D. SĂNDULESCU

La Revue Roumaine de Chimie paraît 10 fois par an. Toute commande de l'étranger pour les travaux parus aus Editions de l'Académie de la République Socialiste de Roumanie sera adressée à ILEXIM — Departamentul Export-Import Carte (Livres)/Departamentul Export-Import Presă (Revues) P.O.B. 136—137, télex 11226, str. 13 Decembrie, 79517 Bucarest, Roumanie

Les manuscrits, les livres et les revues proposés en échange, ainsi que toute correspondance seront envoyés à la rédaction :

REVUE ROUMAINE DE CHIMIE

125, Calea Victoriei, 79717 Bucarest, Roumanie, téléphone 50 76 80

EDITURA ACADEMIEI REPUBLICII SOCIALISTE ROMÂNIA
125, Calea Victoriei, 79717 Bucarest, Roumanie, téléphone 50 76 80

REVUE ROUMAINE
DE
CHIMIE

Tome 28, N° 4 Avril, 1983

ELENA CEAUŞESCU R. BORDEIANU, P. GHIOCA, IRINA CERCHEZ, E. BUZDUGAN and RODICA STANCU, Dilute block copolymer systems. II. Tensile modulus of oil-extended butadiene-styrene block copolymers at large strains 299 323

M. M. GIRGIS, D. P. LAZĂR and E. I. SEGAL, Catalytic oxidation of ammonia. IV. Low temperature oxidation on a nickel oxide catalyst supported on alumina . . . . 325 332 Bc

GH. CIURDARU, MARIA-DOINA RUSU and N. PALIBRODA, Thermally and electron impact induced acyl migration in N- [*ortho*-O-, -S-, -Se-acylphenyl]-amides 333 337

EDUARDO A. CASTRO and FRANCISCO M. FERNÁNDEZ, An improved two-parameter omega technique for molecular orbital calculations. III. Aromaticity of some semibenzenoid and nonbenzenoid hydrocarbons (in Spanish) 339 347

N. CALU and N. FOCA, Complexes of transition metals with 2,2′-diaminoazobenzene. IV. The Co(II)-2,2′-diaminoazobenzene system 349 354

D. NEGOIU and ILEANA GHELASE, Complex compounds of Ni(II) with acetone selenosemicarbazone 355 364

RODICA MICU-SEMENIUC, SILVIA BARBU and MARIA SUZANA MIHAIU, Coordination compounds of thiocarbohydrazone-2-aminobenzaldehyde with Co(II) and Ni(II) salts 365 373

IULIA HAVLIK, T. SIMONESCU and I. HAVLIK, New pyrazolone complex compounds of bis-(methylaminoantipyryl)-ethane . . . . 375 379 Bc

M. RĂILEANU, S. FLOREA and N. MUREŞAN, Solvent effects. II. Solvent influence on the acidity of some nitrophenothiazinic compounds . . . 381 385

OANA PETREUŞ and FLORIN NECULAI POPESCU, Thermal behaviour of macromolecular compounds containing phosphorus and sulfur in their chains and of their mixtures with poly(propene) (in French) . . . . . . 387 395 C

M. S. SUBHANI, Photodecomposition of hypoiodite ion in aqueous solution . . 397 404

S. ARRIBAS JIMENO, M. L. ALVAREZ BARTOLOMÉ and E. ANDRÉS GARCÍA, Analytical study of the precipitates obtained from the anion HgI_4^{2-} and the cations of the first analytical group (Ag^+, Pb^{2+}, Hg_2^{2+} and Tl^+) (in Spanish) 405 412

FASIHUDDIN KAMIL, P. P. SINHA and S. K. SINDHWANI, Complexometric and spectrophotometric determination of copper using phenanthrenequinone monosemicarbazone (PQSC) . . . . 413 417 R

MARIANA BEZDADEA, C. V. UGLEA and I. AGHERGHINEI, Gel permeation chromatography of poly(vinylacetate) . . . . 419 424 R

S. F. A. NAQVI, S. P. MATHUR and V. IYER, Spectrophotometric determination of iron with sodium-*N*-(*O*-sulphonic-benzoyl)-*N*-pyridine in the presence of thiocyanate 425 427

BOOK REVIEWS 429 433

Rev. Roumaine Chim. **28**, *4*, 297–434 (1983), Bucarest

Revue Roumaine de Chimie, **28**, *4*, 299–323 (1983)

DILUTE BLOCK COPOLYMER SYSTEMS. II[1]

TENSILE MODULUS OF OIL-EXTENDED BUTADIENE-STYRENE BLOCK COPOLYMERS AT LARGE STRAINS *

ELENA CEAUŞESCU, R. BORDEIANU, P. GHIOCA, IRINA CERCHEZ,
E. BUZDUGAN and RODICA STANCU
Chemical Research Institute ICECHIM, Spl. Independenţei 202, Bucharest, Romania

Received April 1, 1983

The large-strain tensile modulus of oil-extended linear and star butadiene-styrene block copolymers was investigated, particularly the effects of oil level, polymer structure, pre-stretching, oil composition, and casting solvent. Morphological transitions occurring at critical oil levels are thought to be at the origin of a non-linear dependence of tensile modulus on dilution. An empirical relationship correlating tensile modulus with oil level and composition of base polymer in a broad range of network dilutions was found.

A sizable proportion of the present consumption of butadiene-styrene block copolymers is in the form of oil-extended grades. The dilution of both linear (S—B—S) and star ($(S-B-)_n$) thermoplastic elastomers with mineral oils serves the dual purpose of improving certain mechanical and rheological properties while also increasing the cost efficiency of the product.

Although at present many of the fundamental aspects of the extension of conventional rubbers with oils are well understood, [2-6] surprisingly little attention has been given to the study of physical-mechanical properties of dilute block copolymer systems, despite their obvious practical interest.

Our investigation has been aimed at gaining more information on the effect of extender oil on the large strain tensile modulus of linear and star butadiene-styrene thermoplastic elastomers.

EXPERIMENTAL

Two series of block copolymers were investigated, designated according to their structure by the letters *L* (linear) or *S* (star). The properties of the polymers are given in Table 1.

Polymers *L*—1, *L*—3 and *L*—4 were synthesized by a three-step sequential monomer addition process in toluene with *n*-BuLi as polymerization catalyst. In order to accelerate

---

* Part I of this series has delt with the refractive index and density of oil-extended block copolymers. [1]

TABLE 1

Properties of block copolymers

Polymer	Structure	Styrene content, wt.-%	Molecular weight $\overline{M}_n$, g.mole^{-1}		
			Total	$\overline{M}_B$	$\overline{M}_S$
L—1	linear	34.5	123,200	80,800	21,200
L—2	linear	35.0	108,000	70,200	18,900
L—3	linear	27.8	78,500	57,100	10,700
L—4	linear	40.3	98,000	58,600	19,700
S—1	star	42.7	120,000	68,800	12,800
S—2	star	30.7	141,400	98,200	10,800
S—3	star	50.8	180,000	88,400	22,900

initiation, diphenyl ether was added at a molar ratio DPE/*n*-BuLi = 2. Polymer *L*—2 was substantially similar to *L*—1 in composition and molecular weight, but was obtained by a two-step process in which polystyryllithium synthesized in the first step initiated the polymerization of a butadiene-styrene mixture in the second reaction step. Polymers *S*—1, *S*—2 and *S*—3 were obtained by coupling active S—B—Li chains with a tetrafunctional coupling agent ($SiCl_4$). After synthesis the polymers were stabilized in solution with 2,6-bis-*tert*-butyl-*p*-cresol (0.8 percent with respect to the polymer) and then recovered by steam-hot water stripping. Weighed amounts of polymer were then redissolved in toluene or cyclohexane and known amounts of extender oil were added. From the homogeneous solution 0.8 mm thick polymer films were spin cast using the method previously described.[1]

Three different oils were used, two of them (Oils I and II) being paraffinic-naphthenic and the third being a highly aromatic oil. The properties of the extender oils are given in Table 2.

TABLE 2

Properties of extender oils

Property	Unit	Oil I	Oil II	Oil III
Color	—	colorless	pale yellow	black
Density at 25°	kg.m^{-3}	866.5	897.1	1009.6
Refractive index at 25°	—	1.4740	1.4929	1.5785
Average molecular weight	g.mole^{-1}	418	450	
Kinematic viscosity at 37.8°	m^2.h $^{-1}$	0.134	0.432	
Saybolt viscosity at 100°	deg. Saybolt			118
Structural composition *)				
Aromatic C	wt.—%	3.5	7	45
Naphthenic C	wt.—%	29.9	38	21
Paraffinic C	wt.—%	66.6	55	34

*) Calcd. from n_D, *d*, and *M*

The tensile modulus of the polymers was determined on standard dumbbell specimens with an active length of 20 mm at a jaw separation speed of 0.5 m.min^{-1} (when not stated otherwise) on a Zwick tensile tester, automatically recording during extension the retractive force at extension ratios $\lambda = 4$ and $\lambda = 6$. The tensile modulus is defined as the retractive force divided by the initial cross-section area of the oil-extended sample ($f = F/A_0$). All measurements were performed at 25°.

DTA measurements were carried out on a Mod. Q Derivatograph (MOM-Budapest) at a heating rate of 10°/min using open platinum crucibles. DSC runs were performed on a DuPont instrument, at the same heating rate.

Swelling measurements were performed at 25° by immersion, either gravimetrically or by following with a cathetometer the length increase of polymer strips suspended in extender oil.

RESULTS AND DISCUSSION

1. POLYMER-OIL COMPATIBILITY

In order to evaluate the compatibility of the polymers with extender oils, DTA measurements were performed first on polystyrene homopolymer of molecular weight equal to that of the polystyrene blocks of polymer *L*-1, in the presence of oils I, II, and III. Samples of PS ($\bar{M}_n =$ $= 21{,}200\ \text{g}\cdot\text{mole}^{-1}$) mixed with 30 wt. percent oil were ground and left for 15 hrs at room temperature, then subjected to two heating-cooling cycles in the DTA equipment ($t_{\max} = 175°$). The results are given in Table 3.

TABLE 3

Glass transition temperatures (T_g) of polystyrene-oil systems (30 percent oil), determined by DTA

Oil	1st Cycle	2nd Cycle
—	94	93
Oil I	93	85
Oil II	95	76
Oil III	91	59

It can be seen that in the first cycle, despite the relatively long soaking time of polystyrene in oil, T_g was not affected with the exception of Oil III. The agreement between the value found for the T_g of PS and that reported in literature for a sample of similar mol. wt.[7] is excellent. After annealing the samples at 175° the T_g is reduced the more so the higher the content of aromatic carbon atoms. It follows that in glassy PS the diffusion of aromatic hydrocarbons is slow but above T_g a sizable amount of these hydrocarbons is absorbed in the polymer. The depression of T_g in the second heating cycle can thus be taken as a measure of polystyrene compatibility with the oil.

In block copolymers the glass transition of polystyrene blocks is lower than the T_g of PS homopolymer (87° vs. 94° for PS). This effect was also observed by other investigators[8-12] and was explained by the existence of frozen mechanical stresses of thermal origin arising from the different expansion coefficients of polystyrene and polybutadiene and concentrated in the PS domains[8] (as is known, the T_g of PS decreases under strain with about 8° for each percent of deformation[13]) or, alternatively, by a mechanism of energy transfer of the fast microbrownian motion of polybutadiene chains towards the PS blocks.[10]

The investigation by DSC of a series of *L*-1 — Oil I blends showed somewhat surprisingly an increase in the T_g of the polystyrene blocks. This is taken as an indication that, at least for the polymer-oil system under consideration, no plasticization of the glassy domains occurs or, even if it does, it is masked by a much stronger effect acting in the opposite direction. At any rate, the partition equilibrium of oil between phases is strongly shifted towards PB. The increase in T_g could be followed by DSC in the range from 0 to 60 phr (at higher dilutions the transition became too weak). As seen from Figure 1, despite a rather severe scattering of the data, the trend is unmistakable.

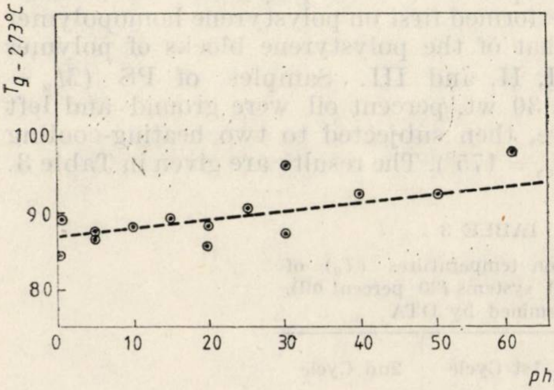

Fig. 1. — Variation of glass transition temperature of polystyrene domains of polymer *L*—1 with extender oil content (Oil I).

If one assumes that the difference between the T_g of PS blocks in pure gum polymers and that of PS homopolymers is due to frozen mechanical stresses, then the effect of oil is explainable by a stress reduction following the lowering of the matrix modulus. Alternatively, the dilution of the matrix would favor an energy transfer of the microbrownian motions of polybutadiene chains towards oil molecules diminishing thus the available energy for the transfer to the glassy domains. A discrimination between the two mechanisms cannot be made based on T_g data alone.

2. MODULUS OF TRIBLOCK COPOLYMERS

2.1. Effect of Oil Level

The modulus of triblock copolymers at first loading is strongly dependent on oil level. Taking the volume fraction of polybutadiene in the oil-extended matrix, φ_R, as a measure of the degree of polymer dilution, it can be seen from the log-log plot given in Figure 2 that, although there is a general decrease of the modulus with increasing dilution, this dependence is not monotonous; after an initially gentler descent a steeper decrease of the modulus at higher degrees of oil-extension follows after a transition interval. The onset of the transition depends on the composition of base polymer, occurring at lower oil contents for polymers richer in butadiene.

The mentioned effect is time-dependent, as seen from Figure 3 in which the tensile modulus of polymer *L*-1 extended with Oil I measured at jaw separation speeds of 0.1 and 1 m·min^{-1} respectively was plotted against φ_R.

The volume fraction of rubber used in the above plots was calculated from $\varphi_R = v_B(1 - w_S)/[v_B(1 - w_S) + v_o w_o]$ (where v_B and v_o are the specific volumes of polybutadiene and oil, w_S is the volume fraction of polystyrene in the base polymer and w_o is the amount of oil, in phr/100). For v_B the value 1.116 $cm^3 \cdot g^{-1}$ was used. [1]

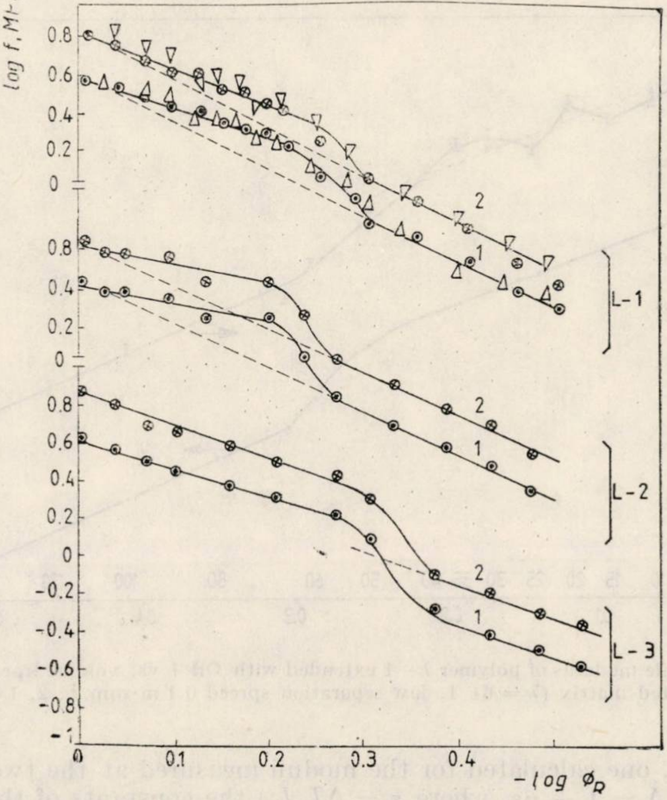

Fig. 2. — Tensile modulus of linear block copolymers vs. volume fraction of rubber in the oil-diluted matrix. 1, $\lambda = 4$; 2, $\lambda = 6$; ⊙, ⊗ Oil I ; Δ, ∇ Oil II.

The most direct treatment of modulus data would be based on the assumption that the Mooney-Rivlin equation[14] holds for the rather complicated system of oil-extended rubber filled with a reinforcing charge (polystyrene domains). Considering the polystyrene phase as being totally rigid, a strain amplification factor has to be taken into account[15] which, in a first approximation, is given by the Guth-Smallwood equation [16]:

$$\gamma \equiv E/E_0 = 1 + 2.5\varphi_S + 14.1\varphi_S^2 \tag{1}$$

where φ_S is the volume fraction of polystyrene domains in the extended rubber (calculated from $\varphi_S = v_S w_S/[v_S w_S + v_B(1 - w_S) + v_o w_o]$, in which

v_S is the specific volume of polystyrene, taken as 0.9416 $\text{cm}^3 \cdot \text{g}^{-1}$ at 25°) and E, E_0 are the elasticity moduli of the filled and unfilled elastomer, respectively. A further, even more drastic approximation, is that such a data treatment is valid for the high strains, λ, and even higher "amplified" strains, Λ, at which tensile modulus was determined in this work.

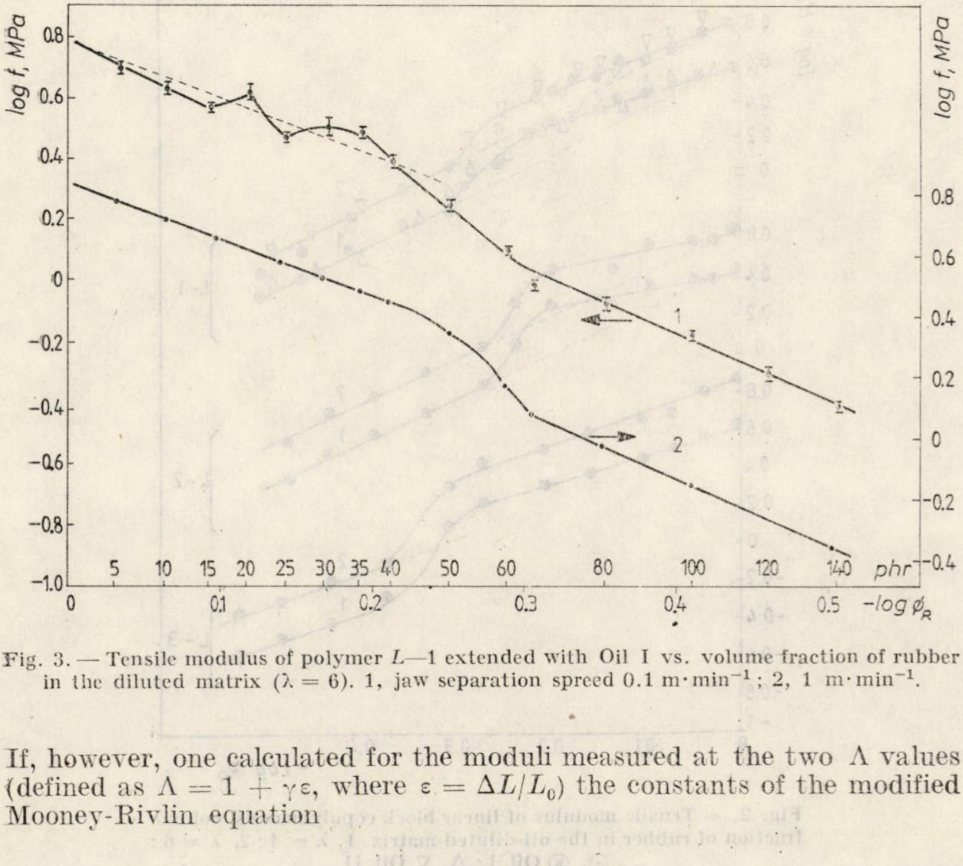

Fig. 3. — Tensile modulus of polymer L—1 extended with Oil I vs. volume fraction of rubber in the diluted matrix ($\lambda = 6$). 1, jaw separation spreed $0.1\ \text{m} \cdot \text{min}^{-1}$; 2, $1\ \text{m} \cdot \text{min}^{-1}$.

If, however, one calculated for the moduli measured at the two Λ values (defined as $\Lambda = 1 + \gamma\varepsilon$, where $\varepsilon = \Delta L/L_0$) the constants of the modified Mooney-Rivlin equation

$$f = (2C_1 + 2C_2/\Lambda)\,(\Lambda - 1/\Lambda^2) \tag{2}$$

a complicated dependence of both $2C_1$ and $2C_2$ on φ_R is found, denying the use of eq. (2) for predicting the modulus of oil-extended S—B—S.

A similar approach was taken by Holden el al.[17] who combined the Mooney-Rivlin equation with the Guth-Smallwood function to yield:

$$f = (2C_1 + 2C_2/\lambda)\,(\lambda - 1/\lambda^2)\gamma \tag{3}$$

Again, this equation applied to our data yielded for $2C_1$ and $2C_2$ values which showed a complicated variation with φ_R.

A more recent equation describing the modulus of oil-extended block copolymers was derived by Leonard[18] from a generalized theory of elasticity:

$$f = RT\nu\varphi_B^{-1/3}\,\varphi_R^{-2/3}\,(\lambda - 1/\lambda^2)\,\gamma/V' \tag{4}$$

where ν = number of elastomer blocks, φ_B = volume fraction of rubber in BAS copolymer and φ_R = volume fraction of rubber in the extended matrix (defined as the ratio V_0/V' where V' is the volume of elastomer after extension and V_0 is the initial volume of elastomer). The Leonard equation does not describe satisfactorily the behaviour of oil-extended S—B—S at first traction, including the rather drastic effect of oil on modulus.

In order to find an empirical equation adequately describing the variation of the tensile modulus with the degree of oil extension, we assumed that the main governing factor is the volume fraction of polystyrene domains, or rather the γ function which actually expresses the reinforcing effect of the domains. Also it was assumed that the modulus depends on the 1/3rd power of φ_R, as predicted by the statistical theory of rubber elasticity.[19-22]

By plotting the ratio $f/\varphi_R^{1/3}$ of oil-extended samples of polymers $L-1$, $L-3$ and $L-4$ at $\lambda = 4$ and $\lambda = 6$ against γ in a log-log diagram, two sets of straight lines of different slope were obtained, as seen in Figure 4.

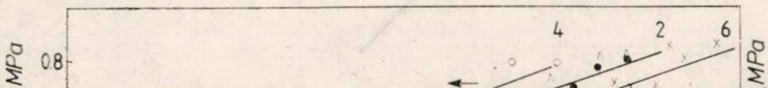

Fig. 4 — Variation of the $f/\varphi_R^{1/3}$ ratio with the Guth-Smallwood function for toluene-cast films of linear polymers. 1, 3, 5, $\lambda = 4$; 2, 4, 6, $\lambda = 6$.
● L—1/Oil I; Λ L—1/Oil II; ○ L—3/Oil I; × L—4/Oil I.

For the same polymer the data for the two extension ratios can be superposed reasonably well by a shift parallel to the $0y$ axis of $\log(\lambda_2 - 1/\lambda_2^2) - \log(\lambda_1 - 1/\lambda_1^2)$. For different polymers the slopes of the two rectilinear branches are respectively equal. By a shift parallel to the abscissa the data obtained for different polymers can be superposed on a master curve. The shift factor is proportional to the inverse of the square root of φ_S (Fig. 5). This dependence reflects the higher dilution of the elastic network of a polymer with higher polystyrene content compared with a polymer with less polystyrene for the same amount of extender oil added.

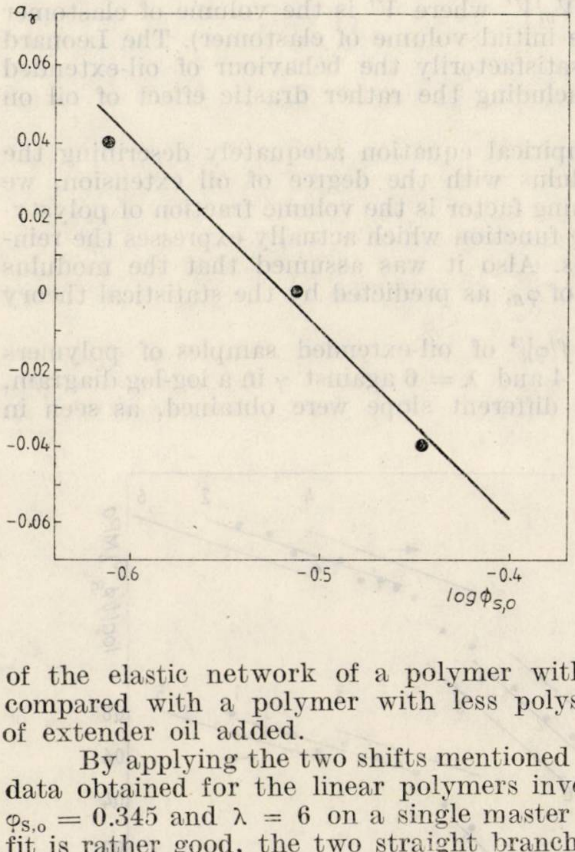

Fig. 5. — Dependence of shift factor on composition of base polymer.

By applying the two shifts mentioned above, all the tensile modulus data obtained for the linear polymers investigated could be reduced to $\varphi_{S,o} = 0.345$ and $\lambda = 6$ on a single master curve given in Figure 6. The fit is rather good, the two straight branches of the curve having slopes of 4/3 for $\gamma > 0.33$ and 4 for $\gamma < 0.28$ with a transition zone in between in which the modulus changes abruptly.

The modulus of oil-extended butadiene-styrene triblock copolymers can thus adequately be described by the following equation :

$$f = (C_1' + C_2'/\lambda)\,(\lambda - 1/\lambda^2)\varphi_R^{1/3}\ (\varphi_{S,o}^{-1/2}\,\gamma)^n \tag{5}$$

with $n = 4/3$ for $\varphi_S > 0.20$

$n = 4$ for $\varphi_S < 0.18$

The exponent n in Eq. (5) constitutes a measure of the retention of the reinforcing capacity of polystyrene domains with increasing dilution by extender oil (the higher the value of n, the faster is the reinforcing capacity lost). A calculation of the two constants in Eq. (5) from the tensile moduli at $\lambda = 4$ and $\lambda = 6$ yielded the values $C_1' = 0.117$ MPa and $C_2' = -0.11$ MPa for the first domain and $C_1' = 2.21 \times 10^{-3}$ MPa and $C_2' = -1.5 \times 10^{-3}$ MPa for the second, with which a good fit with the experimental data was obtained (Fig. 7).

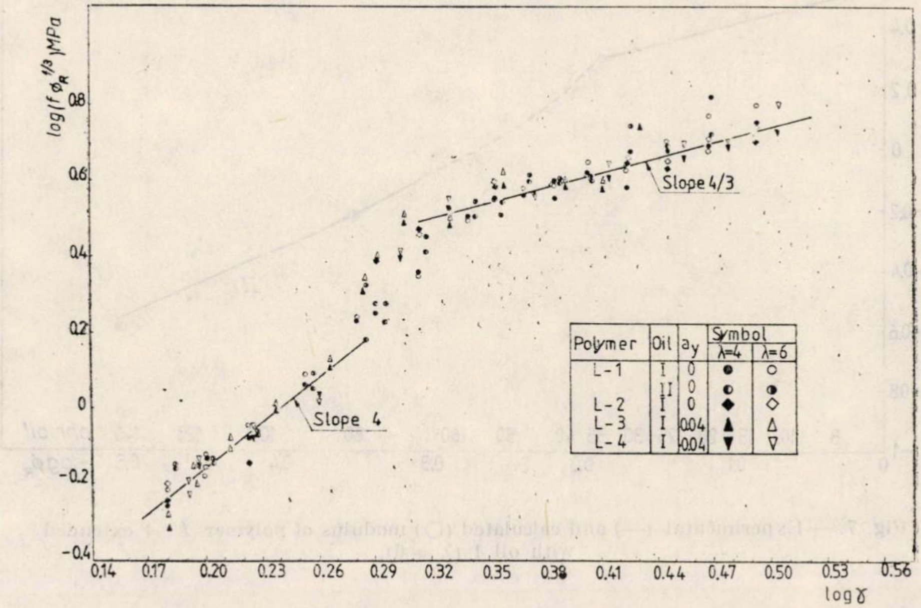

Fig. 6. — Master curve of modulus dependence on the Guth-Smallwood function ($\varphi_{S,0} = 0.345$, $\lambda = 6$).

It would be tempting to use instead of Eq. (5) a simpler equation like Eq. (3) in which, instead of the Guth-Smallwood function (which is strictly applicable for spherical-shaped filler particles), a function allowing for a change in the domain morphology is employed. The Guth function

$$\gamma' = E/E_0 = 1 + 0.67\, p\varphi_S + 1.62 p^2 \varphi_S^2 \tag{6}$$

applies for rigid rodlike filler particles, p being a shape factor (length/diameter).[23,24] If one calculates the ratio p/p_0 (where p_0 is the value of the shape factor at $\varphi_S = \varphi_{S,0}$ and p is its value at a degree of oil extension corresponding to φ_S) for polymers of various initial compositions, the set of curves given in Figure 8 is obtained. It can be seen that for each polymer the ratio p/p_0 should vary in a complicated manner with the volume fraction of glassy domains in order to accomodate the experimental tensile modulus data. The shape of the curves would indicate a transition from elongated domains (lamellae or rods) towards more spherical shapes. It is however interesting to note that the morphological transition seems to be dependent on $\varphi_{S,o}$. At this point a more detailed discussion of the phenomenon would be in order.

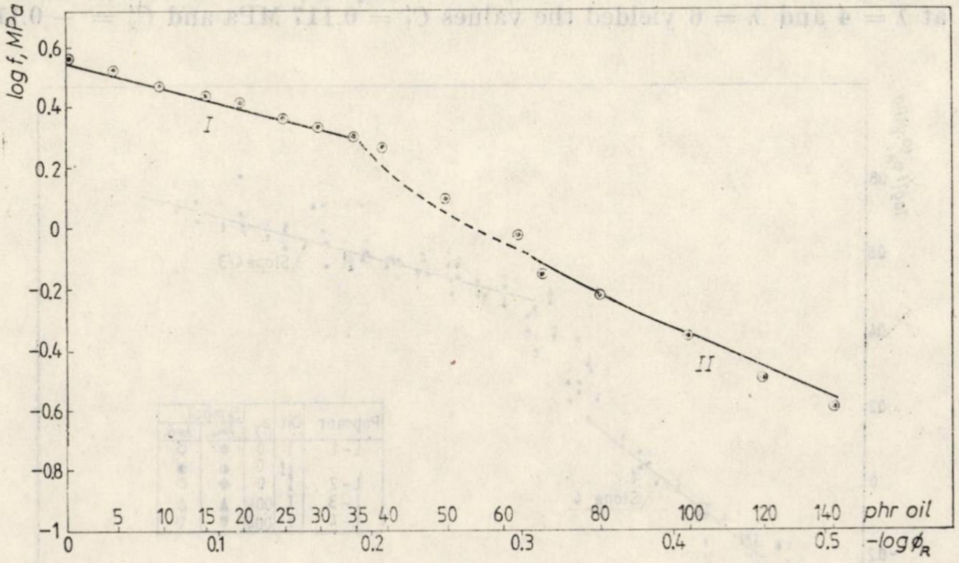

Fig. 7. — Experimental (—) and calculated (○) modulus of polymer *L*—1 extended with oil I ($\lambda = 6$).

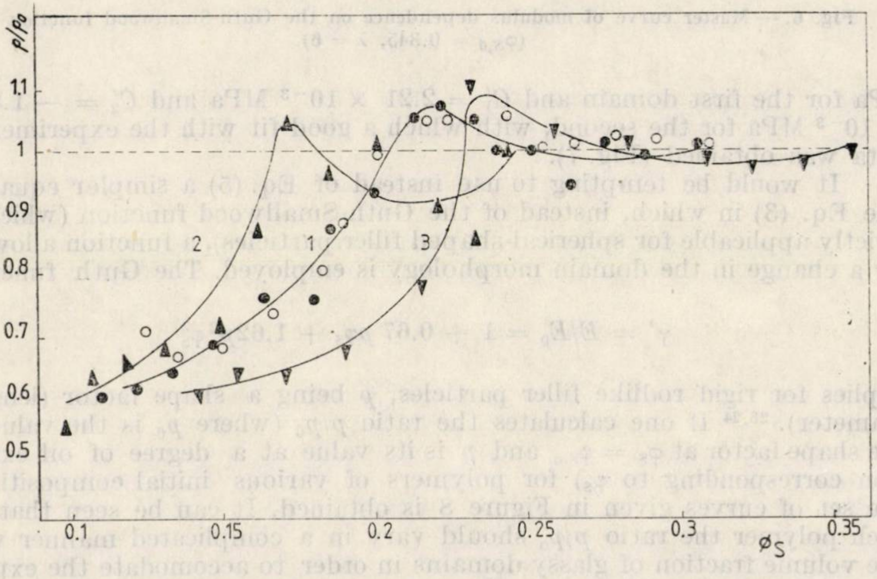

Fig. 8. — Variation of shape factor with volume fraction of polystyrene ($\lambda = 4$). 1, *L*—1 ; 2, *L*—3; 3, *L*—4 ; ●, ▲, ▼, Oil I ; ○, Oil II.

In a block copolymer the morphology of the domains depends primarily on the volume fraction of the disperse phase.[25-28] By diluting the network of a block copolymer with initially lamellar morphology with a selective solvent for polybutadiene (the case of paraffinic-naphthenic extender oils) morphological transitions are expected to occur as rodlike and then spherical domains become thermodynamically increasingly favored.[27] At low oil concentrations in the matrix the polymers investigated in this study probably have, depending on $\varphi_{S,o}$, either a lamellar or rodlike morphology (i.e. containing domains extending over distances considerably longer than their characteristic length) or spherical domains interconnected by polystyrene bridges, in films cast from a common solvent (toluene). At large strains the continuous polystyrene phase is extensively broken but large domain aggregates still remain intact immobilizing part of the elastic matrix. As a consequence the modulus decreases only relatively slowly with the concentration of extender oil, probably on account of decreasing size of domain aggregates. At a certain critical degree of dilution a morphological transition to isolated spherical domains is likely to occur, accompanied by the sudden drop in modulus identified in Figure 2.

It would be reasonable to expect such a transition to occur at the same φ_S for all the polymers investigated. This is, however, not the case as seen from Figure 9 in which the modulus at $\lambda = 6$ was plotted against φ_S for polymers $L-1$, $L-3$ and $L-4$, and also from Figures 3 and 8.

It seems that not only the volume fraction of PS but also the concentration of oil in the elastomeric matrix exerts an influence on the

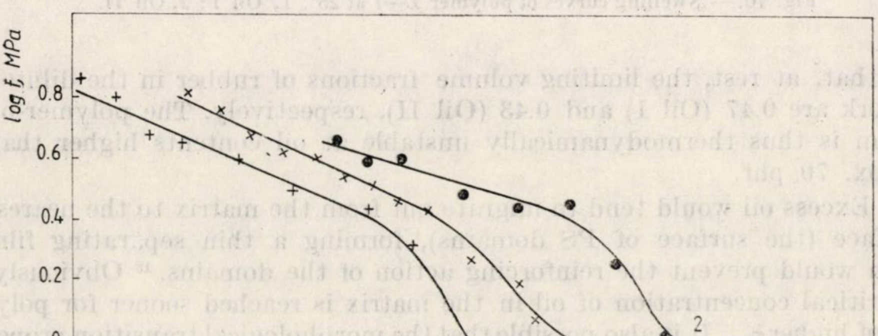

Fig. 9. — Dependence of tensile modulus at $\lambda = 6$ on volume fraction of polystyrene. 1, L—1 ; 2, L—3 ; 3, L—4.

onset of the transition. A possible mechanism for this action was suggested by Leonard[18] who showed by thermodynamic calculations that the reinforcing effect of the domains was supposed to decrease strongly with matrix dilution, becoming nil at $\varphi_R = 0.3-0.5$ with a negative contribution at higher degrees of dilution. According to Leonard at higher oil concentrations oil would separate from the extended matrix forming a distinct phase. From equilibrium swelling measurements performed with polymer $L-1$ with oils I and II at room temperature (Fig. 10) it can be seen that, at rest, the limiting volume fractions of rubber in the diluted network are 0.47 (Oil I) and 0.43 (Oil II), respectively. The polymer-oil system is thus thermodynamically unstable at oil contents higher than approx. 70 phr.

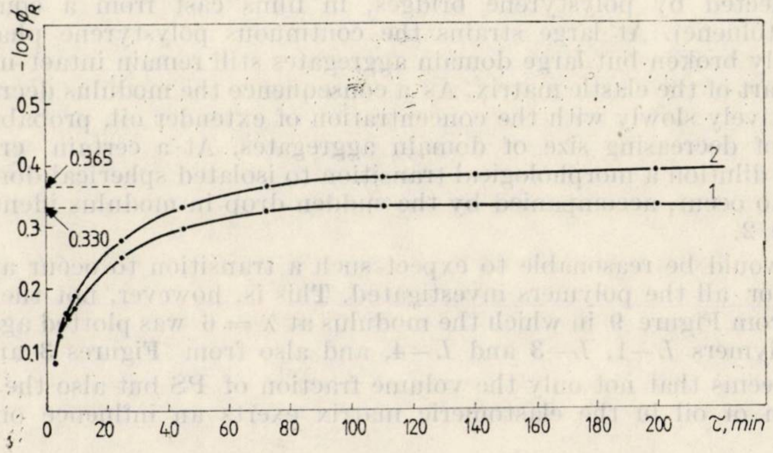

Fig. 10. — Swelling curves of polymer L—1 at 25°. 1, Oil I; 2, Oil II.

Excess oil would tend to migrate out from the matrix to the nearest interface (the surface of PS domains), forming a thin separating film which would prevent the reinforcing action of the domains.[18] Obviously, the critical concentration of oil in the matrix is reached sooner for polymers of higher $\varphi_{S.o}$. It is also possible that the morphological transition proper be assisted by the presence of oil in the matrix beyond a critical concentration.

2.2. Effect of Polymer Structure

In contrast to the other linear polymers investigated, polymer $L-2$, synthesized by a two-step process, is characterized by the presence of unevenly distributed styrene units in the center block, the density of such units increasing towards the second PS end block. The density of styrene units along chain length (defined as the sum of bond lengths in the backbone, $l = \int_0^M \{[l_S P_S + (1 - P_S) l_B]/[M_S P_S + M_B\ (1 - P_S)]\}$, where P_S is the instantaneous wt. fraction of styrene at the chain end of molecular weight M, $l_S = 0.308$ nm and $l_B = 0.595$ nm are the segment lengths of styrene and butadiene, respectively, and M_S and M_B are the mol. wts. of the monomers) calculated by using the mathematical model of the anionic copolymerization of butadiene with styrene described earlier[29] with the reactivity ratios $r_S = 0.0041$ and $r_B = 12.9$[30] is given in Figure 11.

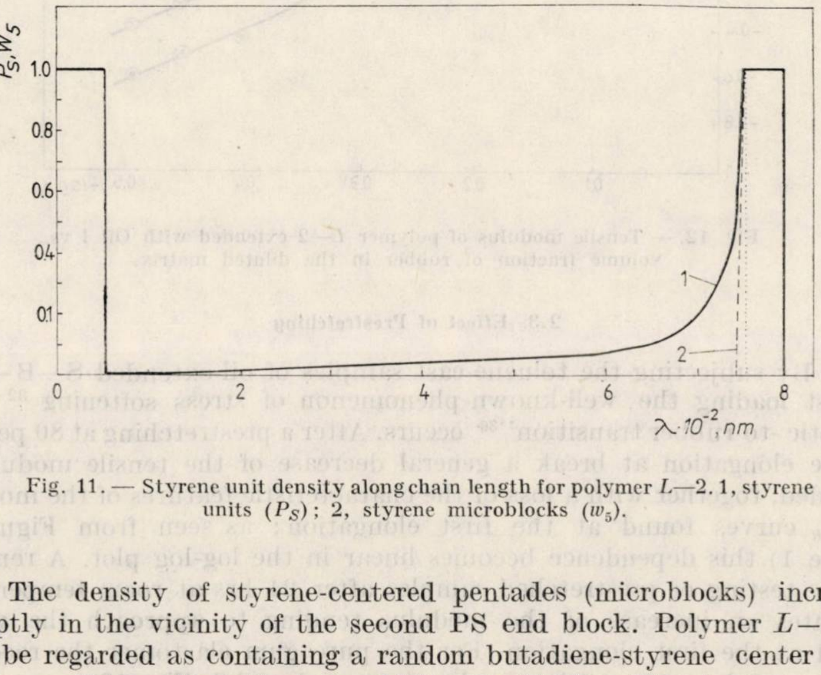

Fig. 11. — Styrene unit density along chain length for polymer L—2. 1, styrene units (P_S); 2, styrene microblocks (w_5).

The density of styrene-centered pentades (microblocks) increases abruptly in the vicinity of the second PS end block. Polymer $L-2$ can thus be regarded as containing a random butadiene-styrene center block and a small transition block in which microblocks of the two monomers are non-uniformly distributed. The correlations between segmental density along the main chain and the thickness of the interphase layer, and between size and structure of interphase layer and mechanical properties are not yet well understood. In any case, the "tapered" or "graded" structure of polymer $L-2$ is likely to lead to a thicker interphase than that of the otherwise similar "pure" triblock copolymer $L-1$.[31]

The modulus of $L-2$ shows a similar variation with the content of extender oil to that of polymer $L-1$ (Fig. 12). However, the transition between the two zones is shifted towards higher oil concentrations. An explanation could be that the thicker interphase layer can be penetrated only superficially by Oil I and thus the apparent φ_s is always larger than that of polymer $L-1$.

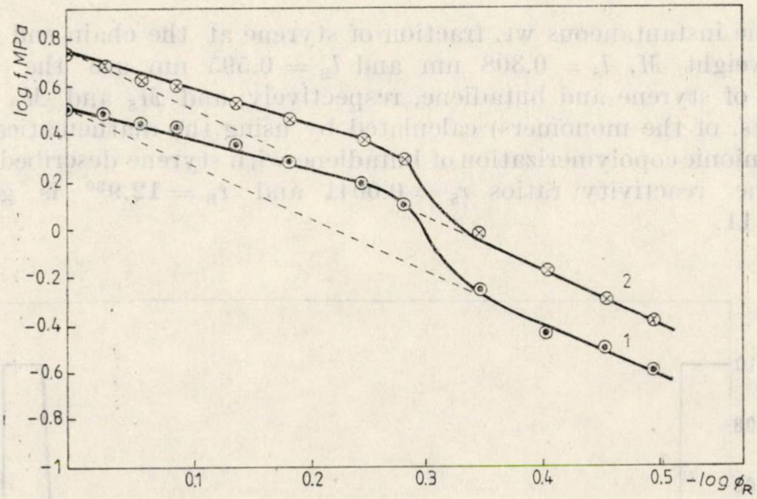

Fig. 12. — Tensile modulus of polymer L—2 extended with Oil I vs. volume fraction of rubber in the diluted matrix.

2.3. Effect of Prestretching

By subjecting the toluene-cast samples of oil-extended S—B—S to a first loading the well-known phenomenon of stress softening [32–35] or "plastic-to-rubber transition"[36] occurs. After a prestretching at 80 percent of the elongation at break a general decrease of the tensile modulus is recorded, together with a loss of the characteristic features of the modulus vs. φ_R curves found at the first elongation; as seen from Figure 13 (curve 1) this dependence becomes linear in the log-log plot. A renewed tensile testing of prestretched samples after 24 hrs at room temperature indicates an increase of the modulus tending to approach the values found at the first elongation. For the pure gum elastomer the recovery of the modulus at $\lambda = 4$ is complete (curves 2 and 3, Fig. 13).

The effect of prestretching can be explained by the disruption of the long-range continuous polystyrene phase discussed above (§ 2.1). In the softened elastomer the polystyrene phase is largely discontinuous and thus the polymer behaves more like a conventional filled crosslinked rubber. Upon resting, even at room temperature, the continuity of the glassy phase is restored to a certain extent but the dilution of the elastic network seems to prevent a complete healing.

In the $f/\varphi_R^{1/3} - \gamma$ plot the discontinuity previously found for virgin samples is absent and the experimental data fit a straight line of slope 3 (Fig. 14).

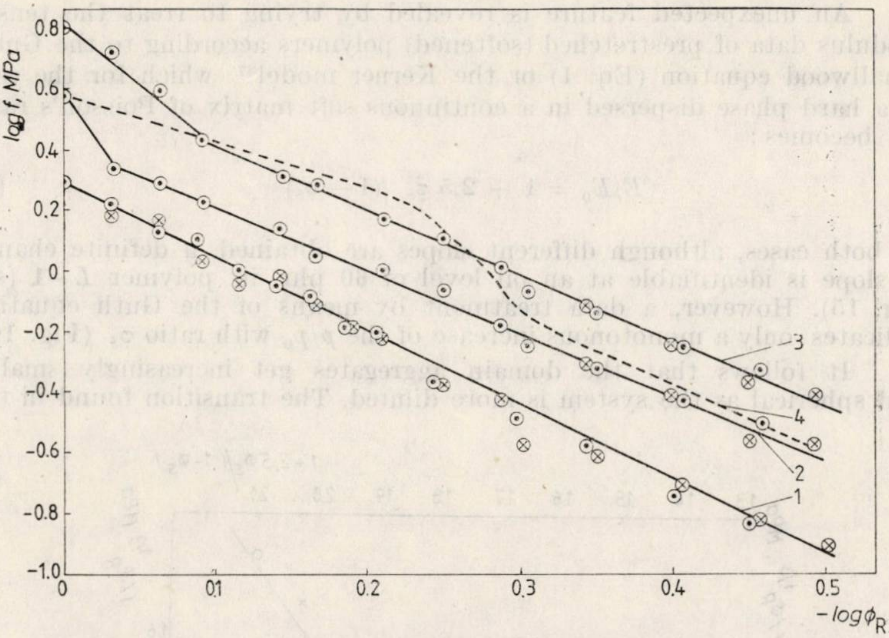

Fig. 13. — Effect of prestretching at 80 % of the elongation at break on modulus of polymer *L*—1. 1, at λ = 4 immediately after the first elongation ; 2, at λ = 4 after first elongation and 24 h recovery ; 3, at λ = 6 after elongation and recovery ; 4, modulus at first elongation ; ⊙ Oil I, ⊗ Oil II.

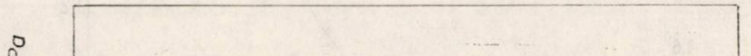

Fig. 14. — Variation of the $f/\varphi_R^{1/3}$ ratio with the Guth-Smallwood function for prestretched samples of polymer *L*—1 extended with Oil I. ○ λ = 4 ; × λ = 6.

An unexpected feature is revealed by trying to treat the tensile modulus data of prestretched (softened) polymers according to the Guth-Smallwood equation (Eq. 1) or the Kerner model[37] which for the case of a hard phase dispersed in a continuous soft matrix of Poisson's ratio 0.5 becomes:

$$E/E_0 = 1 + 2.5\,\varphi_s\ /(1-\varphi_s) \qquad (7)$$

In both cases, although different slopes are obtained, a definite change of slope is identifiable at an oil level of 60 phr in polymer $L-1$ (see Fig. 15). However, a data treatment by means of the Guth equation indicates only a monotonous increase of the p/p_0 with ratio φ_s (Fig. 16).

It follows that the domain aggregates get increasingly smaller and spherical as the system is more diluted. The transition found in the

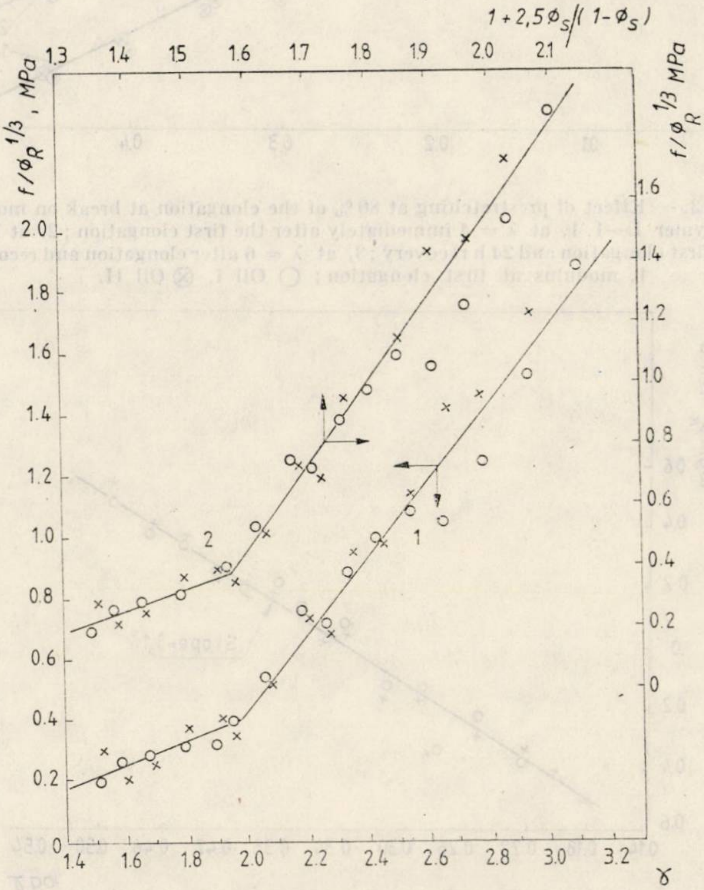

Fig. 15. — Dependence of $f/\varphi_R^{1/3}$ on the Guth-Smallwood (1) and Kerner (2) functions (prestretched samples of polymer L—1).
● Oil I; × Oil II.

Kerner and Guth-Smallwood plots is probably due to the separation of oil from the matrix.

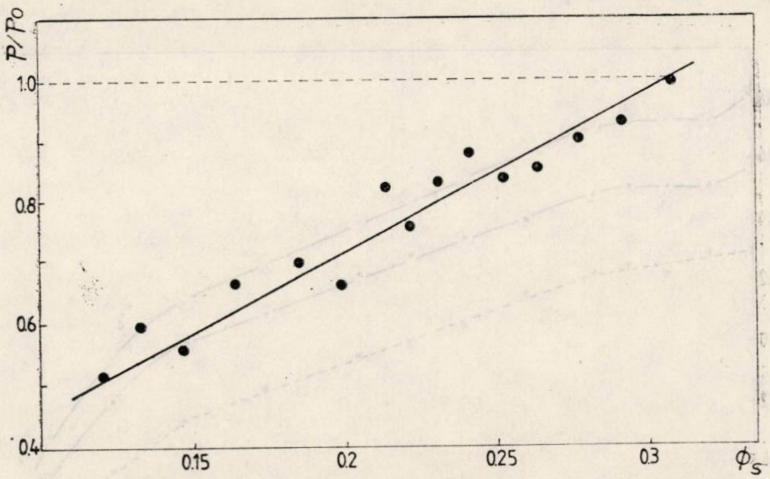

Fig. 16. — Variation of the shape factor with the volume fraction of polystyrene for prestretched samples of polymer *L*—1 cast from toluene.

2.4. Effect of Oil Composition

As seen from the data presented in the preceding sections, the differences between the mechanical properties of polymer samples extended with the two type of naphthenic-paraffinic oils tested are not essential. On the contrary, the use of a highly aromatic oil (Oil III) for the extension of block copolymers leads to strikingly different results.

A first interesting observation is that tensile moduli of S—B—S extended with aromatic oil are higher than expected, considering the plasticizing effect of the aromatic hydrocarbons on polystyrene (the higher compatibility of aromatic oil with PS was demonstrated by the data given in § 1). Thus, in a $f - \varphi_R$ diagram (Fig. 17) the tensile modulus of polymer *L*—1 shows a small decrease at 5 phr followed by a plateau of constant *f* and then, above 20 phr oil a decrease with a slope similar to that of polymers extended with naphthenic-paraffinic oils. At the highest oil levels used (120 and 140 phr) a steep decrease in modulus is noticed.

In the $f/\varphi_R^{1/3} - \gamma$ plot (Fig. 18) the middle portion of the curve has a slope of 5/2, less than that of polymers extended with naphthenic-paraffinic oils, but closer to the slope found for prestretched samples.

The behaviour of S—B—S extended with aromatic oil is probably determined by the increased absorption of oil hydrocarbons in the polystyrene domains, which brings about an increase of their volume. Below 20 phr Oil III this practically compensates the dilution of the polymer by oil and even at higher oil levels it opposes the effect of oil extension.

After a first stretching at $\lambda = 7$ a stress softening occurs (see curve 3, Fig. 17) but the general shape of the curve is little altered.

This can also be seen from curve 2, Figure 18, of a shape similar to that of the plot for virgin polymers and in which the linear portion of the plot has a similar slope.

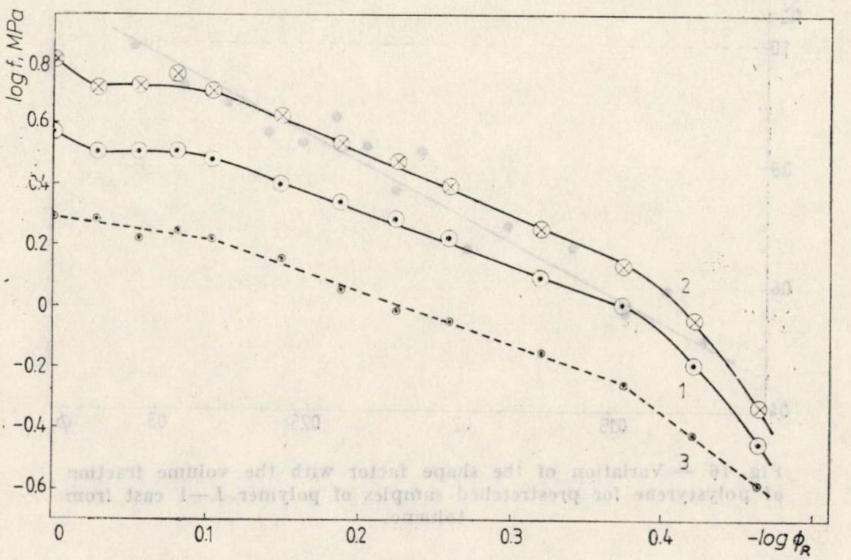

Fig. 17. — Tensile modulus of polymer *L*—1 extended with Oil III vs. volume fraction of rubber in the diluted matrix. 1, λ = 4 ; 2, λ = 6 ; 3, λ = 4 after prestretching at λ = 7.

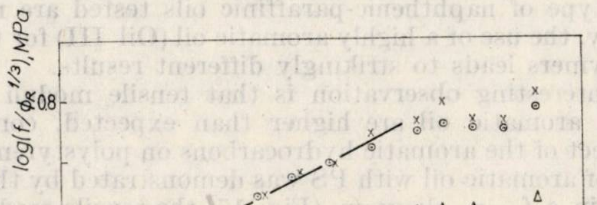

Fig. 18. — Dependence of $f/\varphi_R^{1/3}$ on the Guth-Smallwood function for polymer *L*—1 extended with Oil III. 1, first traction ; 2, after prestretching at λ = 7, ⊙, Δ, λ = 4 ; ×, λ = 6.

It can be assumed that the oil-plasticized polystyrene continuum readily fragmentates under strain throughout the oil concentration range investigated. This fragmentation is probably promoted by the presence of even small amounts of aromatic oil, as seen from the decrease in modulus at 5 phr where the swelling effect is not yet high enough. At least in the case of block copolymers extended with aromatic oils the mechanism suggested by Leblanc[35] involving the participation of the interphase layer in forming the continuous polystyrene superstructure; it is reasonable to assume that this layer is the main locus of swelling with oil and that the breaking of the continuous glassy phase occurs along interphase-interphase boundaries.

If the assumption of strong swelling of the domain-interphase layer system (DILS) by oil is correct, this effect would act against morphological transitions in the material, tending to preserve the initial morphology of the sample by increasing the volume of DILS. This view is supported by the plot based on Eq. (6) (Fig. 19) which indicates a conservation of the shape of the domains (on rather DILS) up to 100 phr Oil III. The abrupt modulus decrease at oil levels above 100 phr could thus be ascribed either to a loss of domain cohesion by the absorption of aromatic hydrocarbons (with a corresponding drop of T_g to near room temperature) or to a morphological transition of the DILS. At 100 phr $\varphi_S = 0.16$. Assuming that below 100 phr the initial morphology was conserved (i.e. that at $\varphi_{S,o} = 0.31$), then a doubling of the volume by swelling has to be assumed. Actually, the volume of the interphase layer is rather important even in the pure gum polymer : the thermodynamic calculations performed by Meier [38] show that the interphase layer constitutes 25 % of the total volume of a block copolymer with $M_{PS} = M_{PB}$ at a total mol. wt. of 10^5 g·mole^{-1}.

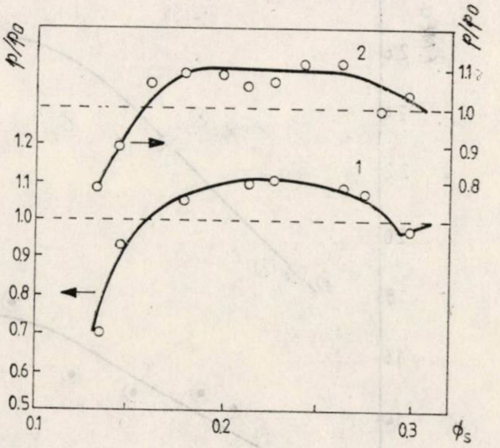

Fig. 19. — Variation of the shape factor with the volume fraction of polystyrene for polymer L—1 extended with Oil III, at $\lambda = 4$. 1, first traction ; 2, after prestretching at $\lambda = 7$.

In a separate set of experiments the tensile modulus of polymer L—1 extended with a constant amount of oil (50 phr) of variable composition (mixtures of Oil I and Oil III in different proportions) was measured. The results are given in Figure 20.

It can be seen that up to approximately 25 percent of aromatic C atoms in oil the modulus shows a continuous increase, but at higher oil aromaticity the effect levels out. This may be interpreted in terms of a partial "saturation" of the DILS or at least of the domain core with aromatic hydrocarbons. The aromatic C level at which the saturation takes place is roughly correspondent to the amount of aromatic oil at which the modulus begins to decrease in samples extended with Oil III alone.

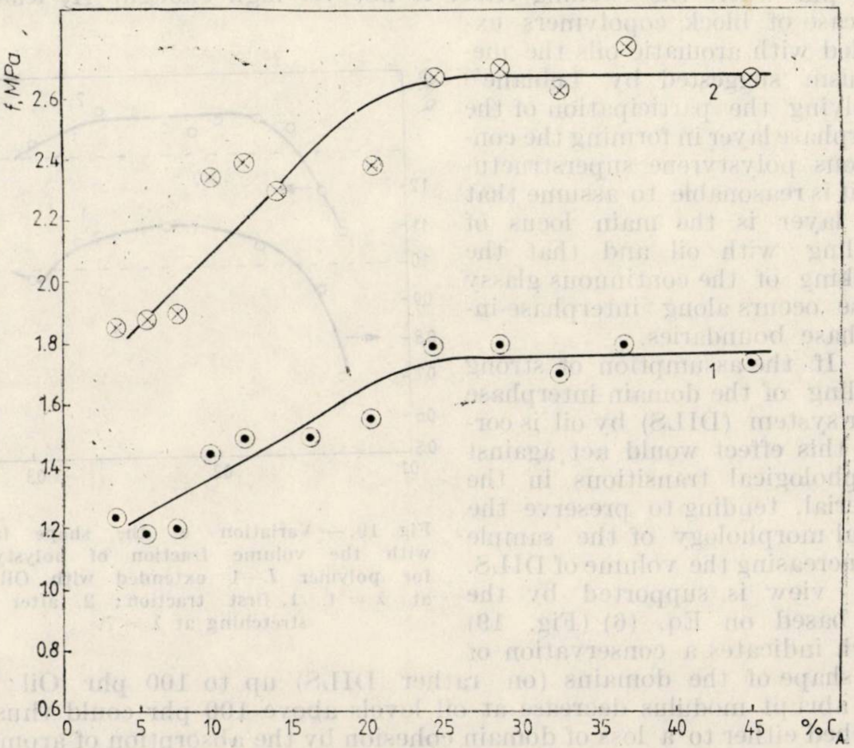

Fig. 20. — Effect of oil composition on the tensile modulus of polymer *L*—1 extended with 50 phr oil. 1, $\lambda = 4$; 2, $\lambda = 6$.

2.5. Effect of Casting Solvent

The profound effect of solvent on the morphology and properties of cast films of block or graft copolymers [28,31,32,39–45] is well known. In films cast from a solvent selective from one of the blocks the opposite blocks collapse and form the discrete domains dispersed in a matrix consisting of the better solvated blocks. Thus, a solvent selective for polybutadiene like cyclohexane (a θ solvent for polystyrene at 34.5°) inhibits an extensive interconnection of the PS domains and thus the formation of a continuous glassy phase. The aspect of the pure gum films cast from cyclohexane is soft and rubberlike in contrast with the leathery aspect of toluene cast films.

The $f - \varphi_R$ plots of cyclohexane cast films of polymer *L*—1 extended with Oil I do not show the features of films cast from toluene. As seen from Figure 21 the plots are linear indicating a monotonous decrease of modulus with oil level at both $\lambda = 4$ and $\lambda = 6$.

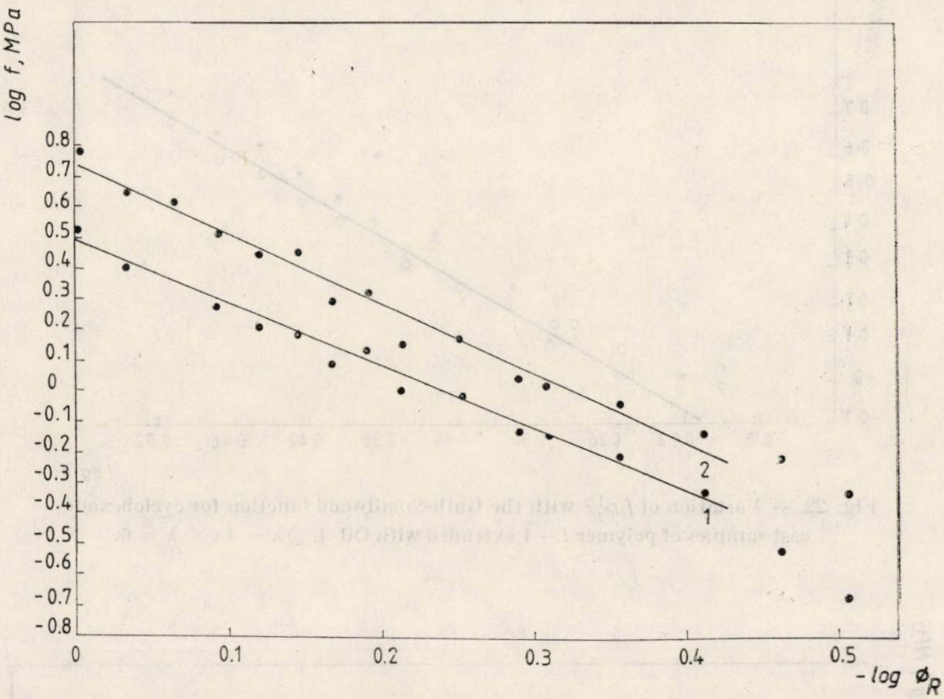

Fig. 21. — Dependence of tensile modulus on oil level for cyclohexane-cast samples of polymer L—1 extended with Oil I. 1, $\lambda = 4$; 2, $\lambda = 6$.

In the $f/\varphi_R^{1/3} - \gamma$ plot (Fig. 22) the experimental points also fit a straight line of slope = 3. It can thus be hypothesized that no morphological transition proper occurs in the series of cyclohexane cast films. Instead, a gradual passage from loose aggregates to isolated PS spheres probably takes place.

3. MODULUS OF STAR BLOCK COPOLYMERS

The effect of oil level on the tensile modulus of star block copolymers is strikingly different from that found for S—B—S block copolymers. This is illustrated by the plots given in Figures 23 and 24.

It can be seen that the dependence of f on φ_R is more complicated than for S—B—S; for all $\varphi_{S,o}$ an initial decrease of f with oil level is recorded, followed by a plateau or even an increase of modulus in the middle range of oil contents. At high oil levels a general decrease of the tensile modulus takes place. Only for $S - 1$, which has the lowest $\varphi_{S,o}$ the $f - \varphi_R$ dependence approaches that of S—B—S. Rather surprisingly,

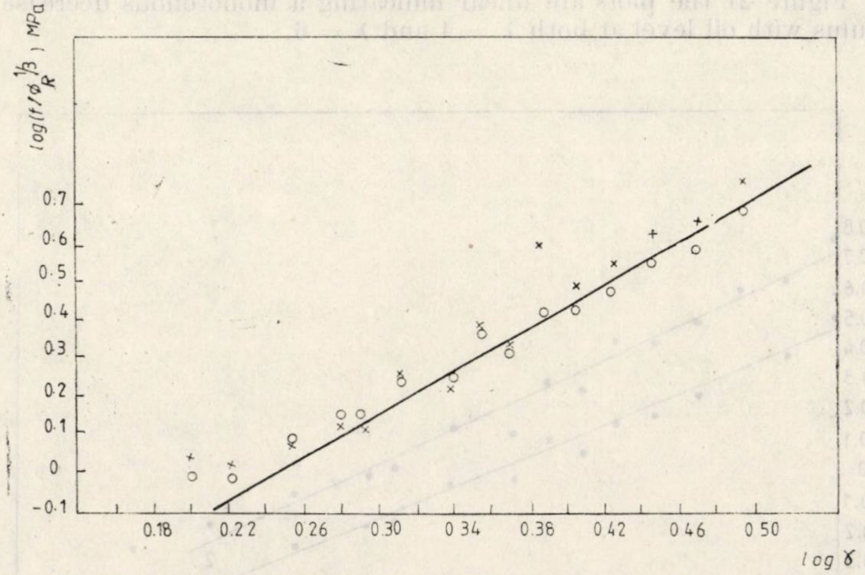

Fig. 22. — Variation of $f/\varphi_R^{1/3}$ with the Guth-Smallwood function for cyclohexane-cast samples of polymer *L*—1 extended with Oil I. ○ $\lambda = 4$; × $\lambda = 6$.

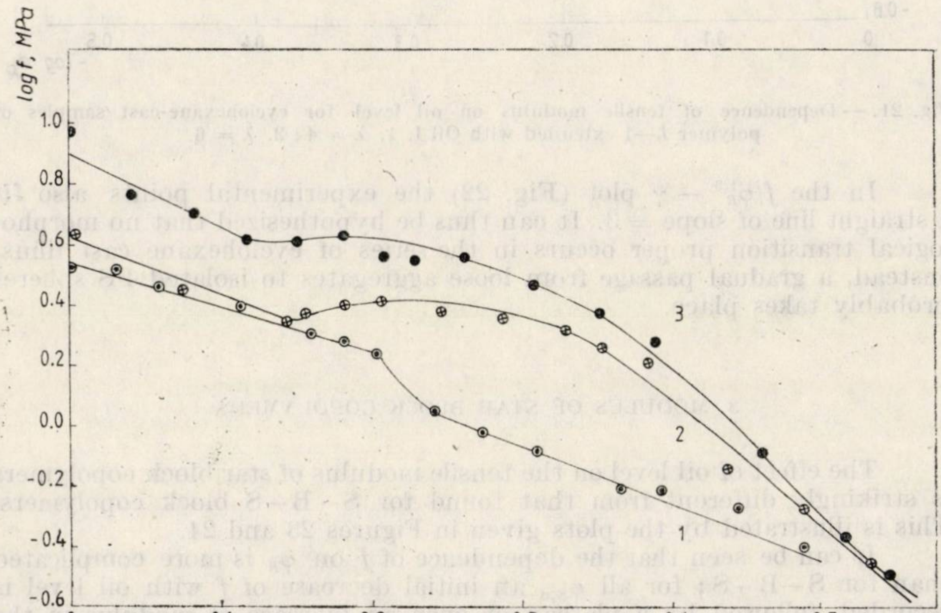

Fig. 23. — Tensile modulus of star block copolymers at $\lambda = 4$ vs. volume fraction of rubber in the matrix extended with Oil I. 1, *S*—1 ; 2, *S*—2 ; 3, *S*—3.

the transition from the initial descending slope of f to the plateau seems to be dependent on φ_R only, at least for the polymers richer in styrene. A possible interpretation of this fact would be that in the case of star block copolymers the controlling factor of the morphological transition assumed to take place is the concentration of oil in the elastomeric matrix rather than the volume fraction of polystyrene domains.

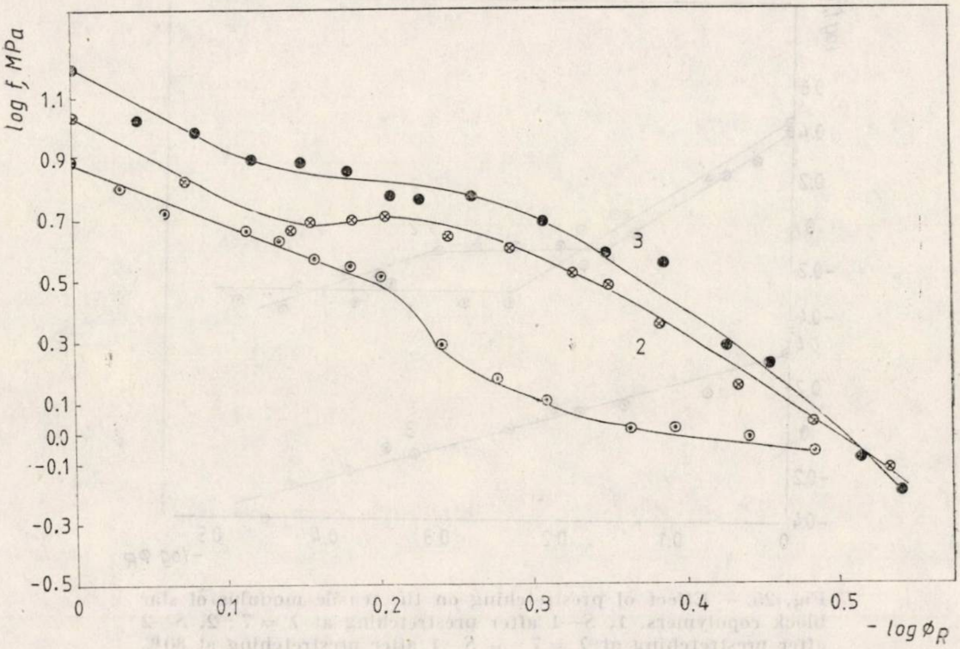

Fig. 24. — Tensile modulus of star block copolymers at $\lambda = 6$ vs. Volume fraction of rubber in the matrix extended with Oil I. 1, S—1 ; 2, S—2 ; 3, S—3.

Investigations on the morphology of star block copolymers [31,46,47] have shown that the regularity of the domains is sharper than in the case of their linear counterparts of similar chemical composition, this being a consequence of better phase separation. The basic domain shapes are similar, except for multichain star block copolymers with a large number of arms where regularly arranged but distorted domains of a characteristic sickle shape have been identified [31]. It may be assumed that morphological transitions would be sharper in the case of star block copolymers, hence an "assisting" effect of oil would be stronger felt. It is also possible that, due to the higher density of the elastic network of star block copolymers (deriving from the presence of a fixed entanglement in the elastomeric block of each molecule), the local oil concentration at the domain/matrix interface is higher under stress than for S—B—S block copolymers at the same overall oil concentration in the rubbery matrix.

The effect of prestretching on the tensile modulus of star block copolymers is illustrated in Figure 25. As in the case of S—B—S, immediately after a first elongation at 80 percent of the elongation at break the features of the initial $f - \varphi_R$ curve are lost (curve 3). If, instead, the polymer is subjected to a first elongation at $\lambda = 7$, then the modulus

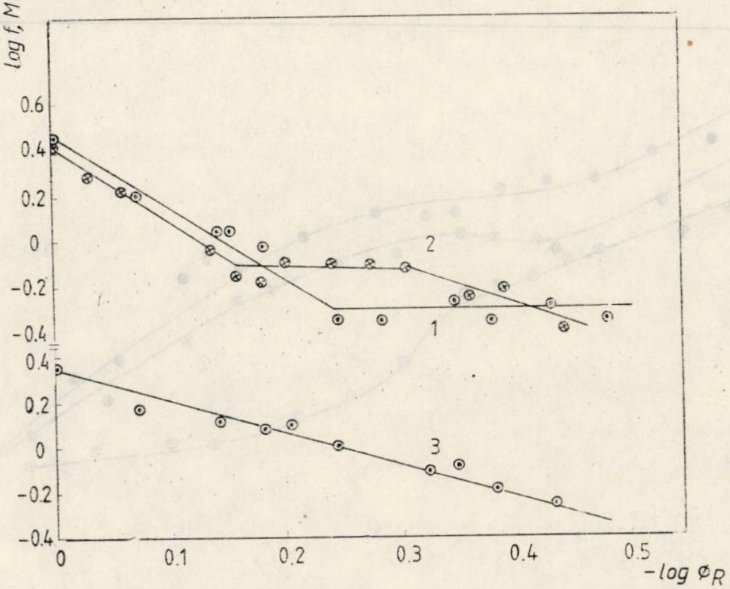

Fig. 25. — Effect of prestretching on the tensile modulus of star block copolymers. 1, S—1 after prestretching at $\lambda = 7$; 2, S—2 after prestretching at $\lambda = 7$; 3, S—1 after prestretching at 80% of the elongation at break.

measured at $\lambda = 4$ (curves 1 and 2) shows an initial decrease followed by a plateau. Hence, the disruption of the initial structure of the material is incomplete at $\lambda = 7$ and, due to the decrease of the modulus of the matrix, the stresses exerted upon the domains decrease and the original morphology is altered less with increasing oil level.

REFERENCES

[1] Part I : E. Ceauşescu, R. Bordeianu, P. Ghioca and M. Bălănescu, *Mat. Plast.*, **17**, 201 (1980).

[2] F. M. McMillan, in "Rubber Technology", M. Morton, ed., Reinhold., New York, 1959, p. 151.

[3] E. B. Storey, *Rubber Chem. Technol.*, **34**, 1402 (1961).

[4] C. Paton, in "Plasticisers, Stabilisers and Fillers", P. D. Ritchie ed., Iliffe, London, 1972, p. 39.

[5] J. M. Heaps, *ibid.*, p. 50.

[6] E. A. Lazurin and L. V. Kosmodem'yanskii, "Manufacture and Properties of Oil-Extended Polymers" (Russ.) Ser. Prom. Sint. Kaut., Tsentr. Nauch.-Issl. Inst. Inform. Tekh.-Ekon. Issl. Neftepererab. Neftekhim. Prom., Moscow, 1979.

[7] A. Rudin, and D. Burgin, *Polymer*, **16**, 291 (1975).
[8] G. Kraus and K. W. Rollman, *J. Polymer Sci., Polymer Phys. Ed.*, **14**, 1133 (1976).
[9] J. K. Gillham and R. F. Boyer, *Polymer Prepr.*, **18** (2), 468 (1977).
[10] P. L. Kumler, S. E. Keinath and R. F. Boyer, *Polymer Prepr.*, **18**, 313 (1977).
[11] S. E. Keinath, P. L. Kumler and R. F. Boyer, *Polymer Prepr.*, **16**, 120 (1975).
[12] D. C. Douglass and V. J. McBrierty, *J. Chem. Phys.*, **54**, 4085 (1971).
[13] R. F. Fedors, *J. Polymer Sci. C*, **26**, 189 (1969).
[14] R. S. Rivlin, in "Rheology", F. R. Eirich ed., Vol. 1, Academic Press, New York, 1956, p. 351.
[15] L. Mullins and N. R. Tobin, *J. Appl. Polymer Sci.*, **9**, 2993 (1965).
[16] H. M. Smallwood, *J. Appl. Phys.*, **15**, 758 (1944).
[17] G. Holden, E. T. Bishop, and N. R. Legge, *J. Polymer Sci. C*, **26**, 37 (1969).
[18] W. J. Leonard, *J. Polymer Sci. Polymer Symp.*, **54**, 237 (1976).
[19] S. M. Gumbrell, L. Mullins and R. S. Rivlin, *Trans. Faraday Soc.*, **49**, 1945 (1953).
[20] P. J. Flory, A. Ciferri and C. A. J. Hoeve, *J. Polymer Sci.*, **45**, 235 (1960).
[21] P. J. Flory and Y.-I. Tatara, *J. Polymer Sci. Polymer Phys. Ed.*, **13**, 683 (1974).
[22] M. Shen, in "Science and Technology of Rubber", F. R. Eirich ed., Academic Press, New York, 1978, p. 155.
[23] E. Guth, "Proc. 2nd Rubber Technol. Conf.", London, 1948, p. 353.
[24] R. F. Fedors, in "The Stereo Rubbers", W. M. Saltman ed., Wiley, New York, 1977, p. 679.
[25] G. E. Molau, in "Block Copolymers", S. L. Aggarwal ed., Plenum Press, New York, 1970, p. 102.
[26] A. E. Skoulios, in "Block and Graft Copolymers", J. J. Burke and V. Weiss eds., Syracuse Univ. Press, Syracuse N.Y., 1973, p. 121.
[27] D. J. Meier, *ibid.*, p. 105.
[28] T. Uchida, T. Soen, T. Inoue and H. Kawai, *J. Polymer Sci.*, A-2, **10**, 101 (1972).
[29] E. Ceaușescu, R. Bordeianu, M. Bălănescu, I. Cerchez, P. Ghioca, G. Benescu and M. Tănăsescu, in E. Ceaușescu "Noi cercetări în domeniul compușilor macromoleculari", Ed. Academiei R.S.R., Bucharest, 1981, p. 225.
[30] R. Ohlinger and F. Bandermann, *Makromol. Chem.*, **181**, 1935 (1980).
[31] S. L. Aggarwal, *Polymer*, **17**, 938 (1976).
[32] J. F. Beecher, L. Marker, R. S. Bradford and S. L. Aggarwal, *J. Polymer Sci., C*, **26**, 117 (1969).
[33] M. Morton, J. E. McGrath and P. C. Juliano, *J. Polymer Sci., C*, **26**, 99 (1969).
[34] E. Pedemonte, G. Dondero, G. C. Alfonso and F. de Candia, *Polymer*, **16**, 531 (1975).
[35] J. L. Leblanc, *J. Appl. Polymer Sci.*, **21**, 2419 (1977).
[36] T. Kotaka, T. Miki and K. Arai, *J. Macromol. Sci.-Phys. B* **17**, 303 (1980).
[37] E. H. Kerner, *Proc. Phys. Soc. (London)*, **69B**, 808 (1956).
[38] D. J. Meier, *Polymer Prepr.*, **15**, 171 (1974).
[39] F. M. Merrett, *J. Polymer Sci.*, **24**, 467 (1957).
[40] M. Shen, E. H. Cirlin and D. H. Kaelble, *Polymer Prepr.*, **11**, 686 (1970).
[41] E. F. Bradford, *Polymer Prepr.*, **11**, 392 (1970).
[42] N. K. Kalfoglou, *J. Appl. Polymer Sci.*, **23**, 2673 (1979).
[43] H. Kawai, T. Soen, T. Inoue, T. Ono and T. Uchida, *Mem. Fac. Eng. Kyoto Univ.*, **33**, 383 (1971).
[44] M. Morton, L. J. Fetters, F. C. Schwab, C. R. Strauss and R. F. Kammereck, "4th Internat. Synth. Rubber Symp.", London, **3**, 70 (1969).
[45] G. S. Fielding-Russell, *Rubber Chem. Technol.*, **45**, 252 (1972).
[46] L.-K. Bi, L. J. Fetters and M. Morton, *Polymer Prepr.*, **15**, 157 (1974).
[47] L.-K. Bi and L. J. Fetters, *Macromolecules*, **8**, 90 (1975).

Revue Roumaine de Chimie, 28, 4, 325–332 (1983)

CATALYTIC OXIDATION OF AMMONIA. IV[1–3]

LOW TEMPERATURE OXIDATION ON A NICKEL OXIDE CATALYST SUPPORTED ON ALUMINA

M. M. GIRGIS*, D. P. LAZĂR** and E. I. SEGAL***

* Faculty of Science, Department of Chemistry, University of Assiut, Egypt
** The Polytechnic Institute of Jassy, Department of Physical Chemistry, Romania
*** The Polytechnic Institute of Bucharest, Chair of Physical Chemistry and Electrochemical Technology, Bucharest, Romania

Received June 22, 1982

The catalytic oxidation of ammonia, with atmospheric oxygen, was studied using an industrial catalyst, type NiO/Al_2O_3. The oxidation process was carried out at atmospheric pressure, using a dynamic method. The influence of the initial temperature of the reactor (T_i), the flow rate of gaseous reaction mixture and NH_3 concentration in the initial NH_3 + air mixture, as well as some specific phenomena due to the exothermal character of the oxidation process are discussed.

INTRODUCTION

According to the literature data, the catalytic oxidation of ammonia, at low temperature (<400°C), using a nickel oxide catalyst is less studied from catalytical point of view, [4–10] as well as kinetically. The lack of information about some details concerning the ammonia oxidation process on a nickel oxide catalyst and the low cost of this catalyst too have prompted the authors to approach this subject.

In the present paper some kinetic aspects of the ammonia oxidation on a solid NiO catalyst supported on Al_2O_3 are reported. Catalytic oxidation of ammonia was carried out using atmospheric oxygen at normal pressure and applying the flow method previously described. [1]

The influence of the initial temperature of the reactor (T_i), of the reaction mixture flow rate and of the percentage content of NH_3 in the reaction mixture upon the conversion degree of ammonia to reaction products were studied. The experiments were accomplished within the temperature range 236 – 362°C, using gaseous reaction mixtures whose composition varied between 12.58 and 22.44% (v/v) ammonia.

EXPERIMENTAL

Characterisation of the catalyst

The main physical features of the pelletized catalyst are summarized in table 1.

TABLE 1

The main characteristics of the pelletized NiO/Al_2O_3 catalyst

1. Morphologic characterization :

Pellet shape	Pellet diameter (cm)	Particle density ($g \cdot cm^{-3}$)	Specific surface area* ($m^2 \cdot g^{-1}$)
Spherical	0.603	1.48	160.8

2. Quantitative composition :

NiO** %(w/w)	Al_2O_3 %(w/w)	Moisture content %(w/w)
33.8	52.7	13.5

3. X-ray analysis :

Using an X-ray diffraction apparatus, type TUR-M 62 (Made in DDR), K_α radiation of molybdenum and Nb filter, from the intense diffraction lines, characteristic of both non-heated sample and sample preheated at 500°C in air for three hours, it was confirmed that this catalyst contains NiO in the crystalline state and Al_2O_3 in amorphous state.

4. TG and TDA analysis :

It has been observed that during the thermal treatment of the catalyst between 40° and 710°, in air, at a heating rate of $12°K.min.^{-1}$, the weight loss was 13.5% (w/w). It has been found that the thermal process is endothermic in nature.

---

* Determined by physical adsorption of Kr, at liquid nitrogen temperature, degasing of the sample at 200°C.

** Precipitation with dimethyl glyoxime.

RESULTS AND DISCUSSIONS

The reaction for ammonia oxidation was already described in a previous paper. [1]

1. *Influence of the initial temperature of the reactor (T_i) over the temperature distribution alongside the reactor*

Using a reaction mixture with 12.58% (v/v) ammonia, at a flow rate of $27.77\ cm^3 \cdot s^{-1}$, the influence of the initial temperature of the reactor (T_i) over the conversion degree of ammonia has been investigated.

When $T_i \geqslant 279°C$, the oxidation of ammonia behaves as a strong exothermal chemical process, being able to disturb the initial temperature distribution of the reactor. This perturbation takes place following a certain "induction period", measured from the moment when the reactant gases entered into the reactor and it appears as a well-marked "temperature peak", initially positioned in the middle of the reactor, completely filled-up with pelletized catalyst. This "temperature peak" slowly moves towards the reactor entrance where becomes stable, simultaneously with noticeable growing in altitude. The time required for the displacement of the "temperature peak" from its formation zone to the point of stabilization is considered as an "autoacceleration period" of the oxidation process. In its steady position, next to reactor entrance, the "temperature peak" continues to grow-up until it reaches a "stationary maximum value" which is characteristic of the steady state of the oxidation process. The direct visual observation of the reactor fully filled with pelletized catalyst allowed to establish that at a distance of 7.5 — 9.5 cm from the reactor entrance, the packing catalyst became incandescent on the whole cross-section of the reactor.

The luminescent zone had a thickness of about 13 mm (equivalent to two catalyst pellets). It must be pointed that within this incandescent zone, the temperature of the reactor is quite moderate (579°C).

In the same manner as for ammonia oxidation on an $Fe_2O_3 - Cr_2O_3$ catalyst,[1-3] this light emission could eventually be attributed to the "cool flame" phenomenon.

When the oxidation process enters the steady state, this light emission becomes exactly superposed over the " temperature peak", i.e. just near the entrance of the gaseous reaction mixture into the reactor.

Using different values for the initial temperature of the reactor (T_i) and computing the ΔT values (as differences between $T_{\max}$ of the "temperature peak" and T_i values) it has been established that $\Delta T = f(T_i)$, as it is shown in figure 1.

Concerning the data given in figure 1, the highest value for ΔT is that corresponding to $T_i = 279°C$. The G. C. analysis of the reaction products proved that the oxidation process starts, also, for a minimum value of T_i equal to 279°C.

During both induction and autoacceleration periods, the dependence upon time of the conversion degree of ammonia, α, exhibits a specific aspect (Fig. 2).

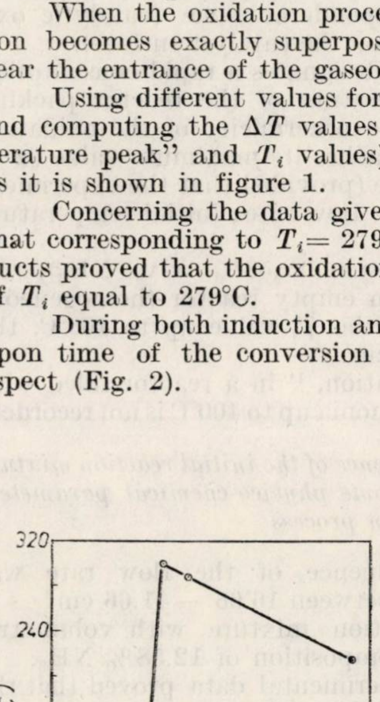

Fig. 1. — Variation of ΔT values vs. T_i (flow rate : 27.77 $cm^3 \cdot s^{-1}$; percentage content of ammonia : 12.58% v/v).

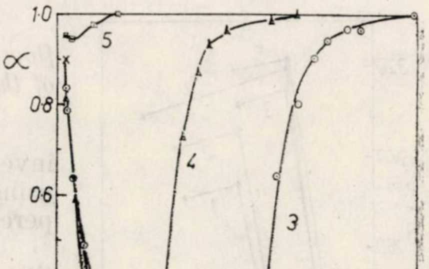

Fig. 2. — Variation of conversion degree (α) vs. reaction time, at different T_i values (flow rate : 27.77 $cm^3 \cdot s^{-1}$; ammonia content : 12.58%, v/v). 1. 236°C ; 2. 269°C ; 3. 279°C ; 4. 290°C ; 5. 362°C.

Firstly, α values decrease with the time elapsed until they reach certain minimum values, characteristic of each T_i value; subsequently α increases again with the time elapsed, until its maximum value ($\alpha = 1.0$). This corresponds to the steady state of the oxidation process, when the conversion of ammonia to reaction products is fully accomplished.

For T_i values smaller than 279°C, the downward fragment of the curves (Fig. 2) can be assigned to some sorption processes of ammonia on the catalyst surface; as for $T_i \geqslant 279°C$, the downward fragment could be assigned both to sorption processes as well as to the true ammonia oxidation process. Along these downward fragments, the temperature of the system increases rather slowly. It is obvious that the lowest values of α in figure 2 indicate the transition from a physically preponderant process (i.e. sorption process) to a chemically preponderant one (catalytic oxidation on the catalyst surface, or initiated on the catalyst surface).

The upward fragment of the curves designates a rapid consumption of ammonia and consequently the temperature of the reactor packing quickly increases owing to the noticeable exothermicity of the oxidation process. When the conversion degree, α, reaches its maximum value ($\alpha = 1.0$), ΔT value reaches also its highest value (provided that the experimental parameters preserve their initial values: flow rate; initial temperature T_i; percentage composition NH_3 : air).

Using the same reaction mixture (i.e. 12.58%, v/v, NH_3), the same flow rate (i.e. 27.77 $cm^3 . s^{-1}$) and an empty reactor (homogeneous kinetic system), it was found that raising the T_i value up to 400°C, the oxidation process of ammonia did not occur.

According to some published information, [11] in a reactor filled with pelletized Al_2O_3 a noticeable oxidation of ammonia up to 400°C is not recorded.

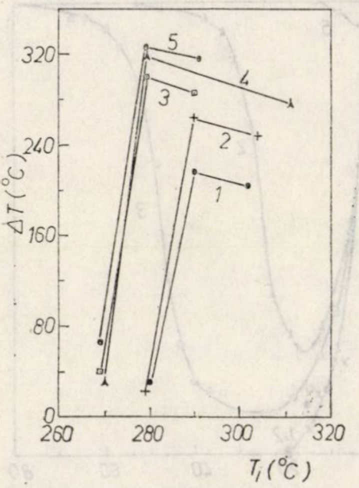

Fig. 3. — Variation of ΔT values vs. T_i, for different flow rates (reaction mixtures with 12.58%, v/v, NH_3). 1. 16.66 $cm^3 \cdot s^{-1}$; 2. 22.22 $cm^3 \cdot s^{-1}$; 3. 27.77 $cm^3 \cdot s^{-1}$; 4. 33.33 $cm^3 \cdot s^{-1}$. 5. 41.66 $cm^3 \cdot s^{-1}$.

2. *Influence of the initial reaction mixture flow rate on some physico-chemical parameters of the oxidation process*

The influence of the flow rate was investigated between 16.66 — 41.66 $cm^3 \cdot s^{-1}$, using a reaction mixture with volumetric percentage composition of 12.58% NH_3.

The experimental data proved that the flow rate variation, within the above mentioned limits, has no significant influence over the general form of ΔT vs. T_i plots (Fig. 3).

However, it was observed that following the increase of the reaction mixture flow rate from 22.22 $cm^3 \cdot s^{-1}$ to 27.77 $cm^3 \cdot s^{-1}$, the initial minimum temperature ($T_{i,\min}$) decreases from 290 to 279°C; also an increase of the corresponding $\Delta T_{\max}$ has been observed.

Investigating, at different $T_{i,\min}$ values, the influence of the flow rate over the temperature distribution alongside the reactor when the oxidation process entered its steady state, it was observed that the increase of the flow rate from 16.66 $cm^3 \cdot s^{-1}$ to 41.66 $cm^3 \cdot s^{-1}$ has no effect on this temperature distribution. For all flow rates used in these experiments, the position of ΔT_{max} exactly located just near the entrance into the reactor.

For flow rate values higher than 22.22 $cm^3 \cdot s^{-1}$, the "temperature peak" formation is associated with the appearance of an incandescent zone, localized in the cross-section of the packed catalyst and extended over about 13 mm, located between 7.5 and 9.5 cm away from the reactor entrance.

When the oxidation process reaches its steady state, the "temperature peak" superposes over the incandescent zone of the catalyst, this last one being located now just at the reactor entrance.

For flow rates smaller than 22.22 $cm^3 \cdot s^{-1}$, the formation of the incandescent zone was not observed.

Figure 4 illustrates the variation of the conversion degree, α, as a function of reaction time, for different flow rates and minimum values of T_i.

From this graphical illustration it has been found that :

— The induction period increases with the flow rate increase.

— When the flow rate exceeds 16.66 $cm^3 \cdot s^{-1}$ an increase of the flow rates determines a corresponding increase of the necessary period for the oxidation process to reach its steady state regime; this period increases from 64 min. for a flow rate of 16.66 $cm^3 \cdot s^{-1}$, to 134 min., for a flow rate of 41.66 $cm^3 \cdot s^{-1}$.

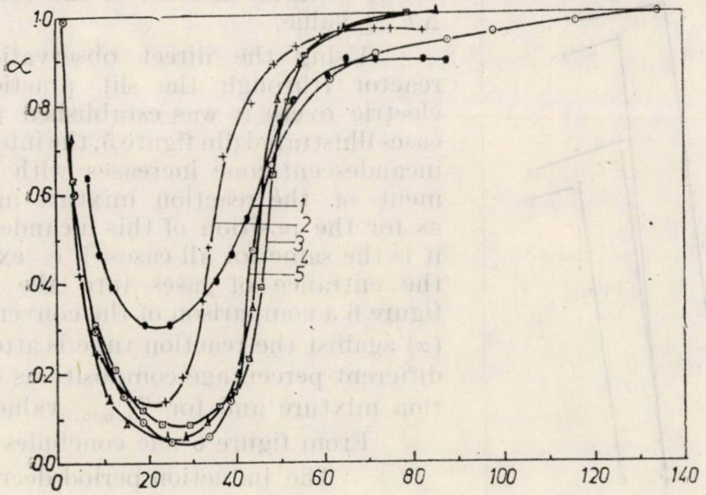

Fig. 4. — Variation of conversion degree (α) vs. reaction time, for different flow rates (reaction mixtures with 12.58 %, v/v, NH_3). 1. 16.66 $cm^3 \cdot s^{-1}$ ($T_i = 290°C$); 2. 22.22 $cm^3 \cdot s^{-1}$ ($T_i = 290°C$); 3. 27.77 $cm^3 \cdot s^{-1}$ ($T_i = 279°C$); 4. 33.33 $cm^3 \cdot s^{-1}$ ($T_i = 279°C$); 5. 41.66 $cm^3 \cdot s^{-1}$ ($T_i = 279°C$).

— The efficiency of the catalyst rises simultaneously with the flow rate increase; the most important increase was observed for the flow rates ranging from 16.66 to 22.22 $cm^3 \cdot s^{-1}$. The maximum value of the efficiency was established for the flow rate equal to 27.77 $cm^3 \cdot s^{-1}$. In the steady state regime, α grows from 0.89 (flow rate 16.66 $cm^3 \cdot s^{-1}$) to 0.96 (flow rate 22.22 $cm^3 \cdot s^{-1}$), then from 0.96 to 1.00 (flow rate 27.77 $cm^3 \cdot s^{-1}$).

Anokhin and Babankov [12] investigated the mass transfer corresponding to the external diffusion during the ammonia oxidation on an Fe_2O_3 — Cr_2O_3 catalyst. These authors proved that for small flow rates, the mass transport is slowed down and, therefore, the catalyst efficiency is poor. This ascertained fact has been confirmed also by Beskov [13] and Stetsovich [14] and can be used to interpret the results shown in figure 4, when the oxidation of ammonia is carried out at T_i higher than the corresponding $T_{i,\,min}$.

3. *Influence of the initial reaction mixture composition on the physico-chemical parameters of the oxidation process*

Influence of the ammonia percentage composition in the initial reaction mixture has been studied at a constant flow rate of 41.66 $cm^3 \cdot s^{-1}$, using reaction mixtures whose ammonia content varied from 12.58 % to 22.44 % (v/v).

The experimental results proved (Fig. 5) that an increase of the ammonia content is connected with a decrease of the initial minimum temperature from 279°C to 260°C and simultaneously, with an increase of the corresponding $\Delta T_{max.}$ value.

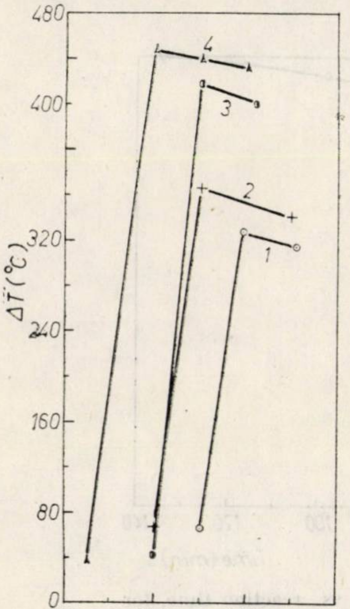

Fig. 5. — Variation of ΔT values vs. T_i (flow rate : 41.66 $cm^3 \cdot s^{-1}$; reaction mixtures of different compositions). 1. 12.58 % (v/v) NH_3 ; 2. 14.04 % (v/v) NH_3 ; 3. 19.50 % (v/v) NH_3 ; 4. 22.44 % (v/v) NH_3.

Using the direct observation of the reactor (through the slit practiced in the electric oven) it was established that for all cases illustrated din figure 5, the intensity of the incandescent zone increases with the enrichment of the reaction mixture in ammonia, as for the position of this incandescent zone, it is the same for all cases, i. e. exactly near the entrance of gases into the reactor. In figure 6 a comparison of the conversion degree (α) against the reaction time is attempted, for different percentage compositions of the reaction mixture and for $T_{i,\,min.}$ values.

From figure 6 one concludes that :

— The induction period decreases when the percentage content of ammonia in the reaction mixture increases.

— The higher the volumetric percentage content of ammonia in the reaction mixture, the smaller is the necessary period to reach the steady state reaction regime.

— The conversion of ammonia to reaction products is complete in all cases, with the exception of the reaction mixture with the composition 22.44% (v/v) NH_3, for which α does not indicate a complete conversion of ammonia for $T_i = 270°C$, and also for $T_i = 280°C$.

This behaviour is assigned to an insufficient amount of oxygen in the reaction mixture, in comparison with the amount required for a complete conversion of ammonia to reaction products.

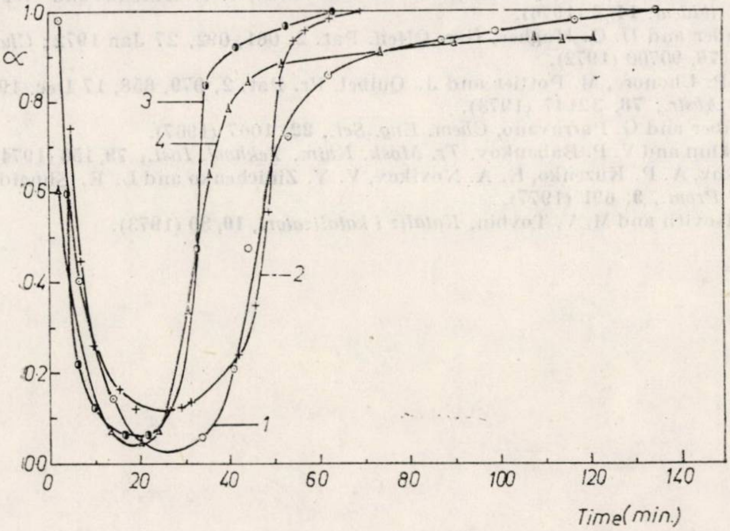

Fig. 6. — Variation of conversion degree (α) vs. reaction time, for the different $T_{i,\min}$. values (constant flow rate 41.66 $cm^3 \cdot s^{-1}$). 1. 12.58% (v/v) NH_3 and $T_i = 279°C$; 2. 14.04% (v/v) NH_3 and $T_i = 270°C$; 3. 19.50% (v/v) NH_3 and $T_i = 270°C$; 4. 22.44% (v/v) NH_3 and $T_i = 260°C$.

CONCLUSIONS

1. Catalytic oxidation of ammonia on a NiO/Al_2O_3 catalyst is a strong exothermal process consisting of two kinetic stages, the first one being predominantly physical in nature, the second one predominantly chemical.

2. The increase of the flow rate leads to the decrease of the $T_{i,\min}$. values, the increase of $\Delta T_{\max}$ values, the increase of the induction period and also the increase of the catalyst efficiency.

3. For flow rates somewhat higher than 22.22 $cm^2 \cdot s^{-1}$, the reaction system becomes incandescent.

4. The increase of the ammonia percentage content of the reaction mixture causes the decrease of the $T_{i,\min}$. values and, on the other hand the increase of $\Delta T_{\max}$ values.

REFERENCES

[1] Part I. M. M. Girgis and D. P. Lazăr, *Rev. Roumaine Chim.*, **25**, 1293 (1980).
[2] Part II. M. M. Girgis, D. P. Lazăr and E. I. Segal, *Rev. Roumaine Chim.*, **26**, 1199 (1981).
[3] Part III. M. M. Girgis, D. P. Lazăr and E. I. Segal, *Rev. Roumaine Chim.*, **26**, 1423 (1981).

[4] N. I. Il'chenko and G. I. Golodets, *Teor. Eksp. Khim.*, **9**, 36 (1973).

[5] N. I. Il'chenko, V. M. Vorotyntsev and I. M. Avilova, *Kinetika i kataliz.*, **17**, 378 (1976).

[6] N. Giordano, E. Cavaterra and D. Zema, *J. Catalysis*, **5**, 325 (1966).

[7] N. F. Kleshchev, V. I. Atroshchenko, N. N. Nechiporenko, A. N. Butenko and N. P. Levshin, *Kataliz i katalizatori*, **14**, 3 (1976).

[8] N. F. Kleshchev, N. N. Nechiporenko, V. I. Atroshchenko, A. N. Butenko and N. P. Levshin, *ibidem*, **14**, 6 (1976).

[9] C. M. Stander and D. O. Hughes, Ger. Offen. Pat. 2, 061, 092, 27 Jan 1972; *Chem. Abstr.*, **76**, 90700 (1972).

[10] M. Senes, P. Lhonore, M. Pottier and J. Quibel, Fr. Pat. 2, 079, 658, 17 Dec. 1971, *Chem. Abstr.*, **78**, 32147 (1973).

[11] T. J. Schriber and G. Parravano, *Chem. Eng. Sci.*, **22**, 1067 (1967).

[12] V. N. Anokhin and V. P. Babankov, *Tr. Mosk. Khim. Tekhnol. Inst.*, **79**, 150 (1974).

[13] V. S. Beskov, A. P. Kuzenko, E. A. Novikov, V. Y. Zinichenko and L. E. Shnaider, *Khim. Prom.*, **9**, 691 (1977).

[14] K. G. Stetsovich and M. V. Tovbin, *Kataliz i katalizatori*, **10**, 30 (1973).

Revue Roumaine de Chimie, 28, *4*, 333–337 (1983)

THERMALLY AND ELECTRON IMPACT INDUCED ACYL MIGRATION IN N-[*ortho*-O-, -S-, -Se-ACYL-PHENYL]-AMIDES

GH. CIURDARU* MARIA-DOINA RUSU* and N. PALIBRODA**
* Institute of Chemistry and **Institute of Stable Isotopes
Cluj-Napoca 3400, Str. Donath 65–103, Romania

Received December 23, 1981

The mechanism similarity of the thermal rearrangement and the main mode of fragmentation in mass spectrometer of N-[*ortho*-O-, -S-, -Se-acyl-phenyl]-amides 1 are discussed.

In our previous papers [1–5] we described the thermal rearrangement of N-[*ortho*-O-, -S-, -Se-acyl-phenyl]-amides **1** to the 4-benzazolines **2** (Scheme 1).

All the data on this reaction [1–6] have indicated a mechanism involving a cyclic transfer of electrons, leading to the unstable intermediate **I** which stabilizes as benzazoline **2** by water elimination (Scheme 1).

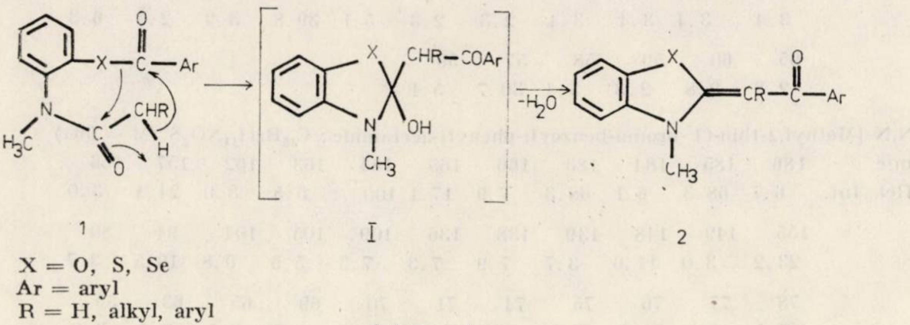

X = O, S, Se
Ar = aryl
R = H, alkyl, aryl

Scheme 1

Taking into account that in many instances there is a parallelism between the thermal processes and electron impact-induced fragmentations, we considered of interest to examine the behaviour of these compounds in the mass spectrometer.

RESULTS AND DISCUSSION

To avoid the thermal rearrangement of the compounds before being subjected to the electronic bombardment, the spectra were recorded at a temperature as low as possible.

The examination of the mass spectra (besides the absence or the presence of a very small peak corresponding to the molecular ion) reveals the absence of the transition $[M-H_2O]^{+\bullet}$, expected in the case in which the

TABLE 1

The mass spectra of the amides **1**

N,N-[Methyl-d_3,2-thiobenzoyl-phenyl]-acetamide ; $C_{16}H_{12}D_3NO_2S$ (M = 288)												
m/e	169	168	167	166	165	153	152	151	150	149	142	
Rel. Int.	3.6	6.9	71.8	7.4	1.6	1.8	2.7	19.2	2.6	7.4	1.3	
	141	139	138	137	127	125	123	122	121	119	113	
	3.2	1.6	2.1	1.3	1.3	1.4	1.8	1.9	1.3	1.0	1.3	
	111	110	109	108	107	106	105	99	98	97	96	
	2.9	3.8	3.7	2.7	1.9	7.2	100	1.9	1.8	7.7	2.0	
	93	91	85	84	83	82	81	80	79	78	77	76
	1.6	1.4	4.2	2.3	5.0	1.8	3.1	1.0	1.8	5.5	29.0	1.0
N,N-[Methyl,2-thiobenzoyl-phenyl]-propionamide ; $C_{17}H_{17}NO_2S$ (M = 299)												
m/e	299	233	180	179	178	177	176	163	162	161	160	
Rel. Int.	0.8	1.1	3.9	11.4	100	31.8	31.8	2.7	15.2	1.1	1.5	
	150	149	148	139	138	137	136	135	134	127	123	
	2.7	4.5	2.7	1.1	3.6	1.5	3.8	3.0	0.7	0.7	1.7	
	122	121	120	119	109	108	107	106	105	95	94	
	9.1	1.5	0.7	0.9	7.4	1.7	1.7	7.9	88.6	2.8	4.5	
	91	85	84	83	82	81	78	77	71	70	69	
	3.4	3.4	3.4	3.4	2.3	2.3	5.1	39.8	3.9	2.3	6.3	
	65	60	59	58	57	56						
	2.8	2.8	2.3	3.4	30.7	5.1						
N,N-[Methyl,2-thio-(4′-bromo-benzoyl)-phenyl]-acetamide ; $C_{16}BrH_{14}NO_2S$ (M = 364)												
m/e	186	185	184	183	166	165	164	163	162	157	156	
Rel. Int.	6.7	68.3	6.1	68.3	7.9	17.1	100	5.5	3.0	24.4	3.0	
	155	149	148	139	138	136	109	105	104	94	80	
	23.2	3.0	11.6	3.7	7.9	7.3	7.3	5.5	9.8	19.5	3.7	
	78	77	76	75	74	71	70	69	65	63	59	
	8.5	15.8	21.9	18.3	4.9	4.3	4.3	4.9	8.5	3.6	3.0	
	57	56	55	52	51	50	45	44	43			
	9.7	5.5	6.1	4.3	8.5	15.8	9.1	26.8	34.1			
N,N-[Methyl,2-thio-(4′-nitro-benzoyl)-phenyl]-acetamide ; $C_{16}H_{14}N_2O_4S$ (M = 330)												
m/e	166	165	164	150	149	148	138	136	120	109	105	
Rel. Int.	3.4	10.7	100	35.0	2.1	34.2	9.4	3.0	8.5	3.4	1.7	
	104	94	92	77	76	75	66	50	45	43		
	25.6	15.4	8.1	3.4	13.7	1.7	2.1	2.6	1.7	18.8		

TABLE 1 (*continued*)

N,N-[Methyl,2-thio-(4′-nitro-benzoyl)-phenyl]-phenylacetamide ; $C_{22}H_{18}N_2O_4S$ (M = 406).

m/e	255	245	242	241	240	239	238	236	226	225	224
Rel. Int.	7.1	5.9	2.4	4.8	17.9	21.4	16.7	3.8	4.8	7.1	33.3
	223	222	173	168	167	166	165	163	162	152	151
	11.9	2.4	7.1	2.4	7.1	13.1	5.9	2.4	4.8	3.6	11.9
	150	149	148	141	140	139	138	137	136	135	134
	100	4.8	8.3	2.4	2.4	11.9	14.3	13.1	13.1	5.9	9.5
	131	129	127	125	124	122	121	120	119.5	119	118.5
	2.4	2.4	9.5	2.4	2.4	2.4	9.5	26.2	14.3	2.4	4.8
	118	112	111.5	109	108	107	106	105	104	103	102
	7.1	4.8	10.7	10.7	4.8	2.4	4.8	9.5	32.1	5.9	2.4
	99	97	96	95	94	93	92	91	90		
	2.4	2.4	2.4	2.4	15.5	4.8	23.8	91.7	7.1		

N,N-[Methyl,2-seleno-(4 -bromo-benzoyl)-phenyl]-acetamide ; $C_{16}BrN_{14}NO_2Se$ (M = 411).

m/e	214	213	212	211	210	209	208	202	200	186	185
Rel. Int.	8.0	4.7	37.3	8.0	19.3	9.3	10.7	10.7	10.0	10.0	100
	184	183	158	157	156	155	148	130	116	107	106
	10.7	100	4.0	29.3	5.3	26.7	9.3	3.3	3.3	6.7	24.0
	105	104	94	78	77	76	75	74	65	63	57
	6.7	12.0	3.3	8.0	16.7	22.7	18.7	5.3	5.3	4.0	3.3
	56	55	52	51	50	44	43				
	3.3	3.3	4.0	9.3	18.7	11.3	32.0				

main way of fragmentation of these compounds parallels their thermal behaviour (Table 1). The spectra are dominated by an unexpected transition, producing the $[M-OCOAr]^+$ ions, which appears to be characteristic of the whole series. The ions are very abundant and in many cases they correspond to the base peak of the spectrum (Table 1). For understanding this transition we have to admit that before it takes place, the molecular ion A rearranges to the species B. In these species the transition $[M-OCOAr]^+$ is favoured because it produces ions of a high stability, the quaternary benzazolium ions C (Scheme 2).

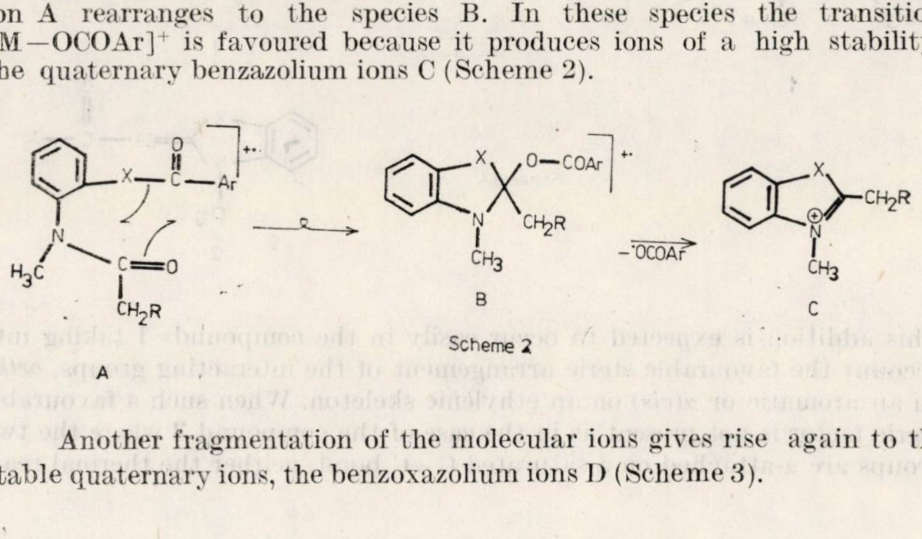

Scheme 2

Another fragmentation of the molecular ions gives rise again to the stable quaternary ions, the benzoxazolium ions D (Scheme 3).

The fission of the esteric (XCOAr) and amidic (RCH_2CON) groups produces the corresponding E and F acylium ions (Scheme 3).

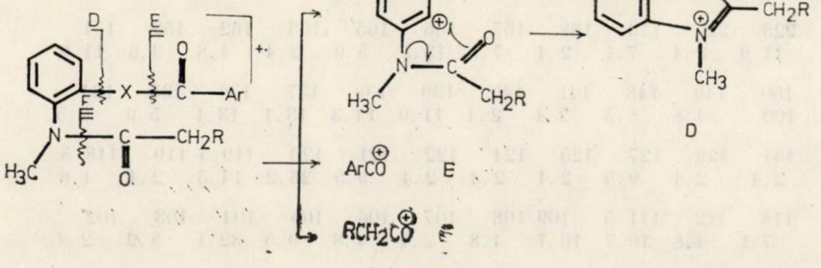
D
E
F
X
O
Ar
N
C
CH_2R
H_3C
O
+·
⊕
N
C
O
H_3C
CH_2R
⊕
N
O
CH_2R
CH_3
D
$Ar\overset{\oplus}{C}O$ E
$RCH_2\overset{\oplus}{C}O$ F

Scheme 3

Although the absence of the $[M-H_2O]^{+\cdot}$ ions in the mass spectra would indicate a different behaviour of these compounds under electron impact and under thermal conditions, the rearrangement of the molecular ion A to the species B (Scheme 2) suggests, however, that the *thermal rearrangement* could follow a similar route. Thus, it is very likely that the first step in *thermal rearrangement* of the compounds **1** to the benzazolines **2** is the internal addition of the esteric group (XCOAr) to the amidic carbonyl, via a 4-centered transition state (Scheme 4).

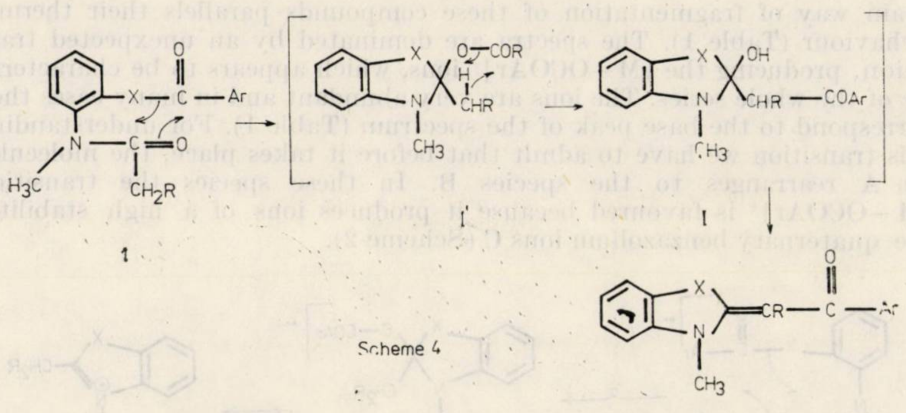
O
X
C
Ar
N
C
O
H_3C
CH_2R
1
X
O
COR
H
N
CHR
CH_3
X
OH
N
CHR
COAr
CH_3
I
O
X
CR
C
Ar
N
CH_3
2

Scheme 4

This addition is expected to occur easily in the compounds **1** taking into account the favourable steric arrangement of the interacting groups, *ortho* on an aromatic or α(*cis*) on an ethylenic skeleton. When such a favourable steric factor is not present as in the case of the compound **3** where the two groups are α-attached on a saturated C—C bond, neither the thermal rearrangement nor the characteristic fragmentation, [M−OCOAr]$^+$, are observed.

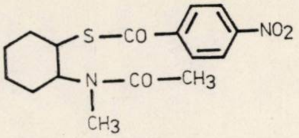

3

In the intermediate I′, resulted in the addition step of the thermal rearrangement, a new acyl migration to the vicinal alkyl group leads to the intermediate I which after water elimination gives the final product, the benzazoline **2** (Scheme 4).

REFERENCES

[1] V. Denes, Gh. Ciurdaru and M. Farcasan, *Chem. Ber.*, **96**, 2691 (1963).
[2] V. Denes, Gh. Ciurdaru and M. Farcasan. *Rev. Roum aine Chim.*, **9**, 375 (1964).
[3] V. Denes, Gh. Ciurdaru and M. Farcasan, *Rev. Roumaine Chim.*, **9**, 867 (1964).
[4] V. Denes, Gh. Ciurdaru and M. Farcasan, *Rev. Roumaine Chim.*, **10**, 1043 (1965).
[5] V. Denes and Gh. Ciurdaru, *Chem. Comm.*, **1970**, 510.
[6] Gh. Ciurdaru, unpublished data.

Revue Roumaine de Chimie, **28**, *4*, 339–347 (1983)

UNA TÉCNICA OMEGA BIPARAMÉTRICA MEJORADA PARA CÁLCULOS CON ORBITALES MOLECULARES III*

AROMATICIDAD DE HIDROCARBUROS SEMIBENCENOIDES Y NO-BENCENOIDES

EDUARDO A. CASTRO* y FRANCISCO M. FERNÁNDEZ

Instituto de Investigaciones Fisicoquímicas Teóricas y Aplicadas, Sección Química Teórica, Sucursal 4 – Casilla de Correo 16, La Plata 1900, Argentina

Recibido: el 4 de April de 1981

Se aplica una Técnica Omega Biparamétrica Mejorada (ITPOT) junto con una Técnica Omega Biparamétrica (TPOT) al cálculo de índices de aromaticidad de algunos hidrocarburos no-alternantes. Los resultados son comparados con los obtenidos por otros métodos, y asimismo se discuten en relación a las propriedades químicas conocidas.

An Improved Two Parameter Omega Technique (ITPOT) and a Two Parameter Omega Technique (TPOT) are applied to the calculation of the aromaticity indices of several non-alternant hydrocarbons. The results are compared with those obtained previously by other methods, and furthermore they are discussed in close relation with the chemical properties.

I. INTRODUCCION

El concepto de aromaticidad es ya más que centenario y aún continúa siendo de interés en la Química Orgánica. Varias propiedades químicas se pueden correlacionar con el carácter aromático. Los espectros electrónicos, las propiedades magnéticas y la reactividad química de un buen número de moléculas orgánicas se pueden analizar en términos de su aromaticidad. [1] Se han propuesto un gran número de índices de aromaticidad y se han intentado diversos enfoques teóricos para fundamentar solidamente el concepto de "carácter aromático". [2–21] Sin embargo, a pesar del gran número de contribuciones originales en el terreno de la correlación teórico-experimental, todavía no se ha podido arribar a la definición de un índice universal de aromaticidad y de un método de cálculo de Orbitales Moleculares asociado, que sean totalmente satisfactorios.

En dos publicaciones recientes[22] hemos presentado una Técnica Omega Biparamétrica Mejorada (ITPOT) para el cálculo de la estructura electrónica pi de especies neutras, iónicas y radicalarias. Esta ITPOT es una modificación de la Técnica Omega Biparamétrica (TPOT) de Mathur y col. [23] y la comparación de resultados mostró una superior calidad de la primera respecto de la segunda y de otros métodos del tipo SCF más elaborados, tales como PPP, CNDO/S2 y SPO. [22] Los resultados obtenidos fueron muy promisorios para correlacionar datos experimentales con valores teóricos.

---

* To whom any correspondence concerning this paper must be addressed.

Recientemente, Aihara [24] introdujo la técnica omega de Wheland y Mann [25-26] en la teoría de grafos de aromaticidad [21] a los efectos de obtener mejores valores de energías de resonancia de hidrocarburos no-alternantes. En sus conclusiones, el autor sugiere la utilización de la técnica omega en la teoría de aromaticidad de Hess y Schaad [6-7] como un medio alternativo respecto del simple modelo de Hückel (HMO) [2] para lograr mejores resultados.

Las técnicas omega biparamétricas TPOT y I TPOT constituyen métodos más elaborados que el método monoparamétrico de Wheland y Mann, ya que tiene en cuenta de un modo más adecuado la repulsión interelectrónica. [22-23] Por todo ello hemos creído de interés evaluar las energías de resonancia según la teoría de Hess y Schaad y las ya clásicas energías de delocalización para varios hidrocarburos nobencenoides y semibencenoides, para los cuales existen datos de sus reactividades químicas, así como de otros tipos de cálculos.

En esta comunicación aplicamos los métodos TPOT y I TPOT para determinar la estructura electrónica pi de 16 hidrocarburos no-alternantes. Con ello evaluamos energías electrónicas totales, energías de delocalización y energías de resonancia. Con ayuda de estos índices, comparamos los resultados con otros similares obtenidos con diferentes métodos del tipo SCF, y asimismo se discuten las propiedades químicas de las moléculas elegidas.

Por otra parte, esta tercera comunicación de la serie acerca de la ITPOT, nos permite encarar un problema diferente a los ya discutidos previamente, y de sus bondades poder inferir la importancia de los métodos omega-biparamétricos como una potencial herramienta, simple y eficiente a la vez, que sirva al químico orgánico experimentalista para complementar su trabajo de laboratorio.

II. METODOS DE CALCULO Y DETALLES COMPUTACIONALES

Las expresiones para los elementos de matriz de Hamilton no-diagonales en las técnicas TPOT y ITPOT son, respectivamente [22]

$$H_{rs}^{\mathrm{TPOT}} = \beta + (1 - p_{rs})\,\omega'\beta \qquad (1)$$

$$H_{rs}^{\mathrm{ITPOT}} = \beta \exp(0.55 p_{rs} - 0.366) \qquad (2)$$

donde ω' es uno de los parámetros omega y cuyo valor asignado es -0.6; β es la integral de resonancia estándar y p_{rs} es el órden de enlace entre el átomo r-ésimo y el átomo s-ésimo.

La fórmula para el elemento de matriz diagonal es la misma en ambos métodos y está dada por

$$H_{rr} = \alpha + (1 - q_r)\omega\beta - 2 \sum_{\substack{s \text{ unido} \\ a\ r}} (1 - q_s)\,\omega'\beta \qquad (3)$$

donde α es la integral de Coulomb estándard, q_r es la carga electrónica pi sobre el átomo r-ésimo y ω es el otro parámetro omega, con valor 1.4.

Como los métodos son iterativos, se debe comenzar con una determinada matriz densidad (cargas y órdenes de enlace). Entonces, primero se calcula la estructura con el HMO, y de la matriz densidad obtenida se pueden determinar los elementos de matriz (1 — 3) y con ellos, a su vez, una nueva matriz densidad. Este proceso se continúa hasta autoconsistencia ó sea hasta que todos los elementos de cargas electrónicas y órdenes de enlace en dos iteraciones sucesivas, no difieran en más de una cota predeterminada (0.001 unidades en nuestro caso). Como es bien sabido, en este tipo de métodos suelen existir problemas de convergencia. [27-28] Por ello se aplicaron los procedimientos de promediación previamente descriptos y empleados, [22] para acelerar la convergencia. El lector interesado en este detalle deberá remitirse a nuestros trabajos previos. [22, 27, 28]

El cálculo de las energías de resonancia por el método de Hess y Schaad [6-7] requiere la determinación de todas las formas resonantes posibles para una dada molécula. La información necesaria para efectuar tal determinación se halla contenida en la matriz topológica de Hückel, de modo que, en principio, esta tarea es realizable desde un punto de vista computacional. Sin embargo,ello constituye una tarea díficil y tediosa, la cual puede ser obviada, tomando una sola estructura como representativa del total, pues los resultados no se ven significativamente modificados al hacer esta aproximación. [29]

La Energía de Delocalización (*ED*) se calculó de acuerdo a la relación [30]

$$ED = E^{\pi} - n E^{\pi}_{et} \qquad (4)$$

donde E^{π} es la energía electrónica pi total de la molécula en cuestión, E^{π}_{et} es la energía electrónica pi del etileno y n es el número de dobles enlaces en la estructura resonante elegida.

La Energía de Resonancia (*ER*) se determinó mediante el método de Hess y Schaad,[6] de acuerdo a la fórmula

$$ER = E^{\pi} - E^{\pi}_{\text{pol acl}} \qquad (5)$$

donde $E^{\pi}_{\text{pol acl}}$ es la energía electrónica pi total de un polieno acíclico referencial, y se calcula sumando directamente las energías de todos sus enlaces. Se emplearon a tal fin los valores dados por Hess y Schaad (ver Tabla I en la Ref. 6).

Cuando se efectúan comparaciones entre moléculas con diferentes números de átomos de electrones pi, es más apropiado analizar las energías de resonancia y de delocalización por electrón pi [6] (ERPE y EDPE, respectivamente, las cuales se definen como

$$\text{EDPE} = \text{ED}/n_{\pi} \qquad (6)$$

$$\text{ERPE} = ER/n_{\pi} \qquad (7)$$

donde n_{π} es el número total de electrones pi.

Asimismo empleamos una medida de la estabilización aromática recientemente propuesta por Aihara [24] que se denomina porciento de energía de resonancia (%ER) y que se define como 100 veces la ER dividida la energía de referencia. Esta cantidad mide el grado de estabilización con el cual un sistema conjugado se comporta aromaticamente como un todo. Debe observarse que el % ER no depende ni del número de electrones pi ni del número de uniones pi existentes en el sistema conjugado.

Creemos importante puntualizar que es difícil efectuar una comparación directa de las aromaticidades calculadas teoricamente, pues no existe una cantidad medible experimentalmente que sea equivalente a la aromaticidad. Sólo existen las ideas cualitativas, pero útiles al fin, de que las especies aromáticas son estables, participan de reacciones de sustitución electrofílica, son planas y pueden ser representadas graficamente por más de una estructura de Kekulé.

III. RESULTADOS Y DISCUSION

Se eligieron 16 hidrocarburos no alternantes, los cuales se presentan en la Figura 1. En la Tabla 1 se dan los resultados para los cálculos de las energías electrónicas pi de los polienos cíclicos asociados a las estructuras resonantes de la Figura 1, y determinados según el método de Hess y Schaad. [6]

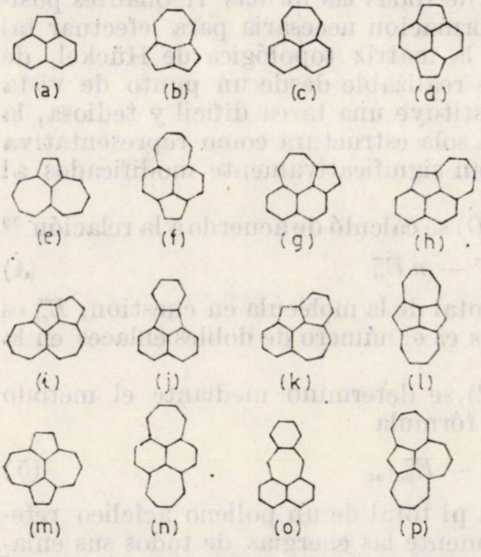

Fig. 1. — (a) Acenaftileno. (b) Aceazulileno. (c) Pleiadieno. (d) Piracileno. (e) Aceheptileno. (f) Acepleiadileno. (g) Naftazuleno. (h) Cicloheptacenaftileno. (i) Pentalenoheptaleno. (j) Fluoranteno. (k) Ciclohaptapentaleno. (l) Dicicloheptaleno. (m) Azupireno. (n) Dipleiadadieno. (o) Benzopleiadieno. (p) Azulenohaptaleno.

En la Tabla 2 se ofrecen las energías electrónicas totales pi calculadas mediante los métodos TPOT y I TPOT. Las energías de delocalización y de resonancia calculadas en este trabajo, junto con otros resultados previos, son ofrecidos en la Tabla 3.

Como en los diferentes métodos se emplean distintas unidades energéticas, los valores absolutos de los índices para una misma molécula, difieren apreciablemente, por lo cual no tiene sentido un análisis cuantitativo diferencial entre los distintos métodos. De modo que nos remitiremos a una discusión cualitativa de los resultados numéricos.

Por definición, aquellos hidrocarburos no-alternantes en los cuales puedan asignarse uno a más sextetos aromáticos, se denominan "hidrocarburos semibencenoides". [31]

Por otra parte, cuando un sistema conjugado resulta de la combinación de anillos pi con un número impar de átomos de Carbono, el hidrocarburo se denomina "no bencenoide". En nuestro conjunto de moléculas escogidas, a, c, d, f, g, h, n, k, j y o son hidrocarburos semibencenoides, y los restantes, o sea b, e, m, l, i y p son no-bencenoides. Es dable esperar que los primeros sean más estables que los segundos debido a su mayor carácter aromático. En términos generales, ésto se ve reflejado en las $(\mathrm{EDPE})_{\mathrm{HMO}}$, ya que el promedio para los primeros es 0.383, mientras que para los segundos es 0.367.

Sin embargo, cuando comparamos en detalle, observamos algunas discrepancias. Así *m*, l e i (no-bencenoides) poseen mayor EDPE que el *n* (semibencenoide). Esta clase de discrepancias que surgen en la simple metodología HMO es la que ha llevado a proponer otros típos de cálculos del SCF para medir la aromaticidad. [32]

De los resultados de la Tabla 3 se observa la existencia de valores negativos para ciertos índices de aromaticidad. Ello ocurre cuando el compuesto presenta un carácter antiaromático. El único valor negativo de EDPE es el correspondiente al compuesto *k*, en concordancia con los resultados de Das Gupta y Das Gupta [31-32] y con los hechos experimentales. En efecto, hasta la fecha, el ciclohepta(def) fluoreno no ha sido sintetizado.

La diferencia entre hidrocarburos semibencenoides y no-bencenoides se ve bastante bien remarcada respecto de la EDPE, tanto en la TPOT como en la I TPOT, ya que para el primer método, los valores medios son 0.205 y 0.123 respectivamente, mientras que para el segundo, dichos promedios son 0.378 y 0.292 respectivamente. Vemos así que al emplear los métodos más elaborados de cálculo respecto del HMO se logra una distinción más neta entre ambos tipos de compuestos. Un análisis similar a lo anterior se puede aplicar al índice ERPE.

Aunque en general los resultados de los distintos métodos se hallan en buena concordancia, existen algunas discrepancias que sería conveniente comentar, así como discutir aquellos casos en que existe evidencia experimental acerca de los estabilidades químicas y espectroscópicas.

De acuerdo a las propiedades químicas, el compuesto f es más aromático que el c. [33] Sin embargo, nuestros resultados afirman lo opuesto. Esta discrepancia ya había sido encontrada por Das Gupta y Das Gupta [31-32] y por Aihara. [24]

El valor *ER*/*CC* para el piracileno (compuesto d) calculado por el método de Dewar-Harguet (0.082) es comparable al de otros hidrocarburos semibencenoides. Pero de acuerdo a los hechos experimentales [34] este hidrocarburo no es aromático, y esto concuerda con lo calculado por nosotros y en concordancia con el valor de *ER*/*CC* (0.045) del método de Dewar y De Llano. [32]

En la comparación de la aromaticidad de las moléculas aceheptileno (*e*) y aceazulileno (*b*), hallamos otro ejemplo donde nuestro método supera discrepancias previas. En efecto, de acuerdo a las propiedades químicas [35-36] el primero es más aromático que el segundo. Esto es lo que predicen nuestros resultados y los de Dewar y De Llano [16], aunque lo opuesto es predicho por el método de Dewar-Harguet. [37]

Las propiedades reportadas del azupireno (m) indican que esta molécula posee un marcado grado de aromaticidad. [38] Los diferentes métodos coinciden completamente en ello. Asi, los índices de EDPE de los métodos

TPOT y I TPOT (0.222 y 0.346 respectivamente) se hallan muy cerca de los valores medios de los hidrocarburos semibencenoides (0.205 y 0.378 respectivamente).

La aromaticidad de la molécula cicloheptacenaftileno (*h*) ha sido estudiada por Reid y col. [39] Estos autores reportaron que la molécula debería poseer un carácter azulénico más que ciclopoliolefínico ; i.e. una marcada aromaticidad. Este resultado concuerda con nuestros valores, así como con los de otros autores. [24, 32]

IV. CONCLUSIONES

Si bien los resultados obtenidos son suficientemente buenos como para otorgar un crédito a los métodos omega biparamétricos en lo atinente a su aplicación al estudio de la aromaticidad, no se pueden extraer todavía conclusiones definitivas. Esto se debe a que el conjunto de moléculas elegidas es relativamente pequeño, y en consecuencia sería necesario ampliar el espectro de posibilidades, incluyendo en un estudio similar, a hidrocarburos aromáticos y analizando los índices de aromaticidad para los tres casos : aromáticos, semiaromáticos y no-aromáticos. Esta tarea se está llevando a cabo actualmente en nuestro laboratorio y los resultados serán presentados prontamente.

Sin embargo un aspecto especialmente importante puesto de relieve en este estudio es que las bondades de las técnicas omega biparamétricas (TPOT y I TPOT) en el estudio de la aromaticidad, son similares a las de otros métodos más elaborados y por ende más trabajosos para llevarlos a la práctica. Aunque para el químico teórico este aspecto es algo irrelevante, no ocurre lo mismo con el químico experimental, para quién cuanto más simple sea el método de cálculo, mejor, en tanto se mantenga un nivel rezonable de credibilidad en tal procedimiento teórico.

REFERENCIAS

* Part II. *Rev. Roumaine Chim.*, **25**, 643 (1980).

[1] Aromaticity, Pseudoaromaticity, Antiaromaticity, Proc. International Symp. (E. D. Bergman and B. Pullman, Editors), Jerusalem, 1971.

[2] E. Hückel, *Z. Physik*, **70**, 204 (1931).

[3] J. W. Armit and R. Robinson, *J. Chem. Soc.* **121**, 827 (1922) ; **127**, 1604 (1925).

[4] R. Robinson, *Tetrahedron*, **3**, 323 (1958).

[5] M. H. Palmer and R. H. Findlay, *Tetrahedron Letters*, **1974**, 253.

[6] B. A. Hess, Jr. and L. J. Schaad, *J. Amer. Chem. Soc.*, **93**, 305 (1971).

[7] B. A. Hess, Jr., L. J. Schaad, and C. W. Holyoke, Jr. *Tetrahedron*, **28**, 3857 (1972) ; **31**, 295 (1975).

[8] J. A. Kruszewski and T. M. Krygowski, *Tetrahedron Letters*, **1970**, 319.

[9] J. A. Kruszewski and T. M. Krygowski, *Acta Chimica*, **18**, 165 (1972).

[10] G. Náray-Szabó and K. Horváth, *Croat. Chem. Acta.*, **49**, 461 (1977).

[11] A. Julg and F. Francois, *Theor. Chim. Acta.* **7**, 249 (1967).

[12] W. T. Dixon, *J. Chem. Soc.*, **1970**, 612.

[13] A. L. H. Chung and M. J. S. Dewar, *J. Chem. Phys.*, **42**, 756 (1965).

[14] D. H. Lo and M. A. Whitehead, *Canad. J. Chem.*, **46**, 2027 (1968).

[15] M. J. S. Dewar and G. J. Gleicher, *J. Amer. Chem. Soc.*, **87**, 685, 692 (1965).

[16] M. J. S. Dewar and C. de Llano, *J. Amer. Chem. Soc.*, **91**, 789 (1969).

[17] M. Randić, *Int. J. Quantum Chem.*, **17**, 549 (1980).

[18] M. Milun and N. Trinajstić. "Proceedings of the Meeting of Croatian Chemists", Zagreb, Croatia, February 1971, p. 72.

[19] M. Milun, Z. Sobotka and N. Trinajstić, *J. Org. Chem.*, **37**, 139 (1972).

[20] S. C. Sharma, A. K. Srivastava and B. Krishna, *JCS Faraday II*, **70**, 168, 172 (1968).

[21] J. Aihara, "The Theory of Aromatic Stabilization", A Source Book (1974—1979), Department of Chemistry, Faculty of Science Hokkaido University, 1980.

[22] E. A. Castro and F. M. Fernández, *Rev. Roumaine Chim.*, **25**, 635, 643 (1980).

[23] S. C. Mathur, D. C. Singh, B. Kumar and S. Mitra, *Int. J. Quantum Chem.*, **11**, 759 (1977).

[24] J. Aihara, *Bull. Chem. Soc. Japan*, **53**, 2689 (1980).

[25] G. W. Wheland and D. E. Mann, *J. Chem. Phys.*, **17**, 264 (1949).

[26] A. Streitwieser, Jr., "Molecular Orbital Theory for Organic Chemists", Wiley, New York, 1961, Chapter 4.

[27] E. A. Castro, *Canad. J. Chem.*, **54**, 3242 (1976).

[28] E. A. Castro, *Anales Asoc. quim. argentina*, **64**, 299 (1976).

[29] B. A. Hess, Jr., and L. J. Schaad, *J. Amer. Chem. Soc.*, **93**, 2413 (1971).

[30] F. L. Pilar, "Elementary Quantum Chemistry", McGraw Hill, New York, 1968, p. 606.

[31] A. Das Gupta and N. K. Das Gupta, *Theor. Chim. Acta*, **33**, 177 (1974).

[32] A. Das Gupta and N. K. Das Gupta, *Tetrahedron*, **28**, 3587 (1972).

[33] V. Boekelheide and G. K. Vick, *J. Amer. Chem. Soc.*, **78**, 653 (1959).

[34] B. M. Trost G. M. Bright, C. Frihart and D. Britelli, *J. Amer. Chem. Soc.*, **93**, 737 (1971).

[35] K. Hafner and J. Schneider, *Liebigs Ann. Chem.*, **624**, 37 (1959).

[36] M. A. Ali and C. A. Coulson, *Mol. Phys.*, **4**, 65 (1961).

[37] M. J. S. Dewar and A. J. Harget, *Proc. Roy. Soc. (London)*, **315A**, 443 (1970).

[38] A. G. Anderson, Jr., A. A. McDonald and A. F. Montana, *J. Amer. Chem. Soc.*, **90**, 2993 (1968).

[39] D. H. Reid, W. H. Stafford and J. P. Ward, *J. Chem. Soc.*, **1955**, 1193.

Revue Roumaine de Chimie, **28**, *4*, 349–354 (1983)

COMPLEXES OF TRANSITION METALS WITH 2,2′-DIAMINOAZOBENZENE. IV[1–3]

THE Co(II)-2,2′-DIAMINOAZOBENZENE SYSTEM

N. CALU and N. FOCA
The Polytechnic Institute, Inorganic Chemistry Department, Splai Bahlui 71, Iassy, Romania

Received December 15, 1981

The paper presents the complex formation in the Co(II)—2,2′-diaminoazobenzene system, studied by spectrophotometric methods. The composition of the complexes is CoL^{2+} and CoL_2^{2+} and the overall formation constant, β_2, is eqaul to $2.22 \times 10^7 l^2 \cdot mol^{-2}$. Their formation reactions are described by second order kinetic equations. The rate constants and activation energies for the two steps, CoL^{2+} and CoL_2^{2+} are $1.31 \times 10^2 l \cdot mol^{-1}$ and $0.69 \times 10^2 l \cdot mol^{-1}$, and 7.2 kcal mol^{-1} and 11.28 kcal mol^{-1}, respectively.

INTRODUCTION

The Cu^{2+}, Ni^{2+}, Pd^{2+}, Co^{2+} and other ions react with 2,2′-diaminoazobenzene[1–3] to form ML^{2+} and ML_2^{2+} type complex compounds (ligand L = 2,2′-diaminoazobenzene).

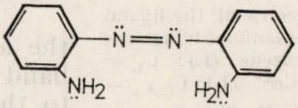

Our studies on these complexes show that the Cu^{2+} and Pd^{2+} ions form directly ML^{2+} complexes while the Ni^{2+} ions form step by step complexes i.e. ML^{2+} and ML_2^{2+}.

In the Co(II)-2,2′-diaminoazobenzene system stepwise complex formation occurs, nevertheless spectrophotometrically only the combination ratio, 1 Co^{2+} : 2L, namely CoL_2^{2+} could be detected.

In this paper we present the results concerning the composition, the stability and the formation kinetics of the CoL_2^{2+} complex ion.

EXPERIMENTAL

For this study, $CoCl_2$ was used as an aqueous solution of 1.10^{-1} mol l^{-1} and pH ≈ 3.5. From this solution, by dilution with ethanol, several solutions with the concentrations ranged between 1.10^{-3} and 1.10^{-4} mol. l^{-1} were prepared.

The ligand was employed as solution in ethanol with the concentrations ranged between $1 \cdot 10^{-3}$ and 1.10^{-5} mol.l^{-1}.

The CoL_2Cl_2 complex was obtained in 90 % ethanol solution, by mixing the $CoCl_2$ and L solution in a 1 : 2 molar ratio Co^{2+}/L. The CoL_2Cl_2 complex formation was complete after about 12 hours.

The UV — VIS spectra of the solution containing the CoL_2Cl_2 complex in 90 % ethanol were measured with a Specord UV — VIS spectrophotometer. The reaction kinetics was studied measuring the absorbance versus time for the solution with Co^{2+} ion and L in the ratio 1 :2 of $1 \cdot 10^{-4}$ mol l^{-1} $CoCl_2$, using $\lambda_{max} = 600$ nm.

RESULTS AND DISCUSSION

The reaction between $CoCl_2$ and 2,2′-diaminoazobenzene gives rise to complex compounds with characteristic UV-VIS spectrum. The reaction develops relatively slowly so that the spectrum modifications could be easily followed in time. The absorption spectra of the reagents and complex formation in the Co(II)-L system are plotted in figure 1.

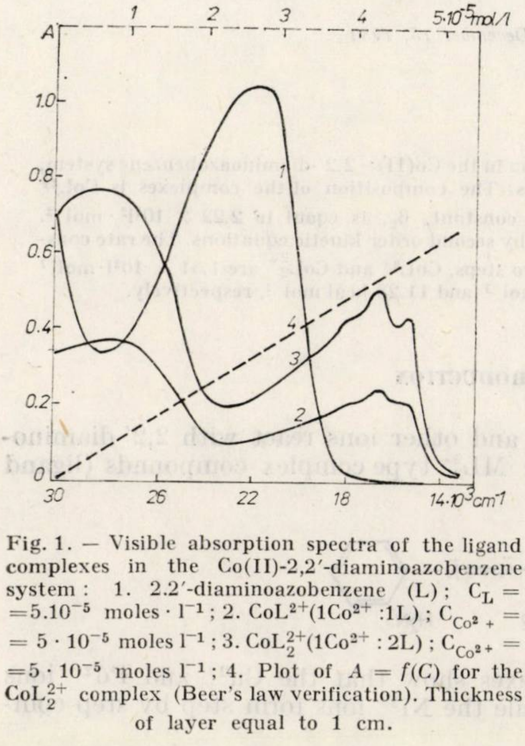

Fig. 1. — Visible absorption spectra of the ligand complexes in the Co(II)-2,2′-diaminoazobenzene system : 1. 2.2′-diaminoazobenzene (L) ; $C_L = 5.10^{-5}$ moles · l^{-1} ; 2. $CoL^{2+}(1Co^{2+} : 1L)$; $C_{Co^{2+}} = 5 \cdot 10^{-5}$ moles l^{-1} ; 3. $CoL_2^{2+}(1Co^{2+} : 2L)$; $C_{Co^{2+}} = 5\ 10^{-5}$ moles l^{-1} ; 4. Plot of $A = f(C)$ for the CoL_2^{2+} complex (Beer's law verification). Thickness of layer equal to 1 cm.

The spectrum of the Co(II) solution and L develops during about 12 hours after mixing, showing that complex formation in this system is slow and requires this long time.

The spectrum of the final complex exhibits significant modifications compared to the starting reactants.

Among these modifications the appearance of an absorption band with $\lambda_{max} = 600$ nm, due to the blue CoL_2^{2+} complex, is noticed. Since the reactants do not exhibit absorption bands in this region, the above mentioned band is characteristic of the CoL_2^{2+} complex (Fig. 1).

The intermediate complex CoL^{2+} absorbs practically in the same region as CoL_2^{2+} (Fig. 1).

Our study on the Co(II)-2,2′-diaminoazobenzene system is based on the absorption band with $\lambda_{max} = 600$ nm for which Beer's law holds for a large concentration range (Fig. 1).

COMPOSITION OF THE COMPLEX FORMED IN THE Co(II)-2,2′-DIAMINOAZOBENZENE SYSTEM

The combination ratio Co(II)-L was determined on the stabilized solutions, by means of several spectrophotometric methods, measuring the absorbance, *A*, of the complex at $\lambda_{max} = 600$ nm.

Thus, the molar ratio method,[4] Job's method [5] and the logarithmic method [6] have been employed. The experimental results are shown in figures 2a—c.

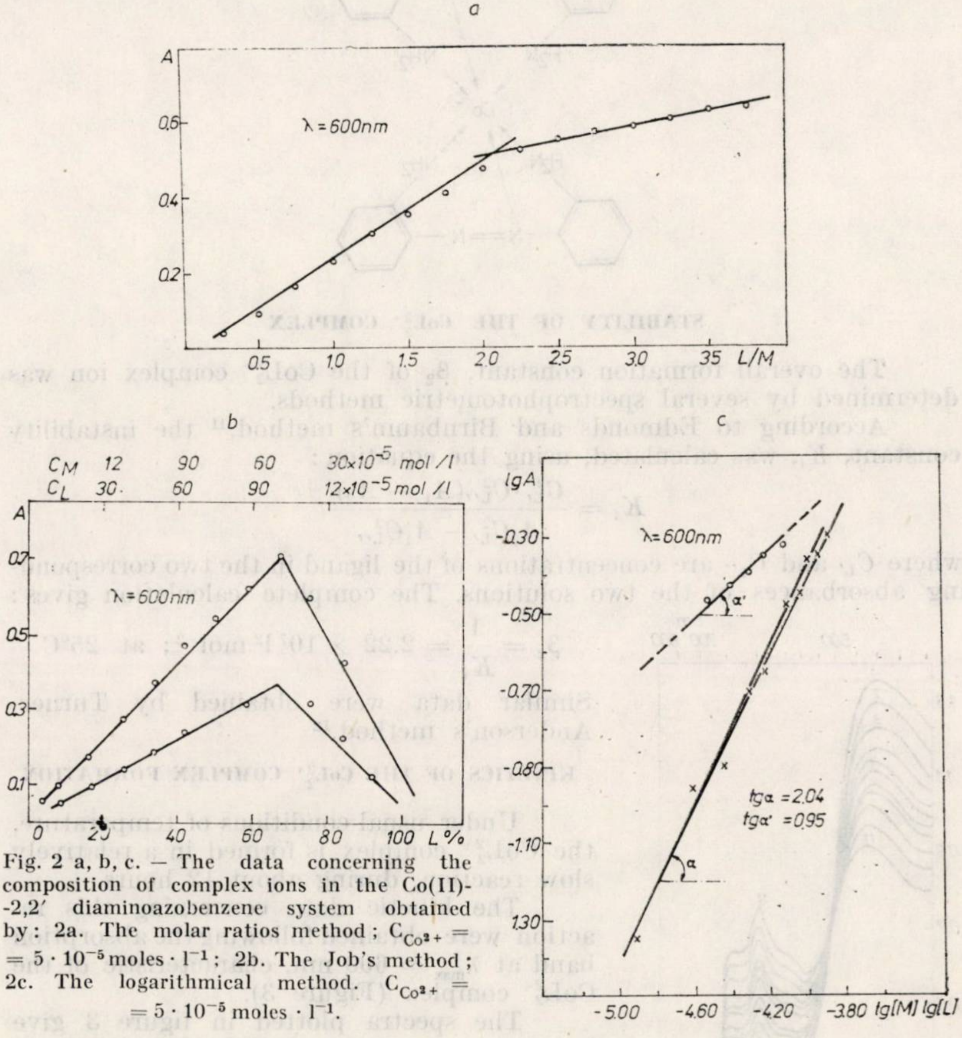

Fig. 2 a, b, c. — The data concerning the composition of complex ions in the Co(II)-2,2′ diaminoazobenzene system obtained by: 2a. The molar ratios method; $C_{Co^{2+}} = 5 \cdot 10^{-5}$ moles · l^{-1}; 2b. The Job's method; 2c. The logarithmical method. $C_{Co^{2+}} = 5 \cdot 10^{-5}$ moles · l^{-1}.

The data are in agreement with the reactions:

$$Co^{2+} + L \rightleftharpoons CoL^{2+}$$

$$CoL^{2+} + L \rightleftharpoons CoL_2^{2+}$$

The spectrophotometric determinations carried out on solutions stabilized for 12 hours, show only the second step of the complex formation, namely the CoL_2^{2+} complex. For this complex the metal-ligand bonds are formed as shown in formula 2.[7–10]

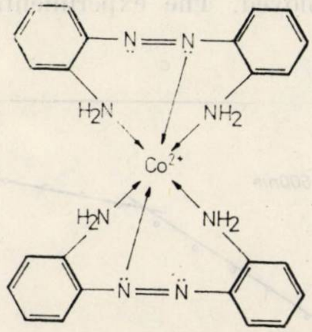

STABILITY OF THE CoL_2^{2+} COMPLEX

The overall formation constant, β_2 of the CoL_2^{2+} complex ion was determined by several spectrophotometric methods.

According to Edmonds and Birnbaum's method,[11] the instability constant, K_i, was calculated, using the equation:

$$K_i = \frac{C_{L'}^2 \cdot C_{L''}^2 (A_1 - A_2)}{A_2 C_{L'}^2 - A_1 C_{L''}^2}$$

where $C_{L'}$ and $C_{L''}$ are concentrations of the ligand in the two corresponding absorbances of the two solutions. The complete calculation gives:

$$\beta_2 = \frac{1}{K_i} = 2.22 \times 10^7 \, l^2 \, mol^{-2}; \text{ at } 25°C$$

Similar data were obtained by Turner-Anderson's method.[12]

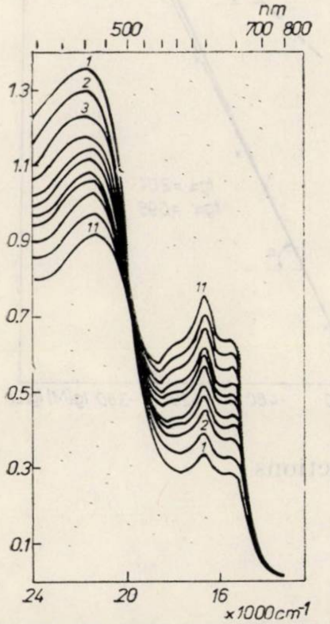

Fig. 3.—The data concerning the evolution of the Co(II)-2.2′-diaminoazobenzene system (1 Co^{2+} : 2L) *versus* time. 1. $t_1 = 1'$ and $10''$, $t_2 = 2'$ ... $t_{11} = 42'$ and $30''$.

KINETICS OF THE CoL_2^{2+} COMPLEX FORMATION

Under usual conditions of temperature, the CoL_2^{2+} complex is formed in a relatively slow reaction, during about 12 hours.

The kinetic data concerning this reaction were obtained following the absorption band at $\lambda_{max} = 600$ nm, characteristic of the CoL_2^{2+} complex (Figure 3).

The spectra plotted in figure 3 give information on the evolution of the Co(II)-L system in time.

At the end of the reaction after 12 hours, at $\lambda_{max} = 460$ nm a minimum appears and the band of the free ligand disappears almost completely. Additionally, some isobestic points are observed in the spectra. The isobestic point with $\lambda_{max} = 515$ nm appears as the ligand disappears accompanied by the CoL_2^{2+} complex formation, illustrated by its band with $\lambda_{max} = 600$ nm.

During the reactions:

$$Co^{2+} + L \rightleftharpoons CoL^{2+}$$

$$CoL^{2+} + L \rightleftharpoons CoL_2^{2+}$$

the conversion, x, was determined on the basis of the relationships:

$$C_i = \frac{A_i}{\varepsilon d} \quad \text{and} \quad x = \frac{C_i}{\nu}$$

Where:

C_i = the concentration of the complex

A_i = the absorbance of the sample at $\lambda_{max} = 600$ nm;

$\varepsilon = 1.34 \times 10^4$ mol l^{-1} cm^{-1}

d = the thickness of the layer (equal to 1 cm);

ν = the stoichiometric coefficient of the Co(II) complex in the above mentioned reaction.

The calculations show that the complex formation in the studied system, develops according to a second order reaction.[13] Thus plotting the equation:

$$\lg \frac{a - x}{b - x} = f(t)$$

where: a and b are the initial concentrations of the reactants; t = the time, gives straight lines (Fig. 4). From their slopes, the reaction rate constants have been calculated

$$K = \frac{\text{tg}\, \alpha}{0.434(a - b)}$$

TABLE 1

The reaction rate constants and activation energies for the reactions in the Co(II)-2,2′-diaminoazobenzene system

Temperature °C	K_1 $l \cdot mol^{-1}s^{-1}$	K_2 $l \cdot mol^{-1}s^{-1}$	E_1 $kcal \cdot mol^{-1}$	E_2 $kcal \cdot mol^{-1}$
18	1.5×10^2	0.38×10^2	7.2	11.28
25	1.32×10^2	0.69×10^2		
35	2.3×10^2	1.1×10^2		

at several temperatures (Table 1).

From the slope of the lines obtained by plotting the equation $\log K = f(1/T)$, where T: the absolute temperature (Fig. 5), the activation energies of the reactions in the Co(II)-L system have been calculated (Table 1).

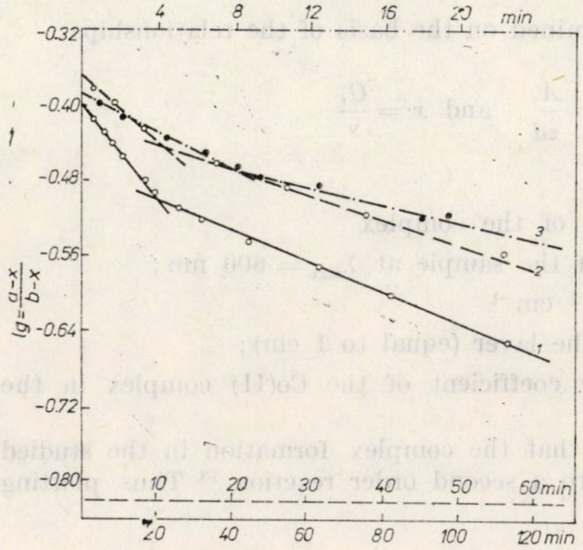

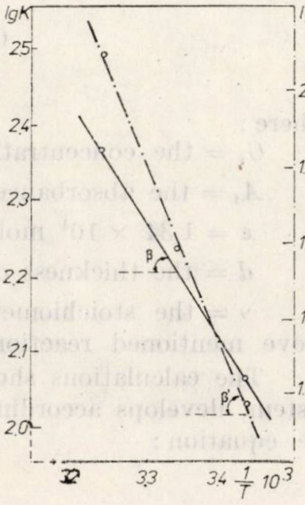

Fig. 4. Variation of $\lg \frac{a-x}{b-x}$ *versus* time, for the complex formation in the 1 Co(II)-2L system: 1 · t = 18°C; 2 · t = 25°C; 3 · t = 35°C.

Fig. 5. Plot of log K *versus* $\frac{1}{T}$.

REFERENCES

[1] N. Calu and N. Foca, *Anal. St. Univ. Iași Secț. I*, **18**, 1 (1972).
[2] N. Calu and N. Foca, *Anal. St. Univ. Iași Secț. I*, **18**, 2 (1972).
[3] N. Calu and N. Foca, *Anal. St. Univ. Iași Secț. I*, **19**, 1 (1972),
[4] J. Yoe and A. Jones, *Ind. Eng. Chem. Anal., Ed.*, **16**, 111 (1944).
[5] P. Job, *Liebigs Ann. Chem.*, **1928**, 113.
[6] H. Bent and C. French, *J. Amer. Chem. Soc.*, **63**, 568 (1941).
[7] A. C. Cope and R. W. Siekman, *J. Amer. Chem. Soc.*, **87**, 3272 (1965).
[8] J. P. Kleiman and M. Dubeck, *J. Amer. Chem. Soc.*, **85**, 1544 (1963).
[9] R. F. Heck, *J. Amer. Chem. Soc.*, **90**, 313 (1968).
[10] M. M. Bagga, P. L. Pauson, F. J. Preston, and R. I. Reed, *Chem. Comm.*, 1965, 543.
[11] S. Edmonds and N. Birnbaum, *J. Amer. Chem. Soc.*, **63**, 1471 (1941).
[12] S. E. Turner and R. G. Anderson, *J. Amer. Chem. Soc.*, **71**, 912 (1949).
[13] I. G. Murgulescu, T. Oncescu and E. Segal, "Introducere în chimia fizică" vol. II, Ed. Acad. R.S.R., București, 1981, p. 49.

Revue Roumaine de Chimie. 28, 4, 355–364 (1983)

COMPLEX COMPOUNDS OF Ni(II) WITH ACETONE SELENOSEMICARBAZONE

D. NEGOIU and ILEANA GHELASE

Faculty of Chemical Technology, Polytechnical Institute of Bucharest, 1, Polizu Street,
78126 – Bucharest, Romania

Received May 6, 1981

Complex compounds of Ni(II) with acetone selenosemicarbazone (Hsesac) of $[Ni_2CH_3COO(sesac)_2(H_2O)_2]CH_3COO \cdot 3H_2O$, $[Ni(sesac)_2] \cdot 0.5H_2O$, $[Ni(sesac)_2]$, $[Ni(sesac)_2Hsesac]$ and $[Ni(Hsesac)_2H_2O]Cl_2 \cdot 0.5H_2O$ types have been synthetized. The compounds were characterized through elemental chemical analysis, determinations of molecular weight and molar electric conductivity, and visible, ultraviolet and IR spectra. The stereochemistry of the complex compounds has been established, as well as the mode of coordination of the ligands.

INTRODUCTION

Since 1968,[1,2] a number of papers have appeared in the literature reporting on new complex compounds of copper, zinc, vanadium, chromium, iron, cobalt, nickel, palladium with selenosemicarbazide and various selenosemicarbazones [3] as ligands. In a previous paper [4] we reported on the synthesis and characterization of cadmium complexes with acetone selenosemicarbazone.

Since the literature has mentioned only one nickel complex with acetone selenosemicarbazone, [5] we found of interest to investigate the ability of Ni(II) ion to form complexes with this ligand.

RESULTS AND DISCUSSION

Complex compounds of nickel with acetone selenosemicarbazone (Hsesac) were obtained from nickel acetate and nickel chloride. Taking into account the (previously established) heat and water sensitivity of cadmium complexes of acetone selenosemicarbazone, [4] all our experiments were carried out in ethyl alcohol solutions, at room temperature, while varying the molar ratio between the central metal ion and the ligand, the pH value of the medium, the nature of the nickel salt and the concentration of the solutions.

When nickel acetate, $Ni(CH_3COO)_2 \cdot 4H_2O$, and acetone selenosemicarbazone (Hsesac) are taken under molar ratio 1 : 1, in saturated ethanolic solution (pH = 7), at room temperature, a microcrystalline gray-greenish complex $[Ni_2CH_3COO(sesac)_2(H_2O)_2]CH_3COO \cdot 3H_2O$ is obtained.

If the molar ratio is Ni : Se = 1 : 2 — under identical conditions — — the compound $[Ni(sesac)_2] \cdot 0.5H_2O$ is obtained, as a greenish-dark brown powder.

If the molar ratio of the reagents is again 1 : 2, while the ethanolic solution is more diluted (pH = 7), the anhydrous complex $[Ni(sesac)_2]$ is obtained, as a microcrystalline powder of dark brown-greenish colour. The complex compound $[Ni(sesac)_2]$ is also formed when the synthesis is carried out at pH = 11, in the presence of ammonia, at room temperature, irrespective of the Ni : Se molar ratio (1 : 1 or 1 : 2).

Towards nickel as a central metal ion in a medium of ethyl alcohol, at pH = 7, acetone selenosemicarbazone is a more powerful *trans*-active ligand than the acetate anion. Thus, in contrast to cadmium,[4] for which it has been possible to obtain a complex of the type $[CdCH_3COO(sesac)(Hsesac)] \cdot 0.5H_2O$, in the case of nickel all attempts undertaken under pH = 7 and the initial molar ratio Ni : Se = 1 : 2 have led only to compounds of the $[Ni(sesac)_2]$ type.

When the molar ratio nickel acetate : acetone selenosemicarbazone is 1 : 3, in a neutral or slightly ammoniacal medium (pH = 8.5), microcrystalline compounds of the $[Ni(sesac)_2Hsesac]$ type, of a brown-greenish colour, are obtained.

When nickel chloride, $NiCl_2 \cdot 6H_2O$, and acetone selenosemicarbazone are used — but only for a Ni : Se = 1 : 1 molar ratio — a yellow-beige microcrystalline complex $[Ni(Hsesac)_2H_2O]Cl_2 \cdot 0.5H_2O$ resulted.

Like for acetates, nickel chloride and cadmium chloride behave differently when complexing with acetone selenosemicarbazone. Thus, while with cadmium chloride, two complex compounds of the form $[(CdClHsesacH_2O)_2]Cl_2$ and $[CdCl(Hsesac)_2]Cl \cdot 0.5H_2O$ were obtained,[4] nickel chloride with acetone selenosemicarbazone forms only the complex $[Ni(Hsesac)_2H_2O]Cl_2 \cdot 0.5H_2O$, despite the fact that the conditions were practically identical.

In each case the yields of the nickel complex compounds with acetone selenosemicarbazone were good, and the syntheses were reproducible (Table 1).

The complex compounds of nickel with acetone selenosemicarbazone are slightly soluble in methyl or ethyl alcohol and almost insoluble in nitrobenzene. They are sensitive to prolonged action of air, sunlight, humidity or warmth. In the absence of these factors, they can be relatively well preserved for some time.

The complex compounds of nickel with acetone selenosemicarbazone are monomers, with the exception of the binuclear compound $[Ni_2CH_3COO(sesac)_2(H_2O)_2]CH_3COO \cdot 3H_2O$.

Molar electric conductivity measurements have shown that the nickel acetone selenosemicarbazone complexes are either electrolytes of the type 1 : 1 and 1 : 2, or non-electrolytes (Table 2).

The electronic spectra of nickel acetone selenosemicarbazone complexes exhibit two absorption bands in the 350 nm and 400—450 nm

TABLE 2

Molar electric conductivity in methanolic solutions

Complex compounds	Concentration mol/l	Molar electric conductivity $\Omega^{-1} \cdot cm^2 \cdot mol^{-1}$	Type of electrolyte
$[Ni_2CH_3COO(sesac)_2(H_2O)_2]CH_3COO \cdot 3H_2O$	$2.65 \cdot 10^{-4}$	70	1 : 1
$[Ni(sesac)_2] \cdot 0.5H_2O$	$5.21 \cdot 10^{-4}$	14	non-electrolyte
$[Ni(sesac)_2]$	$2.71 \cdot 10^{-4}$	14	non-electrolyte
$[Ni(sesac)_2Hsesac]$	$5.01 \cdot 10^{-4}$	11	non electrolyte
$[Ni(Hsesac)_2H_2O]Cl_2 \cdot 0.5H_2O$	$2.61 \cdot 10^{-4}$	171	1 : 2

ranges, the first of these bands being more intense (Figs 1 and 2). These absorption bands are characteristic of square-planar complex compounds of divalent nickel. Thus, on the basis of the energy level diagram for a d^8 ion in a field of square-planar symmetry,[6,7] the relatively intense absorption band in the 15,000–25,000 cm^{-1} range (400–450 nm) may be attributed to the transition: ${}^1A_{2g} \leftarrow {}^1A_{1g}$ $(b_{1g} \leftarrow b_{2g})$, while the more intense band from the 23,000–30,000 cm^{-1} range (350 nm) can be attributed to the transition: ${}^1B_{1g} \leftarrow {}^1A_{1g}$ $(b_{1g} \leftarrow a_{1g})$.

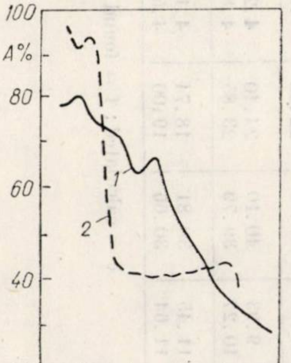

Fig. 1. — Electronic reflectance spectra of compounds:
1. $[Ni(Hsesac)_2H_2O]Cl_2 \cdot 0.5H_2O$,
2. Acetone selenosemicarbazone.

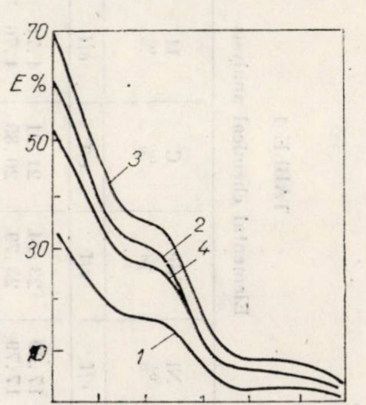

Fig. 2. — Visible absorption electronic spectra of complex compounds:
1. $[Ni_2CH_3COO(sesac)_2(H_2O)_2]CH_3COO \cdot 3H_2O$,
2. $[Ni(sesac)_2] \cdot 0.5H_2O$
3. $[Ni(sesac)_2]$, 4. $[Ni(sesac)_2Hsesac]$.

Just as in the case of cadmium complexes,[4] in the electronic spectra of square-planar complex compounds of nickel with acetone selenosemicarbazone, an absorption band "characteristic of the free ligand" also appears. This band, situated in the 270–285 nm range has been attributed to an $n \rightarrow \pi^*$ transition of lone electron pairs of the selenium atom.[8] This band has been used for the spectrophotometric determinations of molecular weight of the synthetized compounds. It is worth mentioning that the nickel complex of acetone selenosemicarbazone shows a slight hypsochromic shift of the absorption band "characteristic of the free ligand", which is probably determined by the nature of the central metal ion.

In the ultraviolet absorption electronic spectra of Ni(II) compounds: $[Ni_2CH_3COO(sesac)_2(H_2O)_2]CH_3COO \cdot 3H_2O$, $[Ni(sesac)_2]$, $[Ni(sesac)_2] \cdot 0.5H_2O$ and $[Ni(sesac)_2Hsesac]$ an intense absorption band appears at about 235 nm, as a result of a bathochromic shift of the free ligand absorption band, from 212 nm (Fig. 3). This seems to suggest that chelate rings are formed in these compounds, with the selenium ligand coordinated as a bidentate ligand, through σ bonds at the selenium atom and at the hydrazine nitrogen atom.

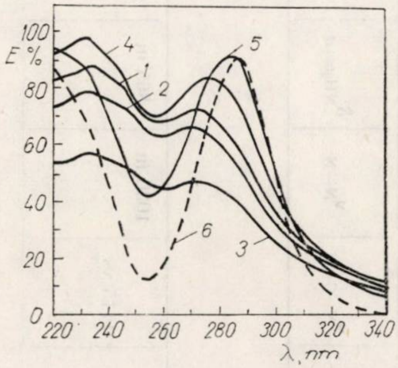

Fig. 3. — Ultraviolet absorption electronic spectra of compounds: 1. $[Ni_2CH_3COO(sesac)_2(H_2O)_2]CH_3COO \cdot 3H_2O$, 2. $[Ni(sesac)_2] \cdot 0.5H_2O$, 3. $[Ni(sesac)_2]$, 4. $[Ni(sesac)_2Hsesac]$, 5. $[Ni(Hsesac)_2H_2O]Cl_2 \cdot 0.5H_2O$, 6. Acetone selenosemicarbazone.

For the complex compound $[Ni(Hsesac)_2H_2O]Cl_2 \cdot 0.5H_2O$ the presence of an absorption band at 220 nm points that acetone selenosemicarbazone coordinates as a bidentate ligand, both at the selenium atom and at the hydrazine nitrogen atom, but only through σ bonds of the $L \rightarrow M$ type.

Vibrational spectra recorded in the 400—4,000 cm^{-1} range confirmed the structures suggested above (Table 3).

As a result of the coordination of acetone selenosemicarbazone ligand with the central metal ion, the greatest shifts of frequencies are produced in the IR spectra for the two neighbouring modes of vibration: $\delta_{NH_2 twist.}$ and $\nu_{C=Se}$.

Thus, in the compounds investigated, which contain a bidentate (chelating) or monodentate ligand through σ bonds at the selenium atom, $\delta_{NH_2 twist.}$ and $\nu_{C=Se}$ are shifted towards lower frequencies with 115 cm^{-1} and with 83—93 cm^{-1}, respectively.

In the case of the compound $[Ni(sesac)_2Hsesac]$ in the IR spectrum the two bands $\delta_{NH_2 twist.}$ and $\nu_{C=Se}$ are unmodified with respect to the free ligand. Likewise, a greater number of modes of vibration appear in the range of vibration frequencies: ν_{NH}, $(\delta_{N-H} + \nu_{C-N})$, ν_{N-C-N}, ν_{N-N}. The $\delta_{as\,CH_3}$ asymmetrical bending vibration is observed at 1 476 cm^{-1}. These observations lead to the conclusion that in the complex compound [Ni(sesac)$_2$Hsesac] one molecule of the ligand coordinates as a monodentate ligand through the amide nitrogen atom.

The presence of coordinated water in the compounds of the type $[Ni(Hsesac)_2H_2O]Cl_2 \cdot 0.5H_2O$ and $[Ni_2CH_3COO(sesac)_2(H_2O)_2]CH_3COO \cdot 3H_2O$ is proved by the bending vibrations $\delta_{H_2O\ wagging}$ at 735 cm^{-1} and at 780 cm^{-1} respectively. The greater value of the second absorption frequency suggests some intramolecular hydrogen bonds in the latter compound.[9]

The presence of crystallization water in $[Ni(sesac)_2] \cdot 0.5H_2O$, $[Ni(Hsesac)_2H_2O]Cl_2 \cdot 0.5H_2O$ and $[Ni_2CH_3COO(sesac)_2(H_2O)_2]CH_3COO \cdot 3H_2O$ proved by chemical methods — drying in an exsiccator under high vacuum, over P_2O_5 in the dark — is also confirmed by IR spectrometry. Thus, for these compounds, wide absorption bands appear in the range of ν_{NH} stretching vibrations, as a consequence of a superposition of the ν_{OH} stretching vibration modes of water molecules[9] with ν_{NH} stretching vibrations of the coordinated ligand. The presence of crystallization water is also proved by some wide absorption bands in the low frequencies range, at 600—400 cm^{-1}.

CONCLUSIONS

The data obtained by electronic and vibrational spectra reveal that, in the complex compounds of nickel with acetone selenosemicarbazone, selenium interacts with the central metal ion forming σ bonds.

Nitrogen atoms — whether hydrazine or amide — of the acetone selenosemicarbazone form only σ bonds of the L → M type, with a Ni(II) ion.

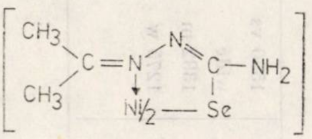

(1)

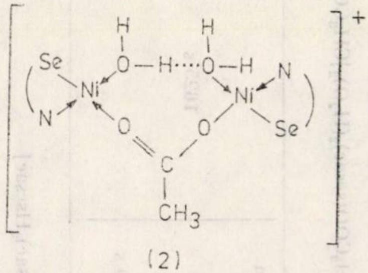

(2)

Acetone selenosemicarbazone coordinates with the nickel central metal ion both as monodentate ligand and as bidentate ligand. It is bidentate in complex compounds $[Ni(sesac)_2]$, $[Ni(sesac)_2] \cdot 0.5H_2O$ and $[Ni_2CH_3COO(sesac)_2(H_2O)_2]CH_3COO \cdot 3H_2O$, according to structures **1** and **2**.

Coordination as a monodentate ligand is achieved either through the selenium atom, or through the atom of amide nitrogen — in the complex compounds $[Ni(Hsesac)_2H_2O]Cl_2 \cdot 0.5H_2O$ and $[Ni(sesac)_2Hsesac]$, which also contain molecules of selenosemicarbazone coordinated as bidentate ligand, according to structures **3** and **4**.

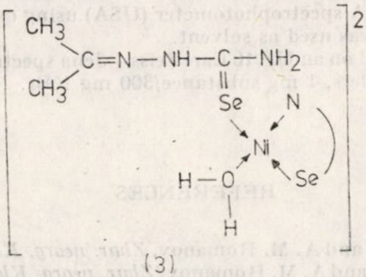

(3)

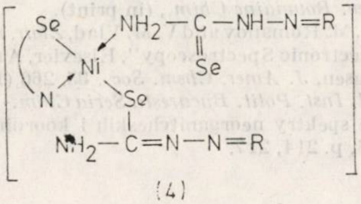

(4)

EXPERIMENTAL DATA

I. Complex compounds synthesis

1. $[Ni_2CH_3COO(sesac)_2(H_2O)_2]CH_3COO \cdot 3H_2O$: To a mixture of 0.74 g $Ni(CH_3COO)_2 \cdot 4H_2O$ and 0.53 g Hsesac, 0.4 cm³ ethyl alcohol is added. The components are mixed for about 15 minutes, when a new compound is formed, as a green-gray precipitate, with a strong smell of acetic acid. After adding 4 cm³ ethyl alcohol (pH = 7), the suspension is mixed and filtered. The precipitate, separated on a filter plate, is washed with 50 drops of ethyl alcohol and then dried in the dark, in the presence of air. The yield is 83%.

2. $[Ni(sesac)_2] \cdot 0.5H_2O$: 0.37 g $Ni(CH_3COO)_2 \cdot 4H_2O$ and 0.53 g Hsesac are mixed. 0.2 cm³ ethyl alcohol is added for moistening and a paste is formed, under continuous mixing. After about 15 minutes, 4 cm³ ethyl alcohol are added (pH = 7), stirring all the time. The precipitate is then filtered, washed with 50 drops of ethyl alcohol and dried. The yield is 94%.

3. $[Ni(sesac)_2]$: To 0.49 g $Ni(CH_3COO)_2 \cdot 4H_2O$ and 0.71 g Hsesac thoroughly mixed, 5 cm³ ethyl alcohol are gradually added (pH = 7). Immediately, a gray-greenish precipitate is formed ; however, the mingling continues for about 20 minutes, for the completion of the reaction. The precipitate is then filtered, washed with 50 drops of ethyl alcohol gradually added, and dried. The yield is 95%.

4. $[Ni(sesac)_2Hsesac]$: To 0.25 g $Ni(CH_3COO)_2 \cdot 4H_2O$ and 0.53 g Hsesac which have been mixed, 0.3 cm³ ethyl alcohol is added. The components are carefully mixed for 30 minutes. A green-gray dense precipitate appears, with a strong smell of acetic acid. Other 2 cm³ ethyl alcohol are added (pH = 7), the stirring is continued for a few minutes and the suspension is filtered. The resulting precipitate is washed with 30 drops of ethyl alcohol and dried. The yield is 92%.

5. $[Ni(Hsesac)_2H_2O]Cl_2 \cdot 0.5H_2O$: 1.19 g $NiCl_2 \cdot 6H_2O$ and 0.89 g Hsesac are mixed with 1.5 cm³ ethyl alcohol. In about 1 minute a yellow-light-beige paste is formed. After mixing the suspension for other 15 minutes, 4 cm³ ethyl alcohol are added (pH = 7) and the suspesnion is immediately filtered. The precipitate is washed with 30 drops of ethyl alcohol and then dried. (In the presence of water the resulting complex compound decomposes). The yield is 67%.

II. Apparatus

For molar electric conductivity measurements, a conductometer of the IRME type (Romania) was used, its cell constant being $c = 0.30738\ \text{cm}^{-1}$. CARLO ERBA methyl alcohol for electronic use, 99.9 % purity and 0.05 % H_2O, was used as solvent.

Electronic reflectance spectra were recorded on a VSU-1 spectrophotometer Carl Zeiss—Jena (East Germany), using magnesium oxide as reference substance.

Electronic absorption spectra (in the ultraviolet and visible ranges) were recorded on a double beam Beckman DK—2A spectrophotometer (USA) using quartz cells with optic path of 1 cm. Absolute ethyl alcohol was used as solvent.

IR spectra were recorded on an UR 10 Carl Zeiss—Jena spectrophotometer (G.D.R.). Solid samples were used as KBr pellets, 1 mg substance/300 mg KBr.

REFERENCES

[1] A. V. Ablov, N. V. Gerbeleu and A. M. Romanov, *Zhur. neorg. Khim.*, **13**, 787 (1968).

[2] A. V. Ablov, N. V. Gerbeleu and A. M. Romanov, *Zhur. neorg. Khim.*, **13**, 3024 (1968).

[3] I. Ghelase, Doctoral Dissertation, Polytechnical Institute of Bucharest, 1979.

[4] D. Negoiu and I. Ghelase, *Rev. Roumaine Chim.*, (in print).

[5] A. V. Ablov, N. V. Gerbeleu, A. M. Romanov and V. M. Vlad, *Zhur. neorg. Khim.*, **16**, 1357 (1971).

[6] A. B. P. Lever, "Inorganic Electronic Spectroscopy", Elsevier, Amsterdam, 1968, p. 343.

[7] H. B. Gray and C. J. Ballhausen, *J. Amer. Chem. Soc.*, **85**, 260 (1963).

[8] D. Negoiu and I. Ghelase, *Bul. Inst. Polit. București, Seria Chim.- Metal.*, **43**, 27 (1981).

[9] K. Nakamoto, "Infrakrasnye spektry neorganitcheskih i koordinatzionnyh soedinenij", Izd. Mir, Moscow, 1966, p. 214, 217.

Revue Roumaine de Chimie, 28, *4*, 365–373 (1983)

COORDINATION COMPOUNDS OF THIOCARBOHYDRAZONE-2-AMINOBENZALDEHYDE WITH Co(II) AND Ni(II) SALTS

RODICA MICU-SEMENIUC*, SILVIA BARBU** and MARIA SUZANA MIHAIU*

* Faculty of Chemical Technology, Arany Ianoş, 11
** Faculty of Pharmacy, Ion Creangă, 12, 3400 Cluj-Napoca, Romania

Received December 25, 1981

Complex halides and pseudohalides of Co(II) and Ni(II) with thiocarbohydrazone-2-aminobenzaldehyde (A—TCH) were synthesized. The combination ratio was 1M : 2X : 1 A—TCH. The compounds were investigated by electronic spectra and diffuse reflectance spectra. IR spectra were recorded and discussed. The magnetic moments were determined. The physico-chemical study suggests that there might be a $D_{4h} \rightleftarrows T_d$ equilibrium for the solid state of Co(II) compounds, while the Ni(II) compounds are square-planar both in the solution and solide state.

INTRODUCTION

Thiocarbohydrazones are compounds with known biological activity and analytical properties which allow various practical applications.[1,2] On the other hand they exhibit interesting coordinative properties due to the presence in the molecule of the azomethine (—N=CH—), hydrazine (—NH—NH_2) and thionic $\left(\rangle C{=}S\right)$ groups.

The coordinative abilities of salicylaldehyde, vanilline, isonicotinaldehyde, nicotinaldehyde and thiophene-2-carbaldehyde thiocarbohydrazones relative to the various salts of 3*d* ions in the 2^+ oxidation state were studied.[3]

The aim of this work is to test the donor complex forming capacity of thiocarbohydrazone-2-aminobenzaldehyde (A—TCH),

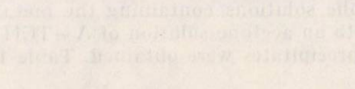

towards Co(II) and Ni(II) halides and pseudohalides.

EXPERIMENTAL

A. Synthesis of the ligand (A–TCH)

The thiocarbohydrazone of 2-aminobenzaldehyde was prepared by condensation of thiocarbohydrazide with 2-aminobenzaldehyde according to the reaction :

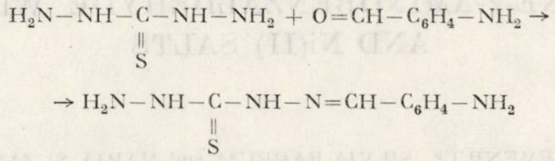

$$H_2N-NH-\underset{\underset{S}{\|}}{C}-NH-NH_2 + O=CH-C_6H_4-NH_2 \rightarrow$$

$$\rightarrow H_2N-NH-\underset{\underset{S}{\|}}{C}-NH-N=CH-C_6H_4-NH_2$$

Commercial grade 2-aminobenzaldehyde was used and thiocarbohydrazide was prepared according to literature. [4]

A methanolic solution of 2-aminobenzaldehyde (6.05 g in 50 ml methanol) was added to an aqueous solution of thiocarbohydrazide (5.3 g in 100 ml H_2O). The molar ratio was 1 : 1. The mixture was heated for 30 minutes on a water bath ; a yellow precipitate was formed and was filtered off. The precipitate was washed with methanol and ethanolic ether and was recrystallized from ethanol. Melting point 218°C with decomposition. The purity of substance was checked by elemental analysis : found % N 33.70 ; %S 15.10 ; %C 45.63 ; %H 5.01 ; requiered : %N 33.49 ; %S 15.31 ; %C 45.93 ; %H 5.26.

The thiocarbohydrazone of 2-aminobenzaldehyde (A–TCH) is insoluble in water, slightly soluble in acetone and ethanol and soluble in dimethylformamide and other basic solvents.

B. Synthesis of the complexes

Commercial grade metal halides were used in the synthesis of the complexes ; iodides and pseudohalides were obtained in solution by stoechiometric mixing of hexahydrated Co(II) and Ni(II) nitrate dissolved in ethanol with the aqueous solution of KI and KOCN or with ethanolic KSCN and KSeCN solution. The resulting potassium nitrate was filtered off.

The complexes were obtained by mixing the ethanolic solutions containing the metal salts (CoF_2 was the only one which dissolved in water) with an acetone solution of A–TCH, the molar ratio being 1 MX_2 : 1A–TCH. Microcrystalline precipitates were obtained. Table 1 contains the properties of complexes thus prepared.

TABLE 1

Some characteristics of the obtained compounds

Compound	Colour	M.P.(dec)°C	Solubility
$CoF_2 \cdot$ A–TCH	brown-red	(220)	dimethylformamide
$CoCl_2 \cdot$ A–TCH	brown-green	(272)	acetone
$CoBr_2 \cdot$ A–TCH	brown	(260)	methanol ; acetone
$CoI_2 \cdot$ A–TCH	brown	220	methanol ; acetone
$Co(NCO)_2 \cdot$ A–TCH	dark green	(180)	methanol ; acetone
$Co(NCS)_2 \cdot$ A–TCH	brown-green	(250)	acetone
$Co(NCSe)_2 \cdot$ A–TCH	brown-red	198	acetone
$NiCl_2 \cdot$ A–TCH	brown-red	(220)	acetone
$NiBr_2 \cdot$ A–TCH	brown	218	acetone
$NiI_2 \cdot$ A–TCH	brown	220	acetone
$Ni(SCN)_2 \cdot$ A–TCH	brown	250	acetone

Elemental analysis of the complexes is given in table 2. The metal content of the complex was determined by gravimetric analysis : cobalt as $CoSO_4$ and nickel as Ni(dimethylglioxime)$_2$. Nitrogen was determined by combustion, sulphur by the gravimetric method, after alkaline oxidation with $KMnO_4$ and $BaSO_4$ precipitation.

TABLE 2

Elemental analysis of the compounds

Compound	%M		%N		%S	
	found	calc.	found	calc.	found	calc.
$CoF_2 \cdot A-TCH$	18.80	19.26	22.81	22.88	10.39	10.46
$CoCl_2 \cdot A-TCH$	17.00	17.38	20.48	20.65	9.70	9.44
$CoBr_2 \cdot A-TCH$	13.40	13.77	16.55	16.36	7.48	7.70
$CoI_2 \cdot A-TCH$	10.92	11.29	13.21	13.41	6.53	6.13
$Co(NCO)_2 \cdot A-TCH$	16.52	16.74	27.89	27.84	8.70	9.09
$Co(NCS)_2 \cdot A-TCH$	15.64	15.34	25.80	25.52	24.40	25.00
$Co(NCSe)_2 \cdot A-TCH$	12.50	12.22	20.42	20.33	7.04	6.64
$NiCl_2 \cdot A-TCH$	16.97	17.33	20.66	20.66	9.20	9.44
$NiBr_2 \cdot A-TCH$	13.44	13.73	16.36	16.37	7.19	7.48
$NiI_2 \cdot A-TCH$	10.95	11.25	13.31	13.42	5.80	6.13
$Ni(SCN)_2 \cdot A-TCH$	14.91	15.30	25.69	25.25	24.72	25.01

The electronic absorption spectra of the complexes were studied with a Specord UV—VIS instrument. For some of the compounds the diffuse reflectance spectra in MgO or $BaSO_4$ pellets were studied (with a VSU—2P instrument provided with a reflection adapter).

The IR spectra were recorded with a Carl Zeiss Jena UR—20 instrument, in KBr pellets. Magnetic properties were determined by Gouy method at room temperature.

RESULTS AND DISCUSSION

The combination ratio was 1M : 2X : 1A—TCH (where M = Co(II) and X = F^-, Cl^-, Br^-, I^-, OCN^-, SCN^-, $SeCN^-$; M = Ni(II) and X=Cl^-, Br^-, I^-, SCN^-) (Table 2). The complexes were air stable except for the iodides, cyanates and selenocyanates which decomposed in a few days. The complexes obtained were thermally stable up to approx. 200°C. At this temperature some of the compounds decompose without melting, other melt with decomposition.

The electronic spectra were recorded in freshly-prepared solutions, obtained by mixing the reagents in the required stoechiometric ratios, in solutions obtained by dissolving the isolated solid complexes and in polycrystalline powders.

The spectrum of the (A—TCH) ligand was recorded in acetone solution and showed the following bands: 48,000; 42,000 (shoulder); 33,500 and 32,500 (doublet); 27,670 and 26,660 (doublet) cm^{-1}. Some of the spectra of the complexes obtained are shown in figures 1 and 2 and summarized in table 3.

The electronic spectra recorded in fresh solutions obtained from synthesis without isolation of the complex in the solid state and in acetone solution of the solid complexes (Table 3) were similar. In the solutions there was a unique symmetry: a pseudotetrahedral symmetry for Co(II) ions [5] and a square-planar symmetry for Ni(II) ions.[6]

The spectra recorded in solution for the Co(II) complexes showed only the ν_3 band ($^4T_1(P) \leftarrow {}^4A_2(F)$) multicomponent (Fig. 1 and Table 3).

The assignments were done by excluding the highest value component, the difference between the components of the ν_3 band being

TABLE 3

Electronic spectra of the compounds (cm^{-1})

Compound		Bands [a)]	Assignment	Bands of the ligand
				48,600
$CoCl_2 \cdot A-TCH$	I*	15,160	$^4T_1(P) \leftarrow {}^4A_2(F)$	42,000
		15,870 sh		33,200
		16,300 sh		26,000
		15,190		
	II*	15,900	$^4T_1(P) \leftarrow {}^4A_2(F)$	
		16,300		
		14,980		49,000
$CoBr_2 \cdot A-TCH$	I*	15,460 sh	$^4T_1(P) \leftarrow {}^4A_2(F)$	42,000
		17,500		32,600
				25,800
		14,920		
	II*	15,615 sh	$^4T_1(P) \leftarrow {}^4A_2(F)$	
		17,500 sh		
		5,500		
		5,900	$^4T_1(F) \leftarrow {}^4A_2(F)$	
		6,230		
	III*	8,400		
		9,000		
		12,200		
		15,400	$^4T_1(P) \leftarrow {}^4A_2(F)$	
		17,700		
		20,000		
$CoI_2 \cdot A-TCH$	I*	14,100		
		15,320	$^4T_1(P) \leftarrow {}^4A_2(F)$	
$Co(NCO)_2 \cdot A-TCH$	I*	15,900		
		17,000	$^4T_1(P) \leftarrow {}^4A_2(F)$	
$Co(NCS)_2 \cdot A-TCH$	I*	16,000		
		17,240	$^4T_1(P) \leftarrow {}^4A_2(F)$	
$Co(NCSe)_2 \cdot A-TCH$	I*	16,200	$^4T_1(P) \leftarrow {}^4A_2(F)$	
		13,000 sh		27,330
		15,670		26,830
$NiCl_2 \cdot A-TCH$	I*	19,330	$^1B_{1g} \leftarrow {}^1A_{1g}$	
		20,660	$^1A_{2g} \leftarrow {}^1A_{1g}$	
		12,840		27,330
		15,500	$^1B_{1g} \leftarrow {}^1A_{1g}$	26,830
$NiBr_2 \cdot A-TCH$	I*	19,250	$^1A_{2g} \leftarrow {}^1A_{1g}$	
		20,750		
		5,800		
		6,500		
		6,800		
		7,400		
$NiBr_2 \cdot A-TCH$	III*	15,550	$^1B_{1g} \leftarrow {}^1A_{1g}$	
		17,800 sh		
		18,200 sh		
		19,600	$^1A_{2g} \leftarrow {}^1A_{1g}$	
		15,420	$^1B_{1g} \leftarrow {}^1A_{1g}$	
$NiI_2 \cdot A-TCH$	I*	18,830	$^1A_{2g} \leftarrow {}^1A_{1g}$	
		20,830		

[a)] sh = shoulder

[*)] I — fresh solution prepared by mixing the reagents
II — acetone solution of the solid
III — diffuse reflectance

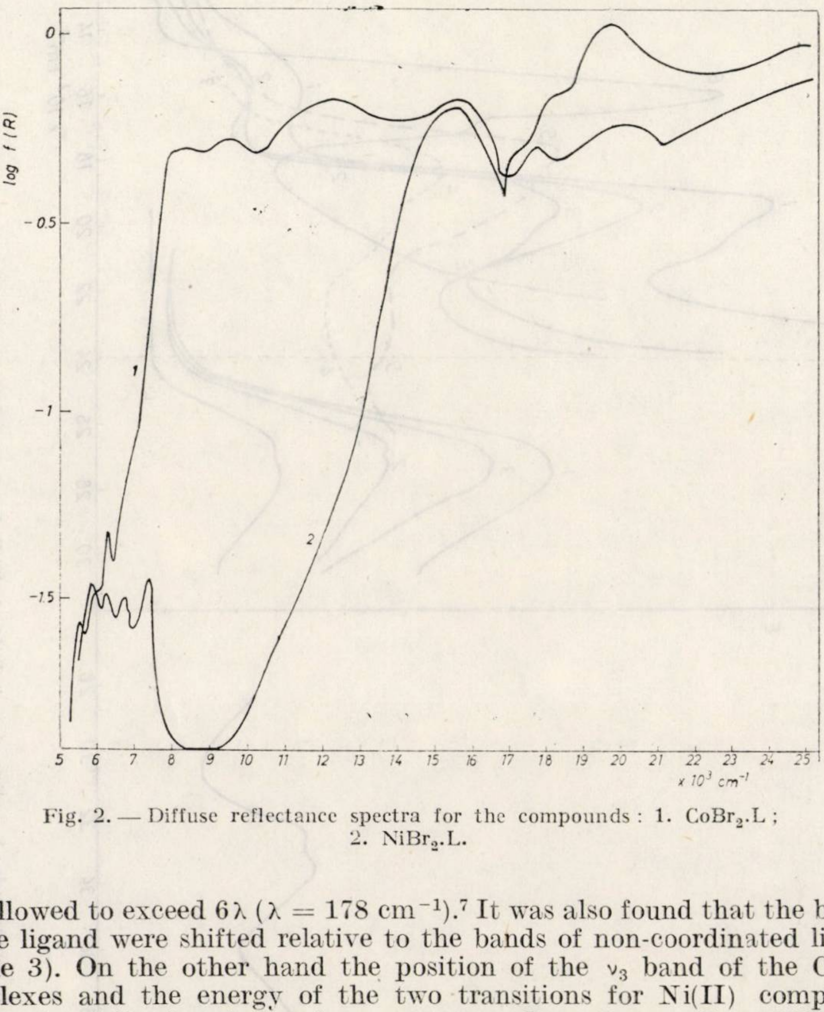

Fig. 2. — Diffuse reflectance spectra for the compounds : 1. $CoBr_2.L$; 2. $NiBr_2.L$.

not allowed to exceed 6λ ($\lambda = 178$ cm^{-1}).[7] It was also found that the bands of the ligand were shifted relative to the bands of non-coordinated ligand (Table 3). On the other hand the position of the ν_3 band of the Co(II) complexes and the energy of the two transitions for Ni(II) complexes lie in the following increasing sequence : $I^- < Br^- < Cl^- < NCO^- < NCS^- < NCSe^-$, which is the order of the ligands in the spectrochemical series, proving that the anions participate in the coordination.

The diffuse reflectance spectra showed several bands which were assigned in table 3. Beside the characteristic bands due to the tetrahedral configuration in solutions, the Co(II) compound (Fig. 2) also showed other bands. These can be correlated with the presence of D_{4h} symmetry species in solid state, there probably being a $T_d \rightleftarrows D_{4h}$ symmetry equilibrium similar to that shown by other Co(II) complexes.[8] The partial change of the central ions from the T_d symmetry (in solution) to D_{4h} symmetry (in solid state) may be correlated with the stiffening of the valence angles due to packing in the solid state and with the steric restrictions imposed by the ligand, following the reduction of free rotation capacity in solid state.

For the Co(II) ions, which remain in T_d symmetry in solid state, the following parameters were calculated according to the Lever method,[10] using the visual estimation of the ν_2 band by the centre of gravity of the multicomponent band[7]: the interelectronic repulsion parameter B' (722 cm^{-1}) which leads to a nephelauxetic parameter $\beta = 0.71$ and crystalline field splitting parameter $10\ D_q = 3{,}610\ cm^{-1}$.

Regarding the $NiBr_2 \cdot A-TCH$ compound (Fig. 2 and Table 3) it is assumed that the planarity of the Ni(II) ions is maintained in solid state but the spectrum contains several bands that might be due to some spin-forbidden transitions, and in the low energy region, to some combination bands or higher harmonics of the vibration bands.

The magnetic moments (Table 4) prove the planarity of the chromophore obtained for the Ni(II) complexes which are diamagnetic. The Co(II) compounds have lower magnetic moments than the spin only value ($\mu = 3.88$ MB). This is not incongruous with chromophore group planarity[9] but also suggests, like the diffuse reflectance spectra, a pos-

TABLE 4

Magnetic moments (BM) and IR spectra of the compounds (cm^{-1})

Compound	$\mu_{(BM)}$	$\nu_{NH_2} + \nu_{NH}$	$\nu_{C=N}$	$\nu_{C=S} + \nu_{C-N}$	ν_{CN}	δ_{NCX}	ν_{CX}
A−TCH	—	3450 3350 3285 3170	1615	785	—	—	—
$CoF_2 \cdot A-TCH$	3.7	3205 sh *	1610	760	—	—	—
$CoCl_2 \cdot A-TCH$	3.7	3450 3420 3200 sh	1610	765	—	—	—
$CoBr_2 \cdot A-TCH$	3.3	3440 *	1615	765	—	—	—
$CoI_2 \cdot A-TCH$	0.71	*	1610	760	—	—	—
$Co(NCO)_2 \cdot A-TCH$	—	*	1615	765	2200	620	—
$Co(NCS)_2 \cdot A-TCH$	—	3310 *	1615	765	2075	480 472	—
$Co(NCSe)_2 \cdot A-TCH$	—	*	1615	765	2095	460	650
$NiCl_2 \cdot A-TCH$	diamag	3430 *	1610	765	—	—	—
$NiBr_2 \cdot A-TCH$	diamag	3300 sh * 3350	1617	750	—	—	—
$NiI_2 \cdot A-TCH$	diamag	*	1610	765	—	—	—
$Ni(NCS)_2 \cdot A-TCH$	diamag	*	1615	760	2110	470	750

---

* The 3400−3100 cm^{-1} region appears as a continuous absorption for the most of the cases with some poor resolutions of the peaks proving the lack of amino group in the coordination.

sible $T_d \rightleftarrows D_{4h}$ equilibrium. The $CoI_2 \cdot A-TCH$ compound showed a peculiar behaviour. Its magnetic moment value ($\mu = 0.71$ MB) (Table 4) cannot be explained.

The IR spectra of the complexes were compared with the spectrum of the non-coordinated ligand. The characteristic bands of the ligand were assigned in comparison with the bands of thiocarbohydrazide.[4] The results are shown in Table 4.

The following three regions may be affected by the coordination of the ligand: 3,400–3,100 cm^{-1} (ν_{NH_2}); 1,600 cm^{-1} (characteristic of the azomethine group) and 800–700 cm^{-1} (where a combination $\nu_{C=S} + \nu_{C-N}$ band was observed).

The changes in the spectra may establish which donor group of the ligand participates in the coordination. It was found that for some compounds *(1; 2; 3; 6; 8; 9)* (Table 4) some bands or shoulders may be located in the ν_{NH_2} range, but generally this region cannot be used to establish the donor atoms, since a continuous absorption appears for all the compounds. In the ~ 1,600 cm^{-1} region no change was observed as compared to the free ligand, consequently the azomethine group is not involved in the coordination. The unique region affected by the formation of complexes is that between 800–700 cm^{-1} where the combined $\nu_{C=S}$ and ν_{C-N} band appears. It confirms the thionic group involvement in the coordination by its sulphur atom. Consequently the ligand forms a fivemembered ring with the metal ion according to structure *A* by the terminal nitrogen of the hydrazide group.

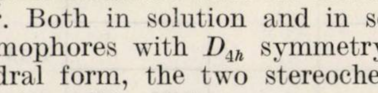

A

As the electronic spectra suggest, the anion coordination permits the formation of a type *A* structure with the metal ions having the coordination number four. Both in solution and in solide state, the Ni(II) compounds give chromophores with D_{4h} symmetry. Co(II) ions exist in solution in a tetrahedral form, the two stereochemical forms occurring simmultaneously only in solide state.

The pseudohalide ions are linked to the Co(II) atom by nitrogen atom, the ν_{CN} frequency being characteristic of this way of coordination [11-13] (Table 4).

According to the ν_{CN} band value [14,15] the thiocyanate ion is coordinated through the sulphur atom in the $Ni(SCN)_2 \cdot A-TCH$ compound (Table 4).

The chromophores thus obtained are of the MX_2NS type (wherf $X = F^-, Cl^-, Br^-, I^-$), of the CoN_3S type and $NiNS_3$ type in the case oe pseudohalide complexes.

REFERENCES

[1] H. W. Stephen and F. J. Wilson, *J. Chem. Soc.*, **1926**, 2531.
[2] S. Barbu and C. Gh. Macarovici, *Rev. Roumaine Chim.*, **26**, 1255 (1981).
[3] S. Barbu, Ph. D. Thesis, Library of Chemical Technology Department, Cluj-Napoca, 1975.
[4] G. R. Burns, *Inorg. Chem.*, **7**, 277 (1968).
[5] F. A. Cotton, D. M. L. Goodgame and M. Goodgame, *J. Amer. Chem. Soc.*, **83**, 4690 (1961).
[6] J. D. Lebedda and R. A. Palmer, *Inorg. Chem.*, **11**, 484 (1972).
[7] F. A. Cotton and M. Goodgame, *J. Amer. Chem. Soc.*, **83**, 1777 (1961).
[8] G. W. Everet and R. H. Holm, *J. Amer. Chem. Soc.*, **87**, 5266 (1965).
[9] F. A. Cotton and R. H. Holm, *J. Amer. Chem. Soc.*, **82**, 2979 (1960).
[10] A. B. P. Lever, *J. Chem . Educ.*, **45**, 711 (1968).
[11] A. H. Norbury and A. I. P. Shinha, *J. Chem. Soc.*, **1968 A**, 1599.
[12] J. Lewis, R. S. Nyholm and P. W. Smith, *J. Chem. Soc.*, **1961**, 4590.
[13] A. Turco, C. Pecile and M. Nicolini, *J. Chem. Soc.*, **1962**, 3008.
[14] A. Sabatini and I. Bertini, *Inorg. Chem.*, **4**, 959 (1965).
[15] M. E. Farago and J. M. James, *Inorg. Chem.*, **4**, 1706 (1965).

Revue Roumaine de Chimie, 28, 4, 375–379 (1983)

NEW PYRAZOLONE COMPLEX COMPOUNDS OF BIS-(METHYLAMINOANTIPYRYL)-ETHANE

IULIA HAVLIK*, T. SIMONESCU** and I. HAVLIK*
* Chemical Research Center, Timişoara, Blvd. Mihai Viteazul, No. 24, Romania
** University of Timişoara, Blvd. Vasile Pârvan No. 4, Timişoara, Romania

Received January 6, 1982

A number of eight new complex compounds of bis-(methylaminoantipyryl)-ethane of the type $ML(SCN)_2$ and $MLX_2 \cdot nMX_2$ (where M — transition metal) have been synthesized. The compounds have been characterized by elemental analysis, chromatography, electronic and vibrational spectra and by magnetic measurements.

In two previous papers we described the preparation of N,N′-bis-(antipyryl)-piperazine, a product obtained by the condensation of aminoantipyrine with 1,2-dibromoethane,[1] as well as the complex compounds of this ligand with different metal ions.[2]

The present work deals with the complex formation of a new ligand, bis-(methylaminoantipyryl)-ethane (L), the preparation of which is the object of a patent application.[3] The methyl group at the N atom from the $\rangle C_4-N$ position in L was introduced with the purpose of blocking the position 4 (a very reactive one) and of obtaining a linear product of condensation.

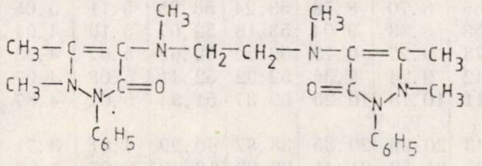

L

The present paper reports on the use of this ligand in the preparation of complexes with $3d^n4s^2$ (where $n = 5-10$) metals (except Cu) and group IIB metals.

EXPERIMENTAL

For the synthesis of complex compounds, metal acetates $MAc_2 \cdot 4H_2O$ (M = Mn, Ni, Co and Ac = Acetate) and $FeSO_4$, $ZnCl_2$, $CdCl_2 \cdot 2H_2O$ and HgJ_2 were used. The syntheses were carried out in ethanol, or in ethanol-water mixtures, at 20°C or 60°C, depending on the solubility of the metal salts and of the resulting complexes. The compounds obtained are of the type $ML(SCN)_2$(M = Mn, Fe, Co, Ni and Zn) and $MLX_2 \cdot nMX_2$(M = Cd, Hg, X = SCN, J, n = 0.5, 1.5, and 2). No complex compounds of the type $ML(SCN)_2$ could be obtained with Cd and Hg, since the solubility of their metal salts is lower than that of their complexes. The determination the halogen content by potentiometric titration for these complexes gave lower results, because of the partial ionization of the salts. Only one example for the synthesis of each type of compounds is illustrated here.

Preparation of $MnL(SCN)_2$: 0.0613 g ($2.5 \cdot 10^{-4}$ M) $MnAc_2 \cdot 4H_2O$ is solved at 60°C, under stirring in 5 ml ethanol. Then 0.0381 g ($5 \cdot 10^{-4}$ M) NH_4SCN, dissolved in 2.5 ml ethanol is added dropwise to obtain $Mn(SCN)_2$; the mixture is stirred continuously at 50—60°C, then 0.1151 g ($2.5 \cdot 10^{-4}$M) ligand L solved in 5 ml ethanol is added dropwise. The formation of the complex started almost immediately, but the compound is kept at + 5°C for two hours, to form easy filtrable crystals. The solid is filtered on a G3 crucible, washed with ethanol and dried at 70°C. The yield of $MnL(SCN)_2$ is 91.03 %. For other compounds similarly prepared the yields are : 68.4 % for $FeL(SCN)_2$ and 96.5 % for $CoL(SCN)_2$.

Preparation of $HgLJ_2 \cdot 1.5\ HgJ_2$: 0.1136 g($2.5 \cdot 10^{-4}$M) HgJ_2 is solved at 60°C, under stirring in 15 ml ethanol. An amount of 0.1151 g ($2.5 \cdot 10^{-4}$M) L, solved in 5 ml ethanol is added. The yellow solution formed is kept at 60°C, stirred, and after 30 min the complex begins to deposit as a yellow precipitate. The system is stirred and warmed cca 30 min and then kept at + 5°C for two hours. The solid is filtered on a G3 crucible, washed with ethanol and dried at 70°C. The yield of $HgLJ_2 \cdot 1.5\ HgJ_2$ is 42.5 %. The yields of $CdL(SCN)_2 \cdot 0.5Cd(SCN)_2$ and $CdLJ_2 \cdot 2CdJ_2$, which are prepared similarly, are 72.5 % and 61.5 %, respectively.

The compounds prepared are insoluble in water, slightly soluble in ethanol, acetone, chloroform.

The results of the elemental analysis and the melting points of the compounds are given in table 1.

TABLE 1

Analytical data of complexes

Compound	Molecular weight	M(%)		C(%)		H(%)		SCN(%) :J(%)		Melting point (°C)
		calcd.	found	calcd.	found	calcd.	found	calcd.	found	
$MnL(SCN)_2$	631.66	8.70	8.78	53.24	53.25	5.11	5.05	18.39	17.82	298
$FeL(SCN)_2$	632.58	8.83	9.04	53.16	52.07	5.10	4.91	18.36	18.24	297
$CoL(SCN)_2$	635.73	9.27	9.13	52.90	52.62	5.07	4.93	18.27	18.36	291
$NiL(SCN)_2$	635.42	9.24	9.36	52.92	52.41	5.08	4.97	18.28	17.99	294—6
$ZnL(SCN)_2$	642.11	10.18	10.25	52.37	51.54	5.02	4.87	18.09	18.45	258
$CdL(SCN)_2 \cdot 0.5Cd(SCN)_2$	803.43	20.99	20.35	38.87	40.29	4.01	3.71	21.69	19.35	246
$CdLJ_2 \cdot 2CdJ_2$	1559.25	21.62	21.41	20.03	19.40	2.07	1.99	48.83	43.22	180
$HgLJ_2 \cdot 1.5HgJ_2$	1602.70	31.29	30.98	19.48	20.05	2.01	1.96	39.59	36.18	165—7

The purity of the compounds was checked by paper chromatography using Whatman paper no.1, a mixture of methylcyclohexane : acetone (in 4 : 5 ratio) as developing solvent and Dragendorff's reagent for detection.

The electronic spectra of the compounds were recorded on a Unicam SP 800 spectrophotometer, in glass cells, using solutions of the samples of $0.7 \cdot 10^{-4}$ M/1 in absolute ethanol.

The vibrational spectrum was registered on a Specord IR 75 spectrophotometer, in the range of 400—4000 cm^{-1}, using the KBr mulls technique.

The magnetic moment was determined on a Gouy balance, at 21°C using $Hg[Co(SCN)_4]$ for calibration.

RESULTS AND DISCUSSIONS

The results of elemental analysis and paper chromatography show that the compounds are pure, free of uncomplexed ligand.

The electronic spectra are given in table 2. In the spectra of the complexes, two ligand maxima are present. The high ε value suggests a charge transfer origin of the bands.

TABLE 2

Electronic spectral data

Compound	Absorption 1		Absorption 2	
	λnm, (cm^{-1})	ε	λnm, (cm^{-1})	ε
L	243 .5(41,070)	17,020	272(36,765)	15,860
$MnL(SCN)_2$	243(41,150)	17,200	271(36,900)	19,400
$FeL(SCN)_2$	244(40,980)	18,370	268(37,300)	21,555
$CoL(SCN)_2$	243 .5(41,070)	17,950	273,5(36,560)	18,750
$NiL(SCN)_2$	243(41,150)	17,980	272 .5(36,700)	21,700
$ZnL(SCN)_2$	243(41,150)	17,980	268 .5(37,240)	20,975
$CdL(SCN)_2 \cdot 0.5Cd(SCN)_2$	245(40,815)	17,150	271(36,900)	20,885
$CdLJ_2 \cdot 2CdJ_2$	228(43,860)	22,460	272(36,765)	20,415
$HgLJ_2 \cdot 1.5\ HgJ_2$	230(43,480)	17,120	271(36,900)	16,825

Table 3 shows the characteristic vibrational bands of the free ligand and those of the complexes. In the case of the $FeL(SCN)_2$, $CdL(SCN)_2 \cdot 0.5\ Cd(SCN)_2$, $CdLJ_2 \cdot 2CdJ_2$ and $HgLJ_2 \cdot 1 \cdot 5HgJ_2$ complexes, the $\nu_{C=O}$ band (at cca 1600 cm^{-1}) disappeared by complexation, and a new band appeared at about 1000 cm^{-1}, which can be attributed to ν_{C-O}. The both pairs of donor atoms coordinate, thus the metal ions are six-coordinated. Due to the complex spatial structure, it is possible that the two pairs of donor atoms may not belong to the same ligand molecule, resulting in the formation of polynuclear compounds of the type:

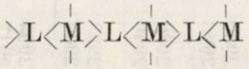

$$>L<\overset{|}{\underset{|}{M}}>L<\overset{|}{\underset{|}{M}}>L<\overset{|}{\underset{|}{M}}$$

In the case of the other compounds, both vibrations corresponding to $\nu_{C=O}$ and $\nu_{C=O}$ are present in the IR spectrum. In these compounds, the metal ion is four-coordinated, being bonded only with one pair of donor atoms $C_5-O\rightarrow$ and $C_4-N\rightarrow$ and the two X anions.

The magnetic data (Table 4) prove that $MnL(SCN)_2$ and $FeL(SCN)_2$ are high spin(O_h or T_d) complexes and $CoL(SCN)_2$ and $NiL(SCN)_2$ are high or low spin(O_h or T_d) complexes.

The results of vibrational spectrum and magnetic measurements suggest the following probable structures for the four complexes: $FeL(SCN)_2O_h$, $MnL(SCN)_2$, $CoL(SCN)_2$ and $NiL(SCN)_2\ T_d$.

CONCLUSIONS

1. Eight new complexes of bis-(methylaminoantipyryl)-ethane with different transition metals have been prepared.

2. The electronic spectra of the compounds have been recorded, compared with the spectrum of the ligand and suggest a charge transfer origin of the bands.

TABLE 4

Magnetic data of complexes

Compound	$\chi_m \cdot 10^6$ cgsu	μ_{eff}(BM)	No. unpaired electrons
$MnL(SCN)_2$	15,091.21	5.98	5
$FeL(SCN)_2$	13,425.92	5.65	4
$CoL(SCN)_2$	8,870.97	4.58	3
$NiL(SCN)_2$	4,137.5	3.27	2

3. The vibrational spectra were used to establish the donor groups. Based on spectroscopic evidence, four-coordination for the d^5, d^7, d^8 and d^{10} (Zn) metal ions complexes and six-coordination for d^6 and d^{10} (Cd and Hg) complexes was established, in agreement with magnetic measurements.

REFERENCES

[1] S. Policec, A. Maurer, I. Havlik, O. Costişor, M. Mracec and C. Csunderlik, *Bul. Inst. Polit. Timişoara*, **25**, 57 (1980).

[2] I. Havlik, T. Simonescu, I. Havlik, A. Maurer and S. Policec, *Bul. Inst. Polit. Timişoara*, in press.

[3] I. Havlik, T. Simonescu, A. Maurer and I. Havlik, Rom. Pat. Appl. 102460, 29 oct. 1980.

Revue Roumaine de Chimie, 28, *4*, 381–385 (1983)

SOLVENT EFFECTS. II[1]

SOLVENT INFLUENCE ON THE ACIDITY OF SOME NITROPHENOTHIAZINIC COMPOUNDS

M. RĂILEANU, S. FLOREA and N. MUREȘAN
University of Craiova, Department of Chemistry, Str. A. I. Cuza, 13,
Craiova, Romania

Received January 19, 1982

Acidity constants of 1,3,7-trinitrophenothiazine-5-oxide, -1,3,7-trinitrophenothiazine-5, 5-dioxide, 1, 3, 7, 9-tetranitrophenothiazine-5-oxide and 1,3,7 9-tetranitrophenothiazine-5, 5-dioxide in tetrahydrofuran, acetonitrile, methylethylketone, dimethylsulphoxide, dimethylformamide and in 0.75 N NaOH in dimethylformamide-water (1 : 3, V/V) were spectrophotometrically determined. It was found that the steric effect at the acidity center from position 10 of these compounds changes the basicity scale of the solvents deduced by Agami and Caillot by utilising the IR spectra of phenylacetylene.

1. INTRODUCTION

In a previous paper [1] the solvent influence on the absorption spectra of some nitroderivatives of phenothiazine (I) was studied and it was established that in some solvents these compounds ionise losing a proton from position 10. It was shown also that the nitrogroups from positions 1 and 9 form intramolecular hydrogen bonds with the hydrogen atom from position 10. Thus chelated structures result which determine a decrease of the acidity in the corresponding nitroderivatives.[2–6]

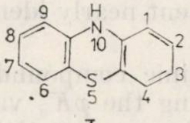

I

In the present paper it has been studied the influence of solvent basicity on the acidity of some phenothiazinic nitroderivatives possessing an intramolecular hydrogen bond. The studied nitroderivatives and the corresponding abbreviations are:

1,3,7-Trinitrophenothiazine-5-oxide (tNPS);
1,3,7-Trinitrophenothiazine-5,5-dioxide (tNPD);
1,3,7,9-Tetranitrophenothiazine-5-oxide (TNPS);
1,3,7,9-Tetranitrophenothiazine-5,5-dioxide (TNPD);

In order to calculate the acidity constants (K_a), the extinctions (E) for absorptions of anions resulted from nitroderivative ionization were read on the spectrophotometer.

Having in view the acid ionization reaction:

$$HA \rightleftharpoons H^+ + A^-$$

and the fact that $[A^-] = [H^+]$, the K_a value can be calculated from relation (1):

$$K_a = \frac{[A^-]^2}{[HA]} = \frac{[A^-]^2}{c - [A^-]} \qquad (1)$$

where c represents the initial concentration of the nitrophenothiazinic compound.

The anion concentrations and the molar extinction coefficients (ε) were calculated from the Lambert-Beer relation (2):

$$E = \varepsilon \cdot 1 \cdot c \qquad (2)$$

where $c = [A^-]$.

It was found experimentally that all the four phenothiazinic nitroderivatives studied ionise completely in the dimethylformamide (DMF) at the concentration order of 10^{-5} M. Under these conditions the absorption band for the unionized form of the nitroderivatives disappears and the molar extinction coefficients are calculated from the extinction values for the wavelengths of the corresponding anions.

The acidity constants in acetonitrile (AN), methylethylketone (MEC), tetrahydrofuran (THF), dimethylsulphoxide (DMSO) and 0.75 N NaOH in DMF$-H_2O$ (1 : 3, V/V) were determined.

2. RESULTS AND DISCUSSIONS

In table 1 the studied substances, the utilized solvents, the spectral data and the acidity constants are presented.

As expected, the molar extinction coefficients for tNPS and tNPD anions, possessing three nitro groups, have very similar values; also the TNPS and TNPD anions, with four nitro groups, present nearly identical molar extinction coefficients.

In table 2 the pK_a values of the nitrophenothiazinic compounds studied in five different solvents are presented. Comparing the pK_a values of TNPS and TNPD in different solvents and having in view that these compounds ionize completely in DMF, it results that the basicity of the utilized solvents increases in the following order:

$$\text{THF} < \text{AN} < \text{MEC} < \text{DMSO} < \text{DMF}$$

Agami and Caillot,[7] utilising the stretch vibrations of the C$-$H group from the phenylacetylene, forming hydrogen bonds with different basic solvents, have found from the IR spectrum shift that the basicity of the solvents mentioned above increases in the following order: AN < < acetone < THF < DMF < DMSO.

The basicity scale of the solvents found by Agami and Caillot is verified also through the displacement of ^{1}H$-$NMR signal of the chloroform in the corresponding solvents.[8-9]

TABLE 1

Spectral data and K_a values of tNPS, tNPD, TNPS and TNPD in different solvents

Substance	Solvent	Conc. $\times 10^5$ (mol/l)	λ(nm)	E	ε	l(cm)	K_a
tNPS	DMF	1.72	500	0.92	53488	1	—
	AN	1.71	500	0.25	—	1	1.76×10^{-6}
	THF	3.42	505	0,08	—	1	6.51×10^{-8}
	MEC	7.26	500	0.06	—	0.5	7.13×10^{-8}
	DMSO	8.38	500	1.24	—	0.5	5.75×10^{-5}
	0.75N NaOH*	5.89	480	1.16	—	0.5	1.21×10^{-4}
tNPD	DMF	1.64	505	0.88	53658	1	—
	AN	1.64	500	0.34	—	1	4.00×10^{-6}
	THF	1.64	505	0.06	—	1	8.20×10^{-8}
	MEC	5.89	500	0.08	—	1	3.86×10^{-8}
	DMSO	5.76	505	0.87	—	0.5	4.16×10^{-5}
	0.75N NaOH*	6.33	480	1.20	—	0.5	1.07×10^{-4}
TNPS	DMF	1.52	480	0.84	55263	1	—
	AN	1.58	480	0.40	—	1	6.12×10^{-6}
	THF	4.45	480	0.28	—	1	6.50×10^{-7}
	MEC	6.63	480	0.70	—	0.5	1.56×10^{-5}
	DMSO	3.28	480	0.88	—	0.5	1.01×10^{-3}
	0.75N NaOH*	5.00	475	1.06	—	0.5	1.25×10^{-4}
TNPD	DMF	1.36	480	0.75	55147	1	—
	AN	1.46	480	0.40	—	1	7.15×10^{-6}
	THF	6.26	480	0.16	—	1	1.40×10^{-7}
	MEC	8.40	480	0.74	—	0.5	1.26×10^{-5}
	DMSO	4.96	480	1.29	—	0.5	7.26×10^{-4}
	0.75N NaOH*	5.79	475	1.22	—	0.5	1.43×10^{-4}

* in DMF – H_2O(1 : 3, V/V)

The disagreement between the basicity scale of the solvents found by us and that established by Agami and Caillot[7] can be explained, having in view that in tNPS, tNPD, TNPS and TNPD the hydrogen atom from position 10 is sterically hindered by the neighbouring nitro groups from positions 1 and 9.

Because of the steric hindrance the solvent molecules with different volumes and structures have a different access at the hydrogen atom from position 10.

TABLE 2

pK_a values of tNPS, tNPD, TNPS and TNPD in different solvents

Solvent / Substance	THF	AN	MEC	DMSO	0.75N NaOH in DMF – H_2O (1 : 3, v/v)
TNPS	6.19	5.21	4.80	2.99	3.90
TNPD	6.85	5.14	4.90	3.11	3.84
tNPS	7.18	5.75	7.15	4.24	3.92
tNPD	7.08	5.40	7.41	4.38	3.97

Indeed, we can admit that the center of acidity from position 10 is more sterically hindered in TNPS and TNPD than in tNPS and tNPD. Although the TNPS and TNPD have a greater acidity than the tNPS and tNPD, we expect a tendency of levelling the acidity of these compounds, if the solvent molecule penetrates more difficult the center of acidity from TNPS and TNPD in comparison with tNPS and tNPD. This phenomenon can be observed in acetonitrile. It is easy to admit that in the absence of sterical hindrance, the acetonitrile, which is a weakly basic solvent on the Agami and Caillot's scale, is not able to level the acidity of nitrophenothiazinic compounds with three and four nitro groups. In the same way the levelling of the acidity of the nitrophenothiazinic compounds with three and four nitro groups in 0.75 N NaOH in DMF—H_2O (1 : 3, V/V) can be explained.

On the contrary, other solvents, namely THF, MEC and DMSO, differentiate the acidity of nitrophenothiazinic compounds with three and four nitro groups, as resulting by comparing the pK_a values. This fact can be explained by admitting that the molecules of these solvents penetrate approximately with the same difficulty the center of acidity sterically hindered by a nitro group from position 9 or by two nitro groups from positions 1 and 9. The contribution of the fourth nitro group to the acidity of the studied compounds in THF, MEC and DMSO is obvious.

The basicity of the HO^- anion and of the DMF molecules from the 0.75 N NaOH solution in DMF—H_2O(1 : 3, V/V) is smaller than the basicity of the pure DMF in which the four nitrophenothiazinic compounds ionise completely. This phenomenon can be easily explained because HO^- anions and the DMF molecules lose from their real basicity by formation of the hydrogen bonds with water. The decrease of the anionic basicity in protic solvents was previously studied by Hammett,[10] Weaver and Hutchison,[11] Cavell, [12,13] and others. It was established that the solvatation capacity of anions by hydrogen bonds increases with their charge density, *i.e.* with the ratio between charge and volume.

From the results obtained in this paper it was found that the basicity scale of the solvents changes, if the acidity centre of the solvated substances is sterically hindered. In this case an apparent basicity instead of the real one is manifested.

EXPERIMENTAL

The anionic extinctions resulted in nitrophenothiazinic compound ionization were read on a Specord UV—VIS Carl Zeiss—Jena spectrophotometer at room temperature.

The nitrophenothiazinic compounds were prepared by methods described in the literature. [14,15]

The solution concentrations were of the 10^{-5} M order.

Spectroscopically pure solvents were utilized.

REFERENCES

[1] Part I : M. Răileanu, S. Florea and M. Sahini, Rev. Roumaine Chim., (in press).
[2] R. Arnold and J. Sprung, *J. Amer. Chem. Soc.*, **61**, 2475 (1939).
[3] M. I. Gornyaev, V. S. Volkov and G. A. Tolsticov, *Zhur. Org. Chim.*, **28**, 2102 (1958).
[4] G. R. Sprengling and C. W. Lewis, *J. Amer. Chem. Soc.*, **75**, 5709 (1953).

[5] M. Davies, *Trans. Faraday Soc.*, **36**, 1114 (1940).

[6] J. G. Lombardino, *J. Org. Chem.*, **32**, 1988 (1967)

[7] C. Agami and M. Caillot, *Bull. Soc. chim. France*, **1969**, 1990.

[8] T. Cuvigny and H. Normant, *Bull. Soc. chim. France.*, **1964**, 2000.

[9] H. Normant, *Angew. Chem.*, **79**, 1029 (1967) ; *Bull. Soc. chim. France.*, **1968**, 791 ; *Uspekhi Khim.*, **39**, 990 (1970).

[10] H. R. McCleary and L. P. Hammett, *J. Amer. Chem. Soc.*, **63**, 2254 (1941).

[11] W. A. Weaver and J. D. Hutchison, *J. Amer. Chem. Soc.*, **86**, 261 (1964).

[12] E. A. S. Cavell, *J. Chem. Soc.*, **1958**, 4217.

[13] E. A. S. Cavell and J. A. Speed, *J. Chem. Soc.*, **1960**, 1453.

[14] M. Răileanu, *Rev. Chim, (București)*, **33**, 1102 (1982).

[15] C. Bodea and M. Răileanu, *Studii și Cercet. Chim. Acad. R.P.R., Fil. Cluj*, **1957**, 303.

Revue Roumaine de Chimie, **28**, *4*, 387–396 (1983)

LE COMPORTEMENT THERMIQUE DES COMPOSÉS MACROMOLÉCULAIRES CONTENANT DU PHOSPHORE ET DU SOUFRE DANS LA CHAÎNE ET DE LEURS MÉLANGES AVEC LE POLYPROPYLÈNE

OANA PETREUȘ et FLORIN NECULAI POPESCU
Institut de chimie macromoléculaire « Petru Poni » Allée Grigore Ghica Vodă n° 41 A — Iassy — Roumanie

Reçu le 14 juin 1980

On expose des données sur le comportement thermique de quelques additifs macromoléculaires organiques ayant dans leur constitution du phosphore et du soufre. On constate que le comportement thermique est aussi influencé par l'halogène qui se trouve dans l'unité structurelle de l'additif macromoléculaire phosphoré. Les résultats de l'analyse thermique des composés qui contiennent du phosphore et du soufre sont comparés avec ceux du polypropylène et des mélanges du polypropylène avec les composés mentionnés. L'interprétation des résultats permet d'établir l'effet du phosphore et du soufre sur la stabilité thermique du polypropylène.

The paper presents data on the thermal behaviour of some macromolecular organic additives containing phosphorus and sulphur in their chains. The influence of halogen in the structural unit of the macromolecular additive has been studied. The results of thermal analysis of these compounds are compared with those of polypropene and of its mixtures with the compounds above-mentioned. Interpretation of results permits the determination of the phosphorous and sulphur effect on the thermal stablility of propene.

Les additifs macromoléculaires contenant du phosphore sont utilisés de plus en plus [1–5] pour l'ignifugation des fibres synthétiques à cause d'une meilleure compatibilité, d'une capacité d'exudation réduite et d'une altération minimale des propriétés mécaniques de la fibre additivée.

Les composés organiques du phosphore et du soufre sont mentionnés dans la littérature comme des agents d'ignifugation hautement résistants à l'action des détergents. [6]

Une des qualités nécessaires des agents d'ignifugation est aussi la stabilité thermique accrue, nécessaire pour assurrer son mélange en état fondu avec les polymères filables.

Les polyphénylephosphonates et les polyphényléthiophosphonates présentent une supériorité bien établie, résistant un temps illimité à 260°, et pour de courtes périodes de temps à des températures au-dessus de 500°.[7,8]

Des motifs d'ordre structural assurent cette supériorité comparativement aux polyphosphonates.[9]

Le présent travail contient quelques aspects liés à la stabilité thermique des polyphényléthiophosphonates et aussi la comparaison de cette stabilité avec celle du polypropylène et de leurs mélanges avec diverses quantités d'additifs.

TABLEAU 1

Analyse élémentaire des polymères étudiés

Notation dans le texte	Formule de l'unité structurelle	P %	S %	Hal. %
S_1	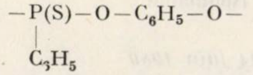 $-\underset{\substack{\vert\\ C_3H_5}}{P}(S)-O-C_6H_5-O-$	12,25	12,84	—
S_2	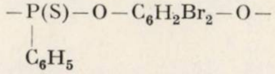 $-\underset{\substack{\vert\\ C_6H_5}}{P}(S)-O-C_6H_2Br_2-O-$	8,02	7,86	40,14
S_3	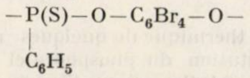 $-\underset{\substack{\vert\\ C_6H_5}}{P}(S)-O-C_6Br_4-O-$	5,28	5,78	56,82
S_4	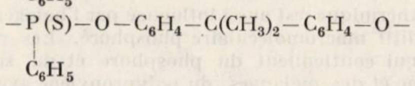 $-\underset{\substack{\vert\\ C_6H_5}}{P}(S)-O-C_6H_4-C(CH_3)_2-C_6H_4-O-$	8,50	8,57	—
S_5	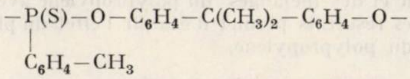 $-\underset{\substack{\vert\\ C_6H_4-CH_3}}{P}(S)-O-C_6H_4-C(CH_3)_2-C_6H_4-O-$	7,94	8,22	—
S_6	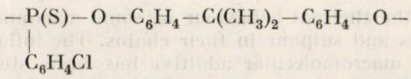 $-\underset{\substack{\vert\\ C_6H_4Cl}}{P}(S)-O-C_6H_4-C(CH_3)_2-C_6H_4-O-$	7,59	6,84	8,93
P_1	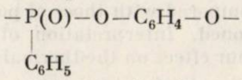 $\underset{\substack{\vert\\ C_6H_5}}{P}(O)-O-C_6H_4-O$	14,00	—	—
P_2	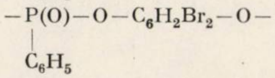 $-\underset{\substack{\vert\\ C_6H_5}}{P}(O)-O-C_6H_2Br_2-O-$	7,99	—	43,20
P_3	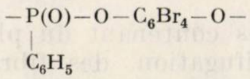 $-\underset{\substack{\vert\\ C_6H_5}}{P}(O)-O-C_6Br_4-O-$	5,42	—	59,59
P_4	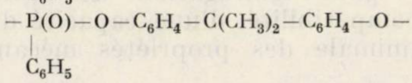 $-\underset{\substack{\vert\\ C_6H_5}}{P}(O)-O-C_6H_4-C(CH_3)_2-C_6H_4-O-$	9,14	—	—

On a soumis aux tests de thermostabilité six composés notés $S_1 - S_6$. On trouve dans le tableau 1 les formules des unités structurelles et les données de l'analyse élémentaire pour le contenu en pour cent en phosphore, soufre et halogène.

Les phosphonites notés conventionnellement $P_1 - P_4$ et qui se trouvent aussi dans le tableau 1 servent pour des déterminations comparatives.

Le polymère d'ignifugation S_5 a été mélangé avec le polypropylène en proportion de 1—5 % et la thermostabilité du mélange a été comparée avec le polymère S_5 et le polypropylène.

I. INFLUENCE DE LA STRUCTURE DES POLYTHIOPHOSPHONATES SUR LA STABILITÉ THERMIQUE

1. Influence du groupement thiophosphonium

Les polyphényléthiophosphonates sont plus stables thermiquement que leurs homologues contenant seulement des liaisons phosphonium dans la chaîne.

En superposant les courbes des pertes en poids de trois polymères phosphorés P_4, S_4 et S_1 (fig. 1) on constate que la température indiquant le commencement de la décomposition du P_4 est de seulement 240°, tandis que S_4 commence à se décomposer à 260° et S_1 résiste jusqu'à 300°C.

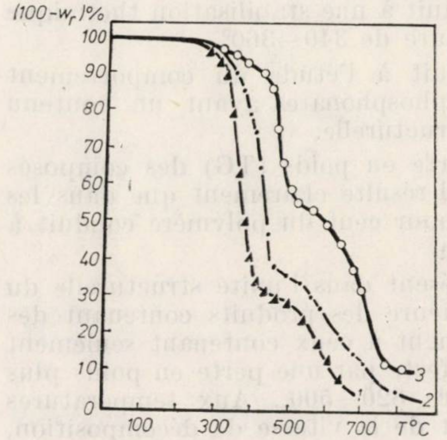

Fig. 1. — Courbes des pertes en poids pour les polymères P_4(▲), S_4(●) et S_1(○)

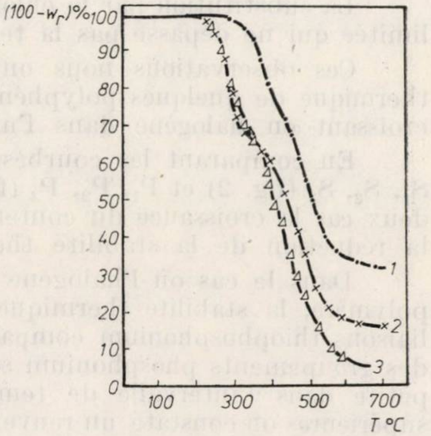

Fig. 2. — Courbes des pertes en poids pour les polymères S_1(●), S_2(×) et S_3(△)

Si on apprécie les pertes en poids pour la température de 500° on constate que P_4 perd 71% de son poids, S_4 perd 64% et S_1 seulement 41%.

En corrélant les données fournies par la figure 1 avec les données obtenues par l'analyse élémentaire (tab. 1). nous pouvons constater qu'à mesure que le contenu en pour cent en phosphore et en soufre rapporté à l'unité structurelle croît, s'amplifie aussi la température à laquelle commence la décomposition. La quantité de résidium croît aussi pour une température donnée.

On peut expliquer la stabilité accrue des produits avec des liaisons thiophosphoniques, comparativement à ceux contenant une liaison phosphonium, par la capacité du soufre de réduire la densité électronique de l'oxygène dans des liaisons du type [10] :

$$S=\overset{|}{\underset{|}{P}}-O$$

Le déficit en électrons de l'oxygène doit se compléter par conjugaison avec le noyau arylique adjacent, qui détermine un renforcement de la liaison $-\overset{\|}{\underset{|}{P}}-O-Ar$ et respectivement de la résistance à la destruction thermique.

2. Influence de la substitution du noyau aromatique contenu dans l'unité structurelle des polythiophosphonates

En analysant les pertes en pour cent en poids des composés S_4, S_5 et S_6 (tableau 2) on observe, en général, que la substitution dans la position « para » du noyau arylique lié au phosphore confère une croissance de la stabilité thermique.

La substitution en « para » du noyau par le groupement méthylique stabilise la molécule et se manifeste par des pertes plus pertites en poids visibles sur les courbes thermogravimétriques. (TG), jusqu'à la température de 900°.

La substitution par le chlore conduit à une stabilisation thermique limitée qui ne dépasse pas la température de 340—360°.

Ces observations nous ont conduit à l'étude du comportement thermique de quelques polyphényléthiophosphonates ayant un contenu croissant en halogène dans l'unité structurelle.

En comparant les courbes de perte en poids (TG) des composés S_1, S_2, S_3 (fig. 2) et P_1, P_2, P_3 (fig. 3) il résulte clairement que dans les deux cas la croissance du contenu en pour cent du polymère conduit à la réduction de la stabilité thermique.

Dans le cas où l'halogène est présent dans l'unité structurelle du polymère, la stabilité thermique supérieure des produits contenant des liaisons thiophosphonium comparativement à ceux contenant seulement des groupements phosphonium se manifeste par une perte en poids plus petite dans l'intervalle de température 320—500°. Aux températures supérieures on constate un renversement de la vitesse de décomposition, les pertes en poids des composés contenant des liaisons phosphonium étant les plus petites.

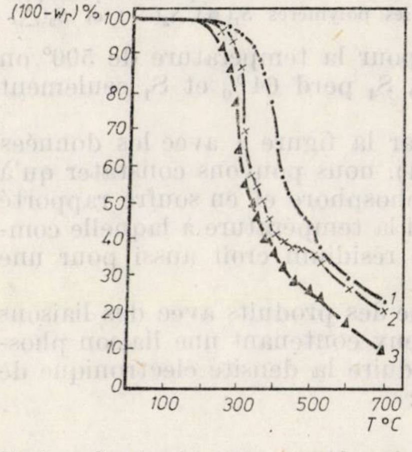

Fig.3. — Courbes des pertes en poids pour les polymères P_1(●), P_2(×) et P_3(▲)

Ces premiers renseignements fournis par l'examen comparatif des courbes de décomposition nous ont montré la nécessité de calculer les énergies d'activation pour les deux zones de décomposition thermique visibles sur la dérivée de la courbe de décomposition thermique (DTG) des produits S et P. Les énergies d'activation calculées sont données dans le tableau 3.

En comparant les énergies d'activation de *la première zone de décomposition* thermique, on constate les choses suivantes :

— Elles sont plus grandes dans le cas des polymères sans halogène, pour les composés ayant des liaisons P = S et plus petites pour les composés ayant des liaisons P = O.

— Dans le cas des polymères ayant deux atomes d'halogène dans l'unité structurelle, les énergies d'activation sont sensiblement égales.

— Elles sont plus grandes dans le cas des polymères contenant quatre atomes d'halogène dans l'unité structurelle, pour les composés ayant des liaisons P = O comparativement à ceux ayant des liaison P = S.

TABLEAU 2

Influence de la substitution du noyau phénylique des polythiophosphonates sur la stabilité termique

T°C	Pertes en pour cent en poids			Ordre de l'influence sur la stabilité thermique
	S_4	S_5	S_6	
300	3,21	1,50	4,44	$CH_3 > H > Cl$
340	8,56	8,50	6,66	$CH_3 > H < Cl$
360	12,84	9,00	9,99	$CH_3 > H < Cl$
380	18,51	11,50	14,43	$CH_3 > H < Cl$
400	24,60	16,00	18,31	$CH_3 > H < Cl$
420	36,38	19,00	23,86	$CH_3 > H < Cl$
440	52,43	24,00	33,30	$CH_3 > H < Cl$
460	62,06	40,00	57,72	$CH_3 > H < Cl$
500	64,20	63,50	65,49	$CH_3 > H > Cl$
600	74,90	72,20	76,59	$CH_3 > H > Cl$
800	94,16	83,00	94,46	$CH_3 > H > Cl$

Pour la deuxième zone de décomposition thermique on peut faire les constatations suivantes :

— Les énergies d'activation sont plus grandes dans le cas des liaisons P=S que dans le cas des liaisons P=O pour les polymères qui n'ont pas d'halogène dans l'unité structurelle.

TABLEAU 3

Energies d'activation associées aux zones de décomposition thermique pour les polyphosphonites et polythiophosphonites

Polymère	Zone de décomposition I			Zone de décomposition II		
	t°C	*TG*	E_A	*t*°C	*TG*	E_A
P_1	240–500	0–55 %	15,98	500–660	53–82 %	65,44
S_1	340–440	0–28	37,27	440–600	28–65	262,16
P_2	200–340	0–45 %	23,54	350–440	45–61 %	98,25
S_2	200–350	0–33	23,54	350–600	33–83	43,54
P_3	240–360	0–50 %	87,31	360–440	50–64 %	262,16
S_3	220–380	0–32	43,54	380–580	32–86	59,14

— Elles sont plus grandes dans le cas des liaisons P=O et comparativement plus petites dans le cas des liaisons P = S, quand il y a deux atomes d'halogène dans l'unité structurelle.

— Avec la croissance en pour cent de l'halogène dans l'unité structurelle, l'énergie d'activations pour les composés contenant des liaisons P=O est beaucoup plus grande que pour la liaisons P=S.

Il paraît donc que la présence de l'halogène a une influence défavorable sur la stabilité thermique dans la seconde zone de décomposition pour le composé contenant des liaisons P=S.

Ces constatations trouvent leur importance dans le choix du meilleur mélange additif ignifugeant – polymère inflammable.

II. EFFET DES ADDITIFS CONTENANT DES LIAISONS P = S SUR LA STABILITÉ THERMIQUE DU POLYPROPYLÈNE

Nous avons étudié la stabilité thermique du polypropylène et des mélanges polypropylène – polythiophosphonates, en conditions dynamiques (hausse de la température = 9°/mn) et aussi en conditions isothermes.

En comparant les courbes TG du polypropylène – additif S_5 (fig. 4) nous avons fait les constatations suivantes:

– La stabilité thermique du polythiophosphonate S_5 est supérieure à celle du polypropylène.

– Le mélange polypropylène – 1 % S_5 présente une légère stabilisation en ce qui concerne le point du commencement de la décomposition mais son résidu de décomposition reste plus petit.

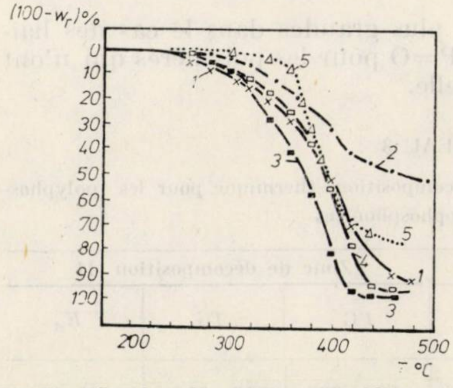

Fig. 4. – Courbes des pertes en poids pour la polypropylène et pour les mélanges polypropylène-polythiophosphonate, en conditions dynamiques. *1*, polypropylène. *2*, polythiophosphonate S_5. *3*, polypropylène +1 %S_5. *4*, polypropylène + 3 % S_5. *5*, polypropylène + 5 %S_5.

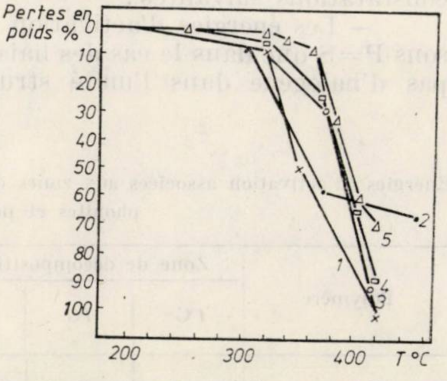

Fig. 5. Courbes des pertes en poids pour le polypropylène et pour les mélanges polypropylène-polythiophosphonate, en conditions isothermes.

– Le mélange polypropylène – 3 % S_5 se décompose plus lentement jusqu'à 400°C. Son résidu de décomposition reste inférieur à celui du polypropylène.

– Le mélange polypropylène – 5 % S_5 présente des modifications essentielles du comportement thermique. Le matériel commence à se décomposer au-dessus de 360° et le résidu de décomposition est plus grand que le résidu du polypropylène, même pour les valeurs mesurées au-dessus de 420°.

Pour les décompositions thermiques dans des conditions isothermes (fig. 5) nous avons constaté les modifications suivantes :

— L'additif S_5 perd en poids plus que le polypropylène jusqu'à proximité de la température de 320°.

— Le mélange à 1 % S_5 est plus stable que le polypropylène, mais les courbes de perte en poids fusionnent à 400°C.

— Les résidus de pyrolyse de mélange avec 3 % et 5 % S_5 sont beaucoup plus grands que ceux du polypropylène.

Dans le tableau 4 sont résumées les données calculées concernant l'augmentation du résidu des produits additivés et aussi la fraction du résidu qui correspond pour l'additif S_5.

Les résultats obtenus de l'analyse thermique comparée aussi aux études concernant le comportement thermique du polypropylène additivé avec des polyphosphonates[11] nous conduisent à attribuer le comportement bien différent des mélanges polypropylène-polythiophosphonate S_5 à l'action conjointe du phosphore et du soufre, dû à leur activation réciproque.

L'analyse élémentaire de l'additif S_5 soumis à la dégradation isotherme fournit les constatations suivantes :

— Pendant la croissance de la température on constate une perte en poids accompagné d'une diminution du pourcentage en carbone et en soufre, celui en hydrogène restant constant tandis que celui en phosphore présentant une très petite croissance.

— A toutes les épreuves dégradées on constate un résidu final infusible. Sa quantité croît avec la température et est lié directement du contenu en phosphore et en soufre.

On arrive à la conclusion que la quantité de résidu formé est due aux possibilités de formation de nouveaux composés thermorésistants du phosphore qui dépendent des conditions de température choisies et de la quantité initiale d'additif dans le mélange. Les réactions qui sont dues à la présence du soufre conduisent à la croissance en résidu bien que celui-ci s'élimine partiellement pendant la pyrolyse.

La croissance du résidu de pyrolyse constatée est plus petite que dans le cas du polypropylène additivé par polyphosphonates.

On doit conclure que ces ignifugeants actionnent principalement dans la formation des produtis gazeaux ayant une inflammabilité réduite, bien qu'ils possèdent du phosphore, connu par sa capacité d'accroître les résidus carbonés infusibles.

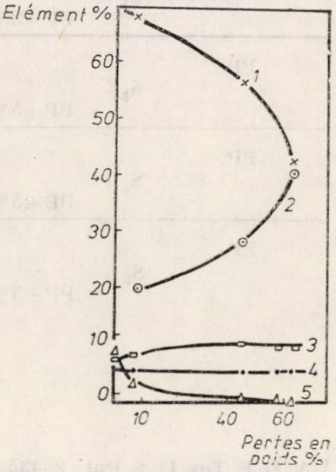

Fig. 6. — Variation du contenu en pour cent des éléments du polythiophosphonate S_5 en fonction de la température de chauffage. *1*, C % *2*, résidu % ; *3*, P % ; *4*, H % ; *5*, S %.

TABLEAU 4

L'effet de l'addition de la polypropylène avec des polythiophosphonite S_5 en différentes concentrations

Polypropylène/Additif/Mélange	t°C	Résidu pour t°C	Croissance du résidu	Additif % dans le résidu
PP	300	90		
S_5	300	96		1,07
PP+1 %S_5	300	89	−1,1	
PP	340	81		
S_5	340	88		1,22
PP+1 %S_5	340	72	−11,11	
PP	420	29		
S_5	420	58		1,93
PP+1 %S_5	420	3	−89,6	
PP	300	90		
S_5	300	96		3,2
PP+3 %S_5	300	90	0	
PP	340	81		
S_5	340	88		3,21
2P+3 %S_5	340	82	+1,23	
PP	420	29		
S_5	420	58		8,28
PP+3 %S_5	420	21	−27,58	
PP	300	90		
S_5	300	96		4,89
PP+5 %S_5	300	98	+8,88	
PP	340	81		
S_5	340	88		4,58
PP+5 %S_5	340	96	+18,51	
PP	420	29		
S_5	420	58		5,61
PP+5 %S_5	420	31	+6,89	

BIBLIOGRAPHIE

[1] A. D. F. Toy, U. S. Pat., 2. 435. 252 (1947) ; *Chem. Abstr.* **42**, 2817 (1948).

[2] D. Coleman (to American Cyanamid Co), Fr. Pat. 1. 520. 998 (12 apr. 1968) ; *Chem Abstr.*, **70**, 107155 (1969).

[3] Y. Masei, X. Kato, M. Shiga, K. Murayama, Y. Iwakuni, N. Fukui et S. Otsui, Ger. Off. Pat. 2. 111. 202 (30 sept. 1971) ; *Chem. Abstr.* **76**, 47329 (1971).

[4] A. Rio et G. Vivant, Fr. Pat. 2. 190. 869 (1974) ; *Chem. Abstr.*, **83**, 60492 (1976).

[5] K. A. Petrov, E. E. Nifantev, L. V. Khakoian et G. Golteev, *Vysokomol. Soedineniya*, **12**, 1799 (1963).

[6] J. J. Anderson, W. N. Byrd jr. et V. C. Camacho, Fr. Pat. 2. 046. 522 (26 nov. 1970) ; *Chem. Abstr.*, **74**, 43109 (1971).

[7] K. R. Eilar et R. I. Wagner, *Chem. Eng. News*, **1962**, 139.

[8] E. M. Zhivukin, V. B. Tobstoguzov, V. U. Kireeb, N. V. Aulova, T. T. Gerasimenko et F. J. Yakobson, *Plasticheskie Massy*, **10**, 19 (1964).

[9] I. B. Hendrickson, D. J. Gram et G. S. Hamond, « Chimie Organică », Editura științifică și enciclopedică, București, 1976, p. 826.

[10] U. Blindheim et T. Gramstad, *Spectrochim. Acta*, **25**A, 1113 (1969).

[11] Fl. Popescu, O. Petreuș, S. Percec et I. Agherghinei, *IMPHOS* (1er Congrès international des Composés phosphorés), Rabat, 17–21 octobre 1977.

Revue Roumaine de Chimie, 28, *4*, 397–403 (1983)

PHOTODECOMPOSITION OF HYPOIODITE ION IN AQUEOUS SOLUTION

M. S. SUBHANI
Department of Chemistry, Faculty of Science, University of Garyounis, P. O. Box : 9480
Benghazi – Libya

Received May 29, 1980
Revised June 30, 1981

The photodecomposition of hypocodite ion in aqueous solution in alkaline medium was carried out using flash photolysis and steady state photolysis techniques. At 313 nm and 253.7 nm the primary products are $O(^1D)$, O^-, I^- and I formed by the following processes (a) and (b)

$$IO^- \xrightarrow{h\nu} \begin{cases} I^- + O(^1D) & \text{(a)} \\ I + O^- & \text{(b)} \end{cases}$$

with $\Phi_a = 0.05$ and $\Phi_b = 0.255 \pm 0.015$ at 313 nm and $\Phi_a = 0.10 \pm 0.016$ and $\Phi_b = 0.44 \pm 0.016$ at 253.7 nm respectively.

A mechanism for photodecomposition of IO^- is proposed.

INTRODUCTION

The flash photolysis technique has been used for investigation of various short lived transient species produced during photolysis of oxychlorine and oxybromine anions [1-6] but little information are available in the literature regarding the photochemistry of oxyodine ainons in aqueous system. The purpose of this paper is to investigate the possible primary processes taking place in the photolysis of IO^- and to establish an overall mechanism involving the primary processes and the subsequent secondary processes leading to end products.

EXPERIMENTAL

All chemicals used were of analar grade and without further purification. Dilute solutions of $NaIO(10^{-3} - 10^{-4}\ M)$ were prepared by readily dissolving solid I_2 in solution containing 0.01 M to 0.4 M NaOH (under these conditions their disproportionation reaction was relatively slow). The solutions were prepared just before irradiation and were saturated with the required gas (O_2, N_2 or Ar) using the usual bubbling procedure described elsewhere.

The flash photolysis set up was the same as described elsewhere. [8,9] The radiations of 313 nm and 253.7 nm were obtained in the same way as described in the literature.[9] The analyses for the IO_3^- and IO_{10}^- were carried out spectrophotometrically as described in the literature. [10]

RESULTS AND DISCUSSIONS

(a) *Flashphotolysis*

On flashphotolysis of 10^{-4}M argon saturated aqueous solution of IO^- at pH 12.8 a transient absorbing species peaking at 495 nm was observed (Fig. 1.). An oxygenated solution of 10^{-4} M IO^- at pH 12.8 was also studied under the same flash photolysis conditions. A complex absorption spectra between 350 nm and 600 nm was recorded (Fig. 2). As no absorption was observed below 400 nm in the Ar-saturated system the complex spectrum was resolved into two spectra on the assumption that below 400 nm the absorption is due to O_3^- only as was identified from its decay kinetics and absorption reported in the literature. [11] The other resolved component of the complex spectrum was identical with that obtained in Ar-saturated system with max = 495 nm and is most probably IO radical similar to that of BrO[2] and ClO [8] radicals and was found to decay by second order kinetics with $2k/E = (4.6 \pm 0.3) \times 10^6$ cm s^{-1}. The two transients O_3^- produced as a result of the primary process

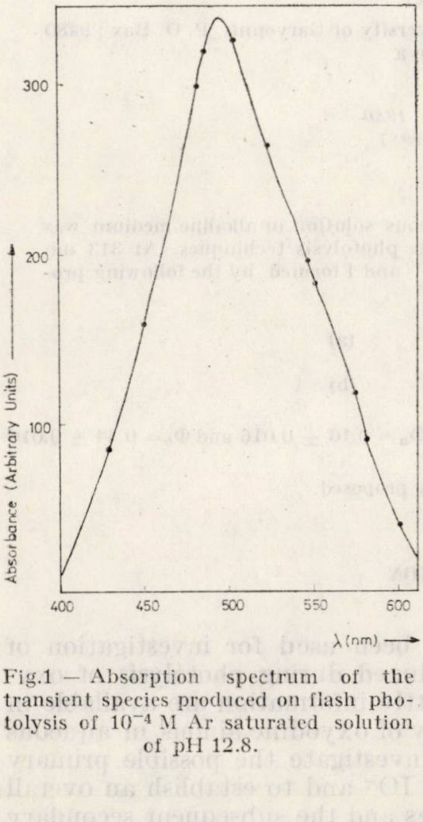

Fig.1 — Absorption spectrum of the transient species produced on flash photolysis of 10^{-4} M Ar saturated solution of pH 12.8.

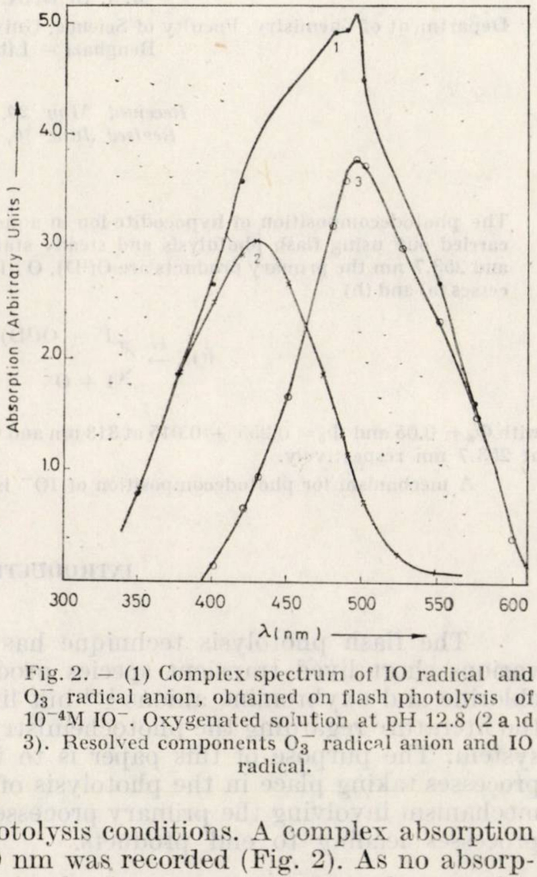

Fig. 2. — (1) Complex spectrum of IO radical and O_3^- radical anion, obtained on flash photolysis of 10^{-4}M IO^-. Oxygenated solution at pH 12.8 (2 and 3). Resolved components O_3^- radical anion and IO radical.

$$IO^- \rightarrow I + O^- \qquad (1)$$

followed by

$$O^- + H_2O \rightarrow OH + OH^- \tag{2}$$

(as this equilibrium is readily established)[12]

$$O^- + O_2 \rightarrow O_3^- \tag{3}$$

$$O^- + IO^- \rightarrow IO + O^{2-} \tag{4}$$

$$OH + IO^- \rightarrow IO + OH^- \tag{5}$$

$$I + IO^- \rightarrow IO + I^- \tag{6}$$

As the concentration of IO^- varied in Ar-saturated system a new transient speciespeaking at 370 nm was observed (Fig. 3) decaying by first order process with rate constant proportional to IO^- (Fig. 4).

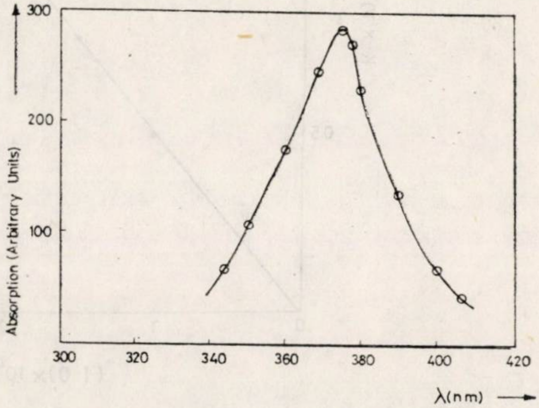

Fig. 3. — Absorption spectrum for the transient Species I_2^-.

The species was identified as I_2^- from its reported absorption spectrum[13] and is produced by the reaction

$$I + I^- \rightarrow I_2^- \tag{7}$$

where iodine atoms are the primary products in the process(1) and IO^- solution always contained equivalent amount of I^- ions. This further supports the primary photolytic process (1) taking place. The pseudo first order decay of I_2^- suggests reaction (8) which is analogous to the reaction of Br_2^- with BrO^-. [14] The rate constants for ractions (4) and (5) were measured as described elsewhere [15] from the pseudo first order decay of O_3^- at PH 12.5 and 13.5 respectively using flash photolysis techniques.

The values are $k_1 = (4.5 \pm 0.2) \times 10^9\ M^{-1}s^{-1}$.

$$k_5 = (4.8 \pm 0.2) \times 10^9\ M^{-1}s^{-1}.$$

$$I_2^- + IO^- \rightarrow 2I^- + IO \tag{8}$$

On flash photolysis of N_2O saturated solution of IO^- at pH 12.8 the yield of IO was found to be the same as that of Ar-saturated system using the same flash energy and the same concentration of IO^-. In the steady photolysis work of N_2O saturated system, no nitrogen traces were detected. Both these observations suggest that the primary photolytic process (9)

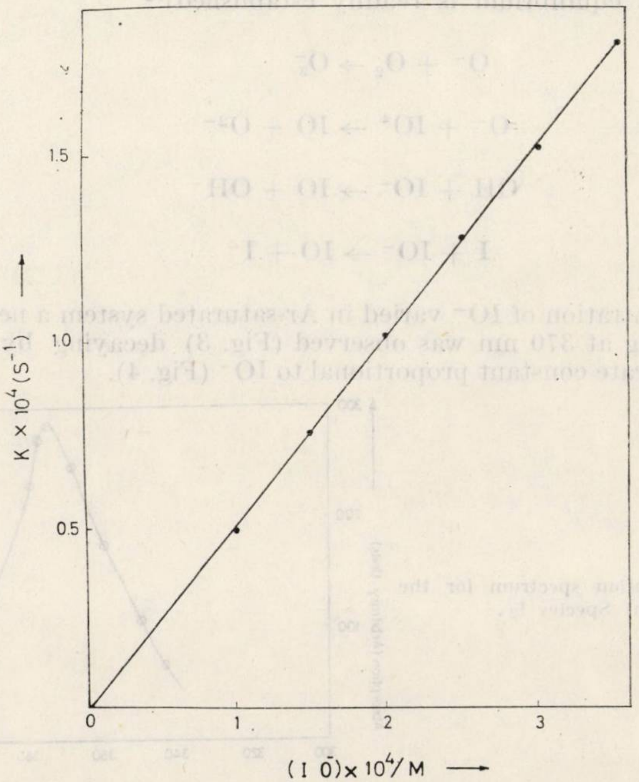

Fig.4. — Dependence of the decay rate of I_2 on (IO^-) in Ar—saturated system.

$$IO^- \rightarrow IO + e_{aq}^- \qquad (9)$$

is not taking place as under the experimental conditions. N_2O would scavenge all the electrons produced in reaction (9) by reaction (10)[16]

$$N_2O + e_{aq}^- \rightarrow N_2 + O^- \qquad (10)$$

In O_2-saturated aqueous solution of IO^- at lower pH no absorption due to O_3 was observed at 260 nm thus ruling out the possibility of another primary process (11)

$$IO^- \rightarrow I^- + O\,(3p) \qquad (11)$$

taking place.

(b) *Steady State Photolysis*

Photolysis was carried out at 313 nm and 253.7 nm and the stable end products observed were IO_3^-, O_2 and I^-. The quantum yields for the disappearance of IO^- and also for the products IO_3^-, I^- and O_2 formed were measured and are shown in table 1.

TABLE 1

Quantum yields for the products formed and for the disappearance of hypoiodite in the photolysis of hypoiodite in aqueous solution

	$pH=12.8, (IO^-) = 10^{-3}-10^{-4}M$	
λ (nm)	313	253.7
$\Phi(^-IO^-)$	0.50±0.01	0.90+0.02
$\Phi(O_2)$	0.10±0.008	0.20±0.006
$\Phi(IO_3^-)$	0.11±0.026	0.18±0.028
$\Phi(I^-)$	0.39±0.024	0.72±0.035

On the basis of the observations made in the flash photolysis work, it seems that the primary process

$$IO^- \rightarrow I + O^- \tag{1}$$

is only responsible for the photodecomposition of IO^-. The possibility of another primary process

$$IO^- \rightarrow I^- + O(^1D) \tag{12}$$

can not be ruled out when we take into consideration the observed O_2 yield. Such type of process has been shown to occur in ClO^- BrO^- systems.[1,2,17]

A possible mechanism which can satisfy the observations made in flash photolysis work and the quantum yield measured in the steady work at 313 nm and 253.7 nm respectively can be suggested as follows :

$$IO^- \xrightarrow{h\nu} I + O^- \tag{1}$$

$$IO \xrightarrow{h\nu} I^- + O(^1D) \tag{12}$$

$$I + IO^- \rightarrow I^- + IO \tag{6}$$

$$O^- + H_2O \rightarrow OH + OH^- \tag{2}$$

$$O^- + IO^- \rightarrow IO + O^{2-} \tag{4}$$

$$OH + IO^- \rightarrow IO - OH^- \tag{5}$$

$$2IO \rightleftarrows I_2O_2 \qquad (13)$$

$$I_2O_2 + 2OH \rightarrow IO^- + IO_2^- + 2H^+ \qquad (14)$$

$$I_2O_2 + IO_2^- \rightarrow IO_3^- + I_2O\downarrow \qquad (15)$$

$$H_2O \rightarrow 2IO^- + 2H^+$$

$$O(^1D) + H_2O \rightarrow H_2O \qquad (16)$$

$$H_2O_2 + IO^- \rightarrow H_2O + O_2 + I^- \qquad (17)$$

Reaction (12) is well known and there is good evidence that (16) represents the fate of $O(^1D)$ in dilute aqueous solution. [18, 19] Thus the primary process (12) is the only process leading to the formation of O_2 through reaction (17).

Expressions relating the quantum yields for the disappearance of IO^- and for the formation of the products IO_3^-, I^- and O_2 are predicted in terms of the primary quantum yields O_1, and O_{12} for the primary photolytic process (1) and (12) respectively.
They are the following

$$\Phi(-IO^-) = (1 + a)\,\Phi + 2\Phi_{12} \qquad (18)$$

$$\Phi(O_2) = 2\Phi_{12} \qquad (19)$$

$$\Phi(IO_2^-) = \Phi_1(1 - a) \qquad (20)$$

$$\Phi(I^-) = 2\Phi_{12} + \Phi_1 \qquad (21)$$

Substituting the data in table 1 into equations (18), (19) and (20) the values of Φ_{12} and of a are obtained at wavelengths 313 nm and 253.7 nm and are shown in table 2.

TABLE 2

Primary quantum yields Φ_1 and Φ_2 and constant 'a' in the photodecomposition of hypoiodite ion in aqueous solution

λ(nm)	313	253.7
Φ_1	0.255±0.015	0.44±0.016
Φ_{12}	0.05±0.015	0. 1±0.016
a	0.57±0.035	0.59±0.05

The values of $\Phi(I^-)$ obtained by substitution of Φ_1 and Φ_2 in equation (21) at 313 nm and 253.7 nm are 0.355 ± 0.015 and 0.64 ± 0.016 respectively. These values are in fair agreement with reported values in table 1.

This agreement provides further support to the proposed mechanism.

REFERENCES

[1] (a) M. S. Subhani and G. V. Buxton, *J. Chem. Soc., Trans Faraday*, **68** 970 (1972) ; (b) M. S. Subhani (Submitted for publication).

[2] O. Amchai, G. Czapski and A. Trinin, *Israel. J. Chem.*, **7**, 351 (1968).

[3] O. Amachai and A. Treinin, *Chem. Phys. Let.*, **3**, 611 (1969).

[4] N. K. Bridge and M. S. Matheson, *J. Phys. Chem.*, **64**, 1280 (1960).

[5] M. S. Matheson and L. M. Forman, *J. Chem. Phys.*, **32**, 1870 (1960).

[6] A. Gitter and A. Treinin, *J. Chem. Phys.*, **42**, 2019 (1965).

[7] M. S. Subhani (Accepted for publicaton) *Rev. Roumaine Chim.*, **25**, 327 (1980).

[8] M. S. Subhani and G. V. Buxton, *J. Chem. Soc.*, **68**, 958 (1972).

[9] M. S. Subhani, *Rev. Roumaine Chim.*, **25**, 851 (1980).

[10] A. John and B. Frank, *J. Sci. Mathes*, **16**, 210 (1961).

[11] G. E. Adams, J. W. Bong and B. D. Michael, *Proc. Roy. Soc.*, **A287**, 321 (1965).

[12] G. V. Buxton, *Trans. Faraday Soc.*, **65**, 2150 (1969).

[13] L. I. Grossweiner and M. S. Matheson, *J. Phys. Chem.*, **61**, 1089 (1957).

[14] G. V. Buxton and F. S. Dainton, (a) *Proc. Roy. Soc.*, **A304**, 427 (1968) ; (b) *Proc. Roy. Soc.*, **A304**, 441 (1968).

[15] M. S. Subhani and T. Kausar, *Rev. Roumaine. Chim.*, **25**, 855 (1980).

[16] M. Anbar and P. Nate, *International J. Appl. Radiation Isotopes*, **18**, 493 (1967).

[17] M. S. Subhani, *Rev. Roumaine Chim.*, **25**, 861 (1980).

[18] H. Taube, *Trans. Faraday Soc.*, **53**, 656 (1957).

[19] F. S. Dainton and P. Fowles, *Proc. Roy. Soc.*, **A287**, 295 (1965).

Revue Roumaine de Chimie, **28**, *4*, 405–412 (1983)

ESTUDIO ANALÍTICO DE LOS PRECIPITADOS OBTENIDOS CON EL ANIÓN HgI_4^{2-} Y LOS CATIONES DEL GRUPO PRIMERO (Ag^+, Pb^{2+}, Hg_2^{2+} Y Tl^+)

S. ARRIBAS JIMENO, M. L. ALVAREZ BARTOLOMÉ y E. ANDRÉS GARCÍA
Departamento de Química Analítica, Facultad de Ciencias, Universidad de Oviedo, Spain

Recibido el 24 de April de 1981

El anión HgI_4^{2-} origina precipitados voluminosos y coloreados con los cationes del grupo primero de la marcha Analítica del SH_2. Aunque han sido descritos por la literatura, no han tenido — aplicaciones analíticas, o éstas han sido escasas. En el presente trabajo se utilizan estos precipitados para ensayos de identificación de Hg(I), Ag(I), Pb(II) y Tl(I), calculando en todos los casos la sensibilidad de los mismos. Asimismo, se ponen a punto sendos métodos volumétricos para las valoraciones de Ag(I) y Hg(I) con dicho anión. El punto final se fija potenciométricamente o con difenilcarbazida como indicador. Especial interés se ha puesto en la determinación del Hg(I) cuyas curvas de valoración potenciométrica son muy características del proceso que tiene lugar ; los distintos precipitados obtenidos en el transcurso de esta valoración se han identificado por vía química y por difracción de rayos X.

The anion HgI_4^{2-} yields coloured bulky precipitates with the first group of the analytical determinations with H_2S. There are still no analytical applications of this observation. We use these precipitates for identifying Hg(I), Ag(I), Pb(II) and Tl(I) and we calculate in all these cases the sensitivity of the method. We also present volumetric methods for determining Ag(I) and Hg(I) by means of the above anion ; the final point of the titration is determined potentiometrically with diphenylcarbazide as indicator. Especially interesting is the determination of Hg(I) by this method. The various precipitates were investigated chemically and by X-ray diffraction.

INTRODUCCIÓN

El estudio del anión tetrayodomercuriato como agente precipitante es antiguo y algunos de los precipitados que con él se obtienen han sido utilizados con fines analíticos, siendo posiblemente los más conocidos los que forma con el catión amonio y con los alcaloides. (Reactivo de Nessler y de Mayer).

Los precipitados voluminosos anaranjados o amarillos, más o menos intensos, que se obtienen al añadir disolución de tetrayodomercuriato potásico sobre Hg(I), Ag(I), Tl(I) o Pb(II) son adecuados para la identificación de estos iones por lo que se ha estudiado la sensibilidad de los ensayos en distintos soportes y a diferentes valores de pH.

Hemos utilizado con fines cuantitativos los que se obtienen con Hg(I) y Ag(I) ya que al seguirse las reacciones de precipitación potenciométricamente, con electrodo de Pt y E.S.C., se obtienen, en ambos casos, claros saltos de potencial, no quedando en el punto de equivalencia cantidades apreciables de mercurio (I) y (II) ni de plata lo que indica que tanto el Hg(I) o la Ag(I) de los problemas como el Hg(II) del reactivo valorante se encuentran precipitados. Conocidos los moles de I^- y de Hg^{2+} de este reactivo se pueden calcular los del problema de acuerdo con la ecuación :

$$(nI^- + mHg^{2+}) + (n - 2m)Me^+ \rightarrow mHgI_2(n - 2m)\,MeI \qquad (A)$$

En esta ecuación *n* representa los moles de yoduro de la disolución de tetrayodomercuriato potásico por lo que, aunque se han escrito totalmente ionizados, debe entenderse que parte estarán unidos a los *m* moles de Hg^{2+} formando el complejo correspondiente. *Me* indica Hg(I) o Ag(I).

En un trabajo reciente Baiulescu y Ciocan [1] al determinar Hg(II), complejado con yoduro, con mercurioso utilizando un electrodo sensible a este ion para realizar la valoración, señalan asimismo que, en el transcurso de la misma, el complejo se destruye precipitando conjuntamente con el yoduro mercurioso el yoduro mercúrico procedente del complejo.

En nuestro trabajo se ponen a punto las determinaciones volumétricas del Hg(I) y de la Ag(I) señalando el punto final potenciométricamente o con difenilcarbazida. Previamente se elige entre una serie de disoluciones de relaciones molares I^-/Hg^{2+} diferentes la más adecuada para efectuar dichas valoraciones.

PARTE EXPERIMENTAL

Se han utilizado los reactivos, aparatos y procedimientos operatorios siguientes :

Reactivos

— HgO sólido, Merck, p.a.

— Acido Acético 2 M, obtenido por dilución del ácido acético concentrado del 99 % en peso, Probus.

— Disolución de $Hg_2(NO_3)_2$ 50,00 · 10^{-3} M, preparada a partir de la sal Merck, p.a., cuya concentración exacta se determina por valoración potenciométrica con NaCl 50,00 · 10^{-3} M, previamente secada durante una hora a 270°C[2] o con azul de bromofenol como indicador.[3]

— Disolución de $AgNO_3$ 50,00 · 10^{-3} M, preparada por pesada exacta de la sal Merck, p.a., una vez seca a 110°C, durante una hora y dilución conveniente.

— Disolución de KI 1,000 M, preparada por pesada exacta de la sal Merck, p. a., una vez seca a 110 °C.

— Indicador difenilcarbazida, al 1 % en etanol.

Aparatos

— Potenciómetro Radiometer Type TTTlc Nº 51758 dotado, para la medida de potenciales, de electrodo de platino Radiometer Type P101, como indicador y electrodo de calomelanos, Radiometer Type K401, como referencia. En la medida de pH se ha utilizado, junto con el E.S.C. un electrodo de vidrio, Radiometer Type G202C en lugar de electrodo de platino. Durante el proceso de valoración se mantiene agitación magnética constante.

— La difracción de rayos X se verifica con un equipo Philips PW1011 dotado de un goniómetro vertical Pw 1050/25 y registro gráfico. Las condiciones habituales de trabajo han sido :

Rendijas	1°, 0,1 mm, 1°
Velocidad de papel	2 cm/min
Velocidad de barrido	2°/min
RM :	4 .10^2 cps
TC :	1 seg.

— Los diagramas se han realizado empleando anticátodo de Cu con una radiación CuKα (λ = 1,5418 Å) y filtro de Ni

— Disoluciones de Ag(I), Pb(II), Hg(I) y Tl(I) en concentración de 0,01 g de elemento por ml.

Procedimientos operatorios

a) *Ensayos de identificación*

Las reacciones se han verificado (a) en tubo de ensayo, (b) en placa de gotas y (c) sobre papel de filtro, añadiendo sobre 1 ml de problema en el caso (a) y sobre una gota ($\simeq$ 0,05 ml) en los casos (b) y (c) 1/2 ml y dos gotas, respectivamente, de disolución de tetrayodomercuriato potásico, $1{,}000 \cdot 10^{-2}$ M, en Hg(II) y relación molar $I^-/Hg^{2+} = 5$. El pH de las disoluciones se ajusta con HNO_3 o NaOH antes de añadir el reactivo precipitante.

b) *Determinaciones volumétricas*

A la disolución problema de Hg(I) o de Ag(I) se añaden unos 10 ml de agua destilada y se procede a realizar la valoración. El punto final de la misma se señala potenciométricamente con electrodo de Pt y con E.S.C., o con difenilcarbazida ; en este caso se añaden unas gotas de indicador antes de comenzar la valoración.

RESULTADOS Y DISCUSION

Reacciones de identificación

La sensibilidad de los ensayos efectuados se exponen en la TABLA 1, expresada en pD. El Pb(II) y el Tl(I) se han estudiado a pH 1,5 — 4 — 10 y además el Pb(II) a pH 13 ya que tal como se ha comprobado en experiencias preliminares, a este valor de pH, aparece un precipitado voluminoso de color amarillo pálido en el que no se observa el color anaranjado característico del HgI_2; sin embargo el análisis cualitativo de dicho precipitado revela la existencia de I^-, Hg(II) y Pb(II) lo que unido a la alcalinidad del medio hace pensar en un yoduro de mercurio y plomo en forma de sal básica no descrito en la bibliografía. El estudio de la Ag(I) se ha hecho a pH 1,5 y 4, pues a valores más altos estará precipitada como Ag_2O. El Hg(I) solo se ha ensayado a pH 1,5 para asegurar su existencia ya que a pH menos ácidos se dismutaría.

Las reacciones más sensibles son las de Hg(I) y Tl(I) seguidas de las de Ag(I) y Pb(II), excepto este último a pH 13, cuya sensibilidad es superior a la Ag(I).

El precipitado anaranjado que se obtiene con el Hg(I) formado por una mezcla de yoduro mercúrico (rojo anaranjado) y yoduro mercurioso (amarillo) permite comprobar que el precipitado de Hg_2I_2 es amarillo y no verde amarillento como indican la mayor parte de los textos usuales de Química Analítica. En efecto si al precipitado anaranjado se añade gota a gota una disolución de KI(0,1 M) se disuelve el HgI_2 por formarse el HgI_4^{2-} con desaparición del color — anaranjado quedando la suspensión de un amarillo vivo(Hg_2I_2) que — adquiere primero color verdoso amarillento y oscurece paulatinamente con más KI. Por tanto el color verdoso amarillento puede ser debido a la mezcla de Hg_2I_2 amarillo y una pequeña cantidad de Hg° que aparece al iniciarse la dismutación del mercurioso.

TABLA 1

Sensibilidad de las reacciones

Ion ensayado	técnica seguida	pH aprox.	Sensibilidad en pD.
Hg(I)	a	1,5	4,3
	b	1,5	4,6
	c	1,5	4,6
Ag(I)	a	1,5	3,3
	b	1,5	3,3
	c	1,5	3,3
	a	4	3,3
	b	4	3,3
	c	4	3,3
Tl(I)	a	1,5	4,3
	b	1,5	4,6
	c	1,5	4,6
	a	4	4,3
	b	4	4,6
	c	4	4,6
	a	10	4,3
	b	10	4,6
	c	10	4,6
Pb(II)	a	1,5	2,7
	b	1,5	2,8
	c	1,5	2,8
	a	4	2,7
	b	4	2,8
	c	4	2,8
	a	10	2,7
	b	10	2,8
	c	10	2,8
	a	13	3,6
	b	13	3,7
	c	13	4

Determinaciones de Hg(I) y Ag(I)

Elección de la disolución valorante

Las disoluciones de tetrayodomercuriato potásico deben prepararse en medio ácido para que sean estables pues en medio alcalino aparecen al cabo de algunos días unos precipitados blancos que impiden su utilización.

La forma más sencilla de preparar dichas disoluciones consiste en disolver HgO en ácido acético 2M y añadir, posteriormente, disolución de KI hasta disolver totalmente el precipitado rojo de yoduro mercúrico inicialmente formado. La relación molar I^-/Hg^{2+} necesaria para conseguirlo es 4,4 ; aunque con relaciones molares superiores también se obtienen disoluciones perfectamente estables. Estas disoluciones pueden prepararse de concentración exacta por simple pesada, siempre que se utilicen reactivos de suficiente garantía. Para comprobar si la exactitud en el procedimiento de valoración depende de la relación molar I^-/Hg^{2+} de las disoluciones, se preparan una serie de 6 comprendidas dentro de los límites 4,4 (mínimo necesario para formar el complejo) y 6 [máximo que puede estar presente sin que se dismute el Hg(I)] para ver con cual de ellas se comete menor error en la valoración del Hg(I) o de la Ag(I).

En todas se mantiene la concentración en Hg(II) constante e igual a $1{,}000 . 10^{-2}$ M y se va aumentando la de I^-. Los errores que se cometen con cada una al valorar potenciométricamente $5{,}00 . 10^{-4}$ moles de Hg(I) o Ag(I) son semejantes y cualquiera de ellas puede servir para efectuar la valoración de estos cationes. Se elige la nº 4 por tener la relación molar I^-/Hg^{2+} más sencilla de números enteros: esta relación es igual a 5 (Tabla 2).

TABLA 2

Errores relativos correspondientes a la valoración de $5{,}00 . 10^{-4}$ moles de Hg(I) y Ag(I) con disolución de tetrayodomercuriato potásico.

Disolución	Molaridad de las disoluciones de tetrayodomercuriato potásico en		ml de complejo necesarios para precipitar $5{,}00 . 10^{-4}$ moles de				% Er	
			teóricos		exper. *			
	$Hg(II) . 10^{-2}$	$I^- . 10^{-2}$	Hg(I)	Ag(I)	Hg(I)	Ag(I)	Hg(I)	Ag(I)
1	1,000	4,40	20,83	20,83	20,98	21,08	+0,7	+1,2
2	1,000	4,60	19,23	19,23	19,32	19,38	+0,5	+0,8
3	1,000	4,80	17,86	17,86	17,88	17,92	+0,1	+0,3
4	1,000	5,00	16,67	16,67	16,58	16,68	−0,5	+0,1
5	1,000	5,20	15,62	15,62	15,48	15,52	−0,9	−0,6
6	1,000	6,00	12,50	12,50	12,42	12,52	−0,6	+0,2

* media aritmética de los volúmenes, cuya diferencia es de 0,05 ml, para los que $\Delta E/\Delta V$ es máximo

Curvas de valoración potenciométrica

La curva de valoración, (1) gráfica 1, que corresponde a la obtenida con la disolución 4, en la determinación del Hg(I) presenta una forma característica que se pone de manifiesto con cualquiera de las disoluciones ensayadas y que se debe a las diferentes etapas en que tiene lugar la precipitación de este catión. Todas presentan un tramo ascendente en que solo precipita el yoduro mercurioso; la disolución se enriquece en Hg(II) y por consiguiente el potencial se eleva; después el Hg(I) del problema y el Hg(II) del reactivo valorante compiten por el I^- y precipitan conjuntamente; mientras esto suceda así el valor del potencial apenas se modifica. Cuando ha precipitado todo el Hg(I), el Hg^{2+} libre precipita como HgI_2 con la adición de nuevos mililitros del reactivo valorante apareciendo el tramo descendente, y una vez ha precipitado todo el yoduro mercúrico se origina un salto de potencial que corresponde al punto final de la valoración.

Estos hechos se han comprobado analizando por vía química los precipitados y disoluciones que corresponden a los diferentes tramos de la curva de valoración 1, gráfica 1, y realizando unos difractogramas sobre los precipitados obtenidos en las diferentes etapas de la citada curva.

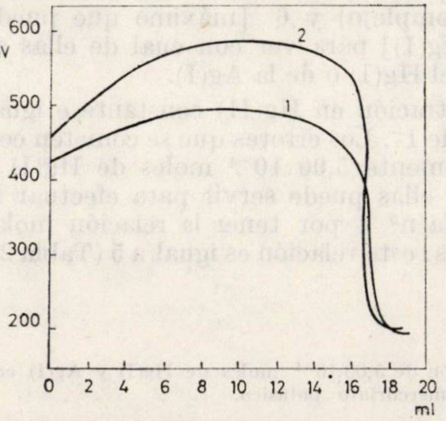

Gráfica 1. — Curvas de valoración con yodomercuriato potásico (disolución nº 4) de : 1 – $5{,}00 . 10^{-4}$ moles de Hg(I) ; 2 – $5{,}00 . 10^{-4}$ moles de Ag(I).$(nI^- + m\mathrm{Hg}^{2+}) + (n-2m)\mathrm{Me}^+ \rightarrow$ $\rightarrow m\mathrm{HgI}_2(n-2m)\mathrm{MeI}$ (A)

En el diagrama de difracción en polvo, realizado sobre el precipitado obtenido al comenzar la valoración, tramo ascendente de la curva, aparecen una serie de picos cuyos valores de "d" en Å, Tabla 3, se corresponden con los tabulados para el yoduro mercurioso puro ; lo que indica que solamente existe este compuesto.

En la 2ª y 3ª muestra, precipitados obtenidos en el segundo tramo, aparecen otros picos nuevos que son más acusados en la 3ª muestra Tabla 3, y cuyos valores de "d" corresponden al yoduro – mercúrico. Finalmente en la 4ª muestra, constituida por un precipitado recogido al finalizar la valoración, se incrementa el número de picos correspondientes al yoduro mercúrico así como la intensidad de los ya existentes de este compuesto.

Estos resultados que completan los obtenidos en los análisis cualitativos realizados, confirman las predicciones teóricas sobre las diferentes etapas en que tiene lugar la precipitación del Hg(I) y que dan lugar a la forma especial que presentan las curvas de valoración potenciométrica.

La curva 2, de la gráfica 1, corresponde a la valoración de $5{,}00.10^{-4}$ moles de Ag(I) con la disolución 4. La forma que presenta, que se pone de manifiesto con cualquiera de las disoluciones ensayadas, es muy parecida a la del Hg(I), 1, si bien aquí el tramo ascendente es un poco más largo debido a la mayor insolubilidad del AgI.

Influencia de distintos factores en los procedimientos de valoración

La exactitud en los procedimientos de valoración no se ve afectada por el pH del medio dentro de los límites estudiados que han sido desde inferior a 1 y hasta 3 para el Hg(I) e inferior a 1 y hasta 5,6 para la Ag(I).

Con ambos métodos de valoración se obtienen resultados reproductibles. Las desviaciones standard, calculadas sobre dos series, de diez muestras cada una que contenían 100,3 mg de Hg(I) y 53,9 mg de Ag(I), son 0,2 y 0,1 respectivamente.

TABLA 3

Relación de los espaciados obtenidos en las muestras correspondientes a las distintas etapas de precipitación del Hg(I).

1ª muestra yoduro mercúrico	2ª y 3ª muestra yoduro mercurioso y yoduro mercúrico	4ª muestra yoduro mercurioso y yoduro mercúrico
dÅ	dÅ	dÅ
4,55	*6,22*	*6,22*
3,47	4,55	4,55
3,03	*4,095*	*4,095*
2,903	*3,56*	*3,56*
2,462	3,47	3,47
2,232	2,903	3,03
2,161	3,03	*3,13*
2,103	*3,01*	2,903
1,877	2,462	*3,01*
1,743	*2,755*	2,529
	2,232	2,462
	2,161	2,232
	2,185	2,755
	2,103	2,161
	1,877	2,103
	2,072	2,185
	1,925	1,877
	1,743	*2,072*
		1,925
		1,859
		1,765
		1,743
		1,595
		1,558
		1,492

cursivas: yoduro mercúrico

Se comprueba la exactitud de las valoraciones sobre diferentes cantidades de Hg(I) o de Ag(I) comprendidas entre 50,2 y 200,6 mg en el caso del Hg(I) y entre 27,0 y 107,9 mg en el de la Ag(I), encontrándose para el caso más desfavorable un error relativo máximo del 0,9 %.

Con el fín de ver si era posible señalar el punto final con un indicador químico se probaron diversos tipos : redox, de adsorción, de oxiadsorción y finalmente metalocrómicos. De todos ellos solo se han obtenido resultados satisfactorios con la difenilcarbazida, siempre que la muestra problema tenga un valor de pH comprendido entre 1,4 y 2 en cuyo caso se obtiene un buen viraje del indicador. [4] Las desviaciones standard son ahora, para las mismas cantidades de Hg(I) y Ag(I) que las utilizadas en las valoraciones potenciométricas, 0,3 y 0,2 respectivamente.

Los iones que mayor interferencia han de causar en estas determinaciones son los que precipitan con el reactivo objeto de nuestro estudio de manera semejante a como lo hacen el Hg(I) o la Ag(I) ; se ha comprobado si es posible determinar uno en presencia de otro, así como en muestras que contengan Pb(II) o Tl(I), encontrándoseque estos cationes dentro de los límites estudiados no interfieren excesivamente las valoraciones del Hg(I) y de la Ag(I) (Tabla 4).

TABLA 4

Determinación volumétrica de Hg(I) y de Ag(I) en presencia de distintas cantidades de Pb(II) o de Tl(I) señalando el punto final potenciométricamente y con el indicador difenilcarazida

mg puestos de :		mg de interferente añadidos	mg encontrados				% de error relativo			
			potenc.		difenilc.		potenc.		difenilc.	
Hg(I)	Ag(I)	Pb(II)	Hg(I)	Ag(I)	Hg(I)	Ag(I)	Hg(I)	Ag(I)	Hg(I)	Ag(I)
100,3	53,9	10,2	99,2	53,3	99,6	53,2	−1,1	−1,1	−0,7	−1,3
100,3	53,9	51,2	99,2	53,5	99,6	53,2	−1,1	−0,7	−0,7	−1,3
100,3	53,9	102,4	99,4	53,5	99,0	53,1	−0,9	−0,7	−1,3	−1,5
100,3	53,9	204,7	99,4	53,5	99,0	53,1	−0,9	−0,7	−1,3	−1,5
		T1(I)								
100,3	53,9	10,2	99,4	53,3	99,0	53,1	−0,9	−1,1	−1,3	−1,5
100,3	53,9	51,1	99,4	53,1	99,0	53,2	−0,9	−1,5	−1,3	−1,3
100,3	53,9	102,2	99,8	53,1	99,0	53,1	−0,5	−1,5	−1,3	−1,5
100,3	53,9	204,4	99,8	53,3	99,0	53,2	−0,5	−1,1	−1,3	−1,3

Sin embargo, no es posible determinar individualmente Hg(I) y Ag(I) en sus mezclas binarias, a no ser que se conozca la concentración de uno de ellos y se calcule el otro por diferencia, ya que el único salto de potencial que se origina en la reacción de precipitación corresponde a la valoración conjunta de ambos iones ; pero pueden determinarse conjuntamente lo que puede resultar de interés en el análisis de determinadas muestras (Tabla 5).

TABLA 5

Valoración potenciométrica conjunta de 100,3 mg de Hg(I) y distintas cantidades de Ag(I)

mg puestos de		moles totales de Hg(I) + Ag(I) puestos. 10^3	moles totales de Hg(I) + Ag(I) encontrados. 10^3	% de error relativo
Hg(I)	Ag(I)			
100,3	5,4	0,550	0,547	−0,5
100,3	27,0	0,750	0,742	−1,1
100,3	53,9	1,000	0,992	−0,8
100,3	107,9	1,500	1,487	−0,9

REFERENCIAS

[1] G. E. Baiulescu y N. Ciocan, *Talanta*, **24**, 37 (1977).
[2] F. Bermejo Martinez, "Química Analítica General Cuantitativa e Instrumental". Vol. 1. 5ª ed. Imprenta del Seminario Conciliar. Santiago de Compostela, 1974, p. 741.
[3] L. V. Zombory, *Z. anorg. Chem*, **184**, 237 (1929).
[4] Op. cit. en 2, p. 618.

Revue Roumaine de Chimie, 28, *4*, 413–417 (1983)

COMPLEXOMETRIC AND SPECTROPHOTOMETRIC DETERMINATION OF COPPER USING PHENANTHRENEQUINONE MONOSEMICARBAZONE (PQSC)

FASIHUDDIN KAMIL, P. P. SINHA and S. K. SINDHWANI
Department of Chemistry, University of Delhi, Delhi-110007, India

Received May 19, 1981

Phenanthrenequinone monosemicarbazone (PQSC) has been successfully used as a metallochromic indicator in the complexometric estimation of copper (II) over the pH range 5.4–7.2, the end-point being sharp and distinct. The optimum range of pH, temperature and the amount of indicator for the success of the titration have been investigated. The 1 : 2 copper(II)–PQSC complex exhibits maximum absorption at 480 nm and Beer's law is obeyed up to 8.9 ppm of copper, the optimum range of concentration for the determination being 1.82–6.76 ppm. The sensitivity of the method over the pH range 7.2–10.0 is 0.008 µg Cu/cm^2. The complexometric and spectrophotometric determinations have also been carried out in the presence of foreign ions and the selectivity has been enhanced by the use of masking agents. Copper has also been determined spectrophotometrically in samples of gun metal.

The titrimetric determination of copper with murexide as indicator [1] presents no difficulty in the direct or back titration in the pH range 5–10. But the end point is not sharp or missing if too much of ammonia is added. This is the case with other indicators also, which is due to strong $[Cu(NH_3)_4]^{2+}$ complex formation as compared to copper-indicator complex. In the case of PAN,[2] the complex is insoluble, heating is required and the colour change is not very sharp. Because of the stability of Cu–PAN complex, the decomposition of the complex by EDTA is very slow. To speed up the reaction, either the solution is heated or the titration is performed in 50% ethanol, methanol or acetone medium.

Phenanthrenequinone monoxime [3] is also a selective indicator for the titrimetric determination of copper, which has been used over the pH range 3.9–5.3. In the present case, PQSC has been used over the pH range 5.4–7.2. The end-point is very sharp and no heating is required as is the case of PAN or PAR.[4,5] To increase the selectivity, masking agents may be used.

Cuproine,[6] neocuproine[7] and bathocuproine[8] are most selective reagents for the spectrophotometric determination of copper as they do not react with other metals. Diethyldithiocarbamate [9] has been used with success and large amounts of Al(III), As(III), Fe(II), Zn(II), Ni(II) and Co(II) do not interfere. 2,2′-Biquinoline [10] is quite a selective reagent for copper and its sensitivity is fairly good (0.010 µg). Dithizone [11] is one of the most popular organic reagents for the spectrophotometric determination of copper. It has the advantage of very high sensitivity and mineral acid reaction medium. It can be used to determine copper directly in the presence of nickel and cobalt. The strong colour of dithizone and the interference due to other metal ions are the disadvantages. In the case of nitroso-R-salt ,[12] the sensitivity is 0.063 $\mu g\ cm^{-2}$ and iron, cobalt, uranyl, palladium, oxalate, citrate and tartrate interfere.

Phenanthrenequinone monosemicarbazone is not so selective as cuproine, neocuproine and bathocuproine, however, the tolerance for platinum metals and some other cations is an advantage of the present method. The method is more sensitive (sensitivity = $0.008 \mu g/cm^2$) than cuproine and 2,2′-biquinoline and the pH range is fairly wide (7.2–10.0). The reagent has been successfully employed in the complexometric and spectrophotometric determination of copper using simple procedures.

EXPERIMENTAL

Apparatus and reagents

Pre-calibrated pipettes, burettes and measuring flasks were used for volume measurements. A Unicam SP 600 spectrophotometer, with 10 mm matched glass absorption cells, was employed for the measurements of absorbance and pH measurements were carried out with an ECIL Expanded Scale pH meter, PH 821A.

A stock solution of copper(II) was prepared by dissolving BDH, AnalaR sample of cupric sulphate pentahydrate in doubly distilled water and standardised gravimetrically by thiocyanate method.

0.5 % solution of PQSC was prepared in dimethylformamide for complexometric and 5×10^{-3} *M* solution of the reagent was prepared in ethanol for spectrophotometric studies.

Acetate buffers were used for pH adjustment, for higher pH values, sodium hydroxide was added.

Reagent grade chloroform and dimethyl formamide were distilled before use. Doubly distilled water was used throughout.

Procedure for complexometric determination of copper

To a sample solution containing 5 μg–25 mg of copper, add 2–3 drops of the indicator (0.5 %) and 3 ml of acetate buffer to bring the pH in the range 5.4–7.2. Dissolve the precipitate obtained in 3–4 ml of DMF and titrate against standard EDTA solution of suitable concentration taken in a microburette. Note the end point when the orange red colour of the solution changes to green.

Procedure for spectrophotometric determination of copper

Take an aliquot of solution containing 18.2–67.6 μg of copper(II), add suitable masking agent, if necessary, when the solution contains any of the interfering cations and then add ten times molar excess of ethanolic solution of PQSC. Adjust the pH between 7.2 and 10.0 with sodium acetate and sodium hydroxide in a total volume of 10 ml and add 10 ml of freshly distilled chloroform. Shake the contents for five minutes on a shaking machine and set aside for equilibration. Pipette out the chloroform layer and centrifuge to remove any droplets of water in the organic layer. Measure the absorbance of extracted chelate at 480 nm against a reagent blank prepared under similar conditions. Calculate the amount of copper from the calibration curve.

RESULTS AND DISCUSSION

Complexometric determination

It was observed from the results that copper (II) can be titrated when the pH is 5.4–7.2. pH 6.2 was maintained in all subsequent studies. Titrations were carried out by adding varying amounts of 0.5% solution of the indicator in DMF. It was found that even one drop of the indicator is sufficient to cause a sharp change at end-point and the addition up to 10 drops has no effect on colour change. In subsequent studies, however, 2–3 drops of the indicator were added. A series of solutions containing fixed amount of copper (II) were prepared, they were cooled and heated to temperatures ranging from 5 to 70°C and titrated under suitable conditions, with standard EDTA solution. The study revealed that the colour change is sharp and instantaneous when temperature is 10–55°C. Subsequent studies have been carried out at room temperature (~30°C).

Precision and interference

To find the precision of the titration procedure, statistical evaluation of the results has been carried out. For this purpose, a series of eight identical solutions were prepared and titrated according to the recommended procedure. The standard deviation was found to be 0.0079, with an average relative deviation of ± 0.22%. The coefficient of variation was 0.31%.

Solutions were prepared containing a fixed amount of metal ion (2.541 mg) and known amounts of foreign ions. The tolerance limits (ppm) of various anions and cations are given in parentheses below: fluoride, chloride, nitrate, perchlorate or sulphate (3000), bromide or phosphate (2000), iodide (1000), nitrite (1500), sulphite (2500), oxalate (100), citrate (500), tartrate (800), borate or phthalate (500), barium (II) or strontium (II) (1500), calcium (II) (900), magnesium (II) (1000), cobalt (II) (10), zinc (II) (100), ruthenium (III) (70) and platinum (IV) (40).

The following cations have been masked successfully in amounts in ppm by the anions indicated in parentheses below: aluminium (III) (200, F^-), iron (III) (500, F^-), silver (I) (100, Cl^-), lead (II) (100, SO_4^{2-}), manganese (II) (200, F^-), thorium (IV) (150, F^-) and tin (II) (500, F^-). Serious interference is caused by cyanide, thiosulphate and nickel (II).

Spectrophotometric determination

A series of solutions containing a fixed amount of copper (II) (1 ml of 1×10^{-3} *M*) and an excess of the ligand (2 ml of $5 \times 10^{-3} M$) were prepared. pH's of the solutions were adjusted by the use of acetate buffers in a total volume of 10 ml by adding sodium hydroxide for higher pH's. The solutions were extracted in 10 ml of chloroform and the absorbances were measured against reagent blanks prepared under similar conditions. The values exhibit maximum absorption at 480 nm. The absorbance was found to remain constant in the pH range 7.2–10.0. In subsequent studies the pH of the solutions was adjusted to 8.0 and absorbances were measured at 480 nm. The absorbance of the complex was found to remain constant for 24 hours after which a slow decrease takes place. A number of solutions containing a fixed amount of copper (II) and varying amounts of the reagent were prepared. The chelates were extracted in 10 ml of chloroform and the absorbances were measured at 480 nm against the corresponding reagent blanks. For full colour development, at least five times molar excess of the reagent is required. However in subsequent studies, ten times molar excess of the reagent was maintained. The system obeys Beer's law up to 8.9 ppm of copper. The optimum concentration range, evaluated by Ringbom method, is found to be 1.82 to 6.76 ppm. The sensitivity of the reaction, as evaluated from Beer's plot is 0.008 μg Cu/cm^2 at 480 nm for $\log I_0/I = 0.001$. The molar absorptivity of the complex is 7.7×10^3. The values of E_m (maximum absorbance in the presence of an excess of regent) and E_s (absorbance of the complex when the metal and reagent are present in the ratio of 1 : n, stoichiometric ratio) obtained from the study of the effect of reagent concentration, are 0.770 and 0.605 respectively. $\alpha (= E_m - E_s/E_m)$ is found to be 0.2143 and the formation constant of the complex comes out to be 1.99×10^9. The stoichiometry of the complex has been determined by Job's[13,14] and mole ratio[15] methods. The maximum occurring at 0.33 mole fraction of metal indicates that copper and PQSC are present in the ratio of 1 :2 in the complex. The same results are obtained by the application of mole ratio method.

Precision and interference

Eight solutions each containing $1 \times 10^{-4} M$ copper (II) were taken and the complex was extracted in chloroform as given under recommended procedure. The mean value of absorbance was found to be 0.77 with standard deviation of 0.0042. The coefficient of variation was 0.545 % with relative average deviation of ±0.4 %.

Solutions containing 6.35 ppm of copper and known amounts of foreign ions were prepared and absorbances of chelates extracted in 10 ml of chloroform were measured at 480 nm against reagent blank and the copper content was then deduced from the calibration curve. The amounts (in ppm) of various ions tolerated are given below in parentheses. Masking agents, wherever used, have been mentioned against each : chloride, nitrate or perchlorate (1000), bromide or fluoride (800), sulphite (500), nitrite (400), phosphate or phthalate (200), citrate (70), borate (300), oxalate (100), barium (II) or strontium (II) (200), calcium (II) (100), zinc (II), cadmium (II) or mercury (II) (5), lead (II) (10, SO_4^{2-}), iron (III) (50, F^-), aluminium (III) (75), magnesium (II) (50), silver (I) (50, Cl^-), ruthenium (III) or platinum (IV) (30), rhodium (III) or iridium (III) (25), osmium (VIII) (8) and thorium (IV) (35, F^-). However, thiosulphate, cobalt (II), nickel (II) and palladium (II) interfere.

Determination of copper in gun metal

Copper was determined spectrophotometrically in samples of gun metal (composition, Cu = 87.1 %, Zn = 2.57 %, Sn = 9.61 %, Pb = 0.35 % and Fe = = 0.06 %), after the addition of fluoride and sulphate as masking agents. The results of this study are given in table 1. The standard deviation of six replicate determinations containing 3.91 ppm of copper (II), was found to be 0.4 %.

TABLE 1

Determination of copper in gun metal

Copper found (ppm)	Cu(II) calcd. (ppm)	% Error
0 .853	0 .860	−0 .81
1 .765	1 .768	−0 .17
2 .846	2 .845	+0 .04
3 .910	3 .910	0 .00
5 .240	5 .235	+0 .09

REFERENCES

[1] G. Schwarzenbach, "Komplexon Methoden", Siegfried & Co., Zofingen, 1948.
[2] I. A. Crişan and A. S. Matei, *Rev. Roumaine Chim.*, **13**, 1347 (1968).
[3] F. Kamil, S. K. Sindhwani and R. P. Singh, *Ann. Chim. (Ital.)*, **68**, 71 (1978).
[4] P. Wehber, *Z. analyt. Chem.*, **166**, 186 (1959).
[5] M. Hnilickova and L. Sommer, *Coll. Czech. Chem. Comm.*, **26**, 2189 (1961).
[6] J. Hoste, *Analyt. Chim. Acta*, **4**, 23 (1950).
[7] G. F. Smith and W. H. Mc Curdy, Jr., *Analyt. Chem.*, **24**, 371 (1952).
[8] G. F. Smith and D. H. Wilkins, *Analyt. Chem.*, **25**, 510 (1953).
[9] Sesiti Ikeda and Hirshi Nagai, *Japan Analysi*, **7**, 76 (1953).
[10] C. E. A. Shanahan and R. H. Senkins, *Analyst*, **86**, 166 (1961).
[11] P. D. Kartz, I. Jay and A. Feldman, *Analyt. Chem.*, **20**, 524 (1952).
[12] Sangal P. Satendra, *J. prakt. Chem.*, **29**, 76 (1965).
[13] P. Job, *Ann. Chim. (Ital.)*, **9**, 113 (1928).
[14] H. Irving and T. B. Pierce, *J. Chem. Soc.*, 2565 (1959).
[15] J. H. Yoe and A. L. Jones, *Ind. Eng. Chem. Analyt. Ed.*, **16**, 111 (1944).

Revue Roumaine de Chimie, 28, *4*, 419–424 (1983)

GEL PERMEATION CHROMATOGRAPHY OF POLY(VINYLACETATE)

MARIANA BEZDADEA[a], C.V.UGLEA[b]* and I. AGHERGHINEI[c]
a The Polytechnic Institute, Iassy, Splai Bahlui 72,6600, Romania
b Synthetic Fiber Works, Research Department, Sos. Tutora, 27, Iassy, Romania
c Institute of Macromolecular Chemistry, "Petru Poni", Aleea Grigore Ghica Vodă, 41 A, Iassy, Romania

Received December 25, 1981

The role of matrix method of poly(vinylacetate) synthesis on the polydispersity degree is investigated. The gel permeation chromatography evidenced the formation of two classes of compounds : a macromolecular one of the "replica" type and an oligomer of the "inclusion" type.

I. INTRODUCTION

The determination of molecular weight distribution is a mean of knowing the influence of the experimental working or synthesis conditions on the species dimensions and frequency in a polymer.

Numerous investigators have used the gel permeation chromatography (GPC) to determine the distribution of molecular weight distribution in poly (vinylacetate) (PVAc).[1-5] The aim of the present paper is to determine by means of GPC the influence of synthesis conditions on the molecular characteristics of PVAc obtained by matrix polymerization.

II. EXPERIMENTAL

1. *Reagents.* Vinylacetate (VAc), freshly distilled (Schuchardt).
Sephadex G-50, Pharmacia, Uppsala, Sweden.
PVAc, commercial products, with characteristics listed in table 1.

2. *Polymerization.* PVAc was obtained by VAc photopolymerization in inert medium, using an equipment provided with a source of UV radiations emmitted by a Hg vapour lamp (500 W) placed at 0.25 m from the ampoule with the sample.

The polymerization was accomplished in the quartz ampoules provided with cooling coils. The monomer was added to the Sephadex, previously swollen in water (water to Sephadex ration : 10/1), in determined quantities.

The separation of polymer from Sephadex was performed by extraction in methanol, filtration, reprecipitation in water and drying under vacuum at 30°C. The details of VAc photopolymerization in Sephadex were reported in a previous paper.[6]

The samples denoted by M in table 1 are obtained without matrix, using distilled water as polymerization medium.

3. *Gel permeation chromatography.* The chromatograms were obtained by using a Knauer apparatus provided with differential refractometer. A glass column ($\varnothing_i = 1.6$ cm, $L = 72$ cm) filled with styrene-divinylbenzene copolymers was used. The calibration method reported by Loy [7] and checked by other authors [8,9] was applied, using a polydisperse "secondary standard", namely a commercial PVAc denoted by PI1 in table 1.

---

* Correspondence author

These data were worked on a Felix C32 computer. The calibration relation was used as follows :

$$\log M = C_1 - C_2 V_{EL} \qquad (1)$$

were M represents the molecular weight, V_{EL} is elution volume and C_1, C_2 are the constants.

To determine the calibration parameters, a gel chromatogram of a polydispersed sample of a known molecular weight has to be obtained. In principle, it is enough to know the values of either $\overline{M}_n$ or $\overline{M}_w$. The determination of the two calibration constants (C_1, C_2) is thus reduced to an optimization iterative calculation of a function of two variables.[7] The obtained values of the two variables are the calibration constants. Loy[7] derived a method for determining C_1 and C_2 constants which involves knowledge of the $\overline{M}_n$ and $\overline{M}_w$ molecular weights, while the dispersion effect due to the imperfections of the column resolution is neglected. By this procedures, the volume of mathematical calculations is significantly reduced. To determine the optimum, the method of unidimensional search was used.[8-11] The iterative calculation of the parameters was stopped when the difference between two successive iterations was $< 10^{-3}$. In this way the values of 4.371 and -0.456 have been determined for C_1 and C_2, respectively, from relation (1).

In figures 1–3 the gel chromatograms of the products obtained are given.

4. *Determination of* $\overline{M}_n$. The osmometric measurements were taken on a Hewlett-Packard 502 osmometer, at 25°C, in benzene. The value of the π/c ratio was determined at four concentrations. To obtain $(\pi/c)_{c \to 0}$ ratio the least square method was applied. The $\overline{M}_w$ values for the commercial polymers were determined by the manufacturer.

III. RESULTS AND DISCUSSION

The influence of the polymerization time, matrix to monomer ratio and temperature on the value and distribution of molecular weight of PVAc was followed. The GPC data indicate that the distribution of molecular weight (DMW) of PVAc obtained by matrix polymerization depends on the synthesis conditions. Here, the selection of the optimum conditions is possible, leading to a polymer with good homogeneity.

The influence of the polymerization time is clearly evidenced by the diminution of the low molecular weight fractions for a reaction duration of 3 h (Fig. 1, A, Table 2). In addition, by comparing our samples with the standard ones (Fig. 1, B), and with the sample M VI the differentiation of the polydispersity degree is quite noticeable and indicative of the role of Sephadex matrix in the synthesis. The matrix to monomer ratio influences the DMW. Thus the increase of this ratio determines the polymer homogeneity, that is the increase of average molecular weight and the diminuation of low molecular weight fractions.

As can be seen in figure 2, the least disperse sample, B, containing 5.44 % low molecular weight fractions, was obtained at the highest matrix to monomer ratio (Table 2). The results concerning the temperature influence are not very important. One may notice the most homogenous polymer to be obtained by matrix polymerization, at – 10°C, with matrix to monomer ratio > 3 (Fig. 3).[13]

IV. CONCLUSIONS

1. The GPC allowed the conclusion to be drawn that the matrix can lead to the formation of two classes of compounds, a macromolecular

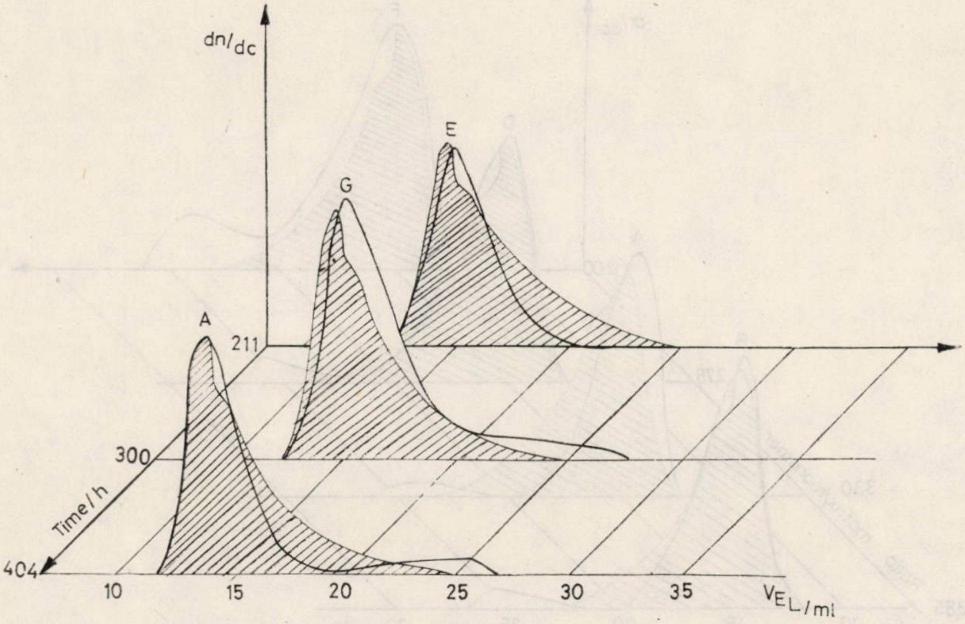

Fig. 1. — A. The influence of the polymerization time on the DMW of PVAc samples A, E and G; hatched curve-industrial sample (PI1)

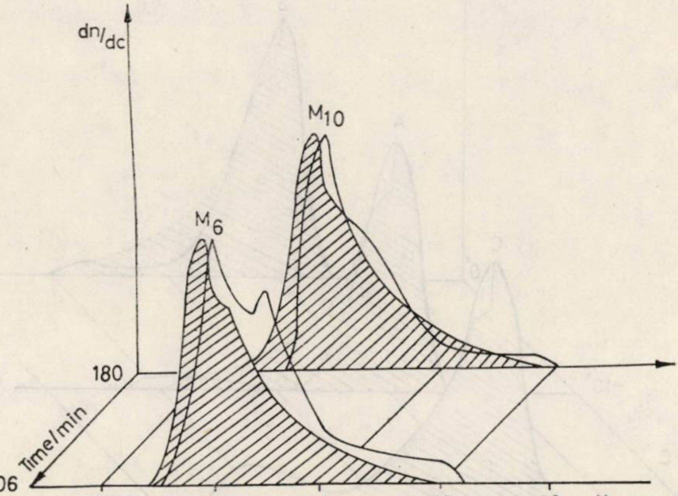

B. Gel-chromatograms of PVAc samples obtained without matrix (MVI, MIX); hatched curve-industrial sample PI1.

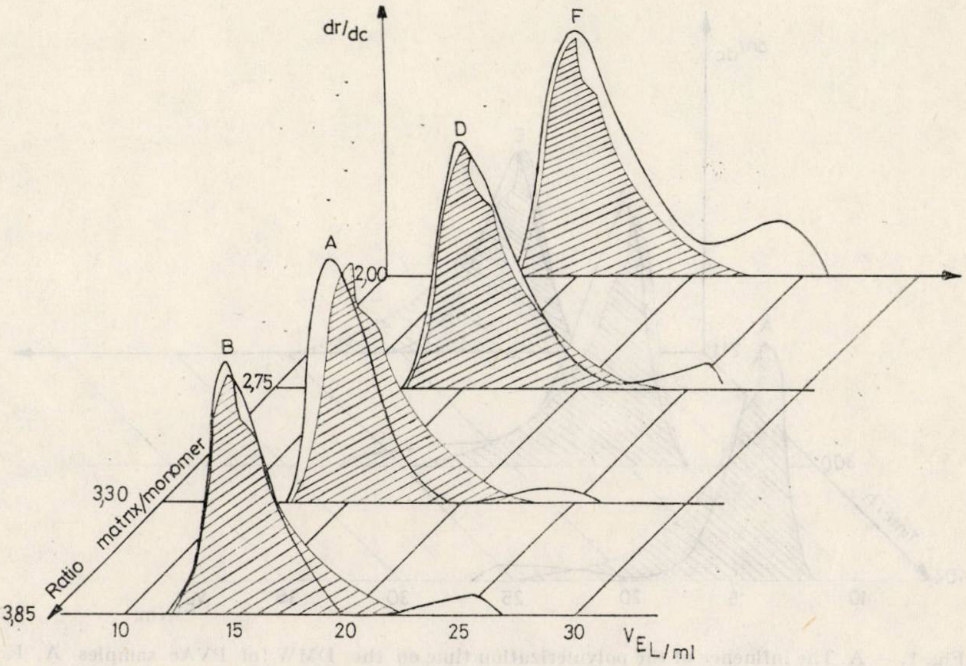

Fig. 2. — The influence of matrix to monomer ratio on the DMW of PVAc sampes A, B, D and F; hatched curve-industrial sample PI1.

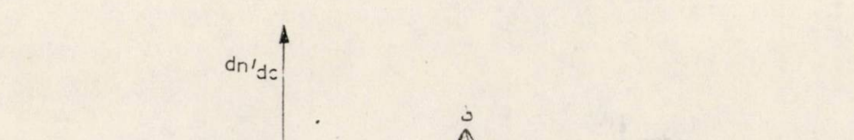

Fig. 3. — The influence of the polymerization temperature on the DMW of PVAc samples A, B and C; hatched curve-industrial sample PI1.

TABLE 2

The characteristics of low molecular weight fractions*

Sample	$\overline{M}_n$	$\overline{M}_w$	$[\eta]$ dl/g	$\overline{M}_w/\overline{M}_n$	$\overline{M}_v$	% in initial sample
A	11 180	23 210	0.12	2.076	19 380	6.97
B	12 060	19 420	0.11	1.61	17 310	5·44
C	9 661	12 050	0.09	1.247	11 470	8.61
D	9 400	12 450	0.09	1.324	11 660	6.98
E	—	—	—	—	—	0
F	11 460	16 460	0.10	1.436	15 290	15.13
G	15 270	24 990	0.13	1.636	22 840	9.58

* Determined from GPC data ; low molecular weight fractions represents the species with elution volume VEL/ml> 20($\overline{M}_n < 10^4$)

one (about 85 % of the total product), resulted from a "replica" type polymerization and an oligomer one (about 15 % of the total product).

2. By taking into account the range of molecular weights of the molecules capable of entering the Sephadex G—50 pores, the oligomers formed can be considered as resulted from an "inclusion" type polymerization.

3. For every sample investigated the macromolecular fraction obtained was found to exhibit a considerably low polydispersity degree.

REFERENCES

[1] A. E. Hamielec, A. C. Ouano and L. L. Nebenhahl, *J. Liquid Chromatog.*, **1**, 527 (1978).
[2] R. Dietz, *Prepr. Short Comm. Makro Mainz*, **2**, S1, 735 (1976) ;
[3] C. M. Atkinson and R. Dietz, *Eur. Polymer J.*, **14**, 185 (1978).
[4] J. Brezinski, *Eur. Polymer J.*, **16**, 85 (1980) ;
[5] R. P. D. D'Amelia and H. Jacom. *Ind. Eng. Chem., Prod. Res. Develop.*, **15**, 303 (1976).
[6] Cr. I. Simionescu and M. Bezdadea, *Bull. Inst. Politehnic Iași, Sect. II*, Tom **XXV**, 93 (1979).
[7] B. R. Loy, *J. Polymer Sci., Polymer Chem. Ed.*, **14**, 2321 (1976).
[8] R. P. Chaplin, J. K. Haken and J. J. Paddon, *J. Chromatogr.*, **171**, 55 (1979).
[9] R. P. Chaplin, W. Ching, *J. Macromol. Sci., — Chem.*, **A14**, 257 (1980).
[10] M. Matsumoto and Y. Ohynagi, *J. Polymer Sci.*, **46**, 441 (1960).
[11] I. Dancea, "Metode de Optimizare", Ed. Dacia, Cluj-Napoca, 1976, p. 24.
[12] Cr. I. Simionescu, M. Bezdadea and N. Hurduc, "Al 2-lea Congres National de Chimie", București, 1981.

Revue Roumaine de Chimie, 28, 4, 425—427 (1983)

SPECTROPHOTOMETRIC DETERMINATION OF IRON WITH SODIUM-*N*-(*O*-SULPHONIC-BENZOYL)-*N*-PYRIDINE IN THE PRESENCE OF THIOCYANATE

S. F. A NAQVI, S. P. MATHUR and V. IYER
Research Laboratories, Govt. College, Beawar-305901, India

Received April 24, 1981

Sodium-N-(O-Sulphonic benzoyl)-N-pyridine forms an orange red complex with iron (III) in the presence of thiocyanate medium. This complex has the maximum absorption at 480 nm with a molar absorptivity 14,600 $l \cdot mole.^{-1}\ cm^{-1}$. Beer's law is obeyed up to 5.2 ppm of iron. The effect of diverse ions is also described.

INTRODUCTION

Ligands containing a pyridine ring system are found to possess analytical applications. [1-5] The newly synthesized ligand sodium-N-(O-sulphonic benzoyl)-N-pyridine is water soluble and results in water soluble complexes with a number of metal ions. The present communication describes the spectrophotometric determination of iron (III) with sodium-N-(O-sulphonic benzoyl)-N-pyridine in the presence of thiocyanate medium. The method is simple, sensitive and rapid for the determination of microgram amount of iron (III). The method is highly selective and can be applied to almost all common ions including those which interfere with the classical thiocyanate method [6].

EXPERIMENTAL

Preparation of sodium N-(O-sulphonic benzoyl)-N-pyridine: equimolar quantities of 2-amino pyridine and O-sulpho benzoic anhydride were taken in benzene and the mixture was stirred mechanically. Alcoholic sodium hydroxide was added to it to get sodium salt of sulphonic acid. It was precipitated by adding ether, filtered under suction and crystallized by dissolving it in a minimum quantity of water and adding excess of alcohol. The purity of compound was established by elemental analysis, thin layer chromatography and IR.

2% W/V fresh solution of reagent in distilled water was prepared each time.

Standard iron solution: ferrous ammonium sulphate (3.929 g) was oxidised in ammoniacal medium with hydrogen peroxide. Ferric hydroxide so formed was dissolved in dilute hydrochloric acid and volume made to one litre. The iron amount was determined gravimetrically.

A 5% (W/V) solution of amonium thiocyanate was used.

Solution of diverse ions

Cation solutions were prepared from reagent grade chloride on nitrate salts. Osmium, tungsten and arsenic oxides were used for preparation of solutions. Anion solutions were prepared from their sodium or potassium salts.

All chemicals used were of A.R. grade.

Apparatus

Absorbance measurements were made with a Beckmann Model DU quartz spectrophotometer. All pH measurements were made with a Cambridge bench type pH meter.

Procedure

An aliquot of iron (III) solution containing 60 µg. of metal was taken into 25 ml measuring flask. A 2 ml of 5% (W/V) thiocyanate solution was added. Suitable amount of 10% hydrochloric acid was added so that after dilution the pH of final solution became 4.5.5 ml of 2% reagent solution was added and the volume made up to the mark with distilled water. The absorbance of orange-red coloured complex was measured at 480 nm against reagent blank.

RESULTS AND DISCUSSION

The absorbance of ternary iron (III)-reagent-SCN complex was found to be maximum at 480—490 nm with molar absorptivity 14.600 1. mole^{1} cm^{-1}. The reagent under similar conditions showed negligible absorbance in the region 480—490 nm.

Beer's law was obeyed up to 5.2 ppm of iron (III) at 480 nm and the optimum concentration range on the basis of Ringbom's plot [7] was 1.2 to 4.6 ppm of metal. Sandell's [8] sensitivity of colour reaction was 0.0053 µg Fe(III)/cm^2. The statistical analysis of the results obtained at three different levels of iron indicated that the system is highly reproducible and shows good accuracy. The relative standard deviation of the method was found to be ± 0.89%.

The optimal range for complex formation was found to be between the pH values 4.2 and 7.4. The colour of the complex was found to be stable for 24 hours. There was no difference in the absorbance of the sample at 25°C and the sample heated to 50°C. At high temperature the colour faded slightly.

The composition of Fe(III) — reagent — thiocyanate was determined by the curve fitting method.[9] The ternary complex so formed showed 1 :1 : 2 (metal : reagent : thiocyanate) composition.

Tolerance of diverse ions

In the determination of Fe(III) at pH 4.5, the effect of diverse ions was studied as described in the procedure. Cl$^-$, Br$^-$, No$_3^-$ So$_4^{-2}$, I$^-$, alkali metals, alkaline earth metals, lanthanides, urea, thiourea and ammonia did not interfere the estimation up to 3000 ppm. The tolerance limits of other ions causing an error less than 2% in the absorbance reading, are shown in parentheses (in ppm) : F$^-$(1700), Po$_4^{-3}$ (1600), Co^{+2} Cr^{+3} and Mn^{+2} (900), Zn^{+2}, Cd^{+2}, Ni^{+2} (1800), Zr^{+4} (600), W^{+6} (400), Mo^{+6} (80), Al^{+3} (1400), V^{+5}(100), Ti^{+4} (100), Cu^{+2} (40), Os^{+8} (150) and As^{+3} (700).

ACKNOWLEDGEMENT. The authors are thankful to Mr. S.T.H. Zaidi, Principal, Govt. College, Beawar (India) for providing research facilities.

REFERENCES

[1] **S. P. Mathur**, V. P. Mehta and M. Hasan, *Chem. Analit*, **24**, 921 (1979).
[2] **S. P. Mathur** and M. R. **Bhandari**, *Rev. Latinoamer. Quim*, **6**, 160 (1975).
[3] **S. P. Mathur**, *J. Inst. Chemists (India)*, **47**, 173 (1975).
[4] **S. P. Mathur**, *Chem. Analit*, **22**, 819 (1977).
[5] W. J. **Holland** and J. **Bozic**, *Talanta*, **15**, 843 (1968).
[6] **E.** B. **Sandell**, "**Colorimetric** Determination of Traces of Metals", Interscience, New York, 1956, p. 524, 537 and 544.
[7] A. **Ringbom**, *Z. analyt. Chem.*, **115**, 332 (1938).
[8] **E. B. Sandell**, "**Colorimetric** Determination of Traces of Metals", Interscience, New York, 1952 p. 53.
L. G. **Sillen**; *Acta Chem. Scand.*, **10**, 185 (1956).

Revue Roumaine de Chimie, **28**, *4*, 429–433 (1983)

COMPTES RENDUS

"Flavonoids and Bioflavonoids, 1981", L. Farkas M. Gabor, F. Kallay, H. Wagner (editors), Akadémiai Kiadó, Budapest, 1982, 534 pages.

The book contains the proceedings of the international Bioflavonoid Symposium (6^{-th} Hungarian Bioflavonoid Symposium) held in Munich, FRG, in September 6–9, 1981.

From the 50 papers, presented in the camera-ready form, in order to make the material rapidly available to all researchers, an important part belongs to well-known Hungarian authors working in this domain. Numerous contributions of renowed scientists from nearly all major schools of international flavonoid research are also included.

As in the previous volumes dedicated to Flavonoid Symposions the main topics attack : the syntheses of flavonoids, the structure elucidations and the biologic actions (biosynthesis, the methabolic pathways in plant, animal and human organisms etc.).

From the numerous very interesting papers we could only mention some examples concerning : 1) the syntheses of flavonoids : "The synthesis of isosophoronol, an isoflavanone from *Sophora tomentosa*" (G. B. Marini-Bettòlo and co-workers), "The first synthesis of acylated flavonoid glycosides" (B. Vermes, H. Wagner), "Synthesis of 6-chlorogenistein" (A. I. Tőkes, A. Lévai), "3-Acylchromones" (F. Eiden), "Synthesis of the oligosaccharides of flavonol-triosides" (H. Wagner and co-workers), "Synthetic studies on some flavanone ether derivatives possessing spasmolytic (R. Ertan) ; 2) the structure elucidations : "Structural elucidation of the flavanolignans hydrocarpin and silandrin by partial synthesis" (H. Wagner and co-workers), "Structure elucidation and hindered rotation of two procyanidins from *Nelia meyeri*" (H. Kolodziej), "^{13}C-NMR spectroscopy of flavonoid O- and C- glycosides" (W. M. Chari) ; 3) the biologic aspects ; "Advances in the pharmacology of benzopyrone derivatives and related compounds" (M. Gabor) a contribution of 38 pages, 104 references, underlining the outstanding results obtained in researches of antiallergic, antiasthmatic action of chromones, of anti-gout and anti-anginal action of benzofuran derivatives, and of antihepatotoxic and spasmoanalgetic effects of some flavones, "Gastric anti-ulcer activity of methyl-3 (+)-catechin" (N. S. Parmar, M. N. Ghosh), "The hepatic metabolism of flavonoids" (I. C. Shaw and co-workers), "Advances in the pharmacology of benzopyrone derivatives and related compounds" (M. Gabor).

Including a lot of different aspects of researches in the flavonoid domain, presenting the newest results of all major schools of flavonoid research, including rich reference lists and being published soon after the Symposium, this book is a very useful aid, providing an up-to-date survey of present knowledge in the field of flavonoids.

M. Banciu

"NMR, Basic Principles and Progress. Oxygen-17 and Silicon-29", Edited by P. Diehl, E. Fluck, R. Kosfeld, Springer-Verlag, Berlin, 1981.

This book is the 17th in the series "NMR. Basic Principles and Progress" of Springer-Verlag and is dedicated to Oxygen-17 and Silicon-29.

It consists of two parts : "Oxygen NMR. Characteristic Parameters and Applications" by J. P. Kintzinger and "^{29}Si-NMR Spectroscopic Results" by H. Marsmann.

The first part begins with experimental considerations regarding the comparison of Fourier transform and continuous wave methods, as well as the chemical shift scale. Then nuclear quadrupole coupling constants, screening constants σ and chemical shifts δ are considered. Some synthetizing tables and graphs are employed to discuss and exemplify the case of compounds that contain oxygen bounded to C, Si, N, P, Sb, O, S, Se, Te, Xe, halogen and to transition elements, respectively. Some theoretical and practical considerations are followed by presentation of experimental results regarding coupling constants and ^{17}O relaxation. The first part of the book is concluded with applications of ^{17}O NMR : ^{17}O as structural probe, as hydrogen bonding probe and as dynamic probe, ^{17}O titration curves, diamagnetic electrolyte solutions and miscellaneous studies.

The second part specializes in theoretical and practical considerations regarding the detection of $^{29}Si-NMR$ signals, ^{29}Si chemical shifts, spin-spin coupling involving ^{29}Si and relaxation effects. It includes a compilation of ^{29}Si chemical shift data, standard compound for chemical shift determination and comprehensive diagrams and tables.

The book is clear and concise, based on a large bibliography, includes the newest contributions (248 entries in the 1st part and 393 in the second) and supplies a sound theoretical basis and an excellent practical guide for all those interested in NMR.

Luminiţa Vlădescu

"*Structure and Bonding*" vol. 37, "*Structural Problems*". Springer-Verlag, Berlin—Heidelberg—New York, 1979, 216 pages.

The 37th volume in the series "Structure and Bonding" published by Springer-Verlag includes three papers on the following topics : Jahn Teller interactions, the frameworks in cubic structure types, and polyhalogen cations.

The first paper ("Local and Cooperative Jahn-Teller Interactions in Model Structures. Spectroscopic and Structural Evidence", by Dirk Reinen and Claus Friebel, 60 pages, 28 figures, 6 tables, 136 references) examines the Jahn-Teller effect, which controls in many cases the structural chemistry of the solid compounds of transition metals. The main features of local and cooperative Jahn-Teller effects are discussed, then the Jahn-Teller interactions are examined in different types of the host lattices, where Ag^{2+}, Cu^{2+}, Cr^{2+}, Mn^{3+}, low spin Co^{2+} and Ni^{3+} are in octahedral coordination. As EPR spectroscopy is the most useful method in analysing the symmetry aspects and static-dynamic transitions in unstable Jahn-Teller solids, some details concerning these subjects are treated in this paper.

The second paper ("The Frameworks of the Cubic Structure Types", by Erwin E. Hellner, 80 pages, 12 figures, 8 tables, 69 references) is the fifth in a series entitled "Relationship Criteria for Crystal Structure Types", and deals with the cubic-type structures. Some aspects of homogeneous sphere packing are correlated with the structure types of the cubic system. A grouping of the structure types in families, main classes and subclasses is proposed. A notation is proposed for each homogeneous lattice which yields directly both the notation for invariant lattice complexes and another one for coordination polyhedra. For heterogeneous structures, a combination of symbols of homogeneous lattices results.

The last paper ("Polyhalogen Cations" by J. Shamir, 70 pages, 29 tables, 148 references) is an excellent review of the preparation, properties and structural data concerning polyhalogen cations. The paper examines both the iso-polyhalogen cations which include a few atoms of a single halogen species and heteropolyhalogen cations, which include a few atoms of two halogens (also known as inter-halogen cations).

In order to establish the structures of the polyhalogen cations, different investigation methods as Raman spectroscopy, single crystal X-ray diffraction, NMR on ^{19}F, absorption and vibration spectra and Mössbauer spectroscopy are presented.

The usual excellence of the title series is also achieved. The clear and concise papers, the extensive bibliography and expressive iconography add to the usefulness of the book to all interested in the particular areas under discussion and in structural chemistry.

Dorel Crişan

"*Advances in Polymer Science*", volume 46, "*Behavior of Macromolecules*", Springer-Verlag, Berlin, Heidelberg, New York, 1982.

This book deals with some of the problems in field of behavior of macromolecules.

The first part is a contribution entitled "The structure of macromolecules adsorbed on interfaces" (65 pages and 128 references) by A. Takahashi and M. Kawaguchi.

This paper is devoted to the studies of polymer adsorption developed within the last two decades. This survey begins with a consideration of the principal theories, confining to those which are amenable to experimental tests (the theories of Hoeve, of Silberberg, of Scheutjens and Fleer). The relations between the root-mean-square thickness and the loop or tail size derived by Hesselink and diffusion equation approach deduced by De Gennes are also discussed. The existing theories allow other important quantities such as the adsorbed amount, the fraction of adsorbed segments, and the surface coverage to be calculated, but the results from different theories are not very different from one another.

The existing theories of the adsorption of polyelectrolyte (the theory of Frisch and Stillinger, the theory of Hesselink) allow effects of the polymer charge density, the surface charge density, and the ionic strength on the adsorption behavior to be predicted.

Chapter C is a brief survey of the typical measuring techniques : hydrodynamic methods, ellipsometry, adsorption isotherms, the ATR method, calorimetry, IR and EPR method.

In chapter D important experimental data on the thickness of the adsorbed polymer layer and the fraction of adsorbed segments are summarized and discussed, along with their comparison with theories. Studies of adsorption of flexible non-ionic polymers (adsorption at the theta point, adsorption from good solvents, attachement of train segments to active sites) by ellipsometry, hydrodynamic methods, by small-angle scattering, by IR spectroscopy and by calorimetry have been developed.

A brief outline of the studies in relation to the adsorption of branched polymers, of blockcopolymers, of polyelectrolytes, of block polyelectrolytes, of polyampholytes and of rod-like macromolecules is given in this section.

The second part of the book is a paper entitled "Polymer elasticity discrete and continuum models" by R.G.C. Arridge and P. J. Barham (50 pages and 112 references).

The purpose of this article is to describe the problems regarding measurements of mechanical properties. Some solutions of equations of elasticity and the application of viscoelasticity to real materials are discussed. The authors show how the classical theory is applied to various test methods and comment on the material problems (the effect of non-linearity, inhomogeneity and anisotropy) and consider how they affect individual tests. There are three principal problems relating to the specimen and test geometry : the end-effects due to gripping the sample, the alignment of the specimen in the test equipment and the shape of the specimen.

The authors present the theories relating to non-homogeneous materials. Inhomogeneous materials may be divided according to the following factors : scale (macroscopic, microscopic), the spatial distribution of the inhomogeneities, local geometry and the elastic symmetry of the inhomogeneities. Special attention is given to the discussion of the representative volume element (RVE) defined by Hill for composite materials. Some calculations and estimates of the size of the RVE are reported for amorphous polymers, amorphous copolymers and semicrystalline polymers. In the last chapter, the methods for calculating the elastic properties of polymers are briefly reviewed.

Chapter 3 of the book is a paper entitled "Secondary relaxations in glassy polymers : hydrophilic polymetachrylates and polyacrylates" (41 pages and 197 references) by J. Kolarik.

This review is concerned with the characterization and classification of molecular motions giving rise to secondary transitions, the dynamics and intensity of relaxation processes observed in dynamic mechanical measurements.

The secondary transitions of glassy polymers can be studied by means of the following methods : dilatometry, infrared spectra, thermally stimulated (dielectric) depolarization, thermoluminiscence, nuclear magnetic resonance, electron spin resonance and dielectric measurements. Dynamic mechanical measurements represent the most universal method because they are able to detect the motion of almost all types of structural units. However, a deeper analysis and a quantitative interpretation of results are impeded by poorly established relations to molecular motions.

Molecular motions which give rise to secondary dispersions in glassy polymers have been tentatively divided into four types : local main-chain motion, side-chain rotations, internal motions within the side chain, molecular motions of/or affected by molecules of a diluent. This review attempts to give a categorization of the diluent-induced secondary relaxations. The classification used is based on the assumption that the motions of diluent molecules are either independent of the molecular mobility of the host glassy polymer or are associated with it in some way. The types of molecular motions have been investigated by J. Kolarik on a series of hydrophilic polymethacrylates and polyacrylates. The author's dynamic mechanical measurements illustrate the effects of polarity, geometrical constraints, comonomers and incorporated diluents on molecular mobility.

Kristiana Goşa

Advances in Polymer Science, volume 45, "*Macromolecules in Solution*" Springer-Verlag, Berlin, Heidelberg, New York 1982, 130 pages

The book contains a review entitled "Interactions between macromolecules in solution and intermacromolecular complexes" by E. Tsuchida and K. Abe. The article contains 123 pages and 595 references.

The macromolecules may interact with each other to form intermolecular complexes in solution due to certain secondary binding forces. The interpolymer complexes display new physical and chemical characteristics different from those of the individual components. Many intermolecular complexes which occur in biological systems are known.

This paper is a critical survey of the literature in relation to the formation, properties and structure of intermacromolecular complexes between synthetic macromolecules mainly.

The polymer-polymer complexes are classified into four classes on the basis of their main interaction forces, i.e. polyelectrolyte complexes, hydrogen-bonding complexes, stereocomplexes and charge-transfer complexes.

Oppositely charged polyelectrolytes interact with each other to form polyelectrolyte complexes in solution. The formation of polyelectrolyte complexes is influenced by the characteristics of the individual polyelectrolyte polymers (properties of ionic sites-strong or weak electrolyte — , position of ionic sites, charge density, rigidity of macromolecular chains) and the chemical environment (e. g. solvent, ionic strength, pH and temperature). The obtained products display specific physico-chemical properties because the electrostatic interaction forces are much stronger than other secondary binding forces. The polyelectrolyte complex is crosslinked by ionic bonds, soluble in certain solvents, relatively hydrophilic and thermoformable (when plasticized).

The authors discuss the results of experimental studies on the formation, properties and structure of complexes formed by hydrogen bonding:

— The formation of interpolymer complex can be regarded as a three-components reaction involving a proton-donating polymer, a proton-accepting polymer and a solvent. The dielectric constant of the solvent may be used as a parameter of the strength of the interaction between the polymer components and solvent.

— In aqueous medium when poly(carboxylic acid)s are used, the formation of complex has a cooperative nature, i.e. the formation and dissociation of polymer complex occur within a narrow range of pH.

— The hydrophobic interactions play an essential role in the stabilization of the polymer complex in water. In organic solvent hydrophobic interactions are negligible.

— In heterogeneous systems, the features of complex formation are quite different from those in homogeneous systems.

The stereocomplex, the complex between stereoregular polymers, has not yet been studied extensively, except for a few systems: poly- (methyl methacrylate) (PMMA)-poly(methacrylic acid) (PMAA) and PMMA-poly(vinyl chloride) (PVC).

The facility of stereocomplex formation is known to be affected by the kind of solvent used. The solvents of stereoregular polymers can be divided into three classes: strongly complexing solvents, weakly complexing solvents and non-complexing solvents.

The ratio of the monomeric units, [iso-PMMA]/[synd-PMMA] of stereocomplex is 1/2 irrespective of the initial mixing ratio and the method of preparation.

Between monomeric units (iso- and synd-) there are: dipol-dipol and/or hydrogen bond-like interactions and van der Waals interactions.

There are only few studies on C—T complexes in interpolymer complexes, because electron-accepting polymers are difficult to synthesize. The properties of the C—T complexes are slightly different from those of each polymer component.

In chapter 4 the authors analyze the cooperativity of complexation among macromolecules. In this paper, the cooperative interactions are defined as interactions between complementary macromolecules when each macromolecule is composed of only one kind of repeating units.

The authors consider that a study of selective intermacromolecular complexation and substitution reaction would be expected to clarify the processes occurring in biological systems.

When the complex molecules are formed they tend to aggregate with each other in the process of time. Supermolecular structure is affected by the type of the polymer component and chemical environment.

In chapter 5 the future development of intermacromolecular complexes tailored to special uses (ecological protection, ultrafiltration membranes, matrix polymerization, mechanochemistry) is pointed out.

The authors believe that the new development and the use of interpolymer complexes will establish a novel field in polymer science.

Kristiana Goşa

NOTE POUR LES AUTEURS

La Revue Roumaine de Chimie publie des articles en anglais, français, russe, allemand ou espagnol. Les auteurs sont priés d'envoyer des articles et des comptes rendus inédits.

Les manuscrits seront dactylographiés à double interligne. La bibliographie, les tableaux et la légende des figures seront placés après le texte.

Si l'article fait partie d'une série numérotée, la partie précédente sera donnée comme première référence.

Chaque article sera précédé d'un résumé comprenant quinze lignes au maximum.

Les références bibliographiques dans le texte seront faites par des exposants sans parenthèses et paraîtront à la fin de l'ouvrage.

Les publications périodiques mentionnées dans la bibliographie seront présentées suivant les prescriptions internationales : le nom de l'auteur précédé de l'initiale du prénom, le titre du périodique abrégé conformément à « Chemical Abstracts » et souligné par une ligne, le numéro du tome indiqué par des chiffres arabes et souligné par deux lignes, suivi de la première page de l'article : à la fin, l'année de la parution sera placée entre parenthèses. Le numéro de la revue ne sera pas indiqué si les pages du volume sont numérotées consécutivement.

Les textes des livres ou traités inclueront : Le nom des auteurs, précédé de l'initiale du prénom, le titre du livre entre guillements et sans être souligné, le numéro du tome précédé par l'abréviation « vol » (ou « Bd. »), le numéro de l'édition, les éditions (the publisher), la localité de la parution du livre, l'année de la parution et la page de la référence précédée(s) par l'abréviation « p. » (ou « S. »).

Les brevets seront indiqués comme suit : l'auteur ou la firme, le pays et le numéro du brevet, la date et la revue (Chem. Abstr.). Par ex. : M. Jones (to Union Carbide Co.), *Brit. Pat.* 601 238, 2 Sept. 1959, *Chem. Abstr.*, **54**, 12808 (1960).

Si la référence n'a pas été lue en original, on indiquera aussi la revue de références consultée.

Les diagrammes seront tracés à l'encre de Chine sur papier calque. Les tableaux et les figures (en nombre strictement nécessaire) ainsi que les courbes dans les figures seront numérotés par des chiffres arabes. Leur explication sera donnée dans la légende des figures. Prière de ne pas inscrire les mêmes données dans les tableaux et les figures. Chaque tableau aura un titre. On indiquera dans le texte la place approximative des tableaux et des figures. Les formules chimiques seront incluses dans le texte ; en outre, elles seront transcrites sur papier calque, à l'encre de Chine.

Les auteurs sont priés d'indiquer les caractères italiques (en soulignant les lettres au crayon), ainsi que toute autre caractère spécial : les préfixes *ortho*, *meta*, *para*, *cis*, *trans*, etc. seront soulignés pour indiquer leurs caractères italiques et ne seront jamais écrits avec des majuscules.

Aucune correction à la main ne sera admise sur le manuscrit. Les corrections seronnt tappées à la machine. Les lettres grecques ou d'autres symboles spéciaux seront insérés à la main à l'encre clairement.

Le manuscrit sera signé par l'auteur.

Le titre-courant aura 50 lettres au maximum.

L'entière responsabilité du contenu des articles appartient aux auteurs.

Sur demande on peut obtenir une note plus complète.

PRINTED IN ROMANIA

TRAVAUX PARUS AUX ÉDITIONS DE L'ACADÉMIE DE LA RÉPUBLIQUE SOCIALISTE DE ROUMANIE

ELENA CEAUŞESCU, **Noi cercetări în domeniul compuşilor macromoleculari** (Nouvelles recherches dans le domaine des composés macromoléculaires), 1981, 536 p.

I. G. MURGULESCU, RODICA VÎLCU, **Introducere în chimie fizică. Vol. III. Termodinamica chimică** (Thermodynamique chimique), 1982, 626 p.

I. G. MURGULESCU, J. PĂUN, **Introducere în chimia fizică. Vol. I.3. Nucleul atomic, reacţii nucleare, particule elementare** (Introduction à la chimie physique. Vol. I.3. Noyau atomique, réactions nucléaires, particules élémentaires), 1982, 606 p.

ELENA JERCAN, **Analiza cromatografică** (Analyse chromatographique), 1982, 286 p.

I. G. MURGULESCU, TATIANA ONCESCU, E. SEGAL, **Introducere în chimia fizică. Vol. II.2. Cinetică chimică şi cataliză** (Introduction à la chimie physique. Vol. II.2. Cinétique chimique et catalyse), 1981, 1024 p.

V. DRĂGUŢAN, A. T. BALABAN, M. DIMONIE, **Metateza olefinelor şi polimerizarea prin deschidere de inel a cicloolefinelor** (La métathèse des oléfines et la polymérisation par ouverture annulaire des cyclooléfines), 1981, 254 p.

LYDIA-MARIA VAICUM, **Epurarea apelor uzate cu nămol activ. Bazele biochimice** (L'épuration des eaux résiduelles à boue active. Les bases biochimiques), 1981, 218 p.

I. GĂLĂŢEANU, **Procese şi metode radiochimice în energetica nucleară** (Processus et méthodes radiochimiques dans l'énergétique nucléaire), 1981, 234 p.

O. IORDACHE, **Procese polistocastice aplicate în fenomenele de transfer** (Processus polystochastiques appliqués aux phénomènes de transfert), 1981, 187 p.

CR. SIMIONESCU, VALERIA GORDUZA, **Polimeri biocompatibili şi biologic activi** (Polymères biocompatibles et biologiquement actifs), 1980, 497 p.

ELENA CEAUŞESCU, **Polimerizarea stereospecifică a izoprenului** (La polymérisation stéréospécifique de l'isoprène), 1979, 307 p.

M. FLORESCU, **Metode ştiinţifice în dezvoltarea industriei chimice moderne** (Méthodes scientifiques dans le développement de l'industrie chimique moderne), 1979, 256 p.

A. T. BALABAN, I. GĂLĂŢEANU, G. GEORGESCU, LIGIA SIMIONESCU, **Compuşi marcaţi şi radiofarmaceutici cu aplicaţii în medicina nucleară** (Composés marqués et radiopharmaceutiques à application en médecine nucléaire), 1979, 495 p.

CONST. GH. MACAROVICI, **Analiza chimică cantitativă anorganică** (L'analyse chimique quantitative inorganique), 1979, 457 p.

I. G. MURGULESCU, E. SEGAL, **Introducere în chimia fizică. (Vol. II.1. Teoria molecular-cinetică a materiei** (Introduction à la chimie physique. Vol. II.1. La théorie moléculaire-cinétique de la matière), 1979, 1036 p.

S. STERNBERG, FL. DANEŞ, **Termodinamica chimică aplicată** (La thermodynamique chimique appliquée), 1978, 400 p.

I. G. MURGULESCU, V. EM. SAHINI, **Introducere în chimia fizică. Vol. I.2. Structura şi proprietăţile moleculelor**(Introduction à la chimie physique. Vol. I.2. La structure et les propriétés des molécules), 1978, 604 p.

I. ZUGRĂVESCU, MAGDA PETROVANU, **N-ylid chemistry**, coédition avec McGraw-Hill International Book Company, U.S.A., 1977, 396 p.

I. G. MURGULESCU, **Introducere în chimia fizică. Vol. I.1. Atomi, molecule, legătură chimică** (Introduction à la chimie physique. Vol. I.1. Atomes, molécules, liaison chimique), 1976, 560 p.

ELENA CEAUŞESCU, **Research work on synthesis and characteristation of macromolecular compounds. Contributions.** 1974, 251 p.

CR. SIMIONESCU, VIORICA RUSAN, V. POPA, **Chimia algelor marine** (La chimie des algues marines), 1974, 212 p., 1 pl.

ISSN 0035—4090

I. P Informaţia c. 2761

43426

Lei 40

$ 75 (pour un abonnement annuel)

0F 1103

04

ACADÉMIE DE LA RÉPUBLIQUE SOCIALISTE DE ROUMANIE

vegyület

R

REVUE ROUMAINE DE CHIMIE

TOME 28

N° 6

Juin 1983

EDITURA ACADEMIEI REPUBLICII SOCIALISTE ROMÂNIA

Rev. Roumaine Chim.

RRCHAX, 28, 6, p. 553–666, (1983) Bucarest

ACADÉMIE DE LA RÉPUBLIQUE SOCIALISTE DE ROUMANIE

COMITÉ DE RÉDACTION

Rédacteur en chef:

I. G. MURGULESCU, membre de l'Académie de la République Socialiste de Roumanie

Rédacteurs en chef adjoints:

A. T. BALABAN et V. EM. SAHINI, membres correspondants de l'Académie de la République Socialiste de Roumanie

Collège de rédaction:

EM. BRATU, ELENA CEAUŞESCU, ECATERINA CIORĂNESCU-NENITZESCU, CR. SIMIONESCU, membres de l'Académie de la République Socialiste de Roumanie; P. SPACU membre corrspondant de l'Académie de la République Socialiste de Roumanie; MARGARETA AVRAM, M. BANCIU, I. HAIDUC,D. I. MARCHIDAN, I. MOLDOVAN, G. NIAC et D. SĂNDULESCU

La Revue Roumaine de Chimie paraît 10 fois par an. Toute commande de l'étranger pour les travaux parus aux Editions de l'Académie de la République Socialiste de Roumanie sera adressée à ILEXIM, — Departamentul Export-Import Carte (Livres)/Departamentul Export-Import Presă (Revues), P.O.B. 136—137, télex 11226, 3, str. 13 Decembrie, 79517 Bucarest, Roumanie.

Les manuscrits, les livres et les revues proposés en échange, ainsi que toute correspondance seront envoyés à la rédaction :

REVUE ROUMAINE DE CHIMIE

Calea Victoriei 125, 79717 Bucarest, Roumanie, téléphone 50 76 80

EDITURA ACADEMIEI REPUBLICII SOCIALISTE ROMÂNIA
125, Calea Victoriei 79717 Bucarest, Roumanie, téléphone 50 76 80

REVUE ROUMAINE DE CHIMIE

Tome 28, N° 6 **Juin, 1983**

MARIANA CIUREANU, FELICIA CORNEA, VICTOR SAHINI and CORNELIA CERCASOV, Studies on the electronic spectra of thioacylpiperidides and -morpholides . . . . 555–564 R

S. STERNBERG, VALERIA PETRESCU, T. VIȘAN and ADINA COTÂRȚĂ, Electrochemical reaction of Cu^{2+} and Cu^{+} in the LiCl–KCl eutectic. I. Galvanostatic study 565–573

AL. CECAL, The use of beta-ray backscattering in the study of the corrosion kinetics of steel samples in acid media . . . . 575–582 Bc

S. STERNBERG, V. BRÂNZOI, LILIANA APĂTEANU and A. MATEESCU, Behaviour at polarization of lead and lead-antimony alloys in sulphuric acid solutions . . . . 583–592 R

M. M. GIRGIS, D. P. LAZĂR and E. I. SEGAL, Catalytic oxidation of ammonia. VI. Low temperature oxidation on a NiO catalyst . . . . 593–596 C

JACEK A. SZYMURA, Determination of metal dispersion of Pd/SiO_2 catalysts by a combination of transmission electron microscopy with X-ray diffraction and chemisorption methods . . . . 597–603 C

RODICA MICU-SEMENIUC, SIMONA POPȘE and IONEL HAIDUC, Some novel salts and ligand properties of the cyclic $P_2S_8^{2-}$ anion 605–614

LUMINIȚA PĂUNESCU, Molecular complexes of safranine O (in French) . . . 615–621

A. A. HAMED, A. ESSAWY, A. F. SHABAN and I. A.G. El-KARIM, Some reactions of Michael adducts of α-cyano-β-benzoyl-β-phenyl ethyl acrylate with ketones 623–629

HANS-HORST GLATT, RADU BACALOGLU, SADIG A. SALEH, DAGMAR SZEIBERT and VERONICA SZENAȘI. Synthesis of heterocycles using derivatives of carbonic acid. IV. Kinetics and mechanism of the formation of 5-amino-5-aryl-1,3,4-oxadiazoles from benzoic acid hydrazides and aryl cyanates (in German) 631–639

M. A. HASSAN, M. M. MOHAMED and M. El-BORAI, Base-catalyzed additions to ethyl 7-hydroxycoumarin-3-carboxylate 641–644

REV. ROUMAINE CHIM. **28**, *6*, p. 553–666 (1983), Bucarest

SIMONA SILBERG, Derivatives of 4-aminomethyl-thiazole. I. The synthesis of 2-aryl-4-aminomethyl-thiazoles 645–651

FLORENTINA C. GEORGESCU, E. I. GEORGESCU, E. G. GEORGESCU and I. ZUGRĂVESCU, Pyrimidinium-ylides. V. The reactions of some carbanion-monosubstituted 4-phenylpyrimidinium-ylides with nitromethane (in French) 653–657

M. A. El-HASHASH, G. H. SAYED and M. Y. El-KADY, Studies on the cyclised products of the Stobbe condensation between *p*-bromopropiophenone and diethyl succinate 659–666

Revue Roumaine de Chimie, 28 , 6. 555–564 (1983)

STUDIES ON THE ELECTRONIC SPECTRA OF THIOACYLPIPERIDIDES AND -MORPHOLIDES

MARIANA CIUREANU, FELICIA CORNEA, VICTOR SAHINI and CORNELIA CERCASOV
National Institute of Chemistry, The Polytechnic Institute of Bucharest,
Bucharest, Bd. Republicii 13, Romania

Received April 22, 1982

The ultraviolet spectra in ethanol and hexane are reported for several classes of thiopiperidides and thiomorpholides. The $n-\pi^*$ and $\pi-\pi^*$ transitions appear at shorter wavelengths than in the corresponding primary thioamides, which can be rationalized in terms of a steric inhibition of the intramolecular resonance. The position of the absorption bands was found to depend on the nature of the aromatic moiety of the molecule ; a bathochromic shift of the absorption maximum of the $(\pi-\pi^*)_1$ transition was observed with increasing conjugation, in the series : phenylthioacetylpiperidide < thiobenzoylpiperidide < thiocinnamoylpiperidide. A similar trend was displayed by the maxima of the corresponding thiomorpholides. This trend, and the influence of the ring substituents in the aromatic moiety of the molecule are discussed in terms of the theoretical results, obtained by the SCF CI procedure.

1. INTRODUCTION

The ultraviolet absorption spectra of thioamides have been the subject of extensive investigation, aiming to establish the influence of the electronic structure, steric constraints and medium effects on the $n-\pi^*$ and $\pi-\pi^*$ transitions.[1-11] The purpose of the present paper is to provide further information on this subject, using the UV absorption spectra of the following compounds :

$Y = CH_2$(I)
a) $X = p-NO_2$
b) $X = m-NO_2$
c) $X = p-Cl$
d) $X = H$
e) $X = p-CH_3\overset{\overset{O}{\|}}{C}NH$
f) $X = o-OH$
g) $X = p-OH$
h) $X = o-OCH_3$
i) $X = p-OCH_3$
j) $X = p-N(CH_3)_2$

$Y = O$(II)
a) $X = p-NO_2$
b) $X = m-NO_2$
c) $X = H$
d) $X = p-CH_3\overset{\overset{O}{\|}}{C}NH$
e) $X = o-OH$
f) $X = o-OCH_3$
g) $X = p-OCH_3$
h) $X = p-|N(CH_3)_2$

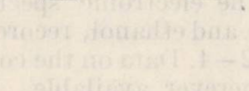

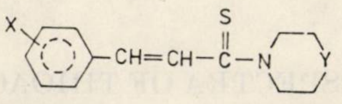

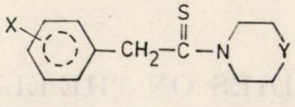

$Y = CH_2$(III)
a) $X = m - NO_2$
b) $X = p - Cl$
c) $X = o - Cl$
d) $X = H$
e) $X = p-CH_3\overset{\overset{O}{\|}}{C}NH$
f) $X = p - OCH_3$
g) $X = o - OCH_3$

$Y = O$(IV)
a) $X = p - NO_2$
b) $X = m - NO_2$
c) $X = p - Cl$
d) $X = o - Cl$
e) $X = H$
f) $X=p-CH_3\overset{\overset{O}{\|}}{C}NH$

$Y = CH_2$(V)
a) $X = p - Cl$
b) $X = p - Br$
c) $X = H$
d) $X = p - CH_3$
e) $X = p-OCH_3$

$Y=O$(VI)
a) $X= m - NO_2$
b) $X = p - Cl$
c) $X = p - Br$
d) $X = H$
e) $X=p-CH_3$

The spectra were also recorded for some of the corresponding primary thioamides.

2. EXPERIMENTAL

The compounds under investigation and some of the related primary thioamides were synthetized and purified as described elsewhere. [12] The identity and purity were checked by chemical analysis, NMR[13] and IR[12] spectra. The ultraviolet spectra were recorded with a Specord UV VIS spectrophotometer. The precision of the wavelength determinations was of ± 1 nm. In order to provide a basis for the interpretation of the spectra, MO calculations were performed using the SCF CI procedure. The first 12 monoexcited singlet configurations were taken into account. The parameters used in the molecular orbital calculations are presented in table 1.

Table 1

Parameter choice for SCF MO calculations

X	I_X(eV)	γ_{XX}(eV)	β(eV)	
$\ddot{N}<$	-28.53	16.57	β_{CN}	-2.32
$\ddot{N}(CH_2)_2<$	-26.50	16.57	β_{CC}	-2.39
$\ddot{O}$	-33.00	20.38	β_{CO}	-2.72
$\dot{O}$	-17.28	15.27	$\beta_{C-C(S)}$	$-1.98\cos\theta$
$\dot{C}$	-11.16	11.14	$\beta_{C=H_2}$	-2.90
$\dot{S}$	-12.86	9.92		
$H_{2(CH_2)}$	-10.25	9.34	β_{N-O}	-2.60
			β_{C-S}	-1.72

As seen from this table, the ionization potential of the thioamide nitrogen was lowered from 28.5 eV to 26.5 eV, in order to account for the presence of the heteroring. The literature data [14,15] were used to provide information on the molecular geometry of the compounds.

3. RESULTS AND DISCUSSION

The electronic spectra of the compounds under investigation in hexane and ethanol, recorded in the 230—700 nm range, are presented in tables 2—4. Data on the corresponding primary thioamides are also presented, wherever available.

Table 4

Electronic spectra of the series V — VI 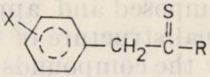

X	Solvent **	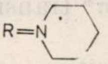				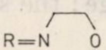				R = NH_2			
		$n \rightarrow \pi^*$		$(\pi \rightarrow \pi^*)_1$		$n \rightarrow \pi^*$		$(\pi \rightarrow \pi^*)_1$		$n \rightarrow \pi^*$		$(\pi \rightarrow \pi^*)_1$	
		λ(nm)	ε	λ(nm)	ε	λ(nm)	ε	λ(nm)	ε	λ(nm)	ε	λ(nm)	ε
m-NO_2	a							275	4.19				
	h							280	4.28				
p-Cl	a			280	4.20			281	4.20	325	2.00	273	4.04
	h			281	4.20			282	4.21	375	2.30	268	4.03
p-Br	a			280	4.19			281	4.21				
	h			281	4.16			282	4.17				
H	a			279	4.21	343*	2.30	280*	4.20	338	2.00	273	4.04
	h	378	2.60	281	4.19			281*	4.17	375	1.60	268	4.03
p-CH_3CONH	a									346	2.00	267	4.05
	h												
p-CH_3	a			279	4.21	345	2.38	279	4.23				
	h			281	4.20			282	4.17				
o-CH_3	a									330	2.00	268	4.06
	h									373	2.00	268	4.06

* Literature data [8-11]

** Solvent : a) ethanol h) heptane c) carbon tetrachloride

An inspection of the data presented in tables 2—4 reveals the existence of one weak band (which generally extends into the visible part of the spectrum) and of one or more strong bands at shorter wavelengths. Based on the low intensity and the important solvatochromic shifts, the first band was assigned to an $n-\pi^*$ transition; for the compounds of the series III—IV (thiocinnamoylpiperidides and -morpholides) this band submerges the strong band at shorter wavelengths, or appears as a shoulder of the latter.

The remaining bands were assigned to $\pi-\pi^*$ transitions, on account of the large intensity and small solvatochromic shifts. For the compounds of the series I—II (thiobenzoylpiperidides and -morpholides) two such bands exist in the region under investigation; a third band was observed in several cases in the region 220 nm or below. The spectra in hexane showed a vibrational structure of the second $\pi-\pi^*$ transition; this structure dissapeared when the spectra were recorded in ethanol.

For the compounds of the series III—IV, there are generally three $\pi-\pi^*$ bands in the investigated spectral range ; the first two bands are sometimes superimposed and appear as a single, broad, unsymmetrical band. The vibrational structure of these bands makes often the assignment very difficult. For the compounds of the series V—VI (phenythioacetylpiperidides and -morpholides) only one $\pi-\pi^*$ transition was observed in the investigated spectral range ; the second $\pi-\pi^*$ transition apears at 220 nm or below.

The assignment of the $\pi-\pi^*$ transitions was made using the theoretical results obtained from SCF MO calculations. Table 5 presents the data obtained in several typical cases, as compared with the experimental results.

Table 5

Experimental and calculated electronic spectra

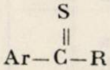

$$\mathrm{Ar-}\overset{\overset{\displaystyle S}{\|}}{C}\mathrm{-R}$$

Ar	λ_{exp} (in hexane) (nm)		λ^*_{calc} (nm)	Assignment of the excited singlet states**
	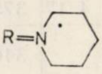	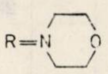		
C_6H_5-	292	291	276	$\Phi_1 = 0.9711\ \Psi_{m,m+1}$
	252	249	232	$\Phi_2 = 0.9269\ \Psi_{m-2,m+1}$
p-$NO_2-C_6H_4$	326	320	337	$\Phi_1 = 0.9439\ \Psi_{m,m+1}$
	259	259	274	$\Phi_2 = 0.9325\ \Psi_{m-3,m+1}$
			254	$\Phi_3 = 0.9598\ \Psi_{m,m+2}$
p-$OCH_3C_6H_4$	283	282	292	$\Phi_1 = 0.9354\ \Psi_{m,m+1}$
			257	$\Phi_2 = 0.3674\ \Psi_{m-2,m+1}-$ $-\ 0.5484\ \Psi_{m-2,m+1}-$ $-\ 0.4217\ \Psi_{m-1,m+1} - 0.4592\ \Psi_{m,m+2}$
	256	255	248	$\Phi_3 = 0.5030\ \Psi_{m-1,m+1} +$ $+\ 0.6983\ \Psi_{m-2,m+1} + 0.3150\ \Psi_{m,m+1}$
$C_3H_5-CH=CH-$	295	297	310	$\Phi_1 = 0.9257\ \Psi_{m,m+1}$
	284	287	267	$\Phi_2 = 0.8720\ \Psi_{m-1,m+1} + 0.3192\ \Psi_{m,m+2}$
	244	244	230	$\Phi_3 = -0.3696\ \Psi_{m-1,m+1} -$ $-\ 0.3084\ \Psi_{m-1,m+2} + 0.8306\ \Psi_{m,m+2}$
$C_6H_5-CH_2-$	279	280	271	$\Phi_1 = 0.9770\ \Psi_{m,m+1}$
			236	$\Phi_2 = 0.3290\ \Psi_{m,m+2} + 0.8716_{m-1,m+1}$

---

* Only those transitions were listed for which the square of the transition moment exceeds 0.1

** The wave functions of the excited singlet states (Φ) were numbered in the order of their increasing energy ; only those configuration were included for which the coefficient is larger than 0.3.

As seen from table 5, the first singlet state contains an overwhelming contribution from a configuration $\Psi_{m,m+1}$, which arises by an electron promotion from the highest occupied MO(φ_m) to the lowest empty one (φ_{m+1}). This transition produces important changes of the π-electron densities in the molecule. Figure 1 presents the electron densities in the ground and first singlet state (Φ_1). It may be seen that there is an electron transfer from the sulphur atom to the aromatic ring. This charge transfer (CT) character of the transition should be made responsible for the blue shift observed when the solvent is changed from an inert to a hydroxylic one; the negative solvatochromic shift is in agreement with Sandstrom's predictions for a CT transition, which lowers the charge density on the sulphur atom.[1,4]

The remaining $\pi-\pi^*$ transitions are benzenoid bands.

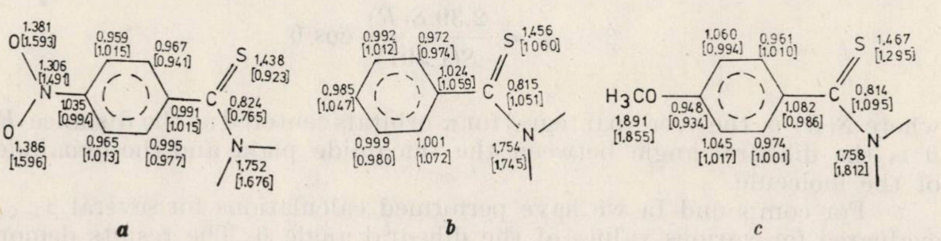
O 1.381 [1.593]
N 1.306 [1.491]
O 1.386 [1.596]
1.035 [0.994]
0.959 [1.015]
0.967 [0.941]
0.991 [1.015]
0.965 [1.013]
0.995 [0.977]
C 0.824 [0.765]
S 1.438 [0.923]
N 1.752 [1.676]
a
0.992 [1.012]
0.972 [0.974]
1.024 [1.059]
0.985 [1.047]
0.999 [0.980]
1.001 [1.072]
S 1.456 [1060]
C 0.815 [1.051]
N 1.754 [1.745]
b
H3CO 1.891 [1.855]
1.060 [0.994]
0.961 [1.010]
0.948 [0.934]
1.082 [0.986]
1.045 [1.017]
0.974 [1.001]
S 1.467 [1.295]
C 0.814 [1.095]
N 1.758 [1.812]
c

Fig. 1. – Charge densities in the ground and first singlet state (in brackets). a) compound 1a; b) compound 1d; c) compound 1i.

Certain generalizations emerge from the results presented in tables 2–4:

3.1. Effect of conjugation

A comparison of the data presented in tables 2–4 reveals a dependence of the maxima of the n–π^* and $\pi-\pi^*$ transitions on the nature of the radical attached to the thioamide group. The following trend was noted for these maxima:
phenylthioacetylpiperidide < thiobenzoylpiperidide < thiocinnamoylpiperidide.
A similar trend was noted for the corresponding series of primary amides or thiomorpholides.

A comparison of the position of the $(\pi-\pi^*)_1$ band in the investigated series of compounds reveals the role of the conjugation between the aromatic ring and the thiocarbonyl group: the shift of this band from 278 nm in thioacetylmorpholide to 287 nm in thiobenzoylmorpholide shows that an increase of conjugation produces a bathocromic shift of this transition. The bathochromic shift is even larger for thiocinnamoylmorpholide, where the aromatic moiety of the molecule is a radical with an extended conjugated system; on the contrary, if the conjugation between the thiocarbonyl group and the benzene ring is prevented by a CH_2 group, the band shifts to blue (273 nm for VId). Our conclusions are supported by the results of SCF CI calculations, as presented in table 5 for several typical examples.

3.2. Effect of the thioamide nitrogen substitution

As seen from tables 2—4, for the series I—IV, both $n-\pi^*$ and $(\pi-\pi^*)_1$ transitions appear at shorter wavelengths than for the corresponding primary thioamides. The hypsochromic shift caused by bulky substituents on the thioamide nitrogen is in agreement with the data reported by other authors: Sandstrom demonstrated that in N,N-dialkylthioamides this shift can be ascribed to a steric inhibition of conjugation;[4] This author concluded, on the basis of theoretical considerations, that steric constraints should prevent a planar configuration, so that the thioamide group and the remainder of the molecule should rotate with respect to each other.

In order to account for this non-planarity of the molecule, we have performed SCF CI calculations using a $\beta_{C-C(S)}$ value evaluated according to the formula:

$$\beta_{C-C(S)} = \frac{2.39\, S(R)}{S(1.397)} \cos\theta$$

where $S(R)$ is the overlap integral for π-orbitals centered at the distance R; θ is the dihedral angle between the thioamide plane and the remainder of the molecule.

For compound Ia we have performed calculations for several $\beta_{C-C(S)}$ evaluated for various values of the dihedral angle θ. The results demonstrated the sensitivity of the first $\pi-\pi^*$ transition to steric constraints: a change in θ from 40° to 25° produced a shift of the band from 276 nm to 286 nm; this shift is about the same as that produced by the replacement of the primary thioamide by a thiomorpholide or a thiopiperidide group.

It should be noted that the hypsochromic shift of the $n-\pi$ and $(\pi-\pi)^*_1$ transitions due to nitrogen substitution is larger for the compounds of the series III—IV than for the series I—II. It may be inferred that steric constraints are larger for the series III—IV, so that a smaller $\beta_{C-C(S)}$ value should be used; the value employed to get the data presented in table 5 is consistent with a torsional angle $\theta=53°$. This value of the angle cannot be checked up, since there are no X ray data on the molecular geometry of these compounds*.

For the series V—VI, there are little or no differences between the spectra of primary and tertiary thioamides. This observation was interpreted in terms of an absence of steric interferences for the compounds of these series.

3.3. Effect of the aromatic ring substitution

An inspection of the data presented in table 4 reveals that the introduction of substituents in the aromatic ring has little or no effect on the position of the $n-\pi^*$ and $\pi-\pi^*$ transitions for the compounds of the series

---

* The value of θ used in our calculations is consistent with the results obtained from ESR data on the anion radicals of compounds III — IV-a.[16] The overall fit of the experimental and calculated hfs was obtained using a $\beta_{C-C(S)}$ value corresponding to an angle of rotation of 60°.

V—VI. This observation can be rationalized in terms of the inhibition of conjugation between the thiocarbonyl group and the aromatic system due to the presence of the methylene group.

For the compounds of the series I—VI, the introduction of an electron-withdrawing substituent in the *para* position of the aromatic ring produces a bathochromic shift of both $n-\pi^*$ and $(\pi-\pi^*)_1$ transitions. The theoretical results account well for the latter effect, as seen from the example presented in table 5 (compound Ia). The introduction of electron-donating substituents should be expected to produce a smaller shift of the $(\pi-\pi^*)_1$ band, also directed to red; this red shift was actually observed for the compounds of the series III—IV (Table 3). For the series I—II it may be observed that a strong electron-releasing substituent such as $N(CH_3)_2$ produces a bathochromic effect, whereas the OH and OCH_3 substituents produce hypsochromic shifts, in disagreement with the theoretical predictions; however, since the theoretical results predicted for the compounds Ig, i.e. the existence of two $\pi-\pi^*$ transitions in the 260—300 nm spectral range, it could be suggested that the observed absorption arises by the overlap of two bands.

A comparison of the spectra of the *ortho*-hydroxy and *ortho*-methoxy derivatives in the series I—II reveals that the $n-\pi^*$ band appears at shorter wavelengths for the former, in agreement with the existence of an intramolecular hydrogen bond (OH ... S).[17] However, this shift is rather small, so that it may be inferred that the hydrogen bond is not very strong and that *o*-hydroxy-derivatives are still twisted around the C—C(S) bond. A similar conclusion was obtained by Berg in the series of N, N-dimethylthiobenzamides. [3] The first $\pi-\pi^*$ transition appears at longer wavelengths in the *ortho*-hydroxy derivatives, as compared with the corresponding *ortho*-methoxy compounds; this is consistent with a decrease of the angle θ owing to hydrogen bond formation.

A comparison of the *ortho* and *para*-methoxy derivatives in the series I—II reveals a larger wavelength for the first $\pi-\pi^*$ transition in the former; this is a rather surprising result, since in the *ortho*-derivatives the steric constraints are larger, so that an inhibition of conjugation would be expected. [18] There are two possibilities to account for this observation: a) the observed band in methoxy-derivatives arises from two overlapping transitions (as discussed before), so that a comparison of the spectra of the two isomers is irrelevant; the steric constraints are able to produce important changes in other molecular parameters besides the torsional angle θ.

REFERENCES

[1] W. Walter and J. Voss, in "The Chemistry of Amides" ed. J. Zabicki, Interscience, London, 1970., p. 283.
[2] S. Sandstrom, *Acta Chem. Scand.*, **16,** 1616 (1962).
[3] U. Berg. *Acta Chem. Scand. B*, **30,** 695 (1976).
[4] B. Persson and J. Sandstrom, *Acta Chem. Scand.*, **18,** 1059 (1964).
[5] G. Kjellin and J. Sandstrom, *Acta Chem. Scand.*, **27**, 209 (1973),
[6] M. Hirota and K. Todokoro, *Chem. Letters*, **1974,** 777.
[7] M. Jansen, *Rec. Trav. chim.* **79,** 454, 1066 (1960).
[8] C. Cercasov, Thesis. Bucharest, 1975.

[9] G. Pappalardo, B. Tornetta, P. Condorelli and A. Bernadini, *Il Farmaco Ed. Sci.*, **22,** 808 (1867).
[10] R. Guepet, P. Piganiol, A. Carayon-Gentil and P. Chabrier, *Bull. Soc. chim. France*, **1965,** 224.
[11] G. Montando and G. Purello, *Ann. Chim.* (*Ital*), **51,** 1361 (1961) ; *ibid.*, **52,** 885 (1962).
[12] F. Cornea, C. Cercasov and M. Ciureanu, *Spectrochim. Acta*, 36A, 775 (1980).
[13] M. Ciureanu, F. Cornea, C. Cercasov and M. Contineanu, *Rev. Chim.* (Bucureşti), **32,** 861 (1981).
[14] J. Voss and W. Walter, *Liebigs Ann. Chem.*, **734,** 1 (1970).
[15] M.A.M. Meester and H. Schenk, *Rec. Trav. chim.*, **90,** 508 (1971).
[16] C. Cercasov, M. Ciureanu, F. Cornea, M. Hillebrand, V. E. Sahini and E. Volanschi, *Org. Magn, Reson.*, 20, 217 (1982).
[17] P. J. Krueger, A. O. Fulea, C. Fulea and F. Cornea, *Spectroscopy Letters*, **8,** 141 (1975).
[18] G. A. Baraniki, G. Derdall and J. T. Edward, *Canad. J. Spectr.*, **18,** 160 (1973).

Revue Roumaine de Chimie, 28, 6, 565–573 (1983)

ELECTROCHEMICAL REACTION OF Cu^{2+} AND Cu^{+} IN THE LiCl – KCl EUTECTIC. I.

GALVANOSTATIC STUDY

S. STERNBERG*, VALERIA PETRESCU*, T. VIŞAN* and ADINA COTÂRŢĂ**
* Physical Chemistry and Electrochemical Technology Department, The Polytechnic Institute, Calea Griviţei 132, Bucharest, Romania
** Institute of Chemical and Biochemical Energetics, ICECHIM, Bucharest, Romania

Received February 26, 1982

A study was carried out on the cathodic process of reducing Cu^{2+} and the anodic process of oxidizing Cu^{+} in varied concentrations of molten LiCl–KCl eutectic in $CuCl_2$ and CuCl. The cathodic reduction took place in two steps : $Cu^{2+} + e = Cu^{+}$ and $Cu^{+} + e = Cu$. The study of the anodic oxidation of Cu^{+} to Cu^{2+} showed that : —at relatively low Cu^{+} and Cu^{2+} concentrations, the $Cu^{+} - e = Cu^{2+}$ process overlaps the discharge of gaseous chlorine ;

— at higher concentrations, the two reactions are clearly separate, the presence of copper ions increasing the chlorine discharge overvoltage, which appears at more positive potentials.

INTRODUCTION

Information in the specialty literature concerning the electrochemical oxido-reduction reaction :

$$Cu^{2+} + e \rightleftarrows Cu^{+} \qquad (1)$$

generally refers to very dilute copper chloride solutions dissolved in the molten LiCl–KCl eutectic.[1–3]

Several of our previous investigations carried out by the cyclic voltametry method, also showed that in such dilute solutions superposal of the anodic oxidation peaks takes place in reactions (2) and (3) :

$$Cu^{+} - e \rightarrow Cu^{2+} \qquad (2)$$

$$Cl^{-} - e \rightarrow 1/2\ Cl_2 \qquad (3)$$

whereas during the cathodic process, apart from the reduction reaction in the homogenous phase :

$$Cu^{2+} + e \rightarrow Cu^{+} \qquad (4)$$

the following reaction may occur:

$$Cu^+ + e \rightarrow Cu \tag{5}$$

For further complete information regarding these reactions, in the present study we extended the concentration range far beyond the concentrations commonly used in chronopotentiometry. The concentrations used are given in table 1. Table 1 shows the $CuCl_2$ and CuCl concentrations dissolved in the LiCl—KCl eutectic. The actual concentrations are also influenced by the disproportionating reaction:

Table 1

The used molten systems LiCl—KCl—$CuCl_2$—CuCl

System	$c_{CuCl_2} \cdot 10^5$ mol/cm^3	$c_{CuCl} \cdot 10^5$ mol/cm^3	Electrode
1	4.59	4.15	Pt
2	9.18	8.3	Pt
3	13.75	12.48	Pt
4	18.37	16.6	Pt
5	27.55	24.9	Pt
6	125.9	113.9	C
7	—	240.5	C
8	234.9	—	C

$$CuCl_2 \rightarrow CuCl + 1/2\, Cl_2 \tag{6}$$

which certainly appears in molten electrolyte.

EXPERIMENTAL

The device used is of classical galvanostatic type (power supply), a cell connected in series with a high ohmic resistance and time-based x—y recorder) as described in the previous papers.[4]

The electrolysis cell is looking like that used by Lantelme et al. [3] The working electrode, for systems 1 — 5 in table 1, was a platinum plate with a 0.3 cm^2 surface area and for systems 6—8 a spectral carbon rod with a 1.75 cm^2 surface. The counter electrode was a carbon rod and the reference electrode consisted of an Ag wire immersed in a molten LiCl — KCl — AgCl mixture (0.1 M). The working atmosphere in the electrolysis cell was purified, dried nitrogen. The LiCl—KCl eutectic was passed through a CCl_4 current for removing humidity. The temperature was maintained at 450°C, for all determinations.

RESULTS AND DISCUSSION

The "zero" potential of the chronopotentiograms and of the curves $I = f(\eta)$ was considered the redox potential established in the absence of current, for each copper ion concentration in the presence of the working electrode irrespective whether Pt or carbon. Therefore, η is the overvoltage that may be either diffusional or charge transfer. The potential of the investigated electrode with regard to the reference electrode (E) varied between 0.65 and 0.7 V in agreement with the Cu^{2+}/Cu^{+} thermodynamical electrode potential in the molten solvents.[1]

Figures 1 and 2 show several typical chronopotentiograms, obtained on the Pt electrode at cathodic polarization. At 3 mA, below the limit current for the appearance of the transient, the reduction of Cu^{2+} to Cu^{+} occurs at a stationary potential, with a very low overvoltage. As the intensity increases to 4.5 and 7 mA, reaction (4) takes place in a nonstationary regime and cathodic transients, τ_{1c}, appear.

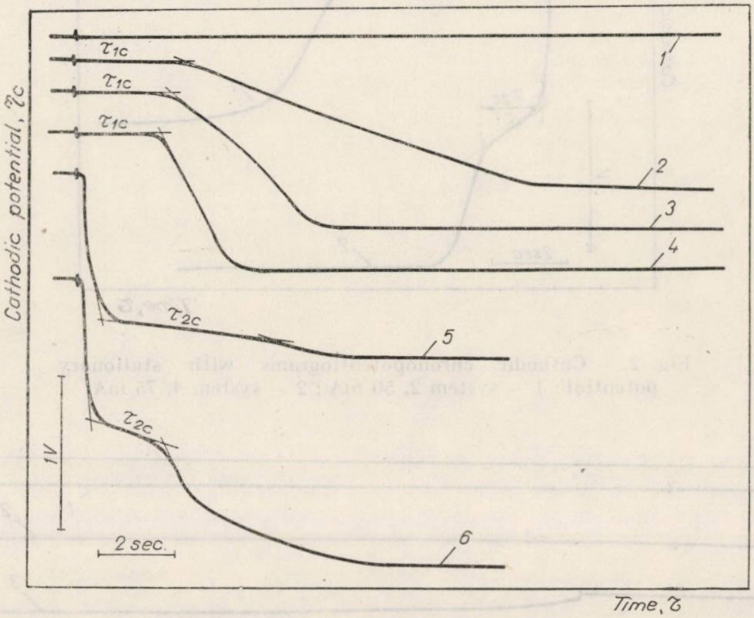

Fig. 1. — Cathodic chronopotentiograms of the system for different current intensities : 1 — 3 mA ; 2 — 4 mA ; 3 — 5 mA ; 4 — 7 mA ; 5 — 15 mA ; 6 — 20 mA.

At potentials of about − 1 V, reaction (5) reducing Cu^{+} to metallic Cu appears. At 20 mA, the transient corresponding to reaction (5), noted τ_{2c}, is evidenced. As τ_{2c} is much greater than τ_{1c}, the two transients cannot, as a rule, be obtained on the same chronopotentiogram.

At a potential of about − 2V the reduction reaction starts

$$Li^{+} + e \rightarrow Li \qquad (7)$$

A similar behaviour was obtained for the other Cu^{+} and Cu^{2+} concentrations. Figure 2 shows the method for the determination of the stationary potential. Several chronopotentiograms, obtained on carbon electrode, at cathodic polarization, are given in figure 3. This figure shows

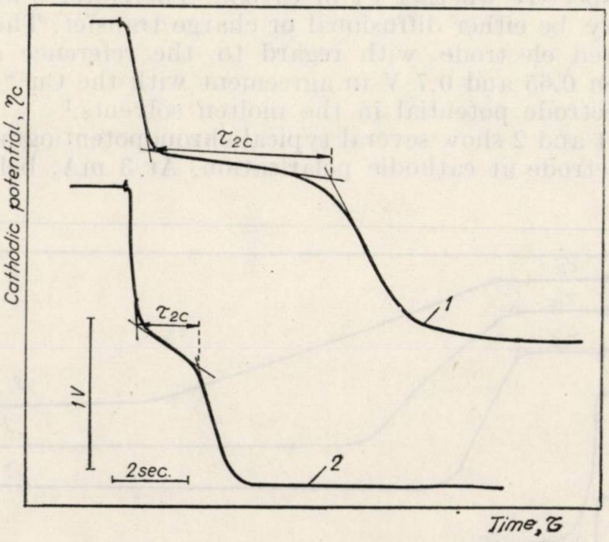

Fig. 2. — Cathodic chronopotentiograms with stationary potential : 1 — system 2, 50 mA ; 2 — system 4, 75 mA.

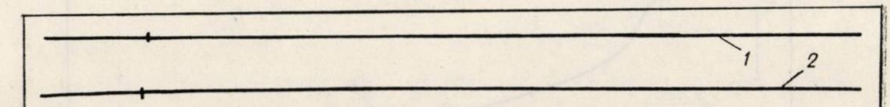

Fig. 3. — Cathodic chronopotentiograms of system 6 for different current intensities : 1 50 mA ; 2 — 125 mA ; 3 200 mA ; 4 — 250 mA ; 5 — 440 mA ; 6 — 550 mA ; 7 — 650 mA ;

that at very high concentrations, reaction (4) develops stationarily up to very high current densites, e.g. 260 mA/cm², and transient τ_{2c} does not appear even at current densities greater than 550 mA/cm².

Figure 4 exemplifies the checking of Sand's equation at a constant concentration (4c):

$$D^{1/2} = \frac{2\,I\,\tau^{1/2}}{n\,F\,\pi^{1/2}\,cS} \tag{8}$$

where D — the diffusion coefficient of the ion, S — the electrode surface; the other magnitudes have their usual meaning.

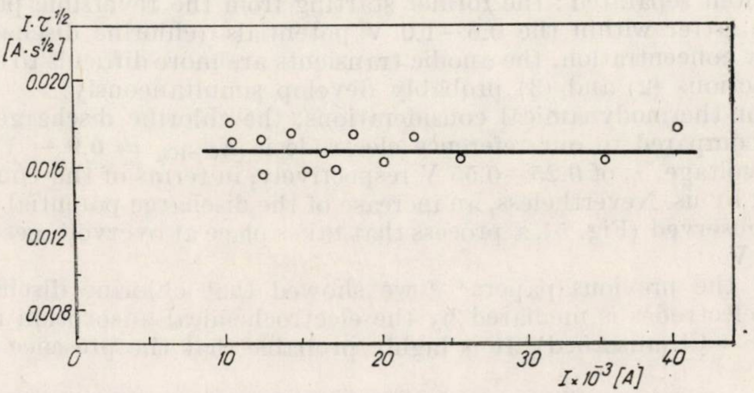

Fig. 4. — Checking Sand's relation for system 4.

Thus, a satisfactory constant of product $\frac{I\tau^{1/2}}{S}$ results on increasing $CuCl_2$ concentration. On the basis of relation (8) the following value is obtained for the diffusion coefficient $D_{Cu^{2+}} = 1.2 \cdot 10^{-5}$ cm²/s.

Owing to the disproportionating reaction, the actual concentrations are only slightly modified, hence this calculation has an orientative character, but the value obtained indicates that reaction (4) is diffusely controlled within a very large range of concentrations both on the Pt and on the carbon electrode.

As concerns the second cathodic transient, τ_{2c}, on the basis of the results obtained in system 1, the following relation can be written:

$$\left(\frac{I\ \tau_{2c}^{1/2}}{I\ \tau_{1c}^{1/2}}\right)^2 = \frac{(0.025)^2}{(0.008)}$$

with which $\tau_{2c}/\tau_{1c} = 10$ is obtained.

The relation proposed by Berzins and Delahay [5] for the two transients of the same chronopotentiogram is:

$$(\tau_1 + \tau_2)^{1/2} - \tau_1^{1/2} = \frac{\pi^{1/2}\,n_2 F\,D_2^{1/2}\,c_2 S}{2\,I} \tag{9}$$

where n_1 and n_2 are the number of electrons in the first and the second chemical reaction respectively, and D_2 is the diffusion coefficient of the ion taking part in the second reaction. In our case $n_1 = n_2 = 1$.

If it is assumed that $D_{Cu^{2+}} = D_{Cu^+}$, then $\tau_{2c}/\tau_{1c} = 3$. It is however, more likely that in the ionic mono-monovalent LiCl–KCl solvent, the two diffusion coefficients differ, i.e. $D_{Cu^{2+}} < D_{Cu^+}$. If it is admitted that $D_{Cu^+} = 2D_{Cu^{2+}}$, then a value of about 4.8 is obtained for ratio τ_{2c}/τ_{1c}. The almost twofold value, obtained experimentally, can be explained by increase of the actual surface following the deposition of metallic copper on the platinum support electrode.

Figure 5 shows several anodic chronopotentiograms (system 7). It is obvious that, at high CuCl concentrations, the two reactions (2) and (3) appear well separated; the former starting from the reversible potential, and the latter within the 0.6–1.0 V potentials (chlorine discharge). At very low concentration, the anodic transients are more difficult to evidence and reactions (2) and (3) probably develop simultaneously.

For thermodynamical considerations, the chlorine discharge potential as compared to our reference electrode is $E_{Cl^-/Cl_2} = 0.9 - 1.0$ V, at an overvoltage, η, of 0.25–0.55 V respectively, in terms of the convention adopted by us. Nevertheless, an increase of the discharge potential of chlorine is observed (Fig. 5), a process that takes place at overvoltages exceeding 0.7 V.

In the previous papers [6–8] we showed that chlorine discharge on carbon electrodes is mediated by the electrochemical adsorption reaction $Cl^- - e \rightarrow Cl$ (adsorbed). It is highly probable that the presence of Cu^{2+}

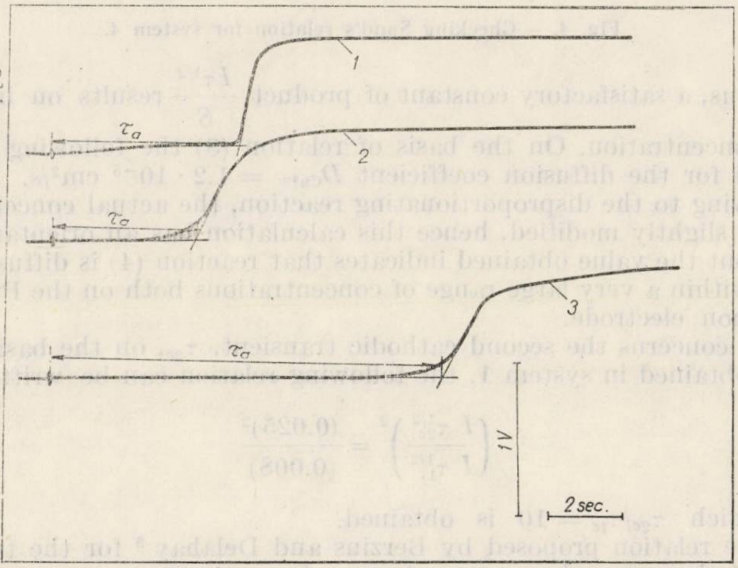

Fig. 5. — Anodic chronopotentiograms of system 7 for different current intensities : 1 — system 5, 100 mA ; 2 — system 5, 200 mA ; 3 — system 7, 600 mA.

and Cu^+ may compete with Cl^- in the adsorption process, which would explain the appearance of a high overvoltage in the discharge of Cl^- in the $LiCl-KCl-CuCl_2-CuCl$ electrolyte.

From the anodic transients obtained for system 7 in table 1, a diffusion coefficient $D_{Cu^+} = 2.3\ 10^{-5}$ cm²/s results, in satisfactory agreement with that obtained by Lantelme et al.;[3] this value is twice the diffusion coefficient $D_{Cu^{2+}}$ calculated by the cathodic method.

The conclusions drawn on the basis of the chronopotentiograms are also confirmed by interpretation of the polarization curves, determined in a galvanostatic stationary regime. The curves of cathodic polarization in the domain of low concentrations are given in figure 6. Two limit currents can be observed on the curves, corresponding to the two cathodic reactions (4) and (5). On anodic polarization, in systems with low CuCl and $CuCl_2$ concentrations, no net limit current can be detected; it is highly probable that, within this concentration range, reactions (2) and (3) occur simultaneously, the concentration of Cu^+ ions being much lower than that of the solvent Cl^- ions.

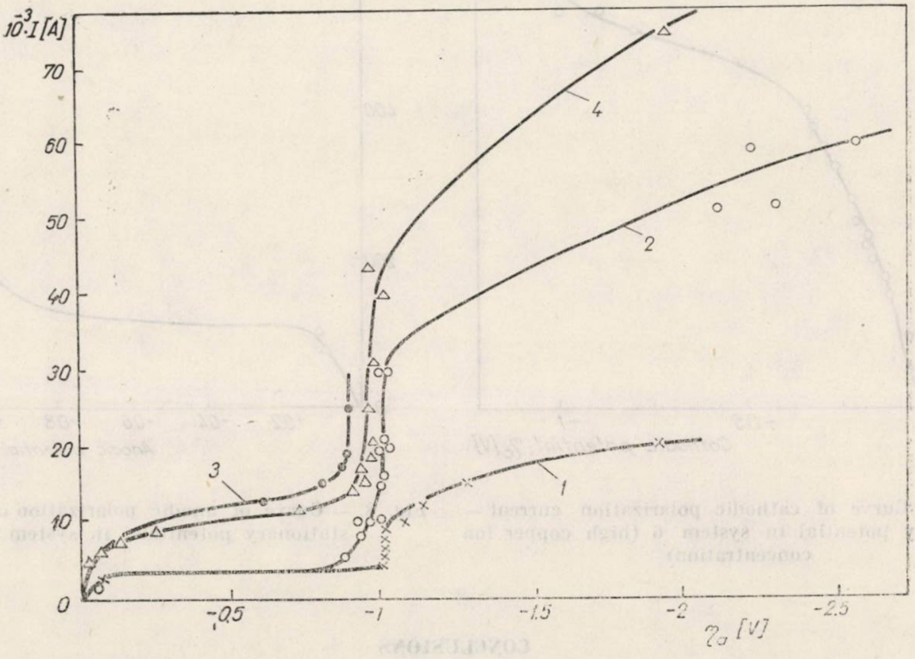

Fig. 6. — Curves of cathodic polarization current — stationary potential of system 1 — 4: 1 — system 1; 2 — system 2; 3 — system 5; 4 — system 4.

From the data in figure 7 it may be seen that within the sphere of high copper concentrations (system 6), the cathodic reaction (4) takes place within a large range of current densities, the limit current being about 500 mA, i.e. about 300 mA/cm².

Figure 8 shows the anodic polarization curves for system 7. The existence of a limit current for reaction (2) is noticed, as well as the same increase of the chlorine discharge overvoltage (reaction 3) by about 0.7V, an increase also observed on chronopotentiograms.

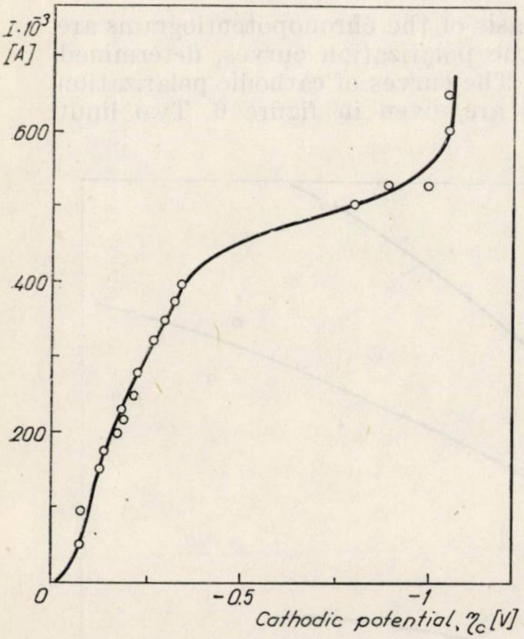

Fig. 7.—Curve of cathodic polarization current—stationary potential in system 6 (high copper ion concentration)

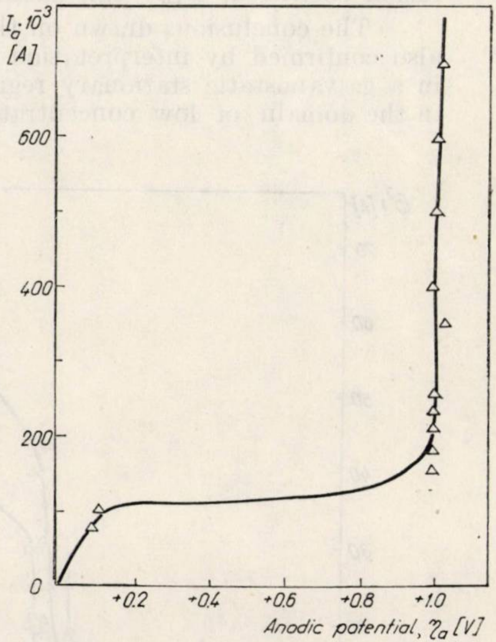

Fig. 8. — Curve of anodic polarization current—stationary potentials, in system 7.

CONCLUSIONS

It was demonstrated that the cathodic process for reducing Cu^{2+} in the molten LiCl-KCl eutectic takes place in two steps: the reduction of divalent copper to monovalent copper at reversible redox potential, and the reduction of monovalent copper to metallic copper at a potential of about — 1V.

The anodic process of oxidizing Cu^{+} to Cu^{2+} at relatively low Cu^{+} and Cu^{2+} concentrations is superposed over the chlorine discharge process. At higher concentrations, over 0.2 mol/l CuCl, the two processes are clearly separated and the presence of the copper ions increases chlorine discharge overvoltage to more positive values, up to 0.7 V, as compared to its discharge conditions in the LiCl-KCl eutectic solvent.

REFERENCES

[1] B. F. Markov, "Termodinamika rasplavlennyh solevyh smesei" Naukova Dumka, Kiev, 1974.

[2] S. Sternberg and T. Vişan, "Electrochemical Studies of Cu (I) and Cu (II) ions in LiCl–KCl Eutectic" in vol. III, International Conference on Molten Salt Chemistry – Proceedings, Wroclaw- Karpacz, Poland, May 28 – June 1, 1976, p. 299–304.

[3] F. Lantelme, J. P. Hanselin and M. Chemla, *Electrochim. Acta*, **22**, 1113 (1977).

[4] S. Sternberg and C. Herdlicka, *Rev. Roumaine Chim.*, **14**, 991 (1969). T. Vişan, D. Geană and S. Sternberg, *Rev. Roumaine Chim.*, **21**, 1155 (1976).

[5] T. Berzins and P. Delahay, *J. Amer. Chem. Soc.*, **75**, 4205 (1953).

[6] S. Sternberg and I. Galasiu, *Electrochim. Acta*, **22**, 9 (1977).

[7] S. Sternberg and V. Petrescu, *Rev. Roumaine Chim.*, **19**, 25 (1974).

[8] S. Sternberg, V. Petrescu and I. Galasiu, *Rev. Roumaine Chim.*, **17**, 1689 (1972).

Revue Roumaine de Chimie, **28**, *6*, 575–582 (1983)

THE USE OF BETA-RAY BACKSCATTERING IN THE STUDY OF THE CORROSION KINETICS OF STEEL SAMPLES IN ACID MEDIA

AL. CECAL

Faculty of Chemical Technology, The Polytechnic Institute of Iași, Splai Bahlui-71, 6600-Iași
Romania

Received May 9, 1982

The present paper deals with the corrosion kinetics of some types of steel : 21 MoC – 11, C – 120 and AUT – 40 in acid media, under several experimental conditions, using a method based on the beta-ray backscattering. The values of the rate constant as well as those of the apparent activation energy were calculated. The experimental data have shown that the corrosion process depends on the chemical composition of the steel samples under study, on temperature and on the nature and concentration of the aggressive medium. For a certain acid medium, the corrosion reaction rate is situated as follows : AUT – 40 > C – 120 > 21 MoC – 11 and for a given type of steel, the same rate is higher in hydrochloric acid and slower in sulphuric and nitric acids.

INTRODUCTION

The use of radioactive tracers in the study of the metallic corrosion under several experimental conditions, has been investigated in the literature. Thus, several monographs and detailed studies [1–4] on the use of radioisotopes, with a view to following the process of corrosion and passivation of metallic surfaces in the presence of either certain aggressive agents or corrosion inhibitors, are reported.

Frasca et al. [5] followed the corrosion of some aluminium bars in different corrosive media, using a method based on the beta-ray backscattering. Miwa and co-workers [6] made an experimental device, based on the absorption of beta rays, to study the thickness of zinc deposited on steel, in order to passivate the latter.

Subramayan at al. [7] investigated the effect of radioactive chromate on the corrosion of mild steel in natrium chloride, while Kuchynka [8] used radioactive tracers to establish the role of sulphur dioxide from the atmosphere, on the corrosion of some steel samples, or to clear up the mechanism of galvanic plating of the metals in electrolytic cells. Kiss and co-workers [9] used techniques based on radioactive tracers, with a view to following, permanently, the development of the corrosion process of some metals and to establish the amount of oxygen absorbed by these metallic samples under several experimental conditions.

Rodin et al. [10] supplied a detailed programme for determining the rate and the dissolving selectivity of certain samples of steel or other alloys, by using the nuclear spectrometry.

This paper is a continuation of some previous studies [11-16] concerning the use of radioisotopes in order to investigate the kinetics of corrosion process of some steel samples, in several aggressive media.

The present paper deals with the kinetics of corrosion reactions of some types of steel, such as : 21 MoC–11, C–120 and AUT–40 in HCl, H_2SO_4 and HNO_3 media, under different experimental conditions, using a technique based on the beta-ray backscattering.

EXPERIMENTAL

Several steel samples of the types : 21 MoC–11, C–120 and AUT–40 were tested. They were bar-shaped and had 1 cm in diameter and 3 cm in height. These samples were ground, washed, cleaned with ethanol and acetone, followed by drying in a desiccator with P_2O_5 under vacuum.

The chemical composition of these three types of steel is presented in table 1.

Table 1

The chemical composition of the steel samples

Sample	C (%)	Mn (%)	Si (%)	S (%)	P (%)	Cr (%)	Mo (%)
21 MoC–11	0.21	1.12	0.28	0.018	0.024	0.90	0.40
C–120	1.96	0.28	0.30	—	—	10.09	—
AUT–40	0.44	1.61	0.26	0.21	0.029	—	—

Amounts of 100 ml of each of the following acid solutions were poured in several Erlenmayer flasks : HCl (2 N, 1 N and 0.5 N), H_2SO_4 (1 N) and HNO_3 (1 N). For each temperature, 3 samples of each of the acid corrosive solution were prepared, since 3 types of steel were taken for study.

In each flask containing aggressive solution, only one steel sample was immersed and from that moment on, the process of steel corrosion practically started.

At certain time intervals, each corrosive solution, containing an immersed steel sample, was transferred in a 150 ml porcelain capsule, which was afterwards placed under the ^{204}Tl beta-source, as shown in Fig. 1.

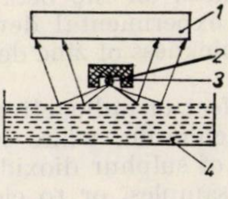

Fig. 1. Experimental device for measuring the activity of beta-ray backscattering : 1. CTC detectors ; 2. lead screen ; 3. ^{204}Tl ; 4. porcelain capsule.

The ^{204}Tl beta-source had a specific activity of 10^6 Bq/g and was obtained from IFIN, Bucharest, as $^{204}TlNO_3$, in solid form.

By means of the three CTC detectors, placed in parallel and connected to a VSP–1960 electronic scalar, the activity of bety-rays emitted by ^{204}Tl and backscattered by the respective solution, was measured. After radioactivity measurement, the solution was again transferred in the respective Erlenmayer flask, so that the corrosion reaction of the steel sample might go on.

The corrosion experiments were carried out at four different temperatures : 293.8, 300.3, 307.5 and 312.9 K.

For each temperature, one could notice that, as the contact time of the steel sample in the aggressive acid solution was longer, the activity of the backscattered rays was implicitly greater, due to the increasing of the concentration of iron ions, in the corrosive solution, after the anodic dissolving of the metallic sample.

Even if the radioisotope ^{204}Tl has a long half-time, for each activity measurement, a correction is however done, taking into account the radioactive decay of this isotope.

RESULTS AND DISCUSSION

The corrosion process of the studied steel samples, may be represented by the reactions : [17–22]

$$Fe \rightarrow Fe^{2+} + 2e^-$$

$$Fe^{2+} \rightarrow Fe^{3+} + e^-$$

namely anodic oxidation of the metallic sample and,

$$3\,H^+ + 3e^- \rightarrow 3/2\,H_2$$

cathodic reduction of the hydrogen ions, with a depolarizing role. The other reactions may be the following :

$$Fe + 2H_2O \rightarrow Fe(OH)_2 + H_2$$

$$Fe^{2+} + H^+ \rightarrow Fe^{3+} + 1/2\,H_2$$

or, in the presence of oxygen :

$$1/2O_2 + H_2O + 2e^- \rightarrow OH^-$$

$$Fe^{2+} + OH^- \rightarrow Fe(OH_2)$$

The reaction of anodic dissolution of the metallic sample may be regarded as a first order reaction [23] ; its integral equation may be represented as follows :

$$\ln \frac{x}{x_0} = kt \tag{1}$$

where x_0 is the initial concentration of the iron ions ($[Fe^{2+}] + [Fe^{3+}]$) in solution and x represents the concentration of the same ions at any instant. Since initially, the concentration $x_0 = 0$, it follows that :

$$\ln x = kt \tag{2}$$

Taking into account that the activity of the backscattered beta-rays is in each and every moment proportional to the concentration of the iron ions in the corrosive solution, as a consequence of the anodic dissolution of the metallic sample immersed in that aggressive medium, that is :

$$R_{(\text{counts/min})} = f([\text{Fe}^{2+}] + [\text{Fe}^{3+}]), \tag{3}$$

it results that :

$$\ln R = kt \tag{4}$$

The graphic plot, ln R *vs.* time, according to relation (4), represents a straight line for any system and from its slope one may calculate the rate constant of the given corrosion reaction of the steel sample in that aggressive medium (k).

The experimental data for the corrosion systems studied, are plotted in Figs 2, 3 and 4.

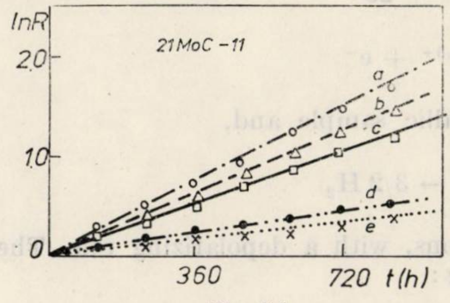

Fig. 2.1

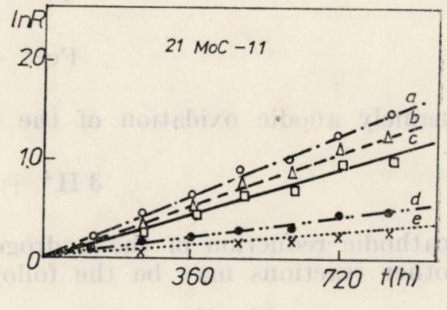

Fig. 2.2

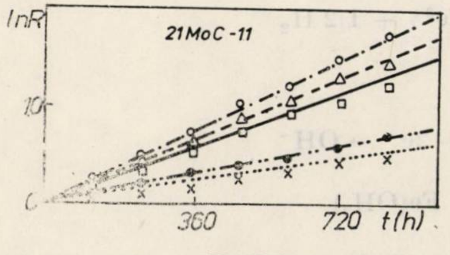

Fig. 2.3

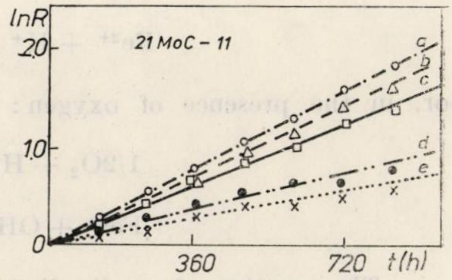

Fig. 2.4

Fig. 2. — 4. Dependence of ln R *vs.* time for the corrosion reactions of the steels :
Fig. 2. — *21 MoC — 11,* by 293.8 K (2—1) ; 300.3 K (2—2) ; 307.5 K (2—3) and 312.9 K (2—4).

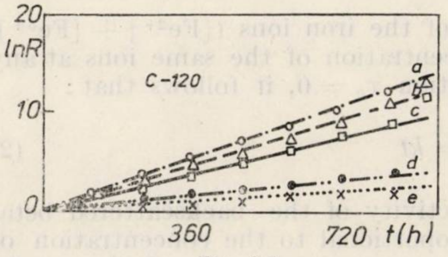

Fig. 3.1

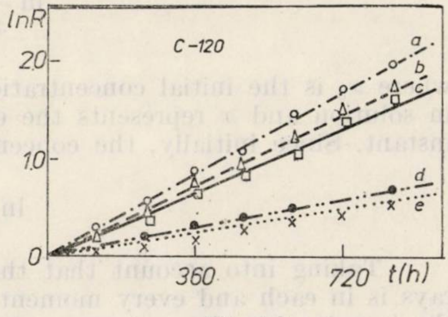

Fig. 3.2

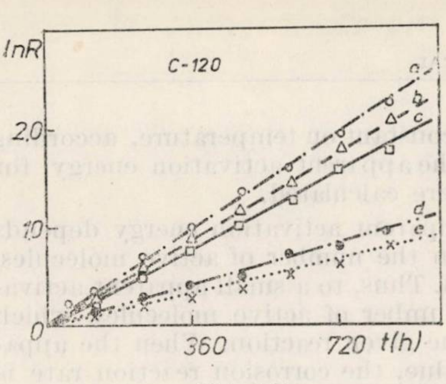

Fig. 3.3

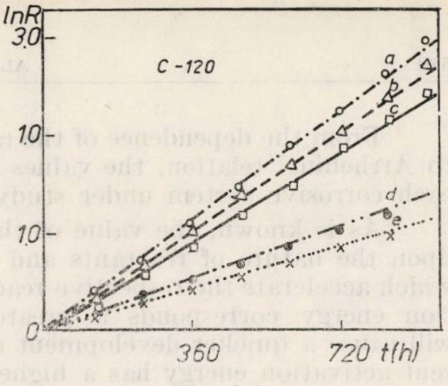

Fig. 3.4

Fig. 3. — *C—120*, by 293.8 K (3—1) ; 300.3 K (3—2) ; 307.5 K (3—3) and 312.9 K (3—4).

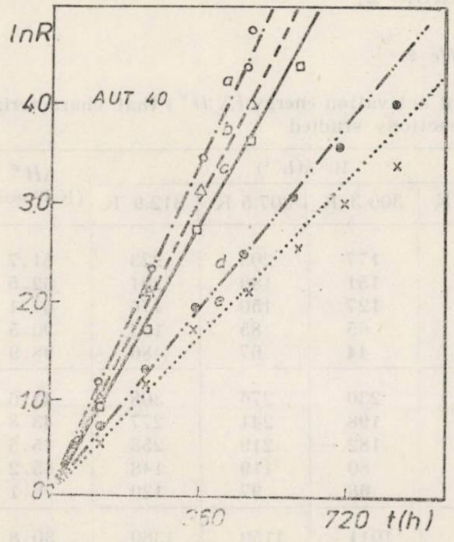

Fig. 4.1

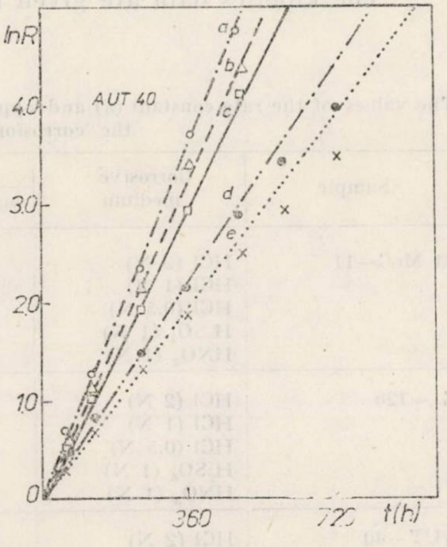

Fig. 4.2

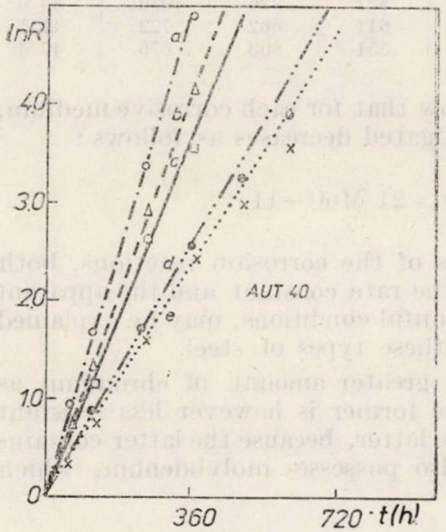

Fig. 4.3

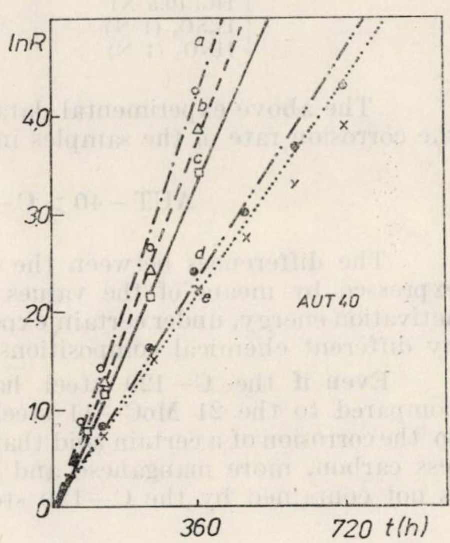

Fig. 4.4

Fig. 4. — *AUT*—40, by 293.8 K (4—1) ; 300.3 K (4—2) ; 307.5 K (4—3) and 312.9 K (4—4). a, b, c, d and e represent the corrosive media : HCl(2N), HCl (1 N), HCl (0.5 N), H_2SO_4 (1 N) and HNO_3 (1 N).

From the dependence of the rate constant on temperature, according to Arrhenius' relation, the values of the apparent activation energy for each corrosive system under study, were calculated.

As is known, the value of the apparent activation energy depends upon the nature of reactants and upon the number of active molecules, which accelerate the respective reaction. Thus, to a small apparent activation energy corresponds a greater number of active molecules, which will cause a quicker development of the given reaction. When the apparent activation energy has a higher value, the corrosion reaction rate is smaller, since in this case there exist in the system fewer active molecules which could favour the development of this reaction.

The kinetics data are given in table 2.

Table 2

The values of the rate constant (*k*) and apparent activation energy ($\Delta H^{\neq}$) that characterize the corrosion reactions studied

Sample	Corrosive medium	$10^5 k(\mathrm{h}^{-1})$				$\Delta H^{\neq}$ (KJ/mol)
		293.8 K	300.3 K	307.5 K	312.9 K	
21 MoC—11	HCl (2 N)	145	177	203	223	61.7
	HCl (1 N)	138	151	180	201	62.5
	HCl (0.5 N)	104	127	150	176	64.1
	H_2SO_4 (1 N)	41	65	85	103	90.5
	HNO_3 (1 N)	28	44	67	80	98.9
C —120	HCl (2 N)	208	230	276	308	41.6
	HCl (1 N)	174	198	241	277	43.8
	HCl (0.5 N)	146	182	219	253	45.5
	H_2SO_4 (1 N)	71	80	119	148	65.2
	HNO_3 (1 N)	51	68	97	120	76.1
AUT—40	HCl (2 N)	933	1011	1150	1380	30.8
	HCl (1 N)	832	905	1046	1155	33.2
	HCl (0.5 N)	765	831	926	1030	36.0
	H_2SO_4 (1 N)	570	611	662	722	42.5
	HNO_3 (1 N)	447	551	603	676	47.4

The above experimental data show that for each corrosive medium, the corrosion rate of the samples investigated decreases as follows :

$$\mathrm{AUT-40} > \mathrm{C-120} > 21\ \mathrm{MoC-11}$$

The differences between the rates of the corrosion reactions, both expressed by means of the values of the rate constant and the apparent activation energy, under certain experimental conditions, may be explained by different chemical compositions of these types of steel.

Even if the C—120 steel has a greater amount of chromium as compared to the 21 MoC—11 steel, the former is however less resistant to the corrosion of a certain acid than the latter, because the latter contains less carbon, more manganese and it also possesses molybdenum, which is not contained by the C—120 steel.

It is known that a reduced amount of carbon, as well as a greater amount of transitional elements (Ni, Cr, V, Mn, Mo, W, etc) confers to the given steel a greater resistance to the corrosive action of a certain aggressive medium.[24–25]

On the other hand, the AUT-40 steel, which contains only manganese and a greater amount of carbon, as compared to the 21 MoC-11 steel, is the least resistant, out of the three types of steels under study, to the action of a given corrosive agent.

For any type of steel, one may notice that the hydrochloric acid has a stronger action than the sulphuric or nitric acids, i.e., the corrosion process rate in these acids is situated as follows:

$$\mathrm{HCl}\ (2\mathrm{N}) > \mathrm{HCl}\ (1\mathrm{N}) > \mathrm{HCl}\ (0.5\mathrm{N}) > \mathrm{H_2SO_4}(1\ \mathrm{N}) > \mathrm{HNO_3}(1\ \mathrm{N})$$

This is explained by the fact that hydrochloric acid, unlike the other two acids,[26–28] does not permit the forming of a protecting layer of oxide or salt on the surface of the metallic sample, under corrosion, because, if these chemical compounds were formed immediately, in the first phase, they would be dissolved in the acid.

In sulphuric acid medium, on the other hand, some hardly soluble compounds may appear on the surface of the steel sample : $Fe_2(OH)_2(SO_4)_2$ or $Fe(OH)_n$. Such compounds have a protecting role, a fact which will slow down the corrosion process, as compared to the first case.

In the presence of nitric acid, corrosion takes place at a lower rate because of the brown layer of iron oxide, deposited on the surface of the metallic sample immersed in this aggressive medium ; this layer has unstoichiometric composition and a greater passivating role than in the previous case. It is also possible that between this oxide layer and the surface of the steel sample, molecules of oxygen deposited by chemosorption will bring about an increase in the thickness of the protecting layer that presents a greater inhibition of the respective corrosion process.

The deviations from the straight line of the points on the respective diagrams corresponding to H_2SO_4 and HNO_3 may be also explained by the growth of these protecting "films" on the metallic surfaces

The above experimental data point out also, that the corrosion reactions of the samples belonging to a certain type of steel, immersed in hydrochloric acid, have different rates, depending on its concentration and temperature. For a greater concentration of HCl, there exist in that system more H^+ ions with an intense depolarizing role (and implicitly a greater number of Cl^- ions able to form iron chloride) ; thus the corrosion process will develop at a higher rate, while a smaller number of H^+ ions, with a less intensive depolarising role, will bring about a slower reaction.

REFERENCES

[1] J. G. N. Thomas, *Werkst. Korr.*, **19**, 957 (1968).
[2] L. A. Medvedeva and I. M. Kolotyrkin, *Zhur. fiz. Khim.*, **31**, 2668 (1957).
[3] K. Schwabe, K. Wagner and C. Weissmantel, *Z. phys. Chem. (Leipzig)*, **206**, 308 (1967).

[4] D. M. Brasher, J. G. Beynon, A. D. Mercer and J. E. Rhoades-Brown, "Proc. 2ème Symp. Européen sur la Inhibiteurs de la Corrosion", 1965, Ferrara, Annali del'Università, 1966.

[5] A. J. Frasca, C. H. Bemisdorfer and C. E. Krause, in "Nucleonics in Aerospace", P. Polishuk ed., Plenum Press Inc., New York, 1968.

[6] H. Miwa, T. Mizukoshi and M. Shimizu, in "Radioisotope Instruments in Industry and Geophysics", Vol. I, IAEA, Vienna, 1966.

[7] N. Subramayan, K. Ramakrishnaiah and S. Iyer Venkatakrishna, *Trans. SAEST* **15**, 317 (1980); *Chem. Abstr.*, **94**, 160718 (1981).

[8] D. Kuchynka, *Strojirenstvi*, **30**, 604 (1980).

[9] L. Kiss, A. I. Molodov, L. M. Varsany, G. N. Markosyan, J. Farkas, V. V. Losev, L. Sziraki and I. A. Safronova, *Zashch. Met.*, **16**, 99 (1980).

[10] N. N. Rodin, O. L. Belov, L. P. Kuznetsov, I. F. Yazikov and V. G. Lambrev, *Vopr. Atom. Nauk. Tekhn. Radiats. Tekhnol.*, **19**, 153 (1980).

[11] Al. Cecal, N. Calu and P. Harabor, *Bull. Soc. chim. France*, **1975**, 176.

[12] Al. Cecal and St. Roșu, *Radiochim., Acta*, **23**, 20 (1976).

[13] Al. Cecal and D. Ciobanu, *Radiochim. Acta*, **28**, 171 (1981).

[14] Al. Cecal, *Isotopenpraxis*, **17**, 328 (1981).

[15] Al. Cecal and V. Stan, *Z. phys. Chem. (Leipzig)*, **263**, 117 (1982).

[16] Al. Cecal and D. Ciobanu, *Radiochem. Radioanal. Letters*, **51**, 9 (1982).

[17] F. Tödt, "Korrosion und Korrosionschutz", Walter de Gruyter, Berlin, 1961.

[18] G. T. Bakhvalov and A. V. Turkovskaya, "Corrosion and Protection of Metals", Pergamon Press, New York, 1965.

[19] N. D. Tomashov, "Theory of Corrosion and Protection of Metals", Mc Millan New York, 1966.

[20] W. Forker, "Elektrochemische Kinetik", Akademie Verlag, Berlin, 1966.

[21] M. Fontana and N. Greene, "Corrosion Engineering", Mc Graw Hill, New York, 1967.

[22] P. Orlowski, "Comment vaincre la Corrosion Métallique", Eyrolles, Paris, 1973.

[23] I. G. Murgulescu, E. Segal and T. Oncescu, "Introducere în Chimia Fizică", Vol. II, 2, Editura Academiei RSR, București, 1981.

[24] J. C. Scully, "The Fundamentals of Corrosion", Pergamon Press, New York, 1966.

[25] L. Oniciu, "Chimie Fizică, Electrochimie", Editura didactică și pedagogică, București, 1977.

[26] U. R. Evans and T. P. Hoar, *J. Electrochem. Soc.*, **99**, 212 (1952).

[27] K. Schwabe, *Electrochim. Acta*, **3**, 663 (1960).

[28] K. C. Tripathi and K. Schwabe, *Rev. Chim. (București)*, **7**, 599 (1962).

Revue Roumaine de Chimie, 28, *6*, 583—592 (1983)

BEHAVIOUR AT POLARIZATION OF LEAD AND LEAD-ANTIMONY ALLOYS IN SULPHURIC ACID SOLUTIONS

S. STERNBERG *), V. BRÂNZOI *), LILIANA APĂTEANU **), and A. MATEESCU***)

*) Dept of Physical Chemistry, The Polytechnic Institute of Bucharest, str. Polizu No. 1, Bucharest, Romania

**) ICECHIM — IECB — Institute of Chemical and Biochemical Energetics, Bucharest, str. Splaiul Independenţei 206, Romania

***) "Acumulatorul" Enterprise, B-dul Biruinţei nr. 98, Bucharest, Romania

Received May 31, 1982

The behaviour of pure lead and lead-antimony at polarization in sulphuric acid solutions of different densities has been studied by potentiodynamic method. The composition of the lead-antimony alloys, the sulphuric acid solution density, the scan rate and the electrode pretreatment effects have been analysed in respect to the formation of the positive electrodes in the lead-acid battery. The experimental results give some information on the formation of the lead oxides and reduction optimums.

INTRODUCTION

The increasing number of the studies referring to the effect of the alloys composition and of some electrolyte [1-10] addition agents on the formation and battery functioning has been determined by the great importance of the lead batteries as power sources.

The present work reports on the electrochemical behaviour of lead and lead-antimony alloys in sulphuric acid solutions of different densities and under different conditions.

The purpose of this work is to give new information on the effect of different factors which could improve the formation and functioning technology of the lead-acid battery.

EXPERIMENTAL

Experiments were carried out by potentiodynamic technique using a RADELKIS potentiostat equipped with an automatic pilot, a microampermeter and an ohmic drop compensator on the cell. Current potential curves were registered by the means of an X—Y recorder. A single compartment glass cell was used to decrease the ohmic resistance, and the working electrode, in the middle of the cell, was surrounded by a platinum gauze as the counterelectrode. This arrangement of the two electrodes created a uniform and intense electric field during the anodic and cathodic polarization.

A Luggin capillary was used to assure the binding between the cell compartment and the reference electrode in order to decrease the ohmic potential drop. The electrochemical cell and the schematical representation of the electronic device were presented in a previous paper[11]. Before each determination the working electrode (lead or lead-antimony and other elementes alloys) was mechanically polished with emery paper of different granulations up to mirror lustre, degreased in benzene, washed with acetone, dried and then immersed in the solution under study. The temperature was maintained constant at 20 ± 0.1 °C.

The electrode was cathodically polarizated for 45 minutes at -2700 mV vs. Hg/Hg_2SO_4 to assure the complete removal of any oxide on the electrode surface and only after that the polarization curves were registered. The polarization curves were obtained starting from potential of -2700 mV and sometimes from $+ 2400$ mV (the latter for the starting from the PbO_2 formation). Many determinations were carried out for each solution till reproducible results were obtained.

All the potentials were measured vs.an Hg/Hg_2SO_4 reference electrode. The potential scan rates were within the 150 — 600 mV/m in range. Sulphuric acid aqueous solutions of different densities were used as basic electrolytes.

RESULTS AND DISCUSSIONS

Figure 1 shows the pure lead polarization curves in 1.05 g/cm³ density sulphuric acid solution, at 600 mV/min potential scan rate. A cycle was obtained by scanning the potential from -2700 mV to $+ 2400$ mV

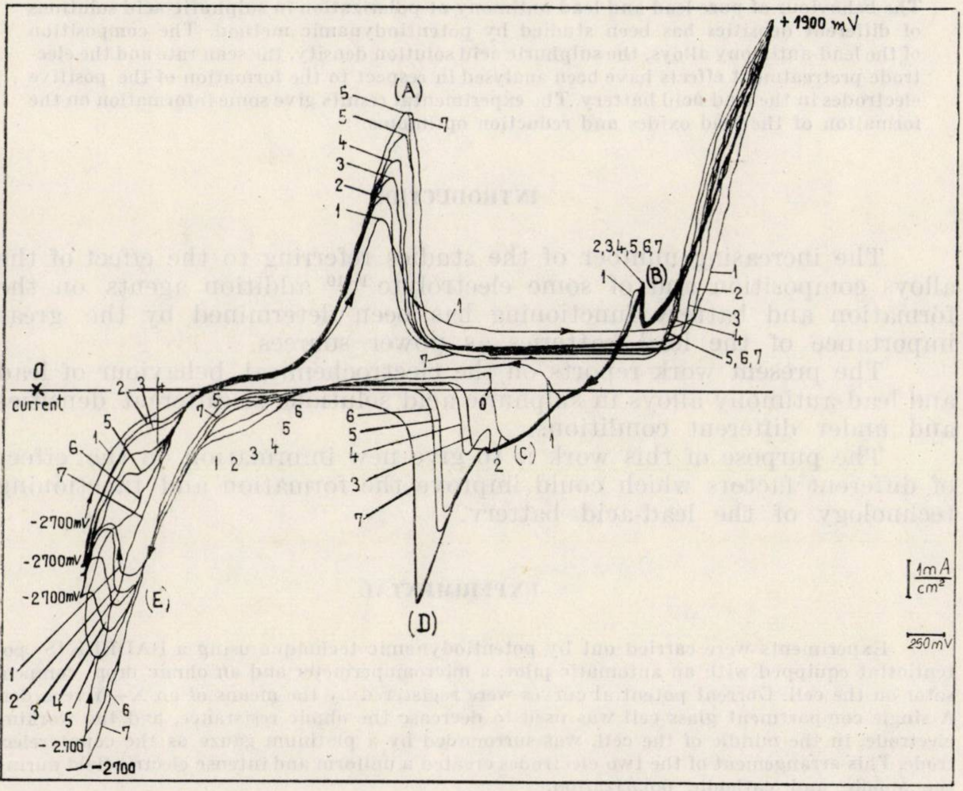

Fig. 1 — Polarization curves of lead in $d = 1.05$ g/cm³ density sulphuric acid solution, at $v =$ 300 mV/min potential scan rate and temperature of 20 ± 0.1°C.

and back to -2700 mV. For each determination a number of 8 cycles has been registered. Analysis of the curves shows the following: on the anodic increasing curve a peak (A) appears within (-1000 mV) – (-600 mV) potential range, then a passive region or about 1550 mV follows, after which the current begins to rise (increases) again (the transpassivation region) on the oxidation of the passive layer to PbO_2 account, simultaneously with the O_2 evolution on the PbO_2 formed.

It is well known that the electric conductibility and the porosity of the PbO_2 formed are much higher than those of the lead sulphate. For this reason the oxygen evolution may occur simultaneously with the PbO_2 formation. The (A) peak to be seen is the lead sulphate formation; the latter forms a dense compact layer on the metal surface, which generates the current drop to a practically constant value on the whole passive range. However, it is found that the passivation current density has a considerable value; therefore some anodic reactions occur within this range, too. The dense lead sulphate film hinders the SO_4^{2-} and HSO_4^- ions penetrability at the metal surface. Thus, between the metal surface and the lead sulphate layer, the alkalinity of the medium will be stressed (increased). This will cause the formation of the basic leady compounds ($PbO \cdot PbSO_4$; $3\ PbO \cdot PbSO_4 \cdot H_2O$; $4PbO \cdot PbSO_4$; $Pb(OH)_2$; $5\ PbO \cdot PbSO_4 \cdot 2H_2O$ etc.) simultaneously with the potential removal towards more and more positive values. At higher potential values than $+1100$ mV, hence below $PbO_2/PbSO_4$ equilibrium electrode potentials, the oxidation of the divalent lead hydrated oxides and sulphates at the $\alpha-PbO_2$ starts. This is a characteristic form of the solutions with higher [12] pH and about $+1200$ mV potentials. The penetrability increases simultaneously with the α-PbO_2 formation and the acidity of the adjacent medium to the metal surface increases again. This fact combined with the further potential removal to more positive values leads to the β-PbO_2 formation (the tetragonal form of the PbO_2) simultaneously with the O_2 evolution. It is known that β-PbO_2 appears at higher potentials being a characteristic of the more acid solutions. Hence, at the anodic scan end a corrosion layer appears, consisting of an inner layer rich in α-PbO_2 and an outer layer (an overlay) rich in β-PbO_2.

The metallographic analysis shows that the dark brown inner layer (rich in α-PbO_2) is dense and compact, while the light brown outer layer (rich in β-PbO_2) is less dense and has a great porosity. Reversing the direction of potential sweep, an oxidation peak (B) within the ($+1000$ mV) – ($+850$ mV) potential range followed by a small reduction peak (C) (rather a shoulder) and two great reduction peaks (D and E) are observed. The oxidation peak (B) which appears at the decreasing anodic sweep could be a remanent oxidation of the passive lead to α-PbO_2. According to other authors [6,7,13] this complex of voltametric peaks (the anodic peak and the cathodic one C) results in the anodic and cathodic simultaneous reactions of the lead ions, occurring within the ($+600$ mV) – ($+1000$ mV) vs. Hg/Hg_2SO_4 potential range, or in a nonstoichiometric oxide formation below the $PbO_2/PbSO_4$ equilibrium potential.

The first reduction peak (C) represents in fact the formed β-PbO_2 reduction, the Pb^{4+} to Pb^{2+} ion reduction respectively. The (D) peak represents the α-PbO_2 and the basic leady compounds reduction, while the (E) peak represents the reduction of the lead sulphate to metallic lead.

Analysis of figure 1 and of table 1 shows that the oxidation (A) peak height increases with the number of cycles and removes to more positive potentials; the oxidation (B) peak is practically keeping constant, while the reduction (C), (D) and (E) peaks remove to more negative potentials, their height increasing with the increase of cycles number. This behaviour can be explained as follows: during the repeat of the potential sweep cycles an activation of the working electrode surface occurs, resulting in a higher active zone formation and in an activation of all oxidation processes at the anodic increasing potential sweep, hence in an increase of all cathodic reduction processes at the reverse potential scan.

Table 1

The peak current density and the peak potential values *vs.* number of cycles

Number of cycle	Scan rate (mV/min)	H_2SO_4 density g/cm³	Working electrode	A		B		D		E	
				E_P (mV)	I_P (mA)	E_P (mV)	I_P (mA)	E_P (mV)	I_P (mA)	E_P (mV)	I_P (mA)
1	300	1.05	Pb	−725	2.25	+ 975	1.35	+475	0.1	−2400	2.45
2	300	1.05	Pb	−675	2.55	+1000	1.45	+100	0.6	−2450	2.7
3	300	1.05	Pb	−650	2.85	+1000	1.45	−100	0.8	−2475	2.85
4	300	1.05	Pb	−600	3.05	+1000	1.45	−150	0.85	−2525	3.20
5	300	1.05	Pb	−550	3.40	+1000	1.45	−275	1.60	−2625	3.55
6	300	1.05	Pb	−550	3.65	+1000	1.45	−325	1.90	−2650	4.51
7	300	1.05	Pb	−525	3.70	+1000	1.45	−475	2.85	−2700	5.00

The potential scan rate decrease resulted, in all cases, in the removal of the peak potential as follows: for the lead sulphate formation (A) peak, the scan rate decrease causes the E_{P_A} removal to more negative values, while E_{P_B}; E_{P_C}; E_{P_D} and E_{P_E} remove to more positive values.

Figure 3 shows the lead-antimony (7.5%) alloy polarization curves, in 1.05 g/cm³ density sulphuric acid solution.

Analysis of the curves in figures 1 and 3 shows that the antimony presence in the alloy results in a supplementary peak appearance on the increasing anodic curve. This oxidation peak appears within the (−450 mV) — (−350 mV) potential range and represents the Sb_2O_3 formation. At the reverse potential sweep another supplementary reduction peak (H) also appears, which represents the antimony oxide to metallic antimony reduction.

Comparatively with the pure lead electrode in the same density sulphuric acid solutions, the antimony presence reduces the (B), (C) and (D) peak height, as far as the antimony amount increases.

It is found that the anodic current average and especially the pasivation current density is less for lead-antimony alloys than for the pure lead and, at the same time for the alloys with higher amounts of antimony than for those with smaller amounts (see Figs 3, 4 and 5). The anodic process inhibition at the antimony addition is pointed out by the passive range increase with at least 150 mV comparatively with pure lead.

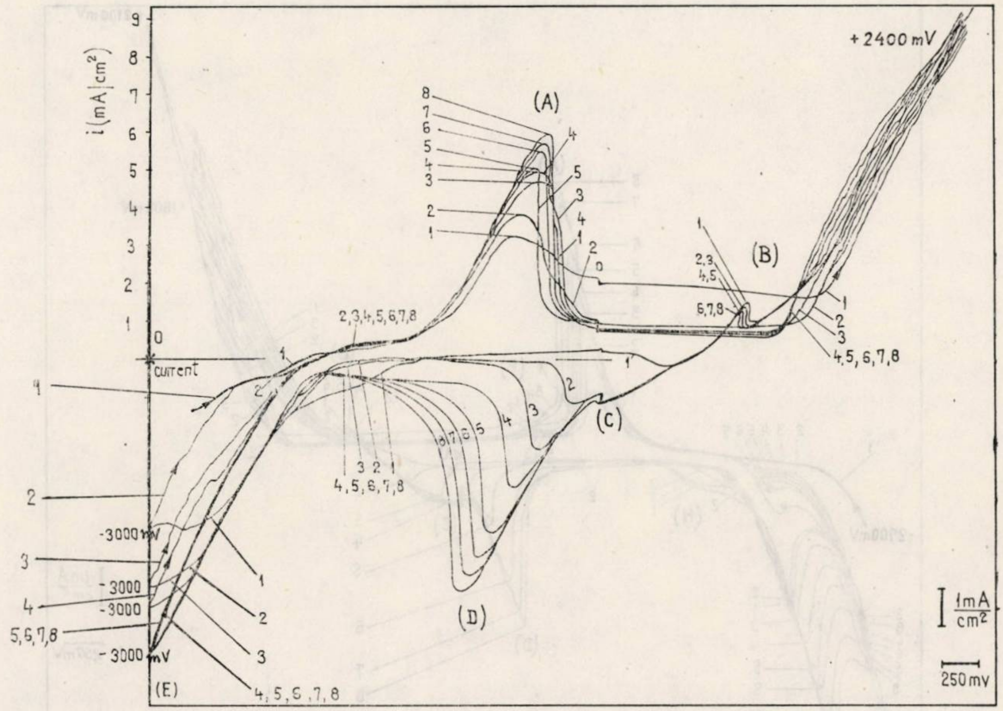

Fig. 2. — Polarization curves of lead in $d=1.05$ g/cm^3 density sulphuric acid solution, at $v=600$ mV/min potential scan rate and temperature of 20 ± 0.1 °C.

These results are in good agreement with those reported in the literature which showed [2,14], that the antimony presence reduces the adhesion between the grid and the α-PbO_2 inner layer, maintains the uniformity of this layer and increases the cohesion between the PbO_2 particles which results in the craking corrosion hinding.

The behaviour of the pure lead and lead-antimony (7.5%) alloy at polarization, in sulphuric acid aqueous solutions of different densities has also been studied.

Sulphuric acid solutions of 1.001 g/cm^2 — 1.12 g/cm^3 have been used. At the sulphuric acid concentration increase, an increase of all peaks strength takes place. The anodic and cathodic current density average is higher for more concentrated solutions, hence an activation of anodic and cathodic processes for both pure lead and lead-antimony (7.5%) alloy takes place.

The increase of the density of the sulphuric acid solution above 1.03 g/cm^3 leads to the decrease of all peaks strength, except for the (D) peak and increases the passive region (increases the oxygen overvoltage). This behaviour is the same for both pure lead and lead-antimony (7.5%) alloy. This can be explained by a stronger passivation of both lead and lead-antimony (7.5%) alloy. Simultaneously with the increase of the sulphuric acid concentration, the $PbSO_4$ to PbO_2 conversion rate decreases. The

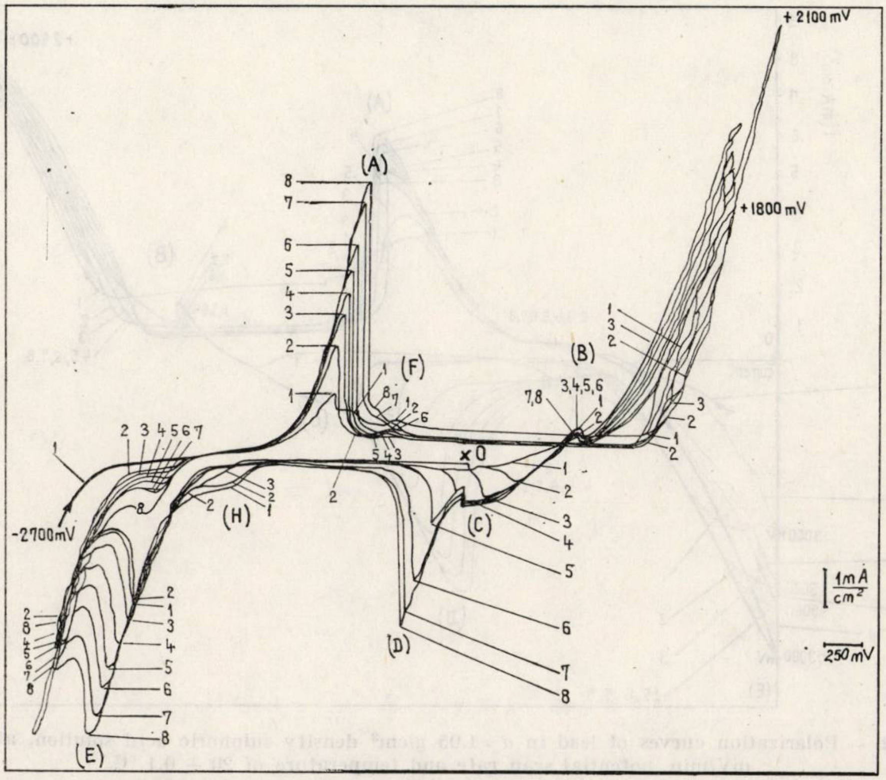

Fig. 3. — Polarization curves of the lead — (2.63 %) antimony alloy in d = 1.05 g/cm³ density sulphuric acid solution at 300 mV/min potential scan rate and at a temperature of 20 ± 0.1 °C.

cathodic (D) peak increase at higher sulphuric acid concentrations is the reflection of a greater anodic oxidation of the lead substrate as a basic leady compound underneath the lead sulphate film.

The penetrability of SO_4^{2-} and HSO_4^- ions through the lead sulphate film decreases with the increase of the sulphuric acid concentration (because the passivation becomes stronger, the $PbSO_4$ layer becomes denser and more compact, thus the alkalinity of the medium between the lead surface and the $PbSO_4$ layer increases), resulting in a higher amount of the basic leady compounds. At the reverse potential sweep these compounds are reducing in the (D) peak potential range, resulting in a higher height of this peak (see comparatively Fig. 1 and Fig. 6). As pointed out before, the antimony addition leads to a stressed decrease of the height of the voltammetric peaks complex, to the decrease of the passive current density and to the extension of the passive region. The silver addition in the lead (7.5 %) antimony alloy leads to the appearance of another oxidation peak on the increasing anodic curve. This new oxidation (G) peak appears at about + 690 mV potential and represents the silver to silver sulphate oxidation. The increasing amount of silver in alloy (see table 2)

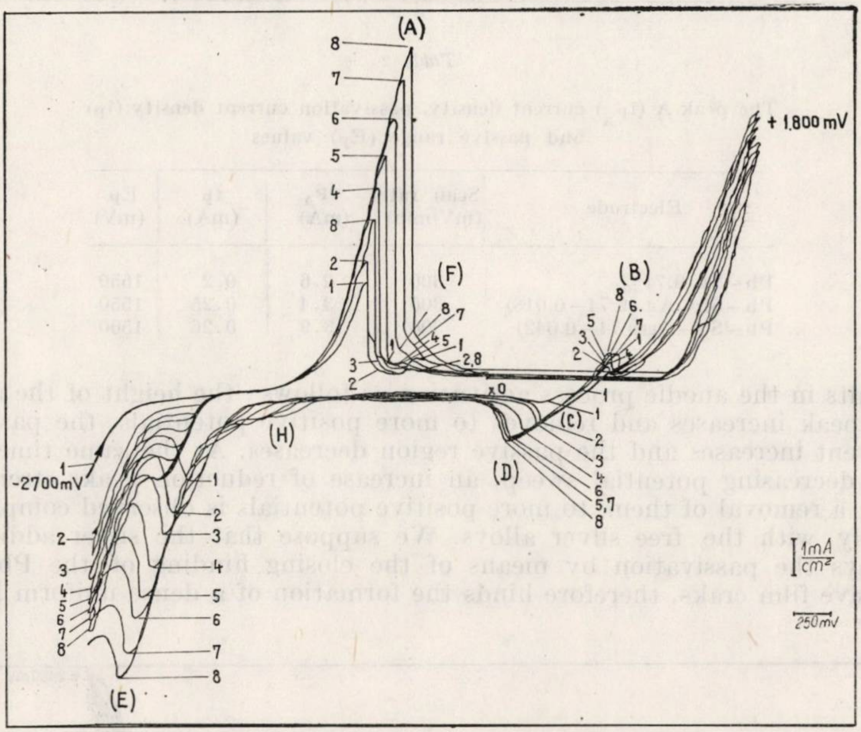

Fig. 4. — Polarization curves of the lead — (7.5%) antimony alloy in d = 1.05 g/cm^3 sulphuric acid solution at 300 mV/min potential scan rate and a temperature of 20 ± 0.1 °C.

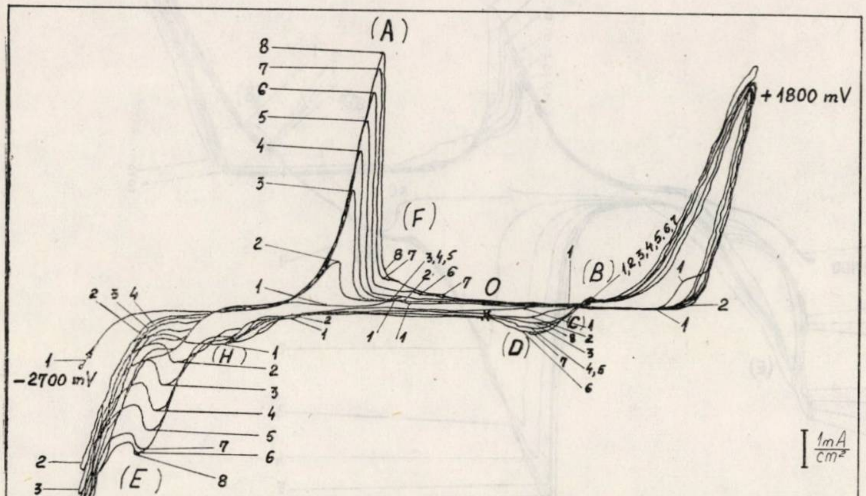

Fig. 5. — Polarization curves of the lead — (9.74%) antimony alloy in d = 1.05 g/cm^3 density sulphuric acid solution, at 300 mV/min potential scan rate and temperature of 20 ± 0.1 °C.

Table 2

The peak A (i_{P_A}) current density, passivation current density (i_P) and passive range (E_P) values

Electrode	Scan rate (mV/min)	i_{P_A} (mA)	i_P (mA)	E_P (mV)
Pb–Sb 9.74%	300	2.6	0.2	1650
Pb–Sb–Ag (9.74–0.018)	300	3.4	0.25	1550
Pb–Sb–Ag(9.74–0.042)	300	3.9	0.26	1500

results in the anodic process activation as follows : the height of the anodic peak increases and removes to more positive potentials, the passive current increases and the passive region decreases. At the same time, at the decreasing potential sweep, an increase of reduction peaks strength and a removal of them to more positive potentials is observed comparatively with the free silver alloys. We suppose that the silver addition delays the passivation by means of the closing hinding of the $PbSO_4$ passive film craks, therefore hinds the formation of a dense uniform lead

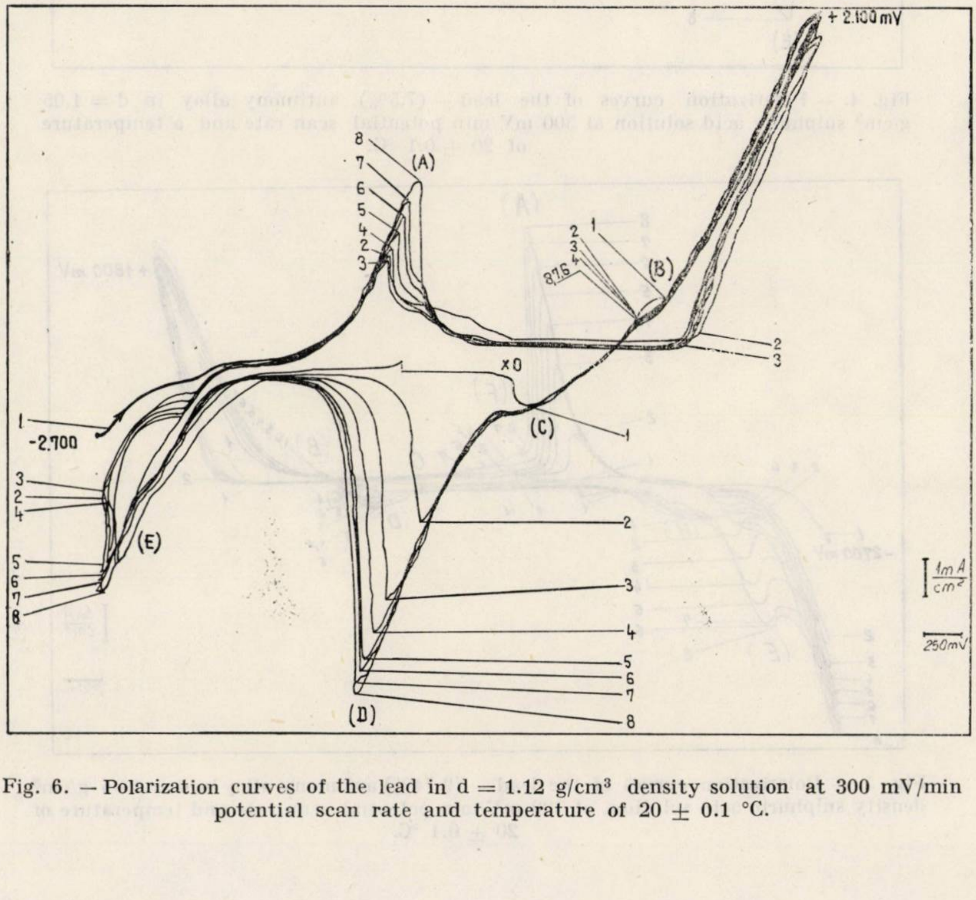

Fig. 6. — Polarization curves of the lead in d = 1.12 g/cm³ density solution at 300 mV/min potential scan rate and temperature of 20 ± 0.1 °C.

sulphate layer. Several authors [14] assume that antimony is filtered outside passive film (it is removed outside these cracks of the passive film), while on the alloy surface first the $PbSO_4$ appears and then, at much more positive potentials of about + 690 mV the silver to Ag_2SO_4 oxidation begins. The fact that the (D) peak is much less than the similar peak for pure lead and lead-antimony free alloys, confirms the assumption of the formation of a complex of lead and silver oxides instead of the basic leady compounds series at the increasing anodic potential sweep. All these assumptions are in agreement with our experimental results (see Fig. 7 and table 2).

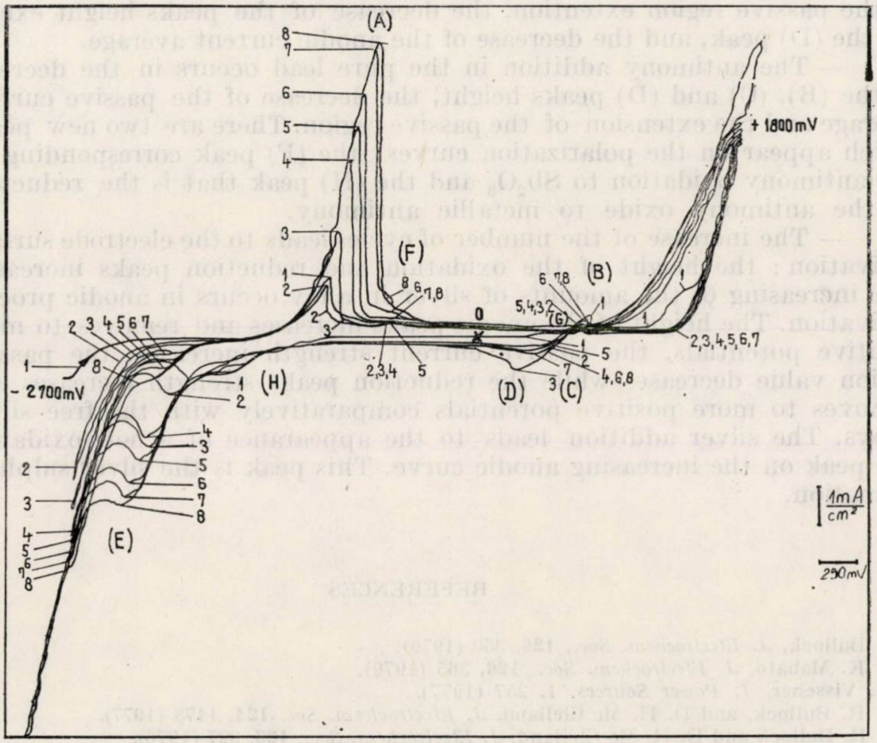

Fig. 7. — Polarization curves of the lead — (9.74%) antimony — (0.012%) silver in d = 1.05 g/cm³ sulphuric acid solution, at 300 mV/min potential scan rate and temperature of 20 ± 0.1 °C.

CONCLUSIONS

— At the pure lead anodic polarization in sulphuric acid solution an oxidation (A) peak has been observed, that is the lead sulphate formation, hence a passive region with a great passivation current formation. This demonstrates the existence of some anodic reactions of the formation of the basic leady compounds and of a transpassive region of the lead sulphate and basic leady compound series to PbO_2 (first α-PbO_2, and then β-PbO_2) oxidation simultaneously with the oxygen evolution.

— At the end of the increasing anodic sweep a corrosion layer consisting of a dense, compact, dark brown and rich in α-PbO_2 inner layer and a less dense, more porous, light-brown and rich in β-PbO_2 outer layer, appear on the lead electrode.

— At the reverse potential sweep a complex of voltammetric peaks is formed due to some simultaneous anodic and cathodic reactions of lead ions.

— The potential scan rate decrease leads in all cases to the decrease of the height peaks.

— The increase of the sulphuric acid solution concentration occurs in the passive region extention, the decrease of the peaks height except for the (D) peak, and the decrease of the anodic current average.

— The antimony addition in the pure lead occurs in the decrease of the (B), (C) and (D) peaks height, the decrease of the passive current average and the extension of the passive region. There are two new peaks which appear on the polarization curves: the (F) peak corresponding to the antimony oxidation to Sb_2O_3 and the (H) peak that is the reduction of the antimony oxide to metallic antimony.

— The increase of the number of cycles leads to the electrode surface activation: the height of the oxidation and reduction peaks increases. The increasing of the amounts of silver in alloy occurs in anodic process activation. The height of the anodic peaks increases and removes to more positive potentials, the passive current strength increases, the passive region value decreases while the reduction peaks strength increases and removes to more positive potentials comparatively with the free silver alloys. The silver addition leads to the appearance of a new oxidation (G) peak on the increasing anodic curve. This peak is the silver sulphate formation.

REFERENCES

[1] R. Bullock, *J. Electrochem. Soc.*, **126**, 360 (1979).
[2] B. K. Mahato, *J. Electrochem. Soc.*, **126**, 365 (1979).
[3] W. Visscher, *J. Power Sources*, **1**, 257 (1977).
[4] K. R. Bullock, and D. H. Mc Clelland, *J. Electrochem. Soc.* **124**, 1478 (1977).
[5] K. R. Bullock and D. H. Mc Clelland, *J. Electrochem. Soc.*, **123**, 327 (1976).
[6] T. F. Sharpe, *J. Electrochem. Soc.*, **122**, 845 (1975).
[7] T. F. Sharpe, *J. Electrochem., Soc.*, **124**, 168 (1977).
[8] A. C. Simon and S. M. Coulder, *J. Electrochem. Soc.*, **121**, 531 (1974).
[9] J. L. Weininger, *J. Power Sources*, **2**, 241 (1977/1978).
[10] R. G. Acton, "Power Sources", D. H. Collins Editor, Pergamon Press, London, p. 133.
[11] V. Brânzoi, *Bull. Inst. Polytech. București, Chimie – Metalurgie*, **3**, 21 (1978).
[12] M. A. Dasoyan and N. A. Aguf, "Sovremennaia teoria svintsovogo akkumuliatora", Energia, Leningrad, 1975.
[13] T. G. Chang, M. M. Wright, and E. M. L. Valeriote, "Power Sources 6", D. H. Collins Editor, Academic Press, London, 1977.
[14] A. A. Abdul Azim, K. M. El-Sobki and A. A. Khedr, *Corrosion Science*, **17**, 415 (1977).

Revue Roumaine de Chimie, 28, *6*, 593–596 (1983)

CATALYTIC OXIDATION OF AMMONIA. VI[1–5]

LOW TEMPERATURE OXIDATION ON A NiO CATALYST

M.M. GIRGIS*, D. P. LAZĂR** and E. I. SEGAL***

* Faculty of Science, Department of Chemistry, University of Assiut, Egypt

** The Polytechnic Institute of Jassy, Department of Physical Chemistry, Romania

*** The Polytechnic Institute of Bucharest, Chair of Physical Chemistry and Electrochemical Technology, Bucharest, Romania

Received July 6, 1982

Catalytic oxidation of ammonia with atmospheric oxygen has been studied using a NiO industrial catalyst. The oxidation process was followed at atmospheric pressure, by applying a dynamic method.

INTRODUCTION

In two previous papers [4,5] the results concerning the catalytic oxidation of ammonia at low temperature ($< 400°C$) on an industrial catalyst of NiO supported on Al_2O_3 were reported.

In the present paper the experimental results of the catalytic oxidation of ammonia using an industrial NiO catalyst without a solid additional support, are reported. The lack of sufficient information regarding the use of this catalyst in the ammonia oxidation process together with its low cost price and the author's interest to compare the catalytic activity of this NiO catalyst without support, at low temperature, with that of NiO catalyst supported on Al_2O_3 appeared among the main reasons for this investigation. The oxidation process was also carried out, at normal pressure, using a laboratory kinetic system described in detail in a previous paper.[1]

EXPERIMENTAL

Characterization of the catalyst

As it was stated before, the used catalyst was of an industrial type. The main physical characteristics of the pelletized catalyst are summarized in table 1.

Table 1

The main characteristics of the pelletized NiO catalyst

1. Morphologic characterization :

Pellet shape	Pellet diameter (cm)	Pellet length (cm)	Pellet density ($g.\ cm^{-3}$)	Specific surface area* ($m^2 \cdot g^{-1}$)
Cylindrical	0.680	0.630	1.45	141.8

2. Quantitative composition :

NiO** (%, g/g)	Humidity (%, g/g)	Binding material (%, g/g)
89.7	8.30	2.0

3. X-ray analysis :

Using an X-ray diffraction equipmeut, type TUR-M 62 (made in D.D.R.), the radiation K_α of molybdenum and Nb filter, it has been observed that on the diffractogram obtained for the non-heated NiO sample, the diffraction lines were absent, denoting an amorphous state for NiO. Following a three-hour heating at 500°C in air, the amorphous NiO turned into its crystalline form.

4. TG analysis :

As a result of the thermal analysis of the catalyst up to 700°C, with a heating rate of 10°. min^{-1}., in air, it was found that between 60° and 315°C, the NiO sample has lost 8.3% in weight and the total lost up to 700°C representing 12.45% (w/w).

* Determined through physical adsorption of krypton, at liquid nitrogen temperature.

** Precipitation with dimethyl glyoxime.

RESULTS AND DISCUSSION

All reported experiments have been worked out using a quartz reactor [1] completely filled with pelletized catalyst, at initial reactor temperatures (T_i) ranging from 188° to 517°C. The gaseous reaction mixture (NH_3 + air) had a percentage volumetric (v/v) content of 12.30% NH_3 and it has been passed through the reactor at a constant flowrate of 27.77 $cm^3.s^{-1}$.

Within the framework above described, for temperatures $T_i \geqslant 280$°C, the oxidation process was so intensely exothermal that, following a certain induction period the initial distribution of the temperature inside the reactor was markedly disturbed. This perturbation has been shaped as a narrow "temperature peak" which, during the reaction time (the so-called "autoacceleration period") shifted toward the entrance of gases into the reactor. Finally, the "temperature peak" stopped at 3–4 cm away from the reactor entrance and after its positional stabilization it continued to grow in altitude since it reached a maximum height. The complete stabilization of the "temperature peak", both in position and in altitude, is a kinetic indication that the system entered into a steady state development.

It must be noticed that the visual observation, through the heater window, permitted to establish that, unlike the catalyst type NiO/Al_2O_3,[4,5] the NiO catalyst does not become incandescent.

Using initial temperatures of the reactor (T_i) comprised between 188° and 517°C and computing, for each temperature T_i, the corresponding $\Delta T_{max.}$ values, the following graphical illustration has been obtained (Fig. 1). It can be seen from this plot that ΔT reached a maximum value for $T_i = 315$°C.

By plotting the time dependence of the conversion degree of ammonia (α), the curves in Fig. 2 were obtained. From this graph it has been found that:

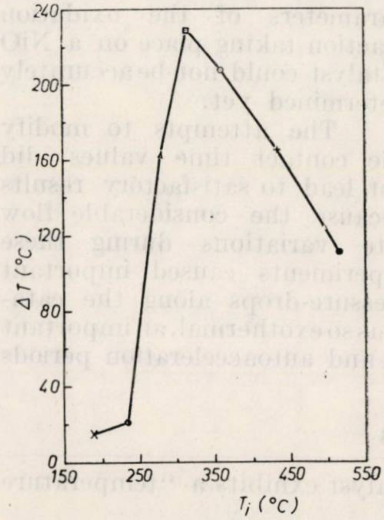

Fig. 1. — Variation of the ΔT values vs. T_i(flow rate: 27.77 $cm^3.s^{-1}$; ammonia content: 12.3 %, v/v).

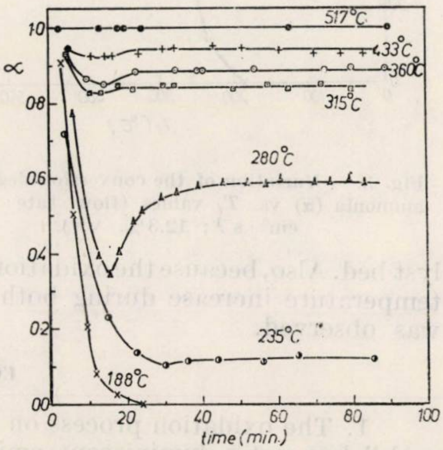

Fig. 2. — Variation of the conversion degree (α) vs. reaction time, for different T_i values (flow rate: 27.77 $cm^3 \cdot s^{-1}$; ammonia content: 12.3 %, v/v).

— catalytic oxidation of ammonia begins at $T_i = 235$°C (with $\alpha = 0.12$); certain more significant values of the conversion degree were obtained only for $T_i = 280$°C (when $\alpha = 0.59$);

— for initial temperatures of the reactor $288° < T_i < 435$°C, the induction period was about 15 min., while the necessary period to reach the stationary state of the oxidation process was about 22 min.;

— for $T_i \geqslant 280$°C, both induction period and autoacceleration period are less evident; the two periods disappear if the initial temperature T_i reaches 517°C;

— in contrast with other industrial catalyst, used in the previous experiments,[1-5] within the same experimental conditions, with this NiO catalyst the complete oxidation process of ammonia (i.e. $\alpha = 1.0$) begins for initial temperatures T_i higher than 400°C (for instance $T_i = 517°C$) instead of $T_i = 315°C$ which corresponds to $\Delta T_{\max}$ value.

As it can be seen in Fig. 3, the variation of the conversion degree (α) as a function of T_i values exhibits a sharp increase between 235° and 315°C; afterwards α grows more slowly up to its maximum value ($\alpha = 1.0$) which is achieved for $T_i = 517°C$.

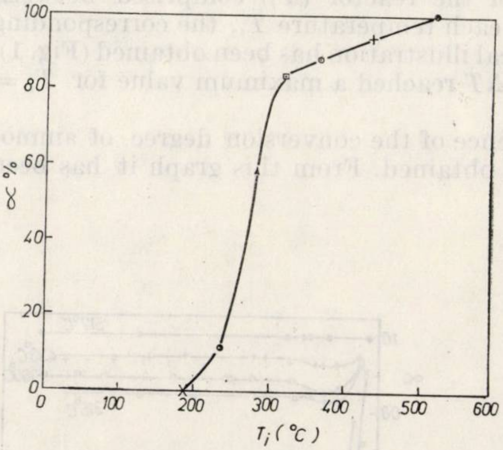

Fig. 3. — Variation of the conversion degree of ammonia (α) vs. T_i values (flow rate: 27.77 $cm^3 \cdot s^{-1}$; 12.3 %, v/v).

Although the steady conversion has values below unity, indicating a less significant contribution of the heterogeneous process to the global oxidation process of ammonia, the kinetic parameters of the oxidation reaction taking place on a NiO catalyst could not be accurately determined yet.

The attempts to modify the contact time values did not lead to satisfactory results because the considerable flow rate variations during these experiments caused important pressure-drops along the catalyst bed. Also, because the oxidation process was so exothermal, an important temperature increase during both induction and autoacceleration periods was observed.

CONCLUSIONS

1. The oxidation process on a NiO catalyst exhibits a "temperature peak" but not a luminiscent emission;

2. Under the same experimental conditions (composition of the reaction mixture and flow rate), the "temperature peak" is closer to the reactor exit for a NiO catalyst in comparison with NiO/Al_2O_3;

3. For the same experimental conditions (see above), the $\Delta T_{\max}$ values on NiO catalyst are obtained for T_i values somewhat higher ($T_i = 315°C$) than that for a NiO/Al_2O_3 ($T_i = 279°C$);

4. The catalytic oxidation of ammonia begins at a lower temperature ($T_i = 235°C$) when a NiO catalyst is used, in comparison with the NiO/Al_2O_3 catalyst for which $T_i = 269°C$;

5. Rising the initial temperature (T_i) of the reactor, both induction and autoacceleration periods disappear somewhat faster on NiO/Al_2O_3 than on NiO catalyst.

REFERENCES

[1] Part I, M. M. Girgis and D. P. Lazăr, *Rev. Roumaine Chim.*, **25**, 1293 (1980).
[2] Part II, M. M. Girgis, D. P. Lazăr, and E. I. Segal, *Rev. Roumaine Chim.*, **26**, 1199 (1981).
[3] Part III, M. M. Girgis, D. P. Lazăr and E. I. Segal, *Rev. Roumaine Chim.*, **26**, 1423 (1981).
[4] Part IV, M. M. Girgis, D. P. Lazăr and E. I. Segal, *Rev. Roumaine Chim.*, **28**, 307 (1983).
[5] Part V, M. M. Girgis, D. P. Lazăr, and E. I. Segal, *Rev. Roumaine Chim*, **28**, 445 (1983).

Revue Roumaine de Chimie, 28, *6*, 597–603 (1983)

DETERMINATION OF METAL DISPERSION OF Pd/SiO_2 CATALYSTS BY A COMBINATION OF TRANSMISSION ELECTRON MICROSCOPY WITH *X*-RAY DIFFRACTION AND CHEMISORPTION METHODS

JACEK A. SZYMURA
Institute of Technology and Chemical Engineering, Technical and Agricultural Academy, 3 Seminaryjna St., 85–326 Bydgoszcz, Poland

Received July 9, 1981

The metal dispersion of Pd/SiO_2 catalysts has been investigated using transmission electron microscopy, X-ray diffraction line broadening and hydrogen chemisorption measurements. A good agreement between the mean palladium particle sizes had been obtained from the three independent techniques that confirmed a proposed chemisorption stoichiometry ratio $H : Pd_s = 1 : 1$ in a wide range of Pd dispersion. The electron micrographs of catalysts showed Pd crystallites as the small spheres which were not distributed uniformly throughout a silica support.

1. INTRODUCTION

Supported metal catalysts consist of small metal crystallites (active phase) dispersed on a high-surface area support. These catalysts are commonly employed in several industrial reactions of hydrocarbon conversion.[1] The elucidation of metal dispersion state on support allows the effective utilization of catalyst in real process.

For characterization of metal dispersion and for crystallite size measurement a number of experimental methods have been used, e.g., selective gas chemisorption,[2–5] transmission electron microscopy TEM, [4–9] X-ray diffraction line broadening XDLB, [5,10,11] and small angle X-ray scattering SAXS. [12,13] In the case of supported Ni and Fe catalysts the magnetic measurements have been applied.[14]

Despite various limitations [15] TEM is the only direct way of investigation on the extremely small metal crystallites with diameters less than 2 nm. [16–18] In TEM a thin layer (< 100 nm) of catalyst to be examined is necessary. For this purpose a number of specimen preparation procedures have been elaborated. [19,20] A principle problem in the electron microscopic studies of these systems usually is the determination of the agreement between the metal dispersion obtained from electron micrographs and the similar one obtained by means of gas chemisorption as an independent method. In the case of a good correlation the electron microscopic data can be used to confirm the proposed chemisorption stoichiometry.[9] Previous X-ray diffraction techniques were also used in connection with TEM or chemisorption measurements.[5,7,14]

Excluding the numerous investigations of other supported metal catalysts, such comparison studies were conducted for following the Pd/support systems: Pd/SiO_2,[21] Pd/Al_2O_3,[22,23] Pd/C,[24-27] and Pd/zeolite.[28]

The aim of the present work is to extend studies of Pd/SiO_2 catalysts to obtain information on palladium dispersion, crystallite shapes and sizes, and their localization on support. The metal particle sizes calculated on the basis of TEM investigation were compared with those obtained from XDLB and H_2 chemisorption in order to verify the validity of $H : Pd_s$ stoichiometry ratio assumed for chemisorption measurement. For TEM studies of Pd/SiO_2 catalysts with various Pd contents an effective, new variant of specimen preparation procedure has been employed.

2. EXPERIMENTAL

2.1. CATALYSTS

The 2.12 wt % and 0.399 wt % Pd/SiO_2 catalysts were prepared by adsorption using the aqueous solutions of $PdCl_2$. The values of specific surface area of silica support and its dominant capillary radius determined from BET measurements were $S = 108.5$ m²/g and $r = 7$ nm respectively. The 5 wt % and 10 wt % Pd/SiO_2 catalysts were supplied by Degussa (Frankfurt, West Germany).

2.2. H_2 Chemisorption

The specific surface area of metal and the mean size of Pd crystallites were determined from H_2 chemisorption as measured by chromatographic pulse method.[3] The catalyst sample, placed in the U-tube was reduced for 2 hrs at 300°C with electrolytic H_2. Then hydrogen was removed by passing argon free from oxygen traces as the carrier gas at the same temperature for 2 hrs. After cooling to ambient temperature (in a stream of argon) hydrogen was introduced by means of a calibrated valve. The volume of chemisorbed H_2 was determined from the number of hydrogen portions adsorbed on metal surface. The values of metal surface areas obtained from chemisorption on pure metal surface were additionally confirmed by gas titration of reduced surface with oxygen and oxidized surface with hydrogen.

2.3. XDLB studies

The fine-ground samples consisting of 0.05 g of catalyst and 0.005 g of freshly roasted MgO have been studied by means of X-ray diffractometer with filtered CuKα radiation and equipped with a proportional counter. The mean crystallite sizes of palladium were determined from the broadening β of the Pd (111) profile. The peak breadth at half-maximum intensity of this profile was measured and the data were corrected for instrumental line broadening using Warren's expression.[10]

2.4. TEM investigation

The small sample of catalyst (ca 0.2 g) ground in an agate mortar was dispersed in ethanol. The freshly cleaved mica plate with deposited suspension was evaporated with 15 nm carbon layer using JEOL JEE—4B vacuum evaporator fitted with rotating and tilting stage. The carbon film with reinforced catalyst particles was then floated off onto a surface of redistilled water and mounted on specimen copper grids Polaron 400 mesh. The investigation of prepared specimen was carried out on Philips EM—300 Transmission Electron Microscope at 100 kV accelerating voltage. The magnification of the instrument was calibrated using the 0.34 nm spacings in graphitized carbon black as the standard.

3. RESULTS AND DISCUSSION

For hydrogen chemisorption the values of Pd surface area S_w in m^2 per gram were calculated from the formula:

$$S_w = \frac{2\,N\,V_m}{cV_N\,kx}$$

where N is Avogadro number, V_m is the volume of adsorbate monolayer in ccm per gram of catalyst, c is the content of Pd on support in wt %, V_N is the mol volume of hydrogen under normal conditions, k is the number of Pd atoms per m^2 of polycrystalline surface $k = 1.27.10^{19}$,[29] and x denotes the stoichiometry of chemisorption (the number of hydrogen atoms chemisorbed per surface Pd atom). According to the earlier investigation [30] H : Pd$_s$ was assumed to be 1 : 1 (Pd$_s$ denotes the surface atom of palladium).

In order to calculate the mean dimension $\bar{d}$(nm) of palladium crystallites from H$_2$ chemisorption data the both spherical and cubic assumptions of geometry of the supported Pd particles were used. Thus the values of $\bar{d}$ are given respectively by equations:

$$\bar{d} = 6 \cdot 10^3/\rho S_w \text{ and } \bar{d} = 5 \cdot 10^3/\rho S_w$$

where ρ is the palladium density in gram per ccm and S_w denotes the specific surface area of palladium.

In the case of X-ray diffraction method the mean crystallite sizes $\bar{d}_x$ were derived from the excess broadening using the Scherrer's formula:

$$\bar{d}_x = K\,\lambda/\beta\cos\Theta$$

in which λ is the radiation wavelength, K is Scherrer's constant chosen as 0.9 (for spherical crystallites and for the lower index planes), Θ is the Bragg angle and β denotes the peak breadth at half-maximum intensity of Pd (111) profile.

In the present study no diffraction lines from palladium were observed for the catalyst containing 0.399 wt % Pd. The similar results were reported by Dorling and Moss [10] in the case of 0.30 and 0.15 wt % Pt/SiO$_2$ systems. The lack of diffraction lines for supported metals in such catalysts is due to the high metal dispersion (crystallites $\leqslant$ 5 nm) and to the low metal content on support ($<$0.5 wt %) less than sensitivity of XDLB method.

For each of the Pd/SiO$_2$ catalysts examined the electron micrographs (e.g., for 2.12 wt % Pd/SiO$_2$ on figure 1) exhibited typical Pd crystallites seen as the dark spots or approximately round objects on silica support. A similar particle morphology for Pd/SiO$_2$ catalyst used in selective oxidation of hydrogen in gas stream was observed by Stetter and Blurton.[31] The present procedure for the preparation of TEM specimens allows the observation of metal particle localization on the support surrounding. It was found that distribution of Pd crystallites is not uniform throughout the pore structure of silica.

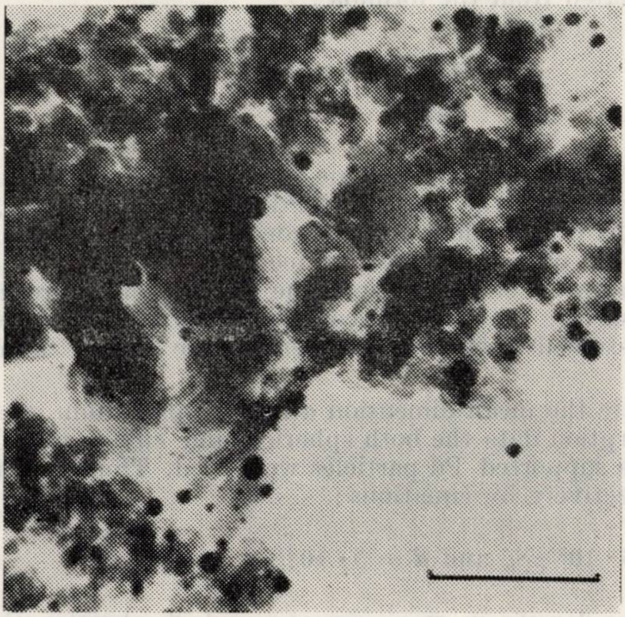

Fig. 1.— Electron micrograph of 2.12 wt% Pd/SiO_2 catalyst (marker indicates 100 nm).

The use of TEM makes possible the full characterization of metal dispersion state in examined catalysts, i.e., determination of crystallite shape and size, calculation of mean crystallite dimension and evaluation of metal particle size distribution. On a few electron micrographs of each catalyst about several hundred (200 — 500) crystallites were identified and then sized in 1 nm increments of dimension. From these data the suitable particle size distribution histograms were derived (Fig. 2a—d). The mean crystallite size based on volume-to-surface ratio $\bar{d}_{vs}$ was calculated from the following equation :

$$\bar{d}_{vs} = \sum_i n_i d_i^3 / \sum_i n_i d_i^2$$

where n_i is the number of crystallites in a suitable increment of dimension whose mean is d_i. On the basis of the values obtained of $\bar{d}_{vs}$ the palladium surface areas were calculated assuming the spherical geometry of metal crystallites :

$$S_w = 6 \cdot 10^3 / \rho \, \bar{d}_{vs}$$

where ρ denotes the density of palladium.

The values of the mean crystallite sizes and metal surface areas for Pd/SiO_2 catalysts obtained with the aid of three independent methods are summarized in table 1. Examining the data closed in this table it may

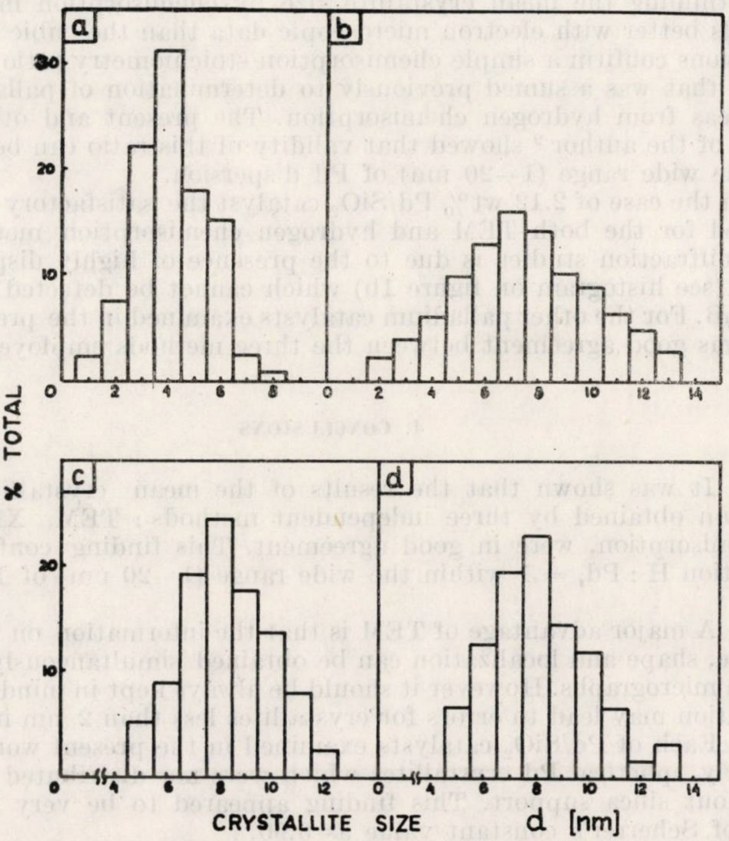

Fig. 2. — The particle size histograms of Pd/SiO$_2$ catalysts : a — 0.399, b — 2.12, c — 5.0 and d — 10.0 wt % Pd.

Table 1

Comparison of the mean crystallite sizes and palladium surface areas for Pd/SiO$_2$ catalysts obtained by employing various methods of metal dispersion measurement

Pd content wt %	H_2 chemisorption				XDLB	TEM	
	V_m(cm^3/g cat.)	S_w(m^2/g)	$\bar{d}$(nm) cubes	$\bar{d}$(nm) spheres	$\bar{d}_x$ (nm)	$\bar{d}_{vs}$(nm)	S_w(m^2/g)
0.399	0.098	108	3.9	4.6		5.0	100
2.12	0.230	49	8.6	10.3	12.6	9.2	54
5.0	0.635	56	7.5	9.0	10.8	8.9	56
10.0	1.290	55	7.6	9.2	11.5	9.1	55

be concluded that the results from TEM investigation are in good agreement with the results of hydrogen chemisorption. Furthermore it is to be pointed out that the spherical assumption of Pd particle geometry made in determining the mean crystallite size by chemisorption method corresponds better with electron microscopic data than the cubic one. These conclusions confirm a simple chemisorption stoichiometry ratio H : Pd_s = = 1 : 1 that was assumed previously to determination of palladium surface areas from hydrogen chemisorption. The present and other recent studies of the author [9] showed that validity of this ratio can be extended over the wide range (1—20 nm) of Pd dispersion.

In the case of 2.12 wt% Pd/SiO_2 catalyst the satisfactory agreement observed for the both TEM and hydrogen chemisorption methods with X-ray diffraction studies is due to the presence of highly dispersed palladium (see histogram on figure 1b) which cannot be detected by means of XDLB. For the other palladium catalysts examined in the present study there was good agreement between the three methods employed.

4. CONCLUSIONS

1. It was shown that the results of the mean crystallite sizes of palladium obtained by three independent methods: TEM, XDLB, and H_2 chemisorption, were in good agreement. This finding confirmed the assumption H : Pd_s = 1 within the wide range (1—20 nm) of Pd dispersion.

2. A major advantage of TEM is that the information on metal particle size, shape and localization can be obtained simultaneously from the electron micrographs. However it should be always kept in mind that such information may lead to errors for crystallites less than 2 nm in size.

3. Each of Pd/SiO_2 catalysts examined in the present work exhibited nearly spherical Pd crystallites which were not distributed uniformly throughout silica support. This finding appeared to be very useful for choice of Scherrer's constant value as 0.90.

4. When using the TEM combined with XDLB and H_2 chemisorption methods a full characterization of metal dispersion state of the supported metal catalysts can be achieved.

REFERENCES

[1] C. L. Thomas, "Catalytic Processes and Proven Catalysts", Academic Press, New York, 1970
[2] H. L. Gruber and A. Hausen, *Kolloid – Z.u.Z. Polymere*, **214**, 66 (1966).
[3] T. Paryjczak and W. K. Jóźwiak, *J. Chromatogr.*, **111**, 443 (1975).
[4] K. Foger and J. R. Anderson, *J. Catalysis*, **54**, 318 (1978).
[5] F. M. Dautzenberg and H. B. M. Wolters, *J. Catalysis*, **51**, 26 (1978).
[6] P. C. Flynn and S. E. Wanke, *J. Catalysis*, **37**, 432 (1975).
[7] H. K. Kuo, P. Ganesan and R. J. DeAngelis, *J. Catalysis*, **64**, 303 (1980).
[8] J. A. Szymura and T. Paryjczak, *React. Kinet. Catal. Lett.*, **12**, 219 (1979).
[9] T. Paryjczak and J. A. Szymura, *Z. anorg. Chem.*, **449**, 105 (1979).
[10] T. A. Dorling and R. L. Moss, *J. Catalysis*, **7**, 378 (1967).
[11] G. B. McVicker, R. L. Garten and R.T.K. Baker, *J. Catalysis*, **54**, 129 (1978).
[12] G. A. Somorjai, Dissertation, University of California, Berkeley, 1960.
[13] T. E. Whyte, P. W. Kirklin, R. W. Gould and H. Heinemann, *J. Catalysis*, **25**, 407 (1972).
[14] M. Boudart, A. Delbouille, J. A. Dumesic, S. K. Khammouma and H. Topsøe, *J. Catalysis*, **37**, 486 (1975).

[15] P. C. Flynn, S. E. Wanke and P. S. Turner, *J. Catalysis*, **33**, 233 (1974).

[16] E. B. Prestridge and D. J. Yates, *Nature*, **234**, 345 (1971).

[17] E. W. Thornton, H. Knözinger, B. Tesche, J. J. Rafalko and B. C. Gates, *J. Catalysis*, **62**, 117 (1980).

[18] J. B. Nagy, M. van Eenoo and E. G. Derouane, *J. Catalysis*, **58**, 230 (1979).

[19] J. W. Sprys, L. Bartosiewicz, R. McCune and H. K. Plummer, *J. Catalysis*, **39**, 91 (1975).

[20] J. A. Szymura and T. Paryjczak, *Wiadomości chem.*, **32**, 175 (1978).

[21] R. L. Moss, D. Pope, B. J. Davis and D. H. Edwards, *J. Catalysis*, **58**, 206 (1979).

[22] T. Paryjczak and S. Karski, *Rocz. Chem.*, **50**, 291 (1976).

[23] R. A. Dalla Betta, R. C. McCune and J. W. Sprys, *Ind. Eng. Chem. Prod. Res. Dev.*, **15**, 169 (1976).

[24] J. A. Szymura, Ph. D. Thesis, Technical University, Łódź, 1979.

[25] D. Pope, W. L. Smith, M. J. Eastlake and R. L. Moss, *J. Catalysis*, **22**, 72 (1971).

[26] D. Pope, D. S. Walker and R. L. Moss, *J. Catalysis*, **28**, 46 (1973).

[27] R. T. Stimek and H. F. Rase, *Ind. Eng. Chem. Prod. Res. Dev.*, **17**, 227 (1978).

[28] G. Dalmai-Imelik, C. Leclercq and I. Mutin, *J. Microsc.*, **20**, 123 (1974).

[29] J. R. Anderson, "Structure of Metallic Catalysts", Academic Press, London — New York — San Francisco, 1975, p. 269.

[30] A. P. Karnaukhov, *Kinetika i Kataliz*, **12**, 1520 (1971).

[31] J. R. Stetter and K. F. Blurton, *Ind. Eng. Chem. Prod. Res. Dev.*, **16**, 22 (1977).

Revue Roumaine de Chimie, **28**, *6*, 605–614 (1983)

SOME NOVEL SALTS AND LIGAND PROPERTIES OF THE CYCLIC $P_2S_8^{2-}$ ANION

RODICA MICU-SEMENIUC, SIMONA POPȘE and IONEL HAIDUC
Chemistry Department, "Babeș-Bolyai" University, R—3400 Cluj-Napoca, Romania

Received February 15, 1982

The reaction of tetraphosphorus decasulfide with aromatic tertiary amines yields salts of the $P_2S_8^{2-}$ anion, namely $[B-H-B^+]_2[P_2S_8^{2-}]$ (with B = α-, β- and γ-picolines) and $[BH^+]_2[P_2S_8^{2-}]$ (with B = 2,6-lutidine and quinoline). In the presence of Ni(II) or Fe(III) carbonates, complexes of the type $Ni(P_2S_8).B$ (with B = pyridine (Py), β-picoline (β-pic), γ-picoline (γ-pic) and quinoline (Quin) and $Fe_2(P_2S_8)_3.2Py$ are formed. The complexes were characterized by IR, electronic and ESR spectra and by thermal analysis. The cyclic anion $P_2S_8^{2-}$ acts as ligand to form presumably polymeric coordination compounds.

INTRODUCTION

The sulfur-containing ligands have been intensively investigated in recent years; among these dithiophosphates, $(RO)_2PS_2^-$, dithiophosphinates, $R_2PS_2^-$ and related compounds focused much attention [1,2] and revealed a considerable variety in their coordination patterns. [3] Our interest in inorganic heterocycles [4] and their potential use as ligands [5] associated with our interest in dithiophosphates and related ligands [3,6–12] lead to the idea that inorganic heterocycles containing PS_2 groups as building units could be of certain interest. The known compounds, falling into this category, include heterocyclic anions I—III, reported in the literature [13–15]:

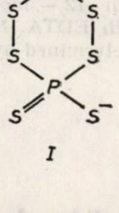

I

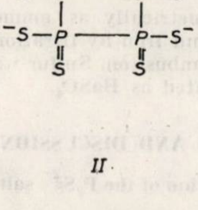

II

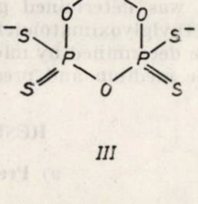

III

Anion I resulted from the reaction of tetraphosphorus decasulfide (P_4S_{10}) with pyridine; it was found, by X-ray diffraction, that the isolable product of this complex reaction is a salt $[Py_2H]_2P_2S_8$ containing a hydrogen-bonded cation $C_5H_5N...H...NC_5H_5^+$ [13]; (Py = pyridine).

Similar cations with other tertiary nitrogen bases are well known in both symmetrical (B..H..B)$^{+}$ [16-19] and asymmetrical (B..H..B')$^{+}$ (where B ≠ B')[17,20] forms, but only another compound containing the P_2S_4 ring has been reported,[21] namely $Br_2(S)_2P_2S_4$.

In this paper we extended the reaction of P_4S_{10} to other tertiary amines, and succeeded in isolating (in low yields) some novel tertiary amine salts of the $P_2S_8^{2-}$ anion. Attempts to use this cyclic anion as ligand met only with moderate success and are reported here.

EXPERIMENTAL PART

The chemicals employed in this work were of reagent grade. The reactions were successful only with fresh and dry P_4S_{10}. The amines had to be dried and distilled over solid KOH before use. The solvents were purified by distillation when necessary.

The infrared spectra were recorded on a UR—20 Carl Zeiss-Jena instrument. ESR spectra were recorded on a JES-3B instrument in the X-band at the room and 77 K temperature and ^1H—NMR spectra on a Tesla BM—487 spectrometer. Electronic spectra were recorded on a VSU-2G Carl Zeiss-Jena instrument and thermal decomposition was followed with a Paulik-Paulik-Erdely derivatograph.

General preparation procedure of $P_2S_8^{2-}$ salts

The preparation was similar to that reported in the literature [13] for the pyridinium salt. Thus, 1g P_4S_{10} was suspended in an excess of tertiary amine (ca. 20 ml) and the mixture was stirred under gentle heating until the solid dissolved completely. The reaction mixture was allowed to cool slowly to room temperature. After ca. 24 hours yellow needle-like crystals were deposited from the mixture. It was noticed that the reacting time was shorter with more basic amines. The crystals were filtered, washed with ether and dried in air. The compounds isolated and their analytical data are listed in table 1.

General preparation procedure for metal complexes

A mixture consisting of ca. 1 g P_4S_{10}, 20 ml tertiary amine and ca. 0.2 g freshly prepared nickel(II) carbonate or freshly mixture obtained reacting iron(III) chloride with sodium carbonate in ethanol, was stirred under heating at < 100°C preferrably on a water bath for ca. 60 minutes. The precipitate formed after cooling was filtered, washed with ethanol and dried in air. The compound isolated and their analytical data are listed in table 2.

In both preparations the temperature must not exceed 100—120°C to avoid decomposition of the cyclic anion. In all reactions evolution of hydrogen sulfide is observed.

Analysis

Phosphorus was determined gravimetrically as ammonium 12 — molybdophosphate, nickel as bis (dimethylglyoximato)nickel and iron by titration with EDTA. Nitrogen, carbon and hydrogen were determined by microcombustion. Sulfur was determined by oxidation with $KMnO_4$ in alkaline medium and precipitated as $BaSO_4$.

RESULTS AND DISCUSSION

a) Preparation of the $P_2S_8^{2-}$ salts

The formation of anion I containing two S—S bonds from tetraphosphorus decasulfide [13] which contains only P—S—P and P=S bonds, is rather intriguing and cannot be completely understood. The low yield suggests that this may be only a secondary process within a complex reaction. For this reason it seemed worthwhile to check whether other tertiary amines give similar products. It was found that the mixtures of P_4S_{10} and tertiary amines in excess, moderately heated until the solid is completely dissolved, deposit pale yellow, needle-like crystals, after cooling and standing for at least 24 hours. The reaction can also be carried at room temperature; in this case the crystalline product appears only after 3—4 days of standing. In both cases, the bulk of the reaction product is a viscous material, which on prolonged storage (5—6 weeks) deposits crystals of the same composition as the first crop. The compounds obtained and their analytical data are listed in table 1.

Table 1

Salts of the $P_2S_8^{2-}$ anion with organic cations*

Cation	M.P. °C	Analysis					
		% P		% N		%S	
		found	(calc.)	found	(calc.)	found	(calc).
$[Py_2H]^+$	105	9.31	(9.75)	8.65	(8.80)	39.70	(40.25)
$[\alpha\text{-pic}_2H]^+$	110	9.10	(8.96)	8.16	(8.09)	36.12	(36.99)
$[\beta\text{-pic}_2H]^+$	100	8.75	(8.96)	7.93	(8.09)	36.25	(36.99)
$[\gamma\text{-pic}_2H]^+$	97	8.45	(8.96)	7.89	(8.09)	36.18	(36.99)
$[2,6\text{-lutH}]^+$	124	11.94	(11.61)	5.34	(5.24)	47.42	(47.94)
$[QuinH]^+$	140	10.59	(10.72)	5.05	(4.84)	43.71	(44.29)

* Abbreviations used: Py = pyridine; pic = picoline; lut = lutidine; Quin = quinoline.

With pyridine and mono-methylpyridines (α-, β- or γ-picoline) salts of the complex organic cations $[B...H...B]^+$ (where B = base) were obtained, whereas with 2,6-dimethylpyridine (lutidine) and quinoline only the salts of the simple cations $[BH]^+$ resulted. The yields were low (ca 10%). With aliphatic or mixed aliphatic-aromatic tertiary amines, like triethylamine or N,N-dimethylaniline, no similar products could be obtained.

The ^{1}H-NMR spectrum of the pyridine derivative exhibits a signal at $\tau = 4.80$ ppm, due to the N...H...N proton.[17] In the ^{1}H—NMR spectrum of the quinoline compound $[QuinH]_2P_2O_8$, in deuterated DMSO solution the $N-H^+$ proton exhibits a signal at $\tau = 0.7$ ppm, in addition to the hydrogen atoms of the heterocyclic nucleus, with the right integrated area ratio (1 : 7).

The *infrared spectra* of the salts afford little structural information. Those containing the $[B-H-B]^+$ cations show poorly resolved peaks within the range 400—700 cm^{-1} and 800—1400 cm^{-1}, as found by other authors for other salts of these cations.[22] The cyclic salts of the $[BH]^+$ cations show better resolved bands. The spectra show little deviation from those of neutral amines.

The *thermal behaviour* of the cyclic salts $[Py_2H]_2P_2S_8$ and $[QuinH]_2P_2S_8$ was followed with the aid of thermogravimetric measurements. The salt $[Py_2H]_2P_2S_8$ shows a single, continuous iweght loss, corresponding to the elimination of pyridine and burning of six equivalents of sulfur. The observed weigth loss is 65.10%, compared to 65.00% calculated.

The compound $[\text{Quin H}]_2P_2S_8$ shows two steps of weight loss (demonstrated by two minima on the DTG curve) and four maxima on the DTA curve. The weight loss of 78.00% corresponds to the burning of the organic part and of sulfur (calculated 72.70%). A part of the P_2O_5 residue is also lost due to its volatility.

b) Coordination compounds of the $P_2S_8^{2-}$ anion

The attempted replacement of the organic cation with transition metals by reacting the cyclic compounds with metal salts failed to give the expected coordination compounds. The only way to obtain such compounds was described in the experimental part. The reaction mixture yields a brown liquid product, from which a red-brown nickel compound and a green iron compound precipitate on standing.

The precipitation of the nickel compound is facilitated if the mixture is treated, after cooling, with a small amount of water (for pyridine and picolines) or acetone (for quinoline). With α-picoline no solid product can be obtained, nor can any iron(III) derivative be isolated from the quinoline reaction. The compounds obtained are listed in table 2.

The metal derivatives do not exhibit sharp melting points and decompose gradually within the temperature intervals shown in table 2. It should be noted that the yields of metal complexes are considerably greater than those of the simple $P_2S_8^{2-}$ salts, obtained from P_4S_{10} and tertiary amines in the absence of the metal.

Table 2

Nickel (II) and iron (III) complexes of $P_2S_8^{2-}$ anion

Compound	Decomposition temperature °C	Yield %	Analysis %		
			%M	% P	% N
			found / calc.	found / calc.	found / calc.
$NiP_2S_8 \cdot$ Py*	180—190	51—52	13.10 / 12.88	13.09 / 13.60	2.78 / 3.07
$NiP_2S_8 \cdot$ β-pic	240—250	45—46	12.05 / 12.49	12.87 / 13.19	2.85 / 2.98
$NiP_2S_8 \cdot$ γ-pic	220—250	50—51	12.00 / 12.49	13.48 / 13.19	2.73 / 2.98
$NiP_2S_8 \cdot$ Quin	230—240	40—41	11.88 / 11.60	11.97 / 12.25	2.50 / 2.77
$Fe_2(P_2S_8)_3 \cdot 2y$	80 (pink) 210	36	8.89 / 9.15	15.45 / 15.19	2.32 / 2.28

* Also : C 12.74 (calcd : 13.16) ; H 1.20 (calcd : 1.09)

Complete elemental analysis of the nickel-pyridine compound suggests the composition $NiP_2S_8 \cdot Py$ (see Table 2). Analytical data for other compounds (metal, P and N% content) are also in agreement with similar compositions, i.e. $NiP_2S_8 \cdot$ base (Table 2). The iron compound has the composition $Fe_2(P_2S_8)_3 \cdot 2Py$; on heating it changes from green to pink at 80°C, and decomposes at ca 210°C with evolution of H_2S, leaving a brown residue.

The nickel(II) compounds obtained are fairly stable and can be stored for long time, without apparent decomposition. The iron(III) compound is less stable.

In order to obtain some information about the nature of the compounds obtained, electronic, infrared, ESR (for the iron compound) spectra were recorded and the thermal decomposition was investigated by the thermogravimetric method.

Electronic spectra. The electronic spectra of nickel compounds, recorded both in DMSO solution and in solid state (in KBr pellets) are very similar and the data are shown in table 3.

Table 3

Electronic spectra of $NiP_2S_8 \cdot L$ adducts (cm^{-1})

Ligand (L)		ν_1	ν_2	Charge transfer
pyridine	solution	14,300	21,800	28,300
	solid	14,000	20,500	27,800
β-picoline	solution	15,000	20,500	27,800
	solid	14,000	21,000	27,000
γ-picoline	solution	14,400	22,000	28,000
	solid	14,100	21,100	27,300

The spectra exhibit absorption bands within the visible range at 14,000 — 15,000 cm^{-1}; 20,000 — 22,000 cm^{-1} and a higher intensity band at 27,000 — 28,000 cm^{-1} which can be assigned to charge transfer transitions. These data are in agreement with a coordination of nickel, in which the metal is surrounded by four sulfur atoms in a plane and a nitrogen atom of the tertiary amine coordinated in an apical position of a square pyramid (IV), thus leading to five-coordinate nickel. Probably the structure is polymeric, with cyclic ligand bridging the five-coordinate nickel atoms in an irregular network.

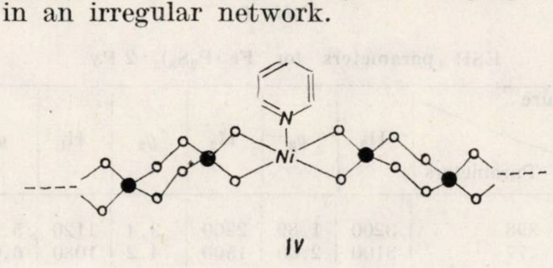

IV

Magnetic properties. The coordination of sulfur to nickel results usually in low spin states, due to high nephelauxetic effect of sulfur, therefore for our nickel(II) compound we expect a singlet state.[23,24] The nickel (d^8) compounds are diamagnetic and ^1H-NMR spectra of the coordinated amine can be recorded in deuterated DMS solutions. Thus, $NiP_2S_8 \cdot Py$ and $NiP_2S_8 \cdot \gamma$-pic exhibited ^1H-NMR spectra, similar to those of the free ligands.[25,26]

$$NiP_2S_8 \cdot Py: \tau = 7.60\,;\ 8.03 \text{ and } 8.70 \text{ ppm.}$$

$$NiP_2S_8 \cdot \gamma\text{-pic}: \tau = 6.18\,;\ 8.01 \text{ ppm.}$$

The iron compound $Fe_2(P_2S_8)_3 \cdot 2Py$ is paramagnetic and its ESR spectrum could be recorded at the room and liquid nitrogen temperature. The spectrum is shown in figure 1 and the *g* parameters are given in table 4

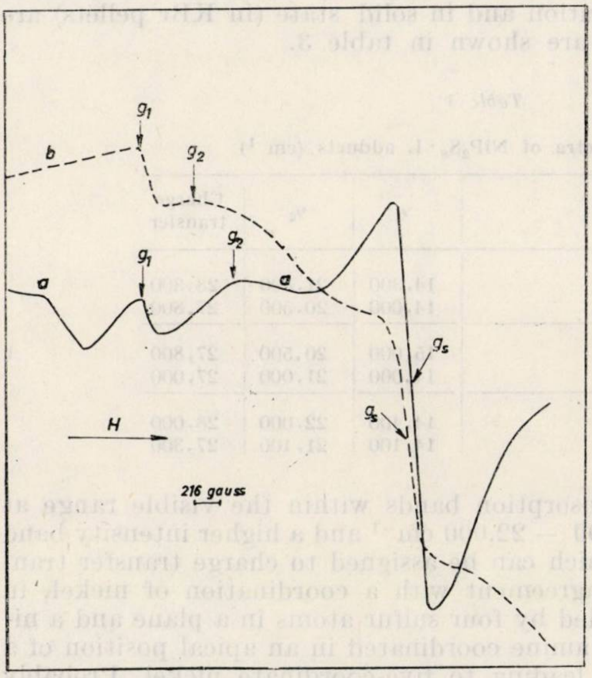

Fig. 1. — ESR spectrum of $Fe_2(P_2S_8)_3 \cdot 2Py$: a) at room temperature ; b) at 77 K.

Table 4

ESR parameters for $Fe_2(P_2S_8)_3 \cdot 2\,Py$

Temperature K / Parameters	H_3	g_3	H_2	g_2	H_1	g_1
398	3200	1.89	2200	3.4	1120	5.42
77	3100	2.00	1500	4.2	1080	6.08

The ESR signals are rather broad, which causes some inaccuracy in determining the value of the g tensor, but the situation is similar to other polycrystalline Fe(III) samples.[27] Their values are within the range which suggests the presence of Fe(III) in the compound studied. [27-29] The g values found for the signal at 77K are in agreement with the theory predictions.[28]

The shape of the ESR spectrum and the g values suggest that the Fe(III) ions do not occupy equivalent positions. The g_1 and g_3 values (Table 4) are in agreement with the presence of an axial symmetry [29] for clustered iron atoms, bonded by two sulfur bridges; a FeS_4N chromophore of C_{4v} local symmetry results. The value of $g \simeq 4$ suggests a rhombic local symmetry [27,30] and a FeS_6 chromophore, i.e. six-coordinated iron.

Infrared spectra. To facilitate the assignment of the absorption bands observed, a normal coordinate analysis for a simplified model (V) containing a S_2PS_2Ni unit was performed. In the calculations the geometry of anion I was used with the molecular dimensions from diffraction data [13] and force constants transferred from dimethyldithiophosphinate anion, $Me_2PS_2^-$ [31] and nickel bis(dimethyldithiophosphinate), $Ni(S_2PMe_2)_2$ [32].

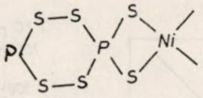

V

The calculated frequencies are not pure or group frequencies but rather combinations of several vibrations modes, as found for other classes of compounds containing the PS_2 group.[31-33] The calculated vibrations are as follows : ν_1 (718 cm^{-1}) — combination of P — S bond stretching in the NiS_2P ring (νPS_4), $\widehat{SPS}$ deformation in the ring (δ PS_4) and (δ PS_6); ν_2(670 cm^{-1}) — combination of νPS_4 with νPS_6 (P —S stretching in the P_2S_6 ring); ν_3 (512 cm^{-1}) — combination of νPS_4, δPS_4, and δPS_6 with a different energy distribution than for ν_1. In addition, the following modes were also obtained: 368 cm^{-1} — combination of νPS_4, νPS_6 and $\delta NiSP$; 347 cm^{-1} — combination of νNiS, δPS_4 and $\delta NiSP$; 281 cm^{-1} — combination of νPS_6, δPS_4 and δPS_6; 276 cm^{-1} — combination of νNiS and $\delta NiSP$.

The observed ν_1 — ν_3 frequencies are listed in table 5, together with their assignment.

It can be seen from table 5 that the experimental values ν_1 are always lower than the calculated ones, the difference being from 1 to 23 cm^{-1}, while ν_2 are larger than expected (with 1 to 30 cm^{-1}); the spread of ν_3 is from -17 to $+13$ cm^{-1} around the calculated value.

Thermogravimetric investigation. The thermogravimetric curves of some of our nickel compounds are shown in figure 2 and their interpretation is given in table 6.

The first process observed is the loss of amine, followed by exothermal oxidation, with stepwise elimination of sulfur, leaving a residue consisting of $Ni_2P_2O_7$ and P_4O_{10}. Part of phosphorus(V) oxide is lost at higher temperatures by sublimation.

Table 5

Calculated and observed infrared absorption bands (cm^{-1})*

Compound	ν_1	$\Delta\nu_1$	ν_2	$\Delta\nu_2$	ν_3	$\Delta\nu_3$
$X = P_2S_8^{2-}$ calculated	718		670		512	
$[Py_2H]_2X$	—	—	670	0	510	− 2
$[\beta\text{-pic}_2H]_2X$	710	− 8	670	0	505	− 7
$[\gamma\text{-pic}_2H]_2X$	713	− 5	680	+10	508	− 4
$[2,6\text{-lutH}]_2X$	717	− 1	700sh	+30	520	+ 8
NiX.Py	695	−23	680	+10	520	+ 8
NiX.β-pic	710	− 8	678	+ 8	495	−17
NiX.γ-pic	710	− 8	—	—	525	+13
NiX · Quin	702	−16	670	0	515	+ 3
$Fe_2X_3.2Py$	712	− 6	682	+12	510	− 2

* $\Delta\nu = \nu_{obs} - \nu_{calcd.}$

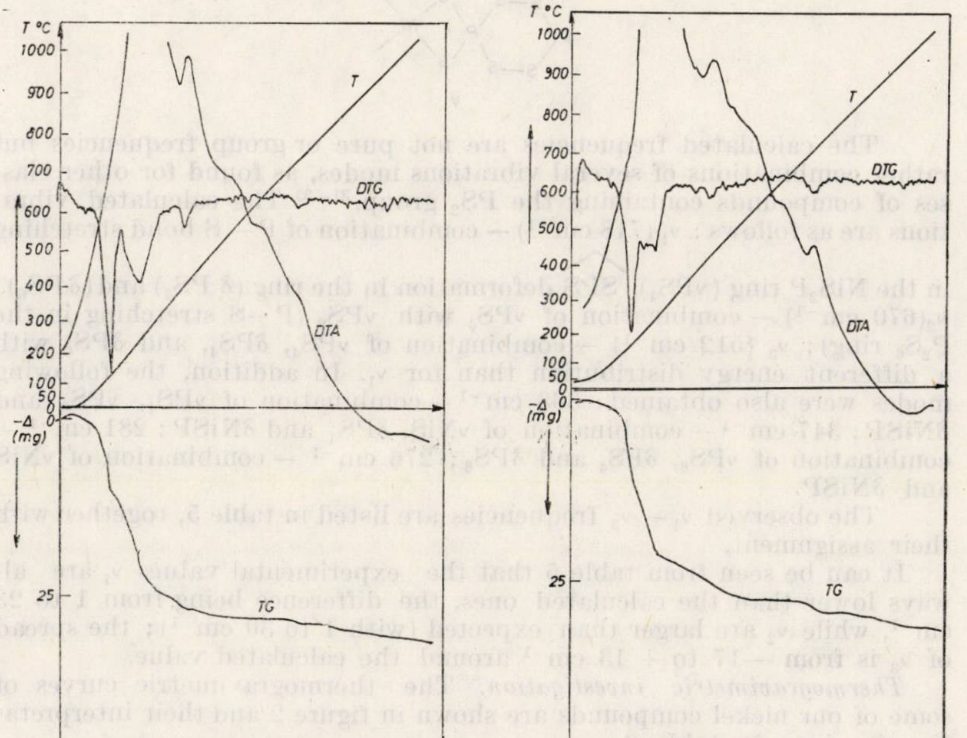

a

b

Fig. 2. — Thermogravimetrical curves : a) NiP_2S_8. Py ; b) NiP_2S_8.(γ-pic).

Table 6

Data of thermogravimetric analysis

Compound	Nature of lost species	Temperature* range °C	Weight loss % found calc.	Residual % found calc.
$NiP_2S_8 \cdot Py$	− pyridine	140	16.00 17.33	—
	− 6S(+ 6O)	250	40.00 38.40	—
	− 2 S	410	51.50 52.44	—
	− P_2O_5	635 710 980	11.50** 4.64***	37.00 36.61
$NiP_2S_8 \cdot \beta$-pic	− β-picoline	140	17.00 19.79	—
	− 6S(+ 6 O)	260	36.00 40.23	—
	− 2S	420	48.00 53.80	—
	− P_2O_5	575 760	20.97** 9.35***	43.00 40.37
$NiP_2S_8 \cdot \gamma$-pic	− γ-picoline	160	17.00 19.79	—
	− 6S(+ 6 O)	250	43.00 40.23	—
	− 2S	430	50.10 53.86	—
	− P_2O_5	615 710	13.90** 4.09***	36.00 35.11

* The processes are all exothermic.

** This corresponds to sublimed P_2O_5 from the sample.

*** This corresponds to P_2O_5 left in the sample.

CONCLUSIONS

From the data obtained it is clear that the cyclic anion $P_2S_8^{2-}$ is able to form some transition metal complexes. The amorphous nature of the products prevents structure determination by diffraction methods and the available spectroscopic data are best understood in terms of an irregular polymeric structure, with five-coordinate nickel atoms or five- and six-coordinate iron atoms, in which the cyclic ligand and additional tertiary amine molecules are attached to the metal. It seems reasonable to assume that nickel is part of a square pyramidal NiS_4N chromophore, with four sulfur atoms at the basal plane. In view of tendency of iron to form iron-sulfur clusters any further assumption about the actual structure of the complex would be pure speculation and we refrain from making further steps in that direction.

ACKNOWLEDGEMENT. The authors are grateful to Dr. I. Silaghi-Dumitrescu for the normal coordinate analysis calculations of the P—S vibrations.

REFERENCES

[1] J. R. Wasson, G. M. Wolterman and J. H. Stoklosa, *Fortschr. Chem. Forsch.*, **35,** 65 (1973).
[2] W. Kuchen and A. Hertel, *Angew. Chem. (Internant. Ed.)*, **8,** 89 (1969).
[3] I. Haiduc, *Revs. Inorg. Chem.*, **3,** 353 (1981).
[4] I. Haiduc, "The Chemistry of Inorganic Ring Systems", Wiley, London, 1970.
[5] I. Haiduc, *Chem. Brit.*, **17,** 330 (1981).
[6] D. B. Sowerby and I. Haiduc, *Inorg. Chim. Acta*, **17,** L15—L16 (1976).
[7] D. B. Sowerby and I. Haiduc, *Inorg. Nucl. Chem. Letters*, **12,** 791 (1976).
[8] S. P. Bone, D. B. Sowerby and I. Haiduc, *J. Chem. Research* (S), **1979,** 69.
[9] R. Micu-Semeniuc, L. Silaghi-Dumitrescu and I. Haiduc, *Inorg. Chim. Acta*, **17,** 5 (1976).
[10] R. Micu-Semeniuc, L. Silaghi-Dumitrescu and I. Haiduc, *Inorg. Chim. Acta*, **19,** 281 (1979).
[11] R. Micu-Semeniuc, L. Silaghi-Dumitrescu, N. Chirilă and I. Haiduc, *Rev. Roumaine Chim.*, **25,** 1025 (1980).
[12] R. Micu-Semeniuc, C. Opriş and I. Haiduc, *Rev. Roumaine Chim.*, **25,** 1489 (1980).
[13] P. C. Minshall and G. M. Sheldrick, *Acta Cryst.*, B, **34,** 1378 (1978).
[14] H. Falius, W. Krause and W. S. Sheldrick, *Angew Chem.*, **93,** 121 (1981).
[15] G. M. Wolf and M. Meisel, *Z. Chem.*, **20,** 452 (1980).
[16] B. Brzezinski and G. Zundel, *Faraday Trans.*, II, **72,** 2172 (1976).
[17] R. Clements and J. L. Wood, *J. Mol. Struct.*, **17,** 265 (1973).
[18] R. Clements, R. L. Dean, T. R. Singh and J. L. Wood, *Chem. Commun*, **1971,** 1125.
[19] B. Brzezinski and M. Szafran, *Roczniki Chem.*, **51,** 1779 (1977).
[20] R. Cements, R. L. Dean and J. L. Wood, *Chem. Comm.*, **1971**, 1127.
[21] F. W. B. Einstein, B. R. Penfold and Q. T. Tapsell, *Inorg. Chem.*, **14,** 186 (1965).
[22] E. Grech, Z. Malarski and L. Sobczky, *Polish J. Chem.*, **52,** 131 (1978).
[23] H. B. Gray in "Transition Metal Chemistry", Edited by R. L. Carlin, E. Arnold Publ., London, 1965 vol. I; 1966, vol. III.
[24] R. Morasi, I. Bertini and L. Sacconi, *Coord. Chem. Rev.*, **11,** 343 (1973).
[25] R. W. Warenhoff, *Canad. J. Chem.*, **43,** 1849 (1965).
[26] J. Abramovitch, *Canad. J. Chem.*, **40,** 2030 (1962).
[27] H. H. Wickman, M. P. Klein and D. A. Shirley, *J. Chem. Phys.*, **42,** 2113 (1965).
[28] T. Castner, G. S. Newel, W. C. Hilton and C. P. Slichter, *J. Chem. Phys.*, **32,** 668 (1960).
[29] D. V. Moon, J. M. Aitke, R. K. MacCrone and G. S. Cielosye, *Physics Chem. Glasses*, **16,** 91 (1975).
[30] R. E. Behringer, *J. Chem. Phys.*, **29,** 573 (1958).
[31] I. Silaghi-Dumitrescu and I. Haiduc, *Rev. Roumaine Chim.*, **25,** 815 (1980).
[32] I. Silaghi-Dumitrescu and I. Haiduc, *Rev. Roumaine Chim.*, **25,** 823 (1980).
[33] W. Rudzinski, G. T. Behnke and Q. Fernando, *Inorg. Chim. Acta*, **16,** 1206 (1977).

Revue Roumaine de Chimie, 28, 6, 615–621 (1983)

COMPLEXES MOLÉCULAIRES DE LA SAFRANINE O

LUMINIȚA PĂUNESCU
Institut Polytechnique, Faculté de Technologie chimique,
Iași, Roumanie

Reçu le: Mars 5, 1982

On a préparé des composés de la safranine O avec le tetraphényle borate de sodium, l'acide picrique, l'ADN, l'ARN et l'acide thiosalicylique. On a effectué pour les nouveaux produits les spectres en IR et UV–VIS. Les données obtenues plaident en faveur de l'obtention des complexes moléculaires proprement dits.

Some compounds of safranine O with : $Na[B(C_6H_5)_4]$, $C_6H_2(NO_2)_3OH$, ADN, ARN, $C_6H_4(SH)COOH$ were prepared and analysed by IR and UV–VIS spectrometry. The obtained compounds can be considered real molecular complexes.

La safranine O fait partie d'une catégorie de substances ayant un substituent phényle sur l'un des atomes d'azote appartenant au noyau central de la phénazine. Ce noyau phénylique, grace à la conjugaison existente entre ses électrons et les électrons p de l'azote phénazinique, peut stabiliser la forme *ortho*-quinoïdique, tandis que le groupement NH_2, présent dans le produit mentionné, peut stabiliser la forme *para*-quinoïdique. On peut donc considérer une résonance entre ces formes, existente malgré la prédominence de la forme p-quinoïdique, conformément aux données fournies par la littérature.[1-3] De plus, la présence de la stucture quinoïdique est soulignée aussi par l'intense coloration de la safranine O, après la théorie Armstrong.[4]

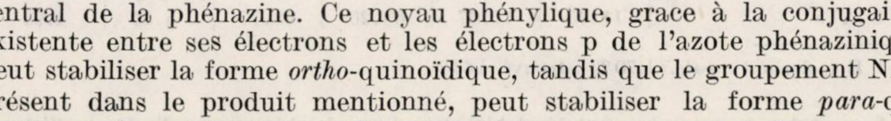

Schéma 1

En solution aqueuse, la safranine O existe comme un cation, donc, il peut réactionner avec des substances formant des anions dans les mêmes conditions.

PARTIE EXPÉRIMENTALE

Nos recherches ont été orientées vers l'obtention des composés de la safranine O avec des différentes substances organiques.

On a utilisé la safranine O produite par Difco Lab., West Molesey, Surrey, U.K. et aussi : $Na[B(C_6H_5)_4]$, l'acide picrique, l'ADN, l'ARN, l'acide thiosalicylique, tous les réactants étant p.a.

Les réactants ont été utilisés sous forme de solutions aqueuses 10^{-1} M, en conservant le pH = 6–7, excepté le dernier cas, quand on a employé un pH = 1 – 2. Après le mélange des solutions, comme résultat de la réaction produite, on a obtenu des précipités qui ont été filtrés, lavés avec de l'eau, alcool éthylique et très peu d'éther éthylique et ensuite, les précipités ont été séchés sous le vide à la température ambiante.

Le tableau 1 présente l'analyse élémentaire des produits obtenus. On peut constater que les résultats sont concordants avec ceux calculés, correspondant à un rapport de combinaison comme celui présenté dans le tableau pour les composés décrits.

Tableau 1

L'analyse élémentaire des composés préparés (l'erreur ne dépasse pas ± 0,5 %)

Composé	N		C		H	
	calc. %	trouvé %	calc. %	trouvé %	calc. %	trouvé %
*$[S.H]\,[B(C_6H_5)_4]$	8,82	8,50	83,27	83,41	6,91	6,33
S·AP	18,04	17,49	57,45	57,12	3,89	3,17
$[S]_x[ADN]_y$		16,82		50,92		4,00
$[S]_x\ [ARN]_y$		16,93		49,50		4,01
S.ATS	11,95	11,07	69,20	68,77	5,16	4,93

* B (colorim.) : calc. 1,70 % ; trouvé 1,63 %.

Les substances préparées sont insolubles dans l'eau, le chloroforme, l'acétone, l'éther éthylique, le tétrachlorure de carbon, le benzène, le nitrobenzène, l'alcool n-butylique, l'alcool isopropylique, l'acétate de butyle, solubles dans 1,2-dichloréthane, le méthyl-éthyl cétone, le cycle héxanone les alcools méthylique et éthylique très solubles dans le propylène- glycol, le DMSO, DMF et le dioxane.

On constate que les composés préparés conservent même dans les solutions (eau : alcool méthylique 1 : 1) le rapport molaire observé pour l'état solide (Fig. 1–2).

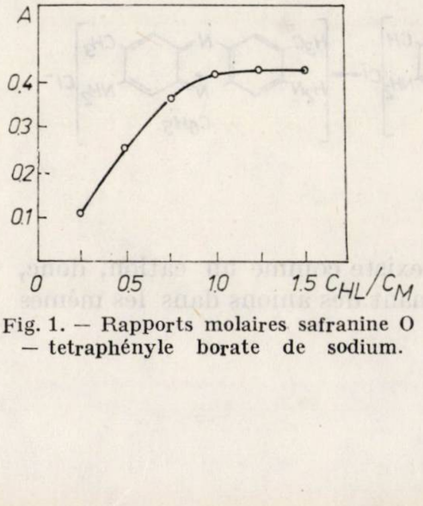

Fig. 1. — Rapports molaires safranine O — tetraphényle borate de sodium.

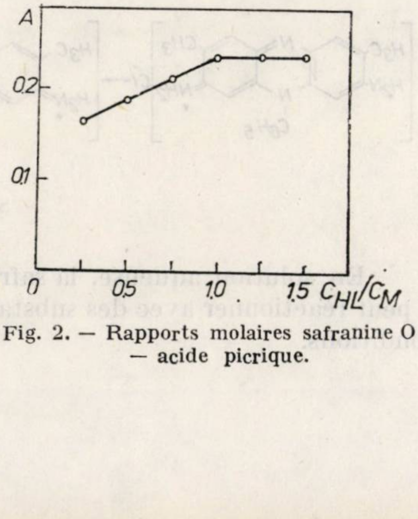

Fig. 2. — Rapports molaires safranine O — acide picrique.

Pour obtenir des informations concernant la nature des produits synthétisés, on a enrégistré leurs spectres IR, employant un spectrophotomètre Perkin-Elmer 577 (200–4000 cm^{-1}), un spectrophotomètre IR Perkin-Elmer 377 (400–4000 cm^{-1}) un spectrophotomètre IR Zeiss-Spekord 71 (700–4000 cm^{-1}) utilisant KBr de pureté spectrale.

En considérant les donnés existentes dans la littérature [5-8] on a pu établir et comparer les bandes ; les résultats figurent dans le tableau 2 (les maximums et les épaulements — entre parenthèses — en cm^{-1}). Les spectres UV–VIS ont été enrégistrés à l'aide d'un spectrophotomètre Unicam SP–800 B un spectrophotomètre UV–VIS Zeiss — Spekord en utilisant le dioxane comme solvent. Le tableau 3 synthètise la présentation des maximums et des épaulements (entre parenthèses ceux-ci) exprimés en nm.

RÉSULTATS ET DISCUSSION

Généralement, l'interprétation des spectres IR appartenant aux molécules polyatomiques (particulièrement dans notre cas) se complique beaucoup par l'accroissement du nombre de degrés de liberté (fonction du nombre des atomes components).

La safranine O a des groupements aminiques primaires mis en évidence par la présence des deux bandes dans la région 3500–3050 cm^{-1} (la littérature donne des renseignements sur les amines primaires [8]), une à 3310–3300 cm^{-1}, et l'autre à 3180–3150 cm^{-1}. On ne doit pas oublier qu'à environ 3298 cm^{-1} existe la bande qui atteste la structure iminique éxocyclique ; [3] elle est visible aussi dans la safranine O que dans les composés préparés, plus évidente pour les spectres IR des composés avec l'ADN, l'acide thiosalicylique et l'ARN. On constate clairement pour tous les composés l'existence de la liaison C=N (pour les azadérivés, elle est mentionnée à 1592–1610 cm^{-1} et à 1518–1520 cm^{-1} avec des variations et supperpositions). [6]

Pour tous les produits préparés on constate la présence des bandes caractéristiques aux phénazines, aussi les déplacements des bandes caractéristiques pour les composés utilisés dans la synthèse.

Prenons comme exemple le composé formé par la safranine O et l'acide picrique. Il est facile à observer le déplacement du doublet caractéristique à l'acide, de 1629, 1608 cm^{-1}[9] à 1620, 1600 cm^{-1} (des bandes fortes). Les bandes attribuées à $\nu_{as(NO_2)}$ et $\nu_{s(NO_2)}$ de l'acide picrique, de 1540 cm^{-1}, respectivement 1350 cm^{-1} se retrouvent déplacées dans le nouveau composé à 1520 cm^{-1} (bande moyenne) et respectivement 1322–1305 cm^{-1} (bande forte) ; la bande caractéristique à l'acide picrique de 3080 cm^{-1}, devient dans le produit très applatie pour 3090–3040 cm^{-1}. La bande moyenne de 3340–3320 cm^{-1}, plus ample et plus déplacée que dans la safranine, plaide en faveur de la présence des liaisons de hydrogène intramoléculaires.

Pour le composé de la safranine O avec l'acide thiosalicylique la liaison C–S donnée dans la littérature [8] à 600–700 cm^{-1} se retrouve ici sous forme d'une bande très forte (à cause de la supperposition avec celle due au cicle phénazinique) à 585 cm^{-1} et une autre moyenne à 669 cm^{-1}. La bande plus faible observée à 2940 cm^{-1} et due à S–H, corresponds aux données fournies par la littérature. [8] Aussi c'est évidente la présence des bandes caractéristiques au carboxyle ionique et pas au groupement COOH (voir la bande forte de 1479 cm^{-1} et celle, plus faible,

Tableau 2

Spectres d'absorption IR

On a noté :
2 — groupement libre NH_2
3 — substituent CH_3 en position 2
4 — liaisons C = N et C = C
5 — caractéristique du noyau phénazinique substitué en position 2
6 — déformations du noyau phénazinique
7 — caractéristique de la substitution de NH_2 en position 2
8 — caractéristique de l'anion dans le composé
9 — caractéristique de l'anion simple

Composé	2	3	4	5	6	7	8	9
$[S.H][B(C_6H_5)_4]$	(3425) 3325 (3200)	(3030) (2910— 2840)	1610 (1600) (1570) (1520) 1480 (1420) (1350) 1321	(875) (825)	(800)	731 701	731 701	740 708
S.AP	(3420) 3340— 3320 3180	2900 2840	1620 1600 (1565) (1540) 1520 1480 1425 (1405) (1370) 1359 1322— 1305	905 880	830— 820 (800)	785 741 (715) 705— 695	1620 1600	1629 1608
$[S]_x[ADN]_y$	3330— 3290 3180— 3120	(2970— 2900)	(1632) 1600 (1520— 1500) 1480 (1450) (1420) (1350) 1320	(910) 880 873	820 800	(780— 770) 745 710 690	1 050	PO_4^{3-} 1080
$[S]_x [ARN]_y$	(3400— 3280) (3180)	(2980— 2900) (2840)	1620— 1590 (1507— 1480) 1470 (1400) (1320)	(940) (880— 870)	825—	770 695	(1100— 1020)	PO_4^{3-} 1080
S.ATS	3320 3300 3160— 3140	(2910— 2900)	(1630) 1600 (1570) (1520— 1500) 1479 1415 (1350) 1330— 1320 (1285)	(885) 870	824 (800)	(760) (740) (730) (710) 690	C—S 669 585 S—H (2940)	C—S 700— 600 S—H pour tio- phénol 2550

Tableau 3

Spectres d'absorption UV – VIS

Composé	Longueurs d'onde maximes	
	complex	réactant anionique
$[S.\ H][B(C_6H_5)_4]$	245	(253)
	272	(260)
$\varepsilon = 22442$ $\lambda = 530$ nm	345	275
	550	(279)
S.AP	(247)	262
	278	(287)
$\varepsilon = 11888$ $\lambda = 530$ nm	375	340
	(435)	420
	537	
$[S]_x[ADN]_y$	248	246
	279	(280)
$\varepsilon = 1000$ $\lambda = 246$ nm	(345)	(325)
	490	
$[S]_x[ARN]_y$	235	253
	(277)	274
$\varepsilon = 1600$ $\lambda = 235$ nm	(334)	(327)
	545	
S.ATS	240	247
	330	304
$\varepsilon = 3400$ $\lambda = 240$ nm	(370)	
	590	

de 1415 cm^{-1}), comme pour la formation d'un complexe genre paires ioniques.

En ce qui concerne les composés formés par la safranine O avec les acides nucléïques (ADN et ARN), les liaisons chimiques produisent des changements conformationaux peu perceptibles dans la constitution de l'ADN, respectivement ARN, avec des rompements des liaisons de hydrogène dans les structures primaire et secondaire [10,11] et avec la formation des deux genres de liaisons [12] : une forte ($K_{asoc} = 10^4 - 10^6$) l'autre faible ($K_{asoc} = 10^3 - 10^4$), sans une certaine spécificité. C'est essentiel à remarquer la présence de la bande caractéristique au PO_4^{3-}, donnée par la littérature [13] à 1080 cm^{-1}; ici, se retrouve pour le composé avec l'ADN à 1050 cm^{-1}, et pour celui avec l'ARN à 1100 – 1020 cm^{-1}. Aussi, la bande caractéristique à $R-O-P \rightarrow O$ existe pour le premier à 1320 cm^{-1} (bande forte) et 1240 – 1230 cm^{-1} (bande moyenne), et pour le deuxième à 1190 cm^{-1} (bande moyenne), respectivement 1320 cm^{-1} (bande moins intense).

On doit souligner pour la majorité des cas, l'apparition d'une bande à environ 1650 cm^{-1}, qui ne peut pas être confondue avec celle de $C=O$, pour les cas où elle existe) qui suggère que l'on peut obtenir des autocomplexes en utilisant la safranine O. [14]

En ce qui concerne les spectres UV – VIS, on peut constater la présence des bandes caractéristiques aux partenaires de réactions, avec les déplacements dus à la réaction, aussi des nouvelles bandes. La bande caractéristique à la safranine O de 523 nm souligne, conformément à la littérature, [3] la présence des espèces protonées de l'azine utilisée ; on ne peut pas dire la même chose pour les composés préparés de la safranine O. On peut penser aux complexes des dérivés moléculaires, après la description des complexes moléculaires (décrits par Mulliken [15]).

Pour tous les composés préparés, on constate la présence de trois grandes régions d'absorbtion, correspondant aux transitions électroniques $\pi - \pi^*$. Malgré les données théoriques de la littérature [16] qui annoncent à longuers d'onde plus grandes l'apparition des transitions $n - \pi^*$, celles-ci semblent être masquées par le troisième groupement de bandes d'absorption, ainsi que les transitions $n - \pi^*$, généralement ne peuvent pas être décelées.[17]

Considérons de nouveau le complexe de la safranine O et l'acide picrique ; l'acide présente les bandes caractéristiques : 262, (287), 340, 420 nm, la safranine O : 243, 277, 523 nm, tandis que pour le complexe, elles existent à : (247), 278, 375, (435), 537 nm, donc des déplacements évidents. Les premières bandes peuvent être attribuées aux transition électroniques $\pi_{\text{cicle}} \rightarrow \pi^*_{NO_2}$, $\pi_{NO_2} \rightarrow \pi^*_{NO_2}$, la troisième, au transfert des charge intermoléculaire caractéristique au complexe $n_{N([S.H]^+Cl^-)} \rightarrow \rightarrow \pi_{NO_2(AP)}$ (voir la littérature [18]). Pour la dernière bande, très intense, considérée pour les azadérivés [19] donnée par la transition $n - \pi^*$,[16] visible aussi pour la safranine O que pour ses complexes, comme on a mentionné déjà on peut affirmer qu'elle est présente par une supperposition (l'absorbtion du groupement III — la troisième région d'absorption $\pi - \pi^*$ [16] — avec la transition $n \rightarrow \pi^*$). De ce point de vue, la situation est analogue aussi pour [S.H] $[B(C_6H_5)_4]$.

En ce qui concerne le préparé avec l'acide thiosalicylique, on constate que si les acides aromatiques présentent deux bandes benzénoïdes plus importantes, ${}^1B_{2u} \leftarrow {}^1A_{1g}$ et ${}^1B_{1u} \leftarrow {}^1A_{1g}$, et aussi une troisième, la bande primaire seconde, très peu évidente $({}^1E_{1u} \leftarrow {}^1A_{1g})$[20] généralement retenant [21,22] seulement la bande de 255 nm, dans le nouveau composé existent les trois bandes avec les déplacements attendus, de plus, l'épaulement de 370 nm, dénotant la formation d'un nouveau produit.

Quand aux acides nucléiques, on constate, sans une grande évidence, la diffusion des bandes, ce qui [23] est compris en termes de perturbation $3\pi\pi^* \leftarrow {}^3n\pi^*$. Pour les composés de la safranine O avec les acides nucleiques, si comme on a mentionné existent deux genres de liaisons des azadérivés avec l'acide nucleique, on considère : [24] les molécules fortement liées sont conçues à être intercalées entre les paires de base successive du hélix, et celles liées faiblement sont conjecturées à être attachées à l'extérieur du hélix par interactions électrostatiques avec les groupements fosfatiques de l'acide nucleique. Spectroscopiquement, il s'agit seulement de deux éspèces de composés liés : le monomère et les dimère. Les spectres UV—VIS plaident, par le déplacement hypsocrome du maximum d'absorbtion dans la région visible du spectre des composés préparés, pour la dimérisation. [25] Ce serait compatible avec un model « sandwich » modifié, pour lequel la supperposition des molécules de l'azaderivé serait incomplète pour permettre l'intercalation d'un des partenaires. Mais toujours, la compréhension du moyen de liaison, aussi que l'effect sur les acides nucléiques est déficitaire jusqu'à présent.

En considérant les spectres IR et aussi UV—VIS, avec le déplacement des bandes appartenant aux composants, et aussi l'apparition des nouvelles bandes (voir le tableau 3), on peut affirmer que les substances formées avec les dérivés organiques peuvent être associés à la catégorie des vrais complexes moléculaires.

BIBLIOGRAPHIE

[1] R. C. Elderfield, « Heterocyclic Componnds », vol. 6, Willey, London, 1957,p. 654—680.

[2] C. Balls, H. Hewitt et A. Newman, *J. Chem. Soc.*, **101**, 1840 (1912) ;
H. Hewitt, A. Newman et J. Winmill, *J. Chem. Soc.*, **95**, 577 (1909).

[3] J-Fernando, W. S. Morgan et J. W. Hausser, *J. Org. Chem.*, **32**, 423 (1967).

[4] K. Venkataraman, « Organic and Biological Chemistry. The Chemistry of Synthetic Dyes », vol. 1, Edit. Fieser, Academic Press, New York, 1952, p. 323—400.

[5] L. J. Bellamy, « The Infrared Spectra of Complex Molecules », (2-nd. Ed) Methuen, London, 1958, p. 277.

[6] C. Stammer et A. Taurins *Spectrochim. Acta*, **19**, 1625 (1963).

[7] H. H. Perkampus et E. Baumgarten, *Z. Elektrochemie*, **64**, 951 (1960).

[8] M. Avram et Gh. D. Mateescu, « Spectroscopia în infraroșu. Aplicații în chimia organică », Edit. Tehnică, București, 1966.

[9] Landolt-Börnstein, « Physikalisch-Chemische Tabellen » 3 Teil, 1951.

[10] M. Tsuboi, « Infrared and Raman Spectroscopy » (« Basic Principles in Nucleic Acids »), vol. 1 Pop Tso Ed., Academic Press, New York, 1974, p. 399—452.

[11] T. Theophanides *Appl. Spectroscopy*, **35**, 461 (1981).

[12] U. Hollstein, et R. J. VAN GEMERT JR., *Biochemistry*, **10**, 497 (1971).

[13] Nakamoto, «Infrared Spectra of Anorganic and Coordination Compounds, Willey, New York, 1966.

[14] F. Guttman et H. Keyser, *Agressologie*, **9**, 27 (1968).

[15] R. S. Mulliken, *J. Amer. Chem. Soc.*, **74**, 811 (1952).

[16] G. M. Badger et I—S. Walker, *J. Chem. Soc.*, (1956), 122.

[17] A. R. Katritzki, « Physical Methods in Heterocyclic Chemistry », Academic Press, New York, 1963, p. 20—45.

[18] R. Merrifield et W. Phillips, *J. Amer. Chem. Soc.*, **80**, 2778 (1958).

[19] H. Hirt et A. Schmidt, *J. Chem. Phys.*, **23**, 600 (1955).

[20] H. H. Jaffé et M. Orchain, « Theory and Applications of Ultraviolet Spectroscopy », Willey, New York, 1964.

[21] I. Pogany et M. Banciu, « Metode fizice în chimia organică », Edit. Științifică, București, 1972.

[22] C. Baloescu et M. Sterescu, « Metode spectrofotometrice de absorbție aplicate la controlul medicamentelor », Edit. Medicală, București, 1975.

[23] R. M. Hochstrasser et C. Marzacco, *J. Chem. Phys.*, **49**, 971 (1968).

[24] R. W. Armstrong, T. Kurucsev, et U. P. Strauss, *J. Amer. Chem. Soc.*, **92**, 3174 (1970).

[25] Z. Balcarova, V. Kleinwächter, M. Waring, L. P. Wakelin et G. Loeber *Stud. Biophys.*, **60**, 119 (1976).

Revue Roumaine de Chimie, 28, 6, 623–629 (1983)

SOME REACTIONS OF MICHAEL ADDUCTS OF α-CYANO-β-BENZOYL-β-PHENYL ETHYL ACRYLATE WITH KETONES

A. A. HAMED, A. ESSAWY, A. F. SHABAN and I.A.G. El-KARIM

Chemistry Department, Faculty of Science, Zagazig University, Zagazig, Egypt

Received July 4, 1981

The reaction of α-cyano-β-benzoyl-β-phenyl ethyl acrylate (**1**) with ketones, namely benzyl methyl ketone, dibenzyl ketone and acetophenone in the presence of sodium methoxide gave the corresponding 1,5-diketones **2a–c**. Michael addition of phenyl benzyl ketone to ester **1** and subsequent cyclization in the presence of sodium methoxide gave 4-carboxy-2, 3, 5, 6-tetraphenyl pyran (**3**), while in the presence of alc. KOH gave 4-carboxy-4-cyano-2,3,5,6-tetraphenyl pyran (**4**). The 1,5-diketone **2a** underwent reactions with hydrazines, amines, hydroxylamine hydrochloride and Grignard reagents to give compounds **8a–c, 9, 10, 11a–d, 12, 13a–c** and **14a–b** respectively. Reaction of ester **1** with ethyl cyanoacetate in the presence of ammonium acetate at 160°C, gave the dihydropyridine derivative **5.** Reaction of **1** with ethyl acetoacetate in the presence of ammonium acetate at 160°C gave adducts **6** and **7.**

In continuation of our previous studies, [1–4] we report in this paper on the reactions of α-cyano-β-benzoyl-β-phenyl ethyl acrylate (**1**) with ketones in the presence of sodium methoxide, and with ethyl cyanoacetate and ethyl acetoacetate in the presence of ammonium acetate.

As a point of interest, it has been found that the ester **1** reacted with ketones under Michael conditions in a similar mechanistic pathway to α, β-unsaturated ketones. Thus ester **1**, reacted with benzyl methyl ketone, dibenzyl ketone and acetophenone in the presence of sodium methoxide to give the corresponding 1,5-diketones (**2a–c**). Michael addition of phenyl benzyl ketone to ester **1** and subsequent cyclization in the presence of sodium methoxide lead to the formation of 4-carboxy-2, 3, 5, 6-tetraphenyl pyran (**3**), while in the presence of alcoholic potassium hydroxide, Michael addition of phenyl benzyl ketone to ester **1** gives 4-carboxy-4-cyano-2,3,5,6-tetraphenylpyran (**4**).

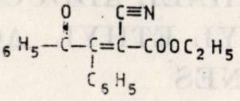

$C_6H_5-\overset{O}{\overset{\|}{C}}-\underset{C_6H_5}{\underset{|}{C}}=\overset{C\equiv N}{\overset{|}{C}}-COOC_2H_5$

1

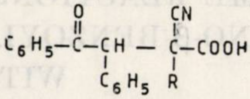

$C_6H_5-\overset{O}{\overset{\|}{C}}-\underset{C_6H_5}{\underset{|}{CH}}-\overset{CN}{\underset{R}{C}}-COOH$

2

a, R = $CHPhCOCH_3$
b, R = $CHPhCOCH_2ph$
c, R = CH_2COPh

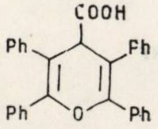

3

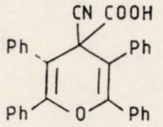

4

The infrared spectra of **2** showed bands characteristic of aroyl carbonyl system at 1660 cm^{-1}, carboxylic carbonyl at 1700 cm^{-1}, $C\equiv N$ at 2220 cm^{-1} and OH at 3300 cm^{-1}. The infrared spectrum of **3** showed the absence of $C\equiv N$ but exhibited ν(CO) carboxylic at 1670 cm^{-1} and ν(OH) carboxylic at 3400 cm^{-1}. The ^1H-NMR spectrum* of **3** showed signals at 5.1—5.3 (*m*, 1H, $>CH-COOH$) and 7.2—7.8 (*m*, 20 H, Ar—H).

The infrared spectrum of **4** exhibited bands at 1690 cm^{-1} (CO carboxylic), 2200 cm^{-1} ($C\equiv N$) and 3340 cm^{-1} (OH carboxylic). The ^1H-NMR of **4** showed signals at 6.7—7.8 (*m*, 20 H, Ar—H) and 8.4 (*s*, 1H, —COO*H*).

Pyridone or hydropyridone derivatives could be synthesized by reaction of **1** with active methylene substrates in the presence of ammonium acetate at 160°C. It has been found that α-cyano-β-benzoyl ethyl cinnamate (**1**) underwent the same mechanistic pathway as in the case of α, β-unsaturated ketones (specially chalcones) to give the corresponding pyridone derivatives. Thus reaction of **1** with ethyl cyanoacetate in the presence of ammonium acetate at 160°C gave the corresponding dihydropyridone derivative **5**. On the other hand compound **1** reacted with ethyl acetoacetate in the presence of ammonium acetate at 160°C to give 3-acetyl-1,2-dihydro-2-oxo-5,6-diphenyl isonicotinamide (**6**) as major adduct together with the minor adduct **7**. The structure of **5** was supported by the infrared spectrum showing bands at 1700 cm^{-1} (CO carboxylic), 1625 (CO cyclic pyridone), 2220 ($C\equiv N$) and 3400 cm^{-1} (NH). The structure of **6** was established with the help of infrared spectrum showing bands at 1680 cm^{-1} (CO acetyl), 1660 cm^{-1} (CO cyclic pyridone), 1640 cm^{-1} (CO amide) and 2930 cm^{-1} (NH). The structure of **7** was established on the basis of infrared spectrum ($\nu(C=O)$ cyclic pyrrolone at 1740 cm^{-1}, $\nu(C=O)$ cyclic pyridone at 1680 cm^{-1}, $\nu(C=N)$ at 1620 cm^{-1} and $\nu(NH)$ at 3240 cm^{-1}).

---

* ^1H-NMR chemical shifts δ in ppm throughout the paper.

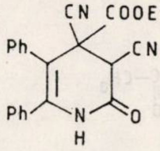

5

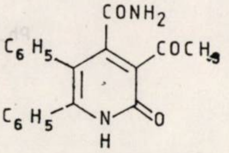

6

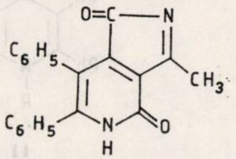

7

Treatment of 1,5-diketone **2a** with hydrazines, namely hydrazine hydrate, phenyl hydrazine and *p*-nitrophenylhydrazine gave the corresponding pyrazoline derivatives (**8a**—**c**). On the other hand it has been found that the reaction of **2a** with phenylhydrazine gave two other products considered to be the pyridazin-3-one derivatives **9** and **10**.

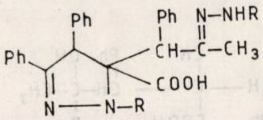

8

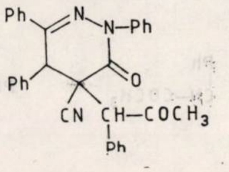

9

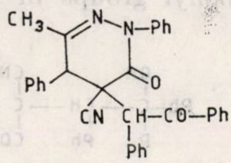

10

a, $R = H$
b, $R = C_6H_5$
c, $R = C_6H_4-NO_2$-*p*

The infrared spectrum of **8c** showed the absence of $\nu C \equiv N$ but exhibited bands at 1700 — 1600 and 3400 cm^{-1} for $C = O$ carboxylic, $C = N$, NH and OH respectively. The infrared spectrum of **9** showed the carbonyl stretching frequency of cyclic amides at 1690 cm^{-1}, $C = N$ stretching frequency at 1620 cm^{-1}, carbonyl stretching frequency of acetyl at 1670 cm^{-1}. As a point of interest, **2a** reacted with amines, namely, methyl amine, benzyl amine, *p*-toluidine and *o*-chloroaniline and gave the corresponding pyridine derivatives **11a**—**d**. The infrared spectrum of **11d** exhibited bands at 1700, 2240 and 3400 cm^{-1} for CO, $C = N$ and OH groups respectively. The ^1H—NMR spectrum of **11a** showed signals at 1.4 (*s*, 6H, $2-CH_3$) and 7.35 (*m*, 15H, Ar—H).

The 1,2-oxazin-6-one derivative **12** was obtained by condensation of the 1,5-diketone **2a** with hydroxyl amine hydrochloride in boiling pyridine. The infrared spectrum of **12** is characterised by bands at

1 700 cm^{-1} (CO cyclic), 1680 cm^{-1} (carbonyl acetyl), 1630 cm^{-1} ($C=N$) and at 2240 cm^{-1} ($C\equiv N$).

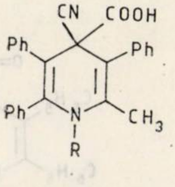

11

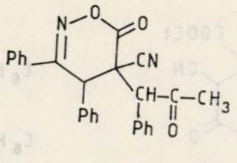

12

a, $R = CH_3-$
b, $R = C_6H_5-CH_2-$
c, $R = C_6H_4-CH_3\text{-}p$
d, $R = C_6H_4 - Cl\text{-}o$

The reaction of 1,5-diketone **2a** with Grignard reagents such as ethylmagnesium iodide, phenyl- and *p*-anisylmagnesium bromides gave the adducts **13a**—**c** *via* addition to carbonyl of benzoyl group. Likewise, other products **14a** and **14b** were obtained *via* the addition of ethylmagnesium iodide and phenylmagnesium bromide to the acetyl and benzoyl carbonyl groups in 1,5-diketone **2a**.

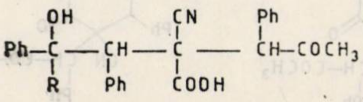

$$Ph-\underset{R}{\overset{OH}{C}}-\underset{Ph}{CH}-\underset{COOH}{\overset{CN}{C}}-\overset{Ph}{CH}-COCH_3$$

13

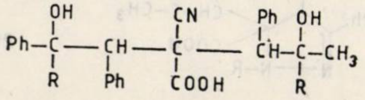

$$Ph-\underset{R}{\overset{OH}{C}}-\underset{Ph}{CH}-\underset{COOH}{\overset{CN}{C}}-\overset{Ph}{CH}-\underset{R}{\overset{OH}{C}}-CH_3$$

14

a, $R = C_2H_5$
b, $R = C_6H_5$
c, $R = C_6H_4 . OCH_3\text{-}p$

a, $R = C_2H_5$
b, $R = C_6H_5$

The infrared spectrum of compound **13a** showed bands characteristic of $C=O$ carboxylic at 1700 cm^{-1}, $\nu(C=O)$ acetyl at 1780 cm^{-1}, $\nu(OH)$ alcoholic at 3320 cm^{-1}, ν OH carboxylic at 3380 cm^{-1} and $\nu(C\equiv N)$ at 2240 cm^{-1}. The ^1H-NMR spectrum of **13c** showed signals at 1.0(*s*, 3H, $-OCH_3$), 2.0(*s*, 3H, $-COCH_3$), 3.5—4.0 (*s*, 2H, $2-\overset{|}{C}H$-ph) and 6.7—7.9 (*m*, 19H, Ar—H). The infrared spectrum of **14b** showed $\nu(CO)$ carboxylic band at 1700 cm^{-1}, $\nu(C\equiv N)$ at 2220 cm^{-1}, OH alcoholic at 3300 cm^{-1} and $\nu(OH)$ carboxylic at 3400 cm^{-1}.

EXPERIMENTAL

All the melting points are uncorrected, IR spectra were carried out using KBr on a Pye Unicam SP 1200 spectrometer, and ^1H-NMR spectra were determined on 5% solutions in $CDCl_3$, dimethyl sulphoxide at 40 MHz with a Varian associates Model V 4300 B. Spectrometer using tetramethyl silan as internal reference.

Reaction of (1) with ketones in NaOMe : formation of 2a–c

A solution of **1** (0.01 mole) and ketones, namely benzyl methyl ketone, dibenzyl ketone or acetophenone (0.01 mole) in methanol (30 ml) was treated with sodium methoxide (0.03 mole). The reaction mixture was refluxed for 4 hrs, then cooled down at room temperature and poured on hydrochloric acid and water. The precipitate which was separated out as a solid was washed with water, dried and crystallized from the proper solvent to give **2a-c** (Table 1).

Table 1

Characterisation of compounds **2a–c, 3, 4, 5, 6, 7, 8a–c, 9, 10, 11a–d, 12, 13a–c, 14a** and **14b**

Compound	m.p. °C	Solvent* Yield (%)	Formula	Analysis (%)	
				Found	Calculated
2a	165	B/P 45	$C_{26}H_{21}NO_4$	C 75.67 H 5.25	75.91 5.11
2b	162	P 50	$C_{32}H_{25}NO_4$	C 78.41 H 5.36	78.85 5.13
2c	160	B/P 40	$C_{25}H_{19}NO_4$	C 75.13 H 5.18	75.57 4.79
3	210	B 50	$C_{30}H_{22}O_3$	C 83.48 H 5.16	83.72 5.12
4	273	P 60	$C_{31}H_{21}NO_3$	C 82.00 H 4.63	81.76 4.62
5	180	B 60	$C_{22}H_{17}N_3O_3$	C 71.30 H 4.66	71.16 4.58
6	222	B 50	$C_{20}H_{16}N_2O_3$	C 72.03 H 4.87 N 8.74	72.29 4.82 8.43
7	85	P 10	$C_{20}H_{14}N_2O_2$	C 76.33 H 4.84 N 8.91	76.43 4.46 8.92
8a	180	B/P 60	$C_{25}H_{24}N_4O_2$	C 71.02 H 5.86	72.82 5.83
8b	75	P′ 40	$C_{37}H_{32}N_4O_2$	C 78.78 H 5.89	78.72 5.67
8c	185	P 55	$C_{37}H_{30}N_6O_6$	C 67.88 H 4.27	67.89 4.59
9	165	P 20	$C_{32}H_{25}N_3O_2$	C 79.32 H 5.13 N 8.63	79.50 5.18 8.69
10	185	B 15	$C_{32}H_{25}N_3O_2$	C 79.87 H 5.36 N 8.62	79.50 5.18 8.69
11a	145	P 40	$C_{27}H_{22}N_2O_2$	C 79.07 H 5.47	79.80 5.42

Table 1 (continued)

Compound	m.p. °C	Solvent* Yield (%)	Formula		Analysis (%) Found	Calculated
11b	125	P′ 50	$C_{33}H_{26}N_2O_2$	C H	82.25 5.58	82.16 5.39
11c	140	B/P 55	$C_{33}H_{26}N_2O_2$	C H	82.55 5.41	82.16 5.39
11d	150	B/P 45	$C_{32}H_{33}N_2O_3Cl$	C H	76.38 5.58	76.49 4.58
12	195	B 60	$C_{26}H_{20}N_2O_3$	C H	76.79 4.86	76.47 4.90
13a	135	P 30	$C_{28}H_{27}NO_4$	C H	76.22 6.20	76.19 6.12
13b	195	P′ 35	$C_{32}H_{27}NO_4$	C H	78.48 5.14	78.52 5.52
13c	220	B/P 45	$C_{33}H_{29}NO_5$	C H	76.20 5.22	76.30 5.58
14a	210	B 15	$C_{30}H_{33}NO_4$	C H	76.37 7.19	76.43 7.00
14b	185	E 10	$C_{38}H_{33}NO_4$	C H	80.19 5.78	80.42 5.82

* B = benzene ; B/P = benzene/light petrol (80—100°) ; P = light petrol (100—120°) ; P′ = light petrol (60—80°C) and E = ethanol.

Synthesis of 4-carboxy-2, 3, 5, 6-tetraphenylpyran (3)

a — A solution of **1** (0.01 mole) and phenyl benzyl ketone (0.01 mole) in warm methanol (70 ml) was allowed to cool at room temperature and potassium hydroxide (3 g, dissolved in one drop of water and 6 ml of ethanol) was added to it. The solution was shaken vigorously for 30 minutes and left at room temperature overnight. The solid thus obtained was filtered, washed with water, and crystallized from an appropriate solvent to give compound **3** (Table 1).

b — A solution of **1** (0.01 mole) and phenyl benzyl ketone (0.01 mole) in methanol (30 ml) was treated with sodium methoxide (0.02 mole). The solution was shaken for 30 min and left at room temperature overnight. The separated solid was crystallized from a proper solvent to give compound **3** (Table 1).

Synthesis of 4-carboxy-4-cyano-2, 3, 5, 6-tetraphenylpyran (4)

To a solution of **1** (0.01 mole) in alcoholic potassium hydroxide 10%, phenyl benzyl ketone (0.01 mole) was added and the reaction mixture was refluxed on water bath for 1 hr. The reaction mixture was cooled down at room temperature then poured on water. The mixture was boiled until a brown oil was separated. The water layer was then removed and the oil was treated with methanol. An orange solid separated which was then filtered, dried and crystallized from a suitable solvent to give compound **4** (Table 1).

Reaction of 1 with esters in ammonium acetate; formation of 5, 6 and 7

A mixture of **1** (0.01 mole), ester (0.01 mole) namely ethyl cyanoacetate or ethyl acetoacetate and ammonium acetate (0.03 mole) was heated at 160°C for 6 hrs, and cooled. The solid that separated was filtered, washed with water, dried and crystallized from the proper solvent to give adducts **5**, **6** and **7** respectively (Table 1).

Reaction of 2a with hydrazines; formation of 8a-e, 9 and 10

A solution of **2a** (0.01 mole) in ethanol (50 ml) was tceated with hydrazine hydrate, phenylhydrazine or *p*-nitrophenylhydrazine (0.01 mole). The solution was heated to boiling for 6 hrs. The product obtained after cooling was crystallized from a suitable solvent to give products **8a**–**e**, **9** and **10** (Table 1).

Action of amines on 2a; formation of pyridine derivatives 11a–d

A mixture of **2a** (0.01 mole), amines (0.01 mole) and ethanol (50 ml) was refluxed for 6 hrs, cooled, acidified by 1 N hydrochloric acid. The solid that separated was filtered, washed with water, dried and crystallized from a proper solvent to give compounds **11a**–**d** (Table 1).

Reaction of 2a with] hydroxylamine hydrochloride; formation of 1, 2-oxazin-6-one derivative 12

A mixture of **2a** (0.01 mole), pyridine (20 ml), hydroxylamine hydrochloride (0.02 mole) and water (2 ml) was refluxed for 10 hrs. The cooled mixture was poured into ice cold dilute hydrochloric acid and the product obtained was crystallized from the suitable solvent to give compound **12** (Table 1).

Reaction of 2a with Grignard reagents; formation of 13a–e, 14a and 14b

A solution of **2a** (0.01 mole) in ether was added to an ethereal solution of ethyl magnesium iodide, phenyl or *p*-anisyl magnesium bromide (0.02 mole). After refluxing the reaction mixture for 3 hrs, it was worked-up as usual to give an oil which was triturated with light petrol and crystallized from a proper solvent to give adducts **13 a**–**e**, **14a** and **14b** (Table 1).

REFERENCES

A. Sammour, M.I.B. Selim, A. Essawy and M. El-Kasaby, *Egypt J. Chem.*, **16**, 197 (1973).

A. Essawy and A. A. Hamed, *Indian J. Chem.*, **16**, 880 (1978).

M. A. El-Hashash and A. Essawy, *Indian J. Chem.*, **17**, 454 (1979).

M. Abdalla, A. Essawy and A. Deep, *Pakistan J. Sci. Ind. Res.*, **20**, 139 (1977).

A. Essawy, M. El-Garby Younes and A.Z.M. Heikal, *Rev. Roumaine Chim.*, (accepted for publication).

Revue Roumaine de Chimie, 28, 6, 631–639 (1983)

HETEROCYCLENSYNTHESEN MIT KOHLENSÄURE-DERIVATEN. IV[1]

KINETIK UND MECHANISMUS DER BILDUNGSREAKTION VON 2-AMINO-5-ARYL-1,3,4-OXADIAZOLEN AUS BENZOESÄURE-HYDRAZIDEN UND ARYLCYANATEN

HANS-HORST GLATT, RADU BACALOGLU, SADIQ A. SALEH, DAGMAR SZEIBERT
und VERONICA SZENAȘI

Polytechnisches Institut „Traian Vuia“ Timișoara, Laboratorium für Organische Chemie, Str. Bocșei 6, 1900 Timișoara, Rumänien

Eingegangen am 8. März 1982

Die Gechswindigkeitskonstanten zweiter Ordnung der 2-Amino-5-aryl-1,3,4-oxadiazolbildung aus kernsubstituierten Benzoesäurehydraziden und Arylcyanaten wurden in dioxanischer Lösung UV-spektroskopisch bestimmt. Im langsamen Schritt der Reaktion findet der nucleophile Angriff des Carboxyl-O-Atoms des Acylhydrazins an das Nitril--C-Atom des Arylcyanates statt. Durch rasche Phenoleliminierung bildet sich das stabile Endprodukt 2-Amino-5-aryl-1,3,4-oxadiazol.

Second order rate constants for the 2-amino-5-aryl-1,3,4-oxadiazole formation from substituted benzoic acid hydrazides and aryl cyanates have been determined in dioxane. In the slow step of the reaction the nucleophilic attack of the acylhydrazine carboxy-O-atom at the aryl cyanate nitrile C-atom takes place, followed by rapid phenol elimination whereby 2-amino-5-aryl-1,3,4-oxadiazole is obtained as a stable product.

Benzoesäurehydrazide reagieren mit Phenylcyanat unter Phenolabspaltung zu den entsprechenden 2-Amino-5-aryl-1,3,4-oxadiazolen **1** :[1–3]

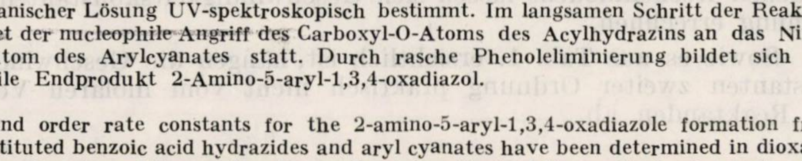

1

In keinem der untersuchten Fälle konnten offenkettige Additionsprodukte abgefangen werden. Zwischenstufen konnten nur im Falle der Addition von 2,2,2-Trichlor – und bzw. 2,2,2-Tribrom-ethylcyanat zu Carbonsäurehydraziden isoliert werden, [3] wobei diese als N′-Carbimidoylcarbonsäurehydrazide **2** formuliert wurden:

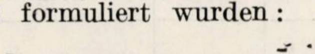

$$R_1-\underset{\underset{O}{\|}}{C}-NH-NH-\underset{\underset{NH}{\|}}{C}-O-Ph$$

2

Die Kinetik der 2-Amino-1,3,4-oxadiazolbildung wurde bisher nur für die Cyclisierung der Acyl(aroyl)hydrazine [4-6] und bzw. 4-Arylsemicarbaziden [7] mit Bromcyan untersucht.

In einer vorangehenden Arbeit dieser Reihe [1] haben wir die präparative Untersuchung der Reaktion der Carbonsäurehydrazide mit Phenylcyanat vorgenommen und waren daher auch an der Kinetik und dem Mechanismus dieser Cyclisierung interessiert.

ERGEBNISSE UND DISKUSSION

Die Reaktionen der Benzhydrazide (0,0197—0,0426 mol) mit Arylcyanaten (0,0196 — 0,0227 mol) wurden in wasserfreiem oder wasserhaltigem Dioxan ($[H_2O] = 0 - 4$ mol) ausgeführt. In diesen Bedingungen bilden sich als einzige Reaktionsprodukte die entsprechenden 2-Amino-5-aryl-1,3,4-oxadiazole und Phenole (siehe Versuchsteil).

Die Reaktionen wurden UV-spektroskopisch verfolgt, anhand der B-Bande des aromatischen Benzolringes, die im Falle der 5-substituierten 2-Amino-1,3,4-oxadiazole um 275 — 320 nm (molarer Extinktionsfaktor 11000 — 21000 [1]) erscheint.

Die Kinetik dieser Reaktion ist bimolekular und anhand eines einfachen Rechenmodells lassen sich Geschwindigkeitskonstanten zweiter Ordnung errechnen.

Sowie es aus Tab. 1. ersichtlich ist, hängen die Geschwindigkeitskonstanten zweiter Ordnung praktisch nicht vom molaren Verhältnis der Reaktanden ab.

Tab. 1

Geschwindigkeitskonstanten zweiter Ordnung für die Reaktionen des Benzoesäurehydrazids mit Phenylcyanat, bei 45° in Dioxan bei verschiedenen molaren Verhältnissen der Reaktanden

$[PhCONHNH_2]$ mol 10^3	$[PhOCN]$ mol 10^3	$\frac{[PhCONHNH_2]}{[PhOCN]}$	k_2 [1/mol min]
19,67	19,96	1,00	1,1596
20,04	20,04	1,00	1,1988
22,42	22,73	1,00	1,0088
16,58	14,20	1,17	0,9610
23,54	19,79	1,19	0,8722
35,16	28,19	1,25	0,8636
25,91	19,92	1,30	0,8289
29,76	19,85	1,50	0,8505
35,67	19,81	1,80	0,8321
42,56	20,08	2,12	0,8414
			$k_{2\,\mathrm{med}} = 0{,}942 \pm 0{,}019$

In Tab. 2. sind die für den Fall der Reaktionen des Benzoesäurehydrazids mit verschiedenen Arylcyanaten in wasserfreiem Dioxan bei

Tab. 2

Bei 45° in Dioxan bestimmte Geschwindigkeitskonstanten zweiter Ordnung der Reaktion des Benzoesäurehydrazids mit Arylcyanaten

X−	σ^{0}*	$[PhCONHNH_2]$ mol 10^3	$[X\text{-}C_6H_4OCN]$ mol 10^3	k_2 [l/mol min]
m-Cl−	0,37	20,00	20,13	5,9603
p-Cl−	0,27	20,18	20,10	3,7571
H−	0,00	20,04	20,04	1,1988
m-CH_3−	−0,07	20,00	20,04	1,1045
p-CH_3−	−0,12	19,81	19,69	0,9619
p-CH_3O−	−0,16	20,00	20,03	0,8409

* Daten aus.[8]

45° bestimmten Geschwindigkeitskonstanten eingetragen. Die entsprechende Hammett-Korrelation ist linear und von folgender Gleichung:

$$\lg k_2 = 1{,}606\ \sigma^0 + 0{,}152\ (r = 0{,}994)$$

Der positive Wert des Parameters ρ aus dieser Gleichung zeigt, dass im langsamen Schritt der Reaktion der elektrophile Angriff des Arylcyanates an das Benzoesäurehydrazid stattfindet. Der absolute Betrag dieses Parameters — 1,61 — ist mit dem für andere Cyclisierungen erhaltenen ρ-Werten vergleichbar (1,50 —1,90).[9–11]

In Tab. 3. sind die für den Falle der Reaktionen der kernsubstituierten Benzhydrazide mit Phenylcyanat bestimmten Geschwindigkeitskonstanten zweiter Ordnung eingereiht. Die Hammett-Korrelierung ist linear und entspricht folgender Gleichung:

$$\lg k_2 = -0{,}357\sigma + 0{,}063\ (r = 0{,}989)$$

Tab. 3

Geschwindigkeitskonstanten zweiter Ordnung der Reaktionen von kernsubstituierten Benzhydraziden mit Phenylcyanat (45°, Dioxan)

X−	σ*)	$[X-C_6H_4-CONHNH_2]$ mol 10^3	$[Ph-OCN]$ mol 10^3	k_2 [l/mol min]
p-O_2N−	0,778	20,00	20,08	0,5641
m-O_2N−	0,710	19,86	20,55	0,6562
p-Cl−	0,227	20,00	20,54	1,0409
m-HO−	0,121	20,00	20,29	1,0065
H−	0,000	20,04	20,04	1 1988
p-CH_3O−	−0,268	20,50	20,51	1,5239
p-H_2N−	−0,660	19,83	19,58	1,8476

*) Datem aus.[8]

Der negative Wert des ρ-Parameters weist auf die Bedeutung der Nucleophilie des Benzhydrazins im langsamen Schritt der Reaktion hin. Der relativ hohe absolute Betrag des ρ-Parameters macht den nucleophilen Angriff des Carboxyl-O-Atoms an das Nitril-C-Atom des Phenylcyanats wahrscheinlich. Ein Angriff der Aminogruppe des Benzhydrazids an das Nitril-C-Atom hätte einen viel kleineren oder sogar fehlenden Benzhydrazid-Substituenteneinfluss auf die Reaktionsgeschwindigkeit erfordert. Der absolute Wert des ρ-Parameters ist etwas grösser als der der 2-Amino-5-aryl-1,3,4-oxadiazolbildung aus Benzhydraziden und Bromcyan (—0,215). [5]

In Tab. 4. sind die für den Fall der Reaktionen des Benzoesäurehydrazids mit 2,6-disubstituierten Arylcyanaten bestimmten Geschwindigkeitskonstanten zusammengetragen.

Tab. 4

Geschwindigkeitskonstanten zweiter Ordnung der Additionen des Benzoesäurehydrazids an 2,6-disubstituierte Arylcyanate (45°, Dioxan)

R—	$[PhCONHNH_2]$ mol 10^3	$[2{,}6\text{-}R_2C_6H_3{-}OCN]$ mol 10^3	k_2 [l/mol min]	$k_{2\,rel}$
H—	20,04	20,04	1,1988	1,000
CH_3—	10,03	19,74	0,2766	0,231
i-Pr—	21,60	18,20	0,0506	0,042

Der zirka 4 mal kleinere Betrag der Konstante im Falle des 2,6-Dimethylphenylcyanates sowie der zirka 24 mal kleinere Wert im Falle des 2,6-Diisopropylphenylcyanates im Vergleich zum unsubstituierten Phenylcyanat zeigt augenscheinlich, dass das Arylcyanat am Übergangszustand beteiligt ist. Für einen acyclischen Übergangszustand sind zweifelsohne wesentlich kleinere Behinderungen zum Erwarten. [12] Die primäre sterische Reaktionsverzögerung sowie der sekundäre Effekt durch sterische Rezonanzhinderung liegt für unseren Fall in der gleichen Richtung. Die bemerkten globalen sterischen Effekte sind als Grössenordnung mit jenen der gekoppelten Phenol und N-Alkylanilin-Addition an Arylcyanate gut vergleichbar. [12] In Tab. 5. sind die für den Fall der Reaktionen *o*-substituierter Benzhydrazide mit Phenylcyanat bei 45° in wasserfreiem Dioxan bestimmten Geschwindigkeitskonstanten zusammengefasst.

Tab. 5

Geschwindigkeitskonstaten der Reaktionen von *o*-substituierten Benzhydraziden mit Phenylcyanat bei 45° in wasserfreiem Dioxan

X—	$[o\text{-}X\text{-}C_6H_4{-}CONHNH_2]$ mol 10^3	$[Ph{-}OCN]$ mol 10^3	k_2 l/mol min]	k_{2rel}
H—	20,04	20,04	1,1988	1,00
HO—	20,00	20,00	0,6099	0,51
CH_3—	20,03	20,29	0,3832	0,32
Cl—	20,00	20,10	0,3176	0,26

Wir haben versucht diese Konstanten mit IR-($\nu_{C=O}$, $\nu^{as}_{NH_2}$, $\nu^{s}_{NH_2}$) — sowie NIR-($3\nu_{C=O}$, $2\nu^{as}_{NH_2}$, $2\nu^{s}_{NH_2}$)-spektroskopischen Befunden zu korrelieren. Alle Korrelationen schlugen jedoch fehl, auch wenn *m*- und *p*-substituierte Benzhydrazide in die Korrelationen miteinbezogen wurden. Aus Tab. 5. ist aber ersichtlich, dass im Falle aller untersuchten *o*-substituierten Benzhydrazide eine Verlangsamerung der Reaktionsgeschwindigkeit eintritt.

Für das *o*-Hydroxyderivat lässt sich diese Verzögerung leicht anhand der in einer vorangehenden Mitteilung festgestellten intramolekularen Assozierung dieses Derivats [1] erklären.

Der elektronenstossende Effekt der Methylgruppe des *o*-Tolylsäurehydrazids müsste dessen Nuceophilie erhöhen, und so zum Anwachsen der Reaktionsgeschwindigkeit führen. Die relative Geschwindigkeitskonstante beiträgt jedoch 0,32 und kann nur als Rezultat eines sterischen primären Effektes verstanden werde. Dieser Effekt ist als Ordnungsgrösse mit dem des für 2,6-Dimethylphenylcyanat gemessenen vergleichbar, und beweist einmal mehr das Eingreifen des Hydrazids im langsamen Schritt der Reaktion.

Im Falle des *o*-Chlor-Derivats liegen der primäre sterische Effekt und der die Herabsetzung der Nucleophilie bewirkende elektronenanziehende Effekt des *o*-Substituenten in der gleichen Richtung und haben so als Globaleffekt das Absinken der Reaktionsgeschwindigkeit ($k_{2\text{rel}} = 0{,}26$). In Tab. 6. sind die für die 2-Amino-5-phenyl-1,3,4-oxadiazolbildung aus Benzhydrazid und Phenylcyanat bei verschiedenen Temperaturen in wasserfreiem Dioxan vermessenen Geschwindigkeitskonstanten sowie scheinbaren Aktivierungsparameter enthalten.

Tab. 6

Geschwindigkeitskonstanten und scheinbare Aktivierungsparameter der Reaktion des Benzhydrazids mit Phenylcyanat in wasserfreiem Dioxan bei verschiedenen Temperaturen

[Ph—CONHNH$_2$] mol 10^3	[Ph—OCN] mol 10^3	T [°C]	k_2 [l/mol min]
23,57	20,00	15	0,2766
23,69	19,93	25	0,4838
23,68	19,96	35	0,6957
23,54	19,79	45	0,8722

$\Delta H^{\neq} = 26{,}6$ kJ/mol

$\Delta S^{\neq} = -147{,}4$ J/mol K

Die scheinbare Aktivierungsenthalpie zeugt für einen Übergangszustand mit guter energetischer Kompensation. Die scheinbare Aktivierungsentropie macht einen Übergangszustand von hoher Ordnung wahrscheinlich. Die Werte dieser Parameter sind in gutem Einklang mit den Litteraturdaten für Reaktionen mit cyclischen Übergangszuständen (30—35 kJ/mol; —90— —180 J/mol K). [9,10] Der Reaktionsmechanismus mit cyclischem Übergangszustand scheint für die nucleophilen Additionen an Arylcyanate allgemein gültig zu sein.

In Tab. 7. sind die für die in wässrigem Dioxan bei 45° bestimmten Geschwindigkeitskonstanten der Reaktionen des Phenylcyanats mit Benzoesäurehydrazid angegeben. Diese Geschwindigkeitskonstanten sind in zufriedenstellender Weise mit der Wasserkonzentration im Dioxan korrelierbar:

Tab. 7

Einfluss der Wasserkonzentration im Dioxan auf die Geschwindigkeitskonstanten der Reaktion des Benzoesäurehydrazids mit Phenylcyanat (45°C)

$[Ph\text{-}CONHNH_2]$ mol 10^3	$[Ph-OCN]$ mol 10^3	$[H_2O]$ mol	k_2 [l/mol min]
23,54	19,79	0,0	0,8722
23,64	20,05	0,6	1,1121
23,58	19,82	1,0	1,1551
23,65	19,86	2,0	1,2690
23,65	19,86	4,0	1,5614

$$k_2 = 0.957 + 0{,}156[H_2O] \quad (r = 0{,}974)$$

Diese Korrelierung beweist einen mässigen Einfluss der Wasserkonzentration auf die Reaktionsgeschwindigkeit. Fehlende oder mässige Polaritätseinflüsse auf die Reaktionsgeschwindigkeit sind ein weiteres Argument für cyclische Übergangszustände.

In gutem Einklang mit den aufgezählten experimentellen Befunden ist folgender Reaktionsmechanismus:

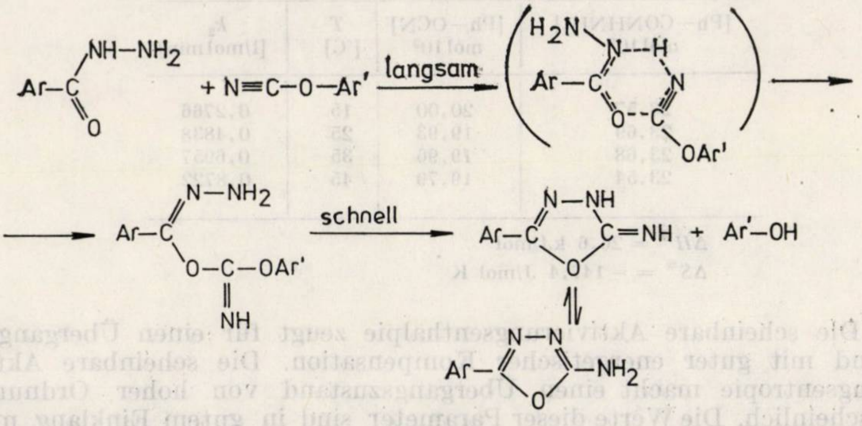

Der Mechanismus besteht im langsamen elektrophilen Angriff des Arylcyanats an das O-Atom des Benzhydrazides, über einen cyclischen Sechszentrenübergangszustand. Die gebildete Zwischenstufe eliminiert rasch das entsprechende Phenol und es bildet sich das stabile Endprodukt 2-Amino-5-aryl-1,3,4-oxadiazol. In der Anwesenheit des Wassers ist der Übergangszustand wie folgt formulierbar:

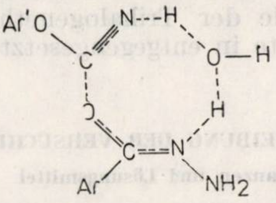

Anhand der IR— und ^{1}H—NMR-Spektren der von Zinner und Mitarb.[3] aus Hydraziden und Arylcyanaten dargestellten Substanzen, die von diesen als N'-Carbimidoylcarbonsäurehydrazide **2** formuliert wurden, sind wir der Meinung, dass deren reelle Struktur die folgende ist:

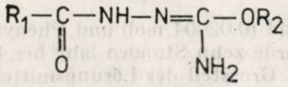

$$R_1-\underset{\underset{O}{\|}}{C}-NH-N{=}\underset{\underset{NH_2}{|}}{C}-OR_2$$

3

So, sind die IR-Banden von um 3370 und bzw. 3200 cm^{-1} der antisymmetrischen und bzw. symmetrischen NH$_2$-Valenzschwingung zuzuschreiben. In den in Literatur[3] angegebenen NMR-Spektren entspricht das Singulett von 9,1 — 10,3 ppm dem sauren Amidproton, während das 2 Protonensingulett von 6,4 — 6,6 ppm der Aminogruppe zuzuschreiben ist. Auf keinen Fall können die benachbarten NH-Gruppen aus **2**, Signale ergeben, die sich in allen neun untersuchten Fällen als Singulett überlappen. Für die Struktur **3** spricht auch die Tatsache, dass durch die Änderung von R$_1$ die Lage des NH-Signals viel bedeutender beeinflusst wird als die des NH$_2$-Signals, während die Änderung von R$_2$ eine umgekehrte Wirkung hat. Für die von uns untersuchten Fälle halten wir jedoch anhand des ρ-Parameters den Angriff des O-Atoms für wahrscheinlicher, können aber den Angriff des N-Atoms nicht gänzlich ausschliessen.

Selbst die Tatsache, dass sogar bei niedrigen Temperaturen[1,3] keine acyclischen Reaktionsprodukte isoliert werden konnten, deutet auf eine Änderung des Reaktionsmechanismus. Im durch nucleophilen Angriff des O-Atoms gebildeten Zwischenprodukt **4** erscheint eine stark nucleophile Aminogruppe, die mit grosser Geschwindigkeit die Cyclisierungsreaktion promoviert.

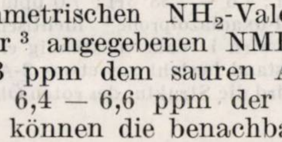

4

Diese Änderung des Reaktionsmechanismus im Falle der Arylcyanate wird nur dann verständlich, wenn man das Anwachsen der Elektronendichte am O-Atom durch den mesomeren Effekt des Arylrestes in Betracht zieht. Im Falle der Trihalogenethylcyanate liegt der induktive Effekt der Alkylreste in entgegengesetzter Richtung.

BESCHREIBUNG DER VERSUCHE

Substanzen und Lösungsmittel

Die Benzhydrazide wurden aus Benzoesäureestern und Hydrazinhydrat[1] gewonnen, durch Umkristallisierung gereinigt.

Die Arylcyanate wurden nach den üblichen Methoden hergestellt,[13] durch Umkristallisierung oder Destillation gereinigt und IR-spektroskopisch sowie gasschromatographisch auf Reinheit geprüft.

Dioxan wurde unter Rückfluss 24 Stunden lang auf Na gekocht, dann abdestilliert.

Reaktionsprodukte

Eine aus Benzoesäurehydrazid (0.02004 mol) und Phenylcyanat (0.02004 mol) gebildete Lösung in wasserfreiem Dioxan wurde zehn Stunden lang bei 45° unter galegentlichem Schütteln gehalten. Dannach wurde der Grossteil des Lösungsmittels i. Vak. abgetrieben. Aus der verbliebenen Lösung fallen nach dem Erkalten farblose Kristalle aus, die aus etwas Methanol umkristallisiert werden. Der Schmelzpunkt von 242° stimmt mit dem des 2-Amino-5-phenyl-1,3,4-oxadiazols überein (242—4° [1]). Die UV- (279 nm, $\varepsilon = 16300$), IR-(NH_2 3300, 3100, 1570, 540, Oxadiazolring 1660, 1025, 975, Benzolring 1590, 1575, 1490, 1305, 1120, 1070, 730, 680 cm^{-1}) und ^{1}H-NMR-Spektren (7,9—7,7 2H ; 7,6 — 7,38 3H ; 7,0 ppm 2H) sind mit denen einer authentischen 2-Amino-5-phenyl-1,3,4-oxadiazolprobe[1] identisch.

Die dioxanische Mutterlauge wird i. Vak. vollständig eigeengt, das rote Öl mit Ether aufgenommen (der kristalline Rückstand besteht aus etwas 2-Amino-5-phenyl-1,3,4-oxadiazol). Nach dem Verdampfen des Ethers wird die Struktur des roten Öls IR-spektroskopisch als Phenol sichergestellt.

Kinetische Messungen. Rechenmodell

Zum Zeitpunkt null der Reaktion werden bei 15—45° thermostatierte Lösungen von Benzhydrazid und Arylcyanat in wasserfreiem oder wässrigem Dioxan ($[H_2O] = 0 - 4$ mol) innig vermischt und weiterhin thermostatiert. Von Zeit zu Zeit werden dem Gemisch je 5—7 µl Proben entnommen, mit je 3 ml Dioxan verdünnt und anschliessend UV-spektroskopisch (Pye Unicam SP 8000) untersucht. Aus der beim Absorptionsmaximum gemessenen Extinktion-Zeit Abhängigkeit lässt sich die Konzentration des sich bildenden 2-Amino-5-aryl-1-3,4-oxadiazols errechnen :

$x = \frac{E_t - E_0}{E_i - E_0} \cdot a$ E_0, E_t, E_i — Extinktion zum Zeitpunkt Null, t und bzw. nach dem Abschliessen der Reaktion ;
x — momentane Produktkonzentration

Geschwindigkeitskonstanten zweiter Ordnung wurden anhand der bekannten Gleichung :

$$\frac{dx}{dt} = k_2(a - x)(b - x),$$

in integrierter Form

$$k_2 = \frac{1}{t} \cdot \frac{1}{a-b} \ln \frac{b(a - x)}{a(b - x)}$$

berechnet.

Die Linearität bleibt bis Umsetzungsgraden von 75 — 90 % erhalten.

LITERATURÜBERSICHT

[1] III. Mitt.: H. H. Glatt, R. Bacaloglu, C. Csunderlik, S. A. Saleh,. F Szeibert und V. Szenaşi, *Bul. ştiinţific tehnic Inst. Polit. „Traian Vuia" (Timişoara), Ser. Chimie*, 1982 unter Druck.

[2] E. Grigat und R. Pütter, *Chem. Ber.*, **97**, 3560 (1964).

[3] G. Zinner, M. Neitzler und I. Holdt, *Arch. Pharm. (Weinheim)*, **311** 1050 (1978).

[4] C. R. Kramer, *Z. Chem.*, **18**, 406 (1978).

[5] C. R. Kramer und J. Dost, *Z. Chem.*, **17**, 451 (9177).

[6] C. R. Kramer, *Z. phys. Chem.*, **259**, 1100 (1978).

[7] C. R. Kramer und L. Beck, *Z. Chem.*, **20**, 25 (1980).

[8] J. E. Leffler und E. Grunwald, „Rates and Equilibria of Organic Reactions", Wiley, New-York, 1969, S. 173.

[9] H. H. Glatt, I. Bacaloglu, T. T. Ky, C. Boeriu, R. Bacaloglu, D. Martin und H. Graubaum, *J. prakt. Chem.*, **322**, 1053 (1980).

[10] H. H. Glatt, I. Bacaloglu, T. T. Ky, R. Bacaloglu und D. Martin, *J. prakt. Chem.*, **1982**, im Druck

[11] D. Martin, K. Nadolski, R. Bacaloglu, und I. Bacaloglu, *J. prakt. Chem.*, **313**, 58 (1971).

[12] I. Bacaloglu, R. Bacaloglu, D. Martin und K. Nadolski, *J. prakt. Chem.*, **316**, 529 (1974).

[13] D. Martin und R. Bacaloglu, „Organische Synthesen mit Cyansäureestern", Akademie-Verlag, Berlin, 1980, S. 11.

Revue Roumaine de Chimie, 28, 6, 641–644 (1983)

BASE-CATALYZED ADDITIONS TO ETHYL 7-HYDROXY-COUMARIN-3-CARBOXYLATE

M. A. HASSAN*, M. M. MOHAMED and M. El-BORAI
Chemistry Department, Faculty of Science, Ain Shams University, Cairo, Egypt

Received June 12, 1981

Base catalyzed additions of cyclic ketones, acetylacetone, benzoylacetone, ethyl cyanoacetate, and ethyl acetoacetate to ethyl 7-hydroxycoumarin-3carboxylate (I) were investigated under different conditions to give the corresponding Michael adducts. The structures of products have been supported by elemental analysis and spectral data.

The C_3-C_4 double bond in ethyl 7-hydroxycoumarin-3-carboxylate (I) is activated by conjugation towards the base catalyzed addition of active methylene compounds.[1]

As an extension of our previous work,[2-4] treatment of ethyl 7-hydroxycoumarin-3-carboxylate (I) with cyclopentanone or cyclohexanone at room temperature in the presence of sodium methoxide gives [1-(2′,4′-dihydroxyphenyl)-1-(2″-oxocyclopentyl/or 2″-oxocyclohexyl)]-methyl malonic acid (IIa and IIb). The IR spectra of II showed well defined absorption bands at 1718 (ν C = O of cyclic ketones), 1724 (ν C=O of dicarboxylic acids), and 3230 cm⁻¹ (ν OH).

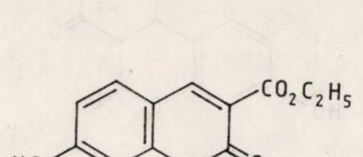

(I)

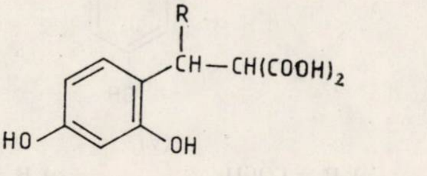

(II)

a) R = 2-oxocyclopentyl
b) R = 2-oxocyclohexyl

Compound I reacts with cyclic ketones at 170°C in the presence of ammonium acetate to give two products : 7-hydroxy-4-(2′-oxocyclopentyl/or 2′-oxocyclohexyl)-coumarin-3-carboxamides (IIIa and IIIb) and 1,2-cyclopent (or cyclohex)-1-ene-4*a*, 10*b*-dihydro-8-hydroxy-4*H* [1] benzopyrano [3,4-*c*] pyridine-4,5-(3*H*)-diones (IVa and IVb). The IR spectra of compounds III showed bands at 1620 (ν C=O of δ-lactones), 1680 (ν C = O of primary amides), 2820 – 2905 (ν cyclic CH), and

3180 – 3440 cm^{-1} (ν OH or NH), while compounds IV showed bands at 1610 (ν C = O of δ-lactones), 1640 (ν C = O of δ-lactam), 2805 – 2900 (ν cyclic CH), and 3420 cm^{-1} (ν NH or OH).

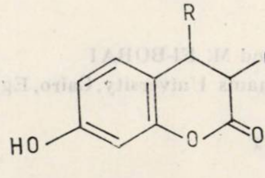

(III)

a) R = 2-oxocyclopentyl
b) R = 2-oxocyclohexyl

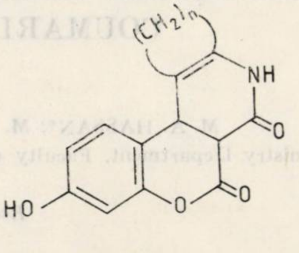

(IV)

a) n = 3
b) n = 4

Treatment of I with acetylacetone or benzoyl acetone at room temperature in the presence of sodium methoxide gives [1-(2′, 4′-dihydroxyphenyl)-1-(acetyl acetonyl/or benzoyl acetonyl)]-methyl malonic acids (Va and Vb), while at 170°C gives 1-acetyl (or benzoyl)-8-hydroxy-4*a*, 10*b*-dihydro-2-methyl-4*H*, 5*H*-pyrano (3,4-*c*) [1] benzopyran-4,5-diones (VIa and VIb) respectively. The IR absorption spectra of compounds V showed bands at 1630 (ν β-diketones), 1738 (ν dicarboxylic acids), and 3265 cm^{-1} (ν OH), while the IR spectra of compounds VI showed bands at 1610 (ν β-diketones), 1635 (ν δ-lactones), 1640 or 1710 (ν acetyl or benzoyl), and 3430 cm^{-1} (ν OH).

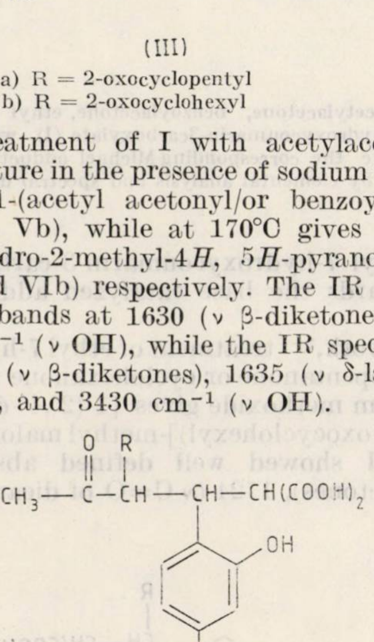

(V)

a) R = $COCH_3$
b) R = COC_6H_5

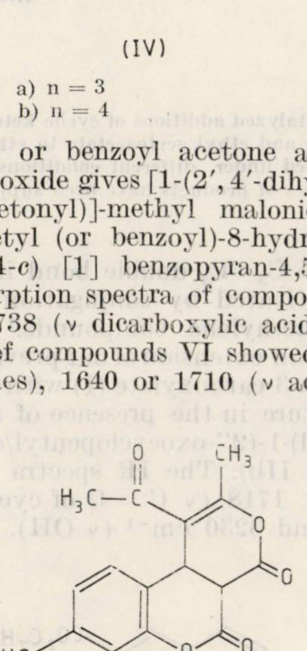

(VI)

a) R = $COCH_3$
b) R = COC_6H_5

Compound I condenses with ethyl acetoacetate, or ethyl cyanoacetate at 170°C in the presence of sodium methoxide to give 1-acetyl (or cyano)-8-hydroxy-1,2,4*a*, 10*b*-tetrahydro-4*H*, 5*H*-pyrano-(3, 4-*c*) [1]-benzopyran-2,4,5-triones (VIIa and VIIb), while in the presence of ammonium acetate under the same conditions it gives 1-acetyl (or cyano)-8-hydroxy-4*a*, 10*b*-dihydro-2*H*, 3*H* [1]-benzopyrano-(3,4-*c*) pyridine-2,4,5 (1*H*, 3*H*)-triones (VIIc and VIId). The IR spectra of VIIa and VIIc showed a band at 1660 cm^{-1} (ν acetyl), compounds VIIb and VIId showed a band at 2230 cm^{-1} (ν C≡N), and compounds VIIc and VIId showed a band at 3340 cm^{-1} (ν NH).

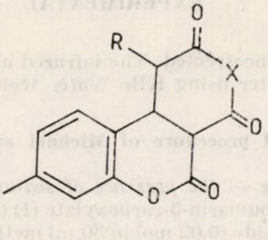

(VII)

	R	X		R	X
a)	$COCH_3$	O	c)	$COCH_3$	NH
b)	CN	O	d)	CN	NH

Table 1

Physical data of compounds II—VII

Compound	m.p. °C	Solvent* (yield %)	Mol. formula	Analysis % Calcd./found		
				C	H	N
IIa	242	dil. E (68)	$C_{15}H_{16}O_7$	58.44 58.67	5.19 5.24	——— ———
IIb	265	E (73)	$C_{16}H_{18}O_7$	59.63 59.82	5.59 5.47	——— ———
IIIa	255	A (58)	$C_{15}H_{15}NO_5$	62.28 62.16	5.19 5.12	4.84 4.77
IIIb	262	A (61)	$C_{16}H_{17}NO_5$	63.37 63.45	5.61 5.53	4.62 4.48
IVa	>300	X (54)	$C_{15}H_{13}NO_4$	66.42 66.58	4.80 4.67	5.17 5.02
IVb	>300	X (59)	$C_{16}H_{15}NO_4$	67.37 67.51	5.26 5.14	4.91 4.88
Va	257	E (52)	$C_{15}H_{16}O_8$	55.56 55.63	4.94 4.87	——— ———
Vb	255	E (46)	$C_{20}H_{18}O_8$	62.18 62.23	4.66 4.54	——— ———
VIa	175	B (48)	$C_{15}H_{12}O_6$	62.50 62.63	4.17 4.23	——— ———
VIb	188	B (57)	$C_{20}H_{14}O_6$	68.57 68.71	4.00 3.88	——— ———
VIIa	258	M (72)	$C_{14}H_{10}O_7$	57.93 57.84	3.45 3.51	——— ———
VIIb	261	E (68)	$C_{13}H_7NO_6$	57.14 57.27	2.56 2.63	5.12 5.00
VIIc	264	E (42)	$C_{14}H_{11}NO_6$	58.13 58.28	3.81 3.76	4.84 4.75
VIId	292	A (44)	$C_{13}H_8N_2O_5$	57.35 57.49	2.94 2.97	10.29 10.13

* A = Acetic acid ; B = Benzene ; E = Ethanol ; M = Methanol and X = Xylene.

EXPERIMENTAL

All melting points are uncorrected. The infrared absorption spectra were determined by Unicam SP 200 G Spectrometer using KBr Wafer technique.

General procedure of Michael addition to I

(a) *At room temperature in the presence of sodium methoxide. Formation of II and V.* A mixture of ethyl 7-hydroxycoumarin-3-carboxylate (I) (0.01 mol), active methylene compound (0.015 mol) and sodium methoxide (0.02 mol in 30 ml methanol) was kept at room temperature for 5 days. The reaction mixture was poured into dilute hydrochloric acid (100 ml, 2%). The solid product that separated was filtered off and washed with water (3 × 50 ml), dried and crystallized from the proper solvent. The results are listed in Table 1.

(b) *At 170°C in the presence of sodium methoxide or ammonium acetate. Formation of III, IV, VI and VII.* A mixture or coumarin I (0.01 mol), active methylene compound (0.015 mol), and sodium methoxide (0.02 mol) or ammonium acetate (2.0 g) was heated in a sealed tube for 4 hrs at 170°. The reaction mixture was stirred with dilute hydrochloric acid (100 ml, 20%), washed with water, dried and crystallized from the proper solvent. The results are listed in Table 1.

REFERENCES

[1] G. F. Koelsch, and M. C. Freerks, *J. Orgn. Chem.*, **18**, 1538 (1953).

[2] M. A. Hassan, M. M. Mohamed, E. A. Soliman, and A. M. Elwy, *Indian J. Chem.*, **18**, 460 (1979).

[3] A. Sammour and M. El-Kady, *Indian J. Chem.*, **12**, 51 (1974).

[4] A. Sammour, M. Abdalla, and M. El-Kady, *Acta Chim. Acad. Sci. Hung.*, **82**, 369 (1974).

Revue Roumaine de Chimie, 28, 6, 645–651 (1983)

DERIVATIVES OF 4-AMINOMETHYL-THIAZOLE. I

THE SYNTHESIS OF 2-ARYL-4-AMINOMETHYL-THIAZOLES

SIMONA SILBERG

Pharmaceutical Faculty, str. Ion Creangă 12, R–3400–Cluj-Napoca, Romania

Received May 19, 1982

The conversion of 2-aryl-4-halomethyl-thiazoles into 4-aminomethyl derivatives by means of Delépine and Gabriel methods was investigated. A comparative evaluation of the preparative efficiency of these two methods in the field of thiazole derivatives pointed out the superiority of the Delépine method. The aminomethyl-thiazoles thus obtained were characterized by derivatization.

The thiazole derivatives carrying a free or substituted amino group linked to the heterocycle by the intermediacy of an alkyl moiety represent in the chemistry of thiazole a chapter that reached only an incipient stage in its development.

A prime reason for the interest in this type of compounds consists in the prospects of obtaining new substances with useful pharmacological properties by the preparation of compounds with antispasmodic and antihistaminic actions.[1,2] Such researches are expected to lead to new aminoalkyl analogues of clomethiazole, (5-(2-chloroethyl)-4-methylthiazole), a drug of well-established therapeutical value,[3] and of other thiazoles with potential biological activity.[4-9]

A survey of the pertinent literature pointed out, along with the indisputable biological usefulness of such compounds, the rather occasional character of the researches in this field; the lack of systematic investigations on the synthesis and properties of aryl-substituted aminoalkyl-thiazoles is particularly conspicuous.

The present paper is the first in a series of reports intended to contribute to this field by carrying out the synthesis and the examination of chemical and physical properties of some aminomethyl derivatives of alkyl-thiazoles.

Our previous investigations [10-12] demonstrated the possibility of using the Sommelet reaction [13-15] for the conversion of 2-aryl- and of 2-arylamino-4-halomethyl-thiazoles into the corresponding aldehydes. The intermediates formed in these reactions, the hexamethylenetetraminium salts, might yield, if subjected to the conditions of the Delépine reaction, [16] 4-aminomethyl-thiazoles of the structural type investigated in this work. Considering the fact that 4-chloromethyl-thiazoles are readily accessible by the Hantzsch cyclization, and that the preparation of hexamethylenetetraminium salts represents a field already largely explored in our previous studies, we chose the Delépine reaction as a first route to 2-aryl-4-aminomethyl-thiazoles. It is to be noted that no data could be found in the literature concerning the application of this reaction in the thiazole chemistry.

In order to check the obtained results and with a view to enlarging the area of preparative methods that can be used for synthesizing the compounds investigated in the present paper (and in the following ones of this series) we studied also the behaviour of the same 4-halomethyl-thiazoles under the conditions of the Gabriel reaction, being thus able to compare the efficiency of the two procedures in the investigated field.

PREPARATION OF 2-ARYL-4-AMINOMETHYL-THIAZOLES BY THE DELÉPINE REACTION

This reaction leads to primary amines by the acid hydrolysis of quaternary ammonium salts obtained by the interaction of reactive haloalkyl derivatives with hexamethylenetetramine: [16-18]

$$R-CH_2X + C_6H_{12}N_4 \longrightarrow RCH_2\,[N_4C_6H_{12}]^+X^- \xrightarrow[H_2O]{HCl} RCH_2NH_3^+\,Cl^- + $$
$$+ 6\,CH_2O + 3\,NH_4Cl$$

The benzylic reactivity of 2-aryl-4-chloromethyl-thiazoles fulfils a prerequisite for the applicability of this reaction in our case. In order to increase the susceptibility of the thiazole compound towards the nucleophilic attack of the nitrogen-containing reagent, we used in some cases the 4-iodomethyl-derivatives, obtained in the usual way from 2-aryl-4-chloromethyl-thiazole and potassium iodide.

For the preparation of the hexamethylenetetraminium salts, the literature [17] recommends the use of 95% ethanol as a reaction medium; in the series investigated, the reactivity of the halogenated compounds is high enough to allow the formation of the salts even in a much less polar solvent, such as chloroform. Under these conditions the starting compounds are very well dissolved, whereas the reaction products — the hexamethylenetetraminium salts — are slightly soluble and separate as crystals. [10] In some cases, when the nature of the aryl substituent on the thiazole ring induced a certain increase of the solubility of the salts in chloroform, dilution with ether was necessary to complete the precipitation.

The 2-aryl-4-halomethyl- and 2-aryl-5-chloro-4-halomethyl-thiazoles **1** were thus readily converted into the hexamethylenetetraminium salts **2** which yielded, upon treatment with concentrated hydrochloric acid, the 4-aminomethyl-thiazoles **3**. The very good yield (over 80—90%) in all the steps of this synthesis, as well as the accessibility of the starting compounds and of the employed reagents, are sufficient reasons to consider the Delépine reaction as a very convenient method for the preparation of aminoalkyl-thiazoles.

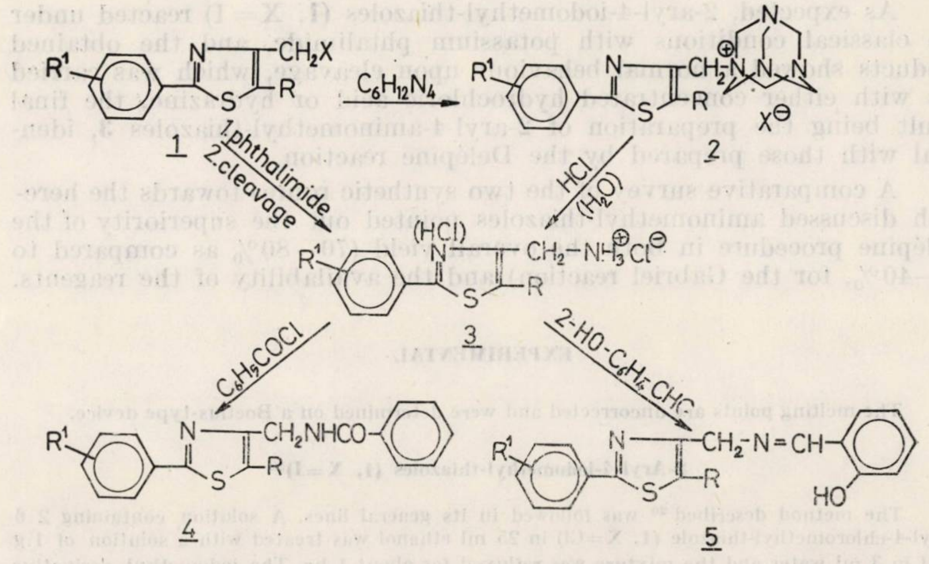

Since the amines thus obtained are compounds of relatively low melting points, they were characterized as hydrochlorides, in the case of 2-aryl-5-chloro-4-aminomethyl-thiazoles (**3**, R=Cl), respectively as dihydrochlorides, in the series of 2-aryl-4-aminomethyl-thiazoles (**3**, R=H), the ring nitrogen of the latters displaying a basicity high enough to ensure the stable bonding of a second molecule of hydrochloric acid.

In order to complete the characterization of the newly prepared compounds, and to enlarge the range of the substances subjected to biological testing in this series, we also prepared the benzoyl derivatives **4** and the Schiff bases **5** with salicylic aldehyde.

PREPARATION OF 2-ARYL-4-AMINOMETHYL-THIAZOLES BY THE GABRIEL REACTION

With a view to assessing the preparative efficiency of the Delépine reaction, a series of experiments were carried out aiming to obtain the same 2-aryl-4-aminomethyl-thiazoles **3** by means of the classical Gabriel method.

There were at least two reasons to prefer this preparative procedure as a reference, namely, the fact that the same starting matters (reactive haloalkyl derivatives) are used in both Gabriel and Delépine methods, and the existence of previous reports concerning the application of the Gabriel method in the thiazole series.

Thus, in 1961, Berlin and Bronovitskaya [19] prepared 2- and 4-aminomethyl-thiazoles by treating chloromethyl-thiazoles with potassium phtalimide, the obtained phtalimido-derivative being cleaved by hydrazinolysis. The same cleavage procedure was also applied to the synthesis of some 2-amino-4-aminoalkyl-thiazoles with longer side-chains,[4] where the phtalimidoderivative was obtained by direct cyclization.

As expected, 2-aryl-4-iodomethyl-thiazoles (**1**, X= I) reacted under the classical conditions with potassium phtalimide, and the obtained products showed a normal behaviour upon cleavage, which was carried out with either concentrated hydrochloric acid or hydrazine, the final result being the preparation of 2-aryl-4-aminomethyl-thiazoles **3**, identical with those prepared by the Delépine reaction.

A comparative survey of the two synthetic routes towards the herewith discussed aminomethyl-thiazoles pointed out the superiority of the Delépine procedure in both the overall yield (70–80% as compared to 30–40%, for the Gabriel reaction) and the availability of the reagents.

EXPERIMENTAL

The melting points are uncorrected and were determined on a Boetius-type device.

2-Aryl-4-iodomethyl-thiazoles (1, X=I)[20]

The method described [20] was followed in its general lines. A solution containing 2 6 2-aryl-4-chloromethyl-thiazole (**1**, X=Cl) in 25 ml ethanol was treated with a solution of 1.g g KI in 3 ml water and the mixture was refluxed for about 1 hr. The iodomethyl derivative separated on cooling as yellowish microcrystals, which were recrystallized from ethanol. Yield 85–95%.

The substances thus prepared are listed in Table 1.

Table 1

2-Aryl-4-iodomethyl-thiazoles (**1**, X=I)

R	R¹	m.p. °C	Molecular formula	N% calculated	N% found
H	H	104–5	$C_{10}H_8INS$	4.65	4.28
H	3-CH_3	67	$C_{11}H_{10}INS$	4.44	4.68
H	4-CH_3	120	$C_{11}H_{10}INS$	4.44	4.52
H	4-Br	130	$C_{10}H_7BrINS$	3.69	3.85
H	4-NO_2	134	$C_{10}H_7IN_2O_2S$	8.09	8.10
H	4-NO_2-3-CH_3	133	$C_{11}H_9IN_2O_2S$	7.78	7.51
H	3-NO_2-4-CH_3	104	$C_{11}H_9IN_2O_2S$	7.78	7.55
Cl	H	73	$C_{10}H_7ClINS$	4.17	4.35
Cl	3-CH_3	53	$C_{11}H_9ClINS$	4.01	4.32
Cl	4-CH_3	119	$C_{11}H_9ClINS$	4.01	3.88
Cl	4-Br	137	$C_{10}H_6BrClINS$	3.38	3.57
Cl	4-NO_2	150	$C_{10}H_6ClIN_2O_2S$	7.36	7.59
Cl	4-NO_2-3-CH_3	118	$C_{11}H_8ClIN_2O_2S$	7.10	7.29
Cl	3-NO_2-4-CH_3	95	$C_{11}H_8ClIN_2O_2S$	7.10	7.17

2-Aryl-4-hexamethylenetetraminomethyl-thiazole chlorides (2)

Two grams of halomethyl-thiazole **1** were treated with 15 ml chloroform and 1.6 g hexamethylenetetramine and the mixture was refluxed on a water bath for about 1 hr. The hexamethylenetetraminium salt **2** separated on cooling, was filtered, and recrystallized from ethanol. Yield 82—96%.

Note. When the spontaneously separated product represents less than 80% of the theoretical yield, the chloroform mother liquor is to be treated with ether; the rest of the salt precipitates and is recovered by filtration. The starting halomethyl-thiazoles are readily soluble in ether and the precipitation of urotropine from such diluted solutions and in the presence of chloroform can be neglected.

The compounds thus obtained are listed in Table 2.

Table 2

2-Aryl-4-hexamethylenetetraminomethyl-thiazole chlorides **(2)**

R	R¹	m.p. °C	Molecular formula	N%	
				calculated	found
H	H	204	$C_{16}H_{20}ClN_5S$	20.02	20.35
H	3-CH_3	200	$C_{17}H_{22}ClN_5S$	19.24	19.48
H	4-CH_3	195	$C_{17}H_{22}ClN_5S$	19.24	19.11
H	4-Br	212	$C_{16}H_{19}BrClN_5S$	16.33	16.56
Cl	H	205	$C_{16}H_{19}Cl_2N_5S$	18.22	18.50
Cl	3-CH_3	213	$C_{17}H_{21}Cl_2N_5S$	17.58	17.41
Cl	4-CH_3	215	$C_{17}H_{21}Cl_2N_5S$	17.58	17.75
Cl	4-Br	210	$C_{16}H_{18}BrCl_2N_5S$	15.12	15.02

2-Aryl-4-aminomethyl-thiazoles, mono- resp. dihydrochlorides (3)

a). Two grams of the hexamethylenetetraminium salts **2** were dissolved in 15—20 ml absolute ethanol and were treated with 4 ml concentrated hydrochloric acid. The mixture was allowed to stay for 12 hrs at room temperature, the separated ammonium chloride was filtered, and the filtrate was evaporated to dryness. The residue was taken in aqueous sodium hydroxide, then diluted with water, the separated brown-yellow substance was extracted with ether and, after the removal of the solvent, the residue was dissolved in absolute ethanol and hydrogen chloride was bubbled into the resulted solution.

The hydrochloride (or dihydrochloride) separated as white crystals and was recrystallized from absolute ethanol.

Yield 80—88%.

b). Two grams of iodomethyl derivative (**1**, X = I) were dissolved in 12 ml absolute ethanol and treated with 1 — 1.2 g potassium phtalimide. The mixture was refluxed for about 10—12 hrs, the solution concentrated by distillation to a small volume and the crystalline mass separated by filtration. The acid hydrolysis was carried out by boiling with concentrated hydrochloric acid for 2 hrs. After cooling, the solution was rendered alkaline with sodium hydroxide, extracted with ether, the solvent removed by evaporation, the residue taken in absolute ether and the hydrochloride precipitated by bubbling a stream of dry hydrogen chloride. After filtration and recrystallization from absolute ethanol this procedure yielded compounds identical to those prepared according to the procedure described above under a). Yield 30—40%

Note. The cleavage of the intermediate phtalimido derivative was also performed by hydrazinolysis under classical conditions.

The substances thus synthesized are given in Table 3.

Table 3

2-Aryl-4-aminomethyl-thiazole dihydrochlorides (**3**, R=H) and 2-aryl-5-chloro-4-aminomethyl-thiazole hydrochlorides (**3**, R=Cl)

R	R¹	m.p. °C	Molecular formula	N% calculated	N% found
H	H	215	$C_{10}H_{12}Cl_2N_2S$	10.64	10.35
H	3-CH_3	214	$C_{11}H_{14}Cl_2N_2S$	10.11	10.41
H	4-CH_3	237	$C_{11}H_{14}Cl_2N_2S$	10.11	10.38
H	4-Br	260	$C_{10}H_{11}BrCl_2N_2S$	8.19	8.35
Cl	H	255	$C_{10}H_{10}Cl_2N_2S$	10.73	10.42
Cl	3-CH_3	198	$C_{11}H_{12}Cl_2N_2S$	10.18	10.20
Cl	4-CH_3	245	$C_{11}H_{12}Cl_2N_2S$	10.18	10.25
Cl	4-Br	256	$C_{10}H_9BrCl_2N_2S$	8.24	8.28

2-Aryl-4-benzoylaminomethyl-thiazoles (4)

The aminomethyl derivatives **3** were benzoylated by treatment with benzoyl chloride in alkaline medium under the usual conditions, and the benzoyl derivatives listed in Table 4 were obtained in practically quantitative yields; they were purified by recrystallization from ethanol.

Table 4

2-Aryl-4-benzoylaminomethyl-thiazoles (**4**)

R	R¹	m.p.°C	Molecular formula	N% calculated	N% found
H	H	118	$C_{17}H_{14}N_2OS$	9.52	9.68
H	3-CH_3	116	$C_{18}H_{16}N_2OS$	9.08	9.27
H	4-CH_3	176	$C_{18}H_{16}N_2OS$	9.08	8.89
H	4-Br	165	$C_{17}H_{13}BrN_2OS$	7.50	7.68
Cl	H	107	$C_{17}H_{13}ClN_2OS$	8.52	8.48
Cl	3-CH_3	120	$C_{18}H_{15}ClN_2OS$	8.17	7.89
Cl	4-CH_3	164	$C_{18}H_{15}ClN_2OS$	8.17	8.01
Cl	4-Br	152	$C_{17}H_{12}BrClN_2OS$	6.87	6.62

The condensation of 2-aryl-4-aminomethyl-thiazoles (3) with salicylic aldehyde

Three grams of **3** were dissolved in 10 ml ethanol and refluxed for 5—15 minutes with 1 g salicylic aldehyde. The Schiff bases **5** separated on cooling as well-formed crystals, pale-yellow flakes, which were recrystallized from ethanol. The yields were practically quantitative.

The compounds thus obtained are listed in Table 5.

Table 5

Schiff bases of 2-aryl-4-aminomethyl-thiazoles with salicylic aldehyde **(5)**

R	R^1	m.p. °C	Molecular formula	N%	
				calculated	found
H	H	87	$C_{17}H_{14}N_2OS$	9 .52	9 .37
H	$3\text{-}CH_3$	60	$C_{18}H_{16}N_2OS$	9 .08	9 .25
H	$4\text{-}CH_3$	104	$C_{18}H_{16}N_2OS$	9 .08	9 .37
H	4-Br	119	$C_{17}H_{13}BrN_2OS$	7 .50	7 .72
Cl	H	98	$C_{17}H_{13}ClN_2OS$	8 .52	8 .17
Cl	$3\text{-}CH_3$	104	$C_{18}H_{15}ClN_2OS$	8 .17	8 .41
Cl	$4\text{-}CH_3$	110	$C_{18}H_{15}ClN_2OS$	8 .17	8 .36
Cl	4-Br	135	$C_{17}H_{12}BrClN_2OS$	6 .87	7 .30

REFERENCES

[1] J. M. Singh, G. P. Saxena and B. N. Tripathi, *Indian J. Appl. Chem.*, **32,** 194 (1969) ; *Chem. Abstr.*, **75,** 20261 (1971).

[2] R. Dahlbom, *Acta Chem. Scand.*, **7,** 374 (1953).

[3] U. H. Lindberg, J. Pedersen and B. Ulff, *Acta Pharm. Suecica*, **4,** 269 (1967).

[4] J. Jonas, *Spisy Prirodovedecke Fak. Univ. Brne*, **447,** 405 (1963) ; *Chem. Abstr.*, **60,** 15852 (1964).

[5] G. Palazzo and M. Tavella, *Gazz. Chim. Ital.*, **92,** 1084 (1962).

[6] K. M. Murav'eva and M. N. Shchukina, *Zhur. obshchei Khim.*, **33,** 3723 (1963).

[7] Merck Co. Inc., *Neth. Appl.* **6,** 607, 593 ; *Chem. Abstr.*, **67,** 32687 (1967).

[8] S. B. Labay, *Invest. Urol.*, **4,** 351 (1967).

[9] T. Okuda and Sh. Ogawa, *Yakugaku Zasshi.*, **77,** 445 (1957) ; *Chem. Abstr.*, **51,** 14687 (1957).

[10] I. Simiti, M. Farkas and S. Silberg, *Chem. Ber.*, **95,** 2672 (1962).

[11] Al. Silberg, I. Simiti, M. Farkas, S. Silberg and H. H. Mantsch, *Rev. Chim. Acad. R. P. Roumaine*, **7,** 513 (1962).

[12] S. Silebrg, Ph. D. Thesis, Institute of Chemistry, Cluj, 1974.

[13] M. Sommelet, *Compt. rend.*, **157,** 852 (1913).

[14] S. J. Angyal, *Org. Reactions*, **8,** 198 (1954).

[15] Ph. Le Hénaff, *Ann. Chim. (Paris)*, **7,** 367 (1962).

[16] M. Delépine, *Bull. Soc. chim. France*, **13,** 358 (1895).

[17] A. Galat and G. Elion, *J. Amer. Chem. Soc.*, **61,** 3585 (1939).

[18] N. Wendler, *J. Amer. Chem. Soc.*, **71,** 375 (1959).

[19] A. J. Berlin and V. P. Bronovitskaya, *Zhur. obshchei Khim.*, **31,** 1356 (1961).

[20] Al. Silberg, I. Simiti, H. Mantsch, *Chem. Ber.*, **94,** 2887 (1961).

Revue Roumaine de Chimie, 28, 6, 653–657 (1983)

PYRIMIDINIUM-YLURES. V[1]

LES RÉACTIONS DE QUELQUES 4-PHÉNYLPYRIMIDINIUM-YLURES CARBANION-MONOSUBSTITUÉS AVEC LE NITROMÉTHANE

FLORENTINA C. GEORGESCU[a], E. I. GEORGESCU[a], E. G. GEORGESCU[b]
et I. ZUGRĂVESCU[c]

[a] Centre de Recherches, Rm. Vilcea, Roumanie
[b] Centre de Chimie Organique, Bucarest, Roumanie
[c] Institut Polytechnique Iassy, Roumanie

Reçu le 31 mars 1982

On a mis en évidence le fait que les réactions des 4-phénylpyrimidinium-ylures carbanion-monosubstitués avec le nitrométhane en milieu alcalin se produit avec la transformation du cycle pyrimidinique. Ainsi, par la réaction des 4-phénylpyrimidinium-ylures **2a**—**2e** avec le nitrométhane en milieu alcalin on obtient 2-phényle-5-nitropyridine **(9)**.

The reactions of carbanion-monosubstituted 4-phenylpyrimidinium-ylides with nitromethane in a basic medium occur with pyrimidine ring transformation. Thus, in the reaction of 4-phenylpyrimidinium-ylides **2a**—**2e** with nitromethane in a basic medium the 2-phenyl-5-nitropyridine **(9)** is formed.

Dans le cadre des recherches plus amples [2] concernant la chimie des azote-ylures nous avons étudié les possibilités de synthèse et la réactivité de quelques 4-phénylpyrimidinium-ylures carbanion-monosubstitués. [1,3,4]

Les 4-phénylpyrimidinium-ylures **2a**—**2e** ont été obtenus par la méthode générale d'obtention des cycloimmonium-ylures,[5] par la déhydrohalogénation des sels quaternaires de 4-phénylpyrimidinium [3] **1a**—**1e** sous l'action des bases.

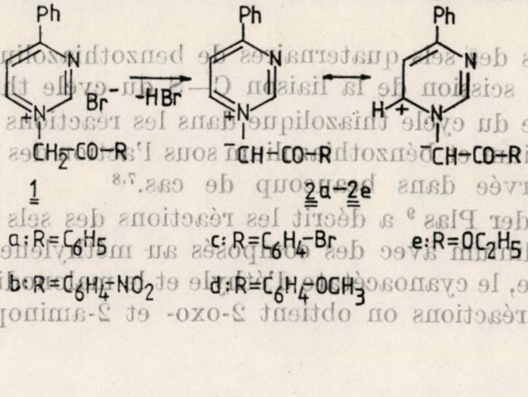

Le caractère dipolaire de ces produits a été demontré par la participation directe aux réactions de cycloadditions [3 + 2] dipolaires avec des acétylènes activés [4] et des oléfines activées.[1]

Pour obtenir de nouvelles données concernant la réactivité de ces produits, nous avons étudié les réactions des 4-phénylpyrimidinium-ylures carbanion-monosubstitués avec des composés nucléophyles comme le nitrométhane.

Etudiant la réactivité des isochinolinium-ylures, Kröhnke et Kiel [6] ont décrit une réaction de cyclisation des respectifs sels quaternaires avec le nitrométhane en milieu alcalin. La réaction se produit par l'attaque de l'anion du nitrométhane sur les isochinolinium-ylures **3**, formés en milieu alcalin par les sels quaternaires respectifs et par le cyclisation aldolique intramoléculaire de l'intérmediaire **4** avec la formation des pyrrolo[2,1-a] isochinolines **5** ou **6**.

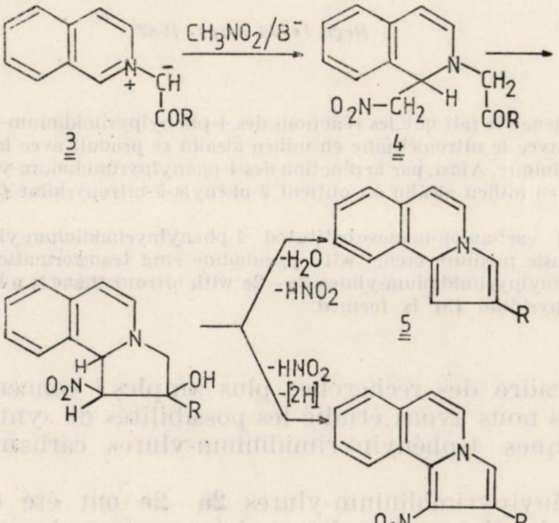

La réaction découle de la même manière dans le cas des chinolinium-ylures.[5]

Dans le cas des sels quaternaires de benzothiazolium la cyclisation est suivie par la scission de la liaison C—S du cycle thiazolique.[6]

L'ouverture du cycle thiazolique dans les réactions des sels quaternaires de thiazolium et benzothiazolium sous l'action des réagents nucléophyles est observée dans beaucoup de cas.[7,8]

H. C. van der Plas [9] a décrit les réactions des sels quaternaires de N-méthylpyrimidinium avec des composés au méthylène actif comme le malonate d'éthyle, le cyanoacétate d'éthyle et le malonodinitrile en milieu alcalin. Par ces réactions on obtient 2-oxo- et 2-aminopyridines substituées. La formation de ces composés implique, de même, une transformation du cycle. L'auteur considère que ces réactions sont caractéristiques aux dérivés pyrimidiniques avec un atome d'azote quaternisé.

En étudiant les réactions des 4-phénylpyrimidinium-ylures **2a**—**2e** avec le nitrométhane en présence de carbonate de sodium anhidre, nous nous sommes attendu aux dérivés pyrrolo[1,2-c]pyrimidiniques **7a**—**7e** ou **8a**—**8e**, éventuellement un mélange de ces deux composés, conformément au mécanisme proposé par Kröhnke et Kiel.[6]

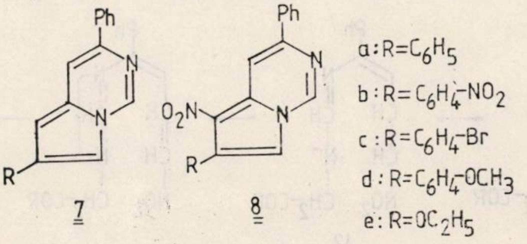

7 8

a : $R=C_6H_5$
b : $R=C_6H_4-NO_2$
c : $R=C_6H_4-Br$
d : $R=C_6H_4-OCH_3$
e : $R=OC_2H_5$

Mais, dans toutes ces réactions on a obtenu le même produit, quoi qu'il soit le substituent du carbanion d'ylure.

L'analyse des spectres IR, ^{1}H-RMN et UV, correlée avec les données de l'analyse élémentaire a indiqué la structure de 2-phényle-5-nitropyridine (**9**) pour ce produit.

Ainsi, le spéctre IR du produit (**9**) présente les bandes d'absorption caractéristiques au groupement nitro (1525 cm^{-1} et 1352 cm^{-1}) ; dans le spectre IR on remarque l'absence de la bande d'absorption caractéristique aux groupements carbonyle.

Le spectre ^{1}H-RMN du produit **9** confirme cette structure. Ainsi, le proton fortement déblindé H-6 apparaît comme un signal sous forme de double doublet avec la constante de couplage $J_{4,6} = 2{,}5$ Hz. Le signal du proton H-4 se présente sous forme de double doublet avec les constantes de couplage $J_{4,6} = 2{,}5$ Hz et $J_{3,4} = 8{,}5$ Hz. Le proton H-3 apparaît comme un signal sous forme de doublet avec la constante de couplage vicinal $J_{3,4} = 8{,}5$ Hz.

Les analyses du produit ont indiqué la formule moléculaire $C_{11}H_8N_2O_2$ qui correspond au nombre des protons du spectre ^{1}H-RMN.

La comparaison du spectre UV du composé **9** (EtOH : λ max. = = 316 nm) avec les spectres UV du *o*-, *m*- et *p*-nitrobiphényle[10] apporte une nouvelle épreuve pour la structure attribuée à ce produit.

La formation du produit **9** dans les réactions des 4-phénylpyrimidinium-ylures **2a**—**2e** avec le nitrométhane en milieu alcalin ne peut pas être expliqué à l'aide du mécanisme présenté au-dessus. Les réactions des ylures **2a**—**2e** avec le nitrométhane impliquent évidemment l'ouverture du cycle pyrimidinique.

Pour expliquer la formation du 2-phényle-5-nitropyridine **(9)**, nous avons proposé le mécanisme ci-dessous présenté.

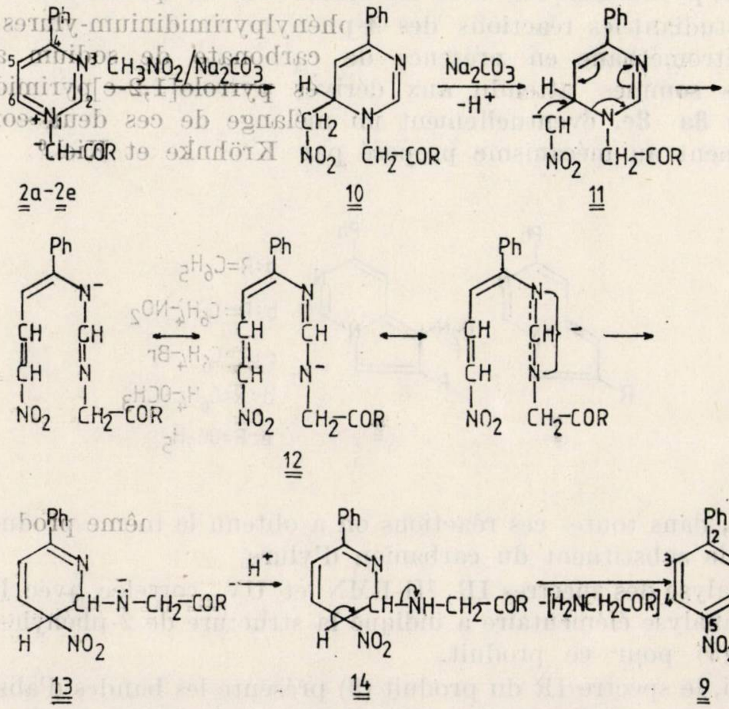

La réaction débute par l'addition de la molécule de nitrométhane aux 4-phénylpyrimidinium-ylures **2a**–**2e** avec la formation du dérivé 1,6-dihydro **10**. On peut former l'intermédiaire **10** relativement facile par l'attaque de l'anion du nitrométhane sur la position 6 au déficit d'électrons du 4-phénylpyrimidinium-ylures. Sous l'action de la base se produit une déprotonation du groupement méthylénique du dérivé 1,6-dihydro **10**. La scission de la liaison N_1-C_6 du cycle pyrimidinique et l'attaque nucléophyle du groupement méthynique de l'intermédiaire **11** sur l'atome de carbon C-2 peuvent être bien acceptés dans ce milieu alcalin et dans les conditions d'altération de la structure aromatique dans l'intermédiaire **11**, respectivement dans l'anion mésomère **12**. Par la scission du groupement α-aminocétonique des intermédiaires **13** et **14** et par le redressement de la structure aromatique, on obtient 2-phényle-5-nitropyridine **(9)**.

L'action de la base s'exerce dans tout le cours de la réaction et n'est pas limitée à la génération « in situ » des ylures **2a**–**2e** dans des sels quaternaires respectifs. Ce fait a été mis en évidence par les réactions directes des 4-phénylpyrimidinium-ylures stables **2b** et **2c** avec le nitrométhane en présence et en l'absence de la base. Ainsi, à des temps égaux de réaction, en présence de base se forme le produit **9** avec un rendement de 40–50%; dans l'absence de la base, le rendement en produit **9** est de 5—10%. La formation du produit **9** dans le dernier cas peut être expliquée par la basicité des ylures **2b** et **2c** (pK_a = 6,4, resp. 7,55 [3]).

Les données présentées montrent que dans la réaction des 4-phénylpyrimidinium-ylures carbanion-monosubstitués **2a**—**2e** avec le nitrométhane en milieu basique a lieu la transformation du cycle pyrimidinique en cycle pyridinique.

On propose un mécanisme pour ce type de réaction.

PARTIE EXPÉRIMENTALE

Les sels quaternaires de 4-phénylpyrimidinium **1a**—**1e** et les 4-phenylpyrimidinium-ylures stables **2b** et **2c** ont été obtenus d'après les procédés décrits dans un travail antérieur. [3]

Les points de fusion ne sont pas corrigés. Les spectres ^{1}H-RMN on été enregistrés sur un spectromètre VARIAN A-60 A et les spectres IR sur un spectromètre PERKIN-ELMER 621.

2-Phényle-5-nitropyridine (9)

a) On ajoute à une solution de 10 mmoles sel quaternaire **1a**—**1e** dans 50 ml nitrométhane 6g de carbonate de sodium anhydre. Le mélange de réaction est porté à reflux pendant 10 heures. Après le refroidissement la solution est filtrée. On chasse sous vide presque tout le nitrométhane. Le résidu est dissout dans le chlorure de méthylène et chromatographié sur Al_2O_3 (activité I). Par élution avec chloroforme on obtient un produit jaune. On récristallise le produit dans du méthanol ; p.f. = 119 — 121°C ; rd. = 40—60%. Analyse ($C_{11}H_8N_2O_2$) : calculé : C% = = 66,0, H% = 4,0 N% = 14,0 ; trouvé : C% 66,04, H% = 4,34, N% = 14,09. Spéctre IR (KBr, cm^{-1}) : 1600, 1525, 1352. Spéctre ^{1}H-RMN ($CHCl_3$, δ, ppm) : 7,33—7,68 (m, 3H, les protons du groupement phényle de la position 2), 7,87 (d, 1 H, H-3, $J_{3,4}$ = 8,5 Hz), 8,00—8,21 (m, 2H, les protons du groupement phényle de la position 2), 8,48 (d.d., 1H, H-4, $J_{3,4}$ = 8,5 Hz, $J_{4,6}$ 2,5 Hz), 9,45 (d, 1 H, H-6, $J_{4,6}$ = 2,5 Hz). Spectre UV (EtOH, λ max) : 316 nm.

b) On ajoute à une solution de 10 mmoles 4-phénylpyrimidinium 1-(*p*-nitrobénzoyl) méthylure **(2b)** et resp. 4-phénylpyrimidinium-1-(*p*-brombénzoyl) méthylure **(2c)** dans 50 ml nitrométhane 3 g de carbonate de sodium anhydre. Le mélange de réaction est porté à reflux pendant 10 heures et traité à la manière décrite au-dessus.

BIBLIOGRAPHIE

[1] F. Georgescu, E. G. Georgescu, F. Chiraleu, E. I. Georgescu et I. Zugrăvescu, *Rev. Roumaine Chim.*, sous press.

[2] I. Zugrăvescu et M. Petrovanu, «Chimia N-ilidelor», Ed. Academiei, București, 1974.

[3] I. Zugrăvescu, F. Georgescu, F. Chiraleu, P. Filip et E. I. Georgescu, *Rev. Chim. (București)*, **31**, 11 (1980).

[4] F. Georgescu, F. Chiraleu, E. I. Georgescu et I. Zugrăvescu, *Rev. Roumaine Chim.*, **26**, 879 (1981).

[5] F. Kröhnke, *Chem. Ber.*, **68**, 1177 (1935).

[6] W. Kiel et F. Kröhnke, *Chem. Ber.*, **105**, 3709 (1972).

[7] W. Friedrich, F. Kröhnke et P. Schiller, *Chem. Ber.*, **98**, 3804 (1965).

[8] W. Friedrich, H. Kehr, F. Kröhnke et P. Schiller, *Chem. Ber.*, **98**, 3808 (1965).

[9] H. C. van der Plas, *Hétérocycles*, **9**, 33 (1978).

[10] D. F. DeTar et H. J. Schleifele, *J. Amer. Chem. Soc.*, **73**, 1442 (1951).

Revue Roumaine de Chimie, **28**, *6*, 659–666 (1983)

STUDIES ON THE CYCLISED PRODUCTS OF THE STOBBE CONDENSATION BETWEEN *p*-BROMOPROPIOPHENONE AND DIETHYL SUCCINATE

M. A. El-HASHASH, G. H. SAYED and M. Y. El-KADY
Department of Chemistry, Faculty of Science, Ain Shams University Cairo, Egypt

Received July 4, 1981

The present investigation deals with the condensation of *p*-bromopropiophenone with diethylsuccinate under the Stobbe condensation conditions. The study was also extended to cover the reaction of the anhydrides obtained from the Stobbe condensations, with anhydrous aluminium chloride (in different solvents), hydrazines and amines.

As a continuation of the recent studies,[1,2] *p*-bromopropiophenone was condensed with diethylsuccinate in the presence of potassium tert-butoxide and yielded a crude oily mixture of half esters. The syntheses of various compounds are given in schemes 1—3. Saponification of the crude half esters gave *trans*- (4'-BrC_6H_4/COOH)-3-carboxy-4-ethyl-4 (4'-bromophenyl)-but-3-enoic acid (**1**) in pure crystalline state as predominant product, indicating that the preceding *trans*- (4'-BrC_6H_4/$COOC_2H_5$)-half ester is the major constituent of the Stobbe condensation products. Beside the crystalline dibasic acid, an oily dibasic acid fraction was also obtained.

The position of the double bond in both crystalline and oily dibasic acids was determined by oxidation with alkaline potassium permanganate; in each case the neutral oxidation product was characterised as the original ketone, [3] indicating that the dibasic acids and the preceding half esters have an alkylidene structure.

Further evidence for the position of the double bond in the dibasic acid **1** has been obtained from its IR spectrum, which shows the characteristic carbonyl stretching frequencies of α,β-unsaturated acids and that of non-conjugated carboxyl groups at 1695 and 1718 cm^{-1} respectively.

The *trans*-(4' -BrC_6H_4/COOH)-configuration assigned to the dibasic acid **1** was proved by the following route. Treatment with acetyl chloride converted the dibasic acid **1** to the corresponding cyclic anhydride **2**. The IR spectrum of the latter exhibited the carbonyl coupling bands expected from cyclic five-membered anhydrides at 1840 and 1770 cm^{-1}. Upon treatment with aluminium chloride in nitrobenzene, **2** gave 6-bromo-1-ethyl-4-hydroxy-2-naphthoic acid (**3**). The IR spectrum of **3** shows strong absorptions at 1685 cm^{-1} (ν C = O) and a broad peak centered at 3300 cm^{-1} (νOH).

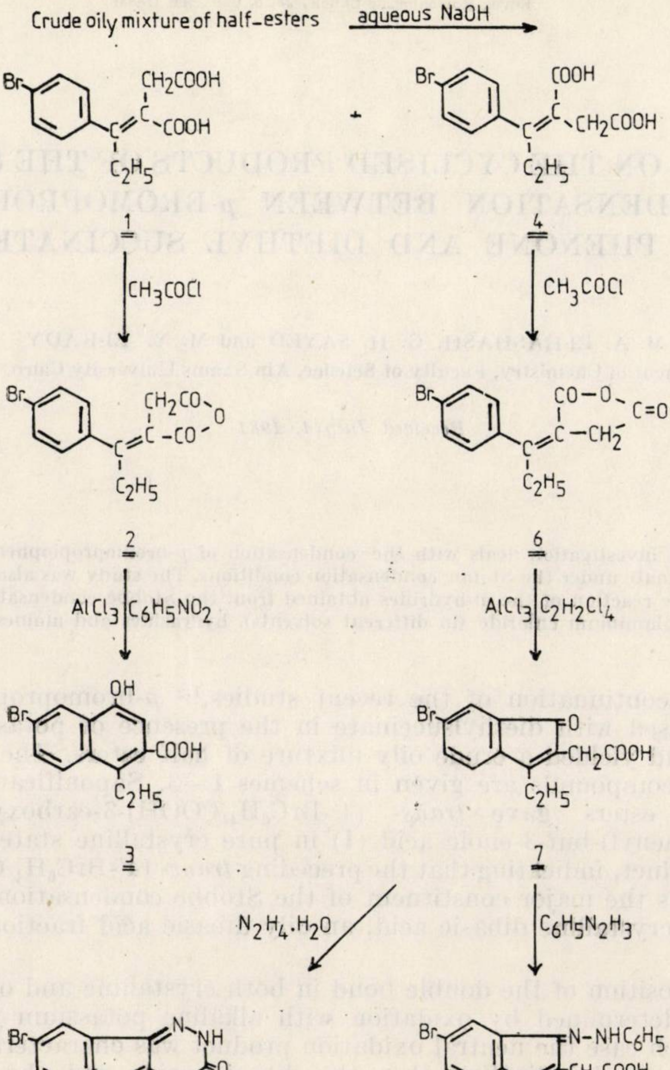
Crude oily mixture of half-esters
aqueous NaOH
CH3COCl
CH3COCl
AlCl3 / C6H5NO2
AlCl3 / C2H2Cl4
N2H4.H2O
C6H5NH2
1
4
2
6
3
7
12
13

Scheme 1

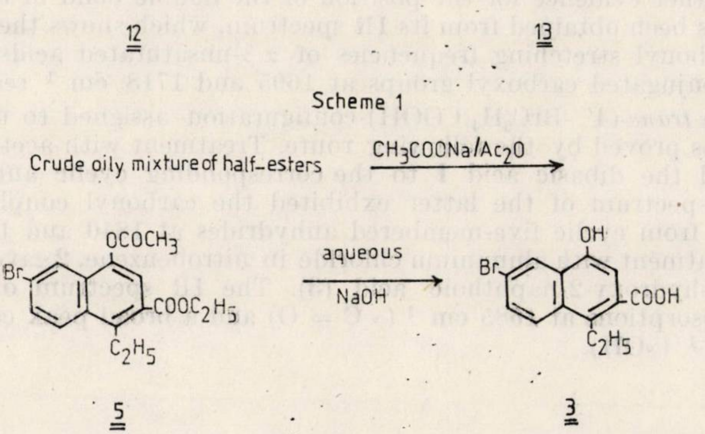
Crude oily mixture of half-esters
CH3COONa/Ac2O
aqueous NaOH
5
3

Scheme 2

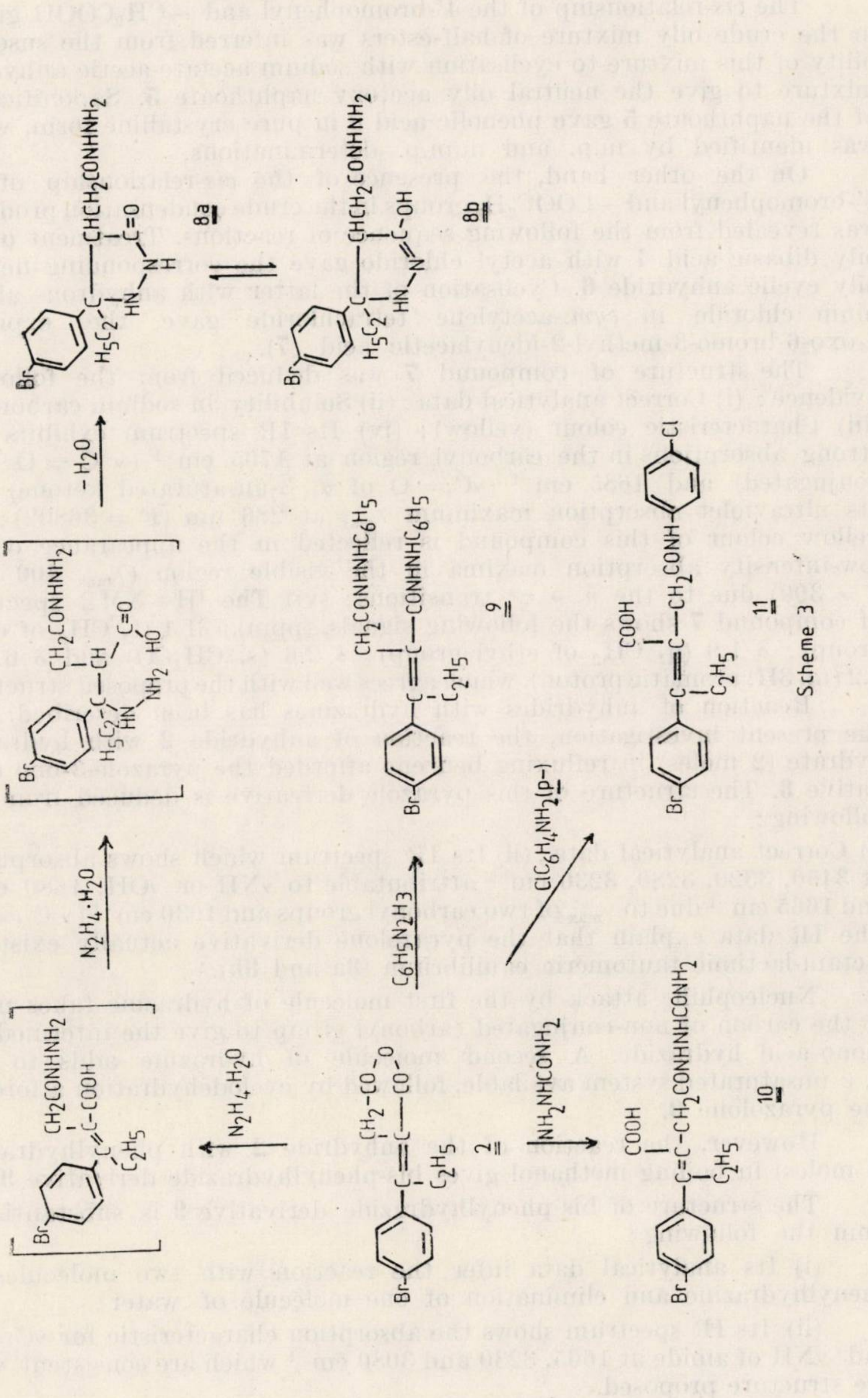
N₂H₄·H₂O
−H₂O
8a
8b
N₂H₄·H₂O
2
C₆H₅NHNH₃
9
ClC₆H₄NH₂(p-)
NH₂NCONH₂
10
11

Scheme 3

The *cis*-relationship of the 4'-bromophenyl and $-CH_2COOH$ groups in the crude oily mixture of half-esters was inferred from the susceptibility of this mixture to cyclisation with sodium acetate-acetic anhydride mixture to give the neutral oily acetoxy naphthoate **5**. Saponification of the naphthoate **5** gave phenolic acid **3** in pure crystalline form, which was identified by m.p. and m.m.p. determinations.

On the other hand, the presence of the *cis*-relationship of the 4'-bromophenyl and $-COOC_2H_5$ groups in the crude condensation products, was revealed from the following sequence of reactions. Treatment of the oily dibasic acid **4** with acetyl chloride gave the corresponding neutral oily cyclic anhydride **6**. Cyclisation of the latter with anhydrous aluminium chloride in *sym.*-acetylene tetrachloride gave the expected 1-oxo-6-bromo-3-methyl-2-idenylacetic acid (**7**).

The structure of compound **7** was deduced from the following evidence : (i) Correct analytical data ; (ii) Solubility in sodium carbonate ; (iii) Characteristic colour (yellow) ; (iv) Its IR spectrum exhibits two strong absorptions in the carbonyl region at 1705 cm^{-1} (ν C = O non-conjugated) and 1685 cm^{-1} (νC = O of α, β-unsaturated ketone) ; (v) Its ultraviolet absorption maximum λ_{max} at 286 nm (F = 36802) ; the yellow colour of this compound is reflected in the appearance of the low-intensity absorption maxima in the visible region (λ_{max} 400 nm ; $\varepsilon = 390$) due to the $n \rightarrow \pi^*$ transitions ; (vi) The ^1H-NMR spectrum of compound **7** shows the following signals, (ppm) ; δ1.1 (t, CH_3 of ethyl group) ; δ 1.9 (q, CH_2 of ethyl group) ; δ 2.6 (s, CH_2CO) and δ 6.9 – 7.2 (m, 3H, aromatic proton), which agrees well with the proposed structure.

Reaction of anhydrides with hydrazines has been described. [4] In the present investigation, the reaction of anhydride **2** with hydrazine hydrate (2 moles) in refluxing benzene afforded the pyrazole-3-one derivative **8**. The structure of this pyrazole derivative is deduced from the following :

(i) Correct analytical data ; (ii) Its IR spectrum which shows absorptions at 3450, 3320, 3280, 3230 cm^{-1} attributable to νNH or νOH, 1680 cm^{-1} and 1665 cm^{-1} due to ν_{max} of two carbonyl groups and 1630 cm^{-1} (ν C = N). The IR data explain that the pyrazolone derivative actually exists in lactam-lactimic tautomeric equilibrium (**8a** and **8b**).

Nucleophilic attack by the first molecule of hydrazine takes place at the carbon of non-conjugated carbonyl group to give the intermediate mono acid hydrazide. A second molecule of hydrazine adds to the α, β-unsaturated system available, followed by cyclodehydration affording the pyrazolone **8**.

However, the reaction of the anhydride **2** with phenylhydrazine (2 moles) in boiling methanol gives bis-phenylhydrazide derivative **9**.

The structure of bis-phenylhydrazide derivative **9** is substantiated from the following :

(i) Its analytical data infer the reaction with two molecules of phenylhydrazine and elimination of one molecule of water ;

(ii) Its IR spectrum shows the absorption characteristic for νC = O and νNH of amide at 1665, 3230 and 3080 cm^{-1} which are consistent with the structure proposed.

The treatment of anhydride **2** with semicarbazide in refluxing pyridine yielded 3-carboxy-4 (4′-bromophenyl)-4-ethyl-but-3-enoic acid carbamoylhydrazide (**10**).

The structure of carbamoylhydrazide derivative **10** was inferred from the following:

(i) Solubility in sodium carbonate solution;

(ii) Its IR spectrum shows ν_{max} of three carbonyl groups at 1705 (for COOH), 1660 (primary amide) and 1640 cm^{-1} (secondary amides) and ν_{max} for NH groups at 3300 and 3100 cm^{-1}, which agree well with the suggested structure.

The acylation of aromatic amines with anhydrides in the presence of dry benzene has been described. [5] In the present investigation, treatment of anhydride **2** with *p*-chloroaniline gave N(4′-chlorophenyl)-3-carboxy-4 (4′-bromophenyl)-4-ethyl-but-3-enoic acid amide (**11**).

The IR spectrum of **11** shows strong absorption at 1690 and 1670 cm^{-1} attributable to ν_{max} of two carbonyl groups, 3310 (intra-molecularly hydrogen bond), 3200 cm^{-1} (bonded NH).

As a point of interest, this work also investigated the reaction of indenyl acetic acid derivative **7** with hydrazines.

Thus, compound **7** reacted with hydrazine hydrate in ethanol and gave the pyridazinone derivative **12**. The IR spectrum of compound **12** showed carbonyl stretching frequency for cyclic amide at 1676 cm^{-1}, νNH 3300 cm^{-1} (broad) and $\nu C{=}N$ at 1610 cm^{-1} which are consistent with the structure proposed.

However, when compound **7** was allowed to react with phenylhydrazine in ethanol, the corresponding phenylhydrazone **13** was obtained. Structure of **13** was inferred from: (i) Its solubility in sodium carbonate solution; (ii) Its IR spectrum which shows strong absorptions at 3300 cm^{-1}, 3210 cm^{-1}, 1715 cm^{-1} and 1630 cm^{-1} attributable to νOH, νNH, $\nu C = O$ and $\nu C = N$ respectively.

EXPERIMENTAL

Melting points are uncorrected, IR spectra were measured with a Pye Unicam infrared spectrophotometer, using KBr Wafer technique, the UV spectrum was recorded on a Coleman Hitachi 124 double beam instrument in ethanol solution, the ^{1}H-NMR spectrum on a Jeol JMN-F 100 pulse Fourier transform instrument in deuterated acetone solution.

Stobbe condensation of *p*-bromopropiophenone with diethylsuccinate

To a gently warmed solution of potassium *tert.*-butoxide (1.1 mole) a solution of diethylsuccinate (1.5 mole) and *p*-bromopropiophenone (1 mole) is added dropwise and the mixture is stirred for two hours in a boiling water-bath. The reaction mixture is cooled and becomes slightly acidic by addition of a few drops of dil. HCl, then concentrated (by aid of a water-pump). The residual product is dissolved in H_2O and acidified by dil. HCl. The residual oily materials were extracted with ether. The ethereal layer is extracted several times with 10% aqueous sodium carbonate solution; the carbonate solution is cooled and acidified by dil. HCl, and the oily precipitate extracted with ether. Evaporation of the dried ether extract gives the crude oily acidic product in 88% yield.

Saponification of the oily half-ester

The oily half ester (25 g) was refluxed with 10 % aqueous sodium hydroxide (*ca.* 8 ml per 1 g half ester) for a period of 4—5 hrs. The alkaline solution was then cooled in ice, acidified with dil. HCl, and the precipitated material taken-up in ether. Evaporation of the dried ether extract gives the oily acidic fraction (20 g; 87 % yield).

By dissolving 20 g of oily acidic fraction in boiling benzene, and preserving overnight, two fractions were obtained : (i) A crystalline solid (14 g), m.p. 156°C (identified as diacid **1**) ; (ii) An oily acidic fraction (*ca.* 6 g) obtained by evaporation of the mother liquor (diacid **4**).

Note : The predominance of E-configurational half-ester *cis*-($4\text{-}BrC_6H_4/CH_2COOH$) can be deduced from the high percentage (70 %) of the corresponding crystalline dibasic acid.

Oxidation of the dibasic acids

To an ice-cold solution of the crystalline or oily dibasic acid (2 g) in 3 % Na_2CO_3 solution (200 ml) a cold 2 % $KMnO_4$ solution (120 ml) was added portionwise with stirring. The reaction mixture was left at room temperature for 24 hrs. The precipitated MnO_2 was filtered. Both filtrate and precipitate were thoroughly extracted with ether followed by benzene. Evaporation of combined organic extracts gave colourless crystals, m.p. 48°C undepressed upon admixture with *p*-bromopropriophenone.

Conversion of diacid 1 to anhydride 2

Diacid **1** (6 g) was refluxed with acetyl chloride (60 ml) for 1 hr. Excess acetyl chloride was then removed by distillation, the last traces being removed by addition of small amounts of light petroleum (b.p. 40—60°C) followed by distillation to give the neutral solid product **2** (*ca.* 5 g; 88 % yield). The results are listed in Table 1.

Action of aluminium chloride on crystalline anhydride 2

To a stirred ice-cold solution of anhydride (5 g) in dry nitrobenzene (50 ml), powdered anhydrous $ALCl_3$ (*ca.* 5 g) was added in one portion and stirring was continued for 6 hrs. The reaction mixture was left aside for two days at room temperature with occasional stirring, then decomposed with ice-cold dil. HCl. The nitrobenzene was removed by steam distillation and the reaction product extracted with ether. The ethereal solution was extracted with 5 % aqueous Na_2CO_3 solution, and the cold alkaline solution was finally acidified. The acidic reaction product was then isolated by extraction with ether. Evaporation of the dried ether extract gave the phenolic acid **3**(1.9 g ; *ca.* 40 % yield). The results are listed in Table 1.

Cyclisation of the crude oily half-esters mixture

A mixture of the half-ester (10 g), freshly fused CH_3COONa (*ca.* 3 g) and acetic anhydride (100 ml) was refluxed for 8 hrs. The excess of acetic anhydride was removed under reduced pressure, water was added and the organic material was extracted with ether. The ethanol solution was successively washed with water, 5 % Na_2CO_3 solution, cold 5 % NaOH solution and finally with water. Evaporation of the dried ether solution gave the neutral cyclisation product **5** as an oily material (6.5 g; 60 % yield).

Saponification of acetoxynaphthoates 5

The acetoxy ester **5** (6.5 g) was refluxed with 10 % aqueous NaOH (70 ml) for 5 hrs. The solution was extracted once with ether to remove the unsaponified material. The alkaline solution was then cooled, acidified with dil. HCl, and the precipitated material was taken up in ether. Evaporation of the dried ethereal solution left the desired phenolic acid **3** (18 g ; 34 % yield) which was identified by m.p. and m.m.p. determinations.

Conversion of the oily diacid 4 to the corresponding oily anhydride 6

The reaction was carried out as described at anhydride **2** (5 g diacid gave 4.2 g neutral oily product *6* ; 89 % yield).

Table 1

Characterisation of the new compounds

Compd.	M.p. °C Colour	Recrystallisation solvent *	Formula	Analysis %		
					Required	Found
1	156 colourless	A	$C_{13}H_{13}O_4Br$	C H	49.84 4.15	49.80 4.21
2	89 colourless	B	$C_{13}H_{11}O_3Br$	C H	52.88 3.73	52.85 3.67
3	168 grey	C	$C_{13}H_{11}O_3Br$	C H	52.88 3.73	52.83 3.75
7	179 yellow	A	$C_{13}H_{11}O_3Br$	C H	52.88 3.73	52.79 3.74
8	197 colourless	D	$C_{13}H_{17}O_2N_4Br$	C H N	45.75 4.99 16.42	45.69 4.94 16.38
9	142 colourless	D	$C_{25}H_{25}O_2N_4Br$	C H N	60.85 5.07 11.36	60.87 5.13 11.42
10	172 colourless	A	$C_{14}H_{16}O_4N_3Br$	C H N	45.41 4.32 11.35	45.36 4.41 11.42
11	176 colourless	B	$C_{19}N_{17}O_3NBrCl$	C H N	53.96 4.02 3.31	53.88 4.11 3.34
12	191 colourless	D	$C_{13}H_{11}N_2OBr$	C H N	53.61 3.78 9.62	53.63 3.82 9.71
13	182 reddish	D	$C_{19}H_{17}N_2O_2Br$	C H N	59.22 4.42 7.27	59.26 4.38 7.32

* A = Benzene ; B = Petroleum ether (100–120°C) ; C = dil. acetic acid ; D = Ethanol.

Action of aluminium chloride on oily anhydride 6

The reaction was carried out using the procedure described for the reaction of **2** except that the nitrobenzene was replaced by acetylene tetrachloride (4.2 g of **6** gave 2 g of **7**; *ca.* 50% yield). The results are listed in Table 1.

Action of hydrazine hydrate on anhydride 2

A solution of anhydride **2** (2.9 g, 0.01 mole) in dry benzene (40 ml) was refluxed with hydrazine hydrate (0.02 mole) for 4 hrs. The reaction mixture was concentrated and cooled. The solid separated was crystallised from the proper solvent and gave the pyrazolone **8**, (2.3 g, *ca.* 67%). The results are listed in Table 1.

Action of phenylhydrazine on anhydride 2

The reaction was carried out as described in reaction with N_2H_4 except that the dry benzene was replaced by methanol (2.9 g of **2** gave 1.6 g of bis-phenylhydrazide **9**; yield 33%). The results are listed in Table 1.

Action of semicarbazide on anhydride 2

The reaction was carried out as described in reaction with N_2H_4 except that dry benzene was replaced by pyridine and the reaction mixture was poured upon ice-dil. HCl. The precipitate obtained was crystallised from the proper solvent and gave the carbamoyl derivative **10** (1.4 g; yield 37%).

Action of *p*-chloroaniline on anhydride 2

The reaction was carried out as described in reaction with N_2H_4 (2.9 g of **2** gave 1.9 g of **11**, 45% yield). The results are listed in Table 1.

Action of hydrazines on the indenyl acetic acid derivative 7

A solution of compound **7** (1.4 g; 0.005 mole), hydrazine hydrate or phenylhydrazine (0.005 mole) in ethanol (40 ml) was refluxed for 5 hrs. The reaction mixture was concentrated and cooled, the separated solids were crystallised from the proper solvent and gave pyridazinone **12** (0.8 g; 57% yield) and phenylhydrazone **13** (0.7 g; 37% yield).

REFERENCES

[1] M. F. El-Newaihy and M. A. El-Hashash, *J. Chem. Soc.* (*C*), **1971**, 2373.
[2] M. A. El-Hashash and A. A. El-Khamry, *Pakistan J. Sci. Res.* (in press).
[3] Collect, *Compt. rend.*, **126**, 1577 (1898).
[4] H. Ferrer, G. B. Bachman and E. H. White, *J. Amer. Chem. Soc.*, **73**, 4716 (1951).
[5] L. E. Coleman, J. F. Bork and H. Dunn, *J. Org. Chem.*, **24**, 135 (1959).

NOTE POUR LES AUTEURS

La Revue Roumaine de Chimie publie des articles en anglais, français, russe, allemand ou espagnol. Les auteurs sont priés d'envoyer des articles et des comptes rendus inédits.

Les manuscrits seront dactylographiés à double interligne. La bibliographie, les tableaux et la légende des figures seront placés après le texte.

Si l'article fait partie d'une série numérotée, la partie précédente sera donnée comme première référence.

Chaque article sera précédé d'un résumé comprenant quinze lignes au maximum.

Les références bibliographiques dans le texte seront faites par des exposants sans parenthèses et paraîtront à la fin de l'ouvrage.

Les publications périodiques mentionnées dans la bibliographie seront présentées suivant les prescriptions internationales : le nom de l'auteur précédé de l'initiale du prénom, le titre du périodique abrégé conformément à « Chemical Abstracts » et souligné par une ligne, le numéro du tome indiqué par des chiffres arabes et souligné par deux lignes, suivi de la première page de l'article ; à la fin, l'année de la parution sera placée entre parenthèses. La numéro de la revue ne sera pas indiqué si les pages du volume sont numérotées consécutivement.

Les textes des livres ou traités inclueront : le nom des auteurs, l'initiale du prénom, le titre du livre entre guillemets et sans être souligné, le numéro du tome précédé par l'abréviation « vol. » (ou « Bd. »), le numéro de l'édition, les éditions (the publisher), la localité de la parution du livre, l'année de la parution et la page de la référence précédée(s) par l'abréviation « p » (ou « S »).

Les brevets seront indiqués comme suit : l'auteur ou la firme, le pays et le numéro du brevet, la date et la revue (*Chem. Abstr.*). Par ex. : M. Jones (to Union Carbide Co.), Brit. Pat. 601 238, 2 sept. 1959 ; cf. *Chem. Abstr.*, **54**, 12808 (1960).

Si la référence n'a pas été lue en original, on indiquera aussi la revue de références consultée.

Les diagrammes seront tracés à l'encre de Chine sur papier calque. Les tableaux et les figures (en nombre strictement nécessaire) ainsi que les courbes dans les figures seront numérotés par des chiffres arabes. Leur explication sera donnée dans la légende des figures. Prière de ne pas inscrire les mêmes données dans les tableaux et les figures. Chaque tableau aura un titre. On indiquera dans le texte la place approximative des tableaux et des figures. Les formules chimiques seront incluses dans le texte ; en outre, elles seront transcrites sur papier calque, à l'encre de Chine.

Les auteurs sont priés d'indiquer les caractères italiques (en soulignant les lettres au crayon), ainsi que tout autre caractère spécial : les préfixes *ortho*, *meta*, *para*, *cis*, *trans*, etc. seront soulignés pour indiquer leurs caractères italiques et ne seront jamais écrits avec des majuscules.

Aucune correction à la main ne sera admise sur le manuscrit. Les corrections seront tapées à la machine. Les lettres grecques ou d'autres symboles spéciaux seront insérés à la main à l'encre clairement.

Le manuscrit sera signé par l'auteur.

Le titre-courant aura 50 lettres au maximum.

L'entière responsabilité du contenu des articles appartient aux auteurs.

Sur demande on peut obtenir une note plus complète.

PRINTED IN ROMANIA

1984 JAN 12

TRAVAUX PARUS AUX ÉDITIONS DE L'ACADÉMIE DE LA RÉPUBLIQUE SOCIALISTE DE ROUMANIE

ELENA CEAUŞESCU, **Noi cercetări în domeniul compuşilor macromoleculari** (Nouvelles recherches dans le domaine des composés macromoleculaires), 1981, 536 p.

L. G. MURGULESCU, RODICA VÎLCU, **Introducere în chimia fizică. III. Termodinamica chimică** (Introduction à la chimie physique, Vol. III, Thermodynamique chimique), 1982, 624 p.

I. G. MURGULESCU, J. PĂUN, **Introducere în chimia fizică, Vol. I. 3. Nucleul atomic, reacţii nucleare, particule elementare** (Introduction à la chimie physique. Vol. I. 3. Noyau atomique, réactions nucléaires, particules élémentaires), 1982, 606 p.

ELENA JERCAN, **Analiza cromatografică** (Analyse chromatographique), 1982, 286 p.

I. G. MURGULESCU, TATIANA ONCESCU, E. SEGAL, **Introducere în chimia fizică, Vol. II.2. Cinetică chimică şi cataliză** (Introduction à la chimie physique. Vol. II.2. Cinétique chimique et catalyse) 1981, 1024 p.

V. DRĂGUŢAN, A. T. BALABAN, M. DIMONIE, **Metateza olefinelor şi polimerizarea prin deschidere de inel a cicloolefinelor** (La métathèse des oléfines et la polymérisation par ouverture annulaire des cyclooléfines), 1981, 254 p.

LYDIA-MARIA VAICUM, **Epurarea apelor uzate cu nămol activ. Bazele biochimice** (L'épuration des eaux résiduelles à boue active. Les bases biochimiques), 1981, 218 p.

I. GĂLĂŢEANU, **Procese şi metode radiochimice în energetica nucleară** (Processus et méthodes radiochimiques dans l'énergétique nucléaire), 1981, 234 p.

OCTAVIAN IORDACHE, **Procese polistocastice aplicate la fenomenele de transfer** (Processus polystochastiques appliqués aux phénomènes de transfert), 1981, 186 p.

CR. SIMIONESCU, VALERIA GORDUZA, **Polimeri biocompatibili şi biologic activi** (Polymères biocompatibles et biologiquement actifs), 1980, 479 p.

ELENA CEAUŞESCU, **Polimerizarea stereospecifică a izoprenului** (La polymérisation stéréospécifique de l'isoprène), 1979, 307 p.

CONST. GH. MACAROVICI, **Analiza chimică cantitativă anorganică** (L'analyse chimique quantitative inorganique), 1979, 457 p.

M. FLORESCU, **Metode ştiinţifice în dezvoltarea industriei chimice moderne** (Méthodes scientifiques dans le développement de l'industrie chimique moderne), 1979, 256 p.

A. T. BALABAN, I. GĂLĂŢEANU, G. GEORGESCU, LIGIA SIMIONESCU, **Compuşi marcaţi şi radiofarmaceutici cu aplicaţii în medicina nucleară** (Composés marqués et radiopharmaceutiques à application en médecine nucléaire), 1979, 495 p.

I. G. MURGULESCU, E. SEGAL, **Introducere în chimia fizică, vol. II. 1. Teoria molecular cinetică a materiei** (Introduction à la chimie physique. Vol. II.1. La théorie moléculaire-cinétique de la matière), 1979, 1036 p.

S. STERNBERG, FL. DANEŞ, **Termodinamica chimică aplicată** (La thermodynamique chimique appliquée), 1978, 400 p.

I. G. MURGULESCU, V. EM. SAHINI, **Introducere în chimia fizică, Vol. I.2. Structura şi proprietăţile moleculelor** (Introduction à la chimie physique. Vol. I.2. La structure et les propriétés des molécules), 1978, 604 p.

I. ZUGRĂVESCU, MAGDA PETROVANU, **N-ylid chemistry**, coédition avec McGraw-Hill International Book Company, U.S.A., 1977, 396 p.

I. G. MURGULESCU, **Introducere în chimia fizică. Vol. I.1. Atomi, molecule, legătură chimică,** (Introduction à la chimie physique, Vol. I. 1. Atomes, molécules, liaison chimique), 1976, 560 p.

ELENA CEAUŞESCU, **Research work on synthesis and characterization of macromolecular compounds. Contributions**, 1974, 251 p.

CR. SIMIONESCU, VIORICA RUSAN, V. POPA, **Chimia algelor marine** (La chimie des algues marines), 1974, 212 p., 1 pl.

ISSN 0035 — 4090

Lei 40

I. P. Informaţia c. 1147

43 426

$ 75 (pour un abonnement annuel)

66 0F1103 104

ACADÉMIE DE LA RÉPUBLIQUE SOCIALISTE DE ROUMANIE

VEGYÉSZ

R

REVUE ROUMAINE DE CHIMIE

REFERÁLVA

TOME 28

N° 7

Juillet 1983

EDITURA ACADEMIEI REPUBLICII SOCIALISTE ROMÂNIA

Rev. Roumaine Chim.

RRCHAX, 28, 7, p. 667–776 (1983), Bucarest

ACADÉMIE DE LA RÉPUBLIQUE SOCIALISTE DE ROUMANIE

COMITÉ DE RÉDACTION

Rédacteur en chef :

I. G. MURGULESCU, membre de l'Académie de la République Socialiste de Roumanie

Rédacteurs en chef adjoints :

A. T. BALABAN et V. EM. SAHINI, membres correspondants de l'Académie de la République Socialiste de Roumanie

Collège de rédaction :

EM. BRATU, ELENA CEAUȘESCU, ECATERINA CIORĂNESCU-NENITZESCU, CR. SIMIONESCU, membres de l'Académie de la République Socialiste de Roumanie : P. SPACU, membre correspondant de l'Académie de la République Socialiste de Roumanie ; MARGARETA AVRAM, M. BANCIU, I. HAIDUC, D. I. MARCHIDAN, I. MOLDOVAN, G. NIAC et D. SĂNDULESCU

La Revue Roumaine de Chimie paraît 10 fois par an. Toute commande de l'étranger pour les travaux parus aux Editions de l'Académie de la République Socialiste de Roumanie sera adressée à ILEXIM — Departamentul Export-Import Carte (Livres)/Departamentul Export-Import Presă (Revues), P.O.B. 136—137, télex 11226, 3, str. 13 Decembrie, 79517 Bucarest, Roumanie

Les manuscrits, les livres et les revues proposés en échange, ainsi que toute correspondance seront envoyés à la rédaction :

REVUE ROUMAINE DE CHIMIE
125, Calea Victoriei, 79717 Bucarest, Roumanie, téléphone 50 76 80

EDITURA ACADEMIEI REPUBLICII SOCIALISTE ROMÂNIA
125, Calea Victoriei, 79717 Bucarest, Roumanie, téléphone 50 76 80

REVUE ROUMAINE
DE
CHIMIE

Tome 28, N° 7 Juillet, 1983

IOAN SĂNDULESCU, IOAN V. NICOLESCU, XU YANDONG and VASILE PÎRVULESCU, Selectivity and other properties of Pd, Mn and Pd-Mn/Al_2O_3 catalysts for styrene hydrogenation . . . . 669–682 R

I. MÎNDRU, MIHAELA OLTEANU, LI DEHE and V. TRANDAFIR, Glass transition of polyblends of collagen hydrolysates and poly(ethyl acrylate) 683–687 Bc

ELENA VOLANSCHI and MELANIA VOICU, ESR and electronic spectra of some nitrosubstituted thioureide anion-radicals . . . . 689–697 C

ANTONIE DINCULESCU, MAHMOUD FAHMY, FILIP CHIRALEU and ALEXANDRU T. BALABAN, Reaction of pyrylium salts with nucleophiles. XVI. New *N*-substituted 2,4,6-trimethylpyridinium salts and their ^1H-NMR spectra 699–705

EMIL STEPAN and ALEXANDRU T. BALABAN, Reactions of pyrylium salts with nucleophiles. XVII. New 2,4,6-trisubstituted bis- and tris-pyridinium salts and their ^1H-NMR spectra 707–714

M. A. HASSAN, A. F. ELKAFRAWY and M. ElBORAI, Some reactions of 2-oxo-1,2,3,4-tetrahydronicotinonitriles 715–718

SIMONA SILBERG and IOAN A. SILBERG, Derivatives of 4-aminomethyl-thiazole. II. New thiazole derivatives of urea and thiourea 719–724

Z. H. KHALIL and A. IBRAHIM, Synthesis and spectral behaviour of benzoxazolium indolo (or benzofurano) quinolinium bisethiodide cyanine dyes . . . . 725–732 R

C. CRISTESCU, *as*-Triazine derivatives with potential therapeutic action. XVII. Synthesis of 5-mercapto-6-azauracil-S-riboside 733–736

C. I. CHIRIAC, A new synthesis of aromatic esters by a direct condensation reaction . . . . 737–739 R

ANA AURELIA BOTAR, A. BARABÁS, I. OPREAN, JULIANNA CSONKA-HORVAI and F. HODOŞAN, Exo- and endohormones. VI. Syntheses of the sex pheromones of some Lepidoptera 741–756

J. HERDAN, LIVIA CRIŞAN, M. LUCA and S. BALIU, New polymers with heterocyclic side groups having antioxidant properties . . . . 757–762 R

ŞTEFAN UNGUREANU, MATEI MACOVEANU and CORNELIU PETRILĂ, Study of the sensitivity of a reactor for vinyl chloride suspension polymerization with constant rate (in German) 763–773

BOOK REVIEW 775–776

|Rev. Roumaine Chim.| **28**, 7, 667–776 (1983), Bucarest

Revue Roumaine de Chimie, 28, 7, 669–682 (1983)

SELECTIVITY AND OTHER PROPERTIES OF Pd, Mn AND Pd-Mn/Al_2O_3 CATALYSTS FOR STYRENE HYDROGENATION

IOAN SĂNDULESCU, IOAN V. NICOLESCU, XU YANDONG, and
VASILE PÎRVULESCU

National Institute of Chemistry, Department of Chemical Technology and Catalysis,
Bucharest, Romania

Received July 21, 1982

In the styrene hydrogenation reaction, the selectivity for ethylbenzene or ethylcyclohexane depends on the nature of the interaction between styrene and the catalyst surface. The modification of selectivity of styrene hydrogenation on supported Pd, Mn and Pd-Mn/γ-Al_2O_3 catalysts was investigated. Some correlations were also established between selectivity and physical and electronic properties, as determined by X-ray diffraction, ESR, magnetic susceptibility measurements, electron microscopy and analysis of X-ray energy dispersion.

Beside its practical importance,[1] the hydrogenation of styrene on supported metal catalysts is also interesting from a theoretical point of view. As a consequence of the presence of two unsaturated systems which can interact with the metal, the reaction may proceed to give either ethylbenzene or ethylcyclohexane, depending on the nature of the interaction, hence on the way in which this metal is dispersed on the support surface.[2]

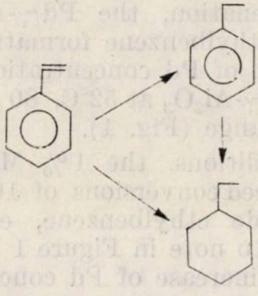

In the case of bimetallic catalysts, this is compounded by the interaction which occurs between the two metals, which is in turn a function of their electronic structure.

In order to correlate the activity and selectivity of supported metal catalysts with the electronic properties of the metal, we investigated the behaviour of the Pd/γ-Al_2O_3, Mn/γ-Al_2O_3 and Pd-Mn/γ-Al_2O_3 catalysts in the hydrogenation reaction of styrene.

EXPERIMENTAL TECHNIQUES

The Pd/γ-Al_2O_3 catalyst was prepared by impregnating γ-Al_2O_3 with an acidic $PdCl_2$ solution ; the samples were then dried at 110°C, calcined at 550°C and reduced in flowing hydrogen at 350°C.

The Mn/γ-Al_2O_3 catalyst was prepared by impregnating γ-Al_2O_3 with a solution of $Mn(NO_3)_2$, followed by drying at 110°C, calcination at 550°C and reduction in flowing hydrogen at 750°C.[3]

The Pd-Mn/γ-Al_2O_3 catalyst was prepared by impregnating the previously mentioned Pd/γ-Al_2O_3 catalyst with a $Mn(NO_3)_2$ solution ; the samples were dried at 110°C, calcined at 550°C and reduced in hydrogen at 750°C.

The reactions were carried out in chromatographic pulse [4,5] in a microreactor, with hydrogen as carrier, subject to the following conditions :

- weight of the catalyst 0.14 g ;
- reaction temperature 40—75°C ;
- hydrogen flow rate 50—150 ml/min ;
- volume of a pulse 0.5—5 µl.

The results related to the activity and to the variation of the activity and selectivity with the nature of the catalyst and the reaction conditions have been published elsewhere.[6]

The physico-chemical and electronic properties of the catalysts were determined by X-ray diffraction, ESR, magnetic susceptibility measurements and electron microscopy, as well as by analysis of X-ray energy dispersion.

X-ray structural measurements were carried out with a TUR-M 62 instrument provided with a HZG-3 diffractometer with electronic recording and a VAZ-522 proportional counter, in the following conditions : CuK_α radiation ; Ni filter ; tube supplied with 35 mA at 40 kV ; $V_{counter} = 0.5°/min$; $v_{paper} = 10$ mm/min ; pulse scale : 1.8×10^4 pulses/min ; statistical deviation : 1 %.

ESR spectra were obtained at room temperature with a Jeol JSB-3B spectrometer operating in the X-band, with 100 kHz frequency modulation. The parameters of the spectra were measured in comparison with a sample of Mn^{2+} in MgO.

Magnetic susceptibility was measured with a magnetic balance by the Faraday method.

To get the surface images and the metal distribution on the surface, a Stereoscan 180 scanning electron microscope, coupled with a Link-type spectrometer for the analysis of energy dispersion of X rays, was used. Images "with elemental contrast" were obtained ; they monitor the metal distribution on the analysed surfaces.

EXPERIMENTAL RESULTS

For styrene hydrogenation, the Pd/γ-Al_2O_3 catalysts showed a 100 % selectivity toward ethylbenzene formation, whereas their activity increased with the increase of Pd concentration (from 5 % for 0.1 Pd/γ-Al_2O_3 to 73 % for 0.5 % Pd/γ-Al_2O_3 at 52°C, 80 ml H_2/min and 3 µl pulses) over the whole working range (Fig. 1).

Under the same conditions, the 1 % Mn/γ-Al_2O_3 and 1 % Mn + Pd/γ-Al_2O_3 catalysts produced conversions of 100 %, but the reaction was no longer selective: beside ethylbenzene, ethylcyclohexane was also obtained. It is interesting to note in Figure 1 the variation of selectivity for ethylbenzene with the increase of Pd concentration from 0 to 0.5 %.

The 1 % Mn/γ-Al_2O_3 catalyst had an 85 % selectivity for ethylbenzene. The presence of 0.1 % Pd increased the selectivity to 92 %, but the continuing increase of Pd concentration decreased significantly the selectivity for ethylbenzene, down to 50.5 % for the 1 % Mn + 0.5 % Pd/γ-Al_2O_3 catalyst.

This modification of selectivity of the bicomponent catalyst with the increase in Pd concentration is difficult to account for, given the acti-

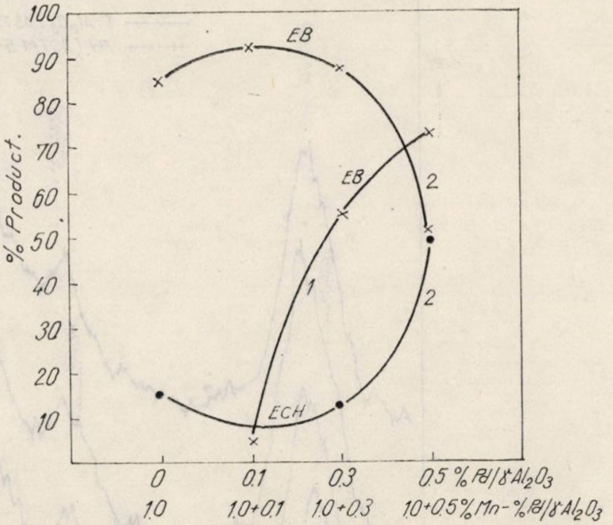

Fig. 1. — Variation of the activity and selectivity in styrene hydrogenation with the nature of the catalyst. *1* — Pd/γ-Al_2O_3 catalysts, *2* — 1.0 % Mn-Pd/γ-Al_2O_3 catalysts, *EB* — ethylbenzene, *ECH* — ethylcyclohexane.

vity of the unicomponent catalysts. In all considered cases of bicomponent catalysts, the conversions were of 100 % (at temperatures exceeding 50°C), and the variation of the selectivity was analogous.

This fact led us to the assumption that an interaction might occur between the two metals supported on γ-Al_2O_3. This interaction is determined by the concentration ratio of the two metals and determines in turn the reaction pathway.

In all the X-ray spectra of the catalysts the lines of γ-Al_2O_3 remained clearly distinguishable. No typical lines of Mn or Pd could be observed, which was taken as a proof that no detectable metallic clusters occur.

However, in the 0.5 % Pd—1 % Mn/γ-Al_2O_3 sample a trend to the appearance of the typical Pd lines was noticed (Fig. 2). We might assume that a certain dispersion of manganese on the alumina surface exists, with clusters too small to be detected by X-ray diffraction. For palladium, an increase of the cluster size occurs when the Pd concentration increases; when the Pd concentration of 0.5 % is reached, sizable clusters could be observed.

To prove the existence of metallic manganese, we recorded the ESR spectra of the reduced catalysts in comparison with the spectrum of a sample of 1 % Mn/γ-Al_2O_3 obtained by impregnation of Al_2O_3 with a solution of manganese nitrate and by (i) drying at 50°C, (ii) calcination at 550°C and (iii) reduction in flowing hydrogen at 750°C. The spectrum of the sample containing dried manganese nitrate had a very strong signal at $g \approx 2$, with a linewidth $\Delta H \sim 400$ G (Fig. 3a). This signal disappears in the spectrum of the sample calcined at 550°C; a weak signal at $g \approx 2$ remains, having a poorly resolved structure of 6 lines ($a_{Mn} \approx$ ≈ 85 G) (Fig. 3b).

The signal of the dried sample can be assigned to the Mn^{2+} ions, the large linewidth being due to their dipole-dipole interaction, with

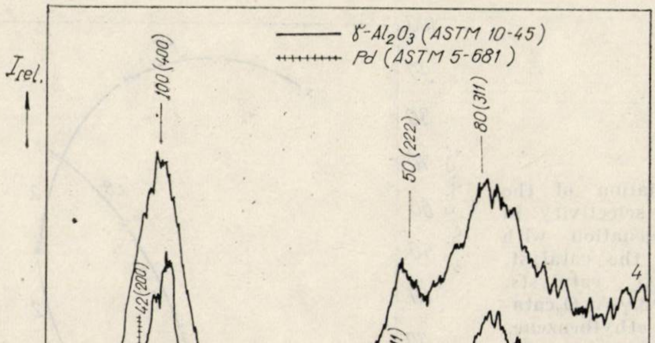

Fig. 2. — X-ray diffraction spectra of the catalysts. *1* — 1.0 %Mn — 0.1 % Pd/γ-Al_2O_3, *2* — 1.0 %Mn — 0.3 % Pd/γ-Al_2O_3, *3* — 1.0 %Mn — 0.5 %Pd/γ-Al_2O_3, *4* — 1.0 % Mn/γ-Al_2O_3.

some contribution from the exchange interaction. Disappearance of the wide line from the spectrum of the calcined sample is due to formation of MnO_2, therefore to the Mn^{2+} oxidation to Mn^{4+}. The typically hyperfine-structured signal still remaining originates in the very low amounts of dispersed Mn^{2+} which was not oxidized.

An unresolved signal of linewidth $\Delta H \sim 200$ G appears at $g \approx 2$ in the spectrum of the reduced 1 % Mn/γ-Al_2O_3 sample (Fig. 4a), about 40 times weaker than in the dried sample. For the reduced samples containing 1 % Mn and increasing amounts of palladium, unresolved spectra were obtained, whose g factor was ≈ 2 and $\Delta H \sim 280$. In these cases, the spectra can be assigned to the Mn^{2+} ions; the relatively small linewidth, as compared to the linewidth in the spectrum of the unreduced sample, indicates a significant contribution of the exchange narrowing to the line's width.

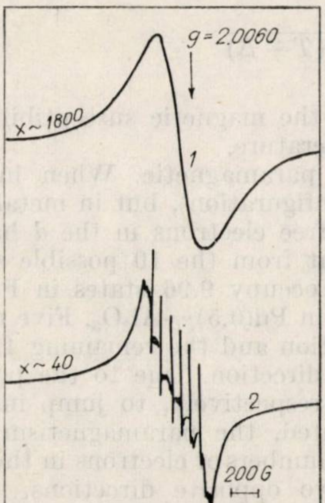

Fig. 3.— The ESR spectra of the samples. *1* — $Mn(NO_3)_2$ (1.0% Mn)/γ-Al_2O_3, dried at 50°C, *2* — $Mn(NO_3)_2$ (1.0%Mn) / γ-Al_2O_3, calcined at 550°C.

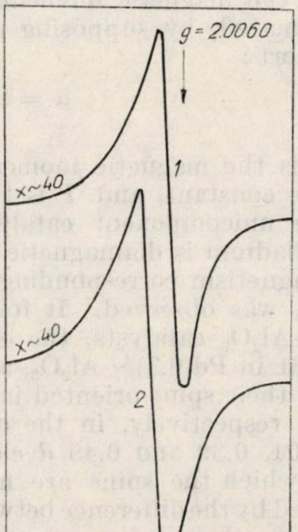

Fig. 4. — The ESR spectra of the catalysts. *1* — 1.0% Mn/γ-Al_2O_3, reduced with hydrogen at 750°C, *2* — 1.0% Mn—0.3% Pd/γ-Al_2O_3, reduced with hydrogen at 750°C.

The very low intensity of the signal of the reduced samples as compared to that of the dried ones suggests that the concentration of Mn^{2+} ions in the catalysts is very low, too low to be significant for the results obtained so far.

Reasons for the existence of metallic manganese were also offered by the magnetic susceptibility data (Table 1). For the unicomponent

Table 1

Magnetic properties of the catalysts

Catalytic system	Total number of *d* electrons	Number of *sp* hybridized electrons	Magnetic susceptibility $\chi \cdot 10$ c.c.s.	Number of free electrons in *d* band
Metallic Pd	10	5.78	—	0.6
0.1% Pd/γ-Al_2O_3	10	5.78	0.458	0.04
0.3% Pd/γ-Al_2O_3	10	5.78	11.624	0.39
0.5% Pd/γ-Al_2O_3	10	5.78	14.519	0.45
Metallic Mn	7	5.78	—	1.22
1% Mn/γ-Al_2O_3	7		7.385	1.12
1%Mn—0.1%Pd/γ-Al_2O_3	—		2.36	—
1%Mn—0.3%Pd/γ-Al_2O_3	—		2.97	—
1%Mn—0.5%Pd/γ-Al_2O_3	—		7.18	—

catalysts the magnetic moments and the number of quasi-free electrons were estimated, by supposing that the metal is uniformly dispersed on the support:

$$\mu = 2.84 \sqrt{\chi_M (T + \Delta)}$$

where μ is the magnetic moment, χ is the magnetic susceptibility, Δ is the Weiss constant, and T is the temperature.

The unicomponent catalysts are paramagnetic. When in atomic state, palladium is diamagnetic ($4d^{10}$ configuration), but in metallic state a paramagnetism corresponding to 0.6 free electrons in the *d* band, per Pd atom, was observed.[7] It follows that from the 10 possible states in the Pd/γ-Al_2O_3 catalysts, the electrons occupy 9.96 states in Pd(0.1)/γ-Al_2O_3, 9,61 in Pd(0.3)/γ-Al_2O_3, and 9.55 in Pd(0.5)/γ-Al_2O_3. Five electrons will have their spins oriented in a direction and the remaining 4.96, 4.61 and 4.55, respectively, in the opposite direction. Due to the possibility of the 0.04, 0.39 and 0.45 *d* electrons, respectively, to jump into the *s* band, in which the spins are not oriented, the paramagnetism will be determined by the difference between the numbers of electrons in the *d* band which have their spins oriented in two opposite directions.

In atomic state, manganese has the configuration d^5, with 5 free electrons, whereas in metallic state 1.22 free electrons were reported.[8] The 1 % Mn/γ-Al_2O_3 catalyst has a paramagnetism corresponding to 1.12 free electrons, therefore very close to that of metallic manganese.

For the bicomponent catalysts Pd-Mn/γ-Al_2O_3, the magnetic susceptibility values consist of contributions from palladium and manganese deposed on the support, and of contributions from other Pd-Mn structures; these contributions are not necessarily additive.

The observed decrease of their magnetic susceptibility in comparison with the values for the unicomponent catalysts suggests a smaller number of free electrons in the bicomponent catalysts. Increase of the magnetic susceptibility with the increase of Pd concentration in the bicomponent catalysts (the ratio Mn : Pd remaining greater than 1) may imply a decrease of the number of interactions between the two metals.

The Pd-Mn system is further compounded by the possibility of formation, in the temperature range in which reduction occurs, of some intermetallic compounds such as PdMn or Pd_3Mn.[9]

The following conclusions could be drawn from the analysis of the electron micrographs and of the X-ray energy dispersion spectra with elemental contrast (Fig. 5a–j):

— The surface of the catalyst is not essentially modified by changes in Pd concentration; in the case of the bicomponent catalysts with 0.3 and 0.5 % Pd, a certain compaction of the surface occurs (Fig. 5a–d).

— In all samples the manganese dispersion is uniform and similar. In Figure 5 we only give the pictures for manganese distribution in the samples with 1 % Mn and 0.5 % Pd + 1 % Mn (Fig. 5e–f).

— Dissimilarities occur for the dispersion of palladium (Fig. 5g–i). Whereas for the catalyst with 0.1 % Pd a uniform dispersion is apparent (Fig. 5i), for the catalysts with 0.3 and 0.5 % Pd the dispersion is no

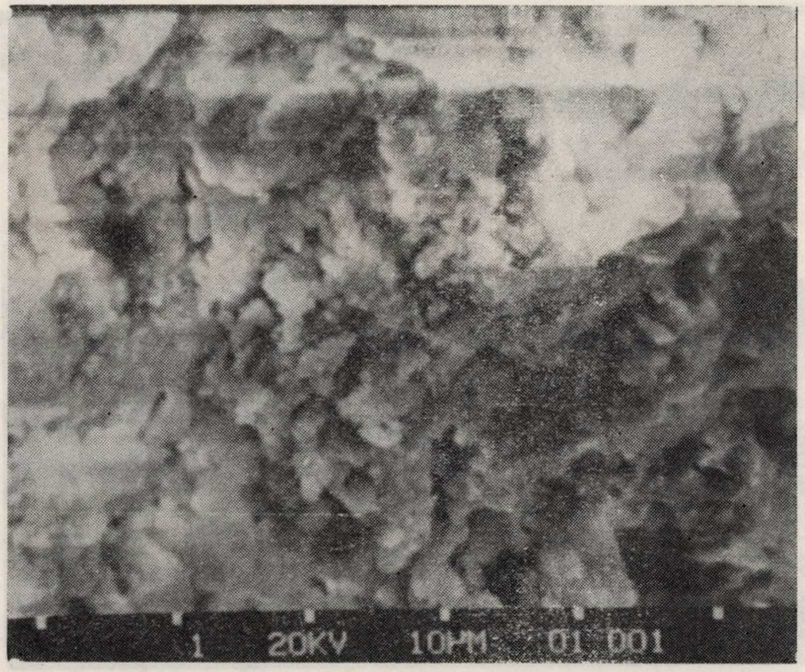
1 20KV 10ΜM 01 D01

Fig. 5 a

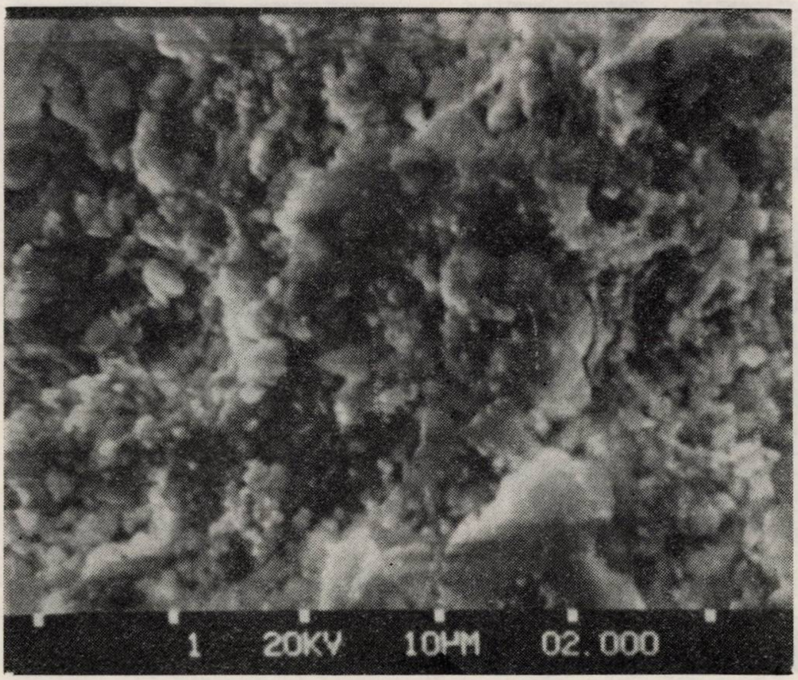
1 20KV 10ΜM 02.000

Fig. 5 b

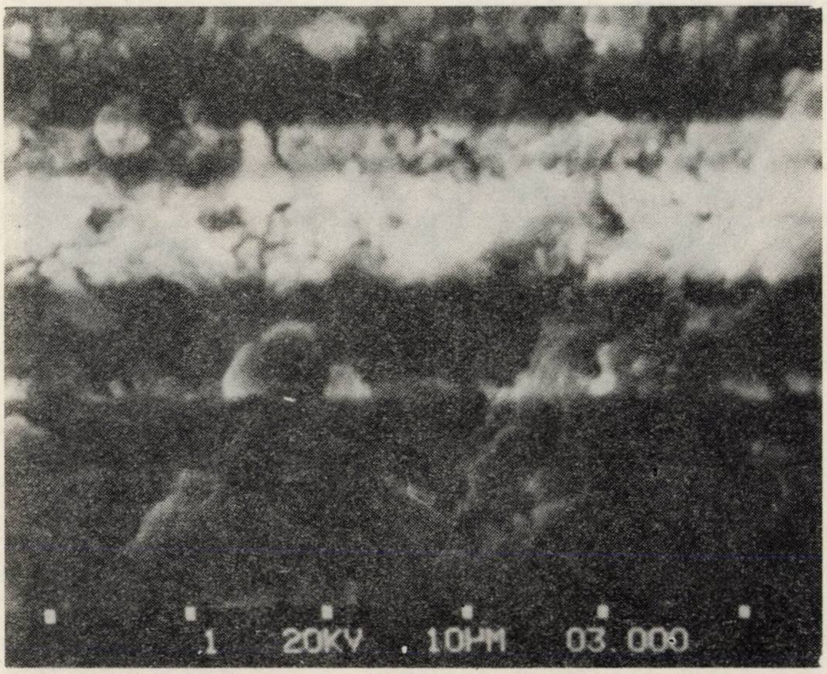
1 20KV .10μM 03.000

Fig. 5 c

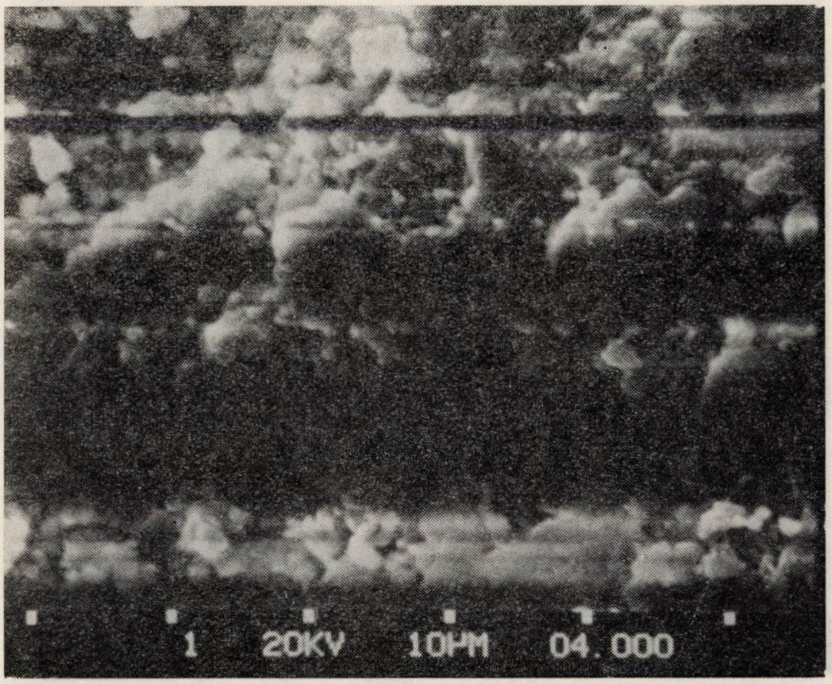
1 20KV 10μM 04.000

Fig. 5 d

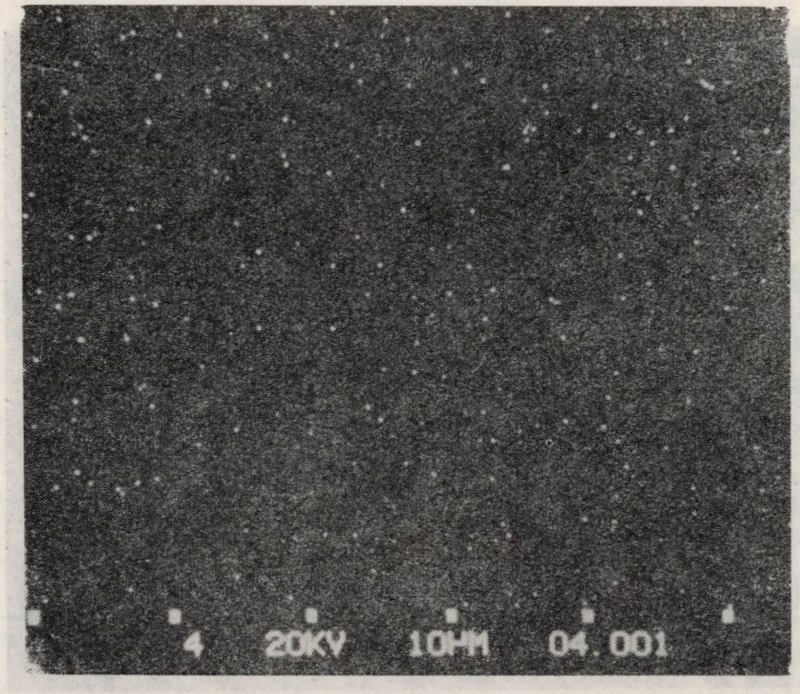
4 20KV 10µM 04.001

Fig. 5 e

4 20KV 10µM 01.002

Fig. 5 f

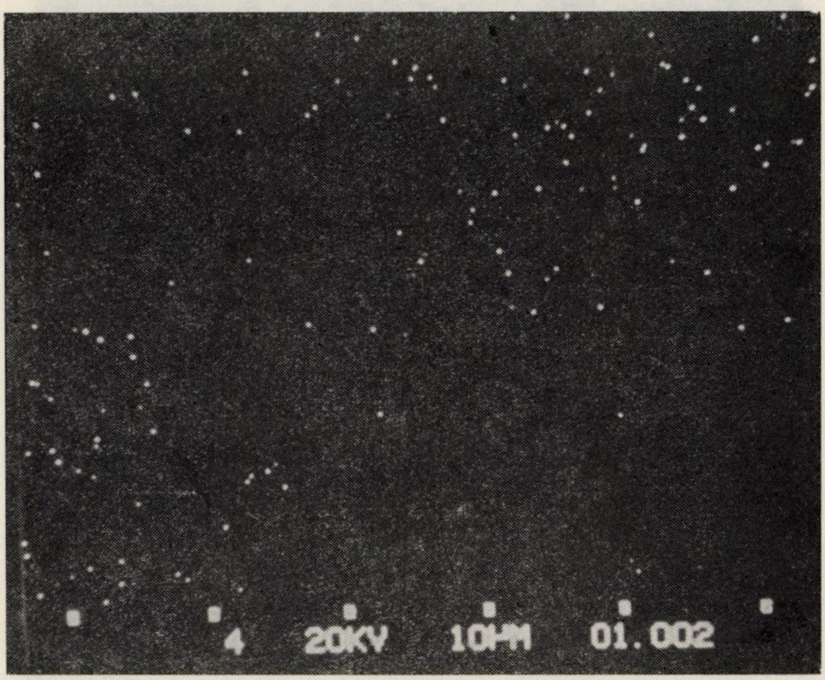
4 20KV 10HM 01.002

Fig. 5 g

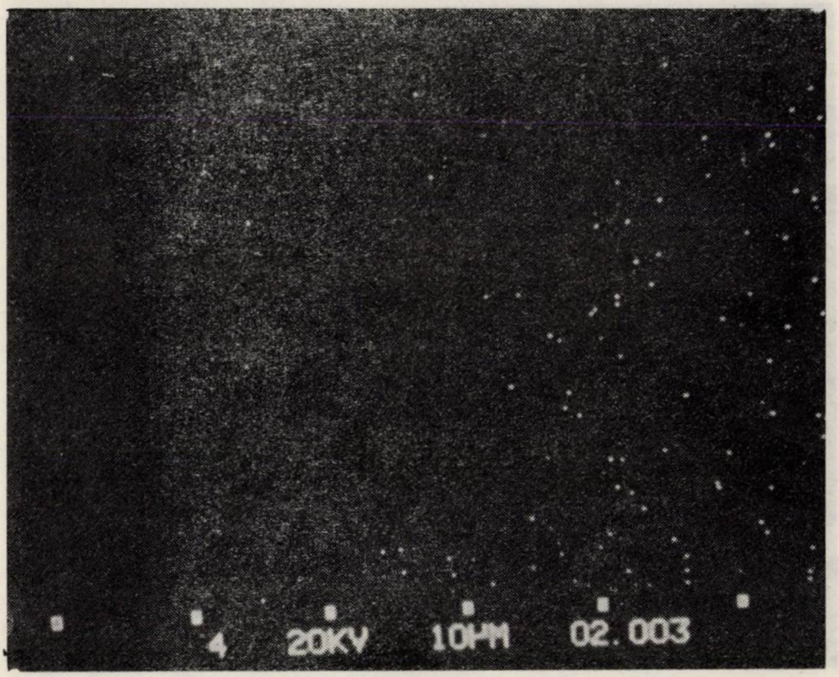
4 20KV 10HM 02.003

Fig. 5 h

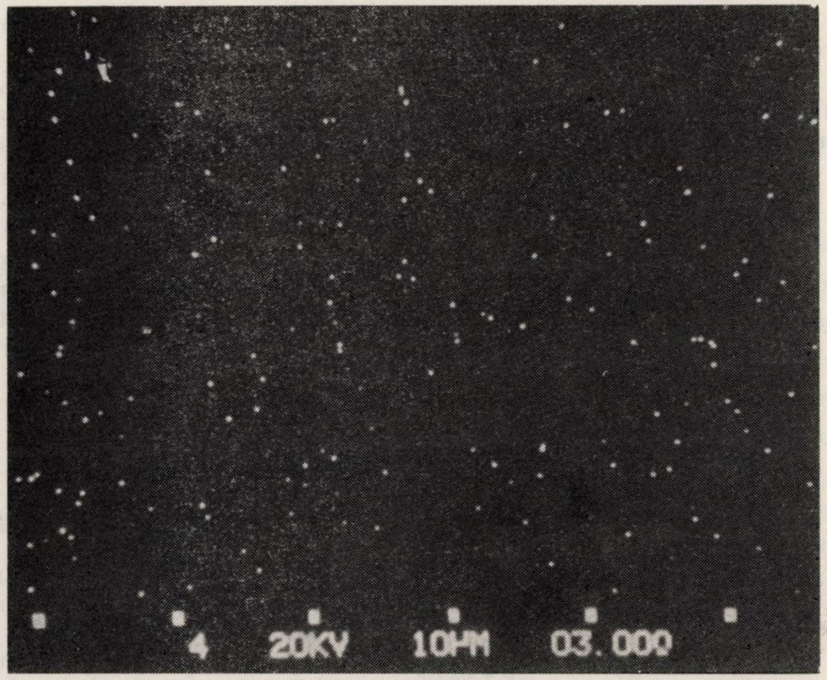

5i

Fig. 5. — Electron microscopy pictures and analysis of X-ray energy dispersion. *a—d*—pictures of the surfaces, *e—f*—dispersion of manganese, *g—i*—dispersion of palladium, *a, f, g* — 1.0 %Mn—0.5 %Pd/γ-Al_2O_3, *b, h* — 1.0 %Mn — 0.3 %Pd/γ-Al_2O_3, *c, i* — 1.0 %Mn—0.1 %Pd/γ-Al_2O_3, *d, e* — 1.0 %Mn/γ-Al_2O_3.

longer uniform, areas with high concentrations of palladium and with no palladium being visible. We may say that the increase of Pd concentration from 0.1 to 0.3 % leads to the formation of small clusters of palladium.

By comparing the pictures for the dispersion of manganese and palladium on the surface of the catalyst it becomes apparent that increase of palladium concentration is accompanied by a decrease of the number of associations between palladium and manganese, due to Pd-cluster formation. This would also account for the increase of magnetic susceptibility which occurs in the bicomponent catalysts when the palladium content increases.

INTERPRETATION OF RESULTS

Studies on the complex combinations of olefins have shown that the metal-ligand interaction occurs as a consequence of an electron density transfer from the occupied π orbitals of the olefin to the empty d orbitals of the metal (σ bond) and of an electron density transfer from the occupied d orbitals of the metal (i.e. d_{xy}, d_{yz}, d_{zx}) to the empty π orbitals localized on the atoms through which the coordinative bond is formed (π bond).[10,11]

Since the π bond is prevalent, we may assume that the unsaturated hydrocarbons are electron acceptors in their interactions.

We may therefore assume that, in the case of the unicomponent catalysts, the interaction between styrene and catalyst takes place between the antibonding π orbitals of vinyl (Pd/γ-Al_3O_2) or of vinyl and the aromatic ring (Mn/γ-Al_2O_3), and the centers of maximum electronic density of the metal, which are supposedly the active centers of the catalyst. In a picture specific to solids, we may suppose that these maxima may be associated with the first Brillouin zones.[12]

For the Pd/γ-Al_2O_3 catalysts, the variation of conversion to ethylbenzene as a function of metal concentration has the same trend as the variation of the magnetic susceptibility (Fig. 6), that is as the variation of the concentration of unpaired electrons of the metal. As palladium concentration increases, sintering of this metal on γ-Al_2O_3 occurs (as shown by the values of magnetic susceptibility and by the analysis of X-ray energy dispersion); this increases the amplitude of the probability density distribution and hence the possibility of an interaction between reactant and catalyst, a fact which was proven by kinetic measurements.[13]

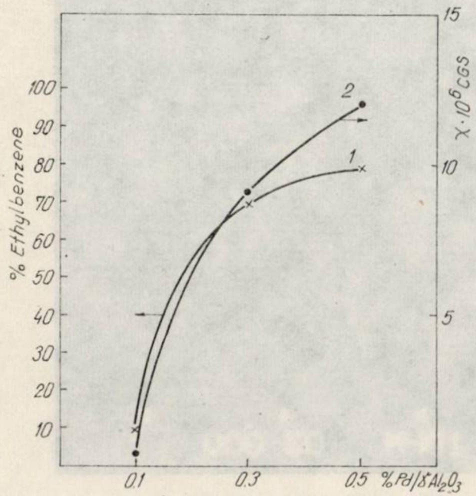

Fig. 6. — Variation of the activity and magnetic susceptibility of the Pd/γ-Al_2O_3 catalysts with palladium concentration.

For the Mn/γ-Al_2O_3 catalysts, the large electronic density allows the practically complete conversion of styrene by interactions with both the vinyl group and the aromatic ring. These interactions may take place either simultaneously or consecutively. The selectivity for ethylbenzene (85 %) suggests that the prevalent interactions are those with the vinyl group.

Much more difficult to account for is the interaction with styrene of the bicomponent catalysts. For the 0.1 % Pd-1 % Mn/γ-Al_2O_3 catalyst, increase of selectivity for ethylbenzene could be determined by a decrease of free electron density (i.e. by a significant decrease of magnetic susceptibility) as a consequence of interactions occurring between palladium and manganese. Owing to the large dispersion of the two metals, the number of these interactions is large and this diminishes the interaction with the benzenic ring.

Increase of Pd concentration to 0.3 % in the bicomponent catalyst (0.3 % Pd-1 % Mn/γ-Al_2O_3) leads to a decrease of selectivity for ethylbenzene. Sintering of palladium on γ-Al_2O_3 occurs, whereas manganese remains uniformly distributed. The number of interactions between Mn and Pd decreases (i.e. the magnetic susceptibility increases) and, as a consequence, the number of formations with free electrons, and implicitly the interaction with the aromatic ring, increase.

At 0.5% Pd concentration (in the 0.5% Pd-1% Mn/γ-Al_2O_3 catalyst), the degree of sintering of palladium increases without affecting the uniform distribution of manganese. The magnetic susceptibility increases, becoming approximately equal to the susceptibility of the 1.0% Mn/γ-Al_2O_3 unicomponent catalyst. However, the large decrease, down to $\sim$ 50%, of the selectivity for ethylbenzene is difficult to explain. Sintering of palladium might possibly induce associations with manganese, whose electronic density is larger than in the system 1% Mn/γ-Al_2O_3, even if the magnetic susceptibility value is smaller than that of the individual components on the support; this would lead to the total hydrogenation of styrene.

Considering, in this complex case, that between the free electron density and the value of magnetic susceptibility a proportionality does not exist, we might infer that in the case of the bicomponent catalyst 0.5% Pd-1% Mn/γ-Al_2O_3 the value of 7.18 of the magnetic susceptibility is given by a density of unpaired electrons greater than that of the individual components.

It seems certain that the modification of styrene interaction with the active centers, induced by the presence of the two metals, depends on the manner in which the two metals interact, which is in turn a function of their distribution on the catalyst surface.

A general conclusion would be that at low values of the free electron density interactions occur only with the vinyl group of styrene and that increase of the number of free electrons leads to an increase of the ethylbenzene concentration (as in the Pd/γ-Al_2O_3 catalyst).

When the number of free electrons increases over a certain upper limit, interactions with the aromatic ring also occur; here, too, increase of the number of free electrons shifts the interaction towards the aromatic ring, increasing the selectivity for hydrogenation to ethylcyclohexane, with practically total conversion of styrene.

Obviously, the possibility that association of palladium with manganese, occurring by sintering of palladium in the bicomponent catalysts, may lead to a modification in the nature of the active centers which favours formation of centers for the total hydrogenation of styrene, cannot be entirely excluded.

CONCLUSIONS

For the Pd/γ-Al_2O_3 catalysts, the activity in the styrene hydrogenation reaction depends on the degree of sintering of palladium on the support and increases with the increase of the number of quasifree electrons. In this case, only interactions with the vinyl group occur, leading to ethylbenzene.

For the Pd—Mn/γ-Al_2O_3 catalysts, the selectivity modification is caused, on the one hand, by the presence of manganese, and on the other, by the modification of the interaction between manganese and palladium induced by palladium sinterization. In these cases hydrogenation to ethylbenzene or to ethylcyclohexane may take place, the pathway being determined by the nature of the interaction between styrene and the active centers and by modifications of the interactions between the two metals.

REFERENCES

M. C. Sze and U. Montclair, U.S. Pat. 3, 493, 492 (1964) ; G. W. Mathews, L. Jackson and B. D. Head, U.S. Pat. 3, 764, 521 (1971).

[2] I. Săndulescu and V. Pârvulescu, *Rev. Chim. (București)*, **11**, 1086 (1979).

[3] P. Pascal, ''Nouveau traité de chimie minérale'', vol. 16, Masson, Paris, 1967.

[4] W. K. Hall and J. A. Hassel, *J. Phys. Chem.*, **67**, 636 (1969).

[5] A. G. Gaziev, B. I. Filinovskii and M. J. Yanovskii, *Kinetika Kataliz*, **5**, 688 (1963).

[6] I. Săndulescu, Xu Yandong and V. Pârvulescu, *Rev. Chim. (București)*, to be published.

[7] H. Kubicka, *J. Catalysis*, **5**, 39 (1966).

[8] G. C. Bond, ''Catalysis by Metals'', Academic Press, London, 1962.

[9] E. Savitsky, V. Poliakova, N. Gorina and V. Roshan, ''Physical Metalurgy of Platinum Metals'', Mir, Moscow, 1978.

[10] G. C. Bond and P.B. Wells, *Adv. Catalysis*, **15**, 91 (1965).

[11] G. Henrici-Olivé and G. Olivé, ''Koordinatsyia i Kataliz'', Mir, Moscow, 1980.

[12] C. Kittel, ''Introducere în fizica corpului solid'', Ed. Tehnică, București, 1973.

[13] I. Săndulescu, V. Pârvulescu and S. Neagu, communication at the ''2nd National Congress of Chemistry'', Bucharest, 1981.

Revue Roumaine de Chimie, 28, 7, 683–687 (1983)

GLASS TRANSITION OF POLYBLENDS OF COLLAGEN HYDROLYSATES AND POLY(ETHYL ACRYLATE)

I. MÎNDRU*, MIHAELA OLTEANU*, LI DEHE** and V. TRANDAFIR***

* Polytechnic Institute of Bucharest, Bd. Republicii 13, Romania
** Shandong Institute of Chemical Engineering, Qingdao China
*** Institute of Leather Research, Bucharest, Romania

Received June 11, 1982

Stable polyblends of collagen hydrolysates and poly(ethyl acrylate) have been obtained and characterized. The mixtures of different compositions are characterized by a single glass transition temperature (T_{gm}), indicating the polymer microcompatibility. The transition temperature has been determined from the temperature variation of Young's modulus and of the dielectric loss. The glass transition temperatures of polyblends vary linearly between the characteristic values of the two polymers, increasing with the collagen hydrolysate content. For the same composition, T_{gm} increases with the average molecular weight of the collagen hydrolysate.

INTRODUCTION

The aim of this contribution was to obtain and characterize some stable polyblends of natural polymers from collagen with synthetic polymers (polyacrylic latexes). The collagen hydrolysates are obtained by hydrolyzing scraps of untanned leather to linear polymers with different molecular weights, corresponding to hydrolysis conditions. The collagen hydrolysates have been the object of numerous studies on obtaining synthetical protein products which are widely used in leather and synthetic leather industries, human and veterinarian medicine, zootechny and cosmetics.[1–5]

Stable systems were obtained by mixing the aqueous solutions of collagen hydrolysates having viscosity average molecular weights between 50,000 – 90,000 with poly (methyl acrylate) and poly (ethyl acrylate) latexes, obtained by radicalic polymerization in emulsion. By evaporating the water from these systems, stable films were obtained, the polymers forming micro-compatible mixtures called in literature polyblends or compounds. As the films obtained from collagen hydrolysates with poly (methyl acrylate) were hard and brittle no matter the composition, only the films obtained from collagen hydrolysates with poly (ethyl acrylate) could be characterized.

The kinetic stability of the fluid mixtures has been determined as a function of the mixing ratio, total polymer concentration and temperature. The kinetic stability of fluid mixtures has been proved by the independence of storing time of the rheological curves obtained with a rotation viscosimeter.[6] The stable mixtures have a pseudoplastic flow, the viscosity coefficient decreases with increasing the shear rate. Stability is maintained for every component ratio up to a concentration of 30 % hydrolysate and a temperature of 60°C.

The polymer micro-compatibility in solid films obtained after removing the water from fluid mixtures has been proved by the existence of a single glass transition temperature determined from the temperature variation of Young's modulus and of the dielectric loss.

EXPERIMENTAL PART

The collagen hydrolysates were obtained from scraps of untanned leather by hydrolysis at 110—115°C and 1.5—2 atm. Three hydrolysates with viscosity average molecular weights of 80,700, 69,195 and 53,350 respectively, have been used. The employed latex had a concentration of 43 % in poly (ethyl acrylate).

The films were obtained by ambient temperature evaporation of the water from mixtures deposited on a well-stretched polyethylene sheet.

The Young modulus has been determined at room temperature from stress-strain curves obtained by means of a Schoper dynamometer at a straining rate of 50 mm/min for different component ratios. The curves show two regions : elastic deformation and cold-drawing.[6] Both Young's modulus and breaking or tensile strength increase with increasing the hydrolysate content but the domain of cold-drawing is narrower. The films obtained from acrylic latex have a behaviour characteristic of a soft and weak type polymer and those obtained from the hydrolysate solution of a hard and brittle one.[7,8] The films obtained from a blend of the two polymers have modified mechanical properties corresponding to polymers of the types hard and strong, hard and tough or soft and tough, according to both component ratio and molecular weight of the hydrolysate. Above the 1/1 ratio the films become brittle. The temperature variation of Young's modulus has been determined from the elongation at small static forces. Sample temperature was varied between —50 and 100°C by means of a cryostat.

The temperature variation of the dielectric loss was determined with an apparatus made in Hungary which has a TT1301-type selective detector and a TT9701-type measuring bridge with a linear frequency range between 0.03—300 kHz. The dynamic dielectric constant ε' and the loss factor ($\mathrm{tg}\delta$) are directly given by the apparatus. The dielectric loss, ε'', is calculated from these quantities :

$$\varepsilon'' = \varepsilon' \,\mathrm{tg}\delta \tag{1}$$

The dielectric measurements were carried out on circular films of 8 cm diameter and 0.1—0.3 cm thicknesses. Cell temperature was varied between—50 and 100°C. The dielectric quantities were determined at a certain temperature as function of the frequency of the applied electrical field and at a certain frequency as function of temperature. Temperature was modified every 5°C and around maximum value every 2.5°C.

In this paper the abbreviation PEA recommended by IUPAC is used for poly (ethyl acrylate).

RESULTS AND DISCUSSIONS

The blends of micro-compatible polymers are characterized by a single value for glass transition temperature, T_{gm}, dependent on blend composition and T_g values of the components.[9] The blends of collagen hydrolysates and poly (ethyl acrylate) are characterized by a single value for T_{gm}, placed in between the glass transition temperatures of PEA and collagen hydrolysate, respectively.

In Figure 1, the temperature variation of Young's modulus is represented for some mixing ratios of collagen hydrolysate of molecular weight $M_v = 70{,}000$ with PEA.

The glass transition temperatures have been determined from the inflexion point on temperature variation curves of Young's modulus, E. The temperature corresponding to the sudden decrease in E is characteristic of polymer transition from the glassy state to the highly elastic one.[10]

The values of Young's modulus at 25°C are listed in Table 1 together with glass transition temperatures determined from the curves in Fig. 1.

Temperature variation curves of the dielectric loss at different frequencies are presented in Figure 2 (a—d) for some blends. Similar curves were also obtained for mixtures with ratios 1/5, 1/6 and 1/7.5. For some blends, the temperature at which a peak is obtained on the curve, considered as glass transition temperature or process α[11], varies with frequency. For 1/1 composition, ε'' increases continuously with both temperature and frequency. The blend loses its dielectric character with the increase in hydrolysate content and the conductivity, characteristic of polymers with a high content of hydrogen bonds, increases accordingly.

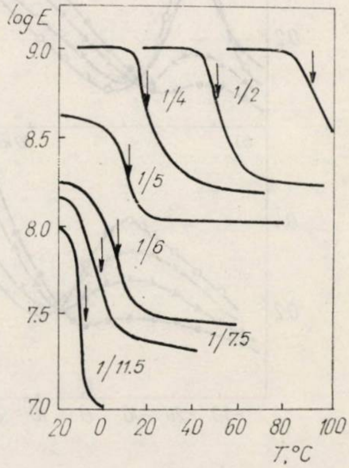

Fig. 1. — Temperature variation of Young's modulus for different mixing ratios of collagen hydrolysates ($M_v = 70{,}000$) and poly (ethyl acrylate).

The glass transition temperatures obtained from the temperature dependence of dielectric properties are given in Table 2.

From the data listed in Tables 1 and 2, a good agreement is noticed for the T_{gm} values obtained using the two experimental methods. The

Table 1

Glass transition temperatures obtained from temperature variation of Young's modulus for blends of collagen hydrolysate ($M_v = 70{,}000$) with poly(ethyl acrylate)

Hydrolysate/PEA ratio	$E \times 10^{-8}$ at 25°C (N/m²)	Glass transition temperature (°C)
1/1	10	90
1/2	9	50
1/4	2.5	20
1/5	0.9	12
1/6	0.39	8
1/7.5	0.25	0
1/11.5	0.10	−10
PEA	0.01	−24

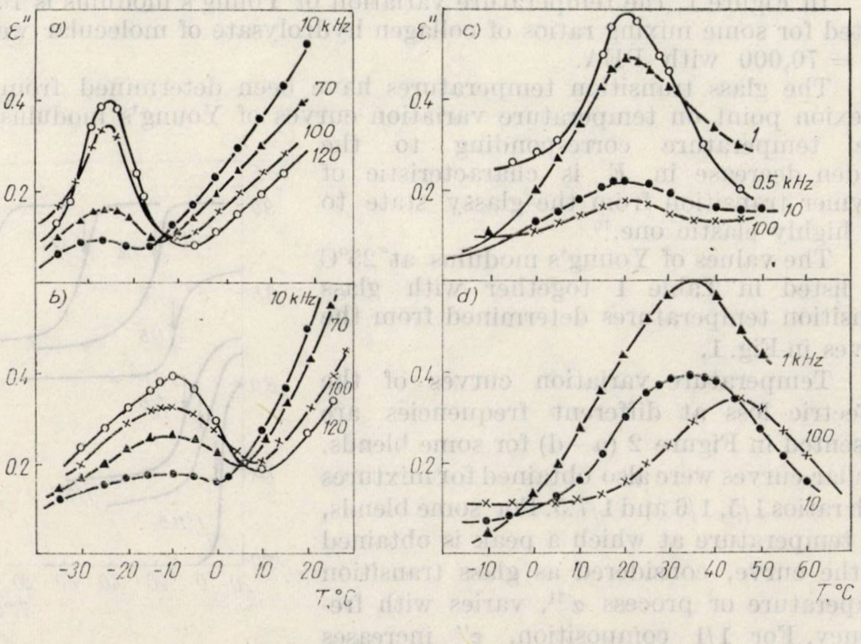

Fig. 2. — Temperature variation of dielectric loss, ε'', for a) PEA ; b) hydrolysate-PEA 1/11.5 ; c) hydrolysate-PEA 1/4 and d) hydrolysate-PEA 1/2. Collagen hydrolysate with $M_v = 70{,}000$.

value of the T_g of PEA as obtained from mechanical and dielectric properties at frequencies higher than 70 kHz coincides with those reported in literature.[12] Plotting the T_{gm} values as a function of the mixing ratio a straight line is obtained (Fig. 3).

By extrapolating the straight line in Fig. 3 one obtains a T_g of 200°C for collagen hydrolysate. For a gelatin with properties alike those of hydrolysate used in the present work, the T_g is 190°C.[13] The mentioned

Table 2

Glass transition temperatures obtained from temperature variation of dielectric loss for blends of collagen hydrolysate ($M_v = 70{,}000$) with poly (ethyl acrylate)

Hydrolysate/PEA	Glass transition temperature (°C)	
	10 kHz	100 kHz
1/2	35	45
1/4	20	20
1/5	11	12
1/6	8	8
1/7.5	0	0
1/11.5	−10	−10
PEA	−26	−24

gelatin film had a water content of 12% with a plasticizing effect. If an extrapolated value is taken into consideration, the linear dependence of T_{gm} upon the blend composition can be described by the relation:

$$T_{gm} = W_1 T_{g_1} + W_2 T_{g_2} \qquad (2)$$

where T_{gm} is blend glass transition temperature, T_{g_1}, T_{g_2} are glass transition temperatures of hydrolysate and PEA and W_1, W_2 are weight fractions of hydrolysate and PEA in blends, respectively.

Similar relations are found for collagen hydrolysates with average molecular weights of 53,350 and 80,700. The increase of the molecular weight of the hydrolysate in the blend produces an increase in Young's modulus values, a narrowing of the range of mixing ratios for which films have an elastic behaviour, as well as a decrease in T_{gm} values.

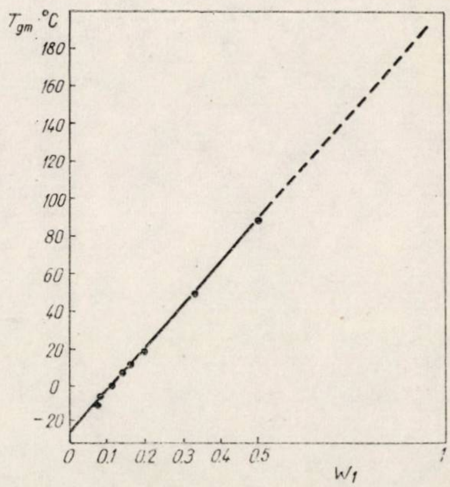

Fig. 3. — Dependence of glass transition temperatures on the blend composition for collagen hydrolysate ($M_v = 70{,}000$) poly (ethyl acrylate) system.

REFERENCES

[1] V. Trandafir, S. Balica and M. Constantinescu, *Ind. Ușoară* **9**, 386 (1979).
[2] M. Condratov, N. Badea and G. Chiriță, *Ind. Ușoară* **8**, 234 (1977).
[3] A. L. Rubin and K. H. Stenzel, *Biomaterials*, 157 (1969).
[4] E. W. Chapman and F. Rodriquez, *A.I. Ch.E. Symp. Ser.*, **73**, 129 (1977).
[5] T. M. Moshkina, E. A. Zimkin and R. I. Karnitskaya, *Uspehi Nauk Fotogr.* **18**, 145 (1977).
[6] M. Olteanu, V. Trandafir, I. Mîndru, M. Leca, I. Ionescu-Bujor and I. Brădescu, *Mat. Plastice*, **1**, 43 (1981).
[7] T. S. Carswell and H. K. Neason, *Modern Plastics*, **21**, 121 (1944).
[8] L. E. Nielson "Mechanical Properties of Polymers" Reinhold Publ. Corporation, New York, 1962.
[9] L. Yu. Zlatkevich and V. G. Nikolskii, *Rubber Chemistry and Technology*, **46**, 1210 (1973).
[10] A. V. Tobolski and M. Takahasahi, *J. Appl. Polymer Sci.*, **7**, 1341 (1963).
[11] P. Hedvig "Dielectric Spectroscopy of Polymers" Academy Kiado, Budapest, 1977, p. 83.
[12] J. Brandrup and E. H. Immergut Ed., "Polymer Handbook", Interscience Publishers, Wiley, New York, 1966, p. III 66.
[13] E. P. Chang and J. C. W. Chien, *J. Polymer Sci.*, **11**, 737 (1973).

Revue Roumaine de Chimie, 28, 7, 689–697 (1983)

ESR AND ELECTRONIC SPECTRA OF SOME NITROSUBSTITUTED THIOUREIDE ANION-RADICALS

ELENA VOLANSCHI* and MELANIA VOICU
Department of Physical Chemistry, Polytechnic Institute
Bd. Republicii 13, Bucharest, Romania

Received June 14, 1982

The ESR and electronic spectra of the anion radicals provided by some nitrosubstituted thioureides are reported and discussed. The determining role of the nitro group as compared to the other structural entities present in the molecule is outlined. The calculated hyperfine splittings and π bond orders account well for the experimental trends.

ESR and optical spectra have already been employed in the study of the electronic structure of anion-radicals containing several substituents.[1-3]. It was stated that when the nitro group is present, it determines both the spin pattern and the position of the energy level of the unpaired electron in the anion-radical.

It is the aim of this paper to report the ESR and optical spectra of the anion-radicals provided by some nitrosubstituted thioureides, a class of physiologically active substances, the electronic structure of which is now investigated in our laboratory.[4]

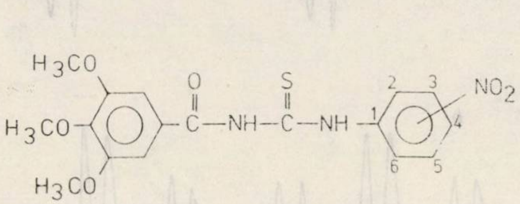

1 2 — nitrophenyl-(3′,4′,5′-trimethoxybenzoyl) — thiouree
2 3 — nitrophenyl-(3′,4′,5′-trimethoxybenzoly) — thiouree
3 4 — nitrophenyl-(3′,4′,5′-trimethoxybenzoyl) — thiouree

The present study aims to reveal, among the different moieties composing these systems (amide, thioamide, phenyl and nitro group) that which conferes the characteristic features to the electronic structure of the anion-radical.

EXPERIMENTAL PART

The synthesis and purification of the compounds is reported in literature.[5-7]

The anion-radicals were obtained by chemical reduction using alkali metals (Li, Na, K) in dimethyl-formamide (DMF), or by electrochemical reduction in dimethylsulfoxide (DMSO), using tetra-*n*-butylammonium perchlorate as supporting electrolyte. The ESR and electronic spectra were registered during the electrolysis, using the techniques previously described.[8]

The electronic spectra were recorded on a SPECORD-UV-VIS spectrophotometer, using 1 cm path-lengths, in the range 350–800 nm.

The ESR spectra were recorded on a JES-3B spectrometer in the X-band frequency. Potassium peroxylamin disulphonate ($a_N = 13.000$ G ; $g = 2.0055$) was used as internal standard. The hyperfine splitting constants (hfs) were checked by simulation using a program written in FORTRAN IV. The spin density calculations were carried out in the frame of the McLachlan approximation, at the Computing Center of the Polytechnic Institute of Bucharest.

RESULTS AND DISCUSSION

The ESR spectra obtained by electrochemical reduction in DMSO (Figs 1–3) were interpreted in terms of the splitting constants listed in Table 1. The assignment of the coupling constants to the different sites is based upon the similitude with calculated hf splittings.

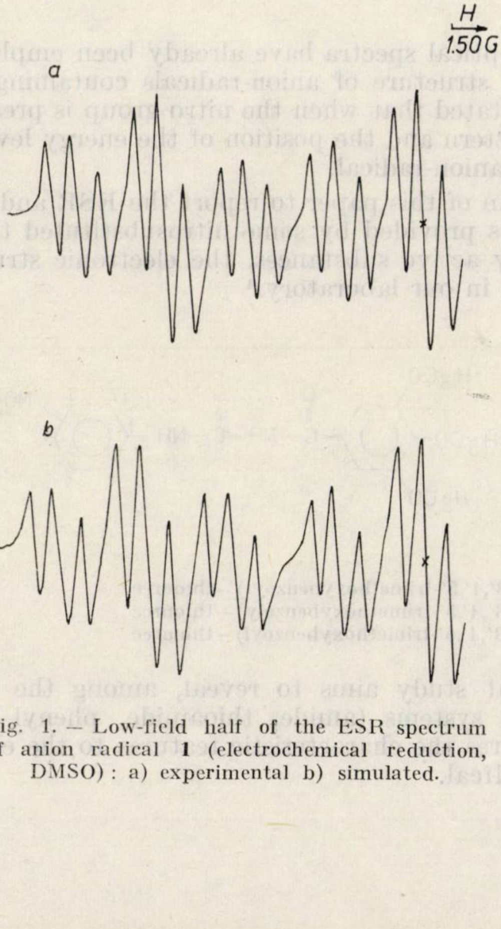

Fig. 1. — Low-field half of the ESR spectrum of anion radical **1** (electrochemical reduction, DMSO) : a) experimental b) simulated.

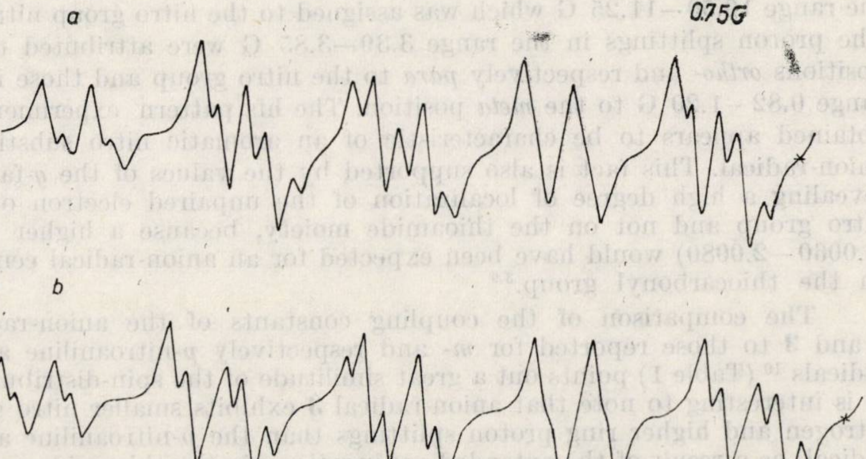

Fig. 2. — Low-field half of the ESR spectrum of anion radical 2 (electrochemical reduction, DMSO): a) experimental; b) simulated.

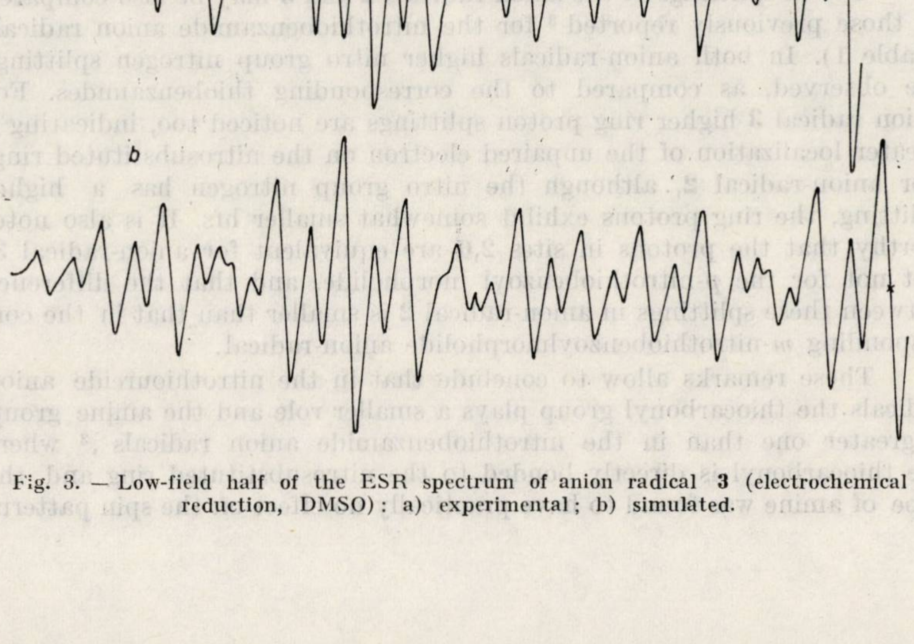

Fig. 3. — Low-field half of the ESR spectrum of anion radical 3 (electrochemical reduction, DMSO): a) experimental; b) simulated.

Examination of the data in Table 1 reveals a nitrogen splitting in the range 10.50—11.25 G which was assigned to the nitro group nitrogen. The proton splittings in the range 3.39—3.85 G were attributed to the positions *ortho*- and respectively *para* to the nitro group and those in the range 0.82—1.20 G to the *meta* position. The hfs pattern experimentally obtained appears to be characteristic of an aromatic nitro substituted anion-radical. This fact is also supported by the values of the *g*-factors, revealing a high degree of localization of the unpaired electron on the nitro group and not on the thioamide moiety, because a higher value (2.0060—2.0080) would have been expected for an anion-radical centered on the thiocarbonyl group.[3,9]

The comparison of the coupling constants of the anion-radicals **2** and **3** to those reported for *m*- and respectively *p*-nitroaniline anion-radicals [10] (Table 1) points out a great similitude of the spin-distributions. It is interesting to note that anion-radical **3** exhibits smaller nitro group nitrogen and higher ring proton splittings than the *p*-nitroaniline anion-radical, as a result of the extended conjugation via the thioamide moiety.

It is also worth noticing that in the ESR spectrum of anion-radical **3** both the thioamide nitrogen and proton exhibit measurable splittings, similar to those reported for *p*-nitroaniline; for anion-radical **2** no hfs from the thioamide nitrogen was detected, although the splitting of the thioamide proton was determined. Since splittings due to the amine protons are usually higher than the corresponding nitrogen splittings [11,12], the spin polarization parameter $Q^{\mathrm{H}}_{\mathrm{NH}}$ being greater than $Q^{\mathrm{N}}_{\mathrm{N}}$, it is explainable why, at an experimental line width of 0.30 G a splitting smaller than 0.36 G could not be resolved.

For anion-radical **1**, the poorer resolution of the experimental spectrum (line-width 0.45 G as compared to 0.30 G for **2**) prevents the detection of the coupling constants due to the thioamide group.

The hf splittings of the anion-radicals **2** and **3** may be also compared to those previously reported [3] for the nitrothiobenzamide anion radicals (Table 1). In both anion-radicals higher nitro group nitrogen splittings are observed, as compared to the corresponding thiobenzamides. For anion radical **3** higher ring proton splittings are noticed too, indicating a greater localization of the unpaired electron on the nitrosubstituted ring. For anion-radical **2**, although the nitro group nitrogen has a higher splitting, the ring protons exhibit somewhat smaller hfs. It is also noteworthy that the protons in sites 2,6 are equivalent for anion-radical **3**, but not for the *p*-nitrothiobenzoyl morpholide, and that the difference between these splittings in anion-radical **2** is smaller than that in the corresponding *m*-nitrothiobenzoylmorpholide anion-radical.

These remarks allow to conclude that in the nitrothioureide anion radicals the thiocarbonyl group plays a smaller role and the amine group a greater one than in the nitrothiobenzamide anion radicals ,[3] where the thiocarbonyl is directly bonded to the nitrosubstituted ring and the type of amine was found to have practically no effect on the spin pattern.

M.O. CALCULATIONS

In order to avoid supplementary and not necessary parameters, only the thioamide and the nitro-containing ring were considered in the spin density calculations. This assumption is justified by the experimental statement that only this part of the anion radical has measurable hf splittings. The parameters and equations used in the spin density calculations are collected in Table 2.

Table 2

Parameters and equations used in the MO calculations

	h	*k*
>C = S	1.0	1.2
– NH –	1.5	0.8
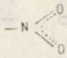	N : 2.2 O : 1.4	N–O : 1.67 C–N : 1.2

$$a_H = |25| \rho_C^\pi \qquad (1)$$

$$a_N^{NO_2} = 99\,\rho_N^\pi - 35.8 \times 2\rho_O^\pi\,{}^{13} \qquad (2)$$

$$a_N^{NH} = |30| \rho_N^\pi\ {}^{11}(a) \quad a_H^{NH} = |35| \rho_N^\pi\ (b) \qquad (3)$$

$$a_N^{NH} = 22.70\,\rho_N^\pi + 3.27 \sum_i \rho_{x_i}\ {}^{12} \qquad (4)$$

$$a_N^{NH} = 24.08\,\rho_N^\pi + 3.70 \sum_i \rho_{x_i}\ {}^{12} \qquad (5)$$

The theoretical hf splittings listed in Table 1 point out an overall good agreement with the experimental ones, and have the general features of a nitro-containing anion radical.

Special discussion is required by the thioamide nitrogen and proton. For the hfs of the thioamide nitrogen several formulae were tried and it was found that a Mc Connell type one (formula 3a Table 2) with Q_N^N in the range 27–35 G[11] leads to values in disagreement with the experiment for anion-radical **3**.

If a Karplus-Fraenkel type formula[14] is used with the spin polarisation parameters suggested in literature[12] for regular (formula 4) and distorted (formula 5) geometries of the anion-radical, values reflecting the experimental trends are obtained (Table 1).

Table 3

π-bond orders for the neutral compounds and their anion radicals

Compound		p_{C-S}	$p_{C(S)-N}$	$p_{N(H)-C}$	p_{C-NO_2}	p_{12}	p_{23}	p_{34}	p_{45}	p_{56}	p_{16}
1	M :	0.825	0.423	0.308	0.389	0.574	0.602	0.685	0.646	0.672	0.642
	A.r :	0.815	0.432	0.284	0.472	0.521	0.543	0.697	0.634	0.632	0.676
2	M :	0.822	0.428	0.279	0.372	0.652	0.611	0.603	0.677	0.663	0.631
	A.r :	0.822	0.429	0.278	0.467	0.674	0.544	0.540	0.700	0.637	0.608
3	M :	0.825	0.424	0.303	0.386	0.622	0.694	0.596	0.596	0.694	0.622
	A.r :	0.812	0.435	0.272	0.469	0.610	0.705	0.540	0.540	0.705	0.610

For the splitting due to the thioamide proton the same situation was encountered; only a two-parameters formula would lead to results in reasonable agreement with experiment.

The differences observed between the spin patterns of the anion radicals **1**—**3** are also reflected by the calculated charge diagrams.

The π-bond orders calculated for the neutral compounds and their anion radicals are presented in Table 3 and reveal noticeable modification of the thioamide group at the reduction only for compounds **1** and **3**. The highest π-bond order ($p_{C(S)-NH}$) is reached in anion radical **3**, pointing out that in this compound the highest conjugation with the thioamide moiety is implied, as reflected by scheme:

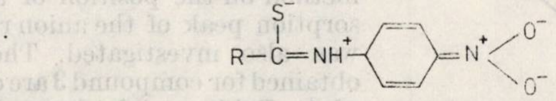

ELECTRONIC SPECTRA

The chemical or electrochemical reduction of compounds **1**—**3** is accompanied by the appearance of one absorption band in the visible range. This band disappears when the solution is open to the air and was therefore ascribed to the anion radical. The electronic spectra registered by the electrochemical reduction in DMSO of the compounds **1** and **3** are presented in figures 4, 5.

The equilibrium between the anion radicals **1** and **3** and the neutral parent compounds is characterised by the isosbestic points at 464.6 and 431.0 nm respectively.

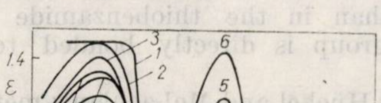

Fig. 4. — Electronic spectra obtained by the electrochemical reduction of **1** in DMSO: 1: initial; 2—6: in time.

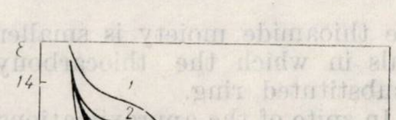

Fig. 5. — Electronic spectra obtained by the electrochemical reduction of **3** in DMSO: 1: initial, 2—6: in time.

The small influence of the thioamide moiety on the electronic structure of the anion radical is revealed also by the absorption spectrum.

The peak of anion radical **3** (510.2 nm) is very close to that found for other *p*-nitrosubstituted amines in the same conditions[2] (i.e. the *p*-nitrodiphenylamine anion radical absorbs at 504 nm).

The influence of the reduction method on the position of the absorption peak of the anion radicals was also investigated. The data obtained for compound **3** are collected in Table 4. A fairly good linear dependence was obtained when the maximum wave number was plotted against the reciprocal of the cation radius (fig. 6) pointing out that the ion-pair interaction may play an important role in these systems even in polar solvents like DMF.

In conclusion it may be stated that in these systems the nitrogroup exerts the determining influence on the electronic structure of the anion-radical. The role of the thioamide moiety is smaller than in the thiobenzamide anion radicals in which the thiocarbonyl group is directly bonded to the nitrosubstituted ring.

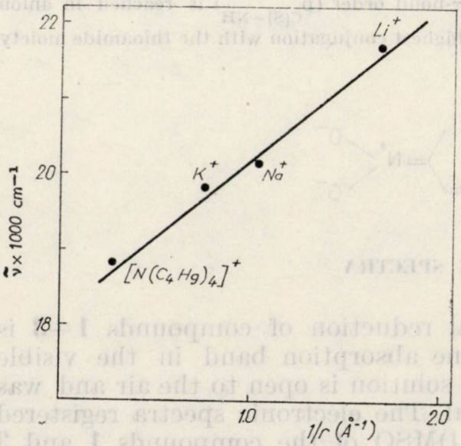

Fig. 6. — Plot of the maximum wave number (cm^{-1}) of anion radical **3** against the reciprocal of the cation radius (A$^{0-1}$).

In spite of the approximations of Hückel and McLachlan's methods, the MO calculations performed account well for the experimental statements.

Table 4

Dependence of the absorption band of anion radical **3** on the counter ion (solvent : DMF)

Cation	r(Å)	$1/r$(Å^{-1})	λ(nm)	$\tilde{\nu}$(cm^{-1})
Li^+	0.60	1.67	461.2	21680
Na^+	0.96	1.04	496.0	20160
K^+	1.33	0.75	504.2	19830
$[N(C_4H_9)_4]^+$	3.50	0.28	531.9	18800

REFERENCES

[1] I. Baciu, M. Hillebrand, V. Em. Sahini and E. Volanschi, *Rev. Roumaine Chim.*, **21**, 485 (1976).
[2] A. Meghea, V. Em. Sahini and E. Volanschi, *Rev. Roumaine Chim.*, **25**, 449 (1980).
[3] C. Cercasov, F. Cornea, M. Ciureanu, M. Hillebrand, V. Em. Sahini and E. Volanschi, *Org. Magn. Resonance*, (in press).

[4] M. Hillebrand, E. Volanschi and A. Missir, *Bull. Inst. Politeh. București, Ser. Chim.-Met.*, **42**, (4), 55 (1980).
[5] A. Missir. *Farmacia*, **25**, 123 (1977).
[6] A. Missir, *Farmacia*, **26**, 183 (1978).
[7] A. Missir, *Farmacia*, **27**, 217 (1979).
[8] E. Volanschi, C. Vlădescu and C. Volanschi, *Rev. Roumaine Chim.*, **19**, 755 (1974).
[9] J. Aarons and F. C. Adam, *Canad. J. Chem.*, **50**, 1390 (1972).
[10] R. D. Allendoerfer and P. H. Rieger, *J. Amer. Chem. Soc.*, **88**, 3711 (1966).
[11] J. P. Malrieu, *J. Chim. phys.*, **62**, 485 (1965).
[12] D. Greatorex, D. B. Jenkins and T. J. Kemp., *J. Chem. Soc. Perkin II*, **1973**, 1762.
[13] P. H. Rieger and G. K. Fraenkel, *J. Chem. Phys.*, **39**, 609 (1963).
[14] M. Karplus and G. K. Fraenkel, *J. Chem. Phys*, **35**, 1312 (1961).

Revue Roumaine de Chimie, 28, 7, 699 – 705 (1983)

REACTION OF PYRYLIUM SALTS WITH NUCLEOPHILES. XVI[1]

NEW *N*-SUBSTITUTED 2,4,6-TRIMETHYLPYRIDINIUM SALTS AND THEIR ^{1}H-NMR SPECTRA

ANTONIE DINCULESCU,[a] MAHMOUD FAHMY,[b,c] FILIP CHIRALEU,[d] and ALEXANDRU T. BALABAN[b,e]

[a] Institute of Chemical and Pharmaceutical Research, Bucharest, Romania
[b] The Polytechnic, Department of Organic Chemistry, Romania
[c] On leave from Tanta University, Faculty of Science, Chemistry Department, Egypt
[d] Centre of Organic Chemistry-ICECHIM, Bucharest, Romania
[e] Correspondence author

Received January 27, 1983

From the reaction of 2,4,6-trimethylpyrylium perchlorate with primary amines, new N-substituted 2,4,6-trimethylpyridinium salts have been obtained. Some of these may have potential biological activity. When the amines were too weakly nucleophilic the reaction was carried out without solvent by melting together the amine and 2,4,6-trimethylpyrylium sulfoacetate which is not explosive. ^{1}H-NMR spectra of pyridinium salts with aromatic N-groups evidence the previously described effect of aromaticity on the chemical shifts of α- and γ-methyl groups.

INTRODUCTION

As known,[2-5] pyrylium salts (I) react with primary amines yielding pyridinium salts (II) according to a sequence of reactions. Each of the intermediate steps from I to II may be neutral or protonated so that the reaction mechanism[6-8] is fairly complicated. The initial ring opening of pyrylium salts is facilitated by the high electronegativity of the oxygen heteroatom, leading to a reduced aromaticity of I, while the final formation of the pyridinium cation has rearomatisation as a driving force. The net result is the replacement of a highly electronegative heteroatom by a less electronegative heteroatom in a six-membered aromatic ring.

This synthesis of pyridinium salts is an excellent method, starting from readily accessible synthons (pyrylium salts),[9] because it gives high yields and may be applied for the preparation of pyridinium salts which are otherwise difficultly accessible. Pyridinium salts are of interest for a variety of reasons :

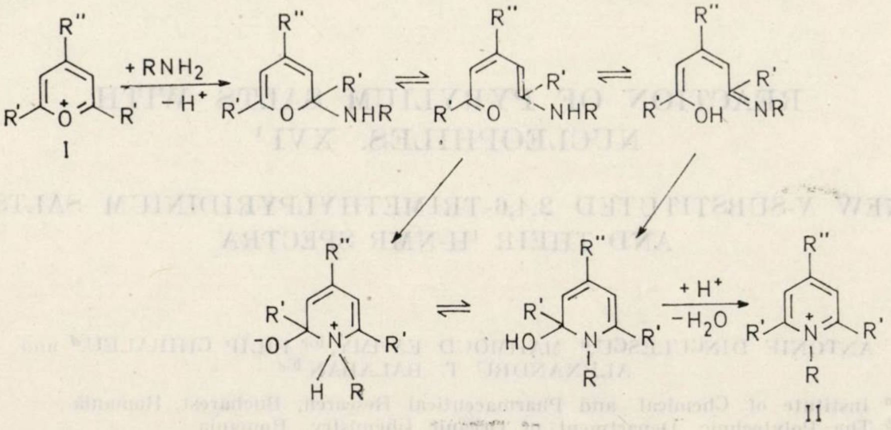

(i) Some of them may have potential biological activity, serving as antidotes for cholinesterase inhibitors, or acting as coccidiostatics. [1,10]

(ii) It was shown [11–13] that from ^{1}H-NMR spectra of N-aryl-2,4,6-trimethylpyridinium salts one may obtain information on the aromaticity of the N-aryl group.

(iii) Katritzky and coworkers, following earlier initial observations,[14] developed the nucleophilic attack on 2,4,6-triarylpyridinium salts into a powerful synthetic method for the formation of a new bond between the attacking nucleophile and the N-substituent.[7] Thus the triarylpyridine acts as a good leaving group leading as a net result in the replacement of NH_2 groups from primary amines by various nucleophiles.

(iv) Some pyridinium salts evidence interesting stereochemical features: atropisomerism of asymmetrically substituted N-arylpyridinium salts,[15] restricted rotation around the N-alkyl bond in N-alkyl-2,4,6-trimethylpyridinium salts,[16] or in similar compounds with isopropyl groups.[17]

The present paper continues to report new pyridinium salts with potential biological activity [1,12,18] and, in addition, it describes a new method for obtaining pyridinium salts from unreactive primary amines and molten 2,4,6-trimethylpyrylium sulfoacetate[19] which, unlike the corresponding perchlorate, avoids the danger of explosions. These experiments were also intended to enlarge the number of N-aryl-substituted compounds for correlating the ^{1}H-NMR data with the aromaticity of the N-aryl group.[11–13]

PREPARATION

Most reactions were carried out with 2,4,6-trimethylpyrylium perchlorate [20] (I, $R' = R'' =$ Me) in ethanol under reflux with excess amine. If the product does not crystallize on cooling, ethyl ether may be added. This has the added advantage of removing most of the unreacted amine; when unreacted 2,4,6-trimethylpyrylium is a contaminant, a good way of eliminating it is to treat the crude product with aqueous ammonia; the pyrylium salt is converted thereby into *sym*-collidine which is readily removed by washing the product with ethyl ether.

When the reaction between 2,4,6-trimethylpyrylium perchlorate and primary amine fails to take place (namely when the amine is too weakly nucleophilic), more energetic conditions had to be used, namely heating the trimethylpyrylium cation with the amine at 160–180° in the absence of a solvent; since, however, pyrylium perchlorates present the danger of explosions,[20,21] in such cases we use another salt, namely 2,4,6-trimethylpyrylium sulfoacetate.[19] This salt, whose anion is $HOOC-CH_2-SO_2-O^-$, is readily available in excellent yield, and has m.p. 115°.[19] One drawback of pyridinium sulfoacetates is their high solubility hence low melting points; therefore after completion of the reaction, the melt was cooled, dissolved in ethanol, and treated with 70% perchloric acid, proceeding thereafter as described above for the purification of the product from unreacted materials.

Table 1 presents the structures, melting points, formulas and elemental analyses of the new pyridinium perchlorates.

^{1}H–NMR SPECTRA

The new pyridinium perchlorates were investigated by means of ^{1}H–NMR spectroscopy in trifluoroacetic acid as solvent at room temperature. The chemical shifts are indicated in Table 2. This table includes two compounds (N-isopropyl-, and N-5-methyl-3-isoxazolyl-2,4,6-trimethylpyridinium) reported earlier.

The following remarks may be made on discussing the data from Table 2:

(a) When N-aryl substituents are present, the γ-methyl group has a remarkably constant chemical shift ($\delta = 2.6-2.8$ ppm). The lowest value (2.61) is evidenced by compound **2** derived from 2-aminobiphenyl; this is due to the sterically-conditioned non-coplanarity of the *ortho*-standing phenyl group (only 2 kcal/mole conjugation energy are lost thereby); this phenyl group shields accordingly all protons on the pyridinium moiety (the effect is evident also for the pyridinium β-aromatic and α-methyl protons of **2**). When an *ortho*-phenyl group is linked to an N-benzenoid ring through the intermediacy of an NH or CO group (compounds **10**, **11**) such sterical constraints disappear and the chemical shifts fall within the normal range.

(b) As first observed earlier,[4,11–13] with non-aromatic N-bonded R groups the α-methyl peak appears at lower fields than the γ-methyl peak but with aromatic R groups the situation is reversed, see comment (c) below. An interesting observation is that whereas the pyridinium salt **1** formed from cyclopentylamine has at room temperature a normal ^{1}H-NMR spectrum, the α-methyl peak of compound (*b*) formed from isopropylamine presents considerable broadening, and at lower temperature two α-methyl peaks appear. This phenomenon has also been observed with other primary amines whose NH_2 group is bonded to a secondary carbon atom and is due to restricted rotation around the $C(sp^3)-N(sp^2)$

Table 2

Chemical shifts (δ values) and multiplicities[a] in ^{1}H-NMR spectra of 2,4,6-trimethylpyridinium perchlorates II (cf. Tabe 1) in trifluoroacetic acid, *D* and RRC values

Comp. (R)	2(6)$-$CH$_3$	4$-$CH$_3$	other CH$_3$	CH$_2$	3(5)$-$CH	other CH	*D*	RRC
(i-Pr *b*)	2.97	2.57	1.83d	—	7.53	5.48m	−0.40	—
1	2.93	2.55	—	2.18	7.48	5.50	−0.38	—
2	2.48	2.61	—	—	7.50	—	0.13	76
3	2.51	2.70	—	—	7.67	—	0.19	88
4	2.50	2.75	—	—	7.85	—	0.25	100
5	2.46	2.71	—	—	7.73	—	0.25	100
6	2.46	2.71	—	—	7.73	—	0.25	100
7	2.38	2.72	2.83	—	7.67	—	0.34	—
8	2.47	2.72	2.88	—	7.72	—	0.25	100
9	2.47	2.72	2.92	—	7.72	—	0.25	100
10	2.49	2.68	—	—	7.67	—	0.19	88
11	2.50	2.68	—	—	7.67	—	0.18	66
12	2.47	2.72	—	—	7.70	—	0.25	100
13	2.50	2.68	—	—	7.58	—	0.18	86
14	2.46	2.68	—	3.13t 2.26t	7.65	—	0.22	94
15	2.48	2.73	—	—	7.75	9.15	0.25	100
16	2.51	2.76	—	—	7.75	9.08	0.25	100
(*c*)	2.62	2.74	2.74	—	7.75	—	0.12	74
17	2.60	2.76	2.08 2.55	—	7.78	—	0.16	82
18	2.73	2.80	4.10	—	7.83	—	0.07	64

[a] If no data are given, the peaks are singlets.

[b] At room temperature the α-methyl peak is broad due to restricted rotation around the N$-$CHMe$_2$ bond.[16,17]

[c] 5-Methylisoxazol-3-yl. Revised assignment for pyridinium salt reported in ref. [3,8], and [11].

bond. Since it was discussed elsewhere,[16,17] this observation will not be further commented here.

(c) The difference between N-alkyl- and N-aryl-2,4,6-trimethylpyridinium salts mentioned in the preceding item is not only a qualitative feature, but can be used to assess quantitatively the aromaticity of the N-aryl group. This group, which is approximately perpendicular to the pyridinium ring, shields the α-methyl protons and deshields the γ-methyl protons. The effect is larger for larger dihedral angles, for larger perimeters of the N-aryl ring, and for higher ring currents in this ring. Of course, these three factors appear combined in the chemical shift difference between α- and γ-methyl protons; however, on comparing N-aryl rings of similar magnitude and with similar steric factors, only the last factor becomes dominant.

It was proposed [11-13] to measure the relative ring current (RRC) of the N-aryl group using the value 100 for an N-phenyl group as standard. The difference *D* between chemical shifts

$$D = \delta(\gamma\text{-CH}_3) - \delta(\alpha\text{-CH}_3)$$

is related to the relative ring current by the relationship

$$\text{RRC} = 200\ (D + 0.25) - T$$

where T is a term accounting for the presence of bulky *ortho*-substituents. In the present paper, we consider $T = 0$.

EXPERIMENTAL

Three methods were used for preparing pyridinium salts.

A. *In refluxing ethanol.* 2,4,6-Trimethylpyrylium perchlorate [20] (20 mmol) and 30 mmol primary amine (molar ratio 1 : 1.5) were refluxed for three hrs in 100 ml ethanol. After cooling, 2 ml of conc. aqueous ammonia were added and the mixture was refluxed for another 10 minutes with active charcoal. After filtration, the pyridinium perchlorate was precipitated by adding ethyl ether (in small amounts, stirring and scratching with a glass rod). The products were obtained in 55—85 % yield and were recrystallised as indicated in Table 1.

With compound **13**, in order to obtain the bis-pyridinium salt, the molar ratio was 1 : 1. With compounds **11** and **12** derived from the highly basic amino-diphenylamines, an excess of pyrylium salt was used (molar ratio 2 : 1); this excess was destroyed by adding the corresponding amount of aqueous ammonia.

B. *In dichloromethane at room temperature.* This method, due to Katritzky *et al.*,[7] is simple and convenient and was applied in modified form for compounds **15** and **17** (also **1**, which however may also be obtained in ethanol at room temperature). Nevertheless, in several cases (for compounds **2**, **9** and **10**), it failed to lead to the desired result, though method A was successful. Our modification consisted in replacing the additional triethylamine (which isometimes difficult to remove completely) by an excess of the primary amine reagent.

The trimethylpyrylium perchlorate (20 mmol) and the primary amine (30 mmol) were stirred in 100 ml methylene dichloride for 3—4 hrs at room temperature. Then 25 ml glacial acetic acid were added and the mixture was stirred for one hr at room temperature. Then the product was precipitated with ethyl ether as described in method A. The yields were 60—80 %. When the addition of ether causes the pyridinium perchlorate to separate as an oil, brief refluxation in isopropanol (to which a few drops of 70 % perchloric acid were added) resulted in the formation of a crystalline product.

C. *In molten state at elevated temperature.* Although two of the isomeric aminobenzonitriles react smoothly with 2,4,6-trimethylpyrylium perchlorate yielding the corresponding pyridinium salts **5** and **6** with *m*- and *p*- standing cyano groups, the *ortho*- isomer does not react in the conditions of method A ; this is probably due to a combination of reduced basicity and steric factors. We therefore applied a more drastic method which, we believe, can be of assistance whenever other methods fail owing to the above two factors.

2-Aminobenzonitrile (5 g, 42 mmol) having m.p. 55°, and 10g (39 mmol) of 2,4,6-trimethylpyrylium sulfoacetate (m.p. 115°) [19] were heated gradually in a porcelain capsule on the sand bath, under continuous stirring with a rod-like thermometer. At 150° an exothermal reaction took place when the deep red molten mixture foamed owing to the evaporation of the resulting water. After the foaming subsided, i.e. after 5—10 minutes, the heating was continued for 10 minutes at 150—160°, then the product was left to cool. When the temperature reached 90—100°, the mixture was poured into a beaker containing 200 ml ethanol. The solution was heated with active charcoal and 2 ml aqueous ammonia, filtered, treated with a slight excess of 70 % perchloric acid, and finally with ethyl ether which was added gradually. The pyridinium perchlorate **4** resulted in 68 % yield.

REFERENCES

[3] Preceding part, A. Dinculescu and A. T. Balaban, *Rev. Roumaine Chim.*, **25**, 1505 (1980).
[1] A. Baeyer and J. Piccard, *Liebigs Ann. Chem.*, **384**, 208 (1911).
[2] R. Lombard and A. Kress, *Bull. Soc. chim. France*, 1458 (1958) ; 1528 (1960).

A. T. Balaban and C. Toma, *Tetrahedron, Suppl. 7*, **1966**, 1. C. Toma and A. T. Balaban, *ibid.* **1966**, 9.

[4] K. Dimroth and K. H. Wolf, "Newer Methods in Preparative Organic Chemistry", vol. 3,
[5] p. 357 (ed. W. Foerst) Academic Press, New York, 1964.

[6] A. T. Balaban and W. Silhan, *Tetrahedron*, **26**, 743 (1970).

[7] A. R. Katritzky, *Tetrahedron*, **36**, 679 (1980) and further references therein.

[8] A. T. Balaban, A. Dinculescu, G. N. Dorofeenko, G. W. Fischer, A. V. Koblik, V. V. Mezheritskii and W. Schroth, "Pyrylium Salts. Syntheses, Reactions and Physical Properties", Adv. Heterocyclic Chem., Suppl. 2., ed. A. R. Katritzky, Academic Press, New York, 1982.

[9] A. T. Balaban, in "New Trends in Heterocyclic Chemistry", Studies in Organic Chemistry No. 3, ed. R. B. Mitra *et al.*, Elsevier, Amsterdam, 1979, p. 79.

[10] A. Dinculescu, S. Cilianu and C. Drăghici, Roum. Pat. 69761 (1977).

[11] A. T. Balaban, A. Dinculescu, H. N. Koutrakis and F. Chiraleu, *Tetrahedron Letters*, **1979**, 437.

[12] A. Dinculescu, H. N. Koutrakis and A. T. Balaban, *Rev. Roumaine Chim.*, **24**, 439 (1979).

[13] A. T. Balaban, A. Dinculescu, F. Iordache, F. Chiraleu and D. Pătrăşcoiu, *Chem. Scripta*, **18**, 230 (1981).

[14] A. B. Susan and A. T. Balaban, *Rev. Roumaine Chim.*, **14**, 111 (1969).

[15] C. Uncuţa and A. T. Balaban, *Rev. Roumaine Chim.*, **21**, 251 (1976).

[16] A. T. Balaban, C. Uncuţa, A. Dinculescu, M. Elian and F. Chiraleu, *Tetrahedron Letters*, **21**, 1553 (1980).

[17] C. Roussel, A. T. Balaban, U. Berg, M. Chanon, R. Gallo, G. Klatte, J. A. Memiaghe, J. Metzger, D. Oniciu and J. Pierrot-Sanders, *Tetrahedron*, (in press).

[18] A. Dinculescu and G. Andreescu, Roum. Pat., 55461 (1972).

[19] A. Dinculescu and A. T. Balaban, *Org. Prep. Proc. Internat.*, **14**, 39 (1982).

[20] A. T. Balaban and C. D. Nenitzescu, *Org. Synth. Coll. Vol.*, **5**, 1156 (1973).

[21] A. Pelter, *Tetrahedron Letters*, **22**, No. 22, i **(1981)**.

Revue Roumaine de Chimie, **28**, 7, 707–714 (1983)

REACTIONS OF PYRYLIUM SALTS WITH NUCLEOPHILES. XVII[1]

NEW 2,4,6-TRISUBSTITUTED BIS- AND TRIS-PYRIDINIUM SALTS AND THEIR ^{1}H-NMR SPECTRA

EMIL STEPAN[a] and ALEXANDRU T. BALABAN[b,c]

[a] Chemical Research Institute, ICECHIM, Splaiul Independenţei 202, Bucharest, Romania

[b] Department of Organic Chemistry-TCH, The Polytechnic, Splaiul Independenţei 313, 76206 Bucharest-16, Romania

[c] Correspondence author

Received January 27, 1983

By reaction of 2,4,6-trimethyl- or triphenyl-pyrylium perchlorates with primary aromatic amines possessing two or three NH_2 groups, twelve new bis-pyridinium salts **2a**–**d**, **5a**–**e**, **6a**–**e** and one tris-pyridinium salt **7** were obtained. However, when *ortho*-chloro groups are present in the diamine, only one amino group reacts leading to mono-pyridinium salts **3** and **4**. A mono-pyridinium salt **8** with nitro and amino groups does not react further with pyrylium cations. The ^{1}N-HMR spectra of all new products are discussed.

1. INTRODUCTION

The discovery that some quaternary ammonium salts may possess selective phytotoxic properties oriented the research towards quaternary salts of 2,2′- and 4,4′-bipyridine. Thus two remarkable herbicides were discovered : 1,1′-ethylene-2,2′-bipyridinium dibromide (diquat), **1A**,[2] and 1,1′-dimethyl-4,4′-bipyridinium dichloride (paraquat), **1B**.[3]

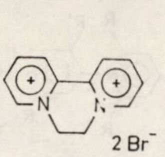

1A

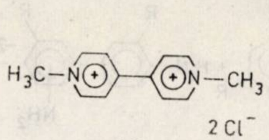

1B

Their effectiveness is correlated with their ability to undergo one-electron reduction to stable radical-cations in aqueous solutions.[4]

A number of 1,1′-polymethylene-bis-(4-formylpyridinium bromide) dioximes, **1C**,[5] are used as chemotherapeutic agents since they reactivate acetylcholinesterase when this enzyme is inhibited by organophosphorus insecticides or by similar compounds.

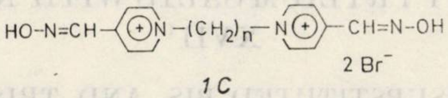

1C

Finally, other biologically active pyridinium compounds are N,N′-(α, ω-polymethylene)-bis-(4-alkylamino-pyridinium) derivatives **1D**, which possess antibacterial and antifungic properties, and are therefore used in dentistry.[6]

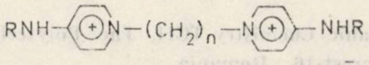

1D

All the above types of pyridinium salts were obtained by quaternizing pyridines with dihaloalkanes. Often this reaction requires elevated temperatures and long reaction times, and leads to the formation of undesired side-products.

We present here an alternative method for synthesizing poly-(2,4,6-trisubstituted pyridinium) salts, starting from the corresponding pyrylium salts and primary aromatic amines. With α, ω-polymethylenediamines, biologically active N,N′-(α, ω-poly-methylene)-bis-pyridinium salts were obtained earlier,[7] under mild conditions and with high yields. We have also obtained [8] new poly-pyridinium derivatives from pyrylium salts; they may form radical-cations by one-electron reduction.

2. PREPARATION OF POLY-PYRIDINIUM SALTS

A. Diamines derived from biphenyl react readily with 2,4,6-trisubstituted pyrylium salts (R = Me or Ph) affording bis-pyridinium salts **2** in good yields (88–96 %), as seen in Table 1.

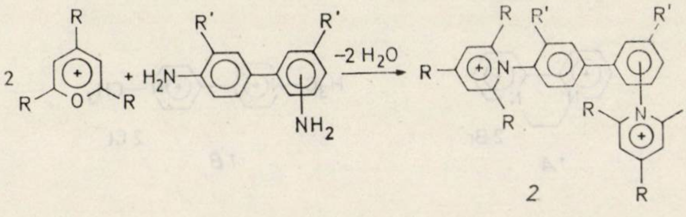

2

	R	*R′*	*Positions of NH$_2$*
a	Me	H	2,4′
b	Me	H	4,4′
c	Me	OMe	4,4′
d	Ph	OMe	4,4′

3,3′-Dimethoxybenzidine reacts more easily than benzidine, despite the steric hindrance, since the methoxy groups enhance the nucleophilicity of amino groups compensating the deactivating effect of the first pyridinium ring, once formed. Neidlein *et al.*[9] reported the preparation of compound **2b**, using different reaction conditions from those reported in the present paper.

However, 3,3′-dichlorobenzidine and 1,4-diamino-2,5-dichlorobenzene do not afford bis-pyridinium salts; their reaction with pyrylium salts under similar conditions to those described above leads to mono-pyridinium salts **3** and **4**, respectively, whose remaining amino group no longer reacts.

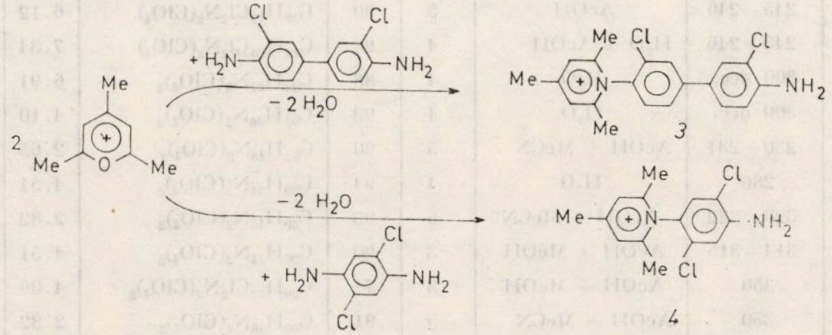

This is probably due to a combination of steric hindrance and electronic effects; the nucleophilicity of the remaining amino group in reaction products **3** and **4** is depressed both by the halogen and, more significantly, by the pyridinium ring.

B. Diamines derived from *p,p′*-diaminodiphenylamine, *p,p′*-diaminodiphenylmethane, or *p,p′*-diamino-1,2-diphenylethane, react normally with pyrylium salts affording in high yields (88–94%, cf. Table 1) bis-pyridinium salts **5**.

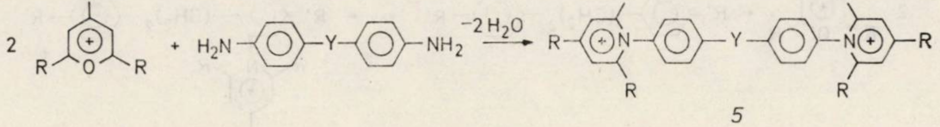

	R	*Y*
a	Me	NH
b	Me	CHPh
c	Ph	CHPh
d	Me	CH_2CH_2
e	Ph	CH_2CH_2

The secondary amine function does not interfere with the formation of the bis-pyridinium salt **5a** (the nucleophilicity of diarylamines is too low to enable them to react with pyrylium salts).

Table 1

The new poly-pyridinium salts

Comp.	M.P. (°C)	Recryst. from	Reaction		Formula	N %	
			Time hrs.	Yield %		Calc.	Found
2a	278–280	H_2O	2	88	$C_{28}H_{30}N_2(ClO_4)_2$	4.72	4.89
2b	350	H_2O	3	93	$C_{28}H_{30}N_2(ClO_4)_2$	4.72	4.85
2c	350	H_2O	2	92	$C_{30}H_{34}N_2O_2(ClO_4)_2$	4.29	4.46
2d	350	AcOH + MeCN	5	96	$C_{60}H_{46}N_2O_2(ClO_4)_2$	2.73	2.71
3	245–246	AcOH	5	90	$C_{20}H_{19}Cl_2N_2(ClO_4)$	6.12	6.14
4	245–246	H_2O + AcOH	4	90	$C_{14}H_{15}Cl_2N_2(ClO_4)$	7.34	7.89
5a	300 dec.	H_2O	4	88	$C_{28}H_{31}N_3(ClO_4)_2$	6.91	6.98
5b	300 dec.	H_2O	4	93	$C_{35}H_{36}N_2(ClO_4)_2$	4.10	4.27
5c	230–231	AcOH + MeCN	5	90	$C_{65}H_{48}N_2(ClO_4)_2$	2.65	2.88
5d	286	H_2O	4	94	$C_{30}H_{34}N_2(ClO_4)_2$	4.51	4.75
5e	320–322	AcOH + MeCN	5	93	$C_{60}H_{46}N_2(ClO_4)_2$	2.82	2.74
6a	314–315	AcOH + MeOH	3	90	$C_{30}H_{34}N_2(ClO_4)_2$	4.51	4.73
6b	350	AcOH + MeOH	3	71	$C_{30}H_{32}Cl_2N_2(ClO_4)_2$	4.06	4.20
6c	350	AcOH + MeCN	5	91	$C_{60}H_{46}N_2(ClO_4)_2$	2.82	2.92
7	320	H_2O	3	92	$C_{46}H_{52}N_3(ClO_4)_3$	4.45	4.72
8	183–185	H_2O	5	75	$C_{22}H_{23}N_4O_4(ClO_4)$	11.05	11.00

C. Similar reactions were observed with diamines derived from 1,2-diphenylethane, having the two amino groups in *o,o'*-positions.

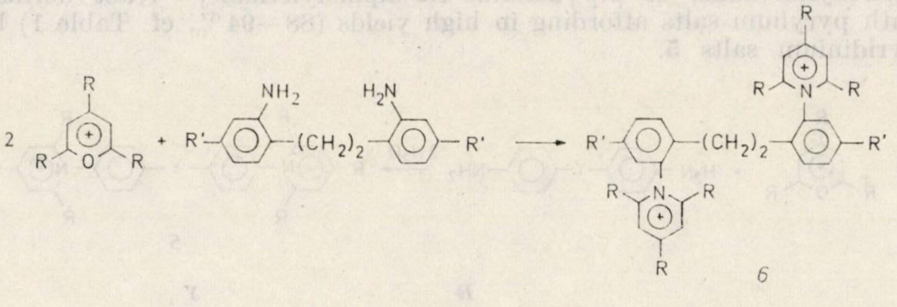

6

	R	R'
a	Me	H
b	Me	Cl
c	Ph	H

Interestingly, though the reactivity and yields are higher (~ 90%) in the absence of chloro substituents R' (for **6a** and **6c**), the presence of such substituents R' does not forbid the formation of bis-pyridinium salt **6b**; it must be stressed, however, that these substituents R′ are situated in *meta*- positions relatively to the amino groups, whereas in the case of compounds **3** and **4** the chloro substituents were *ortho* to the amino groups.

D. With an aromatic triamine derived from triphenylmethane, a tris-pyridinium salt **7** results in 92% yield.

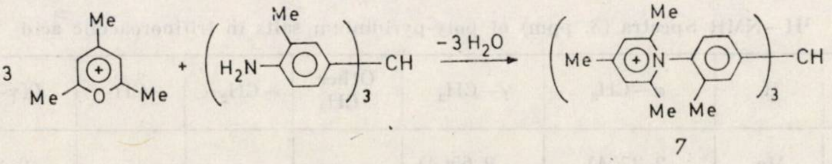

Though there exist *ortho*-methyl substituents relatively to the amino groups, the reaction proceeds normally, as with *o*-toluidine.

E. The attempt to obtain a bis-pyridinium salt similar to **6** with $R' = NO_2$ substituents yielded instead a monopyridinium salt **8**. In this case, unlike **3** and **4**, one cannot assume a through-bond electronic influence of the pyridinium ring on the amino group in **8**, because of the 1,2-ethylenic insulating chain;

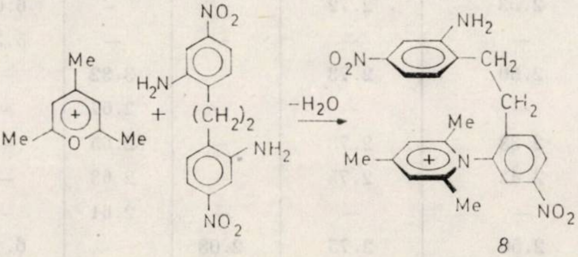

however, owing to the flexibility of this chain, it is conceivable that an intramolecular through-space charge transfer occurs in **8** (in a folded conformation as illustrated) reducing thereby the nucleophilicity of the amino group. Since however, this does not prevent the analogous intermediate monopyridinium salts devoid of nitro groups to react further and to yield **6**, probably the *meta*-standing nitro group in **8** also contributes to this effect. There is a marked difference between the ¹H-NMR chemical shift of methylene groups in **8** and **6**, as it will be seen in Table 2, probably because the electrostatic repulsion between the two pyridinium rings in **6** does not favour a folded conformation as in **8**.

3. ¹H–NMR SPECTRA

The ¹H-NMR spectra of all reported poly-pyridinium perchlorates are presented in Table 2. As indicated earlier,[10] for N-aryl-2,4,6-trimethylpyridinium salts the two rings are not coplanar so that the 2,6-methyl groups (α-positions) are shielded by the aryl group, while any *ortho*-standing alkyl on the aryl group is shielded by the pyridinium ring. Accordingly, α-standing methyl groups in all compounds **2**–**8** resonate at higher fields than γ-methyl groups. We assigned the four methyl singlets of **2a** as indicated in Table 2, on the basis of peak intensity (α-methyls have twice the intensity of γ-methyls) and peak position (A-type protons at higher field than B-type protons).

Table 2

^1H–NMR Spectra (δ, ppm) of poly-pyridinium salts in trifluoroacetic acid

Comp.	R	$\alpha-CH_3$	$\gamma-CH_3$	Other $-CH_3$	$-CH_2-$	$-\overset{\vert}{C}H-$	$D(\gamma-\alpha)$
2a	Me	2.37(A) 2.55(B)	2.65(A) 2.68(B)	—	—	—	0.28(A) 0.13(B)
2b	Me	2.55	2.75	—	—	—	0.20
2c	Me	2.53	2.73	4.07	—	—	0.20
2d	Ph	—	—	3.75	—	—	—
3	Me	2.53	2.77	—	—	—	0.24
4	Me	2.51	2.76	—	—	—	0.25
5a	Me	2.55	2.73	—	—	—	0.22
5b	Me	2.53	2.72	—	—	6.07	0.19
5c	Ph	—	—	—	—	5.38	—
5d	Me	2.50	2.73	—	3.32	—	0.23
5e	Ph	—	—	—	2.67	—	—
6a	Me	2.38	2.73	—	2.65	—	0.35
6b	Me	2.43	2.75	—	2.63	—	0.22
6c	Ph	—	—	—	2.61	—	—
7	Me	2.50	2.75	2.08	—	6.12	0.25
8	Me	2.54	2.75	—	3.45	—	0.21

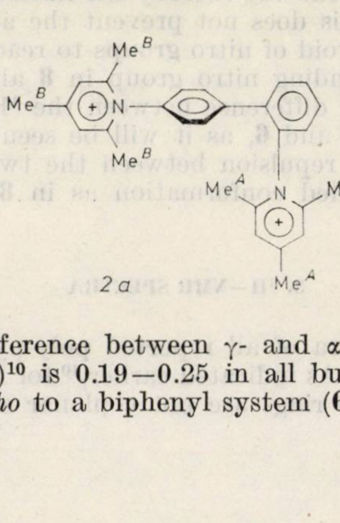

2a

The resulted difference between γ- and α-methyl protons (column headed D in Table 2)[10] is 0.19–0.25 in all but three cases: when the pyridinium ring is *ortho* to a biphenyl system (**6a**, and protons A in **2a**), the *D* value is higher: 0.28 ppm for *A*-protons in **2a**, and 0.35 ppm in **6a**; for *B*-protons in **2a**, the *D*-value is lower (0.13 ppm) for reasons which are not clear, but which are probably connected with the unusual shape of the molecule **2a**, with the phenyl rings orthogonal to each other, hence shielding/deshielding.

The fact that compound **6b** does not present large *D* values like **6a**, is probably the result of a compensating effect of Cl groups, which lower the *D* value (while structure **6** increases this value, as seen for **6a**).

From Table 2 it is apparent that whenever 2,4,6-triphenyl substituents are present, the protons of the side-chains are appreciably shielded (0.3—0.7 ppm). This is evident by comparing the chemical shifts of methoxy-groups in **2c** and **2d**, of methine protons in **5b** and **5c**, or of methylene groups in **5d** and **5e**. Such an effect is not observed in comparing the methylene protons in **6a** and **6c**, again probably due to the unusual conformation of these molecules **6**. The fact that the methylene protons in **8** resonate at lower fields than in **6** has been already mentioned under E above, and has been assigned to conformational differences.

The shielding effect of pyridinium rings on the *ortho*-methyl groups in **7** is paralleled by the NMR spectra of N-*o*-tolyl-2,4,6-trimethylpyridinium salts.[11]

4. EXPERIMENTAL PART

2,4′-Bis-(2,4,6-trimethylpyridininum-N-yl)-biphenyl diperchlorate (**2a**), 2,4′-Diaminobiphenyl dihydrochloride (1.29 g, 5 mmol) in 10 ml methanol was neutralized with the stoichiometric amount of sodium methoxide, then 10 mmol (2.22 g) of 2,4,6-trimethylpyrylium perchlorate[12] was added. After refluxing for 2 hrs with stirring, the product crystallized on cooling, was filtered off and purified by recrystallization with charcoal.

4, 4′-Bis-(2,4,6-trimethylpyridinium-N-yl)-biphenyl diperchlorate, or 1,1′-(1,1′-biphenyl)-4,4′-diylbis (2,4,6-trimethylpyridinium) diperchlorate (**2b**). A suspension of 2.22 g (10 mmol) 2,4,6-trimethylpyrylium perchlorate in 20 ml methanol was treated with 0.92 g (5 mmol) of 4,4′-diaminobiphenyl, and the product was isolated as described above.

4,4′-Bis-(2,4,6-trimethylpyridinium-N-yl)-3,3′-dimethoxybiphenyl diperchlorate (**2c**), was obtained as described for **2b**, using 4,4′-diamino-3,3′-dimethoxybiphenyl.

4,4′-Bis-(2,4,6-triphenylpyridinium-N-yl)-3,3′-dimethoxybiphenyl diperchlorate (**2d**), was prepared as described for **2c**, but replacing the trimethylpyrylium salt by 2,4,6-triphenylpyrylium perchlorate.[13]

4-(2,4,6-Trimethylpyridinium-N-yl)-4′-amino-3,3′-dichlorobiphenyl perchlorate (**3**), was obtained from a suspension of 2.22 g (10 mmol) 2,4,6-trimethylpyrylium perchlorate in 20 ml ethanol and 4,4′-diamino-3,3′-dichlorobiphenyl, irrespective of the molar ratio, under conditions identical with those above. The yield indicated in Table 1 is for equimolar ratios.

N-(2,5-Dichloro-4-aminophenyl)-2,4,6-trimethylpyridinium perchlorate (**4**), was obtained as above with 1,4-diamino-2,5-dichlorobenzene. The yield in Table 1 is for equimolar ratios.

4,4′-Bis-(2,4,6-trimethylpyridinium-N-yl)-diphenylamine diperchlorate (**5a**), was prepared as for **2b** from 4,4′-diaminodiphenylamine, in methanol.

4,4′-Bis-(2,4,6-trimethylpyridinium-N-yl)-triphenylmethane diperchlorate (**5b**), was obtained analogously to **5a**.

4,4-′Bis-(2,4,6-triphenylpyridinium-N-yl)-triphenylmethane diperchlorate (**5c**). A mixture of 1.37 g (5 mmol) 4,4′-diaminotriphenylmethane, 4.08 g (10 mmol) 2,4,6-triphenylpyrylium perchlorate in 30 ml dimethylformamide was stirred at 90°C for 5 hrs. After cooling, the solution was diluted with water, filtered off and purified by recrystallization.

p,p′-Bis-(2,4,6-trimethylpyridinium-N-yl)-1,2-diphenylethane diperchlorate (**5d**), was obtained as described for **2b**, from *p,p′*-diamino-1,2-diphenylethane, in methanol.

p,p′-Bis-(2,4,6-triphenylpyridinium -N-yl)-1,2-diphenylethane diperchlorate (**5e**), was prepared analogously in ethanol.

o,o′-Bis-(2,4,6-trimethylpyridinium-N-yl)-1,2-diphenylethane diperchlorate **(6a)**, was obtained as for **2b**, from *p,p′*-diamino-1,2-diphenylethane in methanol.

o,o′-Bis-(2,4,6-trimethylpyridinium-N-yl)-, p, p′-dichloro-1,2-diphenylethane diperchlorate **(6b)**, was obtained analogously.

o,o′-Bis-(2,4,6-triphenylpyridinium-N-yl)-1,2-diphenylethane diperchlorate **(6c)**, was prepared as for **5c**, using *o,o′*-diamino-1,2-diphenylethane.

4,4′,4″-Tris-(2,4,6-trimethylpyridinium-N-yl)-3,3′,3″-trimethyl-triphenylmethane triperchlorate **(7)**. A suspension of 6.67 g (30 mmol) 2,4,6-trimethylpyrylium perchlorate in 50 ml methanol, was treated with 3.31 g (10 mmol) 4,4′,4″-triamino-3,3′3″-trimethyl-triphenylmethane. After refluxing, the product was isolated as described for **2a**.

o-(2,4,6-trimethylpyridinium-N-yl)-o′-amino-p,p′-dinitro-1, 2-diphenylethane perchlorate **(8)**. 2,4,6-Trimethylpyrylium perchlorate (10 mmol) in 7 ml dimethylformamide was treated with a solution of 10 mmol 2,2′-diamino-4,4′-dinitrodibenzyl in 18 ml dimethylformamide, then stirred at 90°C for 5 hrs. After cooling the mixture was diluted with water, and the product was filtered off and purified, yielding white crystals.

ACKNOWLEDGEMENT. Thanks are expressed to Dr. Filip Chiraleu for recording the ^{1}H-NMR spectra.

REFERENCES

[1] Part XVI, preceding paper.

[2] R. C. Brian, R. F. Homer, J. Stubbs and R. L. Jones, *Nature*, **181**, 446 (1958).

[3] R. C. Brian, G. W. Driver, R. F. Homer and R. L. Jones, *Germ. Pat.*, 1,048,070 (1958) ; *Chem. Abstr.*, **55**, 891 (1961).

[4] R. F. Homer and T. E. Tomlinson, *Nature*, **184**, 2012 (1959).

[5] E. J. Poziomek, B. E. Hackley Jr. and G. M. Steinberg, *J. Org. Chem.*, **23**, 714 (1958).

[6] D. M. Bailey, *Germ. Pat.*, 2,708,331 (1977) ; *Chem. Abstr.*, **88**, 22632 (1978).

[7] A. Dinculescu, A. T. Balaban and E. Stepan, *Roumanian Pat.*, 73,504 (1978).

[8] E. Stepan and A. T. Balaban, *Roumanian Pat.*, 79, 547 (1982).

[9] R. Neidlein and P. Witerzens, *Monatsh. Chem.*, **106**, 643 (1975).

[10] A. T. Balaban, A. Dinculescu, H. N. Koutrakis and F. Chiraleu, *Tetrahedron Letters*, 437 (1979) ; A. T. Balaban, A. Dinculescu, F. Iordache, F. Chiraleu and D. Pătrăşcoiu, *Chem. Scripta*, **18**, 230 (1981) ; A. T. Balaban, *Pure Appl. Chem.*, **5**, 1075 (1982) and further references therein.

[11] C. Uncuţa and A. T. Balaban, *Rev. Roumaine Chim.*, **21**, 251 (1976).

[12] A. T. Balaban and C. D. Nenitzescu, *Org. Synth.*, Coll. Vol. 5, 1106 (1973).

[13] A. T. Balaban, *Compt. rend.*, **256**, 4239 (1963).

Revue Roumaine de Chimie, 28, 7, 715–718 (1983)

SOME REACTIONS OF 2-OXO-1,2,3,4-TETRAHYDRO-NICOTINONITRILES

M. A. HASSAN*, A. F. ELKAFRAWY and M. ElBORAI,

Faculty of Science, Ain Shams and Tanta Universities, Egypt

Received June 15, 1981

Some new 2-oxo-1,2,3,4-tetrahydronicotinonitriles (I) were prepared. The compounds I gave the characteristic reactions of cyano group, e.g. acidic and alkaline hydrolysis, as well as addition of Grignard reagents. Addition of isocyanates to I was also studied.

Recently,[1,2] we have reported that ethyl cyanoacetate condenses with chalcones in the presence of ammonium acetate to give 2(1*H*)-pyridones. The base catalyzed cycloaddition of cyano-acetamide on dibenzylideneacetone or dianisalacetone at 170°C gave 2-oxo-4-phenyl (or *p*-methoxyphenyl)-6-styryl (or *p*-methoxy-styryl)-1,2,3,4-tetrahydronicotinonitriles (I*a* and I*b*).

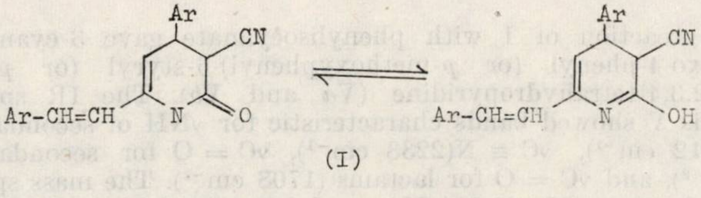

(I)

a) Ar = C_6H_5 b) Ar = $C_6H_4-OCH_3-p$

The IR spectra of I showed the bands characteristic for νC = O(1700 cm^{-1}), νNH and OH (3158, 2872 cm^{-1})[3], νC ≡ N (2229 cm^{-1}) and νC = O conjugated with phenyl group (1650 cm^{-1}).

The alkaline hydrolysis of I*b* gave 4-*p*-methoxyphenyl-6-*p*-methoxystyryl-2-oxo-1,2,3,4-tetrahydronicotinamide (II). The IR spectrum of II showed the absence of stretching frequency of cyano-group and showed a band characteristic for νC = O of primary amides (1683 cm^{-1}). The acid hydrolysis of I*b* gave 4-*p*-methoxyphenyl-6-*p*-methoxystyril-2-oxo-1,2,3,4-tetrahydronicotinic acid (III). The IR spectrum of III showed bands characteristic for νC = O of acids (1715 cm^{-1}), and for νOH of carboxylic group (2920 cm^{-1}).

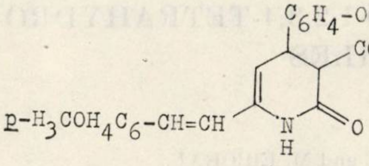

(II)

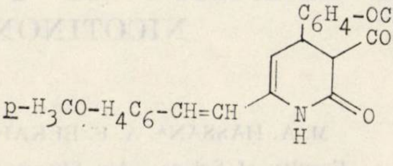

(III)

Treatment of I with Grignard reagents yielded 3-acyl-4-phenyl (or *p*-methoxyphenyl)-6-styryl (or *p*-methoxystyryl)-1,2,3,4-tetrahydro-2-pyridones (IV*a*-*h*). The IR spectra of IV showed bands attributable to chelated OH (3050 cm^{-1}), νC = O of acyl group (1712—1695), and νC=O of δ-lactames (1670—1645 cm^{-1}). The IR data of IV proved that these compounds exist in the lactam-lactimic tautomeric mixture in which the lactam form predominates due to stabilization by chelation.[2]

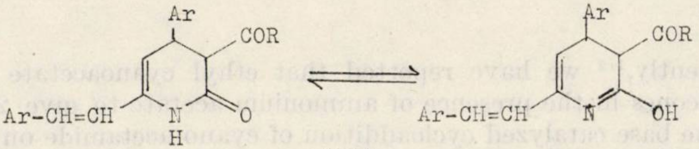

(IV)

a) R = CH_3 ; Ar = C_6H_5
b) R = CH_3 ; Ar = $C_6H_4-OCH_3-p$
c) R = cyclo$-C_6H_{11}$; Ar = C_6H_5
d) R = cycl$-C_6H_{11}$; Ar = $C_6H_4-OCH_3-p$
e) R = C_6H_5 ; Ar = C_6H_5
f) R = C_6H_5 ; Ar = $C_6H_4-OCH_3-p$
g) R = $C_6H_4-OCH_3-p$; Ar = C_6H_5
h) R = $C_6H_4-OCH_3-p$; Ar = $C_6H_4-OCH_3$-*p*

The reaction of I with phenylisocyanate gave 3-cyano-1-formanilido-2-oxo-4-phenyl (or *p*-methoxyphenyl)-6-styryl (or *p*-methoxystyryl)-1,2,3,4-tetrahydropyridine (V*a* and V*b*). The IR spectrum of compounds V showed bands characteristic for νNH of secondary amides (3185, 3212 cm^{-1}), νC ≡ N(2238 cm^{-1}), νC = O for secondary amides (1676 cm^{-2}), and νC = O for lactams (1708 cm^{-1}). The mass spectrum of V*b* showed m/e at 479 (1.8% M$^+$), and 359 (100% M$-C_6H_5NHCO$). The mass spectrum of V is another proof for the predomination of lactamic form.[4]

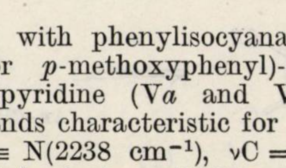

(V)

a) Ar = C_6H_5 b) Ar = $C_6H_4-OCH_3-p$

EXPERIMENTAL

All melting points are uncorrected. The IR absorption spectra were determined on a Unicam SP 200 G spectrophotometer using KBr wafer technique, and the mass spectra were determined on a Varian MAT CH—4B, 70eV-spectrophotometer (direct injection). The physical data of all new compounds are listed in Table 1.

Table 1

Data of compounds I—V

Compd.	M.p. °C	Yield %	Mol. formula	Analysis % Found / Calcd. C	H	N
Ia	310	32	$C_{20}H_{16}N_2O$	79.69 79.98	5.21 5.33	9.22 9.33
Ib	313	37	$C_{22}H_{20}N_2O_3$	73.62 73.33	5.42 5.42	7.84 7.78
II	290	76	$C_{22}H_{22}N_2O_4$	69.61 69.84	5.57 5.82	7.62 7.41
III	302	58	$C_{22}H_{21}NO_5$	69.39 69.66	5.37 5.54	3.47 3.69
IVa	302	72	$C_{21}H_{19}NO_2$	79.78 79.50	5.88 6.02	4.56 4.42
IVb	309	67	$C_{23}H_{23}NO_4$	73.42 73.21	5.93 6.10	3.79 3.71
IVc	238	78	$C_{26}H_{27}NO_2$	80.92 81.04	6.98 7.01	3.74 3.64
IVd	250	74	$C_{28}H_{31}NO_4$	75.36 75.51	7.04 6.97	3.21 3.15
IVe	226	62	$C_{26}H_{21}NO_2$	82.46 82.32	5.47 5.54	3.74 3.69
IVf	232	69	$C_{28}H_{25}NO_4$	76.37 76.54	5.57 5.69	3.27 3.19
IVg	191	74	$C_{27}H_{23}NO_3$	79.41 79.22	5.49 5.62	3.51 3.42
IVh	195	78	$C_{29}H_{27}NO_5$	74.12 74.20	5.59 5.76	3.01 2.99
Va	292	43	$C_{27}H_{21}N_3O_2$	77.54 77.33	4.89 5.01	10.18 10.02
Vb	315	46	$C_{29}H_{25}N_3O_4$	72.91 72.65	5.14 5.22	8.61 8.77

2-Oxo-4-phenyl (or p-methoxyphenyl)-6-styryl (or p-methoxystyryl)-1,2,3,4-tetrahydronicotinonitriles (Ia and b). A mixture of dibenzylideneacetone / or dianisylacetone (0.01 mole), and cyanoacetamide (0.02 mole) was heated in a sealed tube for 6 hrs at 170°C. After cooling, the reaction product was triturated with hot ethanol. The solid that separated was crystallized from acetic acid to give I as yellow crystals.

4-p-Methoxyphenyl-6-p-methoxystyryl-2-oxo-1,2,3,4-tetrahydronicotinamide (II). A mixture of Ib (1.0 g) and alcoholic potassium hydroxide (20 ml, 5 %) was heated for 5 hrs, cooled and poured into dilute hydrochloric acid (100 ml, 2%). The solid that separated out was filtered and crystallized from acetic acid to give II as yellow crystals.

4-p-Methoxyphenyl-6-p-methoxystyryl-2-oxo-1,2,3,4-tetrahydronicotinic acid (III). A mixture of Ib (1.0 g), glacial acetic acid (10 ml), and concentrated hydrochloric acid (10 ml) was heated for 5 hrs, cooled and poured into ice-water mixture. The solid product was filtered off and crystallized from acetic acid to give III.

3-Acyl-4-phenyl (or p-methoxyphenyl)-6-styryl (or p-methoxystyryl)-1,2,3,4-tetrahydro-2-pyridones (IVa-h). A suspension of I (0.01 mole) in dry benzene (50 ml) was added to an ethereal solution of Grignard reagents (0.04 mole). The reaction mixture was refluxed on a steam bath for 4 hrs, left overnight at room temperature, then decomposed with cold solution of (10%) hydrochloric acid. The yellow products IV*a*–*h* were crystallized from acetic acid/ethanol mixture.

3-Cyano-1-formanilido-2-oxo-4-phenyl (or p-methoxyphenyl)-6-styryl (or p-methoxystyryl)-1,2,3,4-tetrahydropyridines (Va and b). A mixture of I (0.01 mole), phenyl isocyanate (0.012 mole) and triethylamine (3 ml) in dry dimethylsulphoxide (50 ml) was stirred at room temperature for about 6 hrs (till it gives clear solution). The reaction mixture was poured into ice-water (100 ml). The solid product was filtered off and crystallized from acetic acid to give V*a* and V*b* as colourless crystals.

REFERENCES

[1] A. Sammour, V. Akhnookh and H. Jahine, *J. Chem. U.A.R.* **13**, 421 (1970.)
[2] S. Sammour, A. Raouf, M. Elkasaby and M. Hassan, *J. prakt. Chem.*, **315**, 1175 (1973).
[3] E. Spinner and J.C.B. White, *J. Chem. Soc.*, **1966**, 991.
[4] A. Lang and E. Cohen, *J. Org. Chem.*, **39**, 1008 (1974).

Revue Roumaine de Chimie, 28, 7, 719–724 (1983)

DERIVATIVES OF 4-AMINOMETHYL-THIAZOLE. II.[1]

NEW THIAZOLE DERIVATIVES OF UREA AND THIOUREA

SIMONA SILBERG* and IOAN A. SILBERG**
* Pharmaceutical Faculty, str. Ioan Creangă 12, R-3400 Cluj-Napoca, România
** IECB–"Babeş-Bolyai" University Research Group, Department of Physical Chemistry, str. Arany Janos 11, R–3400–Cluj-Napoca, Romania

Received May 19, 1982

The synthesis, IR-, ^{1}H-NMR-, and mass spectra of the title compounds are presented, and some aspects of their conformation and reactivity are discussed.

Our previous researches[1,2] demonstrated that 2-aryl-4-aminomethyl-thiazoles **1** can be easily obtained using Delépine (or Gabriel) methods applied to 4-chloromethyl derivatives (directly, or after transformation into their iodomethyl analogs by halogen interconversion), such chloromethyl thiazoles being readily accessible by Hantzsch cyclizations.

As a part of our investigations in the field of 4-aminomethyl-thiazoles, we carried out the addition of **1** to arylisocyanates and arylisothiocyanates, aiming to obtain new thiazole derivatives of urea **2**, respectively of thiourea **3**, potentially useful as starting materials for other syntheses (cf. the following paper of this series) and as biologically active compounds.

There are, indeed, abundant data in the literature (*e.g.*[3–5]) on the pesticidal and antineoplasic actions of various substances containing both the thiazole ring and the urea or thiourea moieties.

It is the purpose of this paper to present the preparation of some **2** and **3** derivatives, as well as their IR-, ^{1}H-NMR-, and mass spectra, which pointed out interesting features of the conformation and behaviour of these compounds.

Synthesis

The 2-aryl-4-aminomethyl-thiazoles **1** displayed a normal primary amine reactivity towards arylisocyanates and arylisothiocyanates; the additions were smoothly effected by a short refluxing of reactants in ethanol. In all cases (see Tables 1 and 2) we obtained practically quantitative yields, and the substances were easily isolated and characterized, owing to their crystallinity and relatively high melting points.

IR spectra

The IR spectra confirmed the normal course of the reaction in this case. The ν (C=O) band appears at 1630–1640 cm^{-1} (solid state) in the spectra of the ureas **2** and usually shows incipient splittings due to hydrogen bonding and vibrational couplings.

Table 1

1-Phenyl-3-(2-aryl-4-thiazolyl-methyl)-ureas, **2**

R	R^1	m·p·°C	Molecular formula	N %	
				Calculated	Found
H	$3-CH_3$	185	$C_{18}H_{17}N_3OS$	12.99	12.80
H	$4-CH_3$	209	$C_{18}H_{17}N_3OS$	12.99	13.23
H	4−Br	225	$C_{17}H_{14}BrN_3OS$	10.82	10.89
Cl	H	190	$C_{17}H_{14}ClN_3OS$	12.22	12.50
Cl	$3-CH_3$	183	$C_{18}H_{16}ClN_3OS$	11.74	11.90
Cl	$4-CH_3$	201	$C_{18}H_{16}ClN_3OS$	11.74	11.61
Cl	4−Br	210	$C_{17}H_{13}BrClN_3OS$	9.94	10.04

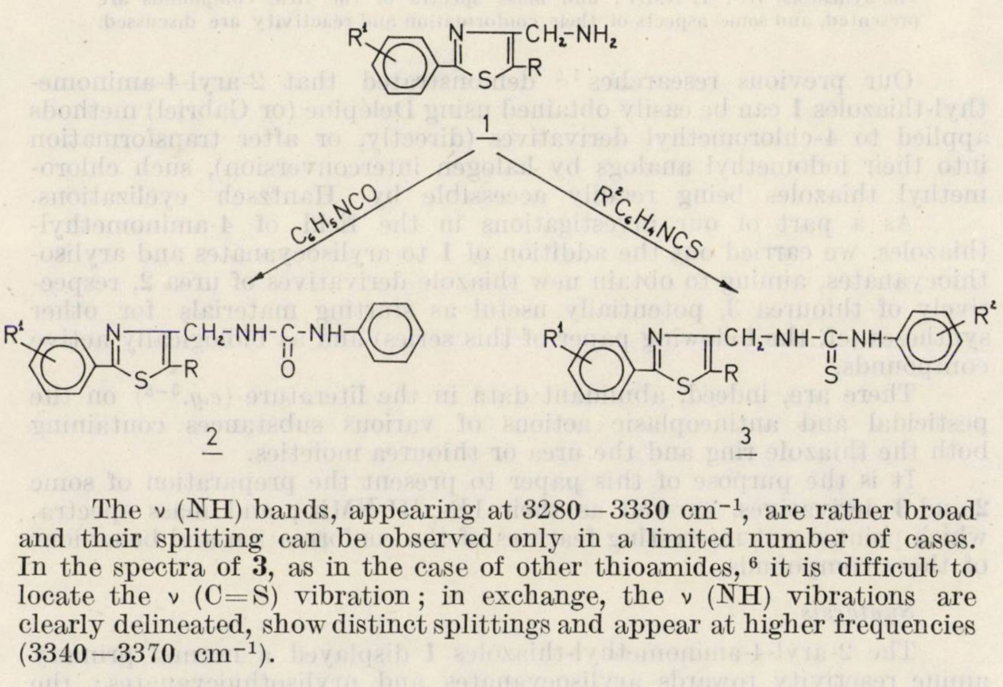

The ν (NH) bands, appearing at 3280—3330 cm⁻¹, are rather broad and their splitting can be observed only in a limited number of cases. In the spectra of **3**, as in the case of other thioamides,[6] it is difficult to locate the ν (C=S) vibration; in exchange, the ν (NH) vibrations are clearly delineated, show distinct splittings and appear at higher frequencies (3340—3370 cm⁻¹).

¹H-NMR spectra

The ¹H-NMR spectra (δ-values) of **2** and **3** show, as expected, similar features; the higher solubility of **3** made them more suitable for a detailed investigation.

Thus, in $CDCl_3$ solutions of **3**, ($R=R^1=R^2=H$), the protons from the *ortho*-positions of the phenyl radical attached to thiazole in position 2 give rise to a multiplet centered at 7.8 ppm, whereas the remainder of the aromatic protons generates a complex multiplet at 7.0—7.5 ppm. Two broad, unresolved signals at 8.32 and 3.1 ppm, which disappear on treatment with D_2O, were assigned to the NH protons adjacent to the

Table 2

1-Aryl-3-(2-aryl-4-thiazolyl-methyl)-thioureas, **3**

R	R¹	R²	m.p.°C	Molecular formula	N% Calculated	N% Found
H	H	4-Br	193	$C_{17}H_{14}BrN_3S_2$	10.39	10.58
H	H	4-Cl	188	$C_{17}H_{14}ClN_3S_2$	11.68	11.91
H	H	4-CH$_3$	151	$C_{18}H_{17}N_3S_2$	12.38	12.56
H	H	4-OC$_2$H$_5$	178	$C_{19}H_{19}N_3OS_2$	11.37	11.11
Cl	H	H	136	$C_{17}H_{14}ClN_3S_2$	11.68	11.46
Cl	H	4-Br	202	$C_{17}H_{13}BrClN_3S_2$	9.58	9.63
Cl	H	4-Cl	203	$C_{17}H_{13}Cl_2N_3S_2$	10.66	10.68
Cl	H	4-CH$_3$	174	$C_{18}H_{16}ClN_3S_2$	11.24	11.23
Cl	H	4-OC$_2$H$_5$	196	$C_{19}H_{18}ClN_3OS_2$	10.40	10.58
H	3-CH$_3$	4-Br	195	$C_{18}H_{16}BrN_3S_2$	10.04	10.29
H	3-CH$_3$	H	125	$C_{18}H_{17}N_3S_2$	12.38	12.54
H	3-CH$_3$	4-Cl	190	$C_{18}H_{16}ClN_3S_2$	11.24	11.48
H	3-CH$_3$	4-CH$_3$	163	$C_{19}H_{19}N_3S_2$	11.89	12.17
H	3-CH$_3$	4-OC$_2$H$_5$	156	$C_{20}H_{21}N_3OS_2$	10.96	10.94
Cl	3-CH$_3$	H	158	$C_{28}H_{16}ClN_3S_2$	11.24	11.25
Cl	C-CH$_3$	4-Br	211	$C_{18}H_{15}BrClN_3S_2$	9.28	9.14
Cl	3-CH$_3$	4-Cl	210	$C_{18}H_{15}Cl_2N_3S_2$	10.29	10.18
Cl	3-CH$_3$	4-CH$_3$	182	$C_{19}H_{18}ClN_3S_2$	10.83	10.61
Cl	3-CH$_3$	4-OC$_2$H$_5$	175	$C_{20}H_{20}ClN_3OS_2$	10.05	10.31
H	4-CH$_3$	H	134	$C_{18}H_{17}N_3S_2$	12.38	12.54
H	4-CH$_3$	4-Br	198	$C_{18}H_{16}BrN_3S_2$	10.04	10.02
H	4-CH$_3$	4-Cl	189	$C_{18}H_{16}ClN_3S_2$	11.24	11.38
H	4-CH$_3$	4-CH$_3$	170	$C_{19}H_{19}N_3S_2$	11.89	11.99
H	4-CH$_3$	4-OC$_2$H$_5$	183	$C_{20}H_{21}N_3OS_2$	10.96	10.90
Cl	4-CH$_3$	H	180	$C_{18}H_{16}ClN_3S_2$	11.24	11.34
Cl	4-CH$_3$	4-Br	214	$C_{18}H_{15}BrClN_3S_2$	9.28	9.51
Cl	4-CH$_3$	4-Cl	211	$C_{18}H_{15}Cl_2N_3S_2$	10.29	10.46
Cl	4-CH$_3$	4-CH$_3$	201	$C_{19}H_{18}ClN_3S_2$	10.83	10.74
Cl	4-CH$_3$	4-OC$_2$H$_5$	193	$C_{20}H_{20}ClN_3OS_2$	10.05	10.20
H	4-Br	H	159	$C_{17}H_{14}BrN_3S_2$	10.39	10.45
H	4-Br	4-Br	211	$C_{17}H_{13}Br_2N_3S_2$	8.70	8.34
H	4-Br	4-Cl	205	$C_{17}H_{13}BrClN_3S_2$	9.58	9.61
H	4-Br	4-CH$_3$	179	$C_{18}H_{16}BrN_3S_2$	10.04	9.85
H	4-Br	4-OC$_2$H$_5$	184	$C_{19}H_{18}NrB_3OS_2$	9.37	9.52
Cl	4-Br	H	175	$C_{17}H_{13}BrClN_3S_2$	9.58	9.41
Cl	4-Br	4-Br	222	$C_{17}H_{12}Br_2ClN_2S_2$	8.12	8.43
Cl	4-Br	4-Cl	216	$C_{17}H_{12}BrCl_2N_3S_2$	8.88	9.00
Cl	4-Br	4-CH$_3$	191	$C_{18}H_{15}BrClN_3S_2$	9.28	9.26
Cl	4-Br	4-OC$_2$H$_5$	210	$C_{19}H_{17}BrClN_3OS_2$	8.70	8.65

methylene and phenyl groups, respectively, as indicated by their chemical shifts. The methylene protons appear as a doublet, $J = 5.0$ Hz, centered at 4.93 ppm; the large splitting and its coalescence after treatment with D_2O clearly show that this is due to the interaction with the NH proton, which seems to be highly localized. Careful investigations revealed the existence of a second splitting, $J = 0.4-0.5$ Hz, of each component of the doublet; this is due to the *cisoid* allylic (benzylic) coupling with the proton from C—5 of the thiazole ring. This small J_{cis} value indicates [7] that the preferred conformation of the radical attached to the thiazole nucleus brings the two CH_2 protons at dihedral angles of 135° and 255°, that is, the projection of the CH_2—NH bond is slightly deviated with respect to a perpendicular line to the thiazole ring plane. The same situation was encountered in the case of other 4-aminomethyl-thiazoles investigated by us [1,2] but not with our thiazole derivatives of phenothiazine,[8] where allylic couplings of the order of 1 Hz were found, pointing out to an important change of the conformation.

Mass spectra

In the mass spectra of both **2** and **3** the molecular ion is always present, but its relative intensity reaches only 33% for urea **2** ($R=R^1=H$) and 50% for thiourea **3** ($R=R^1=R^2=H$). The analysis of the spectra demonstrated that, unlike other compounds with related structures, our substances show only two ways of fragmentation of the molecular ion, namely, the retroadditions corresponding to the two theoretical routes of formation of **2** and **3** from primary amines and isocyanates (respectively isothiocyanates). The fragmentation sequences are practically identical for **2** and **3**, the only difference consisting in the elimination of NCO· radicals from **2** and NCS· from **3**.

It is of interest to note that in the case of the thiazole derivatives of urea the prevailing fragmentation pathway is that leading to the ions of aniline (base peak of the spectrum) and of 2-phenyl-4-thiazolyl-methyl-isocyanate (m/e 216), whereas with the thiourea one finds in the forefront the formation of the ion of phenylisocyanate (base peak) and of 2-phenyl-4-aminomethyl-thiazole (m/e 190).

The most striking peculiarity of the behaviour of our urea and thiourea derivatives upon electron impact consists of the total lack of M—1 ions, which reflect, in the spectra of other phenyl-ureas, respectively thioureas, energetically advantageous cyclizations to heterocyclic structures. [9] This is especially intriguing in the case of **3**, since the formation of benzothiazoles upon oxidation of phenyl-thioureas is commonplace in the chemistry of the latter compounds. [10,11] The absence of M—1 ions is the more surprising as in our case there exists, at least theoretically, a second route towards cyclic ions, by reactions involving an attack to the high electron density from position 5 of thiazole rings.

The observed phenomena prompted us to undertake an investigation of the behaviour of our thiazole derivatives of thiourea **3** upon oxidative cyclization, in order to elucidate the peculiarities of the above reported mass spectra and to establish the reaction pathways of the intermediates formed by loss of electrons from these compounds.

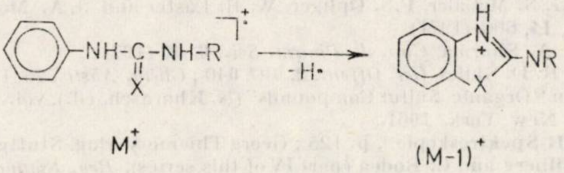

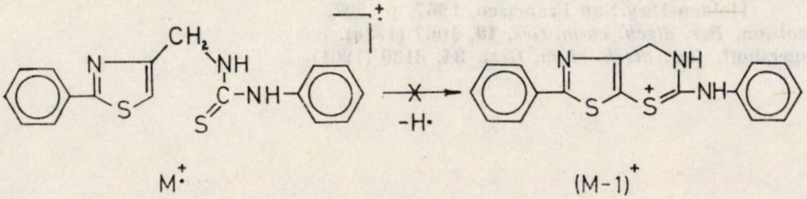

EXPERIMENTAL

Melting points are uncorrected. Infrared spectra were determined in KBr pellets by means of an UR-10 Carl Zeiss Jena recording spectrophotometer. ^{1}H-NMR spectra were obtained on a BS-478 C Tesla 80 MHz spectrometer in $CDCl_3$ solutions, with TMS as internal reference. Mass spectra were recorded with a MAT-311 Varian-Atlas Bremen double focusing spectrometer at 70 eV.

Addition of 2 phenyl-4-aminomethyl-thiazole (1, R = R^1=H) to phenylisocyanate

A solution of 0.7 g **1** (R=R^1=H) hydrochloride in 1.5 ml ethanol was neutralized with an aqueous solution of $NaHCO_3$ then treated with 0.4 ml phenylisocyanate. The mixture was refluxed for 5—10 min, cooled, the white crystalline precipitate filtered and recrystallized from ethanol to give an almost quantitative yield of **2** (R=R^1=H) m.p. 197°.

Found: N, 13.59; $C_{17}H_{15}N_3OS$ requires N, 13.58%

The compounds in Table 1 were similarly prepared.

Addition of 2-phenyl-4-aminomethyl-thiazole to phenylisothiocyanate

A solution of 0.9 g **1** (R=R^1=H) hydrochloride in 2 ml ethanol was neutralized with an aqueous solution of $NaHCO_3$ and treated with 0.4 g phenylisothiocyanate. After 5—10 min of refluxing, the mixture was cooled, the crystalline product filtered off and recrystallized from ethanol or 50% aqueous acetic acid, to give **3** (R=R^1=R^2=H), (almost quantitative yield), m.p. 143°.

Found: N, 13.04; $C_{17}H_{15}N_3S_2$ requires N, 12.91%.

The compounds in Table 2 were similarly prepared.

ACKNOWLEDGEMENTS. Acknowledgements are expressed to Dr. N. Palibroda for recording the mass spectra, to engineer I. Lungu for the ^{1}H-NMR spectra and to Mrs. E. Hamburg for the IR spectra. The elemental analyses were carried out at the Micro-analytical Laboratory of the Institute of Chemistry, Cluj-Napoca.

REFERENCES

1 Part. I. S. Silberg, *Rev. Roumaine Chim.*, **28**, 000 (1983).

2 S. Silberg, Ph. D. Thesis, Institute of Chemistry, Cluj-Napoca, 1974.

3 Th. P. Johnston, G. S. McCaler, P.S. Opliger, W. R. Laster and J. A. Montgomery, *J. Med. Chem.*, **14**, 600 (1971).

4 H. G. Garg and R. A. Sharma, *Can. J. Pharm. Sci.*, **6**, 45 (1971).

5 K. H. Pilgram and R. D. Skiles, *Ger. Offen.*, **2**, *101*, 640 ; *Chem. Abstr.*, **75**, 140835 (1971).

6 L. R. J. Bellamy in "Organic Sulfur Compounds" (N. Kharasch, ed.), vol. 1, p. 52 ; Pergamon Press, New York, 1961.

7 H. Günther, "NMR-Spektroskopie", p. 125 ; Georg Thieme Verlag, Stuttgart, 1973.

8 S. Silberg, I. A. Silberg and C. Bodea (part IV of this series), *Rev. Roumaine Chim.*, **28**, 000 (1983).

9 H. Budzikiewicz, C. Djerassi and D. H. Williams, "Mass Spectrometry of Organic Compounds" Holden-Day San Francisco, 1967, p 507.

10 P. Jacobson, *Ber. dtsch. chem. Ges*, **19**, 1067 (1886).

11 A. Hugershoff, *Ber. dtsch. chem. Ges.*, **34**, 3130 (1901).

Revue Roumaine de Chimie, 28, 7, 725–732 (1983)

SYNTHESIS AND SPECTRAL BEHAVIOUR OF BENZOXAZOLIUM INDOLO (OR BENZOFURANO) QUINOLINIUM BISETHIODIDE CYANINE DYES

Z. H. KHALIL and A. IBRAHIM
Department of Chemistry, Faculty of Science, Assiut University, Assiut, Egypt

Received April 20, 1981

2[2-(3-Benzoxazolium-3-ethiodide)-indolo and/or benzofurano]-quinolinium-1-ethiodide cyanine dyes (VII, 1–10 and X, 1–3) were prepared, *via* interaction of 2[2-(benzoxazolium-3-ethiodide)-1,2-dibromoethenyl]-quinolinium-1-ethiodide (IV) with the appropriate arylamines and/or phenols, under basic conditions. The structures of the synthesized compounds were determined by analytical and spectral data. The biological activity of VII, 3 and X, 1 against bacteria and fungi was tested.

INTRODUCTION

Extensive efforts have been made to prepare new cyanine dyes for their wide application in many fields. They are used as photosensitizers in photographic processes, [1] photochemical solar energy conversions, [2] and as model chromophores in monolayer assemblies. [3] The photochemical instability is a common behaviour of this class of compounds and it was found that conformational changes occur after excitation along the polymethine chain and precede the degradation process. [4] By decreasing the flexibility of the dye molecule *via* chemical rigidization, high fluorescence yields and photochemical stability can be obtained. [5]

The biological activity of cyanine dyes is of interest; they possess bactericidal activity against *Staphylococcus aureus* and *Escherichia coli*. [6] They have anti-cancer activity against P-338 tumor and B-16 melanoma cells. [7]

In our recent study merocyanine dyes showed high efficiency as corrosion inhibitors for aluminium and its alloys in hydrochloric acid solutions, at very low concentrations (3×10^{-5} g/l).[8]

In this work, new dicationic cyanine dyes (VII, 1–10 and X, 1–3) were prepared to study the effect of substitution at the indole nucleus on their spectral behaviour in ethanol. Also, the biological activity of selected compounds towards bacteria and fungi was tested.

RESULTS AND DISCUSSION

Synthesis of 2[2-(benzoxazolium-3-ethiodide)-1,2-dibromoethenyl]-quinolinium-1-ethiodide (IV). This key intermediate was prepared according to the following sequence; selective oxidation of 2-methyl-benzoxazole-3-ethiodide (I) with selenium dioxide in ethanol gave benzoxazolium-3-ethiodide-2-carboxaldehyde (II), its IR spectrum showed a well defined absorption band at 1760 cm^{-1}(νCHO). Interaction of II with 2-methylquinolinium-1-ethiodide in the presence of piperidine, afforded the corresponding styryl cyanine dye III (IR 1625–1620 cm^{-1}($\nu C=C$). Its absorption spectrum in ethanol possesses absorption bands located at λ_{max}nm (ε_{max}) 212 (75000), 242 (72000), 297 (32000), 510 (11500) and 570 (10000). Bromination of III gave the dibromo derivative (IV). Its IR spectrum shows absorption bands at 770 cm^{-1}($\nu C-Br$), 1185, 1100 cm^{-1} ($\nu C-O-C$ cyclic oxazole), 1590 cm^{-1} ($\nu C=N$) and 3000, 2940 cm^{-1} (νN quaternary salts).

Synthesis of 2[2-(3-benzoxazolium-3-ethiodide) indolo]-quinolinium-1-ethiodide cyanine dyes (VII, 1–10). These compounds were achieved *via* the interaction of IV with the appropriate arylamines under basic conditions. The reaction mechanism can be represented as follows:

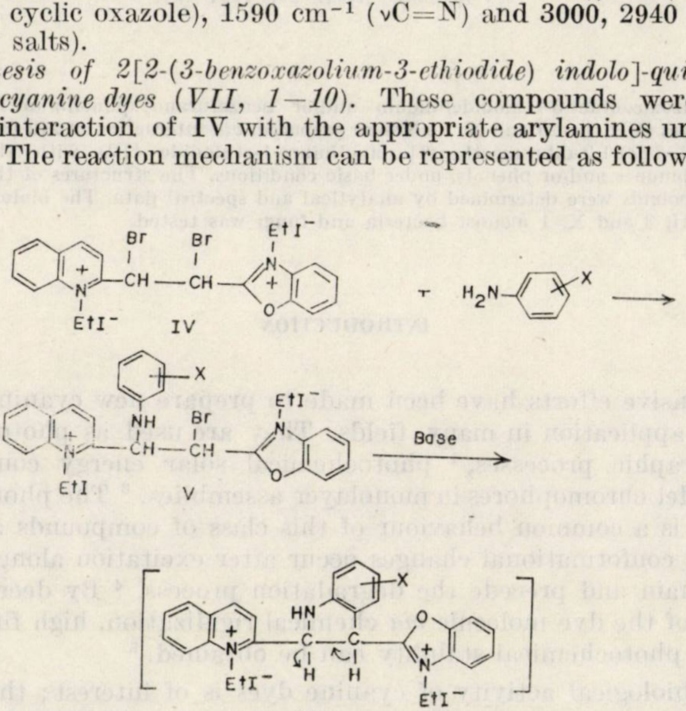

VII, X = H (1); 5-CH_3 (2); 5-OCH_3 (3); 5-Cl (4); 5-NO_2(5); 5-COOH (6); 7-COOH (7); 7-OH (8); 6,7-Benz. (9); 5,6-Benz. (10).

The intermediate compound (V, X, 4-OCH_3) was isolated by refluxing of equimolecular proportions of IV and *p*-anisidine in *n*-butanol. Its IR spectrum possesses absorption bands at 640 cm^{-1} (νC—Br), 3460 cm^{-1} (νNH), 1050 cm^{-1} (νC—O—C cyclic oxazole) and 1580 cm^{-1} (νC=N).

Further reaction of V with excess *p*-anisidine afforded the cyclised product (VI) which was dehydrogenated under the reaction conditions to the cyanine dye (VII, 3).

Acetylation of (VII, 3) gave its monoacetyl derivative VIII. Its IR spectrum shows absorption bands at 1780, 1720 cm^{-1} (νC=O of N acetyl group)[9] and the disappearance of the NH absorption band.

Infrared spectra of (VII, 1—10) possess characteristic bands at 1650, 1590, 1500—1480 cm^{-1} (ν indole ring) and 3500—3450 cm^{-1} (ν NH). Their electron spectra in ethanol 95% have absorption bands in the UV region located at 207 nm, attributed to $\pi-\pi^*$ transitions within benzopyrrole nucleus,[10] 230—270 nm which are assigned to the transitions in benzoxazole,[11] and at 290—325 nm which are due to the transitions of quinoline moiety.[12]

Generally, they have a single broad adsorption band in the visible region located at λ_{max} 450—600 nm which can be ascribed to the charge transfer (C.T.) from the electrons on the nitrogen of the indolyl ring through extended conjugation towards the positive charge on the nitrogen of quinoline residue. This band is largely affected by the type of substituents, c.f. table 1.

Introduction of an electron releasing group (5—CH_3) causes a slight red shift by 5 nm with intensification of the absorption band; this is due to the hyperconjugative effect of the CH_3 group. While a stronger releasing group causes a splitting of the C.T. band to two bands located at λ_{max} 510, 575 nm (ε_{max} 64000 and 5800 respectively). On the other hand, introduction of an electron withdrawing atom (5—Cl) causes a blue shift by 15 nm, while a strong deactivating group (5—NO_2) splits the C.T. bands: the one at a shorter wavelength by 10 nm and the other at a longer wavelength by 11 nm (VII, 5 λ_{max} 465, 486 nm, ε_{max} 90000 and 45000 respectively).

The introduction of a carboxyl group causes a strong red shift relative to (VII, 1), attributed to the solute-solvent interaction of lower excitation energy molecule, absorbing the light at a longer wavelength. The more red shifted one was attributed when the carboxyl group is at 7-position (*ortho* to NH of indole ring).

It is of interest to mention that the absorption bands of cyanine dyes (VII, 9 and 10) are of higher intensities and are more red shifted than the parent compound (VII, 1). This suggests that the naphtyl moiety is of linear type.

Synthesis of 2[2-(3-benzoxazolium-3-ethiodide) benzfurano]-quinolinium-1-ethiodide cyanine dyes (X, 1—3). These were obtained *via* the reaction of IV with phenols in pyridine. The reaction mechanism can be represented as follows:

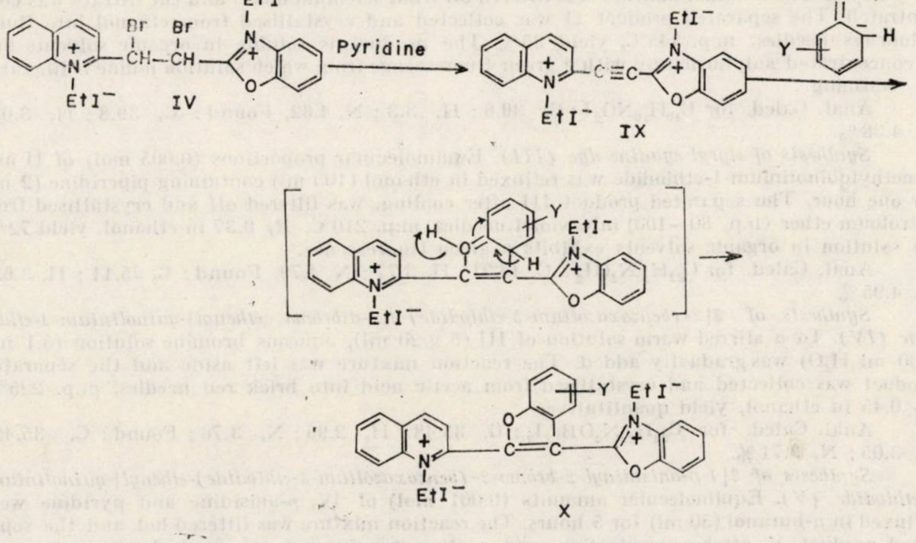

X,Y = 7–OH(1); 6,7–Benz.(2); 5,6–Benz.(3).

Infrared spectra of (X, 1–3) show absorption bands at 870, 950 cm^{-1} (ν furane ring) and 1505 cm^{-1} (νC–O–C cyclic of furane), besides the other characteristic bands of oxazole nucleus.

Their alcoholic solutions give a violet colour in 0.1 molar H_2SO_4 which turned yellow on basification with 0.1 NaOH. This interchangeable colour suggests their possible use as acid-base indicators in photometric titrations.

Their absorption spectra in ethanol 95% show a single broad band in the visible region, located at 570–580 nm.

The biological activity of VII, 3 and X, 1 towards bacteria and fungi. It is noticed from table 3 that benzoxazolium-indolo-quinolinium cyanine dye (VII, 3) is more active than the benzofurano derivative (X, 1), against all of the bacteria under investigation, but *Bacillus cereus*. They have no or slight activity against fungi.

EXPERIMENTAL

The infrared spectra were recorded with a PYE Unicam SP 1100 Spectrophotometer using KBr wafer technique. Absorption spectra in the UV-visible region were recorded on a PYE Unicam SP 8000 Ultraviolet Recording Spectrophotometer using 1 cm matched silica cells. All melting points are uncorrected.

Preparation of 2-methylbenzoxazolium-3-ethiodide (I). A mixture of 2-methylbenzoxazole (15 g) and ethyl iodide (25 g) was gradually heated in a sealed tube at 100°C for 3 hours. The tube was cooled, opened and the product was collected, washed with ether and crystallised from ethanol into fine needles, m.p. 160°C, yield 65%.

Anal. Calcd. for $C_{10}H_{12}NOI$: C, 41.52 ; H, 4.15 ; N, 4.81. Found : C, 41.39 ; H, 4.3 ; N, 4.75 %.

Synthesis of benzoxazolium-3-ethiodide-2-carboxaldehyde (II). This was prepared by refluxing equimolecular proportions (0.01 mol) of I and selenium dioxide in ethanol (15 ml) for 4 hours. The reaction mixture was filtered off from selenium metal and the filtrate was concentrated. The separated product II was collected and crystallised from ethanol into fluffy colourless needles, m.p. 145°C, yield 85 %. The product is soluble in organic solvents and in concentrated sulphuric acid with a green fluorescence from which solution iodine is liberated on warming.

Anal. Calcd. for $C_{10}H_{10}NO_2I$: C, 39.6 ; H, 3.3 ; N, 4.62, Found : C, 39.8 ; H, 3.05 ; N, 4.38 %.

Synthesis of styryl cyanine dye (III). Equimolecular proportions (0.005 mol) of II and 2-methylquinolinium-1-ethiodide was refluxed in ethanol (100 ml) containing piperidine (2 ml) for one hour. The separated product III after cooling, was filtered off and crystallised from petroloum ether (b.p, 80—100) into violet needles, m.p. 210°C, R_f 0.37 in ethanol, yield 72 %. Its solution in organic solvents exhibits a green fluorescence.

Anal. Calcd. for $C_{22}H_{22}N_2OI_2$: C, 45.21 ; H, 3.77 ; N, 4.79, Found : C, 45.11 ; H, 3.65 ; N, 4.95 %.

Synthesis of 2[2-(benzoxazolium-3-ethiodide)-1,2-dibromo ethenyl]-quinolinium-1-ethiodide (IV). To a stirred warm solution of III (5 g/20 ml), aqueous bromine solution (5.1 ml//100 ml H_2O) was gradually added. The reaction mixture was left aside and the separated product was collected and crystallised from acetic acid into brick red needles, m.p. 225°C, R_f 0.45 in ethanol, yield quantitative.

Anal. Calcd. for $C_{22}H_{22}N_2OBr_2I_2$: C, 35.48 ; H, 2.96 ; N, 3.76 ; Found : C, 35.42 ; H, 3.05 ; N, 3.71 %.

Synthesis of 2[1-p-anisidinyl-2-bromo-2-(benzoxazolium-3-ethiodide)-ethenyl]-quinolinium-1-ethiodide (V). Equimolecular amounts (0.001 mol) of IV, *p*-anisidine and pyridine were refluxed in *n*-butanol (50 ml) for 5 hours. The reaction mixture was filtered hot and the separated product V after concentration and cooling was filtered off, washed with ether and crystallised from aqueous ethanol into pale brown crystals, m.p. 235°C, R_f 0.73 in ethanol and 0.59 in ethanol/benzene 50 %, yield 45 %.

Anal. Calcd. for $C_{28}H_{30}N_3O_2BrI_2$: C, 43.41 ; H, 3.88 ; N, 5.43, Found : C, 43.66 ; H, 3.98 ; N, 5.77 %.

Effect of excess arylamine on the intermediate compound (V). A mixture of V (0.0005 mol) and *p*-anisidine (0.001 mol) was refluxed in ethanol (30 ml) for 10 hours. The separated product after cooling and dilution with water was collected and crystallised from aqueous ethanol into brown violet crystals, m p. 266—7°C, R_f 0.83 in ethanol. This was identified by mixed m.p. and R_f values as (VII, 3).

Anal. Calcd. for $C_{28}H_{27}N_3O_2I_2$: N, 5.97, Found : N, 5.82 %.

Synthesis of 2[2-(3-benzoxazolium-3-ethiodide)-indolo]-quinolinium-1-ethiodide cyanine dyes (VII, 1—10). A mixture of IV (0.0005 mol) and arylamines (0.002 mol) was refluxed in ethanol (50 ml) for 10—20 hours. The reaction mixture was filtered hot and the filtrate was acidified with dilute acetic acid. The separated product was collected, washed with boiling water, ether and crystallised from the appropriate solvents. The dicationic cyanine dyes (VII, 1—10) are soluble in alcohols, dioxane, DMF, pyridine and acetic acid, exhibiting a green fluorescence in solutions ; they are insoluble in CCl_4 and water. The results are summarised in table 1.

Acetylation of VII, 3. A mixture of VII, 3 (0.5 g), fused sodium acetate (one g) and acetic anhydride (30 ml) was refluxed for 4 hours. The monoacetyl derivative (VIII) which was separated after cooling and dilution with ice-water, was filtered off and crystallised from acetic acid into pale brownish violet crystals, m.p. 246°C, R_f 0.8 in ethanol, yield 84 %.

Anal. Calcd. for $C_{31}H_{29}N_3O_3I_2$: N, 5.64, Found : N, 5.84 %.

Synthesis of 2[2-(3-benzoxazolium-3-ethiodide)-benzofurano]-quinolinium-1-ethiodide cyanine dyes (X, 1—3). Equimolecular proportions (0.0005 mol) of IV and phenols (catechol, α-/and or β-naphthol) were refluxed in pyridine for 13—18 hours. The reaction mixture was filtered hot and the filtrate was cooled and acidified with dilute acetic acid. The separated products (X, 1—3), were collected and crystallised from the appropriate solvents. They are soluble in organic solvents exhibiting a blue to green fluorescence intensified in dioxane solutions. The results are summarised in table 2.

Biological activity of VII, 3 and X, 1 :

a) *Bacterial suspension* : This was prepared by adding 10 ml of sterile distilled water to a 10 days old culture of the test bacteria grown on Nutrient Agar (N.A.) [13] (beef extract

Table 2

2-[(3-benzoxazolium-3-ethiodide)]benzofurano-quinolinium-1-ethiodide cyanine dyes (X, 1—3)

Comp. X No.	Formula	Solvent for crystallization	Time of reflux, h	m.p. °C	Yield %	Analysis %		Absorption spectra in ethanol 95%
						Calcd.	Found	$\lambda_{nm_{max.}}$ (ε_{max})
						N	N	
1	$C_{28}H_{24}N_2O_3I_2$	Ethanol	13	295	60	4.06	4.19	210(58000), 243(44000), 300(28000), 570(5400)
2	$C_{32}H_{26}N_2O_2I_2$	Aqueous ethanol	18	315	70	3.87	3.98	210(9000), 240(87000), 290(3700), 580(13100)
3	$C_{32}H_{26}N_2O_2I_2$	Ethanol	15	288	65	3.87	3.76	210(6600), 230(6800) 290(2300), 570(6900)

10 g/l, peptone 5 g/l, sodium chloride 5 g/l, agar 17 g/l at pH 7.4. One ml aliquots of the bacterial suspension were added to N.A. Petri dishes (2 plates/test compound). The excess liquid was removed and two filter paper discs (15 mm diameter), containing the test compound (10 mg/100 ml ethylene glycol), were placed on each plate. Plates were then incubated at 37°C, and the inhibition zones were measured after 24 hours. These experiments were repeated 3 times.

b) *Spore suspension.* This was prepared by adding 10 ml of sterile distilled water to a 10 days old culture of the test fungus grown on potato-dextrose+agar or PDA. Potatoes (peeled and sliced) 200 g/l, dextrose (20 g/l), agar (17 g/l) at pH 6.5, slant.[14] The excess liquid was removed and two filter paper discs (15 mm diameter) containing the test compound (same concentrations) were placed on each plate. Plates were incubated at 37°C, and the diameters of the inhibition zones were measured after 5 days. The results are listed in table 3

Table 3

Biological screening of selected dicationic cyanine dyes (VII 3 and X 1), expressed as inhibition zones (diameter in mm)

Organism used	Compound tested No.	
	VII 3	X 1
a) Bacteria species		
Staphylococcus aureus (+ ve)	4	2
Sarcina lutea (+ ve)	6	—
Bacillius cereus (— ve)	1	3
Escherichia coli (— ve)	7	3
b) Fungal species		
Aspergillus egyptiacus	Overgrowth	1
Penicillium cyclopium	—	—
Trichoderma viridi	—	—

REFERENCES

[1] A. H. Herz, *Adv. Colloid Interface Sci.*, **8**, 237 (1977).

[2] A. M. Fox, F. J. Nobs and T. A. Voynich, *J. Amer. Chem. Soc.*, **102**, 4036 (1980) ; F. F. Fan, B. Reichman and A. J. Bard, *ibid.*, 1488 (1980).

[3] O. Inacker, H. Kuhn, D. Mobius and G. Debuch, *Z. phys. Chem. (Frankfurt)*, **101**, 337 (1976).

[4] R. Steiger, R. Kitzing, R. Hanger and H. Stoeckli-Evans, *J. Photogr. Sci.*, **27**, 151 (1974).

[5] L. L. Lincoln and D. W. Heseltine, *U.S. Patent*, 3, 864, 664 (March 22, 1971).

[6] E. P. Opanasenko, G. K. Palli, P. V. Prisyazhnyuk, *Khim-Farm. Zhur.*, **8**, 18 (1974).

[7] H. Nomura, Y. Kozai and I. Minami, *Ger. Offen.*, 2, 919, 447 ; *Chem. Abstr.*, **92**, 122044 (1980).

[8] F. M. El-Cheikh, Z. H. Khalil, and K.K. Kasem (to be published).

[9] J. R. Dyer, "Application of Absorption Spectroscipy of Organic Compounds", Georgia Institute of Technology, 1965.

[10] I. L. Finar, "Organic Chemistry", vol. 1, *Six^th^* Edition, 1962, p. 876.

[11] R. C. Elderfield, "Heterocyclic Compounds", vol. 5, Wiley, New York, 1959, p. 323.

[12] H. Gilman, "Organic Chemistry", vol. 3, Wiley, New York, 1953, p. 167.

[13] E. T. Knudsen and G. W. Rolinson, *Lancet*, **1954**, 1105.

[14] A. H. Riker and R. S. Riker, "Introduction to Research on Plant Diseases", John Swift, St. Louis, 1936.

Revue Roumaine de Chimie, **28**, **7**, 733–736 (1983)

as-TRIAZINE DERIVATIVES WITH POTENTIAL THERAPEUTIC ACTION. XVII*

SYNTHESIS OF 5-MERCAPTO-6-AZAURACIL-S-RIBOSIDE

C. CRISTESCU
Chemical and Pharmaceutical Research Institute,
Şos. Vitan 112, 74351 Bucharest, Romania

Received September 24, 1982

The sodium salt of 5-mercapto-6-azauracil (I) reacts in DMF solution with 2,3,5-tri-0-benzoyl-D-ribofuranosyl chloride (II) to afford a mixture of the two anomeric blocked S-ribosides. The anomeric mixture was purified by column chromatography and the two anomers (III and IV) were separated by fractional crystallization. Debenzoylation of III and IV yielded the free S-ribofuranosides V and VI, respectively.

The 6-azauracil derivatives are intensively studied owing to their similarity to natural pyrimidines. [1] Analogs of natural pyrimidines with a powerful inhibitory activity in biological systems were synthetized. 5-Mercaptouracil [2] and its nucleosides,[3,4] 5-mercaptomethyluracil, [5] 5-mercapto-6-azauracil [6] and its derivatives [7,8] have shown interesting activities in enzymatic, microbiological and animal tumor systems. All these mercaptopyrimidines, which at physiologic pH are esentially ionized, were found to undergo an unusual rapid autoxidation [9] to the corresponding disulfides catalyzed by traces of iron. In the search of "protected" mercapto-derivatives that would require for "deprotection" the action of thioglycosidase,[10] present in tumor cells, several S-glycosides of purines [10,11] and pyrimidines[12] have been prepared. In this paper, the synthesys of 5-mercapto-6-azauracil-S-riboside is described.

The reaction of 2,3,5-tri-0-benzoyl-D-ribofuranosyl chloride[13] (II) with the sodium salt of 5-mercapto-6-azauracil (I) in DMF solution yielded a mixture of the two anomeric blocked S-ribosides (III and IV). The anomeric mixture was purified by column chromatography on silicic acid, and the two anomers were separated by fractional crystallization from toluene solutions.

Debenzoylation of III and IV yielded the free S-ribofuranozides V and VI, respectively.

In the infrared spectrum of the tri-0-benzoyl-derivatives III and IV, the ring carbonyl group bands were found at 1715 and 1730 cm^{-1}. The absorption bands of acyl groups, linked to the ribose residue appears at 1680 cm^{-1} $\bar{\nu}(CO)$, 1260, 1310 cm^{-1} $\bar{\nu}(C-CO)$ and 1098, 1085 cm^{-1} $\bar{\nu}(C-CO)$.

The assignment for the bonding of carbohydrate moiety at the S-atom of the 5-mercapto-6-azauracil ring, is based on the fact that the S-riboside does not exhibit a hypsochromic or bathochromic shift of the absorption maximum in the ultraviolet spectra on passing from acidic to basic medium.[14,15]

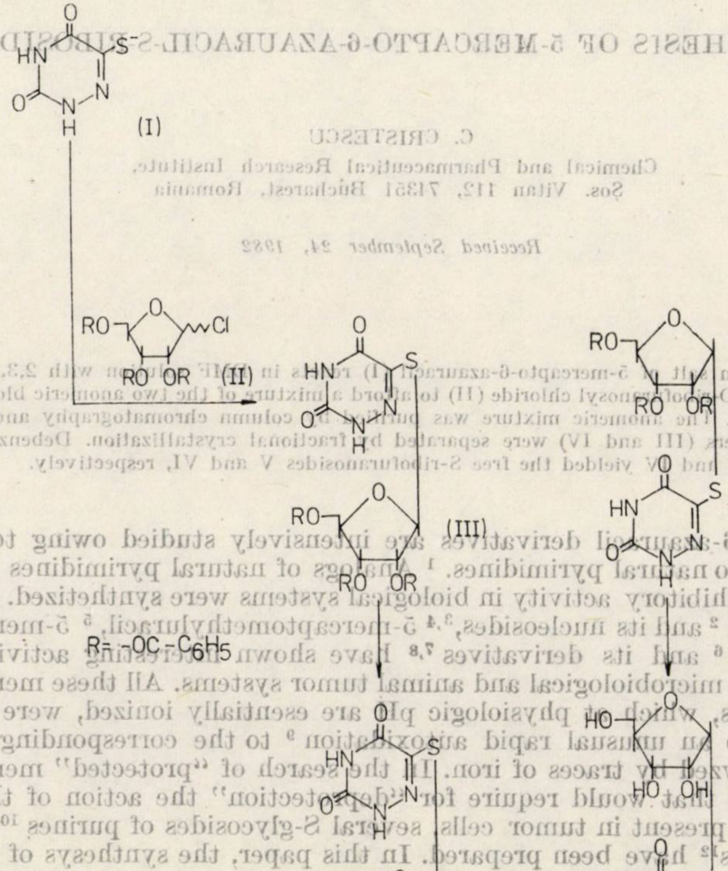

The anomeric configuration was assigned on the basis of the ^1H-NMR spectra of V and VI. The patterns of the anomeric protons appear as a doublet at δ 5.34 ppm ($J_{1',2'} = 2.8$ Hz) for V and δ 6.05 ppm ($J_{1',2'} = 5.0$ Hz) for VI. The position of the signals indicated that the compound V is the β-anomer (the signal at higher field corresponds to the β-anomer in case of ribofuranosides[16]) and the compound VI is the α-anomer.

Preliminary tests of V and VI against the L 1210 Lymphoid leukemia showed no significant inhibitory activity.

EXPERIMENTAL

The melting points were determined on a heating plate microscope and are not corrected. Paper chromatography was performed by the ascending technique on paper Schleicher & Schüll in the solvent systems: S_1, 1-butanol-acetic acid-water (5 : 2 : 3); S_2, 2-propanol-conc. aqueous ammonia-water (7 : 1 : 2); Detection of the compounds was made under ultraviolet light (254 nm). Thin layer chromatography (tlc) was performed on precoated tlc silicagel 60 F_{254} plates (Merck) in the solvent systems: S_3, benzene-ethyl acetate (7 : 3) and S_4, chloroform-methanol (8 : 2). Optical rotation was measured on a Hilger & Watts polarimeter. Ultraviolet spectra were measured on a Pye Unicam SP 1800 ultraviolet spectrophotometer. The ^{1}H-NMR spectra were recorded at 60 MHz on a Varian EM 360 spectrophotometer in D_2O and the chemical shifts are reported as δ values in ppm with DSS as internal reference.

Anomeric S(2′, 3′, 5′-tri-0-benzoyl-D-ribofuranosyl)-5-mercapto-6-azauracils (III and IV)

To a solution of 2,3,5-tri-0-benzoyl-D-ribofuranosyl chloride (II) (prepared from 5.04 g; 10 mM, 1-0-acetyl-2,3,5-tri-0-benzoyl-D-ribofuranose according to Kissman et al.[13]) in anhydrous DMF (15 ml), 2.03 g (10 mM) 5-mercapto-6-azauracil sodium salt[6] previously dissolved in anhydrous DMF (15 ml) was added. The solution was stirred under nitrogen for 20 hours at room temperature. The salt was removed by filtration and the solvent was evaporated *in vacuo*. The residue was dissolved in 1,2-dichloroethane, washed with water, filtered on Celite 535, dried (Na_2SO_4) and the solvent evaporated. The residue was dissolved in benzene and applied to a column packed with 100 g silicic acid. The column was washed with benzene and eluted with a mixture of benzene-ethyl acetate (9 : 1). Fractions containing the product (tlc S_3) were pooled and evaporated. The mixture of the two anomers was obtained as a solid foam (3.25 g; 55 %). Heating this residue in toluene resulted in a rapid dissolution followed by immediate precipitation of III as a white powder (2.068 g; 35 %) with m.p. 162—164°C. Recrystallization from toluene furnished a pure sample, m.p. 168—170°C; $[\alpha]_D^{25}$: − 122°C (c, 2.0, $CHCl_3$); *Rf*: 0.82 (S_1); 0,80 (S_2); 0.14 (S_3) and 0,87 (S_4); $UV_{(ethanol)}$: λ_{max} 220 nm (log ε 4.67 and 304—306 nm (log ε 3.83).

$C_{29}H_{23}N_3O_9S$ Calcd., C, 59.07; H, 3.93; N, 7.12; S, 5.43%
Found C, 59.13; H, 4.11; N, 7.18; S, 5.52%

The toluene mother liquor was concentrated to dryness to give IV as a solid foam (0.709 g; 12 %). This was purified for analysis by repeated recrystallization in from benzene-hexane (1 : 1 v/v, white crystals with m.p. 105—107°C; $[\alpha]_D^{25}$: 140°(c 1, $CHCl_3$); Rf: 0.77 (S_1); 0.73 (S_2); 0.14 (S_3); 0.87 (S_4); $UV_{(ethanol)}$: λ max 220 nm (log ε 4.68) and 304—306 nm (log ε 3.85).

$C_{29}H_{23}N_3O_9S$ Calcd., C, 59.07; H, 3.93; N, 7.12; S, 5.43%
Found, C, 59.18; H, 4.17; N, 7.20; S, 5.57%

S(α-D-ribofuranosyl) 5-mercapto-6-azauracil-(V)

To a suspension of III (1.179 g; 2 mM) in anhydrous methanol (50 ml), sodium methoxide, freshly prepared from sodium metal (4 mg atoms) in methanol (10 ml), was added and the resulting solution was stirred for 10 hours at room temperature. DOWEX 50×8 (H^+) (15 ml wet volume in methanol) was added and the mixture was stirred for 15 minutes. The resine was removed by filtration and the methanol solution was concentrated to 5 ml. The solution was diluted with water (25 ml) and extracted with ethyl acetate ether (2 : 1 v/v; 2×10 ml). The water solution was concentrated and the residue was recrystallized from 2-propanol. Yield 0.467 g (86 %) IV, m.p. 210—212°C $[\alpha]_D^{25}$: −186° (c = 1, H_2O); *Rf*: 0.21 (S_1); 0.33 (S_2); UV: λ max (0.1 N HCl) 302—304 nm (log ε 3.86); λ max (0.1 N NaOH) 302—304 (log ε 3.68); ^{1}H-NMR: anomeric proton δ 5.34 ppm (d, $J_{1',2'} = 2.8$ Hz).

$C_8H_{11}N_3O_6S$ Calcd., C, 34.65; H, 3.99; N, 15.15; S, 11.56%
Found, C, 34.80; H, 4.12; N, 15.25; S, 11.62%

S(α-D-ribofuranosyl)-5-mercapto-6-azauracil(VI)

IV (0.294 g; 0.5 mM) was debenzoylated as described above for III to give VI (0.105g; 76 %). After recrystallization from 2-propanol, the following data were obtained: m.p.146—148°C; $[\alpha]_D^{25}$: 280° (c 0.5, H_2O); *Rf*: 0.17 (S_1); 0.28 (S_2); UV: λ max (0.1 N HCl) 302—

304 nm (log ε 3.70) ; λ max (0.1 N NaOH) 302—304 nm (log ε 3.82) ; ^{1}H-NMR) : anomeric proton δ 6.03 (d, $J_{1',2'} = 5.0$ Hz).

$C_8H_{11}N_3O_6S$ Calcd., C, 34.65 ; H, 3.99 ; N, 15.15 ; S, 11.57%
Found, C, 34.75 ; H, 4.15 ; N, 15.30 ; S, 11.68%

ACKNOWLEDGEMENTS. The author thanks Mrs. Chem. Veronica Vişan of the Analytical Department of our Institute for recording the IR and UV spectra, Mrs. Pharm. Cornelia Ioan for analyses and Dr. D. Ionescu for ^{1}H-NMR spectra.

REFERENCES

* Part. XVI, C. Cristescu and S. Sitaru, *Rev. Roumaine Chim.*, **27**, 943 (1982).
[1] J. Gut, "*Adv. Heterocyclic Chem.*", Vol. 1, A. R. Katritzky, Ed., Academic Press, New York, 1963.
[2] T. J. Bardos, R. R. Herr and T. Enkoji, *J. Amer. Chem. Soc.*, **77**, 960 (1955).
[3] M. P. Kotick, C. Szantay and T. J. Bardos, *J. Org. Chem.*, **34**, 3806 (1969).
[4] G. Sezekeres and T. J. Bardos, *J. Med. Chem.*, **13**, 708 (1970).
[5] A. Giner-Sorolla and L. Medrek, *J. Med. Chem.*, **9**, 97 (1966).
[6] C. Cristescu and J. Marcus, *Pharmazie*, **16**, 135 (1961).
[7] C. Cristescu and V. Badea, *Rev. Roumaine Chim.*, **12**, 913 (1967).
[8] C. Cristescu, *Rev. Roumaine Chim.*, **20**, 1287 (1975).
[9] T. J. Kalman and T. J. Bardos, *J. Amer. Chem. Soc.*, **89**, 1171 (1967).
[10] J. Goodman, J. R. Fouts, E. Bresnick, R. Menegas and G. H. Hitchings, *Science*, **130**, 450 (1959).
[11] D. A. Shuman, A. Bloch, R. K. Robins and M. J. Robins, *J. Med. Chem.*, **12**, 652 (1969).
[12] G. Szekeres and T. J. Bardos, *J. Med. Chem.*, **15**, 1333 (1972).
[13] H. M. Kissman, C. Didaks and R. B. Baker, *J. Amer. Chem. Soc.*, **77**, 18 (1955).
[14] J. Johnas and J. Gut. *Coll. Czech. Chem. Comm.*, **26**, 2155 (1961).
[15] K. Y. Zee-Cheng and C. C. Cheng, *J. Org. Chem.*, **27**, 976 (1962).
[16] J. D. Stevens and H. G. Fletcher Jr., *J. Org. Chem*, **33**, 1799 (1968).

Revue Roumaine de Chimie, 28, 7, 737–739 (1983)

A NEW SYNTHESIS OF AROMATIC ESTERS BY A DIRECT CONDENSATION REACTION

C. I. CHIRIAC
"P. Poni" Institute of Macromolecular Chemistry,
Aleea Gr. Ghica Vodă 41 A, Iași, Romania

Received June 22, 1982

Various aromatic esters are prepared by a direct condensation reaction between triacylborates prepared "in situ" and phenols.

In a previous paper[1] we showed that triaryl borates can react with aromatic acids, affording the corresponding esters.

RESULTS AND DISCUSSION

In this paper, we present a new method for the synthesis of aromatic esters using the reaction between triacylborates and phenols. The reaction was known for the synthesis of amides,[2] but still not for aromatic esters. We used triacylborates prepared "in situ" from triacetylborate and aromatic acids.[2,3] Thus, by the heating of a mixture of triacetyl borate (1 mole), benzoic acid (3 moles) and phenol (3 moles) at 210–220°, phenyl benzoate has been obtained (yield 45–50%). The yield has increased to 70–75%, when the reaction took place in xylene at 210–220° using a Dean-Stark trap for the recirculation of the solvent. This increase of the yield is explained by the removal of water which resulted during the dehydration of boric acid on heating.[4] The removal of water was also necessary in other reactions when boric acid resulted as a by-product.[1,5] In this case, the removal of water is necessary because the triacyl borates are readily hydrolyzed during the reaction.[5,6]

As a result of these investigations and similar to other cases,[1,2,7] we propose the next mechanism of reaction :

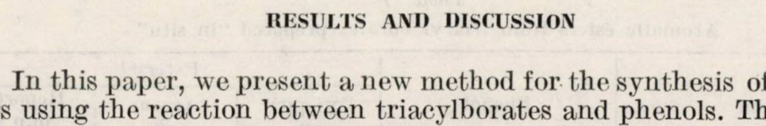

$$\underset{(I)}{3\ \mathrm{Ar{-}COOH}} + (\mathrm{CH_3{-}COO})_3\mathrm{B} \xrightarrow[\text{reflux}]{\text{xylene}} \underset{(II)}{(\mathrm{Ar{-}COO})_3\mathrm{B}} + 3\mathrm{CH_3{-}COOH}$$

$$\mathrm{II} + \underset{(III)}{3\mathrm{Ar'OH}} \xrightarrow[\text{reflux}]{\text{xylene}} \underset{(IV)}{3\ \mathrm{Ar{-}COOAr'}} + \mathrm{B(OH)_3}$$

$$\begin{tikzcd}\mathrm{B(OH)_3} \arrow[d, "-\mathrm{H_2O}(\text{removed by xylene})"] \\ \mathrm{B_2O_3}\end{tikzcd}$$

The presence of water was proved by identification with anhydrous $CuSO_4$.

We supposed, as in other cases,[1,6,7] that this reaction involves a transition state (V):

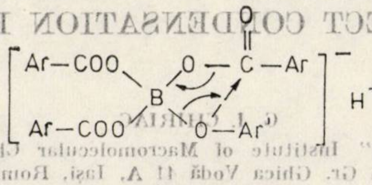

(V)

The general method for obtaining aromatic esters (IV) consists in refluxing a very concentrated solution of aromatic acid (3 moles), triacetyl borate (1 mole) and phenol (3 moles + 10% excess) in xylene as solvent using a Dean-Stark trap for removing the water (4—5 hours). The temperature of the solution is 210—220°, using very little xylene which refluxes during the reaction (at lower temperatures the yield decreases). Using toluene or benzene as solvents, the yield decreases too, because these solvents have boiling points lower than xylene. The excess of phenol, till 10%, contributes at the increase of the yield.

Table 1 shows the aromatic esters obtained in this way.

Table 1

Aromatic esters from triacyl borates prepared "in situ"

Acid	Phenol	Esters[a]		
		Yield[b] °C	M.p.[c] °C	Reported m.p.[d] °C.
C_6H_5-COOH	C_6H_5OH	70	68—70	69—71
C_6H_5-COOH	$p\text{-}Cl-C_6H_4-OH$	66	85—87[e]	86—87
C_6H_5-COOH	$p\text{-}CH_3-C_6H_4-OH$	69	70—72	70—71
C_6H_5-COOH	β-naphthol	76	105—170[c]	105—107
$p\text{-}CH_3-C_6H_4-COOH$	C_6H_5-OH	78	75—77	76—77[8]
$p\text{-}CH_3-C_6H_4-COOH$	$p\text{-}CH_3-C_6H_4-OH$	73	89—91	90—91
$p\text{-}CH_3-C_6H_4-COOH$	β-naphthol	77	135—137[e]	136—138
$p\text{-}CH_3OC_6H_4-COOH$	C_6H_5-OH	71	73—75	75—76[7]
$p\text{-}CH_3OC_6H_4-COOH$	$p\text{-}CH_3-C_6H_4-OH$	74	65—67	66—67[8]
$m\text{-}Br-C_6H_4-COOH$	C_6H_5-OH	62	64—66[e]	65—66

[a] The products were identified by comparison of m.p. and IR spectra with those of authentic samples.

[b] Yields determined by isolation of crude products.

[c] Before recrystallization.

[d] From "Beilsteins Handbuch der organischen Chemie".

[e] After recrystallization.

The yields of this method ranged from 62 to 78% (table 1).

By this new direct synthesis we obtained aromatic esters, which are difficult to obtain by heating of aromatic acids with phenols.

EXPERIMENTAL

Phenyl *p*-toluate

A solution of 4.08 g (3 moles) *p*-toluic acid and 1.88 g (1 mole) triacetyl borate in 20 ml dried xylene was refluxed 1 hour in a 50 ml flask with a Dean-Stark trap for the removal of xylene (15—17 ml) and acetic acid, the latter resulting as a by-product (the temperature of the salt bath was 190—200° , the mixed anhydride between toluic acid and boric acid resulting "in situ". Then 3.1 g (3 moles + 10% excess) phenol and 20 ml dried xylene were added in the flask and the obtained solution was refluxed 4—5 hours with the removal of water by azeotropic distillation using the same, Dean-Stark trap, which was used for the removal of the mixture xylene-acetic acid. The temperature of the salt bath was maintained between 225—235°, when the solution temperature varied between 210—220°, because the solution was very concentrated having only 3—5 ml xylene and the rest remained, all the time, in the Dean-Stark trap, which has a volume of 14—16 ml xylene without recirculation. At the end of the reaction, the solvent was completely removed by heating under vacuum. The resulted ester, still hot(melted), was treated with 2 ml N-methyl-2-pyrrolidone, which prevents the crystallization by cooling at room temperature. This solution was poured into a large volume of water with ice (80—100 ml) under stirring and treated with 5% NaOH solution till pH = 9—10. The product was collected by filtration and washed three times with 30—50 ml water. After drying under vacuum at 40—50°, 5 g phenyl toluate with m.p. 75—77° were obtained (mixed m.p. with pure phenyl toluate underpressed). Yield 78% (calculated on toluic acid employed).

Anal. Calculated for $G_{14}A_{12}O_2$; C, 79.24 ; H, 5.66%. Found : C, 79.11 ; H, 5.43%.

In similar conditions, the other aromatic esters (presented in table 1) were prepared.

REFERENCES

[1] C. I. Chiriac, *Rev. Roumaine Chim.*, (in press).

[2] H. Schulze, U. S. Pat. 2, 898, 353, Aug. 4, 1959 ; *Chem. Abstr.*, **54**, 17, 238 (1960).

[3] A. Pictet, *Ber. dtsch. chem. Ges.*, **36**, 2219 (1903).

[4] M. F. Lapert, *Chem. Rev.*, **56**, 971 (1956).

[5] J. Tani and I. Inone, *Synthesis*, **1975**, 714.

[6] W. H. Miller and A. Scottergood, *J. Amer. Chem. Soc.*, **67**, 2150 (1945).

[7] B. Iselin and W. Rittel, *Helv. Chim. Acta*, **40**, 373 (1957).

[8] H. Rheinboldt, *Quimica*, **1951** (3), 52 ; *Chem. Abstr.*, **1952**, 7552.

Revue Roumaine de Chimie, 28, 7, 741–756 (1983)

EXO- AND ENDOHORMONES. VI[1]

SYNTHESES OF THE SEX PHEROMONES OF SOME LEPIDOPTERA

ANA AURELIA BOTAR, A. BARABÁS, I. OPREAN, JULIANNA CSONKA-HORVAI
and F. HODOŞAN
Institute of Chemistry, str. Fintînele 30, 3400 Cluj-Napoca, Romania

Received June 22, 1982

Eight alken-1-ol acetates and one epoxide, components of the sex pheromone blends of some economically important lepidopterous pests, were synthetized following the acetylenic route of chain build-up. Alternatives to the standard procedures are described. ^{13}C-NMR spectroscopy was used for characterization of the pheromones and the principal intermediate synthons.

INTRODUCTION

In the spectrum of the rapidly developing new methods of the so-called non-conventional pest control much attention has been focused upon the natural compounds called *pheromones*,[2] chemicals carrying important intraspecific biochemical information. Among them, the best known and most advanced in practical applications are the sex attractant pheromones of the Lepidoptera. Most lepidopteran sex attractant pheromones are long-chain normal olefines with an alcohol, acetate or aldehyde end function.[2] In most cases, the natural messenger is a suitable mixture — a so-called "blend" — of several compounds of closely related structure. An important number of syntheses of lepidopteran sex pheromones were reported.[3–6] In the present paper synthetic pathways worked out in our laboratory to obtain alkenol acetates of the general formula $R_1-CH=CH-(CH_2)_n-OAc$ and of one compound possessing an epoxide substructure are described.[7]

RESULTS AND DISCUSSION

All reported syntheses of alkenolic pheromonal compounds can be included in several general schemes. Among these, we selected the route based on alkynic intermediates, which seemed to us the most suitable for large-scale applications.[3–6] This frequently used pathway starts from acetylene, which is first transformed *via* sodation and alkylation in a higher terminal alkyne of suitable chain length. As standard, both reaction steps are carried out in liquid ammonia; sodium amide is prepared *in situ* and then acetylene is added, followed by the suitable alkyl bromide. To bring higher alkyl bromides into solution, during the alkylation step DMSO should be added into the reaction mixture.[8,9] From the alternative procedures described for metallation of acetylene, our attention was attracted to that one which uses dimsyl-sodium as the metallating reagent. This reagent can be prepared at room temperature or slightly above by reacting sodium hydride with a large excess of DMSO used both as a solvent and reactant. Sodation is caried out by bubbling acetylene through this solution. The completion of sodation can be easily determined by adding triphenylmethane to an aliquot of the reaction mixture: when sodation is complete, no red coloration due to triphenylmethylsodium should appear. Alkylation is effected by adding the suitable alkyl bromide into the above reaction mixture at room temperature.[10] This procedure seemed to us especially suitable for large-scale applications and we extensively used it to prepare the 1-alkynes IA—IF, intermediates in pheromone syntheses. Excellent yields were obtained in each case, practically equalling those reported for syntheses in liquid ammonia. We should call attention upon literature indications [11] that the reaction between sodium hydride and DMSO may sometimes become explosive. This could be especially dangerous for large-scale applications. We must however point out that no incident occurred in our laboratory with this reaction, though it was used currently during 7 years with up to 1 mole of sodium hydride per run. Attempts to use commercial sodium amide in DMSO instead of sodium hydride in the synthesis of 7-methyl-1-octyne (IF) produced poor yields.

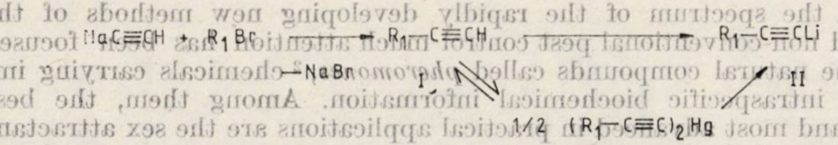

I, II, III:	A	B	C	D	E	F
R_1:	C_2H_5	C_3H_7	C_4H_9	C_5H_{11}	$C_{10}H_{21}$	$-(CH_2)_4CH(CH_3)_2$

The 1-alkynes thus obtained are usually purified by distillation, a procedure which produced poor results in our laboratory: with the highly volatile lower alkynes there were important losses of product during distillation, whereas the higher homologues could not be separated neatly enough from traces of DMSO and from reaction by-products of similar volatilities with the product alkyne. Therefore a chemical purification of the product alkynes was attempted. 1-Alkynes upon reaction with alkalic mercury cyanide solution,[12] or more conveniently with mercuric chloride in an aqueous solution containing potassium iodide and sodium hydroxide (Nessler's reagent)[13] can be quantitatively precipitated as dialkynyl-mercury compounds (III A—F), white solids, easily recrystallizable from organic solvents. These dialkynyl mercury compounds are perfectly stable in air and may easily regenerate the starting alkynes upon reaction with hydrochloric acid[12] or aqueous potassium cyanide,[14] being therefore excellently suited for purifying and stocking 1-alkynes.

The second step of the acetylenic route consists of a second metallation of the intermediate 1-alkyne I, obtained as described above, followed by alkylation to obtain the desired higher alkyne homologue. The 1-alkyne is first lithiated either with lithium amide in liquid ammonia or with butyl-lithium in hexane[15] to yield the alkynyl lithium compounds II. Dialkynyl-mercury derivatives III can be directly lithiated to II by heating them with lithium metal in dioxane.[16] The lithium alkynes II are alkylated with the suitable *omega*-halo alcohols, $Br(CH_2)_nOR_2$, (IV), having their hydroxyl functions appropriately protected during the coupling reaction.

The following series of these intermediate synthons IV were prepared in our laboratory :

$Br-(CH_2)_nOR_2$

IV	a :	R_2*):	THP	n = 4,7,8,10
	b :		*t*-Bu	4,7,10
	c :		Ac	4
	d :		$Si(CH_3)_3$	7

*) THP : tetrahydropyranyl ; *t*-Bu : *t*-butyl ; Ac : acetyl.

Compounds IVa, b, c ($n = 4$) were prepared by opening the tetrahydrofuran ring with acyl halides and zinc chloride.[17] Thus 4-bromobutyl acetate IVc was obtained from tetrahydrofuran and acetyl bromide ; IVc was hydrolyzed with acidulated methanol to yield 4-bromobutan-1-ol, which was subsequently eterified to obtain IVa or IVb ($n = 4$). Compounds IVa, b, d ($n = 7, 8, 10$) were synthetized starting from the appropriated dicarboxylic acids $HOOC-(CH_2)_{n-2}-COOH$. The acids or their ethyl or methyl esters were reduced to the corresponding diols either with $LiAlH_4$ or through catalytic hydrogenation under high pressure. The diols were subsequently one-end brominated[18,19] to the bromoalcohols, then eterified to yield compounds IVa[19], IVb, or IVd[20] ($n = 7, 8, 10$). For large-scale syntheses, *t*-buthyl ethers IVb are especially suitable as they are easily prepared from cheap and readily available isobutylene.

The coupling reaction between the alkynyl-lithium compounds II and the protected bromoalcohols IV is usually carried out either in liquid ammonia or in organic solvents, depending on the lithiation method used.[15] We attempted to execute the lithiation and the subsequent alkylation in a one-pot procedure starting from the dialkynyl-mercury compounds III. Dioxane proved an unsatisfactory solvent for this reaction : by treating di-pentynyl-mercury IIIB with lithium in boiling dioxane, the stoichiometrically expected amount of metallic mercury had separated, but on subsequent adding of 7-bromoheptan-1-ol tetrahydropyranyl ether (IVa, $n = 7$) and boiling prolonged for another 10h, only a 12 % yield of the expected disubstituted alkyne VBa was obtained. Hexamethylphosphoric triamide was added to the reaction mixture, without causing any improvement. THF used as solvent produced essentially the same result ; again only the transmetallation reaction could be carried out. However, good overall results were obtained when the reaction was effected in diglyme; transmetallation was quantitative and fair yields of the disubstituted alkynes V(ABCD)(ab) were obtained.

$R_1-C\equiv C-(CH_2)_n-O-R_2$

V A a :	R_1	C_2H_5	R_2 :	THP	n=10
b :		C_2H_5		*t*-Bu	10
c :		C_2H_5		Ac	10
V B a :		C_3H_7		THP	7
b :		C_3H_7		*t*-Bu	7
c :		C_3H_7		Ac	7
d :		C_3H_7		$Si(CH_3)_3$	7
V C a :		C_4H_9		THP	4, 10
b :		C_4H_9		*t*-Bu	4, 10
c :		C_4H_9		Ac	4, 10
V D a		C_5H_{11}		THP	10
c :		C_5H_{11}		Ac	10

Diglyme as solvent proved to be equally successful in preparing 2-methyl-7-octadecyne $C_{10}H_{21}-C\equiv C-(CH_2)_4-CH(CH_3)_2$, VE from IIIE and 1-bromo-5-methyl hexane. The yields related to the starting mercury dialkynes (III) ranged between 85—90 %. As expected, the *omega*-brom-alcohol-acetates IVc could not be used in this alkylation reaction. The attempted reaction between 4-bromobutan-1-ol acetate (IVc) and hexynyl-lithium (IIC) yielded carbinol VI as the main product:

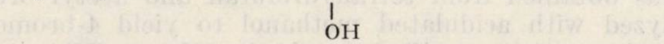

$$CH_3-CH_2-CH_2-CH_2-C\equiv C-\underset{OH}{\overset{CH_3}{C}}-C\equiv C-CH_2-CH_2-CH_2-CH_3$$

VI

Compound VI afforded a characteristic fragmentation pattern in its mass spectrum, as shown in Scheme 1. Structure VI could also be recognized in the $^{13}C-NMR$ spectrum of the sample, as follows: (carbon no. /$\delta-{}^{13}C$

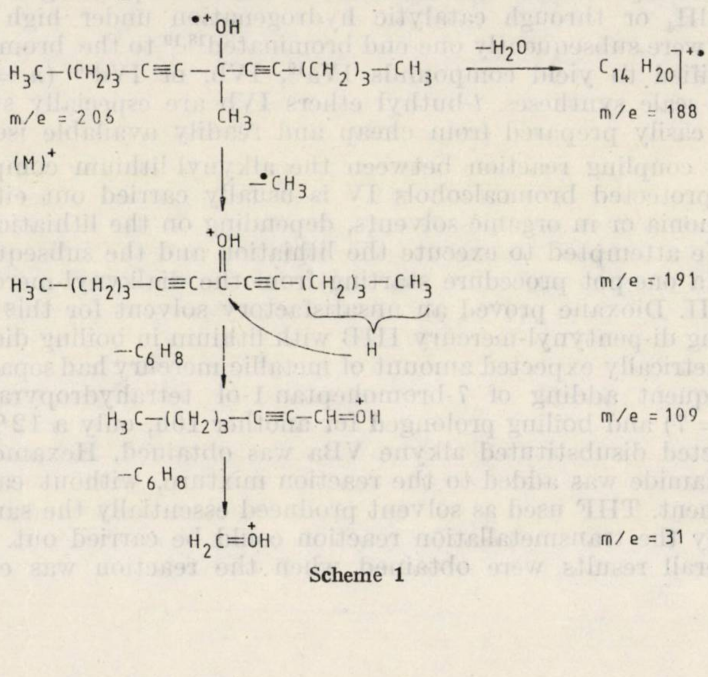
•+OH
H₃C—(CH₂)₃—C≡C—C—C≡C—(CH₂)₃—CH₃
CH₃
m/e = 206
(M)⁺
—H₂O
[C₁₄H₂₀]⁺•
m/e = 188
—•CH₃
+OH
H₃C—(CH₂)₃—C≡C—C—C≡C—(CH₂)₃—CH₃
m/e = 191
H
—C₆H₈
H₃C—(CH₂)₃—C≡C—CH=OH⁺
m/e = 109
—C₆H₈
H₂C=OH⁺
m/e = 31

Scheme 1

in ppm) : 1,13/13.75 ; 2, 12/22.2 ; 3, 11/31.0 ; 4, 10/18.6 ; 5, 6, 8, 9/82.8 ; 7/60.0 ; 7 $-CH_3$/33.1.

Mass spectra of the products of the coupling reaction were in accordance with the expected structures, V. Especially the *t*-butyl ethers V(ABC)b could be easily identified by their mass spectra exhibiting a specific fragmentation pattern (an example is given in Scheme 2), with a characteristic base peak at $m/e = 57$ $(C_4H_9)^+$.

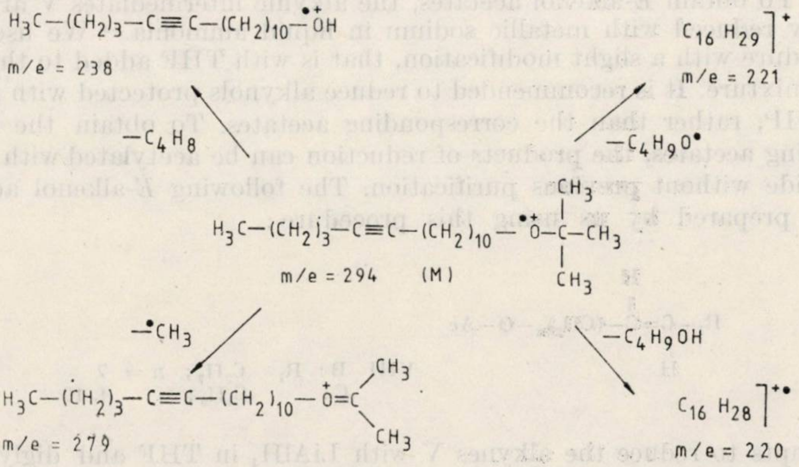

Scheme 2

The last step in the preparation of the alkenol acetate pheromones consisted of the partial hydrogenation of the alkynol ethers or acetates V. Usually this hydrogenation should be effected in a highly stereoselective manner, as the two geometrically isomeric alkenol acetates resulting from the same alkynic precursor exhibit markedly different and often contrasting pheromonal activities. *Z*-Alkenol acetates are usually obtained from the corresponding alkynol acetates V(ABCD)c directly, by catalytic hydrogenation using the so-called Lyndlar catalyst. The alkynol acetates V(ABCD)c are easily prepared from the corresponding *t*-butyl ethers under the action of acetyl chloride in acetic acid. We experienced far better results by using another catalyst known as Ni P—2, obtained by reducing nickel acetate with sodium borohydride and subsequent poisoning with ethylenediamine (EDA).[21] The following *Z*-alkenol acetates were thus prepared :

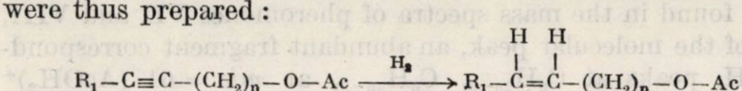

$$R_1-C\equiv C-(CH_2)_n-O-Ac \xrightarrow[\text{Ni P-2/EDA}]{H_2} R_1-\overset{H}{\overset{|}{C}}=\overset{H}{\overset{|}{C}}-(CH_2)_n-O-Ac$$

V(ABCD)c

VII A :	R_1 :	C_2H_5	$n=10$
B :		C_3H_7	7
C :		C_4H_9	4, 10
D :		C_5H_{11}	10

The *Z*-olefine VIIE was analogously obtained starting from VE.

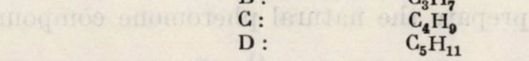

$$C_{10}H_{21}-\overset{H}{\overset{|}{C}}=\overset{H}{\overset{|}{C}}-(CH_2)_4-CH(CH_3)_2$$

VIIE

Using Ni-P—2 catalyst, the hydrogenation takes place quantitatively and with a very high degree of stereoselectivity. The *E*-isomer content of the alkenol acetates VIIABCD thus obtained was found to be less than 0.3%, only VIIE contained about 10% of its *E*-isomer. The Ni P—2 catalyst is remarkably insensitive towards impurities in the substrate or traces of oxygen in the reaction medium. The alkenol acetates thus obtained, if needed can easily be hydrolized to afford the corresponding free alkenols.

To obtain *E*-alkenol acetates, the alkynic intermediates V are commonly reduced with metallic sodium in liquid ammonia.[22] We used this procedure with a slight modification, that is with THF added to the reaction mixture. It is recommended to reduce alkynols protected with *t*-butyl or THP, rather than the corresponding acetates. To obtain the corresponding acetates, the products of reduction can be acetylated with acetyl chloride without previous purification. The following *E*-alkenol acetates were prepared by us using this procedure:

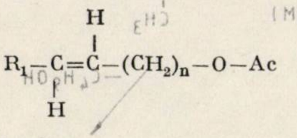

$$R_1-\underset{H}{C}=\overset{H}{C}-(CH_2)_n-O-Ac$$

VIII B : R_1 : C_3H_7 ; $n =$ 7
C : C_4H_9 ; 4, 10

Attempts to reduce the alkynes V with $LiAlH_4$ in THF and diglyme as described by Rossi[23] produced unsatisfactory results, as reduction was not complete even after 55 h heating.

The *Z*-alkenol acetates VIIC ($n = 4, 10$) and VIIB were converted to their *E*-isomers VIIIC ($n = 4, 10$) and VIIIB with the method described by Sonnet and Oliver.[24] In this procedure, the *Z*-olefine is first epoxidated, then treated with triphenyl-bromo-phosphonium bromide. This results in opening of the oxyrane ring; subsequent elimination (E2) of triphenylphosphinoxide leads to the *erythro*-dibromide, which in turn affords the corresponding *E*-olefine upon stereospecific debromination with zinc powder in dimethyl formamide. Samples of *E*-alkenol acetates (VIII) prepared through this procedure were found to contain 97—99% of *E*-isomer.

The expected specific fragmentation pattern, characteristic of alkenol acetates was found in the mass spectra of pheromones VII and VIII, namely absence of the molecular peak, an abundant fragment corresponding to M—AcOH, peaks at C_nH_{2n-2}, C_nH_{2n-3}, at $m/e = 61$ $(AcOH_2)^+$ and 43 $(Ac)^+$ (base peak). The corresponding pairs of geometrical isomers VII (*Z*) and VIII (*E*) afforded in all cases practically identical mass spectra.

To prepare the natural pheromone compound IX, the olefine

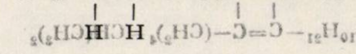

$$C_{10}H_{21}-\underset{H}{C}\overset{O}{-}\underset{H}{C}-(CH_2)_4-CH(CH_3)_2$$

IX

VIIE was epoxidated with perphthalic acid. A fragmentation pattern according to formula IX was found in the mass spectrum of the sample and the expected molecular peak could be observed:

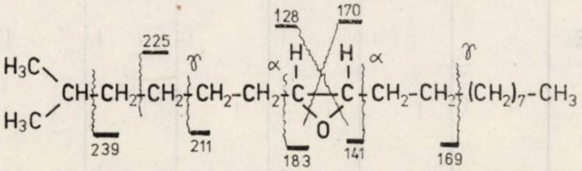

All pheromones prepared and most of the key intermediate synthons were characterized by their $^{13}C-NMR$ spectra. $^{13}C-NMR$ data are summarized in Tables 1—4. Assignments of the observed signals are based on general literature and on a former study[25] on pheromones and pheromone intermediates performed in our laboratory. As it may be seen, $^{13}C-NMR$ spectroscopy affords a very advanced degree of characterization of the samples, as practically every carbon atom could be identified by its unique $^{13}C-NMR$ signal.

The 1-alkynes (I) studied (Table 1) afforded spectra in good accordance with literature data.[26] Formation of the mercury salts (III) results in important deshielding of the alkynic carbons, whereas the chemical shifts of the saturated carbons remain practically unchanged. Further, the neat distinction between the substituted and unsubstituted alkynic carbon in the free 1-alkynes (I), (chemical shift difference $\Delta \approx 17$ ppm) is strongly reduced in the mercury salts ($\Delta \approx 2$ ppm).

The different substituents attached to the hydroxyl functions of the pheromones and the intermediate synthons are easily identified by the resonance signals of their own carbon atoms, as well as by their characteristic influence upon the chemical shifts of carbons in positions 1,2 and 3 of the alcohol they are attached to (see Tables 2 and 3).

The chemical shifts of the carbons *alpha*- to the multiple bonds afford clear evidence concerning the degree of unsaturation of the multiple bond as well as the geometrical isomerism of the olefinic double bonds, a key feature of pheromone structure. As it may be seen in Tables 1, 3 and 4, *alpha*-carbons in alkynic compounds appear with 10—11 ppm more shielded than the corresponding carbons in a saturated carbon chain. Alkynes can be of course identified by the characteristic chemical shift values of the sp-carbons, but these quaternary carbons usually afford very weak signals, which in some cases might be easily overlooked. The chemical shifts of the allylic carbons in an *n*-alkenic chain are heavily dependent on the stereochemistry of the olefinic double bond. The allylic carbons in a *Z*-olefine appear with 2.5—3.0 ppm more shielded, in an *E*-olefine on the contrary, with 2.5—3.0 ppm deshielded as compared with a corresponding saturated chain (see Tables 3 and 4). This stereochemical information cannot be obtained from the chemical shifts of the olefinic carbons themselves; these shifts are practically not influenced by *E—Z* isomerism of the double bond.

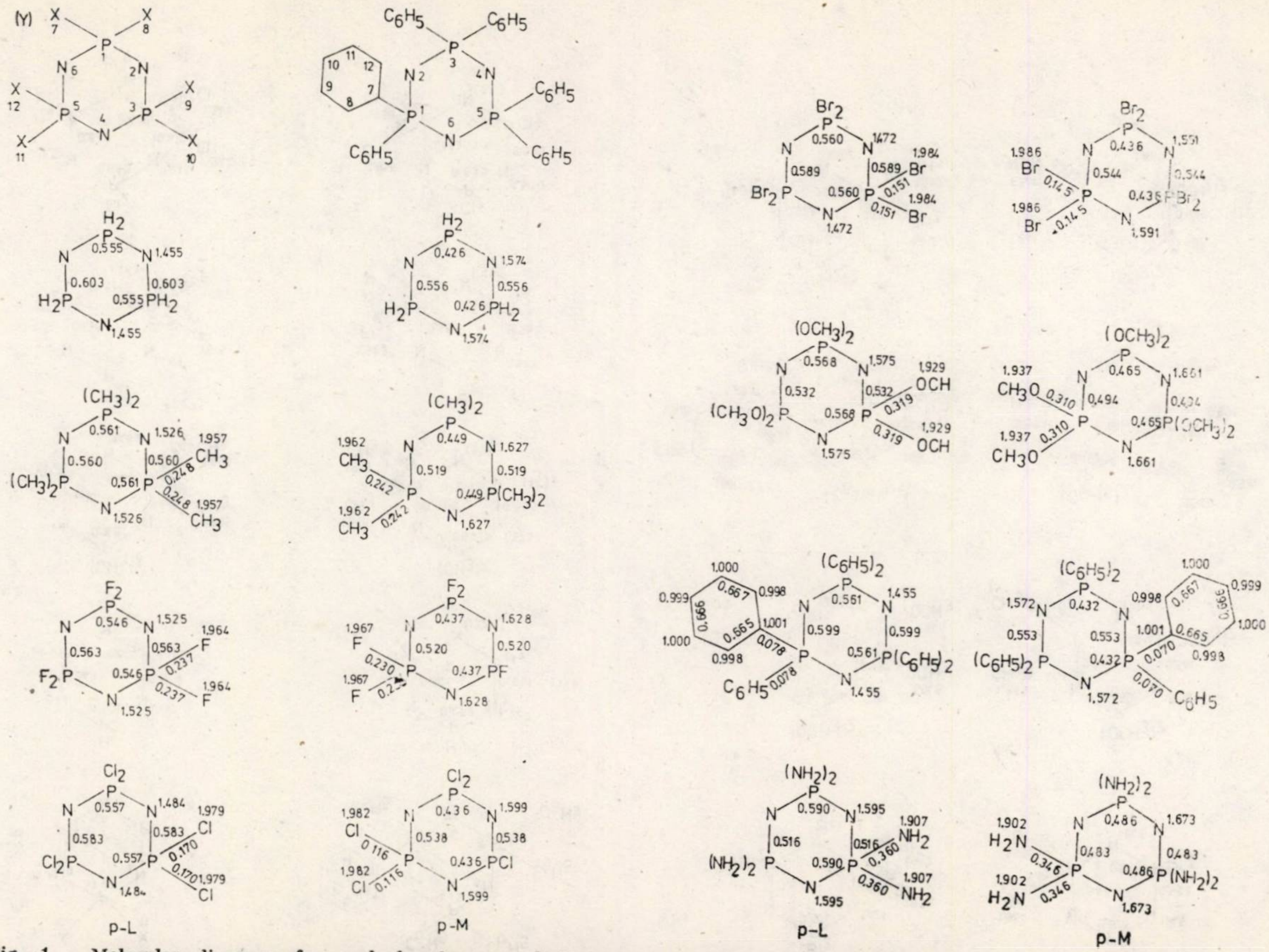
(Y)
X 7
X 8
P 1
N 6
2 N
X 12
X 9
P 5
4 N
3 P
X 11
X 10
C6H5
P 3
N 2
4 N
10 11 12 9 7 8
P 1
6 N
5 P
C6H5
H2
0.555
1.455
0.603
0.603
H2P
0.555 PH2
1.455
0.426
1.574
0.556
0.556
0.426 PH2
1.574
(CH3)2
0.561
1.526
1.957
0.560
0.560
CH3
(CH3)2P
0.561
0.248
0.248
1.957
1.526
0.449
1.962
1.627
0.519
0.519
0.242
0.449 P(CH3)2
1.962
1.627
F2
0.546
1.525
1.964
0.563
0.563
F2P
0.546
0.237
0.237
1.964
1.525
0.437
1.967
1.628
0.520
0.520
0.230
0.437 PF
1.967
1.628
Cl2
0.557
1.484
1.979
0.583
0.583
Cl2P
0.557
0.170
0.170
1.979
1.484
p-L
0.436
1.982
1.599
0.538
0.538
0.116
0.436 PCl
1.982
0.116
1.599
p-M
Br2
0.560
1.472
1.984
0.589
0.589
Br2P
0.560
0.151
0.151
1.984
1.472
0.436
1.986
1.591
0.544
0.544
0.145
0.436 PBr2
1.986
0.145
1.591
(OCH3)2
0.568
1.575
1.929
0.532
0.532
OCH
(CH3O)2P
0.568
0.319
0.319
1.929
1.575
0.465
1.937
1.661
CH3O
0.310
0.494
0.494
0.465 P(OCH3)2
1.937
0.310
1.661
(C6H5)2
1.000
0.667
0.998
0.561
1.455
0.999
0.666
1.001
0.599
0.599
1.000
0.665
0.078
0.561 P(C6H5)2
0.998
0.078
C6H5
1.455
0.432
1.000
1.572
0.998
0.667
0.999
0.666
0.553
0.553
1.001
0.665
1.000
(C6H5)2P
0.432
0.070
0.998
0.070
1.572
(NH2)2
0.590
1.595
1.907
0.516
0.516
NH2
(NH2)2P
0.590
0.360
0.360
1.907
1.595
p-L
0.486
1.902
1.673
H2N
0.483
0.483
0.346
0.486 P(NH2)2
1.902
0.346
1.673
p-M

Fig. 1. — Molecular diagrams for cyclophosphazenes derivates calculated with the Fukui model (p—L — set of parameters for the phosphorus atom taken from literature,[9,12] p—M— set of parameters for the phosphorus atom recommended by Mracec [13]).

TABELLE 1

Chromatographische Trennung der Kupplungsprodukte der H-Säure mit 4-Nitrodiazobenzol

Die Substanz	Farbe der Flecke		*Rf*-Wert	Anteil in % umgesetzter H-Säure					
	in saurem Medium	in alkalischem Medium		*p*H 1	*p*H 2	*p*H 5	*p*H 7	*p*H 8	*p*H 10
4-Nitranilin $\xrightarrow{\text{sauer } (p-)}$ H-Säure (II)	bläulich-rot	blau	0,15	10	5	—	—	—	—
4-Nitranilin $\xrightarrow{\text{sauer } (o-)}$ H-Säure (I)	rot	blau	0,34	85	30	5	5	—	—
4-Nitranilin $\xrightarrow{\text{alk. } (o-)}$ H-Säure (III)	rot	rot	0,47	—	10	50	55	60	70
4-Nitranilin $\xrightarrow{\text{sauer } (o-)}$ H-Säure (V) 4-Nitranilin $\xrightarrow[\text{alk. } (o-)]{}$ H-Säure (V)	grünlich-blau	grünlich-blau	0,53	5	55	40	25	15	10
4-Nitranilin $\xrightarrow{\text{alk. } (p-)}$ H-Säure (IV)	rot	blau	0,58	—	—	5	10	15	15
4-Nitranilin $\xrightarrow{\text{sauer } (o-)}$ H-Säure (VI) 4-Nitranilin $\xrightarrow[\text{alk. } (p-)]{}$ H-Säure (VI)	blau	blau	0,75	—	—	—	5	10	5

TABELLE 4

Chromatographische Trennung der Kupplungsprodukte der I-Säure mit 4-Nitrodiazobenzol

Die Substanz	Farbe der Flecke		*Rf*-Werte	Anteil in % umgesetzter I-Säure					
	in saurem Medium	in alkalischem Medium		*p*H 1	*p*H 3	*p*H 5	*p*H 7	*p*H 8	*p*H 10
4-Nitranilin $\xrightarrow{\text{sauer}}$ I-Säure (VIII)	rötlich-orange	rot-violett	0,55	80	70	—	—	—	—
4-Nitranilin $\xrightarrow{\text{sauer}}$ I-Säure (XI) 4-Nitranilin $\xrightarrow{\text{alk.}}$	violett	violett	0,59	20	15	10	3	—	—
4-Nitranilin $\xrightarrow{\text{alk.}(o-)}$ I-Säure (IX)	gelblich-orange	gelblich-orange	0,63	—	10	65	70	60	42
4-Nitranilin $\xrightarrow{\text{alk.}(p-)}$ I-Säure (X)	rötlich-orange	rot-violett	0,65	—	5	25	27	40	58

TABELLE 5

Chromatographische Trennung der Kupplungsprodukte der I-Säure mit 5-Nitro-2-diazobenzoesäure

Die Substanz	Farbe der Flecke		*Rf*-Werte	Anteil in % umgesetzter I-Säure	
	in saurem Medium	in alkalischem Medium		*p*H = 1	*p*H = 3
5-Nitro-2-aminobenzoesäure $\xrightarrow{\text{sauer}}$ I-Säure	hellrot	violett	0,46	75	35
5-Nitro-2-aminobenzoesäure $\xrightarrow{\text{sauer}}$ I-Säure 5-Nitro-2-aminobenzoesäure $\xrightarrow{\text{alk.}}$	dunkelrot	dunkelrot	0,59	25	40
5-Nitro-2-aminobenzoesäure $\xrightarrow{\text{alk.}(o-)}$ I-Säure	gelblich-orange	gelblich-orange	0,63	—	15
5-Nitro-2-aminobenzoesäure $\xrightarrow{\text{alk.}(p-)}$ I-Säure	orange	violett	0,67	—	10

TABELLE 6

Chromatographische Trennung der Kupplungsprodukte der N-Azetyl-I-Säure mit 4-Nitrodiazobenzol

Die Substanz	Farben der Flecke		*Rf*-Werte	Anteil in % eingesetzter N-Azetyl-I-Säure	
	in saurem Medium	in alkalischem Medium		*p*H = 5	*p*H = 8
4-Nitranilin $\xrightarrow{\text{alk. }(o-)}$ N-Azetyl-I-Säure	gelblich-orange	gelblich-orange	0,65	85	60
4-Nitranilin $\xrightarrow{\text{alk. }(p-)}$ N-Azetyl-I-Säure	gelblich-orange	rot	0,69	15	40

TABELLE 7

Chromatographische Trennung der Kupplungsprodukte der γ-Säure mit 4-Nitranilin

Die Substanz	Farbe der Flecke		*Rf*-Wert	Anteil in % umgesetzter γ-Säure					
	in saurem Medium	in alkalischem Medium		*p*H 1	*p*H 3	*p*H 5	*p*H 7	*p*H 8	*p*H 10
4-Nitranilin $\xrightarrow{\text{sauer}}$ γ-Säure (XII)	violett	violett	0,37	100	85	80	20	5	3
4-Nitranilin $\xrightarrow{\text{alk. }(o-)}$ γ-Säure (XIII)	braun	braun	0,70	—	12	15	70	85	75
4-Nitranilin $\xrightarrow{\text{alk. }(p-)}$ γ-Säure (XIV)	braun	bläulich-braun	0,72	—	3	5	10	10	22

TABELLE 8

Die *p*K-Werte der H-, I- und γ-Säure und einiger ihrer Kupplungsprodukte mit 4-Nitrodiazobenzol

Die Substanz	*p*K-Werte					
	Eigene Bestimmungen		Bestimmungen anderer Autoren			
	pK_{NH_2}	pK_{OH}	pK_{NH_2}	Lit.	pK_{OH}	Lit.
H-Säure	3,45	8,25	3,5	2	8,5	2
4-Nitranilin $\xrightarrow{\text{sauer }(o-)}$ H-Säure (I)	—	6,20	—		6,15	8
I-Säure	4,55	8,60	—		—	
4-Nitranilin $\xrightarrow{\text{sauer}}$ I-Säure (VIII)	—	5,15	—		—	
γ-Säure	4,2	8,75	—		—	

TABLE 1

Adsorption parameters for different binary liquid mixtures on solids calculated according to Eq. (14)

Liquid mixture "1 + 2"	Adsorbent	Temp. °C	Equation (14) for m = 1			Equation (14) for m ≠ 1				Ref. to adsorption system	Ref. to activity coefficients
			n^s [mmole/g]	$L_{12}^{(1)}$	$K_{12}^{(2)}$	m	n^s [mmole/g	$L_{12}^{(1)}$	$K_{12}^{(2)}$		
Chloroform+benzene	boehmite	20	1.021	2.828	2.828	0.921	1.019	4.762	1.566	12	16
Chloroform+carbon tetrachloride	charcoal	20	0.849	19.575	2.287	0.917	0.878	18.777	2.240	13	13
Propyl chloride+carbon tetrachloride	charcoal	20	2.949	0.936	0.601	0.049	2.609	0.820	0.617	13	13
Ethylene dichloride + benzene	charcoal	20	0.983	4.826	0.078	0.731	3.409	1.407	0.529	13	$f_i = 1$
Methyl acetate + benzene	charcoal	20	1.819	1.281	0.217	0.703	1.516	0.700	0.310	13	13
Benzene+ethylene dichloride	activated carbon	30	1.027	18.849	0.743	0.792	1.206	14.372	0.755	14	$f_i = 1$
Pyridine+ethyl alcohol	charcoal	20	2.058	17.255	0.753	0.616	2.944	6.743	1.013	13	$f_i = 1$
Benzene+ethyl alcohol	activated carbon	25	2.225	7.456	1.511	0.791	2.229	5.161	2.303	15	17

TABLE 1

Elemental chemical analysis of complex compounds of cadmium with acetone selenosemicarbazone

COMPLEX COMPOUNDS	Cd %	Se %	C %	H %	N %	Halogen %	O %	Total %	Cryst. H_2O %
	c/f	c/f	c/f	c/f	c/f	c/f	c/f	c/f	c/f
$[(CdClHsesacH_2O)_2]Cl_2$	29.63 29.67	20.81 20.93	12.69 13.10	2.90 3.10	11.07 11.10	18.69 18.05	4.21 —	100.00 95.95	— absent
$[CdCl(Hsesac)_2]Cl.0.5H_2O$	20.50 20.65	28.80 28.61	17.52 17.05	3.47 3.42	15.32 14.92	12.93 13.43	1.46 —	100.00 98.08	1.64 1.79
$[(CdI_2Hsesac)_2]$	20.65 19.85	14.51 15.02	8.82 8.94	1.66 2.18	7.72 8.03	46.64 —	— —	100.00 54.02	— absent
$[CdI_2(Hsesac)_2]$	15.56 15.88	21.87 22.04	13.30 13.65	2.49 2.63	11.63 11.80	35.15 —	— —	100.00 66.00	— absent
$[\{Cd(CH_3COO)(CH_3COOH)(sesac)\}_2]$	27.52 27.85	19.33 19.67	23.52 24.00	3.67 3.77	10.29 10.43	— —	15.67 —	100.00 85.72	— absent
$[CdCH_3COO(sesac)(Hsesac)]0.5H_2O$	20.99 20.77	29.49 29.05	22.44 22.91	3.92 4.30	15.69 15.39	— —	7.47 —	100.00 92.42	1.68 1.43
$[Cd(sesac)_2]$	24.10 24.28	33.86 34.15	20.60 20.05	3.43 3.95	18.01 17.80	— —	— —	100.00 100.23	— absent

c = calculated ; f = found

TABLA 1

Energías electrónicas pi de los polienos acíclicos asociados a las moléculas de la Figura 1 calculadas por el método aditivo de Hess y Schaad [6]

Molécula	Contribución de cada uno de los términos								Energía
	23	22	22′	21	20	12	11	10	
a	—	3	—	2	1	2	4	2	$12\alpha + 16.1463\ \beta$
b	—	3	—	2	1	2	4	2	$12\ \alpha + 16.1463\ \beta$
c	—	4	—	2	1	3	4	2	$14\ \alpha + 18.6822\ \beta$
d	—	2	—	4	1	2	4	4	$14\ \alpha + 19.1646\ \beta$
e	—	4	—	2	1	3	4	2	$14\ \alpha + 18.6822\ \beta$
f	—	3	—	4	1	3	4	4	$16\ \alpha + 21.7005\ \beta$
g	—	3	—	4	1	3	4	4	$16\ \alpha + 21.7005\ \beta$
h	—	4	—	2	2	2	6	3	$16\ \alpha + 21.6960\ \beta$
i	—	4	—	2	2	2	6	3	$16\ \alpha + 21.6960\ \beta$
j	—	4	—	2	2	3	4	4	$16\ \alpha + 21.7254\ \beta$
k	—	3	—	4	1	3	4	4	$16\ \alpha + 21.7005\ \beta$
l	—	4	—	2	2	2	6	3	$16\ \alpha + 21.6960\ \beta$
m	—	4	—	2	2	2	6	3	$16\ \alpha + 21.6960\ \beta$
n	—	4	—	4	1	4	4	4	$18\ \alpha + 24.2364\ \beta$
o	—	4	—	4	1	3	6	3	$18\ \alpha + 24.2070\ \beta$
p	—	4	—	4	1	4	4	4	$18\ \alpha + 24.2364\ \beta$

TABLA 2

Energías electrónicas totales pi calculadas mediante los métodos TPOT [23] y ITPOT [22]

Molécula	Energía (TPOT)	Energía (ITPOT)
a	$12\ \alpha + 13.53198\ \beta$	$12\ \alpha + 15.91724\ \beta$
b	$12\ \alpha + 12.89198\ \beta$	$12\ \alpha + 15.95234\ \beta$
c	$14\ \alpha + 19.62064\ \beta$	$14\ \alpha + 20.65606\ \beta$
d	$14\ \alpha + 15.03052\ \alpha$	$14\ \alpha + 18.93274\ \beta$
e	$14\ \alpha + 15.06808\ \beta$	$14\ \alpha + 18.50732\ \beta$
f	$16\ \alpha + 20.40856\ \beta$	$14\ \alpha + 22.09214\ \beta$
g	$16\ \alpha + 19.72584\ \beta$	$16\ \alpha + 22.22876\ \beta$
h	$16\ \alpha + 21.67894\ \beta$	$16\ \alpha + 22.15546\ \beta$
i	$16\ \alpha + 17.84724\ \beta$	$16\ \alpha + 21.36914\ \beta$
j	$16\ \alpha + 18.85100\ \beta$	$16\ \alpha + 21.91146\ \beta$
k	$16\ \alpha + 15.62390\ \beta$	$16\ \alpha + 20.74188\ \beta$
l	$16\ \alpha + 18.01114\ \beta$	$16\ \alpha + 21.73784\ \beta$
m	$16\ \alpha + 19.54688\ \beta$	$16\ \alpha + 21.54176\ \beta$
n	$18\ \alpha + 19.11696\ \beta$	$18\ \alpha + 24.02560\ \beta$
o	$18\ \alpha + 24.64104\ \beta$	$18\ \alpha + 26.52080\ \beta$
p	$18\ \alpha + 20.27118\ \beta$	$18\ \alpha + 24.40292\ \beta$

TABLA 3

Energías de Delocalización y de Resonancia

Molécula	$EDPE_{HMO}$	$EDPE_{POT}$	$EDPE_{ITPOT}$	$ERPE_{TPOT}$	$ERPE_{ITPOT}$	$ERPE^{(a)}_{Dewar}$	$ERPE^{(a)}_{Hess}$	$ER^{(b)}$	$ER/CC^{(c)}_{D-Marget}$	$ER/CC^{(c)}_{D-de Llano}$
a	0.385	0.128	0.326	−0.218	−0.019	0.090	0.039	0.319	0.105	0.077
b	0.366	0.074	0.033	−0.271	−0.016	0.041	0.018	−0.030	0.042	0.035
c	0.368	0.401	0.475	0.075	0.141	0.080	0.033	0.317	0.091	0.070
d	0.387	0.074	0.352	−0.295	−0.017	0.055	0.019	0.065	0.082	0.045
e	0.351	0.076	0.322	−0.258	−0.013	0.057	0.016	0.018	0.037	0.050
f	0.391	0.276	0.381	−0.081	0.025	0.095	0.034	0.334	0.080	0.080
g	0.389	0.233	0.389	−0.123	0.033	0.062	0.033	0.312	0.082	0.052
h	0.388	0.355	0.385	−0.001	0.029	0.071	0.032	0.317	0.081	0.060
i	0.372	0.115	0.336	−0.241	−0.020	0.038	0.016	0.034	0.040	0.032
j	0.406	0.178	0.369	−0.180	0.012	0.134	0.048	0.567	0.124	0.101
k	0.375	−0.024	0.296	−0.380	−0.060	−0.008	0.018	0.063	0.021	−0.006
l	0.377	0.126	0.359	−0.230	0.003	0.023	0.021	0.117	0.044	0.019
m	0.378	0.222	0.346	−0.134	−0.010	0.035	0.022	0.131	0.048	0.030
n	0.363	0.062	0.335	−0.284	−0.012	0.035	0.017	0.110	0.069	0.030
o	0.375	0.369	0.473	0.024	0.129	0.047	0.030	0.382	0.075	0.041
p	0.356	0.126	0.356	−0.220	−0.009	0.011	0.009	−0.078	0.033	0.010

(a) A. Das Gupta and N.K. Das Gupta, *Tetrahedron*, **28**, 3857 (1972), Tabla 6

(b) J. Aihara, *Bull. Chem. Soc. Japan*, **53**, 2689 (1980).

(c) A. Das Gupta and N.K. Das Gupta, *Theor. Chim. Acta*, **33**, 177 (1974), Tabla 2

TABLE 1

Elemental chemical analysis

Complex compounds	Ni %	Se %	C %	H %	N %	Cl %	O %	Total %	Cryst. H_2O %
	c/f	c/f	c/f	c/f	c/f	c/f	c/f	c/f	c/f
$[Ni_2CH_3COO(sesac)_2(H_2O)_2]CH_3COO\cdot 3H_2O$	17.29	23.24	21.21	4.71	12.36	—	21.19	100.00	7.95
	17.79	23.79	20.85	4.76	11.81	—	—	79.00	8.38
$[Ni(sesac)_2]\cdot 0.5H_2O$	13.93	37.45	22.78	4.03	19.92	—	1.89	100.00	2.13
	14.21	36.90	23.25	4.56	19.76	—	—	98.68	1.85
$[Ni(sesac)_2]$	14.23	38.26	23.28	3.88	20.35	—	—	100.00	—
	14.45	37.95	22.80	4.62	20.10	—	—	99.92	absent
$[Ni(sesac)_2Hsesac]$	9.93	40.10	24.40	4.24	21.33	—	—	100.00	—
	10.27	39.79	23.85	4.84	20.94	—	—	99.69	absent
$[Ni(Hsesac)_2H_2O]Cl_2\cdot 0.5H_2O$	11.45	30.81	18.74	4.10	16.39	13.83	4.68	100.00	1.75
	11.64	30.66	19.00	4.56	16.30	13.32	—	95.48	1.66

c = calculated ; f = found

TABLE 3

Characteristic IR frequencies (in cm^{-1}) and their assignment

Crt. nbr.	ν_{NH}	$\nu_{C=N}$	δ_{NH_2}	δ_{N-H} + ν_{C-N}	δ_{CH_3}	ν_{N-C-N}	ν_{N-N}	$\delta_{NH_2 twist.}$	$\nu_{C=Se}$	δ_{H_2O} *co-ordinated*	Low frequencies
1	Acetone selenosemicarbazone $(CH_3)_2C{=}N{-}NH{-}\underset{\underset{Se}{\Vert}}{C}{-}NH_2$										
	3340 vs 3200 vs 3120 vs	1650 m	1605 vs	1525 vs 1275 vs 1197 s	1475 s 1435 vs 1375 s	1115 vs	1030 m	865 m	775 s	—	615 vs 575 vs 535 s 495 m
2	$[Ni(sesac)_2]$										
	3375 s 3245 s 3130 s 3095 s	1630 vs		1558 s 1330 s 1275 m	1435 m 1371 m	1160 m	1010 w	750 m	692 m	—	—
3	$[Ni(sesac)_2] \cdot 0.5H_2O$										
	3365 s wide 3240 s 3130m 3090m wide	1625 s		1550 s 1325 s 1270 m	1430 w 1371w	1160 w	1010 w	750 m	692 m	—	600 — —400 m strongly extended band

Table 3 (continued)

4	$[Ni(Hsesac)_2H_2O]Cl_2 \cdot 0.5H_2O$									
	3350 m wide 3190 m 3095 m wide	1615 s	1570 m 1280 m	1435 m 1365 m	1165 w	1030 vw	750 w	692 w	735 w	575 w 515 w wide
5	$[Ni_2CH_3COO(sesac)_2(H_2O)_2]CH_3COO \cdot 3H_2O$									
	3420 m wide 3230 s 3140— —3090 s wide	1625 s	1550 vs wide 1332 m 1275 w	1435 s 1371 w	1160 w	1010 w	747 m	682 m	780 w	627 w 556 m wide
6	$[Ni(sesac)_2Hsesac]$									
	3365 s 3300 s 3230 s 3175 s 3127 s 3098 s	1625 vs	1550vs 1525 s 1330 s 1277 m	1476 w 1437 m 1375 m	1160 w 1115 w	1030 w 1010w	865 vw 750 w	775 w 690 w	—	615 m 575 m

Description of absorptions: vs = very strong, s = strong, m = medium, w = weak, vw = very weak.

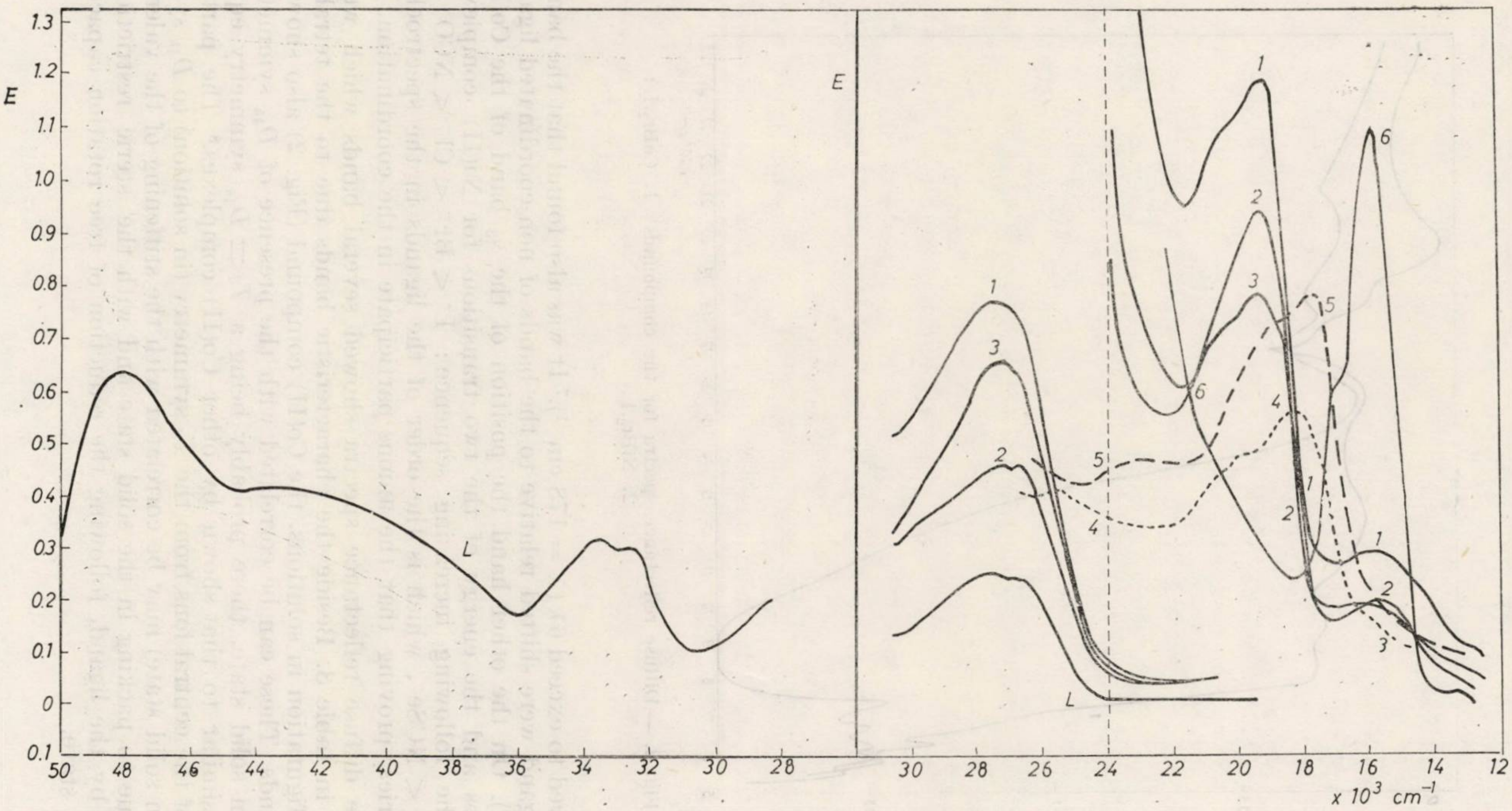

Fig. 1. — The absorption electronic spectra of compounds : L = ligand = A-TCH ; 1. $NiCl_2.L$; 2. $NiBr_2.L$; 3. $NiI_2.L$; 4. $CoCl_2.L$; 5. $CoBr_2.L$; 6. $Co(NCS)_2.L$.

TABLE 3

Assignments of the IR spectra of the ligand and complexes

Compound	$>C=O$		$C-O$	Pyrazolone			ring		$>C_4-NRR_1$	$M-N=C=S$		
					C_3-CH_3		N_2-CH_3		$R=CH_3$, $R_1=-CH_2-$			
	$\nu C=O$	$\delta O=C-N$	$\nu C-O$	$\nu C=C$ $\nu C=N$	νCH_3 as. sym.	δCH_3 as. sym.	νCH_3	δCH_3 as. sym.	$\nu C-N$	$\nu C\equiv N$ or νas, SCN	νCS or νs, SCN	δSCN
L	1630	627	—	1576 1543*	2997 2917	1460 1360	2827	1440 1316	1300 1127	—	—	—
$MnL(SCN)_2$	1607	630	1010	1563 1523*	2980 2943	1473 1353	2847	1436 1340	1303 1143	2027	853	473
$FeL(SCN)_2$	—	—	1010	1563 1537*	2980 2940	1473 1357	2847	1437 1340	1303 1150	2037	853	467
$CoL(SCN)_2$	1613	633	1013	1573 1550*	2993 2900	1480 1363	2853	1443 1350	1317 1130	2053	840	470
$NiL(SCN)_2$	1613	637	1010	1567 1543*	2993 2947	1480 1360	2853	1440 1340	1303 1150	2053	820	473
$ZnL(SCN)_2$	1617	637	1020	1573 1546*	2987 2953	1480 1360	2853	1443 1347	1310 1153	2047	863	483
$CdL(SCN)_2 \cdot 0.5Cd(SCN)_2$	—	—	1013	1567 1543*	2980 2940	1476	2880	1440 1343	1307 1147	2027	857	463
$CdLJ_2 \cdot 2CdJ_2$	—	—	1010	1567 1543*	2967 2933	1480 1360	2853	1440 1343	1307 1147	—	—	—
$HgLJ_2 \cdot 1.5HgJ_2$	—	—	1023	1577 1530*	2967 2940	1480 1363	2850	1447 1313	1150	—	—	—

*shoulder

TABLE 1

The characteristics of the studied samples

Sample	Experimental conditions				$\overline{M}_n$		$\overline{M}_w$		$[\eta]$ dl/g	$\overline{M}_w/\overline{M}_n$***	$\overline{M}_v$
	T°C	Time/h	Matrix / Monomer	Monomer / Water	GPC	0*	GPC	LS**			
A	−10	6.44	3.30	—	112 500	—	666 100	—	0.93	5.923	607 100
B	0	6.00	3.85	—	140 400	—	589 900	—	0.86	4.202	536 200
C	−20	6.00	3.85	—	87 600	—	494 900	—	0.75	5.65	430 500
D	0	4.00	2.75	—	97 950	—	517 900	—	0.78	5.30	453 900
E	−10	3.31	3.00	—	471 800	—	646 600	—	0.93	1.36	609 400
F	−10	5.00	2.00	—	62 600	—	521 700	—	0.76	8.30	434 900
G	−10	5.00	3.00	—	97 800	185 000	479 700	—	0.74	4.90	418 500
MVI	−10	3.26	—	0.33	83 400	—	412 100	—	0.66	4.84	347 100
MIX	−10	5.00	—	0.25	84 750	—	403 800	—	0.66	4.76	346 100
PI1	—	—	—	—	113 000	113 000	425 900	427 000	0.68	3.76	362 000
PI2	—	—	—	—	150 200	145 800	448 100	452 000	0.71	2.98	389 400

* Determined by osmometry;
** Determined by light scattering;
*** From GPC data.

Table 2

Electronic spectra of the series I–II

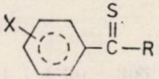

X	Solvent**	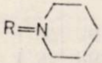						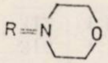						Solvent**	R = NH_2					
		$n \rightarrow \pi^*$		$(\pi \rightarrow \pi^*)_1$		$(\pi \rightarrow \pi^*)_2$		$n \rightarrow \pi^*$		$(\pi \rightarrow \pi^*)_1$		$(\pi \rightarrow \pi^*)_2$			$(n \rightarrow \pi^*)$		$(\pi \rightarrow \pi^*)_1$		$(\pi \rightarrow \pi^*)_2$	
		λ(nm)	ε	λ(nm)	ε	λ(nm)	ε	λ(nm)	ε	λ(nm)	ε	λ(nm)	ε		λ(nm)	ε	λ(nm)	ε	λ(nm)	ε
p-NO_2	a	375	3.39	314	4.07	266	4.27	—	—	307*	3.86	264*	4.24							
	h	391	3.14	326	3.80	259	4.22	400	sh	320	3.66	259	4.04							
m-NO_2	a	—	—	280	4.12	256	4.20	—	—	281	4.08	252	4.18							
	h	397	2.70	290	3.95	254	4.17	398	sh	290	4.00	250	4.16							
p-Cl	a	365	2.60	282	4.05	248	4.11							a	380*	2.44	304*	3.80		
	h	401	2.60	288	3.86	255	3.94							c	415*	2.44	306*	3.88		
H	a	363*	2.47	285*	4.07	242	4.01	366*	2.60	287*	4.05	235	4.00	a	370*	2.40	296*	3.85	241	3.97
	h	400	2.48	293	3.97	252	3.91	400	2.30	291	3.68	249	3.65	c	412*	2.40	298*	3.81	239	3.94
p-CH_3CONH	a	364	3.11	271	4.43	245	4.41	370	2.90	273	4.38	219	4.14							
	h																			
o-OH	a	362	2.70	283	4.20	239	3.89	362	2.60	284	4.15	240	3.86							
	h	388	2.87	296	4.06	244	3.90	389	2.84	296	4.02	245	3.90							
p-OH	a	369	2.82	282	4.23	239	3.92													
		—	—	291	4.18	282	—													
o-OCH_3	a	363	2.47	284	3.76	244	3.52	369	2.60	286	4.20	244	3.90							
	h	394	2.52	288	3.22	249	3.20	389	2.80	289	4.10	249	3.80							
p-OCH_3	a	365	2.84	279	4.22	243	3.99	369	2.84	281	4.20	238	3.93	a	375*	2.65	306*	4.04		
	h	401	2.77	283	4.13	256	4.09	403	2.70	282	4.12	255	4.03	c	407*	2.64	316*	4.19		
p-$N(CH_3)_2$	a	373	3.55	291	4.26	263		374	3.65	293	4.21	253	3.99							
	h	405	3.07	294	4.29	263		408	3.20	298	4.28	258	3.96							

* Literature data [8–11]

** Solvent: a) ethanol h) heptane c) carbon tetrachloride

Table 3

Electronic spectra of the series III–IV 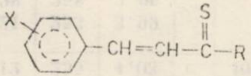

X	Solvent**	R=N 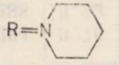								R=N 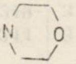								R=NH$_2$			
		n → π*		(π→π*)$_1$		(π → π*)$_2$		(π → π*)$_3$		n→ π*		(π → π*)$_1$		(π → π*)$_2$		(π → π*)$_3$		n → π*		(π → π*)$_1$	
		λ(nm)	ε	λ(nm)	ε	λ(nm)	ε	λ(nm)	ε	λ(nm)	ε	λ(nm)	ε	λ(nm)	ε	λ(nm)	ε	λ(nm)	ε	λ(nm)	ε
p-NO$_2$	a											322	sh	280	4.34						
	h																				
m-NO$_2$	a			270	4.44									272	4.40						
	h			280	4.31	266	4.34	255	4.34					280	4.40						
p-Cl	a	385sh		300	4.33	288	4.37	228	4.11	395	sh	295	4.34			227	4.10	430*	2.44	337*	3.91
	h			309	4.20	299	4.29	254	4.06			307	4.30			250	4.10				
o-Cl	a					283	4.30	254	4.15			300	4.23	286	4.30	234	4.13			337	3.81
	h					279	4.22	251	4.12					282	4.21	247	4.07				
H	a	385sh		288*	4.32			222	4.13	385	sh	294*	4.32			228	4.11	420*	2.49	330*	3.82
	h			295	4.27	284	4.31	244	4.04			297	4.23	287	4.27	244	3.96				
p-CH$_3$CONH	a			315	4.41	306	4.40	234	4.19			294	4.35			238	4.10			345	4.15
	h																				
p-OCH$_3$	a			316	4.35	304	4.34	230	4.15			315	4.27	304	4.26	330	4.10	425*	2.63	342*	4.12
	h			312	4.27	301	4.28	282	4.12			312	4.20	300	4.22	230	4.05				
o-OCH$_3$	a											326	4.27	294	4.30	237	4.23				
	h											321	4.30	302	4.30	238	4.28				

* Literature data [8–11]

** Solvent : a) ethanol h) heptane c) carbon tetrachloride

Table 1

Experimental and calculated ESR parameters (G)

Anion radical		$a_N^{NO_2}$	a_H^2	a_H^3	a_H^4	a_H^5	a_H^6	a_N^{NH}	a_H^{NH}	g-factor	Line-width
1	exp.	11.25	—	3.38	1.20	3.58	0.82	<0.45	<0.45	2.0044	0.45
	calc.	9.71	—	3.92	1.32	4.22	0.86	0.04* 0.51** 0.46***	0.05*		
2	exp.	10.50	3.39	—	3.39	1.08	3.85	<0.30	0.36	2.0047	0.30
	calc.	9.41	3.79	—	3.37	1.15	4.11	0.11* 0.26** 0.23***	0.13*		
3	exp.	10.55	1.27	3.48	—	3.48	1.27	0.70	1.16	2.0048	0.27
	calc.	10.02	1.26	3.56	—	3.56	1.26	0.10* 0.70** 0.63***	0.12*		
4-nitroaniline	exp.[10]	11.49	1.08	3.38	—	3.38	1.08	1.08	0.89	—	—
3-nitroaniline	exp.[10]	10.13	3.46	—	3.01	0.96	3.62	0.21	0.31	—	—
p-nitrothio-benzoyl-morpholide	exp.[3]	8.25	1.00	3.24	—	3.24	0.85	0.70	0.70	2.0046	0.49
m-nitrothio-benzoyl-morpholide	exp.[3]	9.77	3.53	—	3.53	1.12	4.28	0.56	0.56	2.0047	0.56

* Calculated with formula (3), ** — formula (4), *** — formula (5) — (Table 2)

Table 1

2,4,6-Trimethylpyridinium perchlorates (II, R′ = R″ = Me)

Comp.	R	M.p. °C	Formula	N % Calc.	N % Found	Cl % Calc.	Cl % Found	Recryst. solvent	Synthesis method
1	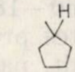	217	$C_{11}H_{18}ClNO_4$	4.82	5.07	12.24	12.50	a	B
2	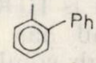	190	$C_{20}H_{20}ClNO_4$	3.74	4.00	9.49	9.35	a	A
3	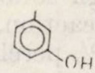	156	$C_{14}H_{16}ClNO_5$	4.45	4.70	11.30	11.50	a	A
4	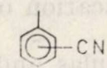	*o* 181	$C_{15}H_{15}ClN_2O_4$	8.67	8.90	10.99	11.25	b	C
5		*m* 225	$C_{15}H_{15}ClN_2O_4$	8.67	8.82	10.99	11.10	b	A
6		*p* 188	$C_{15}H_{15}ClN_2O_4$	8.67	8.43	10.99	10.80	a	A
7	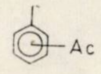	*o* 195	$C_{16}H_{18}ClNO_5$	4.11	4.00	10.44	10.58	a	A
8		*m* 191	$C_{16}H_{18}ClNO_5$	4.11	4.35	10.44	10.60	a	A
9		*p* 146	$C_{16}H_{18}ClNO_5$	4.11	4.20	10.44	10.35	a	A
10	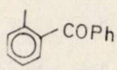	165	$C_{21}H_{20}ClNO_5$	3.48	3.50	8.83	9.00	a	A
11	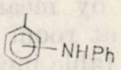	*o* 211	$C_{20}H_{21}ClN_2O_4$	7.20	7.45	9.12	9.30	a	A
12		*p* 270	$C_{20}H_{21}ClN_2O_4$	7.20	7.00	9.12	9.05	c	A
13	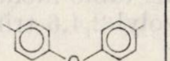	220	$C_{28}H_{30}ClN_2O_5$	4.59	4.75	11.64	11.80	d	A
14	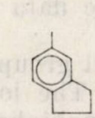	119	$C_{17}H_{20}ClNO_4$	4.14	4.40	10.50	10.25	b	A
15	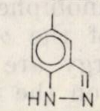	185	$C_{15}H_{17}ClN_3O_4$	12.39	12.50	10.47	10.65	a	B
16	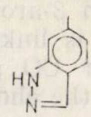	220	$C_{15}H_{17}ClN_3O_4$	12.39	12.42	10.47	10.32	e	B
18	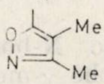	134	$C_{13}H_{17}ClN_2O_5$	8.84	9.00	11.21	11.50	a	A
17	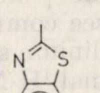	168	$C_{16}H_{17}ClN_2SO_5$	7.28	7.50	9.23	9.15	b	A

a = i-PrOH, b = EtOH, c = H₂O : AcOH (1 : 1), d = i-PrOH : H₂O (3 : 1), and e = i-PrOH : AcOH (3 : 1).

Table 1

2[2-(3-benzoxazolium-3-ethiodide)] indolo-quinolinium-1-ethiodide cyanine dyes (VII,1—10)

Comp. VII N°	Formula	Solvent for crystallisation	Time of reflux (h)	m.p. °C	Yield %	Analysis % Calcd.	Analysis % Found	Absorption spectra in ethanol 95 %
						N	N	$\lambda_{nm_{max.}}(\varepsilon_{max})$
1	$C_{28}H_{25}N_3OI_2$	Ethanol	13	343	65	6.24	6.43	210(128000), 240(100000), 300(40000), 475(5600).
2	$C_{29}H_{27}N_3O_2I_2$	Aqueous ethanol	14	230	70	6.11	6.36	210(182000), 245(138000), 300(84000), 580(8900).
3	$C_{29}H_{27}N_3O_2I_2$	Aqueous ethanol	14	266	72	5.97	5.82	220(117000), 250(68000), 300 (37000), 510(6400), 575(5800).
4	$C_{28}H_{24}N_3OClI_2$	Ethanol	11	276	60	5.94	6.05	207(159000), 238(123000), 295(65000), 460(10100).
5	$C_{28}H_{24}N_4O_3I_2$	Ethanol	10	328	65	7.80	7.72	208(318000), 238(381000), 291 (152000), 465(90000), 486(45000).
6	$C_{29}H_{25}N_3O_3I_2$	Methanol	12	305	75	5.86	5.69	212(118000), 240(108000), 270 (64000), 290(46000), 565(8500).
7	$C_{29}H_{25}N_3O_3I_2$	Ethanol	13	315	70	5.86	5.58	210(13000), 242(108000), 270 (64000), 325(30000), 580(6500).
8	$C_{29}H_{25}N_3O_2I_2$	Ethanol	16	267	75	6.10	6.34	212(179000), 242(161000), 300 (60000), 445(43000), 510(14000).
9	$C_{32}H_{27}N_3OI_2$	Ethanol	18	335	70	5.81	5.97	218(172000), 245(122000), 320(47000), 580(8000).
10	$C_{32}H_{27}N_3OI_2$	Methanol	20	270	65	5.81	5.65	220(332000), 245(208000), 300(100000), 540(28000).

Table 1

^{13}C-NMR Spectra of the alkyne intermediates

Compound		chemical shifts (δ, ppm) of carbons in positions											
		1	2	3	4	5	6	7	8	9	10	11	12
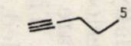	IB	68.4	84.5	20.5	22.0	13.4	—	—	—	—	—	—	—
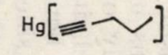	IIIB	109.0	111.2	21.8	22.3	13.7	—	—	—	—	—	—	—
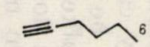	IC	68.4	84.9	18.3	30.9	21.9	13.5	—	—	—	—	—	—
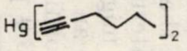	IIIC	109.0	111.0	19.2	30.8	21.8	13.5	—	—	—	—	—	—
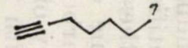	ID	68.1	84.6	18.5	28.4	31.1	22.3	14.0	—	—	—	—	—
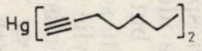	IIID	109.5	111.0	19.8	28.7	31.3	22.3	14.0	—	—	—	—	—
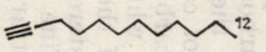	IE	68.5	85.0	18.6	28.9	30.0	29.2	29.5	30.0	29.7	32.3	23.0	14.2
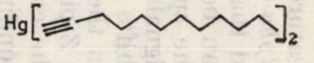	IIIE	108.5	111.0	19.6	29.1	29.8	29.1	29.3	29.8	29.5	32.3	22.8	14.2

Table 2

^{13}C-NMR Spectra of the protected *omega*-bromo-alcohols

Compound		chemical shifts (δ, ppm) of carbons in positions											
		2′	1′	1	2	3	4	5	6	7	8	9	10
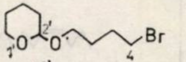	IVa [a] (n = 4)	98.8	—	62.2	30.8	28.4	33.5	—	—	—	—	—	—
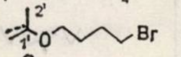	IVb (n = 4)	27.9	73.0	61.0	30.4	29.7	34.2	—	—	—	—	—	—
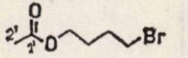	IVc	21.1	172.2	63.6	29.8	27.7	33.5	—	—	—	—	—	—
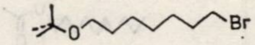	IVb (n = 7)	27.9	72.8	61.8	31.0	28.4	29.0	33.3	26.4	34.1	—	—	—
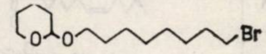	IVa [a] (n = 8)	98.7	—	62.0	30.8	28.2	29.5	29.3	32.9	26.3	33.5	—	—
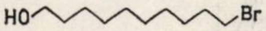		—	—	62.6	32.7	28.2	29.5	29.4	29.4	28.8	32.9	25.8	33.7
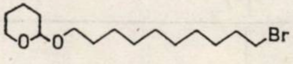	IVa [a] (n = 10)	98.9	—	62.1	30.8	28.2	29.5	29.5	29.5	28.8	32.9	26.2	33.7
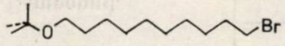	IVb (n = 10)	27.6	72.3	61.6	30.7	28.2	29.4	29.5	29.5	28.8	32.9	26.3	33.6

[a] chem. shifts of the other carbons in the protecting group (position/δ, ppm) : 3′/25.6 ; 4′/19.6 ; 5′/29.8–29.9 ; and 6′/67.4–68.4 ;

Table 3

^{13}C-NMR Spectra of the alkenolic pheromones (VII, VIII) and of their alkynic precursors (V)

Compound		chemical shifts (δ, ppm) of carbons in positions																		
		2′	1′	1	2	3	4	5	6	7	8	9	10	11	12	13	14	15	16	17
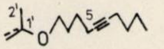	VCb (n = 4)	28.0	73.0	61.5	30.4	26.5	19.0	80.9	81.2	18.8	31.8	22.3	13.8	—	—	—	—	—	—	—
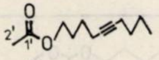	VCc (n = 4)	21.0	171.6	64.4	28.3	27.0	18.7	79.7	81.2	18.7	31.8	22.2	13.7	—	—	—	—	—	—	—
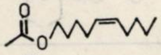	VIIC (n = 4)	21.0	172.2	64.8	28.6	26.4	27.1	130.2	131.4	27.3	32.3	22.6	14.1	—	—	—	—	—	—	—
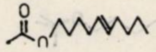	VIIIC (n = 4)	21.1	171.6	64.8	28.5	26.2	32.5	130.2	131.7	32.6	32.3	22.4	14.1	—	—	—	—	—	—	—
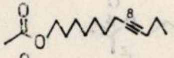	VBc	21.0	171.3	64.2	29.0	26.2	29.0	29.1	29.5	18.9	79.8	79.8	21.0	22.9	13.6	—	—	—	—	—
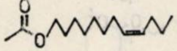	VIIB	21.0	171.6	64.8	28.8	26.0	29.8	29.4	29.4	27.3	129.6	129.8	29.3	23.0	13.8	—	—	—	—	—
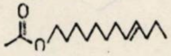	VIIIB	21.1	171.0	64.8	28.8	26.1	29.7	29.3	29.2	32.8	130.6	130.8	35.0	22.9	13.7	—	—	—	—	—
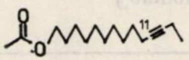	VAc	21.3	174.0	66.0	29.6	26.7	30.3	30.3	29.9	29.9	30.0	29.3	19.3	83.4	81.3	12.8	14.8	—	—	—
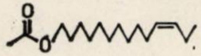	VIIA	20.9	171.1	64.7	28.7	26.0	29.6	29.6	29.6	29.3	29.3	29.8	27.2	129.4	131.6	20.8	14.4	—	—	—

Table 3 (continued)

Compound		chemical shifts (δ, pmm) of carbons in positions																		
		2′	1′	1	2	3	4	5	6	7	8	9	10	11	12	13	14	15	16	17
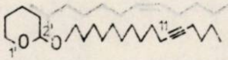	VCa (n = 10)	98.8[a]	—	62.3	28.9	26.3	29.6	29.6	29.6	29.8	29.2	29.2	18.8	80.3	80.3	18.5	31.3	22.0	13.7	—
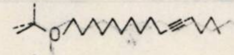	VCb (n = 10)	27.6	72.3	61.7	30.8	26.3	29.6	29.6	29.6	29.2	29.2	28.9	18.8	80.1	80.1	18.5	31.4	22.0	13.7	—
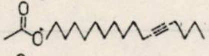	VCc (n = 10)	21.0	171.4	64.7	28.6	25.9	29.4	29.4	29.2	29.2	29.2	28.8	18.7	80.1	80.1	18.4	31.3	21.9	13.6	—
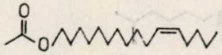	VIIC (n = 10)	20.9	171.2	64.7	28.7	26.0	29.6	29.6	29.6	29.3	29.3	29.8	27.2	129.9	129.9	27.0	32.0	22.4	14.0	—
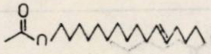	VIIIC (n = 10)	20.9	171.1	64.6	28.7	26.0	29.6	29.6	29.6	29.3	29.3	29.2	31.9	130.3	130.3	32.6	32.3	22.2	14.0	—
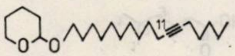	VDa (n = 10)	98.8[a]	—	62.2	28.9	26.3	29.6	29.6	29.6	29.2	29.2	28.9	18.8	80.2	80.2	18.8	29.8	31.2	22.3	14.0
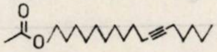	VDc (n = 10)	21.0	171.3	64.7	28.6	25.9	29.5	29.5	29.2	29.2	29.2	28.9	18.8	80.2	80.2	18.8	29.5	31.1	22.3	14.0
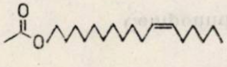	VIID (n = 10)	21.0	171.2	64.7	28.7	26.0	29.6	29.6	29.6	29.6	29.3	29.3	27.2	129.9	129.9	27.2	29.8	31.6	22.6	14.1

[a] chem. shifts of other carbons in the protecting group: (pos/δ, ppm) 3′/25.6 ; 4′/19.7 ; 5′/30.8 and 6′/67.7 ;

Table 4

^{13}C-NMR Spectra of the 2-methyl octadecane derivatives and of some precursor synthons

Compound	chemical shifts (δ. ppm) of carbons in positions											
	1	2	3	4	5	6	7	8	9	16	17	18
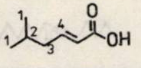	22.5	27.7	41.4	151.8	122.5	173.4	—	—	—	—	—	—
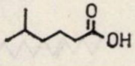	22.5	27.9	38.5	22.8	34.6	180.9	—	—	—	—	—	—
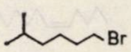	22.5	26.0	38.0	33.0	27.8	33.5	—	—	—	—	—	—
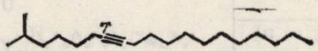 VE	22.8	26.9	38.7	28.2	a,	19.0	80.5	80.5	19.0	32.2	22.9	14.2
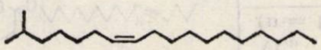 VIIE	22.9	27.5	39.0	28.5	b,	27.7	131.0	131.0	27.7	32.5	23.1	14.3
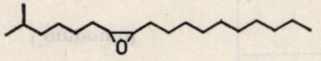 IX[c]	22.8	26.9	39.0	29.6	27.6	28.2	57.3	57.3	28.2	32.2	22.9	14.2

[a] carbons in pos. 5, 10–15 included in a pattern of signals at 29.2, 29.5, 29.6 and 29.9 ppm;
[b] carbons in pos. 5, 10–15 included in a pattern of signals at 29.9, 30.2, 30.3 and 30.6 ppm;
[c] carbon in pos. 10 at 27.1, carbons in positions 11–15 at 29.9 ppm;

Compounds VII, VIII and IX are components of the pheromone blends released by the females of a large number of lepidopterous pests; among these, most important for our country are the following: *Adoxophies orana* [27] (VIIA), *Agrotis segetum* [27] (VIIC $n = 4$), *Anarsia lineatella* [29] (VIIIC), *Grapholitha funebrana* [30] (VIIB, VIIIB) *Grapholitha molesta* [31] (VIIB, VIIIB), *Lymanthria dispar* [32] (IX), *Lymanthria monacha* [33] (IX), *Mamestra brassicae* [34,35] (VIIC, VIID, VIIIC $n = 10$), *Ostrinia nubilalis* [36] (VIIA), *Pammene* spp. [37] (VIIB), *Pandemis heparana* [38] (VIIA), *Peridroma saucia* [39] (VIIC, $n = 10$) and *Tortrix viridana* [40] (VIIA). All pheromonal compounds synthetized as described in this work were experimented and successfully used for practical field survey (and partly for direct control too) of the above pests for periods up to seven years.

EXPERIMENTAL

Mass spectra were recorded on a Varian MAT SN-1 spectrometer at 70 eV and a source temperature of 210°, coupled to a Perkin-Elmer 990 gas-chromatograph. NMR-Spectra were recorded on a Bruker WP-60 FT-NMR instrument equipped with a 14.1 kG electromagnet (60 MHz for ^{1}H, 15.086 MHz for ^{13}C); samples were dissolved in $CDCl_3$ and chemical shifts are related to internal TMS. GLC-Analyses were performed on a Perkin-Elmer F 11 instrument

No details on the syntheses of compounds I(A–E), III(A–E) and IVa, c, d are included here. In preparing these compounds the reported procedures (as indicated above) were generally found satisfactory, even if in some cases during repeated execution we have found some minor modifications to be practical.

Preparation of the omega-bromo-alkan-1-ol t-butyl ethers, IVb: 0.12 Moles *omega*-bromoalkan-1-ol and 150 ml of methylene chloride were placed in an autoclave of 500 ml capacity. The vessel and its content were cooled to −20° and 150 ml of liquid isobutylene were added, followed by 1.5 ml of concd. sulphuric acid. The sealed autoclave was shaken at room temperature for 8 hours. The reaction mixture was then washed with saturated aqueous $NaHCO_3$, the organic layer separated, decolorated with active charcoal and dried over Na_2SO_4. The solution was filtered over a small column filled with active alumina and the solvent removed *in vacuo*. The purity of the product was checked by GLC; usually it could be used in the next step without further purification. The yields ranged between 70–80 %. The samples afforded characteristic ^{1}H-NMR signals at the following δ values: 1.13–1.20 (s, 9H, $-C(CH_3)_3$), 3.31–3.41 (*t*, 2H, $J = 6.0-6.3$ Hz, $-O-CH_2-$), 3.43–3.47 (*t*, 2H, $J = 6.3-6.5$ Hz, $-CH_2-Br$).

Preparation of the alkyn-1-ol t-butyl or tetrahydropyranyl ethers, V(ABCD)(ab): To 15 mmoles of dialkynyl mercury (III) in 40 ml of diglyme, 0.22 g (0.031 gram-atom) of lithium were added. The mixture was heated for 2 hours at 80–100° under inert atmosphere. Without removing the precipitated mercury, 30 mmoles of the appropriated *omega*-bromo-alkan-1-ol *t*-butyl or tetrahydropyranyl ether IVa, b were added dropwise under stirring. The temperature was raised to 100–110° and the stirring continued for 3–5 hours. After cooling to room temperature the solution was decanted, diluted with water and extracted with ethyl ether. The ethereal solution was dried over $MgSO_4$, filtered, the solvent and other volatiles were removed *in vacuo*. The product (yields ranged between 70–80 %) was used in the next step without purification.

Preparation of the alkyn-1-ol acetates, V(ABCD)c: The appropriated *t*-butyl or tetrahydropyranylether V(ABCD)(ab), (20 mmoles) was dissolved in 20 ml of a 1 : 10 mixture of acetyl chloride and glacial acetic acid, and kept at 25–40° for 48 hours. The solution was poured onto ice, extracted with hexane, washed with water and with aqueous $NaHCO_3$. After drying over $MgSO_4$, the solvent was removed and the residue distiilied *in vacuo*. Yields: 75–85 %. ^{1}H-NMR: 2.08 (s, 3H, $-CO-CH_3$), 4.13–4.18 (*t*, 2H, $J = 6.0-6.3$ Hz, $-O-CH_2-$), 0.93–1.13 (*t*, 3H, $-CH_2-CH_3$). *5-Decyn-1-ol acetate* (VCc $n = 4$): b.p. 68–70°/1 mm, $n^{19} = 1.4408$; *8-dodecyn-1-ol acetate* (VBc): b.p. 103°/0.2 mm, $n^{20} = 1.4490$; 11 *tetradecyn-1-ol acetate* (VAc): b.p. 99°/0.07 mm, $n^{22} = 1.4510$; *11-hexadecyn-1-ol acetate* (VCc $n = 10$): b.p. 128°/0.1 mm, $n^{22} = 1.4540$; *11-heptadecyn-1-ol acetate* (VDc): b.p. 129–131°/ /0.1 mm, $n^{20} = 1.4547$.

7-Methyl-7-hydroxy-5,8-tridecadiyne, VI : To 1.6 g (4.4 mmoles) of di-*n*-hexynyl-mercury (IIIC) in 15 ml of diglyme 70 mg (10 matg) of lithium were added. The mixture was heated to 80—100° under inert atmosphere for 2 hours. After cooling to room temperature and without removing the precipitated mercury metal, 1.60 g (8.8 mmoles) of crude 4-bromo-butan-1-ol acetate IVc (or 2.15 g of 4-iodo-butan-1-ol acetate) were added dropwise. After 3h 'shaking the mixture was kept overnight at room temperature, then diluted with water and extracted with ether. The extract was dried over $MgSO_4$ and the solvent removed, obtaining 1.4 g (89 %) of VI, b.p. 120°/3 mm, $n^{20} = 1.4720$.

Hydrogenation of the alkyn-1-ol acetates V(ABCD)c to Z-alken-1-ol acetates, VII(A—D) : A solution of 0.32 g $Ni(CH_3COO)_2$ in 10 ml of ethanol was treated with 1.4 ml of a molar solution of $NaBH_4$ in ethanol. Ethylene diamine (1.15 ml) and 10 mmoles of alkyn-1-ol acetate V(ABCD)c were added and the mixture stirred under hydrogen at room temperature and atmospheric pressure, until the hydrogen uptake ceased. After filtration, the solution was concentrated, diluted with water and extracted with ether. The ethereal solution was washed with water and dried over $MgSO_4$. The solvent was removed and the residue distilled *in vacuo*. The purity of the alken-1-ol acetates VII(A—D) was checked by GLC. Yields : 90—95 %. The progress of the hydrogenation was monitored by TLC on silica gel G, using as eluent mixtures of hexane : ether (from 4 : 1 to 7 : 1) and detecting the spots with iodine vapours. ^{1}H-NMR : 2.03 (2, 3H, $-CO-CH_3$), 4.05 (*t*, 2H, $J = 6.0-6.1$ Hz, $-O-CH_2-$), 5.33—5.35 (m, 2H, $-CH{=}CH-$), 0.90—0.95 (*t*, 3H, $J = 7.0$ Hz, $-CH_2-CH_3$). *Z-5-Decen-1-ol acetate* (VIIC $n = 4$) : b.p. 73—75°/3 mm, $n^{21} = 1.4410$, MS : (*m/e*) 138 $(M\text{-}60)^+$, 110, 95, 81, 67, 54, 43 ; *Z-8-dodecen-1-ol acetate* (VIIB) : b.p. 65—70° 0.01 mm, $n^{20} = 1.4439$, MS : 166 $(M\text{-}60)^+$, 138, 123, 110, 96, 82, 67, 61, 55, 43 ; *Z*-11-*tetradecen*-1-*ol acetate* (VIIA) :, b.p. 88—92°/0.07 mm, $n^{20} = 1.4470$, MS : 194 $(M\text{-}60)^+$, 166, 138, 124, 109, 96, 82, 67, 61, 55, 43 ; *Z*-11-*hexadecen*-1-*ol acetate* (VIIC $n = 10$) : b.p. 130—132°/0.02 mm, $n^{20} = 1.4484$, MS : 222 $(M\text{-}60)^+$, 180, 166, 162, 138, 124, 110, 96, 82, 67, 61, 55, 43 ; *Z*-11-*heptadecen*-1-*ol acetate* (VIID) : $n^{20} = 1.4518$.

Preparation of the E-alkenol acetates VIIIB (n = 7) and VIIIC (n = 4, 10) by reduction of the corresponding alkynol derivatives (V) with sodium in liquid ammonia (exemplified on VIIIC $n = 4$) : 5-Decyn-1-ol *t*-butyl ether (VCb $n = 4$), (140 mmoles) in 400 ml of THF was added dropwise within 1 hour to a solution of 8 g sodium in 400 ml of liquid ammonia. The mixture was stirred for 6 hours, then 20 g of NH_4Cl were added and the ammonia evaporated. The remaining THF solution was concentrated *in vacuo*, the residue treated with ice and extracted with ether. The ethereal solution was washed with water, dried over $MgSO_4$ and the solvent removed. The purity of the crude reduction product was checked by TLC on silica gel G (hexane : ether 10 : 1, detection with methyl red), or quantitatively by GLC (NPGS, 2 m × 4 mm, 180°, $t_R = 5.3$ min.) ; values about 93 % were found. The *E*-5-decen-1-ol *t*-butyl ether thus obtained was treated with 140 ml of an 1 : 10 mixture of acetyl chloride : acetic acid and kept at 35—40° for 48 hours. The resulting dark solution was poured onto ice and extracted with hexane. The extract was washed successively with water, $NaHCO_3$ solution, water again, and dried over $MgSO_4$. The solvent was removed and the residue distilled *in vacuo*, yield 70 %.

Preparation of the E-alkenol acetates VIIIA, VIIIB and VIIIC (n = 4,10) from their Z-isomers through inversion of configuration (exemplified on VIIIC $n = 4$) : *Z*-5-Decen-1-ol acetate (VIIC $n = 4$), (14 mmoles) was treated with an ethereal solution of monoperphthalic acid (17 mmoles) and allowed to stand at room temperature for 24 hours. The precipitated phthalic acid was filtered off, the filtrate washed with 10 % $NaHSO_3$ solution, then with diluted NaOH. After drying over $MgSO_4$ the solvent was removed. The crude *Z*-5,6-epoxidecan-1-ol acetate thus obtained (15 mmoles) was analyzed by GLC (SE 30, 2m × 4 mm, 160°). To a chilled solution of 4.4 g (16.5 mmoles) of triphenylphosphine in 50 ml of methylene chloride 2.7 g (16.5 mmoles) of bromine in 10 ml of methylene chloride were added dropwise. The methylene chloride was then removed and replaced with 60 ml of benzene. The above obtained crude epoxide was added and the solution stirred at room temperature for 4 hours. The solvent was removed and the residue taken up in petroleum ether. The insoluble triphenylphosphinoxide was filtered off, and the solvent removed *in vacuo*. The purity of the crude *vic*-5,6-dibromo-decan-1-ol acetate (12.5 mmoles) thus obtained was checked by GLC (SE 30, 2m × × 4 mm, 180°). To a chilled suspension (5—10°) of 4 g activated zinc powder in 40 ml of DMF containing a few drops of acetic acid, the above obtained crude *vic*-dibromide was added. The mixture was stirred at the same temperature for 2 hours, diluted with water and extracted with hexane. The extract was washed with water, dried, and the solvent evaporated. The residue consisted of 11 mmoles of crude *E*-5-decen-1-ol acetate (VIIIC $n = 4$), containing 98 % of the *E*-isomer as determined by GLC (DPTA, 50 m capillary, 115°, $t_R = 93$ min (*E*), $t_R = 91.6$ min

(*Z*)). This compound could be further purified by distillation, affording a product identical (physical constants, GLC, MS, ^{13}C-NMR) to the samples obtained through reduction as described above.

^{1}H-NMR of the *E*-alkenol acetates (VIII) : 2.03—2.04 (s, 3H, $-CO-CH_3$), 4.06—4.07 (*t*, 2H, $J = 6.0$ Hz, $-O-CH_2-$), 5.43—5.56 (m, 2H, $-CH=CH-$, significantly deshielded as compared to the isomeric *Z*-alkenol acetates VII), 0.90—0.98 (*t*, 3H, $J = 7.5$ Hz, $-CH_2-$ $-CH_3$).

E-5-Decen-1-ol acetate (VIIIC $n = 4$) : b.p. 42—50°/0.03 mm, $n^{20} = 1.4390$, MS : 138 $(M-60)^+$, 110, 95, 81, 67, 61, 54, 43 : *E-8-dodecen-1-ol acetate* (VIIIB) : b.p. 78—81/0.04 mm, $n^{20} = 1.4431$, MS : 166 $(M-60)^+$, 138, 124, 110, 96, 82, 67, 61, 55, 43 ; *E-11-tetradecen-1-ol acetate* (VIIIA) : b.p. 97—100°/0.06 mm, $n^{25} = 1.4457$, MS : 194 $(M-60)^+$, 138, 124, 110, 96, 82, 68, 61, 55, 43 ; *E-11-hexadecen-1-ol acetate* (VIIIC $n = 10$) : b.p. 108—110°/0.05 mm, $n^{20} = 1.4505$, MS : 222 $(M-60)^+$, 194, 180, 166, 152, 138, 124, 110, 96, 82, 67, 61, 55, 43.

2-Methyl-7-octadecane, VE : Di-*n*-dodecynyl mercury, IIIE (9.8 g, 18 mmoles) in 50 ml of diglyme was treated with 0.26 g (0.037 m-g-atoms) of lithium under inert atmosphere at 100—110° for 2 hours. 1-Bromo-5-methyl hexane (7.3 g, 40 mmoles) was added dropwise during 45 min, then the temperature raised to 120—130° under stirring for 6 hours. The mixture was left overnight, decanted, diluted with water and extracted with ethyl ether. The ethereal solution was washed to neutral and dried over $MgSO_4$. The solvent was removed and the residue distilled *in vacuo*, b.p. 120—125°/0.1 mm, yielding 7.8 g (80 %) of VE, $n^{20} = 1.4508$.

2-*Methyl-Z-7-octadecene, VIIE* : this compound was obtained from 2-methyl-7-octadecyne (VE) b) hydrogenation using Ni P-2/EDA catalyst, as described above for *Z*-alkenol acetates (VII). Yield : 98 %, b.p. 127—129°/1 mm, $n^{20} = 1.4482$, *Z*/*E*-ratio 9 : 1, determined by GLC (OV-17, 100 m capillary, 162°, $t_R = 52.2$ min (*Z*), $t_R = 53.7$ min (*E*)) ; ^{1}H-NMR : 1.09 (d, 6H, $J = 6.0$ Hz, $(CH_3)_2CH-$), 2.25 (m, 4H, ($J = 5$ Hz, $-CH_2-CH=CH-CH_2-$), 5.50 (*t*, 2H, $J = 5$ Hz, $-CH=CH-$), 1.08 (*t*, 3H, $J = 7.5$ Hz, $-CH_2-CH_3$) ; MS : 266 $(M)^+$, 251, 238, 210, 182, 168, 147, 133, 125, 111, 97, 83, 69, 57, 43.

Z-7,8-Epoxy-2-methyl-octadecane, IX : 2-Methyl-*Z*-7-octadecene (VIIE), 7.7 g (30 mmoles), was treated with 68 ml of an ethereal solution of minoperphthalic acid (1 ml containing 93 mg of peracid) and kept at room temperature for 24 hours. The mixture was then filtered, the filtrate washed successively with 10 % $NaHCO_3$, diluted NaOH and water. After drying over $MgSO_4$, the solvent was removed. Yield : 95 %, purity 98 %, determined by GLC (OV-17, 1.8 m × 2 mm), b.p. 90—100°/0.0001 mm, $n^{19} = 1.4464$; ^{1}H-NMR : 0.88 (d, 6H, $J = 5.5$ Hz $(CH_3)_2CH-$), 2.68 (m. 2H, 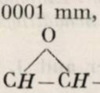 $-\overbrace{CH-CH}^{O}-$), 0.86 (*t*, 3H, $-CH_2-CH_3$). The progress of epoxidation could be monitored by TLC on silica gel G, eluting with cyclohexane : methylene chloride 5 : 1 and detecting with phosphomolybdenic acid.

REFERENCES

[1] Part V : N. Popovici, A. A. Botar, A. Barabás, I. Oprean and F. Hodoşan, *J. prakt. Chem.*, (1982), in press.

[2] M. Jacobson, "Insect Sex Pheromones", Acad. Press, New York, 1972 ; M. C. Birch, "Pheromones", North-Holland Publ. Co., Amsterdam, 1974.

[3] R. Rossi, *Synthesis*, **1977**, 817.

[4] C. A. Henrick, *Tetrahedron*, **33**, 1845 (1977).

[5] K. Mori, "Synthetic Chemistry of Insect Pheromones and Juvenile Hormones", in Recent Developments in the Chemistry of Natural Carbon Compounds, vol. IX, Akad. Kiadó, Budapest, 1979, p. 11.

[6] H. J. Bestmann and O. Vostrowsky, "Chemistry of Insect Pheromones", in "Chemie der Pflanzenschutzmittel", R. Wegler, ed., Bd. 6, Springer Verlag, Berlin, 1980, p. 29.

[7] F. Hodoşan, H. H. Mantsch, I. Goia and A. A. Botar, *Rom. Pat.*, No. 60226, 21 May 1975 ; 1975 ; A. A. Botar and F. Hodoşan, *Rom. Pat.*, No. 63672, 04 Nov 1976 ; A. A. Botar, M. Iacob and F. Hodoşan, *Rom. Pat.*, No. 71231, 15 May 1979 ; A. Gocan, A. A. Botar, M. Iacob, I. Ghizdavu and F. Hodoşan, *Rom. Pat.*, No. 71284, 12 May 1979 ; A. A. Botar, N. Popovici, A. Barabás, G. Dissescu and F. Hodoşan, *Rom. Pat.*, No. 76045, 03 Oct. 1980 ; A. A. Botar, N. Popovici and F. Hodoşan, *Rom. Pat.*, No. 78763, 25 Dec. 1981 ; A. A. Botar, A. Barabás, F. Hodoşan, M. Iacob and I. Ghizdavu, *Rom. Pat.*, No. 78979, 20 Jan. 1982 ; A. A. Botar and F. Hodoşan, *Rom. Pat. appl.*, No. 100851 (1980).

[8] L. Brandsma, "Preparative Acetylene Chemistry", Elsevier Publ. Co., Amsterdam, 1971, p. 15.

[9] E. Müller, "Methoden der organischen Chemie", Bd. V/2a, G. Thieme Verlag, Stuttgart, 1977, p. 357.

[10] L. Brandsma, ref. 8, p. 24 ; E. J. Corey and M. Chaykovsky, *J. Amer. Chem. Soc.*, **84**, 866 (1962) ; B. J. Kriz, M. J. Benes and J. Peska, *Tetrahedron. Letters*, **1965**, 2881 ; K. Sjöberg, *ibid.*, **1966**, 6383.

[11] E. Müller, ref. 9, p. 360 (footnote 5).

[12] T. H. Vaughn, *J. Amer. Chem. Soc.*, **55**, 3453 (1933).

[13] E. Müller, ref. 9, p. 400 ; J. R. Johnson and W. L. McEwen, *J. Amer. Chem. Soc.*, **48**, 469 (1926).

[14] N. A. Nelson and J. C. Wollensak, *J. Amer. Chem. Soc.*, **80**, 6626 (1958).

[15] E. Müller, ref. 9, pp. 362, 364.

[16] B. P. Eisner and P. F. M. Paul, *J. Chem. Soc.*, **1951**, 893.

[17] L. M. Smorgonskii and Ya. L. Goldfarb, *Zhur. obschchei Khim.*, **10**, 1113 (1940) ; *Chem. Abstr.*, **35**, 4011 (1941).

[18] E. F. Degering and L. G. Boatright, *J. Amer. Chem. Soc.*, **72**, 5137 (1950).

[19] A. Butenandt, E. Hecker, M. Hopp and W. Koch, *Liebigs Ann. Chem.*, **658**, 39 (1962).

[20] J. L. Speier, *J. Amer. Chem. Soc.*, **74**, 1003 (1952).

[21] C. A. Brown and V. K. Ahyia, *Chem. Comm.*, **1973**, 553.

[22] M. Schwarz and R. M. Waters, *Synthesis*, **1972**, 567.

[23] R. Rossi and A. Carpita, *ibid.*, **1977**, 561.

[24] P. E. Sonnet and J. E. Oliver, *J. Org. Chem.*, **41**, 3279 (1976).

[25] A. Barabás, A. A. Botar, A. Gocan, N. Popovici and F. Hodoşan, *Tetrahedron*, **34**, 2191 (1978).

[26] W. Hoebold, R. Radeglia and D. Klose, *J. prakt. Chem.*, **318**, 519 (1976).

[27] S. Voerman, A. K. Minks and N. W. Houx, *Environ. Entomol.*, **3**, 701 (1974).

[28] H. Arn, E. Städler, R. Rauscher, H. R. Buser, H. Mustaparta, P. Esjberg, H. Phillipsen, O. Zethner, D. L. Struble and R. Bues, *Z. Naturforsch.*, **35c**, 986 (1980).

[29] W. L. Roelofs, J. Kochansky, E. Anthon, R. Rice and R. T. Cardé, *Environ. Entomol.*, **4**, 580 (1975).

[30] J. Granges and M. Baggiolini, *Rev. Suisse Vitic. Arboric.*, **3**, 93 (1971).

[31] W. L. Roelofs, A. Comeau and R. Selle, *Nature*, **224**, 723 (1969).

[32] B. A. Bierl, M. Beroza and C. W. Collier, *J. Econ. Entomol.*, **65**, 659 (1972).

[33] M. Boness, W. Schulze and U. Skatulla, *Anz. Schädlingskde., Pflanzen Umweltschutz*, **47**, 119 (1974).

[34] D. L. Struble, H. Arn. H. R. Buser, E. Städler and J. Freuler, *Z. Naturforsch.*, **35c**, 45 (1979).

[35] L. Novák, M. Tóth, J. Balla and Cs. Szántay, *Acta. Chim. Acad. Sci. Hung.*, **102**, 135 (1979).

[36] J. A. Klun and T. A. Brindley, *J. Econ. Entomol.*, **63**, 779 (1970) ; J. A. Klun and J. F. Robinson, *ibid.*, **63**, 1281 (1970).

[37] H. P. Chambon and J. d'Anguillar *Ann. Zool.-Ecol. Animal.*, **6**, 423 (1974).

[38] B. Frerot, M. Gallois and J. Einhorn, *Compt. rend. ser. D*, **288**, 1611 (1979).

[39] D. L. Struble, G. E. Swailes, W. F. Steck, E. W. Underhill and M. D. Chisholm, *Environ. Entomol.*, **5**, 988 (1976).

[40] H. Arn, E. Priesner, H. Bogenshütz, H. R. Buser, D. L. Struble, S. Rauscher and S. Voerman, *Z. Naturforsch.*, **34c**, 1281 (1979).

Revue Roumaine de Chimie, 28, 7, 757–762, (1983)

NEW POLYMERS WITH HETEROCYCLIC SIDE GROUPS HAVING ANTIOXIDANT PROPERTIES

J. HERDAN, LIVIA CRIŞAN, M. LUCA and S. BALIU
Institute of Technological Engineering, Research and Design for Refineries
(ICITPR), Ploieşti, Romania

Received April 5, 1982

N-(β-Hydroxyethyl)-S-(2-benzothiazolyl) and N-(β-hydroxyethyl)-S-(2-benzimidazolyl) mercaptoacetamide, **(6a)** and **(6b)**, respectively, were prepared reacting 2-mercaptobenzothiazole and 2-mercaptobenzimidazole with ethyl chloroacetate and subsequently with ethanolamine. The products react with cetyl methacrylate — maleic anhydride copolymer forming macromolecules with heterocyclic side groups **(8a, b)**. The products are free radical scavengers and hydroperoxide decomposers.

It is known that many materials of large practical interest, like polymers, lubricants, natural fats suffer more or less intensive degradation in time, due to the atmospheric oxidation. Atmospheric oxidation is a radicalic chain reaction, involving atmospheric oxygen, leading to hydroperoxides. To limitate the destructive effect of this process antioxidants are used.

They act either by reacting with active peroxy radicals and forming hydroperoxides and an inactive, stable radical and thus breaking off the chain, or as hydroperoxide decomposers. Of great importance are the compounds which are at the same time free radical scavengers and hydroperoxide decomposers. To this class belong several sulfur compounds e.g. dithiocarbamic acid derivatives (**1**) or phosphorodithioates (**2**).[1]

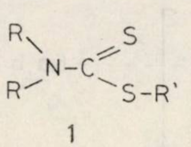

1

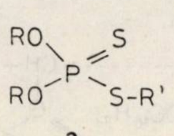

2

2-Mercaptobenzothiazole (**3**) and 2-mercaptobenzimidazole (**4**), with structures related to structure (**1**), also exhibit antioxidant properties.[2-4]

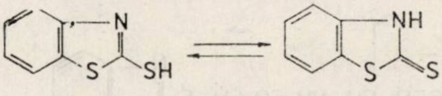

3

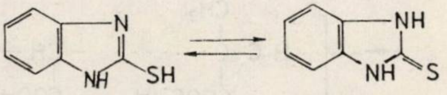

4

The use of these compounds is limited by their reduced solubility in hydrocarbons. To obtain derivatives with improved solubility, the molecules (**3**) and (**4**) were grafted on a macromolecular compound by some polymer-analogous reactions.

As macromolecular compound a cetyl methacrylate-maleic anhydride copolymer was used. The compounds (**3**) and (**4**) were subjected to a sequence of reactions with the view of introducing a β-hydroxyamidic group. The β-hydroxyamidic group offers certain advantages to graft a molecule on a polymer with acid anhydride groups: an easy esterification, at moderate temperature and without acidic catalyst.

Treating 2-mercaptobenzothiazole (**3**) or 2-mercaptobenzimidazole (**4**) with ethyl chloroacetate, in methanol and sodium methoxide, ethyl S-(2-benzothiazolyl) mercaptoacetate (**5a**) and ethyl S-(2-benzimidazolyl) mercaptoacetate (**5b**), respectively are obtained. The mercaptoacetates (**5a, b**) react with monoethanolamine, in boiling xylene, leading to N-(β-hydroxyethyl)-S-(2-benzothiazolyl)mercaptoacetamide (**6a**) and N-(β-hydroxyethyl)-S-(2-benzimidazolyl)mercaptoacetamide (**6b**).

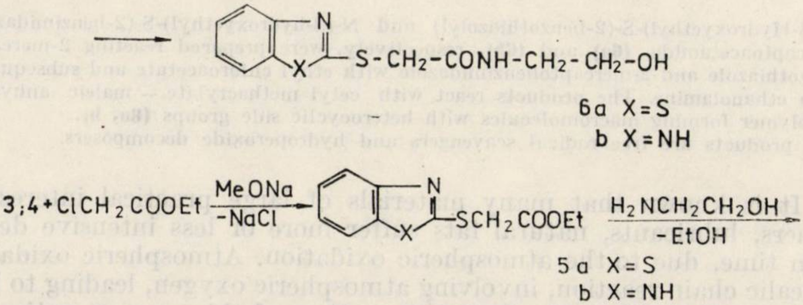

6a X=S
b X=NH

5a X=S
b X=NH

The cetyl methacrylate – maleic anhydride copolymer was prepared by copolymerisation of the monomers, in refluxing xylene, using benzoyl peroxide as initiator. The ratio cetyl methacrylate – maleic anhydride in the copolymer is about 9:1, the molecular weight being 2000 approximately.

N-(β-Hydroxyethyl) mercaptoacetamides (**6a, b**) react with the copolymer (**7**) leading to the modified copolymer (**8 a,b**).

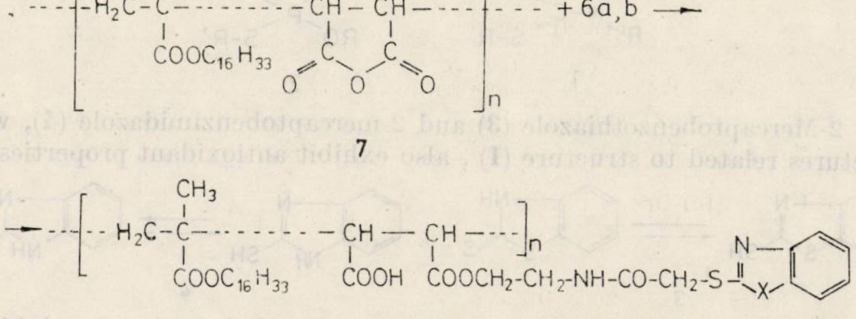

7

8a X-S
b X-NH

The I.R. spectra of the copolymers (**8a, b**) show two peaks at 1560cm^{-1} and 1650 cm^{-1} (amidic C=O) and the absence of the peaks at 1750 cm^{-1} and 1850 cm^{-1}, characteristics of the C=O groups in acid anhydrides.

The compounds (**8a, b**) are completely miscible with hydrocarbons.

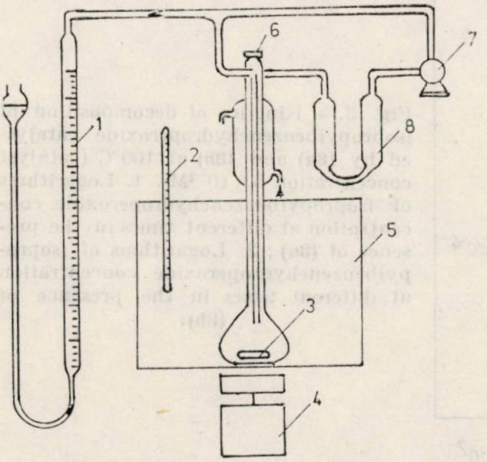

Fig. 1. — Principle of the circulatory oxidation apparatus. 1. Gas burette ; 2. Thermometer ; 3. Stirring bar ; 4. Magnetic stirrer ; 5. Heating bath ; 6. Rubber membrane ; 7. Oxygen pump ; 8. Absorption vessels with silica gel and ascarite.

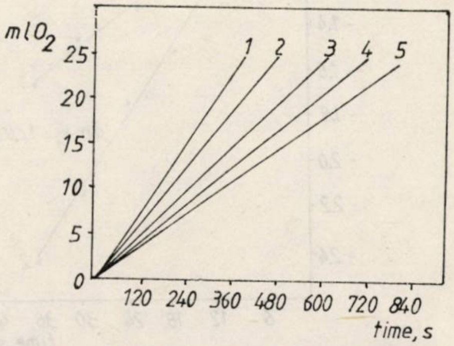

Fig. 2. — Kinetics of oxygen absorption in the initiated oxidation of tetraline containing antioxidants **(8a)** and **(8b)** (α,α-azobisisobutyronitrile concentration 10^{-2}M, temperature 90°C). 1. [**8a**]2 × 10^{-2}M ; 2. [**8a**]4 × 10^{-2}M ; 3. [2,6-di-t-butyl-4-methylphenol] 2 × 10^{-2}M ; 4. [**8b**]2 × 10^{2-}M ; 5. [**8b**]4 × 10^{-2} M

The products acted as chain breakers in oxidation reactions as proved by studying the oxygen absorption rate in the initiated oxidation of tetraline, in the presence of (**8a**) and (**8b**). The oxidation rate was measured with a circulatory oxidation apparatus, presented in figure 1. The reaction temperature was 90°C and α, α-azobisisobutyronitrile, in concentration 0,01 M, was used as initiator.

The kinetic curves of the absorption of oxygen in tetraline containing (**8a**), and (**8b**) in concentration 0.02 and 0.04 M are plotted in figure 2. 2,6-Di-*tert*-butyl-4-methylphenol is used as reference.

We can see that the inhibiting power of the compounds (**8a, b**) is similar to that of the reference compound. 2,6-Di-*tert*-4-methylphenol reacts with the unstable peroxy radicals to form hydroperoxides and the stable aroxyl radical. It seems that (**8a**) and (**8b**) act in a similar way. Also, the method used makes evidence especially of the chain breaking effect of the inhibitors.

The compounds (**8a, b**) act as catalysts in the decomposition of hydroperoxides. This action was observed measuring the decompositin rate of isopropylbenzene hydroperoxide, in chlorobenzene solution, containing (**8a**) and (**8b**), at 100°C. Without catalyst, isopropylbenzenehydroperoxide is stable under these conditions.

In figure 3, log [ROOH] is plotted against time. The reaction is a first order one. The rate constants, calculated by the graphical method, show that compound (**8b**) is a better catalyst than (**8a**).

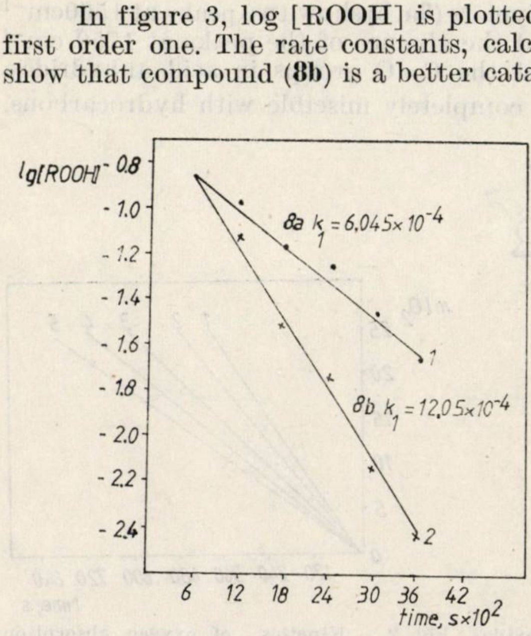

Fig. 3. — Kinetics of decomposition of isopropylbenzenehydroperoxide catalysed by **(8a)** and **(8b)** at 100°C (catalyst concentration 5×10^{-4}M). 1. Logarithms of isopropylbenzenehydroperoxide concentration at different times in the presence of **(8a)** ; 2. Logarithms of isopropylbenzenehydroperoxide concentration at different times in the presence of **(8b)**.

EXPERIMENTAL PART

Ethyl S-(2-benzothiazolyl) mercaptoacetate **5a**. To a stirred solution of 27.6 g (0.165 mol) 2-mercaptobenzothiazole in 150 ml methanol, a sodium methoxide solution, obtained from 3.9 g (0.169 mol) sodium and 30 ml methanol is dropped, during 30 minutes. Then, 21 g (0.17 mol) ethyl chloroacetate are added and the mixture is refluxed during 5 hours. Subsequently, 100 ml benzene and 100 ml water are added, stirring being continued for a few minutes. The benzene layer is separated, washed with water and dried over anhydrous sodium sulphate. Benzene is distilled under reduced pressure and the residue is recrystallised from carbon tetrachloride. Yield : 83 %. M.p. 63—65°C. Found : C, 52.5 ; H, 4.2 ; N, 5.4 %.
$C_{11}H_{11}NO_2S_2$ requires ; C, 52.17 ; H, 4.35 ; N, 5.53 %.

IR ($CHCl_3$) : 1590 cm^{-1} aromatic band, 1610 cm^{-1} C=N band, 1735 cm^{-1} esteric C=O band.

Ethyl S-(2-benzimidazolyl)mercaptoacetate **5b.** The compound **5b** is obtained in 87 % yield similar with **5a**. M.p. 115—117°C. Found : C, 56.3 ; H, 4.8 ; N, 11.7 %. $C_{11}H_{12}N_2O_2S$ requires : C, 55.9 ; H, 5.08 ; N, 11.86 %.

IR($CHCl_3$) : 1592 cm^{-1} aromatic band, 1620 cm^{-1} C=N band, 1740 cm^{-1} esteric C=O band, 3410 cm^{-1} N—H band.

N-(β-Hydroxyethyl)-S-(2-benzothiazolyl)mercaptoacetamide **6a.** 12 g (0.05 Mol) compound **(5a)** and 3.66 g (0.06 mol) monoethanolamine in 20 ml xylene are refluxed during 8 hours. Xylene is distilled under reduced pressure and the product is recrystallised from benzene. Yield 67 %. M.p. 99—102°C, Found : C, 49.0 ; H, 4.5 ; N, 10.5 %. $C_{11}H_{12}N_2O_2S_2$ requires : C, 49.25 ; H, 4.47 ; N. 10.45 %.

I.R. ($CHCl_3$) : 1520 cm^{-1} aromatic band, 1620 cm^{-1} C=N band, 1670 and 1560 cm^{-1} amidic C=O bands, 3300 cm^{-1} O—H band,

N-(β-Hydroxyethyl)-S-(2-benzimidazolyl)mercaptoacetamide **6b.** Compound **(6b)** is prepared as described above, using ethyl S-(2-benzimidazolyl)mercaptoacetate. Yield 78 %. M.p. 58—60°C (benzene). Found C, 52,7 ; H, 4.9 ; N, 16.8 %. $C_{11}H_{13}N_3O_2S$ requires : C. 52.58 ; H, 5.18 ; N, 16.73 %.

I.R. ($CHCl_3$) : 1592 cm^{-1} aromatic band, 1615 cm^{-1} C=N band, 1570 cm^{-1} and 1675 cm^{-1} amidic C=O bands, 3400 cm^{-1} N—H band, 3450 cm^{-1} O—H band.

Cetyl methacrylate — maleic anhydride copolymer **7.** Cetyl methacrylate was prepared by transesterification reaction of methyl methacrylate with cetyl alcohol.[5]

180 g Cetyl methacrylate and 6 g benzoyl peroxide dissolved in 50 ml xylene are mixed with 20 g maleic anhydride in 75 ml xylene. The mixture is dropped during 1 hour into 75 ml refluxing xylene. Heating is continued for 3 hours. The solvent is removed in vacuum. The copolymer is used without further purification. The molecular weight determined by vapour phase osmometry with a Knauer osmometer is about 1870.

I.R. : 1720 cm^{-1} esteric C=O bands ; 1780 cm^{-1} and 1850 cm^{-1} anhydridic C=O bands.

Cetyl methacrylate — maleic acid N-(β-hydroxyethyl)-S-(2-benzothiazolyl) mercaptoacetamide monoester copolymer **8a.** To 15 g cetyl methyacrylate — maleic anhydride copoymer **(7)** containing 0.013 mol maleic anhydride, in 30 ml xylene, 3.48 g (0.013 mol) **(6a)** are added. The reaction mixture is heated at 170°C for 4 hours. Xylene is removed under reduced pressure. The residue is dissolved in n-heptane, the solution is filtered, and n-heptane is distilled. The copolymer **(8a)** is obtained in 87% yield.

I.R. : 1560 cm^{-1} and 1650 cm^{-1} amidic C=O bands ; 1710 cm^{-1} carboxylic C=O band ; 1735 cm^{-1} esteric C=O band.

Cetyl methacrylate — maleic acid N-(β-hydroxyethyl) -S-(2-benzimidazolyl) mercaptoacetamide monoester copolymer **8b.** The compound **(8b)** is prepared similarly with **(8a).** Yield 72%. I.R. : 1560 cm^{-1} and 1650 cm^{-1} amidic C=O bands ; 1710 cm^{-1} carboxylic C=O band ; 1730 cm^{-1} esteric C=O band.

Kinetics of oxygen absorption in the initiated oxidation of tetraline. The air from the circulatory oxidation apparatus is replaced by oxygen and then the temperature is raised to 90°C. The internal pressure is maintained at the same level with the atmospheric pressure. The gas is recirculated with a pump and purified by passing on silica gel and ascarite. Then 5 ml solution of tetraline, containing 10^{-2} mol/l α,α-azobisisobutyronitrile and 2×10^{-2} or 4×10^{-2} mol/l antioxidant are injected through a rubber membrane. On the diagrame, the volume of absorbed oxygen is plotted against time. The oxidation is interrupted when 25 ml oxygen are absorbed.

Kinetics of decomposition of isopropylbenzenehydroperoxide. In a stoppered flask 30 ml solution 0.16 M of isopropylbenzenehydroperoxide in chlorobenzene, containing 5×10^{-4} mol/l antioxidant, are introduced. The flask is placed in a thermostate at 100°C. The hydro-

Table 1

Isopropylbenzenehydroperoxide concentrations at different times in chlorobenzene containing **(8a)** and **(8b)**

Time, s	[ROOH], mol/l	Catalyst	k_1, s^{-1}
600	0.138	**8a** 5×10^{-4}M	6.045×10^{-4}
1200	0.106		
1800	0.078		
2400	0.056		
3000	0.035		
3600	0.023		
600	0.138	**8b** 5×10^{-4}M	12.05×10^{-4}
1200	0.076		
1800	0.031		
2400	0.018		
3000	0.0078		
3600	0.0038		

peroxide concentration is determined by iodometric titration. The logarithms of these concentrations are plotted against time.

ACKNOWLEDGEMENT. Thanks are due to Mr. I. Muntean for recording and discussion of I.R. spectra.

REFERENCES

[1] G. Scott, ''Atmospheric Oxidation and Antioxidants'', Elsevier, London, 1965.

[2] Sh. T. Akhmedov, L. M. Gyul'akhmedov and Gh. A. Yusifov, *Uch. Zap. Azerb. Un.-ta., Ser. Khim.*, **1978**, 50.

[3] J. L. Miesel (Lilly, Eli and Co.), Pat. U.S.A. 4000295 (1976) ; *Chem. Abstr.*, **86**, 140050 (1977).

[4] V. G. Vaidanich and V. Yu. Kazibrid, *Zhur. priklad. Khim.*, **51**, 1430 (1978).

[5] H. Riddle, ''Monomeric Acrylic Esters'', Reinhold, London, 1954.

Revue Roumaine de Chimie, 28, 7, 763–773 (1983)

UNTERSUCHUNG DER EMPFINDLICHKEIT EINES REAKTORS FÜR SUSPENSIONSPOLYMERISATION VON VINYLCHLORID BEI KONSTANTER TEMPERATUR

ŞTEFAN UNGUREANU, MATEI MACOVEANU und CORNELIU PETRILĂ
Fakultät für Technische Chemie, Jassy, Rumänien
Splai Bahlui 71

Eingegangen am August 14, 1981

An hand des mathematischen Modells eines Reaktors fur Suspensionspolymerisation von Vinylchlorid wurde die Zustands- und Austrittsempfindlichkeir im Verhältnis zu den Betriebsparametern untersucht. Als Zustandsvektor betrachtete man die Umsatz und als Austrittvektor die Temperatur des Kühlmittels im Reaktormantel. In Betracht kamen folgende Parameter: Polymerisations-temperatur. Dissoziationskonstante des Initiators, der Wärmedurchgangszahl durch den Mantel und entlang der Oberfläche in Berührung mit der Atmosphäre. Die durch Integrierung der Systeme von Empfindlichkeitsgleichungen erhaltenen Kurvenscharen gestatten eine Voraussage des Reaktorverhaltens bei geringen Veränderungen der im Hinblick auf die optimale Steuerung betrachteten Parameter.

On the basis of a mathematical model of the reactor for vinyl chloride suspension polymerization, we have studied the sensitivity both of the state and of the outlet in comparison with the operational parameters. We have considered conversion as state vector, and temperature of the cooling agent from the reactor coating as outlet vector. The parameters taken into account have been: the polymerization temperature, the dissociation constant of the initiator, the coefficients for heat transfer both through the coating and the surface in contact with the air. The sets of curves obtained by integrating the systems of sensitivity equations allow the estimation of the reactor behaviour of small variations of the used parameters for an optimal governing.

1. EINFÜHRUNG

Die Kenntnis der Empfindlichkeit des Reaktors bei verhältnismässig geringen Abweichungen der Arbeitsparameter hat eine besondere Bedeutung, da die erwährten Abweichungen die Qualitätsnormen des Polymeren bzw. die Ökonomischen Kennwerte der Anlage beeinflussen.

In der vorliegenden Arbeit untersucht man an Hand eines früher erarbeiteten mathematischen Modelles [1] die Empfindlichkeit eines Reaktors fur Suspensionspolymerisation von Vinylchlorid under konstanter Temperatur bei Abweichungen der Temperatur der Reaktionsmasse wie auch des Dissoziationskonstante des Initiators sowie der Wärmedurchgangszahl.

2. MATHEMATISCHES MODELL DES REAKTORS

Das mathematische Modell eines diskontinuierlichen Polymerisationsreaktors wurde auf grund des von Hamielec und Mitarb. [2,3] vorgeschlagenen kinetischen Modelles und der Wärmebilanz erarbeitet und hat die allgemeine Form [1]:

$$\dot{x} = f_{\text{I}} \text{ für } 0 \leqslant x \leqslant x_f$$

$$f_{\text{I}} = \frac{1 + Qx}{(1 - Bx)^{1/2}} \cdot k_1 I_0^{1/2} \exp\left(-\frac{1}{2} k_d t\right) \tag{1}$$

$$\dot{x} = f_{\text{II}} \text{ für } x \geqslant x_f$$

$$f_{\text{II}} = \frac{\overline{P} k_1 I_0^{1/2}}{1 - x_f} \cdot \frac{(1 - x)^2}{(1 - Bx)^{1/2}} \cdot \exp\left(-\frac{1}{2} k_d t\right) \tag{2}$$

$$\frac{\mathrm{d}T}{\mathrm{d}t} = \frac{1}{\sum\limits_{3}^{1} m_i c_i} \left[\frac{m_2^0}{M_{CV}} \cdot \frac{\mathrm{d}x}{\mathrm{d}t} (-\Delta H_R) - \overline{K}_2 A_2 (T - T_R) - \overline{K}_3 A_3 (T - T_a) \right] \tag{3}$$

bei welchen

$$\begin{aligned}
Q &= a_1 + a_2 T + a_3 T^2 \\
k_1 I_0^{1/2} &= 1{,}6\, k_d \\
k_d &= 1{,}786 \cdot 10^{18} \exp\left(-14500 \frac{1}{T}\right) \\
\overline{P} &= \frac{Q x_f + 1}{1 - x_f} \\
x_f &= a_4 + a_5 T + a_6 T^2 \qquad (4) \\
m_2 &= m_2^0 (1 - x) \\
c_2 &= a_7 + a_8 T + a_9 T^2 \\
m_3 &= m_2^0 x \\
\overline{K}_2^{(1)} &= \overline{C} \cdot n_R^{0,67} \cdot D^{0,33} \quad \text{für } x \leqslant x_f \\
\overline{K}_2 &= \overline{K}_2^{(1)} + bx \quad \text{für } x > x_f
\end{aligned}$$

und I_0, B, m_1, m_2^0, c_1, c_3, ΔH_R, M_{CV}, A_2, A_3, $\overline{C}$, D, b, n_R, $\overline{K}_3$, T_a, a_1, $a_2, \ldots, a_9$ sind konstant.

Bei der Ausarbeitung des von den Beziehungen (1) — (4) beschriebenen mathematischen Modells wurden die folgenden Arbeitshypothesen in Betracht gezogen:

— Die Reaktionsmasse bildet eine ideale Mischung; es liegt kein Konzentrations- oder Temperaturgefälle vor;

— als Initiator dient Diisopropylperoxydikarbonat; der Wirksamkeitsfaktor des Initiators ist konstant;

— der Volumendurchfluss des Wärmemittels durch den Reaktorenmantel ist konstant, wobei die Stabilisierung der Temperatur der Reaktions masse durch die Veränderung der Temperatur des Wärmemittels erzielt wird;

— es bildet sich keine Kruste an den Wänden des Reaktors;

— es werden keine zusätzlichen Kühlflächen verwendet;

— man vernachlässigt den von Rühraggregat geleisteten Wärmezusatz;

— das Reaktionsgemisch gelangt zur Polymerisationstemperatur der Zeit $t = 0$.

Der vom mathematischen Model (1) — (4) beschriebene Polymerisationsvorgang läuft in zwei Etappen ab, die zeitlich aufeinander folgen:

— Etappe I, für $0 \leqslant x \leqslant x_f$, wird vom Modell in den Beziehungen (1), (3) und (4) beschrieben;

— Etappe II, für $x \geqslant x_f$, wird vom mathematischen Modell beschrieben, welches von den Beziehungen (2), (3) und (4) gebildet wird.

3. ZUSTANDSEMPFINDLICHKEIT DES POLYMERISATIONSREAKTORS

In oben beschriebenen allgemeinen Fall des mathematischen Modells eines gegebenen Prozesses wird die From eines Systems von Zustandsgleichungen bestimmt:

$$\dot{z} = f(z, p) \tag{5}$$

wobei z- den Zustandsvektor mit n Bestandteilen

p — den Parametervektor, welcher den Zustand beeinflusst, mit m Komponenten, bedeuten.

Die Vektoren der Zustandsempfindlichkeit in bezug auf die Parameter, σ_i, definiert werden durch

$$\sigma_i = \frac{\partial_z}{\partial_{p_i}}, \quad i = 1, 2, \ldots, m \tag{6}$$

Sie ergeben sich als Auflösungen der Systeme von Differentialgleichungen der Empfindlichkeit von folgender Form [4]:

$$\dot{\sigma}_i = F_z \cdot \sigma_i + F_{p_i}, \quad i = 1, 2, \ldots, m \tag{7}$$

unter den Ausgangbedingungen $\sigma_i(t_0) = 0$

In der Beziehung (7) gelten:

F_z ist die Funktionaldeterminante der Derivate ersten Grades der Funktionen f_j in den Punkten z_k mit dem allgemeinen Element j, k von der Form:

$$\partial f_j / \partial z_k, \quad \begin{array}{l} j = 1, 2, \ldots, n \\ k = 1, 2, \ldots, n \end{array}$$

F_{p_i} stellt den Vector der Derivierten der Funktionen f_j in bezug auf p_i vor, mit dem allgemeinen Element j der Form $\partial f_j / \partial p_i$, $j = 1, 2. \ldots, n$.

Der Einfluss der Parametervariationen auf den Vorgangszustand errechnet sich mittels der Beziehung:

$$\Delta z(t) = \sum_{i=1}^{m} \sigma_i(t) \cdot \Delta p_i \tag{8}$$

in welcher

Δp_i – die Veränderlichkeit des Parameters p_i vom Nennwert vorstellt.

In oben dargestellten Modell des Polymerisationsreaktors hat der Zustandsvektor eine einzige Komponente den Umsatzsgrad (x).

Die Parameter, in bezug auf welche Zustandsempfindlichkeit untersucht wurde, sind der Reihe nach die Temperatur (T) und die Dissoziationskonstante des Initiators (k_d).

Die Wahl dieser Parameter ist durch die bekannten Schwierigkeiten gerechtfertigt, die mit der Steuerung der Suspensionspolymerisation von Vinylchlorid in industriellem Maßstab verbunden sind.

Im vorliegenden Falle entstehen die Gleichungssysteme (7):

– für die I. Etappe:

$$\dot{\sigma}_{\mathrm{I},i} = f_{\mathrm{I},x} \cdot \sigma_{\mathrm{I},i} + f_{\mathrm{I},i}, \quad i = 1, 2 \tag{9}$$

unter den Ausgangsbedingungen $\sigma_{\mathrm{I},i}(t_0) = 0$

– für die II. Etappe:

$$\dot{\sigma}_{\mathrm{II},i} = f_{\mathrm{II},x} \cdot \sigma_{\mathrm{II},i} + f_{\mathrm{II},i} \quad i = 1, 2 \tag{10}$$

unter den Ausgangsbedingungen $\sigma_{\mathrm{II},i}(t_0)\mathrm{i} = \sigma_{\mathrm{I},i}(t_f)$.

In den Systemen (9) und (10):

$$\begin{aligned}
f_{\mathrm{I},x} &= \frac{Q(2 - Bx) + B}{2(1 - Bx)^{3/2}} \cdot 1{,}6 . k_d \cdot \exp\left(-\frac{t}{2} k_d\right) \\
f_{\mathrm{I},1} &= \frac{f_{\mathrm{I}}}{1 + Qx}\left[\frac{14500}{T^2}(1 + Qx)\left(1 - \frac{t}{2} k_d\right) + x\,(a_2 + 2a_3 T)\right] \\
f_{\mathrm{I},2} &= \frac{1{,}6(1 + Qx)\left(1 - \frac{t}{2} k_d\right)}{(1 - Bx)^{1/2}} \exp\left(-\frac{t}{2} k_d\right) \\
f_{\mathrm{II},x} &= \frac{1{,}6 . k_d\,(1 + Qx_f)\,(1 - x)\,(B + 3Bx - 4)}{2(1 - x_f)^2\,(1 - Bx)^{3/2}} \exp\left(-\frac{t}{2} k_d\right) \\
f_{\mathrm{II},1} &= \frac{1{,}6(1 - x)^2\, k_d \exp\left(-\frac{t}{2} k_d\right)}{(1 - Bx)^{1/2}\,(1 - x_f)^3}\left\{\frac{14500}{T^2}(1 + Qx_f)\left(1 - \frac{t}{2} k_d\right)(1 - x_f) + \right. \\
&\quad \left. + (a_5 + 2a_6 T)\,[Q(1 + x_f) + 2] + x_f(1 - x_f)\,(a_2 + 2a_3 T)\right\} \\
f_{\mathrm{II},2} &= 1{,}6\,\frac{(1 + Qx_f)\left(1 - \frac{t}{2} k_d\right)(1 - x)^2}{(1 - x_f)^2\,(1 - Bx)^{1/2}} \exp\left(-\frac{t}{2} k_d\right)
\end{aligned} \tag{11}$$

Bei der Integration der Differentialgleichungssysteme (9) und (10) wurde angenommen, dass der Reaktor für die Suspensionspolymerisation von Vinylchlorid unter konstanter Temperatur die folgenden Ausmasse aufweist:

$$D = 1{,}76\ \mathrm{m}; \qquad A_2 = 13\ \mathrm{m}^2$$

$$V = 6.4\ \mathrm{m}^3; \qquad A_3 = 7\ \mathrm{m}^2$$

Die übrigen konstanten Angaben, die im mathematischen Modell verwendet werden, sind:

$B = 0{,}393$; $n_R = 120$ UpM
$m_1 = 2400$ kg; $\overline{K}_3 = 21$ kJ/m$^2\cdot$h.grd
$m_2^0 = 1600$ kg; $a_1 = -181{,}92$
$c_1 = 4{,}19$ kJ/kg.grd; $a_2 = 1{,}145$
$c_3 = 1$ kJ/kg.grd; $a_3 = -0{,}00175$
$\Delta H_R = -100$ kJ/Mol; $a_4 = -1{,}192$
$M_{CV} = 0{,}0625$; $a_5 = 0{,}0141$
$I_0 = 0{,}001$ Mol/Mol $a_6 = -2{,}5\cdot10^{-5}$
$T_a = 293{,}16$°K; $a_7 = 21{,}52$
$\overline{C} = 140$; $a_8 = 0{,}125$
$b = -770$; $a_9 = -4{,}274\cdot10^{-5}$

— Verhältnis Wasser : Monomer = 1,5/1
— Wirksamkeitsfaktor der Startreaktion = 0,8

Die für den Betrieb des Reaktors unter den Nominalparametern erhaltenen Lössungen:

$$p = \begin{pmatrix} T \\ k_d \end{pmatrix} = \begin{pmatrix} 328{,}16\ \mathrm{K} \\ 0{,}1154\ \mathrm{h}^{-1} \end{pmatrix}$$

werden in den Kurven der Abbildung 1 wiedergegeben. Die Lösungen wurden durch Zahlenintegration nach der Runge-Kutta-Methode IV. Grades mittals einer Rechenmaschine FELIX C-256 gefunden.

Wie aus Abbildung 1 hervorgeht steigt die Empfindlichkeitsfunktion sehr rasch während der Reaktion bis zum Zeitpunke, für welchen $x = x_f$ (I. Etappe), wobei sie einen Höchstwert erreicht; dann fällt sie noch rascher ab (II. Etappe). Wie zu erwarten war, ist die Form der Veränderlichkeit ähnlich für die beiden Parameter: $p_1 = T$ und $p_2 = k_d$.

Die erhaltenen Resultate wurden durch Integration der Differentialgleichungen des mathematischen Modelles (1) und (2) für die Temperaturen T bzw. $T \pm 0{,}5°(k_d = 0{,}1154)$ und für k_d bzw. $k_d \pm 1\,\%k_d$ $(T = 328{,}16°)$. Die angefallenen Angaben findet man in Abbildung 2.

Die vergleichende Analyse der in Abbildungen 1 und 2 enthaltenen Informationen zeigt zusammen mit der Anwendung der Beziehung (8) für die beiden in Betracht gezogenen Parameter eine gute Übereinstimmung in der I. Etappe bis in die Nähe des Zeitpunktes t_f, der dem Umsatz x_f entspricht, wo die Kurven x/t einen Knick aufweisen, wie auch nach diesem Zeitpunkt in der II. Etappe.

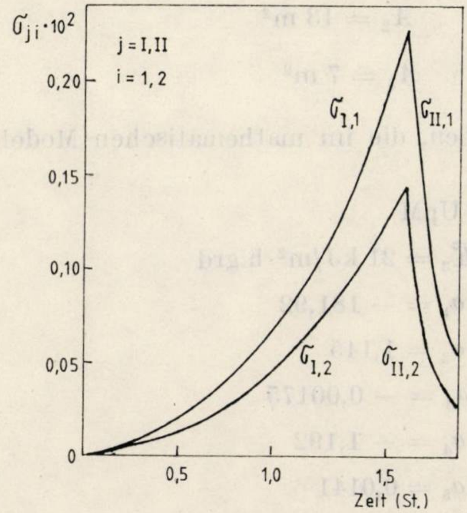

Abb. 1. – Veränderlichkeit der Empfindlichkeitsvektoren σ_{ji}, während des Ablaufes der Suspensionspolymerisationsreaktion von Vinylchlorid. (konstante Polymerisationstemperatur, $T = 328{,}16°K$) $j = I, II$, $i = 1, 2$.

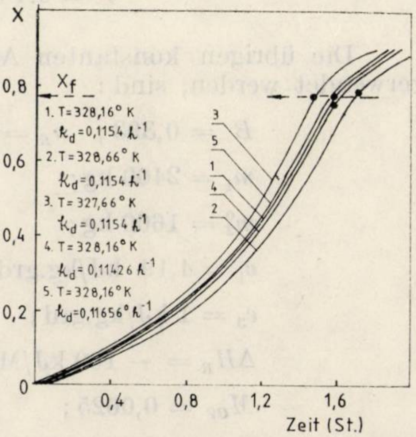

Abb. 2. – Veränderlichkeit dem Umsatz während des Vorganges der Suspensionspolymerisation von Vinylchlorid.

Im Bereiche des Knickpunktes (x_f/t_f) weisen die Empfindlichkeitsberechnungen mittels der Gleichung (8) nur orientativ anwendbar.

4. AUSTRITTSEMPFINDLICHKEIT DES POLYMERISATIONSREAKTORS

Der allgemeine Fall des Austrittes wind von der folgenden Gleichung beschrieben :

$$s = g\,(z,\,p) \tag{12}$$

Die Empfindlichkeitsvelktoren des Austrittes sind im Verhältnis zu den durch [4] definierten Parametern :

$$v_i = \frac{\partial_s}{\partial_{p_i}},\ i = 1, 2, \ldots, n \tag{13}$$

als Lösungen des Systemes von Gleichungen

$$v_i = G_z \cdot \sigma_i + G_{p_i} \tag{14}$$

bestimmt, wobei :

G_z bedeutet die Funktionaldeterminante ersten Grades der Funktionen g_j in den Punkten z_k, mit dem allgemeinen Element j, k mit der

Form $\partial g_j / \partial z_k$, $j = 1, 2, \ldots, n$; $k = 1, 2, \ldots, n$
G_{p_i} ist der Deriviertenvektor der Funktionen g_j in bezug auf p_i mit dem allgemeinen Element j von der Form $\partial g_j / \partial p_i$, $j = 1, 2, \ldots, n$. Der Einfluss der Parametervariationen auf den Austritt errechnet sich mittels der Beziehung

$$\Delta s = \sum_{i=1}^{m} v_i \cdot \Delta p_i \tag{15}$$

Im mathematischen Modell des Polymerisationsreaktors wurde der Austrittsvektor mit einer einzigen Komponente angenommen: $T_R =$ Temperatur des Kühlmittels, welches die Stabilisierung der Reaktorentemperatur bedingt ($\mathrm{d}T/\mathrm{d}t = 0$). Unter diesen Bedingungen ergibt sich aus der Beziehungen (3):

$$g(x, p) = T + \frac{1}{A_2 \overline{K}_2} \left[\frac{m_2^0}{M_{CV}} \cdot \Delta H_R \cdot f(x, p) + \overline{K}_3 A_3 \, (T - T_a) \right] \tag{16}$$

mit

$g = g_{\mathrm{I}}$ und $f = f_{\mathrm{I}}$ für die I. Etappe, bzw. $g = g_{\mathrm{II}}$ und $f = f_{\mathrm{II}}$ für die II. Etappe.

Der Parametervektor, in bezug auf welchen man die Austrittsempfindlichkeit berechnet, hat 4 Komponenten:

$$p = \begin{pmatrix} T \\ k_d \\ \overline{K}_2 \\ \overline{K}_3 \end{pmatrix} \tag{17}$$

Die Gleichungssysteme (14), welche die Elemente der Sensibilitätsvektoren ergeben, nehmen eine besondere Form an:
I. Etappe

$$v_{\mathrm{I},i} = g_{\mathrm{I},x} \cdot \sigma_{\mathrm{I},i} + g_{\mathrm{I},i}, \quad i = 1, 2, 3, 4 \tag{18}$$

mit

$$g_{\mathrm{I},x} = \Delta H_R \frac{m_2^0}{M_{CV}} \cdot \frac{1}{A_2 \overline{K}_2^{(1)}} \cdot f_{\mathrm{I},x}$$

$$\sigma_{\mathrm{I},3} = \sigma_{\mathrm{I},4} = 0$$

$$g_{\mathrm{I},1} = 1 + \frac{1}{A_2 \overline{K}_2^{(1)}} \left[\Delta H_R \frac{m_2^0}{M_{CV}} f_{\mathrm{I},1} + \overline{K}_3 A_3 \right] \tag{19}$$

$$g_{\mathrm{I},2} = \Delta H_R \frac{m_2^0}{M_{CV}} \cdot \frac{1}{A_2 \overline{K}_2^{(1)}} f_{\mathrm{I},2}$$

$$g_{\mathrm{I},3} = -\frac{1}{A_2 (\overline{K}_2^{(1)})^2} \left[\Delta H_R \frac{m_2^0}{M_{CV}} f_{\mathrm{I}} + \overline{K}_3 A_3 (T - T_a) \right]$$

$$g_{\mathrm{I},4} = \frac{A_3}{A_2 \overline{K}_2^{(1)}} (T - T_a)$$

II. Etappe

$$v_{\text{II},i} = g_{\text{II},x} \cdot \sigma_{\text{II},i} + g_{\text{II},i}\,; \quad i = 1, 2, 3, 4 \tag{20}$$

mit

$$g_{\text{II},x} = \Delta H_R \frac{m_2^0}{M_{CV}} \cdot \frac{1}{A_2 \overline{K}_2^2} (\overline{K}_2 \cdot f_{\text{II},x} - b \cdot f_{\text{II}})$$

$$\sigma_{\text{II};3} = \sigma_{\text{II};4} = 0$$

$$g_{\text{II},1} = 1 + \frac{1}{A_2 \overline{K}_2} \left(\Delta H_R \frac{m_2^0}{M_{CV}} \cdot f_{\text{II},1} + \overline{K}_3 A_3 \right)$$

$$g_{\text{II},2} = \Delta H_R \frac{m_2^0}{M_{CV}} \cdot \frac{1}{A_2 \overline{K}_2} \cdot f_{\text{II},2} \tag{21}$$

$$g_{\text{II},3} = - \frac{1}{A_2 (\overline{K}_2)^2} \left[\Delta H_R \frac{m_2^0}{M_{CV}} \cdot f_{\text{II}} + \overline{K}_3 A_3 (T - T_a) \right]$$

$$g_{\text{II},4} = - \frac{A_3}{A_2 \overline{K}_2^2} (T - T_a)$$

Bei der Auflösung der Gleichungssyteme (18) und (20) mit Hilfe von Rechenmaschinen wurde der gleiche in 2 beschriebene Polymerisationsreaktor in Betracht gezogen.

Die für den Betrieb des Reaktors bei der nominellen Parametern erhaltenen Lösungen:

$$p = \begin{pmatrix} 328{,}16 \\ 0{,}1154 \\ 4{,}17 \cdot 10^3 \\ 21{,}0 \end{pmatrix} \tag{22}$$

sind in Abbildungen 3 a, b, c aufgeführt.

Es ist hier zu vermerken, dass in der I. Etappe $v_{\text{I},1}$ und $v_{\text{I},2}$ negativ sind; dieses zeigt dass zum Unterschied vom Einfluss der Parameter $\overline{K}_2$ und $\overline{K}_3$, deren Wachstum z.B. einen Temperaturanstieg T_R bewirkt, die Veränderung der Parameter T und k_d eine Veränderung im umgekehrten Sinn vom T_R beding. Es wird auch der praktisch vernachlässigbare Einfluss von $\overline{K}_3$ auf T_R beobachtet.

Die erhaltenen Resultate wurden dadurch überprüft, dass man die Auswirkungen der Veränderungen der Parameter auf die mittels Formel (15) errechneten Temperatur T_R mit denen verglich, die bei Berechnung der Temperatur T_R bei den Nominalwerten der Parameter und bei den Werten $p_i \pm 1\,\%\, p_i$ erhaltenen werden.

Die Überprüfung ergab eine gute Übereinstimmung, wobei die Genauigkeit in der I. Etappe grösser war.

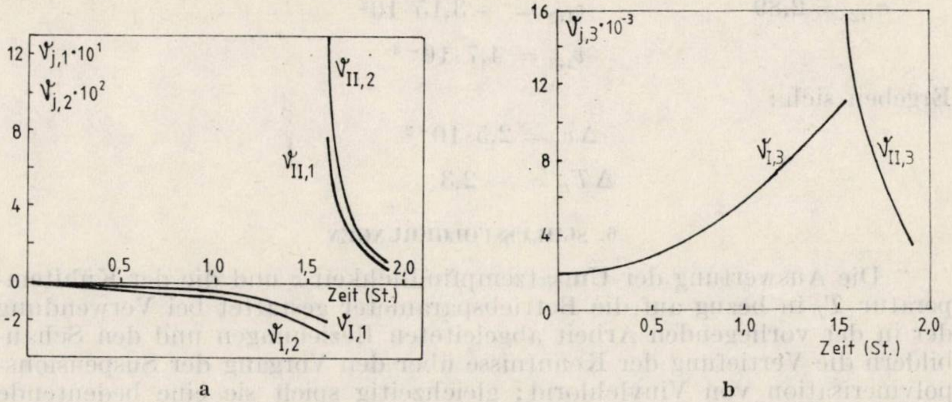

a b

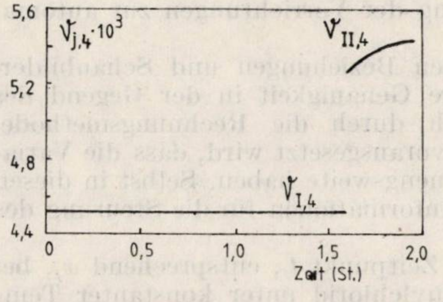

c

Abb. 3 a, b, c — Veränderlichkeit der Vektoren der Austrittesempfindlichkeit $v_{j,i}$ während des Ablaufes des Polymerisationsvorganges von Vinylchloride in Suspension. $j =$ I, II, $i = 1, 2, 3, 4$.

5. ANWENDUNGSBEISPIEL

Gegeben sei ein Polymerisationsvorgang, der sich bei den von (22) genannten Parametern abwickelt. Um den Konjugierten Einfluss der Verkleinerung der Parameter um cca. 1 % ihres Nennwertes, also um

$$\Delta p = \begin{pmatrix} 0{,}55 \\ 1{,}15 \cdot 10^{-3} \\ 41{,}7 \\ 0{,}21 \end{pmatrix} \tag{23}$$

auf den Umsatz x und auf die notige Kühltemperatur T_R nach 0,80 Stunden vom Reaktionsbeginn an zu bestimmen, gelten die Betiehungen (8) und (15):

$$\Delta x = \sum_{i=1}^{2} \sigma_{I,i} \cdot \Delta p_i \tag{24}$$

$$\Delta T_R = \sum_{i=1}^{4} v_{I,i} \cdot \Delta p_i$$

Aus den Kurven in Abbildungen 1 und 3 a, b, c;

$$\sigma_{I;1} = 4{,}49\cdot10^{-2} \qquad v_{I;1} = -\,3{,}88 \qquad v_{I;4} = 4{,}52\cdot10^{-3}$$

$$\sigma_{I;2} = 2{,}89 \qquad v_{I;2} = -\,3{,}15\cdot10^{2}$$

$$v_{I;3} = 4{,}7\cdot10^{-3}$$

Ergeben sich:

$$\Delta x = 2{,}5\cdot10^{-2}$$

$$\Delta T_R = -\,2{,}3$$

6. SCHLUSSFOLGERUNGEN

Die Auswertung der Umsatzempfindlichkeit z und die der Kühltemperatur T_R in bezug auf die Betriebsparameter gestattet bei Verwendung der in der vorliegenden Arbeit abgeleiteten Beziehungen und den Schaubildern die Vertiefung der Kenntnisse über den Vorgang der Suspensionspolymerisation von Vinylchlorid; gleichzeitig spielt sie eine bedeutende Rolle bei der Auswahl und Abstimmung der Vorrichtungen zur automaten Stabilisierung von Parametern.

Der Umstand, dass die erhaltenen Beziehungen und Schaubilder, wie oben gezeigt wurde, eine geringere Genauigkeit in der Gegend des Punktes $x_f(t_f)$ aufweisen, erklärt sich durch die Rechnungsmethode, welche eine Linearisierung bedingt, da vorausgesetzt wird, dass die Variationen der Parameter eine geringe Streuengsweite haben. Selbst in diesen Bereichen erhält man aber nützliche Informationen für die Steurung des Prozesses.

Die Schwierigkeiten, die für den Zeitpunkt t_f, entsprechend x_f, bei der Suspensionspolymerisation von Vinylchlorid unter konstanter Temperatur angegeben werden, sind durch das stetige Ansteigen der Sensibilitätsfunktion während der Reaktionsdauer bis zu $x = x_f$ widergespiegelt, wo sie einen Höchstwert erreicht.

FORMELZEICHEN

$a_1, a_2, \ldots, a_9$	Konstanten
A_2	Oberfläche des Wärmeaustausches bei Vorschung eines Mantels
A_3	Oberfläche des Wärmeaustausches ohne Mantel
b	Konstante
B	Konstante, welche die Volumkontraktion ausdrückt
c	spezifische Wärme
$\bar{C}$	Konstante für eine bestimmte Reaktionsmasse aus einem gegebenen Reaktor
D	Reaktorinnendurchmesser
I_0	Ausgangskonzentration des Initiators
k_1	Geschwindigkeitskonstante der Startsreaktion
k_d	Geschwindigkeitskonstante der Dissoziationsreaktion des Initiators
$\bar{K}_2^{(1)}$	Wärmedurchgangszahl Reaktionsmasse-Wärmemittel für die Umsätze $x \leqslant x_f$
$\bar{K}_2$	Wärmedurchgangszahl Reaktionsmasse-Wärmemittel

$\overline{K}_3$	Reaktionsmasse befindlichen Fluidum und der Umgebung
m	Gewicht
M_{CV}	Molekulargewicht des Vinylchloride
n_R	Rührerdrehzahl im Reaktor
p	Parametervektor, welcher den Zustand beeinflusst, mit m Komponenten
$\overline{P}$	Konstante, die vom Verhältnis der Polymerisationsgeschwindigkeiten in beiden Phassen abhängt
PVC	Polyvinylchlorid
s	Austritt des Polymerisationsreaktors
t	Zeit
T	Temperatur
T_a	Temperatur der Umgebung
T_R	Temperatur des Wärmemittels aus dem Reaktorenmantel
v_i	Empfindlichkeitsvektor des Austrittes
V	Rauminhalt des Reaktors
x	Umsatz $(0 \leqslant x \leqslant 1)$
x_f	Grenzumsatz, bei welchen das freie Monomere aufgebraucht ist
z	Zustandsvektor mit n Bestandteilen
ΔH_R	Polymerisationswärme
σ_i	Vektor der Zustandsempfindlichkeit in bezug auf die Parameter

INDIZES

1	bezieht sich auf Wasser
2	bezieht sich auf Vinylchlorid
3	bezieht sich auf PVC
I	bezieht sich auf die erste Polymerisationsetappe $(0 \leqslant x \leqslant x_f)$
II	bezieht sich auf die zweite Polymerisationsetappe $(x \geqslant x_f)$

EXPONENTEN

0	bezieht sich auf den Zeitpunkt $t = 0$

LITERATUR

[1] M. Macoveanu und C. Petrila, *Bul. Inst. Polit. Iaşi*, in press.

[2] A. H. Abdel-Alim und A. E. Hamielec, *J. Appl. Polymer Sci.*, **16**, 783 (1972).

[3] A. H. Abdel-Alim und A. E. Hamielec, *J. Appl. Polymer Sci.*, **18**, 1603 (1974).

[4] R. Boudarel, J. Delmas, und P. Guichet, "Comande optimale des processus", vol. 1, Ed. Dunod, Paris, 1967.

Revue Roumaine de Chimie, 28, 7, 775 (1983)

COMPTE RENDU

DIETER BRITZ, *Digital Simulation in Electrochemistry*, edited by G. Berthier, M. J. S. Dewar, H. Fischer, K. Fukui, G. G. Hall, H. Hartman, H. H. Jaffé, J. Jortner, W. Kutzelnigg, K. Ruedenberg and E. Scrocco, series "Lecture Notes in Chemistry", Springer-Verlag, Berlin – Heidelberg – New York, 1981.

The book is dealing with a field of great importance for modern electrochemistry. It is hard to imagine any progress in fundamental and applied research in electrochemistry without using computers in order to get the proper results in a time as short as possible.

Written specially for electrochemists, the book of Dieter Britz is a very useful mathematical textbook for many scientists willing to deal with programming. As the author said this book is written for all the scientists "who do not have a friend who will tell them how to do it".

In only 120 pages the author succeeded to describe all the main aspects of the problems treated in nine chapters.

After a short introduction, the author described on chapter 2 the way the current crosses the electrode/electrolyte interface being proportional to the concentration gradient of the species to or from which electrons are being transferred. Digital expressions of diffusion equations have also been developed.

In chapter 3 the author described the procedure of solving the problems of diffusion processes occurring in the bulk of solution and of the way of digitally simulating diffusional transport.

Handling of boundary problems is given in chapter 4 related with controlled current, inert wall boundaries, electrode potential at controlled current, adsorption kinetics and so on.

Implicit techniques and other complications are discussed in chapter 5 dealing mainly with the finite difference method of Richardson, the Crank-Nicolson method and the development of the digital form for unequal intervals.

The problem of accuracy of simulations is more thoroughly treated in chapter 6, when stability is involved.

In chapter 7 the author is dealing with non-diffusional concentration changes.

The Laplace equation and other steady-state systems are presented in chapter 8 giving the mathematical formulation of potential distribution.

In the last chapter of the book some examples of digital simulation programs are given dealing with the potential step experiment, cyclic voltammetry, dropping mercury electrode, adsorption kinetics and ring-disc electrode by the steady state method.

Considering all these aspects the book proves to be a very useful tool for all electrochemists.

N. D. Totir

NOTE POUR LES AUTEURS

La Revue Roumaine de Chimie publie des articles en anglais, français, russe, allemand ou espagnol. Les auteurs sont priés d'envoyer des articles et des comptes rendus inédits.

Les manuscrits seront dactylographiés à double interligne. La bibliographie, les tableaux et la légende des figures seront placés après le texte.

Si l'article fait partie d'une série numérotée, la partie précédente sera donnée comme première référence.

Chaque article sera précédé d'un résumé comprenant quinze lignes au maximum.

Les références bibliographiques dans le texte seront faites par des exposants sans parenthèses et paraîtront à la fin de l'ouvrage.

Les publications périodiques mentionnées dans la bibliographie seront présentées suivant les prescriptions internationales : le nom de l'auteur précédé de l'initiale du prénom, le titre du périodique abrégé conformément à « Chemical Abstracts » et souligné par une ligne, le numéro du tome indiqué par des chiffres arabes et souligné par deux lignes, suivi de la première page de l'article ; à la fin, l'année de la parution sera placée entre parenthèses. Le numéro de la revue ne sera pas indiqué si les pages du volume sont numérotées consécutivement.

Les textes des livres ou traités inclueront : le nom des auteurs, l'initiale du prénom, le titre du livre entre guillemets et sans être souligné, le numéro du tome précédé par l'abréviation « vol. » (ou « Bd. ») le numéro de l'édition, les éditions (the publisher), la localité de la parution du livre, l'année de la parution et la page de la référence précédée(s) par l'abréviation « p » (ou « S »).

Les brevets seront indiqués comme suit : l'auteur ou la firme, le pays et le numéro du brevet, la date et la revue (*Chem. Abstr.*). Par ex. : M. Jones (to Union Carbide Co)., Brit. Pat. 601 238, 2 Sept. 1959 ; cf. *Chem. Abstr.*, **54**, 12808 (1960).

Si la référence n'a pas été lue en original, on indiquera aussi la revue de référence consultée.

Les diagrammes seront tracés à l'encre de Chine sur papier calque. Les tableaux et les figures (en nombre strictement nécessaire), ainsi que les courbes dans les figures seront numérotés par des chiffres arabes. Leur explication sera donnée dans la légende des figures. Prière de ne pas inscrire les mêmes données dans les tableaux et les figures. Chaque tableau aura un titre. On indiquera dans le texte la place approximative des tableaux et des figures. Les formules chimiques seront incluses dans le texte ; en outre, elle seront transcrites sur papier calque, à l'encre de Chine.

Les auteurs sont priés d'indiquer les caractères italiques (en soulignant les lettres au crayon), ainsi que tout autre caractère spécial ; les préfixes *ortho*, *meta*, *para*, *cis*, *trans*, etc. seront soulignés pour indiquer leurs caractères italiques et ne seront jamais écrits avec des majuscules.

Aucune correction à la main ne sera admise sur le manuscrit. Les corrections seront tapées à la machine. Les lettres grecques ou d'autres symboles spéciaux seront insérés à la main à l'encre clairement,

Le manuscrit sera signé par l'auteur.

Le titre-courant aura 50 lettres au maximum.

L'entière responsabilité du contenu des articles appartient aux auteurs.

Sur demande on peut obtenir une note plus complète.

PRINTED IN ROMANIA

ORSZÁGOS MUSZ

1984 FEB 0 9

TRAVAUX PARUS AUX ÉDITIONS DE L'ACADÉMIE DE LA RÉPUBLIQUE SOCIALISTE DE ROUMANIE

ELENA CEAUŞESCU, **Noi cercetări în domeniul compuşilor macromoleculari** (Nouvelles recherches dans le domaine des composés macromoléculaires), 1981, 536 p.

I.G. MURGULESCU, RODICA VÎLCU, **Introducere în chimia fizică, Vol. III. Termodinamica chimică** (Introduction à la chimie physique, Vol. III, Thermodynamique chimique), 1982, 626 p.

I. G. MURGULESCU, J. PĂUN, **Introducere în chimia fizică, Vol. I.3. Nucleul atomic, reacţii nucleare, particule elementare** (Introduction à la chimie physique. Vol. I.3. Noyau atomique, réactions nucléaires, particules élémentaires), 1982, 606 p.

ELENA JERCAN, **Analiza cromatografică** (Analyse chromatographique), 1982, 286 p.

I. G. MURGULESCU, TATIANA ONCESCU, E. SEGAL, **Introducere în chimia fizică. Vol. II. 2. Cinetică chimică şi cataliză** (Introduction à la chimie physique. Vol. II. 2. Cinétique chimique et catalyse), 1981, 1024 p.

V. DRĂGUŢAN, A. T. BALABAN, M. DIMONIE, **Metateza olefinelor şi polimerizarea prin deschidere de inel a cicloolefinelor** (La métathèse des oléfines et la polymérisation par ouverture annulaire des cyclooléfines), 1981, 254 p.

LYDIA-MARIA VAICUM, **Epurarea apelor uzate cu nămol activ. Bazele biochimice** (L'épuration des eaux résiduelles à boue active. Les bases biochimiques), 1981, 218 p.

I. GĂLĂŢEANU, **Procese şi metode radiochimice în energetica nucleară** (Processus et méthodes radiochimiques dans l'énergetique nucléaire), 1981, 234 p.

OCTAVIAN IORDACHE, **Procese polistocastice aplicate la fenomenele de transfer** (Processus polystochastiques appliqués aux phénomènes de transfert), 1981, 186 p.

CR. SIMIONESCU, VALERIA GORDUZA, **Polimeri biocompatibili şi biologic activi** (Polymères biocompatibles et biologiquement actifs), 1980, 479 p.

ELENA CEAUŞESCU, **Polimerizarea stereospecifică a izoprenului** (La polymérisation stéréospécifique de l'isoprène), 1979, 307 p.

CONST. GH. MACAROVICI, **Analiza chimică cantitativă anorganică** (L'analyse chimique quantitative inorganique), 1979, 457 p.

M. FLORESCU, **Metode ştiinţifice în dezvoltarea industriei chimice moderne** (Méthodes scientifiques dans le développement de l'industrie chimique moderne), 1979, 256 p.

A. T. BALABAN, I. GĂLĂŢEANU, G. GEORGESCU, LIGIA SIMIONESCU, **Compuşi marcaţi şi radiofarmaceutici cu aplicaţii în medicina nucleară** (Composés marqués et radiopharmaceutiques à application en médecine nucléaire), 1979, 495 p.

I. G. MURGULESCU, E. SEGAL, **Introducere în chimia fizică, vol. II. 1. Teoria molecular cinetică a materiei** (Introduction à la chimie physique. Vol. II. 1. La théorie moléculaire-cinétique de la matière), 1979, 1036 p.

S. STERNBERG, FL. DANEŞ, **Termodinamica chimică aplicată** (La thermodynamique chimique appliquée), 1978, 400 p.

I. G. MURGULESCU, V. EM. SAHINI, **Introducere în chimia fizică. Vol. I. 2. Structura şi proprietăţile moleculelor** (Introduction à la chimie physique. Vol. I.2. La structure et les propriétés des molécules), 1978, 604 p.

I. ZUGRĂVESCU, MAGDA PETROVANU, **N-ylid chemistry**, coédition avec McGraw-Hill International Book Company, U.S.A., 1977, 396 p.

I. G. MURGULESCU, **Introducere în chimia fizică. Vol. I.1. Atomi, molecule, legătură chimică** (Introduction à la chimie physique, Vol. I.1. Atomes, molécules, liaison chimique), 1976, 560 p.

ELENA CEAUŞESCU, **Research work on synthesis and characterization of macromolecular, compounds. Contributions**, 1974, 251 p.

CR. SIMIONESCU, VIORICA RUSAN, V. POPA, **Chimia algelor marine** (La chimie des algues marines), 1974, 212 p., 1 pl.

ISSN 0035—4090

I. P. „Informaţia" c. 1214

43 426

Lei 40
$ 70 (pour un abonnement annuel)

F 1103 04 Vegyész

ACADÉMIE DE LA RÉPUBLIQUE SOCIALISTE DE ROUMANIE

REVUE ROUMAINE DE CHIMIE

REFERÁLVA

TOME 28
N° 8
Août 1983

EDITURA ACADEMIEI REPUBLICII SOCIALISTE ROMÂNIA

Rev. Roumaine Chim. RRCHAX, 28, 8, p. 777–866 (1983) Bucarest

REVUE ROUMAINE
DE
CHIMIE

Tome 28, N° 8 Août, 1983

I. G. MURGULESCU and GABRIELA MINCU, Kinetics and mechanism of oxido-reduction reaction of the hydroxoaquobisoxalato Co(III) complex with iodide ion in neutral medium . . . . 779–783 R
V. EM. SAHINI and ELENA VOLANSCHI, Electronic structure and UV-spectra of some dibenzo[*b*, *e*]-thiepine derivatives 785–793
ALIN CIOCHINA and RODICA VILCU, Transient hot wire method for absolute and simultaneous measurement of thermal conductivity and thermal diffusivity of fluids . . . . 795–804 R
A. SYAMAL and B. K. GUPTA, New cobalt (II) complexes with tridentate dibasic ONO donor ligands . . . . 805–809 C
FLORICA ZĂLARU, D. IONESCU, AURELIA MEGHEA, FELICIA CORNEA and CONSTANŢA GHEORGHIU, Coordination compounds of Cu(II) with some triazenoimidazole derivates 811–817
R. P. VARMA and A. KUMAR, Conductance behaviour of aqueous solutions of alkaline earth metal butyrates . . . . 819–824 R
Y. M. ISSA, A. M. HINDAWEY, A. L. EL-ANSARY and R. M. ISSA, Spectroscopic investigation of charge transfer complexes of methyl pyridines with aromatic nitrocompounds . . . . 825–830 Bc
GH. SURPĂŢEANU, M. CONSTANTINESCU, C. LUCHIAN, M. PETROVANU, I. ZUGRĂVESCU and A. LABLACHE-COMBIER, Theoretical study on the reactivity of cycloimmonium-ylides. I. Reactivity of monosubstituted carbanion-ylides 831–839
E. I. GEORGESCU, FLORENTINA GEORGESCU, F. CHIRALEU and MAGDA PETROVANU, Dipolar derivatives in the quinazoline series. III. Quaternization of quinazoline with phenacyl bromide (in French) . . . 841–848
A. A. AFIFI, M. A. EL HASHASH and S. S. EL KADY, Synthesis and reactions of some 2-aryl-4-arylidene-5(4)-oxazolones 849–855
C. MIHART, S. RADULY and Z. SIMON, Molecular orbital studies for cyclophosphazene derivatives. IV. All-valence electron calculations by the *HMO* and *DEL RE* methods 857–861
C. I. CHIRIAC, Ethylene chlorophosphite as a new reagent for aromatic amide synthesis by a direct condensation reaction under very mild conditions 863–866 R

|Rev. Roumaine Chim.| **28**, *8*, 777–866(1983), Bucarest

Revue Roumaine de Chimie, 28, 8, 779 – 783 (1983)

KINETICS AND MECHANISM OF OXIDOREDUCTION REACTION OF THE HYDROXOAQUOBISOXALATO Co(III) COMPLEX WITH IODIDE ION IN NEUTRAL MEDIUM

ILIE G. MURGULESCU and GABRIELA MINCU
Institute of Chemistry, Department of Physical Chemistry,
Bd. Republicii 13, Bucharest, Romania

Received June 11, 1982

This paper deals with the kinetics and mechanism of oxidoreduction reaction between $[Co(C_2O_4)_2(H_2O)OH]^{-2}$ and I^- in neutral medium. With the rate constant values obtained at various reactant concentrations and various temperatures are calculated the reaction orders and activation parameters. A reaction mechanism is proposed according to these data.

INTRODUCTION

The oxalato Co(III) comlexes undergo intermolecular redox reaction with I^- catalysed by hydrogen ion. Our previous papers[1,2] dealt with the kinetics and mechanism of the reaction between bisoxalatodiaquo Co(III) complex with I^- in acid medium. The present paper studies the oxidoreduction reaction of hydroxoaquobisoxalato Co(III) complex with iodide ion in neutral medium.

RESULTS

The kinetic data verified a first order law with respect to the complex at all initial complex concentrations for a conversion up to 40% as can be seen in figure 1. The slope of the line calculated by least square method gives a rate constant $k_I = 2.9 \times 10^{-4} s^{-1}$. We carried out our experiments at various excess iodide concentrations. For a great excess iodide ($C_{I^-} = 0.313$ M), the linearity is verified only for a conversion of about 30%. The ratio between the first order rate constant k_I and the excess iodide concentration gives the second order constant $k_{II} = k_I/C_{I^-}$. (Table 1).

This data show that the reaction is first order with respect to the iodide concentration.

From our experiments at various temperatures (20, 25.5, 30 and 35.5°C) the activation parameters are calculated. The plot of log k_{II} versus $1/T$ (Figure 2) gives an activation energy of 19.250 cal/mol and log $A = 11.52$. The calculated activation entropy is -7.8 u.e. at 25°.

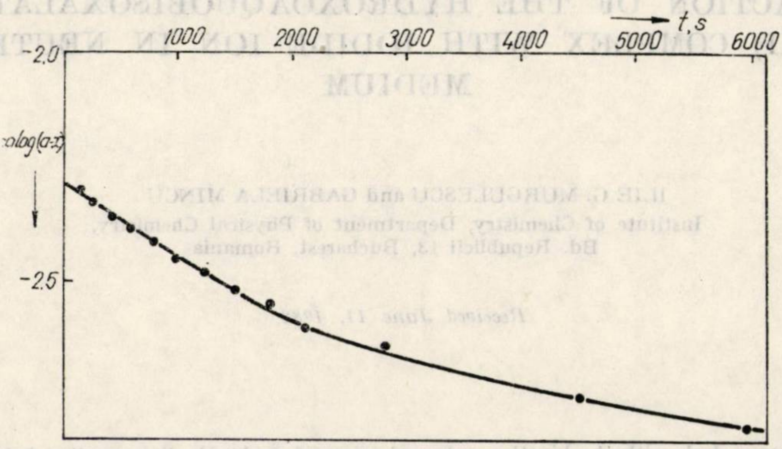

Fig. 1. — Typical first order dependence ($C_C = 5.22\ 10^{-3}$ M, $C_{I^-} = 0.104$ M, $t = 25.5$°C).

Table 1

The rate constants k_I and k_{II} for the reaction between $[Co(C_2O_4)_2(H_2O)OH]^{-2}$ and I^- at different initial reactant concentrations ($t = 25.5$°C)

$C_C \times 10^3$M	$C_{I^-} \times 10$M	$k_I \times 10^4 s^{-1}$	$k_{II} = \frac{k_I}{C_{I^-}} \times 10^3 M^{-1}s^{-1}$
2.61	1.04	2.9	2.8
5.22	1.04	2.8	2.7
7.81	1.04	2.7	2.7
5.22	0.52	1.5	2.8
5.22	1.57	3.7	2.3
5.22	2.09	5.1	2.3
5.22	3.13	7.1	2.3
			$k_{II} = 2.56 \pm 0.24$

DISCUSSION

According to our experimental data we suggest the following reaction mechanism:

$$[Co(C_2O_4)_2(H_2O)OH]^{-2} + H_2O \underset{k_1'}{\overset{k_1}{\rightleftharpoons}} [Co(C_2O_4)(OC_2O_3)(H_2O)_2OH]^{-2} \qquad (a)$$

$$[Co(C_2O_4)_2(H_2O)OH]^{-2}+I^- \xrightarrow{k_2} [Co(C_2O_4)_2(H_2O)OHI]^{-3} \quad (b)$$

$$[Co(C_2O_4)(OC_2O_3)(H_2O)_2OH]^{-2} + I^- \xrightarrow{k_3} [Co(C_2O_4)(OC_2O_3)(H_2O)_2OHI]^{-3} \quad (c)$$

$$[Co(C_2O_4)_2(H_2O)OHI]^{-3} \xrightarrow{k_4} CoC_2O_4 + C_2O_4^{-2} + 1/2I_2 + H_2O + OH^- \quad (d)$$

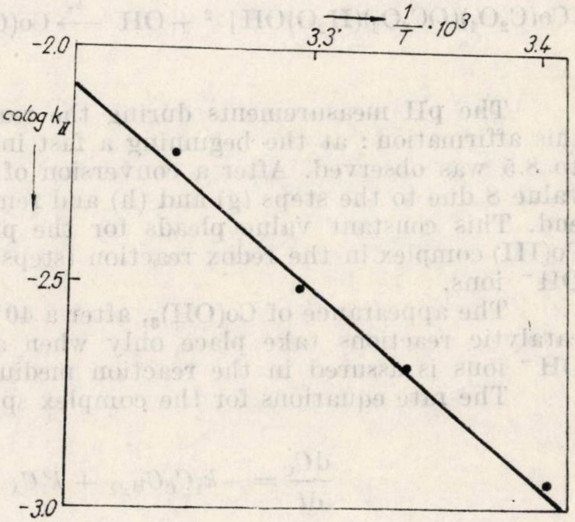

Fig. 2. — The plot of colog k_{II} *versus* $1/T$

$$[Co(C_2O_4)(OC_2O_3)(H_2O)_2OHI]^{-3} \xrightarrow{k_5} CoC_2O_4 + C_2O_4^{-2} + 1/2I_2 + 2H_2O + OH^- \quad (e)$$

The overall reaction is:

$$2[Co(C_2O_4)_2(H_2O)OH]^{-2} + 2\,I^- \xrightarrow{k_{obs}} 2CoC_2O_4 + 2C_2O_4^{2-} + I_2 + 2H_2O + 2OH^- \quad (f)$$

The initial Co(III) complex (C) is involved in the aquation fast preequilibrium (a) giving the aquated complex (A). This behaviour is common for all oxalic complexes of the transition metals.[1,3-7]. The two complexes C and A are simultaneously reduced by I^- in the slow parallel steps (b) and (c). The corresponding intermediate species containing iodine, lead to the final products in the fast steps (d) and (e).

After a conversion of 40% we noted the appearance of a brown precipitate due to $Co(OH)_3$ formation in the reaction medium.

It is known[7] that the hydroxoaquobisoxalato Co(III) complex decomposes at temperatures higher than 50°C according to the reaction:

$$[Co(C_2O_4)(H_2O)OH]^{-2} + H_2O \longrightarrow Co(OH)_3 + 2C_2O_4^{-2} + 2H^+$$

but, for our temperature range, this reaction is practically negligible.

The $Co(OH)_3$ appearance in our case is due to the alkaline catalysed decomposition of the complex in the presence of OH^- ions resulted from steps (d) (and (e) :

$$[Co(C_2O_4)_2(H_2O)OH]^{-2} + OH^- \xrightarrow{k_6} Co(OH)_3 + 2C_2O_4^{-2} + H^+ \qquad (g)$$

$$[Co(C_2O_4)(OC_2O_3)(H_2O)OH]^{-2} + OH^- \xrightarrow{k_7} Co(OH)_3 + 2C_2O_4^{-2} + H_2O + H^+ \qquad (h)$$

The pH measurements during the reaction are in agreement with this affirmation : at the beginning a fast increasing from initial value 7 to 8.5 was observed. After a conversion of 40% it decreases up to the value 8 due to the steps (g) and (h) and remains constant up to reaction end. This constant value pleads for the preponderant consumption of Co(III) complex in the redox reaction (steps (d) and (e)), which generates OH^- ions.

The appearance of $Co(OH)_3$, after a 40% conversion shows that the catalytic reactions take place only when a sufficient accumulation of OH^- ions is assured in the reaction medium.

The rate equations for the complex species C and A are :

$$\frac{dC_C}{dt} = -k_1C_CC_{H_2O} + k_1'C_A - k_2C_CC_{I^-} \qquad (1)$$

$$\frac{dC_A}{dt} = k_1C_CC_{H_2O} - k_1'C_A - k_3C_AC_{I^-} \qquad (2)$$

By summing equations (1) and (2) we get

$$-\frac{d(C_C+C_A)}{dt} = (k_2C_C + k_3C_A)C_{I^-} \qquad (3)$$

Taking into account the equilibrium constant K of the preequilibrium (a) one gets :

$$-\frac{d(C_C+C_A)}{dt} = (k_2C_C + Kk_3C_CC_{H_2O})C_{I^-} \qquad (4)$$

Finaly it can be rewritten :

$$-\frac{d(C_C+C_A)}{dt} = (k_2 + Kk_3C_{H_2O})C_C\,C_{I^-} \qquad (5)$$

Our experimental results led to a similar rate equation namely :

$$-\frac{d(C_C+C_A)}{dt} = k_{obs}\,C_C\,C_{I^-} \qquad (6)$$

The reaction mechanism proposed above describes the electron transfer between Co(III) and I^-.

EXPERIMENTAL

The procedure (clock method) was described in a previous paper.[1] It was not possible to follow the kinetics of this reaction spectrophotometrically, because the reaction medium is not transparent. The hydroxoaquobisoxalato Co(III) complex (Durrant's salt) was obtained as indicated in literature.[7,8] Potassium iodide was BDH analytical reagent . The sodium thiosulphate ("Reactivul") was recrystallized. The solutions were prepared in doubly distilled water. The reactions were performed in a thermostated vessel under continuous magnetic stirring. A concentrated solution of sodium thiosulphate was added with a micropipette, to avoid an excessive dilution of the reaction medium. On the other hand, under these conditions it was not necessary to thermostate the titration reagent (sodium thiosulphate). The concentration of the unreacted complex was calculated taking into account the successive dilution of the medium. All the experiments were performed in excess iodide.

Our experimental technique did not permit to follow the reaction kinetics at higher conversion when the alkaline catalysed decomposition overlaps, because it was not possible to appreciate the colour reaction of I_2 with starch.

REFERENCES

[1] I. G. Murgulescu and G. Mincu, *Rev. Roumaine Chim.*, **23**, 471 (1978).
[2] I. G. Murgulescu, G. Mincu and E. Jurconi, *Rev. Roumaine Chim.*, **25**, 1033 (1980).
[3] G. M. Harris and F. D. Graziano, *J. Phys. Chem.*, **63**, 330 (1959).
[4] T. Oncescu, E. Pantazi and R. Pressel, private communication.
[5] T. Oncescu and E. Jurconi, *Rev. Roumaine Chim.*, **22**, 1471 (1977).
[6] T. Oncescu and E. Jurconi, *Rev. Roumaine Chim.*, **22**, 69 (1979).
[7] T. Oncescu Thesis, 1966.
[8] R. G. Durrant, *J. Chem. Soc.* **1905**, 176.

Revue Roumaine de Chimie, **28**, *8*, 785 – 793 (1983)

ELECTRONIC STRUCTURE AND UV-SPECTRA OF SOME DIBENZO [*b*, *e*]-THIEPINE DERIVATIVES

V. Em. SAHINI and ELENA VOLANSCHI
Department of Physical Chemistry, Polytechnic Institute, Bd. Republicii 13, Bucharest, Romania

Received July, 14, 1982

The results of the MO calculations performed in the framework of the LCAO—HMO and SCF—CI—PPP methods on some derivatives in the dibenzo [*b*, *e*]-thiepine class are reported and discussed in connection with the UV-spectra. The role of the different moieties (heteroatom, methylene, carbonyl group) is outlined by comparison with reference compounds containing only one from these structural entities.

The electronic structure of the dibenzo [*b*,*e*]-thiepine derivatives is of both theoretical and practical interest.

The theoretical interest is determined by the structural peculiarities of this system, i.e. the presence of the heteroatom in a seven-membered ring, which was rather little investigated [1,2] as compared to the five- or six-membered heterocycles, the influence of the oxidation degree of the sulphur atom, the simultaneous presence of donor and acceptor groups in the same molecule, etc.

On the other side, the known pharmacological activity of some derivatives [3,4] confers to this class a practical interest connected to their possible application in the drug production.

Although radicalic species from this class of compounds were already reported,[5] no study is available up to now discussing the electronic spectra and structure of the neutral compounds.

Therefore, it is the aim of this paper to report and discuss the electronic spectra and the results of the MO calculations performed on some derivatives in this series :

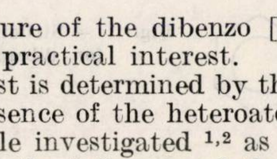

I X = S ; Y = CO
II X = SO ; Y = CO
III X = SO_2 ; Y = CO
IV X = S ; Y = CH_2
V X = O ; Y = CO

MO CALCULATIONS

The MO calculations were performed in the frame of the LCAO-HMO and SCF-Pariser Parr-Pople approximations. In the preliminary HMO treatment the heteroatoms were taken into account using standard parameters (Table 1). The methylene group was considered either in a conjugative (C.M) or an inductive model (I.M.). The sulphoxide and sulphone groups were assumed to furnish two electrons to the aromatic conjugation in a "heteroatom model" (H.M.) The "d-model" (M.d) proposed by Janssen and de Jong[6] was also employed.

The SCF—CI—PPP calculations were carried out using a program written in FORTRAN.[7] Configurational interaction between 16 monoexcited configurations was also included. For the different atomic groups several literature sets of parameters were tried.[8-11] The values finally employed are presented in Table 1.

For the methylene group in site 6 two limiting models were used : in "model A" it was described by a conjugative model and in "model B" its presence was neglected.

As no information was available for the geometry of these componds, a study of the influence exerted by it on the electronic spectrum was necessary. It was performed for compound IV, which was considered folded along the axes in figure 1 with dihedral angles varying from 0° to 40°. It was stated that the SCF—CI calculated transitions differ with less than 0.05 eV from the hypothetical plane molecule, and that the componency of the CI vectors is practically not influenced. Therefore, idealised plane geometries with the distances in Table 1 were used throughout the calculations performed on all the compounds.

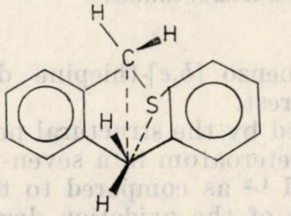

Fig. 1. — Structural model considered for dibenzo [*b*,*e*]-thiepine.

Table 1

Parameters used in the LCAO—HMO and SCF—CI—PPP calculations

	$C=O$	$^{C'}_{C}\rangle C=H_2$		$-O-$	$-S-$	SO	SO_2	
		C.M.	I.M.			H.M.	H.M.	M.d.
h_X	1.00	−0.30	−0.20 (C′)	2.00	1.20	−1.50	−2.60	−1.40(S)
k_{CX}	1.20	2.00	—	0.71	0.42	0.70	0.99	0.90 (SO)
		0.90 (CC′)						0.70 (CS)

X	(Å) r_{CX}	W_X (eV)	(eV) γ_{XX}	(eV) β_{CX}
$\dot{C}$	1.40	−11.42	10.84	−2.30
$\ddot{O}$	1.40	−35.11	21.50	−1.63
$\ddot{S}$	1.75	−20.88	11.90	−1.31
$\dot{O}$	1.22	−17.70	15.34	−2.70
H_2	1.10	−10.25	9.34	−2.70

RESULTS AND DISCUSSION

a) The LCAO—HMO approximation

The electronic transitions calculated in the LCAO-HMO approximation using the different models are presented in Table 2.

The first problem to be discussed is the assignment of the transition at the longest wavelength, which is present in all the compounds containing the carbonyl group. Taking into account that the $n - \pi^*$ transition in benzophenone is in the same range (3.74 eV [12]), this band could be considered as due to such a transition. However, Giovanelli et al. [13] have pointed out that for molecules where donor and acceptor groups are simultaneously present, the lowest energy $\pi - \pi^*$ transition has an intramolecular charge transfer character and is strongly bathochromically shifted; therefore it is usually overlapping the $n - \pi^*$ transition characteristic of the carbonyl group. As the charge diagrams for the fundamental ψ_0 and excited $\Psi_{m,m+1}$ states point out (Fig. 2), the $\Psi_0 \rightarrow \Psi_{m,m+1}$ transition implies an intramolecular charge transfer from the sulphur atom to the carbonyl group, and therefore the longest wavelength band was assigned to this transition.

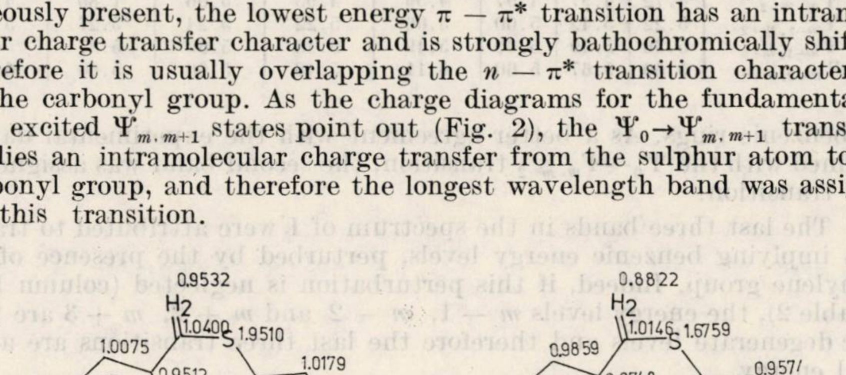
0.9532
H2
1.0400
S 1.9510
1.0075
1.0179
0.9606
0.9512
0.9388
1.0247
1.0321
0.9596
1.0063
0.7379
0.9545
0.9547
1.0131
O
1.4969
Ψo
0.8822
H2
1.0146
S 1.6759
0.9859
0.9571
0.9748
1.0403
0.8941
1.0230
0.9973
1.0304
0.9501
0.9817
1.0247
1.0098
0.8805
O
1.6766
Ψm,m+1
0.9386
H2
1.0220
S 1.6707
1.1388
0.9573
1.1472
0.8290
0.9639
1.0206
0.9995
0.9661
1.2097
0.7382
1.0817
0.9370
0.8646
O
1.4947
Ψm,m+2
0.9165
H2
1.0218
S 1.9216
0.9170
0.9803
0.8473
0.9432
1.0305
1.0109
1.0429
1.0438
0.8155
0.9815
0.9667
1.0028
0.9405
O
1.6168
Ψm-1, m+1

Fig. 2. — Charge diagrams calculated for I in the fundamental Ψ_0, and excited states $\Psi_{m,m+1}$, $\Psi_{m,m+2}$ and $\Psi_{m-1,m+1}$.

The second transition in the spectra of these compounds could be assigned either to a $\Psi_0 \rightarrow \Psi_{m,m+2}$ or to a $\Psi_0 \rightarrow \Psi_{m-1,m+1}$ transition. Examination of the charge diagrams in figure 2 points out that the first may be associated with the conjugation of the heteroatom with the benzenic rings, whereas the second with the conjugation of the carbonyl group to

Table

Experimental (eV) and calculated LCAO–HMO

Compound / Transition	I				II			
	C.M.	I.M.	M.L.	ΔE_{exp}	M.d. C.M.	M.d. I.M.	H.M.	ΔE_{exp}
$\Psi_0 \rightarrow \Psi_{m,\, m+1}$	3.13	3.31	3.27	3.47	3.50	3.66	1.33	3.56
$\Psi_0 \rightarrow \Psi_{m,\, m+2}$	4.72	4.97	4.97	4.59	4.93	5.06	1.80	4.52
$\Psi_0 \rightarrow \Psi_{m-1,\, m+2}$	5.22	5.42	5.60	5.06	5.22	5.24	5.27	5.06
$\Psi_0 \rightarrow \Psi_{m-1,\, m+3}$	5.36	5.49	5.60	5.49	5.48	5.60	5.37	—
$\Psi_0 \rightarrow \Psi_{m-2,\, m+3}$	5.60	5.67	5.60	6.11	5.48	5.60	5.60	6.02

the benzenic rings. As a better agreement with the experimental data is obtained with the $\Psi_0 \rightarrow \Psi_{m,\, m+2}$ transition, the second band was assigned to this transition.

The last three bands in the spectrum of I were attributed to transitions implying benzenic energy levels, perturbed by the presence of the methylene group. Indeed, if this perturbation is neglected (column M.L. in Table 2), the energy levels $m-1$, $m-2$ and $m+2$, $m+3$ are benzenic degenerate levels and therefore the last three transitions are all of equal energy.

Examination of the data in Table 2 points out that the hypsochromic shift observed at the oxidation of the sulphur atom (compounds II and III) is suitably described only by the "d model" (M.d.). It is also noteworthy that the model chosen to describe the sulphoxide or sulphone group does not influence the last three transitions, of a benzenic character.

Special discussion is required by compound V. In this case, although the calculated $\Psi_0 \rightarrow \Psi_{m,\, m+1}$ transition is in the range 3 – 4 eV, it is difficult to admit this assignment since the highest occupied molecular orbital (h.o.m.o.) is no more determined by the heteroatom; therefore in this case, the longest wavelength band has no more an intramolecular charge transfer character and was consequently assigned to an $n-\pi^*$ transition.

b) The SCF–PPP–CI approximation

The electronic transitions and the componence of the CI-eigenvectors calculated for compounds I, IV and V are presented in Tables 3 – 5. The assignment is based upon the energetical criterion and the value of the transition moment (Q^2). The energy of the h.o.m.o. was also listed and compared to the experimental ionization potential from literature.[14] An overall good agreement is observed for both models A and B. For compound I (Table 3), model A reflects better the first transition and the intensity ratio in the experimental spectrum, especially for the bands at 5.06 and 6.11 eV. In both models the longest wavelength transition is a nearly pure $\Psi_0 \rightarrow \Psi_{m,\, m+1}$ transition, as it is reflected by the comparison of the

2

electronic transitions ($\beta = -2.8$ eV)

III				IV		V		
M.d.		H.M.	ΔE_{exp}	C.M.	ΔE_{exp}	C.M.	I.M.	ΔE_{exp}
C.M.	I. M.							
								($n-\pi^*$)
3.52	3.68	1.43	3.67	4.51	4.17	3.37	3.58	3.73
5.03	5.15	1.74	4.71	4.68	4.27	4.94	5.22	4.59
5.32	5.33	5.27	—	4.91	4.77	5.25	5.42	—
5.48	5.60	5.37	5.39	5.02	5.28	5.37	5.55	—
5.48	5.60	5.60	5.93	5.42	5.87	5.60	5.73	5.71

ΔE_{SCF} (column 1) with the ΔE_{CI} values (column 2), and by the corresponding CI-eigenvectors.

The examination of the calculated energy levels points out that the lowest empty molecular orbital (l.e.m.o.) is localized on the carbonyl group, and that the h.o.m.o. is determined by the sulphur atom. Therefore, the intramolecular charge transfer character of the first transition is also evidenced by the SCF—CI—PPP treatment.

For the second band of I, two transitions of different intensities and CI-componency were obtained in the models A and B. However, in both models, the major contribution is due to the excited $\Psi_{m,\,m+2}$ configuration. It is also noteworthy that the configurational interaction does not markedly influence this transition, justifying the LCAO-HMO assignment.

As the last three bands are concerned, the comparison of the ΔE_{SCF} and ΔE_{CI} values and the componency of the CI-eigenvectors reveal the important role of the configurational interaction. Therefore, in this case no reference to the LCAO-HMO preliminary treatment is possible any more.

Examination of Table 4 reveals the major role of the configurational interaction for compound V. It is explainable since for this compound the last occupied levels are perturbed benzenic levels and therefore very near in the energy scale.

For this compound the presence of only two experimental bands (the $n-\pi^*$ transition cannot be accounted for in the framework of this treatment) renders difficult a comparison of the two models. However, model B reflects better the first $\pi-\pi^*$ transition, as compared to model A, which leads to a nearly pure $\Psi_0 \rightarrow \Psi_{m,\,m+1}$ transition at an energy value nearer the $n-\pi^*$ than the first $\pi-\pi^*$ band.

For compound IV (Table 5) a better overall agreement is obtained in the frame of the B model with CI, in comparison with model A. This may be explained by the fact that the assumption of a continuous conjugation in the median ring overestimates the role of the methylene group in this compound.

In order to evidence better the role of the different structural entities on the electronic structure of compounds I, IV and V, reference compounds containing only one of these groups were also calculated with the same

Table 3

Experimental and SCF–PPP calculated electronic transitions for dibenzo [*b*, *e*]-thiepinone (I)

Model A					Model B			
(eV) ΔE_{SCF}	(eV) ΔE_{CI}	Q^2	Ψ_{CI}	(eV) ΔE_{exp}	(eV) ΔE_{SCF}	(eV) ΔE_{CI}	Q^2	Ψ_{CI}
3.40	3.34	0.1078	$0.983\ \Psi_{m,\ m+1}$	3.47	3.23	3.11	0.2082	$0.963\ \Psi_{m,\ m+1} - 0.221\ \Psi_{m,\ m+2}$
4.36	4.17	0.1613	$0.725\ \Psi_{m-1,\ m+1} - 0.361\ \Psi_{m-2,\ m+1} + 0.304_{m-2,\ m+2}$	4.59	4.12	4.16	0.0402	$0.932\ \Psi_{m,\ m+2} - 0.210\ \Psi_{m,\ m+3}$
	4.30	0.7516	$0.946\ \Psi_{m,\ m+2} + 0.155\ \Psi_{m-1,\ m+1}$			4.46	0.0890	$0.731\Psi_{m-3,\ m+1} + 0.311\ \Psi_{m-3,\ m\neg 2} - 0.510\ \Psi_{m-2,\ m+2}$
5.27	4.73	0.8185	$0.509\Psi_{m-1,\ m+1} + 0.616\ \Psi_{m,\ m+3}$	5.06	6.40	5.01	2.5425	$0.496\ \Psi_{m-2,\ m+1} - 0.680\ \Psi_{m,\ m+4} - 0.499\ \Psi_{m-1,\ m+1}$
	4.97	1.9977	$0.729\ \Psi_{m,\ m+4} + 0.496\ \Psi_{m-3,\ m+1}$			5.08	0.5063	$0.704\ \Psi_{m-1,\ m+1} + 0.640\ \Psi_{m-2,\ m+1}$
6.12	5.34	0.7652	$0.795\ \Psi_{m-1,\ m+2} + 0.444\ \Psi_{m,\ m+4} + 0.280\ \Psi_{m-2,\ m+1}$	5.49	6.24	5.93	0.2765	$0.606\Psi_{m-3,\ m+1} - 0.355\ \Psi_{m-3,\ m+3} + 0.583\ \Psi_{m-2,\ m+2} + 0.254\ \Psi_{m-1,\ m+2}$
6.78	6.09	1.3053	$0.699\ \Psi_{m-3,\ m+3} - 0.517\ \Psi_{m-3,\ m+4} - 0.625\ \Psi_{m,\ m+2}$	6.11	6.57	6.05	0.9801	$0.812\ \Psi_{m-1,\ m+4} + 0.321\ \Psi_{m-1,\ m+3} - 0.216\ \Psi_{m-3,\ m+2}$
	h.o.m.o. = 9.05 eV			I.P.$_{exp}$ = 9.21 eV				h.o.m.o. = 9.17 eV

14

Table 4

Experimental and SCF—PPP calculated electronic transitions for dibenzo[*b*, *e*]-oxepinone (V).

Model A					Model B			
(eV) ΔE_{SCF}	(eV) ΔE_{CI}	Q^2	Ψ_{CI}	(eV) ΔE_{exp}	(eV) ΔE_{SCF}	(eV) ΔE_{CI}	Q^2	Ψ_{CI}
4.16	3.98	0.2745	$0.923\Psi_{m,m+1} - 0.234\Psi_{m-1,m+2}$	4.59	4.75	4.26	0.0501	$0.672\Psi_{m,m+1} - 0.497\Psi_{m-1,m+1} - 0.281\Psi_{m,m+4} - 0.272\Psi_{m-1,m+4}$
5.10	4.47	0.6894	$0.567\Psi_{m-2,m+1} - 0.522\Psi_{m-3,m+1}$		6.17	4.69	0.5081	$0.781\Psi_{m-2,m+1} - 0.379\Psi_{m,m+1} - 0.311\Psi_{m-1,m+1}$
5.85	4.95	1.0294	$0.704\Psi_{m-1,m+1} + 0.567\Psi_{m-3,m+1} + 0.258\Psi_{m,m+2}$	—	6.46	5.03	0.2940	$0.666\Psi_{m-1,m+1} + 0.504\Psi_{m,m+1} + 0.482\Psi_{m-2,m+1}$
5.83	5.09	1.3148	$0.819\Psi_{m,m+2} - 0.463\Psi_{m-2,m+1}$	—	6.31	5.59	0.2196	$0.421\Psi_{m-1,m+1} + 0.483\Psi_{m,m+3} - 0.396\Psi_{m,m+4}$
6.78	5.97	1.0382	$0.512\Psi_{m-2,m+2} + 0.369\Psi_{m-1,m+2} + 0.676\Psi_{m,m+4}$	5.71	6.56	5.84	0.3508	$0.523\Psi_{m-3,m+1} - 0.365\Psi_{m-3,m+3} + 0.461\Psi_{m-2,m+2}$

h.o.m.o. = 9.87 eV $I.P_{exp}$ = 9.63 eV[14]   h.o.m.o. = 10.43 eV

Table 5

Experimental and SCF−PPP calculated electronic transitions for dibenzo [*b*, *e*]-thiepine (IV)

Model A				(eV) ΔE_{exp}	Model B			
(eV) ΔE_{SCF}	(eV) ΔE_{CI}	Q^2	Ψ_{CI}		(eV) ΔE_{SCF}	(eV) ΔE_{CI}	Q^2	Ψ_{CI}
3.87	3.81	0.0636	$0.964\,\Psi_{m,\,m+1}$	4.17	3.66	3.49	0.2048	$0.904\,\Psi_{m,\,m+1} - 0.345\,\Psi_{m,\,m+2}$
	4.14	0.2194	$0.892\,\Psi_{m,\,m+2} + 0.294\,\Psi_{m,\,m+3}$			4.01	0.0679	$0.882\,\Psi_{m,\,m+2} + 0.350\,\Psi_{m,\,m+1} - - 0.269\,\Psi_{m,\,m+3}$
4.26	4.39	0.4868	$0.793\,\Psi_{m-1,\,m+1} + 0.394\,\Psi_{m,\,m+4} - - 0.271\,\Psi_{m-1,\,m+2}$	4.27	4.00	4.51	0.2019	$0.789\,\Psi_{m,\,m+4} + 0.383\,\Psi_{m-1,\,m+2}$
						4.55	0.1775	$0.532\,\Psi_{m-3,\,m+1} - 0.503\,\Psi_{m-1,\,m+2} + + 0.451\,\Psi_{m,\,m+4}$
4.75	4.48	0.4385	$0.634\,\Psi_{m,\,m+4} - 0.443\,\Psi_{m-1,\,m+1} + + 0.404\,\Psi_{m-1\; m+3}$	4.77	5.29	4.69	0.5824	$0.944\,\Psi_{m-1,\,m+1}$
5.14	4.99	0.9780	$0.628\,\Psi_{m-1,\,m+2} + 0.464\,\Psi_{m,\,m+4} + + 0.386\,\Psi_{m-1,\,m+3}$	5.28	5.41	5.32	2.8383	$0.651\,\Psi_{m-1,\,m+3} - 0.3353\,\Psi_{m-1,\,m+4} + 0.553\,\Psi_{m-2,\,m+1} + 0.309\,\Psi_{m,\,m+4}$
6.18	5.34	3.2050	$0.588\,\Psi_{m-1,\,m+3} + 0.493\,\Psi_{m-3,\,m+1} - - 0.392\,\Psi_{m-2,\,m+1}$	5.87	6.59	5.67	0.4238	$0.863\,\Psi_{m-1,\,m+4} + 0.182\,\Psi_{m-1,\,m+3}$
						5.87	0.7006	$0.680\,\Psi_{m-1,\,m+2} + 0.644\,\Psi_{m-3,\,m+1}$
	h.o.m.o. = 8.85 eV			I.P.$_{\mathrm{exp}}$ = 8.77 eV[14]				h.o.m.o. = 8.77 eV

method and parameters. Therefore benzophenone, phenylbenzylsulphide, phenylbenzyloxide and diphenylmethane were also calculated.

The results point out that in compound I the highest occupied molecular orbitals are similar to those in phenylbenzylsulphide, whereas the lowest empty MO's are similar to those in benzophenone. In other words the highest occupied MO's are determined by the moiety containing the heteroatom and the lowest empty ones by the moiety containing the carbonyl group. For compound V the situation is similar with regard to the lowest empty MO's, but the highest occupied ones are of a benzenic character, perturbed by the methylene group.

In compound IV the highest occupied MO's are determined by the heteroatom containing moiety, whereas the lowest empty ones by the methylene group.

In conclusion, the analysis of the electronic spectra of compounds I, IV and V by the SCF – CI – PPP treatment, using two limiting models for the methylene group, reveals the following aspects :

— model A gives a better agreement than model B for compound I but not for IV, because it overestimates the role of the methylene group ;

— the heteroatom containing moiety determines the position of the highest occupied MO's in compounds I and IV, but not in V, where the last MO's are determined by the phenyl rings ;

— the perturbation produced by the methylene group is small in the carbonylated compounds, but becomes important in the thiepine derivatives, determining the interruption of the conjugation in the median ring.

REFERENCES

[1] M. J. S. Dewar and Trinajstič, *Tetrahedron*, **26**, 4269 (1970).

[2] T. Toth and L. Klasinc, *Z. Naturforsch.*, **29a**, 1371 (1974).

[3] M. Rajsner and M. Protiva, *Cesk. Farm.*, **11**, 404 (1962).

[4] M. Rajsner, E. Svatek, J. Metysova and M. Protiva, *Coll. Czech. Chem. Comm.*, **34**, 1963 (1969).

[5] E. Volanschi, C. Vlădescu and C. Volanschi, *Rev. Roumaine Chim.*, **19**, 755 (1974).

[6] F. de Jong and M. Janssen, *J. Chem. Soc., Perkin Trans, II*, **5**, 572 (1972).

[7] C. Bendic, M. Hillebrand and V. Em. Sahini, *Rev. Roumaine Chim.*, **23**, 3 (1978).

[8] I. G. Smeyers, *Theor. Chim. Acta*, **28**, 357 (1972).

[9] C. Leibovici, *Theor. Chim. Acta*, **4**, 321 (1966).

[10] T. Morita, *Bull. Chem. Soc. Japan*, **38**, 1638 (1965).

[11] B. Tynland, *Tetrahedron Letters*, **15**, 1789 (1968).

[12] W. L. Dilling, *J. Org. Chem.*, **31**, 1045 (1966).

[13] K. H. Giovanelli, J. Dehler and G. Hohlneicher, *Ber. Bunsenges. physik. Chem.*, **75**, 864 (1971).

[14] V. Constantin, V. Em. Sahini, I. Şerban and C. Vlădescu, *Rev. Roumaine Chim.*, **23**, 163, 315 (1978).

Revue Roumaine de Chimie, 28, 8, 795 – 804 (1983)

TRANSIENT HOT WIRE METHOD FOR ABSOLUTE AND SIMULTANEOUS MEASUREMENT OF THERMAL CONDUCTIVITY AND THERMAL DIFFUSIVITY OF FLUIDS

ALIN CIOCHINA* and RODICA VILCU**

* Centre of Physical Chemistry, ICECHIM, Spl. Independenței No. 202, 79611 Bucharest, Romania.

** The National Institute of Chemistry, Dept. of Physical Chemistry and Electrochemical Technology, Blvd. Republicii No. 13, Bucharest, Romania.

Received February 7, 1983

This paper presents a new computation method together with a new experimental procedure which allow for absolute and simultaneous determination of thermal conductivity and thermal diffusivity of fluids by the transient hot wire method, no matter the diameter of the employed wire and without ab initio knowing the wire physical properties. The validity of the computation method, the simplicity of the experimental procedure and accuracy of the data are proved by the results obtained on six gases at room temperature and atmospheric pressure.

1. INTRODUCTION

The transient hot wire method is intensively employed for determining thermal conductivity of liquids and gases.[1,2] The theory of the method is quite well known[3–20] and the equipment built up by means of modern electronics furnishes very accurate measurements.[9–11,13,14] According to the *classical procedure* of the method, the thermal conductivity has been determined from a linear logarithmic law. Also from the theory of the method it results that by the same classical procedure the fluid thermal diffusivity can be determined as well.[7,21,22] In order to do that, the measurements have to be very accurate and the experimental parameters so chosen as to make sure that determinations are certainly carried out within the validity range of the linear logarithmic law. This last condition must be tested experimentally and by computation. The calculation of the linear logarithmic law domain implies the knowledge of some physical characteristics of both wire and fluid : wire diameter, density and specific heat of wire and fluid, etc., with which some corrections are made for the measured data. *Practically, the validity of the classical procedure of the transient hot wire method is decided upon by the wire diameter, especially in the case of gases.*

We presented in our previous papers the experimental assembly[23−26] and application of the classical procedure by determining the two thermal parameters in liquids [25−28] and gases,[26,29] using a platinum wire with a diameter of 0.015 mm. The results are good for liquids. In order to employ the classical procedure for gases some conditions should be fulfilled [26,29] among which the most important is to use wires with diameters of the order of microns. If one obeys these conditions one has yet to surpass some other experimental difficulties.[26,29] The way the different experimental parameters, involved in establishing the time range over which a linear logarithmic law holds, intervene is strongly contradictory. For this reason, the cells and measuring apparatus have been specialized for determinations in either gases or liquids.

The present paper is aimed at describing the following contributions [26] to the transient hot wire method:

— a new computation method for absolute and simultaneous determination of thermal conductivity, λ, thermal diffusivity, $a = \lambda/(\rho c_p)$, and volumic specific heat, $\rho c_p = \lambda/a$, of the fluids, no matter the wire diameter and without ab initio knowing the wire physical properties;

— a new experimental procedure for absolute and simultaneous measurement of λ, a and (ρc_p) quantities with the same apparatus, transducer and cell, during the same experimental run, on dielectric gases and liquids.

2. BASICS OF THE COMPUTATION METHOD

The temperature rise, $\theta(r_1, t)$, for a wire of radius r_1, at $r = r_1$ and time t counted from the heating turning on time, $t = 0$, against the initial temperature T_0 of the cell at $t = 0$, is given by the relation [30]:

$$\theta(r_1, t) = \frac{q}{4\pi\lambda}\left[\ln\frac{4\tau}{C} + \frac{1}{2\tau}\left(1 + \chi\ln\frac{4\tau}{C}\right) + \cdots\right] \tag{1}$$

or:

$$\Phi(r_1, t) = \frac{1}{\lambda}\left\{\left[1 + \frac{1}{t}\left(u - \frac{A_1}{\lambda}\right)\right]\ln\frac{2t}{uC} + \frac{u}{t}\right\} \tag{2}$$

where: q is the power dissipated per metre of the wire; λ, ρ, c_p and a are thermal conductivity, density, heat capacity and thermal diffusivity of the fluid, respectively; ρ_1 and c_1 are density and specific heat of the wire material, respectively;

$$\tau = at/r_1^2; \quad \chi = 1 - [\rho_1 c_1/(\rho c_p)]; \quad C = 1.781$$

$$\Phi(r_1, t) = (4\pi/q)\,\theta(r_1, t); \quad u = r_1^2/(2a); \quad A_1 = r_1^2 \rho_1 c_1/2 \tag{3}$$

The linear logarithmic law:

$$\theta(r_1, t) = \frac{q}{4\pi\lambda} \ln \frac{4at}{r_1^2 C} \tag{4}$$

is obeyed only for $t_A \leqslant t \leqslant t_B$, where t_A and t_B are limit values for minimum and maximum times, respectively.[25-29]

The computation method, based on eq.(1), uses the $\theta(r_1, t)$ values measured both in the short time range, $t < t_A$, where r_1, a and χ are important, and in the long time range, $(t_A \leqslant) t \leqslant t_B$, where λ is the significant parameter.[26] All quantities involved in computations θ, t, r_1 and A_1 are measured. The wire diameter is measured with an optical microscope. The "wire constant", A_1 is determined from the transient heat transfer equation of the wire heated in vacuo.

2.1. Determination of the "wire constant"

For very short times, the temperature rise of the wire is given by the equation: [12,30,31]

$$\Phi(r_1, t) = \frac{4}{r_1^2 \rho_1 c_1} t \left[1 - \frac{8}{3\sqrt{\pi}} \frac{\lambda}{r_1 \rho_1 c_1 \sqrt{a}} \sqrt{t} \right] \tag{5}$$

The temperature rise of the wire in vacuo($\lambda = 0$) is represented by a straight line which intercepts the origin:

$$\Phi_v(r_1, t) = \frac{4}{r_1^2 \rho_1 c_1} t = \frac{2}{A_1} t \tag{6}$$

2.2. Methods of calculation

The first version of the calculation method consists of an iterative solving of equation (1) by a non-linear regression with two parameters, $P(1)$ and $P(2)$, according to Gauss' method; with relations:

$$y = \Phi(r_1, t); \quad x = t$$

$$P(1) = 1/\lambda; \quad P(2) = 2u = r_1^2/a$$

equation (1) becomes:

$$y = P(1) \left[\left(1 - \frac{2A_1 P(1) - P(2)}{2x} \right) \ln \left(2.246 \frac{x}{P(2)} \right) + \frac{P(2)}{2x} \right] \tag{7}$$

In this version the whole set of experimental (Φ, t) values is computerized. The initial values of $P(1)$ and $P(2)$ parameters are:

$$P^{(0)}(1) = 1/\lambda^{(0)}; \qquad P^{(0)}(2) = r_1^2/a^{(0)} \tag{8}$$

$\lambda^{(0)}$ and $a^{(0)}$ are computed with the following equations[25-29]:

$$\lambda^{(0)} = \frac{\ln t_2 - \ln t_1}{\Phi_2^{(0)} - \Phi_1^{(0)}} \tag{9}$$

$$\Phi_{1,2}^{(0)} = \frac{4\pi}{q}\,\theta(r_1, t_{1,2}) \tag{10}$$

$$a^{(0)} = r_1^2 C/(4t_0) \tag{11}$$

$$\ln t_0 = \ln t_1 - \Phi_1^{(0)}\lambda^{(0)} \tag{12}$$

$$a^{(0)} = \frac{r_1^2 C}{4t_1}\exp\,(\Phi_1^{(0)}\lambda^{(0)}) \tag{13}$$

from pairs (Φ_i, t_i) and (Φ_j, t_j) of the experimental set $(t_{i,j} < t_B)$. At the end of the iterative process the values $P(1)$ and $P(2)$ are found as the best fit for the set of experimental values.

The second alternative of the calculation method does not make use of a computer. The values λ and a are obtained from two pairs of (Φ, t) values, for example (Φ_i, t_i) and (Φ_j, t_j). With equations (9) – (13) the initial quantities $\Phi_i^{(0)}$, $\Phi_j^{(0)}$, $\lambda^{(0)}$, $a^{(0)}$, and $u^{(0)}$ are calculated. With eq. (2) the quantities $\Phi_i^{(1)}$ and $\Phi_j^{(1)}$ corresponding to the first iteration are calculated:

$$\Phi_i^{(1)} = \frac{1}{\lambda^{(0)}}\left\{\left[1 + \frac{1}{t_i}\left(u^{(0)} - \frac{A_1}{\lambda^{(0)}}\right)\right]\ln\frac{2t_i}{u^{(0)}C} + \frac{u^{(0)}}{t_i}\right\} \tag{14}$$

$$\Phi_j^{(1)} = \frac{1}{\lambda^{(0)}}\left\{\left[1 + \frac{1}{t_j}\left(u^{(0)} - \frac{A_1}{\lambda^{(0)}}\right)\right]\ln\frac{2t_j}{u^{(0)}C} + \frac{u^{(0)}}{t_j}\right\} \tag{15}$$

The values $\lambda^{(1)}$ and $a^{(1)}$ corresponding to the first iteration are:

$$\lambda^{(1)} = \lambda^{(0)}\frac{\Phi_j^{(1)} - \Phi_i^{(1)}}{\Phi_j^{(0)} - \Phi_i^{(0)}} \tag{16}$$

$$a^{(1)} = a^{(0)}\exp\left\{\left[\frac{\Phi_i^{(1)}}{\Phi_i^{(1)} - \Phi_j^{(1)}} - \frac{\Phi_i^{(0)}}{\Phi_i^{(0)} - \Phi_j^{(0)}}\right]\ln\frac{t_j}{t_i}\right\} \tag{17}$$

Using $\lambda^{(1)}$, $a^{(1)}$ and $u^{(1)}$ values, the $\Phi_i^{(2)}$ and $\Phi_j^{(2)}$ are re-calculated and, together with $\Phi_i^{(0)}$ and $\Phi_j^{(0)}$ values which remain "reference" values for each iteration, they provide for the new values of $\lambda^{(2)}$, $a^{(2)}$, $u^{(2)}$ and so forth.

3. EXPERIMENTAL PROCEDURE

The steps of the experimental procedure are the following 26;

— measurement of the wire diameter;

— building the measuring cell;

— getting the set of (Φ_v, t) values;

— $R(T_0)$ calibration of the wire in order to determine the temperature coefficient, α_{T_0}, of the wire electrical resistance;

— computation of the "wire constant", A_1;

— getting the set of (Φ, t) values with the cell filled up with the fluid under investigation;

— verifying the accuracy of α_{T_0} value and its stability in time, by measuring the electrical resistance of the "cold" wire at two temperatures, T_0 and T_0' of the cell;

— calculation of the initial values $\lambda^{(0)}$ and $a^{(0)}$ with relations (9) — (13);

— mathematical processing of the experimental data with one of the two versions of the calculation method.

4. EXPERIMENTAL RESULTS AND DATA PROCESSING

The wire diameter was measured with an optical microscope. A mean value, $r_1 = 7.78 \times 10^{-6}$ m was obtained for the wire radius.

The coefficients a, S_a, b, S_b and r for the straight line $t = a\Phi_v + b$ were calculated[26] by the least square method from 94 pairs of experimental (Φ_v, t) values with $2 \leqslant t \leqslant 17$ ms.

$$a = 4.305 \times 10^{-5}; \quad b = 4.18 \times 10^{-4}; \quad r = 0.999964$$

$$S_a = 3.8 \times 10^{-8}; \quad S_b = 7.8 \times 10^{-6}$$

$$a \pm 2S_a = (4.305 \pm 0.008) \times 10^{-5}$$

$$(P = 95\%)$$

$$b \pm 2S_b = (4.2 \pm 0.2) \times 10^{-4}$$

One obtains:

$$A_1 = 2a = (8.61 \pm 0.016) \times 10^{-5} \quad (0.2\%)$$

For $\rho_1 c_1 = 2.86 \times 10^6$ J/(m^{3}K), (tabulated value[7]) the calculated radius of the platinum wire is 7.76×10^{-6} m.

The experimental straight line $t(\Phi_v)$ does not intercept the origin as requested by theory, eq.(6), but it can be made to pass through the origin either by rotation or translation along the abscissa or ordinate. As the calculated radius of the wire is equal to the measured one, the slope of the experimental straight line is correct and then a rotation of the experimental straight line is ruled out. Assuming Φ_v values as correct, the experimental times, *t*(exp), could be higher than those predicted by theory, *t*(*id*), for the following reasons (Fig. 1.a) :

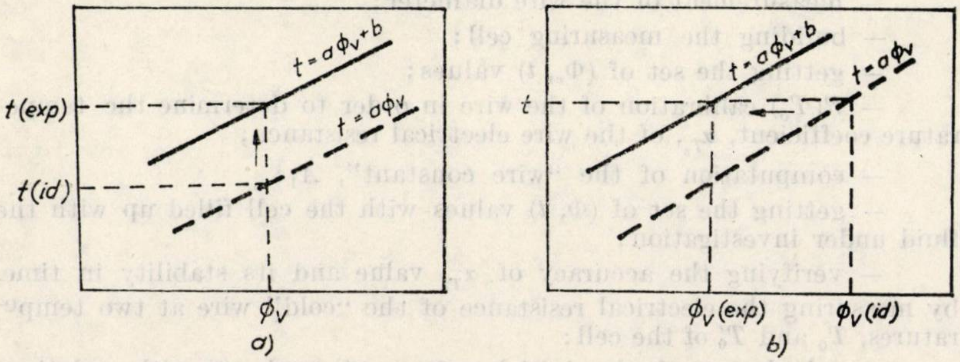

Fig. 1. — Possible causes for inequalities :
t(exp) > *t*(id) and $\Phi_v(\text{exp}) < \Phi_V(\text{id.})$.

a) dissipation into rarefied gas [32,33] (imperfect vacuum, $\lambda \neq 0$);

b) heat losses at the wire ends and by radiation [25–29];

c) delay of the electronic assembly for measuring the transient signal of the transducer.[26)]

Assuming *t* values as correct, the experimental Φ_v (exp) values could be lower than the ideal ones, Φ_v(id), for the following reasons (Fig. 1.b. and eqs (15) — (18) from ref. [29] :

d) the heating pulse value, measured in steady state conditions is higher than the transient value, corresponding to short times [26];

e) the measured value of α_{T_0} is higher than the real one [26,29];

f) the measured value of the wire length is lower than the real one.[26]

The experimental (Φ, *t*) values for argon at 299.8 K and atmospheric pressure [26,29] were computerized using equation (7). Experimental (Φ, *t*) values together with Φ_c values calculated from the regression equation are listed in Table 1.

The following results were obtained [26] by processing the experimental (Φ, *t*) data :

1) initial values calculated by the classical procedure of the method :

$\lambda^{(0)} = 0.0143$; $P^{(0)}(1) = 70$

$a^{(0)} = 1.2 \times 10^{-5}$; $r_1 = 7.76 \times 10^{-6}$; $P^{(0)}(2) = 5.054 \times 10^{-6}$

$2A_1 = 1.722$

The subsequent values resulted after four iterations :

$P(1) = 54.69$; $S_{P(1)} = 0.315$

$P(2) = 2.84 \times 10^{-6}$; $S_{P(2)} = 2.14 \times 10^{-7}$

Table 1

Experimental (Φ, t) values [26,29] and Φ_c values as calculated from the regression straight line

t (s)	Φ (mK/W)	Φ_c (mK/W)
0.2036	638.8	640.5
0.3136	669.2	669.1
0.3371	673.6	673.7
0.3726	680.9	680.0
0.521	701.4	700.6
0.614	711.4	710.5
0.667	715.7	715.5
0.745	722.8	722.0
0.879	731.8	731.7
0.957	736.1	736.6
1.076	743.6	743.4
1.283	753.3	753.5
1.397	757.6	758.4
1.577	764.7	765.3

For $P = 95\,\%$ one obtains :

$$P(1) \pm 2.15 S_{P(1)} = 54.7 \pm 0.7 \qquad (1.3\,\%)$$

$$P(2) \pm 2.15\, S_{P(2)} = (2.8 \pm 0.4) \times 10^{-6} \qquad (14\,\%)$$

$$\lambda = 0.0183 \text{ W/(mK)}\,; \qquad a = 2.1 \times 10^{-5} \quad \text{m}^2\text{/s}$$

2) initial values estimated as order of magnitude :

$$\lambda^{(0)} = 0.01\,; \qquad P^{(0)}(1) = 100$$

$$a^{(0)} = 10^{-5}; \qquad r_1 = 7.76 \times 10^{-6} \qquad P^{(0)}(2) = 5.6 \times 10^{-6}$$

$$2A_1 = 1.722$$

The same values as the above mentioned ones were obtained after six iterations.

At 299.8 K, the values recommended in literature [34-36] are :

$\lambda = 0.0177$ W/(mK)

$a = 2.12 \times 10^{-5}$ m²/s (computed from data [34-36] for λ, ρ, c_p).

It can be noticed that the measured value for thermal conductivity is higher (by 3.4 %) than that recommended, while the measured value for thermal diffusivity coincides with that in literature. By examining relations (15)—(18) (ref. (29)) and observations concerning the possible causes for the translation of the $t(\Phi_v)$ straight line, is results that the measured value of α_{T_0} would be higher (by approximately 3 %) than the real one. [29]

This error might be caused by either a systematic error during the $R(T)$ wire calibration, or, more probably, because this calibration was carried out prior to achieving the set of (t, Φ_v) values. When obtaining those over 100 pairs of (t, Φ_v) values, during releasing each wire heating pulse in vacuo, wire temperature reaches about 350°C at $t = 3$s (pulse duration). These heating-cooling cycles of the wire affect the value of α, especially for very thin wires as those employed by us.[26]

Experimental values, λ and a, together with those recommended in literature [34-36], λ_t and a_t, are given in Table 2, for the set of investigated gases (a_t quantities are calculated from tabulated λ, ρ and c_p values [34-36]).

Table 2

Thermal conductivity and thermal diffusivity of gases — comparative table

Gas	T (K)	λ (W/(mK))	$10^5\ a$ (m^2/s)	λ_t (W/(mK))	$10^5 a_t$ (m^2/s)
Argon	299.8	0.0183	2.10	0.0177	2.12
Nitrogen	295.1	0.0250	2.14	0.0254	2.11
Oxygen	299.8	0.0261	2.33	0.0267	2.26
Hydrogen	300.2	0.179	16.2	0.183	15.8
Carbon dioxide	298.0	0.0161	1.04	0.0164	1.07
Methane	300.1	0.0350	2.31	0.0343	2.38

The accuracy of thermal conductivity measurements is better or equal to 2.3 %, and the accuracy of thermal diffusivity measurements is better or equal to 3.1 %.

5. CONCLUSIONS

The method of calculation and experimental procedure presented are noticeable because:

— eliminate all disadvantages of the classical procedure of the transient hot wire method, especially for gas measurements;

— absolute and simultaneous measurement of the quantities λ, a and ($\rho\ c_p$) becomes feasible in gases as well in liquids;

— eliminate the restriction due to the wire diameter;

— make possible the utilization of thermoresistive metallic wires made of different metals and alloys whose ρ_1, c_1 and λ_1 properties must not be known ab initio.[31] The wires employed have to stand the attack of the investigated fluid;

— short times are used and therefore cell dimensions can be reduced; the uncertainty of a non-detected natural convection is eliminated; the errors due to the heat losses, temperature fluctuations of the cell and vertical temperature gradients in the thermostat are negligible;

— the same cell and experimental set up can be employed for measurements in gases and liquids as well;

— all quantities involved in calculations are absolutely measurable;

— all quantities implicated in computations are measured with the same experimental assembly;

— all quantities involved in calculations are measured in the measurement cell and with cell transducer;

— computerization of the set of experimental (Φ, t) values, first version of the calculation method, is more accurate than processing only two pairs of (Φ, t) values, second version, only because it diminishes the effect of random errors in Φ and t;

— make possible the identification of systematic instrumental errors (equations (15) — (18) from ref. 29);

— initial $\lambda^{(0)}$ and $a^{(0)}$ data can have values correctly estimated only for the order of magnitude (for example:

$$\lambda^{(0)} = 0.01\ \mathrm{W/(mK)} \text{ and } a^{(0)} = 10^{-5}\mathrm{m^2/s} \text{ for gases};$$

$$\lambda^{(0)} = 0.1 - 0.5\ \mathrm{W/(mK)} \text{ and } a^{(0)} = 10^{-7}\mathrm{m^2/s} \text{ for liquids}).$$

A more precise evaluation from relations (9) — (13) has no other effect than to decrease the number of iterations necessary to reach the same final results.

— the computation methods and the experimental procedure are very simple;

— absolute measurement of the specific heat of wire material can be made.

The validity of both calculation method and experimental procedure as well as measurement accuracy of the experimental set up are proved by the values of λ and a obtained on standard gases.

REFERENCES

[1] "Thermal Conductivity", ed. R. P. Tye, vol. II, Academic Press, London, 1969, p. 66 —145.

[2] N. V. Tsederberg, "Thermal Conductivity of Gases and Liquids", Edward Arnold Ltd., London, 1965, p. 1 — 66.

[3] E.F.M. van der Held and F.G. von Drunen, *Physica*, **15**, 865(1949).

[4] D. G. Gillam, L. Romben, H. E. Nissen and O. Lamm, *Acta Chem. Scand.*, **9**, 641 (1955).

[5] J. K. Horrocks and E. Mc Laughlin, *Proc. Roy. Soc.*, **A273**, 259 (1963).

[6] A. F. O. Falcao, *Rev. Port. Quim.*, **7**, 65 (1965).

[7] P. Sale, Thèses, Fac. Sci. Univ. Paris, Paris, 1967.

[8] P. Calvet, Thèses, Fac. Sci. Univ. Paris, Paris, 1967.

[9] J. W. Haarman, Dissertation, Delft, 1969.

[10] E. McLaughlin and J. F. T. Pittman, *Phil. Trans. Roy. Soc. (London)*, **A 270**, 557 (1971).

[11] J. W. Haarman, *Physica*, **52**, 605 (1971).

[12] J. G. Salin, *Acta Acad. Aboensis*, **B 33**, 1 (1973).

[13] P. Barüel, Riso Report No. 263, 1972.

[14] J. J. de Groot, J. Kestin and H. Sookiazian, *Physica*, **75**, 454 (1974).

[15] K. H. Lie, Dissertation, Univ. Karsruhe, 1975.

[16] E. E. Shpilrain, A. S. Umanskii and Yu. A. Gorshkov, *High. Temp. High Pressures*, **7**, 361 (1975).

[17] C. A. N. Castro, W. A. Wakeham and J. C. G., Calado, *Rev. Port Quim.*, **17**, 78 (1975).

[18] J. J. Healy, J. J. de Groot and J. Kestin, *Physica*, **82 C**, 392 (1976).

[19] J. Kestin and W. A. Wakeham, *Physica*, **92 A**, 102 (1978).

[20] H. E. Khalifa, J. Kestin and W. A. Wakeham, *Physica*, **97 A**, 273 (1979).

[21] R. Bachmann, Dissertation, E.T.H. Zürich, 1969.

[22] Y. Nagasaka and A. Nagashima, *Rev. Sci. Instr.*, **52**, 229 (1981).

[23] I. Constantinescu, T.O.N. Moisin, L. P. Dumitrescu and A. Ciochină, Romanian Patent No. 64025 (1975).

[24] R. Vîlcu and A. Ciochină, *Rev. Roumaine Chim.*, **25**, 1113 (1980).

[25] D. Şerbănescu, Gh. Vasu, R. Vîlcu and A. Ciochină, *Rev. Roumaine Chim.*, **26**, 1047 (1981).

[26] A. Ciochină, Teză de doctorat, Inst. Politehnic Bucureşti, Bucureşti, 1982.

[27] R. Vîlcu and A. Ciochină, *Rev. Roumaine Chim.*, **26**, 527 (1981).

[28] R. Vîlcu, A. Ciochină and Gh. Vasu, *Rev. Roumaine Chim.*, **26**, 1355 (1981).

[29] R. Vîlcu, A. Ciochină and Gh. Vasu, *Rev. Roumaine Chim.*, **27**, 313 (1982).

[30] H. S. Carslaw and J. C. Jaeger, "Conduction of Heat in Solids", Oxford Univ. Press, London, 1959, p. 261, 334, 345.

[31] O. Sandberg, P. Andersson and G. Backström, *J. Phys. E., Sci. Instr.*, **10**, 474 (1977).

[32] J. J. C. Picot and A. G. Fredrickson, *Ind. Eng. Chem., Fundamentals*, **7**, 84 (1968).

[33] J. J. C. Picot, *Canad. J. Chem. Eng.*, **47**, 17 (1969).

[34] N. B. Vargaftik, "Spravochnik po teplofizicheskim svoistvam gazov i zhidkostei", Nauka, Moscow, 1972, p. 543.

[35] Y. S. Touloukian, P. E. Liley and S. C. Saxena, "Thermophysical Properties of Matter", vol. 3, TPRC Data Series, Plenum Press, New York, 1970, p. 5.

[36] K. Raznjevic, "Tabele şi diagrame termodinamice", Ed. Tehnică, Bucureşti, 1978, p. 264.

Revue Roumaine de Chimie, 28, *8*, 805 – 809 (1983)

NEW COBALT(II) COMPLEXES WITH TRIDENTATE DIBASIC ONO DONOR LIGANDS

A. SYAMAL* and B. K. GUPTA

Department of Applied Sciences and Humanities, Kurukshetra University, Kurukshetra 132119, Haryana and Department of Chemistry, Regional Engineering College, Kurukshetra 132119, Haryana, India

Received July 10, 1981

A series of new cobalt (II) complexes with the Schiff bases derived from salicylaldehyde, 5-bromosalicylaldehyde, 5-nitro-salicylaldehyde, 3-methoxysalicylaldehyde, 3-ethoxysalicylaldehyde, 3,5-dichlorosalicylaldehyde and *o*-aminobenzylalcohol have been synthesized and characterized on the basis of elemental analyses, conductance, molecular weight, infrared, electronic spectra and magnetic measurements. The Schiff bases behave as dibasic tridentate ONO donor ligands. The complexes are of the type $[Co(OH_2)_2L]_2$ (where LH_2 = Schiff base). The complexes are dimers and nonelectrolytes. The magnetic moments of the complexes are in the range 4.71 – 5.29 B.M. indicating octahedral structure. The $\nu(C=N)$, $\nu(C-O)$ (phenolic) and $\nu(C-O)$ (alcoholic) stretching frequencies have been followed to find out the coordination sites of the ligands. The complexes exhibit electronic spectral bands at around 8800, 18000 and 22 000 cm^{-1} due to the $^4T_{1g}(F) \rightarrow {}^4T_{1g}$, $^4T_{1g}(F) \rightarrow A_{2g}$ and $^4T_{1g}(F) \rightarrow T_{1g}(P)$ transitions respectively, characteristic of octahedral structure.

INTRODUCTION

Considerable attention has been paid to the coordination complexes of tridentate dibasic ligands which influence the metal (II and III) ions to form dimetallic complexes with unusual magnetic properties.[1-3] Such works have been mostly concentrated around $S = 1/2$ systems and relatively less attention has been paid to other spin systems like $S = 3/2$ or $5/2$. Our work on the magnetic exchange behaviour of metal complexes with $S = 1/2$ and $5/2$ systems produced interesting results.[2,4] This prompted us to extend our studies on tridentate dibasic ligands to cobalt (II), an $S = 3/2$ system. We report here new cobalt (II) complexes with the Schiff bases (I) derived from salicylaldehyde, 5-bromosalicylaldehyde, 5-nitrosalicylaldehyde, 3-methoxysalicylaldehyde, 3-ethoxysalicylaldehyde, 3,5-dichlorosalicylaldehyde and *o*-aminobenzylalcohol. The complexes have been characterized by elemental analysis, molecular weight,

---

*** For correspondence.**

conductance, IR and electronic spectra and magnetic susceptibility measurements.

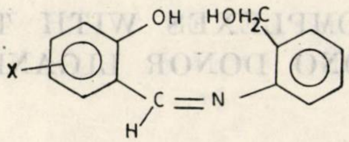

I. X=H, 5-BROMO, 5-NITRO, 3-METHOXY, 3-ETHOXY AND 3,5-DICHLORO

EXPERIMENTAL

Materials and methods

Cobalt (II) acetate tetrahydrate was obtained from BDH. Salicylaldehyde was a product of Sarahhai M. Chemicals. 5-Bromo-salicylaldehyde, 3-ethoxysalicylaldehyde and *o*-aminobenzylalcohol were purchased from Aldrich Chemical Co.(U.S.A.). 5-Nitrosalicylaldehyde and 3,5-dichlorosalicylaldehyde were obtained from Eastman Kodak Co. (U.S.A.). 3-Methoxysalicylaldehyde was procured from Fluka AG(Switzerland).

Physical Measurements and Analyses

The metal content was determined complexometrically by EDTA using Eriochrome Black-T as an indicator. The nitrogen analyses were done microanalytically. Electrical conductance measurements were carried out in methanol with the help of a Toshniwal conductivity bridge (model LO1—O2A) and a dip type cell calibrated with aqueous KCl solutions. The infrared spectra were recorded in KBr pellets using Perkin Elmer-257 Infrared Spectrophotometer calibrated with polystyrene. The molecular weight measurements of the compounds were done by Rast method[5] using diphenyl as solvent. The magnetic measurements were done by the Gouy method and $Hg[Co(NCS)_4]$ was used as the standard. The susceptibility was corrected for diamagnetism and TIP contributions. The electronic absorption spectra were recorded on a Beckman DU-2 Spectrophotometer in methanol.

General method of synthesis of the complexes

Cobalt(II) acetate tetrahydrate (1.25g, 0.006 mole) was dissolved in ethanol (10 ml) and was added to the Schiff base solution (0.005 mole in 10 — 20 ml ethanol). The mixture was refluxed for 3 hrs on a waterbath. The excess solvent was removed by distillation and the separated precipitates were filtered, washed with ethanol, recrystallized from ethanol and dried under vacuum at room temperature. Yield = 60%.

RESULTS and DISCUSSION

Cobalt (II) acetate reacts with the Schiff bases (I) in ethanol to form 1 : 1 complexes of the type $[Co(OH_2)_2L/2$(where LH_2 = Schiff base, I). The analytical, IR and molecular weight data support the above stoichiometry. The complexes are dimers. They behave as non-electrolytes ($\Lambda_M = 1 - 8$ ohm^{-1} cm^2 mole^{-1}) in methanol. The free ligands exhibit a medium intense band at around 2700 cm^{-1} due to the intramolecularly hydrogen bonded OH group. This band disappears in the complexes indicating the breaking of the hydrogen bond and consequent deprotonation and coordination to cobalt ion. The presence of a medium intense IR band at around 3200 cm^{-1} is assigned to the $\nu(OH)$ stretch of coordinated water.[6] The free ligands exhibit a strong band at around 1615 — — 1630 cm^{-1} due to the $\nu(C=N)$ stretch and this band shifts to lower energy by 5 — 40 cm^{-1} in the complexes indicating nitrogen coordination of the ligands.[7] The $\nu(C-O)$ (phenolic) stretch occurs in the free ligands at 1510 — 1550 cm^{-1} and in the complexes this band undergoes a positive shift indicating oxygen coordination of the phenolic OH group.[8] The free ligands exhibit the $\nu(C-O)$ (alcoholic) stretch at 1190 — 1240 cm^{-1} and this band undergoes a negative shift indicating alcoholic oxygen coordination of the Schiff bases.[9] Thus, analytical, IR and conductance data, and valence requirements of the metal ion indicate the dibasic tridentate nature of the ligands.

The electronic spectra of the complexes show three ligand field bands at around 8800, 18000 and 22000 cm^{-1} associated with the transitions $^4T_{1g}(F) \rightarrow {}^4T_{2g}$ (ν_1), $^4T_{1g}(F) \rightarrow {}^4A_{2g}(\nu_2)$ and $^4T_{1g}(F) \rightarrow {}^4T_{1g}(P)$ (ν_3) respectively in an O_h symmetry.[10,11] The low molar extinction coefficient values (Table 1) of these bands are also characteristic of octahedral cobalt (II) complexes.[12] The electronic spectral data rule out a tetrahedral structure for the complexes[10].

The dimeric behaviour of the complexes suggests a μ-bis (Schiff base) tetraaquodicobalt (II), $[Co(OH_2)_2$ (Schiff base)$]_2$ with aquo molecules occupying the *trans* positions of the two octahedral cobalt (II) atoms (see II). The positive shift of the $\nu(C-O)$ (phenolic) stretch to higher energy by 10 — 25 cm^{-1} in the complexes indicates the presence of phenolic oxygen bridge in these dimetallic complexes.[9] The magnetic moments of the complexes occur in the 4.71 — 5.25 B.M. range and are characteristic of magnetically dilute octahedral cobalt (II) complexes.[10]

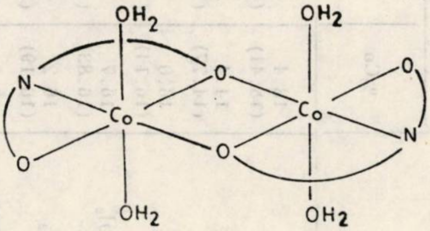

II

ACKNOWLEDGEMENT. The authors are indebted to the University Grants Commission, New Delhi 110002 for support of the work.

Table 1

Analytical, molecular weight, magnetic moment, IR and electronic spectral data of cobalt (II) complexes of Schiff bases[a,b]

Complex	Found (Calcd.)			ν(C=N) complex (ligand)	ν(C–O) (phenolic) complex (ligand)	ν(C–O) (alcoholic) complex ligand)	μ_{eff} B.M. (Temp)	ν_{max} (ε)
	%Co	%N	Mol. Wt.					
$[Co(OH_2)_2(sal\text{-}OABA)]_2$	18.4 (18.41)	4.2 (4.38)	657 (640)	1 600 (1 615)	1540 (1530)	1170 (1190)	4.71 (294)	8850(15), 17860(19), 21740(24)
$[Co(OH_2)_2(5\text{-}bromosal\text{-}OABA)]_2$	14.4 (14.77)	3.3 (3.51)	736 (798)	1 615 (1 620)	1525 (1515)	1175 (1200)	5.13 (293)	8770(17), 17700(20), 21980(23)
$[Co(OH_2)_2(5\text{-}nitrosal\text{-}OABA)]_2$	16.0 (16.14)	7.4 (7.67)	732 (730)	1 595 (1 615)	1570 (1550)	1220 (1240)	5.25 (293)	8810(13), 17390(19), 21500(22)
$[Co(OH_2)_2(3\text{-}methoxysal\text{-}OABA)]_2$	16.7 (16.83)	3.75 (4.00)	690 (700)	1 590 (1615)	1530 (1515)	1175 (1195)	4.97 (294)	
$[Co(OH_2)_2(3\text{-}ethoxysal\text{-}OABA)]_2$	16.2 (16.19)	4.1 (3.85)	754 (728)	1 595 (1 615)	1570 (1545)	1170 (1190)	4.85 (294)	8660(16), 17540(19), 22220(21)
$[Co(OH_2)_2(3,5\text{-}dichlorosal\text{-}OABA)]_2$	15.3 (15.15)	3.4 (3.60)	735 (778)	1 590 (1 630)	1530 (1510)	1190 (1200)	5.29 (291)	

a) Abbreviations : Sal = salicylaldehyde, 5-bromosal = 5-bromosalicylaldehyde, 5-nitrosal = 5-nitrosalicylaldehyde, 3-methoxysal = 3-methoxysalicylaldehyde, 3-ethoxysal = 3-ethoxysalicylaldehyde, 3,5-dichlorosal = 3,5-dichlorosalicylaldehyde

b) IR and electronic spectral data in cm^{-1}.

REFERENCES

[1] D. J. Hodgson, *Progr. Inorg. Chem.*, **19**, 173 (1975).

[2] A. Syamal, *Coord. Chem. Rev.*, **16**, 309 (1975) ; *J. Scient. Indust. Res.*, **26**, 156 (1977).

[3] W. E. Hatfield and R. Whyman, *Transition Metal Chem.*, **5**, 47 (1969).

[4] C.C. Lee, A. Syamal and L. J. Theriot, *Inorg. Chem.*, **10**, 1669 (1970) ; G. O. Carlisle, A. Syamal, K. K. Ganguli and L. J. Theriot, *J. Inorg. Nuclear Chem.*, **34**, 2761 (1972) ; A. Syamal, E. F. Carey and L. J. Theriot, *Inorg. Chem.*, **12**, 245 (1973) ; A. Syamal and L. J. Theriot, *J. Coord. Chem.*, **2**, 193, 241 (1973) ; A. Syamal, *Indian J. Chem.*, **11**, 363 (1973), *Transition Metal Chem.* **5**, 220 (1980) ; A. Syamal and K. S. Kale, *Indian J. Chem.*, **15A**, 431 (1977), **16A**, 46(1978), *Transition Metal Chem.*, **4**, 298 (1979) ; *Inorg. Chem.*, **18**, 992 (1979), *J. Indian Chem. Soc.*, **58**, 186 (1981).

[5] G. F. Mann and B. C. Saunders, "Practical Organic Chemistry", Longmans, London, 1961, p. 435.

[6] J. H. Van Vleck and P. C. Cross, *J. Chem. Phys.*, **1**, 357 (1933) ; G. Sartori, C. Furlani and A. Damiani, *J. Inorg. Nuclear Chem.*, **8**, 119(1958).

[7] F. Maggio, T. Pizzino, V. Romano and G. Dia, *J. Inorg. Nuclear Chem.*, **38**, 602 (1976).

[8] S. J. Gruber, C. M. Harris and E. Sin, *J. Inorg. Nuclear Chem.*, **30**, 1805 (1968).

[9] E. Sinn and C,. M. Harris, *Coord. Chem. Rev.*, **4**, 391 (1969).

[10] F. A. Cotton and G. Wilkinson, "Advanced Inorganic Chemistry", Wiley Eastern Pvt. Ltd., New Delhi, 1972, p. 869.

[11] C. J. Ballhausen, "Introduction to Ligand Field Theory", Benjamin, New York, 1962, p. 258.

[13] S. K. Madan and A. M. Donohue, *J. Inorg. Nuclear Chem.*, **28**, 1617 (1966).

Revue Roumaine de Chimie, 28, *8*, 811 – 817 (1983)

COORDINATION COMPOUNDS OF Cu(II) WITH SOME TRIAZENOIMIDAZOLE DERIVATES

FLORICA ZĂLARU, D. IONESCU *, AURELIA MEGHEA, FELICIA CORNEA and CONSTANŢA GHEORGHIU

Polytechnic Institute, Faculty of Chemical Technology, Bucharest, Romania
***Oncologic Institute, Bucharest, Romania**

Received November 3, 1982

The present paper deals with the preparation and structural problems of new Cu(II) complexes with some triazenoimidazole derivatives. These compounds have been characterized by elemental analysis, conductivity measurements, infrared, UV and visible spectra as well as electron spin resonance spectra. Several conclusions concerning the complexing capacity of the ligands were drawn on the basis of these studies. Molecular models for the new compounds were also proposed.

The imidazole ring is present in a series of natural or synthetic organic compounds and has an important role in biochemistry. It forms the part of the molecule considered to coordinate the metal ions. In the complexing of imidazole and its derivatives, the donor atom is of peculiar interest. It can be the imidazole nitrogen atom N(1) or N(3) or other donor atoms belonging to different functions grafted on the imidazole ring. There are some differences between the donor atoms regarding their complexing capacity owing to some electronic and steric effects[1a,b].

The present paper is designed to obtaining and characterization of some complex Cu(II) compounds using as ligands some triazenoimidazole derivatives of type:

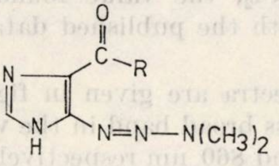

where R = $-OCH_3$, $-NH_2$, $-NHCH_2COOC_2H_5$

in order to follow coordination ability of the ligands and the influence of the triazene group and R substituent on the type of the complex.

RESULTS AND DISCUSSIONS

By treating an ethanolic solution of Cu(II) chloride with the ethanolic solution of the ligand for R = $-OCH_3$, a brown compound was obtained (soluble in water and alcohol) only at a molar ratio of $CuCl_2$:

: L = 1 : 4, while for R = $-NH_2$ and $-NHCH_2COOC_2H_5$ a green khaki compound (sparingly soluble in water) and a yellowish green compound (soluble in water) respectively were separated only at a molar ratio 1 : 1.

The compounds were characterized by elementary chemical analysis, thermodifferential analysis, conductivity measurements; in order to obtain data on the mode of coordination of the ligand and stereochemistry of the central metal ion, the electronic, ESR and IR spectra were recorded within the 700 – 4000 cm^{-1} range both for the ligands and the compounds.

The formulas of the compounds based on the chemical analysis are given in table 1. As proved by thermodifferential analysis (Fig. 1) Cu ClL retains a molecule of solvent. At 130°C the compound loses 15% of its weight as against 14.16% the calculated loss if the $CuLClC_2H_5OH$ formula is admitted to be correct. Conductivity measurements confirm the electrolyte 1 : 2 character for compound $[CuL]Cl_2$, the value found $\Lambda = 234\ \Omega^{-1}\ cm^2\ mol^{-1}$ being in agreement with the published data [2] for a 1 : 2 electrolyte.

Table 1

The compound type and analytical data

Molar ratio Cu : L	Compound for			Cu%		Cl%		N%		C%		H%	
	R_1	R_2	R_3	F	C	F	C	F	C	F	C	F	C
1 : 1	—			7.14	6.93	7.17	7.69	30.1	30.3	36.4	35.9	4.55	4.77
1 : 4	$[CuL_4]Cl_2$												
1 : 1		CuLClS		20.2	19.43	11.1	10.85	25.7	26.3	29.1	29.4	5.01	4.89
1 : 4		—											
1 : 1			$[CuL]Cl_2$	15.5	15.7	17.9	17.6	20.1	20.8	31.1	29.9	4.8	3.97

$R_1 = -OCH_3$, $R_2 = -NH_2$, $R_3 = -NHCH_2COOC_2H_5$; $S = C_2H_5OH$; F = Found, C = Calcd.

The electronic diffuse – reflectance spectra are given in figure 2. All the three compounds present a more or less broad band in the visible-near IR range with a maximum at 800, 840 and 860 nm respectively, and an intense, sharp band in the UV-visible range with absorption maximum at ~360 nm, that can be assigned to the $\pi - \pi^*$ transition, characteristic of the imidazole nucleus [3]. The broad band in the visible range may be assigned to a d-d transition of the Cu(II) ion. It is known that the absorption band, owing to the d-d transition expected for the Cu(II) ion in an octahedral geometry within the 500 – 600 nm range [4], is shifted towards the near IR range when the Cu(II) ion is in a distorted octahedron towards a square planar or in another geometry [5,6]. The maximum absorption position ($\lambda = 800 - 900$ nm) and the broad aspect of the band could be associated with a distorted octahedron axially up to a square planar or square pyramid, in agreement with the literature [7–9] data.

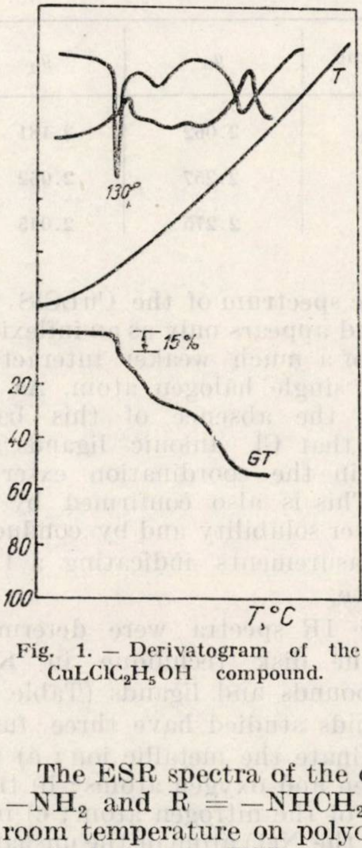

Fig. 1. — Derivatogram of the $CuLClC_2H_5OH$ compound.

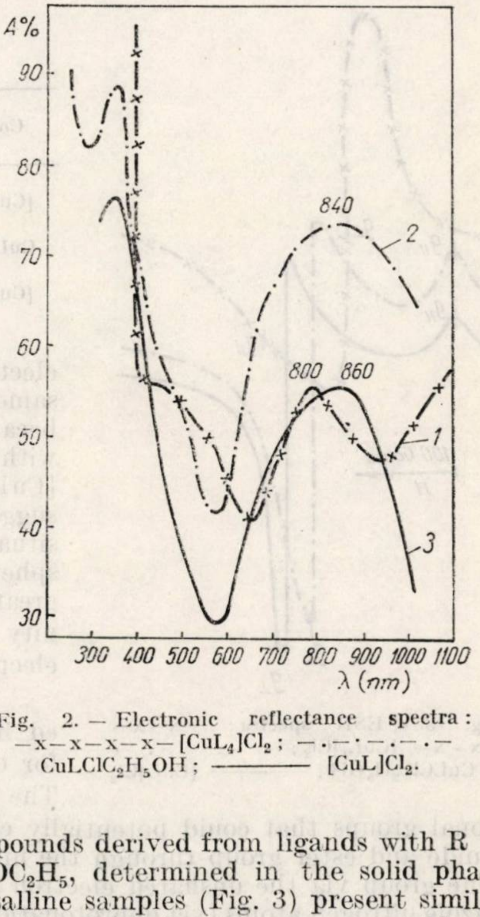

Fig. 2. — Electronic reflectance spectra : —x—x—x—x— $[CuL_4]Cl_2$; —·—·—·—·— $CuLClC_2H_5OH$; ———— $[CuL]Cl_2$.

The ESR spectra of the compounds derived from ligands with $R = -NH_2$ and $R = -NHCH_2COOC_2H_5$, determined in the solid phase at room temperature on polycrystalline samples (Fig. 3) present similar particularly intense ESR signals, with axial anisotropy ($g_{\|} > g_{\perp}$, table 2), resulting from distortion of the octahedral geometry of the Cu(II) ion towards a square planar. For the compound with $R = -NHCH_2COOC_2H_5$, the ESR signal is larger, suggesting less intense anisotropy. For the compound with $R = -OCH_3$ the anisotropic parameters have inverse values as compared to the other two compounds. Anisotropy $g_{\|} < g_{\perp}$ indicates a stronger interaction in the axial direction with regard to the equatorial plan and is characteristic of a hexacoordination with a flattened-octahedral geometry.

This fact suggests that there is a relatively weaker interaction in equatorial plan with imidazole rings of the four ligand molecules, but in axial direction a strong interaction with Cl^- ions. The bulky ligands in plan in comparison with the axial one determine the flattened-octahedral geometry, resulting from ESR spectrum. Moreover, in the electronic spectrum of $[CuL_4]Cl_2$ a strong band at 420 nm appears ; this may be assigned to a charge transfer strong interaction Cu—Cl, and in this way the brown characteristic colour of the compound may be explained. But, in the electronic spectrum of the CuLClS the same band appears only as an inflexion, because of a much weaker interaction with one single halogen atom. As for $[CuL]Cl_2$ the absence of this band suggests that Cl^- anionic ligands are situated in the coordination external sphere. This is also confirmed by its great water solubility and by conductivity measurements indicating a 1 : 2 electrolyte.

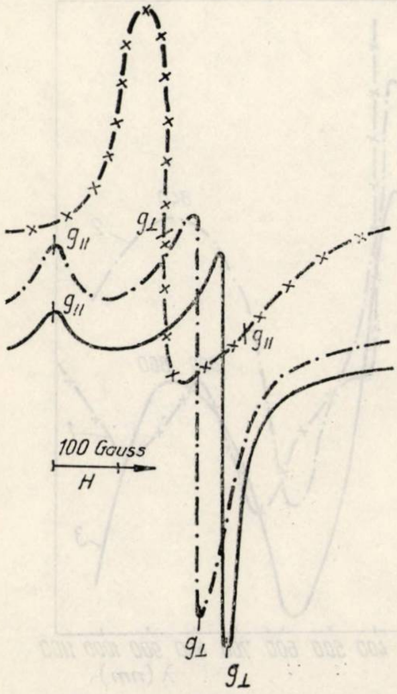

Fig. 3. — ESR spectra ; —x—x—x—x— $[CuL_4]Cl_2$; —·—.—·—.—.— $CuLClC_2H_5OH$; ———— $[CuL]Cl_2$

Table 2

ESR spectral parameters

Compound	$g_{\parallel}$	$g_{\perp}$
$[CuL_4]Cl_2$	2.062	2.181
CuLClS	2.257	2.062
$[CuL]Cl_2$	2.275	2.045

The IR spectra were determined by the disk technique in KBr for compounds and ligands (Table 3). The ligands studied have three functional groups that could potentially coordinate the metallic ion : a) the amide and ester group through the nitrogen and oxygen atoms ; b) triazene group via the unshared electron pair of the nitrogen atom ; c) imidazole nitrogen atoms (via deprotonation of the N(1) atom or the unshared electron pair of the N(3) atom).

A comparison of the IR spectrum of the compounds with that of the ligands points out :

1) For the CuClLS compound, changes appear in the number, position, shape and intensity of the bands characteristic of the amide group within the ν_{NH}, δ_{NH} range[10], as well as within the range of the triazene group [11]. Shifts of the 10 — 20 cm^{-1}, lowering of the intensities, disappearance of the ν_{NH} band characteristic of the associated imidazole (3100 — — 2100 cm^{-1})[12] are observed as well as the existence of a band within the ν_{NH} range pointing to the presence of a secondary amide. These changes might suggest that the amide group participates in complexing by substituting a hydrogen atom from the nitrogen atom, and likewise a nitrogen atom of the triazene group. Correlation of the square planar geometry,

Table 3

IR spectrum and assignments of the main bands, cm^{-1}

R	$-OCH_3$	$-NH_2$		$-NHCH_2COOC_2H_5$		Assignments
L	$[CuL_4]Cl_2$	L	CuLClS	L	$[CuL]Cl_2$	
	3 400 s	3 390 m	3 410 m	3 260 m	3 370 m	νNH asym.
		3 180	—		3 180 m	νNH sym.
3 200 — 2 100	—	3 200 — 2 100	—	3 200 — 2 100	—	ν_{NH} due to the molecular associations[12]
1 700 vs	1 700 s			1 740 vs	1 730 vs	ester ν_{CO}
		1 665 vs	1 650 s	1 670 vs	1 630 vs	amide ν_{CO}
		1 614 vs	1 625 s		1 600 vs	
1 560 vs	1 560 m	1 520 s	1 530 w	1 550 vs	1 550 m	δ_{NH} in plan
1 500 s	1 480 m	1 500 vs	1 500 m	1 470 s	1 500 m	
	1 460 m					
1 400 vs	1 440 vs	1 440 vs	1 440	1 430 m	1 430 w	ν imidazole
1 300 vs	1 340 vs	1 350 vs	1 350 m	1 390 w	1 190 w	cycle [13]
	1 300 sh	1 320 sh	1 320	1 350 sh	1 130 sh	
1 080 vs	1 080 vs	1 080 vs	1 100 m	1 080 vs	1 100 s	ν_{NNN}
940 s	950	965 m	980 w	960 m	990 s	
900 m	900	890 m	905 vw	900 m	900 vw	deformation of the
850 vs	—	870	—	870 m	870 vw	imidazole cycle [13]

S. = C_2H_5OH ; vs = very strong, s = strong, w = weak, vw = very weak, m = medium, sh = shoulder.

suggested by the electronic spectra and ESR, with the changes that appeared in the IR spectrum of the compound, might suggest that the ligand is bidentate and the Cu(II) atom would be in a square planar geometry (Fig. 4).

2) For the CuL Cl_2 compound the following are observed : disappearance of the band within the 3100 — 2100 cm^{-1} range, changes in the position and intensity of the bands due to the amide ν_{CO}(1670 cm^{-1}) and ester ν_{CO} (1740 cm^{-1}) ; all these suggest implication of the oxygen atoms coordination, appearance of the band due to secondary amide ν_{NH} (3180 cm^{-1}) (covered in the ligand spectrum) and changes in the position of the maximum and intensity of the triazene ν_{NNN} band. The data furnished by the IR and electronic spectra and ESR, correlated with literature indications concerning Cu(II) ion stereochemistry [5-9] allow us to postulate that this ligand might function pentadentately in a square pyramid geometry through the triazene nitrogen atoms and the two oxygen atoms of the ester group (Fig. 5).

3) The IR spectrum of the $[CuL_4]Cl_2$ compound exhibits marked changes in number, position of the maxima and intensity of the bands within the 1500 — 1200 cm^{-1} and 1000 — 800 cm^{-1} ranges assigned to

the ν imidazole ring and bending of the ring in the plan, respectively [13]. On the other hand the bands corresponding to the ν_{NNN} (1080 cm^{-1}) and ester ν_{CO} (1700 cm^{-1}) remain unchanged.

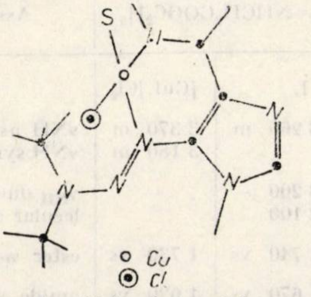

Fig. 4. — Molecular model suggested for the $CuLClC_2H_5OH$ compound.

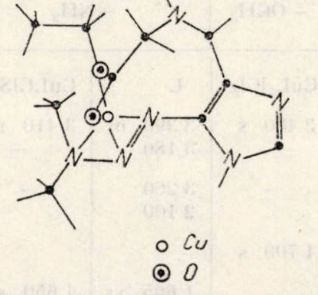

Fig. 5. — Molecular model suggested for the $[CuL]Cl_2$ compound.

The IR correlated with the results of the chemical analysis, the electronic and ESR spectra might suggest that the ligand is monodentate and coordinates by the imidazole N(3) nitrogen atom, the metal ion presenting a flattened octahedron stereochemistry.

In conclusion the following may be stated:

— The R substituent determines the composition and properties of the obtained complex compounds.

— Intermolecular associations existing in ligands disappear by complexing.

— The ligand functions monodentately, bidentately and pentadentately as a function of the R substituent.

— For the ligands with R = $-NH_2$ and $-NHCH_2COOC_2H_5$, the imidazole nitrogen atoms are not involved in coordination.

— The electronic spectra, ESR and molecular models proposed show, for the central metallic ion, an octahedron-like stereochemistry with various degrees of distortion (flattened octahedron, very elongated axial octahedron, square planar and square pyramid).

EXPERIMENTAL

The ligands prepared according to the indications given in[11] and $CuCl_2 2H_2O$ p.a. were used. All the compounds were prepared in the same way from the $CuCl_2$ ethanolic solutions and ligand taken in 1 : 1 and 1 : 4 molar ratios. The compounds obtained were separated by filtration in vacuum, washed in small amounts of ethanol and then dried at room temperature.

$[CuL_4]Cl_2$. The $CuCl_2$ solution (0.17 g in 10 ml ethanol) was added over the ethanolic solution of the ligand (0.75 g and 40 ml ethanol) at 1 : 4 molar ratio. The dark brown solution obtained separates brown crystals by evaporation at the room temperature.

$CuLClC_2H_5OH$. The ethanolic solution of $CuCl_2$ (0.17 g in 10 ml ethanol) is added to the ethanolic solution of the ligand (0.18 g in 26 ml ethanol + 2 ml hot water, pH = 6). The dark green solution obtained separates yellowish khaki microcrystals by evaporation at room temperature till next day.

$[CuL]Cl_2$. The ethanolic solution of $CuCl_2$ (0.17 g in 10 ml ethanol) was added to the ethanolic ligand solution (0.268 g in 60 ml cold ethanol). After two hours, yellowish green crystals were filtered.

The analyses of copper were carried out by Spacu's method. Chlorine analyses were performed by gravimetric standard methods. Conductivity measurements were performed in DMF solution 10^{-3} M with a Radelkis OK 102/1 conductimeter. Diffuse — reflectance spectra were recorded with a Zeiss-Jena VSU-1 spectrophotometer in the range of 220 — 1000 nm using magnesium oxide as reference. Thermodifferential analysis was performed with a Paulik-Paulik Erdey derivatograph in a mixture with Al_2O_3 ($m = 0.057$, $S = 100$ mg, DTA, DTG $= 1/10$, $T = 1200°C$, $\beta = 10°/min$). Infrared spectra of the ligands and the complexes were recorded with a Specord 71 spectrophotometer in the range of 4000 — 700 cm^{-1}. Samples were prepared as KBr disks. The ESR spectra at room temperature were recorded on the polycrystalline powder using an ART-5-IFA spectrograph. The klystron frequency was 9060 MHz and the modulation of the magnetic field 100 Hz. The ESR spectral parameters were calculated versus a Mn(II) standard.

REFERENCES

[1] [a]G. L. Eichhorn, "Inorganic Biochemistry", Vol. 1, Elsevier, 1973, p. 143 ; [b]H. C. Freeman and N. D. Hutchinson, *Acta Cryst.*, **B 35**, 2045 (1979).
[2] W. J. Geary, *Coord. Chem. Rev.*, **7**, 81 (1971).
[3] C. N. R. Rao, "Ultraviolet and Visible Spectroscopy", Batterworths, London, 1967.
[4] D. Polder, *Physica*, **9**, 709 (1942).
[5] B. J. Hathaway and D. E. Billing, *Coord. Chem. Rev.*, **5**, 143 (1970).
[6] B. J. Hathaway, *J. Chem. Soc.* (*A*), **1972**, 1196.
[7] M. C. Lim, Ekk Sinn and B. Martin, *Inorg. Chem.*, **15**, 807 (1976).
[8] D. Mastropaolo, Dana A. Powers, J. A. Potentza and H. J. Schugar, *Inorg. Chem.*, **15**, 1444 (1976).
[9] R. W. Brookes and R. L. Martin, *Inorg. Chem.*, **14**, 528 (1975).
[10] Margareta Avram and Gh. D. Mateescu, "Spectroscopia in infraroșu", Ed.Tehnică, București 1966.
[11] D. Ionescu. "Compuși organici de sinteză cu acțiune biologică", thesis, Bucharest 1981.
[12] H. Zimmermann, *Z. Electrochem.*, **63**, 601 (1959).
[13] R. H. Carlson and T. L. Brown, *Inorg. Chem.*, **5**, 268 (1966).

Revue Roumaine de Chimie, **28**, *8*, 819 – 24 (1983)

CONDUCTANCE BEHAVIOUR OF AQUEOUS SOLUTIONS OF ALKALINE EARTH METAL BUTYRATES

R. P. VARMA and A. KUMAR
Department of Chemistry, D.A.V. College, Muzaffarnagar-251001 (India)

Received July 10, 1981

Specific conductances of aqueous solutions of magnesium, calcium, strontium and barium butyrates have been measured at 35 – 60°C. The data reveal that in addition to an initial CMC (I), a second CMC (II) exists in the concentrated range. The value of CMC(I) decreases with increasing temperature whereas CMC(II) does not vary at all. The variation of molar conductivity λ with concentration, C, of soap in both regions is expressed by an equation : $\log \lambda = A + B \log C$ where A and B are constants. Constant A increases with increasing temperature whereas B does not vary much. Kraus and Bray's type expression has been used to evaluate K and λ_∞. The effect of temperature on these parameters has been studied and thermodynamic parameters i.e. heat of dissociation, ΔH^0, free energy ΔG^0, and entropy, ΔS^0 of dissociation have been evaluated.

INTRODUCTION

Conductance measurements have been exceptionally useful in the field of micelle formation and micelle structure. In the last few years many workers[1-4] from this laboratory have studied the conductance behaviour of aqueous solutions of alkaline earth metal soaps ($> C_5$)mainly in the dilute range of concentration. It is well known [5] that all the properties of soap solutions can be explained by considering the various regions in the soap concentration which is characterised by definite changes in the composition. Therefore, we have attempted to study the conductance behaviour of these soaps of lower fatty acid ($> C_5$) in the entire range of concentration under different conditions.

In the present paper the conductivities of aqueous solutions of alkaline earth metal (magnesium, calcium, strontium and barium) butyrates have been measured at different temperatures, 35 – 60°C, in order to a) determine the CMC of soap solutions : b) confirm the effect of temperature on CMC, if any; c) determine the dissociation constant, K, molar conductivity at infinite dilution, λ_∞ and d) calculate the thermodynamic parameters of dissociation i.e. ΔH^0, ΔG^0 and ΔS^0 respectively.

EXPERIMENTAL

Materials. AnalaR grade magnesium, calcium, strontium and barium carbonates were used. n-Butyric acid obtained from Sigma Chem. Co. U.S.A. was purified by distillation under reduced pressure. The procedure for the preparation of soap and measurement of conductivity of solutions is the same as reported earlier.[1] Water needed for preparation of various solutions was prepared by distilling, twice over alkaline $KMnO_4$.

RESULTS AND DISCUSSION

Specific conductance, k(ohm^{-1} cm^{-1}) of soaps increases with increasing concentration and temperature of the soap solutions. When k is plotted against soap concentration C (moles dm^{-3}) in dilute and concentration range (Table 1) separately at different temperatures, it is observed that the plots (Fig. 1) in the dilute range are characterised by an inter-

Table 1

CMC (mol dm^{-3}) of metal butyrates solutions in the dilute and concentrated range

Soap	Dilute							Concentrated	
	Conc. range (M)	CMC (I) × 10^2						Conc. range (M)	CMC(II)
		35°	40°	45°	50°	55°	60°		
Magnesium	0.01−.10	6.0	5.0	4.0	3.0	2.5	2.0	0.10−.80	0.25
Calcium	0.02−.10	6.2	5.1	4.3	4.0	3.8	3.4	0.10−.50	0.30
Strontium	0.02−.10	6.5	6.0	5.8	5.0	4.7	4.2	0.10−.80	0.35
Barium	0.01−.15	10.0	9.5	9.0	8.4	6.6	6.0	0.15−.80	0.50

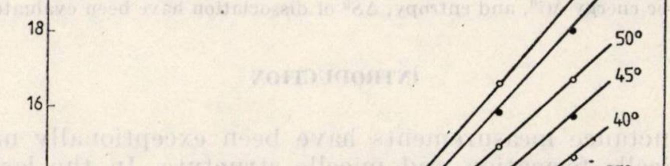

Fig. 1. — Plots of specific conductance, k (ohm^{-1} cm^{-1}) vs. concentration C (mol. dm^{-3}) of barium butyrate in water in dilute range at different temperatures 35 – 60°.

section of two straight lines at a definite concentration indicating the probable formation of micelle. This may be because the long chain ions associate above CMC (I) to form aggregates and the number of the free ions does not decrease as rapidly as at concentration less than CMC (I). The values of CMC (I) of the soaps (Table I) decrease with increasing temperature and are in the order : barium > strontium > calcium > magnesium. This shows that the cations play a definite role. As the size of the cations increases, the CMC increases. The plots (Fig. 2) of k vs. C show the similar nature at higher concentrations of soap but the CMC (II) values (Table I) found in this region are independent of temperature. This second break is obtained due to the formation of neutral colloid.

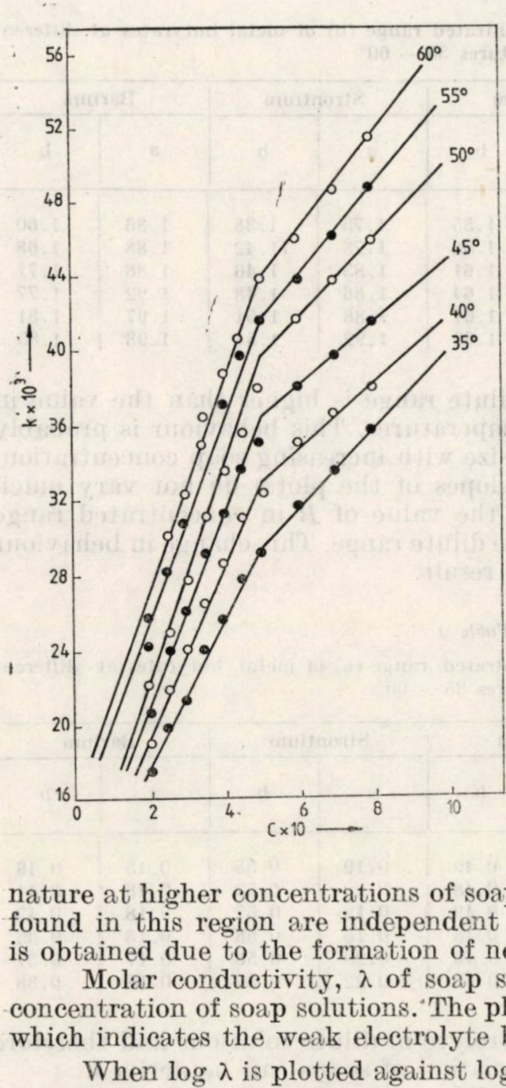

Fig. 2. — Plots of specific conductance, k(ohm^{-1} cm^{-1}) vs. concentration, C(mol. dm^{-3}) of barium butyrate in water in concentrated range at different temperatures 35 — 60°.

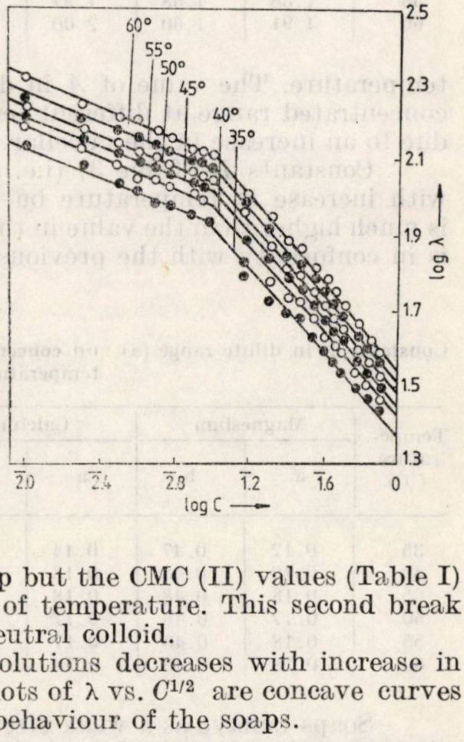

Fig. 3. — Plots of log λ vs. log C of strontium butyrate at different temperatures 35 — 60°.

Molar conductivity, λ of soap solutions decreases with increase in concentration of soap solutions. The plots of λ vs. $C^{1/2}$ are concave curves which indicates the weak electrolyte behaviour of the soaps.

When log λ is plotted against log C the plots (Fig. 3) show an intersection of two straight lines at a definite concentration which is independent of temperature. This concentration is a bridge of dilute and concentrated ranges of soap solutions. The log λ — log C plot indicates the applicability of the following expression in both the regions, dilute and concentrated separately.

$$\log \lambda = A + B \log C \tag{i}$$

where A and B are constants.

Constants A (Table 2), obtained by extrapolating the $\log \lambda - \log C$ plots in dilute and concentrated ranges of soaps increase with increasing temperature. The value of A in dilute range is higher than the value in concentrated range at different temperatures. This behaviour is probably due to an increase in the micellar size with increasing soap concentration.

Table 2

Constants A in dilute range (a) and concentrated range (b) of metal butyrates at different temperatures 35 — 60°

Temperature (°C)	Magnesium		Calcium		Strontium		Barium	
	a	b	a	b	a	b	a	b
35	1.74	1.47	1.88	1.55	1.75	1.38	1.86	1.60
40	1.76	1.48	1.92	1.58	1.78	11.42	1.88	1.68
45	1.81	1.51	1.93	1.61	1.83	1.46	1.88	1.71
50	1.85	1.55	1.95	1.64	1.86	1.48	1.92	1.77
55	1.88	1.58	1.97	1.67	1.88	1.51	1.97	1.81
60	1.91	1.60	2.00	1.69	1.92	1.54	1.98	1.85

Constants B (Table 3) (i.e. slopes of the plots) do not vary much with increase in temperature but the value of B in concentrated range is much higher than the value in the dilute range. This change in behaviour is in conformity with the previous result.

Table 3

Constants B in dilute range (a) and concentrated range (b) of metal butyrates at different temperatures 35 — 60°

Temperature (°C)	Magnesium		Calcium		Strontium		Barium	
	a	b	a	b	a	b	a	b
35	0.17	0.47	0.14	0.49	0.19	0.55	0.15	0.46
40	0.18	0.48	0.13	0.48	0.20	0.52	0.18	0.41
45	0.18	0.48	0.18	0.49	0.19	0.57	0.18	0.42
50	0.17	0.46	0.17	0.48	0.18	0.58	0.18	0.35
55	0.18	0.48	0.17	0.49	0.20	0.58	0.17	0.37
60	0.18	0.49	0.18	0.49	0.22	0.60	0.18	0.38

Soaps behave as a weak electrolyte in dilute solutions and therefore the following expression[6] for dissociation of soaps can be derived.

$$C^2\lambda^2 = \frac{K\lambda_\infty^3}{4\lambda} - \frac{K\lambda_\infty^2}{4} \tag{ii}$$

The plots (Fig. 4) of $C^2\lambda^2$ vs $1/\lambda$ are linear in the dilute range which shows the validity of equation (ii) in these solutions. The values of λ_∞ and K have been evaluated from the slopes and intercepts of the linear plots.

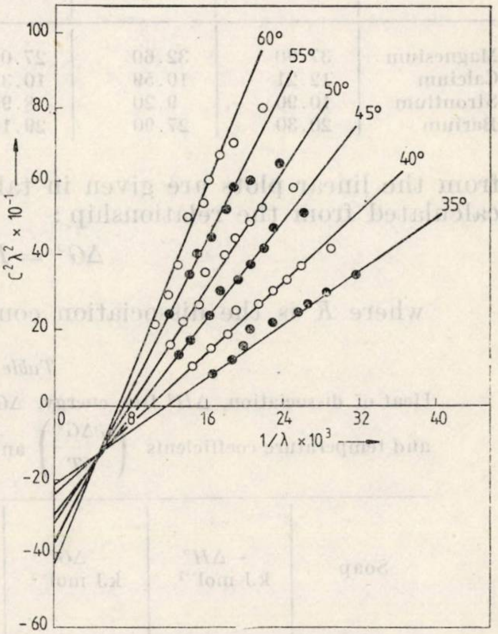

Fig 4. — Plots of $C^2\ \lambda^2$ vs. $1/\lambda$ of strontium butyrate at different temperatures 35 – 60°.

Molar conductivity at infinite dilution (Table 4) increases with increasing temperature. This is due to the increase in ionic mobility despite the fact that the addition of soap increases the viscosity of the solvent. The values of λ_∞ of the soaps at different temperatures are in the order :

Table 4

Molar conductivity at infinite dilution, λ_∞ of metal butyrates at different temperatures 35 — 60°

Soap	35°	40°	45°	50°	55°	60°
Magnesium	68.89	77.55	88.68	97.41	111.29	116.41
Calcium	128.00	141.60	150.30	164.10	172.06	191.89
Strontium	86.59	101.06	113.79	130.00	143.06	157.50
Barium	122.40	126.13	135.82	138.73	148.91	158.00

Calcium > Barium > Strontium > Magnesium

Dissociation constant (Table 5) of barium soap increases with increasing temperature whereas other soaps show the reverse behaviour. The plots of log K vs. $1/T$ are linear. Heats of dissociation, $\Delta H°$, calculated

Table 5

Dissociation constant, $K \times 10^4$ of metal butyrates at different temperatures 35 − 60°

Soap	35°	40°	45°	50°	55°	60°
Magnesium	37.90	32.60	27.00	24.50	20.00	18.90
Calcium	12.21	10.59	10.31	9.36	9.18	8.04
Strontium	10.90	9.20	8.96	7.10	7.04	6.45
Barium	20.30	27.90	29.10	36.00	41.30	44.06

from the linear plots are given in table 6. The free energy, ΔG° can be calculated from the relationship :

$$\Delta G^\circ = RT \ln K \tag{iii}$$

where K is the dissociation constant.

Table 6

Heat of dissociation, ΔH° free energy, ΔG° entropy of dissociation, ΔS° at 35° and temperature coefficients $\left(\frac{\partial \Delta G^\circ}{\partial T}\right)$ and $\left(\frac{\partial \Delta S^\circ}{\partial T}\right)$ of metal butyrates in water

Soap	$-\Delta H^\circ$ kJ mol^{-1}	$-\Delta G^\circ$ kJ mol^{-1}	$-\Delta S^\circ$ J mol^{-1}K^{-1}	$\frac{\partial \Delta G^\circ}{\partial T}$ kJ mol^{-1}K^{-1}	$\frac{\partial \Delta S^\circ}{\partial T}$ Jmol^{-1}K^{-2}
Magnesium	31.59	14.31	−56.10	−.13	.6
Calcium	14.36	17.18	9.16	−.10	.3
Strontium	18.19	17.47	− 2.33	−.11	.4
Barium	−30.63	15.88	151	.045	−.5

The values of entropy (Table 6), ΔS° have also been calculated from ΔH° and ΔG°. Both ΔG° and ΔS° decrease linearly with increasing temperature of barium soap whereas other alkaline earth metal soaps increase. The slopes of these plots vary with nature of metal ions in the soap.

ACKNOWLEDGEMENTS. The authors record their thanks to Dr. K. N. Mehrotra, Reader in the Department of Chemistry, University of Jodhpur, Jodhpur for his keen interest in the work and to the college authorities for providing laboratory facilities.

REFERENCES

[1] R. P. Varma and K. Kumar, *Cellulose Chem. Technol.*, **9**, 23 (1975).
[2] R. P. Varma and P. Bahadur, *Indian J. Chem.*, **10**, 1189 (1972).
[3] R. P. Varma and R. Dayal, *J. Am. Oil. Chem. Soc.*, **53**, 39 (1976).
[4] R. P. Varma and P. Bahadur, *Cellulose Chem. Technol.*, **9**, 393 (1975).
[5] J. W. McBain, *J. Phys. Chem.*, **43**, 671 (1939).
[6] C. A. Kraus and W. C. Bray, *J. Amer. Chem. Soc.*, **35**, 1315 (1913).

Revue Roumaine de Chimie, **28**, *8*, 825 – 830 (1983)

SPECTROSCOPIC INVESTIGATION OF CHARGE TRANSFER COMPLEXES OF METHYL PYRIDINES WITH AROMATIC NITROCOMPOUNDS*

Y. M. ISSA, A. M. HINDAWEY, A. L. EL-ANSARY and R. M. ISSA
Chemistry Department, Faculty of Science, Cairo and
Alexandria Universities. A. R. Egypt

Received January 8, 1982

The charge transfer complexes (C.T.C.) of five methyl pyridines (donors) with three trinitro- and seven dinitro-benzenes (acceptors) were prepared and investigated in the solid state by IR, ^1H-NMR and electronic absorption spectroscopy. The results showed that acidic acceptors form C.T.C. involving $\pi - \pi^*$ and proton transfer interaction, while nonacidic ones are bonded through $\pi - \pi^*$ and $n - \pi^*$ electronic interactions.

INTRODUCTION

Charge transfer complexes of the donor-acceptor type were the subject of some interesting investigations in the last few decades. Most of the complexes investigated with aromatic nitrocompounds as acceptors utilised aniline derivatives, substituted benzenes or condensed ring system compounds as donors.[1-5] Charge transfer complexes of pyridine and few of its derivatives with picric acid were isolated and investigated by IR spectroscopy.[1] The type of bonding in a series of sym-trinitrobenzene complexes with a series of pyridines, including methyl pyridines, and their formation constants were determined using ^1H-NMR spectroscopy.[6]

In the present investigation, the charge transfer complexes of 2-picoline (a), 3-picoline (b), 4-picoline (c), lutidine (d) and collidine (e) as donors and picryl chloride (1), trinitrotoluene (2), 1-F-2,4-di-NO_2 benzene (3), 1-Cl-2,4-di-NO_2 benzene (4), 1,5-di-F-2,4-di-NO_2 benzene (5), picric acid (6), 3,5-dinitrosalicylic acid (7), 3,5-dinitrobenzoic acid (8), 2,4-dinitrophenol (9) and 2,6-diinitrophenol (10) as acceptors are prepared and investigated by IR spectroscopy. The conclusions obtained are supported by the results of both ^1H-NMR and electronic absorption spectra of some complexes.

---

* The preparation of C.T.C. and IR studies were carried out in the Chemistry Department, Faculty of Education, Mekkah, Saudi Arabia.

EXPERIMENTAL

All compounds used in the present investigation were pure laboratory grade (BDH) chemicals. The preparation of the solid C.T. complexes and IR spectroscopic investigation are the same as given before.[4,5] The IR spectra were obtained by the aid of the SP 2000 infrared spectrophotometer (PYE UNICAM) using the KBr disc technique. The accuracy of the apparatus is less than ± 5 cm^{-1} within the 4 000 — 2 000 cm^{-1} range and less than ± 2 cm^{-1} in the lower range. The ^1H—NMR spectra of some donors, acceptors and their C.T. complexes were obtained by the aid of a VARIAN EM-390 NMR spectrophotometer. The electronic absorption spectra were recorded on a UNICAM SP 8000 spectrophotometer using the Nujol Mull technique.

RESULTS AND DISCUSSION

The C.T. complexes isolated can be classified into two groups according to the type of acceptor used.

(A) C.T. complexes with nonacidic acceptors (Table 1)

The IR spectra of this class of compounds display some interesting changes as compared to those of their free constituents. The γ_{CH} bands of the acceptor display a shift to lower wavenumbers whereas those of the donors display on opposite shift. This behaviour denotes an increase of the π-electron density on the acceptor and its decrease on the donor molecules, which results from a $\pi - \pi^*$ interaction.[1,4,5] The increased π-electron density on the acceptor molecules would cause a shift in most of their IR bands to lower wavenumbers. This is the case with the dinitro benzene derivatives (acceptors 3, 4 and 5) while the NO_2-bands of picryl chloride and trinitrotoluene (acceptors 1 and 2) exhibit few exceptions, where some bands display no shifts or were slightly shifted to higher wavenumbers. The shift to higher wavenumbers was explained in the case of aniline derivatives as the results of an $n-\pi^*$ interaction involving the location of an n-electron from the nitrogen lone pair into a π^*-level of one NO_2-group.[1,4] The shifts observed with the NO_2-bands would thus be the resultant of the $\pi - \pi^*$ and $n-\pi^*$ interactions.

The shifts of the NO_2-bands of the acceptors reveal that the $n-\pi^*$ interaction would either be of low magnitude or does not contribute to the bonding in the C.T. complex. The electronic absorption spectra of this class of compounds exhibit only one obvious C.T. band within the wavelength range 380 — 430 nm appearing essentially as a shoulder on the longer wavelength side of the $Ø \rightarrow NO_2$ bands of the acceptor. The band observed would be assigned to the $\pi - \pi^*$ C.T. interaction, which is substantiated by calculating the energy of the C.T. interaction ($E_{C.T.}$) using the relation given by Briegleb.[7] The values determined from the C.T. bands amount to 3.26 — 3.02 eV compared with 3.52 — 3.30 eV calculated from the equation for the C.T. complexes with trinitrotoluene. The absence of n-π^* band, in comparison with the case of aniline derivatives or nitrogen bases, supports the above mentioned conclusion that $n-\pi^*$ interaction would be of low contribution to the bonding in the C.T. complex or even absent. This behaviour can be explained assuming that the n-ionisation potentials in aniline derivatives are lower than the

Table 1

Main bands in the IR spectra of molecular complexes with nonacidic acceptors (cm^{-1})*

Donor	Colour	M.p°C	asym.NO_2	sym. NO_2	γ_{CH} acceptor
(1) Complexes of picryl chloride :					
Free acceptor			1 553, 1 540	1 348	788
a	dark brown	66	1 560, 1 545, 1 535	1 350, 1 340	783
b	canary yellow	100	1 555, 1 545, 1 530	1 345, 1 340	780
c	dark brown	100	1 560, 1 535	1 350, 1 335	m
d	yellowish brown	74	1 560, 1 540, 1 535	1 350, 1 340	785
e	golden yellow	74	1 560, 1 545, 1 535	1 350, 1 345	m
(2) Complexes of trinitrotoluene :					
Free acceptor			1 555, 1 520	1 360	800
a	pale brown	77	1 540, 1 535, 1 518	1 355, 1 350	792
b	pale brown	78	1 545, 1 540, 1 520	1 355, 1 352	793
c	pale brown	75	1 552, 1 535, 1 515	1 355, 1 348	795
d	pale brown	73	1 550, 1 530, 1 515	1 355, 1 348	793
e	pale brown	73	1 545, 1 535, 1 515	1 355, 1 348	792
(3) Complexes of 1-F-2,4-di-NO2 benzene :					
Free acceptor			1 550, 1 545	1 352, 1 348	850, 840, 745
a	yellowish brown	163	1 540, 1 535	1 345	838, 742
b	brown	68	1 545, 1 535	1 350	840, 742
e	yellowish brown	149	1 545, 1 530	1 345	838, 738
(4) Complexes of 1-Cl-2,4-di-NO_2 benzene :					
Free acceptor			1 550, 1 533	1 353, 1 335	852, 836, 758
a	yellowish brown	63	1 545, 1 530	1 350, 1 330sh	852, 832, 750
b	pale violet	208	1 548, 1 528	1 350, 1 330sh	850, 835, 752
d	dark brown	46	1 545, 1 530	1 348, 1 330	850, 832, 748
e	brown	45	1 543, 1 527	1 345, 1 325	847, 832, 745
(5) Complexes of 1,5-di-F-2,4-di-NO_2 benzene:					
Free acceptor			1 548, 1 533	1 350	840, 775
a	golden yellow	69	1 540, 1 530	1 342	835, m
b	olive green	173	1 547, 1 530	1 335	838, m
c	dark brown		1 542, 1 530	1 343	835, m
d	yellowish brown	77	1 540sh 1 530	1 343	832, m
e	yellowish green	78	1 538 1 528	1 342	837, m

* sh : shoulder, m : masked by more intense neighboring bands

first π-ionisation potentials [8] whereas for pyridine and its derivatives or generally for heterocyclic aromatic nitrogen compounds the first π-ionisation potential is lower than the n-ionisation potential.[9]

The ^1H-NMR spectra of the donors display two sets of signals. The first set is observed within the δ 2.6 — 2.3 ppm region and corresponds to the CH_3-groups; the signal appears splitted in the spectrum of donor (e) due to the difference in the character of the three CH_3 groups. The second set at δ 7.6 — 6.9 ppm is due to the protons of the pyridine ring. The ^1H-NMR spectra of the nonacidic acceptors 1 — 5 exhibit one group of signals within the δ 8.7 — 6.8 ppm range resulting from the protons of the phenyl group. In addition, the spectrum of acceptor 2 is also characterized by a signal at δ 2.8 ppm for the CH_3 group. The ^1H-NMR spectra of the molecular complexes can be considered as a superposition of the spectra of their components with their signals being shifted slightly from their positions. The signals of the donor parts are shifted to higher fields by 0.08 — 0.2 ppm while those of the acceptor parts exhibit a counter displacement of 0.1 — 0.18 ppm. Such shifts are due to the decreased electron density on the donor and its increase on the acceptor which results from the intermolecular C.T. interaction. The magnitude of the shifts varies according to the nature of both donot and acceptor. For the same acceptor, the shift varies in the order ($b < a \simeq c < d < e$) whereas for the same donor it is ($3,4 < 5 < 1 < 2$).

Based on the above results, the bonding in C.T. complexes of this type can be represented as follows:

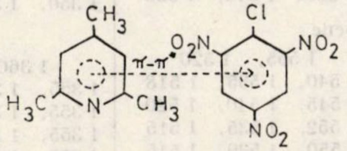

(B) **C.T. complexes with acidic acceptors (Table II)**

The IR spectra of this class of compounds show drastic changes in comparison with those of the simple constituents. All spectra are characterised by a group of broad strongly interacting bands within the $2900 - 2400\ cm^{-1}$ range which are not present in the spectra of the free donors or acceptors. These bands can be assigned to the stretching mode of the group ($=\overset{|}{N}{}^{+}$—H) which is formed through the transfer of a proton from the acidic centre of the acceptor to the nitrogen of the donor. The transfer of the proton from the acceptor is supported by the disappearance of the bands due to the phenolic OH-groups of acceptors 6, 7, 9 and 10 and carboxylic group of acceptor 8.

The γ_{CH} bands of the acceptors are shifted to lower values whereas those of the donors shifted to higher ones. This behaviour is an indication for an intermolecular charge transfer of the $\pi - \pi^*$ type leading to increased electron density on the acceptor and its decrease on the donor. Thus complexes of this class are formed through $\pi - \pi^*$ bonding and proton transfer, hence the C.T. complexes formed belong to compounds of the salt type.[2,3] The higher frequency NO_2-bands of the acceptors are mostly shifted to lower wavenumbers due to the higher polarisation of the NO_2-groups in the C.T. complexes as a result of the increased π-electron density on their rings. The shift of the lower frequency *asym*-NO_2-band (corresponding to the hydrogen bonded NO_2-group)[4] is the resultant of a shift to higher values due to the destruction of the intramolecular hydrogen bonding after proton transfer to the donor molecule and the shift to lower values resulting from the C.T. complex formation. 3,5-Dinitrosalicylic acid exhibits two acidic centers, the proton ofthe phenolic and that of the carboxylic groups; only one of these two protons would be involved in C.T. complex formation. The bands due to the C = O of the COOH group still retain their identity in the spectra of the C.T. complexes and hence the proton involved in C.T. complex formation would be that of the phe-

Table 2

Main bands in the IR spectra of molecular complexes with acidic acceptors (cm^{-1})*

Donor Colour	M.p.°C	ν $=\overset{\backslash}{N}^+-H$	ν_{OH}	$\nu_{C=O}$	asym. NO_2	sym. NO_2	γ_{CH}
(6) Complexes of picric acid :					1 555, 1 540		
Free acceptor					1 530	1 360	784
a yellow	159	— —	—	—	1 550, 1 535	1 340	779
b yellow	147	2 670, —	—	—	1 548, 1 535	1 338	m
c yellow	162	2 780, —	—	—	1 550, 1 535	1 345	780
d yellow	157	2 690, 2 580	—	—	1 550, 1 538	1 345	780
e yellow	152	2 770, 2 680	—	—	1 552, 1 535	1 340	775
(7) Complexes of 3,5-dinitrosalicylic acid :							
Free acceptor			3 570 3 460 3 100	1 700 1 675	1 540, 1 530	1 349	925, 825
a yellow	178	2 780, 2 560	3 090	1 705	1 535	1 345	920, 818
b pale yellow	134	2 840, 2 680	3 090	1 700	1 533	1 350	920, 820
c pale yellow	141	2 730, —	3 080	1 705	1 530	1 345	— 818
d pale yellow	176	2 730, 2 600	3 090	1 705	1 535	1 345	920, 818
e yellow	189	2 730, 2 580	3 090	1 705	1 535	1 343	920, 815
(8) Complexes of 3,5-dinitrobenzoic acid :							
Free acceptor			3 190	1 705	1 555, 1 540	1 350	923, 808, 727
a pale yellow	130	2 760, 2 550	—	—	1 545, 1 530	1 343	920, 795, 725
b pale yellow	131	2 780, 2 580	—	—	1 550, 1 535	1 348	920, 803, 725
c pale yellow	145	2 760, 2 570	—	—	1 545, 1 535	1 345	920, 800, 725
d pale yellow	152	2 740, 2 530	—	—	1 545, 1 535	1 345	918, 798, 725
e pale yellow	152	2 720, 2 480	—	—	1 540, 1 533	1 342	915, 792, 725
(9) Complexes of 2,4-dinitrophenol :							
Free acceptor			3 270	—	1 540, 1 520	1 350	928, 825
a yellow	86	2 760, 2 580	—	—	1 535, 1 528sh	1 345, 1 335	923, 820
b yellow	76	2 780, 2 650	—	—	1 538, 1 530sh	1 345, 1 338	925, 823
c golden yellow	105	2 750, 2 580	—	—	1 530	1 335b	920, 820
d yellow	110	2 750, 2 530	—	—	1 532	1 335b	923, 822
e yellow	105	2 680, 2 490	—	—	1 530	1 335b	920, 820
(10) Complexes of 2,6-dinitrophenol :							
Free acceptor			3 270	—	1 553, 1 537	1 355	828, 765
a orange	65	2 600, 2 400	—	—	1 540	1 348	823, 752
b orange	68	2 700, 2 400	—	—	1 545, 1 540 sh	1 350	825, m
c orange	96	2 680, 2 460	—	—	1 548, 1 543 sh	1 345	m, 750
d orange red	86	2 570, 2 430	—	—	1 545, 1 540 sh	1 342	m, 745
e orange	107	2 680, 2 400	—	—	1 543, 1 535	1 340	820, 745

* b : broadened band, sh : shoulder, m : masked by more intense neighbouring bands.

nolic OH-group. This is in accordance with previous observations in the spectra of C.T. complexes with 3,5-dinitrosalicylic acid.[10]

The electronic absorption spectra of the C.T. complexes belonging to this class of compounds exhibit a single C.T. band within the 360 — 340 nm region which corresponds to the $\pi - \pi^*$ interaction. The band is situated at shorter wavelength as compared with those of class (A); this is attributed to the fact that the donor system is the pyridinium ion and the acceptor is an anion. This causes a higher ionisation potential of the donor and a lower electron affinity of the acceptor which requires a higher energy.

The transfer of a proton from the acceptor to the donor is substantiated by considering the ^1H-NMR spectra of the complexes with acceptor 9. The ^1H-NMR spectrum of 9 displays a group of signals within the δ 8.5 — 6.5 ppm range from which the one at δ.6.60 ppm being rather broad with an integration equivalent to one proton, is assigned to the hydrogen bonded OH group. This signal is not readily affected by deuteration denoting strong intramolecular hydrogen bonding. The other signals correspond to the three protons of the phenyl group. In the ^1H-NMR spectra of the C.T. complexes, the signal at δ 6.60 ppm is no more observed and a new signal with integration equivalent to one proton appears at δ 4.4 — 4.3 ppm which corresponds to the new N^+-H group.

Based on the results obtained, the bonding in complexes of this type with 2,4-dinitrophenol can be formulated as follows :

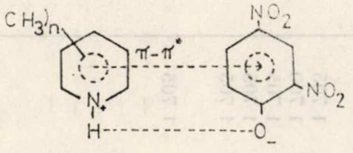

REFERENCES

[1] R. D. Kross and V. A. Fassel, *J. Amer. Chem. Soc.*, **79**, 38 (1957).

[2] G. Briegleb and H. Della, *Z. phys. Chem. (Frankfurt)*, **24**, 359 (1960).

[3] G. Kortum and W. Braun, *Z. phys. Chem. (Frankfurt)*, **28**, 362 (1961).

[4] R. M. Issa and M. M. El-Essawey, *Z. phys. Chem. (Leipzig)*, **253**, 96 (1973) ; *Acta Chim. Acad. Sci. Hung.*, **88**, 341 (1976) ; **92**, 263 (1977).

[5] R. M. Issa, Y. M. Issa and A. M. Hindawey, *Indian J. Chem.*, **19A**, 615 (1980) ; *Monatsh. Chem.*, **111**, 1114 (1980) ; *J. Indian Chem. Soc.*, **57**, 216 (1980).

[6] R. Foster, D. L. Hammick and P. J. Placito, *J. Chem. Soc.*, **1970**, 3881.

[7] G. Briegleb and J. Czekalla, *Z. Elektrochem.*, **58**, 249 (1964).

[8] W. Wheat, "Handbook of Chemistry and Physics" 50th Edit. The Chemical Rubber Co. Ohio, USA (1969—1970).

[9] M. A. El-Bayoumi and O. S. Khalil, *J. Chem. Phys.*, **47**, 4863 (1967).

[10] Y. M. Issa, A. M. Hindawey, R. M. Issa and A. M. G. Nassar, *Rev. Roumaine Chim.*, **25**, 1535 (1980) ; *Gazz. Chim. Ital.*, **111**, 27 (1981).

Revue Roumaine de Chimie, **28**, *8*, 831 – 839 (1983)

THEORETICAL STUDY ON THE REACTIVITY OF CYCLOIMMONIUM–YLIDES. I.

REACTIVITY OF MONOSUBSTITUTED CARBANION-YLIDES

GH. SURPĂŢEANU*, M. CONSTANTINESCU**, C. LUCHIAN*, M. PETROVANU*, I. ZUGRĂVESCU* and A. LABLACHE-COMBIER***

* Polytechnic Institute "Gh. Asachi", Organic Chemistry Department, Jassy, 11, str. 23 August, Romania

** Computer Center of the University "Al. I. Cuza", Jassy, Romania

*** Physical Organic Chemistry Department, University of Lille, France.

Received October 25, 1982

A theoretical study on the reactivity of some monosubstituted carbanion cycloimmonium-ylides is achieved by perturbation and frontier orbital theories. Molecular orbital calculations have been performed by CNDO/2 method. The studied ylides are derived from pyridine, isoquinoline, quinoline, pyridazine, pyrimidine, phthalazine and 4-phenyl-1,2,4-triazole ; the substituent of the ylide carbon atom is always a carbomethoxy group. These monosubstituted carbanion ylides as nucleophilic reagents are theoretically investigated in connection with the protonation and transylidation reactions. The reactivity of these ylides as 1,3-dipoles in 3 + 2 cycloaddition reactions, is also discussed.

The cycloimmonium ylides may be classified by the ylide carbon atom type into monosubstituted, I, and disubstituted, II, carbanion cycloimmonium ylides.[1]

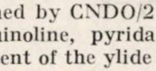

I

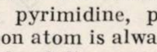

II

In this paper we shall limit our investigation to the monosubstituted carbanion cycloimmonium ylides of the type I.

Generally, in a monosubstituted carbanion ylide the R_1 group is a strong electron withdrawing substituent [2] as CN, COR, CO_2R, CONHR etc. In this case many resonance structures may be suggested:

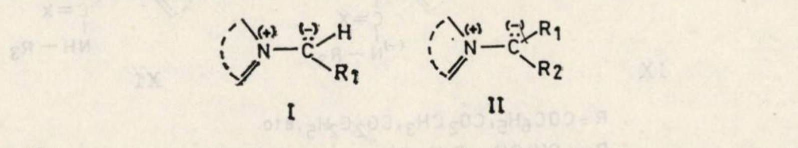

III

The representative chemical properties of these ylides are cleavage of the ylidic bond N^+-C^-, the nucleophilic character of the ylide C atom and 1 — 3 dipolar structure involving the resonance structure IIIb.

Therefore, by the cleavage of the ylidic bond N^+-C^-, intermediate carbenes are formed :[3,4]

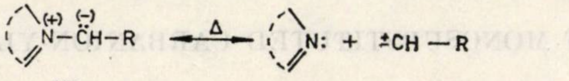
IV V R $(CO_2C_2H_5)$

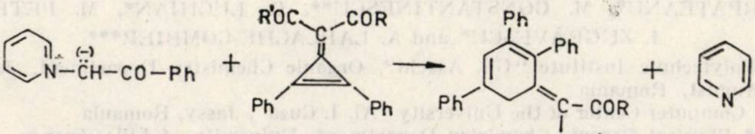
VI VII

The nucleophilic character of cycloimmonium ylides of the type *I* is well-known. In the presence of strong acids, the monosubstituted carbanion ylides are protonated to the ylide C atom, giving the respective cycloimmonium salts.[5,6]

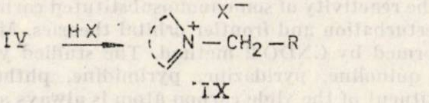
IX

R $(COC_6H_5, CO_2C_2H_5, CN, CONH_2$, etc.)

The first step of the reaction of monosubstituted ylides on isocyanates and isothiocyanates (transylidation reaction) is a nucleophilic attack on the carbon of the double bond C = N or C = S by the ylide C atom, giving finally the disubstituted carbanion ylides XI.[7-9]

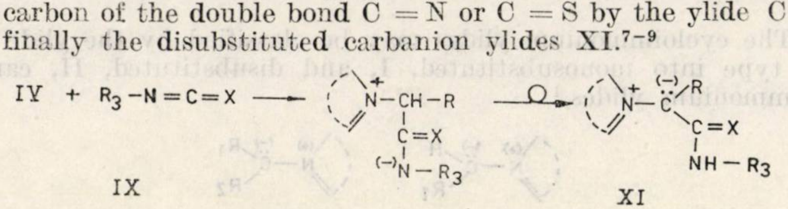
IX XI

$R = COC_6H_5, CO_2CH_3, CO_2C_2H_5$, etc.
$R_3 = CH_2CH_3, C_6H_5$, etc
X = O, S

The monosubstituted ylides as 1,3 dipoles (resonance structure IIIb) undergo 3 + 2 and 3 + 3 cycloadditions. The 3 + 2 cycloadditions of these ylides to symmetrical or unsymmetrical dipolarophiles give new heterocyclic structures [10]:

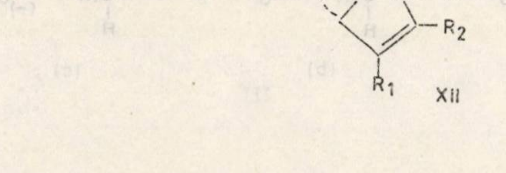
XII

RESULTS AND DISCUSSION

Molecular orbital calculations are applied to explain some aspects of the reactivity of monosubstituted carbanion cycloimmonium ylides. All studied ylides have as common structural element the carbanion — $\diagdown\!\!\!\_\,\ddot{C}H-CO_2CH_3$. This carbanion is bound to a cycloimmonium cation resulted from pyridine, pyridazine, pyrimidine, quinoline, isoquinoline, phtalazine and 4-phenyl-1,2,4-triazole. The total atomic charges, the atomic orbital coefficients corresponding to the frontier molecular orbitals and the molecular orbital energies reported here were carried out by CNDO/2 method,[11] on a Felix C-256 computer.

Table 1 gives the geometries of ylide systems. This table also presents the references on the geometries used. When the references miss, the geometries were approximated taking into account the geometry of some similar compounds or the standard atomic distances corresponding to the hybridization states and the type of the bonds.[15]

Table 2 shows the total atomic charges, Q, the frontier orbital energies for HOMO (the highest occupied molecular orbital) and LUMO (the lowest unoccupied molecular orbital) and the p_z atomic orbital coefficients of some atoms representing virtual reaction centers in monosubstituted carbanion cycloimmonium ylides.

Using the generalized perturbation theory of the second-order the following relation is proposed for the calculation of the interaction energy ΔE between two molecules R and S, by their two atoms k and l, respectively.

$$\Delta E = (q_a + q_b)\,\beta_{ab} S_{ab} + \frac{Q_k \cdot Q_l}{R_{kl} \cdot \varepsilon}\,\alpha - \left(\sum_r^{occ} \sum_s^{unocc} + \sum_r^{unocc} \sum_s^{occ} \right) \frac{2(C_{ra} C_{sb} \beta_{ab})^2}{E_s - E_r} \quad (1)$$

where : — q_a and q_b are the electron populations in the atomic orbitals a and b belonging to the atoms k and l respectively;

— β_{ab} and S_{ab} are the resonance and overlap integrals;

— ε is the local dielectric constant;

— $\sum_r^{occ}$ and $\sum_r^{unocc}$ refer to the molecular orbitals occupied and unoccupied in molecule R, and analogously for the terms $\sum_1^{occ}$ and $\sum_1^{unocc}$ in the molecule S;

— Q_k and Q_l are the total charges on atoms k and l;

— R_{kl} is the distance between the atoms k and l;

— C_{ra} and C_{sb} are the coefficients of atomic orbitals a and b in the molecular orbitals r and s, where r refers to the molecular orbitals on one molecule and s refers to those on the other;

— E_s and E_r are the energies of the molecular orbitals s and r respectively;

— α is a constant ($\alpha = 14.4$) which assures the calculation of the second term of the equation in electron-Volts (eV), when the total atomic charges and the interatomic distances in the atomic units (u.a) and angströms (Å) respectively are given.

Table 1

The geometries of some monosubstituted carbanion cycloimmonium ylides.

Group	Lengths in Å		Angles in degrees		Ref.
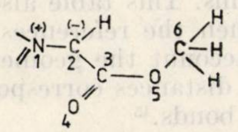	$r_{N_1C_2}$	1.41	$< N_1C_2H_7$	120°	12
	$r_{C_2C_3}$	1.50	$< N_1C_2C_3$	120°	
	$r_{C_3O_4}$	1.22			
	$r_{C_3O_5}$	1.43			
	$r_{O_5C_6}$	1.34			
	r_{CH}	1.08			
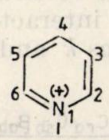	r_{NC}	1.353	$< C_2N_1C_6$	112°	13
	r_{CC}	1.39	$< N_1C_2C_3$	120°	
	r_{CH}	1.08	$< C_2C_3C_4$	119°	
			$< C_3C_4C_5$	120°	
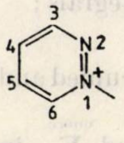	r_{NN}	1.325	$< N_1N_2C_3$	117.2°	
	r_{NC}	1.33	$< N_2C_3C_4$	120°	
	r_{CC}	1.34	$< C_3C_4C_5$	122.4°	
	r_{CH}	1.08			
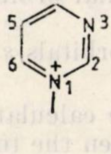	$r_{N_1C_2}$	1.32	$< N_1C_2N_3$	128°	14
	$r_{C_2N_3}$	1.32	$< C_2N_3C_4$	114°	
	$r_{N_3C_4}$	1.32	$< N_3C_4C_5$	125.5°	
	$r_{C_4C_5}$	1.36	$< C_4C_5C_6$	113°	
	$r_{C_5C_6}$	1.36	$< C_5C_6N_1$	125.5°	
	$r_{N_1C_6}$	1.32	$< C_6N_1C_2$	114°	
	r_{CH}	1.08			

Group	Lengths in Å		Angles in degrees		Ref.
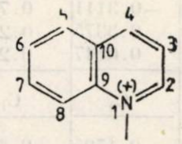	$r_{N_1C_2}$	1.33	$< C_9N_1C_2$	119°	
	$r_{C_2C_3}$	1.38	$< N_1C_2C_3$	121°	
	$r_{C_3C_4}$	1.40	$< C_2C_3C_4$	120°	
	$r_{C_4C_{10}}$	1.42	$< C_4C_{10}C_9$	115°	
	$r_{C_{10}C_5}$	1.42	$< C_{10}C_5C_6$	119.3°	
	$r_{C_5C_6}$	1.35	$< C_5C_6C_7$	121.3°	
	$r_{C_6C_7}$	1.34	$< C_7C_8C_9$	119.3°	
	$r_{C_7C_8}$	1.35	$< C_8C_9C_{10}$	124°	
	$r_{C_8C_9}$	1.42			
	$r_{C_9C_{10}}$	1.39			
	r_{CH}	1.08			
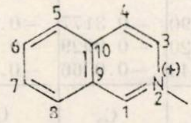	$r_{C_1N_2}$	1.37	$< C_1N_2C_3$	121.6°	
	$r_{N_2C_3}$	1.34	$< N_2C_3C_4$	120.9°	
	$r_{C_3C_4}$	1.36	$< C_4C_{10}C_4$	119°	
	$r_{C_4C_{10}}$	1.42	$< C_{10}C_5C_6$	119.5°	
	$r_{C_{10}C_5}$	1.42	$< C_5C_6C_7$	121.5°	
	$r_{C_5C_6}$	1.36	$< C_6C_7C_8$	121.5°	
	$r_{C_6C_7}$	1.345	$< C_7C_8C_9$	119.5°	
	$r_{C_7C_8}$	1.36	$< C_8C_9C_{10}$	119°	
	$r_{C_8C_9}$	1.42	$< C_{10}C_9C_1$	119°	
	$r_{C_9C_{10}}$	1.39	$< C_9C_1N_2$	120°	
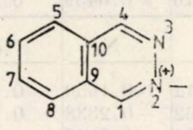	$r_{C_1N_2}$	1.37	$< C_1N_2N_3$	121.6°	
	$r_{N_2N_3}$	1.34	$< N_2N_3C_4$	120.9°	
	$r_{N_3C_4}$	1.36	$< C_4C_{10}C_9$	119°	
	$r_{C_4C_{10}}$	1.42	$< C_{10}C_5C_6$	119.5°	
	$r_{C_{10}C_5}$	1.42	$< C_5C_6C_7$	121.5°	
	$r_{C_5C_6}$	1.36	$< C_6C_7C_8$	121.5°	
	$r_{C_6C_7}$	1.345	$< C_7C_8C_9$	119.5°	
	$r_{C_8C_9}$	1.42	$< C_8C_9C_{10}$	119°	
	$r_{C_9C_{10}}$	1.39	$< C_{10}C_9C_1$	119°	
	$r_{C_1C_9}$	1.40	$< C_9C_1N_2$	120°	
	r_{CH}	1.08			
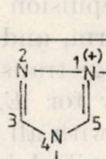	$r_{N_1N_2}$	1.40	$< N_1N_2C_3$	128.5°	16
	$r_{N_2C_3}$	1.30	$< N_2C_3N_4$	106.5°	
	$r_{C_3N_4}$	1.36	$< C_3N_4C_5$	70°	
	r_{CH}	1.08			

Table 2

The frontier orbital energies and the p_z atomic orbital coefficients

No.	Molecule	Frontier orbital and atomic charge	Orbital energy (eV)	Atomic orbital coefficients				
1	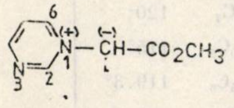			N_1	C_2	C_6	C_i	
		HOMO	−8.79171	−0.0616	−0.3086	−0.3111	0.7271	
		LUMO	2.04585	−0.5711	0.8800	0.3375	0.2545	
		Q		0.2195	0.0143	0.0147	0.2875	
2	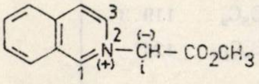			N_2	C_1	C_3	C_i	
		HOMO	−9.08205	0.0955	0.3959	0.1725	−0.6985	
		LUMO	0.5883	−0.4502	0.4651	−0.0717	0.2338	
		Q		0.1940	−0.0113	0.0002	−0.2824	
3	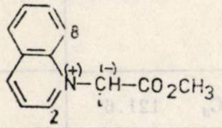			N_1	C_2	C_8	C_i	
		HOMO	−8.8166	0.1104	0.3413	0.0689	−0.7007	
		LUMO	0.7716	0.4810	−0.2921	−0.2983	−0.2519	
		Q		0.2032	0.0019	−0.0042	−0.2719	
4	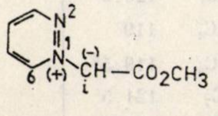			N_1	N_2	C_6	C_i	
		HOMO	−9.5723	0.0259	0.3390	−0.3177	−0.7123	
		LUMO	1.1897	0.5558	−0.4620	−0.0929	−0.2906	
		Q		0.2976	−0.1343	−0.0066	−0.2602	
5	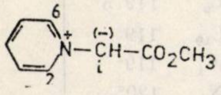			N_1	N_3	C_2	C_6	C_i
		HOMO	−9.4564	0.0828	−0.0594	0.2806	0.2844	−0.7379
		LUMO	1.3796	0.5433	−0.3179	−0.1812	−0.4646	−0.2389
		Q		0.1623	−0.1060	0.0914	0.0714	−0.2999
6	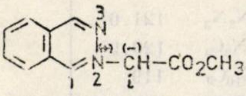			N_2	N_3	C_1	C_i	
		HOMO	−9.1237	−0.0619	−0.1819	−0.4232	0.6738	
		LUMO	0.5514	0.3948	0.1423	−0.4435	−0.2275	
		Q		0.2452	−0.1016	−0.0459	−0.2611	
7	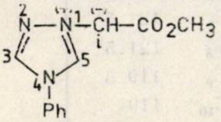			N_2	N_1	N_4	C_5	C_i
		HOMO		0.2442	−0.1112	−0.1650	−0.3825	0.7356
		LUMO		−0.1943	−0.2762	−0.2338	0.3916	0.1326
		Q		−0.0647	0.2432	−0.1246	0.0179	−0.3081

The first term of equation (1) is a closed-shell repulsion term, the second term is a Coulombic repulsion (or attraction) term, and the third term is called either delocalization or overlap or charge-transfer stabilization. This last term has physical significance only for $E_s \neq E_r$. It represents the interaction between all the filled orbitals with all the unfilled ones. When $E_s \approx E_r$ the interaction is better described in charge-transfer terms, and the perturbation is then a first-order one of the form $2C_{ra}C_{sb}\beta_{ab}$.

Equation (1) holds for the change interactions of closed shell systems.[17] For the interaction donor R—acceptor S equation (1) is transformed into : [18–20]

$$\Delta E = \frac{Q_k \cdot Q_l}{R_{kl} \cdot \varepsilon} \propto - \sum_{r}^{occ} \sum_{s}^{unocc} \frac{2(C_{ra} \cdot C_{sb} \cdot \beta_{ab})^2}{E_s - E_r} \qquad (2)$$

The quantities in equation (2) have the same significance as those in equation (1). The largest contribution to the energy ΔE is due to the frontier orbitals HOMO-LUMO interaction.[21] The other orbital interactions owing to the large difference between the corresponding orbital energies $E_s - E_r$, are less significant.

Table 2 shows that all ylide C atoms in monosubstituted carbanion cycloimmonium ylides have negative charges. The values of these charges ranged between −0.2603 and −0.3081. This suggests that in the donor — acceptor charge controlled reactions the ylides act as nucleophilic reagents by the ylide C atoms. The oxygen atoms belonging to the carbanion groups have larger negative charges. Thus, the reactions in which these oxygen atoms should participate as nucleophilic centers do not occur.

The atomic orbital coefficients of ylide carbon atoms in HOMO orbitals have absolute values between 0.6738 and 0.7379 (Table 2). The atomic orbital coefficients of the oxygen atoms belonging to the HOMO orbitals have lower absolute values. Thus, in the single site donor (ylide)— acceptor reactions, the ylide carbon atom is more active. In a donor— acceptor reaction, simultaneously the electrostatic and orbital factors are involved.

Taking into account the experimental data [5–9] and the previous discussion, the monosubstituted carbanion ylides are nucleophilic reagents by the ylide carbon atoms.

On the numerical data in Table 2, the more adequate ylides for the reactions with an electrophilic reagent (acid, isocyanate, isothiocyanate etc.) can be selected.

The monosubstituted carbanion cycloimmonium ylides, by their resonance structures IIIb, participate in the 3 + 2 cycloadditions to double or triple bond dipolarophiles. In this case, it is very important to establish the nature of the 1,3 ylide-dipole. Thus, the values and signs of the atomic orbital coefficients of the ylide C atoms and adjacent atoms to the positive cyclic nitrogen must be analysed.

The 3 + 2 cycloaddition reactions of ylides to dipolarophiles belong to the change reaction class. The interactions energies of these reactions may be estimated by equation (1). In these cases the chorochemistry of the cycloaddition has to be determined.

Next, we shall establish the most probable positions of 1,3 ylide dipoles in the ylidic systems of this study (Table 2).

In pyridinium carbomethoxy methylide **1**, the values of atomic orbital coefficients of the atoms C_2 and C_6 are very close, and so the ylide 1,3-dipole formation is one, either $C_i - C_2$ or $C_i - C_6$.[22,23]

In isoquinolinium carbomethoxy methylide **2** the C_1 atom is more reactive than C_3 atom. The atomic orbital coefficients of C_1 atom, both in HOMO and LUMO orbitals, have higher absolute values than those of C_3 atom. Since the atomic orbital coefficients of C_1 and C_3 atoms in LUMO orbital have contrary signs, it can be accepted that the ylide **2** with a $C_i - C_3$ dipole could participate in the cycloadditions. But, the literature data on the cycloadditions of isoquinolinium-ylides[24,25] refer only to the 1,3 isoquinolinium ylide dipole $C_i - C_1$.

In quinolinium carbomethoxy methylide **3** it is evident that the 1,3-ylide dipole is $C_i - C_1$.

In pyridazinium carbomethoxy methylide **4** the N_2 atom has the absolute atomic orbital coefficient values higher than those of C_6 atom. But experimentally, ylide **4** participates in cycloadditions by the $C_i - C_6$ dipole.[26] Probably, the negative charged N_2 atom determines the nature of the 1,3 pyridazinium ylide dipole.

In the pyrimidinium carbomethoxy methylide **5**, by the atomic orbital coefficient values the C_6 atom is more reactive than C_6 atom. These values are very close in HOMO orbital for C_6 and C_2 atoms but are higher for C_6 atom in LUMO orbital.

In the phtalazinium carbomethoxy methylide **6** both the orbital factors and the experimental data show that the ylide 1,3-dipole $C_i - C_1$ is the most reactive.[27]

A similar case is the 4-phenyl-1,2,4-triazolium ylide **7**. In this molecule the most probable 1,3-ylide dipole is $C_i - C_5$.[28,29]

We outline that the ylides participate in the cycloadditions by the p_z orbitals of 1,3-ylide dipoles.

With the molecular orbital parameters in Table 2 and the same data for different dipolarophiles it can be constructed the orbital correlation diagrams of the cycloadditions.

It is to be mentioned that there is a good agreement between the above theoretical results and the experimental data on the reactivity of the monosubstituted carbanion cycloimmonium ylides. The obtained results suggest the possibility to synthesize new heterocyclic compounds.

REFERENCES

[1] G. Surpăţeanu, J. P. Catteau, P. Carafiloglu and A. Lablache-Combier, *Tetrahedrom Report*, **1976**, 23.

[2] J. Fleming, "Frontier Orbitals and Organic Chemical Reactions", Wiley, London, 1976.

[3] I. Zugrăvescu, E. Rucinschi and G. Surpăţeanu, *Rev. Roumaine Chim.*, **16**, 1099 (1971); *Tetrahedrom Letters*, **1970**, 941.

[4] O. Tsuge, H. Shimoharada and M. Noguchi, *Chemistry Letters*, **1981**, 1899, 1493.

[5] I. Zugrăvescu, M. Constantinescu, G. Surpăţeanu, A. Lablache-Combier and L. Devos, *Rev. Roumaine Chim.*, **24**, 1089 (1979).

[6] G. Surpăţeanu, M. Constantinescu and I. Zugrăvescu, *Rev. Roumaine Chim.*, **23**, 1449 (1978).

[7] F. Kröhnke and H. Kubler, *Chem. Ber.*, **70**, 538 (1937).

[8] A. W. Johnson, "Ylide Chemistry", Academic Press, New York, 1966.

[9] M. Petrovanu, C. Luchian, G. Surpăţeanu and V. Bărboiu, *Tetrahedron* (in press).

[10] I. Zugrăvescu and M. Petrovanu, "Chimia-N-ilidelor", Ed. Academiei, Bucureşti, 1974.

[11] J. A. Pople and D. L. Beveridge, "Approximate Molecular Orbital Theory", McGraw-Hill, New York, 1970.

[12] J. P. Catteau, P. Carafiloglu, A. Lablache-Combier, N. Lethan and G. Surpăţeanu, *Tetrahedron*, **32**, 461 (1976).

[13] B. Bak, L. Hansen and J. Rastrup, *J. Chem. Phys.*, **22**, 2013 (1954).

[14] C. J. B. Clews and W. Cochran, *Acta Cryst.* **1**, 4 (1948).

[15] L. Merritt, R. T. Cady and B. W. Mundy, *Acta Cryst.*, **7**, 473 (1954).

[16] M. E. Senko and D. H. Templeton, *Acta Cryst.*, **11**, 808 (1958).

[17] G. Klopman, "Chemical Reactivity and Reaction Paths", Wiley Intrescience, New York 1974.

[18] R. F. Hudson and G. Klopman, *Tetrahedron Letters*, **12**, 1103 (1967).

[19] G. Klopman and R. F. Hudson, *Theor. Chem. Acta*, **8**, 165 (1967).

[20] G. Klopman, *J. Amer. Chem. Soc.*, **90**, 223 (1968).

[21] K. Fukui, "Theory of Orientation and Stereoselection", Springer Verlag, Berlin, 1975.

[22] R. Huisgen, *Angew. Chem.*, **75**, 604 (1963).

[23] C. A. Henrick, E. Ritchie and W. C. Taylor, *Austral. J. Chem.*, **20**, 2441 (1967).

[24] Y. Kabayashy, T. Kutsumo and Y. Sekine, *Tetrahedron Letters*, **20**, 2441 (1967).

[25] N. S. Basketter and O. Plunkett, *Chem. Commun.*, **1971**, 1578.

[26] T. Sasaki, K. Kanematsu, Y. Yukimoto and S. Ochiai, *J. Org. Chem.*, **36**, 813 (1971).

[27] M. Petrovanu, A. Sauciuc, I. Gabe and I. Zugrăvescu, *Rev. Roumaine Chim.*, **14**, 1153 (1969).

[28] M.Petrovanu, C. Luchian, G. Surpăţeanu and V. Bărboiu, *Rev. Roumaine Chim.*, **24**, 1053 (1979).

[29] M. Petrovanu, C. Luchian, G. Surpăţeanu and V. Bărboiu, *Rev. Roumaine Chim.*, **24**, 733 (1979).

Revue Roumaine de Chimie, **28**, *8*, 841 – 848 (1983)

DÉRIVÉS DIPOLAIRES EN SÉRIE QUINAZOLINIQUES. III[1]

LA QUATERNISATION DE LA QUINAZOLINE AVEC LES BROMURES DE PHÉNACYLE

E. I. GEORGESCU[a], FLORENTINA GEORGESCU[a], F. CHIRALEU[b]
et MAGDA PETROVANU[c]

[a] Centre de Recherches, 1, str. Uzinei, Rîmnicu Vîlcea, Roumanie
[b] Centre de Chimie Organique, Bucarest, Roumanie
[c] Institut Polytechnique, Jassy, Roumanie

Reçu le 14 juin 1982

On a étudié la possibilité d'obtention des sels quaternaires de quinazolinium par la réaction de la quinazoline avec des bromures de phénacyle *p*-substitués. Les sels quaternaires, instables, ont été séparés comme méthanolates (4a-f) ; on a mis en évidence seulement le produit de quaternisation à N-3.

The possibility of the synthesis of the quinazolinium quaternary salts by the reaction of quinazoline with *p*-substituted phenacycle bromides has been investigated. The unstable quaternary salts have been separated as methanolates (4a-f) ; only the quaternisation product at N-3 has been evidenced.

Dans des travaux antérieurs [1,2] on a montré la possibilité d'obtention de quelques dérivés pyrrolo [1, 2—c] quinazoliniques par suite des réactions de cycloaddition [3+2] dipolaire de quelques quinazolinium-3-(p-R-benzoyl)-méthylures généres «in situ» sur des alcynes symétriques ou dissymétriques.

Dans le but d'obtenir des quinazolinium-ylures isolables on a essayé d'appliquer la « méthode du sel » qui consiste dans l'élimination d'acides halogénés à partir des sels de cycloimmonium. [3]

Pour l'obtention des sels quaternaires de quinazolinium on a utilisé, comme pour d'autres hétérocycles d'ailleurs [4], la réaction entre la quinazoline et les bromures de phénacyle *p*-substitués.

En effectuant la réaction de la quinazoline (**1**) avec les bromures de phénacyle (**2**) dans le benzène ou le chloroforme anhydre on a obtenu des produits jaunes claires à points de fusion indéterminés. Par recristallisation de ces produits dans le méthanole, on obtient des produits cristallisés, incolores à points de fusion définis. Les déterminations de structure ont montré que ces produits ne sont pas les sels attendus **3a-f** mais leurs méthanolats **4a-f**. Ces méthanolates **4** peuvent être obtenus facilement si on effectue la réaction de quaternisation de la quinazoline avec les bromures de phénacyle dans du méthanole à la température ambiante.

La formation des méthanolates des sels quaternaires de quinazolinium a été aussi observée dans le processus de quaternisation de la quinazoline avec les iodures de méthyle et d'éthyle.[5,6]

Dans le but d'établir la structure des sels on a parcouru plusieurs étapes. Ainsi, il a été nécessaire de préciser l'atome d'azote sur lequel a lieu la quaternisation.

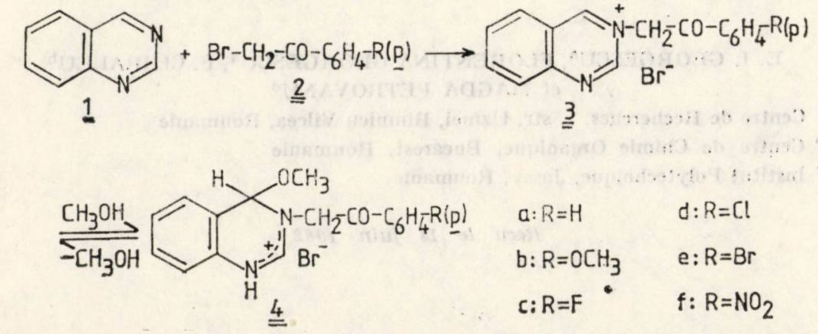

Les données de la littérature indiquent [7] l'obtention d'un mélange de iodure de 3-méthylequinazolinium et de 1-méthylequinazolinium dans la réaction de quaternisation de la quinazoline par l'iodure de méthyle dans un rapport molaire de 5 : 1, l'apparition des deux isomères a été mise en évidence par l'apparition de signaux dans les spectres ^{1}H-RMN du produit quaternisé.

Par contre, les spéctres ^{1}H-RMN des sels **4a-f** indiquent l'obtention d'un seul isomère. Il est connu que, en l'absence des empêchements stériques, la réaction de quaternisation se produit sur l'atome d'azote le plus basique. En ce qui concerne les basicités relatives des deux atomes d'azote de la quinazoline, on a établi [8] que l'atome d'azote N-3 est plus basique que l'atome d'azote N-1 ; donc il est logique que la quaternisation se produise préférentiellement sur l'atome d'azote N-3. Ceci explique le fait que dans la réaction de la quinazoline avec les bromures de phénacyle **2a-f** dans le méthanole on a supposé que la réaction de quaternisation a lieu au niveau de l'azote N-3. Cette supposition a été confirmée tant par les données chimiques, que spectrales.

Dans les spectres IR des bromures **4** les bandes d'absorption des groupements carbonyliques apparaissent entre 1694–1702 cm^{-1}, valeurs normales pour les groupements carbonyles dans les acétophénones substitués.

Dans le spectre ^{1}H-RMN du bromure **4a** dans le DMSO-d$_6$ les deux protons saturés équivalents du groupement CH$_2$ du phénacyle présentent un signal sous forme de singulet élargi à $\delta = 5{,}63$ ppm vers des champs un peu plus bas que les protons saturés à cause du voisinage du groupement benzoylique et de l'atome d'azote N-3. Surprenant est le fait que le signal des protons du groupement $-OCH_3$ en position 4 apparaît sous forme de deux singulets à $\delta = 3{,}0$ ppm et $\delta = 3{,}16$ ppm, le signal à $\delta = 3{,}16$ ppm ayant l'intensité la plus grande. Conformément à l'intégrale, les deux signaux représentent ensemble trois protons. Le signal du proton benzylique H-4 apparaît sous forme de deux singulets, l'un ayant une intensité plus grande à $\delta = 6{,}25$ ppm, et l'autre d'intensité plus faible à $\delta = 6{,}43$ ppm. Les deux signaux représentent conformément à l'intégrale un proton. Le fait que les signaux de ce proton n'apparaissent pas dans la région des protons aromatiques est un argument en faveur de la structure proposée pour le sel **4a**. Le signal du proton H-2 placé entre les deux atomes d'azote apparaît vers des champs plus bas sous forme de deux singulets à $\delta = 8{,}88$ ppm et $\delta = 9{,}08$ ppm qui, conformément à l'intégrale, représente un proton. Le signal à $\delta = 8{,}88$ ppm a une intensité plus grande. Le rapport des intensités des signaux doubles donnés par les protons du groupement OCH_3 en position 4 et les protons H-4 et H-2 est la même. Ce rapport varie en fonction du temps qui s'écoule entre le moment ou l'on trace le spectre et celui de la dissolution de l'épreuve et de la température à laquelle on travaille. Si on fait la solution à la température ambiante et on trace immédiatement le spectre la différence entre les intensités des signaux doubles est tres petite. Après un certain temps, ou après le chauffage de la solution le rapport entre les intensités des signaux doubles augmente beaucoup en faveur des signaux à $\delta = 3{,}16$ ppm, $\delta = 6{,}25$ ppm, respectivement $\delta = 8{,}88$ ppm.

Si on ajoute du D_2O à la solution du bromure **4a** dans le DMSO-d_6 les protons du groupement OCH_3 en position 4 ainsi que les protons H-4 et H-2 présentent dans le spectre ^{1}H-RMN un seul signal sous forme de singulet. Les spectres ^{1}H-RMN des autres bromures **4b-f** sont analogues au spectre décrit (tabl. 1). Le comportement des bromures **4b-f** dans le DMSO-d_6 est parfaitement analogue à celui du bromure **4a**.

Tableau 1

Les spectres ^{1}H-RMN des bromures **4a-f** dans le DMSO-d_6 (δ, ppm)*

nº	Produit R	OCH_3(4)	$-CH_2-$	H−4	Des protons aromatiques	H−2	OCH_3 du phénacyle
4a	H	3,10 s 3,16 s	5,63 s.é.	6,25 s 6,43 s	7,41−7,91 m 8,15−8,32 m	8,88 s 9,08 s	–
4b	OCH_3	2,98 s 3,15 s	5,47 s.é	6,13 s 6,43 s	7,07 d 7,31−7,65 m 8,02 d	8,70 s 8,89 s	3,87 s
4c	F	3,01 s 3,16 s	5,54 s.é	6,15 s 6,35 s	7,25−7,70 m 7,95−8,30 m	8,71 s 8,90 s	–
4d	Cl	3,0 s 3,15 s	5,53 s.é	6,16 s 6,33 s	7,28−8,85 m 8,08 d	8,73 s 8,90 s	–
4e	Br	3,0 s 3,15 s	5,50 s.é	6,13 s 6,33 s	7,35−7,60 m 7,83−8,03 m	8,66 s 8,84 s	–
4f	NO_2	3,04 s 3,16 s	5,65 s.é	6,23 s 6,40 s	7,33−7,65 m 8,39 m	8,78 s 8,96 s	–

* s = singulet, s.é. = singulet élargi ; m = multiplet ; d = doublet.

Comme on l'a constaté, dans le cas du cation de quinazolinium aussi [9], en solution il existe un équilibre entre les bromures **3** et les méthanolates **4**, équilibre qui dépend de l'acidité du milieu. En milieu fortement acide l'équilibre est déplacé en faveur des sels **3**, tandis qu'en milieu acide faible ou neutre les produits d'addition du type **4** sont favorisés.

L'existence de cet équilibre peut expliquer le comportement des bromures **4a-f** dans le DMSO-d_6. Ainsi, il est possible que le DMSO-d_6 se lie en position 4 des bromures **3a-f** formant des produits du type **5a-f** et mettant en liberté le méthanole. Dans ce cas, les signaux des spectres ^{1}H-RMN des méthanolates **4a-f** d'intensité plus faible à $\delta = 3,0$ ppm, $\delta = 6,43$ ppm et $\delta = 9,08$ ppm sont donnés par les protons du groupement OCH_3 en position 4 et par les protons H-4 et H-2 du produit **4a**. Les signaux qui ont une intensité plus grande à $\delta = 7,25$ ppm et $\delta = 8,88$ppm correspondent aux protons H-4 et H-2 appartenant au produit **5a**.

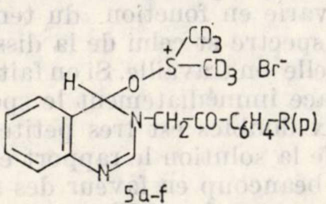

5a-f

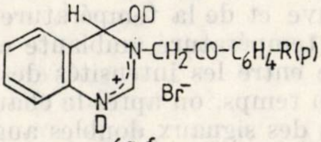

6a-f

Le signal sous forme de singulet à $\delta = 3,16$ ppm a été attribué au méthanole libre.

Lorsque l'on ajoute du D_2O à la solution des bromures **4a** dans le DMSO-d_6 il se forme l'hydrate **6a** beaucoup plus stable en solution en comparaison des produits **5**.

Les spectres ^{1}H-RMN des bromures de 3-(*p*-R-phénacyle)- 4-méthoxy-3,4-dihydroquinazolinium **4a-f** dans l'acide trifluoroacétique représente un argument en faveur de ce comportement. En solutions acides l'équilibre **3** $\underset{-CH_3OH}{\overset{CH_3OH}{\rightleftarrows}}$ **4** est déplacé en faveur des produits **3** ce qui a comme conséquence le fait que les spectres ^{1}H-RMN des méthanolates **4** dans l'acide trifluoroacétique sont en réalité les spectres des produits **3** ayant en plus un signal correspondant au groupement CH_3 du méthanole libre (tab. 2).

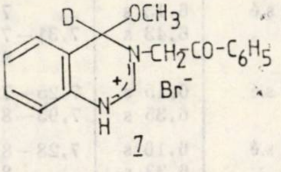

7

Dans ce cas les signaux des protons H-4 n'apparaissent plus dans la région des protons benzyliques mais à des champs beaucoup plus bas. Pour l'attribution des signaux des protons H-2 et H-4 on a synthétisé le produit deutérié **7** par la réaction de la 4-deutério-quinazoline avec le bromure de phénacyle. Le spectre ^{1}H-RMN de ce produit dans l'acide

Tableau 2

Les spectres ^1H-RMN des bromures **4a-f** dans l'acide trifluoroacétique (δ, ppm)*

Produit n°	Produit R	$-CH_2$	Des protons aromatiques	H−2	H−4	$-OCH_3$ du phénacyle	$-CH_3$ du méthanole
4a	H	6,55 s	7,56−7,89 m 8,04−8,56 m	9,46 s	9,77 s	—	4,05 s
4b	OCH_3	6,55 s	7,22 d 8,08−8,63 m	9,53 s	9,81 s	4,10 s	4,06 s
4c	F	6,56 s	7,16−7,53 m 8,11−8,61 m	9,51 s	9,83 s	—	4,06 s
4d	Cl	6,56 s	7,48−7,80 m 7,95−8,62 m	9,50 s	9,78 s	—	4,08 s
4e	Br	6,51 s	7,65−8,61 m	9,48 s	9,75 s	—	4,06 s
4f	NO_2	6,67 s	8,45 m	9,55 s	9,86 s	—	4,08 s

* s = singulet ; m = multiplet.

trifluoroacétique ne présente pas de signal à $\delta = 9,67$ ppm. Ainsi, les signaux sous forme de singulets qui se trouvent à des champs plus bas (valeurs δ comprises entre 9,67 — 9,98 ppm) ont été attribués aux protons H-4, et les signaux sous forme de singulets moins désécrannés (valeurs δ comprises entre 9,43 — 9,58 ppm) ont été attribués aux protons H-2.

Le fait que le réaction de quaternisation a lieu à l'atome d'azote N-3 à été confirmé par des réactions chimiques. Ainsi, par l'oxydation des méthanolates **4a-f** avec l'eau oxygénée en milieu d'acide sulphurique 2N, on a obtenu les 3-(*p*-R-phénacyle)-quinazoline—4(3H)-ones **8a-f**. Il faut mentionner le fait que les produits de structure **8a** et **8e** sont cités dans la littérature,[10] mais en ce qui concerne les données spectrales ^1H-RMN c'est nous qui les avons mis en évidence pour la première fois.

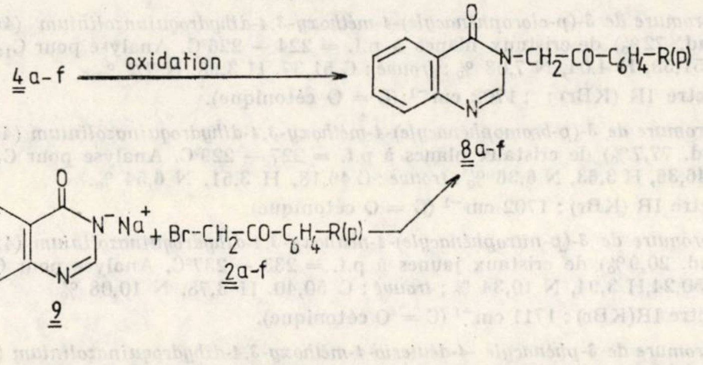

Les produits **8a-f** ont été obtenus aussi dans la réaction du sel de soude de la 4-hydroxyquinazolone (**9**) avec les bromures de phénacycle **2a-f**, méthode indiquée dans la littérature.[10]

Les produits **8a-f** obtenus par les deux méthodes différentes présentent des points de fusion, spectres IR et ^1H-RMN identiques.

Donc, dans la réaction de quaternisation de la quinazoline avec les bromures de phénacyle **2a-f** dans le méthanol, à la place des bromures de 3-(*p*-R-phénacyle)-quinazolinium **3a-f** attendus, on obtient leur méthanolates **4a-f**. Les essais d'obtention des sels **3a-f** à l'état pur ont échoué à cause de la facilité avec laquelle ceux-ci réagissent avec divers agents nucléophyles. Les méthanolates **4a-f** sont stabilisés par une forte résonance de type amidinique.

PARTIE EXPÉRIMENTALE

Le 2-bromo-4'-fluoroacétophénone (**2c**) et le 2-bromo-4'-chloroacetophénone (**2d**) ont été obtenus par la bromuration des acétophénones *p*-substitués respectif, d'après un procédé décrit dans la littérature[11]. La 4-déutérioquinazoline a été obtenue d'après le procédé décrit par Armarego.[12]

Les points de fusion ne sont pas corrigés.

Les spectres IR ont été enregistrés sur un spectrophotomètre Perkin Elmer 621 et les spectres ^{1}H–RMN ont été enregistrés sur un spectromètre Varian A, 60A, avec le TMS comme référence interne.

L'obtention des bromures de 3-(p-R-phénacyle)-4-méthoxy-3,4-dihydroquinazolinium (**4a-f**). A une solution de 1,3 g (10 mmoles) de quinazoline dans 50 ml de méthanol on ajoute 10 moles de bromure de phénacyle *p*-substitué. On agite 5 jours à la température ambiante et on évapore sous vide la moitié du solvant. Le précipité formé est filtré et recristallisé dans du méthanol.

Le bromure de 3-phénacyle-4-méthoxy-3,4-dihydroquinazolinium (**4a**). On obtient 2,92 g de cristaux blancs (rend. 80,9 %) à p.f.= 151 – 153°C. Analyse pour $C_{17}H_{17}N_2O_2Br$: *calculé* : C 56,5, H 4,70, N 7,75 % ; *trouvé* : C 56,75, H 4,82, N 7,60 %.

Spectre IR (KBr) : 1701 (C = O cétonique).

Le bromure de 3-(p-méthoxyphénacyle)-4-méthoxy-3,4-dihydroquinazolinium (**4b**). On obtient 2,78 g de cristaux blancs (rend. 71 %) à p.f. = 176 – 178°C. *Analyse pour* $C_{18}H_{19}N_2O_3Br$: *calculé* : C 55,24, H 4,86, N 7,16 % ; *trouvé* : C 55,15, H 4,35, N 6,97 %.

Spectre IR(KBr) : 1694 cm^{-1} (C = O cétonique).

Le bromure de 3-(p-fluorophénacyle)-4-méthoxy-3,4-dihydroquinazolinium (**4c**). On obtient 2,57 g (rend. 67,8 %) de cristaux blancs à p.f.= 173– 175°C. Analyse pour $C_{17}H_{16}N_2O_2FBr$: *calculé* : C 53,82, H 4,22, N 7,38 % ; *trouvé* : C 53,25, H 4,31, N 7,10 %.

Spectre IR(KBr) : 1701 cm^{-1} (C = O cétonique).

Le bromure de 3-(p-clorophénacyle)-4-méthoxy-3,4-dihydroquinazolinium (**4d**). On obtient 2,85 g (rend. 72 %) de cristaux blancs à p.f. = 224 – 226°C. Analyse pour $C_{17}H_{16}N_2O_2BrCl$: *calculé* : C 51,58, H 4,04, N 7,08 % ; *trouvé* : C 51,37, H 3,98, N 7,2 %.

Spectre IR (KBr) : : 1702 cm^{-1} (C = O cétonique).

Le bromure de 3-(p-bromophénacyle)-4-méthoxy-3,4-dihydroquinazolinium (**4e**). On obtient 3,42 g (rend. 77,7 %) de cristaux blancs à p.f. = 227 – 229°C. Analyse pour $C_{17}H_{16}N_2O_2Br_2$: *calculé* : C 46,36, H 3,63, N 6,36 % ; *trouve* : C 46,18, H 3,51, N 6,54 %.

Spectre IR (KBr) : 1702 cm^{-1} (C = O cétonique).

Le bromure de 3-(p-nitrophénacyle)-4-méthoxy-3,4-dihydroquinazolinium (**4f**). On obtient 0,85 g (rend. 20,9 %) de cristaux jaunes à p.f. = 235 – 237°C. Analyse pour $C_{17}H_{16}N_3O_4Br$: *calculé* : C 50,24,H 3,94, N 10,34 % ; *trouvé* : C 50,40. H 3,78, N 10,08 %.

Spectre IR(KBr) : 1711 cm^{-1} (C = O cétonique).

Le bromure de 3-phénacyle -4-déuterio-4-méthoxy-3,4-dihydroquinazolinium (**7**). On obtient 2,42 g (rend. 67 %) de cristaux blancs à p.f. = 150 – 152°C. Analyse pour $C_{17}H_{16}DN_2O_2Br$: *calculé* : C 56,35, (H + D) 4,97, N 7,73 % ; *trouvé* : C 56,12, (H + D) 4,60, N 7,62 %.

Spectre IR(KBr) : 1701 cm^{-1} (C = O cétonique).

Spectre ^{1}H–RMN(CF_3COOH, δ, ppm) : 4,03 (s, 3H, le groupement CH_3 dans du CH_3OH), 6,51 (s, 2H, le groupement CH_2 du phénacyle), 7,41 – 7,84 (m, 3H, les protons aromatiques), 8,01 – 8,55 (m, 6H, les protons aromatiques), 9,43 (s, 1H, H–2).

L'obtention des 3-(p-R-phénacyle)-quinazolin-4-ones (**8a-f**). A une solution el 1,46 g (10 mmoles) 4-hydroxyquinazoline dans 10 ml méthanol on ajoute 3 ml de solution de méthoxyde de sodium dans le méthanol (1 mol = 300 ml) et on chauffe un peu le mélange pour la complète dissolution. On ajoute 10 mmoles de bromure de phénacyle *p*-substitué **2a-f**, on porte le mélange à reflux pendant 30 minutes et on laisse pendant la nuit à la température ambiante. On filtre le précipité, on le lave sur le filtre avec du méthanol, avec de l'eau et encore à méthanol. On le recristallise dans du méthanol.

3-Phénacylequinazolin-4-one (**8a**). On obtient 2,02 g de cristaux blancs à p.f. = 155 — — 156°C (lit. [10] 149 — 152°C). Rend. 76,5% Analyse pour $C_{16}H_{12}N_2O_2$: *calculé* : C 72,73, H 4,54, N 10,6%; *trouvé* : C 72,58, H 4,42, N 10,68%.

Spectre IR(KBr) : 1705 cm^{-1} (C = O du groupement phénacyle), 1665 cm^{-1} (C = O du cycle).

Spectre ^1H—RMN (DMSO-d_6, δ, ppm) : 5,70 (s, 2H, le groupement CH_2 du phénacyle), 7,45 — 8,33 (m, 9H, les protons aromatiques), 8,45 (s, 1H, H-2).

3-(p-Méthoxyphénacyle)quinazolin-4-one (**8b**). On obtient 2,1 g (rend. 71,4 %) de cristaux blancs à p.f. = 183 — 184,5°C. Analyse pour $C_{17}H_{14}N_2O_3$: *calculé* : C 69,39, H 4,76, N 9,52 %; *trouvé* : C 69,25, H 4,54, N 9,30 %.

Spectre IR (KBr) : 1690 cm^{-1} (C = O du groupement phénacyle), 1660 cm^{-1} (C = O du cycle).

Spectre ^1H—RMN (DMSO-d_6, δ, ppm) : 3,92 (s, 3H, le groupement OCH_3 du phénacyle), 5,66 (s, 2H, le groupement CH_2 du phénacyle), 7,20 (d, 2H, les protons phénylique en ortho près du groupement OCH_3, $J = 9$ Hz), 7,58 — 7,93 (m, 3H, les protons aromatiques), 8,05 — 8,32 (m, 3H, les protons aromatiques), 8,45 (s, 1 H, H-2).

3-(p-Fluorophénacyle)quinazolin-4-one (**8c**). On obtient 1,95 g (rend. 69,1 %) de cristaux blancs à p.f. = 214 — 215°C. Analyse pour $C_{16}H_{11}N_2O_2F$: *calculé* : C % 68,08, H % 3,9, N % 9,93 : *trouvé* : C % 67,81, H % 3,75, N % 9,82.

Spectre IR(KBr) : 1695 cm^{-1} (C = O du groupement phénacyle) 1654 cm^{-1} (C = O du cycle).

Spectre ^1H—RMN (DMSO-d_6, δ, ppm) : 5,65 (s, 2H, le groupement CH_2 du phénacyle), 7,21 — 8,30 (m, 8H, les protons aromatiques), 8,35 (s, 1H, H-2).

3-(p-Chlorophénacyle) quinazolin-4-one (**8d**). On obtient 1,82 g (rend. 60,97%) de cristaux blancs à p.f. = 216 — 217°C. Analyse pour $C_{16}H_{11}N_2O_2Cl$: *calculé* : C 64,32, H 3,68, N 9,38% ; trouvé : C 64,53, H 3,51, N 9,18 %.

Spectre IR (KBr) : 1692 cm^{-1} (C = O du groupement phénacyle) ; 1658 cm^{-1} (C = O du cycle).

Spectre ^1H—RMN (DMSO-d_6, δ, ppm) : 5,65 (s, 2H, le groupement du phénacyle), 7,50 — 8,30 (m, 8H, les protons aromatiques), 8,35 (s, 1 H, H-2).

3-(p-Bromophénacyle)quinazolin-4-one (**8e**). On obtient 2,10 g (rend. 61,3%) de cristaux blancs à p.f. = 210 — 211°C (lit.[10] 209 — 211°C). Analyse pour $C_{16}H_{11}N_2O_2Br$: *calculé* : C 55,97, H 3,21, N 8,16 %; *trouvé* : C 56,03, H 3,16 ; N 8,25 %.

Spectre IR(KBr) : 1698 cm^{-1} (C = O du groupement phénacyle) ; 1658 cm^{-1} (C = O du cycle).

Spéctre ^1H—RMN (DMSO-d_6, δ, ppm) : 5,70 (s, 2H, le groupement CH_2 du phénacycle), 7,56 — 8,35 (m, 8H, les protons aromatiques), 8,40 (s, 1 H, H-2).

3-(p-Nitrophénacyle) quinazolin-4-one (**8f**). On obtient 0,97 g (rend. 31,4%) de cristaux jaunes à p.f. = 227 — 228°C. Analyse pour $C_{16}H_{11}N_3O_4$: *calculé* : C 62,13, H 3,56, N 13,59 %; *trouvé* : C 61,95, H 3,39, N 13,42 %.

Spectre IR (KBr) : 1709 cm^{-1} (C = O du groupement phénacyle) 1665 cm^{-1} (C = O du cycle), 1520 cm^{-1} (NO_2 asymétrique), 1345 cm^{-1} (NO_2 symétrique).

Spectre ^1H—RMN (DMSO-d_6, δ, ppm) : 5,75 (s, 2H, le groupement CH_2 du phénacyle), 7,41 — 8,31 (m, 4H, les protons aromatiques du cycle quinazolinique), 8,38 (s, 4H, les protons aromatiques du cycle phénylique du groupement phénacyle), 8,43 (s, 1 H, H—2).

L'oxydation des bromures de 3-(p-R-phénacyle)-4-méthoxy-3,4-dihydroquinazolinium (**4a-f**). On ajoute à 10 mmoles de bromure de 3-(*p*-R-phénacyle)-4-méthoxy-3,4-dihydroquinazolinium dans 25 ml d'acide sulfurique 2N, 2 ml H_2O_2 30%, on agite pendant 1 h et on laisse un jour à la température ambiante. On apporte le mélange à pH 10 à l'aide de NaOH 2N et puis avec acide acétique à pH 4. On extrait à chloroforme, les extrais se dessèchent sur Na_2SO_4 anhydre et la solution est concentrée sous vide. On précipite à l'éther éthylique, on filtre les précipités et on les recristallise dans du méthanol.

Les produits obtenus ont les points de fusion, les spectres IR et ^1H-RMN identiques à ceux des produits **8a-f** obtenus par la réaction du sel de sodium de la 4-hydroxyquinazoline avec les bromures de phénacyle **2a-f**.

RÉFÉRENCES

[1] Deuxième partie : E. I. Georgescu, I. Druţă et M. Petrovanu, *Bulet. Inst. Politehnic Iaşi* (sous presse).

[2] E. I. Georgescu, I. Druţă et M. Petrovanu, *Rev. Roumaine Chim.*, **26**, 109 (1981).

[3] F. Kröhnke, *Chem. Ber.*, **68**, 1177 (1935).

[4] I. Zugrăvescu et M. Petrovanu, « Chimia N-ilidelor », Ed. Academiei, Bucureşti, 1974.

[5] S. Gabriel et J. Colman, *Chem. Ber.*, **37**, 3643 (1904).

[6] C. Schopf et F. Oechler, *Liebigs Ann. Chem.*, **523**, 1 (1936).

[7] J. W. Bunting et W. G. Meathrel, *Canad. J. Chem.*, **48**, 3449 (1970).

[8] D. D. Perrin, *J. Chem. Soc.*, **1965**, 5590.

[9] W. L. F. Armarego, *J. Chem. Soc.*, **1962**, 561.

[10] R. S. Sinyak, I. A. Mazur et P. M. Kochergin, *Khim. farm. Zhur.*, **10**, 67 (1976).

[11] R. M. Cowper et L. H. Davidson, *Organic Syntheses*., **Coll. Vol. II**, 480 (1943).

[12] W. L. F. Armarego et J. I. C. Smith, *J. Chem. Soc.* (*B*), **1967**, 449.

Revue Roumaine de Chimie, 28, 8, 849 – 855 (1983)

SYNTHESIS AND REACTIONS OF SOME 2-ARYL-4-ARYLIDENE-5(4)-OXAZOLONES

A.A. AFIFI, M. A. EL HASHASH and S.S. EL KADY
Chemistry Department, Faculty of Science, Ain Shams University,
Cairo, Egypt

Received July 4, 1981

2-Aryl-4-arylidene-5(4)-oxazolones 1 reacted with amines in ethanol to give α-arylcarboxamido-β-arylacrylamides 2 and 3 and in acetic acid to give α-4-arylidene imidazolinones 4. Compounds 1 reacted also with hydrazines in ethanol to give the hydrazides 5 while with phenylhydrazine in acetic acid they give the 1 : 2 : 4-triazines 6. The imidazolones 7 resulting from the reaction of 1 with hydroxylamine hydrochloride were converted to the triazines 6. Azidolysis of 1 gave α-[tetrazolyl-(1)]-5-arylacrylic acids 8.

It was previously reported that the reaction of 4-arylidene-2-aryl-5(4)-oxazolones with compounds like $R-NH_2$, $R-NH-NH_2$, etc. takes place by attack at C_5 with concomittant ring opening of the oxazolone ring.[1–4].

In continuation of the previous work,[1,2] some new 2-aryl-4-arylidene-5(4)-oxazolones **1** were prepared according to Erlenmeyer procedure [5] by condensation of the respective aromatic aldehyde with the required aroylglycine in acetic anhydride in the presence of sodium acetate. The infrared spectra of compounds **1** showed strong absorption bands in the region 1800 – 1820 cm^{-1} corresopnding to $\nu_{C=O}$ of azlactone nucleus. The NMR spectrum of compounds **1i** shows the following signals: δ3.2 ppm (s) for *6H* N $(CH_3)_2$, 6.8(s) corresponding to olefinic proton and 7(s), 7.6 (m) and 8.2(m) corresponding to aromatic protons

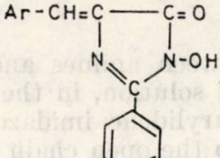

1

Ar	R	Ar	R
a, C_6H_5	Cl	**f,** $C_6H_4NO_2(m)$	CH_3
b, $C_6H_4Cl(o)$	CH_3	**g,** $C_6H_4NO_2(p)$	Cl
c, $C_6H_4Cl(m)$	Cl	**h,** $C_6H_4N(CH_3)_2(p)$	NO_2
d, $C_6H_4Cl(p)$	CH_3	**i,** $C_6H_4N(CH_3)_2(p)$	Cl
e, $C_6H_4Br(0)$	NO_2		

The 4-arylidene-2-aryl-5(4)-oxazolones **1a**, **1c**, **1f** and **1g** reacted readily with various amines in ethanol solution to give the corresponding α-arylcarboxamido-β-arylacrylamides **2** and **3**.[1] The structure of these compounds was supported by elemental analysis and by IR measurements which showed two amide carbonyl bands in the region 1660 – 1650 cm^{-1}, and 1640 – 1630 cm^{-1}, respectively, and two NH bands at 3 380 – 3 320 cm^{-1}.

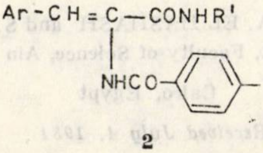

2

Ar	R	R′	Ar	R	R′
a, C_6H_5	Cl	$(CH_2)_3CH_3$	g, $C_6H_4NO_2(m)$	CH_3	C_6H_{11}
b, C_6H_5	Cl	C_6H_{11}	h, $C_6H_4NO_2(m)$	CH_3	$C_6H_3(CH_3)_2(3,4)$
c, C_6H_5	Cl	$CH_2C_6H_5$	i, $C_6H_4NO_2(m)$	CH_3	$C_6H_3(CH_3)Cl(2,5)$
d, $C_6H_4Cl(m)$	Cl	$(CH_2)_3CH_3$	j, $C_6H_4NO_2(m)$	CH_3	$C_6H_4NH_2(o)$
e, $C_6H_4Cl(m)$	Cl	C_6H_{11}	k, $C_6H_4NO_2(m)$	CH_3	$C_6H_4NH_2(p)$
f, $C_6H_4Cl(m)$	Cl	$CH_2C_6H_5$	l, $C_6H_4NO_2(p)$	Cl	$C_6H_4NH_2(o)$
			m, $C_6H_4NO_2(p)$	Cl	$C_6H_4NH_2(p)$

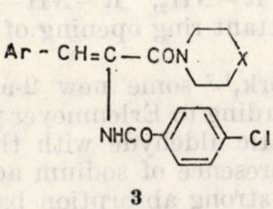

3

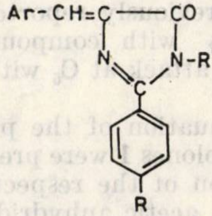

4

Ar	X	Ar	R	R′
a, C_6H_5	CH_2	a, $C_6H_4NO_2(p)$	Cl	$C_6H_4CH_3(p)$
b, C_6H_5	O	b, $C_6H_4NO_2(p)$	H	$C_6H_4CH_3(p)$
c, $C_6H_4Cl(m)$	CH_2			
d, $C_6H_4Cl(m)$	O			
e, $C_6H_4N(CH_3)_2(p)$	O			

When the reaction between amines and 4-arylidene-oxazolones **1** was carried out in acetic acid solution, in the presence of fused sodium acetate, the corresponding 4-arylidene imidazolionones **4** were obtained.[6] It seems that **1** passes first to the open chain structure **2** which recycles to the imidazolinone **4**. This mechanism was verified when some of the open-chain arylacrylamides **2** were heated in acetic acid in the presence of sodium acetate to give the corresponding imidazolinones **4**.

The structure of the imidazolinones **4** was established by elemental analysis and by the fact that they gave no colouration with ferric chloride solution, in contrast to the parent compounds **2**. The structures were also supported by IR measurements which showed stretching frequencies at 1685 cm^{-1} and 1640 cm^{-1} characteristic for $-CONR'-$ and $-C{=}N-$ respectively.

Compounds **1** react with hydrazines in ethanol solution to give the normal hydrazides **5**.[1] The IR spectra of **5** showed $\nu_{C=O}$ of the hydrazide in the region 1680 – 1690 cm^{-1} and a broad ν_{NH} band at 3200 cm^{-1}.

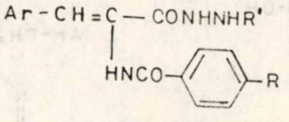

5

Ar	R	R′	Ar	R	R′
a, C_6H_5	Cl	H	e, C_6H_5	Cl	C_6H_5
b, $C_6H_4Cl(m)$	Cl	H	f, $C_6H_4Cl(m)$	Cl	C_6H_5
c, $C_6H_4Br(o)$	NO_2	H	g, $C_6H_4NO_2(m)$	CH_3	C_6H_5
d, $C_6H_4(CH_3)_2(p)$	Cl	H	h, $C_6H_4N(CH_3)_2(p)$	NO_2	C_6H_5

All trials [7] of cyclisation of the hydrazides (**5**, R = H) in the presence of acetic acid and sodium acetate to the corssponding 1 : 2 : 4-triazine derivatives were unsuccessful. It seemed that decomposition took place as indicated by rapid evolution of nitrogen (frothing). The phenylhydrazides **5e** and **5f** were readily cyclised, however, under the above conditions to give the corresponding triazines **6a** and **6b** respectively.[6]

Interaction of oxazolones **1a** and **1c** with phenyl-hydrazine in acetic acid solution and in the presence of sodium acetate gave directly the required 1 : 2 : 4-triatines **6**.

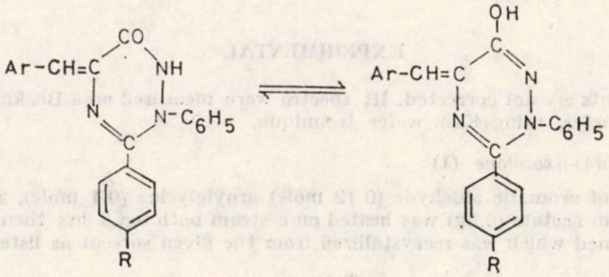

6

Ar	R
a, C_6H_5	Cl
b, $C_6H_4Cl(m)$	Cl

The structure of the triazines **6** was based on analytical data and on IR measurements which showed stretching frequencies at 1650 cm^{-1}, 3280 and 3350 cm^{-1} characteristic for —CONH—, OH and NH— groups respectively. These bands illustrate that compounds **6** exist actually in lactam-lactim tautomeric equilibrium.

The oxazolones **1a, 1c, 1e**, and **1h** reacted with hydroxylamine hydrochloride in pyridine to give 4-arylidene-1-hydroxy-2-aryl-5-imidazolones **7**.[3] Compounds **7** showed in the infrared $\nu_{C=O}$ in the region 1680 – 1 700 cm^{-1}, $\nu_{C=N}$ at 1630 cm^{-1} and ν_{OH} in the region 3 350 – 3 400 cm^{-1}.

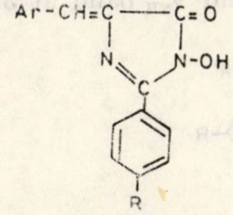

7

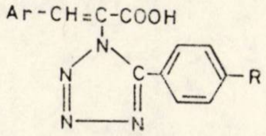

8

Ar	R	Ar	R
a, C_6H_5	Cl	a, C_6H_5	Cl
b, $C_6H_4Cl(m)$	Cl	b, $C_6H_4Cl(m)$	Cl
c, $C_6H_4Br(o)$	NO_2	c, $C_6H_4Br(o)$	NO_2
d, $C_6H_4N(CH_3)_2(p)$	NO_2	d, $C_6H_4N(CH_3)_2(p)$	NO_2

Compounds **7a** and **7b** reacted with phenylhydrazine in ethanol or acetic acid to give the triazines **6**.[3]

4-Arylidene-2-aryl-2-aryl-5(4)-oxazolones **1** reacted with sodium azide in acetic acid to give α-[terazolyl-(1)]—5-aryl cinnamic acid derivative [1] **8**. The IR spectra of **8** showed ν_{OH} stretching frequency in the region 3 300 – 3 350 cm^{-1} (broad), $\nu_{C=O}$ at 1710 cm^{-1} and $\nu_{\text{tetrazolyl ring}}$ at 1 100 – 900 cm^{-1}.

Thus azidolysis of **1** involves opening of C_2—O bond contrary to the normal ring opening of the 5(4)-oxazolone ring (fission of C_5—O bond) in the reaction with all other compounds (viz. RNH_2, $RNH-NH_2$, etc.).

EXPERIMENTAL

Melting points are not corrected. IR spectra were measured on a Beckman IR-20 infrared spectrophotometer, using KBr wafer technique.

2-aryl-4-arylidene-5(4)-oxazolone (1) :

A mixture of aromatic aldehyde (0.12 mole) aroylglycine (0.1 mole), acetic anhydride (20 ml), and sodium acetate (0.5g) was heated on a steam bath for 3 hrs then cooled. A solid product was obtained which was recrystallized from the given solvent as listed in Table 1.

Table 1

Oxazolones 1

Comp	m.p. (°C)	Solvent	Formula	Analysis % Found C	H	N	Required C	H	N
1a	180	Benzene	$C_{16}H_{10}O_2NCl$	67.53	3.30	4.52	67.72	3.52	4.93
1b	160	Benzene	$C_{17}H_{12}O_2NCl$	68.15	4.01	4.51	68.57	4.03	4.70
1c	188	Benzene	$C_{16}H_9O_2NCl_2$	60.03	2.75	4.82	60.37	2.83	4.40
1d	172	Benzene	$C_{17}H_{12}O_2NCl$	68.75	4.22	4.95	68.57	4.03	4.70
1e	225	Benzene	$C_{16}H_9O_4N_2Br$	51.21	2.31	7.12	51.48	2.41	7.50
1f	180	Ethanol	$C_{17}H_{12}O_4N_2$	66.63	3.59	9.38	66.23	3.89	9.09
1g	80	Benzene	$C_{16}H_9O_4N_2Cl$	58.34	2.91	8.74	58.44	2.73	8.52
1h	218	Toluene	$C_{18}H_{15}O_4N_3$	64.38	4.15	12.12	64.09	4.45	12.46
1i	196	Toluene	$C_{18}H_{15}O_2N_2Cl$	66.51	4.34	8.87	66.15	4.59	8.57

Reaction of oxazolones **1** *with amines*

a) *Formation of α-Arylocarboxamido-β-Arylacrylamides*

A solution of **1** (0.01 mole) and the requisite amine (0.01 mole) in ethanol (60 ml) was heated under reflux for 30 min and cooled. The solid products obtained after acidification with dilute hydrochloric acid were filtered and recrystallized from suitable solvent as listed in Table 2.

Table 2

α-Arylcarboxamido-β-arylacrylamides **2** and **3**

Compound	m.p. (°C)	Solvent	Formula	Analysis					
				Found			Required		
				C	H	N	C	H	N
2a	150	Ethanol	$C_{20}H_{21}O_2N_2Cl$	67.11	5.59	7.74	67.32	5.89	7.85
2b	210	Ethanol	$C_{22}H_{23}O_2N_2Cl$	69.24	6.21	7.61	69.01	6.01	7.32
2c	155	Ethanol	$C_{23}H_{19}O_2N_2Cl$	70.92	4.59	7.29	70.67	4.86	7.17
2d	200	Pet. Ether	$C_{20}H_{20}O_2N_2Cl_2$	61.21	5.32	7.56	61.38	5.11	7.16
2e	218	Benzene	$C_{22}H_{22}O_2N_2Cl_2$	63.61	5.21	6.42	63.30	5.27	6.71
2f	170	Benzene	$C_{23}H_{18}O_2N_2Cl_2$	64.73	4.54	6.53	64.94	4.23	6.58
2g	130	Benzene	$C_{23}H_{25}O_4N_3$	67.52	6.23	10.01	67.81	6.14	10.31
2h	220	Ethanol	$C_{25}H_{23}O_4N_3$	69.71	5.21	9.51	69.93	5.36	9.79
2i	136	Benzene	$C_{24}H_{20}O_4N_3Cl$	64.31	4.65	9.11	64.07	4.45	9.34
2j	230	Benzene	$C_{23}H_{20}O_4N_4$	66.59	4.58	13.66	66.35	4.81	13.46
2k	202	Benzene	$C_{23}H_{20}O_4N_4$	66.01	4.58	13.01	66.35	4.81	13.46
2l	290	Acetic acid	$C_{22}H_{17}O_4N_4Cl$	60.12	3.67	12.31	60.48	3.89	12.83
2m	256	Acetic acid	$C_{22}H_{17}O_4N_4Cl$	60.72	3.63	12.32	60.48	3.89	12.83
3a	218	Ethanol	$C_{21}H_{21}O_2N_2Cl$	68.83	5.49	7.02	68.39	5.69	7.59
3b	205	Pet. Ether	$C_{20}H_{19}O_3N_2Cl$	64.51	5.33	7.05	64.77	5.13	7.55
3c	175	Pet. Ether	$C_{21}H_{20}O_2N_2Cl_2$	62.02	4.76	6.72	62.53	4.96	6.95
3d	199	Benzene	$C_{20}H_{18}O_3N_2Cl_2$	59.01	4.24	6.52	59.25	4.44	6.91
3e	235	Benzene	$C_{22}H_{24}O_3N_3Cl$	63.44	5.72	10.63	63.84	5.80	10.16

b) *Formation of* 1 : 2-*diaryl*-4-*arylidene* 2-*imidazolin*-5-*ones*

i) A mixture of oxazolone **1** (0.01 mole), p-toluidine (0.01 mole) and fused sodium acetate (0.3 g) in acetic acid (80 ml) was heated under reflux for one hour. Dilution with water gave the product **4** which was collected and crystallized from ethanol (Table 3).

Table 3

4-Arylidene imidazolinones **4**

Comp.	m.p. (°C)	Formula	Analysis					
			Found			Required		
			C	H	N	C	H	N
4a	120	$C_{23}H_{16}N_3O_3Cl$	66.51	3.62	9.83	66.11	3.83	10.05
4b	145	$C_{23}H_{17}N_3O_3$	72.66	4.44	10.96	71.85	4.32	10.26

Reaction of oxazolones **1** *with hydrazines*

a) *Formation of hydrazides* **5**

A solution of **1** (0.1 mole) and hydrazine hydrate, or phenylhydrazine (0.1 mole) in ethanol (60 ml) was heated under reflux for 1 hr. Acidification with cold dilute hydrochloric acid (pH 5) gave the hydrazides **5** which were collected and crystallized (Table 4).

Table 4

Hydrazides 5

Comp.	m.p.	Solvent	Formula	Analysis Found C	H	N	Requires C	H	N
5a	210	Ethanol	$C_{16}H_{14}O_2N_3Cl$	60.45	4.30	13.00	60.85	4.43	13.31
5b	190	Ethanol	$C_{16}H_{13}O_2N_3Cl_2$	54.72	3.61	12.20	54.85	3.71	12.0
5c	228	Ethanol	$C_{16}H_{13}O_4N_4Br$	47.71	3.22	13.62	47.41	3.21	13.83
5d	202	Benzene	$C_{18}H_{19}O_2N_4Cl$	60.10	5.42	15.70	60.25	5.29	15.62
5e	160	Pet. Ether	$C_{22}H_{18}O_2N_3$	67.21	4.81	10.31	67.43	4.59	10.72
5f	155	Ethanol	$C_{22}H_{17}O_2N_3Cl_2$	61.71	3.72	9.42	61.97	3.99	9.85
5g	178	Benzene	$C_{23}H_{20}O_4N_4$	66.23	4.75	13.23	66.34	4.80	13.46
5h	230	Pet. Ether	$C_{24}H_{23}O_4N_5$	64.41	5.01	15.32	64.71	5.16	15.73

b) *Cyclisation of hydrazides* **5** *to triazines* **6**

a) The hydrazides (**5**; R′=H) (0.01 mole) in acetic acid (60 ml) and in the presence of fused sodium acetate (0.2 g) were heated under reflux for 45 min; much frothing took place. Decomposition of the cold reaction mixture with water gave sticky products from which no crystalline materials were obtained.

b) When the hydrazides **5e** and **5f** were treated as in the above experiment the corresponding 1 : 2 : 4-triazines **6** were obtained (Table 5).

c) The oxazolone **1**(0.01 mole) and phenylhydrazine (0.01 mole) in acetic acid (60 ml) and in the presence of fused sodium acetate (0.3g) were heated under reflux for 1 hr. Dilution with water gave the corresponding 1 : 2 : 4-triazines **6** which recrystallized from the proper solvent (Table 5).

Table 5

Substituted 1 : 2 : 4-triazines 6

Comp.	m.p. (°C)	Solvent	Formula	Analysis % Found C	H	N	Required C	H	N
6a	205	Methanol	$C_{22}H_{16}ON_3Cl$	70.51	4.31	11.74	70.68	4.28	11.24
6b	230	Ethanol	$C_{22}H_{15}ON_3Cl_2$	64.45	3.91	10.01	64.70	3.67	10.29

Reaction of oxazolones with hydroxylamine hydrochloride

A solution of **1** (0.1 mole), pyridine (50 ml) and hydroxylamine hydrochloride (0.1 mole) was heated under reflux for 6 hrs and then cooled. The solid product was filtered off and recrystallized from suitable solvent as listed in Table 6.

Table 6

4-Arylidene-1-hydroxy-2-aryl-5-imidazolones **7**

Comp.	m.p. (°C)	Solvent	Formula	Analysis % Found C	H	N	Required C	H	N
7a	190	Benzene	$C_{16}H_{11}O_2N_2Cl$	64.12	3.51	9.01	64.32	3.68	9.38
7b	200	Benzene	$C_{16}H_{10}O_2N_2Cl_2$	57.48	3.31	8.31	57.65	3.00	8.40
7c	240	Benzene	$C_{16}H_{10}O_4N_3Br$	49.25	2.31	10.52	49.49	2.57	10.82
7d	175	Benzene	$C_{18}H_{16}O_4N_4$	66.45	4.23	15.51	66.46	4.54	15.90

Action of hydrazine on the imidazolones

A solution of imidazolone (0.1 mole) in ethanol or acetic acid was treated with phenylhydrazine (0.1 mole). The reaction mixture was heated under reflux for 3 hrs then cooled. The solid products were filtered off and recrystallized from suitable solvent to the corresponding triazines **6** (m.p. and mixed m.p. ; of Table 5).

Reaction of sodium azide with oxazolones

A solution of **1** (0.1 mole) in hot acetic acid (30 ml) was treated with sodium azide (0.4 mole) dissolved in the least amount of water and the reaction mixture heated under reflux on a steam bath for 3 hrs then poured on crushed ice. The solid product was filtered off and recrystallized from the proper solvent to give **8** (Table 7).

Table 7

Tetrazolyl derivatives

Comp.	m.p.	Solvent 2	Formula	Analysis					
				Found			Required		
				C	H	N	C	H	N
8a	218	Benzene	$C_{16}H_{11}O_2N_4Cl$	58.61	3.31	17.25	58.80	3.36	17.15
8b	209	Acetic	$C_{16}H_{10}O_2N_4Cl_2$	53.38	2.61	15.45	53.18	2.77	15.51
8c	235	Benzene	$C_{16}H_{10}O_4N_5Br$	46.31	2.52	16.53	46.16	2.40	16.83
8d	225	Ethanol	$C_{18}H_{16}O_4N_4$	61.35	4.59	15.81	61.36	4.54	15.90

REFERENCES

[1] A. F. M. Fahmy, A. A. Afifi and I. G. Shenouda, *Pakistan J. Sci.Ind. Res.*, **20**, 150 (1977).

[2] A. F. M. Fahmy, A. A. Afifi and I. G. Shenouda, *Rev. Roumaine Chim.*, **24**, 373 (1979).

[3] A. A. Afifi, G. H. Sayed, H. A. Ahmed and I. G. Shenouda, *Pakistan J. Sci., Ind. Res.*, **20**, 224 (1977).

[4] K. J. Narag and N. J. Ray, *J. Chem. Soc.*, **1931**, 976.

[5] E. Erlenmeyer. *Liebigs. Ann. Chem.*, **316**, 145 (1901).

[6] A. M. Islam, I. B. Hannout, L. M. Souka and H. Aref, *Egypt J. Chem.*, **20**, 473 (1977).

[7] M. Vanghelevici, I. Moise and A. Stefănescu, *Bull. Chim. Soc., Chim. Romania* (2) 3A 85 (1941 –1942) ; *Chem. Abstr.*, **38**, 5500 (1944).

Revue Roumaine de Chimie, 28, 8, 857 – 861 (1983)

MOLECULAR ORBITAL STUDIES FOR CYCLOPHOSPHAZENE DERIVATIVES. IV. [1]

ALL-VALENCE ELECTRON CALCULATIONS BY THE *HMO* AND *DEL RE* METHODS

C. MIHART *, S. RADULY ** and Z. SIMON ***

* Agronomical Institute of Timişoara, Department of Biochemistry, Calea Aradului 119, Timişoara 1900, Romania

**University of Timişoara, Department of Natural Sciences, Bd. V. Pârvan, no. 4, Timişoara, 1900, Romania

***Institute of Medicine Timişoara, Department of Biophysics, Pţa. 23 August no. 2, Timişoara 1900, Romania

Received July 15, 1982

Del Re calculations were performed for nine cyclophosphazene derivatives. Total atomic charges are calculated using the electronic charges given by the HMO study of the previous note. The total atomic charges for the studied compounds present a satisfactory agreement with the chemical shift for $^{31}P-NMR$, with the basicity and with the first ionisation potential.

INTRODUCTION

In the preceding note[1] HMO calculations were performed for cyclophosphazene derivatives by means of the Fukui and Dewar models. A good concordance was obtained for the position of the first UV–absorption maximum, for the polarographic reduction potential, for shortening of bond lengths and for some reactivity characteristics. No agreement was obtained between experimental and calculated values (energy levels, π-electronic charges) for the first ionisation potential, for the chemical shift at the P–atom and for the basicity. These characteristics may depend upon the total electric charges of key atoms and therefore, these charges were calculated by means of the Del Re–method for the σ-electronic systems.

CALCULATION METHOD AND PARAMETERS

Del Re calculations were performed for nine molecules. We have the parameters recommended by Del Re [2] which are listed in Table 1. For the P-atom Pullman's[3] formula, based upon atomic electro-negativities, was used to calculate δ_p^0, while the exchange integrals η_{PN}, η_{PC}, η_{PH} were

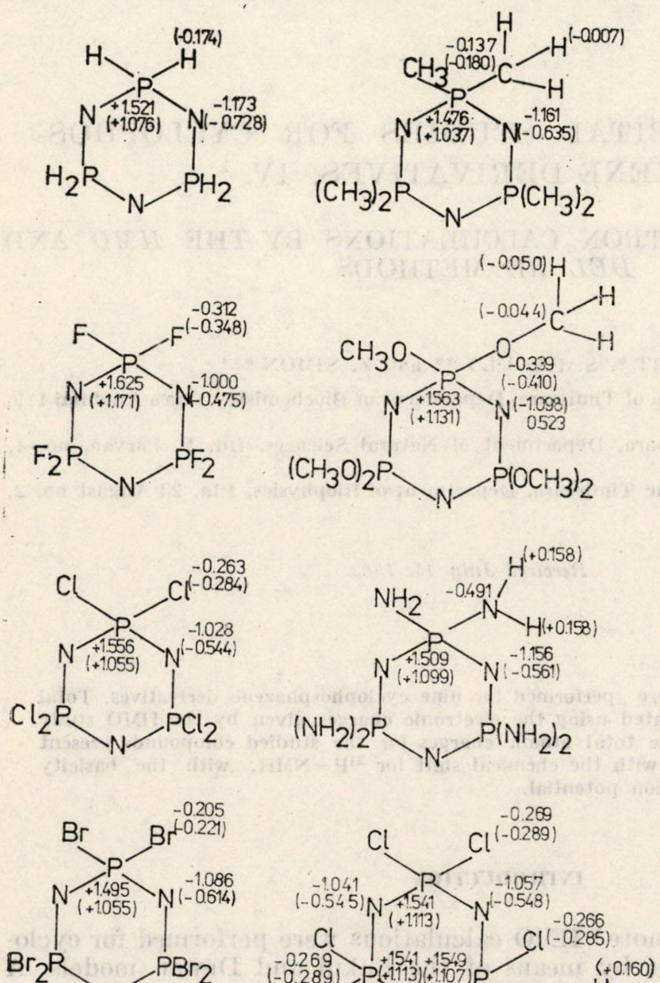
H
H (-0.174)
P
+1.521 (+1.076)
N
N -1.173 (-0.728)
H2P
PH2
N
H
-0.137 (-0.180)
CH3
C
H (-0.007)
H
+1.476 (+1.037)
N
N -1.161 (-0.635)
(CH3)2P
P(CH3)2
N
F
F -0.312 (-0.348)
+1.625 (+1.171)
N -1.000 (-0.475)
F2P
PF2
(-0.050) H
(-0.044) C
H
H
CH3O
O
-0.339 (-0.410)
+1.563 (+1.131)
N (-1.098) 0.523
(CH3O)2P
P(OCH3)2
Cl
Cl -0.263 (-0.284)
+1.556 (+1.055)
N -1.028 (-0.544)
Cl2P
PCl2
H (+0.158)
-0.491 N
NH2
H (+0.158)
+1.509 (+1.099)
N -1.156 (-0.561)
(NH2)2P
P(NH2)2
Br
Br -0.205 (-0.221)
+1.495 (+1.055)
N -1.086 (-0.614)
Br2P
PBr2
Cl
Cl -0.269 (-0.289)
-1.041 (-0.545)
+1.541 (+1.113)
N -1.057 (-0.548)
Cl -0.266 (-0.285)
-0.269 (-0.289)
+1.541 +1.549 (+1.113) (+1.107)
(+0.160) H
-0.484 (-0.584) N
H
-1.057 (-0.548)
H (0.053)
0.105 (-0.107) C
(0.049) H
C -0.059 (-0.059)
H (0.055)
C -0.053 (-0.054)
C6H5
-0.106 (-0.105) C
C
C
H
H
+1.501 (+1.062)
N -1.051 (-0.606)
(C6H5)2P
P(C6H5)2

Fig. 1. — Molecular diagrams for cyclophosphazene derivatives. Numbers in front of atoms represent total atomic charges ($q_{\sigma+\pi}$), numbers in parantheses, σ-electronic charges (q_σ).

considered equal to 1.0 in order to avoid excesive charge-shifts. The total atomic charges and the σ-electronic charges (in parantheses) are listed at the corresponding atoms in figure 1.

Table 1

Parameters for Del Re calculations

a. The electronegativities for atomic valence orbitals :

$\delta^0_P = -0.500$; $\delta^0_H = 0.00$; $\delta^0_{C(sp^3)} = 0.07$; $\delta^0_{C(sp^2)} = 0.12$;

$\delta^0_{-N=} = 0.38$

b. The introductive effect $\gamma_{q(p)}$ of atom p on atom q :

$\gamma_{P(N)} = \gamma_{N(P)} = \gamma_{P(O)} = \gamma_{O(P)} = \gamma_{P(Cl)} = \gamma_{P(Cl)} = \gamma_{P(Br)} = \gamma_{Br(P)} =$

$= \gamma_{(P(F)} = \gamma_{F(P)} = 0.2$;

$\gamma_{C(C)} = \gamma_{C(N)} = \gamma_{N(C)} = 0.1$;

$\gamma_{H(P)} = \gamma_{H(C)} = 0.4$; $\gamma_{P(H)} = \gamma_{C(H)} = 0.3$

c. The exchange integrals :

$\eta_{PN} = \eta_{PC} = \eta_{PH} = \eta_{CH} = \eta_{CC} = 1.000$;

$\eta_{CN} = 0.7$; $\eta_{NH} = 0.45$.

The calculations by the Del Re method were performed on the computer of the Timișoara University acording to a programme written by one of us (S. Raduly).

The π-electronic charges are those obtained in the preceeding note [1] with the Fukui variant and parameters recommended by the literature for the phosphorus atom, by the HMO-method, the variant for which the best results were obtained. We remark that the π-electronic charges calculated with the parameters recommended by Mracec present a very good parallelism to the charges calculated with the literature parameters.

RESULTS AND DISCUSSIONS

Tables 2, 3 and 4 list the chemical shift at the phosphorus atom in NMR (δ^{31}P), the pK_a values (nitrobenzene, 25°C) and the first ionisation potential, respectively, in comparison with π-electronic charges, q_π, σ — electronic charges, q_σ and total atomic charges, $q_{\sigma+\pi}$, of the considered atoms.

The introduction of the total charges $q_{\sigma+\pi}$, instead of the π-electronic charges, improves considerably the agreement between the calculated values and experiment. For the eight compounds of figure 1, for which chemical shifts (δ^{31}P) are available, a remarkable antiparallelism exists between δ^{31} P and $q_{\sigma+\pi}$, with a single notable exception table 2, $r = 0.783$). For the five compounds of table 3 a satisfactory parallelism between

Table 2

Chemical shift at the P-atom ($\delta 31_P$) and atomic charge (q^P)

Compound	$\delta^{31}P$ (ppm)	q^P_π	q^P_σ	$q^P_{\sigma+\pi}$
$(NPBr_2)_3$	+45.4	+0.440	+1.055	+1.495
$(NPF_2)_3$	−13.9	+0.454	+1.171	+1.625
$[NP(C_6H_5)_2]_3$	−14.3	+0.439	+1.062	+1.501
$[NP(NH_2)_2]_3$	−18.8	+0.410	+1.099	+1.509
$N_3P_3Cl_5NH_2$	−19.0	+0.442	+1.107	+1.549
$(NPCl_2)_3$	−20.0	+0.443	+1.113	+1.556
$N_3P_3Cl_5NH_2$	−20.4	+0.428	+1.113	+1.541
$[NP(OCH_3)_2]_3$	−21.7	+0.432	+1.131	+1.563

correlation coefficient $r = 0.783$

Table 3

Basicity (pK_a in nitrobenzene, 25°C) and atomic charge (q^N) and the cyclic N-atom

Compound	pK_a	q^N_π	q^N_σ	$q^N_{\sigma+\pi}$
$[NP(NH_2)_2]_3$	8.25	−0.595	−0.561	−1.156
$[NP(C_2H_5)_2]_3$	6.40	−0.526	−0.635	−1.161
$[NP(C_3H_5)_2]_3$	1.50	−0.445	−0.606	−1.051
$[NP(OCH_3)_2]_3$	−1.90	−0.575	−0.523	−1.098
$(NPCl_2)_3$	−6.00	−0.484	−0.544	−1.028

correlation coefficient $r = 0.856$

Table 4

First ionisation potential (I) and atomic charge (q^N) at the cyclic N-atom.

Compound	I(eV)	q^N_π	q^N_σ	$q^N_{\sigma+\pi}$
$[NP[N(CH_3)_2]_3]_3$	7.85	−0.595	−0.561	−1.156
$[NP(CH_3)_2]_3$	8.35	−0.526	−0.635	−1.161
$[NP(OCH_3)_2]_3$	9.29	−0.575	−0.523	−1.098
$(NPBr_2)_3$	9.56	−0.472	−0.614	−1.086
$(NPCl_2)_3$	10.26	−0.484	−0.544	−1.028
$(NPF)_{23}$	11.40	−0.525	−0.475	−1.000

correlation coefficient $r = 0.881$

the negative charge at the nitrogen atom ($q^N_{\sigma+\pi}$) and the pK_a-value also exists ($r = 0.856$). The ionisation potential, for the six compounds of table 4 increases with the total charge at the nitrogen atom, $q^N_{\sigma+\pi}$, ($r = 0.881$), in good agreement with the assumption of extracting the electron from the lone N-orbital.

CONCLUSIONS

The combination of HMO-method (Fukui variant) with Del Re-method yields realistic results for energy levels and atomic charges, at least as revelative values in series of compounds with similar structure. The energy of frontier orbitals allows to explain the position of the first maximum in the electronic spectra and the behaviour in polarographic reduction of cyclophosphazene derivatives. Bond orders and π-electronic charges also explain the shortening of bond lengths and some reactivity characteristics. Total atomic charges, $q_{\sigma+\pi}$, explain most of the chemical shifts at the P-atom, the basicity and the first ionisation potential of the studied cyclophosphazene derivatives.

A combination of HMO and Del Re methods can be recommended for the theoretical study of large series of molecules and for the calculation of electronic parameters which are to be used in structure-reactivity-biological activity correlations.

REFERENCES

[1] Part III : C. Mihart, M. Mracec and Z. Simon, *Rev. Roumaine Chim.* (1982) in press.
[2] G. Del Re, *J. Chem. Soc.*, **1958**, 4031 ; G. Del Re and B. Pullman, *J. Chem. Phys.*, **62**, 942 (1965).
[3] A. Pullman, *Modern Quantum Chemistry*, **3**, 283 (1965).
[4] M. Mracec, "Doctoral Thesis", Universitatea Timişoara, 1977.

Revue Roumaine de Chimie, 28, 8, 863 – 866 (1983)

ETHYLENE CHLOROPHOSPHITE AS A NEW REAGENT FOR AROMATIC AMIDE SYNTHESIS BY A DIRECT CONDENSATION REACTION UNDER VERY MILD CONDITIONS

C. I. CHIRIAC
"P. Poni" Institute of Macromolecular Chemistry, Aleea Gr. Ghica Vodă 41 A, Iași, Romania

Received June 22, 1982

By a direct condensation reaction of ethylene acylphosphite prepared *in situ* from ethylene chlorophosphite and aromatic acids with aromatic amines, under very mild conditions, aromatic amides resulted in high yields.

A common method for preparing N-monosubstituted amides, utilizes the reaction of primary amines with acyl chlorides. The latter compounds are often prepared by the reaction of a carboxylic acid with phosphorus trichloride or thionyl chloride. In the last time, different investigators have found that the two steps could be combined successfully into a single operation.[1,2]

In previous papers[3,4] we showed that reactive phosphorus compounds can be used as reagents in this field.

RESULTS AND DISCUSSIONS

In this paper we present a new reagent for the synthesis of aromatic amides. We found that ethylene chlorophosphite is a very good reagent in this field. It is very reactive. We obtained aromatic amides in high yields, just at room temperature. Thus a solution of *p*-toluic acid (0.02 mole) in pyridine was treated with ethylene chlorophosphite (0.02 mole) and after one hour *p*-toluidine (0.02 moles + 10% excess) was added. After 10 – 12 hours at room temperature, the yield was 60%, and after 24 hours at the same temperature, the yield was 71% (the room temperature was 15 – 18°).

At temperature higer than 20° (in the summer), the reaction time could be shorter. A practical variant with a shorter time utilises a heating at 45 – 55° for 4 hours.

By the addition of ethylene chlorophosphite to a solution of an aromatic acid in pyridine, a reactive compound results, similar with many other cases.[1–4,5,6]

In this case, the reactive intermediate is an ethylene acylphosphite which was isolated as a hygroscopic compound with m.p. 51 – 54°, in the reaction of benzoic acid with ethylene chlorophosphite. Thus by the addition of a solution of ethylene chlorophosphite in dried benzene to a suspension of sodium benzoate in dried benzene or by the addition of a solution of ethylene chlorophosphite in dried diethyl ether to a solution of benzoic acid in dried diethyl ether, in the presence of pyridine, ethylene benzoyl phosphite results in both cases. As by-products, NaCl in the first case and PyH^+Cl^- in the second one have been obtained. The ethylene benzoylphosphite, isolated and purified, is very reactive with aromatic amines, affording the corresponding amides. For the simplification of this method we prepared *in situ* ethylene acylphosphitea, because the yield and the purity are very good in both cases. Therefore, it was not necessary to isolate these reactive compounds, because pyridine hydrochloride (by-product) does not affect the reaction, like in other cases.[3,4,7] Ethylene acylphosphite can be considered as mixed anhydrides of ethylene phosphorus acid with aromatic acid, and for this reason, they can manifest high reactivity. Tertiary amines play an important role in the reaction. We tried many tertiary amines, but the pyridine was found to be the most suitable base which served also as reaction medium.

As a result of these investigations, we propose the following mechanism of reaction :

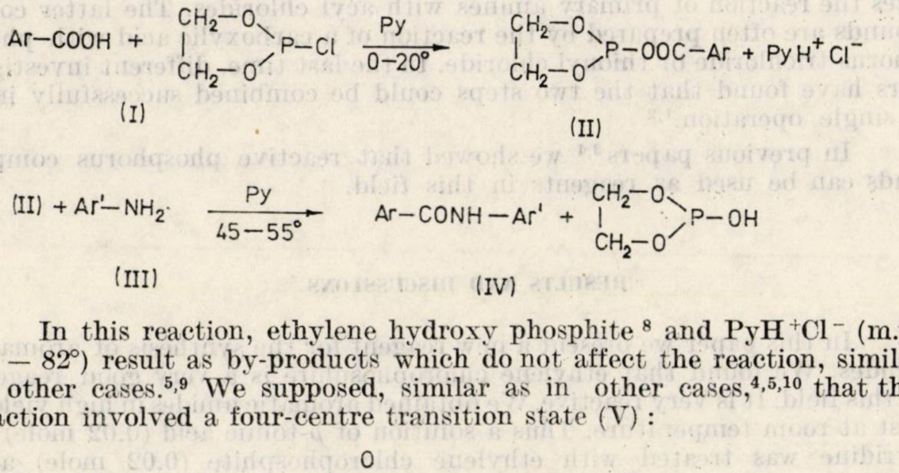

In this reaction, ethylene hydroxy phosphite [8] and PyH^+Cl^- (m.p. 80 – 82°) result as by-products which do not affect the reaction, similar to other cases.[5,9] We supposed, similar as in other cases,[4,5,10] that this reaction involved a four-centre transition state (V) :

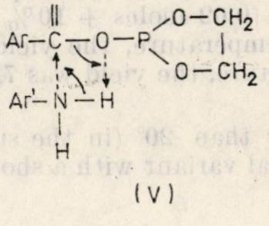

(V)

In a typical procedure, to a solution of one mole (I) in dried pyridine cooled to 0°, one mole ethylene chlorophosphite was added very slowly under stirring (the reaction is exothermic). After one hour, one mole + 10% excess (III) was added and the stirring was continued for four hours at 45 — 55°. The yield was improved when we used a small excess of amines (5 — 10%). The reaction requires a large excess of pyridine in order to assure an efficient stirring, because PyH^+Cl^- and (II) precipitate partially during the reaction at 0 — 20°; then by treatment with (III), the solution becomes clear.

Table 1 shows the amides obtained in this way.

Table 1

Aromatic amides obtained from ethylene acylphosphites prepared *in situ*

Acid	Amine	Amides [a]		
		Yield [b)]%	M.p. [c)] °C	Reported m.p. [d)] °C
p-Toluic	p-Toluidine	95	158—160	159—160
p-Toluic	Aniline	87	144—146	144—145
p-Toluic	2-Naphthylamine	93	172—174	173—174
Benzoic	*p*-Chloroaniline	83	185—187 [e)]	185—187
Benzoic	*p*-Toluidine	88	156—158	157—158
Benzoic	Aniline	86	160—162	161—162
p-Anisic	*p*-Toluidine	92	153—155	153—154
p-Chlorobenzoic	*p*-Toluidine	84	215—217 [e)]	215—216
p-Chlorobenzoic	Aniline	81	193—195	193—194

---

a) The products were identified by comparison of m.p. and IR spectra with those of authentic samples.

b) Yields determined by isolation of the crude products.

c) Before recrystallisation.

d) From "Beilstein Handbuch der organischen Chemie".

e) After recrystallisation.

The large majority of the obtained amides melted, before recrystallisation, within two degrees of the melting points reported in the literature.

By this new direct synthesis, we obtained, in high yields, aromatic amides, which are difficult to obtain by heating aromatic amines with aromatic acids.

EXPERIMENTAL

1. Ethylene benzoylphosphite

Method a

To a stirred cooled suspension of 10 g (0.07 moles) of dried sodium benzoate in 40 ml dried benzene, a solution of 4.5 ml (0.05 moles) of ethylene chlorophosphite [8] in 10 ml dried benzene was added very slowly. Then the mixture was stirred for 12 hours at room temperature. The obtained solution, after centrifugation and decantation, was evaporated under vacuum and magnetic stirring. The obtained precipitate was washed, very fast, three times with 25 — 35 ml dried petroleum ether by decantation and dried under vacuum, giving 8.3 g ethylene benzoylphosphite, a hygroscopic solid with m.p. 51 — 54°. The yield was 84% calculated on ethylene chlorophosphite employed.
Anal. Calculated for $C_9H_9O_4P$; C, 50.94 ; H, 4.24 ; P, 14.62%. Found : C, 50.42 ; H, 4.26 ; P, 14.23%.

Method b

To a solution of benzoic acid (6.1 g, 0.05 moles) in 40 ml dried diethyl ether and dried pyridine (4 ml, 0.05 moles), a solution of ethylene chlorophosphite (4.5 ml, 0.05 moles) in 10 ml dried diethyl ether was added under stirring and cooling. After stirring for 1 — 2 hours at room temperature, the obtained mixture was worked-up as above. The resulted product is similar with the product obtained by the method *a* (PyH^+Cl^- results as by-product with m.p. 80 — 82°).

2. Amide of *p*-toluic acid with *p*-toluidine

To a stirred solution of *p*-toluic acid (2.72 g, 0.02 moles) in dried pyridine (15 ml) cooled to 0°, 1.8 ml (0.02 moles) of ethylene chlorophosphite was added very slowly, when the reactive product resulted *in situ* and pyridine hydrochloride precipitate partially, the solution being very concentrated. The mixture was stirred for 1 — 2 hours at room temperature. Then *p*-toluidine (2.35g, 0.02 moles + 10% excess) was added under stirring and the solution became clear. The obtained solution was heated 4 hours at 45 — 55° and poured into a large volume of water and ice (150 — 200 ml) under stirring. The white amide was collected by filtration, washed with 20 — 30 ml 5% NaOH, 20 — 30 ml 5% HCl, three times with 15 — 20 ml H_2O and dried at 60 — 70° under vacuum. The resulted product (4.3 g) has a m.p. 158 — 160° (mixed m.p. with pure amide undepressed). Yield 95%. The yield was 70% when the reaction mixture was maintained 12 hours at room temperature (with the same m.p.) Anal. Calculated for $C_{15}H_{15}NO$; C, 80.00 ; H, 6.66 ; N, 6.22%. Found ; C, 79.81 ; H, 6.36 ; N, 6,13%.

Under similar conditions, the other amides presented in table 1 were obtained with the exception of benzanilide when 10 ml pyridine were used as solvent.

REFERENCES

[1] T. Wieland and B. Heinke, *Chem. Ber.*, **91**, 483 (1958).
[2] G. W. Anderson and R. W. Young, *J. Amer. Chem. Soc.*, **74**, 5304 (1952).
[3] C. I. Chiriac, *Rev. Roumaine Chimie*, **24**, 609 (1979).
[4] C. I. Chiriac, *Rev. Roumaine Chim.*, **26**, 1001 (1981).
[5] B. Iselin and W. Rittel, *Helv. Chim. Acta*, **40**, 373 (1957).
[6] J. H. Brewster and C. I. Ciotti, *J. Amer. Chem. Soc.*, **77**, 6214 (1955).
[7] C. I. Chiriac and J. K. Stille, *Macromolecules*, **10**, 710 (1977).
[8] H. J. Lucas and F. W. Mitchell, *J. Amer. Chem. Soc.*, **72**, 5491 (1950).
[9] N. Yamazaki, *Tetrahedron Letters*, **1972**, 5047.
[10] H. O. Becker and K. F. Funk, *J. prakt. Chem.*, **14**, 55 (1961).

NOTE POUR LES AUTEURS

La Revue Roumaine de Chimie publie des articles en anglais, français, russe, allemand ou espagnol. Les auteurs sont priés d'envoyer des articles et des comptes rendus inédits.

Les manuscrits seront dactylographiés à double interligne. La bibliographie, les tableaux et la légende des figures seront placés après le texte.

Si l'article fait partie d'une série numérotée, la partie précédente sera donnée comme première référence.

Chaque article sera précédé d'un résumé comprenant quinze lignes au maximum.

Les références bibliographiques dans le texte seront faites par des exposants sans parenthèses et paraîtront à la fin de l'ouvrage.

Les publications périodiques mentionnées dans la bibliographie seront présentées suivant les prescriptions internationales : le nom de l'auteur précédé de l'initiale du prénom, le titre du périodique abrégé conformément à « Chemical Abstracts » et souligné par une ligne, le numéro du tome indiqué par des chiffres arabes et souligné par deux lignes, suivi de la première page de l'article ; à la fin, l'année de la parution sera placée entre parenthèses. Le numéro de la revue ne sera pas indiqué si les pages du volume sont numérotées consécutivement.

Les textes des livres ou traités inclueront : le nom des auteurs, précédés de l'initiale du prénom, le titre du livre entre guillemets et sans être souligné, le numéro du tome précédé par l'abréviation « vol. » (ou « Bd. »), le numéro de l'édition, les éditions (the publisher), la localité de la parution du livre, l'année de la parution et la page de la référence précédée (s) par l'abréviation « p » (ou «S »).

Les brevets seront indiqués comme suit : l'auteur ou la firme, le pays et le numéro du brevet, la date et la revue *(Chem. Abstr.)*. Per ex. : M. Jones (to Union Carbide Co.) Brit. Pat. 610 238, 2 Sept. 1959 : cf. *Chem. Abstr.*, 54, 12808 (1960).

Si la référence n'a pas été lue en original, on indiquera aussi la revue de références consultée.

Les diagrammes seront tracés à l'encre de Chine sur papier calque. Les tableaux et les figures (en nombre strictement nécessaire), ainsi que les courbes dans les figures seront numérotés par des chiffres arabes. Leur explication sera donnée dans la légende des figures. Prière de ne pas inscrire les mêmes données dans les tableaux et les figures. Chaque tableau aura un titre. On indiquera dans le texte la place approximative des tableaux et des figures. Les formules chimiques seront incluses dans le texte ; en outre, elles seront transcrites sur papier calque, à l'encre de Chine.

Les auteurs sont priés d'indiquer les caractères italiques (en soulignant les lettres au crayon), ainsi que tout autre caractère spécial : les préfixes *ortho, meta, para, cis, trans*, etc., seront soulignés pour indiquer leurs caractères italiques et ne seront jamais écrits avec des majuscules.

Aucune correction à la main ne sera admise sur le manuscrit. Les corrections seront tapées à la machine. Les lettres grecques ou d'autres symboles spéciaux seront insérés à la main à l'encre clairement.

Le manuscrit sera signé par l'auteur.

Le titre courant aura 50 lettres au maximum.

L'entière responsabilité du contenu des articles appartient aux auteurs.

Sur demande on peut obtenir une note plus complète.

PRINTED IN ROMANIA

1984 FEB 0 9

TRAVAUX PARUS AUX ÉDITIONS DE L'ACADÉMIE DE LA RÉPUBLIQUE SOCIALISTE DE ROUMANIE

ELENA CEAUŞESCU, **Noi cercetări în domeniul compuşilor macromoleculari** (Nouvelles recherches dans le domaine des composés macromoléculaires), 1981, 536 p.

I. G. MURGULESCU, RODICA VÎLCU, **Introducere în chimia fizică, Vol. III. Termodinamica chimică** (Introduction à la chimie physique. Vol. III, Thermodynamique chimique), 1982, 626 p.

I. G. MURGULESCU, J. PĂUN, **Introducere în chimia fizică, Vol. I. 3. Nucleul atomic, reacţii nucleare, particule elementare** (Introduction a la chimie physique. Vol. I.3. Noyau atomique, réactions nucléaires, particules élémentaires), 1982, 606 p.

ELENA JERCAN, **Analiza cromatografică** (Analyse chromatographique), 1982, 286 p.

I. G. MURGULESCU, TATIANA ONCESCU, E. SEGAL, **Introducere în chimia fizică, Vol. II. 2. Cinetică chimică şi cataliză** (Introduction à la chimie physique. Vol. II.2. Cinétique chimique et catalyse), 1981, 1024 p.

V. DRĂGUŢAN, A. T. BALABAN, M. DIMONIE, **Metateza olefinelor şi polimerizarea prin deschidere de inel a cicloolefinelor** (La métathèse des oléfines et la polymérisation par ouverture annulaire des cyclooléfines), 1981, 254 p.

LYDIA-MARIA VAICUM, **Epurarea apelor uzate cu nămol activ. Bazele biochimice** (L'épuration des eaux résiduelles à boue active. Les bases biochimiques), 1981, 218 p.

I. GĂLĂŢEANU, **Procese şi metode radiochimice în energetica nucleară** (Processus et méthodes radiochimiques dans l'énérgétique nucléaire), 191, 234 p.

OCTAVIAN IORDACHE, **Procese polistocastice aplicate la fenomenele de transfer** (Processus polystochastiques appliqués aux phénomènes de transfert), 1981, 187 p.

CR. SIMIONESCU, VALERIA GORDUZA, **Polimeri biocompatibili şi biologic activi** (Polymères biocompatibles et biologiquement actifs), 1980, 479 p.

ELENA CEAUŞESCU, **Polimerizarea stereospecifică a izoprenului** (La polymérisation stéréospécifique de l'isoprène), 1979, 307 p.

CONST. GH. MACAROVICI, **Analiza chimică cantitativă anorganică** (L'analyse chimique quantitative inorganique), 1979, 457 p.

M. FLORESCU, **Metode ştiinţifice în dezvoltarea industriei chimice moderne** (Méthodes scientifiques dans le développement de l'industrie chimique moderne), 1979, 256 p.

A. T. BALABAN, I. GĂLĂŢEANU, G. GEORGESCU, LIGIA SIMIONESCU, **Compuşi marcaţi şi radiofarmaceutici cu aplicaţii în medicina nucleară** (Composés marqués et radiopharmaceutiques à application en médecine nucléaire), 1979, 495 p.

I. G. MURGULESCU, E. SEGAL, **Introducere în chimia fizică, Vol. II.1. Teoria molecular-cinetică a materiei** (Introduction à la chimie physique. Vol. II.1. La théorie moléculaire-cinétique de la matière), 1979, 1036 p.

S. STERNBERG, FL. DANEŞ **Termodinamica chimică aplicată** (La thermodynamique chimique appliquée), 1978, 400 p.

I. G. MURGULESCU, V. EM. SAHINI, **Introducere în chimia fizică. Vol. I. 2. Structura şi proprietăţile moleculelor** (Introduction à la chimie physique. Vol. I.2. La structure et les propriétés des molécules), 1978, 604 p.

I. ZUGRĂVESCU, MAGDA PETROVANU, **N-ylid chemistry**, coédition avec McGraw-Hill International Book Company, U.S.A., 1977, 396 p.

I. G. MURGULESCU, **Introducere în chimia fizică. Vol. I. 1 Atomi, molecule, legătură chimică** (Introduction à la chimie physique. Vol. I.1. Atomes, molécules, liaison chimique), 1976, 560 p.

ELENA CEAUŞESCU, **Research work on synthesis and characterization of macromolecular compounds. Contributions**, 1974, 251 p.

CR. SIMIONESCU, VIORICA RUSAN, V. POPA, **Chimia algelor marine** (La chimie des algues marines), 1974, 212 p., 1 pl.

ISSN 0035–4090

I. P. INFORMAŢIA c. 1288

43 426

Lei 40

$ 70 (pour un abonnement annuel)

F 1103

Vegyészel

R

ACADÉMIE DE LA RÉPUBLIQUE SOCIALISTE DE ROUMANIE

REVUE ROUMAINE DE CHIMIE

REFERÁLVA

TOME 28

N°s 9—10

Septembre — Octobre 1983

EDITURA ACADEMIEI REPUBLICII SOCIALISTE ROMÂNIA

Rev. Roumaine Chim.

RRCHX, 28, 9 — 10, p. 867 — 950 (1983), Bucarest

ACADÉMIE DE LA RÉPUBLIQUE SOCIALISTE DE ROUMANIE

COMITÉ DE RÉDACTION

Rédacteur en chef :

I. G. MURGULESCU, membre de l'Académie de la République Socialiste de Roumanie

Rédacteurs en chef adjoints :

A. T. BALABAN et V. EM. SAHINI, membres correspondants de l'Académie de la République Socialiste de Roumanie

Collège de rédaction :

EM. BRATU, ELENA CEAUŞESCU, ECATERINA CIORĂNESCU-NENITZESCU, CR. SIMIONESCU, membres de l'Académie de la République Socialiste de Roumanie ; P. SPACU, membre correspondant de l'Académie de la République Socialiste de Roumanie ; MARGARETA AVRAM, M. BANCIU, I. HAIDUC, D. I. MARCHIDAN, I. MOLDOVAN, G. NIAC et D. SĂNDULESCU

La Revue Roumaine de Chimie paraît 10 fois par an. Toute commande de l'étranger pour les travaux parus aux Editions de l'Académie de la République Socialiste de Roumanie sera adressée à ILEXIM — Departamentul Export—Import Carte (Livres)/Departamentul Export—Import Presă (Revues), P.O.B. 133—137, télex 11226, 3, str. 13 Decembrie, 79517 Bucarest, Roumanie

Les manuscrits, les livres et les revues proposés en échange, ainsi que toute correspondance seront envoyés à la rédaction :

REVUE ROUMAINE DE CHIMIE

125, Calea Victoriei, 79717 Bucarest, Roumanie, téléphone 50 76 80

EDITURA ACADEMIEI REPUBLICII SOCIALISTE ROMÂNIA
125, Calea Victoriei, 79717 Bucarest, Roumanie, téléphone 50 76 80

REVUE ROUMAINE
DE
CHIMIE

INFORMÁCIÓS
KÖNYVTÁR

Tome 28, N°s 9—10 Septembre—Octobre 1983

I. G. MURGULESCU, ECATERINA JURCONI and GABRIELA MINCU, Thermal decomposition and oxidoreduction of the trisoxalato Co(III) complex . . . . 869—873 R

MARIANA CIUREANU, V. E. SAHINI, M. CONTINEANU, FELICIA CORNEA and CORNELIA CERCASOV, Internal rotation in charge transfer complexes 875—881 Bc

PAK u SĂP, D. F. ANGHEL and C. LUCA, Electrochemical sensors for anionic surfactants. I. The electrode based on bis [2, 4, 6-tri (2-pyridyl)-1, 3, 5-triazine] iron (II) dodecyl sulphate . . . . 883—890

RODICA VÎLCU, ZOICA CENUȘE, F. GOTHARD and VIELKA LANGSHAW, A new installation for saturation pressure measurement in a multicomponent system (in Spanish) . . . . 891—902 C

I. HAVLIK, C. CSUNDERLIK, A. TOTH and R. BACALOGLU, Synthesis and characterization of 4′-substituted 4-aminoazobenzenes. Determination of basicity constants (in German) . . . . 903—913

M. El-KADY, M. K. El-DEEK, R. M. SALEH and M. G. El-DEIN, Synthesis of 2′-methyl-γ-pyronyl-(5′,-6′, 6, 7)-4-acetonyl-coumarin and its reaction 915—920

AHMED I. KOHDAIR, ABOEL-MAGD A. ABDEL-WAHAB, HUSSAIN S. El-KASHEF, KHAIRY M. HASSAN, AHMED M. El-KHAWAGA and MAHER F. El-ZOHARY, Oxidation of some selected dihydric alcohols 921—931 R

GH. SURPĂȚEANU, M. CONSTANTINESCU, C. LUCHIAN, M. PETROVANU, I. ZUGRĂVESCU and A. LABLACHE-COMBIER, Theoretical aspects on the reactivity of the cycloimmonium-ylides. II. Reactivity of the disubstituted carbanion-ylides . . . . 933—939

JEAN LOUIS BRISSET, Ionic products of H_2O-CH_3CN and CH_3OH-CH_3CN mixtures . . . . 941—949 R

Rev. Roumaine Chim. **28**, *9—10*, 867—950 (1983), Bucarest

Revue Roumaine de Chimie, 28, *9–10*, 869–873 (1983)

THERMAL DECOMPOSITION AND OXIDOREDUCTION OF THE TRISOXALATO Co(III) COMPLEX

I. G. MURGULESCU, ECATERINA JURCONI and GABRIELA MINCU
Institute of Chemistry, Department of Physical Chemistry,
Bd. Republicii 13, Bucharest, Romania

Received June 11, 1982

The kinetics and mechanism of the oxidoreduction reaction of $[Co(C_2O_4)_3]^{3-}$ with I^- ion were investigated at different H^+ ion concentrations and various temperatures. Similar studies on thermal decomposition of the same complex were performed. The catalytic action of H^+ ion, supporting the proposed mechanism, was revealed in both cases.

INTRODUCTION

The kinetics and mechanism of the oxidoreduction reaction of oxalato Co (III) complexes with iodide ion have been the subject of our previous paper in this series. [1-3] In all cases the reaction has been studied at various concentrations of bisoxalato Co (III) complexes and I^-, taking into account the catalytic effect of hydrogen ions and monovalent cations. The general line of the proposed mechanism is common for all oxalic complexes of the transition metals.[4-6] The reaction mechanism consists of aquation and protonation fast preequilibria, followed by the I^- reduction in the slow parallel steps.[1,2] A similar mechanism of an ion pair catalysed dechelation was suggested in order to explain the salt effects on the reaction rate. [3]

The object of the present work is to investigate the oxidoreduction reaction between trisoxalato Co (III) complex and iodide ion in acid medium.

RESULTS

It has already been reported in our previous papers [1-3] that the oxidoreduction reaction of oxalate Co(III) complexes with I^- obeys a first order kinetics rate law so that the rate constant is independent of the complex ion concentration. A typical first order dependence is shown in figure 1.

A similar behaviour was measured with different initial excess concentrations of I^- ion. [3]

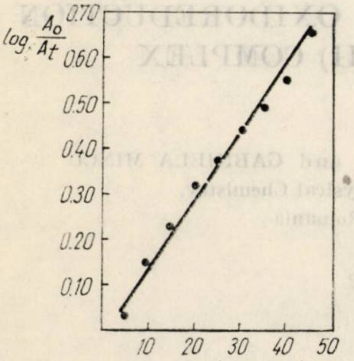

Fig. 1. — First order dependence under the conditions : $C_{complex} = 5 \cdot 3 \times 10^{-3}$ M, $C_{I^-} = 0.6$ M ; $C_{H^+} = 3.4$ M ; $T = 40$°C ; in reference cell KI($C_{I^-} = 0.6$ M) and HCl ($C_{H^+} = 3.4$ M)

Experiments at various hydrochloric acid concentrations were also performed keeping the initial reactant concentration constant ($c_{complex} = 5 \cdot 3 \times 10^{-3}$ M, $c_{I^-} = 0.6$M). Since in all the cases studied, the thermal decomposition of the Co (III) complex takes place in paralel with oxidoreduction reaction, the values of the experimental rate constants (k_{exp}) characterize an overall process. For this reason, similar measurements were made under the same conditions (concentration, temperature, experimental technique) but in the absence of I^- in order to determine the rate constants (k_t) of the thermal decomposition of Co (III) complex. The concentration of the hydrogen ions significantly changes the rate of the decomposition reaction, as well as the overall reaction rate. The acidity dependence of the both reactions is presented in table 1 (columns a and b).

Table 1

Rate constants in acid solutions at different temperatures : a) overall reaction ; b) thermal decomposition ; c) oxidoreduction reaction

C_{HCl} (M)	Rate constants (s^{-1})								
	T = 40°C			T = 45°C			T = 50°C		
	a	b	c	a	b	c	a	b	c
3.40	0.000534	0.000456	0.000078	0.00111	0.000995	0.000115	0.00207	0.00190	0.00017
2.55	0.000405	0.000322	0.000073	0.000891	0.000801	0.000090	0.00148	0.00137	0.00011
1.70	0.000285	0.000240	0.000045	0.000656	0.000607	0.000049	0.00120	0.00113	0.000070
0.85	0.000170	0.000145	0.000025	0.000430	0.000400	0.000030	0.00071	0.000678	0.000032

DISCUSSION

The resulting rate values obtained under various concentration conditions of oxalato complex, iodide and hydrogen ions can be calculated according to the following equation :

$$-\frac{dC_T}{dt} = k_{obs} C_{H_3O^+} C_I \text{-} C_T \qquad (1)$$

Expression (1) is in good agreement with the first order dependence with respect to Co (III) complex (C_T), hydrogen ($C_{H_3O^+}$) and iodide ion (C_{I^-}) concentrations, reveales from our experimental data. Under these conditions we proposed the following mechanism:

$$[Co(C_2O_4)_3]^{3-} + H_3O^+ \underset{k_{-1}}{\overset{k_1}{\rightleftarrows}} [Co(C_2O_4)_2(HC_2O_4)(H_2O)]^{2-} \quad \text{(a) rapid}$$

$$[Co(C_2O_4)_2(HC_2O_4)(H_2O)]^{2-} + I^- \xrightarrow{k_2} [Co(C_2O_4)_2(HC_2O_4)(H_2O)I]^{3} \quad \text{(b) slow}$$

$$[Co(C_2O_4)_2(HC_2O_4)(H_2O)]^{2-} \xrightarrow{k_3} CoC_2O_4 + C_2O_4^{\cdot -} + H_3O^+ + C_2O_4^{2-} \quad \text{(c) slow}$$

$$[Co(C_2O_4)_2(HC_2O_4)(H_2O)I]^{3-} \xrightarrow{k_4} CoC_2O_4 + 2C_2O_4^{2-} + 1/2I_2 + H_3O^+ \quad \text{(d) rapid}$$

$$[Co(C_2O_4)_3]^{3-} + C_2O_4^{\cdot -} \longrightarrow CoC_2O_4 + 2CO_2 + 2C_2O_4^{2-} \quad \text{(e) rapid}$$

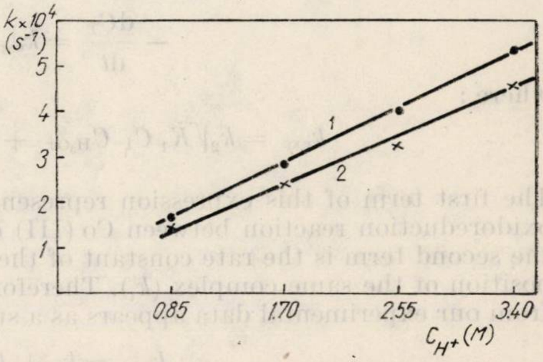

Fig. 2. — Catalytic action of C_{H^+} ion on the reaction rate constant at 40°C; (1) overall reaction; (2) thermal decomposition

On the basis of this mechanism the differential kinetic equation for the Co (III) complex is:

$$-\frac{dC_T}{dt} = k_1 C_T^2 C_{H_3O^+} - k_{-1} C_{TH}^2 + k_5 C_T C_{Ox} \tag{2}$$

where: C_T = concentration of the trisoxalato Co (III) complex;
C_{TH} = concentration of the protonated complex;
C_{Ox} = concentration of the oxalyl radical ion $C_2O_4^{\cdot -}$

By applying stationary state approximation to the intermediates TH, Ox and TI (where TI is the seven-coordinated intermediate) we found:

$$\frac{dC_{TH}}{dt} = k_1 C_T^2 C_{H_3O^+} - k_{-1} C_{TH}^2 - k_2 C_{TH} C_{I^-} - k_3 C_{TH} = 0 \tag{3}$$

$$C_{TH} \simeq \sqrt{K_1} C_{H_3O} C_{H_3O^+} C_T \tag{3'}$$

$$\frac{dC_{TI}}{dt} = k_2 C_{TH} C_{I^-} - k_4 C_{TI} = 0 \tag{4}$$

$$\frac{dC_{Ox}}{dt} = k_3 C_{TH} - k_5 C_T C_{Ox} = 0; \quad C_{Ox} = \frac{k_3 C_{TH}}{k_5 C_T} \tag{5}$$

Taking into account expressions (3) and (3′), equation (2) becomes :

$$-\frac{\mathrm{d}C_{\mathrm{T}}}{\mathrm{d}t} = (k_2C_{\mathrm{I}^-} + 2k_3)\, C_{\mathrm{TH}} \tag{6}$$

$$= (k_2C_{\mathrm{I}^-} + 2k_3) \sqrt{K_1}C_{\mathrm{H_3O^+}}C_{\mathrm{T}} \tag{7}$$

$$= k_{\mathrm{obs}}C_{\mathrm{H_3O^+}}C_{\mathrm{T}} \tag{8}$$

where :

$$k_{\mathrm{obs}} = k_2 \sqrt{K_1}\, C_{\mathrm{I}^-} + 2k_3 \sqrt{K_1} \tag{9}$$

At a given concentration of hydrogen ion, equation (8) can be written as follows :

$$-\frac{\mathrm{d}C_{\mathrm{T}}}{\mathrm{d}t} = k_{\mathrm{exp}}C_{\mathrm{T}} \tag{10}$$

where :

$$k_{\mathrm{exp}} = k_2\sqrt{K_1}\, C_{\mathrm{I}^-}C_{\mathrm{H_3O^+}} + 2k_3 \sqrt{K_1}C_{\mathrm{H_3O^+}} \tag{11}$$

The first term of this expression represents the rate constant (k_r) of the oxidoreduction reaction between Co (III) complex and I^- in acid media; the second term is the rate constant of the acid catalysed thermal decomposition of the same complex (k_t). Therefore, the rate constant calculated from our experimental data appears as a sum of two terms :

$$k_{\mathrm{exp}} = k_r + k_t \tag{12}$$

The k_r values calculated by using relationship (12) are listed in table 1 (column c). The activation energies of the oxidoreduction reaction at different H^+ ion concentrations are shown in table 2 (column c).

Table 2

Activation energies of the reactions studied : a) overall reaction ; b) thermal decomposition ; c) oxidoreduction reaction

C_{HCl} (M)	Activation energies (kcal. mol^{-2})		
	a	b	c
3.40	26.5	29.9	15.1
2.55	27.9	30.0	12.3
1.70	30.2	31.9	8.0
0.85	31.4	32.9	5.5

As can be seen easily from these presentations, the rate constants of the oxidoreduction process are smaller than those of the thermal decompositions under given working conditions. This difference is more pronounced by increasing the temperature. At a low concentration of H^+ ion and a high temperature, the redox reaction becomes negligeable.

It can be said summarized that the contribution of the redox path is less important than thermal decomposition way. This results may be a consequence of the large difference in the activation energy values (table 2, column b and c), which assumes that the constants of the thermal decomposition are characterized by a higher temperature coefficient.

Turning now to the discussion of the kinetic results in light of the suggested mechanism, it is resonable to assume that the rate determining step is represented by the formation of the seven-coordinated intermediate (step b).

In conclusion the oxidoreduction reaction between the trisoxalato Co (III) complex and I^- is more complicated than in the case of other Co (III) complexes previously studied, because this reaction cannot be investigated separately. But mechanistic outline is unique.

EXPERIMENTAL

Solid $[Co(C_2O_4)_3]K_3 \cdot 3H_2O$ was prepared by a standard method,[7] several times recrystallized from ethanol and analyzed for purity. Solutions of complex, KI and HCl were prepared by dissolving reagent in doubly distilled water.

Kinetic runs were made in a SP 800 Pye Unicam spectrophotometer, using a thermostated cell compartment, capable of temperature control ± 0.3°C. The reactions was followed at 40,45 and 50°C. Solutions of complex salt, KI and HCl were preequilibrated with respect to temperature prior to the preparation of the reaction mixture. After mixing and allowing for a suitable period of adjustment inside the spectrophotometer, the time-absorbance data were taken.

REFERENCES

[1] I. G. Murgulescu and G. Mincu, *Rev. Roumaine Chim.*, **23**, 471 (1978).
[2] I. G. Murgulescu and G. Mincu, *Rev. Roumaine Chim.*, **8**, 779 (1983).
[3] I. G. Murgulescu, G. Mincu and E. Jurconi, *Rev. Roumaine Chim.*, **25**, 1033 (1980).
[4] T. Oncescu and E. Jurconi, *Rev. Roumaine Chim.*, **22**, 1471 (1977).
[5] T. Oncescu and E. Jurconi, *Rev. Roumaine Chim.*, **21**, 985 (1976).
[6] N. S. Rowan, R. M. Milburn and M. Z. Hoffman, *Inorg. Chem.*, **11**, 2272 (1972).
[7] S. P. L. Sörensen, *Z. anorg. Chem.*, **11**, 1 (1896).

Revue Roumaine de Chimie, 28, *9–10*, 875–881 (1983)

INTERNAL ROTATION IN CHARGE TRANSFER COMPLEXES

MARIANA CIUREANU, V. E. SAHINI, M. CONTINEANU, FELICIA CORNEA and CORNELIA CERCASOV

National Institute of Chemistry, Polytechnic Institute of Bucharest,
Bucharest, Bd. Republicii 13, Romania

Received July 12, 1982

The results of a DNMR study of the molecular complex formed by iodine with N-(*p*-chlorothiocinnamoyl) piperidine are reported. The activation parameters for the hindered internal rotation about the C—N bond were determined by the line shape analysis method for both the free and complexed donor; the results revealed a considerable increase of the rotational barrier on molecular complexing.

1. INTRODUCTION

The barrier to internal rotation about the C—N bond has been extensively investigated by dynamic NMR. [1-8] Numerous studies were devoted to a systematic examination of the effect of electronic factors and steric constraints on the intramolecular motion. Despite this effort, there are very few information concerning the effect of molecular complexing on the rotational barrier in these compounds. [1,8-10] In a previous paper, [1] we have reported the results of a study performed on the molecular complexes formed by iodine with several donors of the N-(thiobenzoyl) piperidine series; the rotational barriers, determined from coalescence data ($\Delta G^{\neq}_{T_c}$) showed an increase in the complexed donors, as compared with the free molecules. The purpose of the present paper is to provide further information on this subject, using a complete line-shape analysis of the NMR spectra of the molecular complex formed by iodine with N-(p-chlorothiocinnamoyl) piperidine (I). The donor was chosen because of its convenient rotational rates in the absence of iodine; besides, ultraviolet and infrared spectroscopy data demonstrated the high ability of thiocinnamoylpiperidines to form molecular complexes with iodine.[11,12]

2. EXPERIMENTAL

The donor was prepared by the Willgerodt-Kindler method, as described in a previous paper, [11] and was purified by repeated recrystallizations from ethanol. The identity and purity of the compound was checked by chemical analysis, as well as by IR, NMR and UV spectroscopy. Bromophorm was chosen as a solvent because of its high boiling temperature, as well as because it is a very good solvent for thiopiperidines, iodine and for their complexes. In order to avoid acid catalysis by HBr traces which are usually present in bromophorm, the latter was kept over K_2CO_3 and freshly distilled before use. Iodine was purified by repeated sublimation. The solutions of the complex were prepared volumetrically. The equilibrium constants used to obtain the thermodynamic parameters of the complex (ΔH_f, ΔS_f) were determined by a modified form of the Benesi-Hillebrand method.[13]

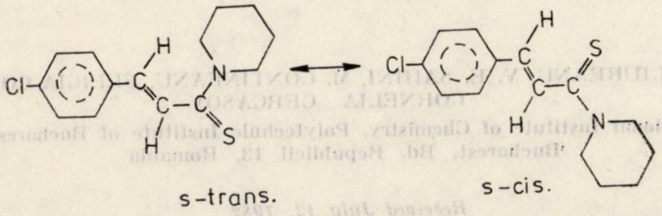

s-trans.   s-cis.

The ^1H—NMR spectra were recorded with a Tesla BD 487C spectrometer operating at 80 MHz in the frequency sweep mode. The chemical shifts measurements were made against internal HDMSO. The temperatures of the variable temperature probe were calibrated against a thermocouple. The precision of the temperature measurements was of 0.5°. The spectra were recorded at a sweep rate of 0.1 $Hz.s^{-1}$ and a scale factor of 5 $Hz.cm^{-1}$.

3. RESULTS AND DISCUSSIONS

The ^1H-NMR spectra of the free molecule, as well as of various donor-acceptor mixtures were recorded in bromophorm at temperatures ranging from 20 to 100°.

Chemical shifts

The assignment of the spectrum of (I) was made according to literature data : [15,14] the resonce signals at 4.21 and 3.77 ppm were assigned to the NCH_2 protons which are *syn*, respectively *anti*, to the C=S group ; in the following discussion, they will be used as sensors for the internal rotation about the C—N bond.

As seen from the example presented in Figure 1, the resonance of the anti NCH_2 is shifted to lower fields on complex formation, whereas the signal of the syn NCH_2 protons undergoes an upfield shift ; therefore, the separation of the maxima in the complex is lowered as compared with the free donor.

In order to provide information on this effect, we have recorded the spectra of various mixtures of (I) with iodine. Figure 2 presents the chemical shift difference of the two maxima ($\Delta = \sigma_s - \sigma_a$) as a function of the ratio $w = \frac{[A]_0}{[D]_0}$ ($[A]_0$ and $[D]_0$ are the initial concentrations of the acceptor and the donor). It may be seen that for $w > 1$, Δ approaches to a constant value. This behaviour can be rationalized in terms of the large formation constant of the complex, as presented in table 1 ; if the acceptor concentration is larger than that of the donor, the latter is practically entierly complexed, so that the observed shifts may be regarded to be the "pure complex shifts".

The observed complexation shifts of the NCH_2 resonances can be interpreted as discussed in a previous paper, [1] in terms of a superposition of three effects :

a) the decrease of the anisotropy of the thiocarbonyl group, which is expected to produce an important shielding of the syn NCH_2 protons.

Table 1

Thermodynamic parameters for the formation equilibrium of the complex

K_{298} 1 mole^{-1}	$-\Delta G^0_{298}$ kJ·mole^{-1}	$-\Delta H^0_f$ kJ·mole^{-1}	$-\Delta S^0_f$ J·mole^{-1}K^{-1}
16500	23.8	26.6	9.17

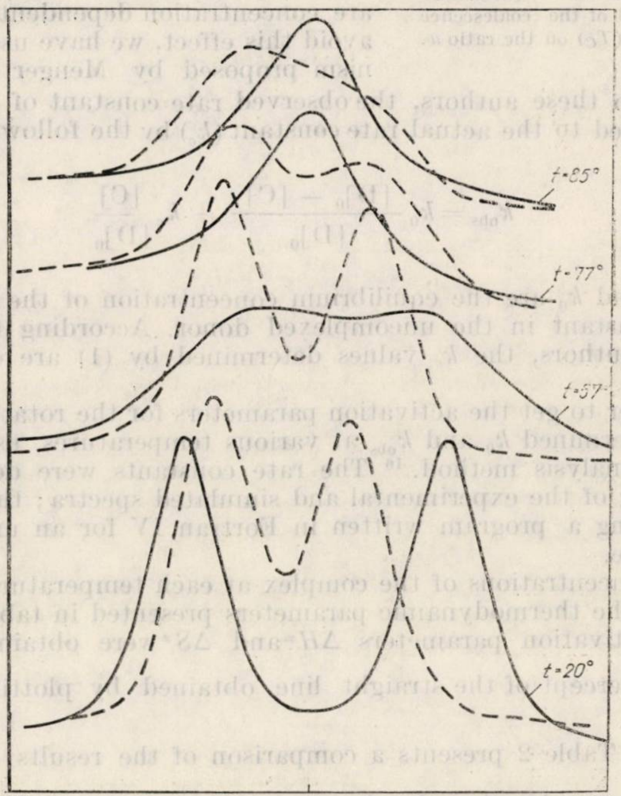

Fig. 1. — Typical examples of NMR spectra of free (——) and complexed (— — —) (I) at several temperatures (4.3 — 3.6 ppm range)

b) the increase of the anisotropy of the C—N bond (owing to the increase of the double bond character) which produces comparable deshieldings of the *syn* and *anti* protons.

Effects a) and b) may be regarded as a consequence of the increase of the weight of the polar structure II (Scheme 1).

c) the decrease of the electron density on the nitrogen atom, owing to the intermolecular charge transfer.

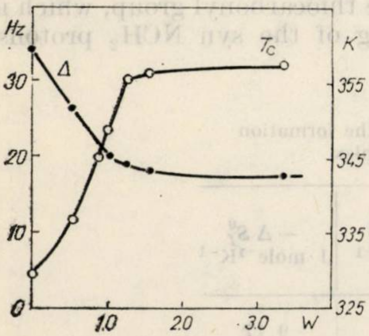

Fig. 2. — Dependence of the signal separation (measured at 20°C) Δ and of the coalescence temperatures (T_C) on the ratio *w*.

Activation parameters for the internal rotation about the C—N bond

The results of a preliminary study on the coalescence temperatures (T_c) of the complex solutions revealed a dependence on the donor/acceptor ratio (Fig. 1). It may be inferred that the observed rate constants are concentration dependent. In order to avoid this effect, we have used the mechanism proposed by Menger and Saito. [9] According to these authors, the observed rate constant of the complex k_{obs}) is related to the actual rate constant (k_c) by the following equation :

$$k_{\text{obs}} = k_0 \frac{[\mathrm{D}]_0 - [\mathrm{C}]}{[\mathrm{D}]_0} + k_c \frac{[\mathrm{C}]}{[\mathrm{D}]_0} \tag{1}$$

where [C] and k_0 are the equilibrium concentration of the complex and the rate constant in the uncomplexed donor. According to the above mentioned authors, the k_c values determined by (1) are concentration independent.

In order to get the activation parameters for the rotational process, we have determined k_0 and k_{obs} at various temperatures, using the total line shape analysis method. [16] The rate constants were determined by visual fitting of the experimental and simulated spectra ; the latter were obtained using a program written in Fortran IV for an uncoupled two site exchange.

The concentrations of the complex at each temperature were calculated using the thermodynamic parameters presented in table 1.

The activation parameters $\Delta H^{\neq}$ and $\Delta S^{\neq}$ were obtained from the slope and intercept of the straight line obtained by plotting $\ln \left(\frac{k}{T}\right)$ versus $\frac{1}{T}$. Table 2 presents a comparison of the results obtained for the free and complexed molecule.

The data presented in table 2 reveal a considerable increase of the rotational barrier on molecular complexing, which is in agreement with previous reports on the charge transfer complexes of various types of amides and thioamides.[8,9] This behaviour is consistent with an increase of the weight of the polar structure II in the complex. This idea is supported by the results obtained theoretically using HMO calculations on

Table 2

Activation parameters for the internal rotation about the C—N bond in free and complexed(I)

	Free donor	Complex
$\Delta H^{\neq}$ (kJ·mole^{-1})	78.3 ± 2.1	94.9 ± 3.0
$\Delta G^{\neq}$ (kJ·mole^{-1})	70.8 ± 0.2	83.9 ± 0.3
$\Delta S^{\neq}$ (J·K^{-1}·mole^{-1})	25.20 ± 2.9	36.7 ± 3.6

a simple whole molecule model : the data reveal an increase of the p_{CN} bond order in the complex, as compared with the free molecule (Table 3).[11] A similar conclusion was obtained from infrared data, which revealed an increase of the frequency of the C—N stretching mode on molecular complexing (Table 3).

Table 3

HMO calculations and infrared spectroscopic data

		Free molecule	Complex
HMO data*	p_{CN}	0.4321	0.4447
	p_{CS}	0.6136	0.3815
	p_{CC}	0.5407	0.6369
IR data**	$\tilde{\nu}_{CS}$(cm^{-1})	1010	972
	$\tilde{\nu}_{CN}$(cm^{-1})	1489	1544

* The parameters used in the HMO calculations are those used in [11]

** The IR spectra were recorded in CCl_4

Selective broadening of the signals

Inspection of the example presented in Figure 1 reveals an important feature of the spectra of the complex solutions : the signal of the *anti* NCH_2 protons is broadened in comparison with the resonance of the *syn* protons. The difference in the line widths of these signals was found to increase with temperature. These observations are in agreement with an exchange between two conformers, due to restricted rotation about the C—C(S) bond (Scheme 2).

The existence of these conformers, as well as their relative populations was studied by Fulea and Krueger [14] for uncomplexed N—(thiocinnamoyl)-piperidines and -morpholines ; for the second class, the population of the s-*trans* conformer was found to be small at lower temperatures,* but to increase at higher temperatures. For the N-(thiocinnamoyl)-piperidine class, the s-*cis* conformer was found to predominate in the whole temperature range.

---

* The relative population of the s-*trans* conformer is 1/15 at —30°C for N-(p-chlorothiocinnamoyl) morpholine.[14]

It seems reasonable to assume that on molecular complexing, a relative stabilization of the minor rotamer (s-*trans*) may occur, since the

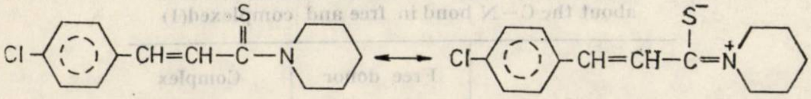

I. II.

iodine coordination defavours sterically the s-*cis* conformer. The increase of the s-*trans* conformer population with the temperature could therefore explain the selective broadening of the *anti* signal at higher temperatures[17] (the separation of the s-*cis* and s-*trans* signals is larger for the *anti* than for the *syn* protons)**.

CONCLUSIONS

The rotational barrier for the hindered internal rotation about the C—N bond was found to increase on molecular complexing. This observation pleads in favour of an increase of the weight of the polar structure II, produced as a consequence of the iodine coordination at the sulphur atom. A tentative explanation of the selective broadening of the *anti* signal was given in terms of an exchange between two rotational conformers (s-*cis* ⇄ s-*trans*).

REFERENCES

[1] M. Ciureanu, F. Cornea, C. Cercasov and M. Contineanu, *Rev. Roumaine Chim.*, **26**, 659, (1981).

[2] W. E. Steward and T. H. Siddall III, *Chem. Rev.*, **70**, 517 (1970).

[3] L. M. Jackman in "Dynamic Nuclear Magnetic Resonance Spectroscopy", Ed. L. M. Jackman and F. A. Cotton, Academic Press, New York, 1975.

[4] M. Ciureanu, V. E. Sahini, F. Cornea, C. Cercasov and M. Contineanu, *Org. Magn. Reson.*, **15**, 148 (1981).

[5] C. Piccini-Leopardi, O. Fabre, D. Zimmermann, J. Reisse, F. Cornea and C. Fulea, *Canad. J. Chem.*, **55**, 2649 (1977).

[6] U. Berg. *Acta Chem. Scand.*, B**30**, 695 (1976).

[7] S. Sandstrom, *J. Phys. Chem.*, **71**, 2318 (1967).

[8] W. Walter, E. Schaumann and J. Voss, *Org. Magn. Reson*, **3**, 733 (1971).

[9] F. Menger and G. Saito, *J. Org. Chem.*, **40**, 2003 (1975).

** It should be noted that the selective broadening of the *anti* signal was observed in a temperature range in which the rotation about the C—C(S) bond is rapid in the free molecule ; however, this observation does not affect the conclusions of the above discussion, since it is reasonable to assume that the activation energy for the internal rotation about the C—C(S) bond increases on molecular complexing.

[10] T. H. Siddal III, E. L. Pye and W. E. Stewart, *J. Phys. Chem.* **74**, 595 (1970).

[11] F. Cornea, C. Cercasov and M. Ciureanu, *Spectrochim. Acta*, **36**A, 775 (1980).

[12] F. Cornea, C. Fulea and S. Moldoveanu, *Rev. Roumaine Chim.*, **19**, 429 (1974).

[13] F. Rossoti and H. Rossoti, "Otpredelenie konstantystoitshivosti i drugih konstant ravnovesia b rastvorov", Izd. Mir, Moskwa, 1965.

[14] A. O. Fulea and P. J. Krueger, *J. Molec. Struct.*, **36**, 253 (1977).

[15] M. Ciureanu, C. Cercasov, F. Cornea and M. Contineanu, *Rev. Chim. (Bucureşti)*, **32**, 861 (1981).

[16] O. Sutherland in "Ann. Rep. on NMR Spectroscopy", vol. 4, Ed. E. F. Mooney, New York, 1971.

[17] A. Liden, C. Roussel, T. Liljefors, M. Chanon, R. E. Carter, J. Metzger and J. Sandstrom, *J. Amer. Chem. Soc.*, **98**, 2853 (1976).

Revue Roumaine de Chimie, **28**, *9–10*, 883–890 (1983)

ELECTROCHEMICAL SENSORS FOR ANIONIC SURFACTANTS. I.

THE ELECTRODE BASED ON BIS[2, 4, 6-TRI(2-PYRIDYL)-1, 3, 5-TRIAZINE] IRON (II) DODECYL SULPHATE

PAK u SĂP, D. F. ANGHEL and C. LUCA
Institute for Chemical Research, Department of Chemical Physics, Splaiul
Independenței 202, R–77208, Bucharest, Romania

Received December 15, 1982

It is proposed a new type of dodecyl sulphate selective electrode based on *bis* [2, 4, 6-tri (2-pyridyl)-1, 3, 5-triazine] iron (II) complex cation. The concentration of the active substance in the membrane mediator (*i.e.* nitrobenzene) was of 10^{-3} M. The electrode has a nernstian slope within the activity range $7.1 \times 10^{-6} - 1.4 \times 10^{-3}$ M of dodecyl sulphate. Its behaviour does not depend on pH in the 4.5 – 9.0 range. The electrode has a good selectivity with respect to inorganic interferents. Among the organic anions, only the surfactant ones do interfere. The sensor allows determination of critical micelle concentration, both in the absence and in the presence of inorganic electrolytes. It has also been used as end-point detector in potentiometric titration of ionic surfactants and to determine the anionic surfactant content of the micellar solutions designed for enhanced oil recovery.

Surfactant-sensitive ion-selective electrodes are specially designed sensors to monitor the changes of surfactant ion activity in the solution. With respect to their active substance, various sensors were proposed. Thus, there are electrodes based on ion-pairs of anionic surfactants with cationic ones [1–12] and basic dyes. [13] Metal/metal soap, [14–16] ion-exchange resins [17–20] and polyvinyl chloride with grafted ionic groups at the end of the macromolecule [21] were used to develop these sensors. Recently, a new type of active substance was introduced. It consists of ion-association compounds of anionic surfactants with transition metal cation complexes. [22–30] The transition metals used were iron, [22–25] cobalt [26–29] and ruthenium, [30] whereas 1,10-phenanthroline, [22–24,26–29] dimethylglyoxime, [26,27,29] diphenylglyoxime [28] and a porphyrine derivative (*i.e.* the hemine dimethyl ester [25]) were the ligands.

In order to extend the field of the active substance of surfactant selective electrodes, the possibility of obtaining a dodecyl sulphate selective electrode based on the complex cation of iron (II) with 2,4,6-tri (2-pyridyl)-1,3,5-triazine was investigated. The electrode was thoroughly characterized and used in anionic surfactant analysis from micellar solutions designed for enhaced oil recovery.

EXPERIMENTAL

Surfactant selective electrode

The complex cation of iron (II) with 2, 4, 6-tri(2-pyridyl)-1, 3, 5-triazine was obtained taking into account the literature data.[31, 32] The metal-ligand molar ratio was of 1 :2, the reaction being made at $pH = 5$ (acetate buffer) in reducing medium (hydroxyl amine chlorohydride). The deep violet coloured complex cation was extracted in nitrobenzene in the presence of dodecyl sulphate so that the concentration of the active substance in the organic phase was of about 10^{-3} M. This solution was used to fill up the electrode reservoir. A liquid-state electrode similar with those previously described[33] was used.

Apparatus

The potential measurements were made by means of an IAMC—Otopeni pH-100 digital pH-meter. The reference electrode was the saturated calomel one.

Reagents

Reagent grade chemicals were used. They were supplied by : SERVA (sodium dodecyl sulphate), AUSTRANAL 2, 4, 6-tri (2-pyridyl)-1, 3, 5-triazine, MERCK (various types of sodium alkyl sulphates and alkane sulphonates, and alkyldimethylbenzylammonium chloride, $M = 365.5$) and FLUKA (Hyamine 1622 and hexadecyldimethylbenzylammonium chloride) All other reagents were supplied by REACTIVUL Bucharest.

To prepare the solutions, distilled water was used.

RESULTS AND DISCUSSION

Electrode characterization

The electrode was calibrated in sodium dodecyl sulphate solutions in the absence and in the presence of inorganic electrolytes. The obtained results are presented in figure 1. In the absence of inorganic electrolyte (Fig. 1, curve 1), the calibration curve has a characteristic feature for these electrodes. At low surfactant levels, near the detection limit, the response is not linear. Between 7.1×10^{-6} and 1.4×10^{-3} M the electrode response is a linear function of dodecyl sulphate activity with a slope of 60 mV/dodecyl sulphate decade. Then, the slope gradually lowers, and at 5.0×10^{-3} M SDS it changes from negative slope (downscale) to positive slope (upscale). Among these zones, the most important is the minimum point that marks the appearance of the micellar aggregates in the solution. However, the critical micelle concentration (CMC) value determined by means of the electrode is lower than the CMC range ($8.0 - 8.4 \times 10^{-3}$M)

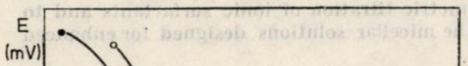

Fig. 1. — Calibration of dodecyl sulphate selective electrode in the absence (1) and in the presence of 0.1 M NaCl (2).

quoted in the literature for sodium dodecyl sulphate.[34] This can be assigned to nitrobenzene employed to develop the liquid membrane of the electrode since such a behaviour was also reported in the case of some other surfactant selective electrodes containing this compound as solvent.[3]

In the presence of inorganic electrolytes (*i.e.* 0.1 M NaCl), the electrode response is linear between 1.0×10^{-5} and 1.0×10^{-3} M SDS (see curve 2 on Fig. 1). Sodium chloride does not affect the electrode slope, but shifts the calibration curve 18 mV towards more positive potential values. Behind CMC (1.0×10^{-3} M SDS), the electrolyte effect is a practical constant response on the electrode. In this case too, the CMC value is lower than the literature one (1.4×10^{-3} M SDS).[34,35]

The influence of hydrogen ions on electrode sensitivity was then determined. To this end, the surfactant concentration was kept constant to 10^{-3}M SDS, and the pH was changed by means of hydrochloric acid and sodium hydroxide. The modification of pH was monitored with a glass electrode. After each pH changing, it was waited until the surfactant selective electrode stabilized its reading. The results are given in figure 2. The recorded e.m.f. *vs.* pH curve points out two plateaus. The first one lies between the pH values of 1.0 and 2.8. It may be assigned to the protonation of the complex used as electrode active substance. The second plateau ranges between 4.5 and 9.0 pH values and agrees well with the pH field within which the iron (II)-2,4,6-tri(2-pyridyl)-1,3,5-triazine complex is not affected by the hydrogen ions from solution.[31,32]

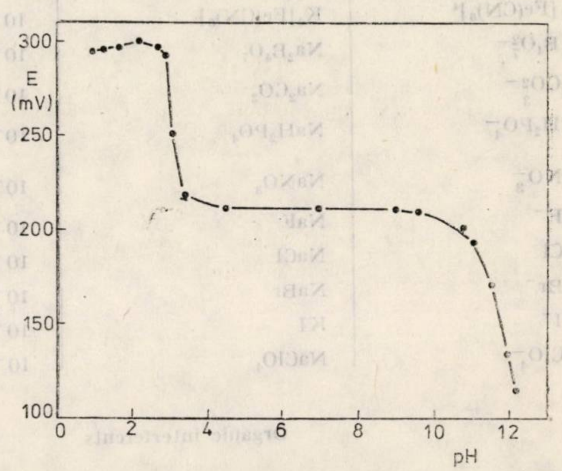

Fig. 2. — The influence of pH on the response of dodecyl sulphate selective electrode.

The selectivity coefficients of dodecyl sulphate selective electrode were determined by using the separate solution method. For a large number of inorganic and organic interferent anions, the results obtained are listed in table 1. The electrode is characterized by a good selectivity towards inorganic anions. Among the organic interferents tested, only those having surface active properties do interfere. For alkyl sulphates and alkane sulphonates, the interference rises as the hydrophobic character of the compounds increases.

Table 1

Selectivity coefficients, $k_{DS^-/A^{n-}}$, of dodecyl sulphate selective electrode

Interferent anion, A^{n-}	Used salt	Interferent concentration	pH	$k_{DS^-/A^{n-}}$
Inorganic interferents				
HPO_4^{2-}	Na_2HPO_4	10^{-3} M	7.3	$<10^{-5}$
$S_2O_3^{2-}$	$Na_2S_2O_3$	10^{-3} M	7.1	$<10^{-5}$
SO_4^{2-}	Na_2SO_4	10^{-3} M	6.1	$<10^{-5}$
NO_2^-	$NaNO_2$	10^{-3} M	5.9	$<10^{-5}$
SO_3^{2-}	Na_2SO_3	10^{-3} M	6.0	$<10^{-5}$
$[Fe(CN)_6]^{4-}$	$K_4[Fe(CN)_6]$	10^{-3} M	7.5	$<10^{-5}$
$B_4O_7^{2-}$	$Na_2B_4O_7$	10^{-3} M	8.7	1.4×10^{-4}
CO_3^{2-}	Na_2CO_3	10^{-3} M	9.7	1.1×10^{-3}
$H_2PO_4^-$	NaH_2PO_4	10^{-3} M	5.0	1.0×10^{-3}
NO_3^-	$NaNO_3$	10^{-3} M	5.5	1.3×10^{-3}
F^-	NaF	10^{-3} M	5.9	1.3×10^{-3}
Cl^-	NaCl	10^{-3} M	5.9	1.3×10^{-3}
Br^-	NaBr	10^{-3} M	5.9	1.7×10^{-3}
I^-	KI	10^{-3} M	5.9	1.4×10^{-3}
ClO_4^-	$NaClO_4$	10^{-3} M	6.0	5.3×10^{-3}
Organic interferents				
$EDTA^{2-}$	Na_2EDTA	10^{-3} M	8.5	$<10^{-5}$
$Citrate^{3-}$	Sodium Citrate	10^{-3} M	5.6	$<10^{-5}$
$C_2O_4^{2-}$	$Na_2C_2O_4$	10^{-3} M	5.6	5.0×10^{-5}
CH_3COO^-	CH_3COONa	10^{-3} M	4.6	2.1×10^{-2}
$C_4H_9SO_3^-$	$C_4H_9SO_3Na$	10^{-3} M	5.6	1.1×10^{-2}
$C_8H_{17}SO_3^-$	$C_8H_{17}SO_3Na$	10^{-3} M	5.6	1.3×10^{-2}
$C_{12}H_{25}SO_3^-$	$C_{12}H_{25}SO_3Na$	10^{-3} M	5.6	1.2×10^{-1}
$C_6H_{13}SO_4^-$	$C_6H_{17}SO_4Na$	10^{-3} M	5.6	2.2×10^{-2}
$C_8H_{11}SO_4^-$	$C_8H_{19}SO_4Na$	10^{-3} M	5.6	4.8×10^{-2}
$C_9H_{19}SO_4^-$	$C_9H_{19}SO_4Na$	10^{-3} M	5.6	8.2×10^{-2}
$C_{10}H_{21}SO_4^-$	$C_{10}H_{21}SO_4Na$	10^{-4} M	5.6	1.5×10^{-1}
$C_{16}H_{33}SO_4^-$	$C_{16}H_{33}SO_4Na$	10^{-4} M	5.6	15.2
$C_{18}H_{37}SO_4^-$	$C_{18}H_{37}SO_4Na$	10^{-4} M	5.6	21.0
$C_{20}H_{37}O_7S^-$	$C_{20}H_{37}O_7SNa$*	10^{-4} M	5.6	2.8
$C_{12}H_{25}C_6H_4SO_3^-$	$C_{12}H_{25}C_6H_4SO_3Na$	10^{-3} M	5.6	1.7

* $C_{20}H_{377}SNa$ is sodium di(2-ethylhexyl) sulphosuccinate

Applications

Since anionic surfactants do interfere in the response of dodecylsulphate selective electrode, the last one has been used as end-point detector in potentiometric titration of ionic surfactants. For example, in figure 3 are shown the curves recorded at potentiometric titration of some sodium alkyl sulphates with alkyldimethylbenzylammonium chloride (BAC). It is to be noted that the potential jump to equivalence rises as the surfactant hydrocarbon chain gets longer. This leads to the conclusion that the solubility products of anionic-cationic surfactant ion-pairs similarly lower.

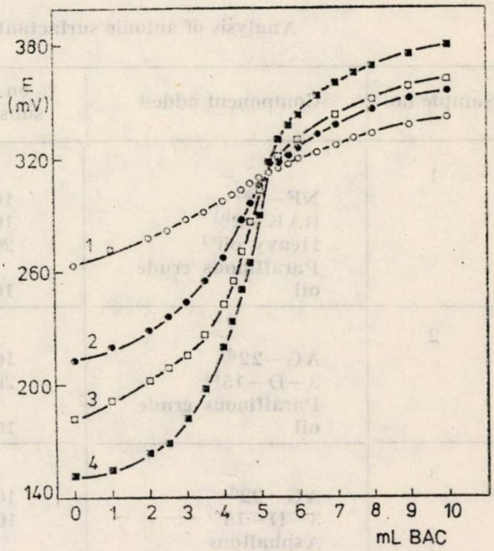

Fig. 3. — Titration curves of various alkyl sulphates with alkyldimethylbenzylammonium chloride (BAC) 0.004 M solution : (1) sodium octyl sulphate, (2) sodium decyl sulphate, (3) sodium dodecyl sulphate and (4) sodium hexadecyl sulphate plus 5% by volume iso-propanol.

Another field of application of the electrode is that of determining anionic surfactants from micellar solutions used in the process of oil recovery. Micellar solutions are thermically stable systems made of water (containing electrolytes), hydrocarbon (usually crude oil), surfactant (of anionic or nonionic type) and cosurfactant. The cosurfactant is a polar organic compound like: alcohols, aldehydes, ketones, ethers, esters etc., containing in the molecule 1—20 atoms of carbon.[36] During the oil displacement tests, the micellar solutions proved to be able of recovering more than 90% of the oil in place.

Because of the crude oil, the micellar solutions are deeply coloured. When they are dispersed in water, turbid and coloured emulsions are obtained. On the other hand, surfactants do contain by-products of their synthesis that made impossible to perform results by classical surfactant analytical methods. In this respect, it is worthy to mention the comparative study of anionic surfactant analysis from micellar solutions by means of three different two-phase titration methods. The reported results were affected by relative errors that sometimes amounted to about 11%.[37]

To determine the influence of various components of the micellar solutions on potentiometric analysis of anionic surfactants, the ingredients were added in turn to the system. The titrant was the 0.004 M hexadecyldimethylbenzylammonium chloride solution because it allows better determination of the equivalence point than Hyamine 1622 does. Table 2 points out the obtained results. It can be noticed that none of the tested ingredients, even if present in higher amounts than practically encountered, do interfere with anionic surfactant analysis (relative error $<2.5\%$). Hence, potentiometric titration can be used to determine the anionic surfactant content of micellar solutions designed for enhanced oil recovery with better results than two-phase titration methods.

Table 2

Analysis of anionic surfactants from micellar solutions

Sample no.	Component added	% on active substance	Active substance (%)	Relative error (%)
1	—	—	9.09	—
	NF$-$3[a)]	100	9.03	-0.66
	RAK$-$2[b)]	100	9.07	-0.22
	Heavy oil[c)]	200	9.10	$+0.11$
	Paraffinous crude oil	100	9.08	-0.11
2	—	—	6.61	—
	AG$-$22[d)]	100	6.55	-0.91
	3$-$D$-$15[e)]	200	6.59	-0.30
	Paraffinous crude oil	100	6.65	$+0.60$
3	—	—	8.47	—
	AG$-$22[d)]	100	8.41	-0.71
	3$-$D$-$15[e)]	100	8.50	$+0.35$
	Asphaltous crude oil	100	8.55	$+0.94$
4	—	—	9.56	—
	p$-$CF$-$2[f)]	150	9.65	$+0.94$
	Heavy oil[c)]	100	9.62	$+0.63$
	Naphthenous crude oil	100	9.52	-0.42
5	—	—	7.78	—
	NF$-$3[a)]	100	7.84	$+0.77$
	Heavy oil[c)]	200	7.76	-0.26
	Asphaltous crude oil	100	7.81	$+0.39$
6	—	—	5.45	—
	NF$-$3[a)]	100	5.38	-1.26
	Heavy oil[c)]	100	5.38	-1.26
	KT$-$56[g)]	100	5.38	-1.26
	Naphthenous crude oil	200	5.40	-0.92

a) NF$-$3 is an alkylphenol polyxyethylene derivative; b) RAK$-$2 is an ethoxylated fatty acid: c) Heavy oil is a residue obtained from butanol preparation by oxo-synthesis; d) AG$-$22 is an ethoxylated fatty alcohol; e) 3$-$D$-$15 is an alcohol mixture mainly containing iso-amyl alcohol; f) *p*$-$CF$-$2 is an ethoxylated *p*-coumylphenol; g) KT$-$56 is a residue obtained as by-product during isoprene synthesis.

CONCLUSIONS

A new type of active substance for liquid-state surfactant selective electrodes was obtained. This substance is *bis*[2,4,6-tri(2-pyridyl)-1,3,5-triazine] iron (II) dodecyl sulphate. The electrode is similar, with respect to performances, to some other metal-complex based dedocyl sulphate selective electrodes previously described in the literature. [22-24] The electrode enables determination of critical micelle concentration both in the presence and in the absence of inorganic electrolytes. However, the obtained CMC values are lower than the literature data. By means of the electrode, an analytical method for determination of anionic surfactant from micellar solutions devoted to enhanced oil recovery process has been proposed. The method is more accurate than the classical two-phase titration procedures.

REFERENCES

[1] C. Gavach and P. Seta, *Analyt. Chim. Acta*, **50**, 407 (1970).

[2] C. Gavach and P. Bertrand, *Analyt. Chim. Acta*, **55**, 385 (1971).

[3] B. J. Birch and D. E. Clarke, *Analyt. Chim. Acta*, **61**, 159 (1972).

[4] B. J. Birch and D. E. Clarke, *Analyt. Chim. Acta*, **67**, 387 (1973).

[5] B. J. Birch, D. E. Clarke, R. S. Lee and J. Oakes, *Analyt. Chim. Acta*, **70**, 417 (1974).

[6] A. G. Fogg, A. S. Pathan and D. T. Burns, *Analyt. Chem. Acta*, **69**, 238 (1974).

[7] A. S. Pathan, *Proc. Soc. Analyt. Chem.*, **11**, 143 (1974).

[8] T. Fujinaga, S. Okazaki and H. Freiser, *Analyt. Chem.*, **46**, 1842 (1974).

[9] G. Popa, B. Geafar and C. Luca, *Rev. Chim.* (București), **25**, 748 (1974).

[10] G. Popa, B. Geafar and C. Luca, *Rev. Chim.* (București), **26**, 512 (1975).

[11] J. E. Newberry and V. Smith, *Colloid Polym. Sci.*, **256**, 494 (1978).

[12] A. Yamauchi, T. Kunisaki, T. Minematsu, V. Tomokiyo, T. Yamaguchi and H. Kimizuka *Bull. Chem. Soc. Jpn.*, **51**, 2791 (1978).

[13] N. Ishibashi and H. Kohara, *Bunseki Kagaku*, **21**, 100 (1972); *Chem. Abstr.*, **76**, 107667 (1972).

[14] F. van Voorst Vader, *Trans. Faraday Soc.*, **57**, 110 (1961).

[15] W. U. Malik and A. K. Jain, *J. Electroanal. Chem.*, **14**, 37 (1967).

[16] W. U. Malik and A. K. Jain, *Austral. J. Chem.*, **22**, 465 (1969).

[17] H. Small, *J. Amer. Chem. Soc.*, **90**, 2217 (1968).

[18] C. Botré, D. G. Hall and R. V. Scoven, *Kolloid Z. Z. Polym.*, **250**, 900 (1972).

[19] B. J. Birch and D. E. Clarke, *Analyt. Chim. Acta*, **69**, 473 (1974).

[20] T. S. Brun, H. Hoiland and E. Vikingstd, *J. Colloid Interface Sci.*, **63**, 590 (1978).

[21] S. G. Cutler, P. Meares and D. G. Hall, *J. Electroanal. Chem.*, **85**, 145 (1977).

[22] D. F. Anghel and N. Ciocan, *Colloid Polym. Sci.*, **254**, 114 (1976).

[23] N. Ciocan and D. F. Anghel, *Tenside Deterg.*, **13**, 188 (1976).

[24] N. Ciocan and D. F. Anghel, *Analyt. Letters*, **9**, 705 (1976).

[25] D. F. Anghel, N. Ciocan and G. Popescu, "Proceeding VII-th International Congress Surface Active Substances", Moscow 1976, Publ. 1977, vol. 1, p. 524.

[26] D. F. Anghel and N. Ciocan, *Analyt. Letters*, **10**, 423 (1977).

[27] D. F. Anghel, G. Popescu and N. Ciocan, *Mikrochim. Acta*, **2**, 639 (1977).

[28] N. Ciocan and D. F. Anghel, *Z. analyt. Chem.*, **290**, 237 (1978).

[29] D. F. Anghel, G. Popescu and F. Niculescu, *Tenside Deterg.* **17**, 171 (1980).

[30] D. F. Anghel, G. Popescu and D. Löwy, Paper submitted to *Rev. Chim.* (București).

[31] P. F. Collins and H. Diehl, *Analyt. Chim. Acta*, **22**, 125 (1960).

[32] B. G. Stephens, H. L. Felkel and W. M. Spinelli, *Analyt. Chem.*, **46**, 692 (1974).

[33] J. Ružička and J. Chr. Tjell, *Analyt. Chem. Acta*, **49**, 346 (1970).

[34] P. Mukerjee and K. J. Mysels, "Critical Micelle Concentrations of Aqueous Surfactant Systems", N. B. S. Publication, National Standard Reference Data Series, National Bureau of Standards, **36**, 51 (1971).

[35] M. L. Corrin and W. D. Harkins, *J. Amer. Chem. Soc.*, **69**, 683 (1947).

[36] S. C. Jones and K. D. Dreher, *Soc. Pet. Eng. J.*, **16**, 161 (1976).

[37] D. F. Anghel and G. Popescu, *Rev. Roumaine Chim.*, **23**, 251 (1978).

Revue Roumaine de Chimie, 28, 9–10, 891–902(1983)

NUEVA INSTALACIÓN PARA MEDIR LA PRESIÓN DE SATURACIÓN EN SISTEMAS MULTICOMPONENTES

RODICA VÎLCU, ZOICA CENUȘE, F. GOTHARD y VIELKA LANGSHAW

Cátedra de Físico Química y Tecnología Electroquímica,
Facultad de Instalaciones e Ingeniería de los Procesos Químicos, Instituto Politécnico de Bucarest, Ave. de la República Nr. 13.

Recibido el 3 de Noviembre de 1982

Una nueva instalación para la determinación de la presión del vapor saturado de mezclas líquidas multicomponentes, en función de la composición de la fase líquida ha sido construída para el intervalo de presión de 10–700 Torr. El principio de funcionamiento está basado en el método estático de medición de la presión del vapor saturado-método isotensioscópico. La instalación está constituída por cuatro partes principales : la célula donde se realiza el equilibrio, el sistema de medir y compensar la presión, el sistema de obtener vacío avanzado (10^{-5} Torr) y el sistema de desgasificación e introducción de las pruebas. Las presiones de saturación medidas en esta instalación tienen una precisión de ± 10^{-2} Torr.

A new static installation based on the isotensioscopic method (10–700 Torr) was designed. It has four principal parts : the equilibrium still, the measurement and compensation system, the vacuum system (10^{-6} Torr) and the degassing and sample introduction device. The precision of saturation pressure was about ± 10^{-2} Torr.

1. INTRODUCCIÓN

Para eliminar algunas desventajas del método de ebullición en masa de las mezclas líquidas, en especial referente a la no realización del estado de equilibrio real y para effectuar mediciones de equilibrio líquido-vapor también a las presiones altas se han realizado aparatos bazados en el principio estático.[1-10]

Estos aparatos junto con las instalaciones aferentes presentan innumerables ventajas debido al hecho que : permiten obtener informaciones amplias sobre el comportamiento de las mezclas en un intervalo grande de temperatura, presión y composición ; de la posibilidad de obtener datos isobáricos a partir de datos isotérmicos ; permite suprimir el análisis de la composición de la fase de vapor en equilibrio, lo que lleva a eliminar algunas fuentes de error vinculadas con la determinación experimental de la composición del vapor (ésta se puede establecer aplicando la ecuación de coexistencia[11] o aplicando otra técnica de cálculo—método Barker[12], método Mixon-Gumowski-Karpenter[13]) ; permite la síntesis de las mezclas con mayor exactitud que el análisis de éstas ; necesita cantidades pequeñas de los compuestos (1—5 g) para realizar las mediciones.

En base a estas consideraciones se ha construído una nueva instalación necesaria para obtener datos experimentales de equilibrio líquido-vapor en condiciones isotérmicas con gran precisión.

La nueva instalación representa la variante óptima, mejorada substancialmente en lo que se refiere al sistema de introducir y desgasificar las pruebas, de medir y compensar la presión de la instalación isotensioscópica[14], descrita detalladamente por R. Vîlcu y colaboradores[15].

La nueva instalación contiene las siguientes modificaciones :

a. se elimina la opción de extraer las pruebas para el analisis de la composición, substituyéndose con la síntesis de las mezclas ;

b. se utiliza una instalación de vacío de tipo IFA AV3 (100 l/s) que contiene una bomba de vacío preliminar (presión límite de 10^{-2} Torr) y una bomba de difusión (presión limite de 10^{-5} Torr) ;

c. se utiliza un solo manómetro MacLeod, el cual se coloca en el centro del tubo, que sirve para las operaciones de evacuación y transferencia de las sustancias entre los differentes dispositivos de la instalación ;

d. se introduce una célula adicional para desgasificar las sustancias necesarias para la síntesis de las mezclas ;

e. se utiliza un dispositivo para preparar ampollas cerradas conteniendo las sustancias en cantidades establecidas ;

f. se utiliza un dispositivo para transferir el contenido de las ampollas cerradas a la célula donde se realiza el equilibrio de fases ;

g. se introduce un dispositivo para preparar cinco ampollas en secuencia ;

h. se reduce al óptimo el volumen total del interior de la instalación disminuyendo la longitud y el diámetro del conducto de transferencia y de la línea de vacío, se reduce al mínimo el número de llaves que unen las partes componentes de la instalación.

2. PARTE EXPERIMENTAL

A. Descripción de la instalación para la determinación de la precision de saturatión

La instalación construida está indicada en la fig. 1.

Ella está provista de cuatro partes principales : la parte esencial de la instalación la constituye la célula de equilibrio, unida al sistema de medición y compensación de la presión, el sistema de obtención de vacío avanzado y el sistema de desgasificación e introducción de las pruebas.

La célula de equilibrio (1) es de construcción especial y está constituida por un vaso troncónico previsto de un brazo lateral unido a uno de los codos del manómetro differencial con mercurio (2) (el mercurio tiene además la función de aislar la prueba del resto de la instalación), los codos del manómetro se comunican entre ellos por medio de la llave r_8. El codo del manómetro (2) que no está unido a la célula de equilibrio, se comunica con el sistema de obtención de vacío, con el sistema de compensación de la presión y con el sistema de desgacificación e introducción de las pruebas. Para agitar el contenido de la célula se introduce una pequeña barra de hierro (14) cubierta de vidrio.

El sistema de obtención del vacío (10), está constituído por una instalación de tipo IFA AV3 (100 l/s) que a su vez está formada por una bomba de vacío preliminar que permite la obtención de una presión de 10^{-2} Torr en la instalación, una bomba de difusión que permite la obtención de una presión de 10^{-5} Torr, instrumentos de medir y controlar el vacío en las diversas porciones de la instalación, el sistema de enfriamiento de la bomba de diffusión y un vaso amortiguador.

El sistema de medir y compensar la presión se une al sistema de obtención de vacío por medio de la trampa (11) que permite la retención por congelamiento con sustancias o mezclas refrigerantes (en el caso de nuestras determinaciones se utilizó nitrógeno líquido) de cualquier vapor o gas condensable, que quede en el trayecto que comunica con la instalación, impidiéndose así la impurificación del aceite de las bombas de vacío.

El sistema de medición y compensación de la presión está constituido por el barómetro (4), que permite medir la presión de vapor del sistema. Las trazas de gas y de vapor que pueda contener el mercurio del barómtro (4), se eliminan conectando el barómetro al sistema de obten-

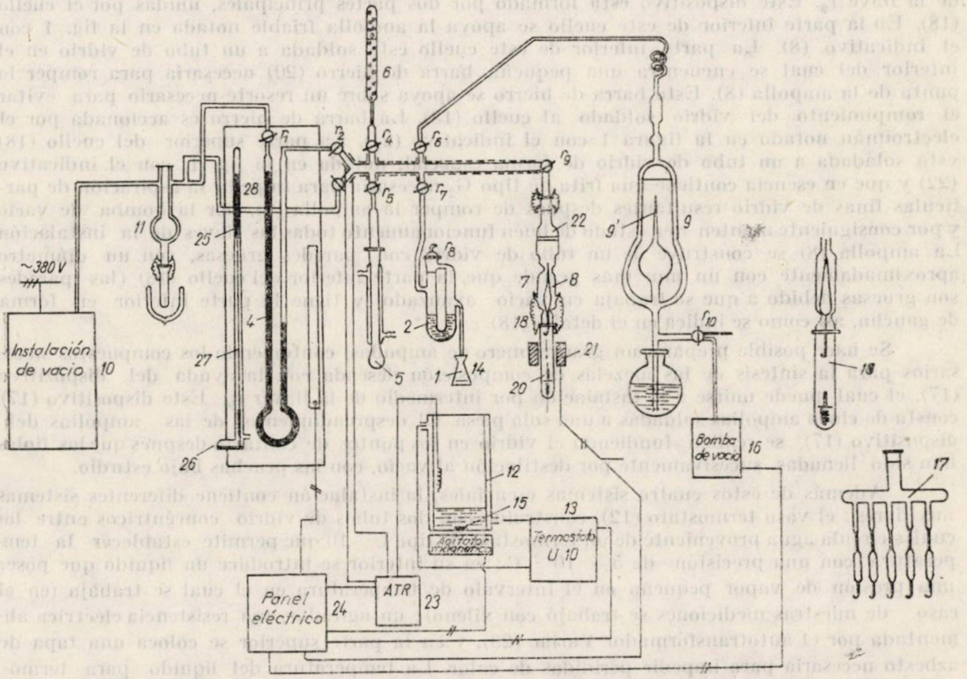

Fig 1. — Instalación para medir la presión de saturación.

ción de vacío por medio de la llave r_1. Esta llave se mantiene cerrada permanentemente después que se ha obtenido en la instalación la presión más baja posible ofrecida por el sistema de obtención de vacío.

El barómetro (4), se une en continuación a la instalación por medio de la llave r_2 ; al mismo tiempo el sistema de obtención de vacío se comunica con la instalación por medio de la llave r_3. La parte de compensación de la presión está prevista de un tubo de vidrio que, por intermedio de la llave r_4, se une a la línea principal de la instalación (3), y con la columna de absorción (6) constituida por un tubo de vidrio de 30 mm de diámetro lleno con gel de silicio activado a la temperatura de 110°C, utilizado para absorber los vapores y eventuales impurezas mecánicas que acompañan al aire introducido para compensar la presión que ejercitan los vapores.

El sistema de medición y compensación de la presión contiene además un manómetro MacLeod, que figura en la instalación con el indicativo (9), con la ayuda del cual se mide el vacío realizado en toda la instalación. El manómetro MacLeod está constituído, esencialmente por el capilar 9′ graduado con precisión (10^{-2} a 10^{-6} Torr) uniendose a la línea principal de la instalación (3), por medio de una espiral de vidrio (que proporciona gran flexibilidad) y a través de la llave r_6. En la parte inferior el manómetro MacLeod está unido por intermedio de la llave con dos pasos r_{10} a la atmósfera y a la bomba de vacío preliminar, que tiene el papel de evacuar el aire introducido en el manómetro durante las mediciones.

El sistema de desgasificación e introducción de las pruebas está provisto de la célula (5), soldada a un condensador ascendente que utiliza como líquido de recirculación agua y está unida a la línea principal de la instalación (3), por medio de la llave r_5.

El sistema de desgasificación e introducción de las pruebas contiene además el dispositivo de transferencia (7) el cual está unido a la línea principal de la instalación por medio de la llave r_9. Este dispositivo está formado por dos partes principales, unidas por el cuello (18). En la parte inferior de este cuello se apoya la ampolla friable notada en la fig. 1 con el indicativo (8). La parte inferior de este cuello está soldada a un tubo de vidrio en el interior del cual se encuentra una pequeña barra de hierro (20) necesaria para romper la punta de la ampolla (8). Esta barra de hierro se apoya sobre un resorte necesario para evitar el rompimiento del vidrio soldado al cuello (18). La barra de hierro es accionada por el electroimán notado en la figura 1 con el indicativo (21). La parte superior del cuello (18) está soladada a un tubo de vidrio de forma especial, notada en la fig. 1, con el indicativo (22) y que en esencia contiene una frita de tipo G_2 necesaria para impedir la aspiración de partículas finas de vidrio resultantes después de romper la ampolla (8), por la bomba de vacío y por consiguiente manten r en estado de buen funcionamiento todas las llaves de la instalación La ampolla (8) se construye de un tubo de vidrio con paredes gruesas, con un diámetro aproximadamente con un mm más grande que la parte inferior del cuello (18) (las parédes son gruesas debido a que se trabaja en vacío avanzado) y tiene la parte inferior en forma de gancho, así como se indica en el detalle (18).

Se hace posible preparar un gran número de ampollas, conteniendo los compuestos necesarios para la síntesis de las mezclas de composición deseada con la ayuda del dispozitivo (17), el cual puede unirse a la instalación por intermedio de la llaver r_9. Este dispositivo (17) consta de cinco ampollas soldadas a una sola piesa. El desprendimiento de las ampollas del dispositivo (17) se realiza fundiendo el vidrio en los puntos de contacto después que las fiolas han sido llenadas sucesivamente por destilación al vacío, con las pruebas bajo estudio.

Además de estos cuatro sistemas esenciales, la instalación contiene diferentes sistemas auxiliares: el vaso termostato (12), construído con dos tubos de vidrio concéntricos entre los cuales circula agua proveniente de un termostato de tipo U — 10 que permite establecer la temperatura con una precisión de 5×10^{-2} °C; en su interior se introduce un líquido que posea una presión de vapor pequeña en el intervalo de temperatura en el cual se trabaja (en el caso de nuestras mediciones se trabajó con xileno); un agitador, una resistencia eléctrica alimentada por el autotransformador Variac (23), y en la parte superior se coloca una tapa de azbesto necesaria para impedir péridiclas de calor. La temperatura del líquido para termostatar, y por consiguiente de la célula de equilibrio se mide con la ayuda de un termómetro de mercurio con precisión de 5×10^{-2} °C. Todos los termómetros de los sistemas auxiliares fueron verificados en comparación con un termómetro de referencia con puntos fijo (punto triple de ebullición del agua) y se eliminaron de la instalación termómetros cuyas escalas no coincidían con las temperaturas de los puntos fijos.

El vaso termostato se apoya sobre un agitador magnético de tipo IOR y tiene el papel de mantener la temperatura del líquido de la célula constante.

En los sistemas auxiliares está incluída, también, una resistencia eléctrica que calienta la línea principal de la instalación, alimentada por un autotransformador, el cual es alimentado a su vez con el panel de control 24.

B. Desgasificacion de las sustancias

La operación más importante para obtener resultados de gran precisión con el método isotensioscópico es la desgasificación de los compuestos que forman el eistema bajo estudio. Para asegurar una desgasificación completa del sistema esta operación se efectúa separadamente para cada compuesto puro en la célula (5), hirviendo el compuesto al vacío y evacuando periódicamente los gases nocondensables después de un congelamiento previo del sistema con nitrógeno líquido.

Para efectuar esta operación, la célula (5), se llena con la sustancia bajo estudio y se une a la instalación por medio del cuello superior de ésta. Se abren las llaves r_5 y r_3 y se evacua parcialmente el aire con la bomba de vacío preliminar. Se cierra la llave r_5 y se realiza un ciclo de ebullición y condensación sucesivas, la ebullición realizándose por la imersión de la célula en un baño con agua tibia y la condensación con la ayuda del condensador (6). Dicha operación tiene una duración de 30 minutos, después de la cual la célula se enfría gradualmente hasta congelar su contenido con nitrógeno líquido. Con la sustancia congelada se abre nuevamente la llave r_5 y se elimina instantáneamente el resto del gas no condensado con la ayuda de la bomba de difusión.

Se cierra la llave r_5, la sustancia alcanza nuevamente la temperatura ambiente, repitiéndose estas operaciones 4—5 veces hasta que se logra la evacuación completa de los gases, la cual se controla midiendo la presión con ayuda del manómetro MacLeod. Estas medidas se realizan abriendo la llave r_6, con la llave r_3 cerrada.

La operación de desgasificación de la sustancia puede ser considerada finalizada si no aparecen más burbujas de gas en el tiempo de descongelamiento, sin embargo es confirma solamente por la reproductibilidad de las presiones de vapor medidas.

El compuesto desgasificado se transfiere de la célula (5) directamente en la célula de equilibrio, si se desea medir la presión de vapor de una sustancia pura. En el caso en que se estudia la presión total de una mezcla, la substancia se transfiere en el dispositivo (17) adaptado para preparar las ampollas, con las cuales se hace la síntesis de las mezclas de composición dada.

C. Introducción de las sustancias en la célula de epuilibrio

La introducción de la sustancia en la célula de equilibrio se realiza del modo siguiente Se llena el manómetro diferencial con mercurio por intermedio de la llave r_8, y se coloca junto con la célula en la instalación. Se evacua el aire abriendo las llaves r_8, r_7 y r_3, primero con la bomba de vacío preliminar después con la bomba de vacío avanzado. El vacío se realiza también en los codos del tubo barométrico por medio de las llaves r_1 y r_2. En el tiempo de la evacuación se calienta la línea principal de la instalación, (3), con ayuda de una resistencia eléctrica montada desde la llaver r_3 hasta la llave r_9, para la desorción de los gases de la superficie interior del tubo. Con el mismo propòsito se calienta la célula de equilibrio y el manómetro diferencial.

La presión alcanzada en la instalación se controla con ayuda del manómetro MacLeod.

Después de evacuar el aire del circuito y de la célula, se cierra la llave r_3 y todas las llaves de la línea principal de la instalación. Se enfría la célula con nitrógeno liquido. Con la célula fría se abre la llave r_7 y después la llave r_5 ó r_9, donde se encuentra la sustancia bajo estudio. Después de transferir las cantidades deseadas de sustancia desgasificada, se cierra inicialmente la llave r_5 (ó r_9) y se esperan algunos segundos para que los gases de la línea se condensen en la célula. La finalización dela transferencia se controla abriendo la llave r_2, y el barómetro (4) no debe mostrar ninguna desnivelacón.

D. Preparación de las ampollas

Las ampollas necesarias para la síntesis de las mezclas de composición deseada se preparan con el dispozitivo (17). El dispositivo permite llenar sucesivamente 5 ampollas en el modo; siguiente : se evacua el aire con la bomba de vacío preliminar, después con la bomba de vacío avanzado y se calienta con la línea donde se realiza la transferancia. Se cierran todas las llaves de la línea principal de la instalación y se enfría la primera ampolla con nitrógeno líquido. Con la ampolla fría se abre la llave r_5 y se transfiera una cantidad de sustancia desgasificada. Se cierra la llave r_5 y se esparan unos minutos para que se condensen todos los gases de la línea en la ampolla. Se cierra la llave r_9 que une el dispositivo con la línea de transferencia. La ampolla se enfría y se desprende fundiendo el vidrio, asegurándose que al fundir el vidrio no quede ningún poro. La sección del vidrio donde se realiza la fundición es una sección capilar. La instalación se lleva de nuevo a la presión de 10^{-5} Torr. Después de verificar esta presión con la ayuda del manómetro MacLeod se enfría la siguiente ampolla y se transfiere otra cantidad de sustancia desgasificada.

Se ejecuta la misma operación para llenar cada ampolla.

Después que la ampolla se desprende, se lleva a la temperatura ambiente, se elimina la humedad condensada en las paredes exteriores y se pesa en una balanza analítica. Antes de pesar la ampolla la parte doblada en forma de gancho se lima ligeramente con carburo de silicio para que al romperse se desprenda un solo fragmento de vidrio. Se procede en forma similar con el segundo compuesto.

E. Síntesis de las mezclas

Las mezclas se preparan transfiriendo el contenido de las ampollas en la célula de equilibrio.

Con este propósito la ampolla llena y pesada se introduce en el dispositivo (7) por medio del cuello (18). Se coloca el dispositivo en la instalación, se evacua el aire abriendo la llave r_9 hasta obtener la presión de 10^{-5} Torr y se calienta el dispositivo para la desorción del vidrio. Se cierra la llave r_9 y se rompe la punta de la fiola con ayuda de la barra de hierro (20), accionada por el electroimán (21).

La transferancia se realiza abriendo inicalmente las llaves r_8 y r_7, con la célula enfriada con nitrógeno líquido y después se abre la llaver r_9. La velocidad de transferencia se puede controlar con la ayuda del mercurio del manómetro diferencial unido a la célula de equilibrio. Después de trafsferir completamente la cantidad de sustancia en la célula de equilibrio, enfriada con nitrógeno líquido, se cierran las llaves r_8 y r_9. Se desprende el dispositivo de transferencia, se recuperan y se pesan los restos de la ampolla quebrada, estableciéndose con precisión la cantidad de sustancia transferida.

En la célula de equilibrio conteniendo uno de los compuestos en cantidad conocida, se transfiere identicamente el contenido de otra ampolla con el otro compuesto. Después de efectuar una serie de mediciones con una mezcla así preparada de cantidades exáctamente pesada de los compuestos, la composición de la mezcla puede ser modificada transfiriendo una nueva cantidad de uno de los compuestos sobre el contenido de la célula de equilibrio, enfriada de antemano a la temperatura del nitrógeno líquido.

F. Medición de la presión de vapor

Para medir la presión de vapor de una sustancia pura o de una mezcla, la célula de equilibrio y el manómetro diferencial se introducen el vaso termostato (12). Se pone en función el agitador, se cierra la llave r_8 que permitió el paso de la sustancias en la célula de equilibrio y se abre la llave r_2 que comunica con el tubo barométrico (4).

Cuando el contenido de la célula de equilibrio alcanza la temperatura del termostato, la presión ejercida por el contenido de la célula crece. Esta presión es compensada introduciendo aire seco por medio de la llave r_4. La compensación de la presión se hace cuidadosamente demanera que los nivéles del mercurio en los codos del tubo barométrico se mantengan casi iguales.

El equilibrio termodinámico se alcanza en 10 – 15 minutos.

La presión de vapor, P, en la superficie del líquido en la célula representa la suma de las presiones hidrostáticas indicadas en la fig. 2.

$$P = (H_1d_1 + H_2d_2 + H_3d_3 + H_4d_4 + H_5d_5)g$$

donde $P_i = H_id_ig$, g es la aceleración de la gravedad = 9,81 ms^{-2} $H_1, H_2 \ldots H_5$ son las alturas indicadas en la fig. 2; d_1 la densidad del mercurio en el tubo barométrico, d_2 la densidad del aire en la porción de la instalación que sen encuentra a la temperatura ambiente, d_3 la densidad del aire en la porción de la instalación que se encuentra en el termostato, d_4 la densidad del mercurio en el manómetro differencial y d_5 la densidad de los vapores en la célula.

Debido a que $(H_3d_3 + H_4d_4 + H_5d_5)$ g/133,32 no sobrepasa el valor de 0,008 Torr, la presión P medida = $(L_1 - L_2) + (L_4 - L_5)$ Torr. Las lecturas se realizaron con la ayuda de un catetómetro con una precisión de 10^{-2} Torr, y se corrigieron con la relación:

$$h_s^0 = h_t(1 + \alpha(t - t_s))$$

donde: h_t es la distancia medida con la escala del catetómetro a la temperatura t; t_s es la temperatura a a cual fue calibrada la escala (= 20°C); α es el coeficiente de dilatación lineal del bronce ($18{,}4 \times 10^{-6}$/°C); y con la relación:

$$h_0^0 = h_t^0/(1 + \beta t)$$

donde β es el coeficiente de expansión volumétrica del mercurio ($181{,}8 \times 10^{-6}/^0C$)

Los manómetros fueron construídos con vidrio Pyrex con diámetro de 18 mm. El barómetro se colocó en una caja de madera y se cubrió con plástico. La temperatura del barómetro se midió con la ayuda de un termómetro de precisión de 0,1°C colocado en la caja entre los codos del tubo barométrico. El menisco del mercurio fue iluminado con una lámpara fluorescente de 40W colocada verticalmente junto a la caja.

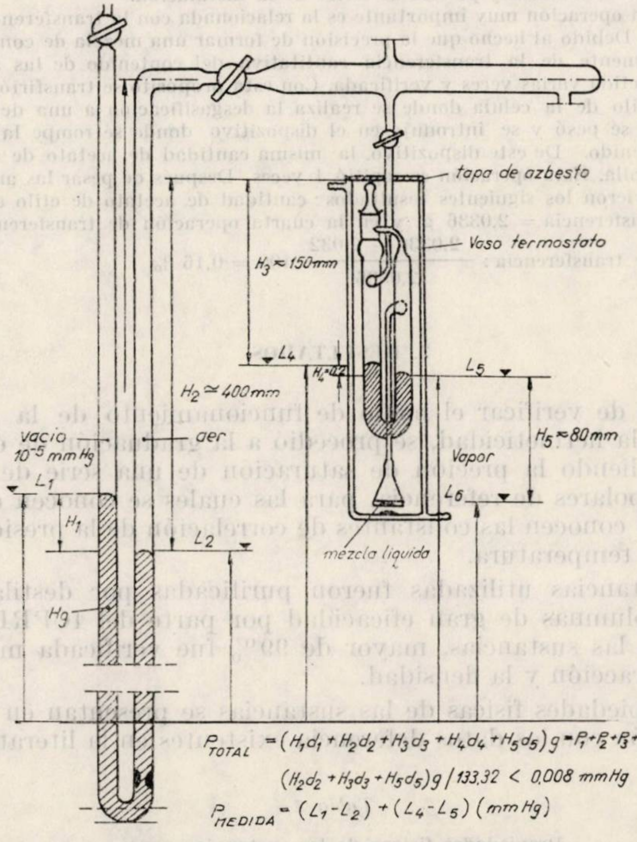
tapa de azbesto
Vaso termostato
$H_3 \approx 150mm$
L_4
$H_4 \approx 2$
L_5
$H_2 \simeq 400mm$
vacío
10^{-5} mm Hg
aer
$H_5 \approx 80mm$
Vapor
L_1
L_6
H_1
L_2
mezcla líquida
Hg
$P_{TOTAL} = (H_1d_1 + H_2d_2 + H_3d_3 + H_4d_4 + H_5d_5)g = P_1 + P_2 + P_3 + P_4 + P_5$
$(H_2d_2 + H_3d_3 + H_5d_5)g / 133{,}32 < 0{,}008$ mmHg
$P_{MEDIDA} = (L_1 - L_2) + (L_4 - L_5)$ (mm Hg)

Fig 2. — Esquema para indicar el modo en que se hacen las mediciones de presión de saturación[20].

La verificación del catetómetro se realizó efectuado 10 mediciones sobre la misma distancia, siendo la media aritmétrica de 414,07 y la desviación estándard de 0,0316.

G. Verificación del modo de funcionamiento de la instalacion

Antes de pasar a la determinación experimental propiamente, se verificó el modo de funcionamiento de todos los sistemas de la instalación para asegurar la obtención de resultados reproductibles. Entre éstas la verificación de que la instalación esté herméticamente cerrada y la transferencia cantitativa son las más esenciales.

La verificación de la hermeticidad consta en medir la velocidad de evacuación del aire de la instalación hasta una presión dada.

Con este propósito, después de realizar el vacío preliminar e instalar una presión de 10^{-2} Torr en la línea principal de la instalación, se realiza vacío avanzado con ayuda de la bomba de difusión hasta 10^{-5} Torr, midiéndose el tiempo necesario para instalar esta presión. Las mediciones se repitieron de 3 en 3 minutos, constatándose que el tiempo necesario para realizar vacío evanzado (10^{-5} Torr), después de instalara la presión de 10^{-2} Torr es de 9—10 minutos.

El control de la hermeticidad de la instalación se realizó también con un tester (VP 23 High Frequency Vacuum and Pore Tester Lybold Herner) con la ayuda del cual se localizaron poros en diferentes soldaduras y puntos de cierre de la instalación.

La segunda operación muy importante es la relacionada con la transferencia cantitativa de las sustancias. Debido al hecho que la precisión de formar una mezcla de composición dada depende esencialmente de la transferencia cantitativa del contenido de las ampollas, esta operación fue repetida varias veces y verificada. Con esta propósito se transfirió una cantidad de acetato de etilo de la célula donde se realiza la desgasificación a una de las ampollas. La ampolla llena se pesó y se introdujo en el dispozitivo donde se rompe la ampolla para transferir su contenido. De este dispozitivo, la misma cantidad de acetato de etilo se transfirió en otra ampolla. Esta operación se repitió 4 veces. Después de pesar las ampollas llenas y vacías se obtuvieron los siguientes resultados : cantidad de acetato de etilo en la primera operación de transferencia = 2,0336 g, y en la cuarta operación de transferencia = 2,032 g.

(Error relativo de transferencia : $\frac{2{,}0336 - 2{,}032}{2{,}0336}\, 100 = 0{,}16\ \%$

3. RESULTADOS

Después de verificar el modo de funcionamiento de la instalación y en especial la hermeticidad, se procedió a la graduación de ésta la cual se realizó midiendo la preción de saturación de una serie de sustancias polares y no polares de referencia, para las cuales se conocen datos de la literatura o se conocen las constantes de correlación de la presión de saturación con la temperatura.

Las sustancias utilizadas fueron purificadas por destilación fraccionada en columnas de gran eficacidad por parte del ICPRP—Ploiești. La pureza de las sustancias, mayor de 99% fue verificada midiendo los indices de refracción y la densidad.

Las propiedades fisicas de las sustancias se presentan en la tabla 1, en comparación con los datos deferencia existentes en la literatura.

Tabla 1

Propiedades fisicas de las sustancias puras

Sustancia	t de ebullición determinada con la ecuación Antoine (C°)	densidad		índice de refración		pureza %
		ρ medida (g/cc)	ρ de referencia (g/cc)	^{n}medido	^{n}de referencia	
benzeno	80,26	0,8790 (20°C)	0,87890[16]	1,4948 (30°C)	1,49486[16]	99,9
acetato de etilo	77,22	0,9000 (20°C)	0,90063[17]	1,3724 (20°C)	1,37239[17]	99,9
n-heptano	98,36	0,6840 (20°C)	0,68367[17]	1,3835 (30°C)	1,39312[17]	99.9

En las tablas (2), (3) y (4) se presentan, en forma comparativa con datos de la literatura, las presiones de saturación de 3 sustancias utilizadas para graduar la instalación, o sea : benzeno, acetato de etilo y n-heptano.

Tabla 2

Presiones de saturación del benzeno medidas y comparadas con datos de la literatura [18]

Temperatura (°C)	Presión medida (Torr)	Datos correlados con la ecuación Antoine	(ΔP/P)	Presión de referencia	(ΔP/P)
22,8	86,52	86,49	0,0003	85,94	0,0067
30,6	122,93	123,02	0,0007	122,60	0,0027
42,8	204,98	204,85	0,0006	204,83	0,0007
50,1	271,91	271,98	0,0003	272,35	0,0016

Los datos experimentales obtenidos fueron correlacionados con una ecuación de tipo Antoine, cuyas constantes se calcularon utilizando el método de los cuadrados mínimos en base a un programa de cálculo. La ecuación tiene la forma :

$$\log P = 6{,}95099 - \frac{1242{,}476}{t + 225{,}0}$$

La desviación relativa media es de 0,031 % en el caso de los datos propios, en comparación con 0,23 % en el caso de los datos obtenidos con la ecuación de Miller [18].

La ecuación propuesta por Miller para el benzeno es :

$$\ln P^s = 133{,}3127518 - \frac{8026{,}2913}{T} + 0{,}023929663T - 20{,}29 \ln T$$

Tabla 3

Presiones de saturación del acetato de etilo medidas y comparadas con datos de la literatura [19]

Temperatura (°C)	Presion medida (Torr)	Datos correlados con la ecuación Antoine	(Δ P/P)	Presión de referencia	(Δ P/P)
15,8	59,51	59,52	0,0002	59,46	0,0008
18,9	69,90	69,94	0,0006	69,86	0,0006
20,4	75,40	75,50	0,0013	75,35	0,0007
30,2	121,50	121,55	0,0004	121,19	0,0026
40,3	190,83	191,97	0,0008	190,45	0,0020

La temperatura de ebullición estándard del benzeno, obtenida de los datos propios es de 80,26°C.

Los datos experimentales obtenidos para el acetato de etilo fueron correlacionados con una ecuación de tipo Antoine, cuyos parámetros fueron calculados con el mismo método utilizado para el benzeno.

La ecuación tiene la forma:

$$\log P = 6{,}94723 - \frac{1167{,}96}{t + 210{,}00}$$

y permite la evaluación de la presión de saturación con una desviación relativa media de 0,0813 %. La temperatura estándard del acetato de etilo es 760 $t_{760} = 77{,}22°C$.

Los valores de referencia fueron calculados utilizando una ecuación Antoine, indicada por Hála [19] con una desviación relativa media de 0,13 %.

$$\log P = 7{,}1019 - \frac{1244{,}95}{t + 217{,}88}$$

En la tabla (4) se presentan los resultados de las medidas de presión de saturación del n-heptano como también los valores correlacionados y los valores de referencia. Correlacionando los datos medidos con la ecuación Antoine se obtiene:

$$\log P = 6{,}96835 - \frac{1305{,}41}{t + 221{,}00}$$

Esta ecuación predice la presión de saturación del n-heptano con una desviación relativa media de 0,26 %, la temperatura de ebullición estándard calculada con esta ecuación es $t_{760} = 98{,}36°C$.

Tabla 4

Presiones de saturación del n-heptano medidas y comparadas con los datos de la literatura [19]

Temperatura (°C)	Presión medida (Torr)	Datos correlados con la ecuación Antoine	($\Delta P/P$)	Presión de referencia	($\Delta P/P$)
18,8	33,44	33,46	0,0006	33,28	0,0048
23,4	42,35	42,37	0,0005	42,19	0,0038
30,2	58,9	59,11	0,0036	58,94	0,0007
35,1	74,5	74,31	0,0026	74,16	0,0046
40,5	95,00	94,69	0,0032	94,57	0,0045

4. CONCLUSIONES

La nueva instalación construída, para medir la presión de saturación de compuestos puros y mezclas líquidas, presenta numerosas mejoras constructivas y funcionales.

Desde el punto de vista constructivo se introdujeron las siguintes mejoras:

— la introducción de las sustancias en la célula de equilibrio y la evacuación del aire de ésta se efectuan sin necesidad de sacar el mercurio, gracias a la introducción de la llave que une une los codos del manómetro diferencial de la célula de equilibrio;

— la eliminación del conducto para extraer las pruebas del liquido de la célula de equilibrio asegura una mayor hermeticidad a la instalación;

— la detección inmediata de modificaciones en la presión causadas por las desajustes de las llaves, se effectúa con el manómetro Mac Leod colocado en la mitad de la linea principal de la instalación;

— se reduce al minimo el número de llaves y de cuellos estandardizados;

— se reduce el volumen de la instalación disminuyendo la longitud y el diámetro de los tubos de enlace a su valor óptimo, la célula de equilibrio y todas las partes componentes de la instalación, lo que permite obtener vacio avanzado aproximadamente en 20 minutos;

— para reducir al minimo los errores en las lecturas de los niveles del mercurio, tant o en el barómetro como en el manómetro diferencial, todas las columnas de mercurio se colocan en un mismo plano, de esta manera se pueden efectuar 4 lecturas sin modificar la posición de la luneta del catetómetro.

Desde el punto de vista funcional se introdujeron las siguientes mejoras:

— se sustituye el análisis final de las mezclas por la sintésis incial de éstas de composición conocida con gran precisión;

— permite llenar cinco ampollas consecutivemente y por consiguiente reducir el tiempo de trabajo;

— se asegura el funcionamiento continuo del aparato anadiendo a una cantidad conocida de uno de los compuestos, cantidades conocidas del otro compuesto, sin necesidad de vaciar la célula de equilibrio;

— se obtienen resultados con una precisión de 10^{-2} Torr en el intervalo de presión comprendido entre 10—700 Torr.

Las mejoras sustanciales introducidas a la instalación permitieron obtener presiones de saturación, así como puede apreciarse en las tablas presentadas, con desviaciones relativas medias más pequenas de centésimas de porcentajes y en buena concordancia con los datos publicados en la literatura.

BIBLIOGRAFIA

[1] M. L. Mc. Glashan y A. G. Williamson, *Trans. Faraday Soc.*, **57**, 588 (1961).
[2] R. W. Hermsen y J. M. Prausnitz, *Chem. Eng. Sci.*, **18**, 485 (1963).
[3] P. J. Maher y B. Smith, *J. Chem. Eng. Data*, **24**, 16 (1979).
[4] E. B. Munday, J. C. Mullins y D. Edie, *J. Chem. Eng. Data*, **25**, 191, (1980).
[5] I. P. C. Li, Y. W. Wong, S. D. Cheng y B. C. Lu, *J. Chem. Eng. Data*, **17**, 492 (1972).
[6] R. P. Tomlins y K. N. Marsh, *J. Chem. Thermodynamics*, **8**, 1185 (1976).
[7] E. Molga y J. Stecki, *J. Chem. Thermodynamics*, **9**, 79, (1977).
[8] J. Jaches, R. P. Phillipe y P. Clechet, *Bull, Soc. chim. France*, **8**, 2860, (1971).
[9] G. Scatchard, M. Wilson y F. Satkewicz, *J. Amer. Chem. Soc.*, **86**, 125 (1964).

[10] J. Ascheroff, D. A. Clayton, y R. Ghearn, *J. Chem. Eng. Data*, **24**, 3 (1979).

[11] H. C. Van Ness, ,,Classical Thermodynamicas of Nonelectrolyts Solutions", Pergamon Press, New York, 1969.

[12] J. A. Barker, *Austral. J. Chem.*, **6**, 207 (1953).

[13] F. O. Mixon, B. Gumowski y B. H. Carpenter, *Ind. Eng. Chem. Fundam.*, **4**, 455 (1965).

[14] F. Gothard, "Echilibre lichid-vapori", vol. **II**, Ed. Academiei, București, 1983.

[15] R. Vîlcu y Z. Cenușe, *Rev. Roumaine Chim.*, **25**, 763 (1980).

[16] J. Timmermans, "The Physico-Chemical Constants of Pure Organic Compounds", Elsevier Co. Inc., New York, 1950.

[17] S. Rașeev y S. Istrati, ,,Constante fizice principale ale hidrocarburilor și ale unor compuși organici", vol. **II**, Ed. Tehnică, București, 1964.

[18] D. C. Miller, *Ind. Eng. Chem.*, **56**, 46 (1964).

[19] E. Hála, I. Wichterle y J. Polak, "Vapour-Liquid Equilibrium Data at Normal Pressures", Pergamon Press, Oxford, 1968.

[20] F. Gothard, N. Neacșu, y Gr. Alexandrescu. Brevet R.S.R. no 65441 07.02.1973.

Revue Roumaine de Chimie, 28, *9–10*, 903–913 (1983)

SYNTHESE UND CHARAKTERISIERUNG EINIGER 4'-SUBSTITUIERTEN 4-AMINOAZOBENZENE. BESTIMMUNG DER BASIZITÄTSKONSTANTEN

I. HAVLIK, C. CSUNDERLIK, A. TOTH und R. BACALOGLU
Chemieforschungszentrum, Bd. Mihai Viteazul 24, 1900 Timișoara, Rumänien

Eingegangen am 26. Februar 1982

Es wurden Syntheseverfahren für 4'-substituierte 4-Aminoazobenzene von hohem Reinheitsgrad ausgearbeitet und diese Verbindungen wurden IR-, UV-VIS, ^{1}H-NMR-spektroskopisch charakterisiert. Es wurden ebenfalls die Basizitätskonstanten bestimmt. Diese physikalischen Eigenschaften wurden zur Bestimmung der elektronischen Struktur der 4'-substituierten 4-Aminoazobenzene benützt.

Synthetic procedures for 4'-substituted 4-aminoazobenzenes of high purity were developed. These compounds were characterized by IR, UV-VIS and ^{1}H-NMR spectroscopy, and their basicity constants were determined. These physical data were employed for discussing the electronic structure of 4'-substituted 4-aminoazobenzenes.

4-Aminoazobenzen und einige seiner 4'-substituierten Derivate sind Verbindungen die schon seit lange bekannt sind und als direkte basische Farbstoffe für Wolle, Seide und gegerbtes Leder oder mit Beizen für Baumwolle und andere Cellulosefasern verwendet wurden (4-Aminoazobenzen : Colour Index 11.000 Solvent Yellow 1 ; 4'-Nitro-4-aminoazobenzen : Colour Index 11.005 Disperse Orange 3 ; 4'-Dimethylamino-4-aminoazobenzen : Colour Index 11.025 Disperse Black 3). [1]

In vorliegender Arbeit wurden Syntheseverfahren ausgearbeitet für 4'-substituierte 4-Aminoazobenzene von hohem Reinheitsgrad, die in kinetischen Modelluntersuchungen für die Herstellung der reaktiven Triazinfarbstoffe Anwendung finden. Die synthetisierten Verbindungen wurden durch Elementaranalyse, IR-, UV-VIS- und KMR-Spektroskopie, sowie auch durch die Bestimmung der Basizitätskonstanten charakterisiert.

ERGEBNISSE UND DISKUSSION

Die 4'-substituierten 4-Aminoazobenzene wurden durch die Kupplungsreaktion der Diazoniumsalze der 4'-substituerten Aniline mit Anilin hergestellt, wobei die Aminogruppe durch die Reaktion mit der Bisulfitverbindung des Formaldehyds geschützt wurde. [2,3,4] Eine Ausnahme bilden die 4'-Dimethylamino- 4'-Hydroxy-4-aminoazobenzene, die durch die Kupplung des diazotierten *p*-Nitroanilins mit Dimethylanilin und Phenol, gefolgt von einer Reduktion mit Natriumsulfid [5] hergestellt wurden. Ebenso wurde 4-Aminoazobenzen durch eine Umlagerung des N^1, N^3-Diphenyltriazens [6] erhalten und die 4-Aminoazobenzen-4'-sulfonsäure durch Sulfonierung des 4-Aminoazobenzens. [4]

Die Verbindungen wurden durch Extraktion, fraktionierte Umkristallisierungen und Umfällen gereinigt, bis sie im Dünnschichtchromatogramm eine einzige Komponente aufwiesen. Die dünnschichtchromatographischen Untersuchungen wurden auf mit Silicagel G „Merck” bedeckten Platten, mit einer Schichtdicke von 0,25 mm durchgeführt und als Laufmittel Methylenchlorid (A) und Benzen-Aceton 16 :1 (B) in Anspruch genommen.

In Tabelle 1 sind die hergestellten Farbstoffe, die R_F-Werte für die zwei Laufmittel, die Schmelzpunkte und die Ergebnisse der Elementaranalyse zusammengefaßt. Man kann feststellen, daß die Verbindungen genügend rein sind, um spektroskopisch untersucht zu werden und um ihre Basizitätskonstanten bestimmen zu können.

In Tabelle 2 sind die Wellenlängen und die molaren Extinktionskoeffizienten der Absorptionsbanden im sichtbaren-UV-Bereich für die synthetisierten Verbindungen, in Methanol und Methylenchlorid enthalten.

Die aromatischen Azoverbindungen können zwei Diastereoisomere — Z und E — aufweisen, wobei das E-Isomer vorzugsweise erhalten wird.[21]

Die Azogruppe aus E-Azobenzen macht sich im Elektronenspektrum durch zwei Banden bemerkbar und zwar, eine verbotene bei verhältnismäßig großen Wellenlängen (443,3 nm in Ethanol), von geringer Intensität ($\lg \varepsilon = 2{,}71$) wegen des $n \rightarrow \pi^*$-Übergangs und eine erlaubte bei kleineren Wellenlängen (319,6 nm in Ethanol) von verhältnismäßig großer Intensität ($\lg \varepsilon = 4{,}33$). [22]

Wird eine elektronenspendende Gruppe in die para-Stellung eines der aromatischen Ringe eingeführt, erscheint ein bedeutender bathochromer Effekt [21, 22] (für 4-Aminoazobenzen der $\pi \rightarrow \pi^*$ -Übergang bei 398 nm [20]).

Die von uns bei Konzentrationen zwischen $4 . 10^{-5}$ M und $8 . 10^{-5}$ M aufgezeichneten Spektren gestatten in allen Fällen die Identifizierung des erlaubten $\pi \rightarrow \pi^*$-Übergangs, der bei einer Wellenlänge von 370 bis 444 nm (Tabelle 2, mit A bezeichnete Absorptionsbanden) und mit einer verhältnismäßig beträchtlichen Intensität ($\lg \varepsilon \cong 4{,}3-4{,}4$) erscheint. Wie gewöhnlich im Falle eines $\pi \rightarrow \pi^* \cong$ Übergangs, ruft eine Verringerung der Lösungsmittelpolarität einen hypsochromen Effekt hervor (Tabelle 2).

Eine Substitution in der 4'-Stellung des 4-Aminoazobenzens von verschiedenen Gruppen hat einen wesentlichen Einfluß auf die Lage der Bande im Spektrum, wobei aber die Intensität — in den Grenzen der experimentellen Fehler — praktisch konstant bleibt. Wird die Wellenlänge als Funktion der Hammet σ^--Parameter aufgetragen, erhält man eine zufriedenstellende Korrelation der Form :

$$\lambda = 33{,}8\sigma^- + 395{,}7 \text{ (nm)} \quad (r = 0{,}960)$$

Tabelle 1

Charakterisierung der synthetisierten 4, 4'-disubstituierten Azobenzene

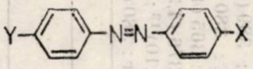

X	Y	Dünnschichtchtromatographie			Schmelzpunkt °C		Elementaranalyse					
		R_f^*(A)	R_f^{**}(B)	Fleckfarbe	bestimmt	Lit.	berechnet			gefunden		
							%C	%H	%N	%C	%H	%N
$(CH_3)_2N$	NH_2	0,38	0,17	braun	194–196	186–187[12]	69,97	6,71	23,31	69,61	6,42	23,11
HO	NH_2	0,13	uneluiert	gelb	191–192,5	–	67,59	5,2	19,71	66,96	4,97	19,56
H_3C	NH_2	0,43	0,38	gelb	156–158	151–152[7] 144–146[8]	74,00	6,2	19,9	74,2	6,00	19,72
H	NH_2	0,44	0,40	gelb	126–127	125–126[10]	73,07	5,62	21,3	73,36	5,67	21,12
Cl	NH_2	0,52	0,44	gelb	194–196	–	62,22	4,35	18,13	60,65	3,91	17,44
H_3C-CO	NH_2	0,32	0,16	gelb-orange	184–186	–	75,31	5,87	18,82	74,6	5,62	18,21
NO_2	NH_2	0,43	0,39	braun	212–214	216[9] 203–205[9]	59,5	4,16	23,13	60,3	4,22	22,65
COO^-Na^+	NH_2	uneluiert	0,44	gelb	unschmelzbar	–	65,0***	4,58***	17,5***	64,0***	4,48***	17,27***
$SO_3^-Na^+$	NH_2	uneluiert	0,19	gelb	unschmelzbar	–	52,17***	3,65***	15,21***	52,09***	3,73***	15,4***
$(H_3C)_2N$	NO_2	0,85	0,73	rot-violett	231–233	225–226[11]	62,21	5,22	20,72	61,76	5,07	20,23
HO	NO_2	0,35	0,22	gelb-orange	222–223,5	–	63,43	4,00	18,49	62,5	3,85	18,22

*) Laufmittel : Methylen chlorid

**) Laufmittel : Benzen – Aceton 16 : 1

***) Es wurden die freien Säuren analysiert

Tabelle 2

Die sichtbaren und ultravioletten Absorptionsspektren der synthetisierten 4, 4′-disubstituierten Azobenzene.

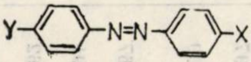

(die Wellenzahl des Absorptionsmaximums in nm und der Logarithmus des molaren Extinktionskoeffizienten — in Klammern).

X	Y	CH_3OH	$C_2H_4Cl_2$	H_2O	Literaturangaben
$(H_3C)_2N$	NH_2	B 256 (4,03) 322 (2,78) A 370 (4,34)	420 (4,48)	—	
HO	NH_2	B 251 (4,02) A 390 (4,39) C 418 (4,47) C 450 (4,47)	A 385 (4,40)	—	HCl 2N : 350 (4,36), 470 (3,83) NaOH 1N : 445(4,46)[18]
H_3C	NH_2	A 389 (4,37)	A 382 (4,40)	—	
H	NH_2	B 248 (3,94) A 390 (4,35)	A 382 (4,33)	—	Ethanol : 248 (3,97)[14] ; 388 (4.41)[18] ; 389 (4,76)[20] Ethylacetat : 380 (4,4)[15] ; Cyclohexan : 365 (4,43)[13] ; Wasser : 376 (4,32), 427 Inflex. (4,10)[13] ; Ethylether : 380 (4,45)[13]
Cl	NH_2	A 392 (4,19)	—	—	
H_3C-CO	NH_2	B 273 (4,12) A 420 (4,34)	A 404 (4,37)	—	
NO_2	NH_2	B 277 (3,98) A 444 (4,36)	273 (3,95) A 426 (4,31)	—	Ethanol : 442 (4,37)[18], 445 ; Wasser : 230 (4,5), 275 (4,5), 350 (4,1),390 (4,0)[19]
COOH	NH_2	B 268 (4,11) A 411 (4,41)	—	A 390 (4,23)	
SO_3Na	NH_2	B 262 (4,04) A 401 (4,39)	—	A 389 (4,03)	
$(H_3C)_2N$	NO_2	B 282 (4,11) A 481 (4,44)	A 482 (4,36)	—	Ethanol : 478 (4,52)[18], 295 (4,1), 479 (4,53)[17] ; Ethanol—HCl: 330 (3,81), 509 (4,79) ; Ethanol—pH0 :510 (4,78) ; pH 2 : 508 (4,7) ; pH 8 : 498 (4,47)[16] ; Benzen : 280 (4,1), 460 (4,5)[18] ; Petrolether : 280 (4,1), 430 (4,5) ; Methanol : 280 (4,1), 480 (4,5)[16]
HO	NO_2	B 256 (3,9) A 382 (5,35)	A 373 (4,37)	—	Ethanol : 385[21]

Solche Korrelationen sind auch im Falle der monosubstituierten Benzene [23] oder sogar der monosubstituierten Azobenzene [20] bekannt, aber in beiden Fällen stellt man eine Brechung der Korrelationsgeraden fest, die genau der nichtsubstituierten Verbindung entspricht. Die elektronenanziehenden oder-abstoßenden Substituenten bestimmen bathochrome Effekte, da sie eine Konjugation im System besitzen.

Im Falle der 4-Aminoazobenzene kann man aber eine einzige lineare Korrelation für alle Substituenten aus der 4'-Stellung erhalten. Ähnliche Korrelationen erhielten wir aufgrund von Daten aus des Fachliteratur [22] für 4' -substituierte 4-Dimethylamino-, 4-Cyanoethyl, ethylamino-, 4-Dicloroethylaminoazobenzene.

$-N(CH_3)_2 \qquad \lambda = 40{,}3\sigma^- + 409{,}5 \qquad (r = 0{,}954)$

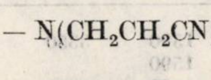

$-\underset{CH_2CH_3}{N}(CH_2CH_2CN) \qquad \lambda = 36{,}1\sigma^- + 400{,}7 \qquad (r = 0{,}980)$

$-N(CH_2CH_2Cl)_2 \qquad \lambda = 34{,}9\sigma^- + 396{,}8 \qquad (r = 0{,}975)$

Die Hammet-Korrelierung mit den σ^--Parametern wiederspiegelt einen wesentlichen direkten konjugierten Einfluß der Substituenten aus der 4'-Stellung auf das ungesättigte System. Der Einfluß der an die Aminogruppe gebundenen Substituenten auf die Proportionalitätsfaktoren beweist, daß die Gruppierungen in die Konjugierung mit den Substituenten aus der 4'-Stellung miteinbezogen sind.

Im Falle des 4'-Hydroxy-4-aminoazobenzens erscheinen zwei Banden bei größeren Wellenlängen als jene für den $\pi \rightarrow \pi^*$-Übergang der Azogruppe bei 418 und 450 nm erwarteten. Beide sind intensive Banden und können dem chinonartigen Tautomer im Gleichgewicht mit dem Benzen-Tautomer zugeschrieben werden[21],[24] (Tabelle 2, mit C bezeichnete Banden).

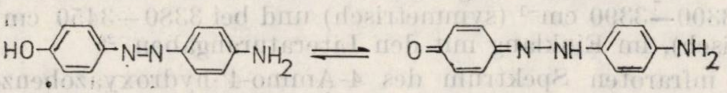

Die Chinon-Tautomere weisen eine bathochrome Verschiebung von 60—70 nm im Vergleich zu den Azo-Tautomeren auf.[21],[24]

In einigen Fällen konnte in den ultravioletten Spektren der substituierten 4-Aminoazobenzene auch eine der Übergangsbanden des aromatischen Rings entsprechende Bande festgestellt werden : die *p*- oder ^1L_a-Bande, [23] welche zwischen 200 und 270 nm ($\lg \varepsilon = 3—4$) für die monosubstituierten Benzene erscheint (Tabelle 2, mit B bezeichnete Banden). Diese Bande liegt bei verhältnismäßig hohen Wellenlängen (240—270 nm), was von neuem eine wesentliche Konjugierung dieser Moleküle beweist.

Die bedeutendsten Banden des IR-Spektrums für 4-Aminoazobenzene sind in Tabelle 3 enthalten. Es konnten die mittelstarken Banden identifiziert werden, die der Valenzschwingung N=N— aus trans-Azobenzen von 1380—1420 cm^{-1} entsprechen. Für einige monosubstituierte Azobenzene wurden solche Banden bei 1400—1420 cm^{-1} gefunden.[25,26]

Werden in die untersuchten Verbindungen elektronenanziehende Substituenten eingeführt, verschiebt sich die Bande gegen größere Wellenzahlen, während durch die elektronenspendenden Substituenten die Bande gegen kleinere Wellenzahlen verschoben wird.[26]

Tabelle 3

Den Azo- und Aminogruppen charakteristischen Banden im IR-Spektrum der 4, 4'-disubstituierten Azobenzene

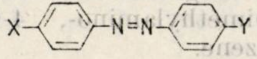

X	Y	ν N=N	ν CN		δ NH$_2$	ν NH$_2$	
$(CH_3)_2N$	NH_2	1400	1220	1150	1590	3350	3450
HO	NH_2	1380	1220	1150	1590		
CH_3	NH_2	1400	1300	1130	1590	3300	3400
H	NH_2	1405	1300	1120	1590	3350	3450
Cl	NH_2	1410	1250	1130	1590	3300	3400
H_3CCO	NH_2						
O_2N	NH_2	1420	1320	1120	1620	3390	3480
COONa	NH_2	1400	1280	1120	1580	3300	3380
SO_3Na	NH_2	1390	1280	1110	1620	3320	3400
$(CH_3)_2N$	NO_2	1420	—	1120	—	—	—
HO	NO_2	1400	—	1140	—	—	—

Es konnten auch zwei Valenzbanden C—N identifiziert werden, eine bei 1330—1280 cm^{-1}, die wir den Ar-NH$_2$-Bindungen zuschreiben und eine bei 1120—1150 cm^{-1}, die der Ar—N= -Bindung entsprechen könnte.[26]

Die NH$_2$-Valenzschwingungen erscheinen für die feste Phase im Bereich 3300—3390 cm^{-1} (symmetrisch) und bei 3380—3450 cm^{-1} (antysymmetrisch), im Einklang mit den Literaturangaben.[26]

Im infraroten Spektrum des 4-Amino-4'-hydroxyazobenzens und des 4-Nitro-4'-hydroxyazobenzens, in festem Zustand, konnte keine Bande über 1600 cm^{-1} identifiziert werden, was die Existenz der Chinon-Tautomere im kristallinen Zustand ausschließt.

Die aromatischen Protonen der 4,4'-disubstituierten Azobenzene bilden zwei Systeme vom Typ A_2B_2 (oder A_2X_2), die verhältnismäßig leicht zu analysieren sind[27]. Die Werte der chemischen Verschiebungen und ihrer in den Spektren gemessenen Kupplungskonstanten sind in Tabelle 4 enthalten.

Die Protonen H_B und H_C aus der 2- bzw. 2'-Stellung sind von der benachbarten N = N-Doppelbindung nicht abgeschirmt und weisen normale chemische Verschiebungen für die anti-Isomere der aromatischen Azoderivate auf[28]. Der Einfluß der Substituenten auf die chemischen Verschiebungen dieser Protonen ist verhältnismäßig klein ($\delta = 7{,}65 - 7{,}85$ ppm mit Ausnahme der mit NO_2-Gruppe substituierten Verbindung, welche diese Protonen mit ungefähr 0,2 ppm gegen niederere Felder verschiebt.

Die Protonen H_A und H_B, hingegen, sind von den Substituenten mehr beeinflußt. In den Derivaten des 4-Aminoazobenzens besitzen die Protonen aus der Nachbarschaft der NH_2-Gruppe (im Benzen um ca 0,5 ppm mehr verschirmt) praktisch gleiche chemische Verschiebungen in allen Verbindungen (6,61—6,77 ppm), was einen vernachläßigbaren Einfluß der Substituenten aus der 4'-Stellung beweist. Die H_D-Protonen aus der Nachbarschaft der Substituenten der 4'-Stellung unterliegen offensichtlich dem Einfluß dieser Substituenten, die (für R_1 = OH, CH_3, $N(CH_3)_2$) mehr oder (für R_1 = CH_3CO, NO_2, COO^-, SO_3^-) weniger verschirmt sind als im 4-Aminoazobenzen. Die Signale der Protonen der R_1 -und R_2-Gruppen haben normale Werte der chemischen Verschiebungen. Im Falle von 4'-Methyl-4-aminoazobenzen hat die Methylgruppe in tieferen Feldern ihre chemischen Verschiebungen (2,43 ppm), was dem anti-Isomer entspricht [29]. In 4'-substituierten 4-Aminoazobenzenen weisen die Aminprotonen den aromatischen Aminen entsprechende chemische Verschiebungen auf, die verhältnismäßig wenig von den Substituenten aus der 4'-Stellung beeinflußt werden. Die Veränderung der chemischen Verschiebungen wird eher von den Konzentrationsänderungen oder vom Lösungsmittel hervorgerufen.

Tabelle 4

hemische Verschiebungen und Kupplungskonstanten der 4'-substituierten 4-Aminoazobenzene

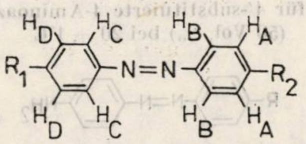

R_1	R_2	A	B	C	D	R_1	R_2	AB	CD
$(CH_3)_2N$	NH_2	6,73	7,68	7,77	6,75	3,06	4,88	8,75	9,25
HO	HH_2	6,72	7,65	7,70	6,91	9,74	5,54	8,75	9,00
CH_3	NH_2	6,77	7,73	7,73	7,30	2,43	4,75	8,75	8,50
H	NH_2	6,71	7,82	7,80	7,48	7,48	4,03	8,75	
CH_3CO	NH_2	6,77	7,78	7,85	8,07	2,65	5,54	8,75	8,50
NO_2	NH_2	6,77	7,82	7,91	8,33	—	5,24	8,75	9,00
COO^-Na^+	NH_2	6,75	7,77	7,85	8,13		6,35	8,75	8,50
$SO_3^-Na^+$	NH_2	6,74	7,71	7,73	7,86	—	6,00	8,75	9,00
NO_2	$N(CH_3)_2$	6,83	7,92	7,98	8,38	—	3,19	9,00	9,25
NO_2	OH	7,01	7,92	8,03	8,42	—	3,74	8,75	9,25

Die Werte der vicinalen Kupplungskonstanten ${}^3J_{AB}$ und ${}^3J_{CD}$ sind ebenfalls gewöhnlich für die aromatischen Kupplungen zwischen den in *ortho*-Stellung stehenden Protonen (8,50—9,25 Hz). Die Substituenten beeinflußen sehr wenig diese Kupplungen.

Die Bestimmung der pK_a-Konstanten der 4′-substituierten 4-Aminoazobenzene wurde spektrophotometrisch in Wasser-Methanol (50 Vol. — %) bei 20±1 °C (Tabelle 5) durchgeführt.

Die pK_a-Werte korrelieren linear mit den Hammet σ-Konstanten, laut Beziehung:

$$pK_a = -0{,}72\sigma + 2{,}463 \qquad (r = 0{,}995)$$

Tabelle 5

Bestimmung der pK_a-Werte für 4′-substituierte 4-Aminoazobenzen in Methanol-Wasser (50 Vol. %) bei 20 ± 1°C

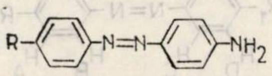

R	σ	Absorptionsmaximum (nm)		pK_a	pK_a(Lit.)
		Neutrales Molekül	Kation		
$(CH_3)_2N$	−0,83	461	504	3,06 ± 0,01	
				1,78 ± 0,01	
HO	−0,37	380	523	2,74 ± 0,01	
CH_3	−0,17	384	507	2,56 ± 0,02	2,82 H_2O[32]
H	0,00	383	499	2,50 ± 0,01	2,76 H_2O[32]
					2,79 H_2O[32]
Cl	0,227	389	501	2,24 ± 0,02	
CH_3CO	0,502	386	353	2,16 ± 0,02	
O_2N	0,778	441	498	1,88 ± 0,01	

Die Korrelierung mit dem σ-Wert beweist, daß die Protonierung des Aminostickstoffs verhältnismäßig wenig auf die direkten konjugativen Effekte der an das zweite Phenylradikal gebundenen Gruppierungen anspricht. Im Falle der *meta*- und *para*-substituierten Aniline war der Wert für ρ unvergleichbar größer (4,56 in Wasser[33], 3,55 in Wasser-Dioxan (70 %)[34] oder 4.03 in Methanol[35]).

Aus dem Vergleich dieser Ergebnisse mit den anhand aus den UV-Spektren abgeleiteten Werten, folgt, daß der konjugative Einfluß der Substituenten aus der 4′-Stellung im angeregten Zustand der 4′-substituierten 4-Aminoazobenzene bedeutender ist als im Grundzustand.

VERSUCHSTEIL

Materialien. Die mit Methyl-, Chlor-, Acetyl-, Nitro- und Carboxylgruppen 4′-substituierten 4-Aminoazobenzene wurden durch Kupplung der Diazoniumsalze der entsprechenden 4′-substituierten Aniline mit dem Kondensationsprodukt des Anilins mit der Bisulfitverbindung des Formaldehyds nach dem in [4] für 4-Amino-4′-nitroazobenzen beschriebenen Verfahren hergestellt.

Die Diazotierung wurde laut Literaturangaben für *p*-Toluidin [4], *p*-Chloranilin [2], *p*-Aminoacetophenon [6] und *p*-Nitroanilin [2] durchgeführt. Die Kupplung und Hydrolyse wurden laut Angaben aus [2] durchgeführt.

Die erhaltenen Ausbeuten hängen von den Substituenten ab und sind folgende: Methyl 92%, Chlor 94%, Acetyl 89%; Nitro 85% und Carboxyl 82%.

Die in 4′ mit Dimethylamino- und Hydroxygruppen substituierten 4-Nitroazobenzene wurden durch die saure Kupplung des diazotierten *p*-Nitroanilins mit Dimethylanilin bzw. mit Phenol erhalten, während die entsprechenden 4-Aminoazobenzene durch Reduktion in ethanol-wäßriger Lösung der Nitroderivate mit Natriumsulfid[5] dargestellt wurden.

Die Kupplungsausbeuten mit *p*-Dimethylanilin (92 %) und Phenol (90%) entsprechen den Literaturangaben.

4-Aminoazobenzen wurde durch Kupplung des diazotierten Anilins mit Anilin und Umlagerung des Diphenyltriazens[6] mit einer Ausbeute von 72% erhalten.

Die 4-Aminoazobenzen-4′-sulfonsäure wurde durch Sulfonierung des 4-Aminoazobenzens[4] mit einer Ausbeute von 20%erhalten. Das Hauptprodukt der Reaktion ist die 4-Aminoazobenzen-3′, 4′ disulfonsäure, die durch fraktionierte Aussalzung abgetrennt wurde.

Die *Reinigung der Farbstoffe* wurde durch eigene Herstellungsmethoden von hochreinen, für kinetische und physikalisch-chemische Bestimmungen notwendigen Verbindungen, wie folgt durchgeführt:

4′-Dimethylamino-, 4′-Hydroxy-, 4′-Methylaminoazobenzen und 4-Aminoazobenzen wurden durch zweifache Umkristallisierung des Rohprodukts aus wäßrigem Ethanol (50 Vol. %) gereinigt. Die Verbindungen kristallisieren als nadelförmige Kristalle (rot-violette Nadeln — das Dimethylaminoderivat, braune — das Methylderivat und orange — Aminoazobenzen) und als braune Plättchen (das Hydroxyderivat).

4′-Dimethylamino- und 4′-Hydroxy-4-nitroazobenzen wurden wiederholt aus 96%igem Ethanol umkristallisiert (rot-dunkelbraune nadelförmige Kristalle; das Hydroxyderivat — rot-purpurne nadelförmige Kristalle).

Das rohe 4′-Chlor-4-aminoazobenzen wurde im Soxhlet-Apparat mit *n*-Butanol extrahiert, die Lösung konzentriert, der kristalline Farbstoff filtriert und auf dem Filter mit 96%igem Ethanol gewaschen, dann getrocknet und zweimal aus Dimethylformamid-Wasser (75/25 V/V) umkristallisiert. Das Produkt erscheint als orange nadelförmige Kristalle.

Reines 4′-Acetylaminoazobenzen wurde durch Eliminieren aus dem Rohfarbstoff der im Lösungsmittel unlöslichen Komponenten durch Suspendieren in kochendem Ethanol, gefolgt von Filtrieren in der Wärme, erhalten. Das Filtrat wurde auf das dreifache Volumen mit Wasser verdünnt und das ausgefallene gelb-orange Produkt einer ähnlichen Reinigung in Dioxan unterworfen. Der Farbstoff wurde als oranges Pulver erhalten.

Reines 4′-Nitro-4-Aminoazobenzen wurde durch Extraktion des Rohprodukts im Soxhlet-Apparat mit *n*-Butanol, Konzentrieren des Filtrats im Vakuum und Abkühlen auf 0°C erhalten. Die kristalline Verbindung wurde durch Filtrieren abgetrennt, im Vakuum getrocknet und dreimal aus Toluen umkristallisiert. Der Farbstoff ist ein rot-dunkelbraunes Pulver.

Die rohe 4-Aminoazobenzen-4′-carbonsäure wurde folgenderweise gereinigt: zuerst wurde sie bei 80° mit einer Natriumcarbonatlösung in das Natriumslaz umgewandelt, dann die Reaktions masse filtriert, um die dunkelgefärbten unlöslichen Komponenten abzutrennen und schließlich durch langsames Abkühlen der Lösung kristallisiert. Der kristalline orange Farbstoff wurde abfiltriert und zweimal wie oben umkristallisiert. Die freie Säure wurde durch Ansäuern, bei pH 1 und 60°, der wäßrigen Lösung des reinen Farbstoffs (Natriumsalz) erhalten und anschließend wiederholt auf dem Filter mit destilliertem Wasser gewaschen und dann getrocknet. Sie erscheint als dunkelviolette Kristalle.

Die 4-Aminoazobenzen-4′-sulfonsäure und ihr Natriumsalz wurden ähnlich wie die Carbonsäure gereinigt. Die freie Säure ist ein graues Pulver, das Natriumsalz ist orange.

Die in der Literatur [30–31] empfohlenen Laufmittel für die Azofarbstoffe eignen sich nicht für die chromatographischen Analyse der in der vorliegenden Arbeit angegebenen Aminoazofarb stoffe, aus welchem Grund ein Studium der chromatographischen Bedingungen durchgeführt werden mußte.

Mit Methylenchlorid (A) und dem System Benzen-Aceton 16 :1 (B) konnte eine wirksame Abtrennung der Aminoazofarbstoffe von den aus der Reaktion hervorgegangenen Nebenprodukten erzielt werden. Die Farbstoffe wurden auf mit Silicagel G „Merck" (0,25 mm Schichtdicke) bedeckten 20 × 20 cm-Platten durch die aufsteigende Methode chromatographiert.

In Tabelle 1 sind die R_F-Werte der Farbstofflecken in den zwei Laufmitteln angegeben.

Ultraviolett-sichtbare Spektren

Die ultraviolett-sichtbaren Spektren wurden an einem UNICAM-Spektrographen in Methanol-, Dichlorethan- und Wasserlösungen, je nach der Löslichkeit der Stoffe, registriert.

Das Methanol wurde vorangehend durch Trocknen des p.a. Produktes „Reactivul" gereinigt, und zwar durch Rückflußkochen über Magnesium und Rektifizierung auf einer versilberten, l m langer Säule (K_p 64°C, Transmittanz 10% bei $\lambda = 202$ nm und 98% bei 250 nm).

Dichlorethan p.a. „Reactivul" wurde 2 stundenlang mit Calciumhydroxyd getrocknet wonach es wie oben rektifiziert wurde (K_p83,5°C, Transmittanz 10% bei 263 nm und 98% bei 270 nm).

Die infraroten Spektren der KBr-Presslinge wurden mit einem Specord IR 75-Spektrographen aufgenommen.

Die NMR-Spektren

Die H^1-NMR-Spektren wurden aus einer 2 – 5%igen Lösung von einem Gemisch von Deuterochloroform-Hexadeuterodimethylsulfoxid, im Volumverhältnis von 3 :1 bis 1 :3, mit einem NMR-Spektrometer, TESLA, BS 487 C bei 80 MHz aufgezeichnet, wobei als interner Standard Tetramethylsilan (TMS) eingesetzt wurde.

Die Basizitätskonstanten wurden spektrophotometrisch an einem Specord UV—VIS. Carl Zeiss Jena-Spektrographen, in Methanol-Wasser (50 Vol. %) bestimmt. Das pH wurde mit einem, mit Glas-und Calomelelektroden versehenen pH-Meter MV-85 gemessen. Die Bestimmungsmethode der pK_a-Werte und die Berechnungen sind die bekannten [36].

Die Elementaranalysen für C, H und N wurden mit einem Perkin Elmer 240 B-Gerät durchgeführt.

Die Schmelzupunkte wurden mit einem Boetius Heiztischmikroskop bestimmt.

Das pH wurde mit einem mit Glaselektrode pH-Meter MV 85 Präcitronic, DDR, gemessen, wobei als Bezugselektrode eine Calomelelektrode eingesetzt wurde.

LITERATURHINWEISE

[1] H. R. Schweizer, "Künstliche organische Farbstoffe und ihre Zwischenprodukte", Springer Verlag, Berlin, 1964.

[2] H. E. Filerz-David und L. Blangey, "Grundlegende Operationen der Farbenchemie", Springer Verlag, Wien, 1952, S. 265.

[3] Ulmann's Encyklopädie der technischen Chemie, Urban-Schwarzenberg, München-Berlin 1958, S. 90.

[4] H. Sanielevici und L. Floru, "Sinteza intermediarilor aromatici și a coloranților", Editura didactică și pedagogică, București, 1971.

[5] I. Reichel und A. Demian, *Stud. Cercet. St. Timișoara*, **3**, 15 (1956).

[6] Houben-Weil, "Die Methoden der organischen Chemie", Leipzig, Georg Thieme Verlag, 10/3, S. 239.

[7] E. Högfeld und T. Biegeleisen, *J. Amer. Chem. Soc.*, **82**, 15 (1960).

[8] R. K. Bukhard und F. A. Moore, *J. Amer. Chem. Soc.*, **77**, 6057 (1955).

[9] "Dictionary of Organic Compounds", London, 1946, vol. III., S. 68.

[10] I. Kuznetov, „Reactivi și produse chimice", Editura tehnică, Moscova, 1956, S. 199.

[11] R. Meldola, *J. Chem. Soc.*, **1884**, 107.

[12] H. Nölting, *Ber. dtsch. chem. Ges.*, **20**, 2994 (1887).

[13] W. F. Forbes und B. Milligan, *Austral. J. Chem.*, **15**, 481 (1962).

[14] L. Pentisnalli, *Ann. Chim. (Ital.)*, **49**, 189 (1959).

[15] A. A. Nesmeianov und D. N. Krovtov, *Doklady Akad. Nauk SSSR*, **142**, 1088 (1962).

[16] A. Zenhausen und H. Zollinger, *Helv. Chim. Acta*, **45**, 1890 (1962).

[17] E. Gerson und E. Heilbronner, *Helv. Chim. Acta*, **45**, 42 (1962).

[18] "Organic Electronic Spectral Data", Wiley-Interscience, New York, 1970.

[19] W. Berends und J. Potshuma, *J. Phys. Chem.*, **66**, 2547 (1962).

[20] H. Mustroph, J. Epperleni und D. Ebert, *J. Signal A, M*, **5**, 439 (1977).

[21] J. Griffiths, "Colour and Constitution of Organic Molecules", Academic Press, New York, 1976.

[22] H. Suzuki, "Electronic Absorption Spectra and Geometry of Organic Molecules, An Application of Molecular Orbital Theory", Academic Press, New York, 1967.

[23] H. H. Jaffé und M. Orchin, "Theory and Application of Ultraviolet Spectroscopy", Wiley, New York, 1964.

[24] I. Y. Bershtein und O. F. Ginzburg, *Russ. Chem. Rev.*, **41**, 97 (1972)

[25] R. Kubler, W. Lütt und S. Weckherlin, *Z. Electrochem.*, **64**, 650 (1960).

[26] N. Coltkup, L. Daly und S. Wiberley, "Introduction to Infrared and Raman Spectroscopy", Academic Press, New York, 1975.
[27] D. H. Grant und R. C. Hirst, *J. Chem. Phys.*, **38**, 470 (1963).
[28] L. H. Jackmann und S. Sternhell, "Application of Nuclear Magnetic Resonance Spectroscopy in Organic Chemistry" 2nd Ed., Pergamon Press, Oxford, 1969, S. 224.
[29] D. L. Welb und H. H. Jaffé, *J. Amer. Chem. Soc.*, **86**, 2419 (1964).
[30] F. H. Polland, G. Nickless, T. J. Samuelson und R. G. Anderson, *J. Chromatog.*, **16**, 231 (1965).
[31] N. N. Naimy, M. J. Namkung und T. L. Feltcher, *J. Chromatog.*, **43**, 537 (1969).
[32] D. D. Perrin, "Dissociation Constants of Organic Bases in Aqueous Solution", London, Butterworth, 1965.
[33] F. G. Bordwell und D. G. Cooper, *J. Amer. Chem. Soc.*, **74**, 1058 (1952).
[34] H. James und J. G. Knox, *Trans. Faraday Soc.*, **46**, 254 (1950).
[35] P. R. Wells, *Chem. Revs.*, **63**, 171 (1963).
[36] A. Albert und E. P. Serjeant, "Ionisation Constants of Acids and Bases", Wiley, London, 1962.

Revue Roumaine de Chimie, 28, 9–10, 915–920 (1983)

SYNTHESIS OF 2'-METHYL-γ-PYRONYL-(5', 6', 6, 7)-4-ACETONYL-COUMARIN AND ITS REACTION

M. El-KADY, M. K. El-DEEK, R. M. SALEH and M. G. El-DEIN
Chemistry Department, Faculty of Science, Ain Shams University, Abbassia, Cairo, Egypt

Received July 10, 1981

6,7 – or (7,8) – (2'-Methyl-4'-proponyl)-4-acetonyl coumarines 5 or 6 were obtained from 6-acetyl of 8-acetyl-7-hydroxy-4-methyl coumarines 3 or 4 by Claisen condensation and ring closure. Compound 5 reacts with aromatic aldehydes to give the corresponding chalcones 7. Reaction of 5 with active methylene compounds (under Michael conditions), Grignard reagents and *p*-benzidine gives Michael adducts 8, 9, chromane derivatives 10 and condensation adducts 11 respectively.

As an extension of our previous studies on coumarin,[1-7] in the present investigation the behaviour of both α-pyrone and γ-pyrone in the 6,7-(2'-methyl-4'-pyronyl)-4-acetonyl coumarin **(5)** and 7, 8-(2'-methyl-4'-pyronyl)-4-acetonyl coumarin **(6)** have been studied. An attractive route used for the construction of such compound is illustrated in the following scheme which involved: (i) acylation of 7-hydroxy-4-methyl coumarin **(1)** yielding 7-acetoxy-4-methyl coumarin **(2)**, (ii) Fries rearrangement of **2** affording 6-acetyl-7-hydroxy-4-methyl coumarin **(3)** and 8-acetyl-7-hydroxy-4-methyl coumarin **(4)**, (iii) the Claisen condensation of **3** or **4** with ethylacetate and ring closure affording **5** or **6**.

The structures of **3**, **4**, **5**, **6** were supported by their spectral data. The IR spectra of **3** and **4** showed bands at 1640 (ν_{CO} of acetyl), 1710 (ν_{CO} of δ-lactone) and at 3300–3480 cm^{-1} (ν_{OH} broad). The IR spectra of **5** and **6** showed bands at 1640 (ν_{CO} of acetonyl), 1680–1700 (ν_{CO} of γ-pyrone), 1710–1720 (ν_{CO} of δ-lactone) and 3000–3100 cm^{-1} (ν_{OH}). The ^1H–NMR spectrum of **5** in deuterated acetone showed signals at $\delta = 2.15$ (*q*, non equivalent *2H*, $-CH_2-COCH_3$), 2.45 (*s*, *3H* of CH_2-COCH_3) 2.40 (*s*, 3H of 2-methyl-γ-pyrone), 5.15 (*s*, 1H of CHa) and at 6.7–6.9 (*m*, 2H of aromatic) and 7.6 (*s*, 1H of CHb). The UV spectra of **5** and **6** showed maxima at λ^{CHCl_3} 278 (ε max 13,810) and at λ^{CHCl_3} 274 (ε max 11,490) respectively. The mass spectrum of **3** exhibited *m/e* 218 (10.95%) while **5** showed *m/e* 284 (0.87%).

Compound **5** reacts with aromatic aldehydes namely, *p*-nitrobenzaldehyde, *m*-nitrobenzaldehyde; piperonal, *m*-chlorobenzaldehyde, benzaldehyde or salicylaldehyde in the presence of piperidine at the boiling

Scheme 1

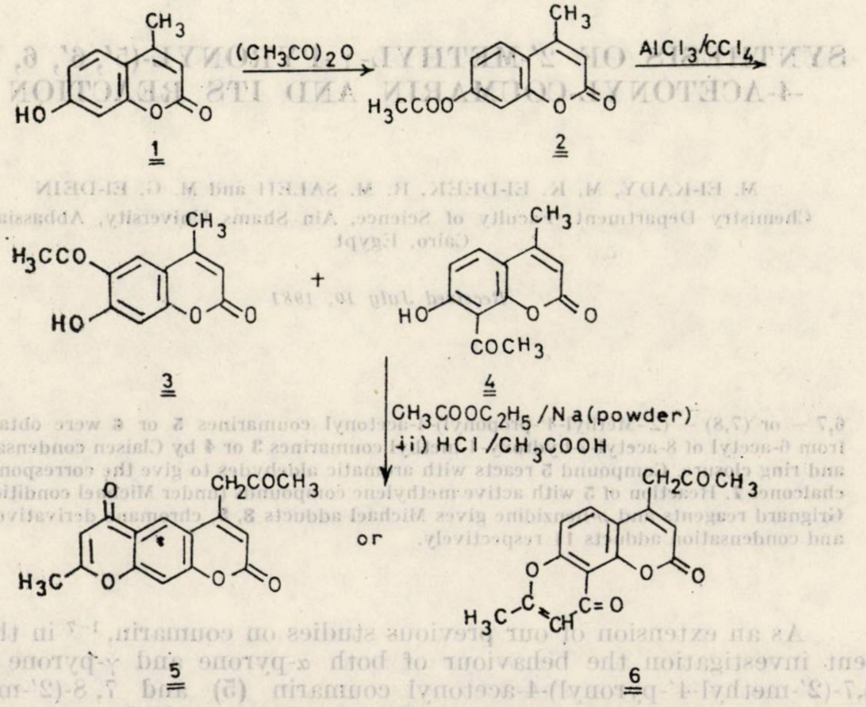

CH3
(CH3CO)2O
HO
O
O
1
CH3
AlCl3/CCl4
H3CCOO
O
O
2
H3CCO
CH3
HO
O
O
3
+
CH3
HO
O
O
COCH3
4
CH3COOC2H5 / Na(powder)
ii) HCl / CH3COOH
O
CH2COCH3
H3C
O
O
O
5
or
CH2COCH3
O
O
O
H3C
C
CH
C=O
6

point of butanol yielding the corresponding chalcones **7a-f**. The formation of **7** may be interpreted from the fact that aromatic aldehydes react readily with the methyl group of 4-acetonyl coumarin only.

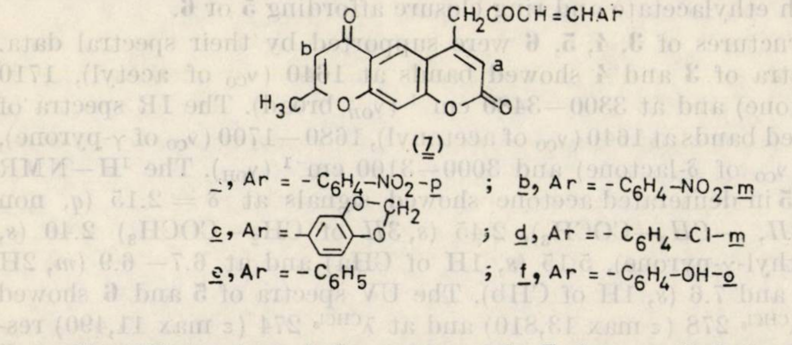

O
CH2COCH=CHAr
b
a
H3C
O
O
O
(7)
a, Ar = - C6H4-NO2-p ; b, Ar = - C6H4-NO2-m
O-CH2
c, Ar =
O
; d, Ar = - C6H4-Cl-m
e, Ar = - C6H5 ; f, Ar = - C6H4-OH-o

The IR spectra of the compounds **7** show well defined absorption bands at 1720—1700 (CO of δ-lactone), 1680—1650 (CO of γ-pyrone), 1660—1640 cm^{-1} (CO of α, β-unsaturated ketone). The ^1H—NMR spectrum of **7a** in CD_3COCD_3 showed signals at 2.0—2.15 (*q*, non equivalent 2*H* of —CH_2—COCH=), 2.45 (*s*, 3H of 2-methyl γ-pyrone), 4.7 (*s*, 1*H*, *CH* Ar), 6.3 (*s*, 1H of CHa), 7.6—7.9 (*m*, 6H of aromatic) and 8—8.2 (broad, 2*H* of CHb and —COC*H*).

As a point of interest the present work investigated the behaviour of **7a** toward active methylene compounds under Michael reaction conditions. Compound **7a** reacts with ethyl cyanoacetate in the presence of sodium ethoxide at room temperature yielding **8**. This result can be explained by the addition of the active methylene compound to the active olefinic double bond of α, β-unsaturated ketone, followed by ring closure, elimination of ethanol and opening of γ-pyrone. The same compound **7a** reacts with cyclopentanone, cyclohexanone, benzyl methyl ketone or acetyl acetone giving the corresponding Michael adducts **9a-c**.

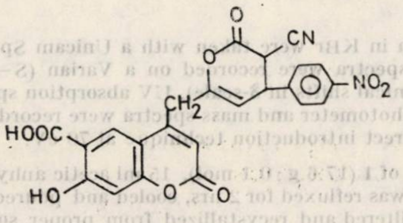

8

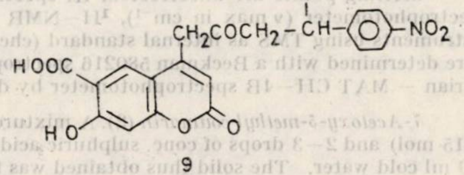

9

a, R = 2-cyclopentanoyl

b, R = 2-cyclohexanoyl

c, R = $-CH_2COCH_2C_6H_5$

The IR spectrum of **8** shows strong absorption bands at 1750—1740 (CO of δ-lactone), 1680 (CO of—COOH), 2300 (C≡N) and at 3300 cm^{-1} (OH, broad). The IR spectra of **9** show well defined absorption bands at 1740—1760 (CO of δ-lactone), 1700 (CO of —COOH), 1660 (CO of ketonic $\nu_{C=O}$ and at 3280—3300 cm^{-1} (OH, broad). The ^{1}H—NMR spectrum of **8** in CD_3COCD_3 showed signals at 2.2—2.35 (broad, 2*H* of CH$_2$), 3.6—3.8 (*m*-broad, 2*H* of CH$_c$ and CH$_d$), 5.4 (*d*, 1*H* of CH$_b$), 6.1 (*s*, 1*H* of CH$_a$), 7.3—7.8 (*m*, 6*H* of aromatic), 9.2 (*s*, 1*H* of OH) and 10.4 (*s*-broad, 1H of COO*H*).

The behaviour of **7a** towards Grignard reagents, namely phenyl magnesium bromide or ethyl magnesium iodide yielded 4-[4′, 4′-diaryl (alkyl)-2-oxo-butanyl]-6-benzoyl (acetyl)-7-hydroxy-2, 2-diaryl (alkyl) chroman ((**10a, b**). Four molecules of Grignard reagent are incorporated in reaction to give **10**.

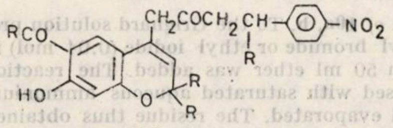

10

a, R = $-C_6H_5$; b, R = $-C_2H_5$

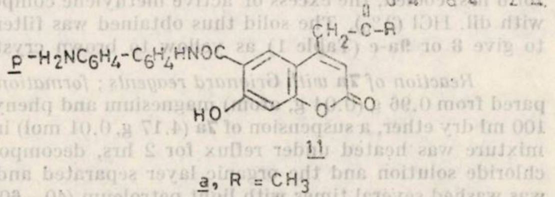
NC$_6$H$_4$-C$_6$H$_4$NH$_2$-p
CH$_2$-C-R
p-H$_2$NC$_6$H$_4$-C$_6$H$_4$HNOC
HO
O
O

11

a, R = CH$_3$

b, R = -CH=CH-⌬-NO$_2$

The IR spectra of **10** showed the absence of ν_{CO} of δ-lactone as well as well defined bands at 1670, 1650 due to ν_{CO} of a ketone and 3320 cm^{-1} due to ν_{OH}. The ^1H-NMR spectrum of **10a** in $CDCl_3$ showed signals at 2.7 (*t*, 1*H* of $-CH_2-CH<$), 3.4−3.5 (*m*, 4*H* of $-CH_2-\overset{\|}{C}-CH_2-$), 5.6 (*s*-broad 1*H* of CH_a), 6.9−7.6 (*m*, 26*H* of aromatic), 8.2 (*s*,-broad 1*H* of OH).

Condensation of **5** or **7a** with benzidine in boiling ethanol gave the corresponding amide **11a, b**. Their IR spectra showed absorption bands at 1750 (δ-lactone), 1650 (CO of amide), 1590 (C=N) and 3240 cm^{-1} (NH).

EXPERIMENTAL

Melting points are uncorrected, IR spectra in KBr were taken with a Unicam Sp 1200 spectrophotometer (ν max in cm^{-1}), ^1H-NMR spectra were recorded on a Varian (S−60T) instruments using TMS as internal standard (chemical shifts in δ-scale), UV absorption spectra were determined with a Beckman 580216 spectrophotometer and mass spectra were recorded on Varian — MAT CH−4B spectrophotometer by direct introduction technique at 70 eV.

7-Acetoxy-5-methyl coumarin (**2**). A mixture of **1** (17.6 g ; 0.1 mol), 15 ml acetic anhydride (0.15 mol) and 2−3 drops of conc. sulphuric acid was refluxed for 2 hrs, cooled and poured into 100 ml cold water. The solid thus obtained was filtered and recystallized from proper solvent to give **2** (Table 1) as colourless crystals in about 85% yield.

The Fries rearrangement of **2** ; *formation of* **3** *and* **4**. To a stirred mixture of finely powdered **2** (21.8 g; 0.1 mol) in 100 ml of acetylene tetrachloride 42 g (0.3 mol) of anhydrous aluminium chloride were added. The temperature of reaction was maintained at 150° for about 2 hrs, the complex was decomposed with ice/HCl and the acetylene tetrachloride evaporated. The product thus obtained was crystallized from proper solvent to give **3** (Table 1) as colourless crystals in about 70% yield. The mother liquids were concentrated and diluted with water to give **4** (Table 1) as colourless crystals in 20% yield.

The Claisen reaction of **3** *and* **4** *and ring closure* ; *formation of* **5** *and* **6**. A solution of **3** and **4** (2.18 g ; 0.01 mol) in dry ethyl acetate (20 ml) was added to finally powdered sodium (0.3 g, 0.013 atom). The mixture was warmed on water-bath and finally boiled under reflux for 1 hr, then poured into ice. The sodium salt of diketone was filtered off and washed with ice/H_2O. The dry product was dissolved in 5 ml acetic acid, 2 ml conc. HCl were added and boiled for 0.5 hr. to effect ring closure. The residue obtained after cooling and dilution with water was filtered off and crystallized from proper solvent to give **5** and **6** (Table 1) as pale yellow crystals in about 50−60 % yield.

Reaction of **5** *with aromatic aldehydes* ; *formation of chalcones* **7a-f**. A solution of **5** (2.84 g, 0.01 mol), *p*-nitrobenzaldehyde, *m*-nitrobenzaldehyde, piperonal, *m*-chlorobenzaldehyde, benzaldehyde or salicyaldehyde (0.015 mol) and piperidine (1 ml) in butanol (30 ml) was refluxed for 3 hrs, cooled and the solid separated was crystallized from suitable solvent to give **7a-f** as pale yellow crystals in about 60−80% yield (Table 1).

Base catalysed reaction of active methylene compounds with **7a** *under Michael reaction conditions* ; *formation of* **8** *and* **9a-c**. A mixture of **7a** (4.17 g ; 0.01 mol), the appropriate active methylene compound (15 ml) and sodium ethoxide (1.36 g, 0.02 mol) was heated at 100° for 6 hrs, cooled, the excess of active methylene compound, evaporated and the residue washed with dil. HCl (2%), The solid thus obtained was filtered and crystallized from proper solvent to give **8** or **9a-c** (Table 1) as yellow to brown crystals in about 40−60% yield.

Reaction of **7a** *with Grignard reagents* ; *formation of* **10a, b**. To the Grignard solution prepared from 0.96 g (0.04 g, atom) magnesium and phenyl bromide or ethyl iodide (0.04 mol) in 100 ml dry ether, a suspension of **7a** (4.17 g, 0.01 mol) in 50 ml ether was added. The reaction mixture was heated under reflux for 2 hrs, decomposed with saturated aqueous ammonium chloride solution and the organic layer separated and evaporated. The residue thus obtained was washed several times with light petroleum (40−60°), and crystallized from a proper solvent to give **10a, b** as colourless crystals (Table 1).

Table 1

Characterisation data of various compounds prepared

Compound	M.p. °C	Mol. formula	Analysis % Found (Calc.) C	H	N
2	186	$C_{12}H_{10}O_4$	66.14 (66,05)	4.67 (4.58)	— —
3	195	$C_{12}H_{10}O_4$	66.28 (66.05)	4.32 (4.58)	— —
4	182	$C_{12}H_{10}O_4$	65.56 (66.05)	4.40 (4.58)	— —
5	179	$C_{16}H_{12}O_5$	67.79 (67.60)	4.36 (4.25)	— —
6	161	$C_{16}H_{12}O_5$	68.29 (67.60)	4.42 (4.25)	— —
7a	114	$C_{23}H_{15}NO_7$	66.59 (66.18)	3.56 (3.59)	3.70 (3.35)
7b	194	$C_{23}H_{15}NO_7$	65.99 (66.18)	3.12 (3.59)	3.15 (3.35)
7c	180	$C_{24}H_{16}O_7$	68.97 (69.23)	4.03 (3.84)	— —
7d	196	$C_{23}H_{15}O_5Cl$	68.09 (67.89)	3.56 (3.69)	— —
7e	198	$C_{23}H_{16}O_5$	74.40 (74.19)	4.60 (4.30)	— —
7f	210	$C_{23}H_{16}O_6$	71.36 (71.13)	4.35 (4.12)	— —
8	173	$C_{23}H_{14}N_2O_9$	60.30 (59.74)	3.24 (3.03)	6.63 (6.06)
9a	220	$C_{25}H_{21}NO_9$	62.80 (62.63)	3.98 (4.38)	3.40 (2.92)
9b	215	$C_{26}H_{23}NO_9$	62.90 (63.28)	4.89 (4.66)	2.99 (2.83)
9c	170	$C_{29}H_{23}NO_9$	65.67 (65.78)	4.70 (4.34)	2.21 (2.64)
10a	181	$C_{43}H_{33}NO_6$	77.97 (78.30)	5.14 (5.00)	2.43 (2.12)
10b	135	$C_{28}H_{33}NO_6$	70.10 (70.14)	6.47 (6.88)	3.70 (2.92)
11a	127	$C_{37}H_{30}N_4O_4$	75.02 (74.74)	4.99 (5.05)	10.36 (9.42)
11b	230	$C_{44}H_{33}N_5O_6$	72.31 (72.62)	3.98 (4.53)	9.62 (9.24)

Solvents used for crystallization were: benzene for **7a, 7b**; ethanol for **3, 7c, 7d, 7e,** methanol for **2, 7f, 8, 9a-e,** aq. ethanol for **4, 10 a, b,** and light petroleum (b.p. 100−120°) for **5** and **6**.

Condensation of **5** *or* **7a** *with p-benzidine; formation of condensation product* **11a, b**. A solution of **5** or **7a** (0.01 mol) and *p*-benzidine (0.01 mol) in 30 ml ethanol was refluxed 4 hrs, cooled and the solid separated was crystalized from methanol to give **11a, b**, as deep yellow crystal (Table 1) in about 60% yield.

REFERENCES

[1] A. Sammour, M.I.B. Selim and M. El-Kady, *U.A.R. J. Chem.* **14**, 261 (1971).

[2] A. Sammour, M. Abdalla and M. El-Kady, *Acta Chim. Acad. Sci. Hung.* **82**, 369 (1974).

[3] A. Sammour and M. El-Kady, *Indian J. Chem.* **12**, 51 (1974).

[4] M. El-Kady, *Pakistan J. Sci. Res.* **31**, 163 (1979).

[5] M. El-Kady and A. I. Essawy, *Pakistan J. Sci. Res.* **30**, 93 (1978).

[6] M. Abdalla, M. El-Kady and A.F. El-Fraragy, *Egypt. J. Chem.*, **20**, 245 (1977).

[7] A. I. Essaway, M. El-Kady and A.Y. Mohamed, *Indian J. Chem.* **19**, 567 (1980).

Revue Roumaine de Chimie, **28**, *9–10*, 921–931 (1983)

OXIDATION OF SOME SELECTED DIHYDRIC ALCOHOLS

AHMED I. KOHDAIR, ABOEL-MAGD A. ABDEL-WAHAB *, HUSSAIN S. El-KASHEF,
KHAIRY M. HASSAN, AHMED M. El-KHAWAGA and MAHER F. El-ZOHARY

Chemistry Department, Faculty of Science, Assiut University, Assiut, Egypt

Received September 30, 1981

Nine dihydric alcohols (1 — 9) with specific structural features were selected and oxidised using different oxidation procedures. The CrO_3/pyridine complex and N-clorosuccinimide/dimethyl sulphide (NCS/DMS) complex were found to oxidise these compounds to the corresponding dicarbonyl products followed by cyclisation via an aldol-like mechanism whenever this process is sterically favoured. Using N-cyclohexyl-N′-(2-morpholinoethyl) carbodiimide metho *p*-toluenesulphonate (19) in DMS dehydration to the corresponding heterocyclic oxygen compound was favoured. Also, equilibration of the diastereoisomers 10 and 11 was observed when the oxidation was performed using CrO_3/pyridine complex.

INTRODUCTION

Recently, much interest was devoted for the oxidation of monohydric alcohols to the aldehyde and ketone stage and many methods were developed lately to accomplish this goal[1-4]. However, the counterpart oxidation of dihydric alcohols was not studied. Because of the importance of this problem in synthesis, particularly when the oxidation products are prone to cyclise under the experimental conditions, wese lected nine different dihydric alcohols with proper structural features and studied their behaviour under the experimental conditions of three different oxidation procedures.

RESULTS AND DISCUSSION

The selected diols are: styrolenediol **(1)**; 1, 4-butanediol **(2)**; *erythro* 2-ethyl-3-methyl-1, 4-butanediol **(3)**; *threo* 2-ethyl-3-methyl-1, 4-butanediol **(4)**; 2-phenyl-1, 4-pentanediol (**(5)**; 1, 5-pentanediol **(6)**; 1,5-hexanediol **(7)**; 1, 6-hexanediol **(8)** and 1,6-heptanediol **(9)**.

Compound **1** was synthesized from styrene according to the procedure of Morgan[5]; **2**, **3**, **4** and **8** were prepared *via* the reduction of diethyl succinate, dimethyl *erythro* 2-ethyl-3-methyl succinate, dimethyl *threo* 2-ethyl-3-methyl-succinate, and diethyl adipate with lithium alu-

---

* To whom all correspondence should be addressed.

Table 1

Synthesis of dihydric alcohols

Dihydric alcohol *	Starting material	Yield (%)	B.P. or (M.P.)		Ref.
			Found	Reported	
Styrolenediol	Styrene	90	(68)	(68)	5
1, 4-Butanediol	Diethyl succinate	79	223	225	10
erythro 2-Ethyl-3-methyl-1,-4-butanediol	*erythro* 2-Ethyl-3-methylsuccinic acid	91	**	**	6
threo 2-Ethyl-3-methyl-1,-4-butanediol	*threo* 2-Ethyl-3-methylsuccinic acid	88	**	**	6
1, 5-Pentanediol	Piperidine	70	236	236	7
1, 6-Hexanediol	Diethyl adipate	85	(41)	(42)	12

* All the prepared diols were found to be chromatographically pure and identical in all respects with authentic samples.

** Boiling points of these diols were not determined as they tend to lose water upon distillation [11].

minium hydride respectively [6]; **6** was prepared from piperidine following Von Braun procedure [7]; **5** was synthesized through condensation of ethyl acetoacetate with ethyl α-bromophenylacetate followed by nucleophilic displacement of the β-carboxylate group with iodide ion, according to the modified technique of Khodair and Kharasch [8], and reduction of the ester of the produced α-phenyllevulinic acid with $LiAlH_4$. Also, this developed technique was successfully used for the preparation of diethyl 2-acetylglutarate and ethyl 6-ketoheptanoate which were converted to **7** and **9**, respectively, through reduction with $LiAlH_4$.

RESULTS AND DISCUSSION OF THE OXIDATION

a) Using CrO_3/pyridine complex [1]

All nine diols were oxidized with CrO_3 complex in CH_2Cl_2 at room temperature for 30 min. under the conditions at which benzyl alcohol, the monohydric alcohol, gave benzaldehyde in 7% yield. Compound **1** gave mainly benzaldehyde (52%) in addition to benzoic acid (20%) and phenylglyoxal (10%). Noteworthy, oxidation of either **3** or **4** gave a mixture of *erythro-* and *threo*-2-ethyl-3-methylsuccinaldehydes (**10** and **11** respectively) in almost the same ratio (1.8 :1) regardless of which isomer was used as starting material. This suggests that equilibration may occur after oxidation under the reaction conditions. Inspection of the Newman's projection formulas of these aldehydes revels that the *erythro* form is thermo-dynamically the most stable isomer as shown from the experimental data (Table 2).

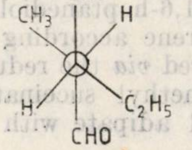

Erythro form

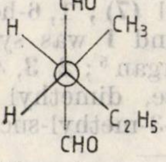

Threo form

Table 2

Results of oxidation of dihydric alcohols

Dihydric alcohol	Reagent	Oxidation products					
		Dicarbonyl compounds		Cyclic products		Other products	
		Structure	%	Structure	%	Structure	%
1	2	3	4	5	6	7	8
$\mathrm{PhCHCH_2OH}$ OH	$\mathrm{CrO_3}$/Pyridine complex	$\mathrm{PhCOCHO}$	10	—	—	PhCHO PhCOOH	52 20
$\mathrm{HO(CH_2)_4OH}$	,,	$\mathrm{OHC(CH_2)_2CHO}$	70	—	—	—	—
$\mathrm{CH_3-CHCH_2OH}$ $\mathrm{C_2G_5-CHCH_2OH}$ *Erythro* isomer	,,	$\mathrm{CH_3CHCHO}$ $\mathrm{C_2H_5-CHCHO}$ + $\mathrm{CH_3CHCHO}$ $\mathrm{OHC-CHC_2H_5}$	42 23	42	—	—	—
$\mathrm{CH_3CHCH_2OH}$ $\mathrm{HOCH_2-CHC_2H_5}$ *Threo* isomer	,,	$\mathrm{CH_3CHCHO}$ $\mathrm{C_2H_5-CHCHO}$ + $\mathrm{CH_3CHCHO}$ $\mathrm{OHC-CHC_2H_5}$	38 23	—	—	—	—
$\mathrm{CH_3CHCH_2CHCH_2OH}$ $\mathrm{OH}\quad\mathrm{ph}$	,,	$\mathrm{CH_3COCH_2CHCHO}$ Ph	20	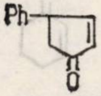 	54	—	—
$\mathrm{HO(CH_2)_5OH}$	,,	$\mathrm{OHC(CH_2)_3CHO}$	75	—	—	—	—

(Table 2 continued)

1	2	3	4	5	6	7	8
$CH_3\underset{OH}{CH}(CH_2)_3CH_2OH$	CrO_3/Pyridine	—	—	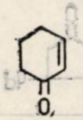	84	—	—
$HO(CH_2)_6OH$	,, ,,	$OHC(CH_2)_4CHO$	32	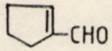	63	—	—
$CH_3\underset{OH}{CH}(CH_2)_4CH_2OH$	,, ,,	$CH_3C(CH_2)_4CHO$	30	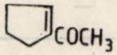	69	—	—
$Ph\underset{OH}{CH}CH_2OH$	Carbodimide/ DMSO	$PhCOCHO$	15	—	—	$Ph\underset{OH}{CH}-CHO$ $PhCOCH_2OH$ $PhCHO$	30 15 10
$HO(CH_2)_4OH$	,,	$OHC(CH_2)_2CHO$	10	—	—	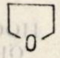	81
CH_3CHCH_2OH $C_2H_5CHCH_2OH$ *Erythro*	,,	CH_3CHCHO C_2H_5CHCHO	12	—	—	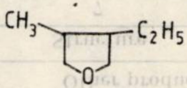 *Cis*	70
						Polymerization product	10

(Table 2 continued)

Dihydric Alcohol	Reagent	Oxidation products					
		Dicarbonyl compounds		Cyclic products		Other products	
		Structure	%	Structure	%	Structure	%
1	2	3	4	5	6	7	8
CH_3CHCH_2OH $HOCH_2CHC_2H_5$	Carbodimide DMSO	CH_3CHCHO $OHCCHC_2H_5$	10	—	—	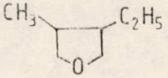 *Trans* Polymerization product	70 10
$CH_3CHCH_2CHCH_2OH$ OH Ph	,,	CH_3COCH_2CHCHO Ph	15		—	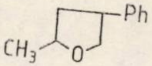 + Dehydration & Polymerization products.	20 60
$HO(CH_2)_5OH$	,,	$OHC(CH_2)_3CHO$	10	—	—	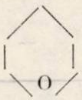	87
$CH_3CH(CH_2)_3CH_2OH$ OH	,,	—	—	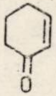	66	—	—
$HO(CH_2)_6OH$	,,	$OHC(CH_2)_4CHO$	67	—	—	unreacted alcohol	20

Table 2 (continued)

1	2	3	4	5	6	7	8
$CH_3CH(CH_2)_4CH_2OH$	Carbodimide/ DMSO	$CH_3CO(CH_2)_4CHO$	45	—	—	$\underset{\substack{\vert\\ OH}}{CH_3CH}(CH_2)_4CHO$ $CH_3CO(CH_2)_5OH$	26 20
$\underset{\substack{\vert\\ OH}}{CH_3CH}CH_2\underset{\substack{\vert\\ Ph}}{CH}CH_2OH$	NCS/DMS	$CH_3COCH_2\underset{\substack{\vert\\ Ph}}{CH}CHO$	15	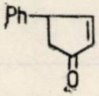	75	—	—
$\underset{\substack{\vert\\ OH}}{CH_3CH}(CH_2)_3CH_2OH$	,,	—	—	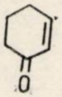	88	—	—
$\underset{\substack{\vert\\ OH}}{CH_3CH}(CH_2)_4CH_2OH$	,,	$CH_3CO(CH_2)_4CHO$	10	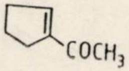	85	—	—

However oxidation of **2** and **6** gave mainly the corresponding aldehydes. On the other hand, oxidation of **5**, **8** and **9** gave mainly the corresponding cyclisation products, 4-phenylcyclopent-2-eneone **(12)**, cyclopent-1-enealdehyde **(13)** and 1-acetylcyclopentene **(14)**, respectively. Also, the corresponding dicarbonyl products, 2-phenyllevulinaldehyde **(15)**, adipaldehyde **(16)** and 5-acetylvaleraldehyde **(17)**, respectively, were obtained. Noteworthy, oxidation of **7** gave only cyclohex-2-eneone **(18)** in 84% yield. The structures of these products were confirmed by comparison with authentic samples and found to be identical in all respects (elemental analysis data ; m.p. ; m.m.p. ; IR as well as glc R.T.).

It is reasonable to assume that the formation of cyclic products can be visualized through intramolecular aldol-like condensation of the dicarbonyl oxidation product, for example :

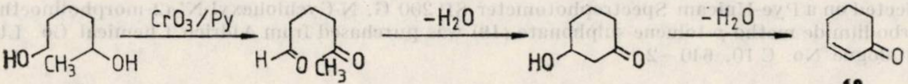

17 **18**

Noteworthy, treatment of either **16** or **17** with 1% NaOH solution at the reflux temperature gave **13** and **14**, respectively.

b) Using Pfitzner-Moffatt procedure [3]

In this procedure, N-cyclohexyl-N′ (2-morpholinoethyl) carbodiimide metho *p*-toluenesulphonate **(19)** in a mixture of DMSO, benzene, pyridine

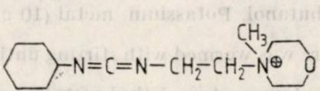

and trifluoroacetic acid was employed under the conditions reported by Pfitzner and Moffatt. [3] The solubility of **19** and its by-products in water solved the problems encountered in the solubility and during the decomposition of the excess dicyclohexylcarbodiimide in Pfitzner-Moffatt procedure. Oxidation of styrolenediol **(1)** afforded a mixture of benzaldehyde (10%), benzoylmethanol (15%), 2-hydroxy-2-phenylethanal (30%) and phenylglyoxal (15%). However, under these conditons **2**, **3**, **4**, **5** and **6** suffered dehydration to the corresponding furan or pyran derivatives, i.e. tetrahydrofuran **(20)**, *cis* 2-ethyl-3-methyltetrahydrofuran **(21)**, *trans* 2-methyltetrahydrofuran **(22)**, 2-methyl-4-phenyltetrahydrofuran **(32)** and tetrahydropyran **(24)**, respectively (See Table 2). On the other hand, cyclic oxygen derivatives of **8** and **9** (1, 6-diols) could not be obtained because of the ring strain in the seven-membered rings, therefore the dialdehydes **16** and **17** are majors. Compound **18** was obtained only from oxidation of **7**.

c) Using N-chlorosuccinimide/dimethysulphide

The simple, highly efficient method of Corey [4] was employed for the oxidation of **5**, **7** and **9**. These compounds were expected to give cyclic unsaturated ketones under the influence of the basic conditions employed. Indeed, oxidation of these compounds resulted into formation of **12**, **18** and **14**, respectively, in high yield (75%, 88% and 85%).

EXPERIMENTAL PROCEDURE

GLC analyses were conducted on a Pye-Unicam gas chromatograph, series 105, using nitrogen gas as a carrier (60 ml/min) and $5' \times \frac{1''}{4}$ column packed with 10% SE 30. All fractional distillations were carried out on a 2-Ft Podbielniak-type column. [9] Melting points were uncorrected and were determined on a Kofler melting point apparatus. IR analysis was effected on a Pye-Unicam Spectrophotometer SP 200 G. N-Cychlohexyl-N′-(2-morpholinoethyl) carbodiimide metho-*p*-toluene-sulphonate (**19**) was purchased from Aldrich Chemical Co. Ltd., Catalogue No. C 10, 640−2.

Synthesis of Diols

The starting diols **1**, **2**, **3**, **4**, **6** and **8** were prepared and purified according to the previously reported procedures and they are all found to be chromatographically pure. Results are found on Table 1.

The other diols **5**, **7** and **9** were synthesised as follows :

Synthesis of 2-phenyl-1,4-pentanediol (5)

Synthesis of **5** was accomplished in several steps as follows :

a — *Preparation of diethyl 2-acetyl-3-phenylsuccinate*

A 3-necked flask, equipped with condenser, mercury sealed stirrer, and dropping funnel, was charged with 400 ml dry *t*-butanol. Potassium metal (10 g, 25 m gram atoms) was added in a period of $\frac{1}{2}$ hr and the mixture was warmed with stirring until the potassium was completely dissolved and then cooled to room temperature. Ethyl acetoacetate (37 g, 25 mmole) was rapidly added followed by the addition of ethyl α-bromophenylacetate [13] (57 g, 25 mmole) in a period of 5 min, and the reaction mixture was refluxed for 4 hrs. At the end of the reflux period, the condenser was arranged for distillation until most of the alcohol was distilled. The residue was cooled, excess water was added and the organic layer was extracted with ether. The ether solution was washed with water, dried over magnesium sulphate, filtered, evaporated and the residue was fractionated using glass column packed with neutral alumina. Diethyl 2-acetyl-3-phenylsuccinate (25 g, 67%, yield) was eluted with benzene-ether mixture (3 :1). IR spectrum revealed characteristic absorptions for the phenyl group at 750 cm^{-1} and 820 cm^{-1}, and for carbonyl groups at 1715 cm^{-1} and 1750 cm^{-1}. Elemental analysis was correct.

b — *Preparation of methyl 2-phenyllevulinate*

A mixture of diethyl 2-acetyl-3-phenylsuccinate (27 g, 10 mmole) and calcium iodide, $CaI_2 \cdot 4H_2O$, (30 g, 7.5 mmole) was heated for four hours at 140−150° C.[8] The neutral extract gave a viscous oil identified as γ-lactone of 2-phenyllevulinic acid [14a] (9 g, 57% yield) ; IR spectrum showed a peak at 1780 cm^{-1} ($\nu_{C=0}$ of γ-lactones). [14b] Hydrolysis of this lactone using potassium hydroxide solution followed by acidification with HCl gave 2-phenyllevulinic acid, m.p. 128°C, lit. [13] m.p. 126°. The original alkaline extract gave after acidification-2-phenyllevulinic acid (6.3 g, 35% yield).

2-Phenyllevulinic acid (38 g, 20 mmole) was esterified by heating under reflux for 20 hrs in 700 ml absolute methanol and 15 ml conc. H_2SO_4. Methyl 2-phenyllevulinate (24 g, 60% yield) had been melted at 69°C, lit. [15a] m.p. 71°C.

c — *Reduction of methyl 2-phenyllevulinate*

Methyl 2-phenyllevulinate (20 g, 10 mmole) was reduced using $LiAlH_4$ (16 g, 40 mmole) in dry ether (200 ml). The product **5** (15 g, 75 % yield) showed no carbonyl absorption and a band at 3500 cm^{-1} (ν_{OH}) appeared instead, GLC analysis at 145°C revealed a single peak at 2.4 min.

Synthesis of 1,5-hexanediol

As described before in the preparation of 2-phenyl-1, 5-pentanediol, ethylacetoacetate (65 g, 500 mmole) was interacted with ethyl β-bromopropionate (90 g, 500 mmole), in the presence of potassium *t*-butoxide (20 g K in, 1l *t*-butanol). Diethyl γ-acetylglutarate (78 g, 68 % yield) was collected at b.p. 159°C/11 mm, lit.[15b] b.p. 162/11 mm).

Hydrolysis of diethyl α-acetylglutarate (23 g, 10 mmole) using $CaI_2 \cdot 4\,H_2O$ (30 g, 7.5 mole) technique gives 5-ketohexanoic acid (5 g, 22 % yield ; b.p. 160°C/15 mm Hg, lit.[15b] b. p. 162°C/15 mmHg ; m.p. of the semicarbazone 174°C, lit[15b] m.p. 175°C), ethyl 5-ketohexanoate (7.5 g, 45 % yield, b.p. 110° C/12 mmHg (220°C), lit.[15b] b.p. 222°C) and unchanged ester (6.8 g, 30 % yield).

Ethyl 5-ketohexanoate (16 g, 10 mmole) was reduced using $LiAlH_4$ (12 g, 30 mmole) to 1,5-hexanediol (12.5 g, 86 % yield). IR-Spectrum revealed a broad peak at 3380 cm^{-1} (νOH) and GLC analysis at 145°C showed a single peak at 2.3 min.

Synthesis of 1,6-Heptanediol

As described before, ethylacetoacetate (65, 500 mmole) was reacted with ethyl γ-bromobutyrate (98 %, 500 mmole) in potassium *t*-butoxide solution (20 g K, 500 mg. atom. in 1 L *t*-butanol). Diethyl α-acetoadipate (98 g., 65 % yield) was collected at 158°/12 mm, lit.[16] b.p. 160°C/12 mm.

Heating of diethyl α-acetoadipate (25 g, 100 m mole) with $CaI_2 \cdot 4H_2O$ (30 g, 75 m mole) at 140°C — 150°C for four hours gave 6-ketoheptanoic acid (5 g, 30 % yield, m.p. and lit.[15c] m.p. 40°C), ethyl 6-ketoheptanoate (9 g, 50 % yield, b.p. 110°C/9 mm, semicarbazone m.p. and lit.[15c] m.p. 107°C).

1,6-Heptanediol was obtained in 78 % yield *via* the reduction of ethyl 6-ketoheptaneoate using $LiAlH_4$. IR-Spectrum gave absorption at 3500 cm^{-1} (ν_{OH}) and GLC analysis at 145°C showed a single peak at 3.1 min.

Oxidation of Dihydric Alcohols with CrO_3/pyridine Complexes[1, 16]

General Procedure

Chromium trioxide (6 g, 60 mmole) was added to a magnetically stirred solution of pyridine (10 ml, 120 m mole) in 200 ml CH_2Cl_2. The deep burgundy solution was stirred for further 30 minutes at room temperature to ensure the formation of the CrO_3/pyridine complex to which a solution of the dihydric alcohol (10 mmole) in 20 ml CH_2Cl_2 was added in one portion, where a tarry black deposit was separated immediately. After stirring for an additional one hour at room temperature, the solution was decanted and the residue was washed with 300 ml of ether.The combined organic solutions were washed with three 100 m portions of 5 % HCl solution, with 100 ml of water and finally dried over anhydrous magnesium sulphate. Evaporation of the solvent, using water pump, afforded the crude reaction products.

Separation and identification of the different products will be described under each individual run.

Oxidation of Dihydric Alcohols with N-cyclohexyl-N′-(2-morpholinoethyl) carbodiimide-metho-*p*-toluene sulphonate/DMSO Reagent[3]

General Procedure

The dihydric alcohol (2 mmole) was dissolved in a mixture of anhydrous DMSO (6 ml), benzene (6 ml), pyridine (3 ml), and trifluoroacetic acid (1 ml). N-cyclohexyl-N′-(2-morpholinoethyl carbodiimide metho-*p*-toluenesulphonate (0.8 g, 4 mmole) was then added in one portion and the reaction mixture was kept overnight at room temperature. At the end of the reaction period, water was added and the liberated organic phase was extracted twice with ether .

The combined ether extract was washed with 5 % Na_2CO_3 solution, with water, dried over $MgSO_4$ and the filtrate was evaporated to dryness leaving the reaction product. Separation and identification of the different products will be described under each individual case.

Oxidation of Dihydric Alcohols with N-chlorosuccinimide/DMS Complex[14]

General Procedure

To a well stirred solution of N-chlorosuccinimide (1.6 g, 6 mmole) in 40 ml dry ether, there were added 6 ml (8.2 mmole) of DMS at 0°C. After the complete addition of the sulphide, a white precipitate was immediately separated. The reaction mixture was cooled to −15°C, using CCl_4-dry ice mixture, and a solution of the dihydric alcohol (2 mmole) in 10 ml dry ether was added dropwise. Stirring was continued for further three hours at −15°C, a solution of triethyl amine (3 mmole) in 50 ml dry ether was then added, the cooling bath was removed and 50 ml ether were added after 5 minutes. The separated organic layer was washed with 10 ml of 10 % hydrochloric acid and with two portions of water. Evaporation of the solvent, after drying over magnesium sulphate, gave the crude reaction product (results being found under each individual experiment).

Results of the oxidation of the diols with CrO_3/pyridine complex

Styrolenediol. The crude product showed no hydroxyl absorption and revealed instead a carbonyl absorption at 1725 cm^{-1}. Alkali washings of the product gave, after acidification, benzoic acid (200 mg, 20 % yield). GLC analysis of the crude product at 145°C showed three peaks : for benzaldehyde (52 % yield) at 1.55 min, for phenylglyoxal (10 %) at 2.75 min., and for benzoic acid (20 % yield) at 4.3 min. The products were found identical in all respects to authentic samples.

1, 4-Butanediol. Chemical analysis showed that the only product is succinaldehyde (70 %), m.p. of the semicarbazone, m.mp and lit.[17] m.p. 268°.

erythro 2-Ethyl-3-methyl-1-1, 4 butanediol. The oxidation product showed IR absorption at 1730 cm^{-1} ($\nu_{C=O}$) and gave semicarbazone derivative, m.p. 268°C. GLC analysis at 145° revealed two peaks at 3.3 min and 3.6 min. identified as *erythro* 2-ethyl-3-methyl succinaldehyde (**10**, 42 % yield) and *threo* 2-ethyl-3-methyl succinaldehyde (**11**, 23 % yield).

threo *2-Ethyl-3-methyl-1,4-butanediol*. As with **3**, the reaction product was found, using authentic samples, GLC and mmp techniques, to be composed of *erythro* 2-ethyl-3-methylsuccinaldehyde (**10**, 38 % yield) and *threo* 2-ethyl-3-methyl succinaldehyde (**11**, 23 % yield).

2-Phenyl-1, 4-pentanediol. GLC analysis of the reaction product at 145° showed a major peak at 0.95 min. and a minor one at 1.9 min. These products were found to be identical in all respects to 4-phenylcyclopent-2-eneone (**12** ; 54 % yield) and 2-phenyllevulinaldehyde (**15** ; 20 % yield). Noteworthy, treatment of the reaction product with 100 ml of 10 % NaOH solution and boiling for 15 min, resulted in the disappearance of **15** and the enrichment of **12**.

1, 5-Pentanediol. The product was found to be identical in all physical and chemical properties with an authentic sample of glutaraldehyde (75 % yield).

1, 6-Hexanediol. The product was found to be 2-cyclohexenone (**18** ; 84 % yield).

1, 6-Hexanediol. GLC analysis showed that the products are 1-cyclopentenealdehyde (**13** ; 63 % yield) and adipaldehyde (**16** ; 32 %). Also, 16 was transformed into **13** upon refluxing with 1 % NaOH solution.

1, 6-Heptanediol. GLC tracing revealed that the reaction product is a mixture of 1-acetylcyclopentene (**14** ; 69 % yield) and 6-keto-1-heptaldehyde (**17** ; 30 yield).

Results of the oxidation of the diols with Carboidiimide/DMSO Reagent

Styrolenediol. GLC analysis of the crude product showed a mixture of four compounds, two of them were found to be benzaldehyde (10 %) and phenylglyoxal (15 %), respectively. The other two compounds were identified as benzoylethanol (15 %) and 2-hydroxy-2-phenylethanal (30 %).

1, 4-Butanediol. GLC tracing revealed that the oxidation products are tetrahydrofuran (81 %) and succinaldehyde (10 %).

erythro-2-Ethyl-3-methyl-1,4-butanediol. GLC analysis proved that the oxidation products are *cis* 3-ethyl-4-methyltetrahydrofuran (major, 70 % yield), *erythro* 2-ethyl-3-methylsuccinaldehyde (minor, 12 % yield) and a trace of polymerization product (10 %) identical with that obtained by heating *erythro* 2-ethyl-3-methylbutan-1, 4-diol above its boiling point.

threo 2-Ethyl-3-methyl-1, 4-butanediol. GLC tracing showed the products to be *trans* 3-ethyl-4-methyltetrahydrofuran (major, 70% yield) and *threo* 2-ethyl-3- methylsuccinaldehyde (minor, 10% yield) in addition to a minor amount of polymerization product (10%).

2-Phenyl-1, 4-pentanediol. GLC analysis at 145°C showed four peaks at 1.7 min., 1.9 min., 5.4 min and 6.3 min. The former two components were identified as 5-methyl-3-phenyltetrahydrofuran (20%) and 2-phenyllevulinaldehyde (15%). The other two peaks were found to correspond to polymerization products (60%).

1, 5-Pentanediol. GLC analysis of the oxidation products showed that they are identical with authentic samples of tetrahydropyran (87%) and glutaraldehyde (10%).

1, 5-Hexanediol. The product was found to be identical in all physical and chemical properties with an authentic sample of 2-cyclohexeneone (66%).

1, 6-Hexanediol. GLC tracing indicated that the reaction products are a mixture of adipaldehyde (67%) and unreacted diol (20%).

1, 6-Heptanediol. The crude product showed both hydroxyl and carbonyl absorptions. GLC analysis at 145° showed a major peak corresponding to 6-keto-1-heptanal (45%) and two minor peaks at 3.1 and 3.5 min. characteristic for the partial oxidation products : 6-hydroxy-1-heptanol (26%) and 6-keto-1-heptanol (20%) respectively.

Results of the oxidation of the Diols with N—chlorosuccinimide/DMS complex

2-Phenyl-1,-4-pentanediol. GLC analysis of the reaction products at 145°C proved that they were 4-phenylcyclopent-2-eneone (**12** ; 75%) and 2-phenyllevulinaldehyde (**15** ; 15% yield).

1, 5-Hexanediol. The oxidation product was found to be 2-cyclohexaneone (**18**, 88% yield).

1. 6-Heptanediol. GLC tracing proved that the oxidation products are 1-1-acetylcyclopentene (**14** ; 85% yield) 6-keto-1-heptanal (**17** ; 10% yield).

REFERENCES

[1] H. H. Sisler, J. D. Bush and O. E. Accountins, *J. Amer. Chem. Soc.*, **70**, 3827 (1948).

[2] (a) J. Rocek and A. E. Radkawsky, *Tetrahedron Letters*, **1968**, 2835 (b) K. B. Wiberg and H. Schafer, *J. Amer. Chem. Soc.*, **91**, 292 (1969).

[3] (a) K. E. Pfitzner and J. G. Moffatt, *J. Amer. Chem. Soc.*, **85**, 3027 (1963) ; (b) *ibid*, **87**, 5661 (1965) ; (c) *ibid*, **87**, 5670 (1965).

[4] (a) E. J. Corey and C.U. Kim, *J. Amer. Chem. Soc.*, **94**, 7586 (1972) ; (b) E. J. Corey and C.U. Kim, *Tetrahedron Letters*, **1973**, 919 ; (c) *ibid*, **1974**, 287.

[5] W. M. L. Evans and L. H. Morgan, *J. Amer. Chem. Soc.*, **35**, 54 (1913).

[6] A. M. Osman, A. I. Khodair, A. A. Swelim and A.A. Abdel-Wahab, *Indian J. Chem.*, **15**B, 782 (1977).

[7] J. Von Brown, *Org. Syn., Coll.*, **1**, 428 (1948).

[8] A. I. Khodair and N. Kharasch, "The American Chemical Society Meeting", Los Angeles, Oct. 28—30 (1975).

[9] W. J. Podbielniak, *Ind. Eng. Chem. Anal. Ed.*, **3**, 177 (1931).

[10] B. Heathcoat, *J. Chem. Soc.*, **1929**, 271.

[11] J. Cason and A. I. Khodair, *J. Org. Chem.*, **31**, 3618 (1966).

[12] A. I. Vogel, "A Text-Book of Practical Organic Chemistry", 3rd editon, Longman, London, 1956, p. 879.

[13] E. Schwenk and D. Papa, *J. Amer. Chem. Soc.*, **70**, 3626 (1948).

[14] (a) G. F. Baddar, S. Sherif, *J. Chem. Soc.*, **1961**, 707.
(b) L. J. Bellamy, "The Infrared Spectra of Complex Molecules", Methuen, London, 1978.

[15] I. Helborn and H. M. Bunbury, "Dictionary of Organic Compounds", Vol. 3, Erye and Spottiswoode London, (b) *ibid*, Vol. 1, 1946 p. 9, (c) *ibid*, 1, 1946, p. 18.

[16] R. Ratcliffe and R. Rodehorst, *J. Org. Chem.*, **35**, 4000 (1970).

[17] R. M. Acheson and R. Robinson, *J. Chem. Soc.*, **1952**, 1127.

Revue Roumaine de Chimie, 28, 9–10, 933–939 (1983)

THEORETICAL ASPECTS ON THE REACTIVITY OF THE CYCLOIMMONIUM-YLIDES. II[1]

REACTIVITY OF THE DISUBSTITUTED CARBANION-YLIDES

GH. SURPĂŢEANU*, M. CONSTANTINESCU **, C. LUCHIAN *, M. PETROVANU*
I. ZUGRĂVESCU * and A. LABLACHE-COMBIER ***
* Polytechnic Institute "Gh. Asachi", Organic Chemistry Department, Jassy, 11, str. 23 August, Romania
** Computer Center of the University "Al. I. Cuza" Jassy, Romania
*** Physical Organic Chemistry Department, University of Lille, France

Received October 25, 1982

Perturbation and frontier orbital theories are applied to explain the reactivity of some disubstituted carbanion cycloimmonium ylides. Molecular orbital calculations have been performed by CNDO/2 method. All studied ylides have as common structural element the carbanion $-C^-(CO_2CH_3)_2$ bonded to a cycloimmonium cation resulted from pyridine, pyridazine, pyrimidine, isoquinoline, phthalazine and 4-phenyl-1, 2, 4-triazole.

The disubstituted carbanion cycloimmonium ylides are represented by the following structure : [2]

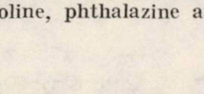

I

in which the cycloimmonium cation is always derived from an azaheterocycle and R_1 and R_2 are electron with drawing substituents as COAr, COOR, CN, CONHR etc.

For these compounds many resonance structures may be considered:

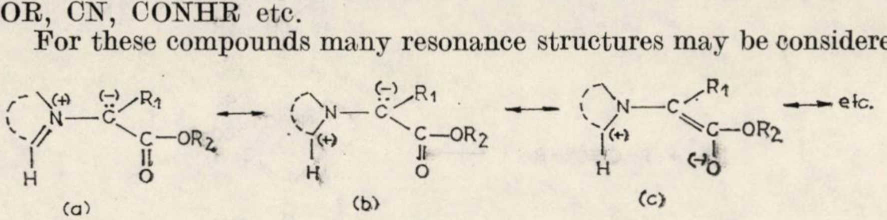

II

The chemical properties of disubstituted cycloimmonium ylides can be rationalized as follows: cleavage of the N^+-C^- bond, nucleophilic character and cycloaddition reactions involving the resonance structures, IIa (3+2 cycloadditions) and IIc (5+2 cycloadditions).

By the cleavage of the ylidic bond, N^+-C^-, the cyclopropanic derivatives are formed via carbene formation. [3,4]

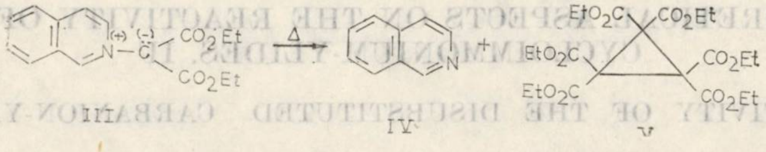

(+)
(−)
CO₂Et
CO₂Et
Δ
EtO₂C
CO₂Et
EtO₂C
CO₂Et
EtO₂C
CO₂Et
III
IV
V

The disubstituted ylides are less nucleophilic reagents than the analogous monosubstituted ylides. Their nucleophilic behaviour can be explained by the influence of the ylide C atom substituents. In some cases the negative charge of the ylide C atom is delocalized on the substituents. Therefore, the protonation of disubstituted ylide VI, in the presence of strong acids (H_2SO_4, $HClO_4$), occurs to the negatively charged carbethoxy oxygen. By the decomposition of the intermediate cycloimmonium salt VII, one obtains the monosubstituted salt X. [5-7]

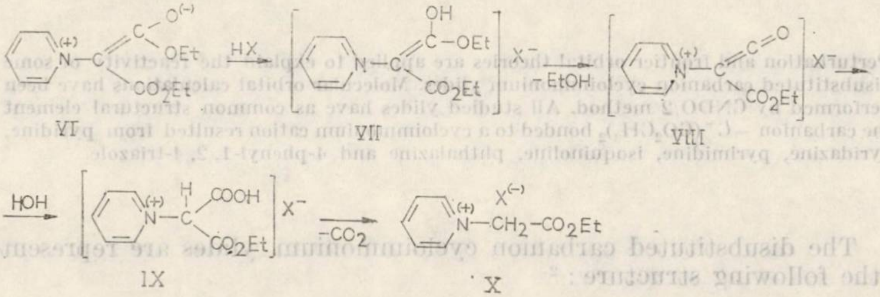

O(−)
OEt
(+)
CO₂Et
HX
OH
C−OEt
CO₂Et
X⁻
−EtOH
(+)
C=O
CO₂Et
X⁻
VI
VII
VIII
HOH
(+)
H
COOH
CO₂Et
X⁻
−CO₂
(+)
X(−)
N−CH₂−CO₂Et
IX
X

By their resonance structures IIb the disubstituted ylides undergo 3 + 2 cycloadditions with double [8,9] or triple bond [10,11] dipolarophiles:

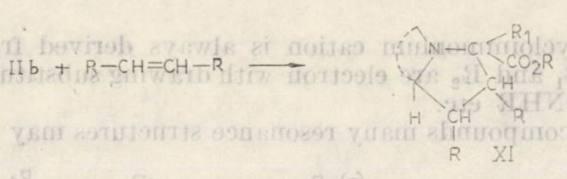

IIb + R−CH=CH−R
R₁
CO₂R
CH
H
CH
R
R
XI

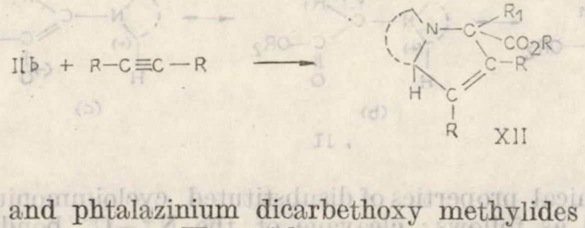

IIb + R−C≡C−R
R₁
CO₂R
C−R
H
C
R
XII

Isoquinolinium and phtalazinium dicarbethoxy methylides react as 1,5 dipole (resonance structure II)c with acetylene dimethyl-dicarboxylate (DMAD) giving oxazepinic compounds: [12,13]

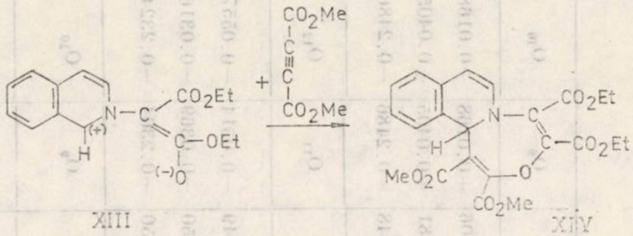

XIII XIV

RESULTS AND DISCUSSION

Perturbation theory has been found to provide a very useful method of understanding diverse organic phenomena. This paper reports applications of perturbation theory to explain the reactivity of disubstituted carbanion cycloimmonium ylides.

The studied ylides are derived from pyridine, isoquinoline, quinoline, pyridazine, pyrimidine, phtalazine and 4-phenyl-1, 2, 4-triazole, all having in common the carbanion—$C^-(CO_2CH_3)_2$. The molecular orbital calculations reported here were carried out by CNDO/2 method, [14] on a Felix C—256 computer.

The geometries of the studied ylides used for these calculations have been approximated taking into account the geometries of the corresponding monosubstituted ylides [1] and the geometry of a carbomethoxy group. [15] The two carbomethoxy groups bonded to the ylide C atom are symmetrically disposed.

Table 1 presents the total atomic charges, Q, the frontier orbital energies for HOMO (the highest occupied molecular orbital) and LUMO (the lowest unoccupied molecular orbital) and the p_z atomic orbital coefficients of some atoms representing virtual reaction centers in disubstituted carbanion cycloimmonium ylides.

Next, the generalized perturbation [16] and frontier molecular orbital[17,18] theories, used in the previous paper [1], are used to discuss the chemical behaviour of disubstituted ylides.

An analysis of Table 1 shows that ylide C atoms are negatively charged, with the values ranged between -0.2214 and -0.2783. These values are lower than those in the corresponding monosubstituted ylides. [1] Also, the atomic orbital coefficients of ylide C atoms in HO and LU orbitals have lower absolute values than those of ylide C atoms in the corresponding monosubstituted ylides. [1] Therefore, it may be appreciated that in the donor-acceptor single site reactions the disubstituted cycloimmonium ylides, by the ylide C atoms, are less nucleophilic reagents than the analogous monosubstituted ylides.

The double bonded O atoms of the carbomethoxy groups in ylide molecules in Table 1, have strong negative charges and higher absolute atomic orbital coefficients values comparatively with the same O atoms in the monosubstituted ylides. [1] Thus, it is understandable the protonation of the disubstituted ylides at the level of these O atoms. [5–7]

Table 1

The frontier orbital energies and p_z atomic orbital coefficients

No.	Molecule	Orbital and atomic charge	Orbital energy (eV)	Atomic orbital coefficients							
				N_1	C_2	C_6	C_i	O_7	O_8	O_9	O_{10}
1	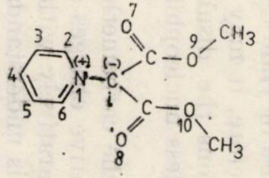 7 O 9 CH3 3 2 (+) (−) C O 4 N C 1 i 5 6 C O 10 O 8 CH3	H O	−10.36980	+0.1071	+0.2434	+0.2435	−0.6411	+0.4306	+0.4306	+0.0168	+0.0168
		L U	0.29018	+0.5739	−0.4063	−0.4062	−0.2048	+0.1381	+0.1381	+0.0405	+0.0405
		Q		+0.0406	+0.0190	+0.0191	−0.2672	−0.3548	−0.3548	−0.2486	−0.2486
				N_2	C_1	C_3	C_i	O_9	O_{10}	O_{11}	O_{12}
2	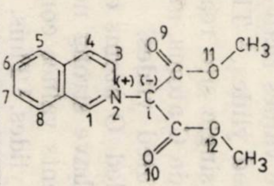 5 4 O 9 11 CH3 6 3 (+) (−) C O 7 N 2 C i 8 1 C O 12 O 10 CH3	H O	−9.70682	−0.1360	−0.3506	−0.1334	+0.6555	−0.3722	−0.3649	−0.0514	−0.0557
		L U	0.23409	−0.4868	+0.5048	+0.0226	+0.1909	−0.1259	−0.1350	−0.0369	−0.0316
		Q		+0.1462	+0.0217	+0.0249	−0.2783	−0.3795	−0.3750	−0.2304	−0.2324
				N_1	N_2	C_6	C_i	O_7	O_8	O_9	O_{10}
3	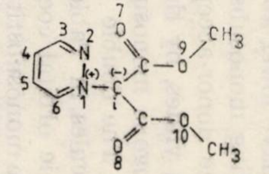 7 O 3 2 CH3 9 4 N (+) (−) C O 5 N C 6 1 i C O 10 O 8 CH3	H O	−10.19021	−0.0476	−0.2895	−0.2661	+0.6671	−0.3811	−0.3949	−0.0469	−0.0342
		L U	0.45075	−0.5650	+0.4808	+0.1708	+0.2287	−0.1596	−0.1553	−0.0444	−0.0392
		Q		+0.2487	−0.0844	+0.0112	−0.2624	−0.3701	−0.3533	−0.2282	−0.2320

				N_1	C_2	C_6	C_i	O_7	O_8	O_9	O_{10}
4	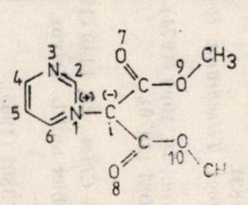	H O	−9.82031	−0.0995	−0.2533	−0.2453	−0.6961	−0.3842	−0.3902	−0.0617	−0.0561
		L U	1.12724	−0.5228	+0.1861	+0.4758	+0.1642	−0.1277	−0.1298	−0.0373	−0.0345
		Q		+0.1881	+0.1154	+0.0873	−0.2639	−0.3990	−0.3956	−0.2307	−0.2325
				N_2	N_3	C_1	C_i	O_9	O_{10}	O_{11}	O_{12}
5	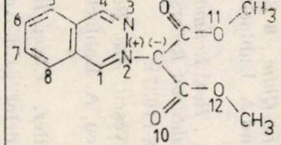	H O	−9.47529	−0.0909	−0.1632	−0.3701	+0.6546	−0.3744	−0.3482	−0.0429	−0.0647
		L U	0.29132	+0.3820	+0.1318	−0.4660	−0.1621	+0.1017	+0.1170	+0.0295	+0.0275
		Q		+0.2648	−0.0765	−0.0272	−0.2214	−0.3899	−0.3918	−0.2353	−0.2284
				N_1	N_2	C_5	C_i	O_6	O_7	O_8	O_9
6	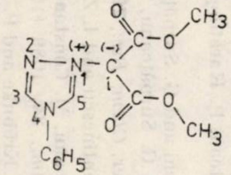	H O	−9.15840	−0.1283	−0.1407	−0.3259	+0.6854	−0.3721	−0.3979	−0.0657	−0.0423
		L U	1.47544	−0.3279	−0.1814	+0.4639	+0.1059	−0.0873	−0.0744	−0.0222	−0.0229
		Q		+0.2300	−0.0838	+0.0562	−0.2624	−0.4129	−0.3899	−0.2319	−0.2412

The absolute atomic orbital coefficient values in HO and LU orbitals of the ylide C atoms (Table 1) are larger than those of the oxygen atoms. This explains the 1,3 dipolar structure (IIb) of these ylides. The available experimental data refer to many $3 + 2$ [8-10] and $3 + 3$ [9,19] cycloaddition reactions of the disubstituted ylides as 1,3 dipoles. Such 1,3 ylidic dipoles are located between ylide C atom and an endocyclic adjacent C atom to the positive cyclic nitrogen. Taking into account the atomic orbital coefficient values there have been established the most probable structures of the 1,3 ylidic dipoles in the molecular systems in this report.

On the basis of the same considerations as in the previous paper[1] the structures of 1,3 dipoles in the disubstituted ylides **1** — **6** are similar positions in molecules as in the analogous monosubstituted ylides.

Thus, in pyridinium dicarbomethoxy methylide **1** the 1,3 dipole is located at $C_i—C_2$ or $C_i—C_6$ atoms (C_2 and C_6 atoms having the same reactivity). In isoquinolinium dicarbomethoxy methylide **2** the i, 3 dipole is $C_i—C_1$. Pyridazinium dicarbomethoxy methylide **3** presents two possibilities for the structure of the 1,3 dipole : $C_i—C_1$ or $C_i—N_3$, but the most probable is $C_i—C_1$ dipole. In pyrimidinium dicarbomethoxy methylide **4**, the 1, 3 dipole is $C_i—C_6$. In phtalazinium dicarbomethoxy methylide **5**, $C_i—C_1$ is the most reactive structure for the 1,3 dipole. In the case of 4-phenyl-1, 2, 4-triazolium dicarbomethoxy methylide **6**, the 1,3 dipole is $C_i—C_5$.

To summarize, the disubstituted carbanion cycloimmonium ylides are less nucleophilic reagents, at the ylide C atom, as the analogous monosubstituted ylides. As 1,3 dipoles the disubstituted ylides are very similar with the monosubstituted ylides. It must be emphasized that a very rigorous investigation of the cycloaddition reactions in orbital terms implies the drawing of the orbital correlation diagrams for each ylide dipole-dipolarophile pair. In the ylide systems with two nitrogen atoms the total energies must be calculated in view of finding the most stable molecular configuration.

The theoretical results in this paper suggest the possibility of synthesis of new azaheterocyclic compounds.

REFERENCES

[1] Part I : Gh. Surpăţeanu, M. Constantinescu, C. Luchian, M. Petrovanu, I. Zugrăvescu and A. Lablache-Combier, *Rev. Roumaine Chim.*, **8** 831, (1983).

[2] G. Surpăţeanu, J. P. Catteau, P. Karafiloglu and A. Lablache-Combier, *Tetrahedron Report*, **1976**, 23.

[3] I. Zugrăvescu, E. Rucinschi and G. Surpăţeanu , *Rev. Roumaine Chim.*, **16**, 1099 (1971).

[4] A. Lablache-Combier and G. Surpăţeanu, *Tetrahedron Letters*, **35**, 3081 (1976).

[5] F. Kröhnke and H. Kubler, *Chem. Ber.*, **70**, 538 (1937).

[6] G. Surpăţeanu, M. Constantinescu and I. Zugrăvescu, *Rev. Roumaine Chim.*, **23**, 1449 (1978).

[7] I. Zugrăvescu, G. Surpăţeanu, M. Constantinescu, A. Lablache-Combier and L. Devos, *Rev. Roumaine Chim.*, **24**, 1089 (1979).

[8] W. Friedrich, H. Kehr. F. Kröhnke and P. Schiller, *Chem. Ber.* **98**, 3808 (1965).

[9] I. Zugrăvescu, and M. Petrovanu, "Chimia N-ilidelor", Ed. Academiei, 1974.

[10] W. J. Linn, O. W. Webster and R. E. Benson, *J. Amer. Chem. Soc.*, **87**, 3651 (1965).

[11] C. A. Henrick, E. Ritchie and W. C. Taylor, *Austral. J. Chem.*, **20**, 2441 (1967).

[12] I. Zugrăvescu, E. Rucinschi and G. Surpăţeanu, *Anal. Sti. Univ. "Al. I. Cuza", Iaşi*, **16**, **f. 1**, 41 (1970).

[13] M. Petrovanu, A. Sauciuc and I. Zugrăvescu, *Anal. Sti. Univ., "Al. I. Cuza", Iași*, **16**, 65 (1970).

[14] J. A. Pople and D. L. Beveridge, "Approximate Molecular Orbital Theory", McGraw-Hill, New York, 1970.

[15] J. M. O. Gorman, W. Shand and V. Schomaker, *J. Amer. Chem. Soc.*, **72**, 4222 (1950).

[16] G. Klopman, "Chemical Reactivity and Reaction Paths," Wiley Interscience, 1974.

[17] K. Fukui, "Theory of Orientation and Stereoselection", Springer-Verlag, Berlin, 1975.

[18] J. Fleming, "Frontier Orbitals and Organic Chemical Reactions" Wiley, New York, 1976.

[19] H. Albrecht, J. Froehlich, U. Hobermoltz and F. Kröhnke, *Tetrahedron Letters*, **37**, 3649 (1967).

Revue Roumaine de Chimie, 28, *9–10*, 941–949 (1983)

IONIC PRODUCTS OF H_2O-CH_3CN AND CH_3OH-CH_3CN MIXTURES

JEAN-LOUIS BRISSET

Laboratoire de Chimie Analytique des Processus Industriels, E.S.P.C.I., 10, rue Vauquelin, 75005 Paris, France

Received July, 13, 1981

Aqueous and methanolic solutions of acetonitrile (AN) have been examined electrochemically. Emf measurements of the cells with junctions

Pt, H_2 / acid or // sat. KCl // sat. KCl / Hg_2Cl_2, Hg
base in S in water

allow the determination of the autoprotolysis products of the mixtures. The values of pK_i continuously increase with the molar fraction X(AN)-for both series of solvents. This confirms that AN has little interaction with the co-solvents considered. The acidity levels of the solvated proton have been determined with reference to a particular extrathermodynamic assumption similar to Popovich's. Agreement with literature data resulting from other assumptions is discussed.

Numerous studies are concerned with the determination of the transfer free energy $\Delta G_t^0\,(i) = {}_sG^\circ(i) - {}_wG^\circ(i)$ of a particular ion (i), mainly H^+, between pure water (W) and some pure organic solvent. An alternative parameter for the transfer is the transfer activity coefficient of i, namely γ_t (i), which is given by

$$\Delta G_t^0(i) = RT \ln \gamma_t(i).$$

The values of $\Delta G^\circ_t(i)$ or $\gamma_t(i)$ are strongly dependent on the extrathermodynamic assumption selected for their determination, as shown by comprehensive papers. [1–5]

The water-acetonitrile (W–AN) mixtures received a limited attention compared to pure solvents, and the physico-chemical data reported in the recent literature are mainly connected with :

- the hydration of undissociated salts in AN, [6]
- spectrophotometric studies of selected indicators, [7–9]
- potentiometric studies of acido-basic systems, [9–13]
- transfer parameters, [14–16] if one excepts conductometric data. [17]

We have determined the autoprotolysis constants of numerous binary mixtures W–AN from emf measurements. We have also calculated the values of $\gamma_t(H^+)$ between water and a given mixture W–AN denoted S, on the basis of a particular extrathermodynamic assumption close to Popovich's. In addition, we report on the MeOH—AN mixtures which are an example of isodielectric media[18] since D varies from 32.6 (Pure MeOH) to 36.5 (pure AN).

RESULTS AND DISCUSSION

A. Autoprotolysis products

If we keep in mind that the deprotonation of CH_3CN is very difficult, we can consider that the concentration of CH_2CN^- can be neglected in both series of mixtures W—AN and MeOH—AN. Consequently only five species occur in the equilibria which govern the mixtures. For the W—AN mixtures, the species H_2O, AN, H_3O^+, ANH^+ and OH^- react together according to

$$2\ H_2O = H_3O^+ + OH^- \qquad K_1$$

$$H_2O + ANH^+ = H_3O^+ + AN \qquad K_2$$

$$H_2O + AN = ANH^+ + OH^- \qquad K_3$$

The autoprotolysis constant of a given mixture is defined from the activities of the anionic and cationic species, $a(S^-) = \Sigma a(j^-)$ and $a(S^+) = \Sigma a(k^+)$ by :

$$K_i = a(S^+) \cdot q(S^-)$$

If one discards the CH_2CN^- ions, K_i takes a simplified expression :

$$K_i = [a(H_3O^+) + a(ANH^+)] \cdot a(OH^-)$$

or

$$K_i = a(H_3O^+) \cdot a(OH^-) \cdot (1 + 1/K_2)$$

Since W and AN react little together, equilibrium 3 is moved to the left and ANH^+ exists in negligible concentration ; a good approximation for K_i is then given by :

$$K_i = a(H_3O^+) \cdot a(OH^-)$$

which is an expression of the autoprotolysis constant similar to that used by Harned[19] or Grunwald[20] for the water-dioxane mixtures.

In order to determine K_i we took again cells with junctions which were already described and used for the study of other hydro-organic mixtures[21].

$$\mathrm{Pt, H_2}\ \Big|\ \begin{array}{c}\text{acid } \textit{or}\\ \text{base in S}\end{array}\ \overset{J' \textit{ or } J''}{\Big\|}\ \begin{array}{c}\text{sat. KCl}\\ \text{in S}\end{array}\ \overset{J}{\Big\|}\ \begin{array}{c}\text{sat. KCl}\\ \text{in W}\end{array}\ \Big|\ \mathrm{Hg_2Cl_2, Hg} \quad (A)\ \textit{or}\ (B)$$

These cells operate with acidic (cell A) or basic (cell B) solutions of known concentrations in a given solvent mixture. The relevant emf values at 25°C are reported in Table 1. The suitable association of cells (A) and (B) leads, for equal concentrations of acid and base to cell (C), the emf E(C) of which is given by :

$$E(C) = (2.3\ RT/F) \cdot (pK_i + 2 \log c + \log \gamma_+ \beta\gamma_-) + E_{J''} - E_{J'},$$

Table 1

Emfs (mV) of cells (A) and (B) in W–AN mixtures ($\theta = 25°C$)

	AN, v/v % / C(M)	10	20	30	40	50	60	70	80
E(A)	$2\ 10^{-1}$	281.5	279.5	278	273	268	261	249	
	10^{-1}	300	298	296	292	286	278	267	256
	$5\ 10^{-2}$	317.5	316	313.5	308.5	301	293	283	272
	$3\ 10^{-2}$	330	329	325	320	312	305	295	284.5
	$2\ 10^{-2}$	339	338	335.5	330	323	314.5	302.5	293
	10^{-2}	357	355	352	347	337.5	329	316	302
	$5\ 10^{-3}$	373	370	368.5	362	355	346	333	316
	$3\ 10^{-3}$	386	383	380	375	369	358	346	326
	$2\ 10^{-3}$	395	394	391	385	378	368	354	336
E(B)	$2\ 10^{-3}$	904.5	920	935	950	964	982	1004.5	(a)
	$3\ 10^{-3}$	920	933	947	961	975	996	1019.5	,,
	$5\ 10^{-3}$	936	947	962	976	990	1009	1033	,,
	10^{-2}	954	966	980	995	1008	1027	1052	,,
	$2\ 10^{-2}$	972	985	997	1012	1025	1044	1069	,,
	$3\ 10^{-2}$	982	995.5	1008	1024	1037	1057	1078	,,
	$5\ 10^{-2}$	994	1007	1020	1036	1048.5	1068	(1086)	,,
	10^{-1}	1010	1024	1037	1052	1065	1085	(a)	,,
	$2\ 10^{-1}$	1026	1040	1052	1068	1082	(a)	,,	,,

(a) demixtion.

$E_{J'}$ and $E_{J''}$ are diffusion potentials the difference in which can be neglected in first approximation.

We assumed then that the mixtures follow the Debye-Hückel theory, i.e. $\log \gamma_+\gamma_-$ is a linear function of the sq. root of the ionic strength $\sqrt{I}$, and we plotted

$$Y = pK_1 + \log \gamma_+\gamma_- = (F/2.3\ RT) \cdot E(C) - 2 \log c$$

against $\sqrt{I}$ for the various sets of values (c ; E(C)). The graphs are linear (Fig. 1), as they are for other mixtures examined with this technique, and they extrapolate to pK_i for $I = 0$. This extrapolation remains however formal since it is impossible to get solutions with a ionic strength lower than the pure mixture. The slopes of the graphs $Y = f(\sqrt{I})$ provide the values of Debye's constant A in the simplified expression of the activity

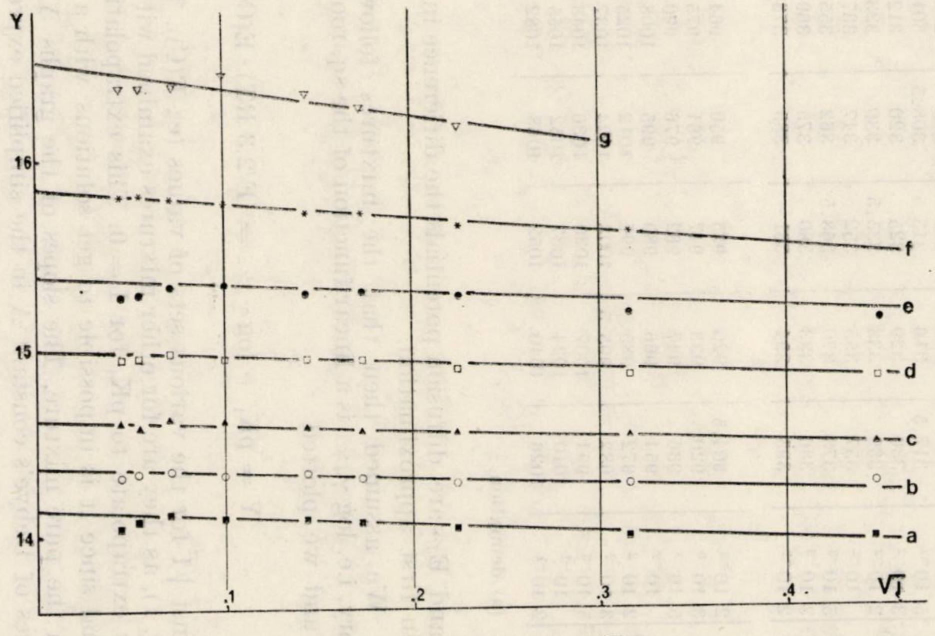

Fig. 1. — Determination of pK_i. Typical plots of $Y = f(\sqrt{I})$ for W—AN mixtures. Graphs $a, b, \ldots$ correspond to solvent composition 10, 20, 30, 40, 50, 60, 70% volume AN.

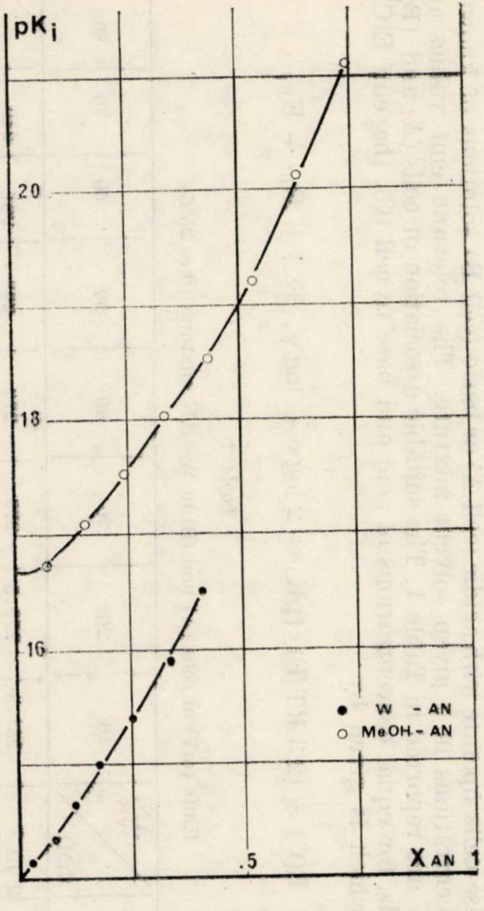

Fig. 2. — Autoprotolysis products of W— AN and MeOH— AN mixtures.

coefficient (i.e. $\log \gamma_+\gamma_- = -(A_+ + A_-)\sqrt{I} = -A\sqrt{I}$). As evident from Table 2, A shows limited variations with the mixture composition, which is not verified for mixtures with strong interactions between the co-solvents.

Table 2

Autoprotolysis products and acidity levels of the proton in W—AN mixtures. (The solvent composition is given in volume AN %)

AN, vol %	10	20	30	40	50	60	70	80	90
X_{AN}	.035	.078	.13	.19	.255	.34	.45	.58	.75
Debye's constant A	−.48	−.40	−.35	−.38	−.45	−.85	−1.38		
pK_i	14.14	14.37	14.62	15.00	15.38	15.87	16.50	(17.35)	
$(f_H{}^a)^\circ$	−.18	−.20	−.25	−.35	−.50	−.65	−.87	−1.30	
$(f_H{}^b)^\circ$	13.98	14.18	14.40	14.65	14.86	15.18	15.58		
$(f_H{}^S)$	7.08	7.19	7.33	7.5	7.68	7.92	8.23		

Figure 2 illustrates the variations of the ionic product with the solvent composition: pK_i continuously increases with the molar fraction in AN, X_{AN}. The MeOH—AN mixtures give similar results (Table 3 and Fig. 2) if one considers MeOH and $MeOH_2^+$ instead of H_2O and H_3O^+. The reported value for the autoprotolysis product of pure AN [22], i.e. 26.5, fits with both graphs and can be considered as the extrapolated value of pK_i to $X_{AN} = 1$.

B. Acidity levels

The difference of the junction potentials $E_{J''} - E_{J'}$, appears in the expression of the emf E(C), and is reasonably neglected in the determination of pK_i since $E_{J'}$, and $E_{J''}$ are diffusion potentials of the same order of magnitude. The junction potential E_J which has its origin in the diffusion of the solvents S and W (or MeOH) remains unknown. The determination of the acidity level of the solvated proton in a given solvent mixture by means of cells (A) and (B) requires that E_J be evaluated. Gaboriaud [23] has reported that the estimation of E_J was equivalent to the use of some particular extrathermodynamic assumption. If we assume that $E_J \sim 0$, then we consider that $\gamma_t(K^+) = \gamma_t(Cl^-)$, which is similar to Popovich's assumption.

The function f_H, which is defined from emf measurements by

$$f_H{}^a = (F/2.3\ RT) \cdot ({}^{S}E(A) - E^\circ_{\text{aq. calomel}})$$

identifies with pH when the solvent S is water, and indicates the variations of the chemical potential of the proton in S, provided the junction potentials be negligible. As previously mentioned [24] the function f_H takes the particular value $(f_H{}^a)^\circ$ when extrapolated to $a(S^+) = 1$. In alkaline media, the corresponding function noted $f_H{}^b$ extrapolates at $(f_H{}^b)^\circ$ for $a(S^-) = 1$. The limit values $(f_H{}^a)^\circ$ and $(f_H{}^b)^\circ$ differ by pK_i and indicate the range of acido-basicity available in the mixture. Table 2 reports also information of the acidity levels of the "neutral" solvents (i.e. without addition of acid or base) which are given by

$$f_H^S = (f_H^a)^\circ + \frac{1}{2}\,pK_i = (f_H^b)^\circ - \frac{1}{2}\,pK_i$$

Table 3

Emfs (mV) of cells (A) and (B) in MeOH—AN mixtures ($\theta = 25°C$)

	AN, vol % / C(M)	10	20	30	40	50	60	70	80
E(A)	$2\ 10^{-1}$	183	176	172	163	150	136	120	104
	10^{-1}	193	188	184	174	161	147	130	115
	$5\ 10^{-2}$	205	199	194	185	172	157	141	125
	$3\ 10^{-2}$	212	205	201	192	178	166	147	133
	$2\ 10^{-2}$	220	214	209	200	184	173	155	138
	10^{-2}	234	225	220	210	195	184	165	150
	$5\ 10^{-3}$	240	234	229	218	204	193	174	161
	$3\ 10^{-3}$	255	245	239	230	215	204	185	169
	$2\ 10^{-3}$	260	253	249	237	223	212	194	176
E(B)	$2\ 10^{-1}$	1055	1070	1090	1102	1120	1151	1182	1232
	10^{-1}	1038	1052	1071	1087	1105	1130	1166	1214
	$5\ 10^{-2}$	1020	1033	1054	1070	1087	1113	1150	1197
	$3\ 10^{-2}$	1007	1020	1041	1056	1073	1099	1137	1180
	$2\ 10^{-2}$	996	1011	1032	1047	1063	1089	1123	1168
	10^{-2}	979	993	1011	1031	1044	1073	1108	1151
	$5\ 10^{-3}$	962	973	996	1012	1026	1057	1090	1137
	$3\ 10^{-3}$	950	960	981	998	1015	1043	1076	1121
	$2\ 10^{-3}$	940	952	970	988	1005	1032	1065	1112

The f_H^S function remains almost independent of the solvent composition: this illustrates the symmetry of the variations of $(f_H^a)^\circ$ and $(f^b_H)^\circ$ with X_{AN}, which was not verified for other mixtures [21] and confirms the weak interactions of the co-solvents in the mixtures.

Literature data relevant to W—AN mixtures enable us to compare $(f_H^a)^\circ$ with other acidity functions. As expected, and discussed for other binary mixtures, [25] a good or a poor agreement is observed depending on whether the basic extrathermodynamic assumptions used are similar or not. Figure 3 reports Douheret's δ° functions (14) and $(f_H^a)^\circ$ which agree better than .4 pH units; Strehlow's $R^\circ(H)$ function fits moderately with Hammett's H° function [26] and shows about 3 pH units discrepancy with the preceeding functions.

The values of the acidity functions $(f_H^a)^\circ$ and $(f_H^b)^\circ$ relevant to MeOH—AN mixtures are listed in Table 4. Comparison with the corresponding function $(f_H^a)^\circ$ related to W—AN solvents shows that the proton is more stabilized by MeOH than by water for a given molar fraction in AN.

Table 4

Autoprotolysis products and acidity levels of the proton in MeOH—AN mixtures.

X_{AN}	.10	.20	.30	.40	.50	.60	.70	75
pK_i	16.85	17.30	17.85	18.40	19.05	19.90	20.73	21.20
$(f_H{}^a)^\circ$	— 2.45	— 2.60	— 2.80	— 3.00	— 3.20	— 3.40	— 3.75	— 3.95
$(f_H{}^b)^\circ$	14.50	14.75	15.10	15.45	15.85	16.40	17.00	17.35
$(f_H{}^S)$	6.00	6.10	6.20	6.25	6.35	6.50	6.62	6.70

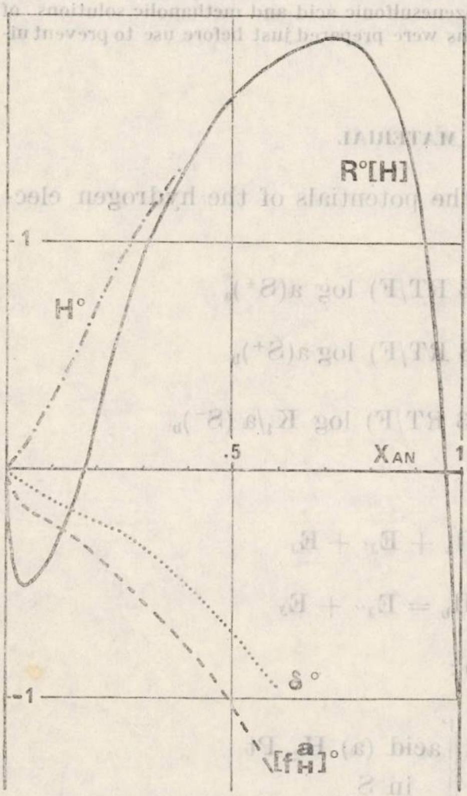

Fig. 3. — Acidity levels of the proton in W—AN mixtures according to various extrathermodynamic assumptions (Y axis in pH units).

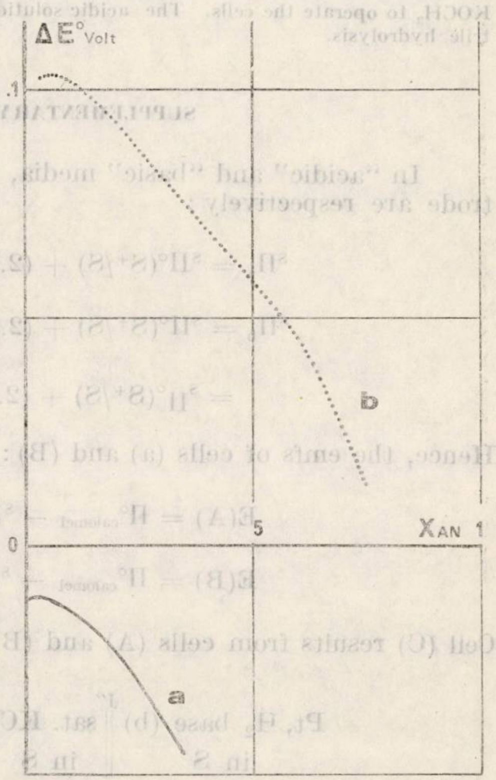

Fig. 4. — Standard emf of cells. a) Bennetto-Spitzer (18); b) this work.

In addition, the standard emf values E°(A) calculated from the corresponding $(f_H{}^a)^\circ$ values (Table 4) are plotted against solvent composition (Fig. 4) and compared to the standard emf of the cells studied by Bennetto and Spitzer[18]

$$H_2/HCl/AgCl,\ Ag.$$

Both graphs are parallel: this gives evidence that chlorhydric and benzenesulfonic acids behave as strong acids in the considered mixtures, and suggests that the junction potentials $E_J + E_{j'}$, remain constant and independent of the solvent composition.

EXPERIMENTAL

The cells have been already described (21). The temperature is fixed at 25 ± ·1°C by circulation of water in a thermostated jacket.

Potentials were measured with an accuracy of ± ·5 mV. Two independent measurements on aqueous mixtures are reproducible within 2 mV, and about 10 mV for non-aqueous solvents.

Solvents were distilled before use and stored under N_2.

Analytical grade solutions of HCl and NaOH were used for the study of W—AN mixtures, but for non-aqueous media we selected benzenesulfonic acid and methanolic solutions of $KOCH_3$ to operate the cells. The acidic solutions were prepared just before use to prevent nitrile hydrolysis.

SUPPLEMENTARY MATERIAL

In "acidic" and "basic" media, the potentials of the hydrogen electrode are respectively :

$$^{S}\Pi_a = {}^{S}\Pi^\circ(S^+/S) + (2.3\ RT/F)\ \log a(S^+)_a$$

$$^{S}\Pi_b = {}^{S}\Pi^\circ(S^+/S) + (2.3\ RT/F)\ \log a(S^+)_b$$

$$= {}^{S}\Pi^\circ(S^+/S) + (2.3\ RT/F)\ \log K_i/a\ (S^-)_b$$

Hence, the emfs of cells (a) and (B) :

$$E(A) = \Pi^\circ_{calomel} - {}^{S}\Pi_a + E_{J'} + E_J$$

$$E(B) = \Pi^\circ_{calomel} - {}^{S}\Pi_b = E_{J''} + E_J$$

Cell (C) results from cells (A) and (B) :

$$\begin{array}{c|c|c} & J'' & J' \\ \text{Pt, } H_2 \text{ base (b)} & \text{sat. KCl} & \text{acid (a) } H_2\text{, Pt} \\ \text{in S} & \text{in S} & \text{in S} \end{array}$$

and the corresponding emf is :

$$E(C) = E_{J''} - E_{J'} + (2.3\ RT/F) \cdot (pK_i + \log a.b + \log \gamma_+ \cdot \gamma_-)$$

The function f_H takes the form :

$$f_H{}^a = (F/2.3\ RT)\ (E(A) - {}^{S}\Pi^\circ_{calomel})$$

$$= (F/2.3\ RT)\ (E_{J'} + E_J - {}^{S}\Pi^\circ(S^+/S) - (2.3\ RT/F) \log a(S^+)_a)$$

$$= -\log a - \log \gamma_+ \ + (F/2.3\ RT)\ (-{}^{S}\Pi^\circ\ (S^+/S) + E_{J'} + E_J)$$

Then

$$f_H^a + \log a = (F/2.3\,RT)(-{}^{S}\Pi^\circ(S^+/S) + E_{J'} + E_J) + \alpha\sqrt{a} = \Phi(\sqrt{a})$$

and similarly

$$f_H^b - \log b = (F/2.3\,RT)(-{}^{S}\Pi^\circ(S^+/S) + E_{J''} + E_J) + pK_1 - \beta\sqrt{b} = \Phi(\sqrt{b}).$$

$(f_H^a)^\circ$ and $(f_H^b)^\circ$ are also obtained from the definition of f_H^a and f_H^b for the particular values $E(A)^\circ$ and $E(B)^\circ$.

J.C. Halle, R. Gaboriaud and R. Schaal, *Bull. Soc. chim. France*, **1969**, 1851.
R. Gaboriaud, J. Chim. phys., **67**, 349 (1970).
R, Gaboriaud and J.L. Brisset, J. Chim. phys., **67**, 1715 (1970).
J.L. Brisset, R. Gaboriaud and R. Schaal, J. Chim. phys., **67**, 1726 (1970).

REFERENCES

1. J. F. Coetzee and J. J. Campion, *J. Amer. Chem. Soc.*, **89**, 2513 (1967).
2. O. Popovych, *Crit. Rev. Anal. Chem.*, **7**, 73 (1970).
3. A. J. Parker, *Chem. Rev.*, **69**, 1 (1969).
4. I. M. Kolthoff, *Pure Appl. Chem.*, **25**, 305 (1971).
5. R. Alexander, A. J. Parker, J. H. Sharp and W. E. Waghorne, *J. Amer. Chem. Soc.*, **94**, 1148 (1972).
6. I. M. Kolthoff, and M. K. Chantooni, *J. Amer. Chem. Soc.*, **89**, 2521 (1967).
7. J. Desbarres, *Bull. Soc. chim. France*, **1965**, 3240.
8. M. K. Chantooni, and I. M. Kolthoff, *J. Amer. Chem. Soc.*, **92**, 2236 (1970).
9. F. Jordan, *J. Phys. Chem.*, **77**, 2681 (1973).
10. R. S. Farinato, R. P. Tomkins and P. J. Turner, *Analyt. Chim. Acta*, **70**, 245 (1974).
11. T. Mussini, P. Longhi and P. Giammario, *Chim. e Indust.*, **53**, 1124 (1971) and **54**, 3(1972).
12. J. A. Lanning and J. Q. Chambers, *Analyt. Chem.*, **45**, 1010 (1973).
13. I. M. Kolthoff and M. K. Chantooni, *Analyt. Chem.*, **39**, 1080 (1967).
14. G. Douheret, *Bull. Soc. chim. France*, **1968**, 3122.
15. B. G. Cox, A. J. Parker and W. E. Waghorne, *J. Phys. Chem.*, **78**, 1731 (1974).
16. C. Moreau and G. Douheret, *J. Chem. phys.*, **71**, 1313 (1974).
17. A. D'Aprano and R. M. Fuoss, *J. Phys. Chem.*, **78**, 400 (1969).
18. H. P. Bennetto and J. S. Spitzer, *Chem. Comm.*, **1971**, 990. ; *J. C. S. Farad. Trans*, **69**, 1491 (1973).
19. S. Harned and L. D. Fallon, *J. Amer. Chem. Soc.*, **61**, 2374 (1939) and **61**, 2377 (1939).
20. G. Baughmann and E. Grundwal D., *J. Amer. Chem. Soc.*, **80**, 3844 (1958).
21. J. L. Brisset, R Gaboriaud and R. Schaal., *J. Chim. phys.*, **68**, 1506 (1971).
22. J. F. Coetzee and G. R. Padmanabhan, *J. Phys. Chem.*, **66**, 1708 (1962). cited in D. Bauer and M. Breant "Electroanalytical Chemistry", A. J. Bard Ed. Vol. 8, p. 324, M. Dekker, New-York, 1975.
23. R. Gaboriaud, *Compt. rend.*, **270C**, 1925 (1970) ; *J. Chim. phys.*, **66**, 10 (1969).
24. supplementary material.
25. J. L. Brisset, *J. Sol. Chem.*, **5**, 587 (1976).
26. J. Vedel, *Ann. Chimie*, **1967**, 335.

AL INFORM

NOTE POUR LES AUTEURS

La Revue Roumaine de Chimie publie des articles en anglais, français, russe, allemand ou espagnol. Les auteurs sont prés d'envoyer des articles et des comptes rendus inédits.

Les manuscrits seront dactylographiés à deux intervalles. La bibliographie, les tableaux et la légende des figures seront placés après le texte.

Si l'article fait partie d'une série numérotée, la partie précédente sera donnée comme première référence.

Chaque article sera précédé d'un résumé comprenant quinze lignes au maximum.

Les références bibliographiques dans le texte seront faites par des exposants sans parenthèses et paraîtront à la fin de l'ouvrage.

Les publications périodiques mentionnées dans la bibliographie seront présentées suivant les prescriptions internationales ; le nom de l'auteur précédé de l'initiale du prénom, le titre du périodique abrégé conformément à « Chemical Abstracts » et souligné par une ligne, le numéro du tome indiqué par des chiffres arabes et souligné par deux lignes, suivi de la première page de l'article : à la fin, l'année de la parution sera placée entre parenthèses. Le numéro de la revue ne sera pas indiqué si les pages du volume sont numérotées, consécutivement.

Les textes des livres ou traités incluront : le nom des auteurs, l'initiale du prénom, le titre du livre entre guillemets et sans être souligné, le numéro du tome précédé par l'abréviation « vol. » (ou « Bd. »), le numéro de l'édition, les éditions (the publisher), la localité de la parution du livre, l'année de la parution et la page de la référence précédée(s) par l'abréviation « p » (ou « S »).

Les brevets seront indiqués comme suit : l'auteur ou la firme, le pays et le numéro du brevet, la date et la revue *(Chem. Abstr)* Par ex. : M. Jones (to Union Carbide Co.), Brit. Pat. 601 238, 2 Sept. 1959, cf. *Chem. Abstr.*, **54**, 12808 (1960).

Les diagrammes seront tracés à l'encre de Chine sur papier calque. Les tableaux et les figures (en nombre strictement nécessaire), ainsi que les courbes dans les figures seront numérotées par des chiffres arabes. Leur explication sera donnée dans la légende des figures. Prière de ne pas inscrire les mêmes données dans les tableaux et les figures. Chaque tableau aura un titre. On indiquera dans le texte la place approximative des tableaux et des figures. Les formules chimiques seront incluses dans le texte : en outre, elles seront transcrites sur papier calque, à l'encre de Chine.

Les auteurs sont priés d'indiquer les caractères italiques (en soulignant les lettres au crayon), ainsi que tout autre caractère spécial : les préfixes *ortho*, *meta*, *para*, *cis*, *trans*, etc. seront soulignés pour indiquer leurs caractères italiques, et ne seront jamais écrits avec des majuscules.

Aucune correction à la main ne sera admise sur le manuscrit. Les corrections seront frappés à la machine. Les lettres grecques ou autres symboles spéciaux seront insérés à la main à l'encre clairement.

Le manuscrit sera signé par l'auteur.

Titre-courant aura 50 lettres au maximum.

L'entière responsabilitè du contenu des articles appartient aux-auteurs.

Sur demande on peut obtenir une note plus complète.

PRINTED IN ROMANIA

1984 FEB 0 9

TRAVAUX PARUS AUX ÉDITIONS DE L'ACADÉMIE DE LA RÉPUBLIQUE SOCIALISTE DE ROUMANIE

ELENA CEAUŞESCU, **Noi cercetări în domeniul compuşilor macromoleculari** (Nouvelles recherches dans le domaine des composés macromoléculaires), 1981, 536 p.

I. G. MURGULESCU, RODICA VÎLCU, **Introducere în chimia fizică. Vol. III. Termodinamica chimică** (Introduction à la chimie physique, Vol. III, Thermodynamique chimique), 1982, 624 p.

I. G. MURGULESCU, J. PĂUN, **Introducere în chimia fizică. Vol. I.3. Nucleul atomic, reacţii nucleare, particule elementare** (Introduction à la chimie physique. Vol. I.3. Noyau atomique, réactions nucléaires, particules élémentaires), 1982, 606 p.

ELENA JERCAN, **Analiza cromatografică** (Analyse chromatographique), 1982, 286 p.

I. G. MURGULESCU, TATIANA ONCESCU, E. SEGAL, **Introducere în chimia fizică. Vol. II.2 Cinetică chimică şi cataliză** (Introduction à la chimie physique. Vol. II.2. Cinétique chimique et catalyse), 1981, 1024 p.

V. DRĂGUŢAN, A. T. BALABAN, M. DIMONIE, **Metateza olefinelor şi polimerizarea prin deschidere de inel a cicloolefinelor** (La métathèse des oléfines et la polymérisation par ouverture annulaire des cyclooléfines), 1981, 254 p.

LYDIA-MARIA VAICUM, **Epurarea apelor uzate cu nămol activ. Bazele biochimice** (L'épuration des eaux résiduelles à boue active. Les bases biochimiques), 1981, 218 p.

I. GĂLĂŢEANU, **Procese şi metode radiochimice în energetica nucleară** (Processus et méthodes radiochimiques dans l'énergétique nucléaire), 1981, 234 p.

OCTAVIAN IORDACHE, **Procese polistocastice aplicate la fenomenele de transfer** (Processus polystochastiques appliqués aux phénomènes de transfert), 1981, 186 p.

CR. SIMIONESCU, VALERIA GORDUZA, **Polimeri biocompatibili şi biologic activi** (Polymères biocompatibles et biologiquement actifs), 1980, 479 p.

ELENA CEAUŞESCU, **Polimerizarea stereospecifică a izoprenului** (La polymérisation stéréospécifique de l'isoprène), 1979, 307 p.

CONST GH. MACAROVICI, **Analiza chimică cantitativă anorganică** (L'analyse chimique quantitative inorganique), 1979, 457 p.

M. FLORESCU, **Metode ştiinţifice în dezvoltarea industriei chimice moderne** (Méthodes scientifiques dans le développement de l'industrie chimique moderne), 1979, 256 p.

A. T. BALABAN, I. GĂLĂŢEANU, G. GEORGESCU, LIGIA SIMIONESCU, **Compuşi marcaţi şi radiofarmaceutici cu aplicaţii în medicina nucleară** (Composés marqués et radiopharmaceutiques à application en médecine nucléaire), 1979, 495 p.

I. G. MURGULESCU, E. SEGAL, **Introducere în chimia fizică, vol II.1. Teoria molecular cinetică a materiei** (Introduction à la chimie physique. Vol. II.1. La théorie moléculaire-cinétique de la matière), 1979, 1036 p.

S. STERNBERG, FL. DANEŞ, **Termodinamica chimică aplicată** (La thermodynamique chimique appliquée), 1978, 400 p.

I. G. MURGULESCU, V. EM. SAHINI, **Introducere în chimia fizică, Vol. I.2. Structura şi proprietăţile moleculelor** (Introduction à la chimie physique. Vol. I.2. La structure et les propriétés des molécules), 1978, 604 p.

I. ZUGRĂVESCU, MAGDA PETROVANU, **N-ylid chemistry**, coédition avec McGraw-Hill International Book Company, U.S.A., 1977, 396 p.

I. G. MURGULESCU, **Introducere în chimia fizică. Vol. I.1. Atomi, molecule, legătură chimică** (Introduction à la chimie physique, Vol. I.1. Atomes, molécules, liaison chimique), 1976, 560 p.

ELENA CEAUŞESCU, **Research work on synthesis and characterization of macromolecular compounds. Contributions**, 1974, 251 p.

CR. SIMIONESCU, VIORICA RUSAN, V. POPA, **Chimia algelor marine** (La chimie des algues marines), 1974, 212 p., 1 pl.

ISSN 0035–4090

I. P. INFORMAŢIA c. 1351

43 426

Lei 40
$ 70 (pour un abonnement annuel)

1103

04 Veggèszet

ACADÉMIE DE LA RÉPUBLIQUE SOCIALISTE DE ROUMANIE

06

REVUE ROUMAINE DE CHIMIE

REFERÁLVA

TOME 28
Nos 11—12
Novembre — Décembre 1983

EDITURA ACADEMIEI REPUBLICII SOCIALISTE ROMÂNIA

Rev. Roumaine Chim. RRCHAX, **28**, *11 – 12*, p. 951–1032 (1983), Bucarest

ACADÉMIE DE LA RÉPUBLIQUE SOCIALISTE DE ROUMANIE

COMITÉ DE RÉDACTION

Rédacteur en chef :

I. G. MURGULESCU, membre de l'Académie de la République Socialiste de Roumanie

Rédacteurs en chef adjoints :

A. T. BALABAN et V. EM. SAHINI, membres correspondants de l'Académie de la République Socialiste de Roumanie

Collège de rédaction ;

EM. BRATU, ELENA CEAUŞESCU ECATERINA CIORĂNESCU-NENITZESCU, CR. SIMIONESCU, membres de l'Académie de la République Socialiste de Roumanie ; P. SPACU membre correspondant de l'Académie de la République Socialiste de Roumanie : MARGARETA AVRAM, M. BANCIU, I. HAIDUC, D. I. MARCHIDAN, I. MOLDOVAN, G. NIAC et D. SĂNDULESCU

La Revue Roumaine de Chimie parait 10 fois par an. Toute commande de l'étranger pour les travaux parus aux Editions de l'Académie de la République Socialiste de Roumanie sera adressée à ILEXIM, — Departamentul Export-Import Carte (Livres)/Departamentul Export-Import Presă (Revues), P.O.B. 136—137, télex 11226, 3, str. 13 Decembrie, 79517 Bucarest, Roumanie

Les manuscrits, les livres et les revues proposés en échange, ainsi que toute correspondance seront envoyés à la rédaction :

REVUE ROUMAINE DE CHIMIE

125, Calea Victoriei, 79717 Bucarest, Roumanie, téléphone 50 76 80

EDITURA ACADEMIEI REPUBLICII SOCIALISTE ROMÂNIA
125, Calea Victoriei, 79717 Bucarest, Roumanie, téléphone 50 76 80

REVUE ROUMAINE DE CHIMIE

Tome 28, N°s 11 — 12 Novembre — Décembre 1983

E. SEGAL, On the diffusion coefficient in binary mixtures of gases . . . . . 953— 955 R
LIANA MARTA, MARIA ZAHARESCU, IOVANCA HAIDUC and C. GH. MACAROVICI, Synthesis of strontium metaniobate by a coprecipitation method . . . . 957— 966 BC
C. B. SHARMA, Kinetics of oxidation of propan-2-ol by chlorine dioxide . . . 967— 975
C. I. CHIRIAC, Triaryl-*s*-triazoles from diaroylhydrazines by a new direct condensation reaction . . . . 977— 980
A. SYAMAL and O. P. SINGHAL, New dioxouranium (VI) complexes with tridentate dibasic Schiff bases prepared from β-diketones and amines . . . 981— 987
C. CRISTESCU, *As*-Triazine derivatives with potential therapeutic action. XVIII. Synthesis of 4-methylthio-5-benzylthio-6-azauridine-5'-phosphate . . . 989— 994
N. POPOVICI, A. BARABÁS and F. HODOȘAN, Exo- and endohormones. VII. Synthesis of *Z*-11-tetradecen-1-ol acetate by phosphonium ylide condensation . . . . 995— 999 BC
LUCIAN ENESCU, MIRCEA D. GHEORGHIU, AURELIA GHENCIULESCU, ILIE G. DINULESCU and MARGARET AVRAM, Reaction of *endo*- and *exo*-benzocyclobutenonorbornenes with methyl propiolate . . . . 1001—1007
N. BÎLBĂ, GH. MIHĂILĂ, P. ONU, D. DRANGA and C. LUCA, Ion exchange selectivity of natural and synthetic zeolites against ammonium . . . . . 1009—1017 R

BOOK REVIEWS . . . . 1019—1022
AUTHOR INDEX . . . . 1023—1031

Rev. Roumaine Chim. **28**, *11—12*, 951 — 1032 (1983), Bucarest

Revue Roumaine de Chimie, **28**, *11–12*, 953–955 (1983)

ON THE DIFFUSION COEFFICIENT IN BINARY MIXTURES OF GASES

E. SEGAL

Chair of Physical Chemistry and Electrochemical Technology,
Faculty of Chemical Engineering, Polytechnical Institute of
Bucharest, Blvd. Republicii 13, Bucharest, Romania

Received February 7, 1983

A critical analysis of different working formulae for the calculation of the diffusion coefficient in binary mixtures is presented.

Heterogeneous reactions, catalytic reactions included, are often limited by the diffusion of the reactants or products to or from the reaction zone. As, at least in the laboratory phase of the investigation of a heterogeneous catalytic reaction we are interested in the kinetic regime, one has either to develop experimental criteria for the kinetic or diffusional regimes or to evaluate by means of calculations their contributions to the progress of the process. Concerning this last aspect of the problem, one has to state that modern theories of transport phenomena were used by people interested in chemical engineering kinetics as a high level tool for the evaluation of the diffusion coefficients from molecular data, taking into account the structure of the molecules as well as their interaction. As an example, Smith[1] in his well known book "Chemical Engineering Kinetics" recommends, for accurate calculations of the diffusion coefficient D_{AB}(cm^{2}s^{-1}) in a binary mixture which consists of gases A and B, the following formula given by Chapman and Enskog[2,3]:

$$D_{AB}^{CE} = 0.0018583 \frac{T^{3/2}\left(\frac{1}{M_A} + \frac{1}{M_B}\right)^{1/2}}{P\sigma_{AB}^2\Omega_{AB}} \tag{1}$$

where T stands for the temperature (K), M_A and M_B for molecular weights, P for the total pressure of the gas mixture (atm), σ_{AB} for the collision diameter and Ω_{AB} for the collision integral.

Table 1 (column VI) lists some results obtained by using formula (1). One can notice a fair good agreement in some cases and a satisfactory one in others between the calculated and experimental values (column V).

Table 1

Comparison between calculated and experimental values of the diffusion coefficients in binary gas mixtures *

Gas mixture	σ_{AB} (A°)	σ^*_{AB} (A°)	T (K)	D_{AB} exp. (cm² s⁻¹)	D_{AB} calculated with formula (1) (cm² s⁻¹)	D^{M-S}_{AB} (cm² s⁻¹)	D^{M-S}_{AB} with σ^*_{AB} (cm² s⁻¹)	D^{C-C}_{AB} (cm² s⁻¹)
N_2-H_2	3.325	—	273.2	0.674	0.656	0.637		
N_2-O_2	3.557	—	273.2	0.181	0.175	0.196		
N_2-CO	3.636	—	273.2	0.192	0.174	0.194		
N_2-CO_2	3.839	—	273.2	0.144	0.130	0.157		
H_2-O_2	3.201	—	273.2	0.697	0.689	0.684		
H_2-CO	3.279	—	273.2	0.651	0.661	0.655		
H_2-CO_2	3.482	—	273.2	0.550	0.544	0.574		
H_2-NO	3.424	—	273.2	0.535	0.532	0.593		0.525
H_2-CH_4	3.425	—	273.2	0.625	0.607	0.616		
$CO-O_2$	3.512	3.70	273.2	0.185	0.175	0.202	0.182	0.178
CO_2-O_2	3.715	4.12	273.2	0.139	0.128	0.157	0.128	0.139
CO_2-CO	3.793	4.22	273.2	0.137	0.128	0.162	0.131	0.143
CO_2-N_2O	3.938	4.66	273.2	0.096	0.092	0.132	0.094	0.117
CO_2-CH_4	3.939	4.39	273.2	0.153	0.138	0.181	0.146	0.150
SO_2-air	3.953	—	753	—	0.285	0.278	—	—

*** The data from columns I, II, IV, V and VI were taken from reference (3), p. 579.**
The data from column III are taken from : S. Dushman, "Scientific Foundations of Vacuum Technique" (Russian edition) Mir Moscow 1969, p. 69, and from reference [2] p. 252. [illegible]*
The data from the last line are taken from reference [1], p. 406—409.

In the present paper we aim to discuss the following problem : to what extent such fields of chemistry as physical chemistry and chemical engineering benefit from the use of formulae like (1) containing the molecular interactions through the collision integral . [2]

For physical chemistry, the advanced theory of transport phenomena could eventually facilitate measurements of molecular interactions from diffusion coefficients. Obviously such coefficients should be determined with the highest possible accuracy. As far as chemical engineering is concerned, in our opinion, the use of formula (1) is not justified. As we are going to show in the following, the diffusion coefficient in binary mixtures can be calculated by some more simple formulae derived in the hypothesis that molecules could be considered as rigid spheres. Firstly let us consider the Maxwell-Stefan formula [4]:

$$D^{M-S}_{AB} = \frac{1}{(3n_A + n_B)\,\pi\sigma^2_{AB}}\left[\frac{8RT}{\pi}\left(\frac{1}{M_A} + \frac{1}{M_B}\right)\right]^{1/2} \tag{2}$$

where n_A, n_B stand for the gas concentrations molecules (cm^{-3}) and R stands for the gas constant. Expressing D_{AB}^{M-S} in $\mathrm{cm}^2\,\mathrm{s}^{-1}$, formula (2) turns into :

$$D_{AB}^{M-S} = 2.13\cdot 10^{-3}\,\frac{T^{3/2}}{P\sigma_{AB}^2}\left(\frac{1}{M_A}+\frac{1}{M_B}\right)^{1/2} \tag{3}$$

According to Chapman and Cowling, the first approximation formula for the diffusion coefficient in binary mixtures without interaction is :

$$D_{AB}^{C-C} = \frac{3}{8\pi n\sigma_{AB}^2}\left[\frac{kT\,(m_A+m_B)}{2\pi m_A m_B}\right]^{1/2} \tag{4}$$

where m_A and m_B — stand for the weights of molecules A and B, or if D_{AB}^{C-C} is expressed in $\mathrm{cm}^2\,\mathrm{s}^{-1}$, the working formula takes the form :

$$D_{AB}^{C-C} = 1.885\cdot 10^{-3}\,\frac{T^{3/2}}{P\sigma_{AB}^2}\left(\frac{1}{M_A}+\frac{1}{M_B}\right)^{1/2} \tag{5}$$

Formula (5) is practically equivalent to formula (1) with $\Omega_{AB} = 1$.

Table 1, column VII, gives the values of D_{AB}^{M-S} according to formula (3). For the binary mixtures with nitrogen the differences with respect to the experimental ones do not exced 10%, the agreement with the experimental values being in some cases even better than for the use of formula (1). A satisfactory agreement is still recorded for the case of the binary mixtures with hydrogen. Higher differences are to be noticed for binary mixtures with CO and CO_2. As one can see in the same table (column IX) the difference becomes lower for diffusion coefficients calculated using formula (5). From column VII of Table 1 it turns out that formula (3) leads to better agreement with experimental data if instead of σ_{AB}, a collision diameter σ_{AB}^* calculated from the values of the viscosity coefficients for individual gases is used.

The critical analysis of the different above mentioned models leads to the following conclusion : the models for evaluation of the diffusion coefficients in binary mixtures based on the rigid sphere approach give results in fair good agreement with experience. Thus in chemical engineering kinetics calculations, it is not necessary to use formulae which contain molecular interactions but simple formulae like (3) and (5), which express with accuracy the diffusion data.

REFERENCES

[1] J. M. Smith, "Chemical Engineering Kinetics", Mc Graw-Hill, New York, 1970, p. 404, 406, 409.

[2] S. Chapman and T. G. Cowling, "The Mathematical Theory of Non-uniform Gases". At the University Press, Cambridge, 1958.

[3] J.O. Hirschfelder, C. F. Curtiss and R. B. Bird, "Molecular Theory of Gases and Liquids", Wiley, New York, 1954, p. 539, 578.

[4] I. G. Murgulescu and E. Segal, "Introduction to Physical Chemistry" (in Romanian) Vol. II, part 1, Ed. Academiei, Bucharest, 1979, p. 164.

Revue Roumaine de Chimie, **28**, *11–12*, 957–966 (1983)

SYNTHESIS OF STRONTIUM METANIOBATE BY A COPRECIPITATION METHOD

LIANA MARTA[a], MARIA ZAHARESCU[b], IOVANCA HAIDUC[c], and C. GH. MACAROVICI[c]

[a] Polytechnic Institute Cluj-Napoca, Baritziu str. 25, Cluj-Napoca, Romania
[b] Center of Physical Chemistry, Spl. Independenţei 202, Bucharest, Romania
[c] Chemistry Department, Babeş-Bolyai University, Arany I. str. 11, Cluj-Napoca, Romania

Received June 18, 1981
Completed April 7, 1983

A novel, non-traditional method for the synthesis of strontium metaniobate is described, based upon coprecipitation of niobic acid and strontium oxalate by treatment of oxalato-niobic acid and strontium nitrate with ammonium hydroxide. The conditions for the quantitative coprecipitation of niobium and strontium have been established. The mechanism of thermal decomposition of the niobic acid-strontium oxalate coprecipitate has been investigated by differential thermal analysis. Strontium metaniobate is formed as final product of thermal decomposition at temperatures above 900°C.

INTRODUCTION

Oxidic compounds are commonly obtained by solid state reaction or sintering, starting from appropriate metal oxides or carbonates. This method has some drawbacks ; it requires high temperatures and long reaction times, and the reaction products do not always have the preestablished composition.

Many oxidic materials have special properties such as ferroelectric, piezoelectric, electrooptical and magnetic behaviour and as such they find many uses in the modern computer and radioelectronic industries, laser technique, piezoceramic technology, etc. These uses require a good reproducibility of the material composition.

Some of the new methods of preparing oxidic compounds avoid some of the disadvantages just mentioned. Two newer general methods seem to show much promise : the thermal decomposition of some coprecipitation products, and the thermal decomposition of coordination compounds, usually with organic acid ligands.

The last two methods were little employed for the synthesis of niobates ; these compounds were almost exclusively obtained previously by solid state reactions. Alkali metal and alkaline earth niobates and tantalates were prepared by hydrolysis of some double alkoxides.[1–4] The coprecipitation method was used for the preparation of Ba, Sr [5] and Pb [6] niobates.

In several previous papers,[7,8] we reported the synthesis of some niobates by thermal decomposition of oxalato-niobate complexes.

The present work describes the synthesis of a strontium niobate based upon the use of coprecipitation. Thus, strontium metaniobate has been obtained by thermal decomposition of the product formed in the coprecipitation of niobic acid with strontium oxalate, in the presence of aqueous ammonia.

RESULTS AND DISCUSSION

The mechanism of coprecipitation in the oxalato-niobic acid-strontium nitrate-ammonium hidroxide system :

$$H_3[NbO(C_2O_4)_3]-Sr(NO_3)_2-NH_4OH$$

In order to establish the optimal conditions for the coprecipitation of niobium and strontium in such a proportion as to afford the final formation of strontium metaniobate, we investigated the processes occurring in a system containing oxalato-niobic acid, strontium nitrate and aqueous ammonia, with the aid of potentiometric and analytical methods.

We established the pH range in which the coprecipitation of strontium and niobium is quantitative, and also the composition of the heterogeneous precipitate formed under these conditions.

The coprecipitation was achieved by treating a mixture of oxalato-niobic acid and strontium nitrate (Nb :Sr = 2 :1 molar ratio) with variable amounts of ammonium hydroxide.

By using the potentiometric method, the pH variation in the system investigated has been determined, as a function of the NH_4OH concentration, at constant concentration of Nb and Sr (2 :1).

The concentration of ammonium hydroxide is expressed by the ratio :

$$R = \frac{[NH_4OH]}{[Sr(NO_3)_2] + [\text{Nb-ox}]}\ ;\ \text{where Nb-ox} = H_3[NbO(C_2O_4)_3]\ \text{(oxalato-niobic acid).}$$

The curves of pH variation for the system investigated as well as for the individual components, on treatment with ammonium hydroxide, are illustrated in Figure 1, as follows :

Curve 1 shows the pH variation during the titration of a solution of oxalato-niobic acid (containing an excess of oxalic acid) with ammonium hydroxide (the $\text{Nb-ox}-H_2C_2O_4-NH_4OH$ system).

Curve 2 shows the pH variation during treatment of a solution of strontium nitrate and oxalic acid, with NH_4OH (the $Sr(NO_3)_2-H_2C_2O_4-NH_4OH$ system).

Curve 3 visualizes the pH change in the complex system containing oxalato-niobate, strontium nitrate, oxalic acid and ammonium hydroxide.

The titration curve exhibits two potential jumps: the first between pH 2.0 and 4.0 with the inflexion point at pH ca. 3.0; the second jump occurs between pH 6.0 and 8.0, with the inflexion point at pH ca. 7. In this system two simultaneous reactions of precipitation take place:

— the precipitation of strontium oxalate, which begins at pH ~ 2:

$$Sr(NO_3)_2 + H_2C_2O_4 + 2NH_4OH \rightleftharpoons SrC_2O_4 + 2NH_4NO_3 + 2H_2O$$

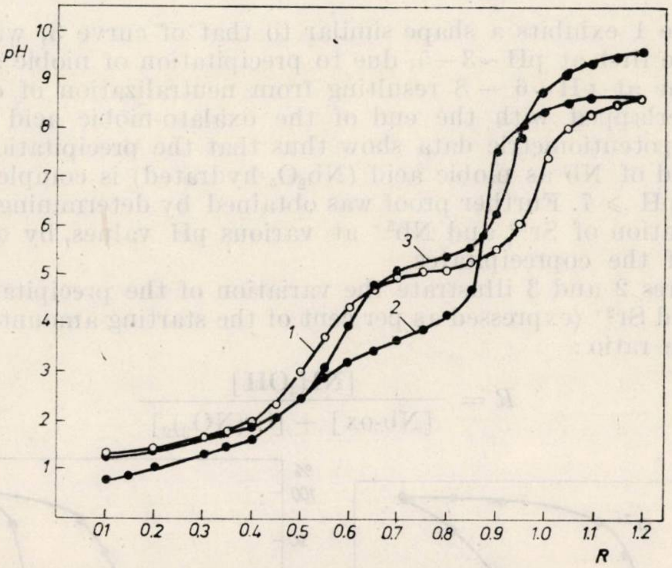

Fig. 1. — Variation of pH as a function of R ratio: 1. Nb-ox—$H_2C_2O_4$—NH_4OH system; 2. $Sr(NO_3)_2$—$H_2C_2O_4$—NH_4OH system; 3. Nb-ox—$Sr(NO_3)_2$—$H_2C_2O_4$—NH_4OH system.

This reaction is complete at pH ~ 7.

— the precipitation of niobic acid, which begins at pH ~ 3 and is quantitative at pH ~ 7:

$$2H_3[NbO(C_2O_4)_3] + 12NH_4OH + nH_2O \rightleftharpoons Nb_2O_5 \cdot nH_2O + 6(NH_4)_2C_2O_4$$

The slope of the potentiometric curve 3 in pH domain of 2 — 4 is due to the overlap of these equilibria.

The second pH-jump on the potentiometric curve 3 is due to the neutralization of oxalic acid, corresponding to an equivalent pH of 6.75.

On curve 2 of the system of $Sr(NO_3)_2$-oxalic acid, the pH variation in the domain of 2.0 — 4.5 indicates the precipitation of strontium oxalate, and the jump between 4.5 and 7.5 corresponds to the neutralization of oxalic acid excess.

Table 1 shows the pH values at the beginning (pH_i) and the end (pH_f) of the precipitation :

Table 1

pH Values at the beginning (pH_i) and the end (pH_f) of the precipitation

$C_{Sr^{2+}}$	$C_{H_2C_2O_4}$	pH_i	pH_f	$pH_{equiv.\ H_2C_2O_4}$
$3.06 \cdot 10^{-2}$M	$2.98 \cdot 10^{-2}$M	0.53	2.93	6.75

Curve 1 exhibits a shape similar to that of curve 3, with two pH jumps : the first at pH ~3–5, due to precipitation of niobic acid, and a sharper one at pH ~6 – 8 resulting from neutralization of oxalic acid, partly overlapped with the end of the oxalato-niobic acid neutralization. The potentiometric data show thus that the precipitation of Sr as oxalate and of Nb as niobic acid (Nb_2O_5-hydrated) is complete (quantitative) at pH $\geqslant 7$. Further proof was obtained by determining the degree of precipitation of Sr^{2+} and Nb^{5+} at various pH values, by quantitative analysis of the coprecipitates.

Figures 2 and 3 illustrate the variation of the precipitation degree of Nb^{5+} and Sr^{2+} (expressed as per cent of the starting amount) as a function of the ratio :

$$R = \frac{[NH_4OH]}{[Nb\text{-}ox] + [Sr(NO_3)_2]}$$

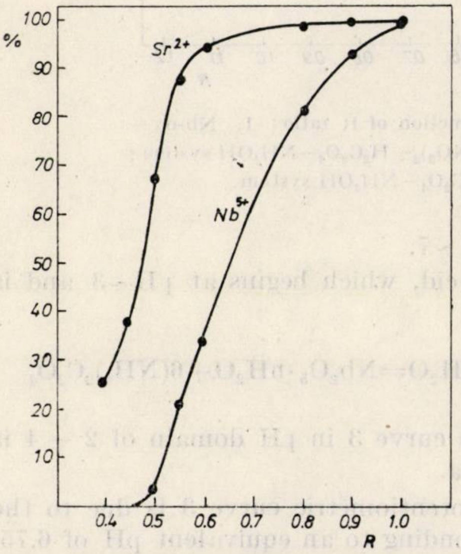

Fig : 2. — Variation of precipitation degree as a funtion of R ratio.

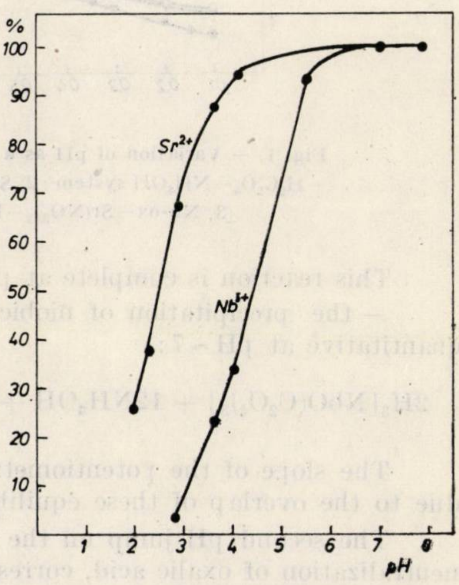

Fig. 3. — Variation of precipitation degree as a function of pH.

and of pH, respectively. The precipitate begins to form at pH ~2 and consists of strontium oxalate only. At pH ~4.2 over 90% of the initial amount of Sr is found in the precipitate, and at pH 6 the precipitation is quantitative, in agreement with potentiometric data.

The precipitation of niobium begins at pH ~2.85, and occurs only to a small extent (ca. 3.4%); at pH ~5.6 about 90% of the niobium is precipitated, and at pH 7 the precipitation is quantitative.

It follows that the quantitative precipitation of both strontium oxalate and niobic acid is complete at $\text{pH} \geqslant 7$.

The precipitation of Sr^{2+} as strontium hydroxide is unlikely, since the latter begins to precipitate only at pH ~13, as calculated for the concentrations used. In addition, it should be noted that the solubility of strontium oxalate ($K_{sp} = 5.6 \times 10^{-8}$) is much lower than that of strontium hydroxide ($K_{sp} = 3.2 \times 10^{-4}$), [9] therefore, the precipitation of strontium hydroxide is not possible in the presence of oxalic acid.

Further proof for the formation of strontium oxalate was obtained by quantitative analysis of the precipitate, which is found to contain oxalate in the theoretical amount.

The formation of strontium metaniobate by the thermal decomposition of the coprecipitate

The formation mechanism of strontium metaniobate by thermal decomposition of the coprecipitate was established with the aid of thermogravimetric and thermodifferential analysis, and X-ray diffraction powder diagrams of the thermal decomposition product.

The TG and DTA curves of pure strontium oxalate have been also recorded and are in agreement with the literature about thermal decomposition of the bivalent metal oxalates.[10,11]

Strontium oxalate, $SrC_2O_4 \cdot H_2O$, loses the crystallisation water before 183°C, with an endothermal effect at 180°C. The decomposition of strontium oxalate, with formation of strontium carbonate and elimination of carbon monoxide, is revealed by a double exothermal effect at 490°C and 520°C. It seems that two simultaneous processes take place: the endothermal decomposition of strontium oxalate, and the exothermal formation of strontium carbonate. The two thermal effects overlap and the endothermal effect is seen as a weak shoulder on the exothermal peak at ~ 495°C on the DTA curve.

The decomposition is accompanied by an important weight loss between 420° and 522 °C (13.72%), which corresponds to the elimination of carbon monoxide, partially oxidized to carbon dioxide. The gaseous product remains partially adsorbed in the solid phase. The stepwise desorption takes place before 1000°C, with a slight weight loss between 522° and 1000°C.[12,13]

The endothermal effect at 922°C, without weight loss is due to a polymorphous transformation of strontium carbonate, from the orthorhombic to the hexagonal form, well established in literature (924°C).

The TG and DTA curves of niobic acid-strontium oxalate coprecipitate are given in Fig. 4. A scheme for the thermal decomposition of pure strontium oxalate, as well as of niobic acid-strontium oxalate coprecipitate is suggested in Table 2.

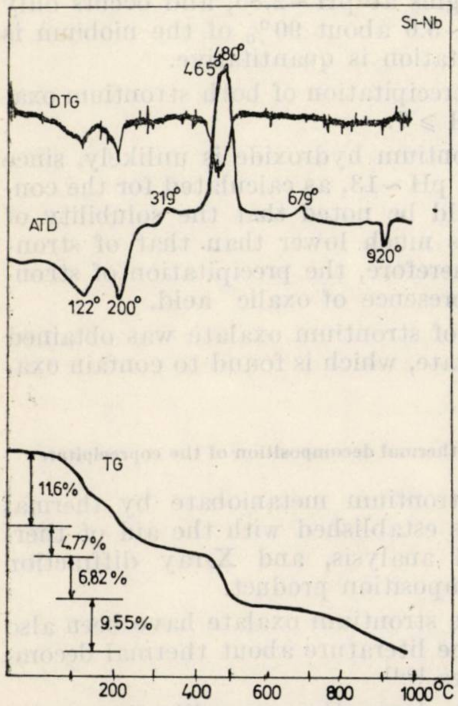

Fig. 4. — TG and DTA curves for niobic acid-strontium oxalate coprecipitate.

The coprecipitate releases the crystallisation water in two steps, as indicated by the two weight losses (at 122° and 200°C) associated with two endothermal effects at 122° and 200°C, respectively.

These weight losses correspond to the dehydratation of strontium oxalate and niobic acid. The water content of the latter is difficult to estimate, since it is a function of the precipitation conditions. The weak exothermal effect at 319°C can be due to a structural reorganization of the niobic acid which takes place in the presence of strontium oxalate.

The decomposition of strontium oxalate, with formation of strontium carbonate is marked by a double exothermal effect at 465° and 480°C. These values are lower than for the pure strontium oxalate. The presence of niobic acid favors the oxalate decomposition.

The exothermal effect at 679°C is due to a reaction between strontium carbonate and dehydrated niobic acid, with formation of strontium metaniobate and carbon dioxide, which remains partly adsorbed on the solid products. Literature data indicate a temperature of 690°C for the formation of strontium metaniobate. [14,15]

Probably, under the experimental conditions, the reaction between strontium carbonate and niobic acid is not quantitative. Thus, the endothermal effect at 920°C due to a polymorphous transformation of strontium carbonate from the orthorhombic to hexagonal form, is still observed, thus showing the presence of $SrCO_3$.

A longer thermal treatment is necessary for the reaction to be complete. The final product of thermal decomposition of the niobic acid-strontium oxalate coprecipitate is strontium metaniobate — $SrNb_2O_6$.

The formation of strontium metaniobate was confirmed by X-ray diffraction powder diagrams and by infrared spectroscopy.

The infrared spectra of the initial coprecipitate and of the thermal decomposition product are given in Table 3.

The infrared spectrum of the coprecipitate exhibits the characteristic bands of the oxalate ion.[16] These bands disappear from the spectrum of the thermal decomposition product, in which only a broad band at ~650 cm^{-1} is present. This band is characteristic for niobates.

Table 2

The thermal decomposition mechanism

Weight loss (TG)			Thermal effects		Compounds
Temperature interval, °C	% loss	Lost species	Endo	Exo	
20°−140°	0.98				$SrC_2O_4 \cdot H_2O$
140°−183°	6.86	H_2O	180°		SrC_2O_4
183°−420°	1.30				
420°−522°	13.72	CO		520°	$SrCO_3 \cdot xCO$ads.
522°−1000°	1.96		922°		$SrCO_3$
					Coprecipitate
20°−122°	5.80		122°		$Nb_2O_5 \cdot nH_2O + SrC_2O_4 \cdot H_2O$
122°−200°	5.80	$(n+1)H_2O$	200°		$Nb_2O_5 + SrC_2O_4$
200°−425°	4.77			319°	
425°−490°	6.82	$CO,(1-x)CO_2$		465° 480°	$Nb_2O_5 + SrCO_3 \cdot xCO_2$ ads.
490°−679°	1.36			679°	$SrNb_2O_6xCO_2$ ads.
679°−1000°	8.55	xCO_2	920°		

Table 3

Infrared spectra

$SrC_2O_4 \cdot H_2O$ (cm^{-1})	Coprecipitate (cm^{-1})	$SrNb_2O_6$ (cm^{-1})	Assignment
510	530		$\delta(O-C=O)$
600	(620)		
		650	$\nu(Nb-O)$-niobate
795	785		$\delta(O-C=O)$
1320	1320		$\nu(C-O)$, $\delta(O-C=O)$
1460	1410		
1640	1640		$\nu(C=O)$, (H_2O)
1670	1670		$\nu(C=O)$
	3360		
	3500		(H_2O)

The X-ray diffraction powder diagram of the thermal decomposition product of the coprecipitate (Table 4) confirms the formation of monoclinic strontium metaniobate.[17]

This diagram is identical with that of strontium metaniobate obtained by a solid state reaction (the traditional method).

Table 4

X-ray diffraction data of the thermal decomposition product of the coprecipitate

d Å	I/I_0	Assignment[17]
5.0178	16	$SrNb_2O_6$ — monoclinic
3.9310	90	
3.6390	13	
3.4476	21	
3.3212	16	
3.2131	16	
3.1400	52	
3.0557	100	
3.0153	56	
2.9435	16	
2.8185	49	
2.7826	49	
2.6018	13	
2.4454	26	
2.3840	16	
2.0633	15	
1.9778	25	
1.9713	30	
1.9232	16	
1.7477	16	
1.6609	34	
1.6343	23	
1.6305	23	
1.6034	11	

EXPERIMENTAL PART

Coprecipitation conditions

A series of oxalato-niobic acid and strontium nitrate solutions, with established concentrations, were prepared in volumetric flasks.

The oxalato-niobic acid solution was obtained by dissolving an amount of freshly precipitated niobic acid in oxalic acid solution. An excess of oxalic acid, corresponding to a ratio Nb : $H_2C_2O_4 \sim 1 : 5$ is necessary to ensure the stability of solution on storage, and to avoid the precipitation of niobic acid.

The exact amount of Nb in this solution was established by gravimetric determination.

The strontium nitrate solution was obtained by dissolving anhydrous strontium carbonate in the stoichiometric amount of nitric acid, and adding water to the mark in a volumetric flask.

The concentrations of the stock solution used in these experiments were the following:

$$C_{Nb-ox} = 6.12 \times 10^{-2} M$$

$$C_{Sr(NO_3)_2} = 3.06 \times 10^{-2} M$$

These values were chosen in order to afford mixing of equal volumes of solution containing niobium and strontium, for a molar ratio 2Nb : 1Sr.

From the stock solutions, 9 series of mixtures were prepared, in stoppered plastic flasks, each containing 10 ml of the niobium and strontium solution ; in each flask a determined volume of titrated 2N ammonium hydroxide solution was added, as shown in Table 5. The amounts of ammonium hydroxide solution were based upon data suggested by the potentiometric curves.

Table 5

Determination of coprecipitation degree

NH_4OH ml	8.0	9.0	10.0	11.0	12.0	16.0	18.0	20.0	22.0
R	0.40	0.45	0.50	0.55	0.60	0.80	0.90	1.0	1.1
pH	2.03	2.3	2.86	3.65	4.11	5.43	5.66	7.9	8.49
Nb %	—	—	3.41	20.31	33.27	81.5	93.25	100	100
Sr %	25.65	37.49	67.6	87.82	94.5	98.9	99.1	100	100

The plastic flasks were closed, the solutions mixed and then left at room temperature for 2—3 hrs, until equilibrium was reached.

The precipitate formed in each flask was filtered. The pH was determined in the filtrates immediately, by the potentiometric method. The precipitates were washed with water and analysed to determine the precipitation degree of Sr^{2+} and Nb^{5+}.

Analysis

Strontium was determined gravimetrically as sulfate. The coprecipitate was dissolved directly from the filter in hydrochloric acid 1 : 1. The solution thus obtained was heated and sulfuric acid 1 : 1 was added, under stirring ; the white precipitate of strontium sulfate was filtered, washed, dried and calcined.

Niobium was determined by precipitation as niobic acid in the filtrate obtained after separation of strontium, by adding ammonia to pH~7, and calcination of the precipitate separated to Nb_2O_5.

Oxalate was determined by permanganometric titration in the solution obtained by dissolving the coprecipitate in sulfuric acid 1 : 1. The titration can be carried out in the presence of strontium sulfate precipitate, with no interference.

The degree of precipitation, i.e. the percentage of Nb^{5+} and Sr^{2+} precipitated in each mixture, from the initial amount of Nb^{5+} and Sr^{2+} was evaluated from the chemical analysis data. These values are given in Table 5, and are plotted in Figures 2 and 3.

The infrared spectra were recorded with a UR 20 Carl Zeiss Jena spectrophotometer in KBr pellets, in the range 4000—400 cm^{-1}.

The X-ray diffraction powder diagrams were recorded with a TUR-M 62 Diffractometer, using $Cu_{K\alpha}$ radiation.

The thermogravimetric and the thermodifferential curves were recorded with a Paulik-Paulik-Erdely Derivatograph, in air, with a temperature increasing rate of 5°/min.

The potentiometric curves recorded with a OP-264 RADELKIS pH-meter with a Radelkis type OP-308 electrode.

REFERENCES

[1] D. C. Bradley, B. N. Chakravarti and W. Wardlav, *J. Chem Soc.*, **1956**, 2381.

[2] R. Gut, *Helv. Chim. Acta*, **47**, 2262 (1964).

[3] G. Daendliker and H. Morawietz, "Decomposition of Organometallic Compounds. Refractory Ceramics, Metals, Metal Alloys", Proceedings Int. Symp. 1967 (Publ. 1968) p. 157.

[4] R. C. Mehorta, M. M. Agrawal and P. N. Kappoor, *J. Chem. Soc.*, **1968,** 2673.

[5] I. V. Vinarov, A. N. Grinberg, I. I. Kovalevskaia and L. Y. Filatov, *Zhur. neorg. Khim.*, **22,** 2054 (1977).

[6] V. A. Titova, I. F. Cherednichenko and N. G. Kisel, *Zhur. neorg. Khim.*, **12,** 1457 (1967).

[7] L. Marta, M. Zaharescu and C. Gh. Macarovici, *Rev. Roumaine Chim.*, **24,** 1115 (1979).

[8] L. Marta, M. Zaharescu and C. Gh. Macarovici, *Rev. Roumaine Chim.*, in print.

[9] W. L. Masterton and E. J. Slowinski, "Chemical Principles", W. B. Saunders Company, Philadelphia, 1966.

[10] E. G. Derouane, Z. Gabelice, R. Hubine and M. J. Hubin-Franskin, *Thermochim. Acta*, **11,** 287 (1975).

[11] B. V. Strijkov, A. V. Lapitskii and L. G. Vlasov, *Zhur. neorg. Khim.*, **7,** (1962).

[12] J. T. Yates and C. V. Garland, *J. Phys. Chem.*, **65,** 617, 746, 901 (1961).

[13] J. H. Taylor and C. H. Amberg, *Canad. J. Chem.*, **39,** 535 (1961).

[14] C. Duval, "Inorganic Thermogravimetric Analysis", Elsevier Publishing Company, Amsterdam, 1963.

[15] V. A. Phelkin, A. V. Lapitskii, V. I. Spitsin and Y. P. Simanov, *Zhur. neorg. Khim.*, **8,** 1784 (1956).

[16] H. Siebert, "Anwendungen der Schwingungsspektroskopie in der anorganischen Chemie", Springer Verlag, Berlin, 1966, p. 80.

[17] J. Ravez and P. Hagenmuller, private comunication.

Revue Roumaine de Chimie, 28, *11–12*, 967–975, (1983)

KINETICS OF OXIDATION OF PROPAN-2-OL BY CHLORINE DIOXIDE

C. B. SHARMA

Chemical Laboratories, D. N. College, Meerut—250002, India

Received July 11, 1981

The kinetics of oxidation of propan-2-ol by chlorine dioxide has been investigated at 35°C. The reaction is of the first order with respect to each propan-2-ol and chlorine dioxide molecule. The apparent second order rate constant is $26.0 \pm 0.1 \times 10^{-4}$ litre mole^{-1} sec^{-1} at 35°C. The influence of various factors, e.g. ionic strength, inorganic salts, pH, acetic acid, D_2O and temperature on the initial rate has been studied. The activation parameters have been calculated and a mechanism involving hydride abstraction has been proposed.

INTRODUCTION

The oxidation of alcohols under different conditions by various oxidising agents e.g. $KMnO_4$, $K_2S_2O_8$, $CeSO_4$, CrO_3, potassium ferricyanide, molybdenum cyanide, and halogens, etc. has been reported in the literature. Some works on the oxidation of alcohols by bromine, [1–3] chlorine, [4] thallic ion,[5] ceric ion,[6] iodine,[7] peroxydisulphate,[8] *t*-butyl hypochlorite[9] and chlorine dioxide[10] has been done in this laboratory. The present paper reports on the oxidation of propan-2-ol by chlorine dioxide in an attempt to obtain information about the mechanism of oxidation of alcohols by chlorine dioxide. The reaction of alcohols with chlorine dioxide is also important from the viewpoint of environmental pollution.

EXPERIMENTAL

All chemicals used were either of B. D. H. (Analar) or Merck (C.P.) grade or of comparable purity; D_2O of isotopic purity $\geqslant 99.45\%$ was supplied by BARC, Trombay, India. All the chemicals were purified by known procedures. Water was purified by passing through an ion exchanger and distillation from alkaline $KMnO_4$. Chlorine dioxide was prepared [11] from potassium chlorate and oxalic acid dihydrate with the addition of small amounts of 4.45 M H_2SO_4.

Kinetic measurements

The reaction was studied at 35°C by adding aqueous chlorine dioxide to an alcohol solution at constant ionic strength ($\mu = 0.2$). The concentration of total oxidant $[OX]_0$ was determined iodometrically. [12] In order to avoid photochemical effects, approach of direct light was minimized by using black bottles for the reaction. Due to the complex nature of the reaction, initial rates (k_0) were calculated. [13]

Products

In a typical experiment propan-2-ol and chlorine dioxide were mixed in the ratio 1 : 1 and kept for 20 hrs at room temperature in a stoppered bottle. The products were isolated as their 2,4-dinitrophenylhydrazones (DNPH). The products separated by g. l. c. and identified by NMR and IR were acetone and monochloroacetone.

RESULTS AND DISCUSSION

Chlorine dioxide does not hydrolyse in aqueous solution. The spectral analysis[14] of ClO_2 solution has shown that the concentration of ClO_2 is unaltered between pH 4.0 and 6.45. The chlorine dioxide molecule remains in the same form[15, 16] in pH range of at least 4.0 to 8.4. Grimley and Gordon[17] found that the absence of light chlorine dioxide water exists mainly in the molecular form in the acidic medium. Only some part of it disproportionates into chlorite ions. They suggested the possibility of the existence of two oxidising agents – ClO_2 and $Cl_2O_4^-$ in highly acidic medium and in the absence of light.

$$ClO_2 + ClO_2^- \rightleftharpoons Cl_2O_4^-$$

At pH 7, the end products[17] of chlorine dioxide in water, will be ClO_2^-, Cl^- and ClO_3^-. Suzuki and Gordon[18] concluded that in the acidic range ClO_2 is the main oxidising agent in the absence of light. First order kinetics has been obtained with respect to both molecular chlorine dioxide (Table 1) and alcohol (Table 2). The main oxidising agent is ClO_2 as the values of $k_0/[ClO_2]$ have been found to be constant (Table 1).

Table 1

Dependence of oxidation rate on the concentration of chlorine dioxide at 35°C

[Propan-2-ol] = 0.100 M ; μ = 0.2

$[ClO_2]$ (M)	$k_0 \times 10^6$ (M sec^{-1})	$\frac{k_0 \times 10^4}{[ClO_2]}$ (sec^{-1})
0.00020	0.054	2.70
0.00025	0.065	2.60
0.00035	0.091	2.60
0.00050	0.129	2.58
0.00060	0.156	2.60
0.00065	0.170	2.61
0.00070	0.182	2.60
0.00080	0.210	2.62

Table 2

Rate constant as a function of propan-2-ol concentration at 35°C
$[ClO_2] = 0.00025M$; $\mu = 0.2$

[Alcohol] (M)	0.100	0.150	0.200	0.250	0.300	0.350	0.400	0.500
$k_0 \times 10^6$ (M sec^{-1})	0.065	0.098	0.130	0.163	0.195	0.228	0.260	0.326
$\frac{k_0 \times 10^7}{[Alc.]}$ (sec^{-1})	6.50	6.53	6.50	6.52	6.50	6.51	6.50	6.52

Efect of H^+ ions

The reaction of propan-2-ol with chlorine dioxide has been studied in the presence of perchloric acid at 35°C. The order with respect to H^+ is one at all hydrogen ion concentrations (Table 3). The initial rate increases in the presence of H^+ ions.

Table 3

Rate constant as a function of perchloric acid concentration at 35°C
[Propan-2-ol] = 0.100 M ; $[ClO_2] = 0.00030$ M ; $\mu = 0.2$

$[HClO_4]$ (M)	0.020	0.035	0.045	0.050	0.065	0.075	0.080
$k_0 \times 10^6$ (M sec^{-1})	0.100	0.174	0.226	0.250	0.326	0.376	0.400
$\frac{k_0 \times 10^6}{[HClO_4]}$ (sec^{-1})	0.500	4.97	5.02	5.00	5.01	5.01	5.00

Rate law

The following rate law is valid :

$$\frac{-d[ClO_2]}{dt} = k_1 \text{ [propan-2-ol]}_0 \text{ [Chlorine dioxide]}_0$$

$$\frac{-d[ClO_2]}{dt} = k_2 \text{ [propan-2-ol]}_0 [ClO_2]_0 [H^+]_0$$

Effect of ionic strength

There is a small influence of change in ionic strength (Table 4) on the reaction rate. This suggests that either two molecules or an ion and a neutral molecule are taking part in the reaction.

Table 4

Dependence of oxidation rate on the concentration of sodium perchlorate at 35°C
[Propan-2-ol] = 0.100 M ; $[ClO_2] = 0.00035$ M

$[NaClO_4]$ (M)	0.200	0.350	0.450	0.600	0.700	0.800	1.00
$k_0 \times 10^6$ (M sec^{-1})	0.091	0.098	0.104	0.110	0.115	0.122	0.131

Effect of inorganic salts

In the oxidation of propan-2-ol by chlorine dioxide at 35°C, it has been found that the anions and cations exert specific effects on the second order rate constant. The results (Table 5) have shown that: (i) chlorides and nitrates accelerate the rate; (ii) potassium bromide and sodium hydrogen phosphate also enhance the reaction rate; and (iii) the sulphates have general tendency to retard the rate.

Table 5

Initial rate constants for the reaction of propan-2-ol with ClO_2 in the presence of different salts at 35°C

[Propan-2-ol] = 0.100 M; $[ClO_2]$ = = 0.00025 M; $\mu = 0.2$

Salt	Concentration (M)	$k_0 \times 10^6$ (M sec^{-1})
NaH_2PO_4	0.050	0.069
$AgNO_3$	0.050	0.078
$NaNO_3$	0.050	0.082
KNO_3	0.050	0.087
KBr	0.050	0.096
NaCl	0.050	0.114
KCl	0.050	0.128
$BaCl_2$	0.050	0.168
$SrCl_2$	0.050	0.183
$AlCl_3$	0.050	0.198
$ZnCl_2$	0.050	0.210
$MnCl_2$	0.050	0.224
$NiCl_2$	0.050	0.244
$ZrOCl_2$	0.050	0.352
Na_2SO_4	0.050	0.060
K_2SO_4	0.050	0.061

Effect of sodium chloride

Chloride ions were found to increase the rate. Therefore, the effect of Cl^- was studied by taking it at constant ionic strength (Table 6). The

Table 6

Rate constant as a function of NaCl concentration at 35°C

[Propan-2-ol] = 0.100 M; $[ClO_2]$ = 0.00025 M; $\mu = 0.2$

[NaCl] (M)	0.025	0.035	0.050	0.075	0.100
$k_0 \times 10$ (M sec)	0.082	0.096	0.114	0.140	0.161
$\dfrac{k_0 \times 10^7}{[\mathrm{Cl}^-]^{\frac{1}{2}}}$ (sec^{-1})	5.19	5.13	5.10	5.11	5.09

rate increases with the concentration of NaCl. The order with respect to NaCl was $\frac{1}{2}$.

$$\frac{-\,d[ClO_2]}{dt} = k'[Alc.]_0\,[ClO_2]_0\,[Cl^-]_0^{\frac{1}{2}}$$

Effect of temperature

The activation parameters are listed in Table 7.

The negative entropies of activation are indicative of a more rigid structure in the transition state than in the ground state. The large negative entropy of activation (greater than 125 JK^{-1}) also suggests the loss of rotational degree of freedom. It also indicates that the transition state is more polar and requires a large extent of solvent immobilization than the ground state.[19]

Table 7

Initial rate constants and thermodynamic activation parameters for the reaction of propan-2-ol with ClO_2 in the absence and presence of perchloric acid

[Propan-2-ol] = 0.100 M ; $[ClO_2]$ = 0.00045 M ; $\mu = 0.2$

Temp. °C	$[HClO_4]$ (M)	$k_0 \times 10^6$ (M sec^{-1})	$k_{int} \times 10^6$ (M sec^{-1})	E_a k J mol^{-1}	$\Delta H^{\neq}$ k J mol^{-1}	$\Delta S^{\neq}$ JK^{-1}	$\Delta G^{\neq}$ kJ mol^{-1}
25	—	0.067	0.064	53.2±2.1	50.7±2.1	−164.5	102.2
35	—	0.117	0.122				
45	—	0.227	0.233				
55	—	0.430	0.428				
25	0.030	0.129	0.125	51.5±2.1	48.6±2.1	−165.4	100.5
35	0.030	0.226	0.237				
45	0.030	0.415	0.431				
55	0.030	0.780	0.758				

Isotope effect

The solvent isotope effect, k_{H_2O}/k_{D_2O}, is 1.78 for the reaction of propan-2-ol with chlorine dioxide. The low value (less than two) of solvent isotope effect indicates that the rate determining step involves the removal of hydride ion[20–23] and not of proton as in the latter case values above two sould have been obtained.[24]

pH-Rate profile

The results have shown that in the oxidation of propan-2-ol with chlorine dioxide in the presence of buffer, the rate decreases with increase of pH between pH's 3.0 and 5.89. The sudden increase in rate between pH 6.3 and 6.7 was observed which is probably due to the reaction of anion of alcohol (RO$^-$) with chlorine dioxide. The rate was maximum at pH

6.7 when studied between pH 5.89 and 8.0. The decrease in rate again at pH 7.5 may be due to the formation of chlorite ion (ClO_2^-) thus decreasing the concentration of ClO_2.

Effect of acetic acid

The results exhibit that in the case of propan-2-ol (Table 8) the rate increases with increase in the percentage of acetic acid up to 50% HOAc and beyond which the rate decreases. The study has been made from 10% HOAc to 80% HOAc. The one possibility is that change in rate may not be due to any solvent effect but may be due to change in the acidity of the reaction medium. ClO_2 oxidations in acidic medium are known to be influenced by $[H^+]$. Thus, the trend in rate may be due to the influence of acidity on the reaction rate. The decrease in rate with increasing acetic acid content may be attributed to a corresponding decrease in $[H^+]$.

Table 8

Dependence of the reaction rate on acetic acid at 35°C

[Propan-2-ol] = 0.100 M ; $[ClO_2]$ = 0.00030 M ; $\mu = 0.2$

% [HOAc]	10	20	30	40	50	60	70	75	80
$k_0 \times 10$ (M sec^{-1})	0.143	0.198	0.232	0.500	0.545	0.460	0.350	0.304	0.254

The solvent-solute interaction is a more probable factor in influencing the rate. While dielectric constant values are no doubt important, several other factors complicate the situation. Uncertain values of dielectric constant in the region of charged species, the structure breaking effect in the solvent system, solvent participation in the reaction, the Rabinowich cage effect and mechanistic changes in environment, all have cumulative effects.

Effect of substituents

A point of great interest in the mechanistic study is the influence of substituent groups. The results show that the electron attracting substituents increase the rate of oxidation. The rate increases regularly with the substitution of methyl groups for hydrogen. This is the expected order for the electron release at the C—H bond of the carbinol group, since methyl groups will tend to increase the electron density at the carbon atom by their general inductive effect. The order of reactivity is : butan-2-ol > propan-2-ol > isobutanol > *n*-butanol > *n*-propanol > ethanol > methanol.

In our case the ρ value has been found to be -1.15. Generally, it is considered that a highly negative ρ value points to an electron deficient carbon centre in the transition state for the reaction.[25-27] Our results are quite similar to the results of the oxidation of aliphatic alcohols by chloramine-T,[28] acid permanganate[29] and bromine[30] where a mechanism involving transfer of a hydride ion from alcohol to the oxidant is suggested.

On the basis of the above results, the following mechanism can be suggested :

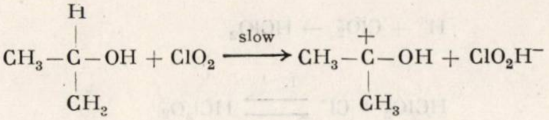

$$CH_3-\overset{\overset{\textstyle H}{|}}{\underset{\underset{\textstyle CH_2}{|}}{C}}-OH + ClO_2 \xrightarrow{\text{slow}} CH_3-\overset{+}{\underset{\underset{\textstyle CH_3}{|}}{C}}-OH + ClO_2H^- \qquad (1)$$

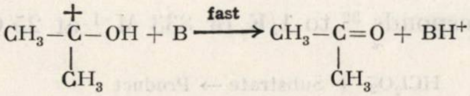

$$CH_3-\overset{+}{\underset{\underset{\textstyle CH_3}{|}}{C}}-OH + B \xrightarrow{\textbf{fast}} CH_3-\underset{\underset{\textstyle CH_3}{|}}{C}=O + BH^+ \qquad (2)$$

where B is base, e.g., water.

$$ClO_2H^- \xrightarrow{\text{fast}} ClO_2^- + H^+ \qquad (3)$$

In the presence of H⁺ ions

H^+ ions react in the following way :

In the presence of H^+ ions the rate enhances probably due to the formation of $[Cl_2O_2]$ from ClO_2^- and H^+ as follows :

$$ClO_2^- + H^+ \rightarrow HClO_2 \qquad (4)$$

$$HClO_2 + HClO_2 \rightarrow HOCl + ClO_3^- + H^+ \qquad (5)$$

$$HOCl + HClO_2 \rightarrow Cl_2O_2 + H_2O \qquad (6)$$

This $[Cl_2O_2]$ perhaps reacts with the substrate to give products.

$$Cl_2O_2 + \text{Alcohol} \rightarrow \text{Products} \qquad (7)$$

In the presence of chloride ions

(i) In the presence of chloride ions the rate enhances probably due to the formation of molecular chlorine as follows :

$$ClO_2^- + H^+ \rightarrow HClO_2 \qquad (8)$$

$$HClO_2 + 3H^+ + 3Cl^- \rightarrow 2Cl_2 + 2H_2O \qquad (9)$$

Once molecular chlorine is formed in the reaction it reacts immediately with the chlorides to form Cl^+ ions.

(ii) It is more probable that both Cl_2 and Cl_2O_2 are formed in the reaction a fact that facilitates the reaction rate as follows :

$$H^+ + Cl^- + HClO_2 \rightarrow 2\ HOCl \qquad (10)$$

$$H^+ + Cl^- + HOCl \rightarrow H_2O + Cl_2 \qquad (11)$$

$$Cl_2 + HClO_2 \rightarrow H^+ + Cl^- + Cl_2O_2 \qquad (12)$$

The steps 10, 11 and 12 are all irreversible since their equilibrium constants[31] are 1.24×10^5, 2.29×10^3 and 1.34×10^6 respectively.

(iii) The acceleration in rate may be due to the formation of $HCl_2O_2^-$ which reacts with the substrate to form the product.

$$H^+ + ClO_2^- \rightarrow HClO_2 \tag{13}$$

$$HClO_2 + Cl^- \xrightleftharpoons{K^{-1}} HCl_2O_2^- \tag{14}$$

The value of K^{-1} corresponds[32] to $1/K$ or $833\ M^{-1}$ at 25°C.

$$HCl_2O_2^- + \text{Substrate} \rightarrow \text{Product} \tag{15}$$

Decrease in rate at higher pH

The rate decreases with decrease of H^+ due to formation of $[Cl_2O_4]^-$ complex as follows:

$$ClO_2 + ClO_2^- \rightleftharpoons [Cl_2O_4]^- \tag{16}$$

The formation constant[33] is about $1.6 M^{-1}$. The rate decreases because ClO_2 is consumed to form a complex which is less reactive than ClO_2.

ACKNOWLEDGEMENT. The author is thankful to the College authorities for providing necessary laboratory facilities and also to U.G.C. (India) for providing a Senior Research Fellowship.

REFERENCES

[1] V. P. Kudesia, *Bull. Soc. Chim. belges.*, **80**, 59 (1971).

[2] V. P. Kudesia, *Ibid*, **80**, 213 (1971).

[3] V. P. Kudesia, *Ciencia e Cultura*, **24**, 61 (1972).

[4] V. P. Kudesia, S. Kant, S. K. Srivastava and D. Prakash, *Acta Ciencia Indica*, **5**, 85 (1979).

[5] V. P. Kudesia, *Bull. Soc. Chim. belges.*, **80**, 211 (1971).

[6] V. P. Kudesia, *Ciencia e Cultura*, **24**, 61 (1971).

[7] V. P. Kudesia, S. K. Sharma and A. Manglik, *React. Kinet. Catal. Lett.*, **15**, 467 (1980).

[8] V. P. Kudesia, *Rev. Roumaine Chim.*, **18**, 1373 (1973).

[9] V. P. Kudesia and B. K. Sharma, *Indian* J. *Chem.*, **16A**, 327 (1978); *Ibid*, **19A**, 82 (1980).

[10] C. B. Sharma, Ph. D. Thesis submitted to Meerut University, Meerut (1980).

[11] W. C. Bray, *Z. phys. Chem.*, **54**, 569 (1906).

[12] E. Grimley, Ph. D. Thesis, University of Iowa (1971).

[13] C. C. Hong and W. H. Rapson, *Canad. J. Chem.*, **46**, 2061 (1968).

[14] V. P. Kudesia, Unpublished results (1980).

[15] M. A. Benarde, B. M. Israel, V. O. Olivieri and M. L. Granstrom, *Applied Microbiology*, **13**, 776 (1965).

[16] R. J. Miltner "Measurement of ClO_2 and Related Products", Water Supply Research Division, Cincinnati, Ohio, 1977, p. 4.

[17] E. Grimley and G. Gordon, *J. Inorg. Nuclear Chem.*, **35**, 2383 (1973).

[18] K. Suzuki and G. Gordon, *J. Inorg. Nuclear Chem.*, **17**, 3115 (1978).

[19] V. P. Kudesia and N. K. Sharma, *React. Kinet. Catal. Lett.*, **16**, 49 (1981).

[20] C. G. Swain, R. A. Wiles and R. F. W. Bader, *J. Amer. Chem. Soc.*, **83, 1945** (1961)
[21] V. P. Kudesia, *Acta Ciencia Indica*, **1**, 294 (1975).
[22] P. T. McTigue and J. M. Sime, *J. Chem. Soc.*, **1963**, 1303.
[23] P.T. McTigue, *Austral. J. Chem.*, **17**, 1210 (1964).
[24] V. P. Kudesia and S. K. Mukherjee, *Indian J. Chem.*, **15A**, 513 (1977).
[25] I.R.L. Barker and P. Auckett, *Chem. Ind.*, **1967**, 193.
[26] N. C. Deno and N. H. Potter, *J. Amer J. Chem. Soc.*, **89**, 3555 (1967).
[27] N. Venkatasubramanian and V. Thiagarajan, *Canad. J. Chem.*, **47**, 694 (1969).
[28] K. K. Banerjee, *Indian J. Chem.*, **16A**, 596 (1978).
[29] K. K. Banerjee, *Bull. Chim. Soc. Japan*, **46**, 3623 (1973).
[30] V. S. Srinivasan and N. Venkatasubramanian, *Indian J. Chem.*, **13A**, 526 (1975).
[31] C. C. Hong and W. H. Rapson, *Canad. J. Chem.*, **46**, 2053 (1968).
[32] R. G. Kieffer and G. Gordon, *Inorg. Chem.*, **7**, 235 (1968).
[33] G. Gordon and F. Emmenegger, *Inorg. Nucl. Chem. Lett.*, **2**, 395 (1966).

Revue Roumaine de Chimie, **28**, *11–12*, 977–980 (1983)

TRIARYL-*s*-TRIAZOLES FROM DIAROYLHYDRAZINES BY A NEW DIRECT CONDENSATION REACTION

C. I. CHIRIAC
"P. Poni" Institute of Macromolecular Chemistry
Aleea Gr. Ghica Vodă 41 A, Iaşi, Romania

Received November 3, 1982

By a direct condensation reaction between phosphoryl triamides prepared *in situ* and diaroylhydrazines in *o*-dichlorobenzene at reflux, 3, 4, 5-triaryl-*s*-triazoles result in high yield.

In a previous paper, [1] we showed that diamides of phenylphosphorous acid can be used in the synthesis of 3, 4, 5-triaryl-*s*-triazoles.

In the present paper we investigate other reagents for the synthesis of the same compounds.

RESULTS AND DISCUSSION

As reagents used for the synthesis of 3, 4, 5-triaryl-*s*-triazoles from diaroylhydrazines, we mention : phenylphosphoazoanilide [2] and aromatic amines/zinc chloride. [3]

By the reaction between phosphorus oxychloride (phosphoryl chloride) and amines, phosphoryl triamides [4] result, which can react with carboxylic acids affording amides. [5] In the present paper, we have investigated if these compounds can be used in the condensation reaction with diaroylhydrazines affording the corresponding triazoles. We have observed that this is possible only at high temperatures (175–185°) in *o*-dichlorobenzene as solvent.

At the beginning, we used pure phosphoryl triamides, [4] but in order to simplify the procedure we prepared this compounds *in situ* from the corresponding aromatic amines and phosphoryl chloride, because the yield and the purity are the same in both cases. By the reaction between an aromatic primary amine (6 moles) and phosphoryl chloride (1 mole) in *o*-dichlorobenzene, phosphoryl amides (1 mole) result *in situ*, which react with diaroylhydrazine (1 mole) in the same solvent at reflux (175–185°C). From the six moles of amine, three are necessary for the formation of triamides of phosphoric acid and three as acceptors for the hydrochloric acid (other acceptors for HCl, e.g. pyridine or other tertiary amines afford impure final products). In the case of 3, 4, 5-triphenyl-1, 2, 4-triazole, the yield is 80–82 % when we use 1 mole phosphoryl trianilide as reagent for 1 mole dibenzoylhydrazine and only 44 – 48 % for 0.5 mole reagent. This shows that two reactive amide groups react under these conditions by cyclisation with dibenzoylhydrazine and the third one is unreactive, similar to other cases.[6,7]

The yield increases with the increasing of the temperature. At temperatures under 170–180°C, the yield decreases very much (at 100–130° being 25–30 %). We have chosen the *o*-dichlorobenzene as a good solvent because it has a high boiling point and is an inert solvent for this reaction. In addition, *o*-dichlorobenzene is a good solvent for the final products (at 170–180°), which precipitate on cooling at room temperature.

As a result of these investigations, we propose the following mechanism of reaction :

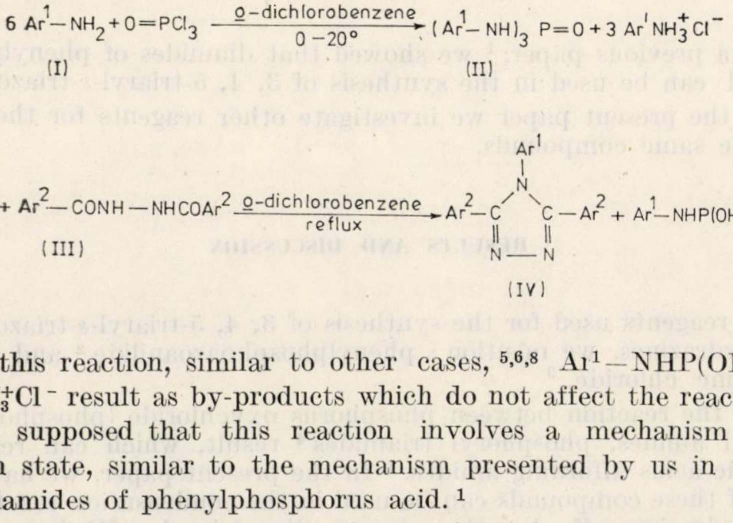

In this reaction, similar to other cases, [5,6,8] $Ar^1-NHP(OH)_2$ and $Ar^1-NH_3^+Cl^-$ result as by-products which do not affect the reaction.

We supposed that this reaction involves a mechanism with a transition state, similar to the mechanism presented by us in the case of the diamides of phenylphosphorus acid. [1]

In a general procedure, to a solution of 6 moles I in dried *o*-dichlorobenzene cooled to 0°, 1 mole phosphoryl chloride was added slowly under stirring (the reaction is exothermic). After 1–2 hours at room temperature, 1 mole III was added and the stirring was continued for 4–5 hours at reflux (175–185°). Then by cooling, the final products IV precipitate. Table 1 shows the triazoles IV prepared by this procedure.

Table 1 shows that the large majority of the final products IV had correct melting points and the yields ranged from 56 to 87 %.

By this simple method we obtained, in high yields, triaryl-*s*-triazoles from diaroylhydrazines.

Table 1

Triaryl-*s*-triazoles obtained from *in situ* prepared phosphoryl triamides and diaroylhydrazines

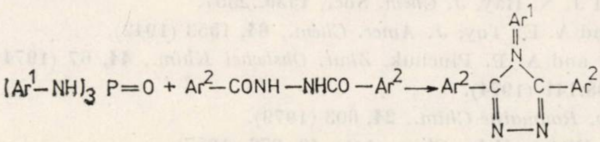

Ar^1	Ar^2	Crude product		Pure product[c]	Reported
		M.p.[a] °C	Yield[b] %	M.p. °C	M.p. °C
C_6H_5	C_6H_5	297–299	84	299–300	299–300[9]
C_6H_5	p-$CH_3OC_6H_4$	249–251	87	250–252	250–252[1]
p-$CH_3-C_6H_4$	C_6H_5	299–301	85	300–302	300–302[3]
m-$CH_3-C_6H_4$	C_6H_5	255–257	81	255–257	254–256[3]
m-$Br-C_6H_4$	C_6H_5	249–254	73	257–259	257–259[1]
o-$Br-C_6H_4$	C_6H_5	292–298	56	300–302	300–302[1]
$1-C_{10}H_7$	C_6H_5	238–244	58	245–247	245–247[3]

a) Before recrystallization.

b) Yields calculated on diaroylhydrazine employed, before recrystallization.

c) The products were identified by comparing the m.p. and IR spectra with those of the authentic samples.

EXPERIMENTAL

3, 4, 5-Triphenyl-*s*-triazole

To a stirred solution of aniline (5.58 g, 0.06 moles) in 20 ml dried *o*-dichlorobenzene cooled to 0°C, phosphoryl chloride (0.9 ml, 0.01 moles) was added slowly, when phosphoryl anilide and $C_6H_5-NH_3^+Cl^-$ precipitate. The mixture was stirred for 1–2 hours at room temperature. Then, dibenzoylhydrazine (2.4 g, 0.01 moles) was added under stirring. The final mixture was stirred and refluxed (175–185°) for 4 hours in an oil (or molten salts) bath at 190–200° (maximum 200°). An efficient stirring is desirable during the heating. The product precipitated on cooling to room temperature was collected by filtration, washed well with 30–50 ml ethyl ether and dried. The obtained product is stirred and heated at 70–90°C with 60–80 ml water and NaOH solution till pH = 9–10 (about 2 hours). After filtration, the same operation is repeated with solution of hydrochloric acid at pH = 1–2. After filtration, the product is washed 2–3 times with 30–40 ml water. After drying at 100–130° under vacuum, 2.5 g crude product (yield 84%) were obtained with m.p. 297–299°C (m.p. of the mixture with an authentic sample of 3, 4, 5-triphenyl-*s*-triazole underpressed).

Anal. Found : C, 80.11 ; H, 4.90 ; N, 14.15%

Calculated for : $C_{20}H_{15}N_3$; C, 80,77 ; H, 5.12 ; N, 14,13%.

Under similar conditions, the other triazoles presented in table 1 were obtained.

REFERENCES

[1] C. I. Chiriac, *Rev. Roumaine Chim.*, **27,** 645 (1982).

[2] E. Klinsberg, *J. Org. Chem.*, **23,** 1086 (1957).

[3] K. L. Bhagot and J. N. Ray, *J. Chem.* Soc., **1930,** 2357.

[4] L. F. Andrieth and A. E. Toy, *J. Amer. Chem.*, **64,** 1553 (1942).

[5] A. P. Marchenko and A. P. Pinchuk, *Zhur. Obshchei Khim.*, **44,** 67 (1974) ; *Chem. Abstr,* **80,** 108.141 (1974).

[6] C. I. Chiriac, *Rev. Roumaine Chim.*, **24,** 603 (1979).

[7] B. Iselin and W. Rittel, *Helv. Chim. Acta*, **40,** 376 (1957).

[8] H. O. Becker and K. F. Funk, *J. prakt. Chem.*, **286,** 55 (1961).

[9] R. Stollé, *J. prakt. Chem.* **73,** 288 (1906).

Revue Roumaine de Chimie, 28, *11–12*, 981–987, (1983)

NEW DIOXOURANIUM (VI) COMPLEXES WITH TRIDENTATE DIBASIC SCHIFF BASES PREPARED FROM β-DIKETONES AND AMINES

A. SYAMAL* and O. P. SINGHAL

Department of Applied Sciences and Humanities, Kurukshetra University, Kurukshetra 132119, Haryana and Department of Chemistry, Regional Engineering College, Kurukshetra 132119, Haryana, India

Received July 14, 1981

Several new dioxouranium (VI) complexes with the dibasic tridentate Schiff bases acac-R (where acac-R is the Schiff base prepared from 2-aminoethanol, *o*-aminobenzylalcohol, *o*-hydroxybenzylamine, 4-amino-1-butanol, benzoylhydrazide or *o*-aminothiophenol and acetylacetone) and benzac-R (where benzac-R is the Schiff base prepared from 2-aminoethanol, *o*-aminobenzylalcohol, *o*-hydroxybenzylamine, 4-amino-1-butanol, benzoylhydrazide, *o*-aminothiophenol or 2-aminoethanethiol and benzoylacetone) have been synthesized by the reaction of an EtOH solution of dioxouranium (VI) acetate dihydrate and the Schiff base. The complexes are of the type $UO_2L.EtOH$ (where LH_2 is the dibasic tridentate Schiff base). The complexes have been characterized on the basis of elemental analyses, IR spectra, conductance, magnetic susceptibility and molecular weight measurements. The complexes are diamagnetic, monomers and octahedral.

INTRODUCTION

Synthesis of dioxouranium (VI) complexes of potentially tridentate Schiff bases derived from β-diketones and amines has been reported in the literature[1,2], but the Schiff bases in these complexes behave as bidentate ligands. These works were not directed to achieve the tridentate behaviour of the Schiff bases. We report here on the successful synthesis of dioxouranium (VI) complexes with the β-diketone Schiff bases which behave as tridentate dibasic ligands. The Schiff bases used in the present paper are structurally represented as follows :

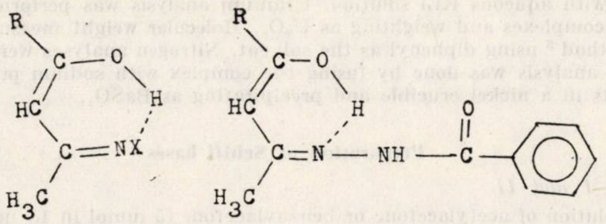

*** Author to whom correspondence should be addressed.**

I. R=CH_3, C_6H_5 II. R=CH_3, C_6H_5

X=$(CH_2)_2OH$, o-$C_6H_4CH_2OH$,

o-$CH_2C_6H_4OH$, $(CH_2)_4OH$

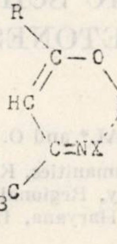

III. R=CH_3 ; X=c-C_6H_4SH

R=C_6H_5 ; X=o-C_6H_4SH, $(CH_2)_2SH$

We would like to indicate that the dioxouranium (VI) complexes with the Schiff bases III are the first examples of dioxouranium (VI) complexes with sulfur donor Schiff bases. The study of metal complexes of sulfur donor Schiff bases is of biochemical interest due to the reported anticancer and antiviral activities of ligands with SN donor set and their metal complexes.

EXPERIMENTAL

Materials

o-Aminobenzylalcohol, 2-aminoethanethiol hydrochloride, 4-amino-1-butanol and o-aminothiophenol were obtained from Aldrich chemical Co. (U.S.A.). Acetylacetone was S.D.'s Lab-Chem reagent. Benzoylacetaone was purchased from Fluka A.G. (Switzerland). Uranylacetate dihydrate was a Hopkins and Williams (U.K.) product. 2-Aminoethanol was a gift from Amines and Plasticizers Ltd., Bombay. o-Hydroxybenzylamine [3] and benzoylhydrazide [4] were prepared according to the published procedures.

Physical Measurements

The IR spectra of the complexes were recorded in KBr pellets on a Beckman IR—20 spectrophotometer calibrated with polystyrene. Electronic spectra were recorded on a Beckman DU-2 spectrophotometer. Electrolytic conductance measurements were made with the help of a Philips PR—9500 conductivity bridge. The conductivity cell with platinum electrodes was calibrated with aqueous KCl solution. Uranium analysis was performed gravimetrically by igniting the complexes and weighting as U_3O_8. Molecular weight measurements were made by the Rast method [5] using diphenyl as the solvent. Nitrogen analyses were done microanalytically. Sulphur analysis was done by fusing the complex with sodium peroxide and sodium hydroxide pellets in a nickel crucible and precipitating as $BaSO_4$.

Preparation of Schiff bases

A. *Schiff bases I and II*

AC_6H_6 solution of acetylacetone or benzoylacetone (5 mmol in 15 ml) was mixed with a C_6H_6 solution of the appropriate amine (5 mmol in 15 ml). The mixture was refluxed for 30 min on a water bath and was then partially evaporated under a fan. The mixture was cooled in ice. The separated crystalline solid was filtered under reduced pressure. On standing at room temperature Schiff bases β-diketone-2-aminoethanol and β-diketone-4-amino-1-butanol turned into oil while the others remained as solids. All the Schiff bases were purified by dissolution of solid precipitate in C_6H_6 and then by cooling in ice. White or yellow crystals of the Schiff bases were formed. The product was then filtered, washed with cold C_6H_6 and dried *in vacuo* at room temperature. Schiff bases β-diketone-2-aminoethanol and β-diketone-4-amino-1-butanol were stored in refrigerator in order to keep them in the solid form. Yield = 60—70%.

B. *β-Diketone-o-aminothiophenol*

A C_6H_6 solution of β-diketone (5 mmol in 15 ml) was mixed with a C_6H_6 solution of *o*-aminothiophenol (0.63 g, 5 mmol in 15 ml). The mixture was magnetically stirred for 1 hr at room temperature. The rest of the procedure was the same as adopted in A above. The Schiff base is stable at room temperature. Yield = 60%.

C. *Benzoylacetone-2-aminoethanethiol*

2-Aminoethanethiol hydrochloride (0.57 g, 5 mmol) was dissolved in EtOH (20 ml) and the solution was treated with an EtHO solution of anhydrous sodium acetate (0.41 g, 5 mmol in 25 ml). The mixture was stirred well to give the sodium chloride precipitate and then filtered off. The filtrate was mixed with an EtOH solution of benzoylacetone (0.81 g, 5 mmol in 20 ml). The mixture was magnetically stirred for 1 hr at room temperature. The rest of the procedure was the same as adopted in A above, except that EtOH was used for recrystallization and washing instead of C_6H_6. The Shiff base is stable at room temperature. Yield = 60%.

Preparation of the complexes

D. *For Complexes with the Schiff bases I and II*

An EtOH solution (10 ml) of the appropriate Schiff base (2 mmol) was treated with an EtOH solution (20 ml) of $UO_2(AcO)_2 . 2H_2O$(0.85 g, 2 mmol). The mixture was boiled under reflux for 2 hrs. The mixture was partially evaporated under a fan and the separated crystalline solid was filtered off under reduced pressure. The complex was purified by dissolution in EtOH and by partial evaporation of the solvent using a fan. The product was filtered off, washed with EtOH and dried *in vacuo* at room temperature. Yield = 60—70%.

E. *For complexes with the Schiff bases III*

The complexes were prepared by adopting the procedure as described in D above, except that the metal ion and ligand solution were stirred magnetically at room temperature for 4 hrs. Yield = 55%.

RESULTS AND DISCUSSION

The analytical data (Table 1) indicate that the complexes are of the type $UO_2L.EtOH$ (where LH_2 = Schiff base and EtOH = C_2H_5OH). The complexes are soluble in methanol, ethanol and chloroform. The molar conductance values of the complexes in methanol ($10^{-3}M$) have been found to be less than 8 ohm^{-1} cm^{2}mol^{-1} indicating their non-electrolytic behaviour. The complexes are monomers and are diamagnetic as expected for $5f^{\circ}$ dioxouranium (VI).

The complexes do not decompose or lose weight on heating at 100°C for hours indicating that ethanol is not lost at this temperature and it is coordinated to uranium. A broad band at 3300—3400 cm^{-1} in the complexes is assigned to the ν (OH) stretch [6] of EtOH. The absence of ν(C=O) frequency in all the Schiff bases except in II indicates that the Schiff bases exist in the enolic form. The presence of hydrogen bonding of both types, inter-molecular (O—H . . . O) as well as intra-molecular (O—H. . . N) has been well established [10] in the Schiff bases having hydroxyl groups. The present Schiff bases exhibit a band at 3000—3200 cm^{-1}, which indi

Table 1

Analytical and molecular weight data of Schiff base complexes*

Complex	Colour	Stoichiometry	M.W.observed (calcd.)	observed (calcd.) %		
				U	N	S
UO_2 (acac-2-aminoethanol)·EtOH	yellow	$C_9H_{17}O_5NU$	435 (457)	52.8 (52.08)	2.9 (3.06)	—
UO_2 (acac-*o*-aminobenzylalcohol).EtOH	yellow	$C_{14}H_{19}O_5NU$	540 (519)	46.6 (45.86)	2.6 (2.70)	—
UO_2 (acac-*o*-hydroxybenzylamine).EtOH	brown	$C_{14}H_{19}O_5NU$	535 (519)	44.7 (45.86)	2.6 (2.70)	—
UO_2 (acac-4-amino-1-butanol).EtOH	yellow	$C_{11}H_{21}O_5NU$	480 (485)	50.2 (49.07)	2.8 (2.89)	—
UO_2 (acac-benzh).EtOH	brown	$C_{14}H_{18}N_2O_5U$	550 (532)	44.1 (44.74)	5.1 (5.26)	—
UO_2 (acac-*o*-aminothiophenol).EtOH	yellow green	$C_{13}H_{17}O_4NSU$	542 (521)	46.7 (45.68)	2.6 (2.69)	6.0 (6.14)
UO_2 (benzac-2-aminoethanol).EtOH	yellow	$C_{14}H_{19}O_5NU$	502 (519)	46.7 (45.86)	2.6 (2.70)	—
UO_2 (benzac-*o*-aminobenzylalcohol). .EtOH	brown	$C_{19}H_{21}O_5NU$	562 (581)	40.1 (40.96)	2.3 (2.41)	—
UO_2 (benzac-*o*-hydroxybenzylamine). EtOH	orange	$C_{19}H_{21}$ O_5NU	570 (581)	40.2 (40.96)	2.3 (2.41)	—
UO_2 (benzac-4-amino-1-butanol).EtOH	yellow	$C_{16}H_{23}O_5NU$	525 (547)	42.6 (43.51)	2.6 (2.56)	—
UO_2 (benzac-benzh).EtOH	brown	$C_{19}H_{20}N_2O_5U$	610 (594)	41.2 (40.07)	4.5 (4.71)	—
UO_2 (benzac-*o*-aminothiophenol).EtOH	yellow green	$C_{18}H_{19}O_4NSU$	571 (583)	39.3 (40.82)	2.3 (2.40)	5.2 (5.49)
UO_2 (benzac-2-aminoethanethiol).EtOH	orange	$C_{14}H_{19}O_4NSU$	554 (535)	45.1 (44.49)	2.7 (2.62)	5.6 (5.98)

* Abbreviations : acac = acetylacetone, benzac = benzoylacetone, benzh = benzoylhydrazide.

Table 2

The IR spectral data of dioxouranium (VI) complexes and their Schiff base ligands*

Complex	ν_{as} (O=U==O)	ν_s(O=U=O)	f_{UO} mdynes A°	R_{U-O} A°	ν (C=N) (azomethine) complex (ligand)	ν (C–O) (enolic) complex (ligand)	ν (C–O) (alcoholic) complex (ligand)	ν (C–O) (EtOH)
UO_2 (acac-2-aminoethanol).EtOH	910	825	6.88	1.74	1625 (1600)	1110 (1130)	1210 (1230)	1060
UO_2 (acac-*o*-aminobenzyalcohol).EtOH	905	a	6.80	1.74	1620 (1600)	1140 (1150)	1195 (1210)	1040
UO_2 (acac-*o*-hydroxybenzylamine).EtOH	905	a	6.80	1.74	1600 (1590)	1115 (1135)	—	1030
UO_2 (acac-4-amino-1-butanol).EtOH	910	a	6.88	1.74	1610 (1600)	1120 (1130)	1200 (1210)	1030
UO_2 (acac-benzH).ETOH	910	830	6.88	1.74	1610 (1600)	1120 (1140)	—	1030
UO_2 (acac-*o*-aminothiophenol).EtOH	920	835	7.03	1.73	1600 (1590)	1120 (1130)	—	1050
UO_2 (benzac-2-aminoethanol).ETOH	910	825	6.88	1.74	1620 (1600)	1115 (1130)	1205 (1230)	1060
UO_2 (benzac-*o*-aminobenzylalcohol).EtOH	900	830	6.73	1.74	1610 (1600)	1125 (1150)	1200 (1215)	1050
UO_2 (benzac-*o*-hydroxybenzylamine).EtOH	900	820	6.73	1.74	1610 (1600)	1140 (1160)	—	1040
UO_2 (benzac-4-amino-1-butanol).EtOH	915	830	6.95	1.74	1620 (1600)	1120 (1150)	1200 (1220)	1060
UO_2 (benzac-benzh).EtOH	900	810	6.73	1.74	1600 (1590)	1120 (1150)	—	1050
UO_2 (benzac-*o*-aminothiophenol).EtOH	925	830	7.11	1.73	1620 (1610)	1130 (1155)	—	1055
UO_2 (benzac-2-aminoethanethiol).EtOH	930	840	7.18	1.73	1595 (1585)	1140 (1150)	—	1040

* All IR bands in cm^{-1}

a = Band masked due to interference with Schiff base ligand.

cates the presence of a hydrogen bonded-OH group in the Schiff bases. The absence of the (C=O) group in the Schiff bases prepared from β-diketones has been previously noticed by several workers.[7,8]

The ν(C—O) (enolic) stretch appears[1,6] at about 1150 cm^{-1} in the Schiff bases. In the complexes this band shifts to lower energy by 10 — 30 cm^{-1} indicating that the oxygen atoms of β-diketone of the ligands coordinate to uranium atom.

The Schiff bases exhibit the ν(C=N) (azomethine) stretch at 1590—1600 cm^{-1}. This band undergoes a positive shift of 10—25 cm^{-1} in the complexes indicating the azomethine nitrogen coordination to uranium. Due to intra-molecular hydrogen bonding (O—H ... N) in the Schiff bases, the ν(C=N) (azomethine) stretch occurs at relatively lower energy.[1] The positive shift occurs on coordination because of the destruction of the hydrogen bonding. The ν(C—O) stretch of ethanol occurs[9] at 1096 cm^{-1} and this band shifts to lower energy at 1030—1060 cm^{-1} indicating the oxygen coordination of ethanol to uranium. Other salient features of the IR spectra of these complexes are summarized below:

ν(*C=O*) *stretch*: The Schiff bases (II) exhibit the ν(C = O) stretch[10] at 1640 — 1650 cm^{-1}. This band disappears in the complexes indicating the destruction of the carbonyl group due to enolisation. The enolisation leads to the formation of the >C=N—N=C< group.

ν(*C—O*) (*phenolic*) *and* ν(*C—S*) (*thiophenolic*) *stretch*: The Schiff bases acac-*o*-hydroxybenzylamine and benzac-*o*-hydroxybenzylamine exhibit the ν(C—O) (phenolic) frequency at 1520 and 1540 cm^{-1} respectively, whereas their dioxouranium (VI) complexes exhibit this band at higher energy[11] (1550 cm^{-1}) indicating the coordination through the phenolic oxygen atom. The ligands acac-*o*-aminothiophenol and benzac-*o*-aminothiophenol exhibit the ν(C—S) stretch[12] at 750 cm^{-1} which moves to higher energy (820 cm^{-1}) on complexation indicating coordination through S atom. The ν(C—O) (phenolic) and ν(C — S) (thiophenolic) stretches undergo positive shifts on complexation due to the maintenance of a ring current arising from electron delocalisation in the chelate ring.

ν(*C — S*) (*thioalcoholic*) *stretch*: The Schiff base benzac-2-aminoethanethiol exhibits the ν(C—S) stretch[12] at 750 cm^{-1} which shifts to 670 cm^{-1} in the complex indicating coordination through the sulfur atom.

ν(*C—O*) (*alcoholic*) *stretch*: The Schiff bases (I) with the exception of acac-*o*-hydroxybenzylamine and benzac-*o*-hydroxybenzylamine exhibit the ν(C—O) (alcoholic) stretch[13] at 1210—1230 cm^{-1}. This band moves to lower energy (1195—1210) cm^{-1}) in the corresponding complexes indicating coordination of the oxygen atom.

All the complexes exhibit a very strong band at 900—930 cm^{-1} characteristic of the ν_{as}(O=U=O) stretch. The ν_s (O=U=O) stretch is observed in the 820—840 cm^{-1} region. The force constant (*f*) for the ν_{as}(O=U=O) vibration was calculated by following the method of McGlynn et al.[14] The force constant values lie in the range 6.73—7.18 mdynes/A° and are comparable with those observed in similar complexes. From these values, the U—O bond distance was calculated by using Jones' equation:[15] $R_{u-0} = 1.08\ f^{-1/3} + 1.17$. The values of U—O bond distance occur in the range 1.73—1.74 A° and are comparable with those observed in similar complexes.

The dioxouranium (VI) complex prepared from ONO donor Schiff base benzac-2-aminoethanol exhibit the $\nu_{as}(O = U = O)$ stretch and $\nu_s(O=U=O)$ stretch frequencies at lower energy (910 and 825 cm^{-1}) in comparison with the dioxouranium (VI) complex prepared from ONS donor Schiff base benzac-2-aminoethanethiol. The latter complex exhibits the $\nu_{as}(O=U=O)$ stretch and $\nu_s(O=U=O)$ stretch frequencies at 930 and 840 cm^{-1} respectively. Sulphur would be expected to bind less strongly than oxygen to the hard Lewis acid UO_2^{2+}, because sulphur has a lower Lewis base strength in comparison with oxygen.[16] The electron density at the U atom in UO_2 (benzac-2-aminoethanol).EtOH is more than the electron density at the U atom in UO_2 (benzac-2-aminoethanethiol). EtOH, because oxygen is a hard Lewis base in comparison with sulphur. An increase in electron density at the U atom would lead to an increase of repulsive force with the non-bonding electrons of the atoms of UO_2^{2+} moiety leading to the weakening of U=O bond.[17] As sulphur allows more electron delocalization, the electron density at U is reduced. The harder oxygen is not so efficient in electron delocalization. A recent study[18] indicating the correlation between the electron delocalization and cathodic reduction potential in dioxomolybdenum (VI) complexes lends support to our observation.

Thus, the analytical and IR data, and valence requirement of the metal ion indicate that the Schiff bases behave as dibasic tridentate ligands coordinating through ONO or ONS donor sets. All the complexes are six-coordinate and we propose an octahedral structure for these complexes.

REFERENCES

[1] R. G. Vijay and J. P. Tandon, *Acta Chim. Acad. Sci. Hung.*, **97**, 369 (1978).

[2] R. K. Mehta, R. K. Gupta and V.C. Singh, *J. prakt. Chem.*, **315**, 843 (1973).

[3] L. C. Raiford and E. P. Clark, *J. Amer. Chem. Soc.*, **45**, 1738 (1923).

[4] L. Gatterman and H. Wieland, "Laboratory Methods of Organic Chemistry", McMillan, London, 1963, p. 153.

[5] F. G. Mann and B. C. Saunders, "Practical Organic Chemistry", Longmans, London, 1961, p. 433.

[6] L. F. Lindoy and S. E. Livingstone, *Inorg. Chem.*, **2**, 1149 (1968).

[7] H. F. Holtzclaw, Jr., J. P. Collman and R. M. Alire, *J. Amer. Chem. Soc.*, **80**, 1100 (1958).

[8] M. F. Richardson and R. E. Sievers, *J. Inorg. Nuclear Chem.*, **32**, 1895 (1970).

[9] H. M. Randall, R. G. Fowler, N. Fuson and J. R. Dangl, "Infrared Determination of Organic Structures", D. Van Nostrand Company, New York, 1961, p. 50.

[10] D. K. Rastogi, S. K. Sahni, V. B. Rana and S. K. Dua, "*J. Coord. Chem.*, **8**, 97 (1978).

[11] S. J. Gruber, C. M. Harris and E. Sinn, *J. Inorg. Nuclear Chem.*, **30**, 1805 (1968) ; T. Tokii, Y. Muto, M. Kato, K. Imai and H. B. Jonassen, *J. Inorg. Nuclear Chem.*, **34**, 3377 (1972).

[12] C. N. R. Rao, "Chemical Applications of Infrared Spectroscopy", Academic Press, New York, 1963, p. 297.

[13] B. B. Mahapatra and B. K. Mahapatra, *J. Inorg. Nuclear Chem.*, **39**, 2291 (1977).

[14] S. P. McGlynn, J. K. Smith and W. C. Neely, *J. Chem. Phys.*, **35**, 105 (1961).

[15] L. H. Jones, *Spectrochim. Acta*, **10**, 395 (1958) ; **11**, 409 (1959).

[16] R. G. Pearson, *J. Amer. Chem. Soc.*, **85**, 3533 (1963).

[17] J. P. Day and L. M. Venanzi, *J. Chem. Soc.*, *A*, **1966**, 1363.

[18] O. A. Rajan and A. Chakravorty, *Inorg. Chim. Acta.*, **37**, 1503 (1979).

Revue Roumaine de Chimie, 28, *11–12*, 989–994 (1983)

A*s*-TRIAZINE DERIVATIVES WITH POTENTIAL THERAPEUTIC ACTION XVIII *

SYNTHESIS OF 4-METHYLTHIO-5-BENZYLTHIO-6-AZAURIDENE--5′-PHOSPHATE**

C. CRISTESCU

Chemical and Pharmaceutical Research Institute,
Şos. Vitan 112, 74351 Bucharest, Romania

Received September 24, 1982

4-Thio-5-benzylthio-6-azauridine (VI) was prepared *via* the silyl modification of the Hilbert-Johnson reaction. Compound VI was converted, *via* the 2′, 3′-O-isopropylidene derivative (IX) to 4-thio-5-benzylthio-6-azauridine-5′-phosphate (X) using phosphoxyl chloride and triethylphosphate. Alkylation of X with methyl iodide led to the title compound.

The carcinostatic activity of 4-thio-5-benzylthio-6-azauracil (I) and 4-methylthio-5-benzylthio-6-azauracil (II) prompted intensive studies in this field.

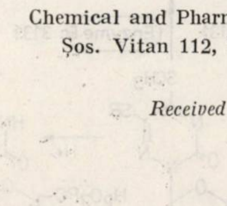

(I)

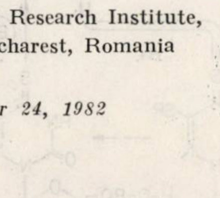

(II)

In order to elucidate the mechanism of their activity, we prepared the nucleoside and its 5′-phosphate derivative. The syntheses of these compounds are reported in this paper. For the synthesis of 4-thio-5-benzylthio-6-azauridine (VI), the silyl modification of the Hilbert-Johnson reaction [1, 2] appeared to be the method of choice.

The reaction of 2(trimethylsilyloxy)-4 (trimethylsilylthio)-5-benzylthio-6-azauracil (III) with 1-O-acetyl-2,3,5-tri-O-benzoyl-D-ribofuranose[3] (IV) in dry 1, 2-dichloroethane, at room temperature, in the presence of anhydrous stannic chloride, afforded the blocked nucleoside (V). The configuration of the blocked nucleoside V at the $C_{(1)}$-carbon atom of the sugar moiety was established by ^1H-NMR spectrum and by comparison with a thionation product of the known blocked 5-benzylthio-6-azauridine. [4]

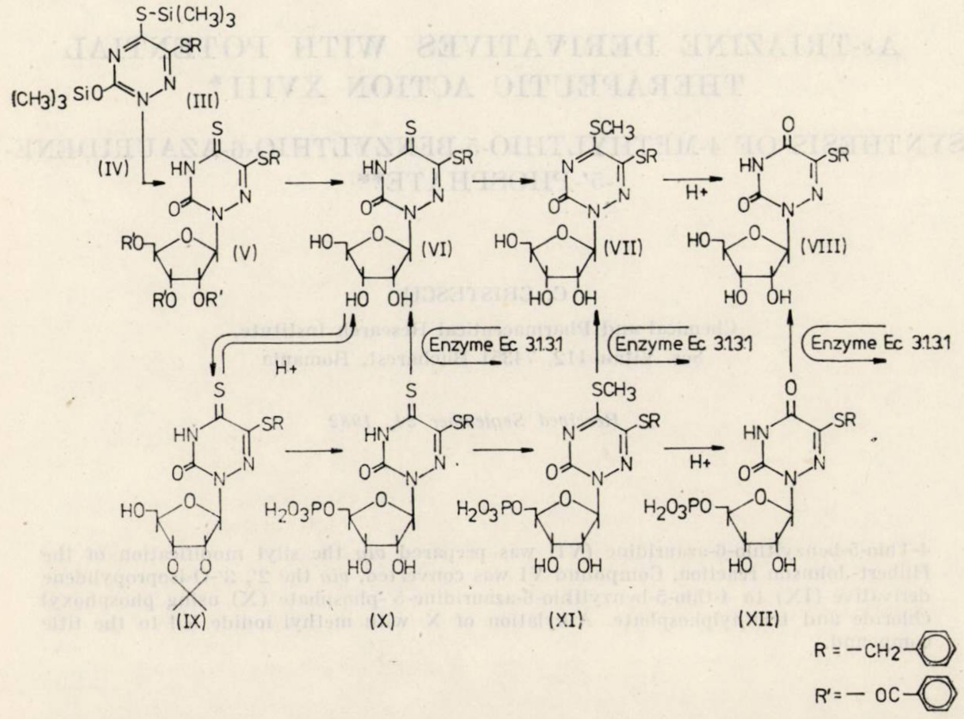

Removal of the blocking groups of V with sodium methoxide in methanol gave a 75% yield of the nucleoside, 4-thio-5-benzylthio-6-azauridine (VI). The UV spectrum of VI either at acid, neutral and alkaline pH shows the characteristic absorption peak of the 4-thio-nucleoside at λ max 324 nm (acid and neutral pH) and 336 nm (alkaline pH). The ready periodic acid oxidation reaction followed quantitatively by means of polarographic method, [5] was in accordance with the structure of compound VI.

Alkylation of VI with methyl iodide in aqueous alcoholic sodium hydroxide solution (1 Ec.) led to 4-methylthio-5-benzylthio-6-azauridine (VII). Compound VII may be subjected to acid hydrolysis to give 5-benzylthio-6-azauridine (VIII) identical in all respects to a sample obtained through another method as described in a previous paper. [4]

Nucleoside VI was converted to its 2′, 3′-O-isopropylidene derivative (IX) in 90% yield by the acid catalyzed reaction with 2,2-dimethoxypropane. The infrared spectrum of the compound containing the isopropylidene group shows two intense bands at 1070 and 1100 cm^{-1}. These bands can be assigned either to the isopropylidene C—O group vibration or to the vibration of the isopropylidene ring coupled with the furanose ring.[6–8] The UV spectrum of IX is identical with that of nucleoside VI. Heating (70°) of the compound IX with 0.5 N hydrochloric acid for 30 minutes affords VI without affecting the 4-thio-group.

The ^{1}H-NMR spectrum of IX exhibited a doublet for the anomeric proton and a difference in the δ values for the methyl groups of the isopropylidene moiety of 0.20 ppm. Such values have been shown[9,10], in the case of ribofuranosyl nucleosides to be consistent with the β-configuration.

The protected 2′,3′-O-isopropylidene derivative, was phosphorylated at the 5'-hydroxy-group using phosphoxyl chloride and triethylphosphate according to Yoshikawa et al[11,12]. Treatment with lithium hydroxide at pH 1.5 and heating at 70° for 30 minutes, removes the blocking group from the resulting 2′,3′-O-isopropylidene-nucleoside-5′-phosphate. The nucleotide, 4-thio-5-benzylthio-6-azauridine-5′-phosphate (X) was converted into the barium salt for storage. A part of the barium salt was converted into the free acid using DOWEX 50 × 8 (H^+). The resulting solution afforded by lyophilisation a crystalline compound. Its UV spectrum shows maximum at 324 nm (acid and neutral pH) and at 336 nm (alkaline pH) and is identical with that of 4-thio-5-benzyl-thio-6-azauridine. Cleavage of 5-phosphoderivative X by *Escherichia Coli* Alkaline Phosphatase (EC 3.1.3.1)[13,14] led to 4-thio-5-benzylthio-6-azauridine which was identified by tlc, paper chromatography and UV spectra.

Alkylation of X with methyl iodide in aqueous alcoholic sodium hydroxide solution (3 Ec.) led to 4-methylthio-5-benzylthio-6-azauridine-5′-phosphate(XI) which was converted to the barium salt. A part of the barium salt was transformed into the ammonium salt using ammonium sulphate. The UV spectrum of XI at acid, neutral and alkaline pH is identical with that of VII. Cleavage of XI by a specific enzymatic degradation method, affords VII identical in all respects to an authentic sample.

Compound XI may be subjected to acid hydrolysis to give 5-benzylthio-6-azauridine-5′-phosphate (XII) identical in all respects to a sample prepared by a different method. [15]

EXPERIMENTAL

The melting point were determined on a heating-plate microscope and are not corrected. Samples for analyses and spectral measurement were dried at 30°/0.1 mm Hg for 8 hours over P_2O_5. Paper chromatography was performed by the ascending tehnique on Schleicher-Schüll 2043 b mgl paper in the following systems : S_1, *n*-butanol-acetic acid-water (5 : 2 : 3) ; S_2, *n*-butanol-water (84 :14) ; S_3, 2-propanol-conc. aqueous ammonia-water (7 : 1 : 2) ; S_4, saturated aqueous solution of ammonium sulphate-1 M ammonium acetate-2-propanole (79 : 19 : 2) ; S_5, ethanol — 1 M ammonium acetate (5 : 2). Detection of the compounds was performed in ultraviolet light (254 nm). Thin layer chromatography (tlc) was performed on precoated Silicagel 60 F_{254} tlc plates (Merck) in the following systems : S_6, benzene-ethanol (9 : 1) ; S_7, benzene-ethyl acetate (7 : 3) ; S_8, benzene-methanol (8 : 2) ; S_9, chloroform-methnaol (8 : 2). The spots were detected in ultraviolet light (254 nm). Preparative column chromatography was performed on a LKB column of silicagel 60 (70—230 mesh). The flow-rate of 2.5 ml per min. was maintained. The fractions were collected at 6 minutes intervals. The ultraviolet absorbing substances in the chromatography were determined in eluates by running registration of UV absorption (UVICORD LKB ; 254 nm). Optical rotation was measured on a Hilger & Watts automatic polarimeter. Ultraviolet spectra were recorded on a Pye Unicam SP 1800 ultraviolet spectrophotometer. IR spectra were recorded on a Zeiss-Jena UR 20 spectrophotometer. The ^{1}H—NMR spectra were recorded at 60 MHz on a Varian EM 360 spectrophotometer in the indicated solvents and the chemical shifts are reported in parts per million (δ) with tetramethylsilane (TMS) or sodium 2,2-dimethyl-2-silapentane-5-sulfonate (DSS) as internal standard.

1(2′,3′,5′-tri-O-benzoyl-β-D-ribofuranosyl)-4-thio-5-benzylthio-6-azaracil (V)

A mixture of 4-thio-5-benzylthio-6-azauracil[16] (5.02 g; 20 mM), hexamethyldisilazane (40 ml) and trimethylchlorosilane (1 ml) was refluxed for 2 hours, with stirring and exclusion of atmospheric moisture. The excess of hexamethyldisilazane was removed in vacuo and the residual oil (III) was dissolved in dry 1,2-dichloroethane (400 ml). To this solution 1-O-acetyl-2, 3, 5-tri-O-benzoyl-D-ribofuranose (8.06 g ; 16 mM) and anhydrous stannic chloride (3.12 g ; 12 mM) were added and the reaction mixture was stirred, with exclusion of atmospheric moisture, for 8 hours at room temperature. The solution was treated with water, the organic layer separated, washed with water, and saturated solutions of sodium hydrogen carbonate again with water and dried (sodium sulphate). The residue remaining after removal of the solvent was purified by column chromatography on silicagel (100 g) with benzene as eluent. The chromatographically homogeneous fractions (tlc S_7, S_8) were collected and evaporated. The crude product was recrystallized from methanol to afford 11.8 g (84%) $\bar{V}$ with a m.p. 158–160° (dec.) ; *Rf*:0.92 (S_1), 0.92 (S_2), 0.93 (S_3), 0.56 (S_7), 0.49 (S_8) ; $[\alpha]_D^{25}$: – 151° (c 1, $CHCl_3$) ; $UV_{(ethanol)}$: λ max 230 nm (log ε 4.72) and 326 nm (log ε 4.09) ; $IR_{(CHCl_3)}$: 1729 cm^{-1} $\bar{\nu}$(CO) 1283, 1320 cm^{-1} $\bar{\nu}$(C.CO) and 1100, 1183 cm^{-1} $\bar{\nu}$ (CO.O) ^1H – NMR ($CDCl_3$) ; 6.8 (1H, d, $J_{1',2'}$ = 2.4 Hz, 1 $H_{1'}$)

$C_{36}H_{29}N_3O_8S$ Calcd., C, 62.14 ; H, 4.20 ; N, 6.03 ; S. 9,21 %

Found C, 62.05 ; H, 4.30 ; N, 6.13 ; S. 9.30 %.

4-Thio-5-benzylthio-6-azauridine (VI)

1.39 g (2 mM) $\bar{V}$ was dissolved in dry methanol (100 ml) and 1 N sodium methoxide (3 ml) was added. The mixture was stirred for 2 hours at room temperature. The solvent was evaporated in vacuo and the resulting oil was dissolved in water (20 ml) and extracted with ethyl acetate-ether (2 : 1 v/v : 2×10 ml). The aqueous layer was treated with DOWEX 50×8 (H^+) at pH 4, filtered and evaporated in vacuo. The residue crystallized from dry ethanol. Yield 0.581 g (75%) compound VI with a m.p. 159–160° ; *Rf*: 0.82 (S_1) ; 0.24 (S_2) ; 0.63 (S_3) ; 0.03 (S_4) ; 0.69 (S5) ; 0.49 (S_9) ; $[\alpha]_D^{25}$: –89.6° (c 1, methanol) ; UV : λ $max_{(EtOH)}$ 324 nm (log ε 4.02) ; λ $max_{(0.1 N HCl)}$: 324 nm (log ε 3.93) ; λ $max_{(0.1 N NaOH)}$ 336 nm (log ε 3.96) ; $IR_{(Kbr)}$: 1689 cm^{-1} $\bar{\nu}$ (CO) ; ^1H–NMR (DMSO–d_6 ; DSS) 5.83 (1 H, d, $J_{1',2'}$ = 2.5 Hz, 1$H_{1'}$)

$C_{15}H_{17}N_3O_5S_2$ Calcd., C, 46.98 ; H, 4.47 ; N, 10.95 ; S, 16.72%

Found C, 47.12 ; H, 4.52 ; N, 10.90 ; S, 16.81%.

4-Methylthio-5-benzylthio-6-azauridine (VII)

4-Thio-5-benzylthio-6-azauridine (0.574 g ; 1.5 mM) was dissolved in ethanol (25 ml) and 1 N sodium hydroxide (1.5 ml) and water (5 ml) was added. The solution was cooled at 10° and a solution of methyl iodide (0.3 ml ; 4.7 mM) in ethanol (5 ml) was added. The mixture was stirred 2 hours at 10° and 2 hours at room temperature and evaporated in vacuo. The dry residue, after recrystalization from methanol-water (1 : 1 v/v) yields 0.460 g (77%) VII with a m.p. 134–136° ; *Rf* : 0.79 (S_1) ; 0.64 (S_2) ; 0.60 (S_3) ; 0.83 (S_5) ; 0.68 (S_9) ; $[\alpha]_D^{25}$: –57° (c 1, ethanol) ; UV : λ $max_{(H_2O)}$ 302–304 nm (log ε 3.55) ; λ $max_{(0.1 HCl)}$: 302 nm (log ε 3.85) ; λ $max_{(0.1 N NaOH)}$ 302 nm (log ε 3.57) ; $IR_{(KBr)}$: 1655 cm^-_1 $\bar{\nu}$(CO).

$C_{16}H_{19}N_3O_5S_2$ Calcd., C, 48.34 ; H, 4.81 ; N, 10.57 ; S, 16.13%.

Found C, 48.40 ; H, 4.85 ; N, 10.65 ; S, 16.21 %.

Hydrolysis : 0.100 g VII was boiled with 5 ml ethanol and 0.5 ml 10% hydrochloric acid for 30 minutes. The solution was evaporated under reduced pressure. The residue was recrystallized from ethanol. Yield 0.078 g (85%) 5-benzylthio-6-azauridine (VIII) with a m.p. 165° without depression on admixture with an authentic sample. The ultraviolet spectra tlc and paper chromatography of the two samples were identical.

2′, 3′-O-Isopropylidene-4-thio-5-benzylthio-6-azauridine (IX)

A solution of 4-thio-5-benzylthio-6-azauridine 61.7 g ; 4.4 mM) in dry acetone (80 ml) and 2,2-dimethoxypropan (6.2 mM) was treated with 4 N hydrochloric acid solution in dioxane until it gave an acidic reaction. The reaction mixture was stirred at room temperature for 30 hours. Excess sodium hydrogen carbonate was added and the solution was stirred until neutral, filtered through Celite 545 and evaporated to dryness. The residue was purified by column chromatography on silicagel (40 g), with chloroform as an eluent. The chromatographically homogeneous fractions (UVICORD λ 254 nm and tlc S_9) were collected and evaporated. The crude product was recrystallized from ethanol to afford 1.68 g (90%) of IX with m.p. 153–155°C ; *Rf* : 0.91 (S_1) ; 0.55 (S_2) ; 0.80 (S_3) ; 0.84 (S_5) ; 0.38 (S_6) ; 0.13 (S_7) ; 0.57 (S_9) ; $[\alpha]_D^{25}$: – 73° (c 1, ethanol) ; UV : λ $\max_{(\mathrm{ethanol})}$ 324 nm (log ε 3.89) ; λ $\max_{(0.1\,\mathrm{N\,HCl})}$ 324 nm (log ε 3.90) ; λ $\max_{(0.1\,\mathrm{N\,NaOH})}$ 336 nm (log ε 4.0) ; $\mathrm{IR}_{(\mathrm{CHCl_3})}$: 1700 $\mathrm{cm^{-1}}$ $\bar{\nu}(\mathrm{CO})$, 2993 $\mathrm{cm^{-1}}$ $\bar{\nu}$ as $(\mathrm{CH_3})$, 2848 $\mathrm{cm^{-1}}$ ν s $(\mathrm{CH_3})$; ^{1}H–NMR (DMSO–d_6, DSS) : 6.00 (1 H, d, $J_{1',2'} =$ = 2.0 Hz, $1\mathrm{H}_{1'}$) ; 1.15, 1.35 (6 H, 2s, 2 $\mathrm{CH_3}$, isopropyl).

$C_{18}H_{21}N_3O_5S_2$ Calcd., C, 51.04 ; H, 4.99 ; N, 9.92 ; S, 15.14%

Found C, 51,10 ; H, 5.20 ; N, 9.96 ; S, 15.21%.

4-Thio-5-benzylthio-6-azauridin-5′-phosphate (X)

Phosphoxyl chloride (1 ml ; 10.95 mM) and dry triethylphosphate (20 ml) were added to IX (1.06 g : 2.6 mM) previously dried in vacuo. The mixture was stirred under anhydrous conditions at 5°. The tlc on silicagel (S_9) indicated that the reaction mixture was complete after 24 hours. Ice (10 g) was added and the mixture was stirred for 30 minutes. The pH was adjustes to 1.5 with 1 N lithium hydroxide and the solution heated under stirring at 70° (bath temperature) for 30 minutes. The resulting solution was extracted with ether (4 × 25 ml). The ethereal solution was extracted with 1 N litium hydroxide (5 ml) and water (2 × 20 ml). The aqueous layer was separated, adjusted to pH 6.5 with 1 N acetic acid, diluted at 100 ml with water and aqueous barium acetate solution (2.63 g in 8 ml water) was added. After cooling to 4° over night, the precipitate was centrifuged, washed with water, 80% ethanol and ether. The resulted barium salt of phosphate X was dried in air. Yield 1.17 g (75%).

The barium salt (0.5 g) was stirred with the upper part of a DOWEX 50 × 8 ($\mathrm{H^+}$) column (10 ml) until the salt dissolved. The column was washed with water and the fraction which contained X (UVICORD λ 254 nm) was lyophilized. The residue was distilled twice with a mixture of ethanol-benzene and twice with a mixture of methanol-benzene. The foamy product was treated with dry ether (10 ml). The mixture was shaked for 3 hours and the ether poured off. The residual crystalline solid, after drying in vacuo afforded 0.356 g (92%) of X with m.p. 113–115° ; *Rf* : 0.61 (S_1) ; 0.14 (S_3) ; 0.36 (S_4) ; 0.19 (S_5) ; $[\alpha]_D^{25}$: –80° (c 1, water) ; UV : λ $\max_{(\mathrm{H_2O})}$ 324 nm (log ε 4.04) ; $\lambda\max_{(0.1\,\mathrm{N\,HCl})}$ 324 nm (log ε 4.04) ; $\lambda\max_{(0.1\,\mathrm{N\,Na\,OH})}$: 336 nm (log ε 3.99) ; $\mathrm{IR}_{(\mathrm{K\,Br})}$: 1690 $\mathrm{cm^{-1}}$ $\bar{\nu}$ (CO) ; ^{1}H–NMR ($\mathrm{D_2O}$, DSS) 5.98 (1 H, d, $J_{1',2'} =$ 3.2 Hz, $1\mathrm{H}_{1'}$)

$C_{15}H_{18}N_3O_8S_2P$ Calcd., C, 38.87 ; H, 3.91 ; N, 9.06 ; S, 13.82 ; P, 6.68%

Found C, 38.91 ; H, 4.18 ; N, 9. 28 ; S, 13.92 ; P, 6.57 %.

Cleavage of X with alkaline phosphatase

A suspension of 80 μ of *Escherichia Coli* alkaline phosphatase (EC 3.1. 3.1) was diluted with 0.25 M TRIS-HCl buffer (380 μl, pH 8). A portion (200 μl) of this solution was added to the substrate (100 μ 1, 1% solution of X in 0.1 N ammonium sulphate) and incubated at 37° for 3 hours. The mixture was heated in a boiling water-bath for 3 minutes and the precipitate was separated by centrifugation. The supernatant showed on the paper chromatogram (elution systems S_1, S_2 and S_3) the main spot of 4-thio-5-benzylthio-6-azauridine.

4-Methylthio-5-benzylthio-6-azauridine-5′-phosphate (XI)

0.2 g (0.432 mM) of X was dissolved in ethanol (4 ml), 1 N sodium hydroxide (1.29 ml ; 1.29 mM) and water (4 ml). The solution was cooled at 10° and a solution of methyl iodide (50 μl) in ethanol (1 ml) was added. The mixture was stirred for 2 hours at 10° and 4 hours at room temperature and evaporated in vacuo. The residue was dissolved in water (6 ml) and an aqueous barium acetate solution (0.2 g in 2 ml water) was added. After cooling to 4° over night, the precipitate was centrifuged, washed with water, 80% ethanol and dried over P_2O_5. Yield 0.180 g (69%) barium salt of phosphate XI.

The barium salt (0.122 g) was supended in water (2 ml) and 40 µl of saturated ammonium sulphate solution was added. The mixture was stirred for 2 hours at room temperature and the precipitate was centrifuged. The supernatant was evaporated in vacuo. The foamy product was shaken for 3 hours with dry ethanol at room temperature. The residual crystalline solid, after drying in vacuo over P_2O_5, afforded 0.090 g (90%) ammonium salt of phosphate XI, white-yellow crystals, very hygroscopic, with a m.p. 105–108° (dec.); *Rf*: 0.65 (S_1); 0.16 (S_3); 0.23 (S_5); $[\alpha]_D^{25}$: $-52°$ (c, 0.5 water); UV : $\lambda\ max_{(H_2O)}$ 302–304 nm (log ε 3.87); $\lambda\ max_{(0.1\ N\ HCl)}$ 302 nm (log ε 3.92); $\lambda\ max_{(0.1\ N\ NaOH)}$ 302 nm (log ε 3.91); $IR_{(KBr)}$: 1660 cm^{-1} ν (CO), 2980 cm^{-1} $\bar{\nu}$ as (CH_3); 2885 cm^{-1} $\bar{\nu}$ s (CH_3).

$C_{16}H_{19}N_3O_8S_2P.NH_4 \cdot H_2O$ Calcd., C, 37.49 ; H, 4.91 ; N, 10,93 ; S, 12.51 ; P, 6.04%

Found C, 37.57 ; H, 5.18 ; N, 11.21 ; S, 12.49 ; P, 6.12%.

Hydrolysis : 0.010 g ammonium salt of phosphate XI was boiled with 10% hydrochloric acid (0.2 ml) for 30 minutes. The solution was evaporated in vacuo and the residue was dissolved in water (0.1 ml) which according to paper chromatography (solvent systems S_1, S_2, S_3) contained 5-benzylthio-6-azauridine-5-phosphate (XII) identical with an authentic sample.

Cleavage of XI with alkaline phosphatase

The ammonium salt of phosphate XI (0.010 g) was dissolved in water (1 ml) and treated with 0.1 M zinc chloride solution (0.1 ml). The cleavage was carried out in the same way as for substance X. The supernatant showed on paper chromatography (solvent systems S_1, S_2, S_3) and tlc (solvent system S_9) the main spot of 4-methylthio-5-benzylthio-6-azauridine identical with an authentic sample.

ACKNOWLEDGMENT : The autor thanks Mrs. Veronica Vişan of the Analytical Department of our Institute for recording the IR and UV spectra, Mrs. Pharm. Cornelia Ioan for elemental analysis and Dr. D. Ionescu for 1 H–NMR spectra.

REFERENCES

* Part XVII : C. Cristescu, *Rev. Roumaine Chim.*, **28**, 733(1983)

** This work has been reported in part as a preliminary communication at the 2-nd National Congress of Chemistry, Bucharest 7–10 Sept. 1981 : C. Cristescu in "Abstracts of Papers" p. 158.

[1] U. Niedballa and H. Vorbrüggen, *Angew. Chem. (Iternat. Ed)*, **9**, 461 (1970).

[2] C. Cristescu, *Monatsch.*, **108**, 1455 (1977).

[3] E. F. Recordo and R. Rinderknecht, *Helv. Chem. Acta*, **47**, 1171 (1959).

[4] C. Cristescu, *Rev. Ro maine Chim.*, **20**, 1287 (1975).

[5] P. Zuman and J. Kruoicka, *Coll. Czech. Chem. Comm.*, **23**, 598 (1958).

[6] S. A. Baker, E. J. Bourne, R. M. Pinkard and D. H. Whiffe, *J. Chem Soc.*, **1959**, 802

[7] S. A. Baker, E. J. Bourne, R. M. Pinkard and D. H. Whiffe, *J. Chem Soc.*, **1959**, 807.

[8] J. Pitha and J. Beranek, *Coll. Czech. Chem. Comm.*, **28**, 1507 (1963).

[9] R. V. Lemieux and D. R. Lineback, *Annu. Rev. Biochem.*, **32**, 155 (1963).

[10] J. L. Imbach, *Ann. N.Y. Acad. Sci.*, **255**, 177 (1975).

[11] M. Yoshikawa, T. Kato, and T. Takenischi, *Tetrahedron Letters*, **1967**, 5065.

[12] M. Yoshikawa, T. Kato and T. Takenischi, *Bull. Soc. Chim. Japan*, **42**, 3505 (1969).

[13] C. I. Hong, A. Nechaev and C. R. West, *J. Med. Chem.*, **22**, 1428 (1979).

[14] H. Rosemeyer and F. Seela, *J. Med. Chem.*, **22**, 1545 (1979).

[15] C. Cristescu in "Abstracts of Papers" 6th Meeting of Chemical and Pharmaceutical Research Institute 1979, p. 23.

[16] C. Cristescu and V. Badea, *Rev. Roumaine Chim.*, **14**, 135 (1969).

Revue Roumaine de Chimie, **28**, *11–12*, 995–999 (1983)

EXO- AND ENDOHORMONES. VII[1]

SYNTHESIS OF *Z*-11-TETRADECEN-1-OL ACETATE BY PHOSPHONIUM YLIDE CONDENSATION

N. POPOVICI, A. BARABÁS and F. HODOȘAN
Institute of Chemistry, 3400 Cluj-Napoca, str. Fîntînele 30, Romania

Received July 21, 1982

From three alternatives tested, condensation between triphenyl propylidene phosphorane (VII) and 10-carbomethoxy decanal (VIII) was found the most convenient procedure for preparing *Z*-11-tetradecen-1-ol acetate (I). The product obtained by this procedure contained the *Z* (I) and *E* (II) isomers of 11-tetradecen-1-ol acetate in a ratio of about 95% to 5% respectively.

INTRODUCTION

The two geometrical isomers, *Z* (I) or *E* (II) of 11-tetradecen-1-ol acetate are known to be components of the sex attractant pheromone blends of a large number of lepidopteran insect species [2], most of them considered as economically important agricultural pests. The proportions of the isomers in the natural pheromonal blends differ from species to species, but many pestiferous insects show a marked preference for mixtures with high proportions (90–97%) of the *Z*-isomer, I. Synthetic procedures

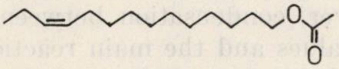

I

to obtain I with a rather high degree of stereoselectivity could therefore be considered of practical interest. The condensation between phosphonium ylides and different carbonyl compounds is known as a convenient means to obtain olefines in a stereochemically dirigeable manner. This procedure widely known as the Wittig reaction was extensively used [3] or stereoselective syntheses of olefinic pheromones. A number of authors[3-5] reported the synthesis of 11-tetradecenyl acetates (mixtures of I with II in different proportions) by the Wittig reaction. I most of these papers however no experimental details on the synthetic procedure were published. As a part of our effort to work out original, simple and practical procedures to obtain alkenol acetates for pheromonal applications, we tested comparatively three possible variations to prepare 11-tetradecen-1-ol acetate with high contents in its *Z*-isomer, I.

RESULTS AND DISCUSSION

In order to obtain an olefine with high *Z*-isomer content, the condensation between the appropriated phosphonium ylide and carbonyl compound should be effected in highly polar aprotic solvents in the presence of strongly alkaline agents.[6] Among the reported base-solvent combinations, most practical seemed to us the use of sodium methoxide in dimethyl formamide (DMF) solution, therefore all condensation runs were effected in this reaction medium. As for the pairs of synthons to be condensed to obtain I, the formally simplest way (referred to as route A) was to condensate propanol III, with the phosphorane obtained from triphenyl-(11-acetoxy-undecyl)-phosphonium iodide, IV.

$$(Ph_3\overset{+}{P}-(CH_2)_{11}-OCOCH_3)I^- \qquad \text{IV}$$

Unfortunately, compound IV could not be obtained in a crystalline form of sufficient and controllable purity, and our attempts to effect the condensation with the crude product obtained from 11-iodo-undecane-1-ol acetate and triphenylphosphine, failed. An alternative possibility (referred to as route B) to prepare I was to condesate propanal III with the phosphorane prepared from triphenyl-(10-carbomethoxy-decyl)-phosphonium iodide, V and subsequent transformation of the condensation product into I, by reduction and acetylation of the end function. The phosphonium salt V is a known[7,8] crystalline compound, easy to be purified. In our attempts however, condensation between III and V always stopped at low conversion values and the main reaction product was the phosphinoxide VI, most probably [2] resulting from hydrolysis of V or of the corresponding phosphonium ylide during working-up of the reaction mixture.

$$(Ph_3\overset{+}{P}-(CH_2)_{10}-COOCH_3)I^- \qquad \text{V}$$

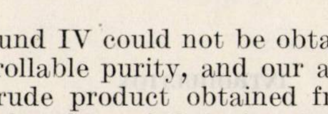

VI

Fair results were however obtained [10] be the third reaction scheme (route C) shown in detail below, in which the key step was the condensation between triphenyl-propylidene phosphirane VII and 10-carbomethoxy-decanal, VIII.

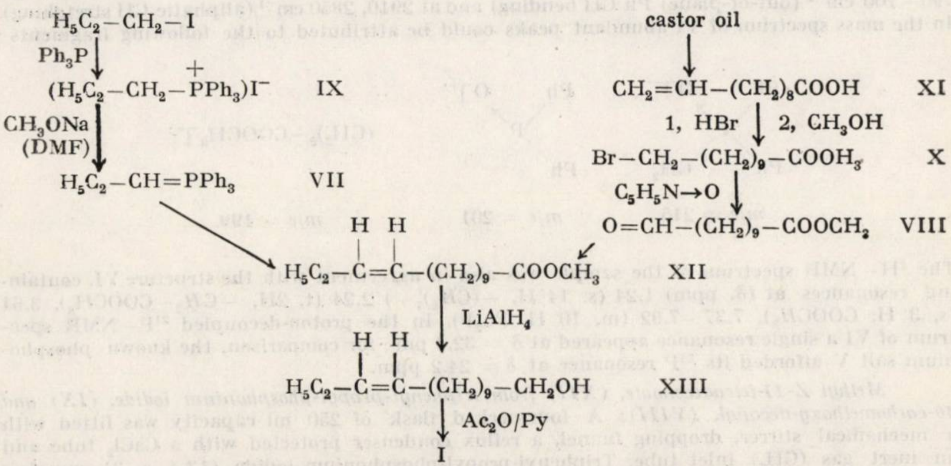
$H_5C_2-CH_2-I$
Ph_3P
$(H_5C_2-CH_2-\overset{+}{P}Ph_3)I^-$ IX
CH_3ONa (DMF)
$H_5C_2-CH=PPh_3$ VII
castor oil
$CH_2=CH-(CH_2)_8COOH$ XI
1, HBr 2, CH_3OH
$Br-CH_2-(CH_2)_9-COOH_3$ X
$C_5H_5N\rightarrow O$
$O=CH-(CH_2)_9-COOCH_3$ VIII
$H_5C_2-\overset{H}{C}=\overset{H}{C}-(CH_2)_9-COOCH_3$ XII
$LiAlH_4$
$H_5C_2-\overset{H}{C}=\overset{H}{C}-(CH_2)_9-CH_2OH$ XIII
Ac_2O/Py
I

Triphenyl-propyl-phosphonium iodide IX was obtained as reported [11] from 1-iodo-propane and triphenylphosphine. The aldehyde VIII was prepared [12] from *omega*-bromo undecanoic acid methyl ester X by oxidation with pyridine N-oxide. The bromo-acid X was prepared [13] from 10-undecenoic acid, XI, which in turn was obtained from castor oil by pyrolysis. [14] The *Z*-11-tetradecenoic ester XII resulting from condensation was reduced as usual with $LiAlH_4$ to the corresponding alcohol, XIII, which in turn was acetylated to yield the pheromone I. A 30% overall yield of I related to XI was obtained.

The pheromone I prepared as above afforded ^1H-and ^{13}C-NMR spectra identical to those of an authentic specimen (95% *Z*-11-tetradecen-1-ol acetate, I, with 5% of the *E*-isomer, II, kindly supplied by the USDA). It was successfully experimented in field and it is currently used in Romania for detection and survey of the following lepidopterous pests: *Adoxophyes orana*, *Ostrinia nubilalis*, *Pandemia heparana* and *Tortryx viridana*.

EXPERIMENTAL PART

Analyses and spectra: GLC-Analyses were performed on a Perkin-Elmer F−11 instrument. For determination of the isomeric purity of the pheromone I (II) and of its precursors XII and XIII a 50 m capillary column packed with Carbowax 20 M was used. Mass spectra were recorded on a Varian MAT 311 spectrometer coupled to a Perkin-Elmer 990 gaschromatograph. All NMR−spectra were recorded on a Bruker WP−60 FT−NMR instrument equipped with a 14.1 kG electromagnet (60 MHz for ^1H, 15.086 MHz for ^{13}C, 24.22 MHz for ^{31}P). Samples were dissolved in $CDCl_3$ ($CHCL_3$ for ^{31}P), the chemical shifts were related to internal TMS (external D_3PO_4 for ^{31}P). IR-Spectra were recorded on a Perkin-Elmer 700 spectrometer.

Syntheses: The precursor synthons to be coupled by the Wittig reaction were obtained as described in the literature (references cited above). No experimental details on the unsuccessful coupling routes A and B will be given here. The diphenyl-(10-carboxymethyl-decyl)-

phosphinoxide VI formed as an undesired by-product of route B, was characterized by its analytical figures (satisfactory for $C_{24}H_{33}PO_3$), m.p. 83° and various spectral data, as given below. The IR-spectrum (KBr pellets) of VI contained strong absorption bands at 1180 cm^{-1} (P—O), at 1745 cm^{-1} ($-COOCH_3$), at 3080 and 3060 cm^{-1} (Ph CH stretching), 790—700 cm^{-1} (out-of-plane) Ph CH bending) and at 2910, 2850 cm^{-1} (aliphatic CH stretching). In the mass spectrum of VI abundant peaks could be attributed to the following fragments:

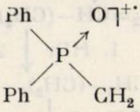

m/e = 215

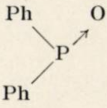

m/e = 201

$(CH_2)_9-COOCH_3]^{+\cdot}$

m/e = 199

The ^1H-NMR spectrum of the sample was also in agreement with the structure VI, containing resonances at (δ, ppm) 1.24 (s. 14 H, $-(CH_2)_7-$) 2.24 (t, 2H, $-CH_2-COOCH_3$), 3.61 (s, 3 H, $COOCH_3$), 7.37—7.92 (m, 10 H, Ph_2P). In the proton-decoupled $^{31}P-NMR$ spectrum of VI a single resonance appeared at $\delta = 32.4$ pm ; for comparison, the known phosphonium salt V afforded its ^{31}P resonance at $\delta = 24.2$ ppm.

Methyl Z-11-tetradecenoate, (XII) from triphenyl-propyl-phosphonium iodide, (IX) and 10-carbomethoxy-decanal, (VIII): A four-necked flask of 250 ml capacity was fitted with a mechanical stirrer, dropping funnel, a reflux condenser protected with a $CaCl_2$ tube and an inert gas (CH_4) inlet tube. Triphenyl-propyl-phosphonium iodide (13.4 g, 31 mmoles) was introduced, covered with 60 ml of anhydrous DMF and stirred until dissolution (about 30 min.) under inert atmosphere. Dry sodium methoxide, 1.4 g (30 mmoles), was then added; the characteristic orange-red colour of the phosphonium ylides (in this case triphenyl-propylidene phosphorane, VII) should immediately appear. The mixture was stirred at room temperature for 2 h, then cooled to 0°C and 4.12 g (20 mmoles) of 10-carbomethoxy decanal (VIII) were added. Stirring was continued for 4 h at 0° and further 12 h at room temperature. The mixture was poured into 500 ml of water and extracted with 5×50 ml of hexane. The extract was washed with water, 10% $NaHCO_3$, saturated NaCl solution and dried over $MgSO_4$. The solvent was removed and the residue distilled, collecting the product boiling at 100—105°/10^{-4} torr, consisted of 2.9 g (63% yield related to VIII).

Being the key intermediate of the synthesis, XII was thoroughly characterized by various analytical methods. Its GLC showed two nearby peaks at t_R values of 32 min. (about 95%, attributed to the *Z*-isomer of XII) and 31.5 min. (about 5%, *E*—XII). The IR-spectrum of the sample contained bands at 3005 and 720 cm^{-1}, characteristic of *Z*-olefines and a weak absorption at 967 cm^{-1}, characteristic of *E*-olefines, along with a strong absorption at 1730 cm^{-1}, due to the carboxymethyl group. ^1H-NMR of XII : 0.97 (t, 3 H, $J = 7.5$ Hz, CH_3-CH_2-), 1.33 (s, about 16 H, $-(CH_2)_8-$,(2.36 (t, 2H, $J=6$ Hz, $-CH_2-COOCH_3$), 3.75 (s, 3 H, $-COOCH_3$), 5.43 (m, 2 H, $-CH=CH-$). $^{13}C-NMR$ of XII : (carbon no./δ, ppm) : 1′/51.0, 1/173.1, 2/33.9, 3/24.8, 4—9/29.1, 10/27.0, 11/128.6, 12/130.8, 13/20.4 and 14/14.3. In the mass spectrum of the sample the following fragment ions can be considered as proofs for structure XII : $m/e = 208$ $(M-CH_3OH)^+$, 180 ($208-C_2H_4$) and 74 (McLafferty transposition of the carbomethoxy end).

In some runs small amounts of a crystalline by-product were isolated (m.p. 100°), which was identified as diphenyl-propyl-phosphinoxide, $Ph_2P(O)CH_2CH_2CH_3$, by its spectra as given below. IR : 1180 cm^{-1} (P—O), 1430 cm^{-1} (CH bending), 3080—3060 cm^{-1} (Ph CH stretching), 790—700 cm^{-1} (Ph out-of-plane CH bending) and 2910, 2850 cm^{-1} (aliphatic CH stretching). ^1H-NMR : 1.00 (t, 3 H, $J = 7.5$ Hz, $-CH_2-CH_3$), 1.25—2.00 (m, 2 H, $-CH_2-CH_2-CH_3$), 1.95—2.70 (m, 2 H, $P-CH_2-$), 7.30—7.95 (m, 10 H, Ph_2P). $^{31}P-NMR$: a single resonance in the proton-decoupled spectrum at $\delta = 32.5$ ppm.

Reduction of methyl Z-11-tetradecenoate, (XII) to Z-11-tetradecen-1-01, (XIII) with $LiAlH_4$: A three-necked flask of 500 ml capacity was equipped with mechanical stirrer, reflux condenser protected with $CaCl_2$ tube and a dropping funnel. A mixture of 0.5 g (13.1 mmoles) of $LiAlH_4$ and 10 ml of diethyl ether was refluxed in the flask for 45 min. under stirring. After cooling, 2.9 g (12 mmoles) of methyl-Z-11-tetradecenoate (XII) in 10 ml of ether were dropped into, under continuous stirring and refluxing. Stirring was continued for another 2 h, then the mixture left standing overnight. The mixture was chilled to 0° and 100 ml of 20% H_2SO_4 were added under stirring. The layers were separated, the water phase extracted with 2×25 ml of ether. The unified ethereal phase was washed with water and 10% $NaHCO_3$

and dried over $MgSO_4$. After removing the solvent, 2 g of crude XIII remained (78 %), which was used in the next step without purification.

Acetylation of Z-11-tetradecen-1-ol, (XIII) to Z-11-tetradecen-1-ol acetate, (I) 2 g (9.3 mmoles) of crude *Z*-11-tetradecen-1-ol (XIII) were dissolved in a mixture of 6 ml acetic anhydride and 6 ml of pyridine and kept at room temperature for 20 h. The mixture was then poured onto ice and extracted with 4×25 ml of diethyl ether. The extract was washed successively with water, 10 % $NaHCO_3$, saturated NaCl solution and water again, then dried over $MgSO_4$. The solvent was then removed and the residue distilled at $75-80°/10^{-4}$ torr, yielding 2.2 g (92 %) of *Z*-11-tetradecen-1-ol acetate, (I).

In the chromatogram of the pheromone I thus obtained, two nearby peaks were assigned to the *Z*-isomer, I, ($t = 33.63$ min, 95 %) and the E-isomer, II, ($t_R = 32.08$ min., 5 %) respectively. In the IR spectrum of the product absorptions at 720 and 3005 cm^{-1} were assigned to the *Z*-olefinic substructure and a small absorption at 967 cm^{-1} to the *E*-olefine. A strong band at 1750 cm^{-1} was attributed to the esteric carbonyl absorption. ^1H-NMR : 0.95 (t, 3 H, $J = 7.5$ Hz, $-CH_2-CH_3$), 1.28 (s, about 15 H, $-(CH_2)_8-$), 1.8–2.2 (m, about 4 H, $-CH_2-$ from positions 10 and 13), 2.05 (s, 3 H, $-O-COCH_3$), 4.05 (t, 2 H, $J = 6.4$ Hz, $-CH_2-O-$), 5.34 (m, 2 H, $-CH=CH-$). $^{13}C-NMR$: (carbon no/δ, ppm) : 2′/20.9, 1′/171.1, 1/64.7, 2/28.7, 3/26.0, 4.5 6 /29.6, 6, 78/29.3, 9/29.8, 10/27.2, 11/129.4, 12/131.6, 13/20.6 and 14/14.4. The measured shifts for C–10 and C–13 in I and XII are proofs for the *Z*-geometry of these compounds. In the mass spectrum of I the following fragments are considered as proofs for the proposed structure (I) : $m/e = 194$ $(M-CH_3COOH)^+$, 166 $(194-C_2H_4)^+$ and 61 $(CH_3COOH_2)^+$.

ACKNOWLEDGEMENTS. Thanks are expressed to Dr. I Oprean for his help in interpreting the mass spectra.

REFERENCES

[1] Part VI : A. A. Botar, A. Barabás, I. Oprean, J. Csonka-Horvai and F. Hodoşan, *Rev. Roumaine Chim.*, **28**,741 (1983).
[2] M. Jacobson, "Insect Sex Pheromones", Acad. Press, New-York, 1972 ; M. Birch, "Pheromones", North-Holland Publ. Co., Amsterdam, 1974.
[3] H. J. Bestmann and O. Vostrowsky, "Chemistry of Insect Pheromones", in "Chemie der Pflanzenschutzmittel", R. Wegler ed., Bd. 6, Springer-Verlag, Berlin, 1980.
[4] W. L. Roelofs and H. Arn, *Nature*, **219**, 513 (1968).
[5] Y. Tamaki, H. Noguchi and T. Yushima, *Appl. Entomol. Zool.*, **6**, 139 (1971).
[6] L. D. Bergelson and M. N. Semiakin, *Angew. Chem. Internat. Ed.*, **3**, 240 (1964).
[7] N. Pietragnini and G. Schiel, *Chem. Ber.*, **97**, 3293 (1964).
[8] G. Schiel, *ibid.*, **99**, 2698 (1966).
[9] U. Schöllkopf, *Angew. Chem.*, **71**, 260 (1959).
[10] N. Popovici, A. Barabás, D. Mustea and E. Maloş, *Rom. Pat.* no. **64550**, 30.08.01978 ; *Chem. Abstr.*, **93**, 176614 (1980).
[11] M. Schlosser and K. F. Christmann, *Liebigs Ann. Chem.*, **708**, 1 (1967).
[12] J. C. Stowe l, *J. Org. Chem.*, **35**,, 244 (1970).
[13] R. G. Jones, *J. Amer. Chem. Soc.*, **69**, 2352 (1947).
[14] E. Atanasova and M. Gardev, *Dokl. Bulg. Akad. Nauk*, **10**, 379 (1957) ; *Chem. Abstr.*, **52**, 14529 (1958).
[15] A. Barabás, A. A. Botar, A. Gocan, N. Popovici and F. Hodoşan, *Tetrahedron*, **34**, 2191 (1978).

and dried over $MgSO_4$. After removing the solvent, 2 g of crude XIII remained (75%), which was used in the next step without purification.

Acetylation of Z-13-tetradecen-1-ol, (XIII) to Z-11-tetradecen-1-ol acetate, (I). 2 g (9.5 mmoles) of crude Z-11-tetradecen-1-ol (XIII) were dissolved in a mixture of 5 ml acetic anhydride and 6 ml of pyridine and kept at room temperature for 20 h. The mixture was then poured onto ice and extracted with 4 × 25 ml of diethyl ether. The extract was washed successively with water, 10% $NaHCO_3$, saturated NaCl solution and water again, then dried over $MgSO_4$. The solvent was then removed and the residue distilled at 72–80°/10^{-4} torr, yielding 2.2 g (92%) of Z-11-tetradecen-1-ol acetate (I).

In the chromatogram of the pheromone I thus obtained, two nearby peaks were assigned to the Z-isomer, I (t_r = 25.63 min, 95%) and the E-isomer, II (t_r = 22.08 min, 5%) respectively. In the IR spectrum of the product absorptions at 730 and 905 cm^{-1} were assigned to the Z-olefinic substructure and a small absorption at 967 cm^{-1} to the E-olefine. A strong band at 1750 cm^{-1} was attributed to the esteric carbonyl absorption. ^1H-NMR: 0.95 (t, 3 H, J = 7.5 Hz, $-CH_3$, CH_2), 1.28 (s, about 15 H, $-(CH_2)_n-$), 1.8–2.2 (m, about 4 H, $-CH_2-$ from positions 10 and 13), 2.03 (s, 3 H, $-O-COCH_3$), 4.05 (t, 2 H, J = 6.4 Hz, $-CH_2-O-$), 5.34 (m, 2 H, $-CH=CH-$). ^{13}C-NMR (carbon no/δ, ppm): 2'/20.9, 1'/171.1, 1/64.7, 2/28.7, 3/26.0, 4.5.6/29.6, 6.7/8/29.3, 9/29.8, 10/27.2, 11/129.4, 12/131.8, 13/20.6 and 14/14.4. The measured shifts for C-10 and C-13 in I and XII are proofs for the Z-geometry of these compounds. In the mass spectrum of I the following fragments are considered as proofs for the proposed structure (I): m/e = 194 ($M-CH_3COOH$)$^+$, 166 ($194-C_2H_4$)$^+$ and 61 (CH_3COOH_2)$^+$.

ACKNOWLEDGEMENTS. Thanks are expressed to Dr. I. Oprean for his help in interpreting the mass spectra.

REFERENCES

[1] Part VI: A. A. Botár, A. Barabás, I. Oprean, J. Csonka-Horvai and F. Hodoşan, Rev. Roumaine Chim., 28, 741 (1983).
[2] M. Jacobson, "Insect Sex Pheromones", Acad. Press, New-York, 1972; M. Birch, "Pheromones", North-Holland Publ. Co., Amsterdam, 1974.
[3] H. J. Bestmann and O. Vostrowsky, "Chemistry of Insect Pheromones", in "Chemie der Pflanzenschutzmittel", R. Wegler ed., Bd. 6, Springer-Verlag, Berlin, 1980.
[4] W. L. Roelofs and H. Arn, Nature, 219, 513 (1968).
[5] Y. Tamaki, H. Noguchi and T. Yushima, Appl. Entomol. Zool., 6, 139 (1971).
[6] L. D. Bergelson and M. M. Shemiakin, Angew. Chem. Internat. Ed., 3, 250 (1964).
[7] N. Pietragalla and G. Sebiel, Chem. Ber., 97, 3293 (1964).
[8] G. Sebiel, ibid., 99, 2098 (1966).
[9] U. Schöllkopf, Angew. Chem., 71, 260 (1959).
[10] N. Popovici, A. Barabás, O. Mustea and E. Matos, Rom. Pat. no. 64750; 20.08.1978; Chem. Abstr., 93, 17681 (1980).
[11] M. Schlosser and K. F. Christmann, Liebigs Ann. Chem., 708, 1 (1967).
[12] J. C. Stowe, J. Org. Chem., 35, 244 (1970).
[13] E. L. Jones, J. Amer. Chem. Soc., 69, 2352 (1947).
[14] L. Alanasova and M. Gardev, Dokl. Bolg. Akad. Nauk, 10, 379 (1957); Chem. Abstr., 52, 11529 (1958).
[15] A. Barabás, A. A. Botár, A. Gocan, N. Popovici and F. Hodoşan, Tetrahedron, 34, 2191 (1978).

Revue Roumanine de Chimie, **28**, *11–12*, 1001–1007 (1983)

REACTION OF *endo* AND *exo*-BENZOCYCLOBUTENONORBORNENES WITH METHYL PROPIOLATE[1]

LUCIAN ENESCU, MIRCEA D. GHEORGHIU, AURELIA GHENCIULESCU,
ILIE G. DINULESCU and MARGARET AVRAM
Laboratory of Organic Chemistry, Polytechnic Institute — TCH, Spl. Independenţei 313,
Bucharest 16, 76206, Romania

Received March 24, 1983

The reaction of *endo* (**1**) and *exo*-benzocyclobutenonorbornene (**2**) with methly propiolate, in the presence of aluminium chloride, gave cycloaddition products **3a** and **4a** respectively, both with preservation of skeleton configuration. The *endo*-benzocyclobutenonorbornene (**1**) gave besides **3a**, the rearranged addition product **5**, in ratio 3 : 1.

In earlier studies concerning the chemistry of *endo* and *exo*-benzocyclobutenonorbornenes **1** and **2** it was established that skeleton rearrangement takes place in the course of reactions involving ionic intermediates.[2,3] Rearrangement occurs during the acid catalysed[4] and photochemical[5] descompositions of diazoketones with *endo* and *exo*-benzocyclobutenonorbornene skeleton. In studies on the behaviour of **1** and **2** in cycloaddition reactions with tert-butylcyanoketene[6] as well as with carbenes[7] and carbenoid species[8], it was demonstrated that the cycloaddition is concerted, occurring without skeletal rearrangement.

Our interest in the synthesis of benzo[*c*]tetracyclo[4.4.1.$0^{2.5}$.$0^{7.10}$] undeca-3.8-dienes **3** and **4** promted us to extend the recently reported cycloaddition reactions of methyl propiolate with alkenes[9] to the alkenes **1** and **2**. Tke greater tendency to rearrangement in ionic conditions of the *endo* isomer **1** with respect to the *exo* isomer **2** may furnish additional information on the concertedness of the cycloadditions with methyl propiolate. As it will be shown later the methyl propiolate complex with aluminium chloride can be viewed as an intermediate between a vinyl cation and ketene, both being able to act as π_{2a} components in the cycloaddition reaction.[10]

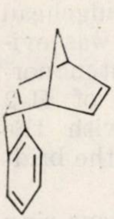
1

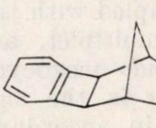
2

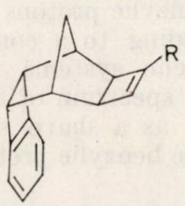

3 R=H
3a R=CO_2CH_3

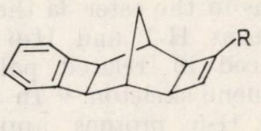

4 R=H
4a R=CO_2CH_3

RESULTS AND DISCUSSION

The reactions of **1** and **2** with methyl propiolate were performed using the standard procedure. The solution obtained from methyl propiolate and anhydrous $AlCl_3$ in methylene chloride was treated with the alkene and kept under stirring at room temperature for 48 hours. The crude reaction mixtures were analysed by GC—MS spectrometry. The compounds were isolated by column chromatography and the structures were ascribed on the basis of ^{1}H-NMR, IR and mass spectral data.

The reaction of *endo*-benzocyclobutenonorbornene (**1**) afforded a mixture of unrearranged cycloadduct **3a** and rearranged addition product **5** in ratio 3 : 1, together with variable amounts of chloro-derivative **6** with rearranged skeleton and unidentified polymeric products.

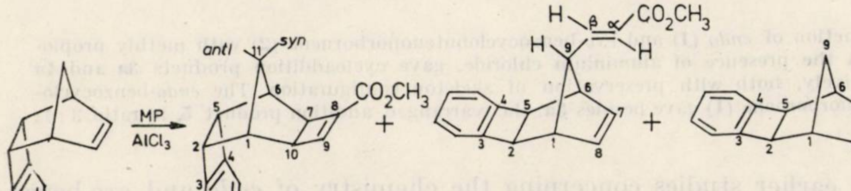

1 3a 5 6

In the reaction of *exo*-benzocyclobutenonorbornene (**2**) with methyl propiolate the cycloadduct **4a** was identified together with unreacted alkene, the chloro-derivative **6** and polymeric products.

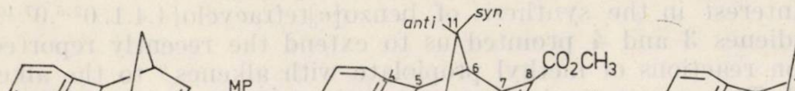

2 4a 6

The *endo* orientation of the benzocyclobutene ring in the ester **3a** as well as the *exo* orientation in the ester **4a** were ascribed on the basis of ^{1}H-NMR spectral pattern of the benzylic protons H-2 and H-5. Thus in the ester **3a** the benzylic protons are coupled with the bridgehead protons H-1 and H-6 leading to a complex multiplet, as it was evidenced in related polycyclic systems with *endo*-benzocyclobutenonorbornene skeleton.[11] In the spectrum of the ester **4a** the signals of H-2 and H-5 protons appear as a sharp singlet, in accordance with the lack of coupling between the benzylic protons of this system and the bridgehead protons.[11]

The *exo* orientation of the annelated carbomethoxycyclobutene ring is supported by the pattern of the signals of the allylic protons H-7 and H-10. These protons present a coupling constant of 3.0 Hz, in accordance with the observed values in other similar systems.[9, 11, 12] It can be noted that in triple resonance experiments by irradiation of H-7 and H-10 the broad singlet of the proton H-11 was narrowed, indicating a long range coupling between H-11-*anti* and H-7 and H-10 occurring only in the *endo* orientation of these protons, i.e. *exo* orientation of four-membered ring.

Further arguments supporting the ascribed structures and stereochemistry for the esters **3a** and **4a** namely for the *exo* orientation of the annelated cyclobutene ring have been provided by lanthanide induced shift experiment using $Eu(fod)_3 \cdot d_{27}$. Thus on icreasing the molar ratio $Eu(fod)_3 \cdot d_{27}$/substrate, the ^{1}H-NMR spectra of the ester **3a** as well as those of the ester **4a** displayed significant diamagnetic shifts for protons H-9, H-7, H-11-*syn* and H-6. The relative molar induced shift (MIS) values for the ester **4a** are presented in table 1 (normalized to the benzylic protons H-2 and H-5). The high induced shift value for H-11-*syn* proton supports the *exo* orientation of the carbomethoxylated cyclobutene ring.

Table 1

^{1}H-NMR chemical shifts and relatve MIS values for protons of the ester **4a**

	H-2 H-4	H-1	H-10	H-9	H-7	H-6	H-11-*anti*	H-11-*syn*	$COOCH_3$
δ [ppm]	3.17	2.12	2.53	6.65	2.83	2.32	0.87	1.26	3.70
MIS rel.	1.00	1.07	2.22	4.69	3.88	2.87	1.41	3.13	7.83

In the ^{1}H-NMR spectrum of the ester **5** the triplet for the protons H-7 and H-8 (coupled with the bridgehead protons H-1 and H-6, $J_{6.7} = J_{1.8} =$ 1·5 Hz) represents a characteristic pattern for the benzocyclobutenonorbornene skeleton.[11] The α-unsaturated proton of the acrylic substituent, partly overlapped by the aromatic signals, is a doublet of doublets with a coupling constant of 17.0 Hz, typical of *trans*-alkene coupling and has also a small coupling with the allylic proton H-9-*anti*. By decoupling the H-9-*anti* proton (at δ 2.13 ppm) the signal of the α-unsaturated acrylic proton becomes a doublet. In accordance with the *exo* orientation of the benzocyclobutene ring, the signal of the benzylic protons H-2 and H-5 appears as a singlet.[11]

Concerning the structure of chlorocompound **6** our results suggest *exo* configuration for benzocyclobutene (the lack coupling between the benzylic protons and the vicinal bridgehead protons) and for the chlorine atom (W-shape long range coupling, $J = 1.5$ Hz of H-7 with H-9-*anti*, as evidenced by double resonance experiments). The ^{1}H-NMR spectral pattern of the chlorocompound is very similar to the earlier reported bromo-derivative with the same structure.[3e]

The mass spectral data of the esters **3a** and **4a** with benzo[*c*]tetracyclo[4.4.1.0^{2,5}.0^{7,10}]undeca-3.8-diene skeleton and of the ester **5** with benzo[*c*]tricyclo[4.2.1.0^{2,5}]nona-3.7-diene skeleton evidence besides the low intensity molecular peak (5–8 %) a base peak at *m/e* 129 identical for the three esters.

The aluminium chloride catalysed reaction of alkenes with methyl propiolate leading to cyclobutene derivatives was described as a concerted $\pi_{2s} + \pi_{2a}$ cycloaddition. It was also shown that norbornene gives beside the cycloaddition products also addition products with rearranged skeleton suggesting an ionic course of this reaction. [9]

The results concerning the behaviour of benzocyclobutenonorbornenes deserve some comments. The propiolic ester takes part in the reaction as a complex with $AlCl_3$ which can be viewed as a polarized molecule with pronounced ionic character (**7a**, **7b**). The triple bond in this complexed molecule is probably of intermediate ionicity between a ketene C=C double bond and a vinyl cation. The ability of ketenes as well as of vinyl cations to take part as π_{2a} partner in cycloadditions is well known.[10]

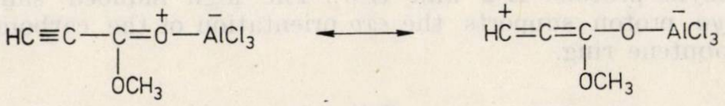

$$HC\equiv C-\underset{\displaystyle OCH_3}{\underset{|}{C}}=\overset{+}{O}-\overset{-}{Al}Cl_3 \longleftrightarrow \overset{+}{HC}=C=\underset{\displaystyle OCH_3}{\underset{|}{C}}-O-\overset{-}{Al}Cl_3$$

7a 7b

If the attack of the vacant *p* orbital of the vinylium ion **7b** takes place in a parallel approach, the dipolar intermediate **8** can result. The proximity of the anionic center to the cationic center favours the four-membered ring closure before any rearrangement can occur.

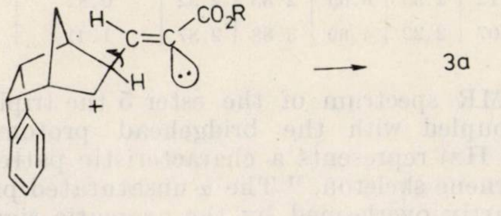

8

Also one may consider the case when the anionic center is far from the cationic center, when the norbornyl cation has enough time to rearrange via the ion **9** into the ester **5**. In the intermediate **9** the vinylium anionic center is in the proximity of the proton H-9 ; an intramolecular proton transfer will lead to the ester **5**.

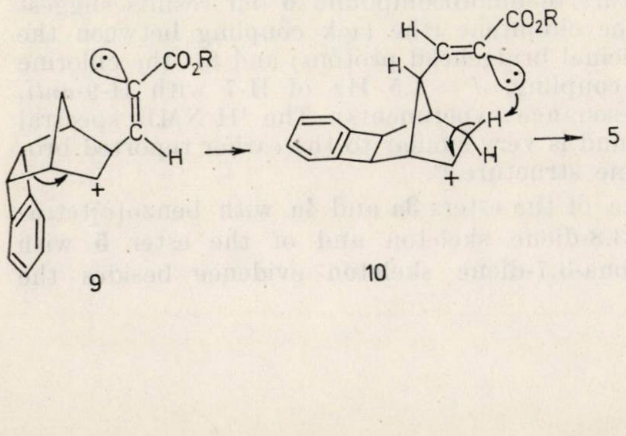

9 10

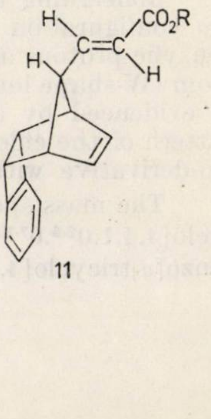

11

The fact that *exo*-benzocyclobutenonorbornene gives only the cycloadduct **4**a and no rearranged addition product such as **11** is attributed to the lower tendency to rearrangement of the *exo*-benzocyclobutenonorbornenic system. It was earlier observed that bromine addition to *exo*-benzocyclobutenonorbornene in less polar media like methylene chloride gave unrearranged adddition product; [3a] rearrangements of the *exo* skeleton to the *endo* form occur only in media with high polarity (solvolytic additions). [3c]

EXPERIMENTAL

IR spectra were recorded on a double beam UR-20 sectrophotometer. ^{1}H-NMR spectra were recorded on a Varian EM-360L spectrometer, using TMS as internal standard. Mass spectra were determined with DP-102 instrument.

Starting materials

Dichloromethane was purified by keeping for 24 hrs on $AlCl_3$; the distilled product was washed with water, dried and finally distilled on $LiAlH_4$.

exo-Benzocyclobutenonorbornene (**2**) was purified by chromatography on silicagel, using petroleum ether (b.p. 35—37°) as eluent.

Methyl propiolate was obtained by esterification of propiolic acid.

Reaction of *endo*-benzocyclobutenonorbornene (1) with methyl propiolate

Into a suspension of 0.7 g (5.25 mmoles) anhydrous aluminium chloride in 20 ml dichloromethane, 1.0 g (12 mmoles) methyl propiolate was added and the mixture was stirred at room temperature until a clear solution results. Alkene **1** (2.3 g, 13.6 mmoles) was dropped and the mixture was stirred at room temperature for 3 days. The mixture was then poured in 20 ml of saturated solution of NaH_2PO_4, stirred for 10 min and 10 % solution of HCl was added until aluminium hydroxide was dissolved. The oragnic layer was separated and the aqueous layer was extracted with dichloromethane for three times. The dichloromethane solution was washed with saturated salt solution, dried and the solvent was removed in vacuo, yielding 3.0 g residue (yellow oil). For this residue, the GC—MS spectrometry analysis shows a content of 45.0 % chloro-derivative **6**, 24.6 % ester **3a** and 8.6 % ester **5**.

The crude product was separated by column chromatography on neutral alumina (activity II).

The first fraction (eluent : petroleum ether, b.p. 35—37°) contains 1.36 g (48.5 %) chloro-derivative **6**, colourless oil with b.p. 88—90°/2 mm.

Mass spectrum (*m*/*e*) : 204 (M^+, $C_{13}H_{13}Cl$, 5 %), 169 (50.8 %), 141 (41.7 %), 129 (100 %), 115 (21.1 %).

^{1}H—NMR spectrum ($CDCl_3$, δ, ppm) : 0.90 (AB system, 1H, H-9-*anti*, $J_{AB} = 11$ Hz), 1.52 (AB system, 1H, H-9-*syn*, $J_{AB} = 11$ Hz), 1.80 (m, 2H, H-8-*exo*, H-8-*endo*), 2.28 (m, 1H, H-1), 2 41 (m, 1H, H-6), 3.03 (s, 2H, H-2, H-5), 3.70 (td, 1H, H-7-*endo*, $J_{7,9\text{-}anti} = 1.5$ Hz, $J_{7,8\text{-}endo} = J_{7,8\text{-}exo} = 5$ Hz).

Further elution with petroleum ether-diethyl ether in ratio 6 : 1 afforded 1.0 g (33.2 %) mixture of **3a** and **5** (cca 3 :1 by NMR), from which by several chromatographies pure **3a** and **5** were obtained.

Methyl *exo*-benzo[*c*]tricyclo[4.2.1.$0^{2.5}$]nona-3.7-dien-9-yl-β-acrylate (**5**), m.p. 79°.

Mass spectrum (*m*/*e*) : 252 (M^+, $C_{17}H_{16}O_2$, 5.2 %), 193 (14 %), 178 (9.3 %), 165 (13 %), 130 (10.8 %), 129 (100 %), 128 (47.8 %), 116 (18.8 %), 115 (12.8 %).

IR spectrum (CCl_4, cm^{-1}) : $\nu_{C=O}$ 1725.

^{1}H-NMR spectrum ($CDCl_3$, δ, ppm) : 2.13 (d, 1H, H-9-*anti*, $J_{9,\beta} = 7.5$ Hz), 2.77 (m, 2H, H-1, H-6), 3.23 (s, 2H, H-2, H-5), 3.63 (s, 3H, $COOCH_3$), 5.62 (dd, 1H, H-α acrylate, $J_{\alpha,9} = 1.5$ Hz), 6.15 (t, 2H, H-7, H-8, $J_{6,7} = J_{1,8} = 1.5$ Hz), 7.00 (dd, 1H, H-β acrylate, $J_{\alpha,\beta} = 17$ Hz, $J_{9,\beta} = 7.5$ Hz), 7.18 (m, 4 aromatic H).

8-Carbomethoxy-*endo*, *exo*-benzo[*c*]tetracyclo [$4.4.1.0^{2.5}0^{7.10}$] undeca-3.8-diene (**3a**), colourless oil.

Mass spectrum (*m/e*) : 252 (M^+, $C_{17}H_{16}O_2$, 8.3 %), 193 (38.5 %), 178 (38.5 %), 165 (25.7 %), 141 (17.1 %), 129 (100 %), 124 (49.2 %), 115 (22.4 %), 102 (25.7 %).

IR spectrum (CCl_4, cm^{-1}) : $\nu_{c=O}$ 1726.

^{1}H-NMR spectrum ($CDCl_3$, δ, ppm) : 1.54 (AB system, 1H, H-11-*anti*, J_{AB} = 12 Hz), 1.92 (AB system, 1H, H-11-*syn*, J_{AB} = 12 Hz), 2.20 (m, 1H, H-1), 2.26 (d, 1H, H-10, J = = 3 Hz), 2.38 (m, 1H, H-6), 2.53 (d, 1H, H-7, J = 3 Hz), 3.50 (m, 2H, H-2, H-5), 3.55 (s, 3H, $COOCH_3$), 6.33 (s, 1H, H-9), 7.00 (m, 4 aromatic H).

Reaction of *exo*-benzocyclobutenonorbornene (2) with methyl propiolate

Working as above, from 0.7 g (5.25 mmoles) anhydrous aluminium chloride, 1.0 g (12 mmoles) methyl propiolate and 2.30 g (13.6 mmoles) *exo*-alkene **2**, in 20 ml dichloromethane, 2.1 g crude product were obtained, which were separated into components by column chromatography on neutral alumina (activity II).

Using as eluent petroleum ether, 0.7 g (33 %) unreacted alkene **2** were obtained in the first fraction and 0.5 g (23.8 %) chloro-derivative **6** in the second.

With a mixture of petroleum ether-diethyl ether 6 : 1, as eluent, 0.4 g (19.0 %) ester **4a** were obtained.

8-Carbomethoxy-*exo*, *exo*-benzo[*c*]tetracyclo[$4.4.1.0^{2.5}.0^{7.10}$] undeca-3.8-diene (**4a**), m.p. 107°.

Mass spectrum (*m/e*) : 252 (M^+, $C_{17}H_{16}O_2$, 10.2 %), 193 (30.0 %), 178 (30.2 %), 165 (19.5 %) 141 (16.5 %), 129 (100 %), 124 (53.9 %), 115 (23.0 %).

IR spectrum (CCl_4, cm^{-1}) : $\nu_{C=O}$ 1730.

^{1}H-NMR spectrum ($CDCl_3$, δ, ppm) : 0.87 (AB system, 1H, H-11-*anti*, J_{AB} = 12 Hz), 1.26 (AB system, 1H, H-11-*syn*, J_{AB} = 12 Hz), 2.12 (m, 1H, H-1), 2.32 (m, 1H, H-6), 2.53 (d, 1H, H-10, *J* = 3 Hz), 2.83 (*d*, 1H, H-7, *J* = 3 Hz), 3.17 (s, 2H, H-2 H-5), 3.70 (s, 3H, $COOCH_3$), 6.65 (s, 1H, H-9), 7.10 (m, 4 aromatic H).

REFERENCES

[1] Part LIV in the series "Investigations in the Cyclobutane Series". For part LIII see : I. G. Dinulescu, A. Ghenciulescu, L. Enescu, E. Olteanu and M. Avram, *Bul. Inst. Politehnic București, Ser. Chim. — Metalurgie*, **43**, (4), 92 (1981).

[2] L. Enescu, H. L. Prasad, N. Ștefan, I. G. Dinulescu, A. Ghenciulescu and M. Avram, *Rev. Roumaine Chim.*, **25**, 535 (1980).

[3] a) M. Avram, I. Pogany, F. Badea, I. G. Dinulescu and C. D. Nenitzescu, *Tetrahedron Letters*, **1969**, 3851.

b) M. Avram, I. Pogany, I. G. Dinulescu, F. Chiraleu and C. D. Nenitzescu, *Rev. Roumaine Chim.*, **15**, 1207 (1970).

c) I. G. Dinulescu, H. L. Prasad, L. Enescu, A. Ghenciulescu and M. Avram, *Rev. Roumaine Chim.*, **24**, 833 (1979).

d) L. Enescu, H. L. Prasad, I. G. Dinulescu, A. Ghenciulescu, F. Chiraleu and M. Avram, *Rev. Roumaine Chim.*, **24**, 999 (1979).

e) A. Ghenciulescu, I. G. Dinulescu, H. L. Prasad, L. Enescu and M. Avram, *Rev. Roumaine Chim.*, **24**, 1159 (1979).

[4] L. Enescu, F. Chiraleu and M. Avram, *Rev. Roumaine Chim.*, **20**, 957 (1975).

[5] L. Enescu and M. Avram, *Rev. Roumaine Chim.*, **22**, 1061 (1977).

[6] M. D. Gheorghiu, C. Drăghici and L. Pârvulescu, *Tetrahedron*, **33**, 3295 (1977).

[7] L. Pârvulescu and M. D. Gheorghiu, *Rev. Roumaine Chim.*, **22**, 1089 (1977).

[8] a) A. Ghenciulescu, L. Enescu, H. L. Prasad, F. Chiraleu, I. G. Dinulescu and M. Avram, *Rev. Roumaine Chim.*, **23**, 1441 (1978).

b) I. G. Dinulescu, L. Enescu, A. Ghenciulescu and M. Avram, *J. Chem. Research (s)*, **1978**, 456.

[9] a) B. B. Snider, D. J. Rodini, R. S. E. Conn and S. Sealfox, J. *Amer. Chem. Soc.*, **101,** 5283 (1979).

b) R. D. Clark and K. G. Untch, J. *Org. Chem.*, **44,** 248 (1979).

c) H. Fienemann and H. M. R. Hoffmann, J. *Org. Chem.*, **44,** 2802 (1979).

d) B. B. Snider, D. M. Rausch, D. J. Rodini, D. Gonzales and D. Spindell, J. *Org. Chem.*, **45,** 2773 (1980).

e) D. M. Reinhold, J. Geevers, W. P. Trompenars, S. Harkema and G. J. van Hummel, *J. Org. Chem.*, **46,** 424 (1981).

[10] R. B. Woodward and R. Hoffmann, "The Conservation of Orbital Symmetry", Verlag Chemie, Weinheim, 1970.

[11] M. Avram, F. Chiraleu and I. Pogany, *Rev. Roumaine Chim.*, **15,** 1219 (1970).

[12] J. Marshall and S. R. Walter, J. *Amer. Chem Soc.*, **90,** 6358 (1974).

Revue Roumaine de Chimie, 28, *11–12*, 1009–1017 (1983)

ION EXCHANGE SELECTIVITY OF NATURAL AND SYNTHETIC ZEOLITES AGAINST AMMONIUM

N. BÎLBĂ, GH. MIHĂILĂ, P. ONU, D. DRANGA and C. LUCA

Department of General and Technological Chemistry, Polytechnic Institute, Splai Bahlui, 71, Iaşi, Romania

Received July 21, 1982

Ion exchange in the $NH_4^+ - NaA$ zeolite, $NH_4^+ - NaX$ zeolite and NH_4^+-clinoptilolite system has been studied. Affinity and selectivity of studied zeolites against NH_4^+ ions are different. The separation factor $\alpha_{Na^+}^{NH_4^+}$ is greater than unit for clinoptilolite, less than unit for NaA zeolite and, for NaX zeolite, up to 60 % ion exchange degree, is greater than unit and, over this value, becomes subunitary. Ion exchange equilibrium is achieved in the first 10–20 minutes without reaching the theoretical ion exchange capacity. The real ion exchange capacity of synthetic zeolites is only 50–62 % from theoretical one. The volcanic tuff with high content of clinoptilolite is selective against NH_4^+ ion, but in natural state its ion exchange capacity is only 0.4 mequiv./g. Its ion exchange treatment with 10 % solution of NaCl leads to an appreciable ion exchange capacity from 0.4 to 1.2 mequiv./g. The volcanic tuff activated on this way can retain about 95 % NH_4^+ ions from solution.

INTRODUCTION

The ammonium ion is one of the main inorganic pollutants of the surface waters having unfavourable consequences over the aquatic environment. For natural waters, ammonia exerts a stress in several ways. Among these ways we can mention its contribution to blue green algae growth causing eutrophication, toxicity for aquatic life, inhibiting the water and food intake for both mammals and plants, reducing the amount of dissolved oxygen in waters due to nitrification process and corrosion of certain metals of construction.[1–3]

The ammonium salts frequently occurred in waste waters dissociate and hydrolyse differently, so that, besides the NH_4^+ ion free NH_3 occurs also and its toxic action is much stronger.

Removal of the ammonium ions from waste waters is carried out by acid-base chemical methods[4–6] or by ion exchange retention using especially natural or synthetic crystalline aluminosilicates.[7–18]

This paper deals with the results achieved in the investigations of the retention of the ammonium ions on volcanic tuffs with high content of clinoptilolite as well as on NaA and NaX synthetic zeolites.

EXPERIMENTAL

Experiments were carried out on the samples of zeolite volcanic tuffs with 60—62 % clinoptilolite mined from Mirşid deposit (Romania)[19] and on NaA and NaX synthetic zeolites obtained by hydrothermal way. Some data proper to these samples are summarized in Table 1.

Table 1

Chemical composition and some properties of the samples

Sample	Chemical composition, %								BET specific surface area, m^2/g	Ion exchange capacity, mequiv/g hydrated
	SiO_2	Al_2O_3	Na_2O	K_2O	CaO	MgO	Fe_2O_3	H_2O 500°		
Volcanic tuff with clinoptilolite	68.54	11.95	0.40	2.80	3.35	0.70	0.86	11.40	46.80	0.4—1.70
Clinoptilolite[20]	65.20	13.20	1.10	8.60	0.10	—	—	11.80	—	2.20
Clinoptilolite[21]	69.10	12.26	2.70	2.11	1.21	0.36	0.56	11.38	—	1.6—1.75
NaA zeolite	32.70	28.50	16.40	—	—	—	—	22.40	640	5.30
NaX zeolite	35.00	23.50	14.50	—	—	—	—	27.00	820	4.70

The samples of natural tuff with granule size of 0.5—1.0 mm were activated thermically in air, for three hours at 500°C, by ion exchange with 10 % solution of NaCl or $CaCl_2$ three times for 24 hours and by acid treatment with 2 % solution of HCl for two hours at 80°C.

The NaA and NaX zeolites, before utilization, were treated with 0.1 N solution of NaCl followed by washing with deionized water until a pH= 10.5—11.0.

The ion exchange isotherms were carried out at 20°C with 0.05 N solution of NH_4Cl for six hours, time enough for equilibrium achievement. Kinetics of the $Na^+ \rightleftarrows NH_4^+$ ion exchange was studied at 20° and 60°C with a ratio liquid to solid equal to 2, 4 and 6 in the case of volcanic tuff and 30 in the case of the NaA and NaX zeolites, using 0.2 mequiv. NH_4^+/ml solution of NH_4Cl. Content of NH_4^+ ions was determined by using the method with formaldehyde and content of Na^+ ions in solution was determined flamphotometrically.

RESULTS AND DISCUSSION

Ion exchange property of zeolites is controlled by the excedentary negative charge of aluminosilicate framework, whose compensation needs cations. Theoretical ion exchange capacity of zeolites to be studied is situated in the order :

$$\text{NaA} > \text{NaX} > \text{clinoptilolite}$$

ant their molar ratios, SiO_2/Al_2O_3, are 1.95, 2.53 and 8.4, respectively. Practical ion exchange capacity of zeolites is controlled by steric factors which take into account the size of exchanging cations and the site that must be occupied in the framework.

The $Na^+ \rightleftarrows NH_4^+$ ion exchange may be represented by the equation :

$$Na^+_{(z)} + NH^+_{4(s)} \rightleftarrows NH^+_{4(z)} + Na^+_{(s)} \qquad (1)$$

Zeolite affinity against Na^+ or NH_4^+ is expressed by the value of the separation factor $\alpha_{Na^+}^{NH_4^+}$, defined by the ratio:

$$\alpha_{Na^+}^{NH_4^+} = \frac{X_{NH^+_{4(z)}} \cdot X_{Na^+_{(s)}}}{X_{Na^+_{(z)}} \cdot X_{NH^+_{4(s)}}} \tag{2}$$

where, X is equivalent fraction of the cation in zeolite (z) or in solution (s).

Since both ions are monovalent ones, the separation factor is identical to the rational coefficient of selectivity $K_{Na^+}^{NH_4^+}$. Taking into account the ion activity coefficient under steady state of the two ions in solution, $\gamma_{Na^+_{(s)}}$ and $\gamma_{NH^+_{4(s)}}$, we can define the rational corrected selectivity coefficient $K_{Na^+}^{\prime NH_4^+}$ as follows:

$$K_{Na^+}^{\prime NH_4^+} = \alpha_{Na^+}^{NH_4^+} \frac{\gamma_{Na^+_{(s)}}}{\gamma_{NH^+_{4(s)}}} \tag{3}$$

Because ion exchange takes place in dilute solutions, $\gamma_{Na^+_{(s)}}$ may be considered equal to $\gamma_{NH^+_{(4s)}}$ and therefore [22]

$$K_{Na^+}^{\prime NH_4^+} \equiv K_{Na^+}^{NH_4^+} \equiv \alpha_{Na^+}^{NH_4^+} \tag{4}$$

The thermodynamic equilibrium constant K_a, of exchange reaction, expressed by Gaines and Thomas' equation [23,24]

$$\ln K_a = \int_0^1 \ln K_{Na^+}^{\prime NH_4^+} \cdot dX_{NH^+_{4(z)}} \tag{5}$$

can be calculated from the plot $\ln K_{Na^+}^{\prime NH_4^+}$ against $X_{NH^+_{4(z)}}$.

The plots $X_{NH^+_{4(z)}}$ *vs* $X_{NH^+_{4(s)}}$ and $\ln K_{Na^+}^{\prime NH_4^+}$ *vs.* $X_{NH^+_{4(z)}}$ give information on the affinity of zeolites against NH_4^+ ion, exchange degree at equilibrium and distribution of NH_4^+ ions in their framework.

Isotherms of the $Na^+ \rightleftarrows NH_4^+$ ion exchange for clinoptilolite,[14] NaA and NaX are represented in Figure 1 and dependence of $\log K_{Na^+}^{\prime NH_4^+}$ on concentration of NH_4^+ in zeolite, in Figure 2.

a. *Ion exchange in the NH_4^+-clinoptilolite system.* Clinoptilolite is a natural aluminosilicate in zeolite series.[25,26] Having zeolite structure, the spatial arrangement of $[SiO_4]$ and $[AlO_4]$ tetrahedrons leads to the formation of some cavities which communicate to one another and to outside through pores of about 3.5 Å in diameter. Due to the fact that $[AlO_4]$ tetrahedrons are carriers of negative charge, clinoptilolite contains mobile enough cations to be easily reversibly exchanged with other cations without crystal structure modification.

The ion exchange isotherm proper to NH_4^+-clinoptilolite system, curve 1 in Figure 1, is of type *a* according to Breck's classification,[26] fact that points out the high affinity of clinoptilolite against ammonium cation. The separation factor $\alpha_{Na^+}^{NH_4^+}$ and rational selectivity coefficient $K_{Na^+}^{NH_4^+}$ are always greater than unit : $\alpha_{Na^+}^{NH_4^+} \equiv K_{Na^+}^{NH_4^+} > 1$.

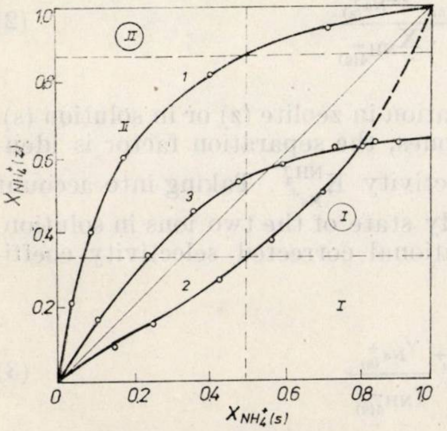

①,② and I, II, show the surface area used to calculate the separation factor, $\alpha_{Na^+}^{NH_4^+}$

Fig. 1. — The ion exchange isotherms for the NH_4^+-zeolite system : 1 — NH_4^+-clinoptilolite at 60°C, for 6 hours at 0.018 total normality ; 2 — NH_4^+ — NaA at 25°C, for 6 hours at 0.05 total normality ; 3 — NH_4^+ — NaX at 25°C, for 6 hours at 0.05 total normality.

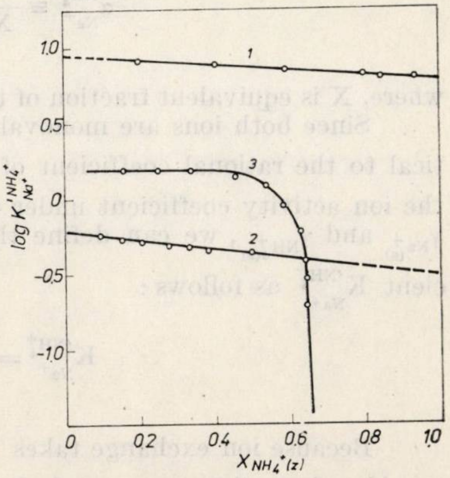

Fig. 2. — Dependence of $\log K'^{NH_4^+}_{Na^+}$ on concentration of NH_4^+ ions in zeolite, at equilibrium. 1 — NH_4^+ — clinoptilolite ; 2 — NH_4^+ — NaA ; 3 — NH_4^+ — NaX.

Plot of $\log K'^{NH_4^+}_{Na^+}$ against concentration of $NH_{4(z)}^+$ ions for the NH_4^+-clinoptilolite system, curve 1, Figure 2, corresponds to a linear correlation controlled by the constant ratio $d\log K'^{NH_4^+}_{Na^+}/dNH_{4(z)}^+$. In this case, the thermodynamic equilibrium constant K_a, can be considered equal to rational corrected selectivity coefficient $K'^{NH_4^+}_{Na^+}$ at the concentration of ammonium ions in zeolite equal to 0.5, for which $K_a = 7.41$.

Shape of the ion exchange isotherm shows a strong interaction between NH_4^+ ions and inner surface of clinoptilolite. The relatively great difference between their ion radii, $r_{Na^+} = 0.98$ Å and $r_{NH_4^+} = 1.4$ Å, allows the preferential exchange of NH_4^+ ion on clinoptilolite. The same selectivity is also in the case of Ca^{2+} and Mg^{2+} ions but it is annuled by K^+ ion ($r_{K^+} = 1.33$ Å).

The zeolite volcanic tuff, mined from Mîrşid deposit (Romania) contains about 60 % clinoptilolite with Ca^{2+}, K^+ and Na^+ and exhibits an ion exchange capacity of about 0.4 mequiv./g at 25°C, after six hours

Ion exchange capacity of natural clinoptilolite and its exchange kinetics depends on purity and can be modified by previous chemical and thermal treatment.

Kinetical curves proper to ion exchange of NH_4^+ on different samples of clinoptilolite volcanic tuff are represented in Figure 3.

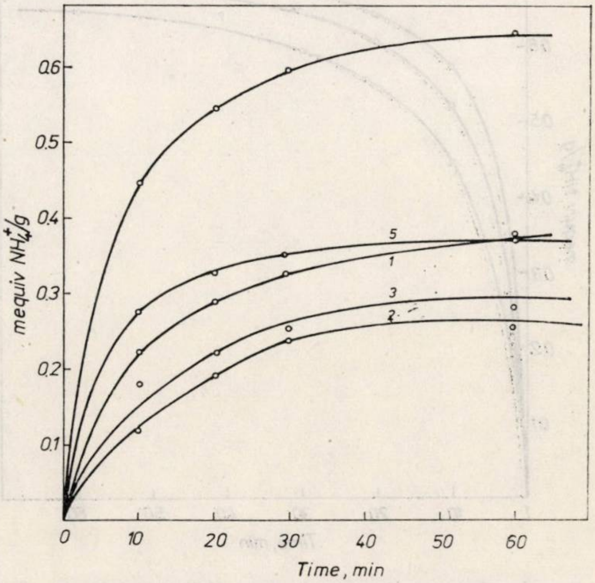

Fig. 3. — Kinetical curves of cation exchange in the NH_4^+-natural and activated volcanic tuff systems at 20°C and a liquid to solid ratio equal to 6 : 1 — natural; 2 — activated thermically at 500°C; 3 — treated with 2% solution of HCl at 80°C; 4 — ion exchanged with 10% solution of NaCl; 5 — ion exchanged with 10% solution of $CaCl_2$.

As it comes out from Figure 3, ion exchange capacity against ammonium ion increases for the samples of zeolite tuff which were previously exchanged with Na^+ ions (Curve 4) whereas those activated thermically and by acid treatment decreases (Curves 2 and 3). The volcanic tuff with Na^+-clinoptilolite exhibits affinity and selectivity against NH_4^+ ion found in solution.

By repeated ion exchange we got samples whose ion exchange capacity becomes as high as 1.2 mequiv./g.

Ion exchange with Ca^{2+} ions takes place at a low rate, so that the tuff sample exhibits a kinetics almost identical to that of natural one (Curve 5).

The acid treatment with hydrochloric acid solution of different concentrations and time, leads to a partial dealuminization of the framework and also a removal of Na^+, K^+, Ca^{2+} and Mg^{2+} ions found especially in channels of zeolite. Consequently, a modification of pore size and pore distribution as well as an increasing of specific surface area [27] and a diminishing of ion exchange capacity against ammonium ions take place.

Thermal activation of the samples at 500°C determines a diminishing of the ion exchange capacity parallel to an increasing of selectivity against ammonium ions found in mixture.

Shape of the kinetical curves shows that ion exchange is accomplished progressively by counter-current diffusion of ions from zeolite and of ammonium ions found in water.

The favourable influence of temperature over ion exchange kinetics on modified volcanic tuff in Na^+ form is represented in Figure 4.

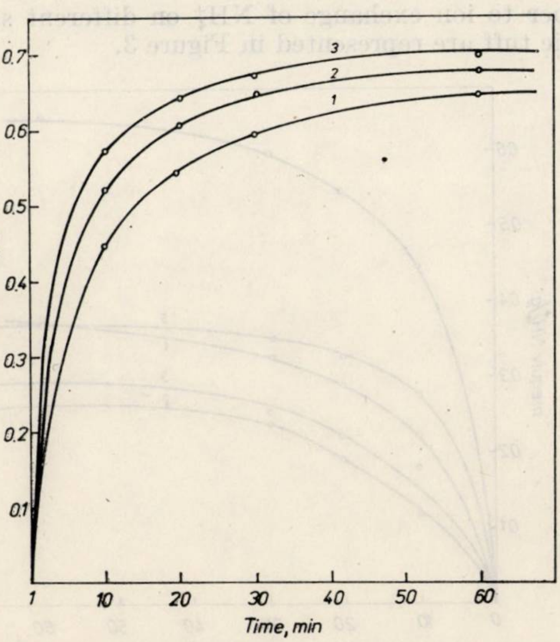

Fig. 4. — Temperature influence over kinetics of the $Na^+ \rightleftarrows NH_4^+$ ion exchange : 1—20°C ; 2—40°C ; 3—60°C.

b. *Ion exchange in the NH_4^+ — NaA zeolite system.* The NaA zeolite is a synthetic crystalline aluminosilicate with threedimensional cubic structure of $[SiO_4]$ and $[AlO_4]$ tetrahedrons containing sodalite cages (β) connected by cubs which generate new cavities, called α, by cuboctaetric type.[28–30] This spatial arrangement determines the porous structure of NaA zeolite in which, under usual conditions, there are found Na^+ cations and zeolite water. Although, all these cations are mobile, their replacing with other ions depends strongly on size and electrical charge of them.

The ion exchange isotherm, proper to the $NH_{4(s)}^+ - Na_{(z)}^+A$ system, curve 2 in Figure 1, is of the type *c* according to Breck's classification what points out a greater affinity of zeolite against Na^+ cation which leaves zeolite, than against NH_4^+ ion. In this case, the separation factor and rational selectivity coefficient are always less than unit :

$$\alpha_{Na^+}^{NH_4^+} \equiv K_{Na^+}^{NH_4^+} < 1$$

The plot, $\log K'^{NH_4^+}_{Na^+}$ *vs.* $NH_{4(z)}^+$, in the case of NaA zeolite, curve 2 in Figure 2, corresponds also to a linear correlation determined by the constant ratio $d\log K'^{NH_4^+}_{Na^+}/dNH_{4(z)}^+$.

Shape of the ion exchange isotherm shows the fact that NaA zeolite is not selective against ammonium ion. The easiest exchangeable Na^+

ions are those located near the four oxygen atoms rings and those found in the center of six oxygen atoms rings which in elementary cell represent about 75%. The Na^+ cations found inside the cavities β cannot participate rapidly to exchange due to NH_4^+ ions with radius equal to 1.4 Å which cannot penetrate through six oxygen atoms rings with the free diameter equal to 2.2 – 2.4 Å. Kinetics of NH_4^+ ion exchange on NaA zeolite is represented in Figure 5, curve 1.

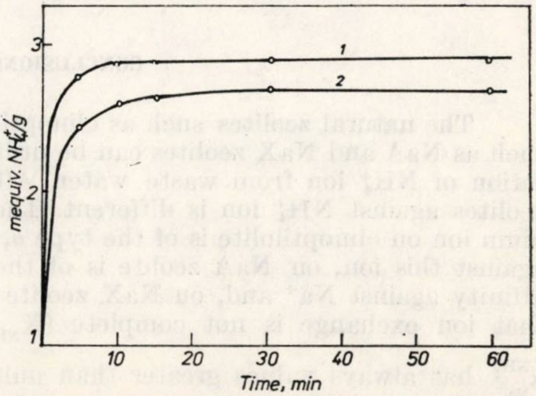

Fig. 5. — Kinetical curves of the $NH_4^+ \leftrightarrows Na^+$ ion exchange on NaA and NaX zeolites at 20°C and a ratio liquid to solid equal to 30 : 1 — 1 — NaA ; 2 – NaX.

It can be seen that ion exchange equilibrium is achieved in the first 10 – 20 minutes and theoretical ion exchange capacity is not realized. The real ion exchange capacity is about 50% from the theoretical one due to low affinity of zeolite against NH_4^+ ion, relatively large size of this ion hydrated with eight water molecules [31], [32] and relatively small size of entrance pores of zeolite cavities.

c. *Ion exchange in the* NH_4^+ *— NaX zeolite system.* The NaX zeolite is a synthetic crystalline aluminosilicate with threedimensional cubic structure of $[SiO_4]$ and $[AlO_4]$ tetrahedrons made up of sodalite cages (β) connected by hexagonal prisms similar to diamond framework, which forms new cavities called supercavities or faujazite cavities. [29,33,34] This spatial arrangement confers to NaX zeolite porous structure, in which, under usual conditions, Na^+ cations and zeolite water are found.

The ion exchange isotherm, characteristic of the $NH^+_{4(s)} - Na^+_{(z)}X^-$ system , curve 3 in Figure 1, is of type *d* according to Breck's classification what shows that ion exchange is not complet, although NaX zeolite exhibited initially a good affinity against NH_4^+ ion. The ion exchange degree realized corresponds to 62%, what indicates that the exchange takes place particularly in supercavities. The NaX zeolite manifests an ion-sieve effect against large cations. The obtained results are in good agreement with those reported by Theng et al. [24] and Tsitsishvili et al. [35] for NH_4^+ ion.

The plot, $\log K'^{NH_4^+}_{Na^+}$ *vs.* $NH^+_{4(z)}$, in the case of NaX zeolite, curve 3 in Figure 2, points out for the ratio $d\log K'^{NH_4^+}_{Na^+}/dNH^+_{4(z)}$ different values and the curve presents a maximum for an ion exchange degree of about

52 %, corresponding to the rapid replacement of unlocated cations in supercavities.

Kinetics of NH_4^+ exchange on NaX, curve 2 in Figure 5, shows that the process takes place rapidly in the first 10–20 minutes and does not correspond to maximum ion exchange capacity.

CONCLUSIONS

The natural zeolites such as clinoptilolite as well as synthetical ones such as NaA and NaX zeolites can be utilized as ion exchangers for separation of NH_4^+ ion from waste water. Affinity and selectivity of studied zeolites against NH_4^+ ion is different. The exchange isotherms of ammonium ion on clinoptilolite is of the type *a*, what points out a good affinity against this ion, on NaA zeolite is of the type *c*, what shows a greater affinity against Na^+ and, on NaX zeolite is of the type *d*, what indicates that ion exchange is not complete ($X_{NH_4^+} < 1$). The separation factor $\alpha_{Na^+}^{NH_4^+}$ has always values greater than unit for clinoptilolite and less than unit for NaA and, for NaX zeolite its value depends on ion exchange degree. Thus, up to 62 % it is greater than unit and for ion exchange degree larger than 62 % it becomes subunitary.

The ion exchange equilibrium is reached during the first 10–20 minutes without theoretical ion exchange capacity to be realized. Therefore, the real ion exchange capacity of NaA zeolite is only about 50 % and that of NaX zeolite is about 62 % from that theoretical one. This fact is in good agreement with the existence of certain sites specific to Na^+ cations which are havily or not at all left, with ion-sieve effect exhibited especially by NaX against large volume cations and with the existence of hydrated cations. The volcanic tuff with high content of clinoptilolite is selective against NH_4^+ ion but in natural state its ion exchange capacity is low. Its treatment by ion exchange particularly with NaCl solution leads to a significant increase of ion exchange capacity from 0.4 to 1.2 mequiv./g. The acid treatment with mineral acids as well as thermic treatment did not improve its ion exchange capacity. By using the clinoptilolite volcanic tuff, the maximum retention degree of NH_4^+ can be about 95 %. The NH_4^+ zeolite can be regenerated with alkaline solution of NaCl or by means of nitrification bacteria which transform ammonium ion in nitric ion.

REFERENCES

[1] O. Y. Ataman and H. B. Mark Jr., *Analyt. Chem.* **49**, 1331 (1977).

[2] G. E. Fogg, W. D. P. Stewart, P. Fay and A. E. Walsby, "The Blue Green Algae", Academic Press, New York, 1973.

[3] P. C. Simson and D. A. Booth, *Physiol. Behav.*, **11**, 329 (1973).

[4] G. Choulat, Pat. Ger. 2, 055, 563 (1972); *Chem. Abstr.*, **77**, 51073 (1972).

[5] T. D. Waite, *J. Environ. Eng. Div. (Am. Soc. Civ. Eng.)*, **105**, (EE 6), 1023 (1979).

[6] Nittetsu Kakoki Co., Ltd., Pat. Jap. 145, 599 (1980); *Chem. Abstr.*, **95**, 12281 (1981).

[7] L. L. Ames, "Proceedings of the 13th Pacific Nortwest Industrial Waste Conference", Washington State Univ., Pullman, 1967, p. 133.

[8] B. W. Mercer, *Water Pollution Control Federation Journal*, **42**, R. 95 (1970).

[9] J. D. Sherman, Ion Exch. Pollut. Control, **2**, 227 (1979) ; *Chem. Abstr.*, **92**, 81656 (1980).

[10] H. Minato, Koatsugasu, 5, 536 (1968) ; *Molec. Sieves Zeolites, Adv. Chem. Ser.*, **101**, *Am. Chem. Soc., Washington*, 311 (1971).

[11] F. A. Mumpton, *Industrial Minerals and Rocks*, **4**, 1262 (1975).

[12] D. W. Breck, Pat. U.S.A. 3, 723, 308 (1973) ; *Chem. Abstr.*, **79**, 45492 (1973).

[13] M. J. Semens, *Environ. Sci. Tech.*, **11**, 255 (1977).

[14] R. M. Barrer, R. Papadopoulos and L. V. C. Rees, *J. Inorg. Nuclear Chem.*, **29**, 2047 (1967).

[15] L. B. Sand and F. A. Mumpton, "Natural Zeolites : Occurrence, Properties, Use", Pergamon Press, New York, 1978, p. 3–27.

[16] J. R. Klieve and M. J. Semens, *Water Res.*, **14**, 161 (1980).

[17] Hitachi Plant Eng. and Construction Co, Ltd, Pat. Jap. 159, 893 (1980) ; *Chem. Abstr.*, **94**, 144913 (1981).

[18] M. Kohei, K. Akinori and K. Hiroo, Sumitomo Jukikai Giho, 28(83) 79, (1980) ; *Chem. Abstr.*, **94**, 162082 (1981).

[19] I. Fodor, P. Piso, A. Bărbat, M. Bengeanu, S. Felvinczi, S. Ciceu and A. Todan, "Symp. New Mining and Dressing Technologies of Non-metallics", Cluj-Napoca, Paper 3.1 (1979).

[20] D. B. Hawkins, R. A. Sheppard and A. J. Gude, "International Conference Zeolite — 76", Tucson, Arizona, June 1976, Pergamon Press, 1978.

[21] N. Hidetsugu, M. Ikuroo, H. Yasutake and O. Hideyo, Kyushu Kogyo Daigaku Kenkyu Hokoku, Kogaku, 40, 145 (1980) ; *Chem. Abstr.* **94**, 160109 (1981).

[22] R. M. Barrer and D. C. Sammon, J. *Chcm. Soc.*, **1955**, 2838.

[23] G. L. Gaines and H. C. Thomas, *J. Chem. Phys.*, **21**, 714 (1953).

[24] B. K. Theng, E. Vansant and J. B. Uytterhoeven, *Trans. Faraday Soc.*, **64**, 3370 (1968).

[25] M. M. Dubinin, N. S. Lojkova and B. A. Onusaitis, "Clinoptilolite", Tbilisi, 1974, p. 5.

[26] D. W. Breck, "Zeolite Molecular Sieves. Structure, Chemistry and Use", Willey, N.Y., 1974, p. 50, 129, 139.

[27] V. Ababi, N. Bîlbă, P. Onu, Gh. Mihăilă, N. Naum and C. Luca, *Bulet. Inst. Polit. Iaşi*, **26**, fasc. 3–4, Secţ. II, 51 (1980).

[28] D. W. Breck, W. G. Eversole, R. M. Milton, T. B. Reed and T. L. Thomas, *J. Amer.Chem. Soc.*, **78**, 5963 (1956).

[29] L. Broussard and D. P. Shoemaker, *J. Amer. Chem. Soc.*, **82**, 1041 (1960).

[30] R. Y. Yanagida, A. A. Amaro and K. Seff, *J. Phys. Chem.*, **77**, 805 (1973).

[31] A. Musinu, G. Paschina and G. Piccaluga, *Chimica e Industria*, **63**, 274 (1981).

[32] R. Caminiti, G. Licheri, G. Piccaluga and G. Pinna, *J. Chem. Phys.*, **68**, 1967 (1978).

[33] D. W. Breck, W. G. Eversole and R. M. Milton, *J. Amer. Chem. Soc.*, **78**, 2338 (1956).

[34] J. V. Smith, *Adv. Chem. Ser.*, **101**, 171 (1971).

[35] G. V.Tsitsishvili, A. Yu. Krupennikova and N. M. Dolaberidze, *Zhur. fiz. Khim.*, **48**, 403 (1974).

Revue Roumaine de Chimie, **28**, *11–12*, 1019–1021 (1983)

COMPTES RENDUS

A. GANDINI and H. CHERADAME, *Cationic polymerisation* (Initiation processes with alkenyl monomers), Advances in Polymer Science, 34/35, Springer-Verlag, Berlin, Heidelberg, New York, 1980.

Cationic polymerisation is, beyond any doubt, the most complex and controversial of all polyadditions. The difficulties specific to this field arise, on the one hand from its kinetic complexity (particularly in the initiation step) and, on the other hand from the high purity of reactants required in experiments. An example (taken from the present review), shows the crucial importance of high purity (for catalysts, monomers, solvents etc.) in order to obtain reliable results, with kinetic or mechanistic significance. As it is known, N-vinylcarbazole has such a tendency towards cationic polymerization, that it can be polymerized by almost any acidic initiator, however weak. In a study now considered as classical, on the polymerization of N-vinylcarbazole by p-chloranil, it was shown that an acidic impurity in the catalyst was in fact responsible for the polymerization, p-chloranil itself being almost inactive as initiator. A concentration as low as 4.10^{-6} mol/l of impurity, gave a polymerization rate much higher than that obtained with $2 \cdot 10^{-2}$ mol/l of carefully purified chloranil, under the same conditions. Equally, serious results can be obtained only starting from the so-called "dry conditions" (less than 10^{-6} mol/l residual water); obviously, the only suitable techniques for this kind of research are high-vacuum techniques.

Perhaps, the best schools dealing with cationic polymerization have earned their reputation mainly due to their high experimental standards. Today, names such as those of P. H. Plesch, J. P. Kennedy, G. A. Olah, D. C. Pepper, T. Saegusa, P. Sigwalt, S. Tazuke, A. Ledwith or S. Okamura are equivalent with the fundamentals of cationic polymerization. Since the early forties, when the first papers related to cationic polymerization have appeared, the great majority of the above-quoted scientists have published (among other papers) reviews on this topic, in order to gather all the experimental evidence to substantiate a sound theory concerning all the aspects of cationic polymerization. Thus, the first book devoted to cationic polymerization appeared in 1953 and is due to P. H. Plesch. So why a new one?

There are several reasons to sustain that this review is quite different from others covering the same problem. The first is the special emphasis put onto initiation, very likely the most controversial point in the field. Second, the experimental results obtained in cationic polymerization are corroborated with relevant aspects from various collateral disciplines, and third, in the last five years a rich experimental material as well as new theoretical points of view have been published.

After describing the purpose of the review in the introductory chapter, the authors present, in the second chapter, the fundamentals of the process. As this work is intended for readers having a certain expertise in the field of polymer syntheses, the authors consider that the experimental techniques as well as the elementary thermodynamic, kinetic and mechanistical aspects are well known. On this basis, the fundamentals presented refer to monomers, catalysts and solvents used, to the role played by temperature and residual impurities. Essential knowledge concerning carbocations (classification, preparation, characterization, thermodynamic stability, reactivity), anions, covalent species, equilibria among active species, cation-radicals are given as well. The experimental technique is presented concisely, underlying the merits or disadvantages of each method.

Chapters III, IV and V are devoted to the initiation by Brönsted acids or iodine by Lewis acids and by carbenium salts and related species respectively. In this part of the review, one should notice the important contribution of the authors in ordering an exceedingly rich experimental material (at the end of the volume, there are around 1000 references, thought as relevant).

The facts are presented in a critical manner, the authors being often sceptical towards some results presented in literature. The importance of cocatalysts is stressed (chapter IV), but alternative mechanisms are presented as well. Several other related reactions are discussed in order to assist the reader in understanding cationic polymerization; among many other examples one notices iodine or acids additions to olefins or Friedel-Crafts reactions.

The following chapters (VI–X) deal with initiation by radiolysis, photochemical ionisation, electrochemical initiation, initiation from a charge-transfer complex or from a polymer (block or graft copolymers are formed). Miscellaneous initiators (perchlorates, chlorides, Grignard reagents, arsenic and phosphorus compounds) are placed in chapter XI. The authors have added a suplementary chapter containing notes in proof, regarding papers published in 1979–80. These new results are presented orderly, according to the scheme used in the previous chapters. A subject index allows the easy finding of a certain topic.

The present work represents a real example of critical inventory of the literature, being a valuable tool for those involved in polymer syntheses.

D. S. Vasilescu

"Solution Behaviour of Surfactants. Theoretical and Applied Aspects", K. L. Mittal and E. J. Fendler, eds., Plenum Press, New York, 1982.

This recent issue published shortly after other two books of similar topic [1, 2], shows the rapid development of colloid chemistry research.

The two volumes of "Solution Behaviour of Surfactants" comprise the proceedings of the symposium with the same title, the third in a series that has been held every two years in USA. The contributions mirror the development of the science of colloids and the increasing diversity of theoretical and practical problems that confront the science of surface-active substance today.

The book comprises 84 contributions of 166 authors from 19 countries ; it is organized in 9 parts.

The first volume presents in parts I and II some general papers and contributions to thermodynamics and kinetics of micellization in aqueous media.

The second volume gathers in the remaining seven parts contributions dealing with : the study of micelles in aqueous media ; mixed micelles ; solubilization phenomena ; micellar catalysis and its inhibition ; reactions in micellar media ; interactions between micellar media ; microemulsions and reactions in microemulsion media ; use of surfactants in analytical chemistry and in tertiar oil recovery, the protection of the environment and other applications.

This diverse topic which extends over 1500 pages is an important source of scientific information about surfactants. The presentation is elegant and the access to the content is easy. Abstracts of discussions that followed communications are available at the end of each part.

Volume 1

The topic of the first volume is organized in two parts, which deal with various aspects of micellization. Part I specializes in the results of investigations on micellar structure and dynamics in microemulsions as well as on the behaviour of surfactant solutions under pressure ; in utilization of fluorescent markers in the study of micellization and in related subjects as : the detergent-biodegradability relationship, the environmental aspects of commercial surfactants, the adsorption of surfactants on zeolites, semiconducting photoactive bilayer membranes, the role of lipids in carcinogenesis.

Part II is devoted to thermodynamics and kinetics of micellization in aqueous media ; it covers subjects as :

— models of micelles and micellization ; the theoretical considerations are supplemented with data on frequency distribution shifts in micellar kinetics, thermodynamic models of the association of ionic surfactants in micelles and in liquid crystalline phases, the thermodynamics of sphere-to-rod transition in alkylsulfate micelles, thermodynamic properties of binary and ternary systems of water-soluble surfactants and the heat capacities of alkyldimethylamine oxides in aqueous solutions ;

— new experimental techniques for the study of micellar behaviour as e.g. : pulse radiolysis, dielectric relaxation spectroscopy, nuclear magnetic resonance, electron spin resonance, near infrared spectroscopy ;

— investigations on various interactions occurring in these systems : the micelle-micelle interaction in aqueous media from the second virial coeficient ; the interaction of cationic and anionic surfactants in the absence and presence of electrolytes ; the thermodynamics of interactions of binary salts with lipids ; the polymer-surfactant interaction, by surfactant selective electrode method ; potentiometric titration in surfactant binding phospholipid vesicles ; hydrophobic interactions of aromatic hydrocarbons induced by surfactants and polyelectrolytes ; applications of hydrophobic bonds in anesthesia and studies related to solubilization and emulsions of biliary lipids in aqueous systems.

This topic whose simple enumeration takes appreciable space is diverse and many of the problems dealt with are recent themes of colloidal chemistry.

It is worth noting the special attention awarded to problems of immediate applications as e.g. the carcinogenic effect of some chemicals, implications of commercial surfactants in health problems and those of hydrophobic bonds in anesthesia. These problems emphasize the wide range of application of surfactant studies to the medical field especially to administering of drugs and to molecular and cellular explanation of certain diseases.

One should finally emphasize the impact of colloidal physical chemistry on biochemistry ; the specific methods of colloidal chemistry apply to biochemical processes.

Volume 2

Unlike the first volume, this volume deals with more diverse problems which are related to practice. Thus, Part III (micelles in non-aqueous media) deals with the structure, solubilizing properties and catalysis by reversed micelles, the association of amphiphilic compounds in non-aqueous solvents by exclusion chromatography, the effect of inverse micelles upon esterification, photon correlation spectroscopy in the study of inverse micelles etc.

Solubilization is studied in Part IV related either to the capacity of solubilization of some micelles or to solubilization of petroleum by micelle and non-solubilization of corn oil in micellar solutions.

The reactions in micelles and micellar catalysis is the topic of Part V which includes : the influence of micelles on chemical reactivity ; the selectivity and equilibrium of some reactions as e.g. selective mercuration of dienes, redox or alkaline hydrolysis reactions ; the kinetic properties of radical ions ; spectral study of aromatic carboxylic acids in micellar environment ; the phosphorescence of stabilized micelle at room temperature ; micellar effects on the radiation chemistry of biologic compounds.

The microemulsions and the reactions in microemulsion media are grouped in Part VI whose topic includes : the dynamics of microemulsions, their features and applications in biological systems ; the chemistry of detergentless microemulsions ; photoinduced electron-transfer across water-in-oil interfaces which is another potential application of photomicellar catalysis.

The last three parts deal with the use of surfactants in analytical chemistry and other uses as e.g. in petroleum industry, building materials, agriculture, medicine, in mineral oil and adhesive industries, in wood, paper, textile and leather industries, etc.

In conclusion, the wide range of studies and applications covered in the two volumes is outstandingly comprehensive and outlines the new horizons of a permanently developing discipline — the colloid chemistry.

1. K. L. Mittal, Editor, "Micellization, Solubilization and Microemulsions", Vols. 1 2, Plenum Press, New York, 1977.
2. K. L. Mittal, Editor, "Solution Chemistry of Surfactants", Vols. 1 2, Plenum Press, New York, 1979.

Georgeta Popescu

Revue Roumaine de Chimie, 28, *11–12*, 1023–1031, (1983)

INDEX DES AUTEURS

A.

ABD ELHALIM M. S., voir SAYED G. H. 493
ABDEL-WAHAB A.-M. A., voir KOHDAIR A. I. 921
AFIFI A. A. and M. A. EL-HASHASH, S. S. EL-KADY, **Synthesis and reactions of some 2-aryl-4-arylidene-5(4)-oxazolones** 849
AGHERGHINEI I., voir BEZDADEA M. 419
ALVAREZ BARTOLOMÉ M. L., voir ARRIBAS JIMENO S. 405
AMBRONO D., voir HUBCA GH. 527
ANDRÉS GARCIA E., voir ARRIBAS JIMENO S. 405
ANGHEL D. F., voir PAK U SĂP 883
APATEANU L., voir STERNBERG S. 583
ARMEANU V. and S. VISAN, **Benzfuroinoxime — an analytical reagent for the microdetermination of uranyl** 45
ARRIBAS JIMENO S. and M. L. ALVAREZ BARTOLOMÉ, E. ANDRÉS GARCIA, **Analytical study of the precipitates obtained from the anion HgI_4^{2-} and the cations of the first analytical group (Ag^+, Pb^{2+}, Hg^{2+} and Tl^+) (in Spanish)** 387
AVRAM M., voir ENESCU L. 1001

B.

BACALOGLU R., voir HAVLIK I. 235
BACALOGLU R., voir HAVLIK I. 903
BAHADUR P. and A. GUPTA, P. LATA, **Conductance behaviour of cationic surfactants in alkanols** 217
BALABAN A. T., voir DINCULESCU A. 699
— , voir J. HERDAN, NEGOITA N. and GRECU N., **4-Substituted 2,6-di-t-butylphenols and their corresponding aroxyls possessing 4-(1-methylene-imidazolyl), 4-(1-methylene-benzimidazolyl) or 4-(1-sulfonyl-benzimidazolyl) groups** . 129
— , voir STEPAN E. 707
BALIU S., voir HERDAN J. 757
BARABAS A., voir BOTAR A. A. 741
— , voir POPOVICI N. 995
BARANWAL B. P., voir SENGUPTA S. K. 487
BARBU S., voir MICU-SEMENIUC R. 365
BEZDADEA M. and C. V. UGLEA, I. AGHERGHINEI, **Gel-permeation chromatography of poly(vinylacetate)** 401
BHATNAGAR B. B., voir VARMA R. P. 115
BILBA N., voir LUCA C. 211
— and GH. MIHAILA, P. ONU, D. DRANGA, C. LUCA, **Ion exchange selectivity of natural and synthetic zeolites against ammonium** 1009
BODEA C., voir SOLBERG S. 243
BORDEIANU R., voir CEAUŞESCU E. 299
BOTAR A. A. and A. BARABAS, I. OPREAN, J. CSONKA-HORVAI, F. HODOSAN, **Exo- and endohormones. VI. Syntheses of the sex pheromones of some Lepidoptera** 741
BRANZOI V. and S. STERNBERG, **Polarization behaviour of copper in CH_3OH + H_2SO_4 solution** 193
— , voir STERNBERG S. 583
BRISSET J. L., **Ionic products of H_2O-CH_3CN and CH_3OH-CH_3CN mixtures** 941
BRUSALIS T., voir PETRESCU S. 451
BUZDUGAN E., voir CEAUŞESCU E. 299

C.

CALU N. and N. FOCA, Complexes of transition metals with 2,2′-diaminoazobenzene. IV. The Co(II)-2,2′-diaminoazobenzene system 331
CASTRO E. A. and F. M. FERNANDEZ, An improved two parameter omega technique for molecular orbital calculations. III. Aromaticity of some semi-benzenoid and non-benzenoid hydrocarbons (in Spanish) 321
CEAUŞESCU E. and R. BORDEIANU, P. GHIOCA, I. CERCHEZ, E. BUZDUGAN, R. STANCU, Dilute block copolymer systems. II. Tensile modulus of oil-extended butadiene styrene block copolymers at large strains 299
CECAL AL., Investigation of corrosion kinetics for steel samples in acid media using a method with radioactive tracers (in German) 91
— , The use of beta-ray backscattering in the study of the corrosion kinetics of steel samples in acid media 575
CENUŞE Z., voir VÎLCU R. 891
CERCASOV C., voir CIUREANU M. 555
— , voir CIUREANU M. 875
CERCHEZ I., voir CEAUŞESCU E. 299
CHIRALEU F. voir GEORGESCU E. I. 841
— , voir DINCULESCU A. 699
— , voir GEORGESCU F. C. 267
CHIRIAC C. I., A new convenient method for synthesis of benzoxazoles by a direct condensation reaction 37
— , A new synthesis of aromatic esters by a direct condensation reaction 737
— , Ethylene chlorophosphite as a new reagent for aromatic amide synthesis by a direct condensation reaction under very mild conditions 863
— , Phenyldichlorophosphite-dimethylformamide. A new reagent for dehydrating aromatic primary amides under mild conditions 33
— , Triaryl-s-triazoles from diarylhydrazines by a new direct condensation reaction. 977
CIOCHINA A. and R. VILCU, Transient hot wire method for absolute and simultaneous measurement of thermal conductivity and thermal diffusivity of fluids . . . 795
CIUPITOIU A., voir HUBCA GH 527
CIUREANU M. and F. CORNEA, V. SAHINI, C. CERCASOV, Studies on the electronic spectra of thioacyl-piperidides and morpholides 555
— and V. E. SAHINI, M. CONTINEANU, F. CORNEA, C. CERCASOV, Internal rotation in charge transfer complexes 875
COBIANU C. and C. PAVELESCU, Deposition kinetics of silicon dioxide from silane and oxygen at low temperature 57
CONSTANTINESCU M., voir SURPATEANU GH. 831
— , voir SURPATEANU GH. 933
CONTINEANU M., voir CIUREANU M. 875
CORNEA F., voir CIUREANU M. 555
— , voir CIUREANU M. 875
— , voir ZALARU F. 811
COTARŢĂ A.. voir STERNBERG S., ... 565
CRISAN L., voir HERDAN J., ... 757
CRISTESCU C., *As*-Triazine derivatives with potential therapeutic action. XVII. Synthesis of 5-mercapto-6-azauracil-S-riboside 733
— , *As*-Triazine derivatives with potential therapeutic action. XVIII. Synthesis of 4-methylthio-5-benzylthio-6-azuridine-5′-phosphate 989
CSONKA-HORVAI J., voir BOTAR A. A. 741
CSUNDERLIK C., voir HAVLIK I. 903

D.

DABROWSKI A. and M. JARONIEC, J. K. GARBACZ, Discussion of the liquid adsorption model involving multilayer formation, surface heterogeneity and nonideality of the bulk solution 201
DANET A., voir POPESCU M.. 65
DEMETRESCU I., voir DRIMER D. 457
DEMIAN B., voir A. SALLO 119
DIMONIE M., voir HUBCA GH. 185
— , voir HUBCA GH. 527

DINCULESCU A. and M. FAHMY, F. CHIRALEAU, A. T. BALABAN, Reaction of pyrylium salts with nucleophiles. XVI. New N-substituted 2,4,6-trimethylpyridinium salts and their ^{1}H—NMR spectra 699
DINULESCU I. G., voir ENESCU L. 1001
DIUDEA M. V., Phenazathionium cations. V. Reactions of 10-(3-phenothiazinylidene)-phenothiazinium cations and their complexes with copper and iron chlorides (in German) 249
DOBOS-ROMAN G., voir MICU-SEMENIUC R. 471
DRAGAN GH., voir HUBCA GH. 527
DRANGA D., voir BILBA N. 1009
DRIMER D. and I. DEMETRESCU, Structure and properties of some carbon fibres in various conditions of utilization 457
DUMITRESCU S. and M. GRIGORAS, Researches in the field of vinyl polymers with aromatic substituents. III. Poly(9-anthryl) methylmethacrylate and its charge transfer complexes 543
DUMITRIU E. and S. OPREA, Catalysis by polymers. IV. The effect of solvent in the esterification reaction of oxiranes with α, β-unsaturated acids 535

E.

EL-ANSARY A. L., voir ISSA Y. M. 825
EL BORAI M., voir HASSAN M. A. 715
EL-DEEK M. K., voir EL-KADY M. 915
EL-DEIN M. G., voir EL-KADY M. 915
EL-HASHASH M. A., voir AFIFI A. A. 849
EL-KADY M. and M. K. EL-DEEK. R. M. SALEH M. G. EL-DEIN, Synthesis of 2′-methyl-γ-pyronyl-(5′, 6′, 6, 7)-4-acetonyl-coumarin and its reaction 915
EL-KADY S. S., voir AFIFI A. A. 849
EL-KARIM I. A. G., voir HAMED A. A. 623
EL-KASHEF H. S., voir KOHDAIR A. I. 921
EL-KHAWAGA A. M., voir KOHDAIR A. I. 921
EL-ZOHARY M. F., voir KOHDAIR A. I. 921
EL-KAFRAWY A. F., voir HASSAN M. A. 715
ENACHE M., voir M. LECA 287
ENESCU L. and M. D. GHEORGHIU, A. GHENCIULESCU, I. G. DINULESCU, M. AVRAM, Reaction of endo- and exo-benzocyclobutenonorbornenes with methyl propiolate 1001
ESSAWY A., voir HAMED A. A. 623
EXNER O., voir SALLO A. 169

F.

FADNIS A.G. and S. K. KULSHRESTHA, Kinetics of ceric ion oxidation 99
FAHMY M., voir DINCULESCU A. 699
FERNANDEZ F. M., voir E. A. CASTRO 339
FERRARI L. and M. RUIZ PASTRANA, Study of acid-base catalysis in the reaction of iodine with acetone. I. Catalysis by bases OH$^-$ and HPO$_4^{2-}$ (in Spanish) . . . 123
FLOREA S., voir RAILEANU M. 381
FOCA N., voir CALU N. 349

G.

GALASIU I., voir PETRESCU S. 451
GARBACZ J. K., voir DABROWSKI A. 201
GEORGESCU E. G., voir GEORGESCU F. C. 267
GEORGESCU E. I., voir GEORGESCU F. C. 267
— and F. GEORGESCU, F. CHIRALEU, M. PETROVANU, Dipolar derivatives in the quinazoline series. III. Quaternization of quinazoline with phenacyl bromide (in French) 841
GEORGESCU F., voir GEORGESCU E. I. 841
GEORGESCU F. C. and E. G. GEORGESCU, F. CHIRALEU, E. I. GEORGESCU, I. ZUGRAVESCU, Pyridinium-ylids. IV. Reactions of carbanion-monosubstituted 4-phenyl-pyridinium-ylids with activated olefins (in French) 267

GHELASE I., voir NEGOIU D. 225
— , voir NEGOIU D. 349
GHELASE I. and D. NEGOIU, Complex compounds of Cd(II) and Ni(II) with furfural selenosemicarbazone 463
GHENCIULESCU A., voir ENESCU L. 1001
GHEORGHIU M., voir GH. HUBCA 185
GHEORGHIU M. D., voir ENESCU L. 1001
GHERGARI L., voir MICU-SEMENIUC R. 471
GHINEA S., voir VLADESCU L. 513
GHIOCA P., voir CEAUSESCU E. 299
GIRGIS M. M. and D. P. LAZAR, E. I. SEGAL, Catalytic oxidation of ammonia. IV. Low temperature oxidation on a nickel oxide catalyst supported on alumina . . 325
— and D. P. LAZAR, E. I. SEGAL, Catalytic oxidation of ammonia. V. Low temperature oxidation on a NiO/Al$_2$O$_3$ catalyst. Influence of the amount of catalyst. Reaction products analysis 445
— and D. P. LAZĂR, E. I. SEGAL, Catalytic oxidation of ammonia. VI. Low temperature oxidation on a NiO catalyst 593
GIURDARU GH. and M. D. RUSU, N. PALIBRODA, Thermally and electron-impact induced acyl migration in N-[*ortho*-O-, -S-, -Se-Acyl-phenyl]-amides 335
GOTHARD F., voir VILCU R. 891
GRECU N., voir J. HERDAN 129
GRIGORAS M., voir S. DUMITRESCU 543
GUPTA A., voir BAHADUR P. 217
GUPTA B. K., voir SYAMAL A. 805

H.

HAIDUC I., voir MARTA L.. 957
— , voir MICU-SEMENIUC R. 605
HAMED A. A. and A. ESSAWY, A. F. SHABAN, I. A. G. EL-KARIM, Some reactions of Michael adducts of α-cyano-β,benzoyl-β-phenyl ethyl acrylate with ketones 623
HASSAN K. M., voir KOHDAIR A. I. 921
HASSAN M. A. and A. F. ELKAFRAWY, M. EL BORAI, Some reactions of 2-oxo-1,2, 3, 4,-tetrahydronicotinonitriles 715
HAVLIK I. and R. BACALOGLU, Nucleophilic substitutions in the 1,3,5-triazine. IX. Kinetics and mechanism of the reaction between 2,4-dichloro-6-phenylazophenylamino-1,3,5-triazine with 4-aminoazobenzene (in German) 235
— and C. CSUNDERLIK, A. TOTH, R. BACALOGLU, Synthesis and characterization of 4′-substituted 4-aminoazobenzenes. Determination of basicity constants (in German). 903
— , voir HAVLIK I. 375
HAVLIK I and T. SIMIONESCU, HAVLIK I., New pyrazolone complex compounds of bis-(methyl-aminoantipyryl)-ethane. 375
HERDAN J. and A. T. BALABAN, N. NEGOITA and N. GRECU, 4-Substituted 2,6-di-t-butylphenols and their corresponding aroxyls possessing 4-(1-methylene-imidazolyl), 4-(1-methylene-benzimidazolyl) or 4-(1-sulfonyl-benzimidazolyl) groups 129
— and L. CRISAN, M. LUCA, S. BALIU, New polymers with heterocyclic side groups having antioxidant properties 757
HERNANDEZ M. D. H., voir SANCHEZ BALLESTERO J. 503
HILA E., voir MICU-SEMENIUC R. 471
HINDAWEY A. M., voir ISSA Y. M. 825
HODOSAN F., voir BOTAR A. A. 741
— , voir POPOVICI N.. 995
HUBCA GH. and M. GHEORGHIU, CR. OPRESCU, M. DIMONIE, Synthesis and polymerization of polyethylene glycol dimethacrylate. VIII. Relations between structure and reactivity of polyethylene glycol dimethacrylates 185
— and GH. IVAN, A. CIUPITOIU, GH. DRAGAN, CR. OPRESCU, M. TOMESCU, D. AMBRONO, M. DIMONIE, Synthesis and polymerization of polyethylene glycol dimethacrylates. IX. Characterization of homo and copolymers of polyethylene glycol dimethacrylates 527

I.

IBRAHIM A., voir KHALIL Z. G. 725
IONESCU D., voir ZALARU F. 811
IONITA S., voir LANGFELD H. W. 151
ISSA R. M., voir ISSA Y. M. 825
ISSA Y. M. and A. M. HINDAWEY, A. L. EL ANSARY, R. M. ISSA, Spectroscopic investigation of charge transfer complexes of methyl pyridines with aromatic nitro compounds 825
IVAN GH., voir HUBCA GH. 527
IYER V., voir NAQVI S. F. A. 425

J.

JAIN P. K., voir VARMA R. P. 15
JARONIEC M., voir DABROWSKI A. 201
JUHASZ A., voir SCHWARTZ R. 499
JURCONI E., voir MURGULESCU I. G. 869

K.

KAMIL F. and P. P. SINHA, S. K. SINDHWANI, Complexometric and spectrophotometric determination of copper using phenanthrenequinone monosemicarbazone (PQSC) 413
KHALIL Z. H. and A. IBRAHIM, Synthesis and spectral behaviour of benzoxazolium indolo (or benfurano) quinolinium bisethiodide cyanine dyes 725
KOHDAIR A. I. and A.-M. A. ABDEL-WAHAB, H. S. EL-KASHEF, K. M. HASSAN, A. M. EL-KHAWAGA, M. F. EL-ZOHARY, Oxidation of some selected dihydric alcohols 921
KUDESIA V. P. and C. B. SHARMA, Effect of structure on the reactivity in the oxidation of aliphatic alcohols by chlorine dioxide 263
KULSHRESTHA S. K., voir FADNIS A. G. 99
KUMAR A., voir VARMA R. P. 819

L.

LABLACHE-COMBIER A., voir SURPATEANU GH. 831
— , voir SURPATEANU GH. 933
LANGFELD H. W. and S. IONITA, Behavoir of some aminonaphtholsulphonic acids in the azo coupling reaction (in German) 151
LANGSHAW V., voir VILCU R. 891
LATA P., voir BAHADUR P. 217
LAZAR D. P., voir M. M. GIRGIS 325
— , voir M. M. GIRGIS 445
— , voir GIRGIS M. M. 593
LAVALE S. C. and K. S. PITRE, Search for the amperometric titration method for the ultramicro and micro estimations of La^{3+} and Ce^{3+} 521
LECA M. and M. ENACHE, Determination of polymer partial solubility parameters by gas-liquid chromatography 287
LEPADATU C. I., voir XU YU XIN 83
LI DEHE, voir MINDRU I. 683
LITEANU C. and R. POPESCU, Study of the behaviour of α, α-diphenyl-β-picrylhydrazyl free radical in chromatography, as admixture to different stationary phases 177
LUCA C., voir BILBA N. 1009
LUCA C., voir PAK U SAP 833
LUCA C. and A. POPA, N. BILBA, GH. MIHĂILĂ, Inclusion compounds of perhydrotriphenylene with higher n-alcohols 211
LUCA M., voir HERDAN J. 757
LUCHIAN C., voir SURPATEANU GH. 831
LUCHIAN C., voir SURPATEANU GH. 933

M.

MACAROVICI C. GH., voir MARTA L. 957
MACOVEANU M., voir UNGUREANU ST. 763

MARCHIDAN S. and I. VARTIRES, I. TANASE, N. D. TOTIR, Determination of trace quantities of cobalt by anodic stripping voltammetry and alternating current polarography 275
— and I. VARTIRES, N. D. TOTIR, Determination of trace quantities of the group V—A elements by anodic stripping voltametry. III. Trace analysis of bismuth 41
MARCU GH., voir ZSAKO J. 107
MARTA L. and M. ZAHARESCU, I. HAIDUC, C. GH. MACAROVICI, Synthesis of strontium metaniobate by a coprecipitation method. 957
MASCAS A., voir STERNBERG S.. 437
MATEESCU A., voir STERNBERG S. 583
MATHUR B. B. L., voir SRIVASTAVA S. P. 27
MATHUR S. P., voir NAQVI S. F. A. 425
MEGHEA A., voir ZALARU F. 811
MICU-SEMENIUC R. and S. BARBU, M. S. MIHAIU, Coordination compounds of thiocarbohydrazone-2-amino-bezaldehyde with Co(II) and Ni(II) salts 365
— and E. HILVA, G. DOBOS-ROMAN and L. GHERGARI, Investigation of some complex metal thiocyanates with chlatration properties 471
— and S. POPSE, I. HAIDUC, Some novel salts and ligand properties of the cyclic $P_2S_8^{2-}$ anion 605
MINCU G., voir MURGULESCU I. G. 779
MINCU G., voir MURGULESCU I. G. 869
MIHAILA GH., voir BILBA N. 1009
MIHAILA GH., voir LUCA C. 211
MIHAIU M. S., voir MICU-SEMENIUC R. 365
MIHART C. and M. MRACEC, Z. SIMON, Molecular orbital studies for cyclophosphazene derivates. III. Comparison of Fukui and Dewar models 3
— and S. RADULY, Z. SIMON, Molecular orbital studies for cyclophosphazene derivatives. IV. All-valence electron calculations by the HMO and DEL RE methods 857
MINDRU I. and M. OLTEANU, LI DEHE, V. TRANDAFIR, Glass transition of polyblends of collagen hydrolysates and poly(ethyl acrylate) 683
MOLDOVEANU S., voir XU YU XIN 83
MORARU L., voir SCHWARTZ R. 499
MRACEC C., voir MIHART C. 3
MURESAN N., voir RAILEANU M. 381
MURGULESCU I. G. and E. JURCONI, G. MINCU, Thermal decomposition and oxidoreduction of the trisoxalato Co(III) complex 869
— and G. MINCU, Kinetics and mechanism of oxidoreduction reaction of the hydroxoaquobisoxalato Co(III) complex with iodide ion in neutral medium . . . 779

N.

NAQVI S. F. A. and S. P. MATHUR, V. IYER, Spectrophotometric determination of iron with sodium-N-(o-sulphonic-benzoyl)-N-pyridine in the presence of thiocyanate 425
NICOLESCU I. V., voir SANDULESCU I. 669
NEGOITA N., voir J. HERDAN 129
NEGOIU D. and I. GHELASE, Complex compounds of Cd(II) with acetone selenosemicarbazone 225
— and I. GHELASE, Complex compounds of Ni(II) with acetone selenosemicarbazone 355
— , voir GHELASE I. 463

O.

OLTEANU M., voir MINDRU I. 683
ONU P., voir BILBA N. 1009
OPREA S., voir DUMITRIU E. 535
OPREAN I., voir A. A. BOTAR 741
OPRESCU CR., voir HUBCA GH. 185
— , voir HUBCA GH. 527

P.

PALIBRODA N., voir CIURDARU GH. 333
PAK U SĂP and D. F. ANGHEL, C. LUCA, Electrochemical sensors for anionic surfactants. I. The electrode based on bis [2,4,6-tri(2-pyridyl)-1,3,5-triazine] iron (II) dodecyl sulphate 883
PĂUNESCU L., Molecular complexes of safranine O (in French) 615
PAVELESCU C., voir COBIANU C. 57
PETRESCU S. and V. PETRESCU, I. GALASIU, T. BRUSALIS, The equation of cathodic polarization in fused salts of halogen-active carbon electrode applied to bromine and iodine 451
PETRESCU V., voir PETRESCU S. 451
— , voir STERNBERG S. 565
PETREUS O. and F. N. POPESCU, Thermal behaviour of macromolecular compounds containing phosphorus and sulfur in their chains and of their mixtures with poly-(propene) (in French) 387
PETRILA C., voir UNGUREANU ST. 763
PETROVEANU M., voir GEORGESCU E. I. 841
— , voir SURPATEANU GH. 831
PARVULESCU V., voir SANDULESCU I. 669
PITRE K. S., voir LAVALE S. C. 521
POPA A., voir LUCA C. 211
POPESCU F. N., voir PETREUS O. 387
POPESCU M. and A. DANET, Mercury (II) complexes of phenyl-α-pyridyltriazine and *p*-nitrophenyl-α-pyridyl-triazene ; properties and analytical application in a spectrophotometric method 65
POPESCU R., voir LITEANU C. 177
POPOVICI N. and A. BARABAS, F. HODOSAN, Exo- and endohormones. VII. Synthesis of Z-11-tetradecen-1-ol-acetate by phosphonium ylide condensation 995
POPSE S., voir MICU-SEMENIUC R. 605

R.

RADULY S., voir MIHART C. 857
RAILEANU M. and A. FLOREA, N.MURESAN, Solvent effects. II. Solvent influence on the acidity of some nitrophenothiazinic compounds 381
RUIZ PASTRANA M., voir FERRARI L. 123
RUSU M.-D., voir CIURDARU GH. 333

S.

SAHINI V., voir CIUREANU M. 555
— and E. VOLANSCHI, Electronic structure and UV-spectra of some dibenzo[*b*, *e*]-thiepine derivatives 785
SALLO A. and B. DAMIAN, O. EXNER, The kinetic and mechanism of the diazo-coupling reaction of 4-chloro-1-naphthol 169
SANCHEZ BALLESTERO J. and M. D. H. HERNANDEZ, Preparation of dispiranic structures. Spectroscopic study of their configuration and transformation into furan derivatives 503
SANDULESCU I. and I. V. NICOLESCU, XU YAN DONG, V. PÎRVULESCU, Selectivity and other properties of Pd, Mn and Pd$-$Mn/Al_2O_3 catalysts for styrene hydrogenation 669
SALEH R. M., voir EL-KADY M. 915
SAYED G. H. and M. S. ABD ELHALIM, Some reactions of 3,4-dichloro-β,benzoyl-N-tolylacrylamide 493
SCHWARTZ R. and A. JUHASZ, S. SELINGER, L. MORARU, Some derivatives of 3β-hydroxy-B-nor-cholest-5-ene 499
SEGAL E. I., On the diffusion coefficient in binary mixtures of gases 953
— , voir M. M. GIRGIS 325
— , voir GIRGIS M. M. 445
— , voir GIRGIS M. M. 593
SELINGER S., voir SCHWARTZ R. 499

SENGUPTA S. K. and B. P. BARANWAL, Preparation and characterization of complexes of bis-(cyclopentadienyl) and bis-(methyl cyclopentadienyl) zirconium (IV) dichloride with carboxylic acids 487
SHABAN A. F., voir HAMED A. A., 623
SHARMA C. B., Kinetics of oxidation of propan-2-ol by chlorine dioxide 967
— , voir KUDESIA V. P. 263
SILBERG I. A. and S. SILBERG, Derivatives of 4-aminomethyl-thiazole. III. Oxidative cyclizations and dethionations in the series of 1-phenyl-3-(2-aryl-4-thiazolylmethyl)-thioureas 139
SILBERG I. A., voir SILBERG S. 243
— , voir SILBERG S. 719
SILBERG S., voir SILBERG I. A. 139
— and I. A. SILBERG, C. BODEA, Derivatives of 4-aminomethyl-thiazole. IV. Thiazole derivatives of phenothiazine 243
— and I. A. SILBERG, Derivatives of 4-aminomethylthiazole II. New thiazole derivatives of urea and thiourea 719
SIMON Z., voir MIHART C. 3
— , voir MIHART C. 857
SIMONESCU T., voir HAVLIK I. 375
SINDHWANI S. K., voir KAMIL F. 413
SINGHAL O. P., voir SYAMAL A. 805
SINGHAL P., voir VARMA R. P. 115
SINHA P. P., voir KAMIL F. 413
SRIVASTAVA S. P. and B. B. L. MATHUR, Kinetics and mechanism of Ag$^+$ catalysed oxidation of isoleucine by peroxydisulphate ion 27
STANCU R., voir CEAUŞESCU E. 299
STEPAN E. and A. T. BALABAN 707
STERNBERG S., voir BRINZOI V. 193
— and V. BRANZOI, L. APATEANU, A. MATEESCU, Behaviour of polarization of lead and lead-antimony alloys in sulphuric acid solutions 585
— and MASCAS A., Temperature dependence of thermal conductivity in Ca(NO$_3$)$_2$.4H$_2$O—nH$_2$O system 437
— and V. PETRESCU, T. VISAN, A. COTARTA, Electrochemical reaction of Cu^{2+} and Cu$^+$ in the LICl—KCl eutectic. I. Galvanostatic study 565
STOICESCU C., Kinetics of decarboxylation of β-pyridylacrylic acids 147
SUBHANI M. S., The study of the reaction between TeO$_3^{2-}$ and BrO$_3^-$ ions in solution 23
— , Radiation chemistry of iodate anion in aqueous solution 281
— , Photodecomposition of hypoiodite ion in aqueous solution 397
SURPATEANU GH. and M. CONSTANTINESCU. C. LUCHIAN, M. PETROVANU, I. ZUGRAVESCU, A. LABLACHE-COMBIER, Theoretical study in the reactivity of the cycloimmonium-ylides. I. Reactivity of the monosubstituted carbanion-ylides 831
— and M. CONSTANTINESCU, C. LUCHIAN, M. PETROVANU, I. ZUGRAVESCU, A. LABLACHE-COMBIER, Theoretical aspects on the reactivity of the cycloimmonium-ylides. II. Reactivity of the disubstituted carbanion-ylides 831
SZYMURA J. A., Determination of metal dispersion of Pd/SiO$_2$ catalyst by a combination of transmission electron microscopy with X-ray diffraction and chemisorption methods 597
SYAMAL A. and B. K. GUPTA, New cobalt(II) complexes with tridentate dibasic ONO donor ligands 805
— and O-P. SINGHAL, New Dioxouranium(VI) complexes with tridentate dibasic Schiff bases prepared from β-diketones and amines 981

T.

TANASE I., voir MARCHIDAN S. 275
TOMESCU M., voir HUBCA GH. 527
TOTH A., voir HAVLIK I. 903
TOTIR N. D., voir MARCHIDAN S. 41
— , voir MARCHIDAN S. 275
TRANDAFIR V., voir MINDRU I. 683

U.

UGLEA C. V., voir BEZDADEA 419
UNGUREANU ST. and M. MACOVEANU, C. PETRILA, Study of the sensitivity of a reactor for vinyl chloride suspension polymerization with constant rate (in German) 763

V.

VARHELYI M., voir ZSAKO J. 107
VARMA R. P. and B. B. BHATNAGAR and P. SINGHAL, Studies on physical properties of alkaline earth metal dodecyl sulphates. I. Conductivity studies of $Ca(SD)_2$ in water-acetone mixtures 115
— and P. K. JAIN, Studies on behaviour of cobalt and calcium soaps. V. Effect of amines on the conductance behaviour in methanol at 35° 15
— and A. KUMAR, Conductance behaviour of aqueous solutions of alkaline earth metal butyrates 819
VARTIRES I., voir MARCHIDAN S. 41
— , voir MARCHIDAN S. 275
VILCU R. and Z. CENUSE, F. GOTHARD, V. LANGHAW, A new installation for the saturation pressure measurement in the multicomponent system (in Spanish) 891
— , voir CIOCHINA A. 795
VISAN S., voir V. ARMEANU 45
VISAN T., voir STERNBERG S. 565
VLADESCU L. and S. GHINEA, Ion exchange chromatographic separations in the presence of Tiron 513
VOICU M., voir VOLANSCHI E. 689
VOICU V. G., Polarographic kinetic study of the oxidation of uranium(V) by vanadium (IV) in sulfonic acid medium 53
VOLANSCHI E., voir SAHINI V. E. 785
— and M. VOICU, ESR electronic spectra of some nitrosubstituted thioureide anion-radicals 689

Z.

ZAHARESCU M., voir MARTA L. 957
ZALARU F. and D. IONESCU, A. MEGHEA, F. CORNEA, C. GHEORGHIU, Coordination compounds of Cu(II) with some triazenoimidazole derivatives 811
ZSAKO J. and M. VARHELYI, GH. MARCU, Electronic spectra of some cis $Co(en)_2AX^{2+}$ type complexes 107
ZUGRAVESCU I., voir GEORGESCU F. C. 267
— , voir SURPATEANU GH. 831
— , voir SURPATEANU GH.. 831

X.

XU YAN DONG, voir SANDULESCU I. 669
XU YU XIN and S. MOLDOVEANU, C. I. LEPADATU, IR analysis of some oil pollutants in water. 83

[illegible]

NOTE POUR LES AUTEURS

La Revue Roumaine de Chimie publie des articles en anglais, français, russe, allemand ou espagnol. Les auteurs sont priés d'envoyer des articles et des comptes rendus inédits.

Les manuscrits seront dactylographiés à double interligne. La bibliographie, les tableaux et la légende des figures seront placés après le texte.

Si l'article fait partie d'une série numérotée, la partie précédente sera donnée comme première référence.

Chaque article sera précédé d'un résumé comprenant quinze lignes au maximum.

Les références bibliographiques dans le texte seront faites par des exposants sans parenthèses et paraîtront à la fin de l'ouvrage.

Les publications périodiques mentionnées dans la bibliographie seront présentées suivant les prescriptions internationales : le nom de l'auteur précédé de l'initiale du prénom, le titre du périodique abrégé conformément à « Chemical Abstracts » et souligné par une ligne, le numéro du tome indiqué par des chiffres arabes et souligné par deux lignes, suivi de la première page de l'article ; à la fin, l'année de la parution sera placée entre parenthèses. La numéro de la revue ne sera pas indiqué si les pages du volume sont numérotées consécutivement.

Les textes des livres ou traités incluеront : le nom des auteurs, l'initiale du prénom, le titre du livre entre guillemets et sans être souligné, le numéro du tome précédé par l'abréviation « vol. » (ou « Bd. »), le numéro de l'édition, les éditions (the publisher), la localité de la parution du livre, l'année de la parution et la page de la référence précédée(s) par l'abréviation « p » (ou « S »).

Les brevets seront indiqués comme suit : l'auteur ou la firme, le pays et le numéro du brevet, la date et la revue *(Chem. Abstr.)*. Par ex. : M. Jones (to Union Carbide Co.), Brit. Pat. 601 238, 2 sept. 1959 ; cf. *Chem. Abstr.*, **54**, 12808 (1960).

Si la référence n'a pas lue en original, on indiquera aussi la revue de références consultée.

Les diagrammes seront tracés à l'encre de Chine sur papier calque. Les tableux et les figures (en nombre strictement nécessaire), ainsi que les courbes dans les figures seront numérotés par des chiffres arabes. Leur explication sera donnée dans la légende des figures. Prière de ne pas inscrire les mêmes données dans les tableaux et les figures. Chaque tableau aura un titre. On indiquera dans le texte la place approximative des tableaux et des figures. Les formules chimiques seront incluses dans le texte ; en outre, elles seront transcrites sur papier calque, à l'encre de Chine.

Les auteurs sont priés d'indique les caractères italiques (en soulignant les lettres au crayon), ainsi que tout autre caractère spécial : les préfixes *ortho*, *meta*, *para*, *cis*, *trans*, etc. seront soulignés pour indiquer leurs caractères italiques et ne seront jamais écrits avec des majuscules.

Aucune correction à la main ne sera admise sur le manuscrit. Les correction seront tapées à la machine. Les lettres grecques ou d'autres symboles spéciaux seront insérés à la main à l'encre clairement.

Le manuscrit sera signé par l'auteur.

Le titre-courant aura 50 lettres au maximum.

L'entière responsabilité du contenu des article appartient aux auteurs.

Sur demande on peut obtenir une note plus complète.

PRINTED IN ROMANIA

1984 FEB 0 9

TRAVAUX PARUS AUX ÉDITIONS DE L'ACADÉMIE DE LA RÉPUBLIQUE SOCIALISTE DE ROUMANIE

ELENA CEAUȘESCU, **Noi cercetări în domeniul compușilor macromoleculari** (Nouvelles recherches dans le domaine des composés macromoléculaires), 1981, 536 p.

I. G. MURGULESCU, RODICA VÎLCU, **Introducere în chimia fizică Vol. III. Termodinamica chimică** (Introduction à la chimie physique, Vol. III, Thermodynamique chimique) 1982, 624 p.

I. G. MURGULESCU, J. PĂUN, **Introducere în chimia fizică, Vol. I. 3. Nucleul atomic, reacții nucleare, particule elementare** (Introduction à la chimie physique. Vol. I. 3. Noyau atomique, réactions nucléaires, particules élémentaires), 1982, 606 p.

ELENA JERCAN, **Analiza cromatografică** (Analyse chromatographique), 1982, 286 p.

I. G. MURGULESCU, TATIANA ONCESCU, E. SEGAL, **Introducere în chimia fizică. Vol. II. 2. Cinetică chimică și cataliză** (Introduction à la chimie physique. Vol. II. 2. Cinétique chimique et catalyse) 1981, 1024 p.

V. DRĂGUȚAN, A. T. BALABAN, M. DIMONIE, **Metateza olefinelor și polimerizarea prin deschidere de inel a cicloolefinelor** (La métathèse des oléfines et la polymérisation par ouverture annulaire des cyclooléfines), 1981, 254 p.

LYDIA-MARIA VAICUM, **Epurarea apelor uzate cu nămol activ. Bazele biochimice** (L'épuration des eaux résiduelles à boue active. Les bases biochimiques,) 1981, 218 p.

I. GĂLĂȚEANU, **Procese și metode radiochimice în energetica nucleară** (Processus et méthodes radiochimiques dans l'énergétique nucléaire), 1981, 234 p.

OCTAVIAN IORDACHE, **Procese polistocastice aplicate la fenomenele de transfer** (Processus polystochastiques appliqués aux phénomènes de transfert), 1981, 186 p.

CR. SIMIONESCU, VALERIA GORDUZA, **Polimeri biocompatibili și biologic activi** (Polymères biocompatibles et biologiquement actifs), 1980, 479 p.

ELENA CEAUȘESCU, **Polimerizarea stereospecifică a izoprenului** (La polymérisation stéréospécifique de l'isoprène, 1979, 307 p.

CONST. GH. MACAROVICI, **Analiza chimică cantitativă anorganică** (L'analyse chimique quantitative inorganique), 1979, 457 p.

M. FLORESCU, **Metode științifice în dezvoltarea industriei chimice moderne** (Méthodes scientifiques dans le développement de l'industrie chimique moderne), 1979, 256 p.

A. T. BALABAN, I. GĂLĂȚEANU, G. GEORGESCU, LIGIA SIMIONESCU, **Compuși marcați și radiofarmaceutuici cu aplicații în medicina nucleară** (Composés marqués et radiopharmaceutiques à application en médecine nucléaire), 1979, 495 p.

I. G. MURGULESCU, E. SEGAL, **Introducere în chimia fizică. Vol. II. 1. Teoria molecular cinetică a materiei** (Introduction à la chimie physique. Vol. II. 1. La théorie moléculaire-cinétique de la matière), 1979, 1036 p.

S. STERNBERG, FL. DANEȘ, **Termodinamica chimică aplicată** (La thermodynamique chimique appliquée), 1978, 400 p.

I. G. MURGULESCU, V. EM. SAHINI, **Introducere în chimia fizică, Vol. 1. 2. Structura și proprietățile moleculelor** (Introduction à la chimie physique. Vol. 1.2. La structure et les propriétés des molécules), 1978, 605 p.

I. ZUGRĂVESCU, MAGDA PETROVANU, **N-ylid chemistry**, coédition avec McGraw-Hill International Book Company, U.S.A., 1977, 396 p.

I. G. MURGULESCU, **Introducere în chimia fizică Vol. I. 1. Atomi, molecule, legătură chimică** (Introduction à la chimie physique, Vol. 1. 1. Atomes, molécules, liasion chimiques), 1976, 560 p.

ELENA CEAUȘESCU, **Research work on synthesis and characterization of macromolecular compounds, Contributions**, 1974, 251 p.

CR. SIMIONESCU, VIORICA RUSAN, V. POPA, **Chimia algelor marine** (La chimie des algues marines), 1974, 212 p., 1 pl.

ISSN 0035–4090

I. P. „Informația" — c. 1410

43 426

Lei 40

$ 75 (pour un abonnement annuel)